HABILITAČNÍ PRÁCE

2018

Ing. Miroslav Lísa, Ph.D.

Univerzita Palackého v Olomouci

Přírodovědecká fakulta

Využití chromatografie a hmotnostní spektrometrie v lipidomické analýze

Ing. Miroslav Lísa, Ph.D.

Univerzita Hradec Králové

Přírodovědecká fakulta

Katedra chemie

Habilitační práce

Obor: Analytická chemie

Hradec Králové 2018

Prohlašuji, že předloženou habilitační práci jsem vypracoval samostatně s využitím informačních zdrojů, které jsou citovány.

V Hradci Králové, dne 9.4.2018 Ing. Miroslav Lísa, Ph.D.

Poděkování

Na tomto místě bych chtěl poděkovat všem kolegům a spolupracovníkům, kteří se podíleli na vzniku publikací tvořících základ mé habilitační práce. Zejména pak bývalým kolegům ze skupiny Hmotnostní spektrometrie na Katedře analytické chemie Univerzity Pardubice, dále všem studentům a zahraničním stážistům, se kterými jsem v průběhu let spolupracoval.

Největší poděkování patří mé rodině, dětem a zejména manželce Haně, která je mi po celou mou vědeckou kariéru důležitou oporou.

Obsah

Seznam zkratek

Ag-HPLC	Argentační chromatografie (Argentation Chromatography)
APCI	Chemická ionizace za atmosférického tlaku (Atmospheric Pressure Chemical Ionization)
DB	Dvojná vazba (Double Bond)
CAD	Aerosolový detektor nabitých částic (Charged Aerosol Detector)
CN	Počet uhlíků (Carbon Number)
ECN	Ekvivalentní počet uhlíků (Equivalent Carbon Number)
ELSD	Detektor rozptylu světla (Evaporative Light Scattering Detector)
ESI	Ionizace elektrosprejem (Electrospray Ionization)
FID	Plamenově-ionizační detektor (Flame Ionization Detector)
GC	Plynová chromatografie (Gas Chromatography)
HILIC	Kapalinová chromatografie hydrofilních interakcí (Hydrophilic Interaction Liquid Chromatography)
HPLC	Vysokoúčinná kapalinová chromatografie (High-Performance Liquid Chromatography)
MALDI	Ionizace laserem za účasti matrice (Matrix Assisted Laser Desorption-Ionization)
MS	Hmotnostní spektrometrie (Mass Spectrometry)
NARP	Nevodné systémy s obrácenými fázemi (Non-Aqueous Reversed Phase)
NP	Normální fáze (Normal Phase)
PCA	Analýza hlavních komponent (Principal Component Analysis)
RP	Obrácené fáze (Reversed Phase)
UHPLC	Ultravysokoúčinná kapalinová chromatografie (Ultrahigh-Performance Liquid Chromatography)
UHPSFC	Ultravysokoúčinná superkritická fluidní chromatografie (Ultrahigh-Performance Supercritical Fluid Chromatography)

Úvod

Cílem lipidomické analýzy je kvalitativní a kvantitativní popis složení lipidů (lipidomu) v organismu, tkáni nebo buňce a sledování jejich interakcí s ostatními lipidy, proteiny a metabolity. Lipidomika je poměrně mladý obor, který byl poprvé definován jako podobor metabolomiky v roce 2003 autory Han a Gross [1]. Tento obor však nabývá rychle na významu, protože lipidy jsou biologicky aktivní látky, které mají celou řadu nezastupitelných rolí v lidském organismu. Představují hlavní zdroj energie, vitamínů rozpustných v tucích a esenciálních mastných kyselin, jsou důležité strukturní komponenty biologických membrán a fungují jako signální molekuly v buněčné komunikaci [2-4]. Nerovnováha lipidů v organismu může mít vliv na vznik a vývoj řady závažných onemocnění, jako jsou obezita, nádorová onemocnění nebo diabetes, proto jsou lipidy v současné době intenzivně studovány jako potenciální biomarkery.

Lipidy jsou definovány jako hydrofobní nebo amfipatické malé molekuly, které vznikají alespoň částečně kondenzací thioesterů a/nebo kondenzací isoprenových jednotek [5, 6]. To představuje širokou škálu látek s odlišnou strukturou, které lze rozdělit do 8 základních kategorií na mastné acyly, glycerolipidy, glycerofosfolipidy, sfingolipidy, sacharolipidy, polyketidy, steroly a prenoly (Obrázek 1). Každá z těchto kategorií dále zahrnuje řadu tříd, podtříd a molekul lipidů, které se navzájem liší funkčními skupinami a navázanými acyly s různou délkou řetězců a počtem dvojných vazeb. Jednotlivé molekuly

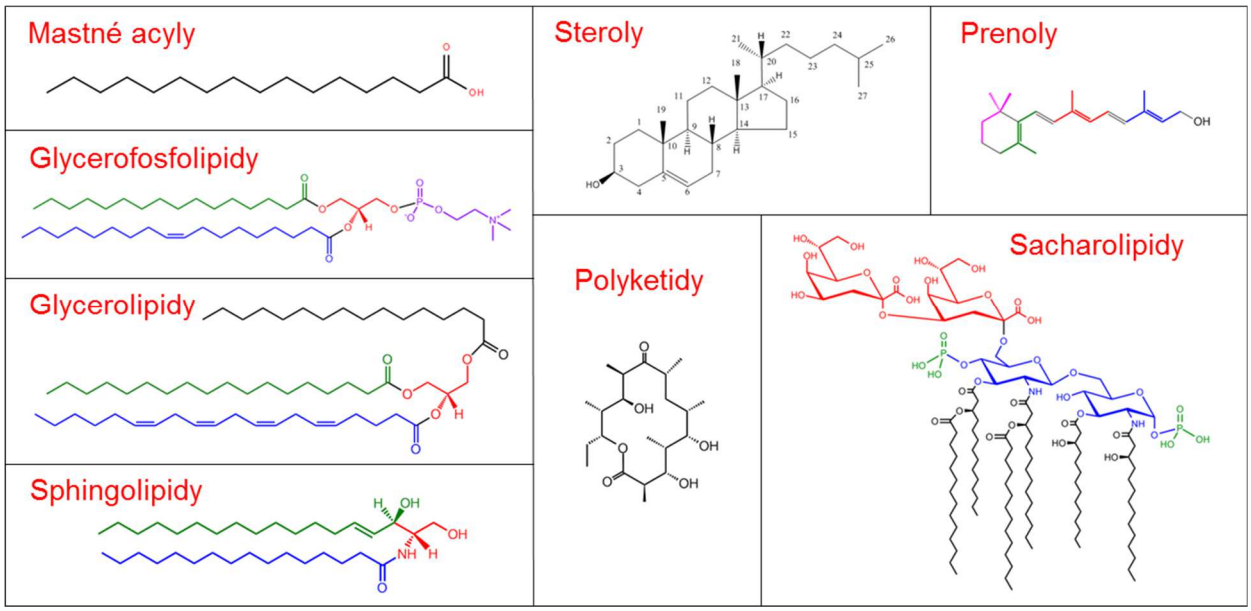

Obrázek 1 Struktury vybraných zástupců 8 základních kategorií lipidů.

lipidů se dále mohou lišit typem izomerie, jako je *cis*-/*trans*- izomerie dvojných vazeb, poloha dvojných vazeb v acylovém řetězci, lineární/větvené řetězce nebo poloha acylu na glycerolovém skeletu (regioizomery a enantiomery), přičemž každý izomer má jinou biologickou aktivitu v organismu. Přírodní vzorky obsahují stovky až tisíce molekul strukturně odlišných lipidů, které jsou ve vzorku zastoupeny v řádově rozdílných koncentracích, což klade velmi vysoké nároky na používané analytické techniky. Chromatografické separace společně s hmotnostní spektrometrií (MS) jsou dnes nejrozšířenější analytické techniky v lipidomické analýze [7, 8], které díky výraznému instrumentálnímu pokroku v posledních letech umožňují získat stále detailnější a přesnější informace o složení lipidů ve vzorku.

Metody lipidomické analýzy mohou být cílené pouze na vybrané a předem známé molekuly lipidů nebo mohou být metody necílené, které se snaží o detailní popis všech lipidů přítomných ve vzorku. V lipidomické analýze se většinou používají dva základní analytické přístupy, a to analýza lipidů založená na chromatografické separaci lipidů a jejich následné MS identifikaci/kvantifikaci a přímá analýza lipidů pomocí MS (někdy nazývaná též shotgun analýza) [7]. Přímá MS lipidomická analýza zahrnuje metody bez separačního kroku. Vzorek lipidů je přímou infúzí zaváděn do iontového zdroje hmotnostního spektrometru, kde jsou všechny lipidy ve vzorku ionizovány najednou. Lipidy jsou identifikovány na základě MS a MS/MS spekter získaných pomocí hmotnostních analyzátorů s vysokou rozlišovací schopností a správností určení hmoty [9-12] nebo častěji pomocí MS/MS skenů založených na charakteristické fragmentaci lipidových tříd měřených pomocí hmotnostních analyzátorů na principu trojitého kvadrupólu [3, 13-15]. Výhodou MS metod je obvykle vyšší prostupnost vzorků a možnost automatizace pro měření rozsáhlých studií v klinické analýze. Nevýhodou těchto metod je obtížná analýza izomerů, izobarických sloučenin a stopových látek ve složitých směsích. Tyto nedostatky nemají metody využívající separační krok před MS detekcí, kde jsou lipidy separovány pomocí vhodného chromatografického módu a identifikovány/kvantifikovány pomocí MS. Díky separaci lipidů je dále potlačen vliv konkurenční ionizace látek v iontovém zdroji, který může být zásadní především pro lipidy s iontovou funkční skupinou. Vysokoúčinná (HPLC) nebo ultravysokoúčinná kapalinová chromatografie (UHPLC) jsou široce využívané chromatografické techniky v lipidomické analýze. Lipidy mohou být separovány v systémech s obrácenými fázemi (RP) na základě složení acylových řetězců, tzn. délky řetězců a počtu dvojných vazeb [16-20]. Kapalinová chromatografie s hydrofilními interakcemi (HILIC) umožňuje separaci lipidů do tříd podle

jejich polarity a náboje, zatímco lipidy lišící se acylovými řetězci jsou eluovány v jednom chromatografickém píku odpovídajícímu lipidové třídě [21-24]. HILIC neumožňuje separaci méně polárních lipidů, které nejsou na koloně zadržovány a eluují v mrtvém objemu kolony. Nepolární lipidy mohou být separovány v systémech s normálními fázemi (NP) podle jejich polarity [22, 24-26], které ale nejsou vhodné pro separaci polárnějších lipidů kvůli jejich silné retenci. Izomery lipidů jsou většinou analyzovány pomocí speciálních chromatografických systémů po alespoň částečné frakcionaci vzorku na lipidové třídy. Pro separaci regioizomerů se používá argentační chromatografie (Ag-HPLC), která je založena na tvorbě slabých reverzibilních komplexů dvojných vazeb lipidů se stříbrnými ionty ve stacionární fázi [27]. Enantiomery lipidů mohou být analyzovány s použitím chirálních kolon [28]. Pro lipidomickou analýzu lze využít i ultravysokoúčinnou superkritickou fluidní chromatografii (UHPSFC), která zaznamenala v posledních letech výrazný rozvoj díky instrumentálnímu pokroku. UHPSFC umožňuje rychlou separaci polárních i nepolárních tříd lipidů v jedné analýze [29] nebo separaci jednotlivých molekul lipidů podle acylových řetězců [30]. Kvantitativní lipidomická analýza přírodních vzorků představuje náročný úkol vzhledem k vysokému počtu lipidů ve směsi s velkými strukturními rozdíly. Nejčastější způsob kvantitativní analýzy využívá neendogenních lipidů jako interních standardů pro jednotlivé třídy lipidů [7]. Jedná se o interní standardy lipidů s krátkými nebo naopak dlouhými acylovými řetězci, kombinace lichých a sudých acylů v molekule nebo izotopicky značené analogy. Koncentrace jednotlivých lipidů jsou vypočteny vztažením jejich signálu k signálu interního standardu o známé koncentraci, který je přidáván ke vzorku před jeho zpracováním. Toto zjednodušení poskytuje přijatelné kvantitativní výsledky a je široce používáno především pro srovnání koncentrací lipidů ve vzorcích pacientů a zdravých dobrovolníků v rámci klinických studií.

Předkládaná habilitační práce se zabývá vývojem a využitím chromatografických a hmotnostně spektrometrických metod pro lipidomickou analýzu široké škály rostlinných, živočišných a biologických vzorků. V práci jsou popsány metody plynové chromatografie (GC), HPLC, UHPLC a UHPSFC s MS detekcí pomocí chemické ionizace za atmosférického tlaku (APCI) a ionizace elektrosprejem (ESI). Metody jsou využity k detailní charakterizaci vybraných tříd lipidů včetně jejich izomerů, pro analýzu celkového lipidového extraktu a pro analýzu klinických vzorků. Habilitační práce je vypracována jako komentář výsledků 29 původních vědeckých prací v mezinárodních vědeckých časopisech, na kterých se autor práce významně podílel plánováním experimentů, experimentální prací, vyhodnocením dat a

publikací výsledků. Práce je členěna do 4 základních kapitol. První kapitola je věnována detailní charakterizaci a kvantitativní analýze triacylglycerolů ve více jak 160 průmyslově významných rostlinných olejích a tucích. Jsou zde popsány možnosti separace triacylglycerolů pomocí kapalinové chromatografie, jejich kvantitativní analýza, charakterizace vlastností vzorků a využití statistické analýzy výsledků pro odhalení falšování olejů. Tato část popisuje soubor přiložených prací P1 – P7. Druhá část práce se zabývá vývojem metod pro analýzu izomerů triacylglycerolů, jako jsou polohové izomery dvojných vazeb, *cis-/trans-* izomery dvojných vazeb, větvení acylového řetězce, regioizomery a enantiomery v rostlinných i živočišných vzorcích (soubor prací P5, P7 – P13). V této části jsou popsány i autorem vyvinuté postupy syntézy standardů regioizomerů a enantiomerů triacylglycerolů pro vývoj analytických metod. Další kapitola je věnována vývoji metod pro necílenou lipidomickou analýzu celkového lipidového extraktu a vybraných důležitých tříd lipidů v biologických vzorcích (soubor prací P14 – P25). V této části jsou popsány vyvinuté HPLC, UHPLC a UHPSFC metody pro HILIC, NP nebo RP separaci celkového lipidového extraktu i vybraných tříd lipidů, retenční chování lipidů v jednotlivých systémech a kvantitativní analýza lipidů. Poslední část práce je věnována aplikaci vyvinutých metod lipidomické analýzy pro analýzu biologických vzorků v rámci klinických studií. Cílem práce je popis vlivu onemocnění na složení lipidomu na základě porovnání vzorků pacientů se zdravými dobrovolníky v rámci klinických studií zaměřených na kardiovaskulární onemocnění a nádorová onemocnění ledvin a prsu (soubor prací P25 – P29). Práce dále obsahuje souhrn vědecko-pedagogické činnosti autora a přiložený soubor prací.

1 Analýza triacylglycerolů

Triacylglyceroly jsou estery glycerolu a vyšších mastných kyselin. Představují nejrozšířenější skupinu nepolárních lipidů, která slouží jako zdroj energie, tepelná a mechanická ochrana důležitých orgánů a především jako zdroj pro tělo esenciálních mastných kyselin přijímaných potravou jako rostlinné a živočišné tuky. Triacylglyceroly se vyskytují jako velmi komplexní směsi obsahující desítky až stovky molekul, což je dané velkým počtem možných kombinací acylů na glycerolovém skeletu. Správná volba chromatografických podmínek je zásadní pro detailní charakterizaci takto složitých směsí triacylglycerolů.

1.1 HPLC separace triacylglycerolů

Triacylglyceroly jsou molekuly nepolárního charakteru, které se navzájem liší esterifikovanými acyly mastných kyselin. Pro jejich analýzu se využívá separace v systémech s obrácenými fázemi pomocí C18 kolon, kde jsou triacylglyceroly separovány na základě hydrofobních interakcí. Vzhledem k jejich nízké polaritě se používají mobilní fáze bez vody, tzv. nevodné systémy s obrácenými fázemi (NARP). Retenční chování triacylglycerolů v NARP systémech lze zobecnit pomocí ekvivalentního počtu uhlíkových atomů (ECN), který vyjadřuje vtah mezi počtem uhlíků ve všech acylových řetězcích (CN) a počtem dvojných vazeb (DB), ECN = CN – 2×DB. Retence triacylglycerolů roste s hodnotou ECN a snížení retence vlivem přítomnosti jedné dvojné vazby odpovídá zkrácení řetězce o dva uhlíky (Obrázek 2). Pro analýzu směsí triacylglycerolů v rostlinných olejích a živočišných tucích byla vyvinuta metoda NARP-HPLC s APCI-MS detekcí (P1). Důslednou optimalizací chromatografických podmínek s použitím sériového zapojení kolon C18 o celkové délce 45 cm a složení mobilní fáze acetonitril – 2-propanol bylo v našich experimentech dosaženo kromě separace triacylglycerolů do skupin ECN i dostatečné separace v rámci jednotlivých skupin. To společně s APCI-MS detekcí umožnilo identifikaci více jak 400 triacylglycerolů složených z 36 acylů mastných kyselin s délkou řetězce 6 až 28 uhlíků a 0 až 6 dvojnými vazbami ve více jak 160 vzorcích rostlinných olejů a živočišných tuků (P1 – P7).

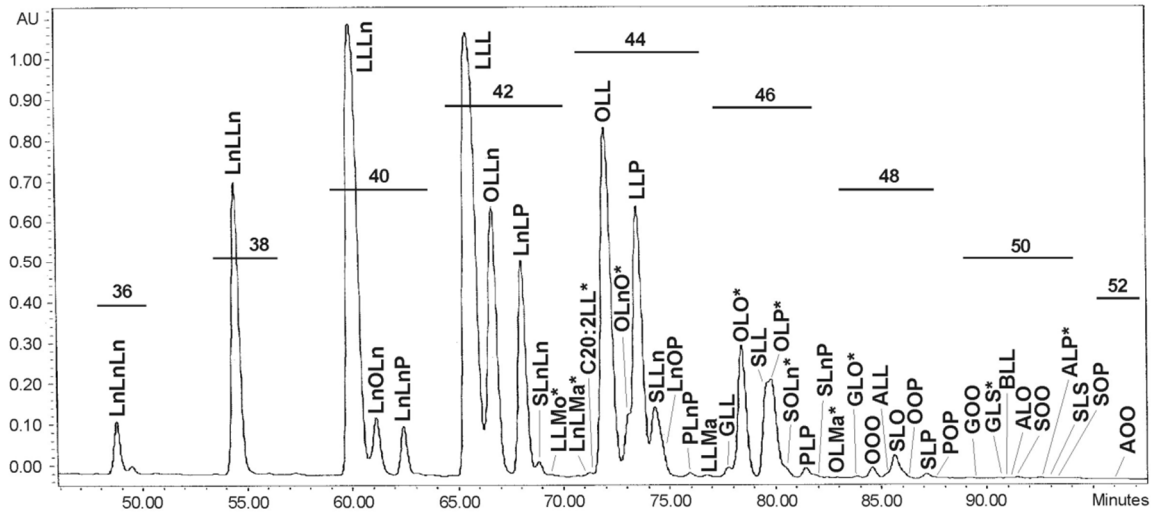

Obrázek 2 NARP-HPLC separace triacylglycerolů oleje z vlašských ořechů (P1).

Část experimentů byla zaměřena na využití nových kolon pro NARP separaci triacylglycerolů (P6). Kolony byly testovány pomocí oleje z černého rybízu, který je charakteristický svou komplexností díky obsahu velkého množství triacylglycerolů a přítomnosti polohových izomerů dvojných vazeb. NARP-HPLC s použitím konvenčních kolon C18 o celkové délce 45 cm, průměrem kolony 3,9 mm a velikostí částic 4 µm poskytuje dostatečné rozlišení triacylglycerolů oleje z černého rybízu, ale nevýhodou tohoto systému jsou poměrně dlouhé retenční časy triacylglycerolů (až 90 min). S použitím C18 UHPLC kolony délky 10 cm a průměru 2,1 mm s velikostí částic 1,7 µm bylo dosaženo téměř 10 násobného zkrácení retenčních časů triacylglycerolů se zachováním chromatografického rozlišení oproti konvenčním kolonám. Zajímavou alternativou pro NARP-HPLC separaci triacylglycerolů je C30 kolona, u které byl pozorován výrazný vliv teploty kolony na separaci. Se změnou teploty kolony může dojít až ke změně elučního pořadí triacylglycerolů, což není pozorováno v NARP systémech s použitím C18 kolon. Pro zvýšení prostupnosti vzorků byla testována monolitická kolona, která umožňuje použití vysokých průtoků mobilní fáze a tím výrazné zkrácení retenčních časů, ale za cenu nižšího chromatografického rozlišení.

Pro detailní analýzu směsí triacylglycerolů byla testována off-line dvourozměrná separace triacylglycerolů v systémech NARP-HPLC a Ag-HPLC (P5). Vzájemná ortogonalita systémů umožňuje separaci většího počtu triacylglycerolů a zároveň i separaci některých izomerů. Triacylglyceroly jsou v první dimenzi separovány podle složení acylů pomocí NARP-HPLC a jejich frakce jsou následně analyzovány v druhé dimenzi pomocí Ag-HPLC podle počtu dvojných vazeb. V off-line uspořádání není omezen čas pro separaci v druhé dimenzi

vzorkovací frekvencí z první dimenze a je možné použít optimalizovanou metodu s delšími retenčními časy. Díky tomu bylo možné dosáhnout v druhé dimenzi nejen separace triacylglycerolů podle počtu dvojných vazeb, ale i rozlišení regioizomerů triacylglycerolů ve vzorku oleje z černého rybízu (Obrázek 3).

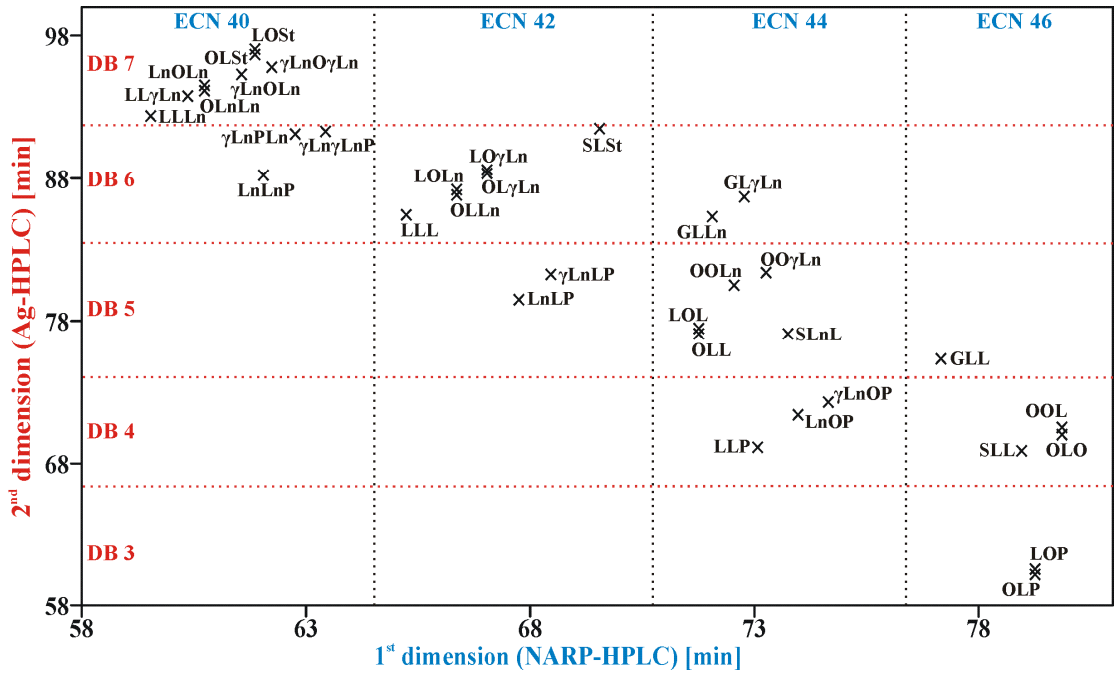

Obrázek 3 Dvoudimenzionální off-line NARP-HPLC x Ag-HPLC/APCI-MS separace oleje z černého rybízu (P5).

1.2 Kvantitativní analýza triacylglycerolů

Důležitou součástí práce byl vývoj metody pro kvantitativní analýzu triacylglycerolů v rostlinných olejích a živočišných tucích, která je obtížná vzhledem ke komplexnosti vzorků. Pro charakterizaci složení acylů mastných kyselin ve vzorku byla použita metoda GC s plamenově-ionizační detekcí (FID) po transesterifikaci triacylglycerolů na methylestery mastných kyselin (P1, P7). Metoda GC/FID analýzy methylesterů poskytuje důležitou informaci o složení mastných kyselin triacylglycerolů a průměrné nutriční hodnotě vzorku. Na druhou stranu tato metoda neumožňuje popsat složení acylů v intaktních triacylglycerolech.

Pro kvantitativní analýzu intaktních triacylglycerolů ve směsi byla vyvinuta metoda založená na odezvových faktorech (P1) pomocí NARP-HPLC separace s APCI-MS detekcí. APCI je ionizační technika vhodná pro analýzu nepolárních triacylglycerolů, která umožňuje

určit molekulovou hmotnost triacylglycerolu a poskytuje i dostatek fragmentových iontů pro identifikaci navázaných acylů mastných kyselin již v hmotnostních spektrech prvního řádu. Metoda kvantitativní analýzy je založená na stanovení odezvových faktorů jednoduchých triaclylglycerolů reprezentujících acyly mastných kyselin zastoupených ve vzorku (např. 18:0/18:0/18:0, 18:1/18:1/18:1, 18:2/18:2/18:2, atd.) vztažením hodnoty směrnice kalibrační přímky ke směrnici trioleinu (18:1/18:1/18:1) jako nejčastěji zastoupenému triacylglycerolu v přírodních vzorcích. Odezvové faktory směsných triacylglycerolů jsou počítány jako aritmetický průměr odezvových faktorů jednoduchých triacylglycerolů odpovídajících přítomným mastným kyselinám, např. 18:0/18:1/18:2 = (18:0/18:0/18:0 + 18:1/18:1/18:1 + 18:2/18:2/18:2)/3. Tato metoda poskytuje dostatečně přesné výsledky porovnatelné s výsledky získanými pomocí konvenční GC/FID metody.

Metoda kvantitativní analýzy triacylglycerolů s využitím odezvových faktorů byla testována pro tři běžné způsoby HPLC detekce triacylglycerolů, tj. APCI-MS, UV detekce při 205 nm a detektor rozptylu světla (ELSD) (P1). APCI-MS umožňuje dostatečně citlivou analýzu pro nasycené i nenasycené triacylglyceroly s možností určení molekulové hmotnosti a složení acylů triacylglycerolu na základě hmotnostních spekter. Nevýhodou UV detekce je špatná citlivost pro zcela nasycené triacylglyceroly, které neobsahují žádnou dvojnou vazbu. ELSD detektor poskytuje dostatečnou citlivost pro analýzu nasycených i nenasycených triacylglycerolů, ale jeho nevýhodou je nelineární závislost odezvy na koncentraci.

V rámci dalších experimentů byl pro HPLC kvantitativní analýzu triacylglycerolů testován aerosolový detektor nabitých částic (CAD) (P2). Tento detektor je typický tím, že jeho odezva je téměř nezávislá na fyzikálně-chemických vlastnostech látek, což umožňuje kvantitativní analýzu bez nutnosti použití odezvových faktorů. Nevýhodou CAD detektoru je silná závislost signálu na složení mobilní fáze při gradientové eluci, která výrazně ovlivňuje odezvu látek. Pro potlačení závislosti CAD signálu na složení gradientu byla použita metoda kompenzace gradientu. Tato metoda spočívá v mísení mobilní fáze před vstupem do CAD detektoru s gradientem mobilní fáze obráceného složení z přídavné pumpy. Tím je dosaženo konstantního složení mobilní fáze vstupující do detektoru a identických podmínek pro detekci látek v průběhu celého gradientu. Výsledné odchylky odezvy triacylglycerolů s CAD detektorem a kompenzací gradientu jsou do 5%, což lze využít pro jednoduchou kvantitativní analýzu triacylglycerolů bez odezvových faktorů.

1.3 HPLC/MS charakterizace složení průmyslově významných olejů

Přírodní směsi triacylglycerolů jsou důležitou komoditou na světových trzích, kvůli jejich širokému uplatnění v různých průmyslových odvětvích. Z tohoto pohledu je znalost jejich složení velmi důležitá. Vyvinutá metoda NARP-HPLC/APCI-MS analýzy byla aplikována na detailní charakterizaci složení triacylglycerolů souboru důležitých rostlinných olejů používaných v průmyslu, kosmetice a výživě (P3, P4). Triacylglyceroly byly identifikovány na základě jejich retenčního chování a APCI-MS spekter a kvantifikovány pomocí metody odezvových faktorů. Detailní znalost složení triacylglycerolů byla využita pro stanovení průměrných parametrů vypovídajících o vlastnostech a nutriční hodnotě vzorku, jako jsou průměrná délka acylového řetězce a počet dvojných vazeb nebo koncentrace esenciálních, nasycených, mononenasycených a polynenasycených acylů mastných kyselin.

Výsledky kvantitativní analýzy triacylglycerolů byly analyzovány pomocí vícerozměrné statistické analýzy dat metodou analýzy hlavních komponent (PCA) (P4). Tato metoda umožňuje posouzení vzájemné podobnosti vzorků na základě porovnání koncentrací všech triacylglycerolů ve vzorcích. PCA analýza kvantitativních dat byla testována i pro odhalení falšování rostlinných olejů na příkladu falšování olivového oleje levnějším olejem slunečnicovým. Za tímto účelem byla analyzována sada vzorků stolních slunečnicových a olivových olejů společně se vzorky olivového oleje s různým přídavkem slunečnicového oleje. PCA analýza NARP-HPLC/APCI-MS dat umožnila identifikaci falšovaného olivového oleje již od přídavku 1% oleje slunečnicového (Obrázek 4).

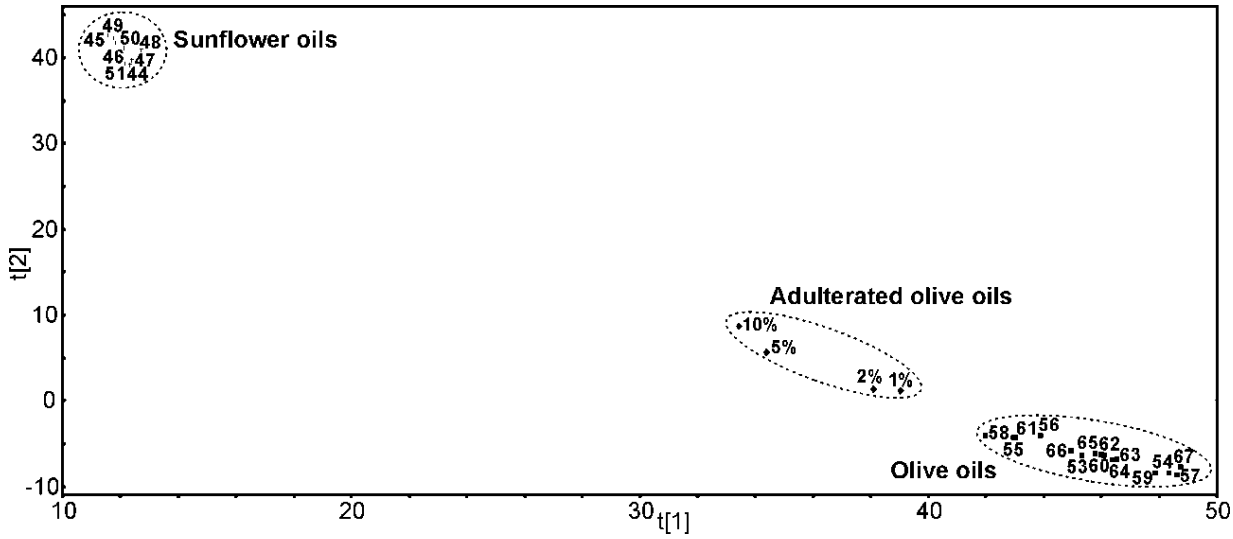

Obrázek 4 PCA analýza složení triacylglycerolů slunečnicového oleje (44-51), olivového oleje (53-67) a olivového oleje s přídavkem 1%, 2%, 5% a 10% slunečnicového oleje (P4).

2 Analýza izomerů triacylglycerolů

Triacylglyceroly se liší složením acylů, ale mohou se vyskytovat i jako různé izomery, jako jsou polohové izomery dvojných vazeb, *cis-*/*trans-* izomery dvojných vazeb, lineární/větvené řetězce nebo regioizomery a optické izomery s různou polohou acylů na glycerolovém skeletu. Znalost složení izomerů je důležitá z hlediska výsledných fyzikálně-chemických vlastností vzorku, ale i vzhledem k různé biochemické aktivitě izomerů v organismu. Metody analýzy izomerů jsou často založeny na přípravě derivátů s následnou LC analýzou produktů, které jsou však časově a technicky náročné. Cílem naší práce byl vývoj nových HPLC/MS metod pro analýzu izomerů intaktních triacylglycerolů.

2.1 HPLC/MS analýza izomerů triacylglycerolů

Přírodní vzorky rostlinných olejů obsahují převážně triacylglyceroly s polynenasycenými acyly s 18 atomy uhlíku a dvojnými vazbami oddělenými jednou methylenovou jednotkou v pozicích Δ9,12 a Δ9,12,15, např. Δ9,12-18:2 (kyselina linolová) a Δ9,12,15-18:3 (kyselina linolenová). Některé rostliny obsahují kromě těchto kyselin i neobvyklé mastné kyseliny s odlišnými polohami dvojných vazeb. Takovým příkladem jsou jehličnany, jejichž olej ze semen obsahuje velké množství triacylglycerolů s neobvyklými acyly mastných kyselin s první dvojnou vazbou v poloze Δ5 a další dvojnou vazbou oddělenou více methylenovými jednotkami, např. Δ5,9-18:2 (kyselina taxolejová), Δ5,9,12-18:3 (kyselina pinolenová). V naší práci bylo zkoumáno složení olejů ze semen modřínu opadavého (*Larix decidua*), smrku ztepilého (*Picea abies*) a jedle bělokoré (*Abies alba*) (P8). Na charakterizaci jejich složení byla aplikována vyvinutá NARP-HPLC/APCI-MS metoda, pomocí které byly triacylglyceroly s neobvyklými acyly mastných kyselin identifikovány na základě odlišného retenčního a fragmentačního chování. Triacylglyceroly obsahující Δ5 polohové izomery dvojných vazeb mají vyšší retenci ve srovnání s jejich běžnými analogy v rostlinných olejích, jako jsou Δ6 a Δ9 izomery. Polohové izomery dvojných vazeb byly rozlišeny i na základě APCI-MS spekter. Spektra Δ5 polohových izomerů triacylglycerolů poskytují fragmentové ionty s identickou m/z jako běžné triacylglyceroly, ale s výrazně odlišnou intenzitou (Obrázek 5). Toho bylo využito pro potvrzení identifikace izomerů triacylglycerolů.

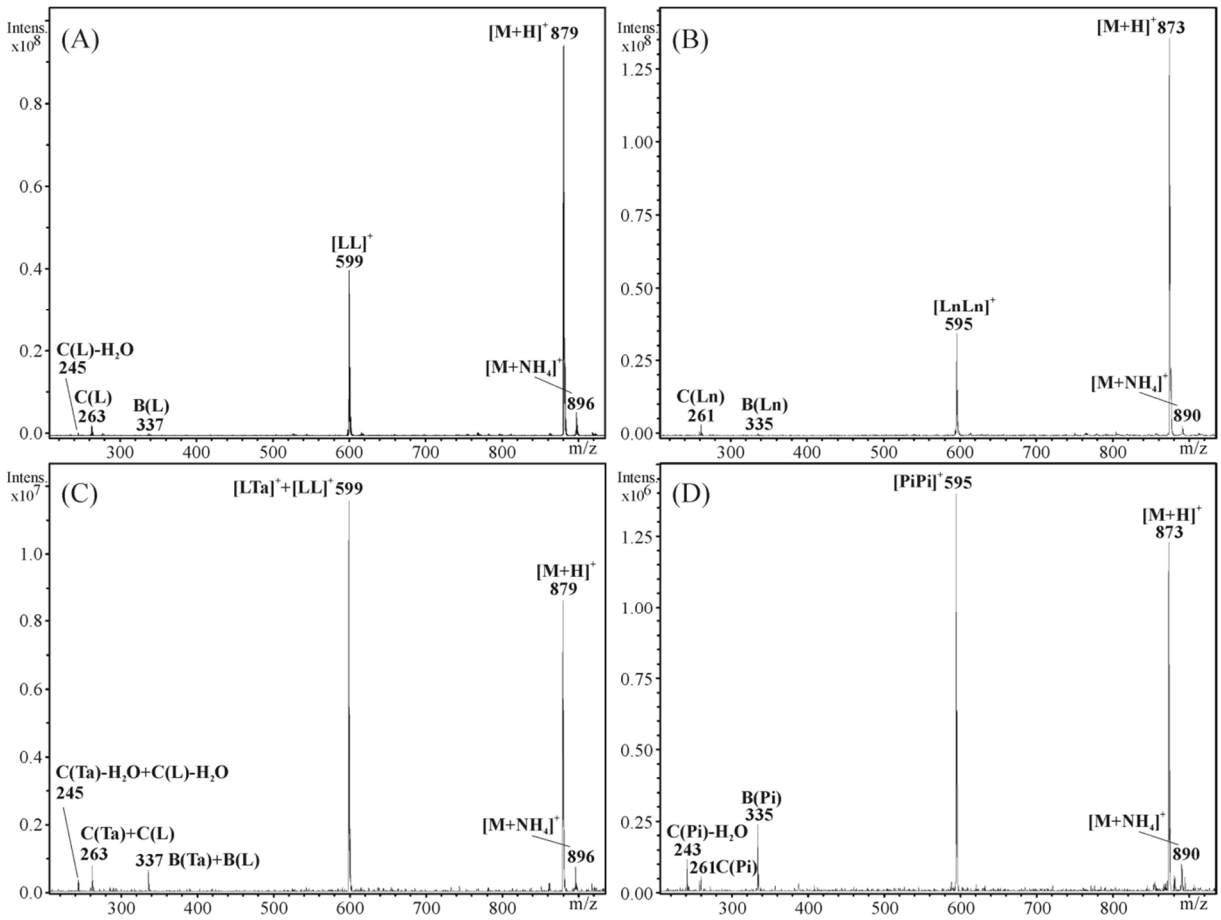

Obrázek 5 APCI-MS spektra triacylglycerolů polohových izomerů dvojných vazeb: (A) standard LLL, (B) standard LnLnLn, (C) LLTa z modřínu opadavého a (D) PiPiPi z jedle bělokoré. L - Δ9,12-18:2; Ln - Δ9,12,15-18:3; Ta - Δ5,9-18:2; Pi - Δ5,9,12-18:3 (P8).

V dalších experimentech bylo studováno složení tuků vybraných živočichů (z jelena, daňka, ovce, muflona, divokého prasete, kohouta, kachny a králíka), které obsahují neobvyklé triacylglyceroly s větvenými řetězci a *trans*- konfigurací dvojných vazeb (P7). Profil složení acylů mastných kyselin byl stanoven pomocí GC/MS a GC/FID metody analýzy methylesterů. Na základě retenčního chování jednotlivých izomerů a naměřených spekter elektronové ionizace bylo celkem identifikováno 29 acylů s větveným řetězcem, 3 s *trans*-konfigurací dvojných vazeb a různé polohové izomery dvojných vazeb. Největší zastoupení acylů s větveným řetězcem (až 16%) a *trans*- konfigurací dvojných vazeb (až 7%) bylo nalezeno v tucích přežvýkavců, což je dáno činností bakterií přítomných v bachoru, které produkují velké množství neobvyklých mastných kyselin. Výsledky GC/MS analýzy byly využity pro identifikaci izomerů intaktních triacylglycerolů pomocí NARP-HPLC/APCI-MS a Ag-HPLC/APCI-MS metod na základě jejich retenčního chování. V NARP-HPLC mají triacylglyceroly s větveným řetězcem nižší retenci v porovnání s jejich lineárními analogy a

trans- izomery mají vyšší retenci než *cis*- izomery. Naopak v Ag-HPLC mají *trans*-izomery nižší retenční časy než *cis*- izomery. Ag-HPLC metoda navíc poskytuje informaci o složení regioizomerů triacylglycerolů.

2.2 Analýza regioizomerů a chirálních izomerů triacylglycerolů

Acyly triacylglycerolů mohou být navázány v polohách *sn*-1, 2 nebo 3 na glycerolovém skeletu. Triacylglyceroly lišící se složením acylů v polohách *sn*-1(3) a *sn*-2 jsou regioizomery a v polohách *sn*-1 a *sn*-3 jsou enantiomery. V přírodních vzorcích se vyskytují směsi těchto izomerů v různém poměru a znalost jejich složení je důležitá z nutričního hlediska kvůli různé biologické dostupnosti acylů ve stereospecifickém prostředí enzymů v organismu. Cílem práce bylo vyvinout metody pro charakterizaci složení intaktních regioizomerů a enantiomerů triacylglycerolů.

Zásadním problémem při analýze regioizomerů a enantiomerů triacylglycerolů je omezená dostupnost standardů regioizomerů, zatímco standardy enantiomerů nejsou komerčně dostupné vůbec. Pro optimalizaci HPLC/MS analýzy izomerů triacylglycerolů byly vyvinuty dva postupy syntézy standardů izomerů, a to metoda syntézy regioizomerů a enantiomerů ve směsi pomocí tzv. randomizační reakce (P9) a metoda syntézy enantiomerů stereospecifickou esterifikací glycerolu (P10). Randomizační reakce má široké uplatnění v průmyslu pro úpravu vlastností olejů a tuků na základě interesterifikace acylů triacylglycerolů. Metoda syntézy směsi standardů je založena na randomizační reakci směsi jednoduchých triacylglycerolů za katalýzy methanolátem sodným (Obrázek 6). Při reakci dochází k opakované náhodné interesterifikaci acylů mezi triacylglyceroly přítomnými ve směsi. Produktem reakce je směs triacylglycerolů se všemi kombinacemi acylů včetně regioizomerů a enantiomerů. Zastoupení produktů je předem dáno zvoleným poměrem acylů ve výchozí směsi. Tímto způsobem lze připravit sadu standardů o vybraném složení pro optimalizaci HPLC metod a charakterizaci retenčního chování triacylglycerolů.

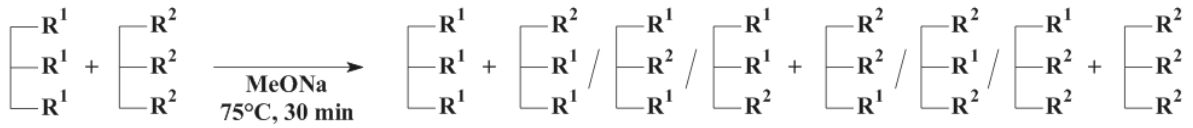

Obrázek 6 Schéma syntézy izomerů metodou randomizace jednoduchých triacylglycerolů (P9).

Syntéza opticky čistých enantiomerů triacylglycerolů je založena na postupné stereospecifické esterifikaci glycerolu mastnými kyselinami (Obrázek 7). Prvním krokem syntézy enantiomerů je esterifikace volné hydroxylové skupiny 1,2- nebo 2,3-isopropyliden-*sn*-glycerolu s chráněnými hydroxylovými skupinami v polohách *sn*-1,2 nebo *sn*-2,3 vybranou mastnou kyselinou. Dále je odstraněna chránící skupina hydroxylových skupin, které jsou v posledním kroku esterifikovány mastnou kyselinou nebo směsí mastných kyselin. Takto lze připravit čistý enantiomer triacylglycerolu nebo opticky čistou směs triacylglycerolů různého složení pro optimalizaci chirální HPLC separace a pro identifikaci enantiomerů ve vzorku na základě retenčních časů.

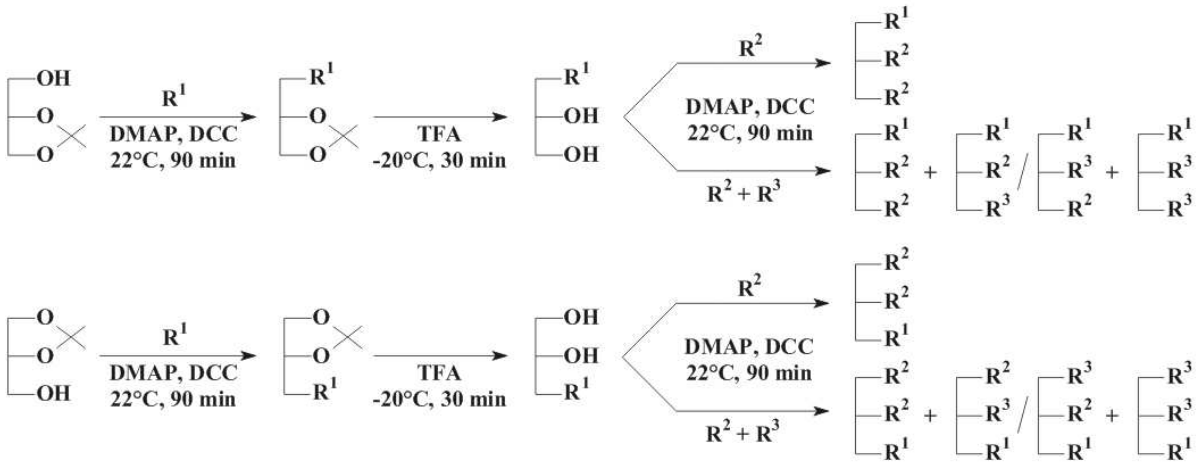

Obrázek 7 Schéma syntézy enantiomerů triacylglycerolů stereospecifickou esterifikací 1,2- a 2,3-isopropyliden-*sn*-glycerolu (P10).

Pro analýzu regioizomerů triacylglycerolů byla vyvinuta Ag-HPLC/APCI-MS metoda s 3 sériově zapojenými iontově-výměnnými kolonami se stříbrnými ionty o celkové délce 75 cm a mobilní fází hexan – 2-propanol – acetonitril (P9). Ag-HPLC umožňuje separaci triacylglycerolů do skupin podle počtu dvojných vazeb, ale i separaci v rámci jednotlivých skupin podle složení acylů. Optimalizované chromatografické podmínky navíc umožňují separaci regioizomerů triacylglycerolů. Izomery jsou ve vzorku identifikovány na základě jejich retenčního chování a pomocí intenzity fragmentových iontů vzniklých neutrální ztrátou mastné kyseliny v APCI-MS spektrech. Neutrální ztráta mastné kyseliny z polohy *sn*-2 je energeticky náročnější v porovnání se ztrátou z *sn*-1 a *sn*-3 poloh, což je ve spektru pozorováno jako nižší intenzita odpovídajícího fragmentového iontu oproti intenzitě očekávané (Obrázek 8).

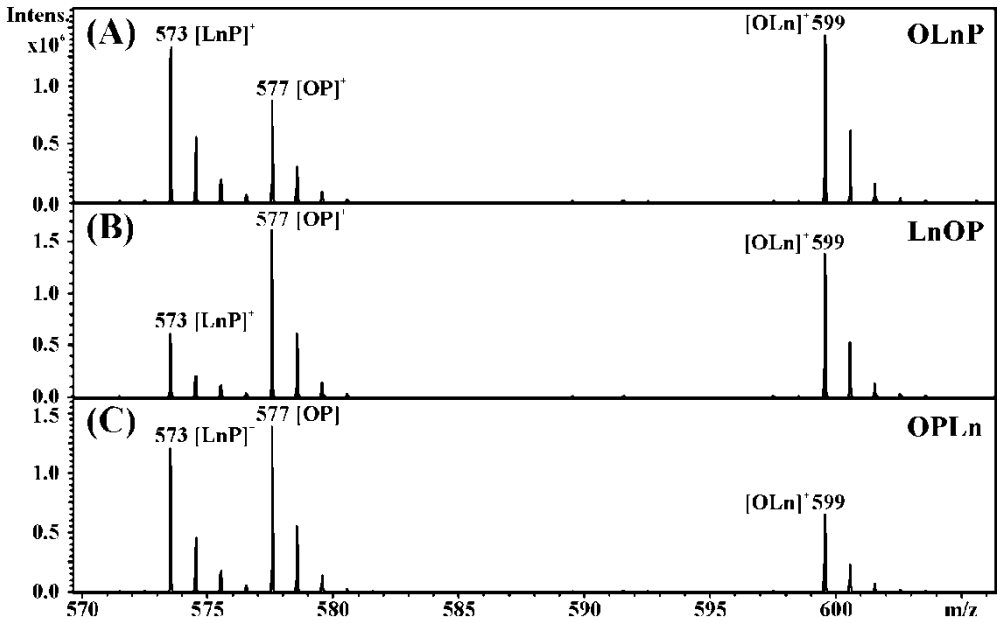

Obrázek 8 Fragmentové ionty v APCI-MS spektrech regioizomerů triacylglycerolů (A) OLnP, (B) LnOP a (C) OPLn (P9).

Detailněji byl prostudován vliv složení mobilní fáze a teploty kolony na Ag-HPLC separaci triacylglycerolů (P11). Byly testovány dvě nejčastější mobilní fáze Ag-HPLC založené na hexanu a dichlormethanu ve směsi s polárnějšími organickými rozpouštědly. Složení mobilní fáze nemá vliv na obecné retenční chování triacylglycerolů, ale byl pozorován velký vliv na retenční pořadí polohových izomerů dvojných vazeb a také odlišné retenční chování triacylglycerolů při změně teploty kolony. Hexanová mobilní fáze poskytuje výrazně lepší výsledky separace regioizomerů, protože umožňuje alespoň částečnou separaci všech testovaných regioizomerů, zatímco dichlormethanová mobilní fáze poskytuje separaci pouze dvou regioizomerních párů.

Vliv konstrukce MS přístroje na zastoupení fragmentových iontů 32 dubletů a 11 tripletů regioizomerů připravených randomizační reakcí 8 jednoduchých triacylglycerolů byl testován pomocí 5 hmotnostních analyzátorů typu kvadrupól, trojitý kvadrupól, iontová past, kvadrupól-analyzátor doby letu a orbitální past (P12). Typ hmotnostního analyzátoru má na zastoupení fragmentových iontů menší vliv v porovnání s ovlivněním počtem dvojných vazeb, jejich polohou a především typem regioizomeru.

Dále byla testována separace regioizomerů triacylglycerolů v plynné fázi pomocí analyzátoru iontové mobility typu diferenční mobilitní spektrometrie s ESI ionizací (P13). Byla vyvinuta metoda analýzy aduktů triacylglycerolů se stříbrnými ionty s použitím 1-propanolu nebo 1-butanolu jako chemického modifikátoru. Optimalizací podmínek bylo

dosaženo separace 4 párů regioizomerů s kombinací nasycených a nenasycených acylů a metoda byla aplikována na určení zastoupení regioizomerů ve vzorku vepřového sádla. Výhodou analýzy regioizomerů s iontovou mobilitou je doba analýzy do 1 minuty, zatímco Ag-HPLC/APCI-MS analýza regioizomerů je řádově v desítkách minut.

Vyvinutou metodou Ag-HPLC analýzy triacylglycerolů s APCI-MS detekcí bylo charakterizováno složení regioizomerů triacylglycerolů ve vzorcích rostlinných olejů a živočišných tuků (P5, P7, P9). Ve vzorcích byla ve většině případů identifikována směs regioizomerů v různém zastoupení v závislosti na typu vzorku. Obecně platí, že rostlinné oleje mají silnou preferenci nenasycených acylů v poloze *sn*-2 s velmi nízkým až nulovým zastoupením izomeru s nasyceným acylem v *sn*-2 poloze. Silná preference nasyceného acylu v poloze *sn*-2 byla naopak identifikována v tuku prasete domácího a prasete divokého, zatímco v ostatních analyzovaných živočišných tucích bylo pozorováno výrazné zastoupení obou regioizomerů s mírnou preferencí nenasycených acylů.

Pro separaci enantiomerů triacylglycerolů byla vyvinuta metoda chirální HPLC/APCI-MS analýzy v systémech s normálními fázemi (P10). Tato metoda je založena na sériovém zapojení dvou chirálních kolon se stacionární fází na bázi celulózy s 3,5-dimethylphenylkarbamát modifikací a gradientu mobilní fáze hexan – 2-propanol. Metoda umožňuje separaci všech enantiomerů triacylglycerolů obsahujících 1 – 8 dvojných vazeb a různé délky acylů s výjimkou enantiomerů s kombinací nasycených a di- nebo trinenasycených acylů v *sn*-1 a *sn*-3 polohách. Dále metoda umožňuje separaci regioizomerů triacylglycerolů a separaci cholesteryl esterů. Retenční chování enantiomerů triacylglycerolů bylo popsáno na základě analýzy směsí připravených randomizační reakcí (Obrázek 9A). Jednotlivé enantiomery byly následně identifikovány porovnáním se standardy připravenými stereospecifickou esterifikací glycerolu (Obrázek 9B). Ve vzorcích byla pozorována preference acylů s vyšším počtem dvojných vazeb v *sn*-1 poloze v rostlinném oleji z lískových ořechů a naopak mírná preference *sn*-3 polohy ve vzorku lidské plazmy.

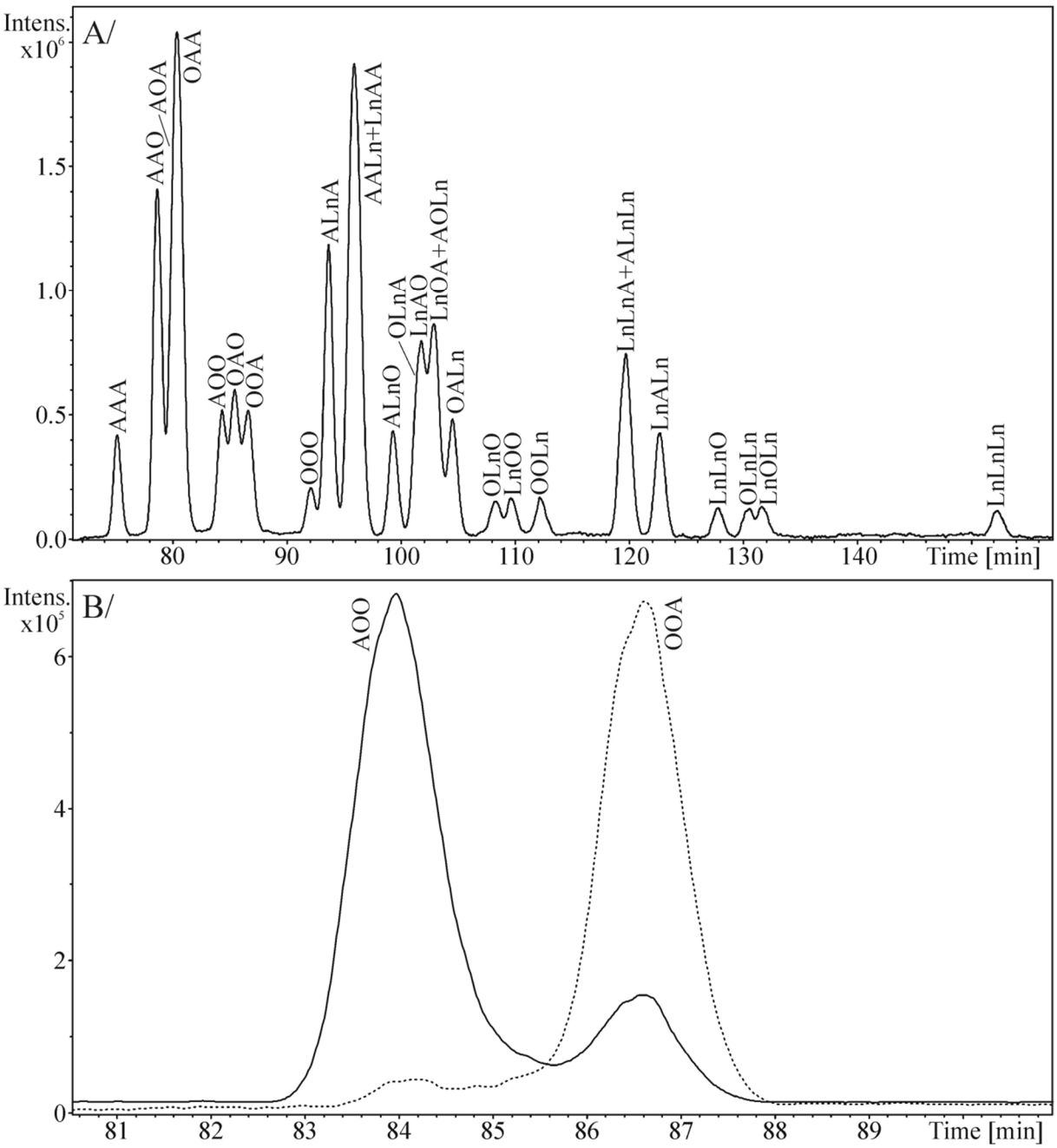

Obrázek 9 Chirální HPLC/APCI-MS analýza standardů enantiomerů triacylglycerolů připravených A/ randomizační reakcí směsi standardů AAA, OOO a LnLnLn a B/ stereospecifickou esterifikací 2,3- a 1,2-isopropyliden-sn-glycerolu (P10).

3 Lipidomická analýza

Snahou necílené lipidomické analýzy je kvalitativní a kvantitativní popis všech lipidů přítomných ve vzorku. Lipidy jsou ze vzorku extrahovány pomocí postupů, které umožňují extrakci co nejširšího spektra lipidů. Takto připravené celkové lipidové extrakty jsou analyzovány pomocí různých analytických metod se snahou o detailní popis lipidomu vzorku. Velmi důležitou roli v analýze lipidů hrají chromatografické techniky a MS detekce. Tato část habilitační práce popisuje vývoj řady (U)HPLC/MS (HILIC, NP a RP), UHPSFC/MS a MS metod pro separaci, identifikaci a kvantitativní analýzu širokého spektra polárních a nepolárních lipidů celkového lipidového extraktu, ale i pro detailní analýzu vybraných důležitých skupin lipidů jako jsou kyselé lipidy, oxylipiny a gangliosidy.

3.1 (U)HPLC/MS analýza celkového lipidového extraktu

Celkový lipidový extrakt je velmi složitá směs lipidů, které se významně liší strukturou, polaritou, složením acylů, izomerií a koncentrací. Lipidy jsou nejčastěji separovány podle polarity na třídy lipidů v HILIC, případně NP systémech nebo podle jejich složení acylů v RP systémech. Separace tříd lipidů a jednotlivých molekul lipidů jsou navzájem ortogonální, čehož lze využít ve vícerozměrných separacích, které přináší detailní informaci o složení lipidů ve vzorku. Za tímto účelem byla vyvinuta metoda dvourozměrné off-line HPLC separace celkového lipidového extraktu různých tkání s MS detekcí (P14). V první dimenzi je celkový lipidový extrakt frakcionován pomocí HILIC separace s použitím silikagelové kolony na jednotlivé třídy lipidů (Obrázek 10A). HILIC metoda umožnila separaci až 19 tříd lipidů včetně 3 regioizomerních párů. Frakce jednotlivých tříd lipidů jsou následně analyzovány v druhé dimenzi v RP systému pomocí C18 kolony, kde jsou lipidy separovány podle složení acylů (Obrázek 10B). Jednotlivé lipidy jsou identifikovány na základě jejich ESI-MS(/MS) nebo APCI-MS spekter. Vyvinutá metoda off-line dvourozměrné separace celkového lipidového extraktu byla aplikována na podrobnou charakterizaci lipidového složení tkání orgánů prasete, jako jsou mozek, srdce, ledviny, játra, plíce, mícha, slezina a žaludek (P15). Celkově bylo v analyzovaných tkáních identifikováno více jak 160 lipidů s různým počtem dvojných vazeb, délkou acylů a různou polohou acylů na glycerolovém skeletu.

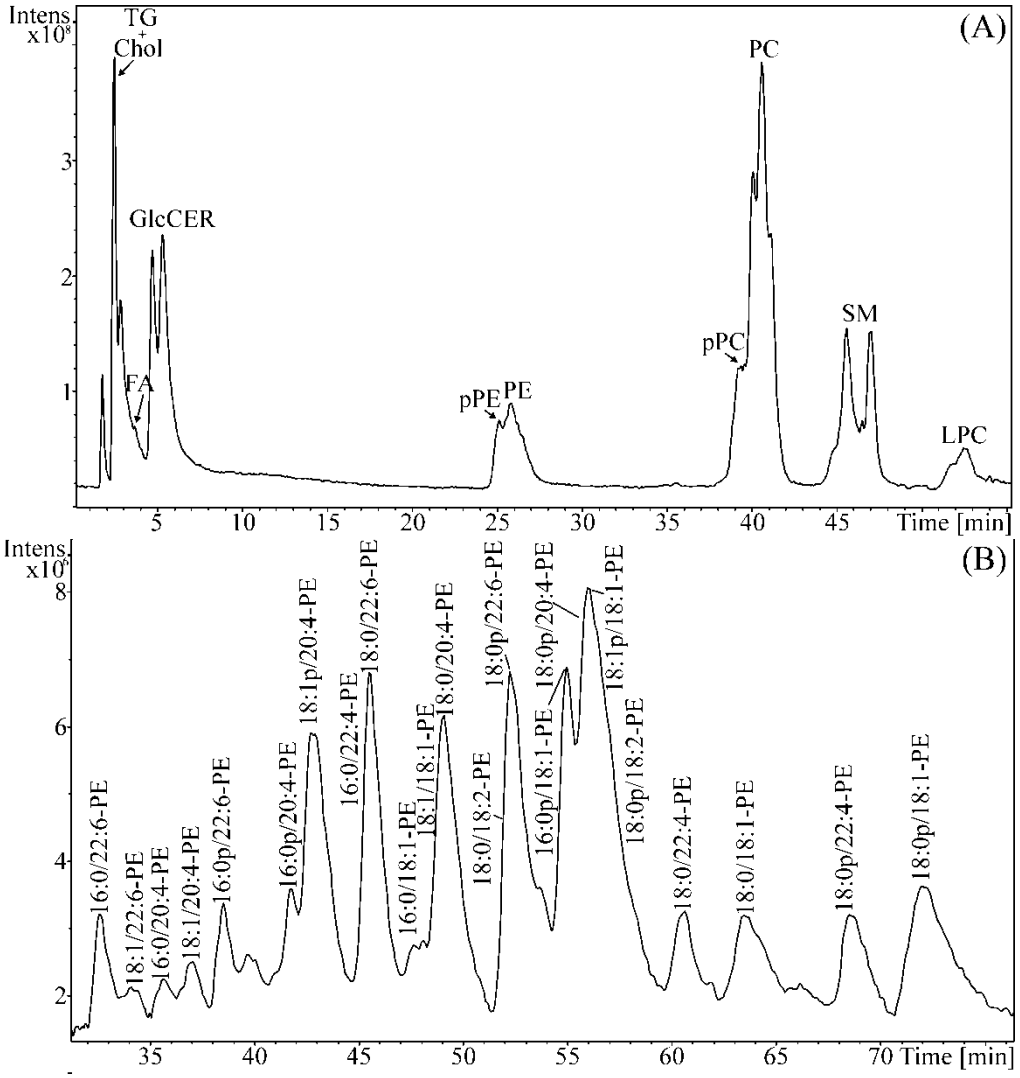

Obrázek 10 Off-line dvourozměrná HPLC separace celkového lipidového extraktu vaječného žloutku. (A) 1. dimenze: HILIC-HPLC/ESI-MS frakcionace celkového lipidového extraktu, (B) 2. dimenze: RP-HPLC/ESI-MS analýza frakce fosfoethanolaminů (P14).

Off-line dvourozměrná separace lipidů poskytuje detailní informaci o složení vzorku, ale neumožňuje plnou automatizaci analýz, které jsou obvykle časově náročné. Cílem další práce bylo vyvinout plně automatickou on-line dvourozměrnou UHPLC separaci lipidů (P16). V on-line uspořádání je v první dimenzi použita C18 kolona pro separaci molekul lipidů podle složení acylů. Frakce z první dimenze jsou plně automaticky převáděny do druhé dimenze pomocí vícecestného ventilu. V druhé dimenzi jsou lipidy separovány podle polarity do tříd pomocí rychlé HILIC metody se silikagelovou kolonou. Metoda on-line UHPLC separace byla použita pro analýzu celkového lipidového extraktu vzorku lidské plazmy a mozku prasete, kde bylo identifikováno 143 lipidů ze 4 kategorií a 10 tříd lipidů (Obrázek 11).

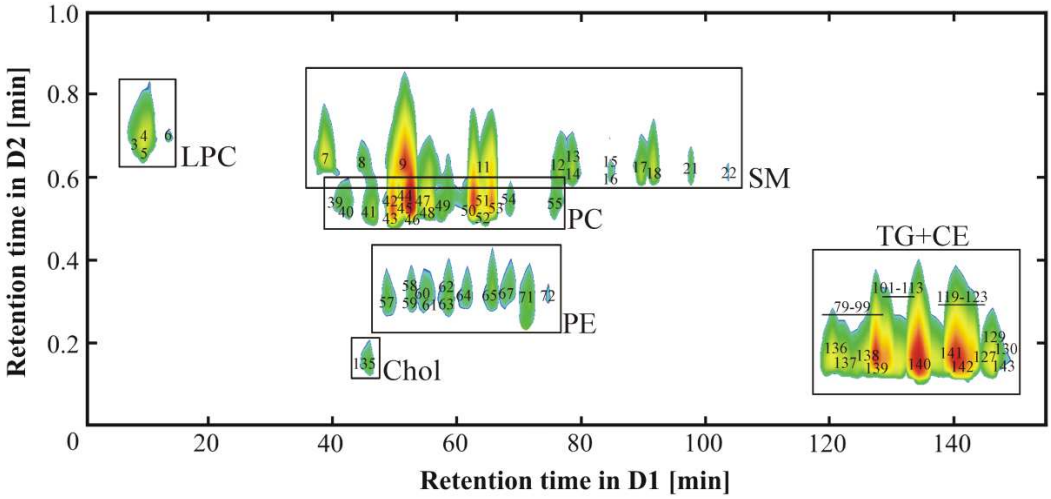

Obrázek 11 On-line dvourozměrná RP-UHPLC x HILIC-UHPLC/ESI-MS separace celkového lipidového extraktu lidské plazmy (P16).

Dále byla pro charakterizaci celkového lipidového extraktu biologických vzorků optimalizována vysokorozlišující RP-UHPLC/ESI-MS metoda založená na spojení dvou 15 cm kolon C18 s velikostí částic 1,7 µm a identifikaci lipidů pomocí ESI-MS a MS/MS spekter měřených s MS analyzátorem s vysokou rozlišovací schopností a správností určení hmoty (P17). Celkem bylo pomocí optimalizované metody identifikováno více jak 400 lipidů ze 14 polárních a nepolárních tříd lipidů z 5 kategorií v lidské plazmě, moči a mozku prasete (Obrázek 12). Dále bylo popsáno retenční chování a relativní retence logických řad identifikovaných lipidů v závislosti na počtu dvojných vazeb a délce acylů, které byly použity jako další kritérium pro správnou identifikaci neznámých lipidů.

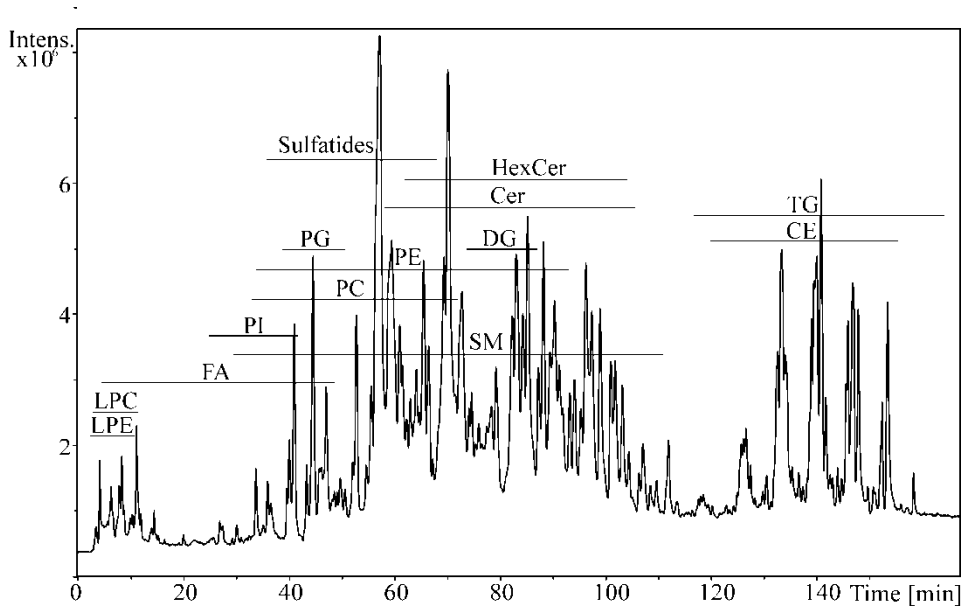

Obrázek 12 RP-UHPLC/ESI-MS analýza celkového lipidového extraktu mozku prasete (P17).

HILIC metody umožňují pouze separaci polárních lipidů, protože nepolární lipidy nejsou v systému zadržovány a eluují nerozlišeny v mrtvém objemu. Pro rychlou analýzu nepolárních lipidů v plazmě, erytrocytech a lipoproteinových frakcích byla vyvinuta NP-UHPLC metoda využívající NP separaci lipidů podle jejich polarity pomocí silikagelové kolony s APCI-MS detekcí (P18). Bylo dosaženo separace cholesteryl esterů, cholesterolu, triacylglycerolů, regioizomerů 1,2- a 1,3-diacylglycerolů a 1-monoacylglycerolů pomocí mobilní fáze hexan – 2-propanol – acetonitril (Obrázek 13). Pro analýzu polárních lipidů byla dále vyvinuta rychlá HILIC-UHPLC/ESI-MS metoda se silikagelovou kolonou a mobilní fází octan amonný – methanol – acetonitril.

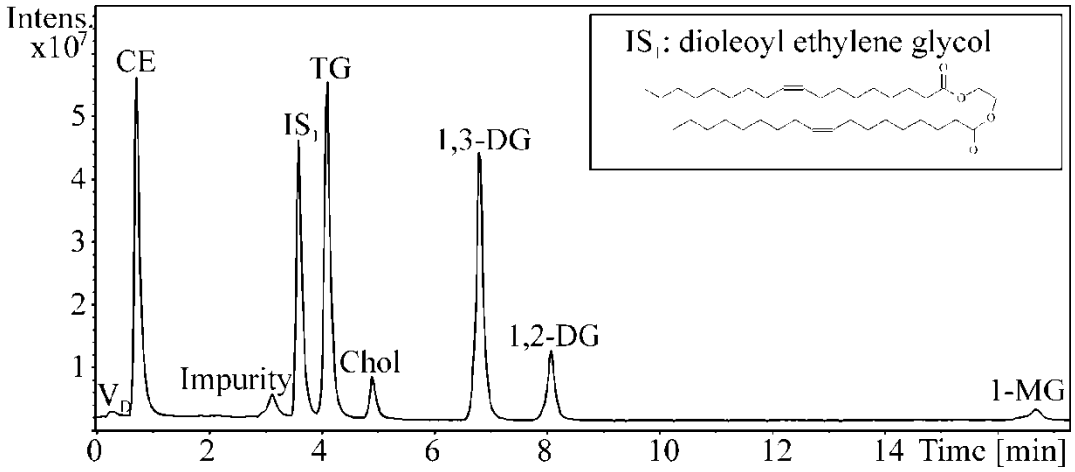

Obrázek 13 NP-UHPLC/APCI-MS analýza standardů nepolárních tříd lipidů (P18).

Kombinace NP a HILIC metod poskytuje ucelenou informaci o složení nepolárních i polárních lipidů ve vzorku, přesto má jejich využití pro lipidomickou analýzu v klinických studiích svá omezení. Jde především o vyšší časovou a finanční náročnost danou analýzou vzorku pomocí dvou UHPLC metod. Pro lipidomickou analýzu polárních a nepolárních lipidů v klinických studiích bylo podrobně studováno využití UHPSFC (P19), která se v poslední době stále častěji prosazuje v různých oblastech omických analýz. UHPSFC separace jsou z principu separace v NP fázích, protože je používán nepolární oxid uhličitý jako mobilní fáze. Z tohoto důvodu byla zvolena separace lipidů podle jejich polarity na jednotlivé třídy pomocí hybridní silikagelové kolony s velikostí částic 1,7 μm a gradientu modifikátoru methanol – voda – octan amonný. Byly optimalizovány všechny chromatografické parametry a popsán jejich vliv na chromatografické chování lipidů. Finální metoda umožňuje separaci až 30 nepolárních a polárních tříd lipidů 6 kategorií v jedné 6 min analýze (Obrázek 14). Metoda

byla aplikována na analýzu komplexního vzorku mozku prasete, kde bylo identifikováno 436 lipidů z 24 tříd. Výsledky UHPSFC analýzy ukázaly, že může být použita jako alternativa k široce používaným metodám přímé MS analýzy a UHPLC/MS pro detailní analýzu lipidů s vysokou prostupností vzorků.

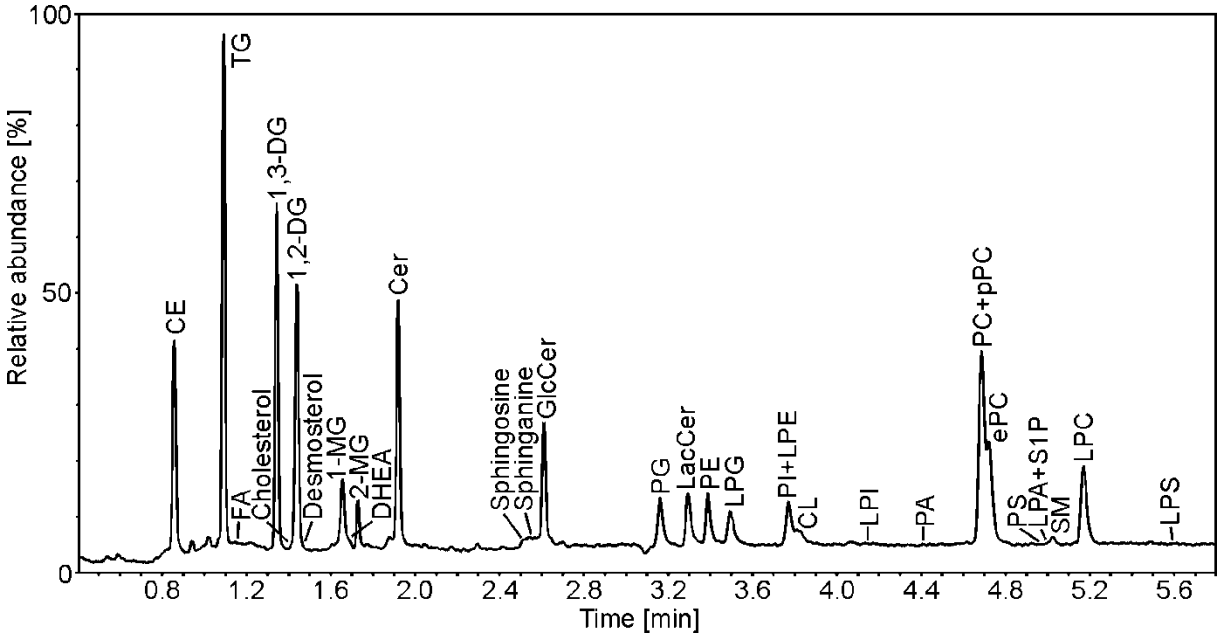

Obrázek 14 UHPSFC/ESI-MS analýza standardů tříd polárních a nepolárních lipidů (P19).

3.2 LC/MS analýza vybraných tříd lipidů

Analýza některých tříd lipidů vyžaduje volbu specifických chromatografických podmínek, protože mají výrazně odlišné retenční chování od ostatních tříd lipidů celkového lipidového extraktu nebo se vyskytují ve velmi nízké koncentraci a nelze je analyzovat vedle ostatních tříd v rámci celkové lipidomické analýzy. Takovým příkladem jsou třídy lipidů kyselého charakteru (tzv. kyselé lipidy), které s použitím běžných chromatografických podmínek vykazují silné sekundární interakce se stacionární fází na bázi silikagelu a dochází k jejich silnému chvostování. V rámci další práce byla optimalizována HILIC-HPLC/ESI-MS metoda pro analýzu kyselých lipidů (P20), konkrétně fosfokyselin, lysofosfokyselin, fosfoserinů a lysofosfoserinů. Především byl optimalizován typ stacionární fáze, pH mobilní fáze a typ a koncentrace aditiva, které mají největší vliv na HILIC separaci lipidů. Finální metoda používá hydridovou kolonu a gradient mobilní fáze acetonitril – octan amonný (pH = 4), který poskytuje dobrý tvar chromatografických píků pro všechny třídy lipidů (Obrázek 15).

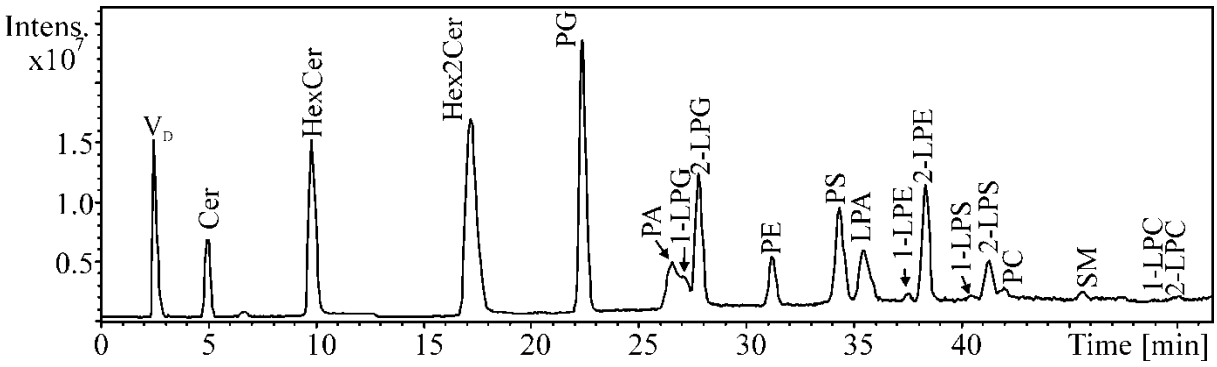

Obrázek 15 HILIC-HPLC/ESI-MS analýza standardů tříd lipidů pomocí hydridové kolony (P20).

Oxylipiny jsou skupina lipidů, která vzniká oxidací polynenasycených mastných kyselin. V porovnání s běžnými lipidy jsou ve vzorcích přítomny ve výrazně nižších koncentracích, proto je pro jejich analýzu nutné použít speciální metody zaměřené pouze na oxylipiny. Za účelem dosažení maximálního chromatogarafického rozlišení a separace izobarických oxylipinů byly porovnávány metody RP-UHPLC/ESI-MS a UHPSFC/ESI-MS analýzy (P21). Finální RP-UHPLC/MS metoda (Obrázek 16) poskytuje separaci více izobarických oxylipinů a vyšší citlivost detekce v porovnání s UHPSFC/MS metodou. Na druhou stranu byl pozorován menší vliv iontové suprese látek lysofosfolipidy přítomnými ve vzorku lidské plazmy pomocí UHPSFC/MS metody.

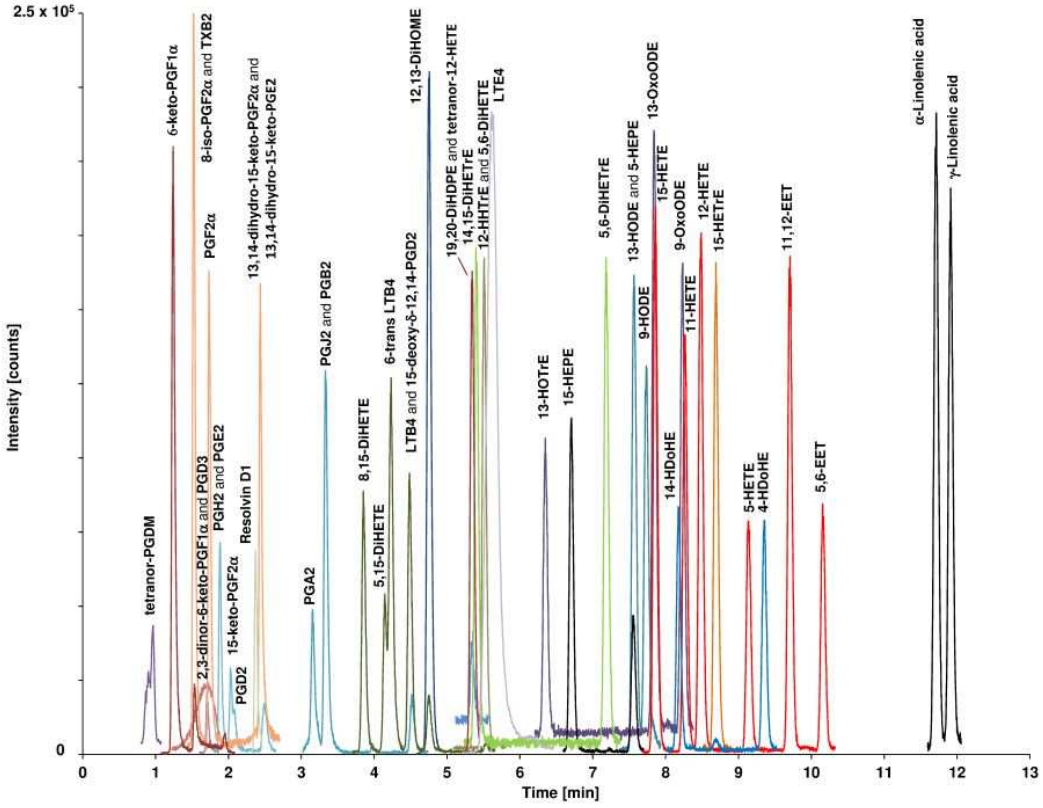

Obrázek 16 RP-UHPLC/ESI-MS analýza standardů oxylipinů (P21).

Gangliosidy jsou důležitou skupinou lipidů, které mají svou nezastupitelnou funkci v buněčných procesech. Pro jejich analýzu v biologických vzorcích byla optimalizována HILIC-HPLC/ESI-MS metoda s cílem dosáhnout dobré separace a dostatečné citlivosti detekce (P22). Vzhledem k nízké koncentraci gangliosidů ve vzorku je důležitým krokem metody jejich extrakce, která se sestává z extrakce směsí chloroform – methanol – voda a následné extrakce tuhou fází pomocí C18 kolony. Finální HILIC metoda je založena na silikagelové koloně a gradientu acetonitril – voda – octan amonný (Obrázek 17). V práci bylo popsáno retenční a fragmentační chování gangliosidů, které bylo využito pro jejich identifikaci ve vzorku mozku prasete, lidské ledviny, plicích, plazmě a erytrocytech, kde bylo identifikováno 145 gangliosidů z 19 tříd společně se 71 sulfatidy a 59 fosfolipidy.

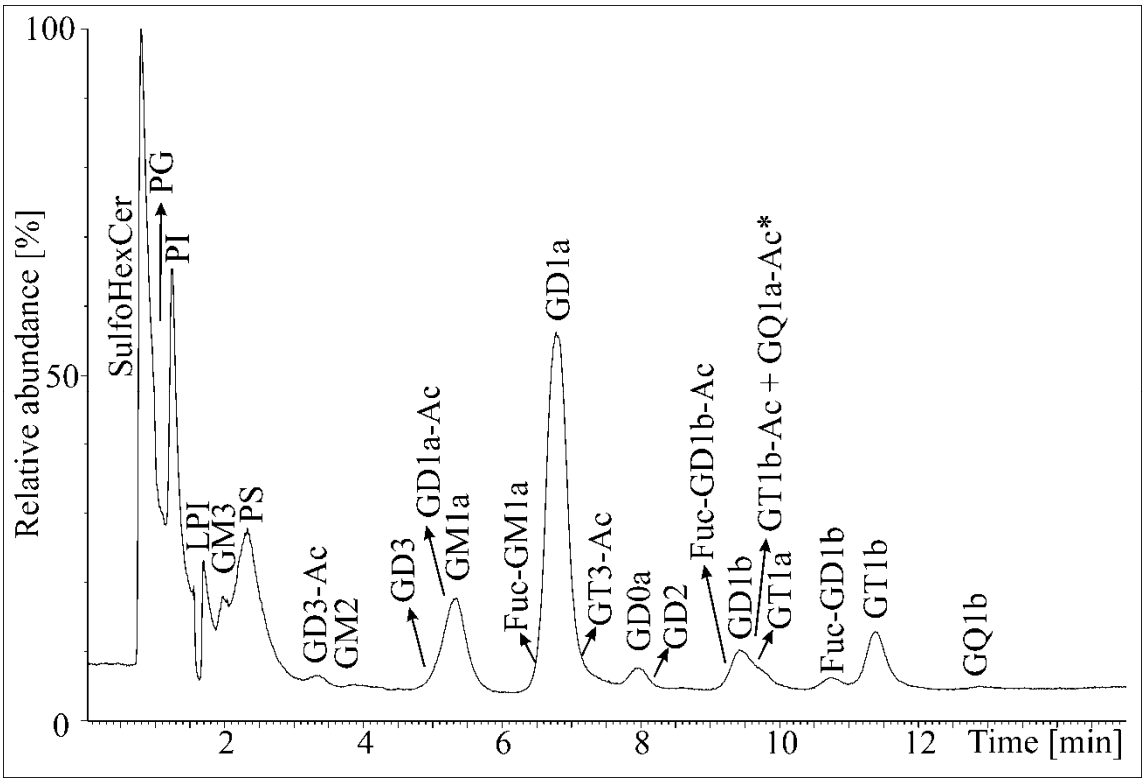

Obrázek 17 HILIC-HPLC/ESI-MS analýza gangliosidů mozku prasete (P22).

3.3 Kvantitativní lipidomická analýza

Kvantitativní lipidomická analýza představuje pro analytického chemika náročný úkol, především kvůli složitosti přírodních matric. Standardně jsou pro kvantitativní analýzu používány jako interní standardy neendogenní lipidy, které byly použity i v naší práci. Byla vyvinuta jednoduchá HILIC-HPLC/MS a NP-HPLC/MS kvantitativní analýza polárních a nepolárních tříd lipidů pomocí jednoho interního standardu (P18, 23). Základní podmínkou

při výběru standardu bylo, že nesmí být přítomný ve vzorku a zároveň musí mít odlišný retenční čas od ostatních lipidů. Sphingosyl fosfoethanolamin d17:1/12:0 byl použit jako interní standard pro HILIC-HPLC/MS analýzu polárních lipidů a dioleoyl ethylenglykol pro NP-HPLC/MS analýzu nepolárních lipidů. Správnost dosažených výsledků byla potvrzena srovnáním dat s daty získanými konvenční kvantitativní analýzou pomocí trojitého kvadrupólu a ^{31}P NMR kvantitativní analýzy lipidů.

Pro kvantitativní analýzu fosfocholinů byla testována MS ionizace laserem za účasti matrice (MALDI) s použitím kyseliny 2,5-dihydroxybenzoové, 1,5-diaminonaphthalenu a 9-aminoakridinu jako matrice (P24). Pro jednotlivé matrice byla studována závislost odezvy fosfocholinů na složení acylů. Za tímto účelem byly syntetizovány směsi standardů fosfocholinů s různou délkou acylů a počtem dvojných vazeb. Nejlepších výsledků pro MALDI kvantitativní analýzu fosfocholinů bylo dosaženo pomocí matrice založené na 9-aminoakridinu.

Pro kvantitativní lipidomickou analýzu velkých sérií biologických vzorků v klinických studiích byly porovnávány metody založené na přímé infúzi ESI-MS a chromatografické separaci s ESI-MS detekcí (P25). Byly testovány tři analytické metody s ohledem na identifikované lipidy, prostupnost vzorků a hodnoty validačních parametrů pro analýzu biologických vzorků zastoupených nádorovou tkání, zdravou okolní tkání, plazmou a erytrocyty pacientů s nádorem ledvin. Metody byly testovány v jedné laboratoři s použitím identických podmínek a postupů zaručující dobrou porovnatelnost výsledků. Pro porovnání byla vybrána HILIC-UHPLC/ESI-MS metoda a metoda přímé infúze ESI-MS jako dvě nejrozšířenější metody pro lipidomickou analýzu společně s UHPSFC/ESI-MS metodou poskytující rychlou a detailní analýzu lipidů. Necílenou analýzou reprezentativních vzorků bylo identifikováno 610 lipidů z 23 tříd. Metoda přímé infúze umožňuje identifikaci největšího počtu tříd lipidů především díky identifikaci kyselých lipidů, které nejsou identifikovány pomocí chromatografických metod. Na druhou stranu UHPSFC metoda poskytuje výbornou citlivost pro nepolární lipidy a nejvyšší prostupnost vzorků s délkou metody 10 min. Metody byly validovány pro kvatitativní analýzu lipidů plazmy s jedním interním standardem pro každou třídu lipidů. Získané výsledky ukazují, že všechny metody poskytují spolehlivé kvantitativní výsledky a mohou být použity pro lipidomickou analýzu biologických vzorků v rámci klinických studií.

4 Lipidomická analýza v klinických studiích

Lipidy jsou biologicky aktivní látky, které mají v organismu celou řadu významných funkcí, a jejich nerovnováha může vést ke vzniku závažných onemocnění, jako jsou kardiovaskulární onemocnění, rakovina, diabetes, atd. Poslední část předkládané habilitační práce se zabývá aplikací vyvinutých HPLC/MS, UHPLC/MS a UHPSFC/MS lipidomických metod na analýzu biologických vzorků v rámci klinických studií zaměřených na popis vlivu onemocnění na složení lipidomu. Cílem studií bylo nalezení takových lipidů, jejichž koncentrace se s onemocněním výrazně mění a které mohou být v budoucnu využity jako biomarkery pro včasnou diagnostiku.

4.1 Postup lipidomické analýzy a zpracování dat

Výsledky každé klinické studie jsou výrazně závislé na způsobu jejího provedení, na analýze, ale i na zpracování naměřených dat. Pro lipidomickou analýzu velkých sérií biologických vzorků jsme optimalizovali postupy pro dosažení správných a přesných výsledků (P25). Prvním krokem studie je příprava reprezentativního vzorku (tzv. pooled sample) smícháním všech nebo vybraných vzorků analyzované série. Reprezentativní vzorek obsahuje průměrnou koncentraci všech lipidů přítomných v analyzovaných vzorcích, které jsou v dalším kroku identifikovány na základě necílené lipidomické analýzy pomocí retenčního chování, MS a MS/MS spekter. Na základě znalosti složení lipidů jsou dále vybrány neendogenní lipidy jako interní standardy pro kvantitativní lipidomickou analýzu. Poté je každá metoda před vlastní studií validována pro příslušnou matrici a zvolené interní standardy za účelem ověření správnosti výsledků. Posledním krokem je cílená kvantitativní analýza identifikovaných lipidů ve všech vzorcích s přídavkem interních standardů.

Nedílnou součástí klinických studií je zpracování velkých objemů naměřených dat. Za tímto účelem jsme optimalizovali postup zpracování dat zahrnující převod naměřených dat do formátu m/z / intenzita a jejich další automatické zpracování pomocí Excel scriptu (data jsou v současné době připravována k publikaci). Automatické zpracování dat zahrnuje identifikaci lipidů na základě porovnání hodnot m/z s databází, izotopickou korekci signálu a výpočet koncentrace lipidů. Důležitým krokem při zpracování dat a výpočtu správné koncentrace lipidů je izotopická korekce signálu, kdy je od signálu lipidu odečten příspěvek M+2 izotopu lipidu s jednou dvojnou vazbou navíc. Koncentrace lipidů jsou poté počítány z jejich intenzit

v ESI-MS spektrech po izotopické korekci vztažením na intenzitu interního standardu o známé koncentraci. Vypočtené koncentrace lipidů jsou finálně analyzovány pomocí vícerozměrných statistických metod, které umožňují srovnání velkého množství dat a nalezení vzájemných rozdílů ve složení lipidů mezi pacienty a vybranými zdravými dobrovolníky.

4.2 Lipidomická analýza vzorků pacientů s kardiovaskulárním onemocněním

Mezi rizikovými faktory kardiovaskulárních onemocnění patří zejména obezita pacientů a vysoká koncentrace cirkulujících lipidů v krvi. Předmětem studie bylo posouzení lipidomického profilu plazmy, erytrocytů a různých lipoproteinových frakcí u zdravých dobrovolníků, obézních jedinců a třech skupin pacientů s kardiovaskulárním onemocněním (P26). Vyvinutá HILIC-UHPLC/ESI-MS metoda byla použita pro kvantitativní analýzu fosfoethanolaminů, fosfoinositolů, sfingomielinů a lysofosfocholinů a NP-UHPLC/APCI-MS metoda pro kvantitativní analýzu cholesteryl esterů, triacylglycerolů, sterolů, 1,3-diacylglycerolů a 1,2-diacylglycerolů. Získaná UHPLC/MS data byla analyzována pomocí různých statistických metod pro nalezení rozdílů ve složení lipidů mezi jednotlivými skupinami a určení lipidů s největším vlivem na rozdělení skupin. U skupiny kardiovaskulárních pacientů se nejvíce zvyšuje koncentrace 1,3-diacylglycerolů 32:1 a 34:1 a naopak snižuje koncentrace sfingomielinu 34:2 a 1,3-diacylglycerolu 32:0. Součástí studie bylo i testování MALDI-MS metody pro rychlou lipidomickou analýzu bez chromatografické separace. Dosažené výsledky MALDI-MS lipidomické analýzy neposkytují dostatečné rozlišení jednotlivých skupin vzorků pomocí vícerozměrné analýzy dat.

4.3 HPLC/MS lipidomická analýza pacientů s nádorem prsu

Další studie byla zaměřena na posouzení vlivu rakoviny prsu na složení lipidů tkáně (P27). Bylo studováno složení lipidů prsní nádorové tkáně, které bylo porovnáváno se složením lipidů ve zdravé okolní tkáni získané na základě histologického vyšetření. Toto porovnání zdravé a nádorové tkáně jednoho pacienta umožňuje přímé srovnání složení, které není ovlivněno biologickou variabilitou mezi jednotlivými pacienty, protože změny ve složení jsou způsobeny pouze nádorem. Pro analýzu polárních lipidů v celkovém lipidovém extraktu byla použita HILIC-HPLC/ESI-MS kvantitativní metoda s jedním interním standardem. Studie byla provedena na 20 vzorcích prsní tkáně získaných z 10 pacientek s nádorem prsu a

data byla zpracována vícerozměrnou statistickou analýzou. Byl pozorován nárůst celkové koncentrace tříd fosfoinositolů, fosfoethanolaminů, fosfocholinů a lysofosfocholinů v nádorové tkáni. Statisticky významné rozdíly mezi jednotlivými lipidy v rámci třídy byly pozorovány především pro vinylether (plasmalogen) lipidy fosfoethanolaminů.

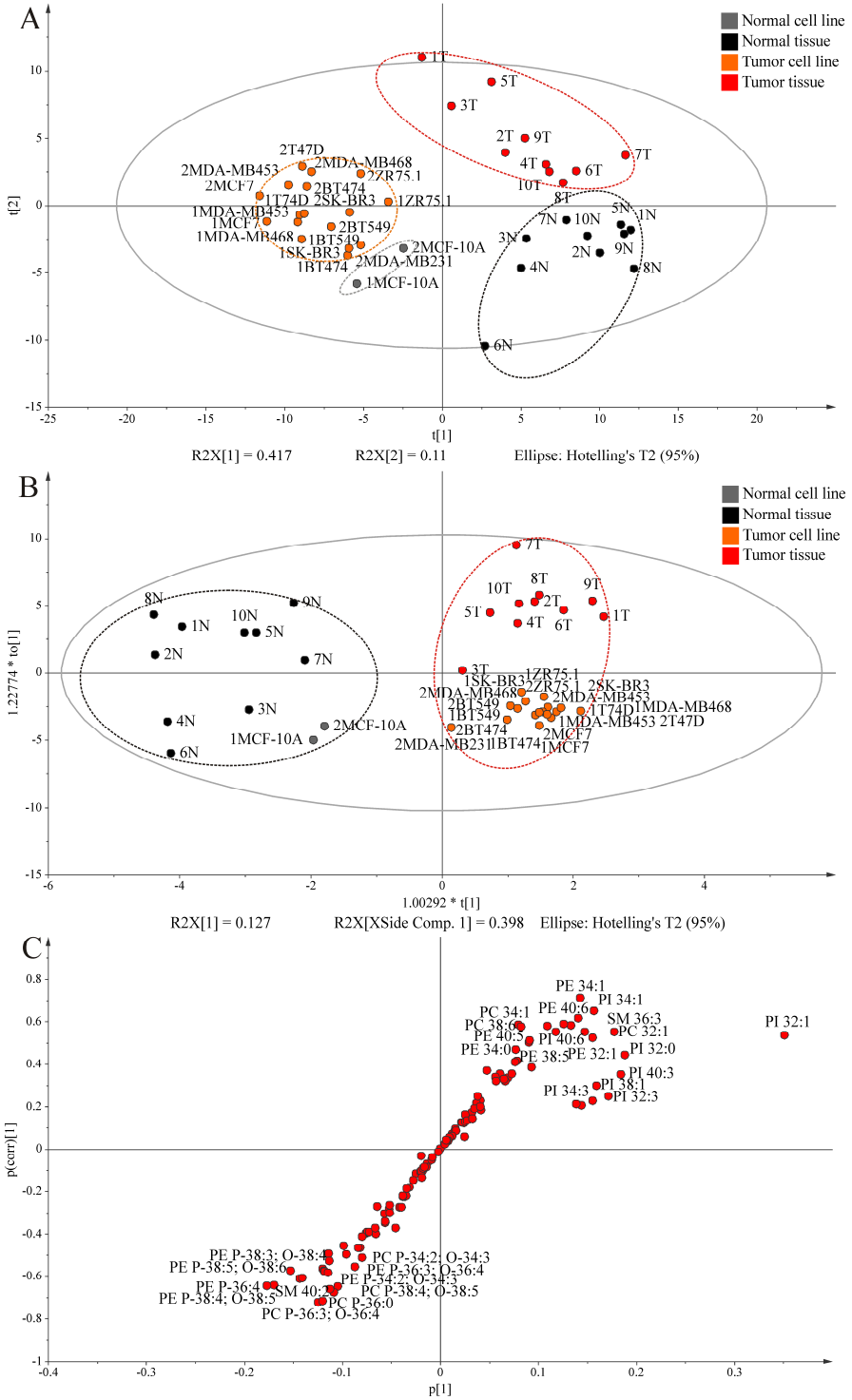

Obrázek 18 Vícerozměrná statistická analýza dat relativního zastoupení lipidů v normálních a nádorových buněčných liniích a tkáních pacientů s nádorem prsu: (A) score-plot metody hlavních komponent, (B) score-plot a (C) S-plot nesupervizované metody nejmenších čtverců (P28).

Nádorová tkáň je směs zdravých a nádorových buněk v určitém poměru, který se může mezi vzorky měnit a tím ovlivňovat výsledky. Z tohoto důvodu byl v další části studie porovnáván stejným způsobem model buněčných linií připravených ze zdravé prsní a nádorové tkáně s nádorovou a okolní zdravou tkání získané po operaci pacientů (P28). Vícerozměrné statistické metody byly použity pro rozlišení skupin vzorků a identifikaci lipidů s největší změnou koncentrace (Obrázek 18). Bylo dosaženo rozlišení skupin vzorků nádorové a zdravé tkáně jak pro vzorky pacientů, tak pro buněčné linie. Nejvíce se v nádorové tkáni zvyšuje koncentrace mononenasycených (např. 32:1 a 34:1) a některých polynenasycených fosfolipidů (např. 40:6), zatímco se snižuje koncentrace polynenasycených fosfolipidů (např. 20:4), plasmalogenů a ether lipidů.

4.4 Lipidomická analýza vzorků pacientů s rakovinou ledvin

Poslední oblast klinických experimentů byla zaměřena na analýzu vzorků pacientů s rakovinou ledvin. Nejdříve byla provedena pilotní studie s cílem popsat rozdíly složení polárních lipidů vzorků nádorové tkáně a okolní zdravé tkáně 20 pacientů s rakovinou ledvin pomocí HILIC-HPLC/ESI-MS metody (P29). Vícerozměrnou statistickou analýzou dat byl pozorován znatelný nárůst zastoupení polárních lipidů obsahujících 4 a více dvojných vazeb ve vzorcích nádorové tkáně v porovnání s okolní zdravou tkání.

Pro další studii byl zvolen větší soubor pacientů a kromě porovnávání složení lipidů v nádorové a okolní zdravé tkáni bylo porovnáváno i složení lipidů plazmy pacientů a zdravých dobrovolníků (výsledky studie jsou v současné době zpracovávány k opublikování). Cílem bylo nalézt korelace ve složení tkání a plazmy, která může být využita pro screening onemocnění. Pro analýzu vzorků byla použita UHPSFC/ESI-MS metoda kvantitativní analýzy lipidů, jejíž výhodou je možnost analýzy nepolárních a polárních lipidů v jedné analýze s vyšší prostupností vzorků. Celkem bylo identifikováno a kvantifikováno 414 lipidů ve 157 vzorcích tkání a 357 lipidů ve 151 vzorcích plazmy. Vícerozměrnou statistickou analýzou dat byly nalezeny lipidy se statisticky významnou změnou koncentrace mezi nádorovou a zdravou okolní tkání. Dále byly popsány významné rozdíly ve složení plazmy v závislosti na pohlaví pacienta, což bylo využito při sestavování jednotlivých modelů.

Další probíhající studie rakoviny ledvin je zaměřena na popis složení gangliosidů v nádorové a okolní zdravé tkáni pacientů pomocí HILIC-UHPLC/ESI-MS metody.

5 Souhrn vědecko-pedagogické činnosti autora

Hlavním vědeckým zaměřením autora jsou kapalinová chromatografie, superkritická fluidní chromatografie a jejich spojení s hmotnostní spektrometrií s aplikací na analýzu malých molekul. Vědecká práce autora zahrnuje především vývoj a validaci analytických metod, vyhodnocení hmotnostních spekter a studium retenčního a fragmentačního chování látek. Hlavní oblastí zájmu autora je cílená a necílená lipidomická analýza rostlinných, živočišných a biologických vzorků. Mezi další témata, kterými se autor ve své vědecké činnosti zabýval, patří analýza různých přírodních látek (např. analýza flavonoidů v nápojích nebo hořkých kyselin v chmelových produktech), analýza metabolitů léčiv, analýza komplexů a analýza vzorků ve spolupráci s průmyslem. Další vědecká činnost autora bude nadále směřována především do oblasti metabolomické analýzy biologických vzorků chromatografickými technikami a hmotnostní spektrometrií.

Autor je spoluautorem 45 publikací v odborných časopisech s počtem citací bez vlastních citací 1172 a h-indexem 21 (dle WoS databáze k 9.4.2018). Celkem polovina prací autora byla publikována v časopisech Analytical Chemistry (5 publikací, IF_{2016} = 6,320) a Journal of Chromatography A (17 publikací, IF_{2016} = 3,981). Tři publikace autora mají více jak 100 citací, dvanáct více jak 50 citací a průměrný počet citací na jeden článek je 29,67. Je spoluautorem 2 přehledových článků z oblasti kapalinové chromatografie a hmotnostní spektrometrie, 7 kapitol v knihách a více jak 200 prezentací na mezinárodních a národních konferencích.

Autor byl od roku 2007 do 2017 zaměstnán jako výzkumný pracovník na Katedře analytické chemie Univerzity Pardubice, kde se částečně podílel na výuce studentů. V letech 2009 až 2014 přednášel povinně volitelný předmět Analýza přírodních látek a v letech 2011 až 2017 povinný předmět Hmotnostní spektrometrie v organické analýze pro studenty magisterského a doktorského studia. Od roku 2017 je autor zaměstnán jako akademický pracovník a vedoucí sekce Analytické chemie na Katedře chemie Univerzity Hradec Králové. Zde přednáší předměty Analytické chemie I a II, Fyzikální chemie I a II a Technologie a ochrana životního prostředí pro studenty bakalářského studia a předměty Hmotnostní spektrometrie, Chromatografické metody a Molekulární a atomová spektroskopie pro studenty navazujícího magisterského studia. Autor je vedoucím 6 obhájených diplomových a 1 bakalářské práce. V současné době je vedoucím 2 bakalářských prací.

Použitá literatura

[1] X.L. Han, R.W. Gross, Global analyses of cellular lipidomes directly from crude extracts of biological samples by ESI mass spectrometry: a bridge to lipidomics, J. Lipid Res., 44 (2003) 1071-1079.

[2] E.A. Dennis et al., http://www.lipidmaps.org/, LIPID MAPS Lipidomics Gateway, in, downloaded September 2017.

[3] O. Quehenberger, A.M. Armando, A.H. Brown, S.B. Milne, D.S. Myers, A.H. Merrill, S. Bandyopadhyay, K.N. Jones, S. Kelly, R.L. Shaner, C.M. Sullards, E. Wang, R.C. Murphy, R.M. Barkley, T.J. Leiker, C.R.H. Raetz, Z. Guan, G.M. Laird, D.A. Six, D.W. Russell, J.G. McDonald, S. Subramaniam, E. Fahy, E.A. Dennis, Lipidomics reveals a remarkable diversity of lipids in human plasma, J. Lipid Res., 51 (2010) 3299-3305.

[4] G. van Meer, D.R. Voelker, G.W. Feigenson, Membrane lipids: where they are and how they behave, Nat. Rev. Molec. Cell Biol., 9 (2008) 112-124.

[5] E. Fahy, S. Subramaniam, H.A. Brown, C.K. Glass, A.H. Merrill, R.C. Murphy, C.R.H. Raetz, D.W. Russell, Y. Seyama, W. Shaw, T. Shimizu, F. Spener, G. van Meer, M.S. VanNieuwenhze, S.H. White, J.L. Witztum, E.A. Dennis, A comprehensive classification system for lipids, J. Lipid Res., 46 (2005) 839-861.

[6] E. Fahy, S. Subramaniam, R.C. Murphy, M. Nishijima, C.R.H. Raetz, T. Shimizu, F. Spener, G. van Meer, M.J.O. Wakelam, E.A. Dennis, Update of the LIPID MAPS comprehensive classification system for lipids, J. Lipid Res., 50 (2009) S9-S14.

[7] T. Čajka, O. Fiehn, Comprehensive analysis of lipids in biological systems by liquid chromatography-mass spectrometry, TrAC, Trends Anal. Chem., 61 (2014) 192-206.

[8] M. Li, L. Yang, Y. Bai, H. Liu, Analytical Methods in Lipidomics and Their Applications, Anal. Chem., 86 (2014) 161-175.

[9] C.J. Fhaner, S.C. Liu, H. Ji, R.J. Simpson, G.E. Reid, Comprehensive Lipidome Profiling of Isogenic Primary and Metastatic Colon Adenocarcinoma Cell Lines, Anal. Chem., 84 (2012) 8917-8926.

[10] H.S. Jonasdottir, S. Nicolardi, W. Jonker, R. Derks, M. Palmblad, A. Ioan-Facsinay, R. Toes, Y.E.M. van der Burgt, A.M. Deelder, O.A. Mayboroda, M. Giera, Detection and Structural Elucidation of Esterified Oxylipids in Human Synovial Fluid by Electrospray Ionization-Fourier Transform Ion-Cyclotron Mass Spectrometry and Liquid Chromatography-Ion Trap-MS3: Detection of Esterified Hydroxylated Docosapentaenoic Acid Containing Phospholipids, Anal. Chem., 85 (2013) 6003-6010.

[11] F. Li, X. Qin, H. Chen, L. Qiu, Y. Guo, H. Liu, G. Chen, G. Song, X. Wang, F. Li, S. Guo, B. Wang, Z. Li, Lipid profiling for early diagnosis and progression of colorectal cancer using direct-infusion electrospray ionization Fourier transform ion cyclotron resonance mass spectrometry, Rapid Commun. Mass Spectrom., 27 (2013) 24-34.
[12] K. Schuhmann, R. Almeida, M. Baumert, R. Herzog, S.R. Bornstein, A. Shevchenko, Shotgun lipidomics on a LTQ Orbitrap mass spectrometer by successive switching between acquisition polarity modes, J. Mass Spectrom., 47 (2012) 96-104.
[13] L.A. Heiskanen, M. Suoniemi, H.X. Ta, K. Tarasov, K. Ekroos, Long-Term Performance and Stability of Molecular Shotgun Lipidomic Analysis of Human Plasma Samples, Anal. Chem., 85 (2013) 8757-8763.
[14] P. Wiesner, K. Leidl, A. Boettcher, G. Schmitz, G. Liebisch, Lipid profiling of FPLC-separated lipoprotein fractions by electrospray ionization tandem mass spectrometry, J. Lipid Res., 50 (2009) 574-585.
[15] K. Yang, H. Cheng, R.W. Gross, X. Han, Automated Lipid Identification and Quantification by Multidimensional Mass Spectrometry-Based Shotgun Lipidomics, Anal. Chem., 81 (2009) 4356-4368.
[16] E.J. Ahn, H. Kim, B.C. Chung, G. Kong, M.H. Moon, Quantitative profiling of phosphatidylcholine and phosphatidylethanolamine in a steatosis/fibrosis model of rat liver by nanoflow liquid chromatography/tandem mass spectrometry, J. Chromatogr. A, 1194 (2008) 96-102.
[17] O. Berdeaux, P. Juaneda, L. Martine, S. Cabaret, L. Bretillon, N. Acar, Identification and quantification of phosphatidylcholines containing very-long-chain polyunsaturated fatty acid in bovine and human retina using liquid chromatography/tandem mass spectrometry, J. Chromatogr. A, 1217 (2010) 7738-7748.
[18] M. Narvaez-Rivas, Q.B. Zhang, Comprehensive untargeted lipidomic analysis using core-shell C30 particle column and high field orbitrap mass spectrometer, J. Chromatogr. A, 1440 (2016) 123-134.
[19] K. Sandra, A.d.S. Pereira, G. Vanhoenacker, F. David, P. Sandra, Comprehensive blood plasma lipidomics by liquid chromatography/quadrupole time-of-flight mass spectrometry, J. Chromatogr. A, 1217 (2010) 4087-4099.
[20] Y. Sato, I. Suzuki, T. Nakamura, F. Bernier, K. Aoshima, Y. Oda, Identification of a new plasma biomarker of Alzheimer's disease using metabolomics technology, J. Lipid Res., 53 (2012) 567-576.

[21] I. Losito, R. Patruno, E. Conte, T.R.I. Cataldi, F.M. Megli, F. Palmisano, Phospholipidomics of Human Blood Microparticles, Anal. Chem., 85 (2013) 6405-6413.
[22] P. Olsson, J. Holmback, B. Herslof, Separation of Lipid Classes by HPLC on a Cyanopropyl Column, Lipids, 47 (2012) 93-99.
[23] M. Scherer, G. Schmitz, G. Liebisch, High-Throughput Analysis of Sphingosine 1-Phosphate, Sphinganine 1-Phosphate, and Lysophosphatidic Acid in Plasma Samples by Liquid Chromatography-Tandem Mass Spectrometry, Clin. Chem., 55 (2009) 1218-1222.
[24] U. Sommer, H. Herscovitz, F.K. Welty, C.E. Costello, LC-MS-based method for the qualitative and quantitative analysis of complex lipid mixtures, J. Lipid Res., 47 (2006) 804-814.
[25] P.M. Hutchins, R.M. Barkley, R.C. Murphy, Separation of cellular nonpolar neutral lipids by normal-phase chromatography and analysis by electrospray ionization mass spectrometry, J. Lipid Res., 49 (2008) 804-813.
[26] D.G. McLaren, P.L. Miller, M.E. Lassman, J.M. Castro-Perez, B.K. Hubbard, T.P. Roddy, An ultraperformance liquid chromatography method for the normal-phase separation of lipids, Anal. Biochem., 414 (2011) 266-272.
[27] B. Nikolova-Damyanova, Retention of lipids in silver ion high-performance liquid chromatography: Facts and assumptions, J. Chromatogr. A, 1216 (2009) 1815-1824.
[28] M. Lísa, M. Holčapek, Characterization of Triacylglycerol Enantiomers Using Chiral HPLC/APCI-MS and Synthesis of Enantiomeric Triacylglycerols, Anal. Chem., 85 (2013) 1852-1859.
[29] M. Lísa, M. Holčapek, High-Throughput and Comprehensive Lipidomic Analysis Using Ultrahigh-Performance Supercritical Fluid Chromatography-Mass Spectrometry, Anal. Chem., 87 (2015) 7187-7195.
[30] E. Lesellier, A. Latos, A.L. de Oliveira, Ultra high efficiency/low pressure supercritical fluid chromatography with superficially porous particles for triglyceride separation, J. Chromatogr. A, 1327 (2014) 141-148.

Přílohy

(P1) M. Holčapek*, **M. Lísa**, P. Jandera, N. Kabátová, Quantitation of Triacylglycerols in Plant Oils Using HPLC with APCI-MS, Evaporative Light-Scattering, and UV Detection, **J. Sep. Sci.** 28 (12) (2005) 1315-1333.

IF_{2005} = 1,829, 105 citací (údaje k 9.4.2018)

(P2) **M. Lísa**, F. Lynen, M. Holčapek, P. Sandra*, Quantitation of Triacylglycerols from Plant Oils Using Charged Aerosol Detection with Gradient Compensation, **J. Chromatogr. A** 1176 (2007) 135-142.

IF_{2007} = 3,641, 54 citací (údaje k 9.4.2018)

(P3) **M. Lísa**, M. Holčapek*, Triacylglycerols Profiling in Plant Oils Important in Food Industry, Dietetics and Cosmetics Using High-Performance Liquid Chromatography - Atmospheric Pressure Chemical Ionization Mass Spectrometry, **J. Chromatogr. A** 1198 (2008) 115-130.

IF_{2008} = 3,756, 128 citací (údaje k 9.4.2018)

(P4) **M. Lísa**, M. Holčapek*, M. Boháč, Statistical Evaluation of Triacylglycerol Composition in Plant Oils Based on High-Performance Liquid Chromatography - Atmospheric Pressure Chemical Ionization Mass Spectrometry Data, **J Agric. Food Chem.** 57 (2009) 6888-6898.

IF_{2009} = 2,469, 63 citací (údaje k 9.4.2018)

(P5) M. Holčapek*, H. Velínská, **M. Lísa**, P. Česla, Orthogonality of Silver-Ion and Non-Aqueous Reversed-Phase HPLC/MS in the Analysis of Complex Natural Mixtures of Triacylglycerols, **J. Sep. Sci.** 32 (2009) 3672-3680.

IF_{2009} = 2,551, 36 citací (údaje k 9.4.2018)

(P6) **M. Lísa**, M. Holčapek*, H. Sovová, Comparison of Various Types of Stationary Phases in Non-Aqueous Reversed-Phase High-Performance Liquid Chromatography-Mass Spectrometry of Glycerolipids in Blackcurrant Oil and Its Enzymatic Hydrolysis Mixture, **J. Chromatogr. A** 1216 (2009) 8371-8378.

IF_{2009} = 4,101, 20 citací (údaje k 9.4.2018)

(P7) **M. Lísa**, K. Netušilová, L. Franěk, H. Dvořáková,V. Vrkoslav, M. Holčapek*, Characterization of fatty acid and triacylglycerol composition in animal fats using silver-ion and non-aqueous reversed-phase high-performance liquid chromatography / mass spectrometry and gas chromatography / flame ionization detection, **J. Chromatogr. A** 1218 (2011) 7499-7510.

IF_{2011} = 4,531, 51 citací (údaje k 9.4.2018)

(P8) **M. Lísa**, M. Holčapek*, T. Řezanka, N. Kabátová, HPLC/APCI-MS and GC/FID Characterization of Δ5-Polyenoic Fatty Acids in Triacylglycerols From Conifer Seed Oils, **J. Chromatogr. A** 1146 (1) (2007) 67-77.

IF_{2007} = 3,641, 51 citací (údaje k 9.4.2018)

(P9) **M. Lísa**, H. Velínská, M. Holčapek*, Regioisomeric Characterization of Triacylglycerols Using Silver-Ion HPLC/MS and Randomization Synthesis of Standards, **Anal. Chem.** 81 (2009) 3903-3910.

IF_{2009} = 5,214, 65 citací (údaje k 9.4.2018)

(P10) **M. Lísa***, M. Holčapek, Characterization of Triacylglycerol Enantiomers Using Chiral HPLC/APCI-MS and Synthesis of Enantiomeric Triacylglycerols, **Anal. Chem.** 85 (2013) 1852-1859.

IF_{2013} = 5,825, 46 citací (údaje k 9.4.2018)

(P11) **M. Lísa***, R. Denev, M. Holčapek, Retention Behavior of Isomeric Triacylglycerols in Silver-ion HPLC: Effects of Mobile Phase Composition and Separation Temperature, **J. Sep. Sci.** 36 (2013) 2888-2900.

IF_{2013} = 2,594, 5 citace (údaje k 9.4.2018)

(P12) M. Holčapek*, H. Dvořáková, **M. Lísa**, A. J. Girón, P. Sandra, J. Cvačka, Regioisomeric analysis of triacylglycerols using silver-ion liquid chromatography - atmospheric pressure chemical ionization mass spectrometry: comparison of five different mass analyzers, **J. Chromatogr. A** 1217 (2010) 8186-8194.

IF_{2010} = 4,194, 51 citací (údaje k 9.4.2018)

(P13) M. Šala, **M. Lísa**, J. L. Campbell, M. Holčapek*, Determination of triacylglycerol regioisomers in porcine adipose tissue using differential mobility spectrometry, **Rapid Commun. Mass Spectrom.** 30 (2016) 256-264.

IF_{2016} = 1,998, 10 citací (údaje k 9.4.2018)

(P14) **M. Lísa**, E. Cífková, M. Holčapek*, Lipidomic profiling of biological tissues using off-line two-dimensional high-performance liquid chromatography - mass spectrometry, **J. Chromatogr. A** 1218 (2011) 5146-5156.

IF_{2011} = 4.531, 89 citací (údaje k 9.4.2018)

(P15) E. Cífková, M. Holčapek*, **M. Lísa**, Nontargeted lipidomic characterization of porcine organs using hydrophilic interaction liquid chromatography and off-line two-dimensional liquid chromatography-electrospray ionization mass spectrometry, **Lipids** 48 (2013) 915-928.

IF_{2013} = 2,353, 22 citací (údaje k 9.4.2018)

(P16) M. Holčapek*, M. Ovčačíková, **M. Lísa**, E. Cífková, T. Hájek, Continuous comprehensive two-dimensional liquid chromatography–electrospray ionization mass spectrometry of complex lipidomic samples, **Anal. Bioanal. Chem.** 407 (2015) 5033-5043.

IF_{2015} = 3,125, 20 citací (údaje k 9.4.2018)

(P17) M. Ovčačíková, **M. Lísa**, E. Cífková, M. Holčapek*, Retention behavior of lipids in reversed-phase ultrahigh-performance liquid chromatography - electrospray ionization mass spectrometry, **J. Chromatogr. A** 1450 (2016) 76-85.

IF_{2016} = 3,981, 13 citací (údaje k 9.4.2018)

(P18) M. Holčapek*, E. Cífková, B. Červená, **M. Lísa**, J. Vostálová, J. Galuszka, Determination of Nonpolar and Polar Lipid Classes in Human Plasma, Erythrocytes and Plasma Lipoprotein Fractions Using Ultrahigh-Performance Liquid Chromatography - Mass Spectrometry, **J. Chromatogr. A** 1377 (2015) 85-91.

IF_{2015} = 3,926, 18 citací (údaje k 9.4.2018)

(P19) **M. Lísa***, M. Holčapek, High-Throughput and Comprehensive Lipidomic Analysis Using Ultrahigh-Performance Supercritical Fluid Chromatography-Mass Spectrometry, **Anal. Chem.** 87 (2015) 7187-7195.

IF_{2015} = 5,886, 40 citací (údaje k 9.4.2018)

(P20) E. Cífková, R. Hájek, **M. Lísa**, M. Holčapek*, Hydrophilic interaction liquid chromatography-mass spectrometry of (lyso)phosphatidic acids, (lyso)phosphatidylserines and other lipid classes, **J. Chromatogr. A** 1439 (2016) 65-73.

IF_{2016} = 3,981, 13 citací (údaje k 9.4.2018)

(P21) R. Berkecz, **M. Lísa**, M. Holčapek*, Analysis of oxylipins in human plasma: comparison of ultrahigh-performance liquid chromatography and ultrahigh-performance supercritical fluid chromatography coupled to mass spectrometry, **J. Chromatogr. A** 1151 (2017) 107-121.

IF_{2016} = 3,981, 1 citací (údaje k 9.4.2018)

(P22) R. Hájek, R. Jirásko, **M. Lísa**, E. Cífková, M. Holčapek*, Hydrophilic Interaction Liquid Chromatography−Mass Spectrometry Characterization of Gangliosides in Biological Samples, **Anal. Chem.** 89 (2017) 12425-12432.

IF_{2016} = 6,320, 1 citací (údaje k 9.4.2018)

(P23) E. Cífková, M. Holčapek*, **M. Lísa**, M. Ovčačíková, A. Lyčka, F. Lynen, P. Sandra, Nontargeted quantitation of lipid classes using hydrophilic interaction liquid chromatography

- electrospray ionization mass spectrometry with single internal standard and response factor approach, **Anal. Chem.** 84 (2012) 10064-10070.

IF_{2012} = 5.695, 45 citací (údaje k 9.4.2018)

(P24) V. Chagovets, **M. Lísa**, M. Holčapek*, Effects of fatty acyls chain lengths, double bond number and matrix on phosphatidylcholine responses in matrix-assisted laser desorption/ionization mass spectrometry, **Rapid Commun. Mass Spectrom.** 29 (2015) 2374-2384.

IF_{2015} = 2,226, 0 citací (údaje k 9.4.2018)

(P25) **M. Lísa***, E. Cífková, M. Khalikova, M. Ovčačíková, M. Holčapek, Lipidomic Analysis of Biological Samples: Comparison of Liquid Chromatography, Supercritical Fluid Chromatography and Direct Infusion Mass Spectrometry Methods, **J. Chromatogr. A** 1525 (2017) 96-108.

IF_{2016} = 3,981, 0 citací (údaje k 9.4.2018)

(P26) M. Holčapek*, B. Červená, E. Cífková, **M. Lísa**, V. Chagovets, J. Vostálová, M. Bancířová, J. Galuszka, M. Hill, Lipidomic analysis of plasma, erythrocytes and lipoprotein fractions of cardiovascular disease patients using UHPLC/MS, MALDI-MS and multivariate data analysis, **J. Chromatogr. B** 990 (2015) 52-63.

IF_{2015} = 2,687, 11 citací (údaje k 9.4.2018)

(P27) E. Cífková, M. Holčapek*, **M. Lísa**, D. Vrána, J. Gatěk, B. Melichar, Determination of lipidomic differences between human breast cancer and surrounding normal tissues using HILIC-HPLC/ESI-MS and multivariate data analysis, **Anal. Bioanal. Chem.** 407 (2015) 991-1002.

IF_{2015} = 3,125, 16 citací (údaje k 9.4.2018)

(P28) E. Cífková, **M. Lísa**, R. Hrstka, D. Vrána, J. Gatěk, B. Melichar, M. Holčapek*, Correlation of lipidomic composition of cell lines and tissues of breast cancer patients using hydrophilic interaction liquid chromatography – electrospray ionization mass spectrometry and multivariate data analysis, **Rapid Commun. Mass Spectrom.** 31 (2017) 253-263.

IF_{2016} = 1.998, 2 citací (údaje k 9.4.2018)

(P29) E. Cífková, M. Holčapek*, **M. Lísa**, D. Vrána, B. Melichar, V. Študent, Lipidomic differentiation between human kidney tumors and surrounding normal tissues using HILIC-HPLC/ESI-MS and multivariate data analysis, **J. Chromatogr. B** 1000 (2015) 14-21.

IF_{2015} = 2,687, 24 citací (údaje k 9.4.2018)

Michal Holčapek[1]
Miroslav Lísa[1]
Pavel Jandera[1]
Naděžda Kabátová[2]

[1]Department of Analytical Chemistry, Faculty of Chemical Technology, University of Pardubice, Pardubice, Czech Republic
[2]Central Institute for Supervising and Testing in Agriculture, Brno, Czech Republic

Quantitation of triacylglycerols in plant oils using HPLC with APCI-MS, evaporative light-scattering, and UV detection

The main constituents of plant oils are complex mixtures of TGs differing in acyl chain lengths, number and positions of double bonds, and regioisomerism. A non-aqueous reversed-phase HPLC method with acetonitrile–2-propanol gradient and 30+15 cm NovaPak C_{18} columns makes possible an unambiguous identification of the highest number of TGs ever reported for these oils, based on positive-ion APCI mass spectra. A new approach to TG quantitation is based on the use of response factors with three typical detection techniques for that purpose (APCI-MS, evaporative light-scattering detection, and UV at 205 nm). Response factors of 23 single-acid TGs (saturated TGs from C7 to C22, 7 unsaturated TGs), 4 mixed-acid TGs, diolein and monoolein are calculated from their calibration curves and related to OOO. Due to differences between saturated and unsaturated acyl chains, the use of response factors significantly improves the quantitation of TGs. 133 TGs containing 22 fatty acids with 8–25 carbon atoms and 0–3 double bonds are identified and quantified in 9 plant oils (walnut, hazelnut, cashew nut, almond, poppy seed, yellow melon, mango, fig, date) using HPLC/APCI-MS with a response factor approach. Average parameters and relative fatty acid concentrations are calculated with both HPLC/APCI-MS and GC/FID.

Key Words: Plant oil; Vegetable oil; Triacylglycerol; Quantitation; Response factor

Received: February 21, 2005; revised: June 3, 2005; accepted: June 16, 2005

DOI 10.1002/jssc.200500088

1 Introduction

Plant oils are complex mixtures of various compound classes, where the main constituents are triacylglycerols (TGs) consisting of saturated and unsaturated fatty acids (FAs), such as oleic (O), linoleic (L), linolenic (Ln), stearic (S), palmitic (P), *etc.*, differing in their acyl chain lengths and their stereochemical positions *sn*-1, 2, or 3 on the glycerol skeleton, and in the number and positions of the double bonds in the acyl chains. They may also differ in *cis*/*trans* configuration of double bonds and *R/S* optical isomerism of TGs with three different acyl chains. The standard notation of TGs employs the initials of the fatty acid trivial names arranged in the order of their positions on the glycerol skeleton. Mostly, *sn*-1 and *sn*-3 positions are not discriminated. Information about the distribution and type of FAs on the glycerol backbone is quite important for lipid digestion and metabolism, because FAs at the *sn*-1 and *sn*-3 positions are digested first by lipases yielding *sn*-2 monoacylglycerols and free FAs [1, 2].

Non-aqueous reversed-phase high-performance liquid chromatography (NARP HPLC) has been widely used for the separation of complex natural lipid samples [3–25]. The retention in NARP HPLC increases with increasing equivalent carbon number (ECN) defined as the total carbon number (CN) in all acyl chains minus two times the number of double bonds (DB), *i.e.*, ECN = CN – 2DB. Under optimized separation conditions, the separation of most TGs within the same ECNs group is also possible, for example the critical pair LLL/OLLn or the group of OOO, OOP, OPP, and PPP can be resolved [3–5]. The separation of TGs differing in the position(s) of double bond(s) is also feasible [6]. On the other hand, NARP HPLC is not suitable for the separation of three types of isomerism, *i.e.*, regioisomers, *R/S* isomers, and *cis*/*trans*

Correspondence: Dr. Michal Holčapek, University of Pardubice, Faculty of Chemical Technology, Department of Analytical Chemistry, Nám. Čs. Legií 565, 532 10 Pardubice, Czech Republic. Phone: +420 46 6037087. Fax: +420 46 6037068.
E-mail: Michal.Holcapek@upce.cz.

Abbreviations: NARP HPLC, non-aqueous reversed-phase high-performance liquid chromatography; MS, mass spectrometry; APCI, atmospheric pressure chemical ionization; ESI, electrospray ionization; ELSD, evaporative light-scattering detection; GC, gas chromatography; FID, flame ionization detection; TG, triacylglycerol; DG, diacylglycerol; MG, monoacylglycerol; FA, fatty acid; ECN, equivalent carbon number; CN, carbon number; DB, double bond; sn, stereochemical numbering; RF, response factor; Cy, caprylic acid; C, capric acid; La, lauric acid; M, myristic acid; Po, palmitoleic acid; P, palmitic acid; Mo, margaroleic acid; Ma, margaric acid; Ln, linolenic acid; L, linoleic acid; O, oleic acid; S, stearic acid; G, gadoleic acid; A, arachidic acid; B, behenic acid; Lg, lignoceric acid.

isomers. Various mobile phase systems, mostly in gradient elution mode, are described in the literature, such as 2-propanol/acetonitrile [3, 7, 8], 2-propanol/acetonitrile/hexane [9, 25], acetone/acetonitrile [5, 10–13], acetonitrile/chloroform [14], 100% propionitrile [4], acetonitrile/dichlormethane [15–21], *etc.* The common feature of the mentioned separation systems is a low polarity of mobile phase components, because TGs are not soluble in water or common aqueous–organic mobile phases used in reversed-phase HPLC. An aqueous–organic step at the beginning of gradient may improve the chromatographic resolution of more polar acylglycerols (di- and monoacylglycerols) without sacrificing the resolution of TGs [9].

The alternative separation technique frequently employed in the lipid analysis is silver ion HPLC in normal-phase systems. The separation principle of this technique is based on the strong interactions between silver ions and π-electrons from the double bonds [26]. Ag^+ HPLC is very successful in the separation of lipids differing in the number [26, 27] and positions of double bonds [28] and *cis*/*trans* isomerism, too [29]. The retention increases in order of increasing number of double bonds, but the method has a low separation selectivity for lipids differing only in the saturated part of molecules, which are usually not separated [26–29] and the reproducibility is low. Numerous studies can be found in the literature on the separation of various lipid classes using silver ion HPLC [26–29 and citations therein]. The separation mechanism of silver ion chromatography is complementary to NARP HPLC, so that off-line or on-line coupling of these two separation modes should considerably improve the number of resolved compounds. Recent results on 2D separation of TGs in plant oils [12] are encouraging, but the number of identified TGs for a given plant oil is still lower than with a properly optimized NARP system. Further improvements in this area are likely in the near future.

In addition to NARP and silver ion HPLC, capillary electrochromatography [25], supercritical fluid chromatography [30–31], and subcritical fluid chromatography [32] have also been successfully applied for the separation of complex TG mixtures with similar chromatographic resolution to NARP or in the case of capillary electrochromatography even slightly better resolution for TGs with higher ECNs [25].

Among the detection techniques not providing structural information, evaporative light-scattering detection (ELSD) is the most widespread in TG analysis [33, 34], but the non-linear response of this detector is a clear disadvantage for the quantification. The other possibility is UV detection at very low wavelengths (*e.g.*, 205 nm) [3, 8, 9], which requires the use of HPLC gradient-grade solvents, but provides a linear response unlike ELSD. The blank gradient should be subtracted to avoid baseline drift during the gradient. Refractive-index detection is often used in routine analyses [35–37], but it cannot be applied for gradient analyses typically used for complex TG mixtures and nowadays is often replaced by ESLD or MS detection.

The coupling of HPLC and mass spectrometry (HPLC/MS) is a powerful tool in lipid analysis, because it provides both structural information and usually also the highest sensitivity among all available chromatographic detectors [9]. Atmospheric pressure chemical ionization (APCI) is the most frequently used ionization technique for TG analysis because of easy coupling to non-aqueous mobile phase systems used in NARP HPLC and high ionization efficiency for non-polar TG molecules. The presence of both protonated molecules $[M+H]^+$ and fragment ions $[M+H-R_iCOOH]^+$ is important for structure elucidation [3, 4, 7–14, 17–23]. Electrospray ionization (ESI) mass spectra exhibit $[M+Na]^+$ and $[M+K]^+$ ions instead of protonated molecules and also fragment ions, such as $[M+Na-R_iCOOH]^+$ and $[M+Na-R_iCOONa]^+$, but in a lower relative intensity [3, 21, 27]. The abundance of molecular adducts with alkali metal ions significantly depends on the salt content in the solution. Coupling with Ag^+ HPLC may require the use of post-column make-up flow of other polar solvent both for ESI and APCI, because typical mobile phases contain more than 98% of hexane [12, 29], which is not favorable for the ionization process. APCI mass spectra provide information on the predominant fatty acid in the *sn*-2 position. The precise ratio of regioisomers can also be obtained by the measurement of calibration curves with both positional isomers [11, 14]. In principle, the same approach is applicable with ESI.

The chromatographic quantitation of TGs is usually based only on the relative areas of chromatographic peaks neglecting potential differences in the relative responses of TGs differing in the number of double bonds and acyl chain lengths. The obvious advantage of such an approach is its simplicity, but it may lead to significant systematic errors in the determination of TG concentration. Due to the enormous number of TGs occurring in natural samples, the calibration curves can be constructed only for a small part of identified single-acid TGs. To our best knowledge, only few authors [17, 37] have attempted to quantify complex natural TG mixtures using a more sophisticated approach than normalized chromatographic peak areas or a limited number of TG standards. The first approach [17] is based on the measurement of calibration sets of SSS, OOO, LLL, LnLnLn, PPP, and PoPoPo with APCI-MS and the use of response factors calculated in different ways and related to deuterated d_{12}-PPP standard. The other approach [37] used for isocratic HPLC with refractive index detection relies on the use of RFs determined with authentic single-acid TG standards and related to OOO.

The main goal of our work to develop a method suitable for reliable quantitation of TGs in complex natural samples based on the comparison of three frequently used detection techniques for gradient elution HPLC of TGs (APCI-MS, ELSD and UV at 205 nm). First, the HPLC separation has to be carefully optimized to achieve the highest possible chromatographic resolution and to reduce the number of possible coelutions. Then, the RFs of authentic standards of single-acid TGs are determined by comparing their calibration curves. The model for the calculation of RFs for mixed-acid TGs with APCI-MS is proposed and applied for the determination of TG composition in 9 edible plant oils prepared in the laboratory – walnut, hazelnut, cashew nut, almond, poppy seed, yellow melon, mango, fig, and date plant oils. The quantitative results for TGs in some plant oils are compared with validated gas chromatography–flame ionization detection (GC/FID) determination of fatty acid methyl esters (FAMEs) obtained by transesterification of TGs.

2 Experimental

2.1 Materials

Acetonitrile, 2-propanol and hexane were purchased from Merck (Darmstadt, Germany). De-ionized water was prepared with a Demiwa 5-roi purification system (Watek, Ledeč nad Sázavou, Czech Republic). The solvents were filtered through a 0.45-μm Millipore filter and degassed by continuous stripping with helium. The standards of trimyristin (MMM, C14:0), tripalmitin (PPP, C16:0), tripalmitolein (PoPoPo, C16:1), trimargarin (MaMaMa, C17:0), triolein (OOO, C18:1), trilinolein (LLL, C18:2), α-trilinolenin (α-LnLnLn, C18:3) and the mixture of tri-, di-, and monoolein were purchased from Sigma-Aldrich (St. Louis, USA); tristearin (SSS, C18:0), γ-trilinolenin (γ-LnLnLn, C18:3), model mixtures of TG standards GLC#435 (all saturated single-acid TGs from C7 to C22) and GLC#406 (C16:0, C18:0, C18:1, C18:2, C18:3, C20:0, C20:1 and C22:1), model mixture of FAMEs standards GLC#85 (C4:0, C6:0, C8:0, C10:0, C11:0, C12:0, C13:0, C14:0, C14:1, C15:0, C15:1, C16:0, C16:1, C17:0. C17:1, C18:0, C18:1, C18:1T, C18:2, C18:3, C18:3γ, C20:0, C20:1, C20:2, C22:0, C22:1, C20:3, C20:4, C22:2, C22:6 and C24:1), GLC#1A (C16:0, C18:0, C18:1, C18:2 and C18:3), and GLC#06A (C16:0, C18:0, C20:0, C22:0 and C24:0) were purchased from Nu-Chek-Prep (Elysian, USA).

2.2 Chromatographic and detection conditions

The chromatographic apparatus consisted of a Model 616 pump with a quaternary gradient system, a Model 996 diode-array UV detector, a Model 717+ autosampler, a thermostated column compartment, and a Millennium chromatography manager (all from Waters, Milford, MA, USA). The final HPLC method for the analyses of all plant oils and the calculation of RFs used the following conditions: two chromatographic columns Nova-Pak C_{18} (300 × 3.9 and 150 × 3.9 mm, 4 μm, Waters) connected in series, flow rate 1 mL/min, injection volume 10 μL, column temperature 25°C, and mobile phase gradient with the steepness 0.65%/min: 0 min–100% acetonitrile, 106 min–31% acetonitrile–69% 2-propanol, 109 min–100% acetonitrile. The injector needle was washed with the mobile phase before each injection. The column hold-up volume t_M was 3.20 min for the system with 30 + 15 cm Nova-Pak columns. The UV detection at 205 nm and positive-ion APCI-MS connected in series were used in most experiments. All UV chromatograms were baseline subtracted using the analysis with a blank injection. The Esquire 3000 ion trap analyzer (Bruker Daltonics, Bremen, Germany) was used in the mass range *m/z* 50–1200 with the following setting of tuning parameters: pressure of the nebulizing gas 70 psi, drying gas flow rate 3 L/min, the temperatures of the drying gas and APCI heater were 350°C and 400°C, respectively. For quantitative evaluation of all standards and samples, reconstructed ion current chromatograms in the region *m/z* 300–1200 were used. Individual reconstructed ion current chromatograms were used to support the identification of coeluting peaks. A Sedex 75 (Alfortville, France) was employed for determination of response factors with evaporative light-scattering detection (ELSD) (connected in series with UV detector) using a nebulizing temperature of 60°C; the flow rate and pressure of nitrogen were 10 L/min and 2.4 bar, respectively.

2.3 Sample preparation

10–15 g of each sample (walnut, hazelnut, cashew nut, almond, poppy seed, yellow melon seed, mango stone, fig stone, and date seed) was weighed and then carefully crushed in a mortar to fine particles, which were mixed with 15 mL of hexane, and the mixture was stirred occasionally for 15 min. The solid particles were filtered out using a coarse filter paper and then the extract was filtered again using a fine filter with 0.45-μm pores. From the filtered extract, hexane was evaporated overnight at room temperature yielding a pure plant oil. The oil samples were dissolved in an acetonitrile–2-propanol–hexane mixture (2:2:1, *v/v/v*) to prepare a 3% solution (*w/v*); 10 μL of this solution was injected for HPLC analysis.

2.4 Calibration curves and limits of detection

The stock solutions of unsaturated TGs (PoPoPo, OOO, LLL, and LnLnLn) at the concentration 3 g/L and of saturated TGs (MMM, PPP, MaMaMa, and SSS) at 0.15 g/L were dissolved in acetonitrile–2-propanol–hexane mixture (2:2:1, *v/v/v*). These solutions were diluted with the same solvent mixture yielding the working solutions at 5,

10, 50, 100, and 150 mg/L for saturated and 5, 10, 100, 300, and 500 mg/L for unsaturated TGs. For the standard mixture of tri-, di- and monoolein, the stock solution at 3.33 g/L in acetonitrile–2-propanol–hexane mixture (2:2:1, *v/v/v*) was diluted with the same solvent mixture for the calibration set of 50, 100, 300, and 500 mg/L. All calibration curves were measured using a 10 μL injection volume of working solutions in three repeated analyses with three detection techniques (APCI, ELSD, and UV at 205 nm), and the average peak areas were used for the construction of calibration curves. For reliable quantitation, concentrations of individual TGs in analyzed samples should not be higher than a verified linear range, because negative deviations from the linear calibration dependences in APCI-MS were observed for high concentrations in this and previous [17] work. Samples with TGs concentrations outside the linear calibration range must be diluted. The limits of detection (LOD) at $S/N = 3$ were determined with the injection volume 10 μL and averaged for particular saturation groups: APCI-MS – 2 mg/L for saturated, 3 mg/L for monounsaturated, 2 mg/L for diunsaturated, and 1 mg/L for triunsaturated; ELSD – 4 mg/L for saturated, 10 mg/L for monounsaturated, 14 mg/L for diunsaturated, and 15 mg/L for triunsaturated TGs; UV detection – 100 mg/L for saturated, 13 mg/L for monounsaturated, 4 mg/L for diunsaturated, and 2 mg/L for triunsaturated.

2.5 Preparation of fatty acid methyl esters and their gas chromatographic analysis with flame ionization detection

Fatty acid methyl esters (FAMEs) were prepared from TGs in plant oils using a standard procedure with sodium methoxide [38]. FAMEs mixtures were analysed by gas chromatography–flame ionization detection (GC/FID) on a Varian CP 3800 with a CP-8410 autosampler and a CP-1177 injector (Varian Analytical Instruments, Walnut Creek, CA, USA) using a BTR-Carbowax-30W-0.5F silica capillary column, 30 m length, 0.32 mm ID, 0.5 μm film thickness (Quadrex, Woodbridge, CT, USA). GC conditions were as follows: injection volume 1 μL, split ratio 1:40, flow rate of nitrogen as a carrier gas 0.7 mL/min, temperature program: initial temperature 160°C hold for 6 min, then ramp to 200°C at 20 K/min, hold for 10 min, ramp to 240°C at 5 K/min and hold for 20 min with a total analysis time of 46 min. Injector and detector temperatures were 250 and 270°C, respectively.

3 Results and discussion

3.1 Nomenclature and general conventions about TGs

Table 1 summarizes all fatty acids (FAs) identified in individual TGs together with their trivial names, abbreviations, carbon numbers (CN), double bond (DB) numbers, and equivalent carbon numbers (ECN). **Table 2** lists ECNs, molecular weights (MWs), RFs measured with APCI-MS, retention times t_R, and the relative retention r measured using the HPLC method with 45 cm total column length for 133 TGs identified in 9 plant oils consisting of 22 fatty acids. The masses and structures of fragment ions have been described in our previous work [3]. Plant oils usually contain a mixture of regioisomers. Three identical acyl chains on the glycerol backbone (single-acid $R_1R_1R_1$ type) provide only a single ion $[M+H-R_1COOH]^+$, while mixed-acid $R_1R_1R_2$ type produces two different $[M+H-R_1COOH]^+$ and $[M+H-R_2COOH]^+$ ions with a statistical abundance ratio of 1:2, and the $R_1R_2R_3$ type has three different $[M+H-R_1COOH]^+$, $[M+H-R_2COOH]^+$, and $[M+H-R_3COOH]^+$ ions with a statistical abundance ratio of 1:1:1. Neutral loss of R_iCOOH from the equivalent side positions *sn*-1 and *sn*-3 is preferred over cleavage from the middle position *sn*-2, which can be applied for determination of the acid predominant in the *sn*-2 position [3, 4, 8–11, 14]. The type (mainly unsaturation degree) may also influence the relative intensity of $[M+H-R_iCOOH]^+$ ions, so the published data [3, 11, 14, 21] on the ratios of authentic standards of selected regioisomers are taken into consideration for the empirical determination of *sn*-2 acyl chain. For precise determination of regioisomeric

Table 1. Systematic and trivial names of fatty acids found in TGs of studied plant oils listed with their abbreviations, carbon numbers (CN), double bond (DB) numbers, and equivalent carbon numbers (ECN).

Systematic name	Trivial name	Abbreviation	CN:DB	ECN
Octanoic	Caprylic	Cy	C8:0	8
Decanoic	Capric	C	C10:0	10
Dodecanoic	Lauric	La	C12:0	12
Tetradecanoic	Myristic	M	C14:0	14
Pentadecanoic	–	–	C15:0	15
Hexadecanoic	Palmitic	P	C16:0	16
cis-9-Hexadecenoic	Palmitoleic	Po	C16:1	14
Heptadecanoic	Margaric	Ma	C17:0	17
cis-10-Heptadecenoic	Margaroleic	Mo	C17:1	15
Octadecanoic	Stearic	S	C18:0	18
cis-9-Octadecenoic	Oleic	O	C18:1	16
cis-9,12-Octadecadienoic	Linoleic	L	C18:2	14
cis-9,12,15-Octadecatrienoic	Linolenic	Ln	C18:3	12
Nonadecanoic	–	–	C19:0	19
Eicosanoic	Arachidic	A	C20:0	20
cis-11-Eicosenoic	Gadoleic	G	C20:1	18
cis-11,14-Eicosadienoic	–	–	C20:2	16
Heneicosanoic	–	–	C21:0	21
Docosanoic	Behenic	B	C22:0	22
Tricosanoic	–	–	C23:0	23
Tetracosanoic	Lignoceric	Lg	C24:0	24
Pentacosanoic	–	–	C25:0	25

Table 2. Triacylglycerols (TG) identified in studied plant oils listed with their equivalent carbon numbers (ECN), molecular weights (MW), retention times t_R, relative retention *r*, and response factors (RF) determined with APCI-MS.

TG	ECN	MW[a)]	t_R	*r*[b)]	*RF*
LnLnLn	36	872	48.3	0.800	0.40
LnLLn	38	874	54.0	0.901	0.46
LaLLa		718	54.8	0.915	4.22
LaOC		692	55.3	0.924	8.22
MOCy		692	55.9	0.934	26.07
MLaLa		666	56.6	0.947	4.95
LnLnMo	39	862	57.7	0.966	0.54
LnLnC15:0		836	58.7	0.984	0.85
LLLn	**40**	**876**	**59.6**	**1.000**	**0.51**
LLLa		798	60.3	1.012	2.39
LnOLn		876	60.6	1.018	0.60
OOCy		746	61.4	1.032	25.48
MLLa		746	61.5	1.034	3.13
LaOLa		720	61.8	1.039	4.36
LnLnP		850	62.1	1.044	0.71
POCy		720	63.0	1.060	25.59
PLaLa		694	63.8	1.074	4.47
MMLa		694	63.8	1.074	3.86
LnLMo	41	864	63.3	1.066	0.59
LLL	**42**	**878**	**65.3**	**1.000**	**0.57**
LLPo		852	65.7	1.006	0.82
OLLn		878	66.4	1.018	0.66
LLM		826	66.7	1.023	1.30
OLLa		800	67.0	1.027	2.54
OOC		774	67.6	1.037	6.54
LnLP		852	67.8	1.040	0.76
MLM		774	68.2	1.047	2.04
PLLa		774	68.3	1.048	2.64
SLnLn		878	68.5	1.052	0.47
MOLa		748	68.5	1.052	3.27
SOCy		748	69.9	1.074	25.35
PMLa		722	70.7	1.087	3.38
LLMo	43	866	69.0	1.060	0.65
LLC15:0		840	70.3	1.081	0.96
LnLMa		866	70.7	1.087	0.59
C20:2LL	44	906	70.8	0.985	0.50
OLL		**880**	**71.8**	**1.000**	**0.71**
OLPo		854	72.2	1.006	0.97
OLnO		880	72.6	1.012	0.80
LLP		854	73.1	1.019	0.82
OLM		828	73.7	1.028	1.45
SLLn		880	73.8	1.029	0.53
LnOP		854	74.0	1.032	0.91
OOLa		802	74.1	1.034	2.68
ALnLn		906	74.3	1.036	0.40
PLM		802	75.1	1.048	1.55
SLLa		802	75.2	1.050	2.41
MOM		776	75.5	1.054	2.18
POLa		776	75.6	1.055	2.79
PLnP		828	75.7	1.057	1.01
OLMo	45	868	75.6	1.055	0.79
LLMa		868	76.3	1.066	0.65
MoLP		842	76.4	1.067	0.90
OLnMa		868	77.0	1.076	0.74
GLL	46	908	77.2	0.991	0.50
OLO		**882**	**77.9**	**1.000**	**0.86**
OOPo		856	78.3	1.005	1.11
SLL		882	79.0	1.015	0.58
OLP		856	79.3	1.019	0.96
GOLa		830	79.4	1.020	2.47
ALLn		908	79.6	1.023	0.46
OOM		830	79.7	1.024	1.59
POPo		830	79.8	1.025	1.22
SOLn		882	80.0	1.028	0.67
BLnLn		934	80.1	1.029	0.42
PLP		830	80.9	1.040	1.07
SLM		830	80.9	1.040	1.32
PPoP		804	81.3	1.046	1.32
POM		804	81.3	1.046	1.70
SOLa		804	81.3	1.046	2.55
SLnP		856	81.4	1.047	0.78
OOMo	47	870	81.5	1.048	0.94
OLMa		870	82.3	1.059	0.79
C21:0LLn		920	82.3	1.059	0.45
MoOP		844	82.7	1.064	1.04
C23:0LnLn		948	82.9	1.067	0.40
GLO	48	910	83.1	0.989	0.64
OOO		**884**	**84.0**	**1.000**	**1.00**
ALL		910	84.8	1.010	0.51
GOM		858	85.0	1.012	1.38
BLLn		936	85.1	1.014	0.48
SLO		884	85.1	1.014	0.73
OOP		858	85.4	1.017	1.11
SLP		858	86.6	1.032	0.83
BLLa		858	86.6	1.032	2.36
SLnS		884	86.9	1.036	0.54
AOLa		832	87.0	1.037	2.48
POP		832	87.0	1.037	1.21
SOM		832	87.0	1.037	1.46
PPP		806	88.7	1.058	1.32
C23:0LLn	49	950	87.8	1.047	0.46
OOMa		872	88.4	1.054	0.94
MaOP		846	89.7	1.071	1.04
GOO	50	912	89.0	0.979	0.79
GLS		912	89.9	0.990	0.51
BLL		938	90.0	0.991	0.53
LgLLn		964	90.2	0.993	0.46
ALO		912	90.4	0.995	0.66
GOP		886	90.4	0.995	0.89

Table 2. Continued ...

SOO		**886**	**90.8**	**1.000**	**0.87**
ALP		886	91.8	1.011	0.76
SLS		886	91.9	1.013	0.60
SOP		860	92.3	1.017	0.98
AOM		860	92.3	1.017	1.39
BOLa		860	92.3	1.017	2.50
SPP		834	94.4	1.041	1.08
C23:0OLa	51	874	94.7	1.045	2.48
SOMa		874	95.0	1.048	0.81
LgLL	52	966	94.9	0.988	0.51
BLO		940	95.5	0.995	0.68
GOS		914	95.7	0.997	0.66
AOO		**914**	**96.0**	**1.000**	**0.80**
LgLM		914	96.7	1.008	1.25
BLP		914	96.8	1.009	0.78
ALS		914	96.9	1.010	0.53
LgOLa		888	97.1	1.012	2.48
AOP		888	97.5	1.016	0.91
SOS		888	97.6	1.017	0.74
SSP		862	99.7	1.040	0.85
C19:0OS	53	902	100.2	1.045	0.70
LgLO	54	968	100.5	1.048	0.66
BOO		942	101.0	1.054	0.82
LgLP		942	101.9	1.064	0.76
BLS		942	102.0	1.065	0.55
AOS		916	102.6	1.071	0.67
SSS		890	104.6	1.093	0.61
C23:0OO	55	956	103.3	1.079	0.80
LgOO	56	970	105.5	1.102	0.80
LgLS		970	106.5	1.113	0.53
LgOP		944	106.9	1.117	0.91
BOS		944	107.0	1.119	0.69
C25:0OO	57	984	107.7	1.126	0.80
C23:0OS		958	109.2	1.142	0.67

[a] For better clarity, the decimal places are neglected in this table.

[b] Relative retention $r = (t_R - t_M)/(t_S - t_M)$, where t_M is 3.20 min and t_S are retention times of standards for particular ECN groups (printed in bold), *i.e.*, LLLn for ECN = 41 and lower, LLL for ECN = 42 and 43, OLL for ECN = 44 and 45, OLO for ECN = 46 and 47, OOO for ECN = 48 and 49, SOO for ECN = 50 and 51, AOO for 52 and higher.

ratios, the accurate determination of calibration curves for both regioisomeric standards is essential [11, 14]. The *sn*-2 acids in TGs are denoted according to the prevailing acids identified in the studied plant oils, *e.g.*, OLP corresponds to linoleoyl prevailing in the *sn*-2 position. TGs marked with asterisk (*e.g.*, OLP*) signify that the determination of middle *sn*-2 acid is not unambiguous due to: 1) the coelution with other TG with the same masses of $[M+H-R_iCOOH]^+$ ions, 2) the concentrations of regioisomers being similar, 3) the concentration of TG being so low that *sn*-2 acid cannot be determined clearly. The positions *sn*-1 and *sn*-3 are considered as equivalent, because these regioisomers cannot be distinguished by NARP HPLC or mass spectrometry, so acids in *sn*-1 and *sn*-3 positions are ordered by decreasing mass, *i.e.*, SLO (not OLS). Identified TGs are sorted into three groups: major TGs (>5 weight% in a particular oil), minor TGs (>0.5% and <5%), and trace TGs (<0.5%), which is found useful for easier comparison and discussion of results. These conventions are used through the whole paper including figures and tables.

3.2 Quantitation using the response factor approach

Natural TG (or lipid in general) samples contain very complex mixtures, but commercial standards are available only for a limited range of TGs, mostly single-acid type $R_1R_1R_1$. Moreover, less common TGs are expensive and polyunsaturated TGs are prone to oxidation, hence quantitation based on the calibration curves for all TGs is practically impossible even if only major TGs are taken into account. For this reason, a suitable approach for the quantitation of complex TG mixtures with a limited range of authentic TG standards (mainly single-acid type) is sought in this work. TGs with different number and positions of double bonds, and lengths of acyl chains, differ in the relative responses with common HPLC detection techniques used for TGs (APCI-MS, ELSD, and UV at 205 nm). This leads to systematic errors in the quantitation based on the relative peak areas. The main goal of our work is to improve the accuracy and precision of TG quantitation using appropriate RFs. For this purpose, the calibration curves of 23 single-acid TGs were measured **(Table 3**) and the RFs of mixed-acid TGs calculated. The RF of OOO, as one of the most widespread natural TGs, is set to RF = 1.00 for all detection techniques and other RFs are expressed relative to this standard value. The use of calibration curves with 5 calibration points should provide better precision than the RFs based on a single point only. For detection techniques providing linear concentration responses (*e.g.*, APCI-MS and UV), the ratio of calibration slopes *a*(OOO)/*a*(TG) is used for the calculation of RFs of individual TGs. For detection techniques with non-linear detector response (*e.g.*, ELSD), the ratios of *y* values *y*(OOO)/*y*(TG) at different concentration levels have to be used instead of calibration slopes. The ratios of *y* values decrease slightly with increasing concentration (**Table 4**), but RFs are relatively stable within a limited concentration range (50–500 mg/L) with the relative standard deviations always lower than 3.2%. RFs should not be used for concentrations outside this range because of non-linear dependence. This is, of course, a serious draw-

Table 3. Response factors (RF) of 23 single-acid TG standards, 4 mixed-acid TG standards and representatives of diacylglycerols (diolein, OO) and monoacylglycerols (monoolein, O) determined with APCI-MS, ELSD and UV detection at 205 nm[a)].

TG (CN : DB)	APCI				ELSD					UV			
	a	*b*	r^2	RF	*a*	*b*	*c*	r^2	RF	*a*	*b*	r^2	RF
C7 : 0	0.229	−0.001	0.995	97.20	1.692	0.038	0.006	1.000	0.32	0.223	−0.001	1.000	7.57
C8 : 0	0.299	0.004	0.992	74.44	1.235	0.281	0.002	1.000	0.44	0.217	0.001	1.000	7.77
C9 : 0	0.572	0.004	0.998	38.91	1.118	0.776	−0.010	0.998	0.48	0.211	0.004	0.997	8.00
C10 : 0	1.263	−0.006	0.991	17.62	0.980	0.951	−0.005	0.999	0.55	0.230	0.009	0.991	7.33
C11 : 0	2.052	0.001	0.995	10.85	1.493	1.289	−0.021	1.000	0.36	0.215	0.006	0.991	7.85
C12 : 0	3.684	−0.007	0.999	6.04	1.990	1.936	−0.039	1.000	0.27	0.243	−0.002	0.994	6.94
C13 : 0	5.166	−0.010	0.998	4.31	3.569	2.032	0.040	1.000	0.15	0.208	0.003	1.000	8.11
C14 : 0	8.033	0.010	0.999	2.77	7.835	1.141	−0.001	0.999	0.07	0.237	0.001	1.000	7.12
C15 : 0	12.700	0.024	0.999	1.75	8.091	1.705	0.013	1.000	0.07	0.227	0.002	0.999	7.43
C16 : 0	16.904	0.303	0.994	1.32	12.778	1.948	−0.009	1.000	0.04	0.241	0.001	0.997	7.00
C16 : 1	16.749	0.715	0.991	1.33	0.447	2.004	−0.119	0.993	1.16	2.132	−0.002	0.999	0.79
C17 : 0	27.590	−0.082	0.995	0.81	14.665	2.697	−0.028	1.000	0.04	0.241	−0.003	0.997	7.00
C18 : 0	36.451	−0.539	0.998	0.61	20.143	2.342	−0.053	1.000	0.03	0.261	−0.004	0.991	6.46
C18 : 1	**22.258**	**1.540**	**0.991**	**1.00**	**0.526**	**1.600**	**0.023**	**1.000**	**1.00**	**1.687**	**0.001**	**0.999**	**1.00**
C18 : 2	39.268	1.563	0.992	0.57	1.084	1.119	−0.075	0.992	0.49	10.512	0.058	0.999	0.16
αC18 : 3	55.618	2.733	0.993	0.40	1.853	0.800	0.008	0.997	0.29	22.788	0.482	0.995	0.07
γC18 : 3	76.808	2.212	0.993	0.29	1.670	1.134	−0.052	0.994	0.32	35.709	0.416	0.996	0.05
C19 : 0	45.635	−0.883	0.970	0.49	23.896	2.602	−0.085	0.999	0.02	0.287	−0.005	1.000	5.88
C20 : 0	56.277	−1.512	0.974	0.40	37.033	1.600	−0.086	0.999	0.01	0.303	−0.002	1.000	5.57
C20 : 1	62.552	0.012	1.000	0.36	4.637	2.038	0.004	1.000	0.12	1.960	−0.008	0.998	0.86
C21 : 0	56.605	−1.986	0.958	0.39	25.331	3.418	−0.149	0.997	0.02	0.322	−0.003	1.000	5.24
C22 : 0	48.118	−1.695	0.958	0.46	7.698	1.871	−0.079	0.995	0.07	0.278	−0.002	1.000	6.07
C22 : 1	52.990	0.059	0.999	0.42	7.018	1.284	0.006	1.000	0.08	1.394	0.003	0.996	1.21
OPP	19.697	0.232	0.997	1.13	–	–	–	–	–	0.912	−0.002	0.997	1.85
POP	20.230	0.263	0.994	1.10	–	–	–	–	–	1.163	−0.010	1.000	1.45
OPO	21.198	0.173	0.996	1.05	–	–	–	–	–	1.268	−0.009	0.995	1.33
OOP	21.822	0.274	0.996	1.02	–	–	–	–	–	1.638	−0.006	1.000	1.03
OO	9.676	−0.035	1.000	2.30	0.483	0.972	-0.039	0.999	1.10	2.270	0.006	1.000	0.74
O	1.655	−0.354	1.000	13.45	0.225	0.180	-0.023	0.996	2.39	3.061	0.035	1.000	0.55

a) RFs are expressed relative to OOO, which is set to 1.00 for all detection techniques. For APCI-MS and UV detection, *a* and *b* values are coefficients of the linear calibration dependence $y = a \cdot x + b$ and RFs are calculated as $RF(TG) = a_{OOO}/a_{TG}$, because *b* values can be neglected. For ELSD, *a*, *b*, and *c* values are coefficients of the quadratic calibration dependences $y = a \cdot x^2 + b \cdot x + c$ and RFs are calculated as the arithmetic mean of y_{OOO}/y_{TG} ratios calculated at 50, 100, 200, and 500 mg/L for OOO and individual TGs. r^2 is the value of coefficient of determination, *y* corresponds to the peak areas and *x* is the concentration in g/L.

back for reliable quantitation of lipid samples. Moreover, the differences among RFs are as high as two orders of magnitude. The non-linear response of ELSD and large differences among individual TGs do not allow us to find a suitable model for the calculation of RFs of mixed-acid TGs. It has been found during our measurements that various parameters (nebulizing gas flow rate and temperature, detector type, mobile phase composition) may have a notable effect on RFs, which causes low method robustness.

The responses of saturated TGs with UV detection at low wavelengths are very low. Unfortunately, LODs of the order of 10^2 mg/L are not sufficient in practice, which basically disqualifies the applicability of the UV detector for the quantitation of natural samples containing saturated TGs. Moreover, considerable differences are observed among RFs of saturated (5.24–8.11), monounsaturated (0.79–1.21), and polyunsaturated (0.05–0.16) TGs. When only one double bond is introduced into a saturated TG molecule, the response is notably increased, for example RF(PPP) = 7.00, RF(OPP) = 1.85, and RF(POP) = 1.45. If the RFs of mixed-acid TGs are calculated as an arithmetic mean of individual FA contributions, then the calculated value is completely misleading, for example RF(OPP or POP) = (2 × RF(PPP) + RF(OOO))/3 = 5.00.

Table 4. Calculation and statistical evaluation of response factors for triacylglycerols and diacylglycerol diolein (OO) and monoacylglycerol monoolein (O) using ELSD.

TG (CN : DB)	Response factors						
	Concentration level [mg/L]				Arithmetic mean	Standard deviation	Relative standard deviation [%]
	50	100	200	500			
C7 : 0	0.330	0.320	0.316	0.313	0.32	0.006	2.0
C8 : 0	0.450	0.438	0.432	0.428	0.44	0.008	1.9
C9 : 0	0.492	0.481	0.476	0.473	0.48	0.007	1.5
C10 : 0	0.559	0.548	0.542	0.539	0.55	0.008	1.4
C11 : 0	0.367	0.360	0.356	0.354	0.36	0.005	1.4
C12 : 0	0.275	0.270	0.267	0.265	0.27	0.004	1.4
C13 : 0	0.155	0.151	0.149	0.148	0.15	0.003	1.8
C14 : 0	0.071	0.069	0.068	0.068	0.07	0.001	1.7
C15 : 0	0.069	0.067	0.066	0.065	0.07	0.001	2.1
C16 : 0	0.044	0.042	0.042	0.041	0.04	0.001	2.7
C16 : 1	1.146	1.161	1.168	1.173	1.16	0.010	0.9
C17 : 0	0.038	0.037	0.036	0.036	0.04	0.0008	2.1
C18 : 0	0.028	0.027	0.026	0.026	0.03	0.0008	2.8
C18 : 1	**1.000**	**1.000**	**1.000**	**1.000**	**1.00**	–	–
C18 : 2	0.504	0.495	0.490	0.487	0.49	0.006	1.3
α-C18 : 3	0.299	0.291	0.288	0.285	0.29	0.005	1.8
γ-C18 : 3	0.330	0.322	0.319	0.316	0.32	0.005	1.6
C19 : 0	0.023	0.023	0.022	0.022	0.02	0.0005	2.5
C20 : 0	0.015	0.015	0.014	0.014	0.015	0.0005	3.2
C21 : 0	0.022	0.021	0.021	0.021	0.02	0.0004	2.2
C20 : 1	0.119	0.116	0.115	0.114	0.12	0.002	1.8
C22 : 0	0.072	0.070	0.069	0.069	0.07	0.001	1.7
C22 : 1	0.079	0.077	0.076	0.075	0.08	0.001	1.8
OO	1.111	1.100	1.095	1.091	1.10	0.007	0.7
O	2.441	2.390	2.364	2.348	2.39	0.035	1.5

Therefore, simple averaging is not suitable for that purpose and some weighting factors have to be introduced to balance the different contributions from saturated and unsaturated acyl chains. Such a model would be very laborious and due to the insufficient sensitivity for saturated TGs, this approach was abandoned as meaningless and our attention was focused on APCI-MS.

The responses with APCI-MS are linear, the sensitivity is sufficient for all TGs regardless of the degree of unsaturation and the differences among individual TGs usually found in natural plant oils are much lower compared to the other two detection techniques (Table 3). When only common acyl chain lengths (C14–C22) are considered, then all RFs are within the approximate range of 0.4–2.8. For shorter FAs, the increase of RFs is observed, but these FAs are not found in common plant oils (or at maximum at trace levels) except in date seed oil. **Figure 1** illustrates a dependence of RFs of saturated TGs on carbon number with the inset showing details of unsaturated TGs. In the case of APCI-MS, the arithmetic mean is applicable for the calculation of RFs of mixed-acid TGs (for FAs C14

Table 5. Concentrations [mg/g] of 133 triacylglycerols (TG) identified in 9 plant oil samples using the APCI-MS detection and response factor approach.

TG	Walnut	Hazelnut	Cashew	Almond	Poppy seed	Yellow melon	Mango stone	Fig seed	Date seed
LnLnLn	6							57	
LnLLn	35							77	
LaLLa									36
LaOC									17
MOCy									48
MLaLa									9
LnLnMo								<0.1	
LnLnC15:0								<0.1	
LLLn	97				17		<0.1	60	
LLLa									15
LnOLn	13							82	
OOCy									39
MLLa									38
LaOLa									121
LnLnP	11							62	
POCy									28
PLaLa									5
MMLa									4
LnLMo					1			0.1	
LLL	135	15	17	24	203	115	1	29	1
LLPo		0.3	1						
OLLn	68	2			9	0.3	0.4	101	
LLM									6
OLLa									37
OOC									16
LnLP	53				8	2	0.3	72	
MLM									7
PLLa									25
SLnLn	2							21	
MOLa									92
SOCy									14
PMLa									5
LLMo	1			0.3	1				
LLC15:0						1			
LnLMa	<0.1							<0.1	
C20:2LL	<0.1				0.2			<0.1	

Table 5. Continued ...

OLL	111	58	55	103	137	133	7	55	3
OLPo		0.4	0.4						
OLnO	18	2	1				1	43	
LLP	85	15	31	30	153	116	2	38	0.3
OLM									12
SLLn	12							20	
LnOP	14		1				2	35	
OOLa									110
ALnLn								2	
PLM									4
SLLa									15
MOM									39
POLa									47
PLnP	1				< 0.1		< 0.1	1	
OLMo		< 0.1	< 0.1	1	< 0.1				
LLMa	0.4		< 0.1	< 0.1	1	2		< 0.1	
MoLP				< 0.1					
OLnMa								< 0.1	
GLL	2		< 0.1		1	1		0.1	
OLO	52	133	93	149	59	64	17	32	7
OOPo		2	1						
SLL	16		26		26	39	3	8	
OLP	33	53	39	88	58	56	8	16	2
GOLa									18
ALLn								4	
OOM									35
POPo		0.2	0.1						
SOLn	3						2	5	
BLnLn								3	
PLP	4	2	13	4	7	8	1	0.3	0.2
SLM									3
PPoP			< 0.1						
POM									25
SOLa									22
SLnP	< 0.1						1	0.1	
OOMo		2		1					
OLMa	< 0.1	< 0.1	0.3	0.4	< 0.1	< 0.1		< 0.1	
C21 : 0LLn								< 0.1	

Table 5. Continued ...

MoOP		0.3	<0.1	1					
C23:0LnLn								<0.1	
GLO	0.1	<0.1	0.1		<0.1	0.3	<0.1	<0.1	<0.1
OOO	18	243	113	213	13	19	29	12	13
ALL	4				2	4		0.1	
GOM									2
BLLn								1	
SLO	11	9	46	10	11	22	16	3	4
OOP	9	141	85	86	10	13	28	9	17
SLP	2	3	12	<0.1	2	6	9	<0.1	<0.1
BLLa									2
SLnS							2	<0.1	
AOLa									6
POP	1	13	31	3	2	1	13	1	6
SOM									10
PPP						<0.1	<0.1		
C23:0LLn								<0.1	
OOMa		2	1	0.3		<0.1	0.4		<0.1
MaOP			<0.1						
GOO	<0.1	3	2	0.3	<0.1	<0.1	0.4	<0.1	1
GLS	<0.1								
BLL			0.2		<0.1	<0.1		<0.1	
LgLLn								<0.1	
ALO	<0.1	1		<0.1	<0.1	1	0.1	<0.1	0.3
GOP							1		1
SOO	3	41	81	19	2	6	81	2	7
ALP	<0.1				<0.1	<0.1		<0.1	<0.1
SLS	<0.1		5		<0.1	2	12	<0.1	<0.1
SOP	<0.1	9	38	1	1	<0.1	74	<0.1	2
AOM									3
BOLa									8
SPP			<0.1			<0.1	<0.1		
C23:0OLa									<0.1
SOMa							1		<0.1
LgLL					<0.1	<0.1			
BLO			1			<0.1	<0.1		0.2
GOS							1		
AOO	<0.1	2	8	<0.1		<0.1	8	<0.1	2

Table 5. Continued ...

LgLM									<0.1
BLP						<0.1			<0.1
ALS			0.3			<0.1	0.1		<0.1
LgOLa									1
AOP		<0.1	1			<0.1	1		1
SOS		1	19			<0.1	143		0.2
SSP							1		
C19:0OS							<0.1		
LgLO							0.1		
BOO							2		
LgLP							<0.1		
BLS							<0.1		
AOS							18		
SSS							2		
C23:0OO							<0.1		
LgOO							2		
LgLS							<0.1		
LgOP							2		
BOS							4		
C25:0OO							<0.1		
C23:0OS							<0.1		

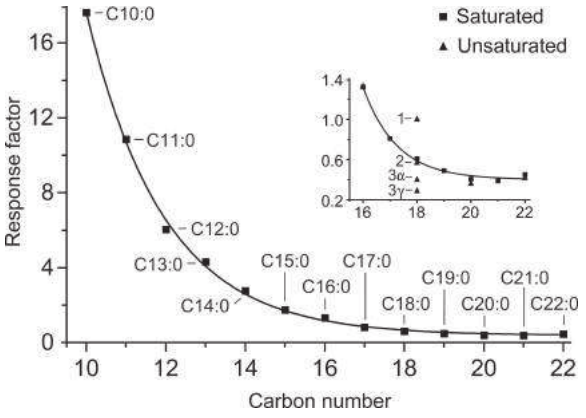

Figure 1. Dependence of response factors of saturated single-acid TGs measured by APCI-MS on the carbon number in the acyl chain (fitted with the equation $y = 2925 \times \exp(-0.5134x) + 0.3824$, $R^2 = 0.999$). Unsaturated single-acid TGs are shown in inset detail.

and higher), for example the calculated value for RF(OOP or OPO) = 1.11 *vs.* experimental values RF(OOP) = 1.02 and RF(OPO) = 1.05. The approach is validated by comparison with the standard GC/FID method (discussed in Section 3.3). RFs of 133 TGs occurring in studied plant oils are calculated this way (listed in Table 2) and the individual peak areas are multiplied by the corresponding RF yielding the real concentration of TG in a given plant oil. Each oil is analysed in triplicate, then the concentrations are averaged, and final values for 9 studied oils are shown in **Table 5**.

The calculation of RFs of mixed-acid TGs neglects the differences – if any – between the regioisomers. Based on our measurements of OPO/OOP and OPP/POP regioisomers, these differences are low with UV detection and nearly negligible with APCI-MS (Table 3). Anyway, distinguishing RFs for both regioisomers would not be beneficial in practice, because the natural lipid sources typically contain both regioisomers in a certain ratio (not identical for all plant oils and animal fats) and regioisomers coelute in all NARP HPLC systems.

3.3 Comparison of HPLC/APCI-MS and GC/FID results of plant oils

APCI-MS is used for the determination of TG relative concentrations in 9 plant oils (Table 5): walnut oil (**Fig. 2.a**),

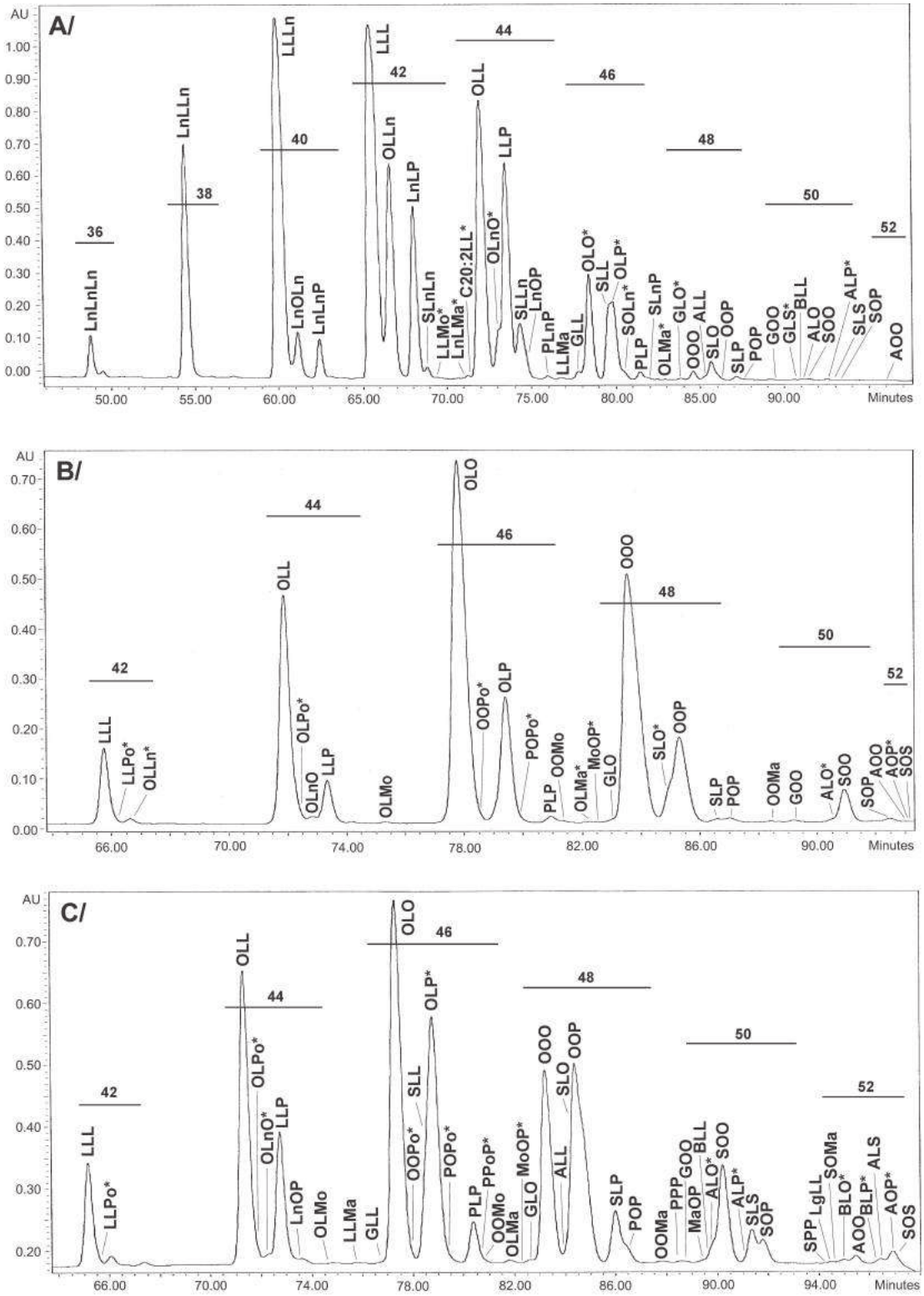

Figure 2. Chromatographic separation of plant oils: A) walnut; B) hazelnut; C) cashew nut. Experimental conditions: 30 + 15 cm Nova-Pak columns connected in series, UV detection at 205 nm, flow rate 1 mL/min, column temperature 25°C, injection volume 10 μL, mobile phase gradient 0 min–100% acetonitrile, 106 min–31% acetonitrile–69% 2-propanol, 109 min–100% acetonitrile. Numbers correspond to ECNs.

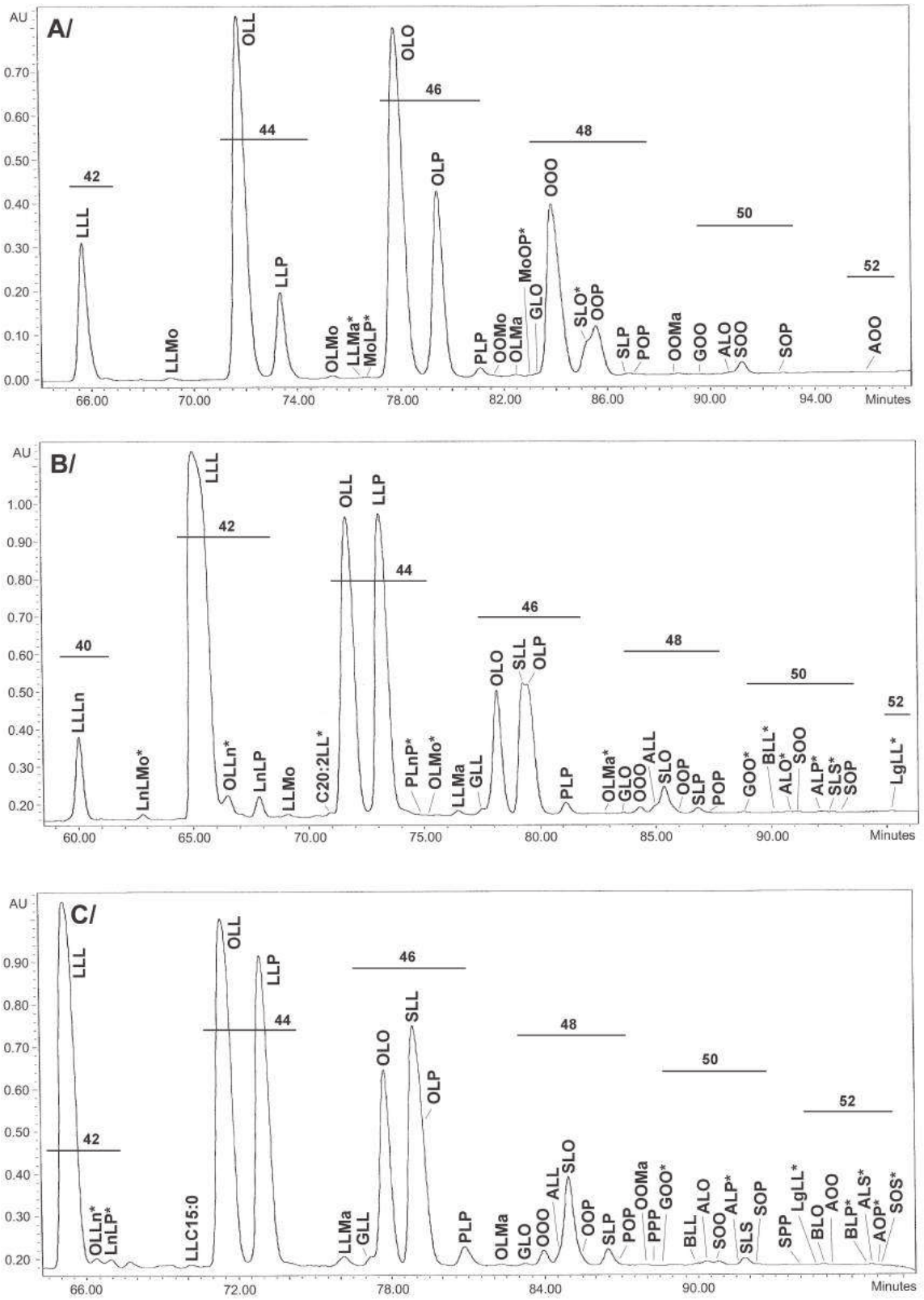

Figure 3. Chromatographic separation of plant oils: A) almond; B) poppy seed; C) yellow melon. All conditions are identical to those for **Figure 2**.

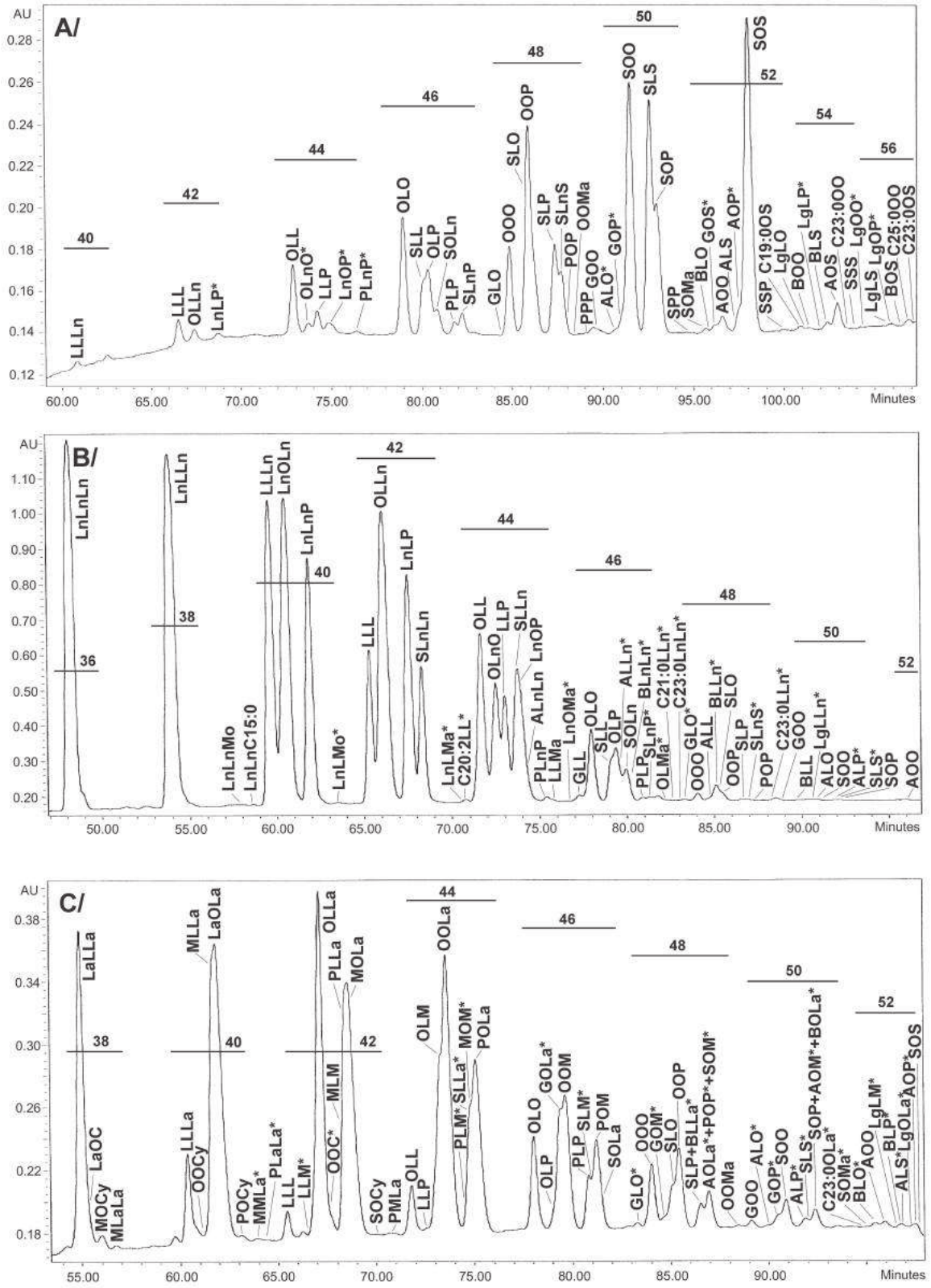

Figure 4. Chromatographic separation of plant oils: A) mango stone; B) fig seed; C) date seed. All conditions are identical to those for **Figure 2**.

Table 6. Comparison of relative concentrations [weight%] of individual FAMEs calculated from GC/FID[a] and from HPLC/APCI-MS of TGs[b].

Fatty acid	Walnut		Hazelnut		Cashew		Almond		Poppy seed		Yellow melon		Fig seed	
	GC	LC	GC	LC	GC	LC	GC	LC	GC	LC	GC	LC	GC	LC
C14:0	< 0.05	–	< 0.05	–	< 0.05	–	0.05	–	< 0.05	–	0.06	–	< 0.05	–
C15:0	< 0.05	–	< 0.05	–	–	–	< 0.05	–	< 0.05	–	< 0.05	0.05	< 0.05	–
C16:0	6.81	8.42	7.05	10.50	11.97	12.94	6.70	9.44	8.62	10.88	8.76	10.88	6.89	8.75
C16:1	0.08	–	0.26	0.08	0.36	0.09	0.56	–	0.12	–	0.08	–	0.07	–
C17:0	< 0.05	< 0.05	0.05	0.09	0.11	0.05	0.05	< 0.05	0.06	0.05	0.08	0.05	0.05	< 0.05
C17:1	< 0.05	< 0.05	< 0.05	0.09	< 0.05	< 0.05	< 0.05	0.13	< 0.05	0.09	–	–	< 0.05	< 0.05
C18:0	1.74	2.01	2.45	2.87	11.69	11.73	1.23	1.37	1.86	1.95	5.22	1.95	2.61	2.34
C18:1	17.28	19.33	77.40	63.39	57.02	51.92	67.35	62.09	14.86	18.53	22.88	18.53	19.23	20.00
C18:2	60.58	53.40	12.17	17.53	17.06	22.58	23.56	26.97	73.25	66.73	61.55	66.73	29.70	28.97
C18:3[c]	12.65	16.53	0.07	0.18	0.14	0.09	< 0.05	–	0.66	1.61	0.20	1.61	40.68	39.52
C20:0	0.07	0.17	0.11	0.14	0.87	0.44	0.06	< 0.05	0.10	0.10	0.22	0.10	0.18	0.25
C20:1	0.18	0.09	0.12	0.14	0.16	0.10	0.07	< 0.05	0.07	0.05	0.13	0.05	0.28	–
C20:2	< 0.05	< 0.05	< 0.05	–	–	–	–	–	< 0.05	< 0.05	< 0.05	–	< 0.05	–
C22:0	< 0.05	< 0.05	< 0.05	–	0.18	0.05	< 0.05	–	< 0.05	< 0.05	0.05	< 0.05	0.07	0.18
C24:0	< 0.05	–	< 0.05	–	0.18	< 0.05	< 0.05	–	< 0.05	< 0.05	< 0.05	< 0.05	< 0.05	< 0.05
Others	0.42	–	0.21	–	0.25	–	0.30	–	0.28	–	0.69	–	0.14	–
Av. rel. error [%][d]	–	16.3	–	32.0	–	12.4	–	18.6	–	16.1	–	29.5	–	7.8

a) Calculated according to Ref. [39].
b) Calculated as the sum of relative contributions of individual FAs in identified TGs.
c) C18:3 is the sum of α- and γ-linolenic acid, when the relative concentration of γ-linolenic acid is always lower than 0.1%.
d) Calculated as average relative difference between LC and GC determinations for fatty acids $\geqslant$ 1%.

hazelnut oil **(Fig. 2.b)**, cashew nut oil (**Fig. 2.c**), almond oil (**Fig. 3.a**), poppy seed oil (**Fig. 3.b**), yellow melon seed oil (**Fig. 3.c**), mango stone oil (**Fig. 4.a**), fig seed oil (**Fig. 4.b**), and date seed oil (**Fig. 4.c**). TGs are identified on the basis of their molecular weights determined from the presence of protonated molecules $[M+H]^+$ in APCI mass spectra, characteristic fragment ions $[M+H-R_iCOOH]^+$ providing an easy identification of individual acids and the position of the most abundant acid in the middle *sn*-2 position, too. Finally, the correctness of the identification is verified by the retention order and relative retention (see Table 2). For the unambiguous identification of trace peaks, the reconstructed ion current records of selected *m/z* values are used to clearly confirm the presence or absence of selected ions in particular peaks, which makes it possible to solve coelutions and even to identify peaks at trace levels.

The *sn*-2 position corresponds to the prevailing acid, but mostly both regioisomers are present. The regioisomeric purity could be determined on the basis of calibration curves of both authentic standards. Concerning the discrimination of OLL vs. LOL (or other TGs differing only by two mass units), the contribution of two ^{13}C atoms to the A+2 ions has to be subtracted first, for example the formula of $[OO]^+$ is $C_{39}H_{71}O_4$ and the theoretically calculated abundance of isotopic peak A+2 is 10.5%. When in previously published data [20] on OLL ($[OL]^+ : [LL]^+ = 100:70$) and LOL ($[OL]^+ : [LL]^+ = 100:23$) regioisomeric pairs are also taken into account, then the distribution of oleoyl and linoleoyl in the *sn*-2 position is close to 1:1 (*e.g.*, almond oil – $[OL]^+ : [OO]^+ = 100:56$, cashew oil – 100:55, and hazelnut oil – 100:53).

To verify the precision and accuracy of the HPLC/APCI-MS method, 7 plant oils were transesterified using a standard procedure with sodium methoxide and analyzed by GC/FID [39]. First, the RFs of a wide range of FAMEs were measured by GC/FID (see Experimental part), then the relative concentrations of individual FAs were calculated. For all identified TGs in plant oils, the relative weight contributions of individual FAs are summarized and compared with GC/FID results (**Table 6**). This comparison is somewhat affected by the fact that trace FAs are not identified in HPLC/APCI-MS, because one FA may be distributed among many different combination in TGs, which results in TG concentrations below the detection limit. Further, the coelution of trace TGs with more abundant

Table 7. Comparison of average carbon numbers (aCN), equivalent carbon numbers (aECN) and double bond (aDB) numbers, total TG weight%, and the number of identified TGs in 9 plant oils calculated from GC/FID analyses (GC) and HPLC/APCI-MS analyses (LC).

Plant oil source	Latin name	Total TGs [%, *w/w*]	No. of TGs	Average parameter					
				aCN		aECN		aDB	
				GC	LC	GC	LC	GC	LC
Walnut	*Juglans regia L.*	82	43	17.77	17.82	14.26	14.32	1.77	1.75
Hazelnut	*Corylus avellana L.*	75	30	17.82	17.78	15.78	15.71	1.02	1.04
Cashew	*Anacardium occidentale*	73	46	17.76	17.74	15.92	15.80	0.92	0.97
Almond	*Prunus dulcis*	72	25	17.81	17.80	15.50	15.49	1.15	1.16
Poppy seed	*Papaver somniferum L.*	73	33	17.78	17.77	14.51	14.66	1.64	1.56
Yellow melon seed	*Cucumis melo L.*	61	37	17.70	17.77	14.77	14.89	1.47	1.44
Mango stone	*Mangifera indica L.*	49	53	–	17.86	–	16.69	–	0.58
Fig seed	*Ficus carica L.*	85	54	17.85	17.82	13.82	13.91	2.01	1.96
Date seed	*Phoenix dactylifera*	98	66	–	15.26	–	14.18	–	0.53
Average relative error [%] [a]				–	0.2	–	0.6	–	2.6

[a] Calculated as average relative difference between LC and GC determinations.

TGs with the same or similar retention times may complicate the identification of trace FAs. GC determination is free of such problems, because FAMEs elute well separated in a single peak unlike the distribution of FAs among many TGs with different retention times in HPLC. If we keep in mind all sources of potential errors, then the correlation is acceptable. The average relative errors are similar to those in the previous publication on TG quantitation [17]. To our best knowledge, Ref. [17] is the only work published in the literature on the systematic use of RFs for TG determination in complex natural mixtures.

Table 7 summarizes so-called average parameters calculated for plant oils on the basis of GC/FID and HPLC/APCI-MS data, *i.e.*, average carbon number (aCN), average double bond (aDB) number, and average equivalent carbon number (aECN). There is excellent agreement (average relative errors are 0.2, 0.6, and 2.6%) between both methods. Except for date seed oil (15.26), the aCN is very close to the typical 18 carbon atoms in the FA moiety and nearly identical for all samples (from 17.70 to 17.85), which is caused by the prevailing presence of oleic, linoleic, and linolenic fatty acids. Higher differences can be found in the aDB number (from 0.53 to 2.01) and aECN (from 13.82 to 16.69). These average values are useful for the characterization of the type of natural oil, as indicated by our preliminary results on a wider range of various plant oils (this work is in progress). The total TG content in date seed oil (98%) seems to be slightly overestimated, which may be due to the presence of FAs with shorter acyl chains with higher RFs probably associated with increased systematic error in the calculation of RFs of corresponding mixed-acid TGs.

3.4 Analysis of complex mixtures containing tri-, di-, and monoacylglycerols

In this work, 23 single-acid TGs were measured and their RFs determined. RFs of mixed-acid TGs were calculated for APCI-MS. Finally, the RFs of diolein as a representative of diacylglycerols and monoolein as a representative of monoacylglycerols were determined using pure standards (Table 3). The RF ratios of OOO/OO and OOO/O are used for the calculation of RFs of DGs or MGs and then applied for the quantitation of these acylglycerol classes. In this approximation, the differences between positional isomers 1,2-DGs *vs.* 1,3-DGs and 1-MGs *vs.* 2-MGs are neglected. If a more reliable quantitation is needed, then the whole procedure as for TGs should be repeated, including the discrimination between regioisomers.

The chromatographic system optimized for the analysis of TGs used in this work can also be applied for the analysis of more polar acylglycerols, such as DGs and MGs. **Fig. 5** shows the separation of the reaction mixture of biodiesel production from rapeseed oil by transesterification with methanol at half-reaction time. The groups of TGs and DGs are fully separated including the separation of 1,3-DG and 1,2-DG positional isomers, where 1,3-DG is eluted first. There is some peak overlap in the region of MG and methyl esters of FAs. If the analysis of these more polar acylglycerols is the main goal, then initial gradient delay or an initial step with aqueous acetonitrile could improve the separation, similarly to our previous work with aqueous-organic gradient mobile phases [9]. **Table 8** lists concentrations of TGs, DGs, and MGs deter-

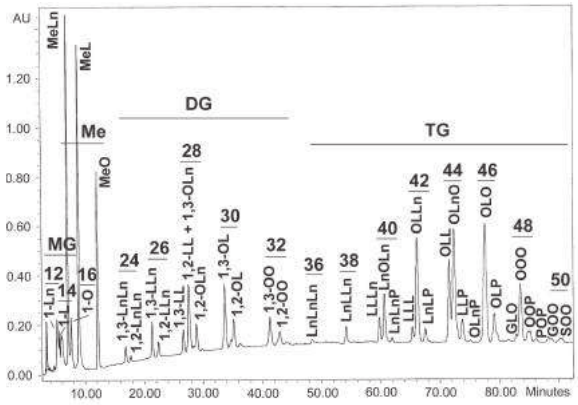

Figure 5. Chromatographic separation of the reaction mixture of rapeseed oil transesterification with methanol containing the groups of tri- (TG), di- (DG), and monoacylglycerols (MG) and methyl esters (Me) of fatty acids. All conditions are identical as for Fig. 2.

mined with APCI-MS in the transesterification mixture of rapeseed oil.

4 Conclusion

A NARP HPLC separation method with acetonitrile–2-propanol mobile phase gradient has been developed and used for unambiguous identification of 133 TGs in 9 plant oils. A knowledge of plant oil composition, including the identification of *sn*-2 acids and reliable quantitation, is very important from a nutritional point of view. Based on the comparison of three detection techniques (APCI-MS, ELSD, and UV at 205 nm), APCI-MS detection is recommended for the analysis and quantitation of TGs for the following reasons: a) unambiguous identification even for strongly coeluting and trace peaks; b) determination of acid prevailing in *sn*-2 position or possible quantitation of regioisomers based on the calibration curves; and c) linear calibration curves (unlike ELSD) with relatively low differences among common C14–C22 fatty acids (unlike UV and ELSD detection). UV detection cannot be recommended because of large differences between saturated and unsaturated TGs and insufficient sensitivity for saturated TGs. Concerning the differences between saturated and polyunsaturated TGs, polyunsaturated TGs have significantly higher relative responses than saturated ones with UV detection (absorption of UV light by unsaturated chains), slightly higher with APCI-MS (easier ionization of π-electrons), but lower with ELSD (probably because less light is scattered by folded conformations of unsaturated chains). The total amount of TGs in the studied plant oils lies in the range of 49% (mango stone oil)–98% (date seed oil). The remaining part (*i.e.*, 2–51%) corresponds to more polar lipids and other compound classes present in these oils. The suggested HPLC/APCI-MS approach

Table 8. Concentrations [mg/g] of individual triacylglycerols (TGs), diacylglycerols (DGs) and monoacylglycerols (MGs) determined with APCI-MS detection in the reaction mixture of transesterification of rapeseed oil with methanol.

Compound	*c* [mg/g]	Compound	*c* [mg/g]
TGs		**DGs**	
LnLnLn	0.3	1,3-LnLn	2
LnLLn	3	1,2-LnLn	0.1
LLLn	8	1,3-LLn	5
LnOLn	19	1,2-LLn	2
LnLnP	4	1,3-LL	4
LLL	6	1,2-LL	5
OLLn	33	1,3-OLn	12
LnLP	6	1,2-OLn	5
OLL	26	1,3-OL	9
OLnO	52	1,2-OL	2
LLP	8	1,3-OO	38
OLnP	1	1,2-OO	14
OLO	61	**MGs**	
OLP	17	1-Ln	4
GLO	2	1-L	5
OOO	85	1-O	31
OOP	22		
GOO	5	POP	1
SOO	8		

with RFs is applicable to the characterization of plant oils, as confirmed by acceptable correlation with validated GC/FID method for FAMEs. GC/FID and HPLC/APCI-MS results are used for the calculation of averaged parameters (aCN, aECN, and aDB), which can characterize the type of plant oil. GC/FID of transesterified FAMEs is an established method for the determination of FA composition; however, unlike the HPLC/APCI-MS method presented in this work, it does not provide any information on TG composition.

Acknowledgments

This work was supported by the grant project No. MSM0021627502 sponsored by the Ministry of Education, Youth and Sports of the Czech Republic and projects Nos. 203/04/0917 and 203/05/2106 sponsored by the Grant Agency of the Czech Republic.

References

[1] D.M. Small, *Ann. Rev. Nutr.* **1991**, *11*, 413–434.

[2] W.M. Willis, A.G. Marangoni, *Biotechnol. Genetic Eng. Rev.* **1999**, *16*, 141–175.

[3] M. Holčapek, P. Jandera, P. Zderadička, L. Hrubá, *J. Chromatogr. A* **2003**, *1010*, 195–215.

[4] H.R. Mottram, S.E. Woodbury, R.P. Evershed, *Rapid Commun. Mass Spectrom.* **1997**, *11*, 1240–1252.

[5] J.S. Perona, V. Ruiz-Gutierrez, *J. Chromatogr. B* **2003**, *785*, 89–99.

[6] P. Laakso, *J. Amer. Oil Chem. Soc.* **1997**, *74*, 1291–1300.

[7] J.D.J. van den Berg, N.D. Vermist, L. Carlyle, M. Holčapek, J.J. Boon, *J. Sep. Sci.* **2004**, *27*, 181–199.

[8] M. Holčapek, P. Jandera, J. Fischer, *Crit. Rev. Anal. Chem.* **2001**, *31*, 53–56.

[9] M. Holčapek, P. Jandera, J. Fischer, B. Prokeš, *J. Chromatogr. A* **1999**, *858*, 13–31.

[10] A. Jakab, K. Héberger, E. Forgács, *J. Chromatogr. A* **2002**, *976*, 255–263.

[11] A. Jakab, I. Jablonkai, E. Forgács, *Rapid Commun. Mass. Spectrom.* **2003**, *17*, 2295–2302.

[12] P. Dugo, O. Favoino, P.Q. Tranchida, G. Dugo, L. Mondello, *J. Chromatogr. A* **2004**, *1041*, 135–142.

[13] J. Parcerisa, I. Casals, J. Boatella, R. Codony, M. Rafecas, *J. Chromatogr. A* **2000**, *881*, 149–158.

[14] L. Fauconnot, J. Hau, J.M. Aeschlimann, L.B. Fay, F. Dionisi, *Rapid Commun. Mass. Spectrom.* **2004**, *18*, 218–224.

[15] S. Héron, A. Tchapla, *OCL-Oleagineux Corps Gras Lipides* **1994**, *1*, 219–228.

[16] S. Héron, A. Tchapla, *Fingerprints of Triacyglycerols from Oils and Fats by HPLC Isocratic Elution and Evaporative Light Scattering Detection*, ELSD Sedex 45, Sedere, Alfortville, France, 1994.

[17] W.C. Byrdwell, E.A. Emken, W.E. Neff, R.O. Adlof, *Lipids* **1996**, *31*, 919–935.

[18] W.E. Neff, W.C. Byrdwell, K.R. Steidley, G.R. List, G. Snowder, *J. Liq. Chromatogr. Rel. Technol.* **2002**, *25*, 985–998.

[19] W.E. Neff, W.C. Byrdwell, G.R. List, *J. Liq. Chrom. Rel. Technol.* **2001**, *24*, 837–854.

[20] W.E. Neff, W.C. Byrdwell, *J. Chromatogr. A* **1998**, *818*, 169–186.

[21] W.C. Byrdwell, W.E. Neff, *Rapid Commun. Mass. Spectrom.* **2002**, *16*, 300–319.

[22] W.C. Byrdwell, *Lipids* **2001**, *36*, 327–346.

[23] H. Kallio, K. Yli-Jokipii, J.P. Kurvinen, O. Sjövall, R. Tahvonen, *J. Agric. Food Chem.* **2001**, *49*, 3363–3369.

[24] S. Morera Pons, A. Castellote Bargalló, C. Campoy Folgoso, M.C. López Sabater, *Eur. J. Clin. Nutr.* **2000**, *54*, 878–882.

[25] P. Sandra, A. Dermaux, V. Ferraz, M.M. Dittmann, G. Rozing, *J. Microcolumn Sep.* **1997**, *9*, 409–419.

[26] W.W. Christie, *J. Chromatogr.* **1988**, *454*, 273–284.

[27] P.J.W. Schuyl, T. de Joode, M.A. Vasconcellos, G.S.M.J.E. Duchateau, *J. Chromatogr. A* **1998**, *810*, 53–61.

[28] P. Laakso, P. Voutilainen, *Lipids* **1996**, *31*, 1311–1322.

[29] R.O. Adlof, A. Menzel, V. Dorovska-Taran, *J. Chromatogr. A* **2002**, *953*, 293–297.

[30] P. Sandra, A. Medvedovici, Y. Zhao, F. David, *J. Chromatogr. A* **2002**, *974*, 231–241.

[31] L.G. Blomberg, M. Demirbuker, P.E. Andersson, *J. Am. Oil Chem. Soc.* **1993**, *70*, 939–946.

[32] E. Lesellier, J. Bleton, A. Tchapla, *Anal. Chem.* **2000**, *72*, 2573–2580.

[33] S. Héron, M. Dreux, A. Tchapla, *J. Chromatogr. A* **2004**, *1035*, 221–225.

[34] T. Andersen, A. Holm, I.L. Skuland, R. Trones, T. Greibrokk, *J. Sep. Sci.* **2003**, *26*, 1133–1140.

[35] K. Aitzetmuller, M. Gronheim, *J. High Res. Chromatogr.* **1992**, *15*, 219–226.

[36] G.N. Jham, B. Nikolova-Damyavova, M. Viera, R. Natalino, A.C. Rodriques, *Phytochem. Analysis* **2003**, *14*, 310–314.

[37] A.A. Carelli, A. Cert, *J. Chromatogr.* **1993**, *630*, 213–222.

[38] S. Hamilton, R.J. Hamilton, P.A. Sewell: Extraction of lipids and derivative formation. In: *Lipid Analysis: A Practical Approach*. R.J. Hamilton, S. Hamilton, Eds. Oxford, NY, IRL Press at Oxford University Press, 1992, pp. 51–52.

[39] Animal and plant fats and oils. Analysis of fatty acid methyl esters by gas chromatography, ČSN ISO 5508, Czech Standards Institute, 1994, Prague.

Available online at www.sciencedirect.com
ScienceDirect
Journal of Chromatography A, 1176 (2007) 135–142
JOURNAL OF CHROMATOGRAPHY A
www.elsevier.com/locate/chroma

Quantitation of triacylglycerols from plant oils using charged aerosol detection with gradient compensation

Miroslav Lísa [a], Frédéric Lynen [b], Michal Holčapek [a], Pat Sandra [b,*]

[a] *Department of Analytical Chemistry, Faculty of Chemical Technology, University of Pardubice, Nám. Čs. legií 565, 53210 Pardubice, Czech Republic*
[b] *Department of Organic Chemistry, Faculty of Science, Ghent University, Krijgslaan 281 S4, B-9000 Gent, Belgium*

Received 17 September 2007; received in revised form 17 October 2007; accepted 24 October 2007
Available online 1 November 2007

Abstract

Quantitative analysis of triacylglycerols (TGs) in plant oils and animal fats by normalization of peak areas can lead to erroneous results due to the large response differences with common HPLC detectors between the various TGs. The charged aerosol detector (CAD), that generates an almost universal response for non-volatile compounds, was combined with non-aqueous reversed-phase HPLC (NARP-HPLC) to develop a simple quantitative method, without need for RFs, for the analysis of complex natural TG mixtures from plant oils. Two 25 cm Hypersil ODS columns, connected in series, and a mobile phase gradient composed of acetonitrile, 2-propanol and hexane were used. Mobile phase compensation was applied, by mixing of the column effluent with the inversed gradient delivered by a second HPLC pump, for the suppression of the response dependency of the analytes on the mobile phase composition. Calibration curves of 16 saturated (from C7:0 to C22:0) and 3 unsaturated (C18:1, C18:2, C18:3) single-acid TG standards were measured and their RFs were compared with a previously described method using atmospheric pressure chemical ionization-mass spectrometry (APCI-MS). The variation in response of the most common TGs (containing fatty acid chains from 12 to 19 carbons) could be reduced to less than 5% making the combination of NARP-HPLC with CAD and mobile phase compensation an adequate tool for fast quantitative analysis of TGs in common plant oils.

Keywords: HPLC; Charged aerosol detection; Triacylglycerols; Triglycerides; Plant oils

1. Introduction

Natural plant oils are complex mixtures of various non-polar compounds of which the triacylglycerols (TGs) make up to 90% of the content. TGs are triesters of fatty acids (FAs) and glycerol differing in length of the FA chains, in the number, position and *cis*/*trans* configuration of the double bonds (DBs), in the position of the FAs on the glycerol skeleton (regioisomers) and in optical isomerism for TGs containing three different FAs. TGs from plant oils represent an important part of the human diet, because they serve as a source of energy and of essential FAs that are used for the synthesis of lipid membranes. Knowledge of the qualitative and quantitative composition of TGs in plant oils is important for dietetical and nutritional reasons because of the influence of the different properties of each FA to the human organism.

The identification of TGs in plant oils which can contain several hundred types is challenging and requires an efficient separation before mass spectrometric characterization. High-performance liquid chromatography (HPLC) has been widely used for this purpose. Normal-phase HPLC with silver ion embedded columns (Ag-HPLC) allows for the separation of TGs differing in the number and position of the DBs [1–4]. The retention of the TGs thereby increases with increasing number of DBs. With non-aqueous reversed-phase HPLC (NARP-HPLC) [5–27] TGs differing in acyl chain lengths and in number and position of the DBs can be separated. The retention thereby increases with increasing equivalent carbon number (ECN) which is defined as the total carbon number in all acyl chains minus two times the amount of DBs, i.e. ECN = CN − 2DB. Under optimized conditions, the separation of the TGs in a single ECN group can also be achieved [10,16,19,23,24]. Relatively

* Corresponding author.
E-mail address: pat.Sandra@richrom.com (P. Sandra).

0021-9673/$ – see front matter © 2007 Elsevier B.V. All rights reserved.
doi:10.1016/j.chroma.2007.10.075

apolar solvents are usually used for the analysis of the TGs because of their insolubility in water and in common reversed-phase HPLC solvents. Typically combinations of acetonitrile (ACN)/2-propanol [14,16,22–24,26], ACN/2-propanol/hexane [11,12], ACN/acetone [8,13,15,17,19,20], propionitrile [10], ACN/chloroform [21] and ACN/dichloromethane [7,9,25] are used as mobile phases in gradient or isocratic NARP-HPLC mode.

The quantitation of TGs from natural mixtures is complicated by the large structural variation of the species leading to much differing detector response factors with common HPLC detectors, such as mass spectrometry, UV or evaporative light scattering detection (ELSD). Simple quantitation based on the relative peak areas while neglecting the differences in response factors is widely used in lipid analysis. However, the differences in chain lengths, the number and position of the DBs and other structural differences lead to highly different responses with common detectors used for TG analysis like UV absorbance at low wavelengths, ELSD and APCI-MS. It has been demonstrated that quantitation without taking the response factors (RFs) into consideration leads to large errors in the results depending on which detector is being used [23]. On the other hand, precise quantitation using the RFs obtained from calibration curves of each pure TG can be time consuming, expensive or not possible because of the lack of TG standards.

Nevertheless, several quantitation approaches based on the (partial) knowledge of the RFs have been developed for quantitation of TGs in plant oils. A method using APCI-MS and RFs has been described for the analysis of TGs in a wide range of plant oils and fats [23,27]. The RFs of fatty acids in the TGs were thereby calculated by the calibration curves of 23 single-acid TG standards and subsequently related to triolein. The RFs of TGs with a mixed fatty acid composition were then calculated as the arithmetic mean of the RFs of fatty acids in each TG. In another approach [9], the RFs of TGs with certain fatty acids were calculated by comparison of the fatty acid composition calculated from the TG composition using APCI-MS to the fatty acid composition obtained by a calibrated GC/FID method of transmethylated TGs. The RFs of TGs with a mixed fatty acid composition were then calculated by multiplication of the RFs of the fatty acids present in the TG. RFs have also been calculated by comparison of the RFs of randomized samples to the RFs of their statistically expected composition. All of these approaches yield satisfactory precision for quantitation of TGs in natural mixtures, but they are complicated and time consuming.

The quantitation of TGs using detectors of which the response is almost independent of the analyte structure allows simpler and faster quantitation without the need of RFs. HPLC combined with flame ionization detection (FID) [5–7,9] and with refractive index (RI) detection have been used for quantitation of TGs in plant oils [8,18]. Both detectors, however, do not allow gradient analysis and moreover they exhibit low sensitivity and robustness as they are highly dependent on the mobile phase composition, temperature or pressure variations during analysis.

Aerosol-based detectors like ELSD [25] and charged aerosol detection (CAD) [28–31] are gaining interest as they are almost universal detectors which can be used in combination with gradient analysis. Drawbacks of ELSD are that it requires non-linear calibration and sometimes lacks sensitivity [12]. The quantitation of a number of TGs by HPLC–ELSD was demonstrated whereby a non-linear equation was used for quantification of unknowns as opposed to the internal normalization method often wrongly applied in HPLC–ELSD as such [25]. Isocratic analysis was thereby performed on an oil containing nine TGs.

Just like for the ELSD, the response of the CAD is almost independent on the structure of non-volatile compounds [29], but it strongly depends on the amount of organic solvent in the mobile phase as it influences the transport efficiency of the nebulizer and the generated signal [32]. The responses of individual lipid classes may significantly differ [31], if the gradient compensation is not employed. The increasing response of more retained compounds in gradient elution is hindering quantitative analysis without knowledge of the RFs [33–35]. This response dependency can, however, be corrected by mixing of the column effluent with the inversed gradient delivered by a second HPLC pump, before introduction into the CAD. In this way, a constant mobile phase composition is reaching the detector [33,35]. The dilution of the analytes by mixing with the inversed mobile phase gradient thereby does not cause a loss of sensitivity because of the mass sensitivity of CAD.

The goal of this work was the development of a simple approach for the quantitation of TGs in complex natural mixtures from plant oils using NARP-HPLC in the gradient mode combined with universal CAD and mobile phase compensation. For this purpose, calibration curves of various single-acid saturated (from C7:0 to C22:0) and unsaturated (C18:1, C18:2, C18:3) TG standards were measured with and without gradient compensation and the response dependency on the length of fatty acid chains and on the number of DBs using CAD was evaluated. The developed method is applied to the analysis of real samples of complex TG mixtures from plant oils.

2. Experimental

2.1. Materials and samples

Acetonitrile and 2-propanol (LC–MS grade) were purchased from Biosolve (HA Valkenswaard, The Netherlands). Hexane was LC grade and was obtained from Sigma–Aldrich (St. Louis, USA). The TG standard mixtures GLC#435 (saturated single-acid TGs from C7:0 to C22:0) and GLC#437 (single-acid TGs C16:0, C18:0, C18:1, C18:2, C18:3 and C20:0) were purchased from Nu-Chek-Prep (Elysian, USA). Nitrogen 4.0 which was used as nebulizing gas for the CAD was purchased from Messner (Mechelen, Belgium). Samples of sunflower (*Helianthus annuus*), soybean (*Glycine soja*), grape seed (*Vitis vinifera*), sesame (*Sesamum indicum*) and linseed (*Linum usitatissimum*) oils were prepared in the laboratory by the following procedure. Each sample was carefully crushed in a mortar to obtain fine particles, which were then mixed with hexane. The mixture was stirred occasionally for 15 min. The solid particles were filtered out using filter paper and then the extract was filtered again using a syringe filter with 0.45 μm pores. Hexane was evaporated from the filtered extract yielding the pure plant oil. Samples of olive

(*Olea europea*) and palm oils (*Elaeis guineensis* Jacq.) were purchased from Augustus Oils Ltd. (Hampshire, England). The oil samples were dissolved in hexane to obtain a final concentration of 600 mg/L. Four microliters of this solution was injected for HPLC analysis.

2.2. Instrumentation

Experiments were performed on an HP1050 system from Agilent Technologies (Waldbronn, Germany) equipped with a quaternary gradient pump, autosampler and controlled by Chemstation software. A second HP1050 quaternary gradient pump programmed with the control panel and started by an external signal from the first HP1050 Series system was used for gradient compensation according to ref. [33]. Effluents from both pumps were connected using a T-piece before the Corona CAD detector (ESA Analytical, Aylsbury, Buckinghamshire, England). Data from the CAD detector were processed by a Peak Simple Chromatography Data System model 202 and Peak Simple software (both from SRI Instruments, Torrance, CA). The following parameters were used for the CAD. The acquisition range was set at 100 pA, the low filter was kept constant and the N_2 pressure was 35 psi. The data acquisition was triggered automatically using the external start signal from the LC autosampler and finished after a predetermined time. TGs in plant oils were identified using HPLC coupled to mass spectrometry. The chromatographic apparatus consisted of a Model 616 pump with a quaternary gradient system, a model 996 diode-array UV detector, a model 717+ autosampler, a thermostated column compartment and a Millennium chromatography manager (all from Waters, Milford, MA, USA) combined with an Esquire 3000 ion trap analyzer (Bruker Daltonics, Bremen, Germany) equipped with a positive-ion atmospheric pressure chemical ionization (APCI) source. The following tuning parameters were used. The pressure of the nebulizing gas was 70 psi, the drying gas flow rate was set at 3 L/min, the temperatures of the drying gas and APCI heater were 350 °C and 400 °C, respectively.

2.3. HPLC conditions

Separations were carried out on two Hypersil ODS columns (250 mm × 4.6 mm I.D., 5 μm, Thermo Electron, San Jose, CA, USA) connected in series and equipped with a precolumn containing the same sorbent. The flow rate of mobile phase was set to 1 mL/min with the following gradient composition used for each analysis: 0 min – 20% A + 80% B, 80 min – 75% A + 25% B, where A is 2-propanol:hexane (1:1, v/v) and B is ACN. The column temperature was 30 °C and the injection volume was 4 μL. Each analysis was repeated three times. Two identical Hypersil ODS columns including the precolumn were connected to the second HPLC pump. The flow rate was thereby also set at 1 mL/min and an inverse gradient composition was applied for compensation i.e. 0 min – 80% A + 20% B, 80 min – 25% A + 75% B. With compensation a flow rate of 2 mL/min mobile phase is introduced into the CAD. Nebulization of the mobile phase at that high flow rate is problem free and within the CAD manufacturers' recommendations.

2.4. Calibration curves, response factors and limits of detection

The stock solutions were prepared by dissolving the GLC#435 and GLC#437 samples in hexane to obtain final concentrations of 63 mg/L (higher concentrations could not be prepared because of low solubility of saturated TGs from C18 to C22) and 333 mg/L of each TG, respectively. The calibration curves were constructed at six concentration levels: 2, 5, 10, 20, 40 and 63 mg/L for GLC#435 and 2, 10, 50, 100, 200 and 333 mg/L for GLC#437. The RFs of the TGs using CAD with mobile phase compensation were calculated as the ratio of the slope of the calibration curve to the slope of the curve obtained for triolein. The limit of detection (LOD) was determined according to the U.S. Environmental Protection Agency (EPA) recommended procedure [36]. Four microliters of a standard solution containing 2 mg/L of each analyte (which leads to an approximate S/N value of 10) was injected seven times and standard deviations of peak areas were calculated. LODs are obtained by multiplying the measured standard deviations by three.

3. Results and discussion

3.1. TG response factors with charged aerosol detection (CAD)

Aerosol-based detectors, such as ELSD and CAD, are nearly universal detectors providing non-volatile compounds are analyzed. TGs have extremely low vapour pressures so they can be detected with a good sensitivity. CAD provides some further benefits in terms of increased dynamic range and sensitivity compared to ELSD, hence this detector was used to develop a simple approach for quantitative TG analysis in plant oils. Two standard TG mixtures containing 16 saturated and 3 unsaturated single-acid TGs were therefore measured. The chromatograms (Fig. 1A and C) show an increasing baseline signal and TG response during gradient elution which is in agreement with previously published data [33,34]. The increased response is caused by an improved transport efficiency of the nebulizer [32] leading to a higher number of ions reaching the detector because of the increasing content of apolar solvent in the gradient.

This non-uniform response of TGs during gradient elution prohibits reliable quantitative analysis. For this reason, the response dependency was corrected by using the gradient mobile phase compensation method [33]. Briefly, the effluent from the HPLC column is mixed by a T-piece installed before the detector with the inverse gradient delivered by the second HPLC pump. The mobile phase reaching the CAD has a constant composition and therefore constant conditions are obtained for nebulizing the mobile phase with target analytes during the gradient elution. Fig. 1B and D show the separation of the standard TG mixtures using CAD with mobile phase compensation. RFs of TG standards analyzed using CAD with and without the gradient mobile phase compensation were calculated based on the peak areas obtained from the analysis of TGs at one concentration level. The response factors of the TGs are calculated as

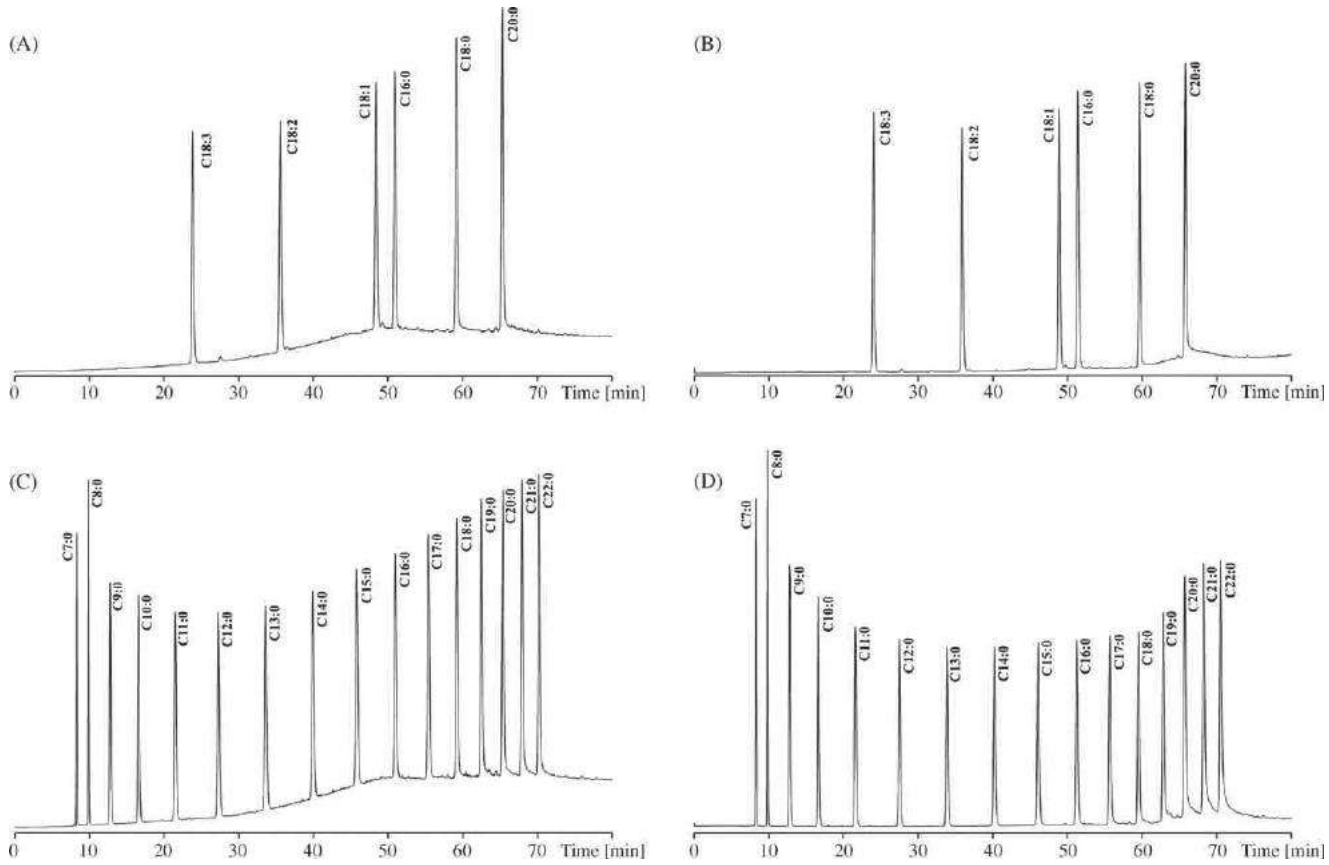

Fig. 1. HPLC separation of equal amounts of each single-acid triacylglycerol (TG) standard using charged aerosol detection: (A) analysis of the TG mixture #437 without and (B) with mobile phase compensation, (C) analysis of the TG mixture #435 without and (D) with mobile phase compensation. Conditions: two Hypersil ODS columns (250 mm × 4.6 mm, 5 μm) connected in series. Flow rate: 1 mL/min. Column temperature: 30 °C. Further details in Section 2.

the ratio of the TG peak areas to the peak area of triolein. The latter was selected because it is one of the most common TGs in nature. The mobile phase compensation significantly improved the response uniformity. For example, the response factor of TG C9:0 changed from 0.69 for the analysis without compensation to 0.83 for the analysis with compensation, for C10:0 from 0.75 to 0.85, for C18:0 from 1.15 to 1.02, for C18:3 from 0.84 to 0.92, etc.

Calibration curves were constructed for 19 single-acid TG standards using CAD with mobile phase compensation to determine the dependency of the response factors of the TGs on the chain length and on the number of DBs in the fatty acid chains. Table 1 shows the results obtained for the series of single-acid TG standards. Contrary to a precedent report [33,34] where the calibration curves required plotting on logarithmic co-ordinates to obtain linearity, in this work the equation of linear dependency, $y = ax + b$, fitted very well on linear co-ordinates, with correlation coefficients of 0.997 and better for all analyzed TG standards. For this reason, the calibration curves were considered linear in the studied concentration range (from LOD to 330 mg/L for the unsaturated TGs and from LOD to 67 mg/L for the saturated TGs). The response factors of the TGs slightly increased with increasing carbon number from 0.54 for the TG containing heptanoic acid (C7:0) to 1.38 for the TG containing behenic acid (C22:0). The lower response obtained for the TGs containing short acyl chains is probably not caused by an increased volatility as they still remain large molecules with very low volatilities [33]. This is also supported by observing the standard deviation of the peak areas, which would be expected to be worse for the volatile compounds using CAD. However, the latter is stable for all analyzed TGs over the whole concentration range (data not shown).

It can be observed from these data that the RFs using the CAD show a slight dependency on the number of carbon atoms in the TG molecules (Fig. 2). This is mainly the case for the TGs with acyl chains ranging from C7:0 to C11:0 with RFs ranging from 0.54 to 0.89 and for TGs containing chains from C20:0 to C22:0 with RFs ranging from 1.11 to 1.38. The dependency of the RFs is lower for TGs containing FAs with 12–19 carbon atoms in the acyl chain with values ranging from 0.94 to 1.05, which is an excellent result for compounds differing by 21 methylene units on the whole TG. The RFs obtained for the single-acid TGs containing FAs with 9–20 carbon atoms show a 20% variation which is still a good result for compounds differing by 33 methylene units and cover an almost doubling of the molecular mass (from 512 to 974 g/mol). The RFs of TGs containing 0, 1, 2 or 3 double bounds were also compared. For the TGs containing three stearic acid chains (C18:0) a response of 1.02 was obtained. For the di- (C18:2) and tri-unsaturated (C18:3) equivalents, a response of 0.98 and 0.92 were obtained, respectively. Hence, the presence

Table 1
Calibration parameters of 19 single-acid triacylglycerol (TG) standards using charged aerosol detection with mobile phase compensation with their corresponding retention times t_R and response factors (RFs)

TGs	t_R (min)	a	b	r^2	RFs-CAD	RFs-APCI[a]
C7:0	8.3	15.3	−31.0	0.999	0.54	97.20
C8:0	10.1	20.9	−12.1	0.999	0.74	74.44
C9:0	12.9	23.6	3.1	0.999	0.83	38.91
C10:0	16.7	24.3	15.4	0.997	0.86	17.62
C11:0	21.6	25.3	16.8	0.997	0.89	10.85
C12:0	27.4	26.7	23.4	0.997	0.94	6.04
C13:0	33.8	27.5	26.5	0.997	0.97	4.31
C14:0	40.1	27.1	31.6	0.997	0.95	2.77
C15:0	46.0	27.9	25.9	0.997	0.98	1.75
C16:0	51.1	28.8	21.5	0.997	1.01	1.32
C17:0	55.6	28.7	32.4	0.997	1.01	0.81
C18:3	24.1	26.2	78.7	0.999	0.92	0.40
C18:2	35.8	27.9	97.2	0.999	0.98	0.57
C18:1	**48.6**	**28.4**	**123.2**	**0.998**	**1.00**	**1.00**
C18:0	59.3	29.1	28.4	0.998	1.02	0.61
C19:0	62.8	29.7	5.7	0.998	1.05	0.49
C20:0	65.5	31.6	−2.5	0.998	1.11	0.40
C21:0	68.2	36.2	−71.6	0.999	1.27	0.39
C22:0	70.5	39.2	−89.6	0.998	1.38	0.46

a and b were obtained from the linear regression according to $y = ax + b$, where y represents the peak areas, x is the concentration in mg/L and r^2 is the correlation coefficient of the curve. The RFs of the TGs using charged aerosol detection (RFs-CAD) and atmospheric pressure chemical ionization (RFs-APCI) are related to triolein (C18:1) which is set to 1.00.

[a] Data from ref. [23].

and the amount of double bounds have only a minor influence on the response. The RFs of the saturated and unsaturated single-acid TG standards with carbon chains containing 12–19 atoms show a variation of only 5% except for C12:0 (6%) and C18:3 (8%) which is an acceptable result for most quantitative applications. Hence, simple quantitative analysis based on the relative peak areas without the knowledge of the RFs becomes possible for plant oil analysis.

In Table 1, the RFs obtained by CAD are also compared with the RFs measured with atmospheric pressure chemical ionization coupled to ion trap mass spectrometry [23]. The RFs of the

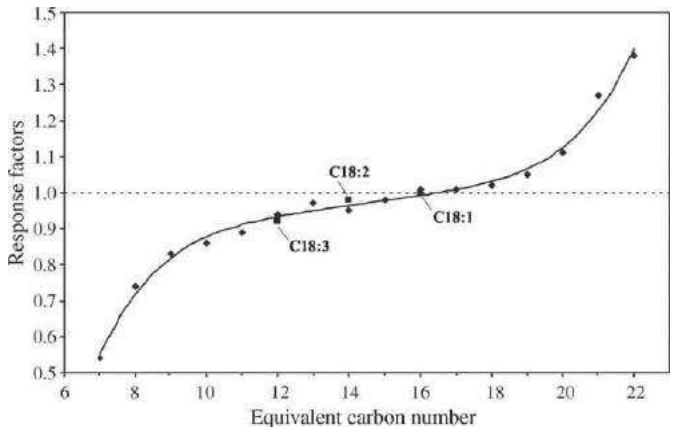

Fig. 2. Dependence of response factors obtained with corona charged aerosol detection on the equivalent carbon number of TGs. All TG standards are saturated except for oleic (C18:1), linoleic (C18:2) and linolenic (C18:3) fatty acids.

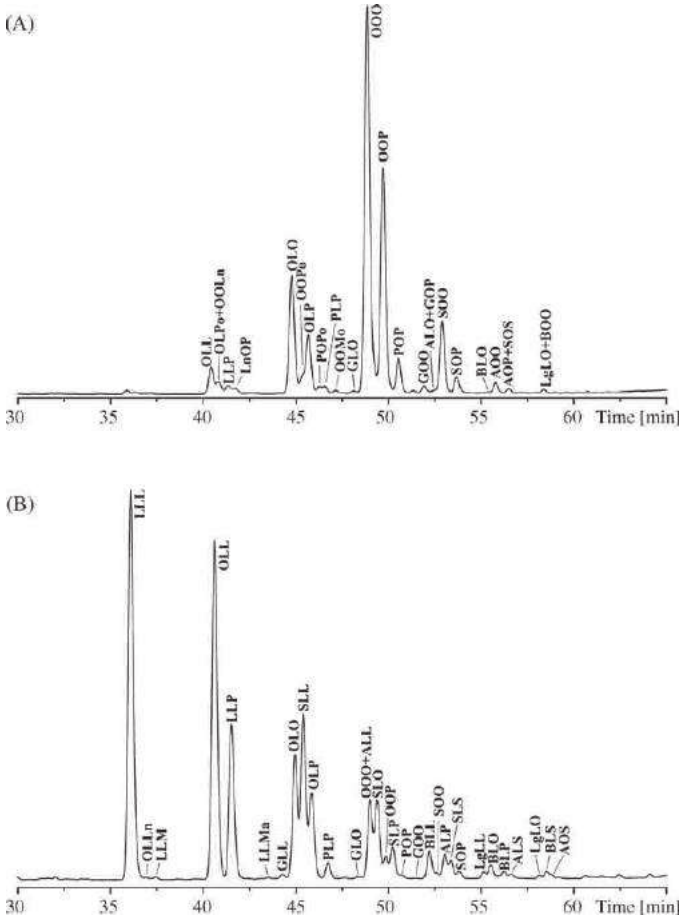

Fig. 3. Representative separations of studied plant oils using charged aerosol detection with mobile phase compensation: (A) olive oil (*Olea europea*) and (B) sunflower oil (*Helianthus annuus*). Conditions: two Hypersil ODS columns (250 mm × 4.6 mm I.D., 5 μm) connected in series. Flow rate: 1 mL/min. Column temperature: 30 °C. Further details in Section 2.

TGs measured with APCI-MS show large differences. This is mainly the case for the TGs with shorter fatty acids due to the strong discrimination of low *m/z* values in the ion trap analyzer. In comparison to CAD, the RFs using APCI-MS can therefore

Table 2
Systematic and trivial names of fatty acids found in triacylglycerols of the studied plant oils listed with their abbreviations, carbon numbers (CN), number of double bond (DB) and equivalent carbon numbers (ECN)

Systematic name	Trivial name	Abbreviation	CN:DB	ECN
Tetradecanoic	Myristic	M	C14:0	14
Hexadecanoic	Palmitic	P	C16:0	16
cis-9-Hexadecenoic	Palmitoleic	Po	C16:1	14
Heptadecanoic	Margaric	Ma	C17:0	17
cis-10-Heptadecenoic	Margaroleic	Mo	C17:1	15
Octadecanoic	Stearic	S	C18:0	18
cis-9-Octadecenoic	Oleic	O	C18:1	16
cis-9, 12-Octadecadienoic	Linoleic	L	C18:2	14
cis-9, 12, 15-Octadecatrienoic	Linolenic	Ln	C18:3	12
Eicosanoic	Arachidic	A	C20:0	20
cis-11-Eicosenoic	Gadoleic	G	C20:1	18
cis-11, 14-Eicosadienoic	–	–	C20:2	16
Docosanoic	Behenic	B	C22:0	22
Tetracosanoic	Lignoceric	Lg	C24:0	24

Table 3
Triacylglycerols (TGs) identified in the studied plant oils listed according to their equivalent carbon number (ECN), retention times (t_R) and relative peak areas

TGs	ECN	t_R (min)	Relative peak areas (%)						
			Olive	Sunflower	Palm	Soybean	Grape	Sesame	Linseed
LnLnLn	36	24.1							19.9
LnLLn	38	27.8				1.5			13.4
LLLn	40	31.8				8.5	0.3	0.1	4.1
LnOLn		32.3				0.6			14.5
LnLnP		33.1				0.4			5.8
LLL	42	35.8		26.2		16.9	31.3	10.0	0.6
OLLn		36.3		0.1		5.3		0.3	7.7
LLM		37.2		0.1					
LnLP		37.3				4.0	0.1	0.1	7.5 + SLnLn
LLMo	43	38.3				0.1			
C20:2LL	44	39.6				0.1	0.1		
OLL		40.3	2.2	23.1	0.4	14.6	23.0	18.2	1.2
OOLn		40.6	1.1 + OLPo			1.1		0.3	7.4
LLP		41.2	0.7	9.6	1.8	12.8	12.9	6.6	
SLLn		41.4				1.1			2.6
LnOP		41.8	0.5		0.4				3.2
PLM		42.6			0.3				
PLnP		42.6				0.3			0.3
LLMa	45	43.2		<0.1		0.2	0.2		
GLL	46	44.0		0.2		0.2	0.4	0.1	0.2
OLO		44.6	11.0	7.1	1.4	5.6	7.1	17.2	2.2
OOPo		45.1	0.9						
SLL		45.2		9.9		4.0	8.5	3.4	0.3
OLP		45.6	5.5	4.9	8.6	7.8	6.7	9.9	3.5 + SOLn + BLnLn
OOM		46.0			0.4				
POPo		46.1	0.5						
PLP		46.3	0.5	0.9	8.7	2.5	0.2	1.5	
POM		46.4			1.6				
SLnP		46.4							0.5
PPM		46.9			0.7				
OOMo	47	46.9	0.2						
OLMa		47.4				0.2		0.1	
GLO	48	47.9	0.2	< 0.1		0.2	0.1	0.2	
OOO		48.6	41.8	4.3 + ALL	3.6	1.9 + ALL	1.4 + ALL	10.1	2.0
SLO		49.1		4.3	1.0	3.0	4.1	5.5	0.6
OOP		49.5	22.2	1.1	19.7	1.6	1.6	6.3	0.9
SLP		49.9		1.6	1.9	1.7	0.4	1.5	0.4
SLnS		50.4							0.2
POP		50.5	2.9	0.3	28.8	0.7	0.3	1.2	
PPP		51.3			8.4				
GOO	50	51.6	0.6	< 0.1					
BLL		51.9		1.5		0.4		0.3	
ALO		52.2	0.1 + GOP		0.2 + GOP		0.1	0.4	
SOO		52.5	6.1	0.3	2.7	0.2	0.8	3.4	0.7
ALP		52.8		1.2		0.6	0.2	0.7	0.1
SLS		53.1		0.8		0.5	0.2		0.2
SOP		53.5	1.3	0.4	6.2	0.5		1.4	
SPP		54.3			1.9				
LgLL	52	54.8		0.3		0.1			
BLO		55.2	0.1	0.7		0.2			
AOO		55.5	0.9		0.2			0.3	
BLP		56.0		0.3		0.2			
ALS		56.3		0.2		0.2			
AOP		56.3	0.4 + SOS		0.8 + SOS			0.7 + SOS	
APP		56.9			0.3 + SSP				
LgLO	54	58.1	0.3 + BOO	0.2				0.2 + BOO	
BLS		58.3		0.3		0.1			
AOS		58.6		0.1		0.1			

Table 4
Comparison of the relative amounts (wt%) of fatty acids (FAs) widely present in plant oils based on the measured triacylglycerol composition in the analyzed samples using HPLC/CAD and HPLC/APCI-MS

FAs	Olive		Sunflower		Palm		Soybean		Grape		Sesame		Linseed	
	CAD	APCI[a]	CAD	APCI[a]	CAD	APCI[a]	CAD	APCI[a]	CAD	APCI[a]	CAD	APCI[a]	CAD	APCI[a]
C16:0	12.0	11.8	6.8	7.7	47.6	40.6	11.6	11.7	7.2	9.4	10.3	10.9	7.1	6.9
C18:0	2.5	2.6	6.3	5.2	4.7	4.6	4.0	3.4	4.8	3.7	5.1	5.0	2.0	3.7
cis-9-C18:1	75.7	73.9	21.4	23.0	37.1	41.4	18.8	19.2	19.4	22.2	41.5	40.9	19.9	20.8
cis-9,12-C18:2	7.9	8.5	63.6	61.5	9.1	10.3	56.1	51.8	68.1	63.2	41.8	41.5	17.3	15.9
cis-9, 12,15-C18:3	0.5	0.8	<0.1	0.1	0.1	0.2	8.5	12.5	0.1	0.6	0.3	0.6	53.7	52.3
Others	1.4	2.4	1.9	2.5	1.4	2.9	1.0	1.4	0.4	0.9	1.0	1.1	<0.1	0.4

[a] Data from ref. [27].

not be neglected and have to be used for quantitative analysis of TGs in plant oils.

3.2. Quantitation of TGs in plant oils by NARP-HPLC/CAD

TGs from plant oils are an important part of the human diet and knowledge of the oil composition is therefore relevant from a nutritional point of view. NARP-HPLC combined with CAD and mobile phase compensation was used for the quantitation of TGs in plant oils (Fig. 3). TGs are generally noted by the initial of the FA trivial names (Table 2) arranged according to their *sn*-1, 2 and 3 positions. Identified TGs are listed in Table 3. *Sn*-1 and *sn*-3 positional isomers cannot be resolved in NARP-HPLC and are therefore considered equivalent. FAs in these positions are therefore arranged in order of decreasing molecular weights (for example, a TG containing two oleic and one linoleic acid group is noted as OOL). FAs in *sn*-2 position can be differentiated by characteristic differences in the ratio of the fragment ions by APCI-MS [16,23,24].

The retention times of TGs in NARP-HPLC depend on the acyl chain lengths and on the number and position of the DBs according to the equivalent carbon number (ECN = CN − 2DB). In this work, TGs with the same ECN were also partially separated with only a few overlapping peaks (Fig. 3 and Table 3) in this way providing sufficient separation for quantitation using CAD detection. As discussed above, the RFs of the TGs containing FAs with 12–19 carbon atoms and 0–3 double bonds range from 0.92 to 1.05 drastically simplifying quantitation. The main constituents of TGs in plant oils [23,24,26,27] are saturated fatty acids with 16 (palmitic) and 18 carbon atoms (stearic) and unsaturated fatty acids with 18 carbon atoms containing 1 (oleic acid), 2 (linoleic acid) or 3 double bonds (linolenic acid). Their total content in common plant oils make up 93–100% of the total FA content with a mean value of 98%. FAs with shorter or longer acyl chains or containing more DBs are unusual and typically they comprise only one fatty acid in the TGs. They are usually present at trace concentration levels in natural plant oils (up to 0.5%) with a few known exceptions, i.e. coconut oil contains 77% of the C6:0–C14:0 fatty acids and date seed oil contains 39% of the C8:0–C14:0 fatty acids. This means that the simple quantitation with CAD is applicable for a wide range of natural plant oils.

Table 3 lists concentrations of identified TGs in seven plant oils based on the relative peak areas using CAD and the gradient mobile phase compensation while neglecting the TG response factors. The FA content calculated from the TG composition using CAD and the gradient mobile phase compensation method is given in Table 4. These results are in a good agreement with the results obtained using a quantitative APCI-MS method with knowledge of the RFs [27]. The latter were previously confirmed by a validated GC/FID method [23].

3.3. Reproducibility and limit of detection

Universal detectors typically provide a lower reproducibility and sensitivity in comparison to common more selective HPLC detectors. The reproducibility of the results obtained with NARP-HPLC/CAD and mobile phase compensation was calculated from five consecutive analyses of single-acid TG standards and expressed as the relative standard deviation (RSD) of the peak areas. The mean values of the calculated RSDs were 5.8% at a concentration of 2 mg/L, 1.3% at 10 mg/L and 0.4% at 333 mg/L. The limit of detection with mobile phase compensation was calculated according to the U.S. EPA recommended procedure [35]. The LODs ranged from 0.1 to 0.5 mg/L with an average value 0.3 mg/L for the 19 TGs. The injection volume of 4 μL used for each analysis corresponds to 1.2 ng of analyte injected on column, which is an excellent result for a nearly universal detector. No explicit differences in the reproducibilities and LODs were observed among the TGs containing saturated, unsaturated, long or short fatty acid chains.

4. Conclusions

The recently introduced CAD was used for the quantitative analysis of TGs in complex natural mixtures. Because the response of the CAD depends on the composition of the mobile phase, gradient elution cannot be used for reliable quantitative analysis without knowledge of response factors. The mobile phase compensation method was used to improve the response uniformity of the analyzed TG standards under gradient elution conditions. The response factors of TGs containing saturated and unsaturated fatty acids from 12 to 19 carbon atoms showed

only 5% variation, which is sufficient for simple quantitative analysis without the need of response factors. The developed measuring method was applied for the quantitation of TGs in seven common edible plant oils containing mainly saturated and unsaturated fatty acids with 16 and 18 carbon atoms. Good reproducibility and excellent limits of detection with a nearly universal response was achieved. Compared to previously published quantitative methods based on the knowledge of RFs, the current method is cheaper (no TG standards are needed), faster (no calibration curves are required for the determination of relative concentrations) and the obtained precision is acceptable for most analytical purposes.

Acknowledgments

The European Community is kindly acknowledged for providing a grant within the Socrates program 2006. M.L. and M.H. acknowledge the support of projects MSM0021627502 sponsored by the Ministry of Education, Youth and Sports of the Czech Republic and 203/06/0219 sponsored by the Czech Science Foundation.

References

[1] W.W. Christie, J. Chromatogr. 454 (1988) 273.
[2] P. Laakso, P. Voutilainen, Lipids 31 (1996) 1311.
[3] P.J.W. Schuyl, T. de Joode, M.A. Vasconcellos, G. Duchateau, J. Chromatogr. A 810 (1998) 53.
[4] R.O. Adlof, A. Menzel, V. Dorovska-Taran, J. Chromatogr. A 953 (2002) 293.
[5] F.C. Phillips, W.L. Erdahl, J.A. Schmit, O.S. Privett, Lipids 19 (1984) 880.
[6] K.V.V. Nurmela, L.T. Satama, J. Chromatogr. 435 (1988) 139.
[7] M.A.M. Zeitoun, W.E. Neff, E. Selke, T.L. Mounts, J. Liq. Chromatogr. 14 (1991) 2685.
[8] A.A. Carelli, A. Cert, J. Chromatogr. 630 (1993) 213.
[9] W.C. Byrdwell, E.A. Emken, W.E. Neff, R.O. Adlof, Lipids 31 (1996) 919.
[10] H.R. Mottram, S.E. Woodbury, R.P. Evershed, Rapid Commun. Mass Spectrom. 11 (1997) 1240.
[11] P. Sandra, A. Dermaux, V. Ferraz, M.M. Dittmann, G. Rozing, J. Microcolumn Sep. 9 (1997) 409.
[12] M. Holčapek, P. Jandera, J. Fischer, B. Prokeš, J. Chromatogr. A 858 (1999) 13.
[13] J. Parcerisa, I. Casals, J. Boatella, R. Codony, M. Rafecas, J. Chromatogr. A 881 (2000) 149.
[14] M. Holčapek, P. Jandera, J. Fischer, Crit. Rev. Anal. Chem. 31 (2001) 53.
[15] A. Jakab, K. Héberger, E. Forgács, J. Chromatogr. A 976 (2002) 255.
[16] M. Holčapek, P. Jandera, P. Zderadička, L. Hrubá, J. Chromatogr. A 1010 (2003) 195.
[17] A. Jakab, I. Jablonkai, E. Forgács, Rapid Commun. Mass Spectrom. 17 (2003) 2295.
[18] G.N. Jham, B. Nikolova-Damyavova, M. Viera, R. Natalino, A.C. Rodrigues, Phytochem. Anal. 14 (2003) 310.
[19] J.S. Perona, V. Ruiz-Gutierrez, J. Chromatogr. B 785 (2003) 89.
[20] P. Dugo, O. Favoino, P.Q. Tranchida, G. Dugo, L. Mondello, J. Chromatogr. A 1041 (2004) 135.
[21] L. Fauconnot, J. Hau, J.M. Aeschlimann, L.B. Fay, F. Dionisi, Rapid Commun. Mass Spectrom. 18 (2004) 218.
[22] J.D.J. van den Berg, N.D. Vermist, L. Carlyle, M. Holčapek, J.J. Boon, J. Sep. Sci. 27 (2004) 181.
[23] M. Holčapek, M. Lísa, P. Jandera, N. Kabátová, J. Sep. Sci. 28 (2005) 1315.
[24] M. Lísa, M. Holčapek, Chem. Listy 99 (2005) 195.
[25] S. Héron, M.-G. Maloumbi, M. Dreux, E. Verette, A. Tchapla, J. Chromatogr. A 1161 (2007) 152.
[26] M. Lísa, M. Holčapek, T. Řezanka, N. Kabátová, J. Chromatogr. A 1146 (2007) 67.
[27] M. Lísa, M. Holčapek, J. Chromatogr. A, in preparation.
[28] R.W. Dixon, D.S. Peterson, Anal. Chem. 74 (2002) 2930.
[29] P.H. Gamache, R.S. McCarthy, S.M. Freeto, D.J. Asa, M.J. Woodcock, K. Laws, R.O. Cole, LC–GC Eur. 18 (2005) 345.
[30] A. Cascone, S. Eerola, A. Ritieni, A. Rizzo, J. Chromatogr. A 1120 (2006) 211.
[31] R.A. Moreau, Lipids 41 (2006) 727.
[32] Z. Cobb, P.N. Shaw, L.L. Lloyd, N. Wrench, D.A. Barrett, J. Microcolumn Sep. 13 (2001) 169.
[33] T. Górecki, F. Lynen, R. Szucs, P. Sandra, Anal. Chem. 78 (2006) 3186.
[34] C. Brunelli, T. Górecki, Y. Zhao, P. Sandra, Anal. Chem. 79 (2007) 2472.
[35] A. de Villiers, T. Gorecki, F. Lynen, R. Szucs, P. Sandra, J. Chromatogr. A 1161 (2007) 183.
[36] U.S. EPA. Definition and Procedure for the Method Detection Limit, Revision 1.11, Environmental Protection Agency: Washington, DC, 1984, 40 CFR Part 136, Appendix B.

Journal of Chromatography A, 1198–1199 (2008) 115–130

Contents lists available at ScienceDirect

Journal of Chromatography A

journal homepage: www.elsevier.com/locate/chroma

Triacylglycerols profiling in plant oils important in food industry, dietetics and cosmetics using high-performance liquid chromatography–atmospheric pressure chemical ionization mass spectrometry

Miroslav Lísa, Michal Holčapek*

Department of Analytical Chemistry, Faculty of Chemical Technology, University of Pardubice, Nám. Čs. Legií 565, 53210 Pardubice, Czech Republic

ARTICLE INFO

Article history:
Received 9 February 2008
Received in revised form 13 May 2008
Accepted 16 May 2008
Available online 22 May 2008

Keywords:
Triacylglycerol
Plant oil
Fat
Lipid
Profiling
Food
Nutrition
HPLC/MS
APCI

ABSTRACT

Optimized non-aqueous reversed-phase high-performance liquid chromatography method using acetonitrile–2-propanol gradient elution and the column coupling in the total length of 45 cm has been applied for the high resolution separation of plant oils important in food industry, dietetics and cosmetics. Positive-ion atmospheric pressure chemical ionization mass spectrometry is used for the unambiguous identification and also the reliable quantitation with the response factors approach. Based on the precise determination of individual triacyglycerol concentrations, the calculation of average parameters important in the nutrition is performed, i.e. average carbon number, average double bond number, relative concentrations of essential, saturated, monounsaturated and polyunsaturated fatty acids. Results are reported in the form of both chromatographic fingerprints and tables containing relative concentrations for all triacylglycerols and fatty acids in individual samples. In total, 264 triacylglycerols consisting of 28 fatty acids with the alkyl chain length from 6 to 26 carbon atoms and 0 to 4 double bonds have been identified in 26 industrial important plant oils.

1. Introduction

Triacylglycerols (TGs) are natural compounds synthesized by the esterification of glycerol with FAs under the enzymatic catalysis. In human organism, they serve as a source of energy stored in fat tissues, thermal and mechanical protective layer surrounding important organs, source of essential FAs (linoleic and linolenic acids), fat-soluble vitamins and other non-polar compounds. They form an important part of human diet and their imbalances can lead to several human diseases, i.e. coronary heart disease, dyslipidaemia, obesity or inborn errors of metabolism. The deficiency of essential FAs necessary for the biosynthesis of long-chain polyunsaturated FAs important for cell membranes leads to problems in nearly every tissue in the body. The main sources of TGs in the human diet are oil plants and especially oils prepared from them [1,2]. The total world production of oil plants in 2006 according to the Food and Agriculture Organization of the United Nations (FAO) reached 743 million tonnes [3]. The biggest producer of oil plants is the USA with almost 15% of the world production followed by Indonesia (14%), China (11%), Malaysia (11%), Brazil (8%), India (7%), Argentina (6%) and 27 European Union member states (5%). Plant seeds can contain from 10–20% oil (wheat germs, soybean) up to 45–65% for highly oily seeds (peanuts, almonds, walnuts) [1]. Some oils are also prepared from plant pulps (palm, olive, avocado). Almost 80% of the total world production of edible oils (127 million tonnes) is represented by 4 plant oils only, i.e. palm (29%), soybean (28%), rapeseed (14%) and sunflower (8%) oils [3]. Other important edible plant oils are peanut, cottonseed, coconut, palmkernel maize, olive and sesame oils [4] with the total production 1–4%. The final use of plant oils depends on their composition and the comprehensive triacylglycerol profiling brings valuable information in this respect.

Individual FAs can differ in the number of carbon atoms (CNs), number of double bonds (DBs) and *cis*-/*trans*-configuration of DBs. Hundreds of natural FAs have been identified so far in the nature and their combinations in TGs, different stereochemical positions *sn*-1, 2 or 3 on the glycerol backbone (regioisomers) or *R*/*S* optical configuration of TGs esterified in *sn*-1 and *sn*-3 positions by two different FAs (optical isomers) lead to enormous complexity. Two techniques of high-performance liquid chromatography (HPLC) are widely used in the analysis of TG mixtures, silver ion normal-phase HPLC (Ag-HPLC) and non-aqueous reversed-phase HPLC

* Corresponding author. Tel.: +420 46 603 7087; fax: +420 46 603 7068.
E-mail address: Michal.Holcapek@upce.cz (M. Holčapek).

0021-9673/$ – see front matter © 2008 Elsevier B.V. All rights reserved.
doi:10.1016/j.chroma.2008.05.037

(NARP-HPLC). Ag-HPLC is widely used for the separation of lipids containing DBs due to the formation of week reversible complexes with silver ions [5,6]. In Ag-HPLC, TGs are separated according to the number [5,7], position [8] and *cis*-/*trans*-configuration [9,10] of DBs. The retention of TGs increases with the increasing number of DBs and TG regioisomers can also be separated under carefully optimized chromatographic conditions [10–14]. In NARP-HPLC [15–30], TGs are separated according to acyl chain lengths and the number of DBs. The retention of TGs is governed by the equivalent carbon number (ECN), which is defined as ECN = CN − 2DB. The separation of most TGs within one ECN group is feasible [19,22,23,25–27] under optimized chromatographic conditions [25,26]. The separation of *cis*-/*trans*-isomers [18,21], DB positional isomers [17,27,29] or partially separated regioisomers [24] has also been reported in NARP-HPLC.

UV detection at low wavelengths (205 or 210 nm) [18,20,22,25,30,31] is used for the detection of common TGs. UV detection provides a linear response, but very low sensitivity for saturated TGs disables their quantitation [25]. Evaporative light-scattering detection (ELSD) [15,20,25,32] is an alternative detection technique used for lipids, but the non-linear response is a disadvantage for the quantitative analysis [20,25]. Moreover, large differences among individual RFs of FAs complicate a simple calculation of RFs of mixed-acid TGs [25]. Charged aerosol detection (CAD) is a new HPLC detection technique with almost universal response for non-volatile compounds with a growing importance in the lipid analysis [28,33,34]. Mass spectrometry (MS) coupled to HPLC is the most powerful tool for the identification of lipids. Atmospheric pressure chemical ionization (APCI) provides best results for TGs [16,17,19–22,25–27] because of the full compatibility with common NARP conditions, easy ionization of non-polar TGs and the presence of both protonated molecules $[M+H]^+$ and fragment ions $[M+H-R_iCOOH]^+$. The spectra interpretation can be simplified by the software algorithm combining $[M+H]^+$ and $[M+H-R_iCOOH]^+$ information [35]. Predominant FA in *sn*-2 position can be determined from APCI mass spectra based on the lower cleavage preference from this position [19,20,22,36,37]. The precise ratio of regioisomers can be obtained by the measurement of calibration curves with both positional isomers [22,37,38]. APCI-MS provides a linear calibration [16,25] and comparable sensitivity for saturated and unsaturated TGs [25]. The first APCI-MS quantitative approach [16] calculates RFs of FAs by comparison of FA composition calculated from the TG composition using HPLC/APCI-MS with FA composition from GC/MS analysis of methyl esters after the transesterification. RFs of mixed-acid TGs were calculated by multiplication of RFs of FAs present in TGs. RFs were also calculated from the comparison of TG composition of randomized sample with their statistically calculated composition. In another approach [25], RFs of 23 single-acid TG standards are calculated from calibration parameters of these TGs related to triolein as one of the most widespread TGs in nature. RFs of mixed-acid TGs are calculated as the arithmetic mean of RFs of individual FAs present in each TG. The precision of the method is verified by validated GC/FID analysis of methyl esters.

The main goal of our work is the detailed analytical characterization of TG composition in a wide range of plant oils important in food industry, dietetics and cosmetics by means of our previously developed method for their NARP-HPLC separation and quantitation based on RFs approach with APCI-MS detection [25]. Average parameters of FA contents in all TGs are calculated including average equivalent carbon number (aECN), average carbon number (aCN), average number of double bonds (aDB), relative concentrations of essential, saturated, monounsaturated and polyunsaturated FAs.

2. Experimental

2.1. Materials

Acetonitrile, 2-propanol (HPLC gradient grade), hexane (HPLC grade), trimyristin, tripalmitin, tripalmitolein, trimargarin, triolein, trilinolein, α-trilinolenin were purchased from Sigma–Aldrich (St. Louis, MO, USA). Tristearin, γ-trilinolenin, model mixtures of TG standards GLC435 (all saturated single-acid TGs from C7 to C22) and GLC406 (C16:0, C18:0, C18:1, C18:2, C18:3, C20:0, C20:1 and C22:1) were purchased from Nu-Chek-Prep (Elysian, MN, USA). Solvents were filtered through a 0.45 μm Millipore filter and degassed by continuous stripping with helium. Samples of palm oil (*Elaeis guineensis*), peanut oil (*Arachis hypogaea*), cottonseed oil (*Gossypium hirsutum*), olive oil (*Olea europaea*) and cocoa butter (*Theobroma cacao*) were purchased from Augustus Oils (Bordon, UK) and samples of kukui oil (*Aleurites moluccana*) and wheat germ oil (*Triticum vulgare*) were purchased from Fragrant Earth (Glastonbury, UK). Plant oils from rapeseed (*Brassica napus*), soybean (*Glycine max*), sunflower (*Helianthus annuus*), coconut palm (*Cocos nucifera*), maize (*Zea mays*), sesame (*Sesamum indicum*), safflower (*Carthamus tinctorius*), grape seed white (*Vitis vinifera*), grape seed red (*Vitis vinifera*), linseed (*Linum usitatissimum*), avocado pear (*Persea americana*), blackcurrant (*Ribes nigrum*), redcurrant (*Ribes rubrum*), borage (*Borago officinalis*) and evening primrose (*Oenothera biennis*) were prepared in our laboratory according to the following procedure. 10–15 g of seeds were carefully crushed in a mortar to fine particles, which were mixed with 15 mL of hexane. The mixture was stirred occasionally for 15 min. The solid particles were filtered out using a rough filter paper and then the extract was filtered again using a fine filter with 0.45 μm pores. From the filtered extract, hexane was evaporated yielding pure plant oil. Oil samples were dissolved in an acetonitrile–2-propanol–hexane mixture (1:1:1, v/v/v) to prepare the initial solution of plant oil with the concentration 10 g/L. Then this solution was diluted with the same solvent mixture to prepare the working solution with the concentration of each TGs within the calibration range. 10 μl of diluted solution was injected in triplicate for HPLC analysis.

2.2. HPLC/APCI-MS conditions

The chromatographic apparatus consisted of a Model 616 pump with a quaternary gradient system, a Model 996 diode-array UV detector, a Model 717+ autosampler, a thermostated column compartment and a Millennium chromatography manager (all from Waters, Milford, MA, USA). The HPLC conditions: two chromatographic columns Nova-Pak C_{18} (300 mm × 3.9 mm and 150 mm × 3.9 mm, 4 μm, Waters) connected in series, a flow rate of 1 mL/min, an injection volume of 10 μL, column temperature of 25 °C and a mobile phase gradient with the slope of 0.65%/min: 0 min—100% acetonitrile, 106 min—31% acetonitrile–69% 2-propanol, 109 min—100% acetonitrile. The injector needle was washed with the mobile phase before each injection. The column hold-up volume, t_M, was 3.20 min for the system with 300 + 150 mm Nova-Pak C_{18} columns. The UV detection at 205 nm and positive-ion APCI-MS were coupled in series. The Esquire 3000 ion trap analyzer (Bruker Daltonics, Bremen, Germany) in the mass range *m*/*z* 50–1200 was used with the following setting of tuning parameters: pressure of the nebulizing gas of 70 psi, the drying gas flow rate of 3 L/min, temperatures of the drying gas and APCI heater were 350 °C and 400 °C, respectively. The reconstructed ion current chromatograms in the region *m*/*z* 300–1200 were used for the peak integration. Presented peak areas correspond to averaged values from three consecutive chromatographic runs. Individual reconstructed ion current chromatograms

were used to support the identification and apportionment of coeluting peaks.

3. Results and discussion

3.1. Chromatographic behavior of triacylglycerols

The retention of TGs in NARP-HPLC systems increases with increasing ECN reflecting the relation between CNs and DBs in all acyl chains, i.e. ECN = CN − 2DB. Most of TGs within one ECN group are also separated in this work including the partial separation of critical pairs of TGs, i.e. SLO (t_R = 85.1 min) and OOP (85.4) with ECN = 48. The retention behavior of TGs in one ECN group is strongly influenced by the FA composition in individual TGs, mainly by the unsaturation degree and acyl chain lengths. For example, the group of OOO (t_R = 84.0 min), OOP (85.4), POP (87.0) and PPP (88.7) with ECN = 48 is well resolved in our optimized chromatographic system. The retention of TGs within one ECN group increases with decreasing DB number in acyl chains, i.e. with replacing of oleic acid by palmitic acid or linoleic acid by palmitoleic acid, as demonstrated by retention times of pairs LLL (t_R = 65.3 min) and LLPo (65.7) with ECN = 42, OLL (71.8) and OLPo (72.2) with ECN = 44, OLO (77.9) and OOPo (78.3) with ECN = 46, etc.

Retention times of identified TGs collected by the analysis of 26 natural samples (Figs. 1–3) together with the knowledge of effects of individual FAs on the retention behavior are very useful for the confirmation of positive identification or the prediction of retention times of unknown TGs. Retention times of identified TGs in the wide range of analyzed samples are used for the identification of TGs containing FAs with unusual positions of DBs (double bond positional isomers). As shown previously [27], TG double bond positional isomers have shifted retention times in comparison to common TGs containing FAs with the same number of CNs and the same number of DBs. Characteristic shifts in their retention factors (Δk) can be used for the identification of TGs containing Δ5 polymethylene interrupted FAs in conifer seed oils, and unusual gamma-linolenic acid (Δ6,9,12–18:3, γLn) in blackcurrant (*R. nigrum*) and redcurrant (*R. rubrum*) (Fig. 2C) oils. In NARP-HPLC systems, TGs containing γLn have a higher retention in comparison to TGs containing only Ln (Table 1), for example pairs of DB positional isomers LnLnLn (t_R = 48.3 min) and LnLnγLn (49.0), LnLSt (49.4) and γLnLSt (50.1), LnLLn (54.0) and LnLγLn (54.7), etc. The differences in retention factors of TGs containing one γLn and TGs containing only Ln are constant with an average value Δk = 0.22. Differences in retention factors for TGs containing two and three γLn acids correspond approximately two times and slightly more than three times of Δk value of one γLn, i.e. Δk = 0.44 and Δk = 0.72, respectively. TGs containing only γLn without any Ln have been identified in borage (*B. officinalis*) (Fig. 2D) and evening primrose (*O. biennis*) (Fig. 3B) oils, which does not enable the direct comparison of both DB positional isomers containing Ln and γLn as for blackcurrant and redcurrant oils. The presence of γLn in TGs has been identified based on shifted retention times and additionally confirmed by the retention time of commercial standard of γLnγLnγLn. Retention times of all TGs in analyzed oils are in agreement with retention times from other analyzed samples and

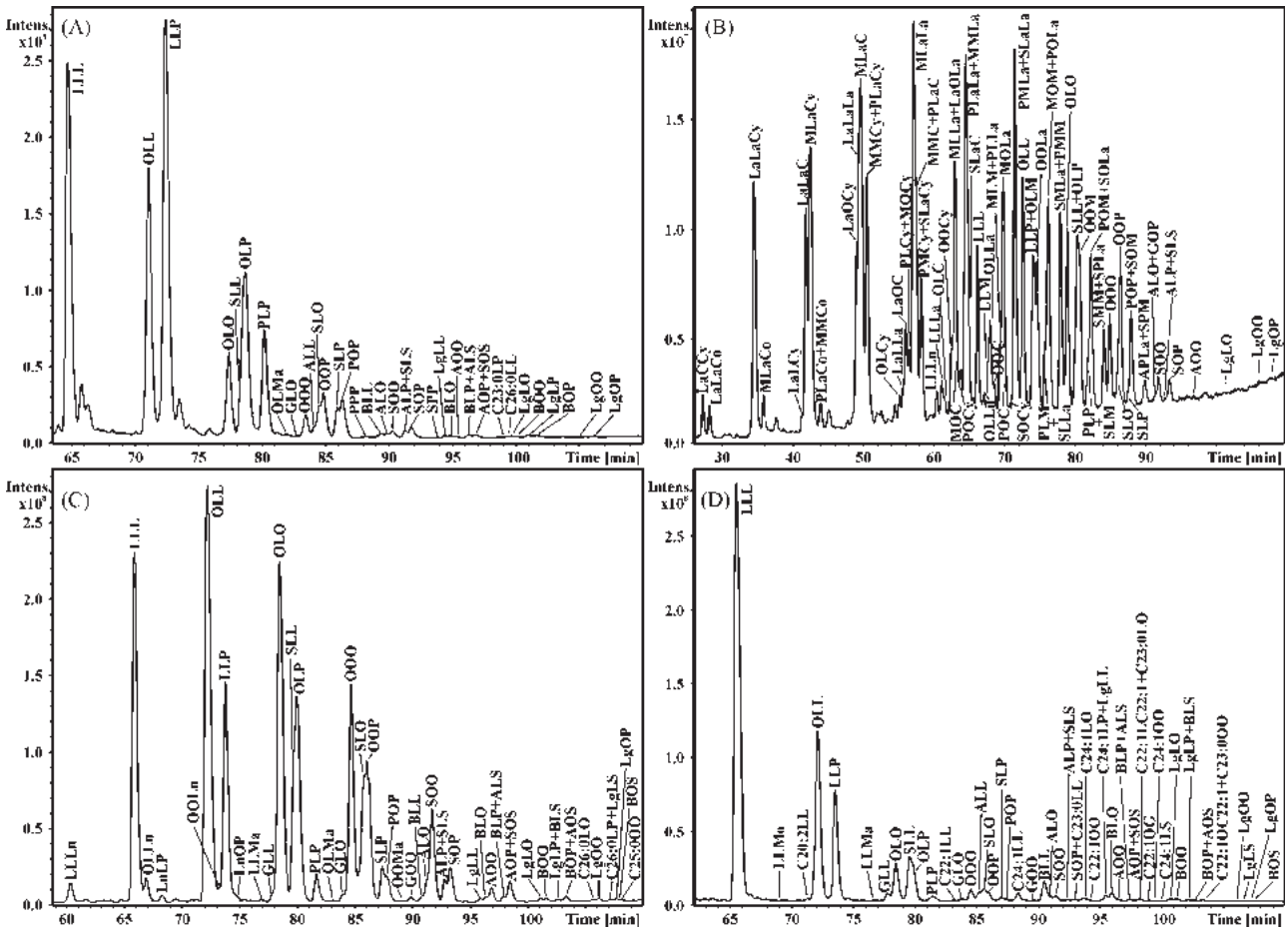

Fig. 1. NARP-HPLC/APCI-MS analysis of plant oils: (A) cottonseed (*Gossypium hirsutum*), (B) coconut (*Cocos nucifera*), (C) sesame (*Sesamum indicum*) and (D) safflower (*Carthamus tinctorius*).

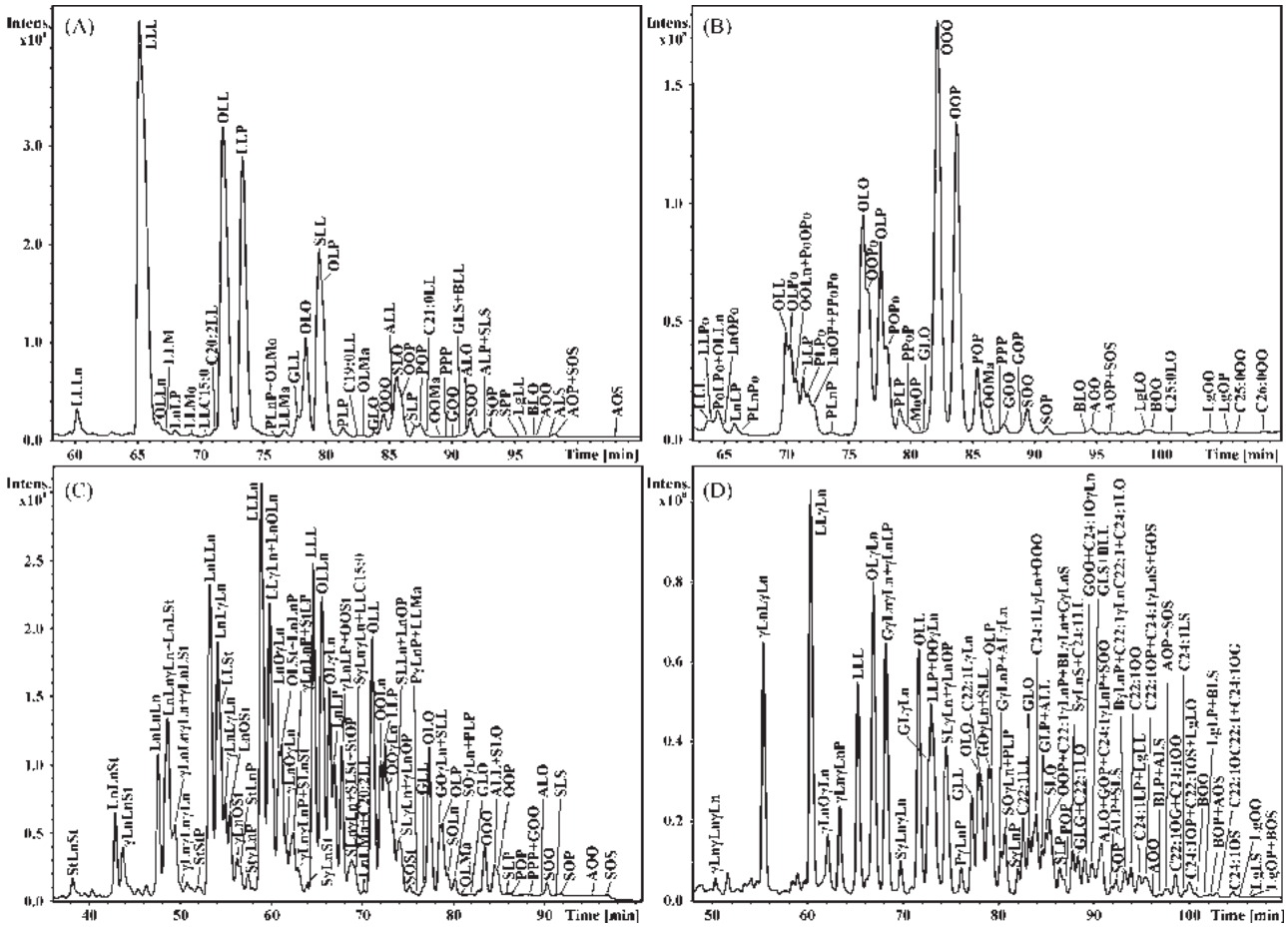

Fig. 2. NARP-HPLC/APCI-MS analysis of plant oils: (A) grape seed-red (*Vitis vinifera*), (B) avocado (*Persea americana*), (C) redcurrant (*Ribes rubrum*) and (D) borage (*Borago officinalis*).

showed very good reproducibility at least during several months of work. Each TG has been positively identified based on the agreement of retention times and the presence and relative abundances of characteristic ions in their APCI mass spectra, i.e. $[M+H]^+$ and $[M+H-R_iCOOH]^+$ ions. The DB positions are determined by the use of identical standards for common FAs, but in case of unusual FAs (e.g. C20:2, C22:1 and C24:1) the DB positions are deduced only from literature data without supporting experimental data.

3.2. APCI-MS profiling of triacylglycerol composition in natural mixtures

In analyzed samples, TGs have been identified using positive-ion APCI-MS based on both protonated molecules $[M+H]^+$ used for the molecular weight assignment and fragment ions $[M+H-R_iCOOH]^+$ used for the identification of individual FAs. The standard notation of TGs using initials of FA trivial names (Table 2) arranged according to their *sn*-1, *sn*-2 and *sn*-3 positions has been used. FAs in *sn*-1 and *sn*-3 positions cannot be resolved using NARP-HPLC/APCI-MS and they are considered as equivalent. FAs in these positions are arranged according to their decreasing molecular weights, for example TG containing oleic, palmitic and linoleic acids with linoleic acid in *sn*-2 position is designated as OLP but not PLO. Unlike to *sn*-1 and *sn*-3 positions, the FA in *sn*-2 position can be identified according to the ratio of fragment ions $[M+H-R_iCOOH]^+$, because the neutral loss of FA from the middle *sn*-2 position is less favored in comparison to *sn*-1 and *sn*-3 positions and therefore it provides the fragment ion with lower relative abundance than statistically expected. In nature, regioisomers are present in mixtures and relative abundances of fragment ions are composed from fragment ions of all isomers. Relative abundances of $[M+H-R_iCOOH]^+$ fragment ions also depend on the number of DBs and CNs, thus the precise determination of FA in *sn*-2 position can be achieved only by using regioisomeric standards, but not all of them are commercially available. Therefore, only predominant FAs in the *sn*-2 position are designated. In agreement with previously published data, the *sn*-2 position in plant oils is preferentially occupied by unsaturated FAs, mainly linoleic acid.

Properly optimized chromatographic conditions together with APCI-MS detection enable successful identification of the largest number of TG species in natural complex mixtures, for example 88 TGs identified in borage oil (comparing to 79 TGs reported in ref. [8]), 77 in blackcurrant oil (56 in ref. [8]), 66 in soybean oil (52 in ref. [22]; 39 in ref. [19]; 26 in ref. [16]; 12 in ref. [36]), 61 in evening primrose oil (39 in ref. [8]; 21 in ref. [19]), etc. Totally, 264 TG species have been unambiguously identified in 26 analyzed plant oils, which is the largest number of identified TGs reported so far.

3.3. APCI-MS quantitation of triacylglycerols

Our previously developed HPLC/APCI-MS method of quantitative analysis of TGs using RFs [25] has been applied for the quantitation of TGs in natural samples. Briefly, RFs of individual FAs (Table 2) are calculated from calibration parameters of 23 commercially available single-acid TG standards of $R_1R_1R_1$ type (i.e. single-acid saturated TGs from C7:0 to C22:0 and

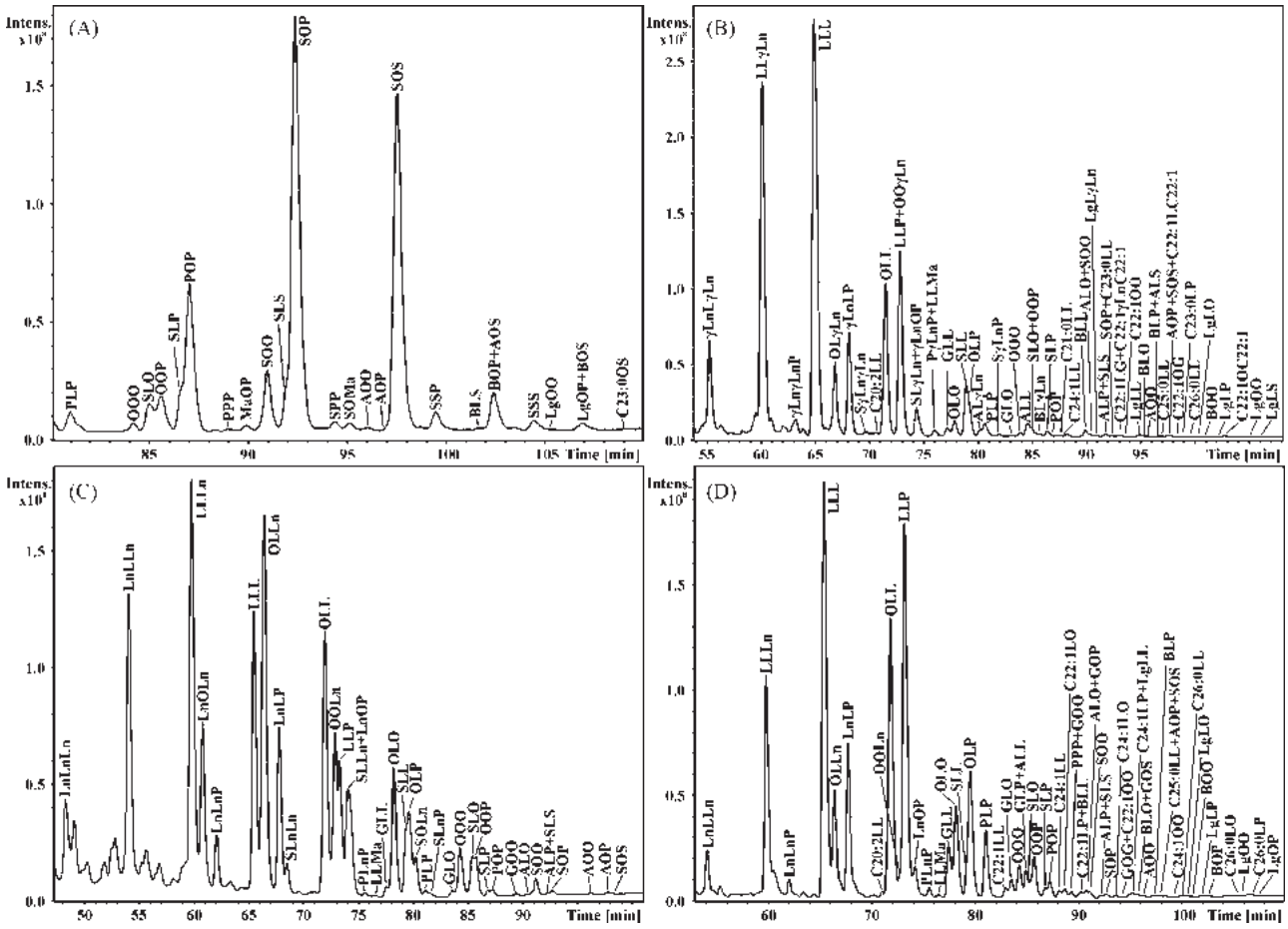

Fig. 3. NARP-HPLC/APCI-MS analysis of plant oils: (A) cocoa butter (*Theobroma cacao*), (B) evening primrose (*Oenothera biennis*), (C) kukui (*Aleurites moluccana*) and (D) wheat germ (*Triticum vulgare*).

unsaturated single-acid TGs C16:1, C18:1, C18:2, C18:3, γC18:3, C20:1 and C22:1) using the ratios of individual TGs calibration slopes to the calibration slope of triolein, for example $RF(LLL) = a_{LLL}/a_{OOO}$. RFs of mixed-acid TGs are calculated as the arithmetic mean of RFs of FAs present in TGs, for example RF(OLP) = (RF(OOO) + RF(LLL) + RF(PPP))/3. Single-acid TG standards from 9 identified trace FAs are not available, therefore their RFs have been approximated by the following way. RFs of saturated FAs, i.e. hexanoic (C6:0), tricosanoic (C23:0), tetracosanoic (C24:0), pentacosanoic (C25:0) and hexacosanoic (C26:0) acids, have been calculated from the equation $y = 2959\exp(-0.5134x) + 0.3824$ ($R^2 = 0.999$) corresponding to the dependence of RFs of 16 saturated TGs on their CNs, where y is RF and x is number of CNs. RF of stearidonic acid (C18:4) has been calculated from the equation corresponding to the dependence of RFs of unsaturated TGs with 18 CNs and 1 (OOO), 2 (LLL) and 3 (LnLnLn) DBs on the number of DBs, i.e. $y = 1.615\exp(-0.4904x)$ ($R^2 = 0.988$), where y is RF and x is number of DBs. RF values of monounsaturated palmitoleic (C16:1, RF = 1.33) and saturated palmitic (C16:0, 1.32) acids with the same CNs, gadoleic (C20:1, 0.36) and arachidic (C20:0, 0.40) acids, or erucic (C22:1, 0.42) and behenic (C22:0, 0.46) acids are very similar, therefore RFs of margaroleic (C17:1) and nervonic (C24:1) acids have been considered the same as their saturated analogues, i.e. RF(C17:1) = RF(C17:0) and RF(C24:1) = RF(C24:0). Similarly, RF of diunsaturated C20:2 acid has been considered the same as its monounsaturated analogue, i.e. RF(C20:2) = RF(C20:1). It should be emphasized that TGs containing these FAs are present in analyzed samples only at trace levels at maximum few tenth % with the exception of 1.49% nervonic acid in borage oil (Table 2). In all cases, FAs with approximated RFs form only one-third of mixed-acid TGs.

3.4. Triacylglycerol and fatty acid composition in analyzed samples

Table 1 lists HPLC/APCI-MS quantitative results of 264 TGs from the analysis of 26 plant oils important in different branches of nutrition and cosmetic industries. Identified TGs are composed of 28 FAs with 6–26 CNs and 0–4 DBs (Table 2). ECNs of all identified TGs range from 32 to 58. Only 6 TGs (PLP, OOO, OOP, POP, SOO and SOP) are detected in all samples. The number of TGs (Table 3) ranges from simple almond oil and cacao butter containing only 25 TGs to very complex blackcurrant oil with 77 TGs, redcurrant oil with 78 TGs or borage oil with 88 TGs. Identified TGs in analyzed samples can be divided into three main groups according to their concentrations. Usually about 5–6 TGs form the main constituents in each sample at the relative concentration level >5% (Table 3). From 6 (in almond and hazelnut oils) to 39 (in redcurrant and borage oils) TGs represent minor constituents with relative concentrations from 0.5 to 5.0%. Trace TG species (<0.5%) are present in a wide range from 9 TGs in cocoa butter up to 51 TGs in coconut oil.

As shown previously [25], FA composition calculated from TG composition using NARP-HPLC/APCI-MS is in a good agreement with FA composition from validated GC/FID analysis of fatty acid methyl esters after the transesterification of TGs by sodium methanoate. Therefore, FA composition of analyzed plant oils has been calculated directly from TG composition using HPLC/APCI-

Table 1
Relative concentrations [%] of all triacylglycerols identified in individual plant oils, their retention times t_R and equivalent carbon numbers

Triacylglycerol	t_R [min]	ECN	Palm	Rapeseed	Soybean	Sunflower	Peanut	Cotton	Coconut	Maize	Olive	Sesame	Almond[a]	Safflower	Grape seed—white
LaCCy	26.5	30							1.8						
LaLaCo	27.4								2.2						
LaLaCy	33.7	32							13.3						
MLaCo	35.0								3.1						
StLnSt	38.8														
LaLCy	40.5								0.5						
LaLaC	41.0	34							2.8						
MLaCy	41.6								15.2						
PLaCo	43.1								<0.1						
MMCo	43.1								0.8						
LnLnSt	43.5														
γLnLnSt	44.2														
LaOCy	48.2	36							6.2						
LnLnLn	48.3			0.1											
LaLaLa	48.6								3.5						
MLaC	49.0								1.8						
LnLnγLn	49.0														
LnLSt	49.4														
MMCy	49.6								4.0						
PLaCy	49.6								7.9						
γLnLnγLn	49.7														
γLnLSt	50.1														
γLnγLnγLn	50.6														
StStP	52.6														
LnLLn	54.0	38		0.7	2.3										
OLCy	54.3								1.0						
LnLγLn	54.7														
LaLLa	54.8								0.1						
LLSt	55.1														
LaOC	55.2								1.3						
γLnLγLn	55.4														
PLCy	55.5								0.5						
MOCy	55.7								1.9						
LnOSt	56.1														
MLaLa	56.2								1.9						
MMC	56.7								2.4						
PLaC	56.7								0.9						
γLnOSt	56.8														
StLnP	57.2														
PMCy	57.4								2.0						
SLaCy	57.4								4.7						
StγLnP	58.0														
LnLnC15:0	58.7	39													
LLLn	59.6	40		1.4	8.6				<0.1	1.6		0.4			0.9
LLLa	60.3								0.1						
LLγLn	60.4														
OLC	60.7								0.2						
LnOLn	60.8			3.0	1.3										
OOCy	61.5								1.9						
LnOγLn	61.6														
MLLa	61.8								0.1						
OLSt	61.9														
LaOLa	62.1								1.8						
LnLnP	62.1			0.6	0.9										
γLnOγLn	62.3														
MOC	62.4								0.2						
γLnLnP	62.8														
POCy	63.0								1.5						
StLP	63.1														
γLnγLnP	63.5														
PLaLa	63.7								0.8						
MMLa	63.7								1.7						
SLnSt	63.8														
SLaC	64.0								0.9						
SγLnSt	64.5														
LnLMo	63.3	41													
LnLnMa	65.6														

Table 1 (*Continued*)

Triacylglycerol	t_R [min]	ECN	Palm	Rapeseed	Soybean	Sunflower	Peanut	Cotton	Coconut	Maize	Olive	Sesame	Almond[a]	Safflower	Grape seed—white
LLL	65.3		0.3	1.2	13.9	24.5	4.6	17.0	0.1	17.5		11.0	3.3	43.3	25.8
LLPo	65.7														
PoLPo	66.2														
OLLn	66.4			8.3	7.1	0.4	0.6		<0.1	2.1		0.7			0.6
LnOPo	66.7														
LLM	66.8					0.6			0.1						0.3
GLnLn	66.8														
OLγLn	67.1														
OLLa	67.2								0.4						
OOC	67.7								0.2						
LnLP	67.8			1.6	6.1		0.2			1.0		0.3			0.2
PLnPo	68.2														
GγLnγLn	68.2														
MLM	68.5	42							0.1						
SLnLn	68.5				0.2										
γLnLP	68.5														
PLLa	68.6								0.2						
OOSt	68.6														
MOLa	68.9								1.1						
POC	69.2								0.3						
SLnγLn	69.2														
SLSt	69.6														
StOP	69.8														
SOCy	69.8								0.1						
SγLnγLn	69.9														
PMLa	70.5								1.7						
SLaLa	70.6								0.4						
LLMo	69.0				0.4	0.1				0.1			0.1	0.1	0.1
LLC15:0	70.3	43													0.1
LnLMa	70.7														
C20:2LL	70.8				0.2	0.1	0.1			0.1				0.1	0.1
OLL	71.8		1.0	7.3	12.9	21.4	16.2	14.3	0.3	22.1	3.1	17.2	13.9	19.8	21.5
GLLn	72.1														
OLPo	72.2										0.4				
OOLn	72.6			13.5	1.2						1.6	0.3			
PoOPo	72.7														
GLγLn	72.8														
LLP	73.1		2.7	1.4	13.3	12.1	6.3	28.7	0.2	16.0	1.2	8.5	4.0	13.6	15.4
OOγLn	73.3														
OLM	73.4		1.2						0.2						
PLPo	73.5														
SLLn	73.8				1.5										
OOLa	73.8								0.7						
LnOP	74.0	44	0.6	3.9	1.7					0.6	0.7	0.3			
PPoPo	74.1														
ALnLn	74.3														
SLγLn	74.5														
γLnOP	74.7														
PLM	74.9		0.7						0.1						
SLLa	75.0								<0.1						
MOM	75.3								0.4						
POLa	75.4								0.7						
PLnP	75.4		0.1	0.4	0.5					0.1					
SOSt	75.9														
PγLnP	76.1														
SMLa	77.0								0.5						
PMM	77.0								0.4						
OLMo	75.6					<0.1	0.1			<0.1			0.1		<0.1
LLMa	76.3	45			0.3	0.3	0.1			0.1		0.1	<0.1	0.1	0.3
MoLP	76.4						0.2						<0.1		
GLL	77.2			<0.1	0.2	0.3	1.2			0.4		0.2		0.5	0.6
OLO	77.9		2.5	15.7	5.3	7.3	14.3	4.8	0.3	10.7	10.0	15.2	20.1	4.8	8.0
C22:1LγLn	78.3														
OOPo	78.3			0.4							2.2				
GOγLn	78.8														
SLL	79.0				2.7	7.1	1.0	1.8	<0.1	1.8		2.1		2.9	5.4
OLP	79.3		9.0	4.4	5.6	6.3	8.1	12.1	0.3	8.7	5.3	9.7	11.8	3.9	8.9
ALLn	79.6														
OOM	79.7		1.7						0.4						
POPo	79.8										0.8				
SOLn	80.0			1.0	0.7						0.1				
BLnLn	80.1														
GγLnP	80.2	46													
ALγLn	80.3														

Table 1 (*Continued*)

Triacylglycerol	t_R [min]	ECN	Palm	Rapeseed	Soybean	Sunflower	Peanut	Cotton	Coconut	Maize	Olive	Sesame	Almond[a]	Safflower	Grape seed—white
SOγLn	80.7														
PLP	80.9		5.8	0.3	1.6	0.8	1.2	8.1	0.1	2.2	0.4	1.4	0.6	0.7	0.4
SLM	80.9								<0.1						
PPoP	81.3														
POM	81.3		3.9						0.4						
SOLa	81.3								0.2						
SLnP	81.4			0.1	0.3										
SγLnP	82.1														
SMM	83.1								0.2						
SPLa	83.1								0.1						
PPM	83.2		0.5												
OOMo	81.5						0.1				0.2		0.3		
C19:0LL	82.1					<0.1									<0.1
OLMa	82.3	47		<0.1	0.1	<0.1	0.1	0.1		<0.1		0.1	0.1		0.1
MoOP	82.7												0.2		
C23:0LnLn	82.9														
C22:1LL	82.5						0.2							<0.1	
GLO	83.1			0.8	0.1	0.1	1.5	<0.1		0.3	0.1	0.1	0.3	0.2	0.2
C24:1LγLn	83.7														
OOO	84.0		5.3	20.3	1.7	4.1	11.8	1.4	0.2	4.4	39.3	10.2	28.5	1.5	2.1
GLP	84.7				0.2		0.7			0.2					
ALL	84.8				0.2	0.6	0.4	0.2		0.5				0.5	0.3
BLLn	85.1				0.3										
SLO	85.1		1.2	0.6	1.7	3.5	1.2	1.1	<0.1	1.0		3.9	1.4	1.3	3.1
OOP	85.4		20.3	5.5	1.8	1.6	6.3	3.4	0.3	3.8	20.7	6.9	11.5	1.0	2.8
C22:1γLnP	85.5														
BLγLn	85.8	48													
GγLnS	85.9														
SLP	86.6		1.0	0.1	1.0	1.2	0.3	1.3	<0.1	0.4		1.2	0.1	0.4	0.3
ALnP	86.8														
SLnS	86.9														
POP	87.0		24.5	0.4	0.7	0.4	0.9	3.3	0.2	1.0	3.0	1.3	0.5	0.1	0.4
SOM	87.0								<0.1						
SγLnS	87.6														
PPP	88.7		5.3				0.1	0.1		0.1					<0.1
APLa	88.8								0.1						
SPM	88.9								<0.1						
C21:0LL	87.4						<0.1								<0.1
C25:0LnLn	88.3														
OOMa	88.4	49	0.1	0.3	<0.1		0.1					<0.1	0.1		<0.1
SLMa	89.3				<0.1										
MaOP	89.7		<0.1												
C24:1LL	87.9													0.5	
GLG	88.5														
C22:1LO	88.6						0.2								
GOO	89.0			1.4	<0.1	<0.1	1.4			0.1	0.7	0.2	0.1	<0.1	<0.1
C24:1OγLn	89.3														
C22:1LP	89.8														
GLS	89.9														<0.1
BLL	90.0			0.1	0.3	1.5	2.2	0.1		0.1	0.1	0.1		1.3	<0.1
LgLLn	90.2				0.1										
ALO	90.4		<0.1	0.2	0.1	0.3	0.6	0.1	<0.1	0.6	0.1	0.4	0.1	0.3	0.1
GOP	90.4		0.1	0.4			0.6		<0.1		0.2				
BOLn	90.6	50													
C24:1γLnP	90.6														
SOO	90.8		3.0	2.0	0.9	1.6	1.6	0.4	<0.1	0.5	5.9	3.9	2.6	0.5	1.2
LgLγLn	90.9														
ALP	91.8		0.2	<0.1	0.2	0.2	0.2	0.2	<0.1	0.2		0.3		<0.1	<0.1
SLS	91.9			<0.1	0.2	0.5	0.1	0.1	<0.1	0.1		0.3		0.1	0.1
BLnP	92.1														
ALnS	92.2														
SOP	92.3		5.7	0.2	0.2	0.3	0.3	0.7	<0.1	0.1	1.3	1.6	0.2	0.1	0.4
BγLnP	92.8														
SPP	94.4		1.4					<0.1							<0.1
C23:0LL	92.4				0.2	0.1	<0.1							0.1	<0.1
C23:0OLn	93.2	51													
SOMa	95.0														

Table 1 (*Continued*)

Triacylglycerol	t_R [min]	ECN	Palm	Rapeseed	Soybean	Sunflower	Peanut	Cotton	Coconut	Maize	Olive	Sesame	Almond[a]	Safflower	Grape seed—white
C22:1LG	93.1														
C22:1γLnC22:1	93.2														
C24:1LO	93.3			0.2										0.2	
GOG	93.9			<0.1											
C22:1OO	94.0						0.2							<0.1	
C24:1LP	94.6													<0.1	
LgLL	94.9			<0.1	0.1	0.4	1.0	0.1		0.2	<0.1	0.1		0.3	<0.1
C22:1OP	95.3														
BLO	95.5		0.1	0.3	0.2	0.8	2.8	0.1		0.2	0.1	0.1		0.7	<0.1
C24:1γLnS	95.6														
GOS	95.7	52													
LgOLn	95.8														
AOO	96.0		0.2	0.9	0.1	0.1	0.9	<0.1	<0.1	0.3	1.1	0.5	0.1	0.1	0.1
BLP	96.8		<0.1	<0.1	0.1	0.1	1.0	0.1		<0.1		<0.1		0.1	
ALS	96.9			<0.1	0.1	0.1		<0.1		<0.1		0.1		0.1	<0.1
LgLnP	97.1														
BLnS	97.2														
AOP	97.5		0.4	0.1	0.1		0.2	0.1		0.1	0.2	0.2		<0.1	0.1
SOS	97.6		0.4	0.1	0.1	0.2	0.1	0.1		0.1	0.2	0.6		0.1	0.1
APP	99.6		0.2												
SSP	99.7		0.1												
C25:0LL	97.4														
C23:0LO	97.9	53			<0.1	0.1								<0.1	
C21:0OO	98.4										<0.1				
C23:0LP	99.5				<0.1			<0.1							
C22:1LC22:1	97.7													0.1	
C22:1OG	98.7													<0.1	
C24:1OO	98.9			<0.1										<0.1	
C24:1LS	99.9													<0.1	
C26:0LL	100.1				<0.1	<0.1	0.2	<0.1							
C24:1OP	100.3														
C22:1OS	100.5														
LgLO	100.5	54	<0.1	0.1	0.1	0.2	1.6	<0.1	<0.1	0.2	0.1	0.1		0.2	
C26:0OLn	100.7														
BOO	101.0		0.1	0.5	0.1	0.4	2.3	<0.1		0.1	0.5	0.1		0.2	
LgLnS	101.8														
LgLP	101.9		<0.1	<0.1	0.1	0.1	0.4	0.1		0.1		<0.1		<0.1	
BLS	102.0				<0.1	0.1	0.3					<0.1		<0.1	
BOP	102.4		0.1	<0.1	0.1	<0.1	0.4	0.1			<0.1	0.1		<0.1	
AOS	102.6		0.1	<0.1	<0.1	<0.1	0.4				<0.1	0.1		<0.1	<0.1
SSS	104.6														
C25:0LO	102.6	55													
C23:0OO	103.3			<0.1		<0.1	<0.1				0.1			<0.1	
C22:1OC22:1	103.1													0.1	
C24:1OG	103.2														
C24:1OS	104.9														
C26:0LO	105.0						0.3					<0.1			
LgOO	105.5	56	0.1	0.2	<0.1	0.1	1.7	<0.1	<0.1	0.1	0.2	0.1		0.1	
C26:0LP	106.3				<0.1		0.1					<0.1			
LgLS	106.5				<0.1	<0.1	0.1					<0.1		<0.1	
LgOP	106.9		0.1	<0.1	<0.1	<0.1	0.3	<0.1	<0.1	0.1	<0.1	<0.1		<0.1	
BOS	107.0			<0.1	<0.1	<0.1	0.2					<0.1		<0.1	
C25:0OO	107.7	57									<0.1	<0.1			
C23:0OS	109.2														
C26:0OO	109.7	58					0.4				0.1				

Triacylglycerol	t_R [min]	ECN	Grape seed—red	Hazelnut[a]	Linseed	Poppy seed[a]	Walnut[a]	Avocado pear	Blackcurrant	Redcurrant	Borage	Cocoa butter	Evening primrose	Kukui oil	Wheat germ
LaCCy	26.5	30													
LaLaCo	27.4														
LaLaCy	33.7	32													
MLaCo	35.0														
StLnSt	38.8									0.1					
LaLCy	40.5														
LaLaC	41.0	34													
MLaCy	41.6														
PLaCo	43.1														
MMCo	43.1														
LnLnSt	43.5									0.8					
γLnLnSt	44.2									0.7					

Table 1 (*Continued*)

Triacylglycerol	t_R [min]	ECN	Grape seed—red	Hazelnut[a]	Linseed	Poppy seed[a]	Walnut[a]	Avocado pear	Blackcurrant	Redcurrant	Borage	Cocoa butter	Evening primrose	Kukui oil	Wheat germ
LaOCy	48.2														
LnLnLn	48.3				14.3		0.8		0.8	1.7				1.9	
LaLaLa	48.6														
MLaC	49.0														
LnLnγLn	49.0								0.9	1.0					
LnLSt	49.4	36							1.6	2.1					
MMCy	49.6														
PLaCy	49.6														
γLnLnγLn	49.7								0.9	0.4					
γLnLSt	50.1								0.8	0.7					
γLnγLnγLn	50.6								0.2	0.1	0.1				
StStP	52.6								0.2	0.1					
LnLLn	54.0				11.9		4.2		3.2	4.9				6.6	1.3
OLCy	54.3														
LnLγLn	54.7								3.6	2.9					
LaLLa	54.8														
LLSt	55.1								1.7	2.1					
LaOC	55.2														
γLnLγLn	55.4								2.0	0.9	3.6		3.4		
PLCy	55.5														
MOCy	55.7	38													
LnOSt	56.1								0.7	1.4					
MLaLa	56.2														
MMC	56.7														
PLaC	56.7														
γLnOSt	56.8								0.5	0.5					
StLnP	57.2								0.6	0.5					
PMCy	57.4														
SLaCy	57.4														
StγLnP	58.0								0.7	0.4					
LnLnC15:0	58.7	39			0.3										
LLLn	59.6		1.0		4.6	2.4	11.6		6.2	7.6				11.0	6.5
LLLa	60.3														
LLγLn	60.4								3.9	3.9	7.4		17.2		
OLC	60.7														
LnOLn	60.8				14.5		1.6		2.7	2.3				5.1	
OOCy	61.5														
LnOγLn	61.6								2.1	2.1					
MLLa	61.8														
OLSt	61.9								1.3	1.7					
LaOLa	62.1														
LnLnP	62.1	40			8.9		1.4		0.8	1.1				1.6	0.6
γLnOγLn	62.3								0.9	0.6	1.3				
MOC	62.4														
γLnLnP	62.8								1.5	0.7					
POCy	63.0														
StLP	63.1								1.5	1.4					
γLnγLnP	63.5								1.4	0.4	2.0		0.7		
PLaLa	63.7														
MMLa	63.7														
SLnSt	63.8								0.1	0.1					
SLaC	64.0														
SγLnSt	64.5									0.1					
LnLMo	63.3	41				0.2									
LnLnMa	65.6				0.1										
LLL	65.3		27.2	2.0	1.0	27.4	16.3	0.4	6.3	6.3	4.7		28.9	7.5	15.3
LLPo	65.7			0.1				0.3							
PoLPo	66.2							0.4							
OLLn	66.4		0.6	0.3	8.1	1.3	8.1	0.6	5.1	7.5				13.6	4.2
LnOPo	66.7							0.4							
LLM	66.8		0.4												
GLnLn	66.8				0.2										
OLγLn	67.1								4.8	4.0	7.9		4.5		
OLLa	67.2														
OOC	67.7														
LnLP	67.8		0.2		4.0	1.1	6.4	0.4	3.8	3.3				6.1	6.6
PLnPo	68.2							0.2							
GγLnγLn	68.2										0.2				
MLM	68.5	42													
SLnLn	68.5				4.3		0.3							0.6	
γLnLP	68.5								5.0	1.4	6.9		6.7		

Table 1 (*Continued*)

Triacylglycerol	t_R [min]	ECN	Grape seed—red	Hazelnut[a]	Linseed	Poppy seed[a]	Walnut[a]	Avocado pear	Blackcurrant	Redcurrant	Borage	Cocoa butter	Evening primrose	Kukui oil	Wheat germ
PLLa	68.6														
OOSt	68.6									2.0					
MOLa	68.9														
POC	69.2														
SLnγLn	69.2								0.2	0.2					
SLSt	69.6								0.2	0.4					
StOP	69.8								0.4	0.4					
SOCy	69.8														
SγLnγLn	69.9								0.3	0.1	0.5		0.1		
PMLa	70.5														
SLaLa	70.6														
LLMo	69.0		0.1			0.2	0.1								
LLC15:0	70.3	43	0.1							0.1					
LnLMa	70.7						0.1			<0.1					
C20:2LL	70.8		0.1			0.1	0.1		0.2	<0.1			0.1		0.1
OLL	71.8		20.7	7.6	2.0	18.5	13.2	3.3	6.7	7.2	7.2		10.4	10.2	13.5
GLLn	72.1								0.2						
OLPo	72.2			0.1				3.4							
OOLn	72.6			0.3	7.9		2.1	1.2	0.9	3.1				5.8	0.5
PoOPo	72.7							0.7							
GLγLn	72.8								0.5		1.4				
LLP	73.1		18.0	2.0	1.1	20.7	10.2	1.9	5.1	3.2	4.8		14.7	4.9	19.8
OOγLn	73.3								1.5	1.9	3.5		0.3		
OLM	73.4														
PLPo	73.5							1.7							
SLLn	73.8				1.7		1.4		0.4	0.9				2.5	
OOLa	73.8														
LnOP	74.0	44			4.2		1.8	1.0	1.3	1.1				2.7	1.8
PPoPo	74.1							0.4							
ALnLn	74.3				<0.1										
SLγLn	74.5								0.8	0.7	2.0		1.1		
γLnOP	74.7								2.3	0.9	3.2		0.4		
PLM	74.9														
SLLa	75.0														
MOM	75.3														
POLa	75.4														
PLnP	75.4		<0.1		0.4	<0.1	0.2	0.2						0.1	0.5
SOSt	75.9								0.1	0.2					
PγLnP	76.1								0.1	<0.1	0.9		0.2		
SMLa	77.0														
PMM	77.0														
OLMo	75.6		<0.1	0.1		0.1									
LLMa	76.3	45	0.2			0.3	0.1		<0.1	<0.1			0.2	<0.1	0.1
MoLP	76.4														
GLL	77.2		0.5		<0.1	0.2	0.2		0.6	0.1	1.8		0.4	0.2	1.4
OLO	77.9		5.9	17.1	2.0	8.0	6.2	10.3	3.7	4.2	3.5		1.3	5.9	5.2
C22:1LγLn	78.3										1.4				
OOPo	78.3			0.3				6.9							
GOγLn	78.8								0.3	<0.1	0.5				
SLL	79.0		5.6		0.3	3.6	2.0		0.9	0.9	2.0		2.6	1.3	1.1
OLP	79.3		8.3	7.0	0.6	7.9	4.0	9.4	2.3	2.0	3.8		1.9	3.8	7.1
ALLn	79.6								0.1						
OOM	79.7														
POPo	79.8			0.1				4.2							
SOLn	80.0				2.6		0.4			0.4				1.2	
BLnLn	80.1				0.1										
GγLnP	80.2	46									0.6				
ALγLn	80.3								0.1		0.2		0.2		
SOγLn	80.7								0.3	0.3	0.9				
PLP	80.9		0.6	0.4	<0.1	1.0	0.6	1.3	0.5	0.1	1.3	1.8	1.3	0.3	4.1
SLM	80.9														
PPoP	81.3							0.5							
POM	81.3														
SOLa	81.3														
SLnP	81.4				0.3		0.1							0.1	
SγLnP	82.1										0.5		0.1		
SMM	83.1														
SPLa	83.1														
PPM	83.2														

Table 1 (*Continued*)

Triacylglycerol	t_R [min]	ECN	Grape seed—red	Hazelnut[a]	Linseed	Poppy seed[a]	Walnut[a]	Avocado pear	Blackcurrant	Redcurrant	Borage	Cocoa butter	Evening primrose	Kukui oil	Wheat germ
OOMo	81.5			0.4											
C19:0LL	82.1		<0.1												
OLMa	82.3	47	0.1	0.1		0.1	<0.1		<0.1	<0.1					
MoOP	82.7			0.1				<0.1							
C23:0LnLn	82.9				<0.1										
C22:1LL	82.5										1.5				0.3
GLO	83.1		0.1	0.1	<0.1	0.1	0.1	<0.1	0.3	0.1	1.2		0.1	0.1	0.6
C24:1LγLn	83.7										0.7				
OOO	84.0		1.5	31.8	1.8	1.8	2.2	23.7	1.2	1.6	3.3	0.7	0.3	2.5	1.7
GLP	84.7										0.9				0.6
ALL	84.8		0.3			0.3	0.5		0.1	0.1	0.1		0.6		0.3
BLLn	85.1				<0.1										
SLO	85.1		2.7	1.2	0.1	1.6	1.3		0.7	0.5	1.3	0.7	0.4	1.1	0.3
OOP	85.4		2.5	18.5	1.2	1.5	1.2	20.2	0.9	0.8	2.2	3.9	0.2	1.9	2.7
C22:1γLnP	85.5										0.6				
BLγLn	85.8	48									0.2		0.1		
GγLnS	85.9										0.2				
SLP	86.6		0.4	0.5	0.1	0.4	0.3		0.1	0.1	0.8	1.9	0.4	0.2	0.3
ALnP	86.8				<0.1										
SLnS	86.9				0.1										
POP	87.0		0.9	1.8	0.2	0.4	0.2	4.2	0.2	0.1	0.6	16.6	0.1	0.3	1.2
SOM	87.0														
SγLnS	87.6										0.2				
PPP	88.7		<0.1					0.2		<0.1		0.1			0.1
APLa	88.8														
SPM	88.9														
C21:0LL	87.4		<0.1										<0.1		
C25:0LnLn	88.3				<0.1										
OOMa	88.4	49	<0.1	0.3	<0.1			<0.1							
SLMa	89.3														
MaOP	89.7											0.4			
C24:1LL	87.9										0.8		<0.1		0.2
GLG	88.5										0.2				
C22:1LO	88.6										0.7				0.2
GOO	89.0		<0.1	0.4	<0.1	<0.1	<0.1	0.3	0.1	<0.1	0.8			0.1	0.2
C24:1OγLn	89.3										0.4				
C22:1LP	89.8														0.1
GLS	89.9		<0.1				<0.1				0.4				
BLL	90.0		<0.1			<0.1	<0.1		0.1		0.4		0.3		0.1
LgLLn	90.2				<0.1										
ALO	90.4		0.1	0.2		0.1	0.1		0.1	<0.1	0.1		0.1	<0.1	0.1
GOP	90.4	50						0.3			0.5				0.2
BOLn	90.6				0.1										
C24:1γLnP	90.6										0.3				
SOO	90.8		1.0	5.4	0.8	0.4	0.4	1.0	0.3	0.4	1.6	4.4	<0.1	0.6	0.2
LgLγLn	90.9												<0.1		
ALP	91.8		<0.1		<0.1	0.1	0.1		<0.1		0.1		0.1	<0.1	<0.1
SLS	91.9		0.1		<0.1	<0.1	0.1		<0.1	<0.1	0.1	1.2	0.1	<0.1	<0.1
BLnP	92.1				<0.1										
ALnS	92.2				<0.1										
SOP	92.3		0.6	1.3	0.1	0.2	<0.1	0.3	0.1	0.1	0.6	36.4	<0.1	0.2	0.2
BγLnP	92.8										0.1				
SPP	94.4		<0.1									0.9			
C23:0LL	92.4								<0.1				<0.1		
C23:0OLn	93.2	51			<0.1										
SOMa	95.0											0.6			
C22:1LG	93.1												<0.1		
C22:1γLnC22:1	93.2										0.1		<0.1		
C24:1LO	93.3										0.5				0.1
GOG	93.9														<0.1
C22:1OO	94.0										1.0		<0.1		<0.1
C24:1LP	94.6										0.6				0.1
LgLL	94.9		<0.1			<0.1			<0.1		0.1		0.1		0.1
C22:1OP	95.3										0.6				
BLO	95.5		<0.1		<0.1			0.1	<0.1				0.1		0.1
C24:1γLnS	95.6										0.1				
GOS	95.7	52									0.2				<0.1
LgOLn	95.8				<0.1										
AOO	96.0		<0.1	0.4	<0.1		<0.1	0.2	<0.1	<0.1	0.1	0.2	0.1	<0.1	<0.1
BLP	96.8										<0.1		<0.1		0.1

Table 1 (*Continued*)

Triacylglycerol	t_R [min]	ECN	Grape seed—red	Hazelnut[a]	Linseed	Poppy seed[a]	Walnut[a]	Avocado pear	Blackcurrant	Redcurrant	Borage	Cocoa butter	Evening primrose	Kukui oil	Wheat germ
ALS	96.9		<0.1		<0.1						<0.1		<0.1		
LgLnP	97.1				<0.1										
BLnS	97.2				<0.1										
AOP	97.5		0.1	<0.1				<0.1			0.1	0.9	<0.1	<0.1	<0.1
SOS	97.6		0.1	0.1	0.1			<0.1		<0.1	0.1	23.5	<0.1	<0.1	<0.1
APP	99.6														
SSP	99.7											1.6			
C25:0LL	97.4												<0.1		<0.1
C23:0LO	97.9	53													
C21:0OO	98.4														
C23:0LP	99.5												<0.1		
C22:1LC22:1	97.7												0.1		
C22:1OG	98.7										0.3		<0.1		
C24:1OO	98.9										<0.1				<0.1
C24:1LS	99.9										0.1				
C26:0LL	100.1												<0.1		<0.1
C24:1OP	100.3										0.1				
C22:1OS	100.5										0.3				
LgLO	100.5	54			<0.1			0.1			0.1		<0.1		0.1
C26:0OLn	100.7				<0.1										
BOO	101.0				<0.1			0.1			0.1		<0.1		<0.1
LgLnS	101.8				<0.1										
LgLP	101.9										<0.1		<0.1		0.1
BLS	102.0										<0.1	0.1			
BOP	102.4				<0.1						<0.1	0.7			<0.1
AOS	102.6		<0.1		<0.1						<0.1	1.9			
SSS	104.6											0.7			
C25:0LO	102.6	55						<0.1							
C23:0OO	103.3														
C22:1OC22:1	103.1										0.1		0.1		
C24:1OG	103.2										0.1				
C24:1OS	104.9										0.2				
C26:0LO	105.0														<0.1
LgOO	105.5	56			<0.1			0.1			0.1	0.1	<0.1		<0.1
C26:0LP	106.3														<0.1
LgLS	106.5										<0.1		<0.1		
LgOP	106.9							<0.1			<0.1	0.3			<0.1
BOS	107.0										<0.1	0.4			
C25:0OO	107.7	57						<0.1							
C23:0OS	109.2											<0.1			
C26:0OO	109.7	58						0.1							

[a] Data from ref. [25].

MS (Table 2) to compare their FA profiles in individual samples. Analyzed samples are composed almost exclusively by FAs with 16 (palmitic and palmitoleic acids) and 18 (stearic, oleic, linoleic, linolenic, gamma-linolenic and stearidonic acids) carbon atoms with the total concentration in samples from 97.01% in palm oil to 99.82% in kukui oil. The lower concentrations of C16 and C18 FAs have been observed only in borage (91.86%) and peanut (90.81%) oils with higher concentration of FAs with long acyl chains (C20 and longer) and coconut oil (23.45%) with well-known high content of short-chain FAs (C6:0 to C14:0). The most abundant FAs present in all analyzed samples are palmitic acid (C16:0) with concentration from 5.76% in redcurrant oil to 40.57% in palm oil, stearic acid (C18:0) from 0.46% in avocado oil to 34.51% in cocoa butter, oleic acid (C18:1) from 7.66% in evening primrose oil to 73.85% in olive oil, linoleic acid (C18:2) from 1.89% in cocoa butter to 73.96% in safflower oil and arachidic acid (C20:0) from 0.03% in coconut oil to 1.05% in cocoa butter.

3.5. Nutritional parameters of analyzed plant oils

Physical and nutritional properties of plant oils are given by FA composition in TGs. Various contents of saturated and unsaturated FAs in TG mixtures result in their different melting points under room temperature (oils vs. fats), oxidation stability, digestion or relation to the harmful low-density lipoprotein (LDL) cholesterol. The average composition of FAs can be expressed by average parameters calculated from TG composition in individual samples (Table 3). Values of calculated average parameters can be compared with values of relevant parameters of FAs, i.e. ECN = 16, CN = 18 and DB = 1 for oleic acid (C18:1), etc. For example, aECN = 15.88, aCN = 17.76 and aDB = 0.94 for olive oil correspond to the high content of oleic acid with 18 CNs and 1 DB, in fact with the total content of oleic acid 73.85%. Other example of aECN = 14.21, aCN = 17.82 and aDB = 1.81 for evening primrose oil corresponds to the high content of linoleic acid with 18 CNs and 2 DBs, in fact with the total content of linoleic acid 67.49%. aECN values of analyzed samples range from 14 to 16 with several exceptions. Coconut oil with aECN = 12.10 is typical by high content of short-chain FAs with the low ECN value. Lower aECN values of linseed (aECN = 13.68), redcurrant (13.82) and blackcurrant (13.91) oils are caused by high content of linolenic acid (ECN = 12) or linolenic and gamma-linolenic (ECN = 12) acids in case of blackcurrant and redcurrant oils. In contrast, the higher value of cocoa butter (aECN = 16.72) results from the high content of stearic acid with ECN = 18. Plant oils are composed predominantly by FAs

Table 2
Relative concentrations [%] of individual fatty acids in analyzed plant oils calculated from HPLC/APCI-MS of triacylglycerols with their response factors (RF)

Fatty acid	Symbol	CN:DB	RF	Palm	Rape	Soybean	Sunflower	Peanut	Cotton	Coconut	Maize	Olive	Sesame	Almond[a]	Safflower	Grape seed—white
Caproic	Co	6:0	134.76							1.37						
Caprylic	Cy	8:0	74.44							15.60						
Capric	C	10:0	17.62							3.70						
Lauric	La	12:0	6.04							37.05						
Myristic	M	14:0	2.77	2.36			0.18			18.80						0.08
–	C15:0	15:0	1.75													0.03
Palmitoleic	Po	Δ9–16:1	1.33		0.13							1.10				
Palmitic	P	16:0	1.32	40.57	6.51	11.66	7.69	9.47	22.12	7.33	11.95	11.75	10.86	9.47	6.60	9.40
Margaroleic	Mo	Δ9–17:1	0.81			0.12	0.06	0.12			0.04	0.08		0.23	0.02	0.05
Margaric	Ma	17:0	0.81	0.03	0.09	0.13	0.11	0.08	0.02		0.04		0.05	0.09	0.03	0.12
Stearidonic	St	Δ6,9,12,15–18:4	0.23													
α-Linolenic	Ln	Δ9,12,15–18:3	0.40	0.23	12.87	12.52	0.14	0.27		0.01	1.73	0.77	0.63			0.60
γ-Linolenic	γLn	Δ6,9,12–18:3	0.29													
Linoleic	L	Δ9,12-C18:2	0.57	10.26	19.21	51.76	61.52	35.63	57.27	2.20	55.99	8.53	41.52	27.03	73.96	63.20
Oleic	0	Δ9-C18:1	1.00	41.36	57.67	19.18	22.94	43.50	18.15	10.73	27.41	73.85	40.91	61.65	15.15	22.21
Stearic	S	18:0	0.61	4.59	1.46	3.41	5.15	1.94	1.93	3.18	1.44	2.57	4.95	1.43	1.86	3.69
–	C19:0	19:0	0.49				<0.01									0.01
–	C20:2	Δ11,14–20:2	0.36			0.05	0.03	0.04			0.02				0.04	0.04
Gadoleic	G	Δ9–20:1	0.36	0.05	0.97	0.16	0.15	1.90	0.01	<0.01	0.34	0.34	0.16	0.04	0.25	0.28
Arachidic	A	20:0	0.40	0.38	0.45	0.32	0.49	0.92	0.25	0.03	0.65	0.49	0.59	0.06	0.40	0.25
–	C21:0	21:0	0.39					0.02				0.01				0.01
Erucic	C22:1	Δ13–22:1	0.42					0.22							0.12	
Behenic	B	22:0	0.46	0.07	0.40	0.42	1.14	3.49	0.15		0.16	0.28	0.19		0.95	0.02
–	C23:0	23:0	0.40		0.02	0.08	0.06	0.03	0.01			0.04			0.05	<0.01
Nervonic	C24:1	Δ15–24:1	0.40		0.08										0.33	
Lignoceric	Lg	24:0	0.40	0.10	0.14	0.18	0.33	1.99	0.08	<0.01	0.23	0.16	0.13		0.24	0.01
–	C25:0	25:0	0.39									0.01	<0.01			
Cerotic	C26:0	26:0	0.39			0.01	0.01	0.38	0.01			0.02	0.01			

Fatty acid	Symbol	CN:DB	Grape seed—red	Hazelnut[a]	Linseed	Poppy seed[a]	Walnut[a]	Avocado pear	Blackcurrant	Redcurrant	Borage	Cocoa butter	Evening primrose	Kukui oil	Wheat germ
Caproic	Co	6:0													
Caprylic	Cy	8:0													
Capric	C	10:0													
Lauric	La	12:0													
Myristic	M	14:0	0.13												
–	C15:0	15:0	0.03		0.08					0.03					
Palmitoleic	Po	Δ9–16:1		0.20				6.52							
Palmitic	P	16:0	10.50	10.60	6.90	10.95	8.67	16.75	9.23	5.76	10.97	27.03	9.02	7.29	16.52
Margaroleic	Mo	Δ9–17:1	0.03	0.18		0.16	0.04	0.01							
Margaric	Ma	17:0	0.10	0.10	0.04	0.12	0.07	0.01	0.03	0.03		0.32	0.06	0.01	0.02
Stearidonic	St	Δ6,9,12,15–18:4							3.54	5.32					
α-Linolenic	Ln	Δ9,12,15–18:3	0.61	0.19	52.32	1.68	16.59	1.32	15.80	20.10				25.56	8.06
γ-Linolenic	γLn	Δ6,9,12–18:3							13.73	9.20	18.41		13.04		
Linoleic	L	Δ9,12-C18:2	65.07	17.61	15.89	66.05	52.69	13.48	37.86	36.34	35.42	1.89	67.49	39.36	54.85
Oleic	0	Δ9-C18:1	19.36	67.83	20.82	18.58	19.34	60.98	17.29	21.20	22.88	34.58	7.66	24.95	17.81
Stearic	S	18:0	3.63	2.91	3.65	2.10	2.19	0.46	1.52	1.86	4.18	34.51	1.71	2.66	0.76
–	C19:0	19:0	0.01												
–	C20:2	Δ11,14–20:2	0.05			0.04	0.02		0.07	0.02			0.04		0.05
Gadoleic	G	Δ9–20:1	0.24	0.18	0.11	0.12	0.15	0.20	0.73	0.09	3.37		0.17	0.13	1.11
Arachidic	A	20:0	0.21	0.20	0.06	0.17	0.24	0.07	0.16	0.05	0.28	1.05	0.36	0.04	0.21
–	C21:0	21:0	0.01										0.01		
Erucic	C22:1	Δ13–22:1									2.53		0.15		0.21
Behenic	B	22:0	0.02		0.09	0.01	<0.01	0.06	0.03		0.35	0.45	0.16		0.12
–	C23:0	23:0			0.01				<0.01			0.01	0.02		
Nervonic	C24:1	Δ15–24:1									1.49		0.01		0.13
Lignoceric	Lg	24:0	<0.01		0.03	0.02		0.10	0.01		0.12	0.16	0.09		0.10
–	C25:0	25:0			<0.01			0.02					<0.01		0.01
Cerotic	C26:0	26:0						0.02					0.01		0.04

[a] Data processed from ref. [25].

Table 3
Number of identified triacylglycerols and fatty acids, average parameters, the relative concentration of essential fatty acids [%] (linoleic and linolenic acids) and of saturated (Sat), monounsaturated (Mono) and polyunsaturated (Poly) fatty acids [%] in all analyzed oils calculated from NARP-HPLC/APCI-MS results

Plant	Number of TGs/FAs	Major TGs (>5%)	aECN	aCN	aDB	Essential FAs [%]	Sat [%]	Mono [%]	Poly [%]
Oil palm	41/11	POP,OOP,OLP,PLP,SOP,OOO,PPP	15.85	17.07	0.61	10.49	48.10	41.41	10.49
Rape	55/13	OOO,OLO,OOLn,OLLn,OLL,OOP	15.20	17.91	1.36	32.08	9.07	58.85	32.08
Soybean	66/14	LLL,LLP,OLL,LLLn,LnLP,OLP,OLO	14.59	17.79	1.60	64.28	16.21	19.46	64.33
Sunflower	50/16	LLL,OLL,LLP,OLO,SLL,OLP	14.97	17.90	15.16	61.66	15.16	23.15	61.69
Peanut	60/16	OLL,OLO,OOO,OLP,LLP,OOP	15.69	18.05	1.18	35.90	18.32	45.74	35.94
Cotton	38/11	LLP,LLL,OLL,OLP,PLP	14.93	17.55	1.31	57.27	24.57	18.16	57.27
Coconut palm	85/13	MLaCy,LaLaCy,PLaCy,LaOCy	12.10	12.36	0.13	2.21	87.06	10.73	2.21
Maize	46/12	OLL,LLL,LLP,OLO,OLP	14.90	17.78	1.44	57.72	14.4	27.79	57.74
Olive	37/15	OOO,OOP,OLO,SOO,OLP	15.88	17.76	0.94	9.30	15.33	75.37	9.30
Sesame	49/12	OLL,OLO,LLL,OOO,OLP,LLP,OOP	15.29	17.79	1.25	42.15	16.78	41.07	42.15
Almond[a]	25/8	OOO,OLO,OLL,OLP,OOP	15.49	17.80	1.15	27.03	11.05	61.92	27.03
Safflower	55/14	LLL,OLL,LLP	14.67	17.94	1.63	73.96	10.13	15.87	74.00
Grape vine white	46/17	LLL,OLL,LLP,OLP,OLO,SLL	14.81	17.81	1.50	63.80	13.62	22.54	63.84
Grape vine red	46/16	LLL,OLL,LLP,OLP,OLO,SLL	14.77	17.78	1.51	65.68	14.64	19.63	65.73
Hazel[a]	30/10	OOO,OOP,OLO,OLL,OLP,SOO	15.70	17.77	1.04	17.80	13.81	68.39	17.80
Linseed (Flax)	63/13	LnOLn,LnLnLn,LnLLn,LnLnP,OLLn,OOLn	13.68	17.86	2.09	68.21	10.86	20.93	68.21
Opium poppy[a]	33/12	LLL,LLP,OLL,OLO,OLP	14.67	17.77	1.55	67.73	13.37	18.86	67.77
Walnut[a]	43/11	LLL,OLL,LLLn,LLP,OLLn,LnLP,OLO	14.34	17.82	1.74	69.28	11.17	19.53	69.30
Avocado pear	44/14	OOO,OOP,OLO,OLP,OOPo	15.57	17.52	0.97	14.80	17.49	67.71	14.80
Blackcurrant	77/14	OLL,LLL,LLLn,OLLn,LLP,γLnLP	13.91	17.82	1.94	53.66	10.98	18.02	71.00
Redcurrant	78/12	LLLn,OLLn,OLL,LLL	13.82	17.88	2.00	56.44	7.73	21.29	70.98
Borage	88/11	OLγLn,LLγLn,OLL,γLnLP	14.90	17.98	1.56	35.42	15.90	30.27	53.83
Cacao	25/9	SOP,SOS,POP	16.72	17.47	0.37	1.89	63.53	34.58	1.89
Evening primrose	61/17	LLL,LLγLn,LLP,OLL,γLnLP	14.21	17.82	1.81	67.49	11.44	7.99	80.57
Kukui nut tree	38/8	OLLn,LLLn,OLL,LLL,LnLLn,LnLP,OLO,OOLn,LnOLn	14.25	17.85	1.80	64.92	10.00	25.08	64.92
Wheat germ	61/15	LLP,LLL,OLL,OLP,LnLP,LLLn,OLO	14.67	17.70	1.51	62.91	17.78	19.26	62.96

[a] Data processed from ref. [25].

with 18 CNs which also correspond to aCN ranging from 17.40 to 18.00 in plant oils. Exceptions are found for coconut oil (aCN = 12.10) with the high content of short-chain FAs, palm oil (aCN = 17.07) with the high content of palmitic acid or peanut oil (aCN = 18.05) with the higher content of long-chain FAs from C20 to C24. The content of saturated and unsaturated FAs in samples is a valuable nutritional parameter in human diet. In analyzed samples, aDB range from 0.9 to 1.9 except for highly saturated coconut (aDB = 0.13), cacao butter (0.37) and palm (0.61) oils or highly unsaturated blackcurrant oil (1.94), redcurrant oil (2.00) and linseed oil (2.09).

Other important nutritional parameters of analyzed plant oils are expressed by the sums of essential, saturated, monounsaturated and polyunsaturated FAs (Table 3). FAs with DBs positions Δ12 and Δ15 (ω3 and wω6 FAs) are essential for human and have to be obtained by food, therefore their content in plant oils correlates with the nutritional value of these oils. The sum of essential FAs in most samples is found in the wide interval from 10 to 70%, except for 1.89% in cacao butter, 2.21% in coconut oil, 9.3% in olive oil and 73.96% in highly essential safflower oil. The sum of saturated FAs in analyzed plant oils ranges from 10 to 25% in common plant oils except 7.73% in redcurrant oil, 9.07% in rapeseed oil or highly saturated oils with 48.10% of saturated FAs in palm oil, 63.53% in cocoa butter and 87.06% in coconut oil. In analyzed samples, the sum of monounsaturated FAs is in the range from 15 to 65% except for 7.99% in evening primrose oil, 10.73% in coconut oil, 67.71% in avocado oil, 68.39% in hazelnut oil and 75.37% in olive oil. The sum of polyunsaturated FAs range from 10 to 70% in samples except for 1.89% in cocoa butter, 2.21% in coconut oil, 9.30% in olive oil, 70.98% in redcurrant oil, 71.00% in blackcurrant oil, 74.00% in safflower oil and 80.57% in evening primrose oil.

4. Conclusions

This work reports the quantitation of TGs in 26 plant oils important in food, nutrition and cosmetic industries according to the ref. [4]. The APCI-MS quantitation is based on the use of response factors calculated according to the calibration slopes of standards of individual single-acid TGs. This method is based on optimized NARP-HPLC separation providing the highest separation selectivity, as demonstrated by the fact that the number of positively identified TGs in our works is significantly higher than reported by others including two-dimensional separations. This is the first case when both intact TGs identification/quantitation and total/average FA profiles are reported and compared with the assessment of nutritional parameters of individual plant oils. Chromatograms are used as fingerprints (i.e. qualitative aspect) of individual oils in contrast to Table 1 showing precise quantitative composition including low abundant TGs. Table 2 presents quantitative results of FAs identified in TGs, while Table 3 summarizes average parameters to explored obtained data from different points of view.

Acknowledgments

This work was supported by the grant project No. MSM0021627502 sponsored by the Ministry of Education, Youth and Sports of the Czech Republic and projects Nos. 203/06/0219 and 203/08/1536 sponsored by the Czech Science Foundation.

References

[1] FEDIOL, The EU Oil and Proteinmeal Industry, Brussels, 2008, http://www.fediol.be, downloaded on 7 February 2008.
[2] F.D. Gunstone, Modifying Lipids for Use in Food, Woodhead Publishing, Cambridge, 2006.
[3] Food and Agricultural Organization of the United Nations (FAO), Rome, 2008, http://www.fao.org, downloaded on 1 February 2008.
[4] Cyberlipid center, C. Leray, Paris, 2008, http://www.cyberlipid.org, downloaded on 7 February 2008.
[5] W.W. Christie, J. Chromatogr. 454 (1988) 273.
[6] B. Nikolova-Damyanova, W.W. Christie, B.G. Herslöf, J. Chromatogr. A 694 (1995) 375.

[7] P.J.W. Schuyl, T. de Joode, M.A. Vasconcellos, G. Duchateau, J. Chromatogr. A 810 (1998) 53.
[8] P. Laakso, P. Voutilainen, Lipids 31 (1996) 1311.
[9] R.O. Adlof, A. Menzel, V. Dorovska-Taran, J. Chromatogr. A 953 (2002) 293.
[10] R. Adlof, G. List, J. Chromatogr. A 1046 (2004) 109.
[11] R.O. Adlof, J. High Resolut. Chromatogr. 18 (1995) 105.
[12] P. Février, A. Binet, L. Dufossé, R. Grée, F. Yvergnaux, J. Chromatogr. A 923 (2001) 53.
[13] M.B. Macher, A. Holmqvist, J. Sep. Sci. 24 (2001) 179.
[14] P. Kalo, A. Kemppinen, V. Ollilainen, A. Kuksis, Int. J. Mass Spectrom. 229 (2003) 167.
[15] S. Héron, A. Tchapla, Finger Prints of Triacylglycerols From Oils and Fats by HPLC Isocratic Elution and Evaporative Light Scattering Detection (brochure), ELSD Sedex 45, Sedere, Alfortville, France, 1994.
[16] W.C. Byrdwell, E.A. Emken, W.E. Neff, R.O. Adlof, Lipids 31 (1996) 919.
[17] P. Laakso, J. Am. Oil Chem. Soc. 74 (1997) 1291.
[18] J.T. Lin, C.L. Woodruff, T.A. McKeon, J. Chromatogr. A 782 (1997) 41.
[19] H.R. Mottram, S.E. Woodbury, R.P. Evershed, Rapid Commun. Mass Spectrom. 11 (1997) 1240.
[20] M. Holčapek, P. Jandera, J. Fischer, B. Prokeš, J. Chromatogr. A 858 (1999) 13.
[21] H.R. Mottram, Z.M. Crossman, R.P. Evershed, Analyst 126 (2001) 1018.
[22] M. Holčapek, P. Jandera, P. Zderadička, L. Hrubá, J. Chromatogr. A 1010 (2003) 195.
[23] J.S. Perona, V. Ruiz-Gutierrez, J. Chromatogr. B 785 (2003) 89.
[24] S. Momchilova, K. Tsuji, Y. Itabashi, B. Nikolova-Damyanova, A. Kuksis, J. Sep. Sci. 27 (2004) 1033.
[25] M. Holčapek, M. Lísa, P. Jandera, N. Kabátová, J. Sep. Sci. 28 (2005) 1315.
[26] M. Lísa, M. Holčapek, Chem. Listy 99 (2005) 195.
[27] M. Lísa, M. Holčapek, T. Řezanka, N. Kabátová, J. Chromatogr. A 1146 (2007) 67.
[28] M. Lísa, F. Lynen, M. Holčapek, P. Sandra, J. Chromatogr. A 1176 (2007) 135.
[29] J.D.J. van den Berg, N.D. Vermist, L. Carlyle, M. Holčapek, J.J. Boon, J. Sep. Sci. 27 (2004) 181.
[30] M. Holčapek, P. Jandera, J. Fischer, Crit. Rev. Anal. Chem. 31 (2001) 53.
[31] K. Aitzetmuller, M. Gronheim, J. High Resolut. Chromatogr. 15 (1992) 219.
[32] S. Héron, M.G. Maloumbi, M. Dreux, E. Verette, A. Tchapla, J. Chromatogr. A 1161 (2007) 152.
[33] A. Cascone, S. Eerola, A. Ritieni, A. Rizzo, J. Chromatogr. A 1120 (2006) 211.
[34] R.A. Moreau, Lipids 41 (2006) 727.
[35] J. Cvačka, E. Krafková, P. Jiroš, I. Valterová, Rapid Commun. Mass Spectrom. 20 (2006) 3586.
[36] A. Jakab, K. Heberger, E. Forgács, J. Chromatogr. A 976 (2002) 255.
[37] A. Jakab, I. Jablonkai, E. Forgács, Rapid Commun. Mass Spectrom. 17 (2003) 2295.
[38] L. Fauconnot, J. Hau, J.M. Aeschlimann, L.B. Fay, F. Dionisi, Rapid Commun. Mass Spectrom. 18 (2004) 218.

6888 J. Agric. Food Chem. 2009, 57, 6888–6898
DOI:10.1021/jf901189u

JOURNAL OF AGRICULTURAL AND FOOD CHEMISTRY
ARTICLE

Statistical Evaluation of Triacylglycerol Composition in Plant Oils Based on High-Performance Liquid Chromatography−Atmospheric Pressure Chemical Ionization Mass Spectrometry Data

Miroslav Lísa,[†] Michal Holčapek,*[,†] and Michal Boháč[‡]

[†]University of Pardubice, Faculty of Chemical Technology, Department of Analytical Chemistry, Studentská 573, 53210 Pardubice, Czech Republic, and [‡]Bruker Daltonics, s.r.o., Zdráhalova 1753/10, 61300 Brno, Czech Republic

The statistical evaluation of triacylglycerol profiles in plant oils based on high-performance liquid chromatography mass spectrometry (HPLC/MS) analysis enables the differentiation of various plant oils on the basis of the multidimensional data matrix. A data set of 93 oil samples from 60 varieties of plants composed from 355 triacylglycerols is evaluated using the principal component analysis. Analyzed samples are resolved in the principal component analysis plot, and similarities among some types of plant oils are visualized by the formation of clusters. The authentication of plant oils is tested with model samples of olive oil adulterated with sunflower oil at different concentration levels. Our HPLC/MS method using the statistical multivariate data analysis of a large data matrix enables a clear identification of adulterated olive oils already from 1% of added sunflower oil as an adulterant.

KEYWORDS: High-performance liquid chromatography; mass spectrometry; atmospheric pressure chemical ionization; triacylglycerol; plant oil; adulteration; authentication; statistics; principal component analysis

INTRODUCTION

Plant oils are an important commodity in world markets because of their widespread utilization in many branches of industry, cosmetics, and nutrition. They are produced from oil plants representing almost 10% of the world production of all crops according to the Food and Agriculture Organization of the United Nations (*1*). The annual production of edible plant oils has increased in the past decade by more than 50% to 127 million tonnes a year (*1*) and is still increasing annually. Edible plant oils are mixtures of lipids composed mainly from triacylglycerols (TGs) with the content up to 95%. They serve as an important source of fatty acids in the human diet, mainly essential fatty acids necessary for the biosynthesis of long-chain polyunsaturated fatty acids important for the synthesis of cell membranes in the human body. A diet with 70 g of fat per day for female adults and 90 g for male adults corresponding to 30−35% of daily energy coming from fats is now considered as consistent with good health (*2*). In reality, the consumption of oils and fats in USA and EU is about 130 g per day per person (*3*).

Prices of plant oils are given by many parameters, mainly by the production cost and the quality of plant oils. Higher prices of high-quality plant oils can lead to the effort of falsification by cheaper oils with a lower quality and less beneficial nutritional properties (e.g., expensive virgin olive oil adulterated by cheaper sunflower oil); therefore, their authentication is of great interest nowadays. Many authentication methods use the measurement of oil fingerprints without any separation and sample pretreatment steps, e.g., Raman spectroscopy (*4*, *5*), infrared spectroscopy (*6*, *7*), nuclear magnetic resonance spectroscopy (*8*, *9*), matrix-assisted laser desorption/ionization mass spectrometry (MS) (*10*, *11*), electrospray ionization (ESI) MS (*12*, *13*), atmospheric pressure photoionization MS (*13*), and so forth. Although the fingerprint methods are fast and simple, some plant oils have similar fingerprints differing only in low concentration components not detectable this way. TGs are compounds suitable for the authentication of plant oils because they are the main components of plant oils with several tens of different species occurring at different concentration levels. They are characterized by fatty acids esterified on the glycerol skeleton and their properties, i.e., carbon number (CN), double bond (DB) number, the configuration and position of DBs in acyl chains, and the stereochemical position of fatty acids on the glycerol skeleton. TG profiles differ for each type of plant oil which is used for authentication based on chromatographic separation, i.e., gas chromatography/isotopic ratio mass spectrometry (*14*), gas chromatography/flame ionization detection (GC/FID) (*15*, *16*), high-performance liquid chromatography (HPLC)/refractive-index detection (*17*), HPLC/atmospheric pressure chemical ionization (APCI) MS (*10*, *18*−*20*), and off-line two-dimensional HPLC/MS (*21*).

The highest number of identified TGs in plant oils have been reported using nonaqueous reversed-phase (NARP) HPLC with APCI-MS detection (*22*, *23*). In NARP-HPLC mode, TGs are separated according to the equivalent carbon number (ECN)

*Corresponding author. Department of Analytical Chemistry, Faculty of Chemical Technology, University of Pardubice, Studentská 573, 53210 Pardubice, Czech Republic. Tel: +420466037087. E-mail: Michal.Holcapek@upce.cz.

 Published on Web 07/09/2009

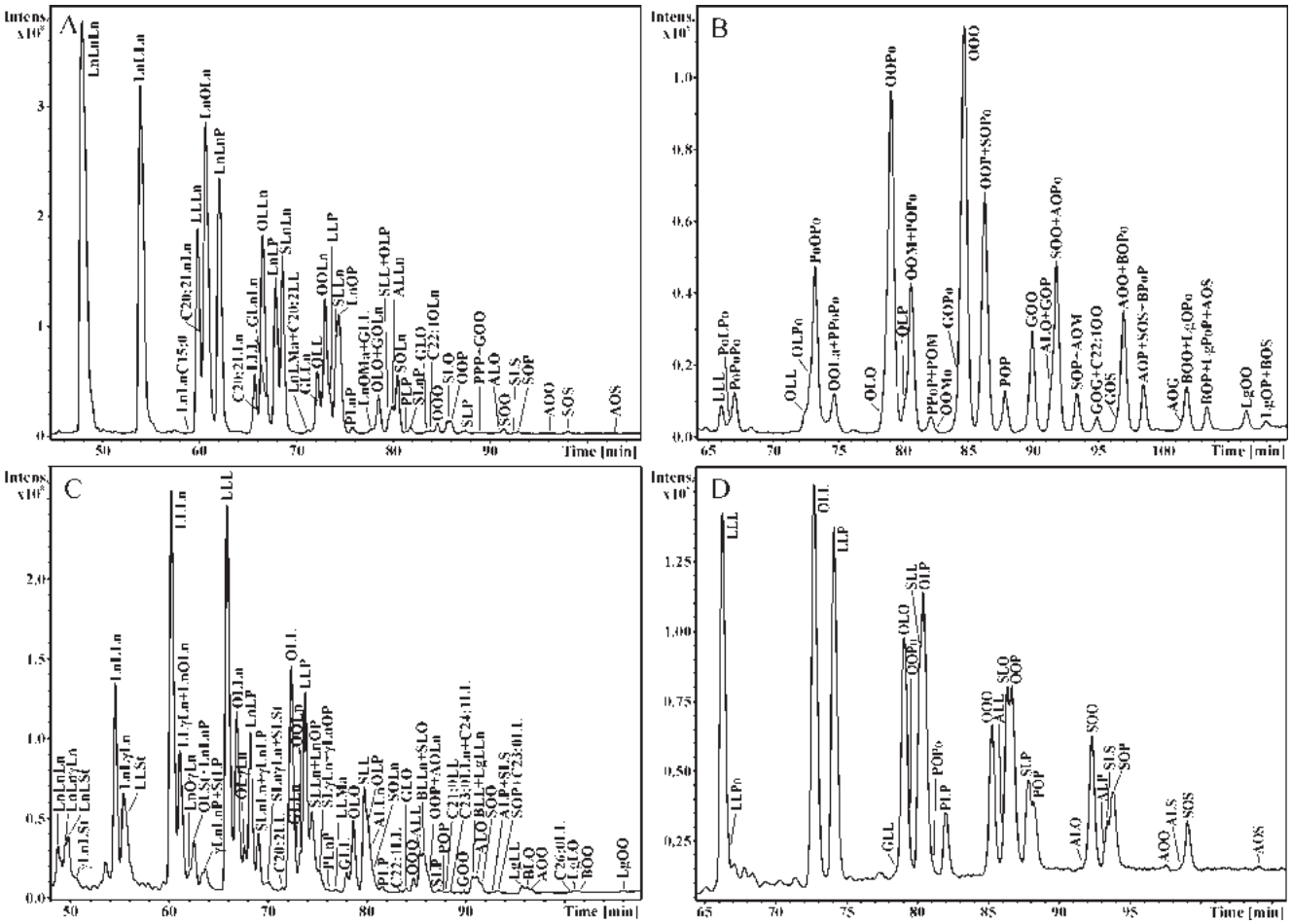

Figure 1. NARP-HPLC/APCI-MS analysis of plant oils: (**A**) kiwi seed (*Actinidia deliciosa*), (**B**) macadamia nut (*Macadamia integrifolia*), (**C**) hemp (*Cannabis sativa*), and (**D**) Brazil nut (*Bertholletia excelsa*).

defined as ECN = CN − 2DB. The separation of almost all TGs within one ECN group (*22*, *23*) or TGs with different positions of DBs (*24*) have been reported. The complementary separation mode, silver-ion chromatography, is based on the formation of weak complexes of silver ions with DBs, which is used for the separation of unsaturated TGs differing in the number and position of DBs. Silver-ion HPLC suffers from a lower reproducibility of retention times and a lower selectivity for saturated TGs in comparison to that in NARP-HPLC, but it enables the separation of TG regioisomers ($R_1R_1R_2$ vs $R_1R_2R_1$) (*25*, *26*). APCI is the most suitable ionization technique for the HPLC/MS analysis of TGs because of the excellent sensitivity and the structural information based on protonated molecules $[M+H]^+$ and $[M+H-R_iCOOH]^+$ fragment ions observed already in full-scan APCI mass spectra. Low abundance of protonated molecules in APCI mass spectra of saturated TGs can be improved by the formation of ammonium adducts $[M + NH_4]^+$ due to the postcolumn addition of ammonium acetate (*27*). Ratios of fragment ions $[M + H - R_iCOOH]^+$ are used for the determination of prevailing fatty acids esterified in the *sn*-2 position because of the lower abundance of fragment ions corresponding to the neutral loss of fatty acid from this position (*28*−*32*). ESI can be also used for the detection of TGs, but $[M + H]^+$ ions in the spectra are replaced by adducts with alkali metal ions $[M+Na]^+$ and $[M+K]^+$ or ammonium adducts $[M + NH_4]^+$ depending on the mobile phase composition (*30*, *33*). Fragment ions $[M + H - R_iCOOH]^+$ are also present in full-scan ESI mass spectra but with lower relative abundances in comparison to that in APCI. Moreover, ESI is less convenient for NARP systems typical for HPLC analysis of TGs.

Simple comparison of TG concentrations of pure and adulterated samples is not often sufficient proof for the authentication of plant oils because of the complexity of the data matrix. The statistical evaluation is a powerful tool for processing of large data sets, which enables the discrimination of different samples. Different multivariate statistical methods are used for the evaluation of TG composition and the detection of adulteration of plant oils, such as principal component analysis (PCA) (*9*, *13*), partial least-squares analysis (*6*, *7*), linear discriminant analysis (*10*, *19*, *20*), hierarchical cluster analysis (*15*), etc. PCA (*34*) uses a simple mathematical procedure for easy transformation of a high number of possibly correlated (covariant) variables into the smaller number of uncorrelated variables called principal components (PCs). PCA is mathematically defined as an orthogonal linear transformation that transforms the data to a new coordinate system in such a way that the greatest variance by any projection of the data shows on the first coordinate (PC1), the second greatest variance on the second coordinate (PC2), etc. PCA is theoretically the optimum transform for a given data set in the least-squares terms. Unlike standard multiple linear regression methods, PCA is not sensitive to any covariance in the data, which is quite common for MS based data sets.

The main goal of this work is the statistical evaluation of full TG profiles in a wide range of natural plant oils and the application of an elaborated PCA method for the identification of adulteration of expensive olive oils by cheaper sunflower oils

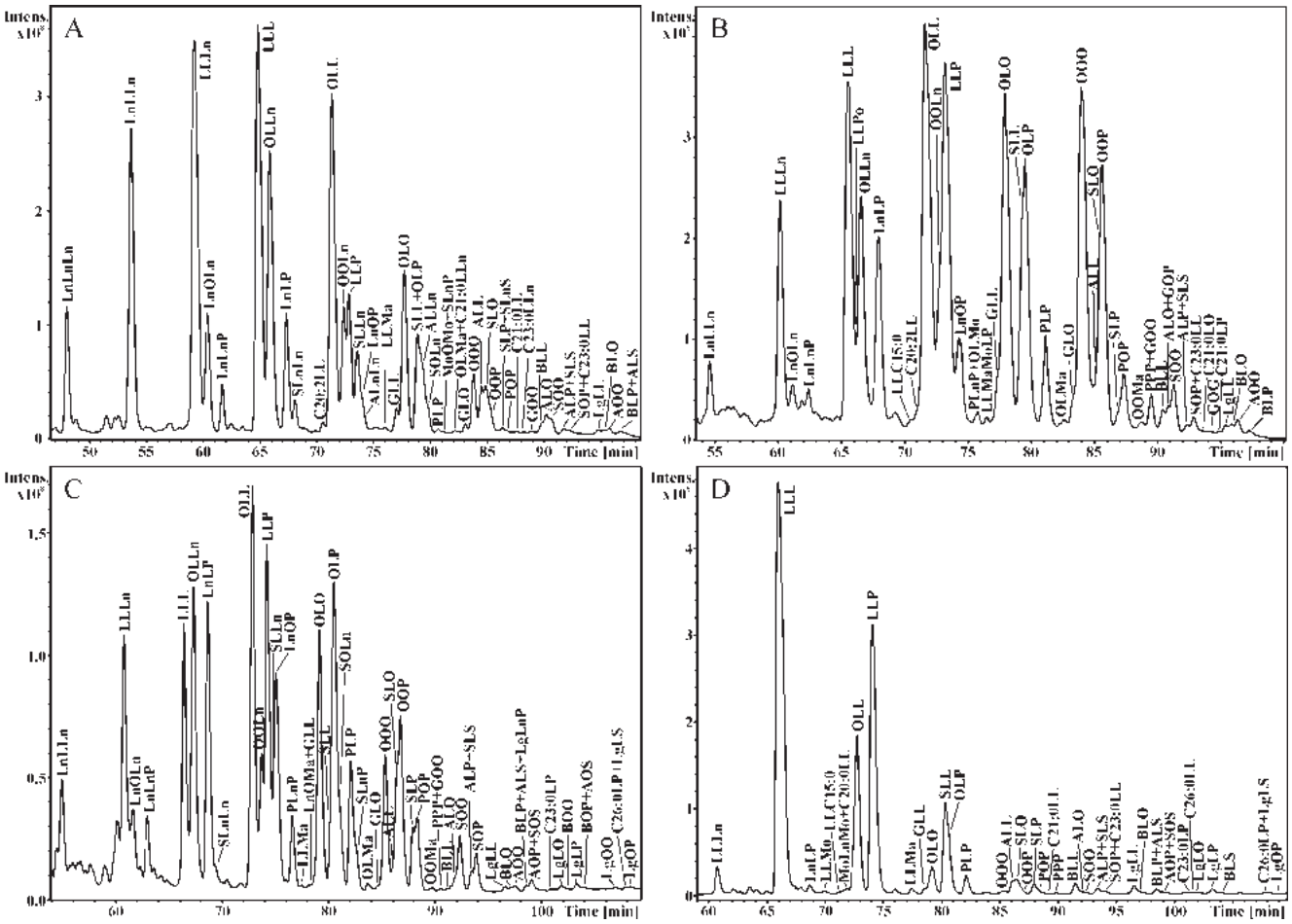

Figure 2. NARP-HPLC/APCI-MS analysis of plant oils: (**A**) dog rose (*Rosa canina*), (**B**) sweet chestnut (*Castanea sativa*), (**C**) lemon (*Citrus limon*), and (**D**) bell pepper (*Capsicum annuum*).

already at low concentration levels of added adulterant. TG concentrations are obtained by our previously developed NARP-HPLC method and precise quantitation with APCI-MS detection and response factor approach (*22*). To our best knowledge, TG profiles of such high numbers of plant oil samples of different types and origin are reported and statistically evaluated for the first time resulting in a robust method for the authentication of olive oils.

MATERIALS AND METHODS

Materials. Acetonitrile, 2-propanol (both solvents are of HPLC gradient grade), and hexane (HPLC grade) were purchased from Sigma-Aldrich (St. Louis, MO, USA). Solvents were degassed by continuous stripping with helium during the analysis. Samples of camellia oil (*Camellia sinensis*), rice oil (*Oryza sativa*), and coffee butter (a mixture of *Coffea arabica* seed oil and hydrogenated vegetable oil) were purchased from Augustus Oils (Bordon, UK). Samples of apricot kernel oil (*Prunus armeniaca*), camellia oil (*Camellia sinensis*), raspberry oil (*Rubus idaeus*), argan oil (*Argania spinosa*), black cumin oil (*Nigella sativa*), macadamia nut oil (*Macadamia integrifolia*), moringa oil (*Moringa ovalifolia*), and tamanu oil (*Calophyllum tacamahaca*) were purchased from Fragrant Earth (Glastonbury, UK). Plant oils from mango (*Mangifera indica*), kiwi (*Actinidia deliciosa*), dog rose (*Rosa canina*), hazelnut (*Corylus avellana*), sweet chestnut (*Castanea sativa*), pumpkin (*Cucurbita pepo*), Brazil nut (*Bertholletia excelsa*), lemon (*Citrus limon*), bell pepper (*Capsicum annuum*), grapefruit (*Citrus paradisi*), cucumber (*Cucumis sativus*), blackcurrant (*Ribes nigrum*), mandarin orange (*Citrus reticulata*), hemp (*Cannabis sativa*), blueberry (*Vaccinium myrtillus*), melon cantaloupe (*Cucumis melo cantalupensis*), papaya (*Carica papaya*), buckwheat (*Fagopyrum esculentum*), pistachio (*Pistacia vera*), and peanut (*Arachis hypogaea*) were prepared in our laboratory according to the following procedure (*22*−*24*). Ten to 15 g of seeds were carefully crushed in a mortar to fine particles. Then 15 mL of hexane was added, and this mixture was stirred occasionally for 15 min. The solid particles were filtered out using a course filter paper, and the extract was filtered again using a fine filter (0.45 μm). From the filtered extract, hexane was evaporated using a mild stream of nitrogen to yield pure plant oil. Samples of cooking oils, i.e., 2 soybean oils (*Glycine max*), 2 rapeseed oils (*Brassica napus*), 8 sunflower oils (*Helianthus annuus*), and 15 olive oils (*Olea europaea*), were purchased at local stores and used without any modification. Four model samples of adulterated olive oil were prepared by addition of 1, 2, 5, or 10% (weight) of sunflower oil to olive oil. Oil samples were dissolved in an acetonitrile/2-propanol/hexane mixture (1:1:1, v/v/v) to prepare the initial solution of plant oil with the concentration 10 g/L. Then initial solutions were diluted with the same solvent mixture to prepare the working solution at the concentration of all TGs within the calibration range. Ten microliters of working solution was injected for the HPLC analysis in triplicate.

HPLC/MS Conditions. The chromatographic apparatus consisted of a Model 616 pump with a quaternary gradient system, a Model 996 diode-array UV detector, a Model 717+ autosampler, a thermostatted column compartment, and a Millennium chromatography manager (all from Waters, Milford, MA, USA). The HPLC conditions were used according to ref *22*: two chromatographic columns Nova-Pak C_{18} (300 × 3.9 and 150×3.9 mm, 4 μm, Waters) connected in series, a flow rate of 1 mL/min, an injection volume of 10 μL, and a column temperature of 25 °C, and a mobile phase gradient with a slope of 0.65%/min with 0 min, 100% acetonitrile; 106 min, 31% acetonitrile/69% 2-propanol; 109 min, 100% acetonitrile. The injector needle was washed with the mobile phase before each injection. The column hold-up volume, t_M, was 3.20 min for the system with 300+150 mm Nova-Pak C_{18} columns. The UV detection at

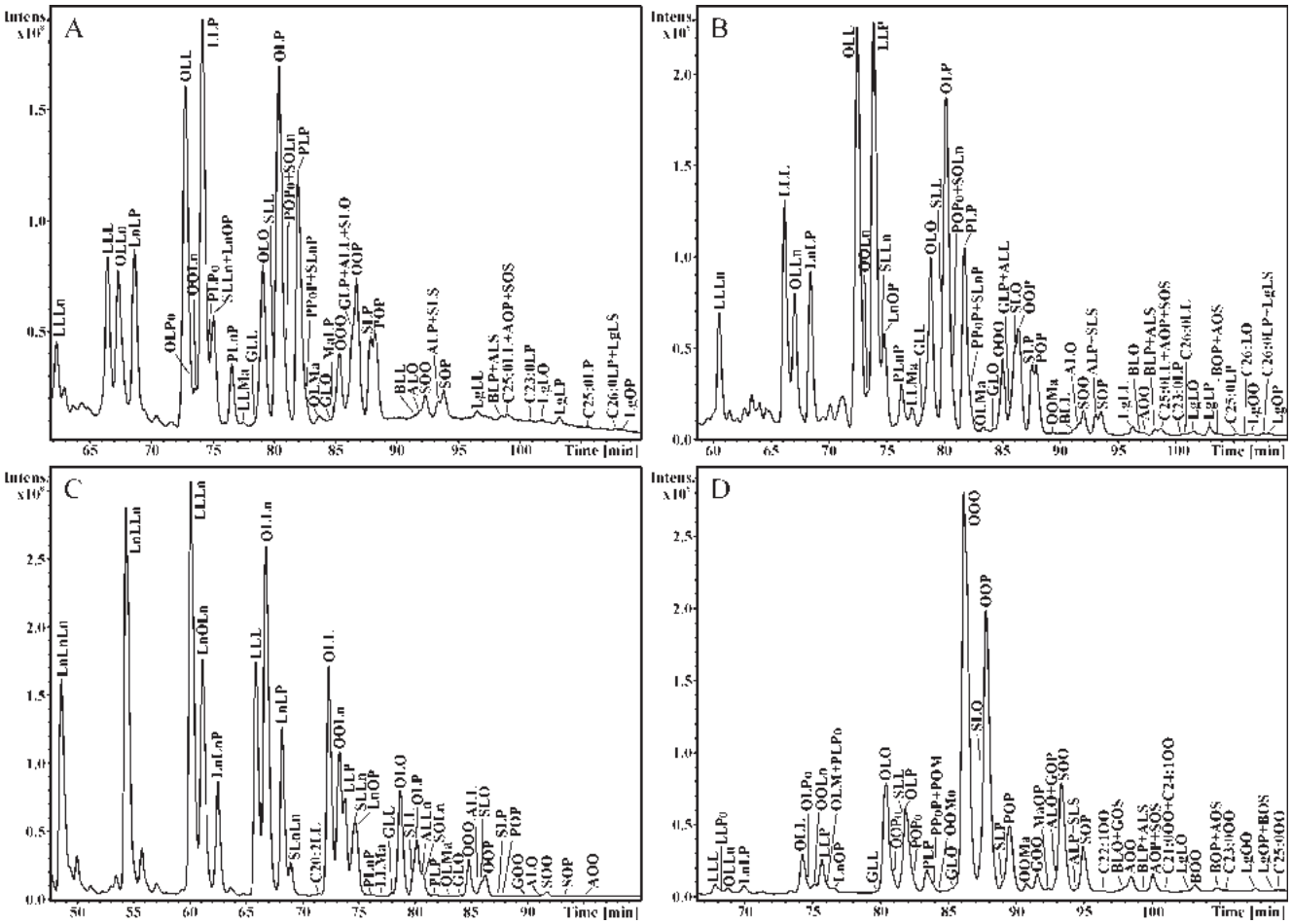

Figure 3. NARP-HPLC/APCI-MS analysis of plant oils: (**A**) grapefruit (*Citrus paradisi*), (**B**) mandarin orange (*Citrus reticulata*), (**C**) blueberry (*Vaccinium myrtillus*), and (**D**) papaya (*Carica papaya*).

205 nm and positive-ion APCI-MS were coupled in series. The Esquire 3000 ion trap analyzer (Bruker Daltonics, Bremen, Germany) in the mass range m/z 50−1200 was used with the following setting of tuning parameters: the pressure of the nebulizing gas was 70 psi, the drying gas flow rate was 3 L/min, and temperatures of the drying gas and APCI heater were 350 and 400 °C, respectively. Reconstructed ion current chromatograms in the region m/z 300−1200 were used for the peak integration. Presented peak areas correspond to averaged values from three consecutive chromatographic runs. Individual reconstructed ion current chromatograms were used to support the identification and quantitation of coeluting peaks.

Multivariate Data Analysis. In our calculations, 93 plant oils and 4 adulterated olive oils were objects (rows), and relative peak areas of 355 identified TGs were variables (columns). The data set for multivariate statistical analysis was processed using multivariate statistical package Simca-P (Umetrics, Umea, Sweden) without any additional pretreatment. The variability of data values was tested, and 13 columns were automatically excluded from original 355 variable columns because of their zero variability. Fifteen samples of olive oils, 8 sunflower oils, and 4 samples of adulterated olive oils were used for the authentication of plant oils using the same procedure. The final data set for the authentication of plant oils consisted of 27 objects and 62 variables. The following samples were processed in this paper: 1, kiwi; 2, macadamia nut; 3, hemp; 4, Brazil nut; 5, 6, mango; 7, dog rose; 8, 9, 10, hazelnut; 11, sweet chestnut; 12, pumpkin; 13, lemon; 14, bell pepper; 15, grapefruit; 16, cucumber; 17, 18, blackcurrant; 19, mandarin orange; 20, blueberry; 21, melon cantaloupe; 22, papaya; 23, buckwheat; 24, pistachio; 25, 26, peanut; 27, 28, camellia; 29, rice; 30, coffee butter; 31, apricot kernel; 32, raspberry; 33, argan; 34, black cumin; 35, moringa; 36, tamanu; 37, 38, 39, soya; 40, 41, 42, rapeseed; 43, 44−51, sunflower; 52, 53−67, olive; 68, palm; 69, cotton; 70, coconut palm; 71, corn; 72, sesame; 73, almond; 74, safflower; 75, grape wine white; 76, grape wine red; 77, linseed; 78, poppy seed; 79, walnut; 80, avocado pear; 81, redcurrant; 82, borage; 83, cacao butter; 84, evening primrose; 85, kukui nut; 86, wheat germ; 87, cashew nut; 88, yellow melon; 89, fig; 90, date; 91, European larch; 92, Norway spruce; 93, European silver fir. The data on new samples are shown in Tables, and the remaining data are taken from our previous works (*22*−*24*).

RESULTS AND DISCUSSION

NARP-HPLC/APCI-MS Analysis of Plant Oils. The separation of TGs from plant oils is quite a challenging task because of the presence of numerous TG species with similar physicochemical properties. NARP-HPLC separation mode is used for the separation of TG complex mixtures of plant oils based on our previously optimized conditions (*22*), i.e., the column coupling in the total length of 45 cm, the mobile phase of acetonitrile/2-propanol, and column temperature of 25 °C. TGs are resolved according to the ECN, and most TGs are clearly separated within individual ECN groups according to esterified fatty acids, i.e., saturation, DB position, and fatty acid chain lengths. **Figure 1** illustrates four examples of HPLC/MS separation of TGs in plant oils with high (kiwi seed oil, **Figure 1**A) and low (macadamia nut oil, **Figure 1**B) concentrations of polyunsaturated fatty acids, and the separation of plant oils with high (hemp oil, **Figure 1**C) and low (Brazil nut oil, **Figure 1**D) number of TG species. **Figures 2**−**4** show HPLC/MS chromatograms of some unusual plant oils, whose chromatograms have not been reported in the literature so far. Other HPLC/MS chromatograms are available in Supporting Information (Figures S1−S5). Individual TGs are identified

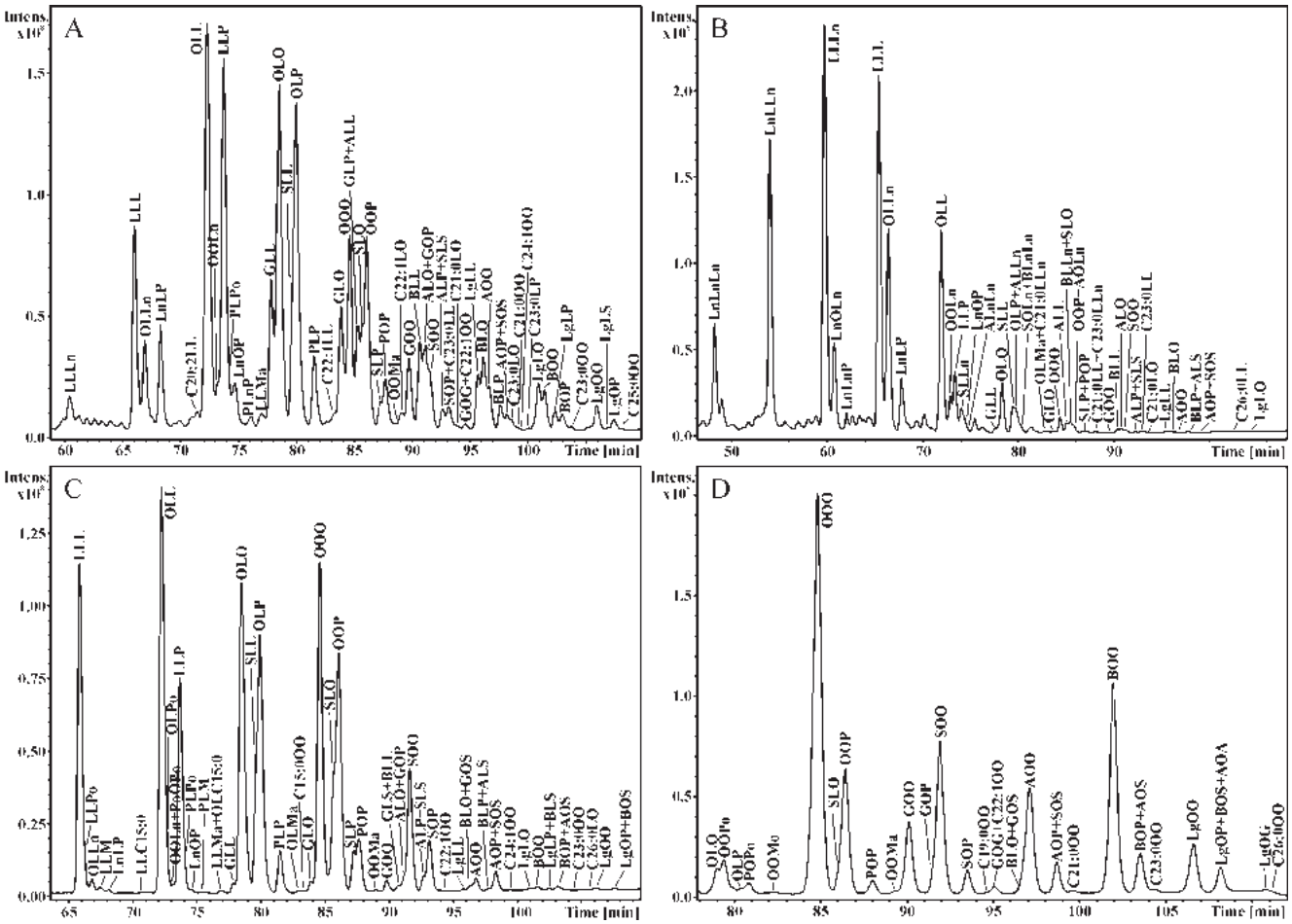

Figure 4. NARP-HPLC/APCI-MS analysis of plant oils: (A) buckwheat (*Fagopyrum esculentum*), (B) raspberry (Rubus idaeus), (C) argan (Argania spinosa) and (D) moringa (Moringa ovalifolia).

on the basis of their positive-ion APCI mass spectra using $[M + H]^+$ ions for the molecular weight determination and $[M + H - R_iCOOH]^+$ fragment ions for the identification of individual fatty acids. It is well known (*28*−*32*) that the cleavage of fatty acid from the *sn*-2 position on the glycerol skeleton is less preferred in comparison to *sn*-1/3 positions resulting in a lower abundance of corresponding $[M + H - R_iCOOH]^+$ fragment ions, which is used for the determination of prevailing fatty acid in the *sn*-2 position. We have found a preference of unsaturated fatty acids (mainly linoleic acid) in the *sn*-2 position for analyzed plant oils, in agreement with the literature data. Fatty acids in *sn*-1/3 positions cannot be resolved using NARP-HPLC/APCI-MS, and they are considered as equivalent in this work. Fatty acids in these positions are arranged according to their decreasing masses.

TG composition of various plant oils has been characterized using optimized NARP-HPLC separation with APCI-MS detection. APCI-MS is applicable also for the identification of trace and chromatographically nonresolved species based on the high sensitivity and possibility of utilization of extracted ion chromatograms, which results in the identification of the highest number of TG species in individual plant oils ever reported (**Table 1**). The number of identified TGs ranges from 26 TGs in Brazil nut and camellia oils as examples of relatively simple oils up to 80 TG species identified in blackcurrant oil as the example of a rather complex oil. The number of TG species in individual oils partially corresponds with the number of fatty acids present in TGs, e.g., 18 fatty acids are identified in hemp oil as one of the most complex oils containing 70 TGs. In total, 355 TG species are identified in 93 plant oils composed from 35 fatty acids with 6 to 26 carbon atoms and 0 to 4 DBs.

TGs in analyzed plant oils are quantified using the APCI-MS response factor approach for the quantitation of TGs in natural samples described previously (*22*). Briefly, the response factors of individual fatty acids are calculated as the ratio of calibration slopes of corresponding single-acid TG standards (type $R_1R_1R_1$) to the calibration slope of triolein as one as the most common TGs in nature. Response factors of mixed TGs (type $R_1R_2R_3$) are calculated as the arithmetic mean of response factors of presented fatty acids in TGs. Concentrations of individual TGs in analyzed plant oils are listed in Supporting Information (Tables S1 and S2). The quantitation of coeluting peaks is supported by reconstructed ion chromatograms of protonated molecules and individual diacylglycerol fragment ions. Precise concentrations of TGs in individual plant oils using HPLC/MS response factor quantitation approach can be used for the calculation of their fatty acid composition (**Tables 2** and S3 (Supporting Information)) and nutritional parameters (**Tables 1** and S4 (Supporting Information)), as confirmed previously (*22*) by the comparison with fatty acid composition determined with validated GC/FID analysis of fatty acid methyl esters prepared by the transesterification of TGs. **Table 1** lists average parameters calculated from HPLC/MS results of TGs, i.e., average equivalent carbon number (aECN), average carbon number (aCN), double bond (aDB) number, and sums of essential fatty acids (linoleic and linolenic), 18 and 16 carbon fatty acids, and saturated, monounsaturated, and polyunsaturated fatty acids. aECN ranges from 13.59 to 16.65, aCN

Table 1. Number of Identified Triacylglycerols (TGs) and Fatty Acids (FAs), Average Equivalent Carbon Number (aECN), Average Carbon Number (aCN), Average Double Bond (aDB) Number, the Relative Weight Concentration [%] of Essential Fatty Acids (Linoleic and Linolenic Acids), Fatty Acids with 18 (C18) and 16 (C16) Carbon Atoms, and Saturated (Sat), Monounsaturated (Mono), and Polyunsaturated (Poly) Fatty Acids in Analyzed Plant Oils Calculated from NARP-HPLC/APCI-MS of Triacylglycerols

oil	no.	number of TGs/FAs	aECN	aCN	aDB	essential FAs [%]	C18 + C16 FAs [%]	Sat [%]	Mono [%]	Poly [%]
Kiwi	**1**	47/11	13.59	17.83	2.12	70.7	99.4	11.7	17.3	71.0
Macadamia nut	**2**	45/13	15.82	17.53	0.85	2.9	91.0	17.5	79.6	2.9
Hemp	**3**	70/18	14.03	17.87	1.89	70.7	98.0	12.9	11.8	75.3
Brazil nut	**4**	26/7	15.38	17.66	1.14	39.9	99.9	24.9	35.2	39.9
Mango	**6**	53/13	16.57	17.86	0.65	8.2	96.5	44.2	47.6	8.2
Dog rose	**7**	51/14	14.27	17.93	1.83	69.7	98.4	8.2	22.0	69.8
Hazelnut	**9**	30/10	15.62	17.83	1.10	21.3	99.2	11.1	67.6	21.3
	10	30/10	15.72	17.84	1.06	17.6	99.1	11.4	71.0	17.6
Sweet chestnut	**11**	49/16	15.04	17.72	1.34	44.2	98.7	16.4	39.3	44.3
Pumpkin	**12**	31/9	15.01	17.71	1.35	56.0	99.0	19.9	24.1	56.0
Lemon	**13**	58/12	14.90	17.62	1.36	46.9	99.3	23.0	30.1	46.9
Bell pepper	**14**	44/16	14.61	17.77	1.58	74.5	98.4	15.9	9.6	74.6
Grapefruit	**15**	51/14	15.07	17.46	1.19	44.7	99.2	29.9	25.5	44.7
Cucumber	**16**	45/13	14.54	17.62	1.54	72.1	99.1	20.0	7.9	72.1
Blackcurrant	**18**	80/14	13.76	17.85	2.05	57.5	99.3	8.9	15.2	75.9
Mandarin orange	**19**	56/14	15.03	17.55	1.26	48.1	98.8	26.4	25.5	48.1
Blueberry	**20**	37/9	13.94	17.86	1.96	70.0	99.7	7.9	22.0	70.0
Melon cantaloupe	**21**	37/11	14.70	17.76	1.53	68.6	99.5	15.6	15.8	68.6
Papaya	**22**	55/17	15.93	17.66	0.87	9.4	97.9	22.4	68.2	9.4
Buckwheat	**23**	59/16	15.51	17.92	1.20	39.4	92.0	21.5	39.0	39.5
Pistachio	**24**	40/11	15.28	17.81	1.27	38.5	99.1	11.5	50.0	38.5
Peanut	**26**	60/16	15.60	17.94	1.17	37.9	92.9	21.2	40.8	37.9
Camellia	**27**	26/12	15.87	17.80	0.97	9.5	99.1	12.5	78.0	9.5
	28	26/12	15.88	17.82	0.97	8.8	99.2	11.6	79.6	8.8
Rice	**29**	48/12	15.30	17.66	1.18	38.1	97.9	20.6	41.3	38.1
Coffee butter	**30**	68/14	14.05	15.01	0.48	20.5	57.6	72.3	7.2	20.5
Apricot kernel	**31**	27/10	15.40	17.86	1.23	31.1	99.8	7.3	61.7	31.1
Raspberry	**32**	51/13	13.91	17.94	2.02	79.7	99.4	4.8	15.5	79.7
Argan	**33**	60/16	15.45	17.71	1.13	33.3	98.8	19.5	47.2	33.3
Black cumin	**34**	35/9	14.89	17.80	1.45	58.8	96.6	15.0	23.5	61.5
Moringa	**35**	33/16	16.65	18.24	0.80	0.9	86.4	22.1	77.0	0.9
Tamanu	**36**	43/12	15.40	17.79	1.19	41.7	98.6	21.7	36.6	41.7
Soya	**38**	66/14	14.86	17.79	1.47	56.9	98.5	16.8	26.3	56.9
Rapeseed	**41**	55/13	15.29	17.90	1.31	30.8	97.9	9.6	59.6	30.8
Sunflower	**44**	50/16	14.91	17.88	1.49	61.9	97.9	13.3	24.8	61.9
Olive	**53**	37/15	15.90	17.75	0.92	7.5	98.5	15.8	76.7	7.5

from 17.46 to 18.24, aDB from 0.48 to 2.12, and the sum of C18 and C16 fatty acids from 86.4% to 99.8%, showing that plant oils are composed almost exclusively from TGs containing fatty acids with 16 and 18 carbon atoms and 0 to 4 DBs, i.e., palmitic (ECN; CN; DB-16; 16; 0), stearic (18; 18; 0), oleic (16; 18; 1), linoleic (14; 18; 2), and linolenic (12; 18; 3) acids (**Tables 2** and S3 (Supporting Information)). Remaining fatty acids with low or usually trace concentrations represent long or short-chain acids, odd-number acids, and acids with unusual DB positions. Higher differences are found among the sums of essential (from 0.9% to 79.7%), saturated (from 4.8% to 72.3%), monounsaturated (from 7.2% to 79.6%), and polyunsaturated (from 0.9% to 75.9%) fatty acids differing significantly for individual oils, and therefore, these parameters can be used for fast consideration of nutritional values or possible industrial applications.

PCA of TG Composition. The evaluation of TG profiles is an important step in the quality control of plant oils. The concentration of individual TG species can be used for simple comparison of various plant oils, but such comparison is not practical due to a high number of detected TGs. For detailed characterization, the comparison of all TG species in all analyzed samples is necessary, which leads to the complex multidimensional data set. Multivariate data analysis using PCA is used for the evaluation of TG composition in all analyzed samples. First, PCA analysis using TG concentrations based on APCI-MS response approach and TG relative peak areas are compared. No significant differences in resulting PCA plots are found, and therefore, relative peak areas are used for further PCA analysis of all samples. The final data set contains 93 plant oils (i.e., objects) of 60 different types characterized by relative peak areas of 355 identified TG species (i.e., variables). Thirteen variables are excluded from the data set because of their zero variability corresponding to the content of this variable in all plant oils lower than the limit of detection (0.01%). Data values of other 342 variables range between 0.01% and 49.32%, i.e., in the range of 3.5 orders of magnitude. Hence, no scaling, normalization, or centering is applied, and the data set without any modification is taken for the direct PCA analysis. Multivariate data set of 342 nonredundant variables is visualized as a set of coordinates in a multidimensional data space with $N = 342$ (one axis per variable) dimensions.

Figure 5 shows the score plots of the first (t[1]) and second (t[2]) PCs of the general PCA model with a good resolution of analyzed samples. These two variables describe 82% of the total variability in the data set, where the first PC t[1] describes 52% and second PC t[2] 30% of the total variability. Other PCs describe significantly lower variability, e.g., t[3] has 4% and t[4] 3% of the total variability. The projection of PCs t[3] and t[4] (Figure S6 (Supporting Information)) shows only a small variance among analyzed samples, and most of samples are grouped around the

Table 2. Relative Weight Concentrations [%] of Individual Fatty Acids in Analyzed Plant Oils Calculated from HPLC/APCI-MS of Triacylglycerols

		Cy	C	La	M		P	Po	Ma	Mo	S	O	L	Ln	γLn	St		A	G			B			Lg			
oil	no.	C8:0	C10:0	C12:0	C14:0	C15:0	C16:0	C16:1	C17:0	C17:1	C18:0	C18:1	C18:2	C18:3	C18:3	C18:4	C19:0	C20:0	C20:1	C20:2	C21:0	C22:0	C22:1	C23:0	C24:0	C24:1	C25:0	C26:0
Kiwi	**1**					0.01	8.5		0.03		3.1	17.1	17.1	53.6				0.04	0.2	0.3			0.02					
Macadamia nut	**2**			0.2	1.4		8.0	18.9		0.1	3.3	57.9	2.9					2.8	2.6			1.3	0.1		0.5			
Hemp	**3**						8.6		0.02		2.6	11.5	49.5	21.2	3.2	1.4		1.0	0.3	0.03	<0.01	0.5	0.01	0.03	0.1	0.01		<0.01
Brazil nut	**4**						16.3	0.08			8.5	35.1	39.9					0.1	0.02									
Mango	**6**						10.7		0.3		30.3	47.3	7.4	0.8			0.03	1.7	0.3			0.5		0.04	0.6		0.03	
Dog rose	**7**						4.6		0.04	0.01	2.4	21.7	47.9	21.8				1.0	0.3	0.07	0.01	0.1		0.03	0.04			
Hazelnut	**9**						7.8	0.6	0.1	0.2	3.0	66.5	20.8	0.5				0.2	0.3									
	10						7.5	0.3	0.1	0.2	3.5	70.2	17.3	0.3				0.3	0.3									
Sweet chestnut	**11**					0.04	14.3	0.08	0.1	0.04	1.5	38.6	37.1	7.1				0.3	0.6	0.06	0.01	0.1		0.04	0.03			
Pumpkin	**12**						14.5		0.1		4.5	24.0	56.0					0.6	0.06			0.2			0.04			
Lemon	**13**						18.8		0.08		3.5	30.1	33.4	13.5				0.3	0.03			0.08		<0.01	0.2			0.01
Bell pepper	**14**					0.06	12.5		0.1	0.2	2.1	9.3	73.7	0.8				0.4	0.07	0.08	0.01	0.3		0.03	0.3			0.05
Grapefruit	**15**						25.9	0.8	0.2		3.2	24.6	38.6	6.1				0.3	0.05			0.02		0.01	0.2		0.01	0.01
Cucumber	**16**				0.4		17.5		0.1		1.7	7.8	68.3	3.8				0.2	0.09			0.04			0.05		0.01	0.01
Blackcurrant	**18**						7.7		0.02		1.1	14.7	40.9	16.6	14.6	3.7		0.1	0.5	0.07		0.01		<0.01	<0.01			
Mandarin orange	**19**						22.1	0.4	0.2		3.3	24.9	42.6	5.5				0.3	0.2			0.1		0.02	0.3		0.03	0.05
Blueberry	**20**						6.6		0.02		1.1	22.0	35.7	34.3				0.2	0.06	0.02								
Melon cantaloupe	**21**					0.05	11.8		0.08		3.4	15.7	67.8	0.8				0.2	0.09			0.06			0.02			
Papaya	**22**				0.2		16.6	0.9	0.2	0.06	4.5	66.5	8.9	0.5				0.6	0.7		0.02	0.2	0.03	0.01	0.07		0.01	
Buckwheat	**23**						14.7	0.2	0.06		2.0	35.7	36.9	2.5				1.1	3.0	0.08	0.04	2.0	0.1	0.2	1.4		0.02	
Pistachio	**24**						9.7		0.05	0.1	1.5	49.4	38.2	0.3				0.1	0.5			0.1			0.05			
Peanut	**26**						12.6		0.09	0.08	2.7	39.7	37.6	0.3				1.1	1.0	0.04	0.01	3.1	0.05	0.03	1.5			0.1
Camellia	**27**						10.0	0.08	0.08	0.08	2.3	77.2	9.2	0.3				0.06	0.6				0.03		0.07			
	28						9.1	0.07	0.06	0.07	2.4	78.8	8.5	0.3				0.04	0.6				0.03		0.03			
Rice	**29**				0.4		16.5	0.7			2.5	40.1	36.1	2.0				0.5	0.5			0.2			0.4			0.1
Coffee butter	**30**	5.1	1.5	24.4	10.1		17.6		0.01		12.3	7.2	19.7	0.8				0.9	0.03			0.3			0.06			
Apricot kernel	**31**						6.2	0.3	0.03	0.1	1.0	61.2	31.0	0.05				0.06	0.06									
Raspberry	**32**						3.4		0.02		0.8	15.5	52.9	26.8				0.3	0.04		0.01	0.2		0.01	0.02			<0.01
Argan	**33**				0.1	0.05	14.0	0.4	0.05		4.7	46.4	33.1	0.2				0.3	0.4			0.2	0.01	0.01	0.07			0.01
Black cumin	**34**						12.4				2.3	23.1	58.8					0.2	0.4	2.7		0.06			0.04			
Moringa	**35**						6.4	1.2	0.05	0.04	4.7	73.2	0.9				0.02	3.4	2.5		0.06	5.8	0.07	0.05	1.6			0.01
Tamanu	**36**						11.2	0.03	0.08	0.03	9.3	36.4	41.7					0.8	0.1		0.02	0.3			0.04			
Soya	**38**						12.1		0.04	0.03	3.3	26.2	49.7	7.2				0.4	0.1	0.02		0.6		0.1	0.2			0.01
Rapeseed	**41**						7.1	0.2	0.1		1.6	58.2	21.2	9.6				0.4	1.1			0.3		0.01	0.1	0.09		
Sunflower	**44**				0.3		7.6		0.05	0.08	3.8	24.6	61.5	0.4			<0.01	0.4	0.1	<0.01		0.8		0.06	0.3			0.01
Olive	**53**						12.5	1.3		0.1	2.3	74.9	6.5	1.0				0.5	0.4		0.03	0.3		0.05	0.1		0.01	0.01

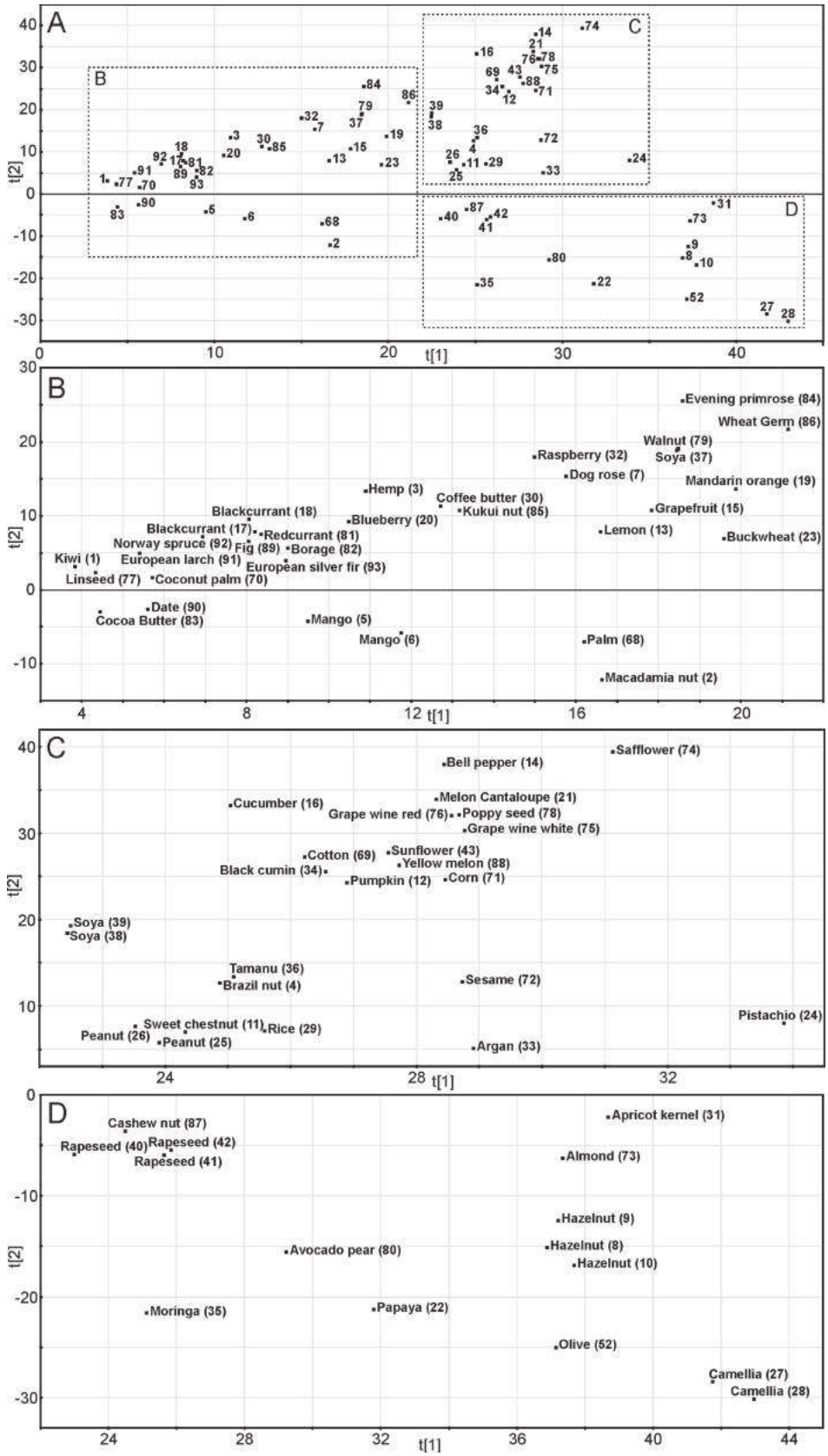

Figure 5. Projection of principal components t[1] and t[2] in two-dimensional scatter plot for all measured samples (**A**) and zooms of individual regions (**B**, **C**, and **D**).

zero of both PCs. Only samples with significantly different composition containing high concentrations of TGs with highly unsaturated (linseed, kiwi and blueberry oils) or saturated (cacao butter and mango oils) fatty acids are clearly distinguished from other samples in Figure S6 (Supporting Information). The projection of analyzed samples using t[1] and t[2] PCs provides

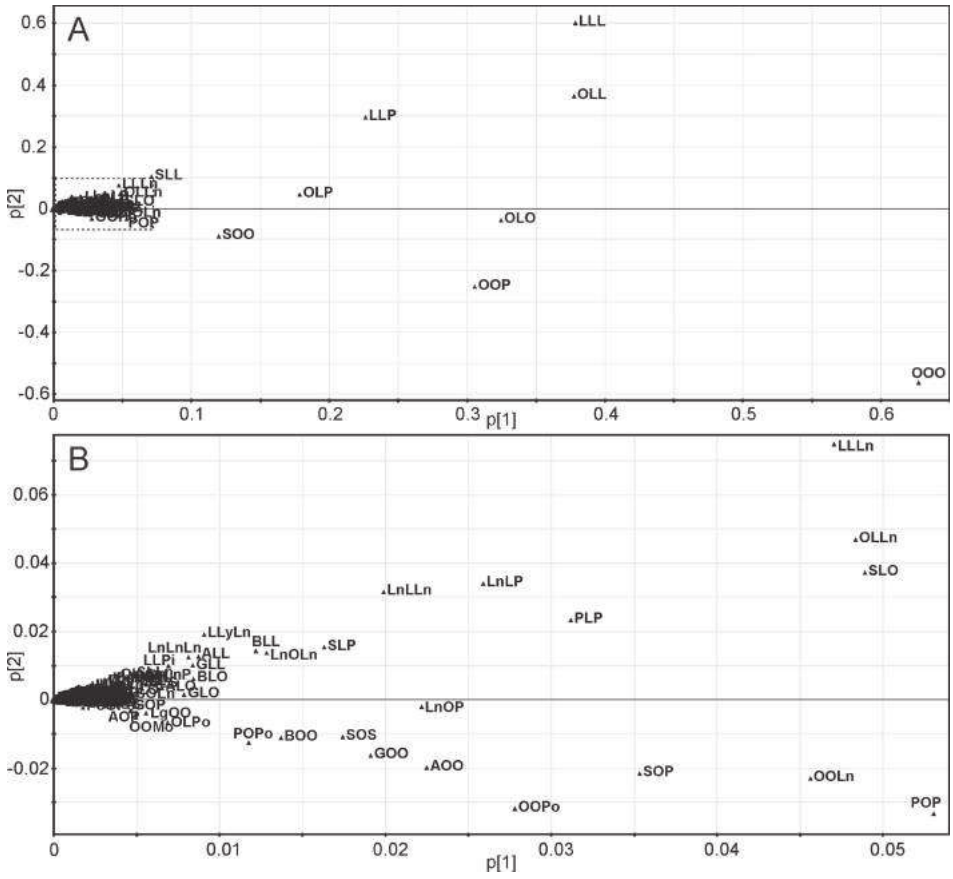

Figure 6. Projection of variables p[1] and p[2] in two-dimensional loadings plot for all measured samples showing the major variables representing TG concentrations (**A**) and zoomed area (**B**).

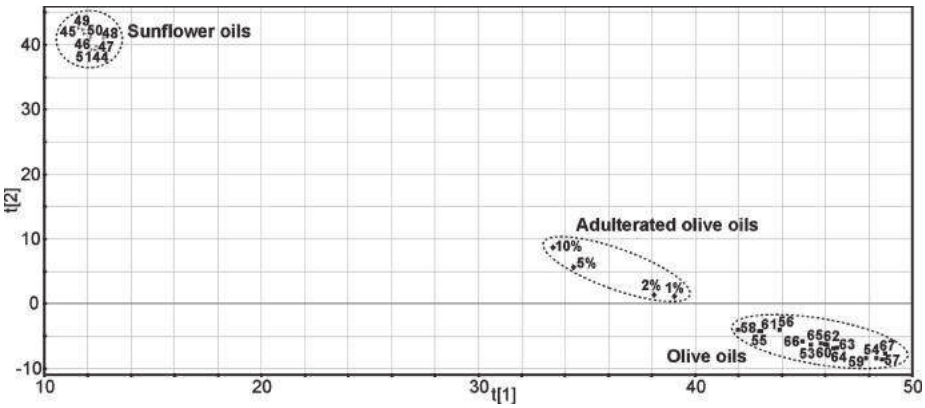

Figure 7. Projection of principal components t[1] and t[2] in two-dimensional scatter plot for analyzed sunflower (44−51) and olive (53−67) cooking oils and four samples of adulterated olive oil by 1%, 2%, 5%, or 10% of sunflower oil.

significantly better resolution of analyzed samples for the comparison of their properties. Samples of one type of plant oil having similar TG composition form narrow clusters, e.g., different samples of hazelnut and camellia oils (**Figure 5D**). Samples with similar TG profiles are grouped in small regions in the PCA plot, e.g., samples of blackcurrant and redcurrant oils (**Figure 5B**). Similar positions of various samples in the PCA plot indicate their similar properties, e.g., Brazil nut and tamanu oils in **Figure 5C**. Their similar properties can be confirmed by the comparison of their average parameters and sums of fatty acids for individual plant oils calculated from TG composition (**Table 1**), i.e., aECN of Brazil nut oil/tamanu oil = 15.38/15.40, aCN = 17.66/17.79, aDB = 1.14/1.19, C18 + C16 fatty acids = 99.9%/98.6%, polyunsaturated fatty acids = 39.9%/41.7%, etc. **Figure 6** shows variables (TG concentrations) in our PCA, and their variance model mostly affects the variability of samples. The most significant variable is the concentration of OOO with more than 60% positive effect on t[1], while −55% effect on t[2]. Other important variables are LLL, OLL, OLO, OOP, LLP, OLP, and SOO. These eight variables are the most significant parameters for the statistical differentiation among plant oils.

Authentication of Olive Oil. Olive oil is one of the most expensive plant oils used in dietetics. For its healthy properties, it is an important ingredient in the so-called Mediterranean diet of southern nations. High prices of olive oils can lead some merchants to illegal falsification by cheaper plant oils, which decrease

their nutritional value. Most favorable oils for adulteration are plant oils with similar TG composition, which are difficult to distinguish using common analytical techniques. The TG composition of hazelnut, camellia, or papaya oils is relatively close to olive oil composition, but they are still clearly distinguished using our HPLC/MS method and PCA analysis (**Figure 5D**). Moreover, their prices and small quantity production in comparison to those of the most common plant oils are not favorable for falsification. The utilization of low-price plant oils produced in large quantities in the same geographical region is more favorable, e.g., sunflower oil. The set of 8 sunflower and 15 olive cooking oils, and 4 model samples of adulterated olive oil by 1%, 2%, 5%, or 10% of sunflower oil (Table S2, Supporting Information) is tested to develop an unambiguous method to identify adulteration even at very low amounts of adulterant. **Figure 7** shows the scores plot of the first (t[1]) and second (t[2]) PCs of all cooking and model adulterated oil samples. This data set is represented by 27 objects (oil samples) and 62 variables (TG concentrations) with significant variability. PCs t[1] and t[2] account for 99.6% of total variability, where t[1] represents 73.5% and t[2] represents 26.1% of total variability. Samples of sunflower oil have small differences in TG composition and form a small cluster clearly distinguished from other samples in the PCA plot. Samples of olive oil have a wider distribution in comparison to the cluster of sunflower oils because of slightly different TG composition of different types (virgin oil, pomace oil, etc.) and different origin of samples, which are not differentiated in this study. Anyway, a clear resolution of sunflower and olive oil samples and their grouping into small clusters enable the resolution of model samples of adulterated olive oil by sunflower oil (**Figure 7**). Samples of adulterated olive oil with increasing concentrations of sunflower oil have an increasing distance from the olive oil cluster in the PCA plot. Even the adulteration of olive oil by 1% of sunflower oil can be clearly visualized in a PCA plot regardless of the fact that different types and origin of olive oils are neglected. This approach is well suitable for the detection of possible adulteration in tested samples.

The presented results demonstrate the utilization of HPLC/MS analysis and statistical evaluation in the quality control of plant oils. A carefully optimized HPLC/MS method is used for detailed characterization of TG profiles of plant oils. PCA evaluation of multidimensional data matrix of TG profiles enables the comparison of all analyzed samples and the resolution of samples with similar properties. PCA analysis is used for the authentication of expensive olive oil. PCA enables the detection of adulterated olive oil starting from 1% of added sunflower oil as an adulterant.

ABBREVIATIONS USED

CN, carbon number; DB, double bond; ECN, equivalent carbon number; ESI, electrospray ionization; MS, mass spectrometry; NARP-HPLC, nonaqueous reversed-phase high-performance liquid chromatography; PC, principal component; PCA, principal component analysis; TG, triacylglycerol; fatty acid abbreviations, Cy, caprylic (CN:DB, C8:0); C, capric (C10:0); La, lauric (C12:0); M, myristic (C14:0); C15:0, pentadecanoic; P, palmitic (C16:0); Po, palmitoleic (Δ9-C16:1); Ma, margaric (C17:0); Mo, margaroleic (Δ9-C17:1); S, stearic (C18:0); O, oleic (Δ9-C18:1); L, linoleic (Δ9,12-C18:2); Ln, α-linolenic (Δ9,12,15-C18:3); γLn, γ-linolenic (Δ6,9,12-C18:3); St, stearidonic (Δ6,9,-12,15-C18:4); C19:0, nonadecanoic (C19:0); A, arachidic (C20:0); G, gadoleic (Δ9-C20:1); C20:2, eicosadienoic (Δ11,14-C20:2); C21:0, heneicosanoic (C21:0); B, behenic (C22:0); C22:1, erucic (Δ13-C22:1); C23:0, tricosanoic (C23:0); 24:1, nervonic (Δ15-C24:1); Lg, lignoceric (C24:0); C25:0, pentacosanoic (C25:0); C26:0, hexacosanoic (C26:0).

Supporting Information Available: HPLC/MS chromatograms of analyzed plant oils (Figures S1−S5), projection of PCs t[3] and t[4] (Figure S6), relative weight concentrations of triacylglycerols (Tables S1 and S2) and fatty acids (Tables S3), average parameters (Table S4) of analyzed plant oils. This material is available free of charge via the Internet at http://pubs.acs.org.

LITERATURE CITED

(1) Food and Agricultural Organization of the United Nations (FAO), Rome, 2009. http://www.fao.org.
(2) FEDIOL, Brussels, 2009. http://www.fediol.be.
(3) Gunstone, F. Introduction: Modifying Lipids-Why and How? In *Modifying Lipids for Use in Food*, 1; Gunstone, F., Ed.; Woodhead Publishing Ltd: Cambridge, England, 2006; pp 1−8.
(4) Li-Chan, E. Developments in the detection of adulteration of olive oil. *Trends Food Sci. Technol.* **1994**, *5*, 3–11.
(5) Baeten, V.; Pierna, J. A. F.; Dardenne, P.; Meurens, M.; Garcia-Gonzalez, D. L.; Aparicio-Ruiz, R. Detection of the presence of hazelnut oil in olive oil by FT-Raman and FT-MIR spectroscopy. *J. Agric. Food Chem.* **2005**, *53*, 6201–6206.
(6) Lai, Y. W.; Kemsley, E. K.; Wilson, R. H. Quantitative-analysis of potential adulterants of extra virgin olive oil using infrared-spectroscopy. *Food Chem.* **1995**, *53*, 95–98.
(7) Galtier, O.; Dupuy, N.; Le Dréau, Y.; Ollivier, D.; Pinatec, C.; Kister, J.; Artaud, J. Geographic origins and compositions of virgin olive oils determinated by chemometric analysis of NIR spectra. *Anal. Chim. Acta* **2007**, *595*, 136–144.
(8) Hidalgo, F. J.; Zamora, R. Edible oil analysis by high-resolution nuclear magnetic resonance spectroscopy: recent advances and future perspectives. *Trends Food Sci. Technol.* **2003**, *14*, 499–506.
(9) Aursand, M.; Standal, I. B.; Axelson, D. E. High-resolution C-13 nuclear magnetic resonance spectroscopy pattern recognition of fish oil capsules. *J. Agric. Food Chem.* **2007**, *55*, 38–47.
(10) Jakab, A.; Nagy, K.; Heberger, K.; Vekey, K.; Forgács, E. Differentiation of vegetable oils by mass spectrometry combined with statistical analysis. *Rapid Commun. Mass Spectrom.* **2002**, *16*, 2291–2297.
(11) Calvano, C. D.; Palmisano, F.; Zambonin, C. G. Laser desorption/ionization time-of-flight mass spectrometry of triacylglycerols in oils. *Rapid Commun. Mass Spectrom.* **2005**, *19*, 1315–1320.
(12) Wu, Z. G.; Rodgers, R. P.; Marshall, A. G. Characterization of vegetable oils: Detailed compositional fingerprints derived from electrospray ionization Fourier transform ion cyclotron resonance mass spectrometry. *J. Agric. Food Chem.* **2004**, *52*, 5322–5328.
(13) Gomez-Ariza, J. L.; Arias-Borrego, A.; Garcia-Barrera, T. Use of flow injection atmospheric pressure photoionization quadrupole time-of-flight mass spectrometry for fast olive oil fingerprinting. *Rapid Commun. Mass Spectrom.* **2006**, *20*, 1181–1186.
(14) Woodbury, S. E.; Evershed, R. P.; Rossell, J. B.; Griffith, R. E.; Farnell, P. Detection of vegetable oil adulteration using gas-chromatography combustion isotope ratio mass-spectrometry. *Anal. Chem.* **1995**, *67*, 2685–2690.
(15) Řezanka, T.; Řezanková, H. Characterization of fatty acids and triacylglycerols in vegetable oils by gas chromatography and statistical analysis. *Anal. Chim. Acta* **1999**, *398*, 253–261.
(16) Destaillats, F.; de Wispelaere, M.; Joffre, F.; Golay, P. A.; Hug, B.; Giuffrida, F.; Fauconnot, L.; Dionisi, F. Authenticity of milk fat by fast analysis of triacylglycerols - Application to the detection of partially hydrogenated vegetable oils. *J. Chromatogr., A* **2006**, *1131*, 227–234.
(17) Lee, D. S.; Lee, E. S.; Kim, H. J.; Kim, S. O.; Kim, K. Reversed phase liquid chromatographic determination of triacylglycerol composition in sesame oils and the chemometric detection of adulteration. *Anal. Chim. Acta* **2001**, *429*, 321–330.
(18) Parcerisa, J.; Casals, I.; Boatella, J.; Codony, R.; Rafecas, M. Analysis of olive and hazelnut oil mixtures by high-performance Liquid chromatography-atmospheric pressure chemical ionisation mass spectrometry of triacylglycerols and gas-liquid chromatography of non-saponifiable compounds (tocopherols and sterols). *J. Chromatogr., A* **2000**, *881*, 149–158.

(19) Jakab, A.; Héberger, K.; Forgács, E. Comparative analysis of different plant oils by high-performance liquid chromatography-atmospheric pressure chemical ionization mass spectrometry. *J. Chromatogr., A* **2002**, *976*, 255–263.
(20) Nagy, K.; Bongiorno, D.; Avellone, G.; Agozzino, P.; Ceraulo, L.; Vékey, K. High performance liquid chromatography-mass spectrometry based chemometric characterization of olive oils. *J. Chromatogr., A* **2005**, *1078*, 90–97.
(21) Dugo, P.; Kumm, T.; Fazio, A.; Dugo, G.; Mondello, L. Determination of beef tallow in lard through a multidimensional off-line non-aqueous reversed phase-argentation LC method coupled to mass spectrometry. *J. Sep. Sci.* **2006**, *29*, 567–575.
(22) Holčapek, M.; Lísa, M.; Jandera, P.; Kabátová, N. Quantitation of triacylglycerols in plant oils using HPLC with APCI-MS, evaporative light-scattering, and UV detection. *J. Sep. Sci.* **2005**, *28*, 1315–1333.
(23) Lísa, M.; Holčapek, M. Triacylglycerols profiling in plant oils important in food industry, dietetics and cosmetics using high-performance liquid chromatography-atmospheric pressure chemical ionization mass spectrometry. *J. Chromatogr., A* **2008**, *1198*, 115–130.
(24) Lísa, M.; Holčapek, M.; Řezanka, T.; Kabátová, N. High-performance liquid chromatography-atmospheric pressure chemical ionization mass spectrometry and gas chromatography-flame ionization detection characterization of Δ5-polyenoic fatty acids in triacylglycerols from conifer seed oils. *J. Chromatogr., A* **2007**, *1146*, 67–77.
(25) Adlof, R. O. Analysis of triacylglycerol positional isomers by silver ion high-performance liquid-chromatography. *J. High Resolut. Chromatogr.* **1995**, *18*, 105–107.
(26) Lísa, M.; Velínská, H.; Holčapek, M. Regioisomeric characterization of triacylglycerols using silver-ion HPLC/MS and randomization synthesis of standards. *Anal. Chem.* **2009**, *81*, 3903–3910.
(27) Cvačka, J.; Hovorka, O.; Jiroš, P.; Kindl, J.; Stránský, K.; Valterová, I. Analysis of triacylglycerols in fat body of bumblebees by chromatographic methods. *J. Chromatogr., A* **2006**, *1101*, 226–237.
(28) Mottram, H. R.; Woodbury, S. E.; Evershed, R. P. Identification of triacylglycerol positional isomers present in vegetable oils by high performance liquid chromatography atmospheric pressure chemical ionization mass spectrometry. *Rapid Commun. Mass Spectrom.* **1997**, *11*, 1240–1252.
(29) Holčapek, M.; Jandera, P.; Zderadička, P.; Hrubá, L. Characterization of triacylglycerol and diacylglycerol composition of plant oils using high-performance liquid chromatography-atmospheric pressure chemical ionization mass spectrometry. *J. Chromatogr., A* **2003**, *1010*, 195–215.
(30) Byrdwell, W. C.; Neff, W. E. Dual parallel electrospray ionization and atmospheric pressure chemical ionization mass spectrometry (MS), MS/MS and MS/MS/MS for the analysis of triacylglycerols and triacylglycerol oxidation products. *Rapid Commun. Mass Spectrom.* **2002**, *16*, 300–319.
(31) Fauconnot, L.; Hau, J.; Aeschlimann, J. M.; Fay, L. B.; Dionisi, F. Quantitative analysis of triacylglycerol regioisomers in fats and oils using reversed-phase high-performance liquid chromatography and atmospheric pressure chemical ionization mass spectrometry. *Rapid Commun. Mass Spectrom.* **2004**, *18*, 218–224.
(32) Leskinen, H.; Suomela, J. P.; Kallio, H. Quantification of triacylglycerol regioisomers in oils and fat using different mass spectrometric and liquid chromatographic methods. *Rapid Commun. Mass Spectrom.* **2007**, *21*, 2361–2373.
(33) McAnoy, A. M.; Wu, C. C.; Murphy, R. C. Direct qualitative analysis of triacylglycerols by electrospray mass spectrometry using a linear ion trap. *J. Am. Soc. Mass Spectrom.* **2005**, *16*, 1498–1509.
(34) Jolliffe, I. T. *Principal Component Analysis*; Springer-Verlag: New York, 1986.

Received April 8, 2009. Revised manuscript received June 12, 2009. Accepted June 15, 2009. This work was supported by the grant project no. MSM0021627502 sponsored by the Ministry of Education, Youth and Sports of the Czech Republic and projects nos. 203/06/0219 and 203/09/P249 sponsored by the Czech Science Foundation.

Michal Holčapek
Hana Velínská
Miroslav Lísa
Petr Česla

Department of Analytical Chemistry, Faculty of Chemical Technology, University of Pardubice, Pardubice, Czech Republic

Received June 3, 2009
Revised July 9, 2009
Accepted August 6, 2009

Research Article

Orthogonality of silver-ion and non-aqueous reversed-phase HPLC/MS in the analysis of complex natural mixtures of triacylglycerols

The goal of this work is the study of possibilities of two basic separation modes used in the analysis of complex triacylglycerol (TG) samples of plant oils and animal fats, *i.e.* non-aqueous reversed-phase (NARP) and silver-ion HPLC coupled with atmospheric pressure chemical ionization mass spectrometry (APCI-MS). The orthogonality of both separation modes is tested for complex TG mixtures containing fatty acids (FAs) with different acyl chain lengths, different number, positions and geometry of double bonds (DBs) and different regioisomeric positions of FAs on the glycerol skeleton. The retention in NARP mode is governed by the equivalent carbon number, while the retention in silver-ion chromatography increases with the increasing number of DBs with a clear differentiation between *cis*- and *trans*-FAs. Moreover, silver-ion mode enables at least the partial resolution of regioisomeric TG mixtures including *cis*-/*trans*-regioisomers, as illustrated on two examples of randomization mixtures. Off-line 2D coupling of both complementary modes (NARP in the first dimension and silver-ion in the second dimension) yields the superior chromatographic selectivity resulting in the highest number of identified TGs ever reported for studied samples. Off-line 2D chromatograms are processed with the home-made software providing various ways of data visualization.

Keywords: 2D liquid chromatography / Regioisomers / Silver-ion chromatography / *Trans* fatty acids / Triacylglycerols
DOI 10.1002/jssc.200900401

1 Introduction

Triacylglycerols (TGs) from plant oils and animal fats are an important part of human diet due to their high nutritional value. They are the source of energy, essential FAs (linoleic and linolenic acids), fat-soluble vitamins (A, D, E and K), *etc.* [1–4]. Natural samples of TGs are complex mixtures of tens up to hundreds of TG species with different physico–chemical properties given by the type of esterified FAs. TGs are characterized by the total carbon number (CN) and the number, position and configuration (*cis*-/*trans*-) of double bonds (DBs) in FA acyl chains. TGs can also differ in the stereospecific positions of FAs on the glycerol skeleton (*sn*-1, 2 or 3) yielding TG regioisomers. If TG has different FAs in *sn*-1/3 positions, then the carbon atom in the *sn*-2 position becomes a chiral center. The combination of different FAs and above mentioned types of isomerism in TGs lead to an enormous number of TG species in natural samples. The characterization of natural mixtures based on the determination of esterified FAs is not sufficient to describe all physico–chemical and nutritional properties of samples. The determination of stereospecific positions of FAs in TGs is important due to the stereospecific environment in the human organism. Another issue is the identification of *trans*-FAs (TFAs) in TGs, which are assumed to have harmful health effects. The characterization of TGs in complex natural mixtures including the determination of different types of isomerism is a challenging task requiring the combination of various separation modes, careful optimization of separation conditions and the use of appropriate detection technique.

Non-aqueous reversed-phase (NARP) HPLC coupled to MS enables the identification of the highest number of TG species in natural samples [5–19]. The retention of TGs depends on the equivalent carbon number (ECN) defined as the total CN in all acyl chains minus two times the number of DBs. The retention of TGs increases depending on the

Correspondence: Professor Michal Holčapek, University of Pardubice, Faculty of Chemical Technology, Department of Analytical Chemistry, Studentská 573, 53210 Pardubice, Czech Republic
E-mail: Michal.Holcapek@upce.cz
Fax: +420-466-037-068

Abbreviations: A, arachidic; **APCI,** atmospheric pressure chemical ionization; **CN,** carbon number; **DB,** double bond; **2D,** two-dimensional; **E,** elaidic; **ECN,** equivalent carbon number; **FA,** fatty acid; **G,** gadoleic; **L,** linoleic; **Ln,** alpha-linolenic; **γ-Ln,** gamma-linolenic; **M,** myristic; **Ma,** margaric; **Mo,** margaroleic; **NARP,** non-aqueous reversed-phase; **O,** oleic; **P,** palmitic; **Po,** palmitoleic; **S,** stearic; **St,** stearidonic; **TFA,** *trans*-fatty acid; **TG,** triacylglycerol

ECN. Under optimized NARP-HPLC conditions (*i.e.* column packing, column length, separation temperature, mobile phase gradient, *etc.*) [11, 13], TGs within one ECN group can be separated according to the length and unsaturation of FAs, the position [12, 16, 19] and configuration of DBs [17, 20]. NARP system has a lower selectivity for the separation of TG regioisomers and their partial separation is feasible only with the multiple column coupling and very long retention times in the range of 100–200 min [21, 22], which is not practical for the routine use.

TGs differing in the DB number are well separated using silver-ion normal-phase HPLC [23–29]. This method is based on the formation of weak reversible complexes of silver ions immobilized on the stationary phase (impregnated silica or ion-exchange column) with π electrons of DBs during the sample elution throughout the chromatographic column. The retention of TGs increases with increasing unsaturation of TGs and it is also affected by the position [26, 28] and geometry [23, 29] of DBs and partially by the length of acyl chain [26]. The steric availability of DBs for the interaction with silver ions in regioisomers enables their separation under carefully optimized conditions [23, 26], *i.e.* column packing and column length, mobile phase composition or gradient steepness. The identification of TG regioisomers is also possible using MS detection based on different relative abundances of fragment ions formed by the neutral losses of FAs from *sn*-1/3 and *sn*-2 positions [10, 18, 30–33]. This approach is often applied for the assignment of prevailing FA in the *sn*-2 position, however the calibration curves for mixtures of both regioisomers have to be measured for the quantitative determination of *sn*-2 occupation [10, 30–32] using the same instrument and ionization technique. Standards of regioisomers are commercially available only at very limited range and their synthesis by the randomization procedure from mono-acid TG standards enables to measure relative abundances of fragment ions for pure compounds [26]. Atmospheric pressure chemical ionization (APCI) is the most frequently used ionization technique for TGs analysis due to their non-polar character, but the electrospray ionization can be applied as well due to the formation of ammonium adducts [34].

The combination of NARP and silver-ion separations in 2D chromatography using either on-line [35–37] or off-line [38–40] mode with APCI-MS detection promises the identification of the highest number of TGs in complex mixtures from plant oils and animal fats. On-line separation with silver-ion separation in the first dimension and NARP in the second dimension enables the fast separation of TGs in two chromatographic modes without the intervention of operator. In contrast, off-line setup requires the fraction collection in the first dimension and their analysis in the second dimension is more laborious, but the retention window in the second dimension is not limited by the fraction collection time in the first dimension.

The main goal of our work is the development of off-line 2D HPLC/MS method applicable for the separation of the highest possible number of TGs including the resolution of TG regioisomers and TGs containing TFA. TGs are separated in the first NARP dimension according to the ECN and collected 1 min fractions are then analyzed with silver-ion HPLC in the second dimension followed by APCI-MS identification. The possibility of off-line 2D HPLC for a wide range of TGs is illustrated with complex TG mixtures prepared by the randomization procedure. Selected examples of complex plant oil (blackcurrant oil) and animal fat (beef tallow) are discussed.

2 Materials and methods

2.1 Materials

Acetonitrile, 2-propanol and hexane (HPLC gradient grade solvents) and sodium methoxide were purchased from Sigma-Aldrich (St. Louis, MO, USA). Standards of tripalmitin (PPP, C16:0), tristearin (SSS, C18:0), triolein (OOO, 9-C18:1), trielaidin (EEE, 9*t*-C18:1), trilinolein (LLL, 9,12-C18:2), trilinolenin (LnLnLn, 9,12,15-C18:3) and triarachidin (AAA, C20:0) were purchased from Nu–ChekPrep (Elysian, MN, USA). Blackcurrant oil was prepared in the laboratory using the extraction with hexane according to ref. [10]. Beef tallow was prepared from the fat tissue using the same procedure after the homogenization of tissue with hexane in a homogenizer.

2.2 Randomization

Standards of mixed-acid TGs ($R_1R_1R_2$, $R_1R_2R_2$, *etc.*) were prepared from mono-acid triacyglycerols ($R_1R_1R_1$) using the randomization procedure according to Ref. [26]. Briefly, the mixture of 25 mg of OOO, 25 mg of EEE and 100 mg of sodium methoxide were weighed into a dry boiling flask with the addition of 2 mL of hexane dried with molecular sieves. The mixture was heated for 30 min in a water bath under the reflux condenser at constant temperature 75°C. Then, the reaction mixture was extracted with water and three times with 1 mL of methanol to remove sodium methoxide. The hexane phase containing the randomized analyte was used for the HPLC analysis. The same procedure was applied for the mixture of 15 mg of PPP, 15 mg of SSS, 15 mg of OOO, 15 mg of LLL, 15 mg of LnLnLn, 15 mg of AAA and 180 mg of sodium methoxide.

2.3 NARP-HPLC

NARP-HPLC experiments were performed on a chromatographic apparatus consisting of a Model 616 pump with a quaternary gradient system, a Model 996 diode-array UV detector, a Model 717+ autosampler, a thermostated column compartment and a Millenium chromatography manager (all from Waters, Milford, MA, USA). Samples

were analyzed using the following HPLC conditions: two chromatographic columns Nova-Pak C_{18} (300 × 3.9 and 150 × 3.9 mm, 4 μm, Waters) connected in series, a flow rate of 1 mL/min, an injection volume of 10 μL, column temperature of 25°C and UV detection at 205 nm. The mobile phase gradient with the slope of 0.65%/min was used for the analysis of TGs from plant oils (method 1) according to ref. [11]: 0 min–100% acetonitrile, 106 min–31% acetonitrile + 69% 2-propanol, 109 min–100% acetonitrile. The maximum backpressure at the end of gradient was about 270 bars. The mobile phase gradient with the slope of 0.33%/min was used for the analysis of TGs from animal fats (method 2): 0 min–80% A + 20% B, 121 min–40% A + 60% B, 122 min–80% A + 20% B, where A was acetonitrile and B was a mixture of hexane–2-propanol (1:1, v/v). The injector needle was washed with the mobile phase before each injection. The column hold-up volume, t_M, was 3.20 min for the system with 300+150 mm Nova-Pak C_{18} columns. The automated fraction collector Gilson FC203B (Middleton, WI, USA) was used for collecting 1 min fractions in the NARP mode using 2 mL vials. Solvents from collected fractions were evaporated using a mild stream of nitrogen and then fractions were redissolved in 150 μL of the initial mobile phase used for the silver-ion HPLC. These fractions were subsequently analyzed by silver-ion HPLC/MS.

2.4 Silver-ion HPLC

Silver-ion HPLC experiments were performed on the liquid chromatograph Agilent 1200 Series (Agilent Technology, Waldbronn, Germany). The final silver-ion HPLC method for the analysis of plant oils and animal fats used the following conditions [26]: three silver-ion columns ChromSpher Lipids (250 × 4.6 mm, 5 μm, Varian, Palo Alto, CA, USA) connected in series, the flow rate of 1 mL/min, the injection volume of 1 μL, column temperature of 25°C, and the mobile phase gradient: 0 min–100% A, 140 min–61% A + 39% B, where A is the mixture of hexane–2-propanol–acetonitrile (99.8:0.1:0.1, v/v/v) and B is the mixture of hexane–2-propanol–acetonitrile (96:2:2, v/v/v). Mobile phases were prepared fresh every day. Silver-ion columns were conditioned at 50 μL/min of the initial mobile phase composition overnight and then at 1 mL/min for one hour before the first analysis. The injector needle was washed with the mobile phase before each injection. The chromatographic system was equilibrated between injections for 30 min. The hybrid quadrupole time-of-flight analyzer micrOTOF-Q (Bruker Daltonics, Bremen, Germany) with positive-ion APCI was used in the mass range 50–1200 *m/z* with the following tuning parameters: the flow of the nebulizing and drying gas 5 and 3 L/min, respectively, temperatures of the drying gas and APCI heater 300 and 400°C, respectively. Reconstructed ion current chromatograms were used to support the identification of coeluting peaks.

2.5 Evaluation of 2D data

2D data were processed using the software developed in the laboratory [41] based on the Python programming language with Matplotlib 2D plotting library. The data from mass spectrometer were exported as netCDF files. Reconstructed ion chromatograms were converted into the ASCII format and the matrix with rows corresponding to the fraction collection period was created. 2D chromatograms were constructed as contour plots with the first dimension retention times from NARP-HPLC on the *x*-axis and the second dimension retention times from silver-ion HPLC on the *y*-axis. Retention data of all TGs detected in this work are summarized in Table 1.

3 Results and discussion

3.1 Comparison of retention mechanisms in NARP and silver-ion HPLC

First, the optimum TG test mixture has been selected for the demonstration of possibilities and limits of both NARP and silver-ion separation modes. Two types of isomerism are critical for the HPLC separation, *i.e.* regioisomerism ($R_1R_1R_2$ *versus* $R_1R_2R_1$) and geometrical isomerism of DBs (*cis- versus trans-*). Therefore, mono-acid TGs containing *cis*-FA (oleic acid, 9-C18:1, O) and *trans*-FA (elaidic acid, 9*t*-C18:1, E) have been randomized according to the procedure described in our previous work [26] yielding a randomization mixture of TGs at identical concentration ratios: OOO, OOE, OEO, EOO, OEE, EOE, EEO and EEE. Doublets OOE/EOO and OEE/EEO are enantiomers and hence they cannot be resolved in non-chiral environment, so their coelution must be expected in both studied systems. NARP systems provide the partial separation of species differing in the total number of TFA, but regioisomers are coeluting under these conditions (Fig. 1A). On the other hand, silver-ion mode yields more than sufficient separation of TGs differing in the total number of TFA but also partial separation of regioisomers EOE/OEE and OOE/OEO (Fig. 1B). It is interesting to note that the retention of TFAs is slightly higher in NARP mode, but significantly lower in silver-ion compared with *cis*-FAs. It is in agreement with well-known fact that the physico-chemical properties of TFA are closer to saturated FAs due to the linear arrangement of alkyl chains containing *trans*-DB similarly as for saturated chains. This simple rule is generally valid for the retention of all TGs in both separation modes, which helps in the planning of optimal conditions for 2D separation of target analytes and also the data interpretation.

The second example (Fig. 2) is the randomization mixture of the same amounts of six mono-acid TGs (PPP, SSS, OOO, LLL, LnLnLn and AAA) with different number of DBs and lengths of FA acyl chains providing theoretically $n^3 = 216$ (for $n = 6$) of different TGs considering all types of isomerism [26]. When enantiomers are neglected, there is

Table 1. Retention times of all TGs detected in silver-ion mode and NARP mode for studied samples in this work

TG[a)]	DB	t_R in silver-ion mode (min)[b)]	ECN	t_R in NARP mode (min)	
				Method 1[c)]	Method 2[d)]
AAA	0	16.9	60	117.5	–
AAS[e)]		17.1	58	113.4	–
AAP[e)]		17.5	56	109.0	–
ASS[e)]		17.5	56	109.1	92.2
SSS		17.6	54	104.6	86.2
ASP[e)]		17.6	54	104.7	86.5
SSMa[e)]		17.8	53	–	83.2
APP[e)]		17.9	52	99.6	–
SSP[e)]		17.9	52	99.7	79.8
SPMa[e)]		18.1	51	–	76.5
SPP[e)]		18.3	50	94.4	72.9
SMaM[e)]		18.5	49	–	67.8
PPP		18.7	48	88.7	65.5
SPM[e)]		18.7	48	–	65.6
AOA	1	36.1	56	107.4	–
AOS		36.9	54	102.6	84.8
SGS		36.9	54	–	84.4
SC19:00[e)]		37.3	53	–	81.8
AOP		37.3	52	97.5	78.2
SOS		37.3	52	97.6	78.3
SGP		37.3	52	–	77.8
SOMa		37.5	51	–	74.8
SOP		37.7	50	92.3	71.3
POMa		37.9	49	–	67.7
SMoP		37.9	49	–	67.8
POP		38.1	48	87.0	63.8
SOM		38.1	48	–	64.0
POC15:0		38.3	47	–	60.2
PPoP		38.4	46	–	56.1
POM		38.4	46	81.3	56.2
AAO		38.6	56	107.4	–
GSS		38.6	54	–	84.4
ASO[e)]		38.6	54	102.6	84.8
GSP[e)]		38.9	52	–	77.8
APO[e)]		38.9	52	97.5	78.2
SSO		38.9	52	97.6	78.3
SMaO[e)]		39.1	51	–	74.8
SPO[e)]		39.3	50	92.3	71.3
OPMa[e)]		39.7	49	–	67.7
SPMo[e)]		39.6	49	–	67.8
OPP		39.7	48	87.0	63.8
OSM[e)]		39.7	48	–	64.0
PC15:00[e)]		39.9	47	–	60.2
PPPo		40.0	46	–	56.1
OPM[e)]		40.0	46	81.3	56.2
SOE	2	48.6	50	–	70.8
EOP		48.9	54	–	63.2
ALA		50.9	54	102.2	–
ALS		51.1	52	96.9	–
ALP		51.4	50	91.8	–
SLS		51.4	50	91.9	–
SLP		51.7	48	86.6	62.9
PLP		52.0	46	80.9	55.2
AAL		52.1	54	102.2	–
ASL[e)]		52.2	52	96.9	–

Table 1. Continued

TG[a)]	DB	t_R in silver-ion mode (min)[b)]	ECN	t_R in NARP mode (min)	
				Method 1[c)]	Method 2[d)]
APL[e)]		52.5	50	91.8	–
SSL		52.5	50	91.9	–
SPL[e)]		52.8	48	86.6	62.9
GSO		52.8	52	–	76.3
AOO		52.8	52	96.0	76.7
LPP		53.0	46	80.9	55.2
GPO		53.1	50	–	69.1
SOO		53.1	50	90.8	69.6
OOMa		53.2	49	–	66.0
OOP		53.4	48	85.4	62.0
OAO		53.8	52	96.0	–
OSO		54.0	50	90.8	69.6
OMaO		54.2	49	–	66.0
OPO		54.3	48	85.4	62.0
OPMo		54.5	47	–	58.3
OMO		54.6	46	–	54.4
OPPo		54.6	46	–	54.8
ALnA	3	58.3	52	97.3	–
ALO		58.6	50	90.4	–
ALnS		58.6	50	92.2	–
SLnS		58.7	48	86.9	–
ALnP		58.9	48	86.8	–
SLnP		59.0	46	81.4	55.2
SLO		59.2	48	85.1	61.4
AOL		59.2	50	90.4	–
OLMa		59.4	47	–	57.6
OPoPo		59.8	44	–	47.5
PLnP		59.8	44	75.4	–
OLP		59.8	46	79.3	53.6
SOL		59.8	48	85.1	61.4
AALn		60.1	52	97.3	–
LOP		60.5	46	79.3	53.6
OAL		60.7	50	90.4	–
ASLn[e)]		60.7	50	92.2	–
SSLn		61.0	48	86.9	–
APLn[e)]		61.1	48	86.8	–
OSL		61.2	48	85.1	61.4
OOO		61.6	48	84.0	60.5
SPLn[e)]		61.7	46	81.4	55.2
OPL		61.8	46	79.3	53.6
LnPP		61.9	44	75.4	–
ALL	4	68.6	48	84.8	–
ALnO		68.6	48	85.4	–
SLL		69.0	46	79.0	–
LLP		69.4	44	73.1	45.6
AOLn		69.7	48	85.4	–
OLO		70.0	46	77.9	52.0
LAL		70.0	48	84.8	–
OOL		70.4	46	77.9	52.0
LSL		70.4	46	79.0	53.2
SLnO		70.4	46	80.0	–
SOLn		70.7	46	80.0	–
LPL		70.8	44	73.1	45.6
OLnP		70.9	44	74.0	–
OALn		71.2	48	85.4	–
γLnOP		71.4	44	74.0	–

Table 1. Continued

TG[a)]	DB	t_R in silver-ion mode (min)[b)]	ECN	t_R in NARP mode (min)	
				Method 1[c)]	Method 2[d)]
OSLn		71.8	46	80.0	–
OPLn		72.2	44	74.0	–
LnOP		72.2	44	74.7	–
GLL	5	75.3	46	77.2	–
ALnL		76.6	46	79.6	–
ALLn		76.7	46	79.6	–
OLL		77.0	44	71.8	–
SLnL		77.1	44	73.8	–
SLLn		77.3	44	73.8	–
LOL		77.4	44	71.8	–
LALn		78.2	46	79.6	–
LSLn		78.8	44	73.8	–
LLnP		79.3	42	67.8	–
LnLP		79.5	42	67.8	–
OLnO		79.7	44	72.6	–
OOLn		80.4	44	72.6	–
LPLn		80.9	42	67.8	–
γLnLP		81.2	42	68.5	–
OOγLn		81.3	44	73.3	–
GLLn	6	85.3	44	72.1	–
LLL		85.4	42	65.3	–
GLγLn		86.6	44	72.8	–
OLnL		86.7	42	66.4	–
OLLn		86.8	42	66.4	–
ALnLn		87.0	44	74.3	–
LOLn		87.2	42	66.4	–
SLnLn		87.5	42	68.5	–
LnLnP		88.2	40	62.1	–
LOγLn		88.6	42	67.1	–
LnALn		88.7	44	74.3	–
LnSLn		89.2	42	68.5	–
LnPLn		89.7	40	62.1	–
γLnPLn		91.1	40	62.8	–
γLnγLnP		91.5	40	63.5	–
SLSt		91.5	42	69.6	–
LLnL	7	92.1	40	59.6	–
LLLn		92.3	40	59.6	–
LLγLn		93.7	40	60.4	–
OLnLn		94.1	40	60.8	–
LnOLn		94.5	40	60.8	–
γLnOLn		95.2	40	61.6	–
γLnOγLn		95.8	40	62.3	–
OLSt		96.6	40	61.9	–
LOSt		97.0	40	61.9	–
LnPSt		98.1	38	57.2	–
LLnLn	8	101.6	38	54.0	–
LnLLn		101.8	38	54.0	–
γLnLLn		102.6	38	54.7	–
LLSt		104.3	38	55.1	–
γLnLγLn		104.4	38	55.4	–
LnOSt		105.4	38	56.1	–
γLnOSt		106.0	38	56.8	–
StPSt		108.5	36	52.6	–
LnLnLn	9	110.1	36	48.3	–
LnLSt		111.0	36	49.4	–
γLnLnLn		111.4	36	49.0	–

Table 1. Continued

TG[a)]	DB	t_R in silver-ion mode (min)[b)]	ECN	t_R in NARP mode (min)	
				Method 1[c)]	Method 2[d)]
γLnLSt		112.5	36	50.1	–
γLnγLnLn		112.9	36	49.7	–
γLnγLnγLn		114.3	36	50.6	–
LnLnSt	10	120.2	34	43.5	–
γLnLnSt		121.9	34	44.2	–
γLnγLnSt		123.1	34	44.9	–

a) Abbreviations used for fatty acids: **A**–arachidic (C20:0); **E**–elaidic (Δ9*trans*-C18:1), **G**–gadoleic (Δ9-C20:1), **L**–linoleic (Δ9,12-C18:2), **Ln**–alpha-linolenic (Δ9,12,15-C18:3), γ-**Ln**–gamma-linolenic (Δ6,9,12-C18:3), **M**–myristic (C14:0), **Ma**–margaric (C17:0), **Mo**–margaroleic (Δ9-C17:1), **O**–oleic (Δ9-C18:1), **P**–palmitic (C16:0), **Po**–palmitoleic (Δ9-C16:1), **S**–stearic (C18:0), **St**–stearidonic (Δ6,9,12,15-C18:4).

b) Silver-ion HPLC – three ChromSpher Lipids columns in the total length 75 cm, flow rate 1 mL/min, injection volume 1 μL, column temperature 25°C, mobile phase gradient: 0 min–100% A, 140 min–61% A + 39% B, where A is the mixture of hexane–2-propanol– acetonitrile (99.8:0.1:0.1, v/v/v) and B is the mixture of hexane–2-propanol–acetonitrile (96:2:2, v/v/v).

c) NARP method 1 – two chromatographic columns Nova-Pak C_{18} in the total length 45 cm, flow rate 1 mL/min, injection volume 10 μL, column temperature 25°C, mobile phase gradient: 0 min–100% acetonitrile, 106 min–31% acetonitrile + 69% 2-propanol, 109 min–100% acetonitrile.

d) NARP method 2 – mobile phase gradient: 0 min–80% A + 20% B, 121 min–40% A + 60% B, 122 min–80% A + 20% B, where A is acetonitrile and B is the mixture of hexane–2-propanol (1:1, v/v), other conditions are identical as for method 1.

e) These regioisomers cannot be resolved.

still $(n^3+n^2)/2 = 126$ different TGs. Figure 2A shows the NARP chromatogram, where some groups are strongly coeluting and they can be resolved only by reconstructed ion current chromatogram of appropriate m/z values due to APCI-MS detection. Regioisomers are not resolved in this mode; therefore, we use peak annotations with the asterisk for non-resolved regioisomers (Fig. 2). The retention is driven by the ECN with the partial or sometimes full separation inside ECN groups. Silver-ion chromatogram (Fig. 2B) shows quite different picture, where the retention is governed by the DB number, while the carbon chain length has only a minor effect on the retention. The unique feature of silver-ion chromatography is the ability to separate regioisomers under optimized conditions. The illustrative example of retention mechanism in this separation mode is the TG group containing one DB (Fig. 2B), which forms a mirror-like picture of two quintuplet peaks AOA/AOS/AOP+SOS/SOP/POP and AAO/ASO/APO+SSO/SPO/OPP. The regioisomeric position has a stronger effect on the retention than the carbon chain length. Unsaturations in the side *sn*-1/3 positions enable a stronger interaction with silver ions and hence higher retention than

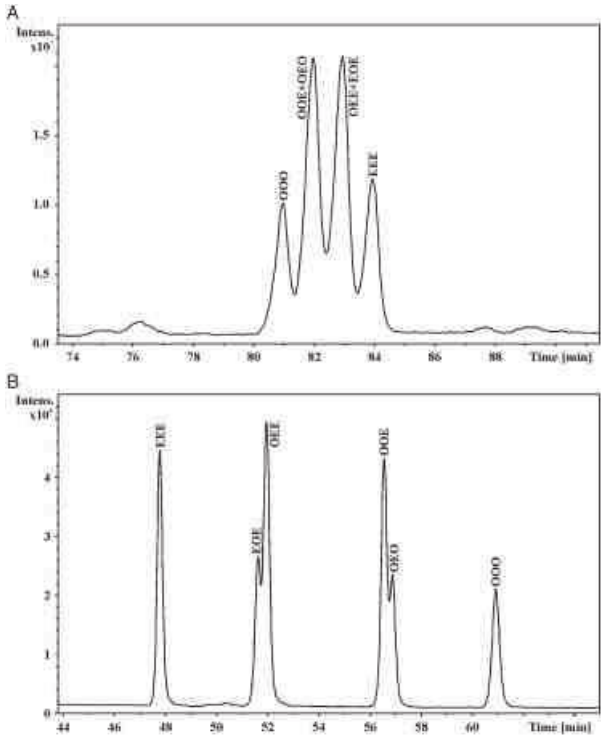

Figure 1. HPLC chromatograms of the randomization mixture of triolein (OOO, 9-C18:1) and trielaidin (EEE, 9*t*-C18:1) with APCI-MS detection: (A) NARP-HPLC using the method 1 – two Nova-Pak C_{18} columns in the total length 45 cm, flow rate 1 mL/min, column temperature 25°C, gradient of acetonitrile–2-propanol, (B) silver-ion HPLC – three ChromSpher Lipids columns in the total length 75 cm, flow rate 1 mL/min, column temperature 25°C, gradient of hexane–2-propanol–acetonitrile, see Section 2 for more details.

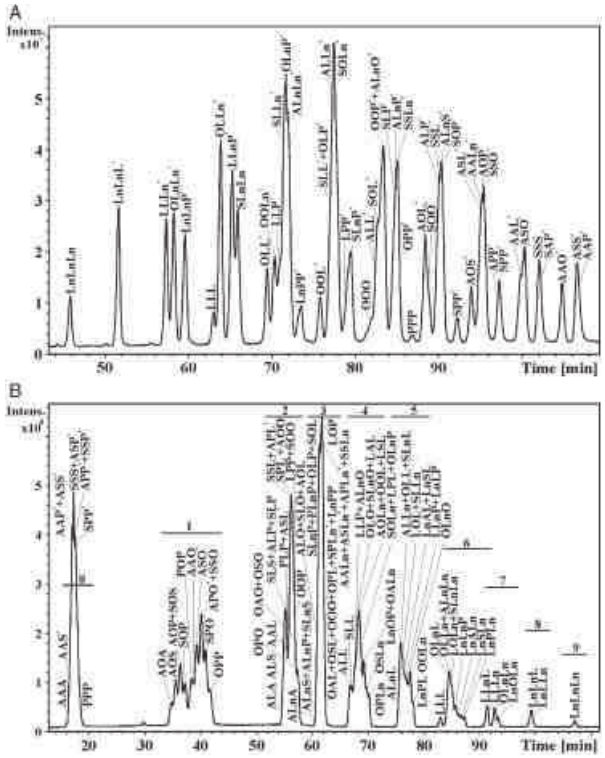

Figure 2. HPLC chromatograms of the randomization mixture of PPP, SSS, OOO, LLL, LnLnLn and AAA: (A) NARP chromatogram using the method 1, (B) silver-ion chromatogram with labeled DB groups, conditions identical as for Fig. 1. Non-resolved regioisomers are labeled with the asterisk.

regioisomers with the same unsaturation in the middle *sn*-2 position, for example POP < OPP. The longer saturated alkyl chain means the lower retention in silver-ion mode (A < S < P). Figure 3 is a compilation of 2D record obtained from NARP and silver-ion data showing relatively good coverage of 2D separation space. Colored labeling of DB and ECN groups improves the visualization of this plot containing labeled sections for 0–7 DBs and 40–54 ECNs, which is in total 64 sections out of which 27 sections are occupied by peaks of TGs, while the remaining 37 are empty, which is affected by the initial choice of mono-acid TGs used for the randomization. Figure 3 shows only the zoomed region of whole 2D chromatogram to enable a reasonable visibility of annotation. The full data are summarized in Table 1.

On the other hand, silver-ion chromatograms provide rather complex records of many strongly overlapping peaks within individual DB groups complicating the interpretation. If the silver-ion separation is coupled in off-line 2D separation with NARP, then the superior chromatographic performance is obtained providing the separation, identification and quantitation of the highest number of TG isomers. On-line 2D limits the analysis time in the second dimension typically to 1 min according to time used for the modulation, but this time is not sufficient either for the silver-ion separation of regioisomers or good resolution in NARP mode. Therefore, off-line 2D coupling enables to explore the full separation power of both dimensions resulting in the highest possible number of identified TGs at cost of higher total analysis time of 3 days running for 24 h per day automatically in case of blackcurrant oil including all steps, *i.e.* automated fraction collection in the first dimension and half an hour equilibration between individual injections in the second dimension.

3.2 Analysis of TGs in plant oils

Blackcurrant oil is one of the most complex plant oils analyzed in our laboratory [10, 11, 13–16, 26] containing a high proportion of essential FAs and both α- and γ-linolenic acids; therefore, this sample is selected for 2D analysis as a chromatographic challenge. Figure 4A depicts a zoomed region of 2D separation of blackcurrant oil, where the first dimension is NARP method 1 using the coupling of two NovaPak C_{18} columns in the total length of 45 cm. Collected 1 min fractions by automated fraction collector are then analyzed in the second dimension by silver-ion chromatography using the coupling of three ChromSpher Lipid columns in the total length of 75 cm (see Section 2 for more

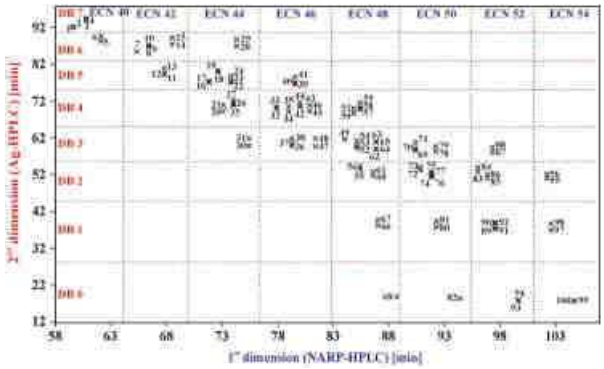

Figure 3. Reconstructed 2D plot compiled from NARP and silver-ion data shown in Fig. 2. Peak annotation:1-LLnL; 2-LLLn; 3-OLnLn; 4-LnOLn; 5-LnLnP; 6-LnPLn; 7-LLL; 8-OLnL; 9-OLLn; 10-LOLn; 11-LLnP; 12-LnLP; 13-LPLn; 14-SLnLn; 15-LnSLn; 16-OLL; 17-LOL; 18-OLnO; 19-OOLn; 20-LLP; 21-LPL; 22-SLnL; 23-SLLn; 24-LSLn; 25-OLnP; 26-LnOP; 27-OPLn; 28-ALnLn; 29-LnALn; 30-PLnP; 31-LnPP; 32-OLO; 33-OOL; 34-SLL; 35-LSL; 36-OLP; 37-LOP; 38-OPL; 39-ALnL; 40-ALLn; 41-LALn; 42-SLnO; 43-SOLn; 44-OSLn; 45-PLP; 46-LPP; 47-SLnP; 48-SPLn+PSLn; 49-OOO; 50-ALL; 51-LAL; 52-SLO; 53-SOL; 54-OSL; 55-OOP; 56-OPO; 57-ALnO; 58-AOLn; 59-OALn; 60-SLP; 61-SPL+PSL; 62-ALnP; 63-APLn+PALn; 64-SLnS; 65-SSLn; 66-POP; 67-OPP; 68-PPP; 69-ALO; 70-AOL; 71-OAL; 72-SOO; 73-OSO; 74-ALP; 75-APL+PAL; 76-SLS; 77-SSL; 78-ALnS; 79-ASLn+SALn; 80-SOP; 81-SPO+PSO; 82-SPP+PSP; 83-AOO; 84-OAO; 85-ALS; 86-ASL+SAL; 87-ALnA; 88-AALn; 89-AOP; 90-APO+PAO; 91-SOS; 92-SSO; 93-APP+PAP; 94-SSP+SPS; 95-AAL; 96-ALA; 97-AOS; 98-ASO+SAO; 99-SSS; 100-APS+ASP+PAS.

details). Fractions without detected peaks in the first dimension are not analyzed in the second dimension to save instrumental time. 2D plot shows colored labeling of 3–7 DBs and 40–46 ECNs (in total 20 sections), where 50% of them contain chromatographic peaks. Peaks in other boxes cannot be expected, because such combinations are not common in the nature.

The home-made software [41] has been previously used for the processing of comprehensive 2D chromatograms, but this work extends its applicability also for the successful visualization of off-line 2D data (Fig. 4B). The *z*-axis (out of plane) is in the logarithmic scale because of better visualization of small peaks. Another way of the presentation of 2D data is three-dimensional chromatogram shown in Fig. 6. Each presentation style of 2D data shown here has some advantages and drawbacks. Dot plots (Figs. 4A and 6A) are well suited for the precise observation of retention times in both dimensions, but the information on peak intensities and chromatographic resolution is lost. Three-dimensional presentation (Fig. 5) shows quickly an overall appearance of 2D record. Contour plots (Figs. 4B and 6B) are something in between, because retention times can be determined relatively easily from these records, the chromatographic resolution can be seen, but some problems may be with small and/or coeluting peaks. For these reasons, contour plots are considered the most suitable for the visualization of 2D chromatograms [35–37, 41].

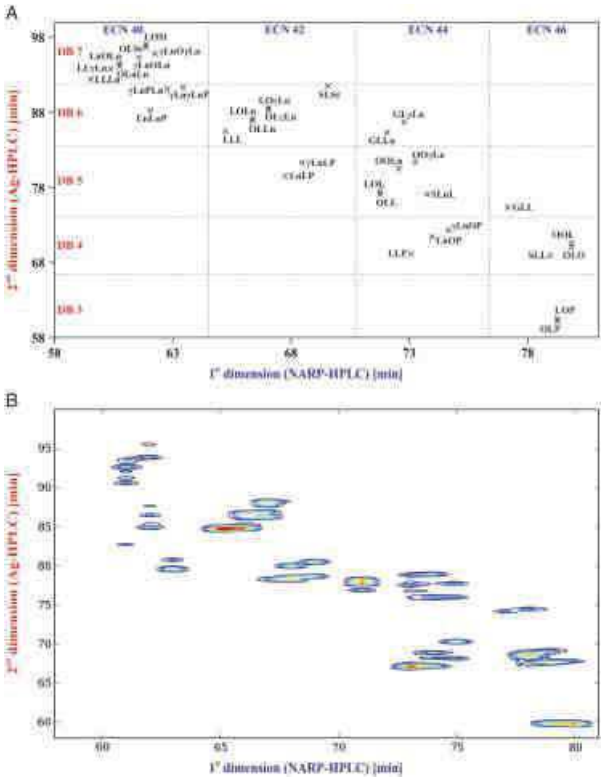

Figure 4. Off-line 2D chromatograms of blackcurrant oil using NARP in the first dimension and silver-ion mode in the second dimension after the fraction collection each minute: (A) dot plot with the peak annotation and DB and ECN labeling, (B) contour plot showing peak intensities, NARP and silver-ion conditions identical as for Fig. 1.

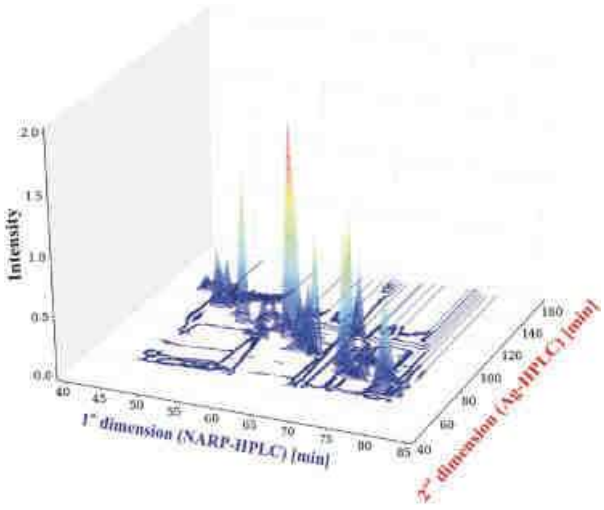

Figure 5. Three-dimensional presentation of 2D chromatogram of blackcurrant oil, conditions identical as for Fig. 1.

3.3 Analysis of TGs in animal fats

Some animal fats are known for their content of TFAs, which are monitored in our diet due to possible negative

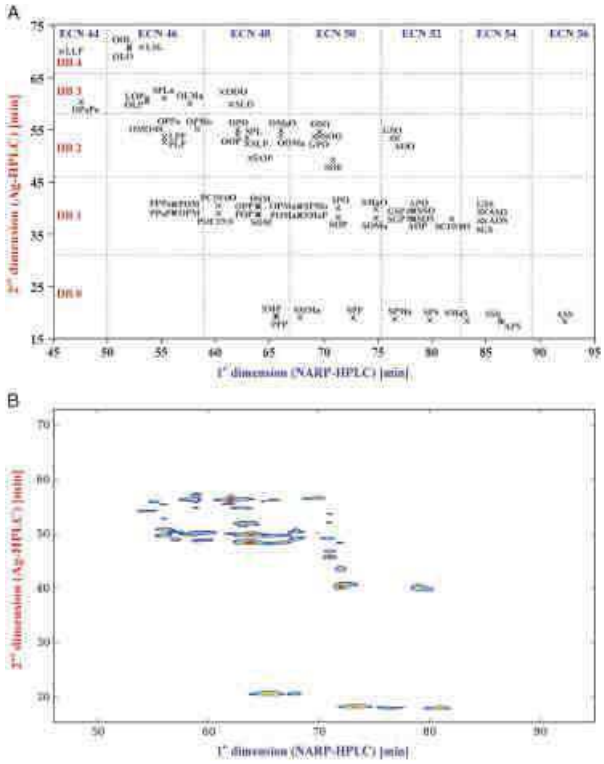

Figure 6. 2D chromatograms of beef tallow using NARP method 2 for the first dimension and silver-ion mode for the second dimension after the fraction collection each minute: (A) dot plot with the peak annotation and DB and ECN labeling, (B) contour plot showing peak intensities.

health effects if consumed in higher amounts. Beef tallow (Fig. 6) contains mainly saturated and monounsaturated FAs with a significant portion of TFA, which can be easily identified in the silver-ion mode due to significantly lower retention in comparison with *cis*-FAs. In principle, NARP separation mode is also applicable for the separation of *cis*-/*trans*-isomers, but the resolution is much worse in comparison with the silver-ion mode. There is also a notable amount of FAs containing the odd number of carbon atoms (*i.e.* C17:0, C17:1, C19:0) unlike to plant oils, where odd number FAs are present only at trace levels. For a better clarity, odd number ECN groups are not labeled in Fig. 6A, *e.g.* SMaO and SOMa with ECN = 51 and DB = 1 can be found in the section corresponding to ECN = 50.

4 Concluding remarks

This work demonstrates the potential of off-line 2D combination of NARP-HPLC in the first dimension followed by the silver-ion HPLC analysis of collected fractions in the second dimension. This experimental setup provides the highest separation capacity of TGs in complex natural samples of plant oils and animal fats, as demonstrated on selected examples of blackcurrant oil as a highly complex plant oil containing both α- and γ-Ln and beef tallow as a representative of animal fats containing also TFAs. The randomization synthesis of regioisomeric TG standards with the selected composition has played an important role in the method development. NARP mode enables the separation of highly complex TG mixtures according to their ECN and also inside individual ECN groups, while the retention in silver-ion mode is governed mainly by the number and geometry of DBs with possible resolution of regioisomers. Both systems show quite good complementary as a prerequisite for 2D analysis. The disadvantage of presented approach is long total analysis time, therefore this method is recommended only for highly detailed characterization of complex samples, but not intended for the routine quality control of TG mixtures of lower complexity.

This work was supported by the grant project No. MSM0021627502 sponsored by the Ministry of Education, Youth and Sports of the Czech Republic and projects Nos. 203/09/0139 and 203/09/P249 (ML) sponsored by the Czech Science Foundation.

The authors have declared no conflict of interest.

5 References

[1] Food and Agricultural Organization of the United Nations (FAO), Rome. http://www.fao.org (accessed May 2009).

[2] FEDIOL, The EU Oil and Proteinmeal Industry, Brussels, Belgium. http://www.fedioil.be (accessed May 2009).

[3] Leray, C. Cyberlipid Center, Paris. http://www.cyberlipid.org (accessed May 2009).

[4] Scheeder, M., in: Gunstone, F.D. (Ed.), *Lipids from Land Animals in Modifying Lipids for Use in Food*, Woodhead Publishing, Cambridge 2006, pp. 28–55.

[5] Byrdwell, W. C., Emken, E. A., Neff, W. E., Adlof, R. O., *Lipids* 1996, *31*, 919–935.

[6] Cvačka, J., Hovorka, O., Jiroš, P., Kindl, J., Stránský, K., Valterová, I., *J. Chromatogr. A* 2006, *1101*, 226–237.

[7] Héron, S., Tchapla, A., Finger Prints of Triacylglycerols from Oils and Fats by HPLC Isocratic Elution and Evaporative Light Scattering Detection, ELSD Sedex 45, Sedere, Alfortville, France 1994.

[8] Holčapek, M., Jandera, P., Fischer, J., *Crit. Rev. Anal. Chem.* 2001, *31*, 53–56.

[9] Holčapek, M., Jandera, P., Fischer, J., Prokeš, B., *J. Chromatogr. A* 1999, *858*, 13–31.

[10] Holčapek, M., Jandera, P., Zderadička, P., Hrubá, L., *J. Chromatogr. A* 2003, *1010*, 195–215.

[11] Holčapek, M., Lísa, M., Jandera, P., Kabátová, N., *J. Sep. Sci.* 2005, *28*, 1315–1333.

[12] Laakso, P., *J. Am. Oil Chem. Soc.* 1997, *74*, 1291–1300.

[13] Lísa, M., Holčapek, M., *Chem. Listy* 2005, *99*, 195–199.

[14] Lísa, M., Holčapek, M., *J. Chromatogr. A* 2008, *1198*, 115–130.

[15] Lísa, M., Holčapek, M., Boháč, M., *J. Agric. Food Chem.* 2009, *57*, 6888–6898.

[16] Lísa, M., Holčapek, M., Řezanka, T., Kabátová, N., *J. Chromatogr. A* 2007, *1146*, 67–77.

[17] Mottram, H. R., Crossman, Z. M., Evershed, R. P., *Analyst* 2001, *126*, 1018–1024.

[18] Mottram, H. R., Woodbury, S. E., Evershed, R. P., *Rapid Commun. Mass Spectrom.* 1997, *11*, 1240–1252.

[19] van den Berg, J. D. J., Vermist, N. D., Carlyle, L., Holčapek, M., Boon, J. J., *J. Sep. Sci.* 2004, *27*, 181–199.

[20] Lin, J. T., Woodruff, C. L., McKeon, T. A., *J. Chromatogr. A* 1997, *782*, 41–48.

[21] Momchilova, S., Itabashi, Y., Nikolova-Damyanova, B., Kuksis, A., *J. Sep. Sci.* 2006, *29*, 2578–2583.

[22] Momchilova, S., Tsuji, K., Itabashi, Y., Nikolova-Damyanova, B., Kuksis, A., *J. Sep. Sci.* 2004, *27*, 1033–1036.

[23] Adlof, R., List, G., *J. Chromatogr. A* 2004, *1046*, 109–113.

[24] Adlof, R. O., *J. High Res. Chromatogr.* 1995, *18*, 105–107.

[25] Christie, W. W., *J. Chromatogr.* 1988, *454*, 273–284.

[26] Lísa, M., Velínská, H., Holčapek, M., *Anal. Chem.* 2009, *81*, 3903–3910.

[27] Schuyl, P. J. W., de Joode, T., Vasconcellos, M. A., Duchateau, G., *J. Chromatogr. A* 1998, *810*, 53–61.

[28] Laakso, P., Voutilainen, P., *Lipids* 1996, *31*, 1311–1322.

[29] Adlof, R. O., Menzel, A., Dorovska-Taran, V., *J. Chromatogr. A* 2002, *953*, 293–297.

[30] Byrdwell, W. C., Neff, W. E., *Rapid Commun. Mass Spectrom.* 2002, *16*, 300–319.

[31] Fauconnot, L., Hau, J., Aeschlimann, J. M., Fay, L. B., Dionisi, F., *Rapid Commun. Mass Spectrom.* 2004, *18*, 218–224.

[32] Leskinen, H., Suomela, J. P., Kallio, H., *Rapid Commun. Mass Spectrom.* 2007, *21*, 2361–2373.

[33] Mottram, H. R., Evershed, R. P., *Tetrahedron Lett.* 1996, *37*, 8593–8596.

[34] McAnoy, A. M., Wu, C. C., Murphy, R. C., *J. Am. Soc. Mass Spectrom.* 2005, *16*, 1498–1509.

[35] Dugo, P., Kumm, T., Crupi, M. L., Cotroneo, A., Mondello, L., *J. Chromatogr. A* 2006, *1112*, 269–275.

[36] Mondello, L., Tranchida, P. Q., Staněk, V., Jandera, P., Dugo, G., Dugo, P., *J. Chromatogr. A* 2005, *1086*, 91–98.

[37] van der Klift, E. J. C., Vivó-Truyols, G., Claassen, F. W., van Holthoon, F. L., van Beek, T. A., *J. Chromatogr. A* 2008, *1178*, 43–55.

[38] Dugo, P., Kumm, T., Fazio, A., Dugo, G., Mondello, L., *J. Sep. Sci.* 2006, *29*, 567–575.

[39] Dugo, P., Favoino, O., Tranchida, P. Q., Dugo, G., Mondello, L., *J. Chromatogr. A* 2004, *1041*, 135–142.

[40] Dugo, P., Kumm, T., Lo Presti, M., Chiofalo, B., Salimei, E., Fazio, A., Cotroneo, A., Mondello, L., *J. Sep. Sci.* 2005, *28*, 1023–1030.

[41] Česla, P., Hájek, T., Jandera, P., *J. Chromatogr. A* 2009, *1216*, 3443–3457.

Journal of Chromatography A, 1216 (2009) 8371–8378

Contents lists available at ScienceDirect

Journal of Chromatography A

journal homepage: www.elsevier.com/locate/chroma

Comparison of various types of stationary phases in non-aqueous reversed-phase high-performance liquid chromatography–mass spectrometry of glycerolipids in blackcurrant oil and its enzymatic hydrolysis mixture

Miroslav Lísa [a], Michal Holčapek [a,*], Helena Sovová [b]

[a] University of Pardubice, Faculty of Chemical Technology, Department of Analytical Chemistry, Studentská 573, 532 10 Pardubice, Czech Republic
[b] Institute of Chemical Process Fundamentals of the ASCR, v. v. I., Rozvojová 135, 165 02 Prague, Czech Republic

ARTICLE INFO

Article history:
Received 29 July 2009
Received in revised form
23 September 2009
Accepted 25 September 2009
Available online 1 October 2009

Keywords:
Ultra high-performance liquid chromatography
C_{30} stationary phase
Triacylglycerol
Lipid
Blackcurrant oil
Enzymatic hydrolysis

ABSTRACT

The selection of column packing during the development of high-performance liquid chromatography method is a crucial step to achieve sufficient chromatographic resolution of analyzed species in complex mixtures. Various stationary phases are tested in this paper for the analysis of complex mixture of triacylglycerols (TGs) in blackcurrant oil using non-aqueous reversed-phase (NARP) system with acetonitrile–2-propanol mobile phase. Conventional C_{18} column in the total length of 45 cm is used for the separation of TGs according to their equivalent carbon number, the number and positions of double bonds and acyl chain lengths. The separation of TGs and their more polar hydrolysis products after the partial enzymatic hydrolysis of blackcurrant oil in one chromatographic run is achieved using conventional C_{18} column. Retention times of TGs are reduced almost 10 times without the loss of the chromatographic resolution using ultra high-performance liquid chromatography with 1.7 μm C_{18} particles. The separation in NARP system on C_{30} column shows an unusual phenomenon, because the retention order of TGs changes depending on the column temperature, which is reported for the first time. The commercial monolithic column modified with C_{18} is used for the fast analysis of TGs to increase the sample throughput but at cost of low resolution.

1. Introduction

The selection of appropriate column during the development of chromatographic method for the separation of complex mixtures of triacylglycerols (TGs) in plant oils and animal fats containing tens to hundreds of species with small differences in physicochemical properties is a crucial step to achieve the highest separation selectivity. Properties of TGs are given by the number, position(s) and configuration (*cis*-/*trans*-) of double bonds (DBs), acyl chain lengths, and stereochemical position (*sn*-1, 2 and 3) of fatty acids (FAs) on the glycerol skeleton (regioisomers and optical isomers) [1]. Individual chromatographic techniques do not allow the separation of all types of TG isomers and usually some compromise has to be made. Two main chromatographic techniques are used in the analysis of TG mixtures, i.e., silver-ion chromatography and non-aqueous reversed-phase high-performance liquid chromatography (NARP-HPLC). The silver-ion chromatography [2–9] is based on the formation of weak reversible complexes of silver ions with π electrons of DBs of unsaturated TGs. Ion-exchange or silica columns impregnated with silver ions are usually used with hexane-based mobile phases. In silver-ion chromatography, retention times of TGs are influenced by the number, position [5,8] and configuration [2,7,9] of DBs in acyl chains and partially by the acyl chain lengths [5]. The resolution of TG regioisomers ($R_1R_1R_2$ vs. $R_1R_2R_1$) using silver-ion chromatography is possible under carefully optimized chromatographic conditions [2,5,7].

The highest number of identified TGs has been reached in NARP-HPLC with atmospheric pressure chemical ionization (APCI) mass spectrometry (MS) using the connection of C_{18} columns in the total length 45 cm and acetonitrile–2-propanol gradient [10–14]. In the NARP-HPLC system with the conventional C_{18} column, TGs are separated according to the equivalent carbon number (ECN) defined as the total number of carbon atoms (CN) minus two times the number of DBs, i.e., ECN = CN − 2DB. Retention times of TGs increase with the increasing ECN and TGs inside one ECN group are separated according to the composition of attached FAs, mainly the lengths of acyl chains and the number of DBs. The separation of TGs differing in the position [14–16] and configuration [17,18] of DBs or partial resolution of regioisomers [19,20] has been reported as well. Long hydrophobic alkyl chains of C_{30} stationary phase provide stronger interactions of non-polar compounds containing the long

* Corresponding author. Tel.: +420 46 6037087; fax: +420 46 6037068.
E-mail address: Michal.Holcapek@upce.cz (M. Holčapek).

0021-9673/$ – see front matter © 2009 Elsevier B.V. All rights reserved.
doi:10.1016/j.chroma.2009.09.060

alkyl chain resulting in at least comparable or even better resolution in comparison to conventional C_{18} stationary phase. C_{30} columns are widely used for the separation of non-polar carotenoids or vitamins [21–23], but no separation of TGs using these columns has been reported so far.

NARP-HPLC separations of TGs using conventional C_{18} columns with 3–5 μm particle size provide good results but at the cost of long retention times in the range of tens of minutes. Nowadays, an effort to reduce the analysis time is of great interest due to the requirement on higher sample throughput. Decreasing the particle size enables to reduce the retention time in comparison to conventional columns. Columns with sub-two micron particles are used for ultra high-performance liquid chromatography (UHPLC) analysis with significantly shorter retention times at the same chromatographic resolution [24]. On the other hand, the use of sub-two micron particles results in higher system backpressure, therefore the special chromatographic system designed for higher pressures have to be used for UHPLC analysis. Monolithic stationary phases are characterized by large-sized through-pores resulting in the low flow resistance and the lower system backpressure. Its higher permeability enables the utilization of higher flow rates and increase of the sample throughput. Silica-based monoliths modified by C_{18} alkyl phase have been used for the analysis of TGs from plant oils [25].

The main goal of our work is the comparison of different NARP systems for the separation of TGs in complex natural samples. Conventional C_{18}, sub-two micron C_{18} particles, C_{30} column and C_{18} monolithic column in NARP systems are tested using blackcurrant oil containing the complex mixture of TGs including DB positional isomers. The analysis time, retention behavior, chromatographic resolution and the number of identified TGs using individual columns are discussed. NARP-HPLC system is also applied for the analysis of mixture of more polar hydrolysis products after the partial enzymatic hydrolysis of TGs in blackcurrant oil.

2. Experimental

2.1. Materials

Acetonitrile, 2-propanol (both HPLC gradient grade) and hexane (HPLC grade) were purchased from Sigma–Aldrich (St. Louis, USA). The solvents of mobile phase were degassed by continuous stripping with helium during the analysis. The hydrolysis of blackcurrant oil was performed with immobilized *sn*-1 and *sn*-3 selective enzyme in supercritical carbon dioxide [26]. The oil was extracted from seeds donated by Zemcheba (Chelčice, Czech Republic) and its main fraction containing TGs [27] was used. The reaction was carried out in a continuous-flow packed-bed reactor at temperature 40 °C and pressure 15 MPa with oil dissolved in supercritical carbon dioxide saturated with water. The enzyme Lipozyme was supplied by Fluka Chemie AG (Buchs, Switzerland). Blackcurrant oil and its hydrolysis mixture were dissolved in an acetonitrile–2-propanol–hexane mixture (1:1:1, v/v/v) at the concentration of 1% (w/v) and 10 μl was injected for the analysis in triplicate.

2.2. Chromatographic and detection conditions

2.2.1. HPLC analysis

All HPLC experiments were performed using the chromatographic apparatus consisting of a Model 616 pump with a quaternary gradient system, a Model 996 diode-array UV detector, a Model 717+ autosampler, a thermostated column compartment and a Millennium chromatography manager (all from Waters, Milford, MA, USA). NARP-HPLC conditions for the analysis of TGs with conventional C_{18} column were used according to Ref. [10], i.e., two chromatographic columns Nova-Pak C_{18} (150 mm × 3.9 mm and 300 mm × 3.9 mm, 4 μm, Waters) connected in series, a flow rate of 1 mL/min, an injection volume of 10 μL, column temperature of 25 °C and a mobile phase gradient with a slope of 0.65%/min: 0 min-100% acetonitrile, 106 min-31% acetonitrile + 69% 2-propanol, 109 min-100% acetonitrile. ProntoSil C_{30} column (250 mm × 4.6 mm, 3 μm, Bischoff, Leonberg, Germany) was used for the analysis of TGs with the same HPLC conditions as for conventional C_{18} column. Experiments with monolithic stationary phase were performed using Chromolith Performance RP-18e column (100 mm × 4.6 mm, Merck, Darmstadt, Germany), the flow rate of 5 mL/min, the injection volume of 5 μL, column temperature of 25 °C and the isocratic elution with the mobile phase composition 85% acetonitrile + 15% 2-propanol. T-piece with the split ratio 1:4 was used for splitting of the flow rate before APCI-MS. The column hold-up volume, t_M, was measured with uracil – 3.20 min for the system with 300 + 150 mm Nova-Pak C_{18} columns and 3.00 min for the system with 250 mm C_{30} ProntoSil column. The injector needle was washed with the mobile phase before each injection. The UV detection at 205 nm and APCI-MS were coupled in series. The Esquire 3000 ion trap analyzer (Bruker Daltonics, Bremen, Germany) in the mass range m/z 50–1200 was used with the following setting of tuning parameters: the pressure of the nebulizing gas of 70 psi, the drying gas flow rate of 3 L/min, temperatures of the drying gas and APCI heater were 350 and 400 °C, respectively.

2.2.2. UHPLC analysis

NARP-UHPLC experiments were performed on an Acquity UPLC system consisting of binary pump, diode-array UV detector, autosampler, thermostated column compartment and Empower chromatography data software (Waters, Milford, MA, USA). Acquity BEH C_{18} column (150 mm × 2.1 mm, 1.7 μm, Waters) was used with the flow rate of 0.4 mL/min, the injection volume of 1 μL, column temperature of 30 °C and the mobile phase gradient with the slope of 2%/min: 0 min-100% acetonitrile, 23 min-54% acetonitrile + 46% 2-propanol, 24 min-100% acetonitrile. Mobile phase gradient with the slope of 2%/min and the following composition: 0 min-80% acetonitrile + 20% 2-propanol, 14 min-52% acetonitrile + 48%

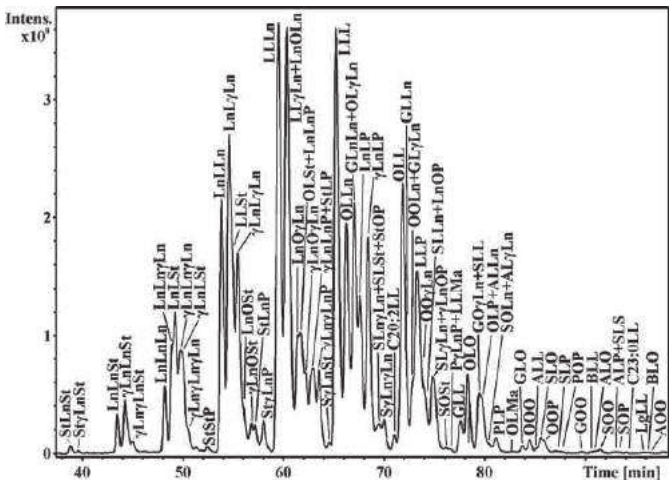

Fig. 1. NARP-HPLC/APCI-MS analysis of triacylglycerols in blackcurrant oil using conventional C_{18} column. *Conditions*: two Nova-Pak C_{18} columns (150 mm × 3.9 mm and 300 mm × 3.9 mm, 4 μm) connected in series, APCI-MS detection in positive-ion mode, flow rate 1 mL/min, column temperature 25 °C, gradient 0 min-100% acetonitrile, 106 min-31% acetonitrile + 69% 2-propanol (see Section 2 for more details and the explanation of used notation of identified TGs).

Table 1
Triacylglycerols (TG) identified in the blackcurrant oil with their equivalent carbon numbers (ECN), molecular weights (MW), retention times (t_R) and relative retention (r) using conventional C_{18} column and C_{30} column with column temperatures 25 and 40 °C.

TG	ECN	MW	C_{18} (25 °C)		C_{30} (25 °C)		C_{30} (40 °C)	
			t_R (min)[a]	r[b]	t_R (min)[a]	r[b]	t_R (min)[a]	r[b]
StLnSt	32	868	38.8	0.631	33.5[c]	0.598	25.2[c]	0.543
StγLnSt		868	39.5	0.644	n.d.	–	n.d.	–
LnLnSt	34	870	43.5	0.715	38.5[c]	0.696	29.4[c]	0.645
γLnLnSt		870	44.2	0.727	n.d.	–	n.d.	–
γLnγLnSt		870	44.9	0.739	n.d.	–	n.d.	–
LnLnLn	36	872	48.3	0.800	43.5[c]	0.794	33.9[c]	0.756
LnLnγLn		872	49.0	0.812	n.d.	–	n.d.	–
LnLSt		872	49.4	0.819	43.7[c]	0.798	34.2[c]	0.763
γLnLnγLn		872	49.7	0.824	n.d.	–	n.d.	–
γLnLSt		872	50.1	0.832	n.d.	–	n.d.	–
γLnγLnγLn		872	50.6	0.840	n.d.	–	n.d.	–
StStP		846	52.6	0.876	n.d.	–	n.d.	–
LnLLn	38	874	54.0	0.901	48.8[c]	0.898	38.9[c]	0.878
LnLγLn		874	54.7	0.913	n.d.	–	n.d.	–
LLSt		874	55.1	0.924	51.1	0.943	40.9[c]	0.927
γLnLγLn		874	55.4	0.926	n.d.	–	n.d.	–
LnOSt		874	56.1	0.938	51.1[c]	0.943	40.9[c]	0.927
γLnOSt		874	56.8	0.950	n.d.	–	n.d.	–
StLnP		848	57.2	0.957	58.2	1.082	45.2[c]	1.032
StγLnP		848	58.0	0.972	58.8	1.094	n.d.	–
LLLn	40	876	59.6	1.000	54.0[c]	1.000	43.9[c]	1.000
LLγLn		876	60.4	1.014	n.d.	–	n.d.	–
LnOLn		876	60.8	1.022	56.2[c]	1.043	45.8[c]	1.046
LnOγLn		876	61.6	1.035	n.d.	–	n.d.	–
OLSt		876	61.9	1.041	56.4	1.047	46.1	1.054
LnLnP		850	62.1	1.044	63.2	1.180	50.2[c]	1.154
γLnOγLn		876	62.3	1.048	n.d.	–	n.d.	–
γLnLnP		850	62.8	1.057	63.8	1.192	n.d.	–
StLP		850	63.1	1.062	64.3	1.202	50.6	1.164
γLnγLnP		850	63.5	1.069	64.5	1.206	n.d.	–
SγLnSt		876	64.5	1.087	n.d.	–	n.d.	–
LLL	42	878	65.3	1.000	59.2	1.000	49.1	1.000
OLLn		878	66.4	1.018	61.4[c]	1.039	51.0[c]	1.041
GLnLn		904	66.8	1.024	63.4	1.075	53.0	1.085
OLγLn		878	67.1	1.029	n.d.	–	n.d.	–
LnLP		852	67.8	1.040	69.0	1.174	55.6[c]	1.141
γLnLP		852	68.5	1.052	69.7	1.187	n.d.	–
SLnγLn		878	69.2	1.063	75.1	1.283	60.2[c]	1.241
SLSt		878	69.6	1.069	n.d.	–	n.d.	–
StOP		852	69.8	1.072	n.d.	–	n.d.	–
SγLnγLn		878	69.9	1.074	75.7	1.294	n.d.	–
C20:2LL	44	906	70.8	0.985	n.d.	–	n.d.	–
OLL		880	71.8	1.000	66.5	1.000	56.0	1.000
GLLn		906	72.1	1.004	68.4[c]	1.030	58.0[c]	1.038
OOLn		880	72.6	1.012	68.7[c]	1.035	58.1[c]	1.040
GLγLn		906	72.8	1.015	n.d.	–	n.d.	–
LLP		854	73.1	1.019	74.7	1.129	61.0	1.094
OOγLn		880	73.3	1.022	n.d.	–	n.d.	–
SLLn		880	73.8	1.029	81.0	1.228	65.6[c]	1.181
LnOP		854	74.0	1.032	77.1	1.167	63.0[c]	1.132
SLγLn		880	74.5	1.039	81.8	1.241	n.d.	–
γLnOP		854	74.7	1.042	77.8	1.178	n.d.	–
SOSt		880	75.9	1.060	n.d.	–	n.d.	–
PγLnP		828	76.1	1.063	n.d.	–	n.d.	–
LLMa	45	868	76.3	1.066	n.d.	–	n.d.	–
GLL	46	908	77.2	0.991	73.5	0.997	62.9	0.998
OLO		882	77.9	1.000	73.7	1.000	63.0	1.000
GOγLn		908	78.8	1.012	n.d.	–	n.d.	–
SLL		882	79.0	1.015	86.8	1.185	70.8	1.130
OLP		856	79.3	1.019	82.6	1.126	68.3	1.088
ALLn		908	79.6	1.023	n.d.	–	n.d.	–
SOLn		882	80.0	1.028	n.d.	–	n.d.	–
ALγLn		908	80.3	1.032	n.d.	–	n.d.	–
PLP		830	80.9	1.040	n.d.	–	n.d.	–
OLMa	47	870	82.3	1.059	n.d.	–	n.d.	–

Table 1 (*Continued*)

TG	ECN	MW	C_{18} (25 °C)		C_{30} (25 °C)		C_{30} (40 °C)	
			t_R (min)[a]	r[b]	t_R (min)[a]	r[b]	t_R (min)[a]	r[b]
GLO		910	83.1	0.989	80.6	0.997	69.5	0.994
OOO		884	84.0	1.000	80.8	1.000	69.9	1.000
ALL		910	84.8	1.010	n.d.	–	n.d.	–
SLO	48	884	85.1	1.014	n.d.	–	n.d.	–
OOP		858	85.4	1.017	90.6	1.126	75.2	1.079
SLP		858	86.6	1.032	n.d.	–	n.d.	–
POP		832	87.0	1.037	n.d.	–	n.d.	–
GOO		912	89.0	0.979	n.d.	–	n.d.	–
BLL		938	90.0	0.991	n.d.	–	n.d.	–
ALO		912	90.4	0.995	n.d.	–	n.d.	–
SOO	50	886	90.8	1.000	n.d.	–	n.d.	–
ALP		886	91.8	1.011	n.d.	–	n.d.	–
SLS		886	91.9	1.013	n.d.	–	n.d.	–
SOP		860	92.3	1.017	n.d.	–	n.d.	–
C23:0LL	51	952	92.4	1.018	n.d.	–	n.d.	–
LgLL		966	94.9	0.988	n.d.	–	n.d.	–
BLO	52	940	95.5	0.995	n.d.	–	n.d.	–
AOO		914	96.0	1.000	n.d.	–	n.d.	–

[a] n.d. means not detected.
[b] Relative retention is defined as $r = (t_R - t_M)/(t_S - t_M)$, where t_M is 3.2 min for the system with C_{18} column and 3.0 min for the system with C_{30} column and t_S are retention times of standards for particular ECN groups, i.e., LLLn (ECN = 32–40), LLL (42), OLL (44, 45), OLO (46, 47), OOO (48), SOO (50, 51) and AOO (52).
[c] Coelution of triacylglycerols containing Ln and γLn acids.

2-propanol, 15 min-80% acetonitrile + 20% 2-propanol was used for fast UHPLC analysis. The baseline drift in UV chromatograms was suppressed using the chromatographic software.

2.3. Notation of identified species

TGs, diacylglycerols (DGs) and monoacylglycerols (MGs) were annotated using initials of trivial names of FAs arranged according to their *sn*-1, *sn*-2 and *sn*-3 positions, i.e., **P**, palmitic (C16:0); **Ma**, margaric (C17:0); **S**, stearic (C18:0); **O**, oleic (Δ9-C18:1); **L**, linoleic (Δ9,12-C18:2); **Ln**, linolenic (Δ9,12,15-C18:3); **γ-Ln**, gamma-linolenic (Δ6,9,12-C18:3); **St**, stearidonic (Δ6,9,12,15-C18:4); **A**, arachidic (C20:0); **G**, gadoleic (Δ9-C20:1); **C20:2**, eicosadienoic (Δ9,11-C20:2); **B**, behenic (C22:0); **C23:0**, tricosanoic (C23:0); **Lg**, lignoceric (C24:0).

3. Results and discussion

3.1. NARP-HPLC analysis of TGs and enzymatic hydrolysis products using conventional C_{18} column

Blackcurrant oil is one of the most complex plant oils typical by high content of linolenic (Δ9,12,15-C18:3, Ln) and gamma-linolenic (Δ6,9,12-C18:3, γLn) acids, both with 3 DBs but in different positions in the acyl chain (i.e., DB positional isomers). Blackcurrant oil is selected as a testing TG mixture based on its complexity which is challenging for NARP-HPLC technique commonly used in the analysis of natural TG mixtures. TG composition is determined using NARP-HPLC method with two conventional C_{18} columns (4 μm particles) in total length 45 cm, acetonitrile–2-propanol gradient and column temperature 25 °C according to our previous optimization [10]. The conventional C_{18} columns provide the separation of TGs according to the ECN and TGs within one ECN group are separated based on the saturation degree and the length of acyl chains of attached FAs (Fig. 1). DB positional isomers are also well resolved in this NARP-HPLC system, where TGs with γLn acid have higher retention in comparison to TGs containing Ln acid (Table 1), e.g., LnLnLn (t_R = 48.3 min) and LnLnγLn (t_R = 49.0 min), etc. The average difference between TGs containing one γLn instead of Ln is about 0.7 min. TG species are identified based on the retention behavior and masses of protonated molecules $[M+H]^+$, low abundant ammonium adducts $[M+NH_4]^+$ and $[M+H-R_iCOOH]^+$ fragment ions observed in their positive-ion full scan APCI mass spectra. Prevailing FA in *sn*-2 position is determined based on lower relative abundances of $[M+H-R_iCOOH]^+$ fragment ions arising by the cleavage of FA from this position in comparison to *sn*-1 and *sn*-3 positions [28,29]. *Sn*-1 and *sn*-3 positions cannot be resolved in NARP-HPLC system and are considered as equivalent. Totally, 83 TGs including DB positional isomers have been identified in this work which is the highest number of identified TGs reported so far in comparison to 56 TGs reported in Ref. [8] or 21 in Ref. [28].

The NARP system is also applied for the analysis of more polar glycerolipids (DGs and MGs) and FAs (Fig. 2) prepared by partial enzymatic catalyzed hydrolysis of blackcurrant oil in supercritical carbon dioxide during the preparation of FAs used as food supplements. The hydrolysis mixture containing unreacted TGs and reaction products DGs, MGs and FAs are analyzed in one analytical run without any fractionation. Fig. 2(A) illustrates HPLC separation of hydrolysis mixture using the conventional C_{18} column, where groups of TGs and DGs are clearly resolved with the partial coelution of polar MGs and FAs. The coelution of these polar compounds is given by the same ECN, because the retention in NARP systems is mainly governed by hydrophobic interactions with only limited effect of polarity. For better separation of FAs and MGs species, acetonitrile/water isocratic step at the beginning of gradient can improve the separation [29] or normal-phase chromatography on silica yields a class separation of individual lipid classes based on their polarity [30]. On the other hand, the excellent resolution of TGs would be partially lost by the addition of water in the initial part of gradient (data not shown). The partial resolution of FA and MG groups is still sufficient for the identification of individual species based on their APCI mass spectra. Deprotonated molecules $[M-H]^-$ in negative-ion and $[M+H-H_2O]^+$ ions in positive-ion full scan APCI mass spectra are used for the identification of FAs and MGs, respectively. In total, 6 FAs, 4 MGs and 27 DGs have been identified in the hydrolysis mixture. A zoomed region of this separation (Fig. 2(B)) illustrates that individual DG species are well resolved according to their ECN including the separation of DGs within individual ECN groups and *sn*-1,2- and *sn*-1,3-DG regioisomers. 1,2- and 2,3-DGs are optical isomers, which cannot be resolved in non-chiral sys-

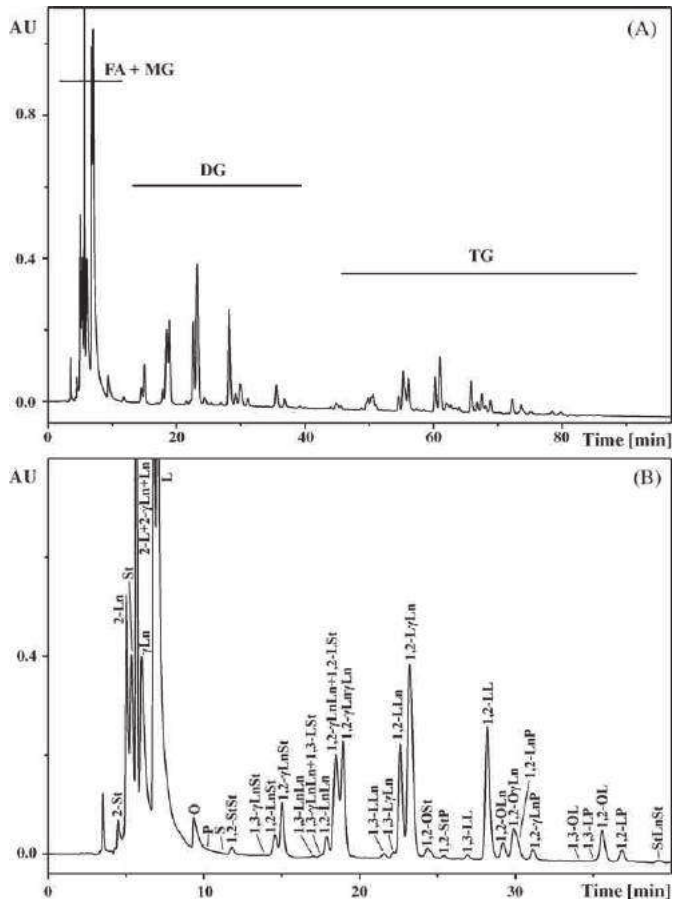

Fig. 2. NARP-HPLC analysis of triacylglycerols (TG) hydrolysis products after the partial enzymatic hydrolysis of blackcurrant oil by *sn*-1/3 selective enzyme Lipozyme using conventional C_{18} column (A) and detail of separation of fatty acids (FA), monoacylglycerols (MG) and diacylglycerols (DG) (B). Conditions identical as for Fig. 1.

tem and therefore they are considered equivalent in this work, i.e., 1,2-DG corresponds to the mixture of 1,2- and 2,3-DGs. Masses of protonated molecules $[M+H]^+$ and $[M+H-H_2O]^+$ fragment ions in positive-ion full scan APCI mass spectra are used for the identification of individual DG species. Non-specific chemical hydrolysis of TGs provides three DG regioisomers (1,3-, 1,2- and 2,3-DG) in ratio 1:1:1. 1,2- and 2,3-optical isomers cannot be separated in NARP-HPLC, hence the final chromatogram contains two peaks of DG regioisomers at the ratio 1,3-DG:1,2-DG = 1:2 (not shown). In this study, *sn*-1 and *sn*-3 specific enzyme Lipozyme is used for the hydrolysis of TGs providing almost exclusively one peak of 1,2-DG regioisomer (Fig. 2(B)). Peaks of 1,3-DGs have very low relative peak areas (1–5%) in comparison to 1,2-DGs (95–98%), which confirms expected specificity of this enzyme (Table 2).

3.2. NARP-UHPLC analysis of TGs in blackcurrant oil

The NARP-HPLC using conventional C_{18} column in total length 45 cm with 4 μm particles provides an excellent resolution of TGs, but retention times up to 96 min are rather long (Table 1). The goal of method transfer to UHPLC has been to maintain the resolution, while the analysis time should be reduced as much as possible. UHPLC method has been developed with the help of the software supplied with UHPLC system from Waters for the method transfer from the conventional HPLC to UHPLC system. Consequentially, we have tested effects of individual chromatographic parameters on the separation, i.e., flow rate, column temperature,

Table 2
Relative peak areas (UV at 205 nm) of 1,3- and 1,2-diacylglycerol regioisomers identified in the hydrolysis mixture of triacylglycerols after the partial enzymatic hydrolysis of blackcurrant oil by *sn*-1/3 selective enzyme Lipozyme.

Diacylglycerol	1,3-Diacylglycerol		1,2-Diacylglycerol	
	t_R (min)	Peak area (%)	t_R (min)	Peak area (%)
γLnSt	13.8	1.2	14.9	98.8
LnLn	16.9	5.2	17.8	94.8
γLnLn + LSt	17.4	1.3	18.4	98.7
LLn	21.5	3.6	22.5	96.4
Lγ Ln	22.1	1.8	23.1	98.2
LL	26.9	2.6	28.1	97.4
OL	34.0	1.6	35.5	98.4
LP	35.1	5.0	36.7	95.0

gradient steepness, initial composition and sample injection volume. The flow rate in the range of 0.2–0.4 mL/min has no significant effect on the chromatographic resolution, because it corresponds to the flat region in van Deemter curve of sub-two micron particle columns [24]. Increased column temperature had tremendous negative effect on the chromatographic resolution of TGs in NARP-HPLC mode [10,11], but this effect is not so significant in UHPLC. Therefore, higher column temperature can be used to reduce the system backpressure in UHPLC, which enables higher flow rates and decreased analysis time. The gradient steepness and initial gradient composition have relatively low effect on the resolution, but significant effect on the analysis time. Therefore, a compromise between the resolution and analysis time is made. Maximum

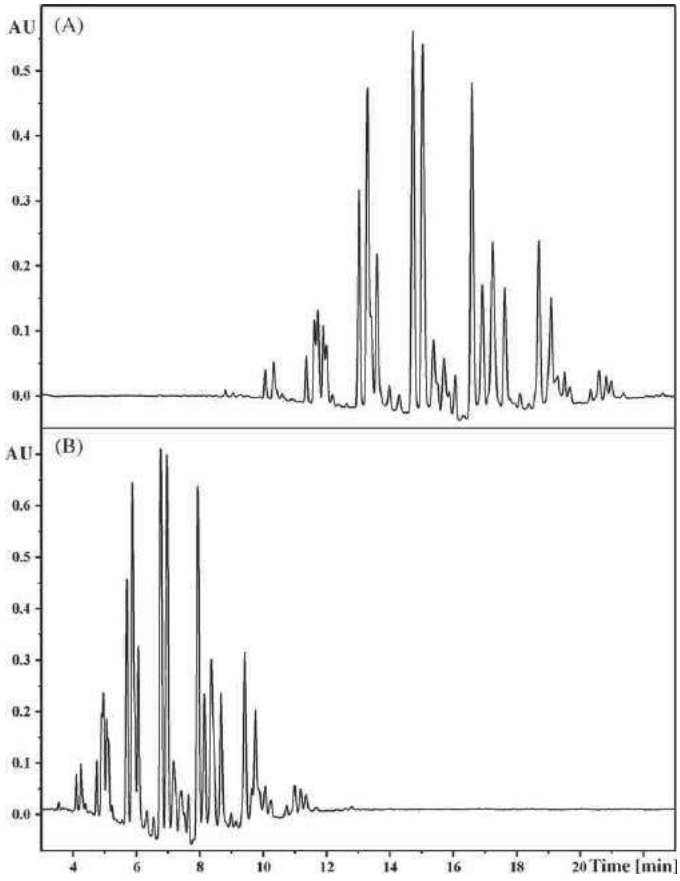

Fig. 3. NARP-UHPLC analysis of triacylglycerols in blackcurrant oil using two gradients: (A) 0 min-100% acetonitrile, 23 min-54% acetonitrile + 46% 2-propanol and (B) 0 min-80% acetonitrile + 20% 2-propanol, 14 min-52% acetonitrile + 48% 2-propanol. *Conditions*: Acquity UPLC BEH C_{18} column (150 mm × 2.1 mm, 1.7 μm), UV detection at 205 nm, flow rate 0.4 mL/min, column temperature 30 °C.

sample injection volume without any effect on the resolution is 2 μL.

Final NARP-UHPLC separation of TGs in blackcurrant oil using the flow rate 0.4 mL/min, column temperature 30 °C, the slope of gradient of 2% 2-propanol/min, 100% acetonitrile as initial mobile phase and 1 μL injection volume provides a similar picture as with conventional HPLC but within 22 min (Fig. 3(A)). The analysis time is significantly reduced by the change of initial gradient composition to 80% acetonitrile + 20% 2-propanol (Fig. 3(B)). TGs are eluted within 12 min with only small loss of resolution. DB positional isomers are separated with average difference between TGs containing one γLn instead of Ln about 0.16 min. The magnification of critical TG groups for the separation (Fig. 4) shows that UHPLC provides better resolution, as demonstrated on the group with ECN = 36 at the beginning of gradient (compare HPLC chromatogram in Fig. 4(A) with UHPLC in Fig. 4(C)) and ECN = 44 at the end of run (compare Fig. 4(B) and (D)). Moreover, retention times of TGs in UHPLC are reduced almost 10 times in comparison to the conventional HPLC providing significantly higher sample throughput.

3.3. NARP-HPLC analysis of TGs using C_{30} column

C_{30} column is tested for the analysis of TGs using the same chromatographic conditions as for the conventional C_{18} column (Fig. 5(A)). The total analysis time using 25 cm C_{30} column with 3 μm particles is comparable to conventional NARP-HPLC analysis but with significantly lower resolution and the number of identified TG species decreased to 38 from initial 83 with C_{18} column (Table 1). TGs containing only unsaturated FAs are separated according to ECN. In contrast to C_{18} column, DB positional isomers (Ln vs. γLn) for TGs with three unsaturated chains are not resolved using C_{30} column and they elute in one peak. The ECN retention mechanism is changed for TGs containing already one saturated FA on the glycerol skeleton. The retention of these TGs is higher in comparison to TGs containing only unsaturated FAs and they elute in higher ECN groups, e.g., StLnP with ECN = 38 elutes between ECN groups 40 and 42, etc. This phenomenon is probably due to the stronger interaction of straight saturated chains of FAs with long alkyl chains of C_{30} stationary phase. Stronger interactions of saturated alkyl chains also enable the partial separation of DB positional isomers unlike to TGs containing only unsaturated FAs.

The change of column temperature in conventional NARP-HPLC system with C_{18} columns affects retention times of TGs at the same level without changing the retention order [10]. By the way we have never seen changes in the retention order of TGs among our extensive NARP C_{18} studies and data published by other groups. The situation is different with C_{30} column. Fig. 5 shows the comparison of TG analysis using C_{30} column at 25 °C (A) and 40 °C (B) column temperature. The retention of TGs containing at least one saturated FA chain significantly decreases in comparison to

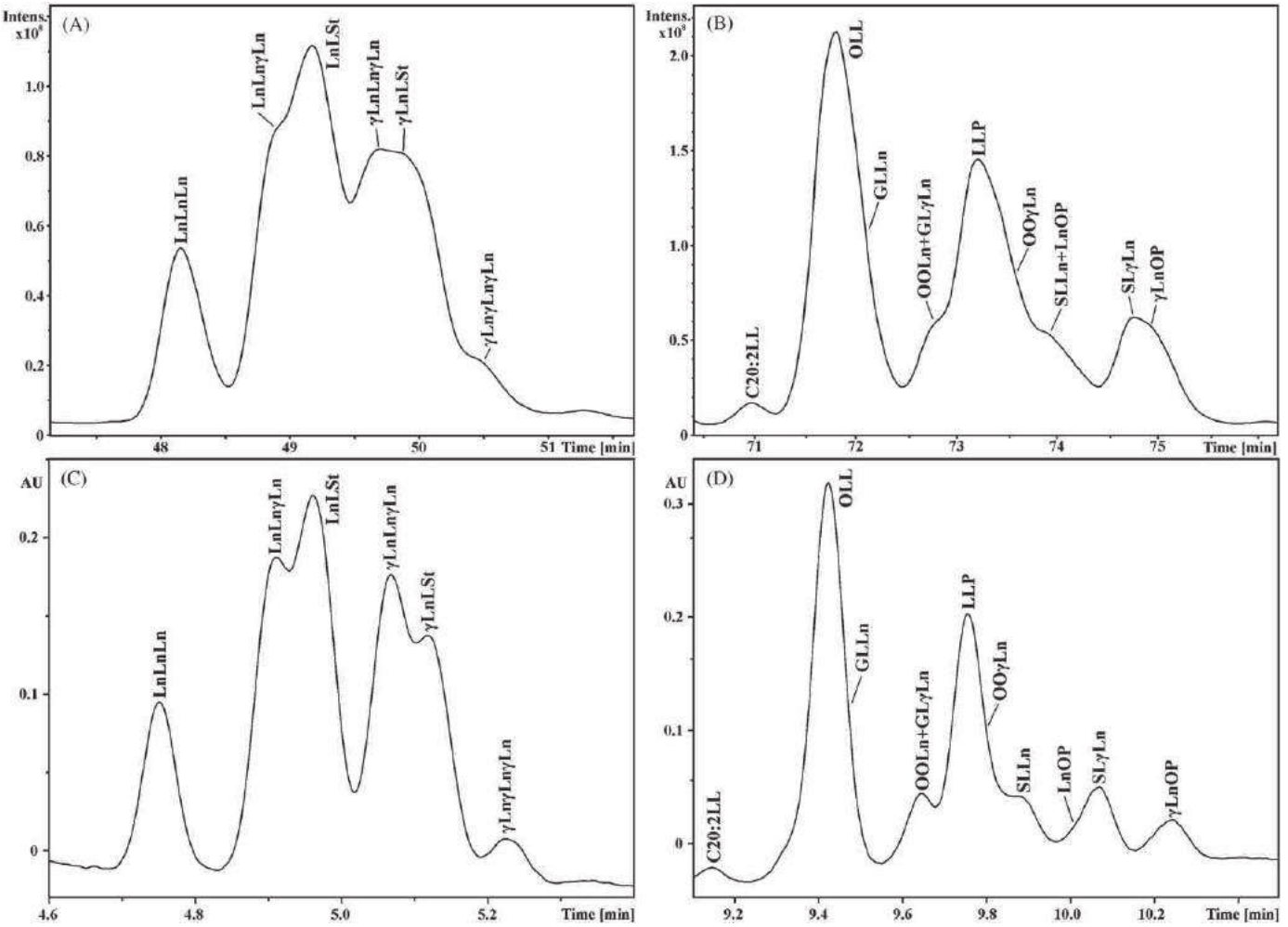

Fig. 4. Details from NARP-HPLC (A and B) and NARP-UHPLC (C and D) separations of critical groups of TGs in blackcurrant oil for comparison of the separation at the beginning of the chromatographic run (A and C) and at the end of gradient (B and D). Conditions identical as for Figs. 1 and 3.

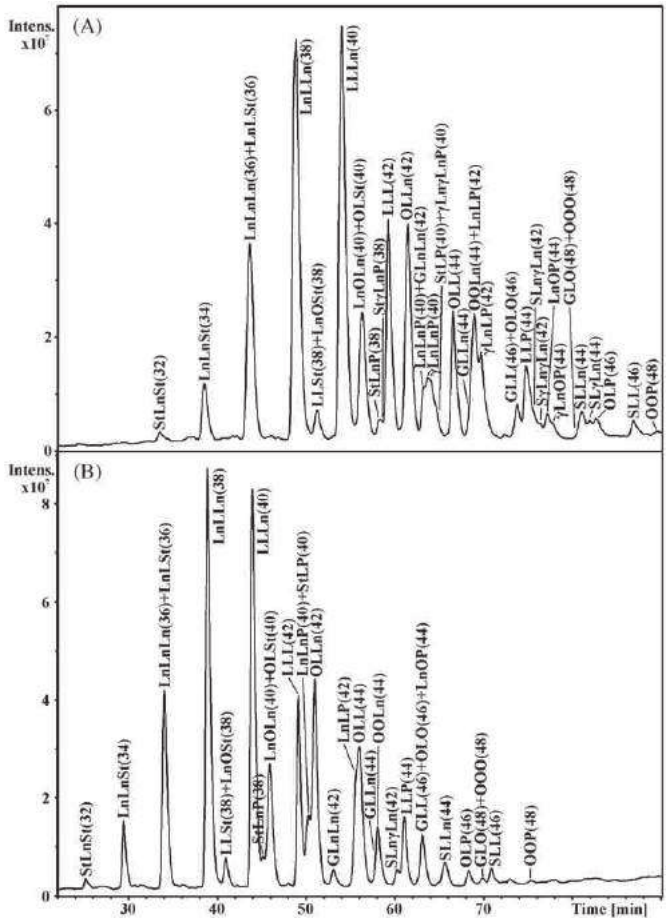

Fig. 5. NARP-HPLC/APCI-MS analysis of triacylglycerols in blackcurrant oil using C_{30} column and column temperatures: (A) 25 °C and (B) 40 °C. *Conditions*: ProntoSil C_{30} column (250 mm × 4.6 mm, 3 μm), APCI-MS detection in positive-ion mode, flow rate 1 mL/min, gradient 0 min-100% acetonitrile, 106 min-31% acetonitrile + 69% 2-propanol.

TGs containing only unsaturated FAs at higher column temperature resulting in changed retention order, e.g., StLnP with ECN = 38 elute in group ECN = 40. Moreover, the resolution of DB positional isomers for TGs containing saturated FAs is completely lost and they elute in one peak. Shifts of retention times of TGs with different column temperature can be visualized by relative retention (Table 1) with higher difference for TGs containing one saturated FA, e.g., $\Delta r = 0.050$ for StLnP in comparison to $\Delta r = 0.014$ for LnOSt, etc. C_{30} stationary phase is strongly temperature dependent and the conformation of C_{30} alkyl chains partially changes at higher temperature from straight *trans n*-alkyl conformation to gauche confirmation [21] which probably causes lower interactions with saturated acyl chains. Changes in the gradient steepness or in the gradient composition only shift retention times, but without notable effect on the chromatographic resolution of TGs unlike to the temperature dependence.

3.4. NARP-HPLC analysis of TGs using the monolithic column

Silica-based monolithic columns modified by C_{18} alkyl phase are used for the analysis of TGs in the blackcurrant oil using acetonitrile–2-propanol isocratic elution (Fig. 6). Low flow resistance of monolithic columns enables the utilization of high flow rates (5 mL/min) to increase the sample throughput. The retention of TGs increases with increasing ECN, but individual groups are not clearly separated. Only 21 TG species with higher concentration

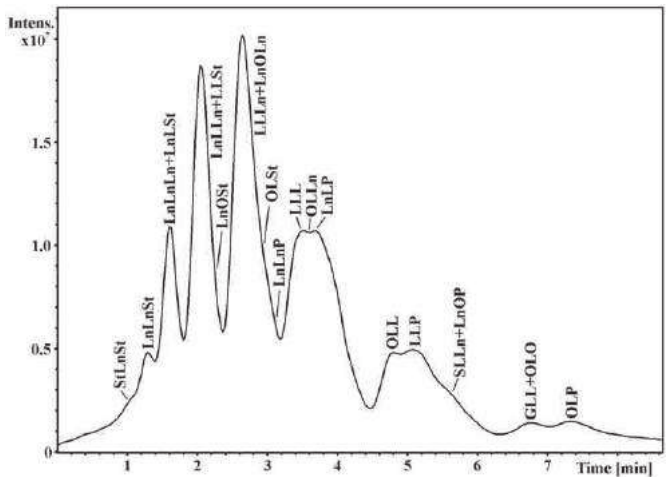

Fig. 6. NARP-HPLC/APCI-MS analysis of triacylglycerols in blackcurrant oil using C_{18} monolithic column. *Conditions*: Chromolith Performance RP-18e column (100 mm × 4.6 mm), flow rate 5 mL/min, column temperature 25 °C, isocratic elution with 85% acetonitrile and 15% 2-propanol, T-piece splitting 1:4 before positive-ion APCI-MS detection.

are identified in the blackcurrant oil in comparison to 83 TGs identified with the conventional C_{18} column. On the other hand, the total analysis time of TGs using C_{18} modified monolithic column is only 8 min, which is 12 times lower in comparison to conventional NARP-HPLC with C_{18} columns. Therefore, this simple and fast separation can be used only for rough determination of TG profiles.

4. Conclusions

This work demonstrates the utilization of different stationary phases in the analysis of TGs using NARP system with acetonitrile–2-propanol gradient. Blackcurrant oil containing high number of TG species including DB positional isomers is used for the characterization of chromatographic behavior of TGs on different columns. Conventional C_{18} column in the total length of 45 cm enables the separation and identification of 83 TGs species including DB positional isomers. This system is successfully applied for the separation of TGs with their more polar hydrolysis products in one analytical run. DG regioisomers are resolved in this system and their relative peak areas confirm the stereoselectivity of enzyme Lipozyme. The separation of TGs using NARP-UHPLC analysis enables almost 10 times reduction of the total analysis time with slightly improved chromatographic resolution in comparison to the conventional NARP-HPLC. The analysis of TGs using C_{30} column provides only 38 identified TG species and no resolution of DB positional isomers of unsaturated TGs. Higher column temperature using C_{30} column causes a change in the retention order of TGs containing saturated FAs which is a phenomenon reported for the first time. Monolithic stationary phase modified by C_{18} alkyl chains enables fast separation of TGs into ECN groups which is applicable only for the determination of rough TG profile.

Acknowledgments

This work was supported by the grant project no. MSM0021627502 sponsored by the Ministry of Education, Youth and Sports of the Czech Republic and projects nos. 203/09/P249 and 203/09/0139 sponsored by the Czech Science Foundation. Authors thank to Czech representatives of Waters Company for a loan of the UHPLC system.

References

[1] W.W. Christie, Scottish Crop Research Institute, The Lipid Library, http://www.lipidlibrary.co.uk/ (downloaded on September 23, 2009).
[2] R.O. Adlof, G. List, J. Chromatogr. A 1046 (2004) 109.
[3] R.O. Adlof, J. High Resol. Chromatogr. 18 (1995) 105.
[4] W.W. Christie, J. Chromatogr. 454 (1988) 273.
[5] M. Lísa, H. Velínská, M. Holčapek, Anal. Chem. 81 (2009) 3903.
[6] P.J.W. Schuyl, T. de Joode, M.A. Vasconcellos, G. Duchateau, J. Chromatogr. A 810 (1998) 53.
[7] M. Holčapek, H. Velínská, M. Lísa, P. Česla, J. Sep. Sci., 32 (2009) in press.
[8] P. Laakso, P. Voutilainen, Lipids 31 (1996) 1311.
[9] R.O. Adlof, A. Menzel, V. Dorovska-Taran, J. Chromatogr. A 953 (2002) 293.
[10] M. Holčapek, M. Lísa, P. Jandera, N. Kabátová, J. Sep. Sci. 28 (2005) 1315.
[11] M. Lísa, M. Holčapek, Chem. Listy 99 (2005) 195.
[12] M. Lísa, M. Holčapek, J. Chromatogr. A 1198 (2008) 115.
[13] M. Lísa, M. Holčapek, M. Boháč, J. Agric. Food Chem. 57 (2009) 6888.
[14] M. Lísa, M. Holčapek, T. Řezanka, N. Kabátová, J. Chromatogr. A 1146 (2007) 67.
[15] P. Laakso, J. Am. Oil Chem. Soc. 74 (1997) 1291.
[16] J.D.J. van den Berg, N.D. Vermist, L. Carlyle, M. Holčapek, J.J. Boon, J. Sep. Sci. 27 (2004) 181.
[17] J.T. Lin, C.L. Woodruff, T.A. McKeon, J. Chromatogr. A 782 (1997) 41.
[18] H.R. Mottram, Z.M. Crossman, R.P. Evershed, Analyst 126 (2001) 1018.
[19] S. Momchilova, Y. Itabashi, B. Nikolova-Damyanova, A. Kuksis, J. Sep. Sci. 29 (2006) 2578.
[20] S. Momchilova, K. Tsuji, Y. Itabashi, B. Nikolova-Damyanova, A. Kuksis, J. Sep. Sci. 27 (2004) 1033.
[21] K. Albert, Trends Anal. Chem. 17 (1998) 648.
[22] L.C. Sander, K.E. Sharpless, M. Pursch, J. Chromatogr. A 880 (2000) 189.
[23] P. Dugo, M. Herrero, D. Giuffrida, C. Ragonese, G. Dugo, L. Mondello, J. Sep. Sci. 31 (2008) 2151.
[24] A. de Villiers, F. Lestremau, R. Szucs, S. Gelebart, F. David, P. Sandra, J. Chromatogr. A 1127 (2006) 60.
[25] A. Jakab, E. Forgacs, Chromatographia 56 (2002) 69.
[26] H. Sovová, M. Zarevúcka, P. Bernášek, M. Stamenic, Chem. Eng. Res. Des. 86 (2008) 673.
[27] H. Sovová, M. Zarevúcka, Chem. Eng. Sci. 58 (2003) 2339.
[28] H.R. Mottram, S.E. Woodbury, R.P. Evershed, Rapid Commun. Mass Spectrom. 11 (1997) 1240.
[29] M. Holčapek, P. Jandera, J. Fischer, B. Prokeš, J. Chromatogr. A 858 (1999) 13.
[30] J. Cvačka, O. Hovorka, P. Jiroš, J. Kindl, K. Stránský, I. Valterová, J. Chromatogr. A 1101 (2006) 226.

Journal of Chromatography A, 1218 (2011) 7499–7510

Contents lists available at ScienceDirect

Journal of Chromatography A

journal homepage: www.elsevier.com/locate/chroma

Characterization of fatty acid and triacylglycerol composition in animal fats using silver-ion and non-aqueous reversed-phase high-performance liquid chromatography/mass spectrometry and gas chromatography/flame ionization detection

Miroslav Lísa[a], Kateřina Netušilová[a], Lukáš Franěk[a], Hana Dvořáková[a], Vladimír Vrkoslav[b], Michal Holčapek[a,*]

[a] University of Pardubice, Faculty of Chemical Technology, Department of Analytical Chemistry, Studentská 573, 53210 Pardubice, Czech Republic
[b] Institute of Organic Chemistry and Biochemistry, Academy of Sciences of the Czech Republic, v. v. i., Flemingovo nám. 2, 166 10 Prague 6, Czech Republic

ARTICLE INFO

Article history:
Available online 20 July 2011

Keywords:
Silver-ion HPLC
Non-aqueous reversed-phase HPLC
Triacylglycerol
Ruminant
Trans-fatty acid
Branched fatty acid

ABSTRACT

Fatty acid (FA) and triacylglycerol (TG) composition of natural oils and fats intake in the diet has a strong influence on the human health and chronic diseases. In this work, non-aqueous reversed-phase (NARP) and silver-ion high-performance liquid chromatography with atmospheric pressure chemical ionization mass spectrometry detection and gas chromatography with flame-ionization detection (GC/FID) and mass spectrometry detection are used for the characterization of FA and TG composition in complex samples of animal fats from fallow deer, red deer, sheep, moufflon, wild boar, cock, duck and rabbit. The FA composition of samples is determined based on the GC/FID analysis of FA methyl esters. In total, 81 FAs of different acyl chain length, double bond (DB) number, branched/linear, *cis*-/*trans*- and DB positional isomers are identified. TGs in animal fats contain mainly monounsaturated and saturated FAs. High amounts of branched and *trans*-FAs are observed in the samples of ruminants. In NARP mode, individual TG species are separated including the separation of *trans*- and branched TGs. Silver-ion mode provides the separation of TG regioisomers, which enables the determination of their ratios. Great differences in the preference of unsaturated and saturated FAs in the *sn*-2 position on the glycerol skeleton are observed among individual animal fats. Unsaturated FAs are preferentially occupied in the *sn*-2 position in all animal samples except for wild boar with the strong preference of saturated FAs in the *sn*-2 position.

1. Introduction

The composition of dietary triacylglycerols (TGs) and their fatty acids (FAs) has significant effects on the prevention or genesis of serious chronic diseases, such as cardiovascular diseases, diabetes, and cancer [1–3]. The correct ratio of saturated and polyunsaturated fatty acids in plant or animal tissues in our diet is especially important, as reflected by recommended daily income of these FAs by some national health organizations, *e.g.*, National Institute of Health in USA. The presence of unusual FAs with special biochemical properties should be also taken into account [4,5]. Wide differences in the FA composition can be found among various types of animal adipose tissues, *e.g.*, ruminants, poultry or fish. Animal fats are characterized by a high content of saturated FAs that have higher temperature and oxidation stability in comparison to unsaturated FAs, but on the other hand their higher content in the diet increases the risk of coronary heart diseases. On the other hand, fish oils are a predominant source of ω-3 polyunsaturated FAs, mainly eicosapentaenoic (Δ*5,8,11,14,17*-C20:5, EPA) and docosahexaenoic (Δ*4,7,10,13,16,19*-C22:6, DHA) acids, precursors of eicosanoids that reduce the inflammation in the body and they also play a crucial role in the prevention of atherosclerosis or heart attack [6]. In the natural samples, *cis*-configuration of double bonds (DBs) is predominant, but small amounts of FAs (<5%) with *trans*-configuration (*trans*-FAs) are present in ruminant meats and milk as products of rumen bacteria. Other products of rumen bacteria are odd- and branched-chain FAs having the important role to maintain an optimal fluidity of the microbial cell membrane or FAs with conjugated DBs as an intermediate in the biohydrogenation of unsaturated acids [4,7].

Nutrition properties of TG mixtures are given by their FA composition differing in acyl chain lengths and number, position and

* Corresponding author. Tel.: +420 466 037 087; fax: +420 466 037 068.
E-mail address: Michal.Holcapek@upce.cz (M. Holčapek).

0021-9673/$ – see front matter © 2011 Elsevier B.V. All rights reserved.
doi:10.1016/j.chroma.2011.07.032

configuration (*cis*-/*trans*-) of DBs. The most widespread method for the analysis of FA profiles is gas chromatography with flame ionization detection (GC/FID) of fatty acid methyl esters (FAMEs) after the catalyzed transesterification of TGs. This method enables fast, simple and reliable characterization of very complex samples based on FA profiles. High-performance liquid chromatography (HPLC) with mass spectrometry (MS) detection is a powerful tool for the characterization of TGs in complex natural mixtures. Two chromatographic techniques are most widespread in the analysis of TGs in natural samples, *i.e.*, non-aqueous reversed-phase (NARP) HPLC and silver-ion chromatography. In NARP-HPLC [8–22], retention times of TGs increase with the increasing equivalent carbon number (ECN) defined as the carbon number (CN) in all acyl chains minus twice the number of DBs (ECN = CN − 2DB). The separations of TGs differing in the position [15,17,22] and configuration [20–23] of DBs or the partial resolution of regioisomers [24] and TGs containing linear and branched FAs [25] have been reported as well. The retention times of TGs can be significantly reduced without the loss of resolution by the use of ultra-high performance liquid chromatography with sub-two micron particles column [26,27].

Silver-ion chromatography [28–34] is based on the formation of weak reversible complexes of silver ions impregnated on the silica or mostly bounded to the ion-exchange stationary phase with π electrons of DBs of unsaturated TGs. The mixture of hexane/acetonitrile is a typical mobile phase used in silver-ion chromatography but with a poor reproducibility due to the low miscibility of these solvents. The addition of 2-propanol into the mobile phase improves the miscibility of these solvents which provides a better reproducibility of retention times among analyses within one or more days [33]. Chlorinated mobile phases are also frequently used in silver-ion HPLC using dichloromethane or dichloroethane with the addition of other polar modifiers at low concentration, typically acetonitrile, acetone, and methanol [31,32,35]. In silver-ion chromatography, separation of TGs is governed mainly by the number of DBs. Double bond positional isomers [32,33], *cis*-/*trans*-isomers [23,28,30] or regioisomers ($R_1R_1R_2$ vs. $R_1R_2R_1$) [23,28,33] can be also separated. The orthogonality of silver-ion and NARP modes can be demonstrated in two dimensional separation for very complex samples in on-line [36–38] or off-line [23,39,40] setup.

The main goal of this work is the characterization of FA and TG composition of selected animal samples important in the nutrition and foodomics. NARP-HPLC and silver-ion HPLC with APCI-MS detection are used for the analysis of TGs according to acyl chain lengths and the number of DBs and FA composition of samples is determined using GC/FID analysis of FAMEs after the transesterification of TGs. The composition of TGs and unusual FAs in analyzed animal fats is discussed.

2. Materials and methods

2.1. Materials

Acetonitrile (HPLC gradient grade), 2-propanol, hexane (both HPLC grade) and sodium methoxide were purchased from Sigma–Aldrich (St. Louis, MO, USA). Model mixtures of FAME standards GLC#617 (C4:0, C6:0, C8:0, C10:0, C11:0, C12:0, C13:0, C14:0, Δ*9*-C14:1, C15:0, Δ*10*-C15:1, C16:0, Δ*9*-C16:1, C17:0, Δ*10*-C17:1, C18:0, Δ*9*-C18:1, Δ*9t*-C18:1, Δ*9,12*-C18:2, Δ*9t,12t*-C18:2, Δ*6,9,12*-C18:3, Δ*9,12,15*-C18:3, C20:0, Δ*11*-C20:1, Δ*11,14*-C20:2, Δ*8,11,14*-C20:3, Δ*11,14,17*-C20:3, Δ*5,8,11,14*-C20:4, Δ*5,8,11,14,17*-C20:5, C21:0, C22:0, Δ*13*-C22:1, Δ*13,16*-C22:2, Δ*7,10,13,16*-C22:4, Δ*4,7,10,13,16*-C22:5, Δ*7,10,13,16,19*-C22:5, Δ*4,7,10,13,16,19*-C22:6, C23:0, C24:0, Δ*15*-C24:1) and GLC#566 (C8:0, C10:0, C11:0, Δ*10*-C11:1, C12:0, C13:0, Δ*12*-C13:1, C14:0, Δ*9*-C14:1, C15:0, C16:0, Δ*9*-C16:1, C17:0, Δ*10*-C17:1, C18:0, Δ*9*-C18:1, Δ*11t*-C18:1, Δ*9,12*-C18:2, Δ*6,9,12*-C18:3, Δ*9,12,15*-C18:3, C19:0, C20:0, Δ*11*-C20:1, Δ*11,14*-C20:2, Δ*8,11,14*-C20:3, Δ*11,14,17*-C20:3, Δ*5,8,11,14*-C20:4, Δ*5,8,11,14,17*-C20:5, C21:0, C22:0, Δ*13*-C22:1, Δ*13,16*-C22:2, Δ*13,16,19*-C22:3, Δ*7,10,13,16*-C22:4, Δ*4,7,10,13,16*-C22:5, Δ*7,10,13,16,19*-C22:5, Δ*4,7,10,13,16,19*-C22:6, C23:0, C24:0, Δ*15*-C24:1) were purchased from Nu-Chek-Prep (Elysian, MN, USA). Standards of methyl 15-methylheptadecanoate (*ai*C18:0) and methyl 16-methylheptadecanoate (*i*C18:0) were purchased from Larodan Fine Chemicals (Mälmo, Sweden). Samples of adipose tissues from fallow deer (*Dama dama*), red deer (*Cervus elaphus*), sheep (*Ovis aries*), moufflon (*Ovis musimon*), wild boar (*Sus scrofa*), cock (*Gallus gallus*), duck (*Anas platyrhynchos domesticus*) and rabbit (*Oryctolagus cuniculus*) were obtained from the local veterinarian. The amount of 20 g of the sample was crushed in a homogenizer with 20 mL of hexane for 10 min. The mixture was filtered and hexane was evaporated under a mild stream of nitrogen yielding the pure animal fat.

2.2. NARP-HPLC/APCI-MS

NARP-HPLC experiments were performed on a chromatographic apparatus consisting of a Model 616 pump with a quaternary gradient system, a Model 996 diode-array UV detector, a Model 717+ autosampler, a thermostated column compartment and a Millennium chromatography manager (all from Waters, Milford, MA, USA). Samples were analyzed using the following HPLC conditions: two chromatographic columns Nova-Pak C_{18} (300 mm × 3.9 mm and 150 mm × 3.9 mm, 4 μm, Waters) connected in series, a flow rate of 1 mL/min, an injection volume of 10 μL, column temperature of 25 °C and the mobile phase gradient according to Ref. [23]: 0 min – 80% A + 20% B, 121 min – 40% A + 60% B, 122 min – 80% A + 20% B, where A is acetonitrile and B is a mixture of hexane–2-propanol (1:1, v/v). The injector needle was washed with the mobile phase before each injection. The column hold-up volume, t_M, was 3.2 min for the system with 300 + 150 mm Nova-Pak C_{18} columns.

The Esquire 3000 ion trap analyzer (Bruker Daltonics, Bremen, Germany) with positive-ion APCI was used in the mass range *m/z* 50–1200 with the following setting of tuning parameters: pressure of the nebulizing gas 70 psi, drying gas flow rate 3 L/min, temperatures of the drying gas and APCI heater were 350 °C and 400 °C, respectively. Individual reconstructed ion current chromatograms were used to support the identification of coeluting peaks.

2.3. Silver-ion HPLC/APCI-MS

Silver-ion HPLC experiments were performed on a liquid chromatograph Agilent 1200 Series (Agilent Technology, Waldbronn, Germany). Samples were analyzed using the following HPLC conditions according to Ref. [33]: three silver-ion chromatographic columns ChromSpher Lipids (250 mm × 4.6 mm, 5 μm, Varian, Palo Alto, CA, USA) connected in series, the flow rate of 1 mL/min, the injection volume of 1 μL, column temperature of 25 °C, and the mobile phase gradient: 0 min – 100% A, 140 min – 61% A + 39% B, where A is the mixture of hexane–2-propanol–acetonitrile (99.8:0.1:0.1, v/v/v) and B is the mixture of hexane–2-propanol–acetonitrile (96:2:2, v/v/v). The mobile phase was prepared freshly every day. Silver-ion columns were conditioned at 50 μL/min using the initial mobile phase composition overnight and at 1 mL/min for 1 h before the first analysis. The injector needle was washed with the mobile phase after each injection. The chromatographic system was equilibrated between injections for 45 min.

The hybrid quadrupole time-of-flight (QqTOF) analyzer micrOTOF-Q (Bruker Daltonics, Bremen, Germany) with positive-

ion APCI was used in the mass range *m/z* 50–1200 with the following tuning parameters: flow of the nebulizing and drying gas 5 and 3 L/min, respectively, temperatures of the drying gas and APCI heater 300 °C and 400 °C, respectively.

2.4. GC/FID and GC/MS analyses of FAMEs

FAMEs were prepared using a standard procedure with sodium methoxide according to Ref. [41]. Briefly, the amount of 5 mg of the sample and 1 mL of 0.25 M sodium methoxide in methanol was heated on a water bath for 10 min at 65 °C. After the reaction, water saturated with sodium chloride was added and then FAMEs were extracted from the mixture using hexane.

GC/FID experiments were performed on the gas chromatograph with flame ionization detection Agilent 7890 (Agilent Technologies, Waldbronn, Germany) using TR-FAME column (70% cyanopropyl polysilphenylene-siloxane), 30 m length, 0.25 mm ID, 0.25 μm film thickness (Thermo Scientific, Waltham, USA). GC conditions were as follows: the injection volume was 1 μL, the split ratio was 1:15, the flow rate of nitrogen as a carrier gas was 1.3 mL/min, the temperature program: the initial temperature 140 °C, ramp to 235 °C at 4 °C/min. Injector and detector temperatures were 250 °C and 280 °C, respectively. Table 1 shows the arithmetic mean values of relative weight concentrations calculated from three replicate measurements.

GC/MS experiments were performed on a gas chromatograph Agilent 6890N coupled to Agilent 5975B mass spectrometer (both Agilent Technologies) using the identical TR-FAME column as for GC/FID experiments. GC conditions were as follows: the injection volume was 1 μL, the split ratio was 1:15, the flow rate of helium as the carrier gas was 1.2 mL/min, the temperature program: the initial temperature 100 °C, ramp to 235 °C at 3 °C/min, the injector temperature was 250 °C. The MS detection conditions: temperatures of ion source and quadrupole were 230 °C and 150 °C, respectively, electron ionization with electron energy 70 eV was used in the mass range *m/z* 25–600.

2.5. Definition of abbreviations

Identified TG species are annotated using initials of FA trivial names (or by CN:DB) arranged according to their stereochemical positions (*sn*-1, *sn*-2 and *sn*-3), *e.g.*, 1-octadecenoyl-2-octadecadienoyl-3-hexadecanoyl-*sn*-glycerol is annotated as OLP. *Sn*-1 and *sn*-3 positions cannot be resolved in this work and FAs in these positions are arranged according to their decreasing molecular masses. The positions and number of branching in TGs cannot be exactly determined by HPLC/MS, therefore we annotate such TGs with a prefix *b*, for example *b*SSS means that this TG contains three C18:0 acyl chains and one or more of them are branched C18:0 acid(s) with unknown position(s) of branching. The regioisomeric positions of branched FAs are not determined. Abbreviations of FAs: M – myristic (C14:0); P – palmitic (C16:0); Po – palmitoleic (Δ*9*-C16:1); Ma – margaric (C17:0); Mo – margaroleic (Δ*9*-C17:1); S – stearic (C18:0); O – oleic (Δ*9*-C18:1); Va – vaccenic (Δ*11t*-C18:1); L – linoleic (Δ*9,12*-C18:2); Ln – linolenic (Δ*9,12,15*-C18:3); A – arachidic (C20:0); G – gadoleic (Δ*9*-C20:1). FAs in GC/FID chromatograms are annotated using CN:DB with position(s) and *cis*-/*trans*- (*t*) configuration of DBs and branching (*i* – iso, *ai* – anteiso, *b* – branched FA with unknown position(s) of branching). Unsaturated and branched FAs identified by GC/MS without identical standards are annotated without position(s) of DBs and branching, respectively.

3. Results and discussion

3.1. NARP-HPLC/APCI-MS

NARP-HPLC method with APCI-MS detection using C_{18} column in the total length of 45 cm, separation temperature 25 °C and the gradient of acetonitrile/2-propanol/hexane [23] is used for the analysis of TGs from animal fats (Figs. 1A and 2A, Table S1). Retention times of TGs in NARP-HPLC are given by the total number of carbon atoms and DBs in TGs usually expressed by ECN value, *i.e.*, ECN = CN − 2DB. The retention of TGs increases with the increasing ECN, while the length and unsaturation of individual fatty acyls in TGs affect their retention inside individual ECN groups. TGs with the higher number of DBs have lower retention times than saturated TGs with the same ECN, *e.g.*, OOO (t_R = 60.5 min) has slightly lower retention in comparison to OOP (62.0 min), POP (63.8 min), or even PPP (65.5 min), all with ECN = 48 (Table S1). TG isomers with *cis*- and *trans*-configuration of DBs are also separated using NARP-HPLC method (Figs. 1A and 2A). *Trans*-FAs have the straight arrangement of acyl chains with similar physicochemical properties as for saturated FAs, therefore TGs containing *trans*-FAs are more retained in NARP-HPLC than *cis*-TGs, *e.g.*, SOO with t_R = 69.6 min and its *trans*-isomer SOVa with t_R = 70.8 min (Table S1).

Peaks of isomers of saturated TGs with the same CN of fatty acyls and shifted retention times are identified in ruminant samples. These isomers correspond to TGs containing branched (*b*) FAs as confirmed by GC/FID data, where numerous *b*FAs in ruminant samples are found. TG isomers containing linear and *b*FAs provide identical APCI mass spectra without any diagnostic fragment ions or measurable differences in relative abundances of ions, therefore they cannot be differentiated based on mass spectra only. On the other hand, NARP-HPLC/APCI-MS data are used for the resolution of both isomers based on shifts in retention times determined using reconstructed ion current chromatograms (RICs) of $[M+H–RCOOH]^+$ ions as shown in Fig. 3. TGs with *b*FAs have slightly lower retention times in comparison to their linear analogs (Fig. 3B), *e.g.*, *b*SSP (t_R = 78.7 min) containing *b*FA has lower retention time than SSP (79.8 min) containing linear acyl chains with the same CN:DB. Only one peak of *b*TGs with the same CN is identified in NARP-HPLC chromatograms from ruminant fats in contrast to expected combinations of *b*FAs with different positions and number of branching identified in GC/FID experiments, therefore all isomers of *b*TGs coelute in one peak. This is in agreement with the literature [25], where TGs with *iso*- and *anteiso*-FAs are not separated under the gradient elution, only TGs containing two or three *b*FAs are partially separated under the isocratic elution with extremely long retention times in the range of hundreds of minutes.

APCI full-scan positive-ion mass spectra of analyzed TGs provide $[M+H]^+$ and $[M+NH_4]^+$ ions and also abundant fragment ions $[M+H–RCOOH]^+$ formed by cleavage of FAs from glycerol. Ratios of $[M+H–RCOOH]^+$ fragment ions are used for the determination of prevailing FA in the *sn*-2 position according to well known rule that the neutral loss of FA from this position provides the fragment ion with a lower relative abundance in comparison to *sn*-1 and *sn*-3 positions [12,13,42].

3.2. Silver-ion HPLC/APCI-MS

Samples of animal fats are analyzed using three ion-exchange based silver-ion HPLC columns connected in series in the total length of 75 cm and hexane/2-propanol/acetonitrile gradient [33]. TGs are separated into groups according to their number of DBs. The higher number of DBs means stronger interactions with silver ions in the stationary phase resulting in higher retention times (Figs. 1B and 2B, Table S1). TGs inside individual DB groups are partially separated according to acyl chain lengths, as demonstrated

Table 1
Relative weight concentrations [%] of FAs[a] identified in analyzed samples from GC/FID of FAMEs, their retention times (t_R) and response factors (RF).

t_R (min)	Fatty acid[b]	RF	Fallow deer	Red deer	Sheep	Moufflon	Wild boar	Cock	Duck	Rabbit
4.3	C10:0	1.33	0.1	0.1	0.1	0.1	0.1			0.1
4.9	C11:0	1.24				0.1				
5.1	*i*C12:0	1.16[c]				0.2				
5.4	*b*C13:0	1.11[c]				0.3				
5.6	C12:0	1.16	0.1	0.4	0.1	0.1	0.1	0.1	<0.1	0.2
5.9	*b*C13:0	1.11[c]				0.4				
6.0	*i*C13:0	1.11[c]		0.1						
6.1	*b*C14:0	1.07[c]				0.4				
6.4	C13:0	1.11	0.1	0.1		0.1				<0.1
6.5	*b*C14:0	1.07[c]				0.1				
6.8	*b*C14:0	1.07[c]				0.3				
6.9	*i*C14:0	1.07[c]	1.1	0.3	0.1	0.1				0.1
7.0	*b*C15:0	1.03[c]				0.3				
7.2	*b*C15:0	1.03[c]				0.2				
7.4	C14:0	1.07	4.8	5.7	2.1	2.8	1.3	0.5	0.7	3.4
7.6	*b*C14:0	1.07[c]	0.1		<0.1	0.8				
7.7	*b*C14:0	1.07[c]				0.4				
7.8	*b*C14:0	1.07[c]	0.1			0.9				
7.9	*b*C14:0	1.07[c]	0.1			0.4				
8.0	*i*C15:0	1.03[c]	0.4	0.8	0.2					0.1
8.1	Δ*9*-C14:1	1.11	0.2	<0.1				0.1	0.1	0.1
8.3	*ai*C15:0	1.03[c]	0.6	1.0	0.2					0.2
8.5	*b*C16:0	1.00[c]				0.1				
8.6	C15:0	1.03	2.0	1.6	0.6	1.6	<0.1	0.1	0.1	1.1
8.8	C15:1	1.00	0.1	0.1	0.1					0.3
8.9	*b*C16:0	1.00[c]	0.1			0.9				
9.0	*b*C16:0	1.00[c]	<0.1			0.7				
9.3	*i*C16:0	1.00[c]	9.5	0.4	0.2	0.6				0.5
9.6	*b*C17:0	0.99[c]	0.3			0.4				
9.9	C16:0	1.00	25.0	24.8	19.8	16.0	25.7	19.8	21.6	33.5
10.1	C16:1	1.00[c]		0.1	0.1			0.1	0.1	0.1
10.2	*b*C17:0	0.99[c]	0.1			1.0				
10.3	*b*C17:0	0.99[c]	0.2	0.2	0.1	0.4			<0.1	
10.4	*b*C17:0	0.99[c]	0.1		0.1	0.9				
10.5	C16:1	1.02[c]	0.6	0.8	0.6	1.5	0.3	0.5	0.5	0.4
10.6	Δ*9*-C16:1	1.02	1.1	0.7	0.6	2.2	2.5	2.5	4.3	3.0
10.7	*i*C17:0	0.99[c]	0.4	0.5	0.4					
10.9	*ai*C17:0	0.99[c]	1.5	0.7	0.8	1.4	0.1		0.1	0.3
11.1	C17:1	0.99[c]	0.1	0.3						
11.2	*b*C18:0	0.97[c]				0.1				
11.3	C17:0	0.99	3.1	1.5	2.2	2.6	0.2	0.3	0.2	1.4
11.6	C16:2	0.99[c]	<0.1	<0.1	0.1					<0.1
11.9	Δ*10*-C17:1	0.99	0.4	0.1	0.5	2.7	0.2	0.1	0.1	0.7
12.0	*i*C18:0	0.96	2.0	0.1	0.2	0.7				0.1
12.2	*ai*C18:0	0.97				0.1				
12.7	C18:0	0.97	22.2	36.7	31.6	7.7	11.7	10.5	5.1	8.5
13.0	Δ*9t*-C18:1	0.98	0.3	0.4	0.8	0.5	0.1	0.3	0.3	0.1
13.1	Δ*11t*-C18:1	0.98[c]	1.0	2.7	5.6	2.3				0.2
13.2	Δ9-C18:1	0.98	15.8	12.3	25.8	34.5	38.2	49.5	48.8	23.2
13.3	Δ*11*-C18:1	1.00	0.3	0.7	0.5	0.7	2.8	2.2	1.7	1.1
13.4	C18:1	0.98[c]	0.1	0.2	0.1	0.1				0.1
13.5	C18:1	0.98[c]	0.5			0.2	0.1	<0.1	0.1	0.1
13.6	Δ*9t,12t*-C18:2	0.99		0.5	0.8	0.3				0.1
13.7	C18:1	0.98[c]	0.3	0.2	0.4	0.7				
13.9	C18:2	0.98[c]	0.1	<0.1	0.1	0.4		0.1	0.1	<0.1
14.1	C19:0	1.00	0.4	0.6	0.6	0.5		0.1	0.1	0.2
14.2	Δ*9,12*-C18:2	0.98	1.4	1.8	1.3	2.0	12.3	10.2	12.7	13.3
14.5	C18:2	0.98[c]		0.1						
14.6	C19:1	1.00[c]	0.1	0.2	0.2	0.3	<0.1	0.1	0.1	0.2
14.8	Δ*6,9,12*-C18:3	0.97						0.1	<0.1	<0.1
15.3	Δ*9,12,15*-C18:3	0.97	0.9	1.2	1.0	1.4	1.3	0.7	1.1	5.5
15.5	C20:0	0.97	0.5	0.5	0.2	0.1	0.2	0.2	0.1	0.2
15.7	C18:2	0.98[c]	0.1	0.1	0.7	1.5	0.1		0.1	0.1
15.9	C18:4	1.00[c]	0.2	0.2	0.2	0.2		0.1	0.2	
16.0	Δ*11*-C20:1	0.98	0.1	0.1	0.1	0.1	1.0	1.0	0.4	0.3
16.2	C20:1	0.98[c]			0.1	0.1	<0.1			
16.6	C18:3	0.97[c]			0.1	0.1				
16.7	C20:2	0.97[c]						0.1	0.1	
16.9	C21:0	0.96	0.1	0.1						
17.0	Δ*11,14*-C20:2	0.97		<0.1		<0.1	0.6	0.1	0.1	0.1
17.6	Δ*8,11,14*-C20:3	0.96				<0.1	0.1	0.1	0.1	<0.1
18.0	Δ*5,8,11,14*-C20:4	0.99	0.1	<0.1	<0.1	<0.1	0.1	0.1	0.3	0.1
18.1	Δ*11,14,17*-C20:3	0.96		<0.1		<0.1	0.3			0.1
18.2	C22:0	0.93	0.1	0.1	<0.1					<0.1
18.7	C22:1	0.95[c]							<0.1	

Table 1 (*Continued*)

t_R (min)	Fatty acid[b]	RF	Fallow deer	Red deer	Sheep	Moufflon	Wild boar	Cock	Duck	Rabbit
18.8	Δ*13*-C22:1	0.95					<0.1	<0.1		
19.2	Δ*5,8,11,14,17*-C20:5	0.97			<0.1					
19.6	C23:0	0.96	0.1	0.1						
20.8	C24:0	0.96	0.1	0.1						
20.9	Δ*7,10,13,16*-C22:4	0.96					0.1	0.1	0.1	0.1
22.0	Δ*7,10,13,16,19*-C22:5	0.97	0.2		0.1	0.1	0.1	0.1	0.1	0.2
	Others	1.00[c]	0.7	0.7	0.5	4.3	0.4	0.2	0.5	0.6

[a] Standard deviations of all relative weight concentrations in this table are <0.03 as calculated from three replicates.
[b] FAs are annotated using CN:DB with position(s) and *cis*-/*trans*- (*t*) configuration of DBs and branching (i – iso, ai – anteiso, b – branched FA with unknown position(s) of branching). Unsaturated and branched FAs identified by GC/MS without identical standards are annotated without position(s) of DBs and branching, respectively.
[c] The response factor of FAs without an identical standard is set the same as for the standard with the identical CN:DB, *e.g.*, iC13:0 and bC13:0 is the same as for C13:0.

on retention times of the pair of SOS (37.3 min) and SOP (37.7 min), both with DB = 1 differing by two methylene units, *i.e.*, the difference in retention is approximately 0.4 min per two methylene units (Table S1). RICs of protonated molecules, ammonium adducts and fragment ions from HPLC/APCI-MS analysis are used for the identification of TGs in highly complex animal fats (*e.g.*, Figs. 3 and 4) even for peaks with the high number of coeluted species, for example in the group of TGs with DB = 0 with very small differences in retention times of individual saturated TGs coeluting in one peak. In silver-ion HPLC, *trans*-FAs have lower retention times in comparison to *cis*-isomers with the same CN:DB, but they elute before the DB minus one group, for example SSS (t_R = 17.6 min, without DB) < SVaS (t_R = 26.8 min, 1 *trans*-DB) < SOS (t_R = 37.3 min, 1 *cis*-DB). Differences of retention times between *cis*- and *trans*-TGs decrease for the higher number of DBs, but they still elute in separated groups between two DB groups with all *cis*-FAs and the identification of *trans*-TGs in the sample can be done even without the need of MS detection.

Silver-ion HPLC method enables the baseline separation of TG regioisomers up to three DBs and at least the partial resolution of regioisomers with four to seven DBs. Regioisomers with the higher number of DBs in fatty acyls in outer positions (*sn*-1 and *sn*-3) are retained more strongly in comparison to TGs with the same unsaturation in the *sn*-2 position (Fig. 4C and D), *e.g.*, SLS (t_R = 51.4 min) and SSL (52.5 min). All TG regioisomers are at least partially separated except for $R_1R_2R_3$ and $R_2R_1R_3$ type regioisomers, where R_1 and R_2 are different saturated FAs that elute in one peak, *e.g.*, SPO and OSP regioisomers are not resolved. The determination of exact composition of individual regioisomers by a simple integration of their peak areas is impossible in highly complex animal samples due to the coelution with other species. For this reason, RICs of protonated molecules and $[M+H–RCOOH]^+$ fragment ions are used to support the proper determination of regioisomeric ratios (Fig. 4). The precision of this procedure is limited by the huge number of isobaric species in the samples and the increment of A+2 isotopic peaks to the intensity of reconstructed ion currents, but it still provides acceptable results for most biochemical applications. Fig. 4 shows a different procedure for the rough determination of regioisomeric composition inside DB groups with the different unsaturation level of individual FAs, *i.e.*, saturated (Sa), monounsaturated (Mo) and diunsaturated (D) FAs. The ratio of regioisomers is determined based on the ratio of peak areas of both groups of regioisomers. It is confirmed that the ratio for all pairs within particular unsaturation groups of regioisomers is similar, as illustrated on the example shown in Fig. 4A and B. The validity of this presumption has been confirmed by the peak areas of individual regioisomers from RICs of fragment ions, as illustrated on selected examples in Fig. 4C, 4D. Regioisomers with unsaturated FAs in the *sn*-2 position, *i.e.*, SaMoSa (Fig. 4A), SaDSa and MoMoSa (Fig. 4D), have higher relative concentrations in comparison to peaks of isomers with unsaturated FAs in *sn*-1/3 positions, *i.e.*, SaSaMo, SaSaD and MoSaMo. This procedure for the rough determination of regioisomeric ratios together with known retention rules in silver-ion HPLC can be easily applied with any HPLC detector, if an HPLC/MS system is not available in the laboratory.

3.3. Analysis of FA composition using GC/FID

The FA composition of animal fats is characterized by the GC/FID analysis of FAMEs after the transesterification of TGs with sodium methoxide (Figs. 1C and 2C, Table 1). At first, the carrier gas flow rate, initial temperature and temperature program have been carefully optimized using complex FAME standard mixtures to achieve the separation of maximum number of species including the separation of all types of isomerism, *i.e.*, *cis*-/*trans*-, linear/branched and DB positional isomers. Individual FAs are identified based on retention times of identical standards or electron ionization (EI) mass spectra from GC/MS analysis. Positions of DBs and branching of some isomers without commercially available standards cannot be clearly identified due to the lack of diagnostic fragment ions in EI mass spectra. These FAs are annotated by their CN:DB but without positions of DBs and branching, *e.g.*, *b*C17:0 in Fig. 1C.

In optimized GC/FID method, all FAMEs including different isomers are baseline or at least partially separated. Retention times of FAMEs increase with the increasing acyl chain length and the number of DBs. Positions of DBs in the acyl chain (DB positional isomers) also influence retention times of FAMEs. DB positional isomers with a greater distance between the first DB and the ester group are retained more strongly, for example C18:1 positional isomers Δ*9*-C18:1 with t_R = 13.2 min and Δ*11*-C18:1 with t_R = 13.4 min (Table 1). FAMEs containing *trans*-configuration of DBs have lower retention times in comparison to their *cis*-isomers, as demonstrated on elaidic (Δ9*t*-C18:1) and oleic (Δ*9*-C18:1) FAs with retention times 13.0 and 13.2 min, respectively. Branched FAs have the lower retention in comparison to their linear analogs. For example, FAs containing 18 carbon atoms that are methyl branched on the first (*iso, i*) or the second (*anteiso*, *ai*) carbon atom have lower retention times in comparison to their C18:0 linear analog, *i.e.*, *i*C18:0 (t_R = 12.0 min), *ai*C18:0 (t_R = 12.2 min) and C18:0 (t_R = 12.7 min). Some *b*FAs are identified based on retention shifts and EI mass spectra, but the determination of branching position or the number of branching in multibranched FAs is not possible without identical standards, which are not commercially available.

Peak areas of FAMEs in GC/FID chromatograms are used for the determination of FA profiles in analyzed animal fats. These areas are multiplied by response factors (RFs) of identical standards related to the palmitic acid. Response factors of individual FAMEs are in the range from 0.93 to 1.03 for FAs with 15 to 24 carbon atoms and 0 to 5 DBs including all isomers, *i.e.*, positional and *cis*-/*trans*-DB isomers and linear/branched isomers of acyl chains (Table 1). Higher differences of RF values can be observed only for FAs with short acyl chains (Δ*9*-C14:1 – 1.11, C14:0 – 1.07, C13:0 – 1.11, C12:0 – 1.16, C11:0 – 1.24 and C10:0 – 1.33), but it is still acceptable for the reliable quantitation due to the low concentration of these FAs.

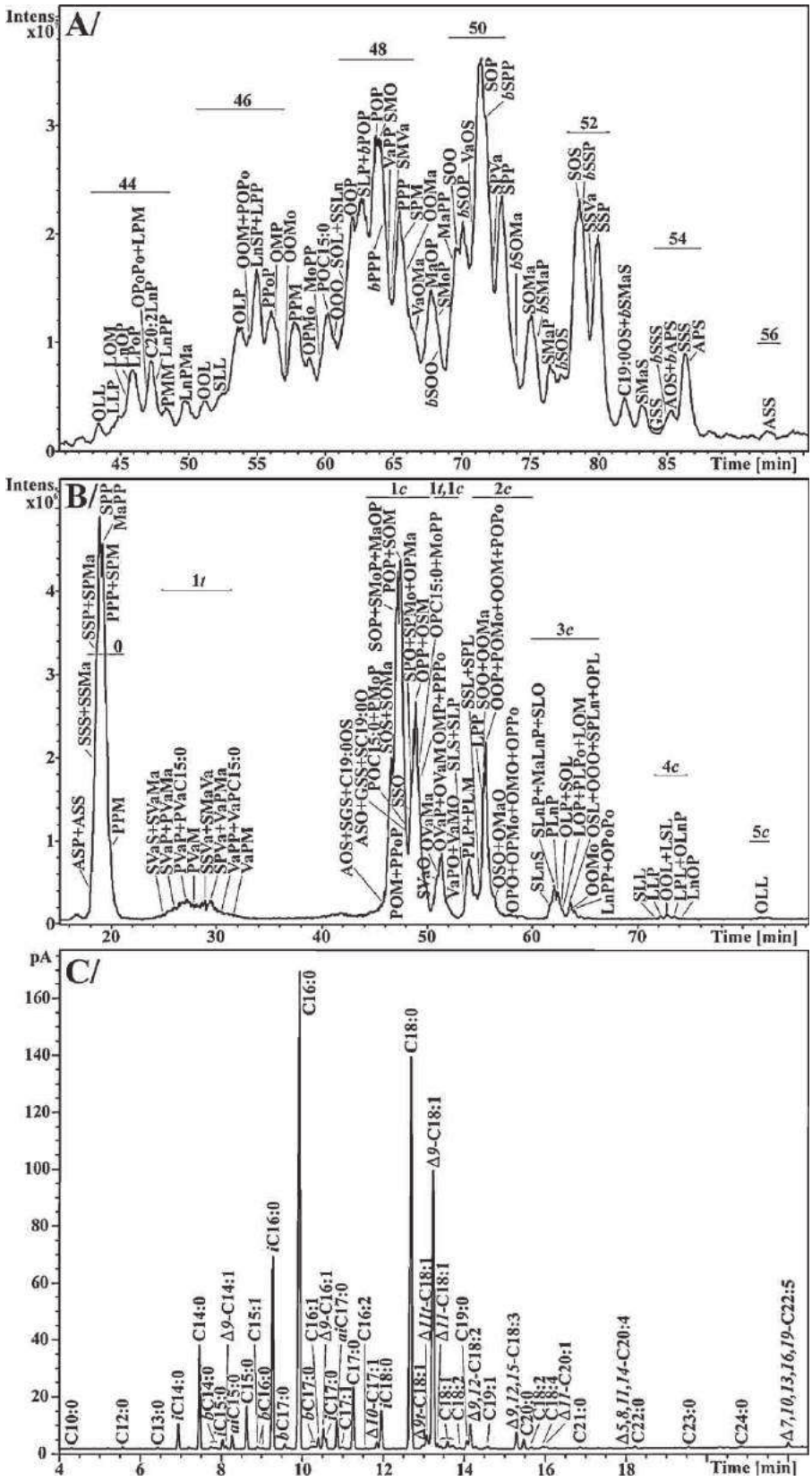

Fig. 1. Analysis of fallow deer (*Dama dama*): (A) NARP-HPLC/APCI-MS analysis of TGs, (B) silver-ion HPLC/APCI-MS analysis of TGs, and (C) GC/FID analysis of FAMEs. NARP-HPLC conditions: two Nova-Pak C18 columns (300 and 150 mm × 3.9 mm, 4 μm) connected in series, flow rate 1 mL/min, column temperature 25 °C, gradient 0 min – 80% A + 20% B, 121 min – 40% A + 60% B, 122 min – 80% A + 20% B, where A is acetonitrile and B is a mixture of hexane–2-propanol (1:1, v/v). Silver-ion HPLC conditions: three ChromSpher Lipid columns (250 mm × 4.6 mm, 5 μm) connected in series, flow rate of 1 mL/min, column temperature 25 °C, gradient 0 min – 100% A, 140 min – 61% A + 39% B, where A is the mixture of hexane–2-propanol–acetonitrile (99.8:0.1:0.1, v/v/v) and B is the mixture of hexane–2-propanol–acetonitrile (96:2:2, v/v/v). GC/FID conditions: TR-FAME column (30 m length, 0.25 mm ID, 0.25 μm film thickness), the flow rate of nitrogen as a carrier gas 1.3 mL/min, temperature program: the initial temperature 140 °C, ramp to 235 °C at 4 °C/min.

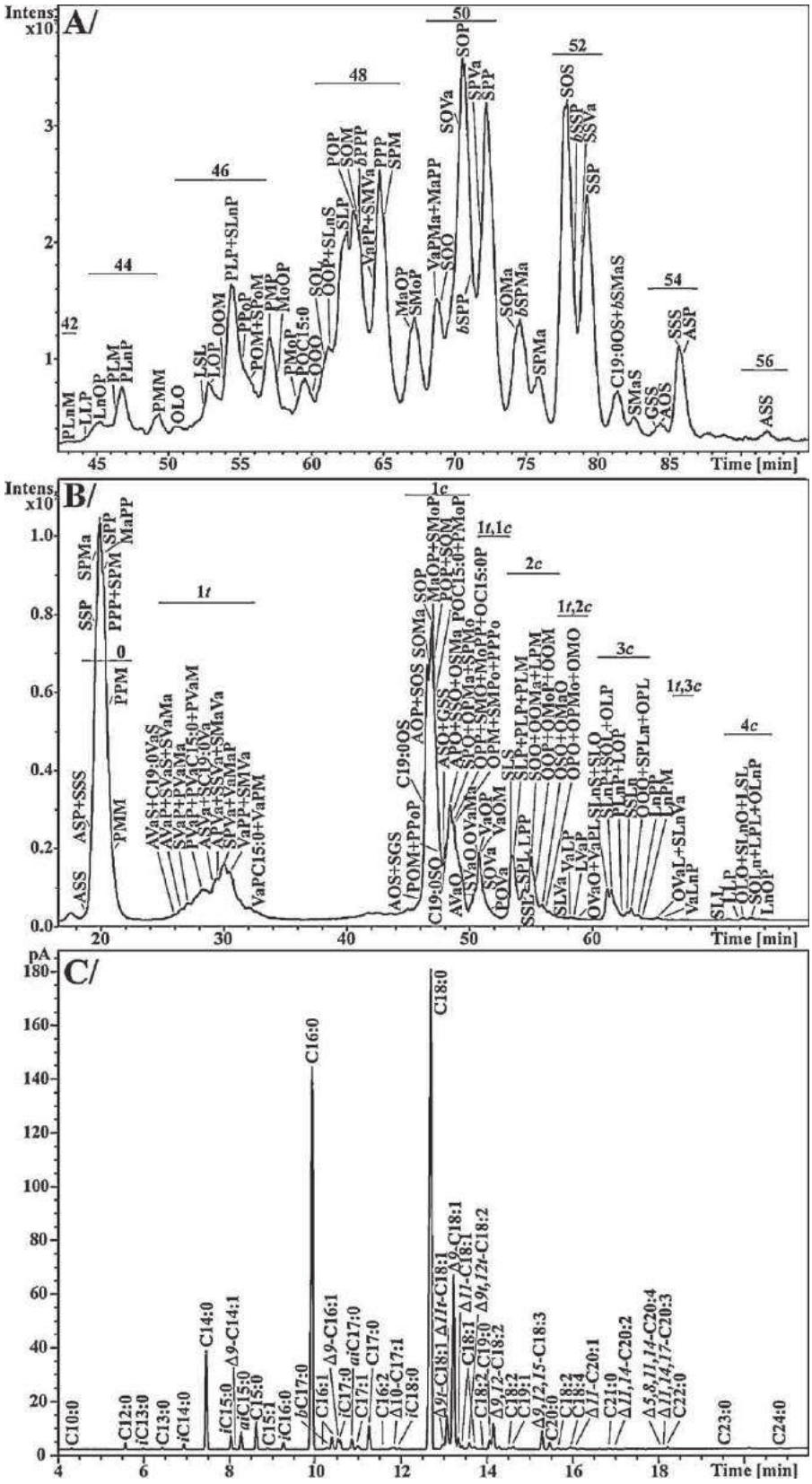

Fig. 2. Analysis of red deer (*Cervus elaphus*): (A) NARP-HPLC/APCI-MS analysis of TGs, (B) silver-ion HPLC/APCI-MS analysis of TGs, and (C) GC/FID analysis of FAMEs. HPLC and GC conditions are identical as for Fig. 1.

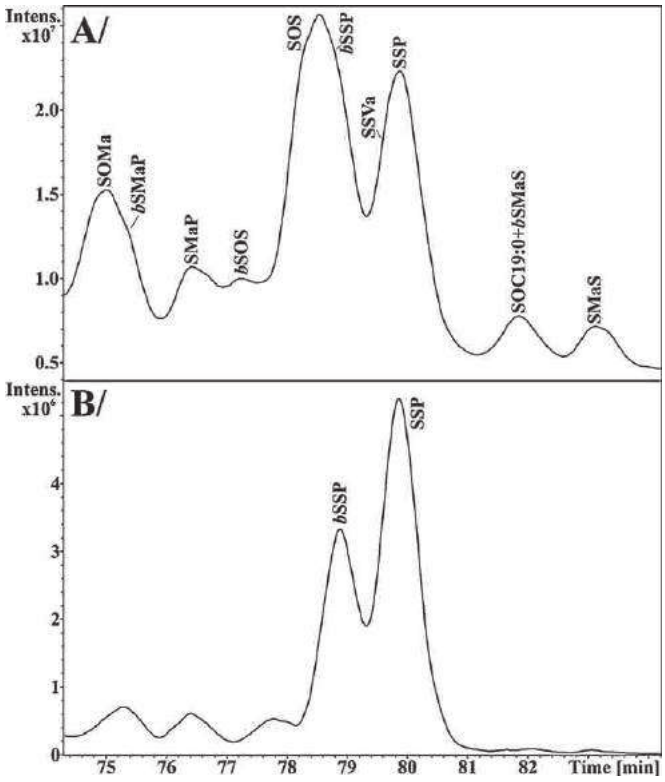

Fig. 3. NARP-HPLC/APCI-MS identification of TGs containing linear (SSP) and branched (*b*SSP) FAs using the total ion current chromatogram (A) and the reconstructed ion current chromatogram (m/z = 579) corresponding to the ion $[M+H–RCOOH]^+$ for the neutral loss of C18:0 (B) in fallow deer (*Dama dama*) sample. HPLC conditions are identical as for Fig. 1.

Response factors of FAs without identical standards are set identical as the closest FAME standard with the same CN:DB values.

3.4. Analysis of animal fats

NARP-HPLC, silver-ion HPLC and GC-FID methods have been applied for the analysis of animal fats from fallow deer (Fig. 1), red deer (Fig. 2), wild boar (Fig. 5), duck (Fig. 6), sheep (Fig. S1), moufflon (Fig. S2), cock (Fig. S3) and rabbit (Fig. S4) samples to achieve the maximum information for the characterization of FA and TG composition of these samples. Tables 1 and 2 show the FA composition of analyzed fats using GC/FID method. Properly optimized GC/FID method provides the separation and identification of a wide range of FAs even in complex animal fats. In total, 81 FAs have been detected in 8 animal fats ranging from 29 in wild boar to 61 in moufflon (Table 2). The number of identified FAs in individual animal samples is significantly higher than in most common fatty samples, for example from 7 to 18 FAs have been identified in a wide range of plant oils [18,43]. The enormous complexity of animal samples is given by the presence of many *cis*-/*trans*-, positional and branched FA isomers. Ruminant fats (fallow deer, red deer, sheep and moufflon) are rather complex due to the action of bacteria in their rumen that produce a number of unusual FAs, mainly branched and natural *trans*-FAs. 29 *b*FAs have been detected in all ruminants, from which 25 *b*FAs are found in the most complex moufflon sample. The most abundant *b*FAs are *i*C16:0 with the concentration up to 9.5%, *ai*C17:0 up to 1.5% and *i*C18:0 up to 2.0% in fallow deer. The concentration of *b*FAs in ruminant fats ranges between 2.2% in sheep and 16.6% in fallow deer in comparison to the trace amount in samples of omnivores (wild boar, cock and duck) with the concentration < 0.1% (Table 2). The highest concentration of *b*FAs is observed in samples of wild animals, *i.e.*, fallow deer (16.6%) and moufflon (12.0%), given

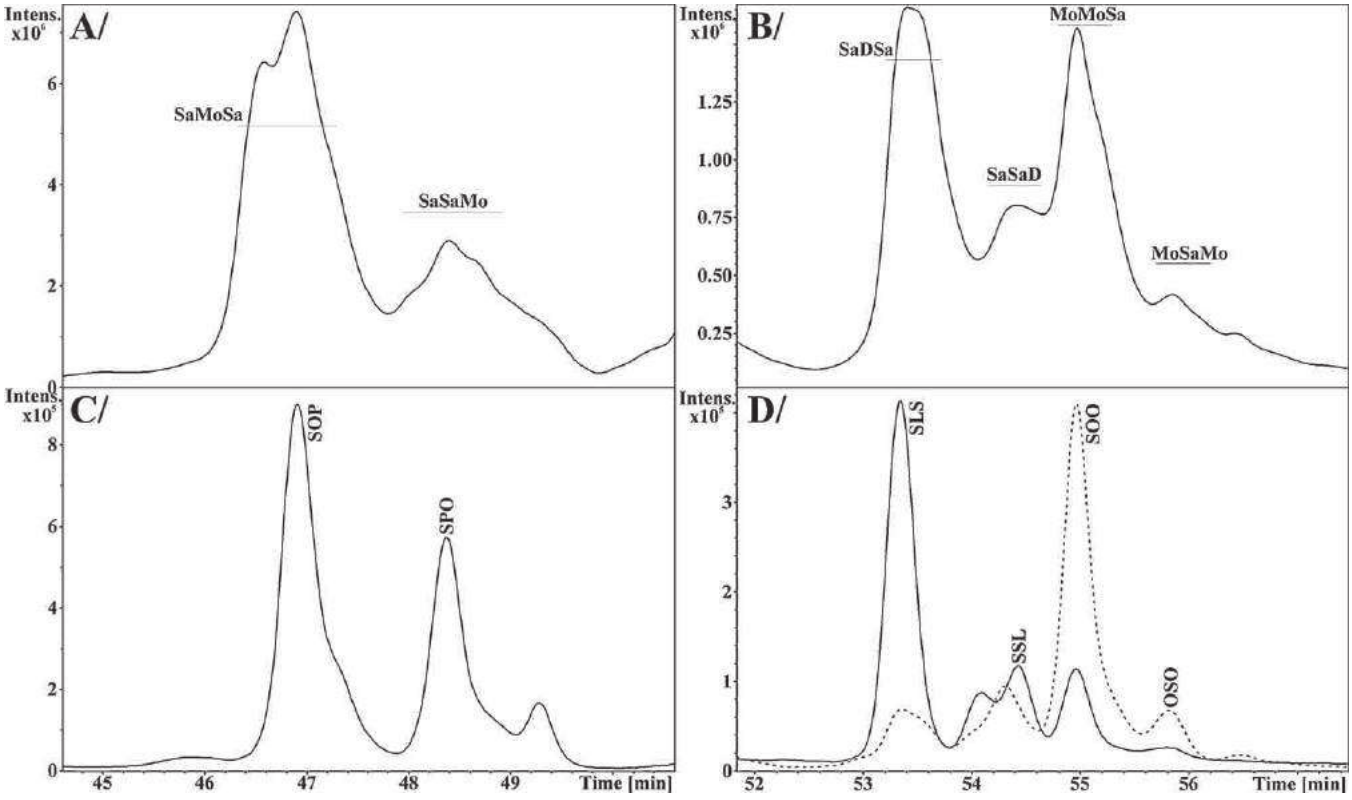

Fig. 4. Determination of TG regioisomers ratios in red deer (*Cervus elaphus*) using silver-ion HPLC/APCI-MS. Total ion chromatograms of regioisomers with 1 (A) and 2 (B) DBs and reconstructed ion current chromatograms of regioisomers SOP/SPO (m/z = 579) (C) and SLS/SSL (m/z = 605) and SOO/OSO (m/z = 607, dash line) (D). Sa – saturated, Mo – monounsaturated and D – diunsaturated FAs. HPLC conditions are identical as for Fig. 1.

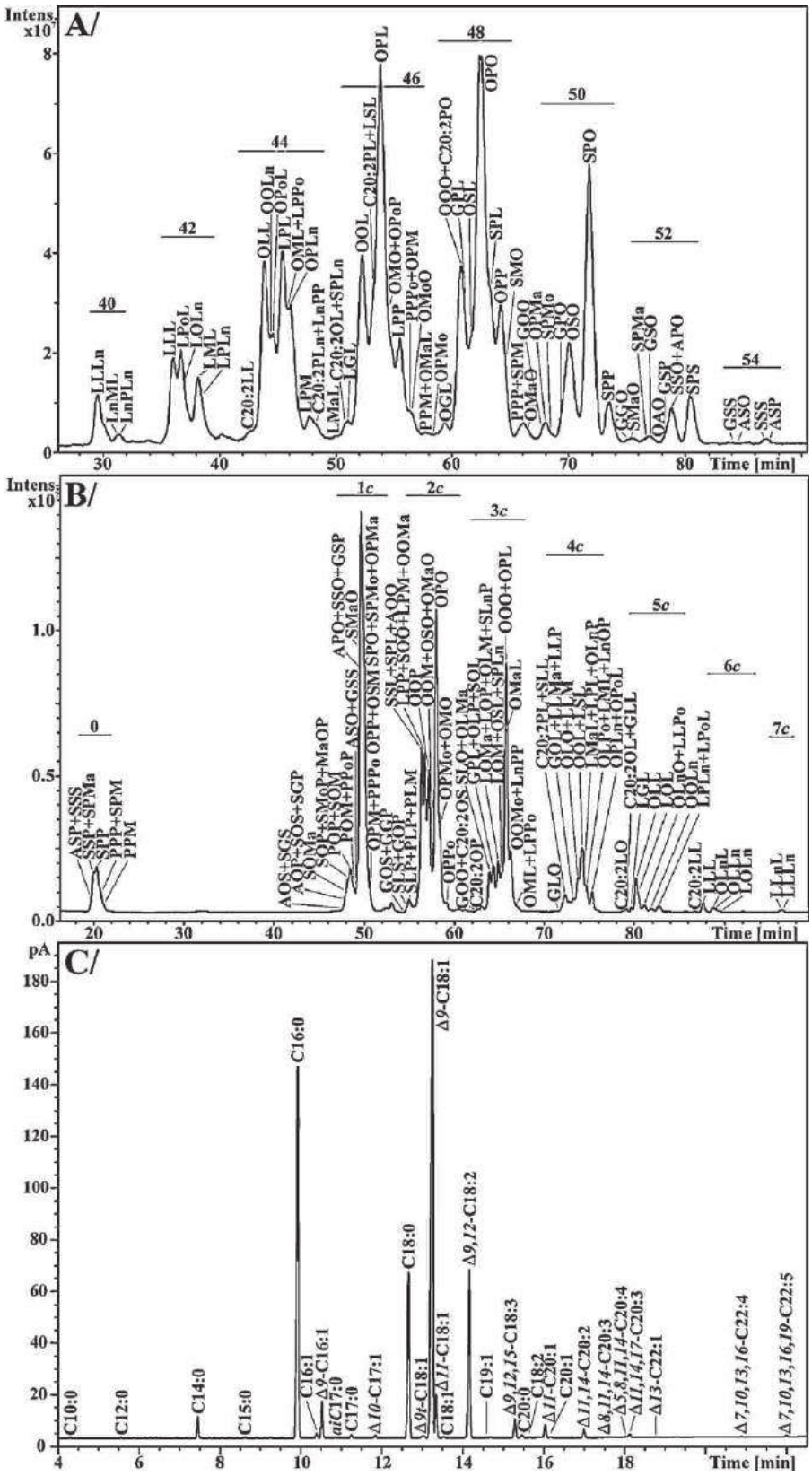

Fig. 5. Analysis of wild boar (*Sus scrofa*): (A) NARP-HPLC/APCI-MS analysis of TGs, (B) silver-ion HPLC/APCI-MS analysis of TGs, and (C) GC/FID analysis of FAMEs. HPLC and GC conditions are identical as for Fig. 1.

probably by their different diet. Three naturally occurring *trans*-FAs are identified in analyzed animal fats (*i.e.*, Δ*9t*-C18:1, Δ*11t*-C18:1 and Δ*9t,12t*-C18:2). Ruminant samples contain *trans*-FAs from 1% up to 7%, where vaccenic acid (Δ*11t*-C18:1) with the concentration up to 5.6% in sheep sample is the most abundant *trans*-FA. On the other hand, their concentrations in herbivore (rabbit) and omnivore samples are only trace (at most 0.4% of *trans*-FAs in rabbit).

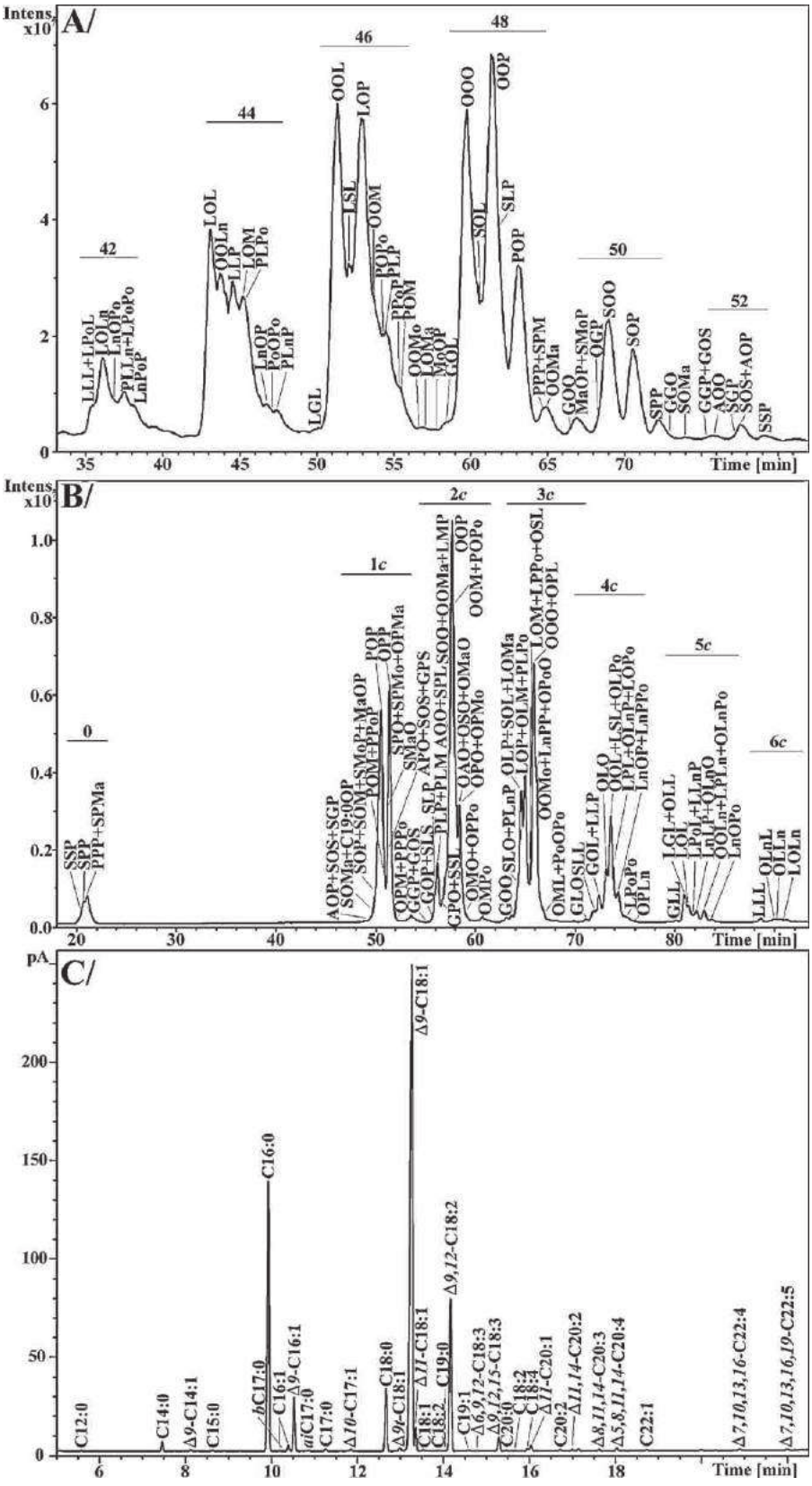

Fig. 6. Analysis of duck (*Anas platyrhynchos domesticus*): (A) NARP-HPLC/APCI-MS analysis of TGs, (B) silver-ion HPLC/APCI-MS analysis of TGs, and (C) GC/FID analysis of FAMEs. HPLC and GC conditions are identical as for Fig. 1.

Table 2 shows the sums of FAs identified in analyzed samples. All samples of animal fats are composed mainly from saturated (28–76%) and monounsaturated (19–57%) FAs, while the content of polyunsaturated FAs is rather low (3–20%) in contrast to common plant oils composed mainly from mono- (15–65%) and polyunsaturated (10–70%) FAs with low concentration of saturated FAs

Table 2
The number of identified FAs and the relative weight concentrations [%] of saturated, monounsaturated, polyunsaturated, essential (linoleic and linolenic acids), branched and *trans*-FAs in analyzed samples using GC/FID analysis of FAMEs.

	Number of FAs	Saturated FAs (%)	Monounsaturated FAs (%)	Polyunsaturated FAs (%)	Essential FAs (%)	Branched FAs (%)	*Trans*-FAs (%)
Fallow deer	53	75.4	21.1	2.9	2.3	16.6	1.3
Red deer	49	76.4	18.9	4.0	3.0	4.0	3.5
Sheep	45	59.7	35.3	4.5	2.3	2.2	7.1
Moufflon	61	43.6	45.9	6.1	3.5	12.0	3.2
Wild boar	29	39.4	45.4	14.8	13.6	0.1	0.1
Cock	31	31.7	56.3	11.7	10.9	0	0.3
Duck	34	28.0	56.5	15.0	13.8	0.1	0.3
Rabbit	44	50.0	29.8	19.7	18.8	1.3	0.4

Table 3
Relative peak areas [%] of DB groups (*c* – *cis*-, *t* – *trans*-) in analyzed samples from silver-ion HPLC/APCI-MS.

	DB group											
	0	1*t*	1*c*	1*t*,1*c*	2*c*	1*t*,2*c*	3*c*	1*t*,3*c*	4*c*	5*c*	6*c*	7*c*	8*c*
Fallow deer	31.8	5.1	44.0	4.1	11.9		2.6		0.4	0.1			
Red deer	36.3	13.7	34.5	4.1	8.2	0.1	2.7	0.1	0.3				
Sheep	17.7	13.5	33.3	11.8	17.8	0.8	3.8	0.5	0.7	0.1			
Moufflon	9.3	2.5	39.1	6.8	28.9	3.3	8.1	0.5	1.4	0.1			
Wild boar	4.4		31.1		32.3		20.3		8.2	2.8	0.8	0.1	
Cock	2.6		27.0		33.8		24.3		9.8	2.2	0.3		
Duck	2.7		22.4		32.5		27.0		11.6	3.2	0.6		
Rabbit	11.1		29.1		26.0		18.1		10.0	3.9	1.3	0.4	0.1

Table 4
Regioisomeric composition of selected TGs in animal fats compared to sunflower oil as a representative plant oil.

Regioisomers	Sunflower oil[a]	Pig[a]	Cattle[b]	Fallow deer	Red deer	Sheep	Moufflon	Wild boar	Cock	Duck	Rabbit
POP/OPP	100/0	8/92	63/37	66/34	74/26	61/39	76/24	10/90	78/22	52/48	51/49
OOP/OPO	98/2	12/88	94/6	87/13	77/23	94/6	95/5	18/82	87/13	53/47	67/33
PLP/LPP	100/0	1/99	61/39	57/43	64/36	65/35	0/0	8/92	53/47	56/44	52/48
LLP/LPL	97/3	9/91	62/38	61/39	57/43	54/46	59/41	9/91	52/48	58/42	54/46
OLP/LOP/OPL	63/36/1	3/12/85	49/36/15	50/38/12	57/28/15	56/34/10	46/30/24	6/9/85	54/37/9	41/36/23	47/35/18

[a] Data from Ref. [33].
[b] Data from Ref. [23].

(10–25%) [18,43]. Animal fats also contain low concentrations of essential FAs (linolenic and linoleic acids) from 2.3% up to 18.8%, which is significantly lower than in plant oils. High concentrations of saturated FAs and low content of essential and other polyunsaturated FAs in animal fats is not favorable in the human diet due to the potential for the cardiovascular diseases. On the other hand, they contain FAs with special functions in the human organism, such as *b*FAs and vaccenic acid (precursor of conjugated linolenic acids), therefore the reasonable proportion of both animal and plant fats in the human diet is recommended.

FA profiles from GC/FID experiments are used for the simple characterization of animal fats, but the information about the composition of TGs is completely lost. NARP and silver-ion HPLC together with APCI-MS enables the separation and identification of intact TGs in analyzed samples providing information about their FA composition. TGs with 38 up to 56 ECN values are identified in animal fats using NARP-HPLC/APCI-MS method including TGs with branched and *trans*-FAs (Table S1) that are identified based on their different retention behavior. TGs with 0 up to 8 *cis*-DBs are separated using silver-ion HPLC. TGs containing one *trans*-DB and combinations with up to four *cis*-DBs are identified in rumen samples thanks to their significantly lower retention times in comparison to *cis*-TGs. Table 3 shows the relative peak areas of particular DB groups from silver-ion HPLC that are in agreement with the FA composition from GC/FID analysis (Tables 1 and 2).

Silver-ion HPLC/APCI-MS data provide information about the composition of TG regioisomers, which is important information for the nutrition due to the stereospecificity of human lipases and therefore different bioavailability of FAs on the glycerol skeleton. The preference of FAs with different unsaturation degree in the *sn*-2 position strongly depends on the origin of the sample. Table 4 shows the comparison of regioisomeric composition of TGs with common saturated, mono- and diunsaturated FAs in sunflower oil and animal fats. Plant oils have a very strong preference of unsaturated FAs in the *sn*-2 position with negligible concentration of regioisomers with saturated FAs in the *sn*-2 position [33]. In contrast to plant oils, pig and wild boar samples have an inverse regioisomeric composition with the strong preference of saturated FAs in the *sn*-2 position, for example regioisomers of PLP/LPP with the ratio 100/0 in sunflower vs. 1/99 in pig and 8/92 in wild boar samples, *etc*. Other animal samples have the preference of unsaturated FAs (mono and diunsaturated FAs) in the *sn*-2 position, but the high amount of regioisomers with saturated FAs in the *sn*-2 position is also present in the samples, *e.g.*, ratio of POP/OPP isomers in the samples range between 78/22 in cock and 51/49 in rabbit. Saturated FAs in the *sn*-2 position in red deer (Fig. 2B) and sheep (Fig. S1B) samples are preferred only in TGs containing one DB with *trans*-configuration, *i.e.*, TGs containing vaccenic acid, which preferentially occupies *sn*-1/3 positions.

4. Conclusions

The detailed characterization of TG composition of 8 animal fats using NARP-HPLC/APCI-MS, silver-ion HPLC/APCI-MS and GC/FID methods is described in this work. 81 FAs including a high number of branched/linear and *cis*-/*trans*-DB isomers have been detected using GC/FID method. NARP mode enables the identification of

intact TGs containing branched and *trans*-FAs due to the different retention behavior in comparison to their linear and *cis*-FAs analogs. The ratios of TG regioisomers are determined based on silver-ion HPLC data. Unsaturated FAs are preferred over saturated FAs in the *sn*-2 position in ruminant and herbivore samples, while saturated FAs are strongly preferred in the *sn*-2 position in wild boar sample. The combination of three analytical techniques is time consuming, but it brings the maximum information content about highly complex animal samples including the identification of different types of isomerism. We have identified 282 TGs including regioisomers, 21 of them containing *b*FAs and 55 *trans*-FAs.

Acknowledgments

This work was supported by the Grant Project No. MSM0021627502 sponsored by the Ministry of Education, Youth and Sports of the Czech Republic and the Project no. 203/09/0139 sponsored by the Czech Science Foundation.

Appendix A. Supplementary data

Supplementary data associated with this article can be found, in the online version, at doi:10.1016/j.chroma.2011.07.032.

References

[1] G. van Meer, EMBO J. 24 (2005) 3159.
[2] M. Lipkin, B. Reddy, H. Newmark, S.A. Lamprecht, Annu. Rev. Nutr. 19 (1999) 545.
[3] C.L.E. Yen, S.J. Stone, S. Koliwad, C. Harris, R.V. Farese, J. Lipid Res. 49 (2008) 2283.
[4] M.W. Pariza, Y. Park, M.E. Cook, Prog. Lipid Res. 40 (2001) 283.
[5] M.U. Jakobsen, A. Bysted, N.L. Andersen, B.L. Heitmann, H.B. Hartkopp, T. Leth, K. Overvad, J. Dyerberg, Atheroscler. Suppl. 7 (2006) 9.
[6] A.P. Simopoulos, Exp. Biol. Med. 233 (2008) 674.
[7] Y. Chilliard, F. Glasser, A. Ferlay, L. Bernard, J. Rouel, M. Doreau, Eur. J. Lipid Sci. Technol. 109 (2007) 828.
[8] W.C. Byrdwell, E.A. Emken, W.E. Neff, R.O. Adlof, Lipids 31 (1996) 919.
[9] J. Cvačka, O. Hovorka, P. Jiroš, J. Kindl, K. Stránský, I. Valterová, J. Chromatogr. A 1101 (2006) 226.
[10] M. Holčapek, P. Jandera, J. Fischer, Crit. Rev. Anal. Chem. 31 (2001) 53.
[11] M. Holčapek, P. Jandera, J. Fischer, B. Prokeš, J. Chromatogr. A 858 (1999) 13.
[12] M. Holčapek, P. Jandera, P. Zderadička, L. Hrubá, J. Chromatogr. A 1010 (2003) 195.
[13] M. Holčapek, M. Lísa, P. Jandera, N. Kabátová, J. Sep. Sci. 28 (2005) 1315.
[14] E. Kofroňová, J. Cvačka, V. Vrkoslav, R. Hanuš, P. Jiroš, J. Kindl, O. Hovorka, I. Valterová, J. Chromatogr. B 877 (2009) 3878.
[15] P. Laakso, J. Am. Oil Chem. Soc. 74 (1997) 1291.
[16] M. Lísa, M. Holčapek, Chem. Listy 99 (2005) 195.
[17] M. Lísa, M. Holčapek, T. Řezanka, N. Kabátová, J. Chromatogr. A 1146 (2007) 67.
[18] M. Lísa, M. Holčapek, J. Chromatogr. A 1198 (2008) 115.
[19] M. Lísa, F. Lynen, M. Holčapek, P. Sandra, J. Chromatogr. A 1176 (2007) 135.
[20] H.R. Mottram, Z.M. Crossman, R.P. Evershed, Analyst 126 (2001) 1018.
[21] H.R. Mottram, S.E. Woodbury, R.P. Evershed, Rapid Commun. Mass Spectrom. 11 (1997) 1240.
[22] J.D.J. van den Berg, N.D. Vermist, L. Carlyle, M. Holčapek, J.J. Boon, J. Sep. Sci. 27 (2004) 181.
[23] M. Holčapek, H. Velínská, M. Lísa, P. Česla, J. Sep. Sci. 32 (2009) 3672.
[24] S. Momchilova, Y. Itabashi, B. Nikolova-Damyanova, A. Kuksis, J. Sep. Sci. 29 (2006) 2578.
[25] O. Schreiberová, T. Krulikovská, K. Sigler, A. Čejková, T. Řezanka, Lipids 45 (2010) 743.
[26] M. Lísa, M. Holčapek, H. Sovová, J. Chromatogr. A 1216 (2009) 8371.
[27] H.M. Leskinen, Rapid Commun. Mass Spectrom. 24 (2010) 1.
[28] R. Adlof, G. List, J. Chromatogr. A 1046 (2004) 109.
[29] R.O. Adlof, J. High Resol. Chromatogr. 18 (1995) 105.
[30] R.O. Adlof, A. Menzel, V. Dorovska-Taran, J. Chromatogr. A 953 (2002) 293.
[31] W.W. Christie, J. Chromatogr. 454 (1988) 273.
[32] P. Laakso, P. Voutilainen, Lipids 31 (1996) 1311.
[33] M. Lísa, H. Velínská, M. Holčapek, Anal. Chem. 81 (2009) 3903.
[34] P.J.W. Schuyl, T. de Joode, M.A. Vasconcellos, G. Duchateau, J. Chromatogr. A 810 (1998) 53.
[35] B. Nikolova-Damyanova, B.G. Herslof, W.W. Christie, J. Chromatogr. 609 (1992) 133.
[36] P. Dugo, T. Kumm, M.L. Crupi, A. Cotroneo, L. Mondello, J. Chromatogr. A 1112 (2006) 269.
[37] L. Mondello, P.Q. Tranchida, V. Stanek, P. Jandera, G. Dugo, P. Dugo, J. Chromatogr. A 1086 (2005) 91.
[38] E.J.C. van der Klift, G. Vivó-Truyols, F.W. Claassen, F.L. van Holthoon, T.A. van Beek, J. Chromatogr. A 1178 (2008) 43.
[39] P. Dugo, O. Favoino, P.Q. Tranchida, G. Dugo, L. Mondello, J. Chromatogr. A 1041 (2004) 135.
[40] I. Francois, A.D. Pereira, P. Sandra, J. Sep. Sci. 33 (2010) 1504.
[41] S. Hamilton, R.J. Hamilton, P.A. Sewell, in: R.J. Hamilton, S. Hamilton (Eds.), Lipid Analysis: A Practical Approach, Oxford University Press, Oxford, NY, IRL, 1992.
[42] H.R. Mottram, R.P. Evershed, Tetrahedron Lett. 37 (1996) 8593.
[43] M. Lísa, M. Holčapek, M. Boháč, J. Agric. Food Chem. 57 (2009) 6888.

Available online at www.sciencedirect.com
ScienceDirect
Journal of Chromatography A, 1146 (2007) 67–77
JOURNAL OF CHROMATOGRAPHY A
www.elsevier.com/locate/chroma

High-performance liquid chromatography–atmospheric pressure chemical ionization mass spectrometry and gas chromatography–flame ionization detection characterization of Δ5-polyenoic fatty acids in triacylglycerols from conifer seed oils

Miroslav Lísa [a], Michal Holčapek [a,*], Tomáš Řezanka [b], Naděžda Kabátová [c]

[a] *Department of Analytical Chemistry, Faculty of Chemical Technology, University of Pardubice, Nám. Čs. Legií 565, 53210 Pardubice, Czech Republic*
[b] *Institute of Microbiology, Vídeňská 1083, 14220 Prague, Czech Republic*
[c] *Central Institute for Supervising and Testing in Agriculture, Hroznová 2, 656 06 Brno, Czech Republic*

Received 4 September 2006; received in revised form 23 January 2007; accepted 25 January 2007
Available online 6 February 2007

Abstract

Edible conifer seeds can serve as a source of triacylglycerols (TGs) with unusual Δ5 unsaturated polymethylene interrupted fatty acids (UPIFAs), such as *cis*-5,9-octadecadienoic (taxoleic), *cis*-5,9,12-octadecatrienoic (pinolenic), *cis*-5,11-eicosadienoic (keteleeronic) and *cis*-5,11,14-eicosatrienoic acids (sciadonic). Conifer seed oils from European Larch (*Larix decidua*), Norway Spruce (*Picea abies*) and European Silver Fir (*Abies alba*) have been analyzed by non-aqueous reversed-phase high-performance liquid chromatography (NARP-HPLC) with atmospheric pressure chemical ionisation (APCI)-MS detection. The influence of different positions of double bonds in Δ5-UPIFAs on the retention and fragmentation behavior is described and used for the successful identification of TGs in each oil. TGs containing Δ5-UPIFAs have a higher retention in comparison with common TGs found in plant oils with single methylene interrupted Δ6(9)-FAs and also significantly changed relative abundances of fragment ions in APCI mass spectra. Results obtained from HPLC/MS analyses are supported by validated GC/FID analyses of fatty acid methyl esters after the transesterification. The total content of Δ5-UPIFAs is about 32% for European Larch, 27% for Norway Spruce and 20% for European Silver Fir. In total, 20 FAs with acyl chain lengths from 16 to 24 carbon atoms and from 0 to 3 double bonds have been identified in 64 triacylglycerols from 3 conifer seed oils.

Keywords: Conifer seed oil; Triacylglycerol; Triglyceride; Delta 5-Olefinic; Polyenoic fatty acid; HPLC/MS

1. Introduction

Triacylglycerols (TGs) are natural compounds consisting of saturated and unsaturated fatty acids (FAs) differing in their acyl chain lengths, in the number and positions of double bonds (DBs), in the *cis*/*trans* configuration of DBs, in positional isomerism and *R*/*S* optical isomerism of TGs containing three different FAs. The standard notation of TGs is based on the initials of FA trivial names (see Table 1), arranged in the order of their stereochemical positions on the glycerol skeleton. In addition to saturated and monounsaturated FAs, common plant oils contain polyunsaturated FAs most frequently with 18 carbon atoms and single methylene interrupted DBs [1–5], i.e. *cis*-9,12-octadecadienoic (linoleic acid) and *cis*-9,12,15-octadecatrienoic (linolenic acid). TGs with unusual FAs, such as those containing conjugated DBs (e.g. conjugated linolenic acids) [6] or unsaturated polymethylene interrupted fatty acids (UPIFAs) [7–14], can be found in some taxonomical groups.

Gymnosperms (*Gymnospermae*) includes trees and shrubs and they are commonly known as conifers. This large taxonomical group is known for the presence of unusual FAs with the first site of unsaturation at the fifth carbon atom (Δ5-UPIFAs) and *cis* (Z) configuration, such as *cis*-5,9-octadecadienoic (taxoleic), *cis*-5,9,12-octadecatrienoic (pinolenic),

* Corresponding author. Tel.: +420 46 603 7087; fax: +420 46 603 7068.
E-mail address: michal.holcapek@upce.cz (M. Holčapek).

0021-9673/$ – see front matter © 2007 Elsevier B.V. All rights reserved.
doi:10.1016/j.chroma.2007.01.122

Table 1
Systematic and trivial names of fatty acids found in triacylglycerols of studied conifer seed oils listed with their abbreviations, carbon numbers (CN), double bond (DB) numbers and equivalent carbon numbers (ECN)

Systematic name	Trivial name	Abbreviation	CN:DB	ECN
Hexadecanoic	Palmitic	P	C16:0	16
cis-9-Hexadecenoic	Palmitoleic	Po	C16:1	14
Heptadecanoic	Margaric	Ma	C17:0	17
Octadecanoic	Stearic	S	C18:0	18
cis-9-Octadecenoic	Oleic	O	C18:1	16
cis-11-Octadecenoic	Vaccenic	Va[a]	C18:1	16
cis-9,12-Octadecadienoic	Linoleic	L	C18:2	14
cis-5,9-Octadecadienoic	Taxoleic	Ta[a]	C18:2	14
cis-9,12,15-Octadecatrienoic	Linolenic	Ln	C18:3	12
cis-5,9,12-Octadecatrienoic	Pinolenic	Pi[a]	C18:3	12
Nonadecanoic	–	–	C19:0	19
Eicosanoic	Arachidic	A	C20:0	20
cis-9-Eicosenoic	Gadoleic	G	C20:1	18
cis-11,14-Eicosadienoic	–	–	C20:2	16
cis-5,11-Eicosadienoic	Keteleeronic	Ke[a]	C20:2	16
cis-8,11,14-Eicosatrienoic	–	–	C20:3	14
cis-5,11,14-Eicosatrienoic	Sciadonic	Sc[a]	C20:3	14
Docosanoic	Behenic	B	C22:0	22
Tricosanoic	–	–	C23:0	23
Tetracosanoic	Lignoceric	Lg	C24:0	24

[a] Suggested abbreviations used in this work.

cis-5,11-octadecadienoic (ephedrenic), *cis*-5,11-eicosadienoic (keteleeronic), *cis*-5,11,14-eicosatrienoic (sciadonic), *cis*-5,9,12,15-eicosatetraenoic (coniferonic) and *cis*-5,11,14,17-eicosatetraenoic (juniperonic) acids. Sciadonic acid has been identified in *Podocarpus nagi* seed oil as early as in 1962 [15]. The presence of the following Δ5-UPIFAs has been reported in Gymnosperm plants: keteleeronic and sciadonic acids in *Ginkgo biloba* [16,17], pinolenic acid in *Larix leptolepsis* [18] and *Pinus koraienesis* [19], taxoleic and sciadonic acids in *Taxus baccata* [20], sciadonic acid in *Toreya nucifera* [19,21], ephedrenic, keteleeronic, sciadonic and juniperonic acids in *Ephedra campylopoda* [22], ephedrenic and sciadonic acids in *Ginkgo biloba* [23], pinolenic acid in *Picea abies* [24], taxoleic, pinolenic, coniferonic, sciadonic and juniperonic acids in many species of conifers [25].

In contrast to several papers dealing with methyl esters of Δ5-UPIFAs (e.g. reviews [7,8,11]), much less attention has been paid to intact TGs that contain those Δ5-UPIFAs. ^{13}C nuclear magnetic resonance (NMR) spectroscopy of oils from three *Taxus* and one *Torreya* species has confirmed that Δ5-olefinic acids are apparently excluded from the *sn*-2 position which is characteristic for all *Gymnosperm* species analyzed so far [12]. ^{13}C NMR spectroscopy of the seed oil from two *Ephedra* species shows that Δ5-UPIFAs are excluded from the *sn*-2 position, a characteristic common to all analyzed *Conipherophytes* species (more than 30 species), with the possibility of an exclusive esterification at the *sn*-3 position [13]. The chemical degradation of conifer seed oils followed by gas chromatographic analysis of dibutyroyl derivatives of monoacylglycerols reveals that seed oils of 18 species from 5 conifer families contain Δ5-olefinic acids esterified mainly at primary positions (i.e. *sn*-1 and *sn*-3) of the glycerol backbone, whereas less than 8% of Δ5-olefinic acids are esterified in the secondary position (i.e. *sn*-2) [14].

Non-aqueous reversed-phase high-performance liquid chromatography (NARP-HPLC) has been widely used for the separation of complex natural lipid samples [1–5,26–41]. The retention in NARP-HPLC increases with increasing equivalent carbon number (ECN) defined as the total carbon number (CN) in all acyl chains minus two times the number of DBs, i.e. ECN = CN − 2DB. Under optimized separation conditions, the separation of most TGs within the same ECN group is also possible, for example the critical pair LLL/OLLn or the group of OOO, OOP, OPP and PPP can be well resolved [1,2,4,5,26,27]. The separation of TGs differing in the positions of DBs is also feasible [28]. On the other hand, NARP-HPLC is not suitable for the separation of three types of isomerism, i.e. regioisomers, *R*/*S* isomers and *cis*/*trans* isomers. Various mobile phase systems, mostly in gradient elution mode, are described in the literature, such as 2-propanol/acetonitrile [1–3,27,29], 2-propanol/acetonitrile/hexane [30,31], acetone/acetonitrile [26,31-34], 100% propionitrile [4], acetonitrile/chloroform [5], acetonitrile/dichloromethane [35–41], etc.

The coupling of HPLC and mass spectrometry (MS) is a powerful tool in lipid analysis, because it provides both structural information and usually also the highest sensitivity among all available chromatographic detectors [30]. Atmospheric pressure chemical ionization (APCI) is the most frequently used ionization technique for TG analysis because of easy coupling to non-aqueous mobile phase systems and high ionization efficiency for non-polar species. The presence of both protonated molecules $[M+H]^+$ and fragment ions $[M+H-R_iCOOH]^+$ is important for structure elucidation [1–5,26–42]. Electrospray ionization (ESI) mass spectra exhibit $[M+Na]^+$ and $[M+K]^+$ adduct ions instead of protonated molecules and also some fragment ions, such as $[M+Na-R_iCOOH]^+$ and $[M+Na-R_iCOONa]^+$, but with lower relative abundances

[1,42]. If ammonium ion is added to the eluent, then the formation of $[M + NH_4]^+$ adduct ions is preferred, which simplifies the subsequent fragmentation in comparison to alkali metal adducts [40,41]. Coupling with silver-ion HPLC may require the use of post-column make-up flow of polar solvent both for ESI and APCI, because typical mobile phases contain more than 98% of hexane [34] or other non-polar solvent, which is not favorable for the ionization process. APCI mass spectra provide information on the predominant FA in the *sn*-2 position [1–5,29–33]. The precise ratio of regioisomers can also be obtained by the measurement of calibration curves with both positional isomers [5,33].

The main goal of our work is the identification of TGs from three representative conifer seed oils containing Δ5-UPIFAs isolated in our laboratory—European Larch (*Larix decidua*), Norway Spruce (*Picea abies*) and European Silver Fir (*Abies alba*). First, the retention behavior of TGs with unusual Δ5-UPIFAs in NARP-HPLC and the fragmentation behavior in positive-ion APCI mass spectra are described and used for the positive identification of TGs in each oil. Then, the pine seed oils are transesterified using a standard procedure with sodium methoxide and analyzed by a validated gas chromatography—flame ionization detection (GC/FID) method for the analysis of FAMEs and concentrations of individual FAs and also average parameters are calculated and used for the characterization of individual oils.

2. Experimental

2.1. Materials

Acetonitrile, 2-propanol, hexane and standards of 1,2,3-tri-(*cis*-9,12-octadecadienoyl)glycerol (trilinolein) and 1,2,3-tri-(*cis*-9,12,15-octadecatrienoyl)glycerol (trilinolenin) were purchased from Sigma-Aldrich (St. Louis, USA). The solvents were filtered through a 0.45 μm Millipore filter and degassed by continuous stripping with helium. The standards of *cis*-5,9-octadecadienoic (taxoleic) methyl ester, *cis*-5,9,12-octadecatrienoic (pinolenic) methyl ester and FAMEs standard mixture Me100 (C4:0, C6:0, C8:0, C10:0, C11:0, C12:0, C13:0, C14:0, C14:1, C15:0, C15:1, C16:0, C16:1, C17:0. C17:1, C18:0, C18:1, C18:1T, C18:2, C18:2T, C18:3, C18:3γ, C20:0, C20:1, C20:2, C20:3, C20:3γ, C20:4, C20:5, C21:0, C22:0, C22:1, C22:2, C22:6, C23:0, C24:0 and C24:1) were purchased from Larodan Fine Chemicals (Mälmo, Sweden).

2.2. HPLC conditions

The chromatographic apparatus consisted of a Model 616 pump with a quaternary gradient system, a Model 996 diode-array UV detector, a Model 717 + autosampler, a thermostated column compartment and a Millennium chromatography manager (all from Waters, Milford, MA, USA). The HPLC conditions: two chromatographic columns Nova-Pak C_{18} (300 mm × 3.9 mm and 150 mm × 3.9 mm, 4 μm, Waters) connected in series, a flow rate of 1 mL/min, an injection volume of 10 μL, a column temperature of 25 °C and a mobile phase gradient with a slope of 0.65%/min: 0 min—100% acetonitrile, 106 min—31% acetonitrile—69% 2-propanol, 109 min—100% acetonitrile. The injector needle was washed with the mobile phase before each injection. The column hold-up volume, t_M, was 3.20 min for the system with 300 + 150 mm Nova-Pak C_{18} columns. The UV detection at 205 nm and positive-ion APCI-MS were coupled in series. The Esquire 3000 ion trap analyzer (Bruker Daltonics, Bremen, Germany) in the mass range *m*/*z* 50–1200 was used with the following setting of tuning parameters: the pressure of the nebulizing gas of 70 psi, the drying gas flow rate of 3 L/min, temperatures of the drying gas and APCI heater were 350 and 400, respectively. The isolation width *m*/*z* = 2 and the collision amplitude 0.8 V were used for HPLC/MS/MS experiments. The reconstructed ion current (RIC) chromatograms in the region *m*/*z* 300–1200 were used for the peak integration. Presented peak areas correspond to averaged values from three consecutive chromatographic runs. Individual reconstructed ion current chromatograms were used to support the identification and apportionment of coeluting peaks.

2.3. Sample preparation

The conifer seeds from European Larch (*Larix decidua*), Norway Spruce (*Picea abies*) and European Silver Fir (*Abies alba*) were collected in early summer 2005 in the Bohemian Forest. Ten to fifteen grams of seeds were weighed and then carefully crushed in a mortar to fine particles, which were mixed with 15 mL of hexane, and the mixture was stirred occasionally for 15 min. The solid particles were filtered out using a rough filter paper and then the extract was filtered again using a fine filter with 0.45 μm pores. From the filtered extract, hexane was evaporated at room temperature yielding a pure plant oil. The oil samples were dissolved in an acetonitrile–2-propanol–hexane mixture (2:2:1, v/v/v) to prepare 3% solution (w/v), 10 μl of this solution was injected for HPLC analysis.

2.4. Preparation of fatty acid methyl esters and their GC/FID analysis

Fatty acid methyl esters (FAMEs) were prepared from TGs in conifer seed oils using a standard procedure with sodium methoxide [43]. FAME mixtures were analyzed by GC/FID on a Varian CP 3800 with an autosampler CP-8410 and an injector CP-1177 (Varian Analytical Instruments, Walnut Creek, CA, USA) using silica capillary column BTR-Carbowax-30 W-0.5 F, 30 m length, 0.32 mm I.D., 0.5 μm film thickness (Quadrex, Woodbridge, CT, USA). GC conditions were as follows: the injection volume was 1 μL, the split ratio was 1:40, the flow rate of nitrogen as a carrier gas was 0.7 ml/min, the temperature program was as follows: the initial temperature was 160 °C, held for 6 min, then a ramp to 200 °C at 20 °C/min, held for 10 min, ramp to 240 °C at 5 °C/min, held for 28 min with the total analysis time of 54 min. Injector and detector temperatures were 250 and 270 °C, respectively.

3. Results and discussion

3.1. Nomenclature for TGs containing common FAs and unusual Δ5-UPIFAs

Table 1 summarizes all FAs identified in individual TGs in conifer seed oils together with their trivial names, abbreviations, carbon numbers (CN), double bond (DB) numbers and equivalent carbon numbers (ECN). Table 2 lists ECNs, nominal molecular weights (MWs), retention times t_R, relative retention r and retention factors k measured using the HPLC method with 45 cm total column length for 64 TGs identified in three conifer seed oils consisting of 20 FAs. The masses and structures of fragment ions have been described in our previous works [1,2,27]. Plant oils usually contain a mixture of regioisomers. Three identical acyl chains on the glycerol backbone (single-acid $R_1R_1R_1$ type) provide only a single ion $[M+H-R_1COOH]^+$, while mixed-acid $R_1R_1R_2$ type produces two different $[M+H-R_1COOH]^+$ and $[M+H-R_2COOH]^+$ ions with the statistical abundance ratio 2:1, and the $R_1R_2R_3$ type has three different $[M+H-R_1COOH]^+$, $[M+H-R_2COOH]^+$ and $[M+H-R_3COOH]^+$ ions with the statistical abundance ratio 1:1:1. The neutral losses of R_iCOOH from the primary positions *sn*-1 and *sn*-3 are preferred, compared to the cleavage from the secondary *sn*-2 position. This characteristic can be used for the determination of the predominant FA in the *sn*-2 position for plant oils containing common unsaturated FAs [1–5,33]. This approach works well for polyenoic FAs with common DB positions, but for unusual DB positions (e.g. Δ5-UPIFAs) the regioisomeric standards are needed for reliable identification of sn-2 FA or even the quantitation of the ratio of individual FAs in sn-2 position. The presence of Δ5-UPIFAs changes the observed ratio of $[M+H-R_iCOOH]^+$ ions. In this work, the determination of *sn*-2 FAs on the basis on well established rules [1,33,25,42] is done for TGs consisting of common FAs. However, the assignment of FA prevailing in individual stereochemical positions for TGs containing Δ5-UPIFAs is based only on previous literature evidence [9,10] that Δ5-UPIFAs preferentially occupy the *sn*-3 position, but the analytical data supporting this assignment are not available because of the total absence of mixed-acid TG standards with Δ5-UPIFAs.

The positions *sn*-1 and *sn*-3 are considered as equivalent, because these regioisomers cannot be distinguished by NARP-HPLC or mass spectrometry, so acids in primary *sn*-1 and *sn*-3 positions are ordered only by decreasing mass, i.e. SLO but not OLS. An exception is Δ5-UPIFAs assigned preferentially to *sn*-3 position based on earlier data [9,10,12–14]. The term "common FAs" is used throughout this work for FAs with even number of carbon atoms and sites of unsaturation at positions 9, 12 and 15 (e.g. oleic acid C18:1Δ9, linoleic acid C18:2Δ9,12 or linolenic acid C18:3Δ9,12,15) or saturated FAs.

3.2. Chromatographic behavior of TGs containing Δ5-UPIFAs

It is well known that the retention of TGs in NARP systems depends on the acyl chain lengths and the number of double

Table 2
Triacylglycerols (TG) identified in studied conifer seed oils listed with their equivalent carbon numbers (ECN), molecular weights (MW), retention times (t_R), relative retention r, retention factors (k) and differences in retention factors (Δk)

TG	ECN	MW[a]	t_R	r[b]	k[c]	Δk[d]
LnLnLn[e]	36	872	48.3	0.800	14.09	0
PiLnPi		872	51.1	0.849	14.97	0.88
PiPiPi		872	52.4	0.872	15.38	1.29
LnLLn[e]	38	874	54.0	0.901	15.88	0
LnLPi		874	55.4	0.926	16.31	0.43
PiLPi		874	56.8	0.950	16.75	0.87
LLLn	40	**876**	**59.6**	**1.000**	17.63	0
LnOLn[e]		876	60.6	1.018	17.94	0
LLPi		876	61.0	1.025	18.06	0.43
C20:3LPi		902	61.6	1.035	18.25	–
C20:3LnTa		902	62.1	1.044	18.41	–
LnLnP[e]		851	62.1	1.044	18.41	0
TaLPi		876	63.1	1.062	18.72	1.09
PiOPi		876	63.5	1.069	18.84	0.90
PPiPi		850	64.9	1.094	19.28	0.87
LLL	42	**878**	**65.3**	**1.000**	19.41	0
C20:2LLn[e]		904	65.4	1.002	19.44	0
OLLn		878	66.4	1.018	19.75	0
C20:3LL		904	66.2	1.014	19.69	–
C20:2LPi		904	66.7	1.023	19.84	0.40
LLTa		878	67.1	1.029	19.97	0.56
LOPi		878	67.6	1.037	20.13	0.38
PLLn[e]		852	67.8	1.040	20.19	0
SLnLn[e]		878	68.5	1.052	20.41	0
PLPi		852	69.0	1.019	20.56	0.37
TaOPi		852	69.5	1.068	20.72	0.97
PTaPi		852	70.9	1.090	21.16	0.97
SPiPi		878	71.2	1.095	21.25	0.84
LnLMa	43	866	70.7	1.087	21.09	0
C20:2LL	44	906	70.8	0.985	21.13	0
OLL		**880**	**71.8**	**1.000**	21.44	0
GLLn[e]		906	72.1	1.004	21.53	0
C20:3LO		906	72.5	1.010	21.66	–
OOLn[e]		880	72.6	1.012	21.69	0
LLP		854	73.1	1.019	21.84	0
GLPi		906	73.3	1.022	21.91	0.38
OLTa		880	73.5	1.025	21.97	0.53
SLLn[e]		880	73.8	1.029	22.06	0
OOPi		880	73.9	1.031	22.09	0.40
LnOP[e]		854	74.0	1.032	22.13	0
PLTa		854	74.9	1.045	22.41	0.57
SLPi		880	75.1	1.048	22.47	0.41
POPi		854	75.4	1.052	22.56	0.43
C19:0LPi	45	894	76.7	1.071	22.97	–
C20:2LO	46	908	77.0	0.988	23.06	–
GLL		908	77.2	0.991	23.13	0
OLO		**882**	**77.9**	**1.000**	23.34	0
C20:3OO		908	78.6	1.009	23.56	–
SLL		882	79.0	1.015	23.69	0
OLP		856	79.3	1.019	23.78	0
OOTa		882	79.7	1.024	23.91	0.57
SOLn[e]		882	80.0	1.028	24.00	0
BLnLn[e]		934	80.1	1.029	24.03	0
SOPi		882	81.3	1.046	24.41	0.41
BPiPi		934	82.7	1.064	24.84	0.81
C19:0OPi	47	896	82.7	1.064	24.84	–
GLO	48	910	83.1	0.989	24.97	0
OOO		**884**	**84.0**	**1.000**	25.25	0
ALL		910	84.8	1.010	25.50	0
SLO		884	85.1	1.014	25.59	0
BLLn[e]		936	85.1	1.014	25.59	0

Table 2 (*Continued*)

TG	ECN	MW[a]	t_R	r[b]	k[c]	Δk[d]
OOP		858	85.4	1.017	25.69	0
BLPi		936	86.3	1.028	25.97	0.38
AOPi		910	86.8	1.035	26.13	–
POP		832	87.0	1.037	26.19	0
PPP		806	88.7	1.058	26.72	0
C23:0LLn[e]	49	950	87.8	1.047	26.44	0
C23:0LPi		950	88.9	1.061	26.78	0.34
GOO	50	912	89.0	0.979	26.81	0
BLL		938	90.0	0.991	27.13	0
LgLLn[e]		964	90.2	0.993	27.19	0
ALO		912	90.4	0.995	27.25	0
SOO		**886**	**90.8**	**1.000**	27.38	0
LgLPi		964	91.5	1.008	27.59	0.40
SOP		860	92.3	1.017	27.84	0
LgLL	52	966	94.9	0.988	28.66	0
BLO		940	95.5	0.995	28.84	0
AOO		**914**	**96.0**	**1.000**	29.00	0
LgLO	54	968	100.5	1.048	30.41	0
BOO		942	101.0	1.054	30.56	0

[a] For simplicity, nominal masses are listed in this table and throughout the text.

[b] Relative retention $r = (t_R - t_M)/(t_S - t_M)$, where t_M is 3.20 min and t_S are retention times of standards for particular ECN groups (printed in bold), i.e. LLLn for ECN = 41 and lower, LLL for ECN = 42 and 43, OLL for ECN = 44 and 45, OLO for ECN = 46 and 47, OOO for ECN = 48 and 49, SOO for ECN = 50 and 51, AOO for 52 and higher.

[c] Retention factor $k = (t_R - t_M)/t_M$, where t_M is 3.20 min.

[d] Differences between retention factors (Δk) for TGs containing FAs with common DB positions (e.g. Δ-9,12,15) and unusual DB position in Δ5. Value "0" means that this TG has only FAs with common DB positions.

[e] TGs from different plant oils [2,44] not identified in conifer seed oils, but listed here because of the calculation of Δk.

bonds according to the equation ECN = CN − 2DB, but this equation does not reflect the fact that optimized separation systems also enable quite good resolution within particular ECN groups. The retention order of TGs consisting of common FAs within one ECN group is also known [1,2,27,37], in contrast to unusual TGs containing Δ5-UPIFAs measured in this work. Fig. 1 illustrates the chromatograms of analyzed conifer seed oils with APCI-MS detection. The average differences in retention factors Δk for the presence of Δ5-UPIFAs are the following: $\Delta k = 0.40$ for one, $\Delta k = 0.86$ for two and $\Delta k = 1.29$ for three pinolenic acids and $\Delta k = 0.56$ for one taxoleic acid (all data are shown in Table 2). For the presence of both pinolenic and taxoleic acids in one TG species, the observed shift $\Delta k = 0.97$ for TaOPi and PTaPi fits well with the sum of contributions for Pi and Ta, $\Delta k = 0.40 + 0.56 = 0.96$. Retention differences are used for the identification of these TGs together with the determination of MWs based on $[M+H]^+$ ions and the characteristic ratios of diagnostic ions, as discussed later in more detail. It is likely that relative retention is similar in other NARP chromatographic systems and hence it may be used for the identification of Δ5-UPIFAs by analogy. To support the hypothesis that the composition of mobile phases in different NARP systems using C18 column packing has a negligible effect on the retention order, we have compared the retention order of TGs in several tens of publications published by different research groups (all references in this and our previous publications) and we have not found even a single case where the retention order is changed regardless of the NARP solvent system. Of course, the resolution and the number of coelutions depend strongly on the separation system, but the order of TG peaks is never changed. This may be explained by the fact that TG molecules do not contain any polar or ionizable functional groups and therefore changed chromatographic conditions have comparable effects on all TGs, because the only functionalities are triester groups and double bonds for unsaturated acyl chains. This information is very useful for transferring relative retention characteristics among different NARP systems applicable for the identification of unknown TGs. It has initiated our effort to collect relative retention data for an extensive range of TGs consisting of common, unusual and also very rare FAs [44].

Table 3 shows average relative peak areas from three consecutive runs for 64 identified TGs in pine seed oils. It should be emphasized that these values are calculated without the use of response factors (unlike our previous work [2]), because the standards of Δ5-UPIFAs are not available, therefore these values are only semi-quantitative. Unfortunately, the extrapolation of response factors for TGs with common positions of DBs (e.g. LLL and LnLnLn) is impossible due to the unknown response differences between common FAs and Δ5-UPIFAs. Peak areas are integrated in the reconstructed ion current chromatograms in the range 300–1200 m/z, but for strongly overlapping peaks (e.g. PLTa, SLPi and POPi in Fig. 1A), the RIC chromatograms of individual $[M+H]^+$, $[M+H-R_iCOOH]^+$ and $[R_iCO]^+$ ions are used to distinguish contributions of particular TGs to such unresolved chromatographic peaks. Peak areas calculated this way are reproducible among different runs and the same way of data processing enables the direct comparison of results with our other works [2,44].

GC/FID data (Table 4) show the presence of other Δ5-UPIFAs (keteleeronic and sciadonic), but these acids are not identified in any TG, because the trace relative concentrations of these acids are distributed among different TGs and therefore the HPLC/MS technique cannot detect such trace FAs in TG combinations. Moreover, potential coelutions with dominant TGs may complicate their identification. The comparison of our data with previous work [8] shows a very good correlation.

3.3. APCI mass spectra of TGs containing Δ5-UPIFAs

The APCI ionization and fragmentation behavior of TGs with common positions of DBs is well known from numerous publications (e.g. [1,2] and citations therein). Briefly, the protonated molecule $[M+H]^+$ is the base peak for TGs with many DBs, while the fragment ion $[M+H-R_iCOOH]^+$ is the base peak for more saturated TGs. Relative abundances of $[M+H-R_iCOOH]^+$ ions can be used for the determination of the prevailing FA in the *sn*-2 position, because the neutral loss from this position is energetically disfavored, hence the corresponding fragment ion $[M+H-R_2COOH]^+$ has a decreased relative abundance in comparison to the statistically expected value (Table 5). For TGs containing only common FAs, this rule can be roughly applied even without regioisomeric standards which are rather expensive or often unavailable. Some

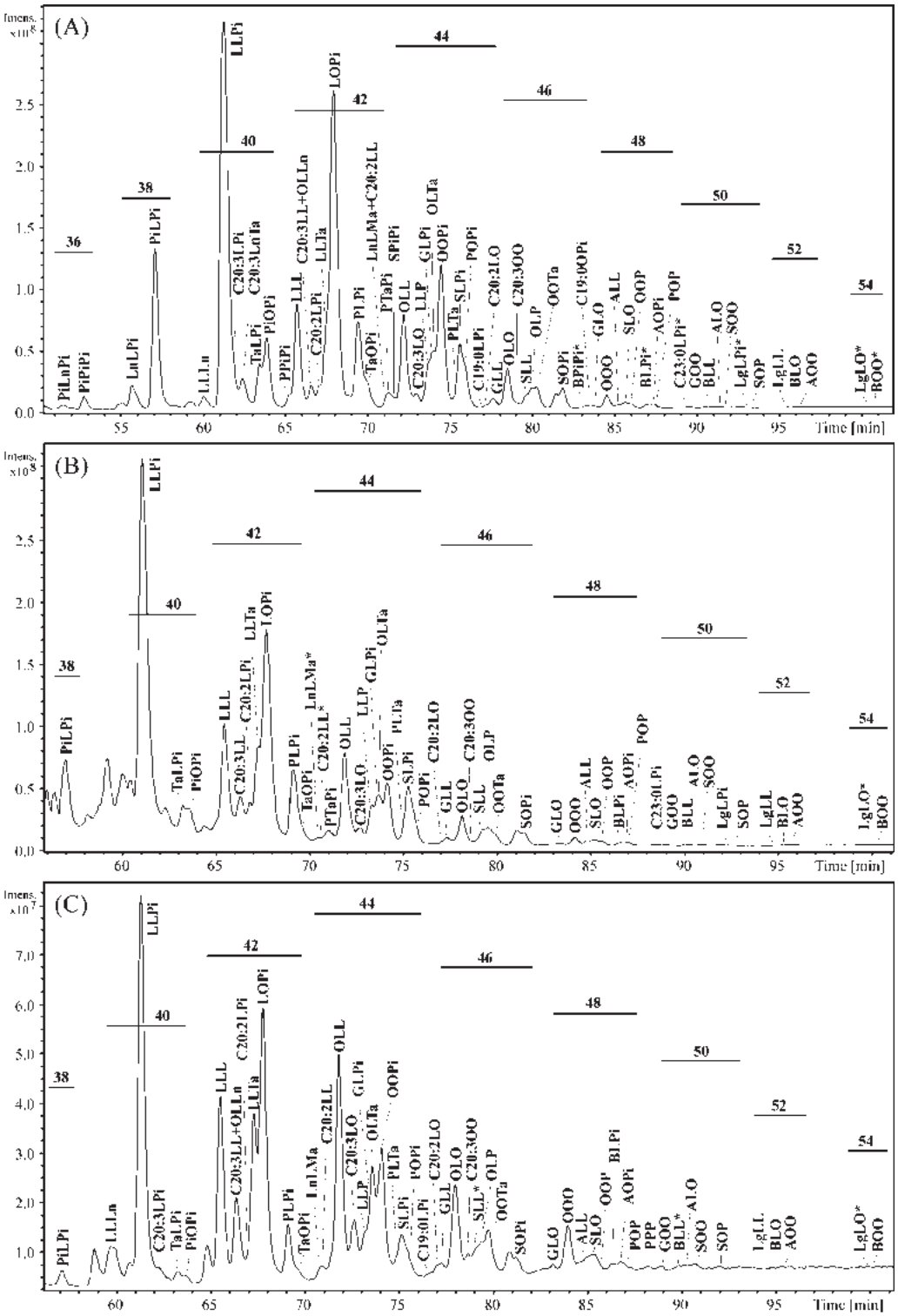

Fig. 1. Chromatographic separation of conifer seed oils: (A) European Larch (*Larix decidua*), (B) Norway Spruce (*Picea abies*), (C) European Silver Fir (*Abies alba*). Experimental conditions: 30 + 15 cm Nova-Pak C_{18} columns connected in series, APCI-MS detection, flow rate 1 mL/min, column temperature 25 °C, injection volume 10 μl, the mobile phase gradient 0 min—100% acetonitrile, 106 min—31% acetonitrile—69% 2-propanol, 109 min—100% acetonitrile. Numbers correspond to ECNs.

differences may be found for different instruments [2,5,33,42] and different ionization techniques [2]. Unfortunately, this rule can fail for TGs containing unusual TGs, for example Δ5-UPIFAs. Figs. 2 and 3 highlight the differences between standards of common TGs (LLL in Figs. 2A and 3A, LnLnLn in Figs. 2B and 3B) and their isomers with the shifted position of DB from Δ6 to Δ5 identified in European Larch (LLTa in Figs. 2C and 3C, PiPiPi in Figs. 2D and 3D) both in

Table 3
Average relative peak areas from three consecutive runs in percent for 64 triacylglycerols (TG) identified in studied conifer seed oils using HPLC/APCI-MS

TG	European Larch (*Larix deciduas*)	Norway Spruce (*Picea abies*)	European Silver Fir (*Abies alba*)
PiLnPi	0.2	–	–
PiPiPi	0.5	–	–
LnLPi	1.3	–	–
PiLPi	6.6	4.2	0.7
LLLn	0.6	–	1.2
LLPi	22.8	29.5	19.3
C20:3LPi	0.8	–	0.7
C20:3LnTa	1.3	–	–
TaLPi	1.6	0.6	0.6
PiOPi	3.4	0.9	0.3
PPiPi	0.4	–	–
LLL	5.1	7.3	0.9
OLLn	1.0	–	4.2
+C20:3LL[a]		2.5	
C20:2LPi	0.7	1.4	0.4
LLTa	2.8	4.1	6.6
LOPi	16.9	16.6	14.0
PLPi	4.3	4.0	2.5
TaOPi	1.3	0.7	0.5
PTaPi	0.7	0.8	–
+LnLMa	0.7		
+C20:2LL[a]			
SPiPi	0.3	–	–
OLL	4.7	5.9	11.0
C20:3LO	0.6	0.8	2.8
LLP	0.6	1.7	1.5
GLPi	1.1	1.6	1.6
OLTa	1.4	1.3	3.3
OOPi	7.4	3.9	6.5
PLTa	0.6	0.4	0.5
SLPi	2.0	3.0	1.7
POPi	1.6	1.2	1.0
C19:0LPi	0.1	–	0.1
C20:2LO	0.1	<0.1	0.3
GLL	0.5	0.4	0.4
OLO	1.9	1.8	4.9
C20:3OO	0.2	0.1	0.7
SLL	0.4	0.8	1.0
OLP	0.7	0.9	1.0
OOTa	0.9	0.6	2.5
SOPi	0.9	0.8	0.6
BPiPi	0.1	–	–
+C19:0OPi[a]		–	–
GLO	0.1	0.1	0.3
OOO	0.6	0.5	2.4
ALL	0.1	0.2	0.3
SLO	0.2	0.3	0.5
OOP	0.2	0.2	0.8
BLPi	0.1	0.2	0.3
AOPi	0.2	0.2	0.4
+POP[a]			
PPP	–	–	<0.1
C23:0LPi	<0.1	<0.1	–
+GOO[a]		0.1	
BLL	<0.1	0.1	0.1
ALO	<0.1	0.1	0.2
SOO	0.1	0.1	0.3
LgLPi	<0.1	<0.1	–
SOP	<0.1	<0.1	<0.1
LgLL	<0.1	<0.1	<0.1
BLO	<0.1	<0.1	0.1
AOO	<0.1	<0.1	0.1
LgLO	<0.1	<0.1	<0.1
BOO	<0.1	<0.1	<0.1

Value "<0.1" means that the peak area is lower than 0.1%, but TG is still positively identified.
[a] Sum of coeluting peaks.

first-order (Fig. 2) and tandem (Fig. 3) mass spectra. The first-order mass spectra of unusual Δ5-UPIFAs show a significantly changed ratio of $[M+H]^+/[M+H-R_iCOOH]^+$ ions. This ratio is changed from 100/42% for LLL (Fig. 2A) to 74/100% for LLTa (Fig. 2C), and from 100/25% for LnLnLn (Fig. 2B) to 87/100% for PiPiPi (Fig. 2D). TGs containing unusual FAs also provide increased relative abundances of fragment ions $[B]^+$, $[B-H_2O]^+$, $[C]^+$ and $[C-H_2O]^+$, other examples are listed in Table 5. The differences observed in tandem mass spectra of $[M+H]^+$ ions are even more pronounced (Fig. 3), because the base peaks for common TGs (Figs. 3A and B) are $[B-H_2O]^+$ ions, but $[B]^+$ ions are base peaks for TGs containing Δ5-UPIFAs (Fig. 3C and D). The same difference of relative abundances is observed for $[C]^+/[C-H_2O]^+$ pair of fragment ions. Summarizing the information from the retention times, MW determination and fragmentation behavior in first-order and tandem mass spectra, Δ5 positional isomers can be unambiguously identified in unknown samples of natural TGs mixtures.

Fig. 4 depicts APCI mass spectra of $R_1R_2R_3$ type (LOPi) and $R_1R_1R_2$ type (LLPi) TGs containing one Δ5-UPIFA from the analysis of European Larch. In case of TGs containing only common FAs, the statistical ratio 1:1:1 for $R_1R_2R_3$ type and 2:1 for $R_1R_1R_2$ type would be shifted towards lower relative abundance of $[R_1R_3]^+$ ion, because the neutral loss from *sn*-2 position is energetically disfavored and therefore the fragment ion corresponding to the neutral loss from sn-2 position has a lower relative abundance than statistically expected. Thanks to the literature data [8,9] showing that Δ5-UPIFAs occupy almost exclusively *sn*-3 position, one may expect either OLPi or LOPi species. The relative ratio of $[LPi]^+/[OPi]^+/[OL]^+ = 9/11/100\%$ (Fig. 4A) indicates that both species are present at comparable relative abundances with small preference for LOPi. The precise ratio of LOPi/OLPi may be obtained only if both stereochemical standard are available. If the mixed spectrum of LOPi/OLPi is compared with the TG analogue with common DB positions (i.e. LOLn/OLLn) measured on the same instrument under identical conditions (Table 5), then observed relative abundances for $[OL]^+/[OLn]^+/[LLn]^+$ are in the ranges 60–100/84–100/43–100% in contrast to values for LOPi/OLPi mixtures—$[OL]^+/[OPi]^+/[LPi]^+ = 100/14$–$24/13$–$17\%$. The relative abundance of the fragment ion corresponding to the neutral loss of Δ5-UPIFA is significantly higher (approximately four times, see data in Table 5) compared to TGs containing only common FAs. Similar behavior is observed for all TGs containing pinolenic or taxoleic acid (Table 5).

3.4. Comparison of HPLC/APCI-MS and GC/FID results of conifer seed oils

To verify the validity of HPLC/MS results on TGs, conifer seed oils have been transesterified with sodium methoxide to obtain methyl esters of individual FAs, which are subsequently analyzed by a validated GC/FID method. Standards of the whole range of FAMEs are used to obtain response factors according to the previously described method [45]. Table 4 shows quantitative results on FAs relative contents determined in this work

Table 4
Relative concentrations of individual FAMEs in weight percent calculated from GC/FID according to Ref. [45]

Fatty acid	European Larch (*Larix deciduas*)		Norway Spruce (*Picea abies*)		European Silver Fir (*Abies alba*)
	Our results	Wolff et al. [8]	Our results	Wolff et al. [8]	
16:0	2.28	2.80	2.73	2.78	2.69
Δ9-16:1	0.06	0.43	0.10	0.20	<0.06
17:0	<0.06	–	<0.06	–	<0.06
18:0	1.26	1.46	1.76	1.49	1.71
Δ9-18:1	17.59	18.76	13.68	13.41	23.68
Δ11-18:1	0.81	0.97	1.08	1.55	0.13
Δ9,12-18:2	43.30	43.10	46.61	49.89	42.23
Δ5,9-18:2	2.73	2.20	3.42	3.25	5.09
Δ9,12,15-18:3	0.52	0.56	0.22	0.21	0.83
Δ5,9,12-18:3	28.45	27.39	22.81	24.67	12.61
19:0	0.08	–	<0.06	–	0.11
20:0	0.18	0.23	0.30	0.24	0.50
Δ9-20:1	0.39	0.40	0.37	0.31	0.50
Δ11,14-20:2	0.36	0.35	0.61	0.58	0.32
Δ5,1 1-20:2	0.16	0.14	0.08	0.05	0.36
Δ8,11,14-20:3	0.28	–	0.15	–	0.16
Δ5,11,14-20:3	0.58	0.51	0.82	0.94	1.91
22:0	0.07	0.10	0.12	0.19	0.71
23:0	<0.06	–	<0.06	–	0.06
24:0	<0.06	–	<0.06	–	<0.06
Others	0.83	0.60	5.03	0.24	6.40
Σ of Δ5-UPIFAs	31.92	30.24	27.13	28.91	19.97

Value "<0.06" means that this TG is positively identified in this sample, but the peak area is lower than 0.06%.

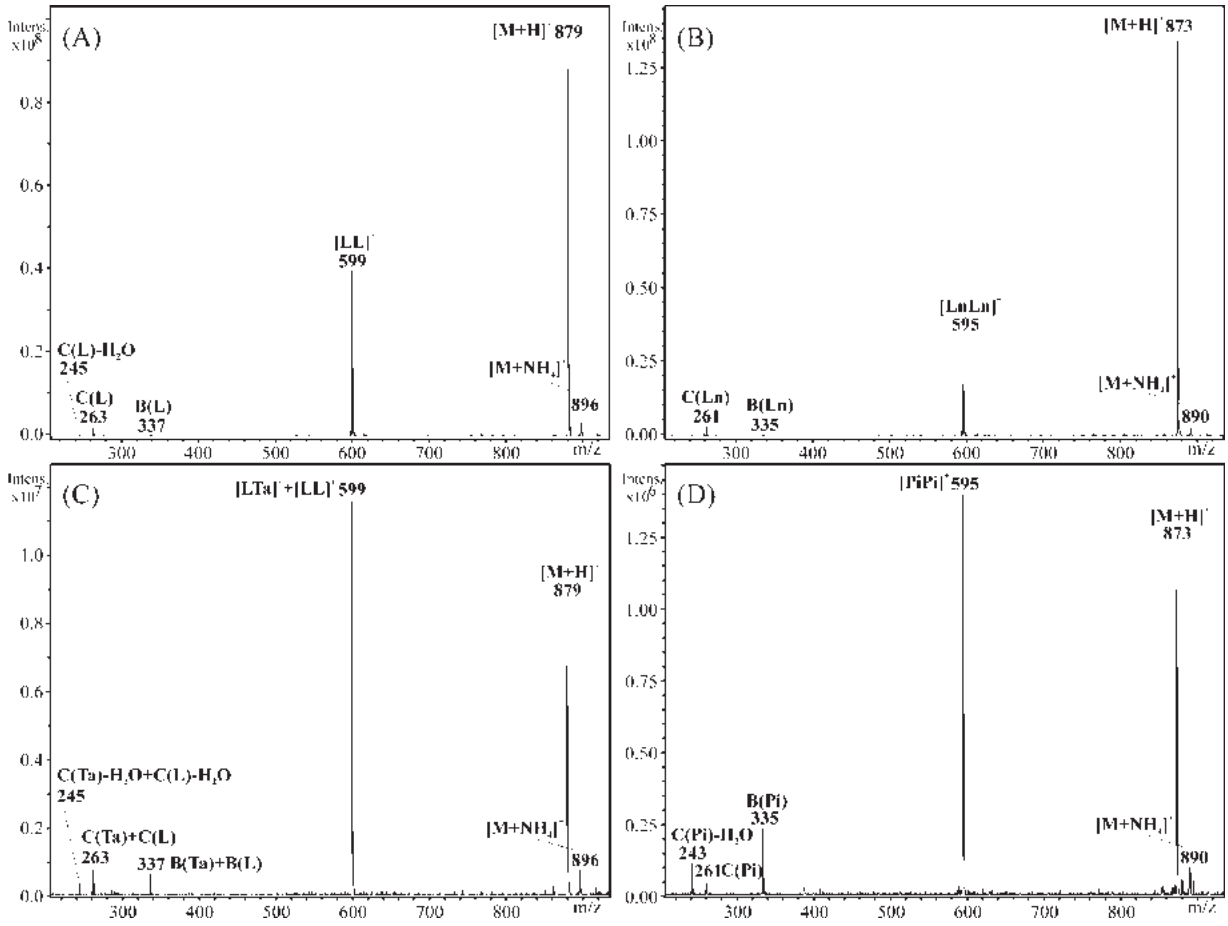

Fig. 2. Comparison of APCI first-order mass spectra of TG isomers with different double bond positions: (A) LLL standard, (B) LnLnLn standard, (C) LLTa from European Larch, and (D) PiPiPi from European Larch. Notation of ions is explained in the text and ref. [1].

Table 5
Comparison of relative ratios of fragment ions A ($[M+H-R_iCOOH]^+$) and $[M+H]^+$ ions for TGs containing only common polyunsaturated FAs (linolenic acid C18:3Δ-9,12,15 and linoleic acid C18:2Δ-9,12) vs. TGs containing unusual Δ5-UPI FAs (pinolenic acid C18:3Δ-5,9,12 and taxoleic acid C18:2Δ-5,9)

TGs	Relative ratios of fragment ions A (%)				Relative ratios of $[M+H]^+$ and most abundant fragment ion A (%)	
$R_1R_1R_2$[a]	R_1R_1	50	R_1R_2	100	$[M+H]^+$	Ion A
OOP[b]	OO	68	OP	100	9	100
OPO[b]	OO	21	OP	100	9	100
OPP[b]	PP	80	OP	100	6	100
POP[b]	PP	24	OP	100	2	100
LnLLn[c]	LnLn	42–50	LLn	100	100	13–32
PiLPi[d]	PiPi	9–13	LPi	100	90–93	100
LLLn[c]	LL	57–74	LLn	100	100	14–37
LLPi[d]	LL	100	LPi	26–33	100	68–83
OLnLn[c]	LnLn	40–56	OLn	100	100	17–47
PiOPi[d]	PiPi	9–11	OPi	100	63–83	100
OOLn[c]	OO	40–71	OLn	100	100	39–64
OOPi[d]	OO	100	OPi	21–32	36–45	100
OLO[c]	OO	47–75	OL	100	33–45	100
OOTa[d]	OO	100	OTa	35–40	10–12	100

$R_1R_2R_3$[a]	R_1R_2	100	R_1R_3	100	R_2R_3	100	$[M+H]^+$	Ion A
OLLn[c]	OL	60–100	OLn	84–100	LLn	43–100	100	12–30
OLPi[d]	OL	100	OPi	14–24	LPi	13–17	74–86	100
LnLP[c]	LP	71–95	LnP	52–76	LLn	100	100	14–30
PLPi[d]	LP	100	PiP	11–14	LPi	21–24	82–84	100
OLnP[c]	OP	62–100	LnP	46–72	OLn	95–100	100	28–69
POPi[d]	OP	100	PiP	8–11	OPi	22–23	20–29	100
SOLn[c]	SO	95–100	SLn	62–93	OLn	78–100	100	33–61
SOPi[d]	SO	100	SPi	14–27	OPi	14–19	19–23	100

[a] Theoretical (i.e. statistical) ratio of fragment ions.
[b] Regioisomeric TG standards.
[c] TGs containing only common polyunsaturated FAs (linolenic acid C18:3Δ-9,12,15 and linoleic acid C18:2Δ-9,12), data obtained from measurements of other 13 plant oils [2,44].
[d] TGs containing unusual Δ5-UPIFAs (pinolenic acid C18:3Δ-5,9,12 and taxoleic acid C18:2Δ-5,9).

for European Larch, Norway Spruce and European Silver Fir. The comparison with earlier published data [8] confirms a good mutual agreement. The results of GC/FID are very important for the identification of TGs with different position of DBs, because the relative concentrations of pinolenic and taxoleic acids can be correlated with their occurrence in TGs. Such TGs have identical MWs and observed ions as for analogues with common FAs (i.e. L and Ln), but the retention times both for GC and HPLC are shifted and the ratio of characteristic ions in APCI mass spectra is changed.

Our last work on the quantitation of TGs by HPLC/MS and transesterified FAMEs by GC/FID has shown [2] that both methods provide comparable results in the calculation of average parameters. In this work, only GC/FID average parameters (Table 6) are calculated because of the absence of Δ5 TGs standards, so the response factors can not be determined for TGs containing one, two or three Δ5-UPIFAs.

For the identification of methyl esters of Δ5-UPIFAs, the standards are available only for pinolenic and taxoleic acids, but keteleeronic and sciadonic acids are identified on the basis of

Table 6
Average carbon numbers (aCN), average equivalent carbon numbers (aECN) and average double bond (aDB) numbers, and the number of identified TGs in three conifer seed oils calculated from GC/FID analyses

Conifer seed oil source	Latin name	No. of TGs	Average parameter		
			aCN	aECN	aDB
European Larch	*Larix decidua*	63	17.85	13.82	2.01
Norway Spruce	*Picea abies*	51	17.09	13.32	1.89
European Silver Fir	*Abies alba*	53	16.90	13.56	1.67

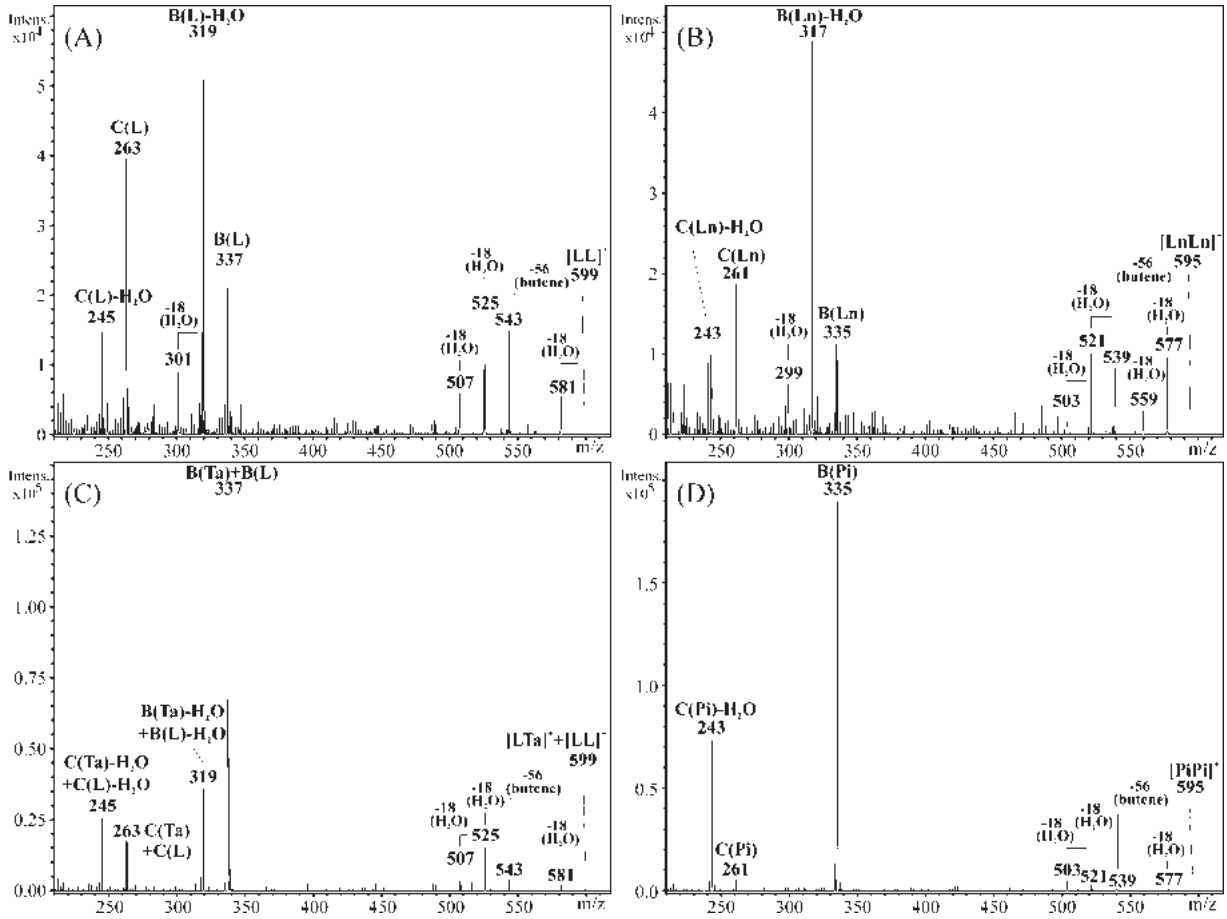

Fig. 3. Comparison of APCI tandem mass spectra of TG isomers with different double bond positions: (A) MS/MS of ion $[LL]^+$ at *m/z* 599 for LLL standard, (B) MS/MS of ion $[LnLn]^+$ at *m/z* 595 for LnLnLn standard, (C) MS/MS of ions $[LTa]^+$ and $[LL]^+$ at *m/z* 599 for LLTa from European Larch, and (D) MS/MS of ion $[PiPi]^+$ at *m/z* 595 for PiPiPi from European Larch. Notation of ions is explained in the text and ref. [1].

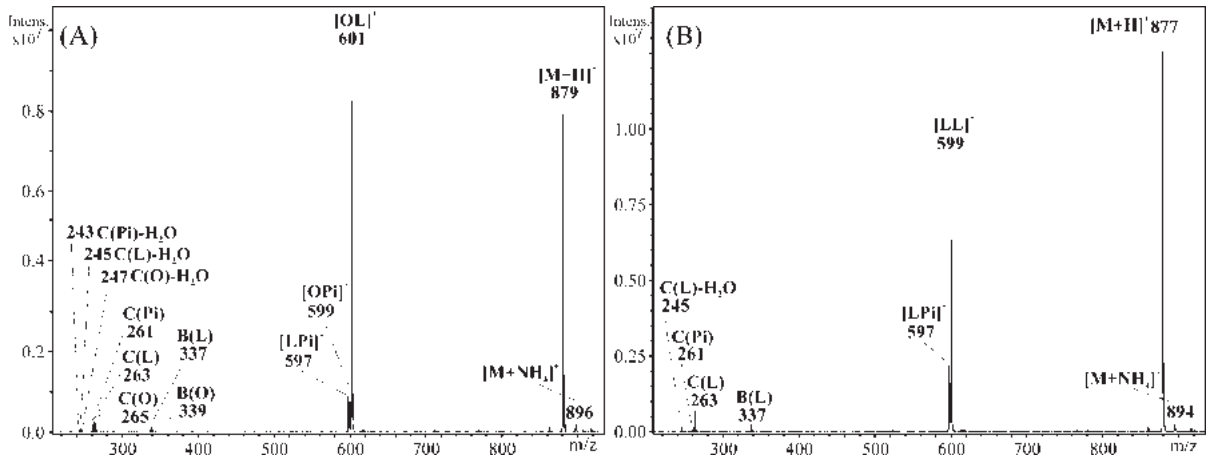

Fig. 4. Comparison of APCI first-order mass spectra of: (A) a mixture of LOPi/OLPi from European Larch, (B) LLPi from European Larch. Notation of ions is explained in the text and ref. [1].

characteristic shifts in retention times and determined MWs in accordance with previous literature data [11–14]. The relative concentrations of Δ5-olefinic FAs in pine seed oils are rather high (32% for European Larch, 27% for Norway Spruce and 20% for European Silver Fir). The dominant Δ5-UPIFA is pinolenic acid which represents approximately 90% of total Δ5 content in studied conifer seed oils.

4. Conclusions

Our HPLC/APCI-MS method has been successfully applied for the identification of 64 TGs consisting of 20 FAs in three conifer seed oils (European Larch, Norway Spruce and European Silver Fir) from the Gymnosperms taxonomical group known for a high content of D-5 olefinic acids (i.e. taxoleic, pinolenic,

keteleeronic and sciadonic). These unusual Δ5-UPIFAs are found in 32 identified TGs. A validated GC/FID method of transesterified oils has been used to confirm HPLC/MS results on TGs and for the calculation of average parameters useful for the characterization of a given plant oil. This is the first time when the study of intact TGs containing Δ5-UPIFAs in conifer seed oils is reported together with their retention characteristics in addition to previously known FA concentrations measured after the transesterification. APCI mass spectra of TG containing Δ5-UPIFAs provide useful information for distinguishing them from common polyenoic FAs in addition to the shifts in retention times. Differences in relative retention, characteristic features in first-order and tandem mass spectra and molecular weight determination can be applied for the positive identification of unknown TGs containing Δ5-UPIFAs in complex natural samples.

Acknowledgments

This work was supported by the grant project No. MSM0021627502 sponsored by the Ministry of Education, Youth and Sports of the Czech Republic and projects Nos. 203/06/0219 and 203/05/2106 sponsored by the Grant Agency of the Czech Republic. Authors would like to thank anonymous reviewers for their useful comments how to improve this paper.

References

[1] M. Holčapek, P. Jandera, P. Zderadička, L. Hrubá, J. Chromatogr. A 1010 (2003) 195.
[2] M. Holčapek, M. Lísa, P. Jandera, N. Kabátová, J. Sep. Sci. 28 (2005) 1315.
[3] J.D.J. van den Berg, N.D. Vermist, L. Carlyle, M. Holčapek, J.J. Boon, J. Sep. Sci. 27 (2004) 181.
[4] H.R. Mottram, S.E. Woodbury, R.P. Evershed, Rapid Commun. Mass Spectrom. 11 (1997) 1240.
[5] L. Fauconnot, J. Hau, J.M. Aeschlimann, L.B. Fay, F. Dionisi, Rapid Commun. Mass Spectrom. 18 (2004) 218.
[6] A. Müller, K. Düsterloh, R. Ringseis, K. Eder, H. Steinhart, J. Sep. Sci. 29 (2006) 358.
[7] R.L. Wolff, W.W. Christie, Eur. J. Lipid Sci. Technol. 104 (2002) 234.
[8] R.L. Wolff, L.G. Deluc, A.M. Marpeau, J. Am. Oil Chem. Soc. 73 (1996) 765.
[9] J. Gresti, C. Mignerot, J. Bézard, R.L. Wolff, J. Am. Oil Chem. Soc. 73 (1996) 1539.
[10] R.L. Wolff, E. Dareville, J.C. Martin, J. Am. Oil Chem. Soc. 74 (1997) 515.
[11] R.L. Wolff, O. Lavialle, F. Pedrono, E. Pasquier, F. Destaillats, A.M. Marpeau, P. Angers, K. Aitzetmuller, Lipids 37 (2002) 17.
[12] R.L. Wolff, F. Pedrono, A.M. Marpeau, W.W. Christie, F.D. Gunstone, J. Am. Oil Chem. Soc. 75 (1998) 1637.
[13] R.L. Wolff, W.W. Christie, F. Pedrono, A.M. Marpeau, N. Tsevegsuren, K. Aitzetmuller, F.D. Gunstone, Lipids 34 (1999) 855.
[14] F. Destaillats, P. Angers, R.L. Wolff, J. Arul, Lipids 36 (2001) 1247.
[15] T. Takagi, J. Am. Oil Chem. Soc. 41 (1964) 516.
[16] J.L. Gellerman, H. Schlenk, Experientia 19 (1963) 522.
[17] H. Schlenk, J.L. Gellerman, J. Am. Oil Chem. Soc. 42 (1965) 504.
[18] R.D. Plattner, G.F. Spencer, R. Kleiman, Lipids 10 (1975) 413.
[19] V.A. Seher, M. Krohn, Y.S. Ko, Fette Seifen Anstrichm 79 (1977) 203.
[20] R.V. Madrigal, C.R. Smith Jr., Lipids 10 (1975) 502.
[21] Y. Koyama, Y. Okada, Y. Toyama, Nippon Kagaku Zasshi 89 (1968) 95.
[22] R. Kleiman, C.F. Spencer, F.R. Earle, I.A. Wolff, Chem. Ind. 31 (1967) 1326.
[23] J.L. Gellerman, H. Schlenk, Lipids 4 (1969) 484.
[24] R. Ekman, Phytochemistry 19 (1980) 321.
[25] G.R. Jamieson, E.H. Reid, Phytochemistry 11 (1972) 269.
[26] J.S. Perona, V. Ruiz-Gutierrez, J. Chromatogr. B 785 (2003) 89.
[27] M. Lísa, M. Holčapek, Chem. Listy 99 (2005) 195.
[28] P. Laakso, J. Am. Oil Chem. Soc. 74 (1997) 1291.
[29] M. Holčapek, P. Jandera, J. Fischer, Crit. Rev. Anal. Chem. 31 (2001) 53.
[30] M. Holčapek, P. Jandera, J. Fischer, B. Prokeš, J. Chromatogr. A 858 (1999) 13.
[31] P. Sandra, A. Dermaux, V. Ferraz, M.M. Dittmann, G. Rozing, J. Microcolumn Sep. 9 (1997) 409.
[32] A. Jakab, K. Héberger, E. Forgács, J. Chromatogr. A 976 (2002) 255.
[33] A. Jakab, I. Jablonkai, E. Forgács, Rapid Commun. Mass Spectrom. 17 (2003) 2295.
[34] P. Dugo, O. Favoino, P.Q. Tranchida, G. Dugo, L. Mondello, J. Chromatogr. A 1041 (2004) 135.
[35] J. Parcerisa, I. Casals, J. Boatella, R. Codony, M. Rafecas, J. Chromatogr. A 881 (2000) 149.
[36] S. Héron, A. Tchapla, OCL-Oleagineux Corps Gras Lipides 1 (1994) 219.
[37] S. Héron, A. Tchapla, Fingerprints of Triacyglycerols from Oils and Fats by HPLC Isocratic Elution and Evaporative Light Scattering Detection, ELSD Sedex 45, Sedere, Alfortville, France, 1994.
[38] W.C. Byrdwell, E.A. Emken, W.E. Neff, R.O. Adlof, Lipids 31 (1996) 919.
[39] W.E. Neff, W.C. Byrdwell, K.R. Steidley, G.R. List, G. Snowder, J. Liq. Chromatogr. Rel. Technol. 25 (2002) 985.
[40] W.E. Neff, W.C. Byrdwell, G.R. List, J. Liq. Chrom. Rel. Technol. 24 (2001) 837.
[41] W.E. Neff, W.C. Byrdwell, J. Chromatogr. A 818 (1998) 169.
[42] W.C. Byrdwell, W.E. Neff, Rapid Commun. Mass Spectrom. 16 (2002) 300.
[43] S. Hamilton, R.J. Hamilton, P.A. Sewell, in: R.J. Hamilton, S. Hamilton (Eds.), Lipid Analysis: A Practical Approach, IRL Press at Oxford University Press, Oxford, NY, 1992, pp. 51–52.
[44] M. Lísa, M. Holčapek, in preparation.
[45] Animal and plant fats and oils. Analysis of fatty acid methyl esters by gas chromatography, ČSN ISO 5508, Czech Standards Institute, Prague, 1994.

Anal. Chem. **2009,** *81,* 3903–3910

Regioisomeric Characterization of Triacylglycerols Using Silver-Ion HPLC/MS and Randomization Synthesis of Standards

Miroslav Lísa, Hana Velínská, and Michal Holčapek*

Department of Analytical Chemistry, Faculty of Chemical Technology, University of Pardubice, Nám. Čs. Legií 565, 53210 Pardubice, Czech Republic

Silver-ion normal-phase high-performance liquid chromatography (HPLC) provides a superior separation selectivity for lipids differing in the number and position of double bonds in fatty acid chains including the resolution of triacylglycerol (TG) regioisomers under optimized conditions. Our silver-ion HPLC method is based on the coupling of three columns in the total length of 75 cm and a new mobile phase gradient consisting of hexane−acetonitrile−2-propanol which provides better resolution and also reproducibility in comparison to previously used mobile phases. In our work, the chemical interesterification (randomization) of single-acid TG standards is used for the generation of regioisomeric series of TGs, because it provides a random distribution of fatty acids in TGs at well-defined concentration ratios. The baseline separation of regioisomeric TG pairs containing up to three double bonds and the partial separation of TG regioisomers with four to seven double bonds are reported for the first time. Our silver-ion high-performance liquid chromatography/mass spectrometry (HPLC/MS) method is applied for the regioisomeric characterization of complex samples of plant oils and animal fat, where the results clearly demonstrate different preference of *sn*-2 occupation in plants (mainly unsaturated fatty acids) versus animal fat (mainly saturated fatty acids).

Triacylglycerols (TGs) are the main constituents of plant oils[1−3] and animal fats[4] characterized by the total carbon number (CN), the type and stereospecific position of fatty acids, and the number, position, and configuration of double bonds (DBs) in acyl chains. Fatty acids are digested in the human or animal organism with the assistance of the stereospecific lipases, where fatty acids from *sn*-1 and *sn*-3 position are cleaved first yielding 2-monoacylglycerols. The stereospecific analysis of TGs is a long-standing and challenging problem in the lipid analysis, but it is of high importance due to the different availability of fatty acids for the human body depending on *sn* positions. Concerning the overall characterization of TGs in complex natural mixtures, the best results are obtained with nonaqueous reversed-phase (NARP) high-performance liquid chromatography (HPLC) coupled to mass spectrometry (MS), where the highest number of identified TGs has been reported for the coupling of chromatographic columns in the total length of 45 cm and the mobile phase gradient consisting of acetonitrile−2-propanol.[5−7] The retention depends on the equivalent carbon number (ECN) defined as the total CN in all acyl chains minus 2 times the number of DBs, but the optimized NARP systems can resolve most TGs even within one ECN group with the exception of positional isomers. The partial separation of regioisomers in NARP mode is feasible only with multiple column coupling and very long retention times in the range of 100−200 min,[8,9] which is not practical for routine analysis.

The main possibilities of regiospecific analysis of TGs are the following: (1) silver-ion HPLC,[10−13] (2) MS,[5−7] (3) enzymatic hydrolysis (e.g., pancreatic lipase, phospholipase A_2)[14] followed by some analytical technique (e.g., silver-ion HPLC), and (4) derivatization[15] followed by chiral HPLC (complicated, laborious, not suitable for complex mixtures). Silver-ion normal-phase HPLC is a powerful technique for the separation of lipids differing in the number and position of DBs. The principle of this method is based on the capability of unsaturated organic compounds to create weak reversible complexes with transition metals, such as a silver ion. Silver ions are integrated into the silica stationary phase (preferably on the basis of ion-exchange mechanism) interacting with π electrons of DBs during the sample elution throughout the chromatographic column. The retention of each sample compound primarily depends

* Corresponding author.

(1) FEDIOL, The EU Oil and Proteinmeal Industry, Brussels, Belguim. http://www.fediol.be (accessed Dec 2008).
(2) Scheeder, M. In *Lipids from Land Animals in Modifying Lipids for Use in Food*; Gunstone, F. D., Ed.; Woodhead Publishing: Cambridge, 2006.
(3) Leray, C. Cyberlipid Center, Paris. http://www.cyberlipid.org (accessed Dec 2008).
(4) Food and Agricultural Organization of the United Nations (FAO), Rome. http://www.fao.org (accessed Dec 2008).
(5) Lísa, M.; Holčapek, M. *J. Chromatogr., A* **2008**, *1198−1199*, 115–130.
(6) Holčapek, M.; Jandera, P.; Fischer, L.; Prokeš, B. *J. Chromatogr., A* **1999**, *858*, 13–31.
(7) Holčapek, M.; Lísa, M.; Jandera, P.; Kabátová, N. *J. Sep. Sci.* **2005**, *28*, 1315–1333.
(8) Momchilova, S.; Itabashi, Y.; Nikolova-Damyanova, B.; Kuksis, A. *J. Sep. Sci.* **2006**, *29*, 2578–2583.
(9) Momchilova, S.; Tsuji, K.; Itabashi, Y.; Nikolova-Damyanova, B.; Kuksis, A. *J. Sep. Sci.* **2004**, *27*, 1033–1036.
(10) Christie, W. W. *J. Chromatogr.* **1988**, *454*, 273–284.
(11) Schuyl, P. J. W.; De Joode, T.; Vasconcellos, M. A.; Duchateau, G. S. M. J. E. *J. Chromatogr., A* **1998**, *810*, 53–61.
(12) Adlof, R. O. *J. High Resolut. Chromatogr.* **1995**, *18*, 105–107.
(13) Adlof, R. O.; List, G. *J. Chromatogr. A* **2004**, *1046*, 109–113.
(14) Janssen, H. G.; Hrnčiřík, K.; Szórádi, A.; Leijten, M. *J. Chromatogr., A* **2006**, *1112*, 141–147.
(15) Kuksis, A.; Itabashi, Y. *Methods* **2005**, *36*, 172–185.

10.1021/ac900150j CCC: $40.75
Published on Web 04/14/2009

on the number of DBs, but it is also affected by the steric availability of DBs for the interaction with silver ions. The retention increases with increasing number of DBs with the secondary separation according to the position and geometry of DBs. Off-line or online two-dimensional (2D) HPLC of relatively complementary separation modes in NARP and silver-ion HPLC is a highly promising method for the analysis of TGs.[16,17]

The different ratios of $[M + H - R_iCOOH]^+$ fragment ions in atmospheric pressure chemical ionization (APCI) mass spectra of positional isomers (regioisomers) of TGs was first reported in 1996[18] and later on applied for HPLC/APCI-MS characterization of prevailing fatty acids in *sn*-2 position in plant oils.[19] All MS approaches are based on the fact that the neutral loss of fatty acid from the *sn*-2 position yields the fragment ion with a lower relative abundance compared to cleavages from the side *sn*-1/3 positions. It is often applied for the assignment of prevailing fatty acids in the *sn*-2 position, but for the quantitative determination of *sn*-2 occupation the calibration curves for mixtures of both regioisomers have to be measured[20−23] using the same instrument and ionization technique. APCI is the most frequently used ionization technique for TG analysis due to their nonpolar character, but electrospray ionization (ESI) can be applied as well due to the formation of ammonium adducts.[24−26]

If the TG has different fatty acids in *sn*-1 and *sn*-3 positions, then the carbon atom in the *sn*-2 position becomes a chiral center. Common analytical techniques working in a nonchiral environment cannot differentiate between *sn*-1 and *sn*-3 enantiomers; therefore, they are generally treated as equivalent due to the lack of suitable analytical techniques for their analysis.[3,5,19,21] No chiral separation of intact TGs have been reported so far with the exception of synthetic TGs containing very different fatty acids C8:0 versus C22:5 or C22:6,[27] which is not a combination occurring in nature. Due to the absence of any official recommendation for the designation of *sn*-1/3 isomers, we list them in the order of decreasing masses in accordance with our previously proposed rule,[20] e.g., OLP but not PLO. In case of isobaric fatty acids in *sn*-1/3 positions, the more common fatty acid is listed first, e.g., LnOγLn but not γLnOLn.

The chemical interesterification (so-called randomization) has been used in many industrial applications in fat and oil processing.[28] It changes physicochemical properties of natural oils with the assistance of fatty acids already present in TGs in a given oil or fat. The degree of change is based on the reaction temperature, reaction time, and catalysts used. The most common catalyst in this process is sodium methoxide, but it is possible to use bases, acids, and some metal ions as well. Sodium methoxide has the highest reactivity, but on the other hand, it is very sensitive to any trace of water, which stops the reaction due to the hydrolysis of sodium methoxide. In the first reaction step, the bonds between glycerol and fatty acids are cleaved yielding a mixture of diacylglycerols (DGs), monoacylglycerols (MGs), and fatty acids. These species subsequently undergo the interesterification reactions providing a random distribution of fatty acids in newly formed TGs.

The main goal of our work is the development of a silver-ion HPLC/MS method applicable for the separation and quantitation of regioisomeric ratios of TGs in complex mixtures. TG regioisomeric pairs are separated by the optimized silver-ion HPLC method, identified based on characteristic differences in their APCI mass spectra, and quantified according to the ratio of chromatographic peak areas. The randomization procedure plays an important role in generating the series of regioisomeric standards. Applications to complex natural samples of plant oils and animal fats containing different TG regioisomers are demonstrated.

EXPERIMENTAL SECTION

Materials. Acetonitrile, 2-propanol, methanol, ethanol, propionitrile, ethylacetate, hexane (solvents are HPLC gradient grade), and sodium methoxide were purchased from Sigma-Aldrich (St. Louis, MO). Standards of tripalmitin (PPP, C16:0), triolein (OOO, Δ9-C18:1), trilinolein (LLL, Δ9,12-C18:2), and trilinolenin (LnLnLn, Δ9,12,15-C18:3) were purchased from Nu-ChekPrep (Elysian, MN). Palm and olive oils were purchased from Augustus Oil Limited (Hampshire, England).

Sample Preparation. An amount of 10−15 g of the sample (sunflower or blackcurrant seeds, fat tissue from pig) was weighed, and then seeds were carefully crushed in a mortar to fine particles, whereas fat tissue was crushed in a homogenizer. Then 15 mL of hexane was added, and this mixture was stirred occasionally for 15 min. The solid particles were filtered out using a course filter paper, and the extract was filtered again using a fine filter (0.45 μm). From the filtered extract, hexane was evaporated using a mild stream of nitrogen to yield pure plant oil or animal fat.

Randomization. Amounts of 50 mg of each TG standard and 100 mg of sodium methoxide were weighed into a dry boiling flask with the addition of 2 mL of hexane dried with molecular sieves. The mixture was heated for 30 min in a water bath under the reflux condenser. The reaction temperature was kept constant at 75 °C. Then, the mixture was extracted with water and three times with 1 mL of methanol to remove sodium methoxide. The hexane phase containing randomized analyte was injected into the silver-ion HPLC system.

(16) Dugo, P.; Favoino, O.; Tranchida, P. Q.; Dugo, G.; Mondello, L. *J. Chromatogr., A* **2004**, *1041*, 135–142.
(17) Van der Klift, E. J. C.; Vivó-Truyols, G.; Claassen, F. W.; Van Holthoon, F. L.; Van Beek, T. A. *J. Chromatogr., A* **2008**, *1178*, 43–55.
(18) Mottram, H. R.; Evershed, R. P. *Tetrahedron Lett.* **1996**, *37*, 8593–8596.
(19) Mottram, H. R.; Woodbury, S. E.; Evershed, R. P. *Rapid Commun. Mass Spectrom.* **1997**, *11*, 1240–1252.
(20) Holčapek, M.; Jandera, P.; Zderadička, P.; Hrubá, L. *J. Chromatogr., A* **2003**, *1010*, 195–215.
(21) Byrdwell, W. C.; Neff, W. E. *Rapid Commun. Mass Spectrom.* **2002**, *16*, 300–319.
(22) Fauconnot, L.; Hau, J.; Aeschlimann, J. M.; Fay, L. B.; Dionisi, F. *Rapid Commun. Mass Spectrom.* **2004**, *18*, 218–224.
(23) Leskinen, H.; Suomela, J. P.; Kallio, H. *Rapid Commun. Mass Spectrom.* **2007**, *21*, 2361–2373.
(24) McAnoy, A. M.; Wu, C. C.; Murphy, R. C. *J. Am. Soc. Mass Spectrom.* **2005**, *16*, 1498–1509.
(25) Cvačka, J.; Hovorka, O.; Jiroš, P.; Kindl, J.; Stránský, K.; Valterová, I. *J. Chromatogr., A* **2006**, *1101*, 226–237.
(26) Malone, M.; Evans, J. J. *Lipids* **2004**, *39*, 273–284.
(27) Iwasaki, Y.; Yasui, M.; Ishikawa, T.; Irimescu, R.; Hata, K.; Yamane, T. *J. Chromatogr., A* **2001**, *905*, 111–118.
(28) Marangoni, A. G.; Rousseau, D. In *Food Lipids*; Akoh, C. C., Min, D. B., Eds.; Marcel Dekker: New York, 2002; pp 301−333 and references therein.

Silver-Ion HPLC. HPLC was performed on a liquid chromatograph Agilent 1200 series (Agilent Technology, Waldbronn, Germany). The final HPLC method for analyses of plant oils and animal fats used the following conditions: three silver-ion chromatographic columns ChromSpher Lipids (250 mm × 4.6 mm, 5 μm, Varian, Palo Alto, CA) connected in series, the flow rate of 1 mL/min, the injection volume of 1 μL, column temperature of 25 °C, and the mobile phase gradient of 0 min 100% A, 140 min 61% A + 39% B, where A is a mixture of hexane−2-propanol−acetonitrile (99.8:0.1:0.1, v/v/v) and B is the mixture of hexane−2-propanol−acetonitrile (98:2:2, v/v/v). The mobile phase was prepared fresh every day before analyses. Silver-ion columns were conditioned at 50 μL/min of the initial mobile phase composition overnight and at 1 mL/min for 1 h before the first analysis. The injector needle was washed with the mobile phase before each injection. The chromatographic system is equilibrated between injections for 30 min. The hybrid quadrupole time-of-flight (QqTOF) analyzer micrOTOF-Q (Bruker Daltonics, Bremen, Germany) with positive-ion APCI was used in the mass range m/z of 50−1200 with the following tuning parameters: flow of the nebulizing and drying gas 5 and 3 L/min, respectively, temperatures of the drying gas and APCI heater 300 and 400 °C, respectively. Reconstructed ion current chromatograms were used to support the identification and quantitation of coeluting peaks.

Fatty Acid Abbreviations. M, myristic (C14:0); C15:0, pentadecanoic; Po, palmitoleic (Δ9-C16:1); P, palmitic (C16:0); Mo, margaroleic (Δ9-C17:1); Ma, margaric (C17:0); St, stearidonic (Δ6,9,12,15-C18:4); Ln, α-linolenic (Δ9,12,15-C18:3); γLn, γ-linolenic (Δ6,9,12-C18:3); L, linoleic (Δ9,12-C18:2); O, oleic (Δ9-C18:1); S, stearic (C18:0); C20:2, eicosadienoic (Δ11,14-C20:2); G, gadoleic (Δ9-C20:1); A, arachidic (C20:0); B, behenic (C22:0); C23:0, tricosanoic (C23:0); Lg, lignoceric (C24:0).

RESULTS AND DISCUSSION

Optimization of Silver-Ion HPLC of TGs. It is well-known that the silver-ion chromatography suffers from a lower reproducibility of retention times in comparison to reversed-phase systems.[29] In the present work, the maximum attention has been paid to the optimization of chromatographic performance in terms of regioselectivity, reproducibility, and robustness. The most important parameters are the selection of column type and mobile phase composition. The optimization of mobile phase composition starts from the hexane−acetonitrile system which is the most widespread system used in silver-ion HPLC[13,30] providing the best results concerning the regioisomeric resolution.[12] The critical problem of this frequently used mobile phase is a low mutual miscibility of these solvents and the evaporative changes of prepared mobile phases, which significantly contributes to the reproducibility problems.[29] This knowledge has driven us to test the different mobile phase compositions with the goal to achieve a better separation selectivity and reproducibility of retention times for TGs. Extensive experiments with the combination of different polar modifiers (2-propanol, ethanol, propionitrile, and ethylacetate) in hexane[31] have shown that it is not easy to improve the selectivity of the hexane−acetonitrile systems. Almost comparable resolution is obtained with hexane−propionitrile systems, where the reproducibility problems are not encountered (in agreement with ref 32), but the serious drawback of this method is the toxicity of propionitrile. We discourage the use of propionitrile because of the health hazard in the laboratory. Other tested systems show poor regioisomeric selectivity. On the basis of these experiments, we have decided to add the third solvent to the hexane−acetonitrile system to improve the mutual miscibility while keeping the chromatographic performance, which has been achieved with the hexane−acetonitrile−2-propanol system. Then, the optimization

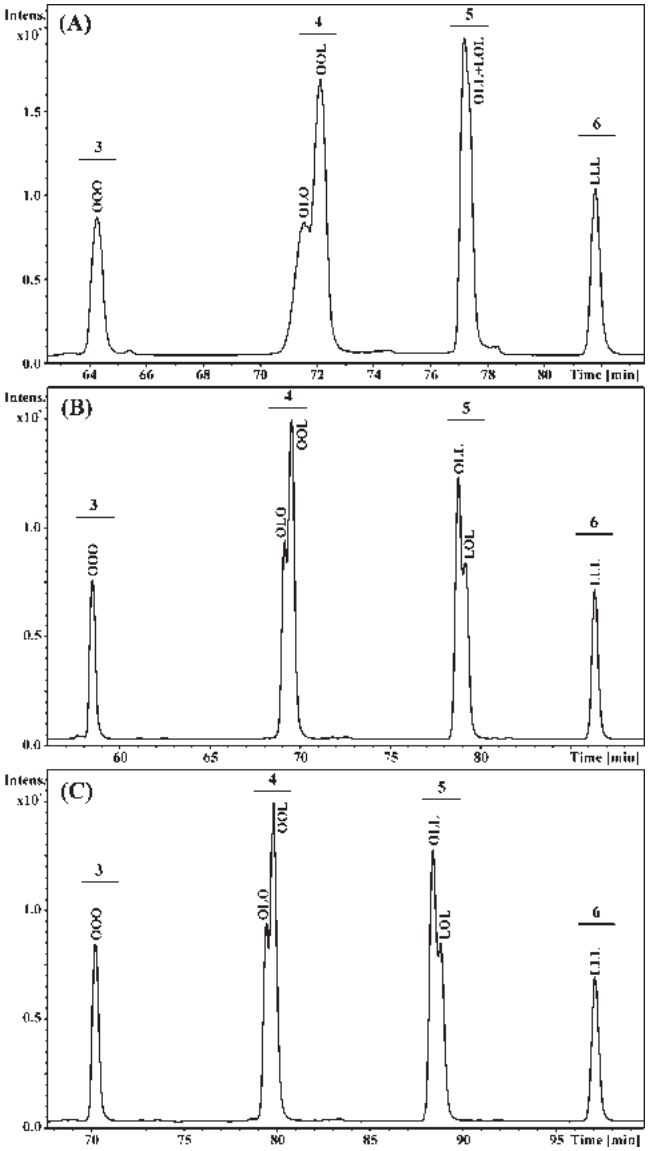

Figure 1. Effect of separation temperature on silver-ion HPLC/APCI-MS analysis of TGs in the randomization mixture of OOO/LLL: (A) 15, (B) 25, and (C) 40 °C. Other chromatographic conditions are described in the Experimental Section.

(29) Harfmann, R. G.; Julka, S.; Cortes, H. J. *J. Sep. Sci.* **2008**, *31*, 915–920.
(30) Nikolova-Damyanova, B. Silver-ion HPLC of fatty acids and triacylglycerols. In *HPLC of Acyl Lipids*; Lin, J.-T., McKeon, T. A., Eds.; HNB Publishing: New York, 2005; pp 221−268.
(31) Velínská, H. Diploma Thesis, University of Pardubice, Pardubice, Czech Republic, 2008.
(32) Müller, A.; Düsterloh, K.; Ringseis, R.; Ender, K.; Steinhart, H. *J. Sep. Sci.* **2006**, *29*, 358–365.
(33) Jakab, A.; Jablonkai, I.; Forgács, E. *Rapid Commun. Mass Spectrom.* **2003**, *17*, 2295–2302.

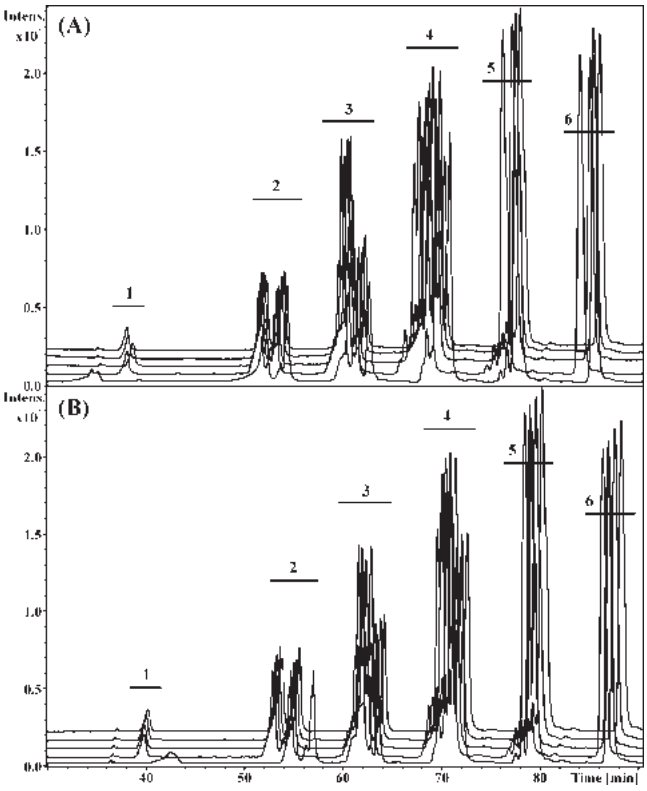

Figure 2. Separation reproducibility for sunflower oil analysis: (A) five consecutive injections in the first day; (B) five consecutive injections in the second day. Chromatographic conditions are described in the Experimental Section.

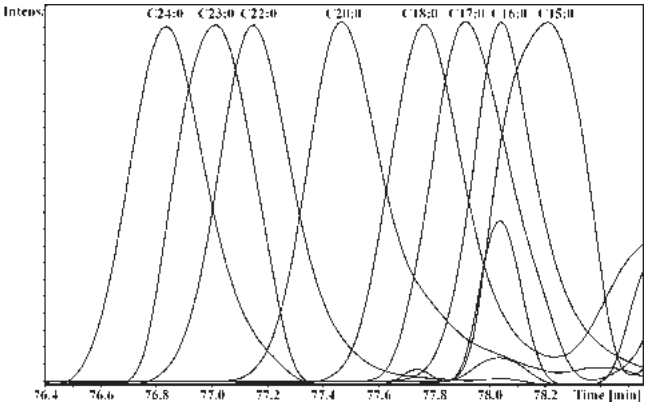

Figure 3. Effect of the fatty acid chain length on the retention in silver-ion HPLC/APCI-MS analysis of TGs in randomized sunflower oil shown by reconstructed chromatograms of $[XL]^+$ ions for XLL type TGs, where X is saturated fatty acid from C15:0 to C24:0.

of gradient conditions has been performed[31] resulting in the final method described in the Experimental Section.

The commercial silver-ion ChromSpher Lipids column provides the best performance and separation selectivity in the lipid analysis based on our previous experiences and the literature data as well.[12,13,16,17,25] An increased length of chromatographic column can improve the chromatographic resolution, as demonstrated earlier in NARP[20] or silver-ion[13] separations of TGs. Unlike NARP systems, the back pressure is not a limiting factor here, because the mobile phases typically consist of hexane with a low percentage of polar modifier. The limiting factors are mainly long retention times associated with the extended column length and

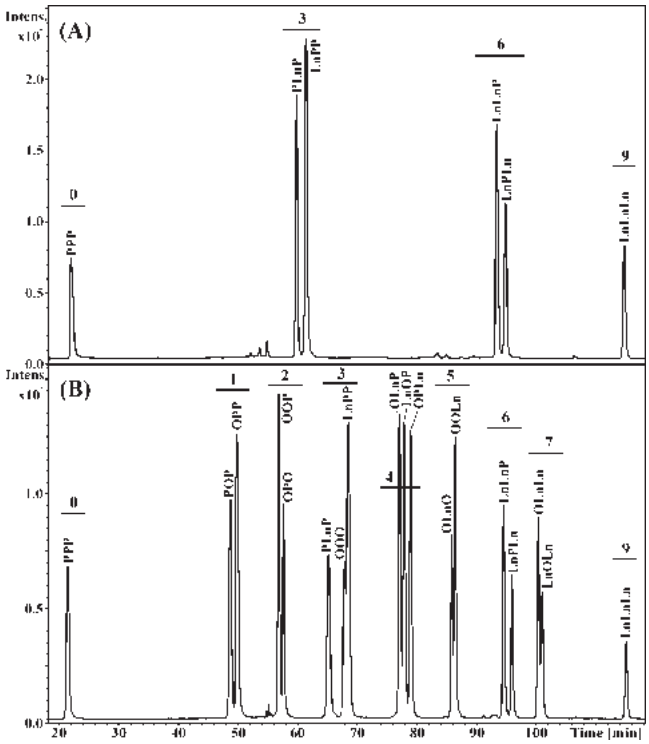

Figure 4. Silver-ion HPLC/APCI-MS analysis of randomization mixtures: (A) PPP/LnLnLn; (B) PPP/OOO/LnLnLn.

peak-broadening effects for multiple column coupling. On the basis of these considerations, the comparison of one, two, and three 25 cm ChromSpher Lipids columns connected in series has been performed (Supporting Information Figure S1). Retention times are approximately doubled and tripled for coupling of two or three columns but not exactly due to different retention characteristics of individual commercial columns.

The chromatographic resolution of lipids in NARP systems is significantly affected by temperature; generally, an improvement is observed at lower temperature. Contrary to NARP chromatographic systems, the retention in silver-ion HPLC increases with increased temperature (Figure 1). Peak shapes at low temperature (e.g., 15 °C in Figure 1A) are distorted. There is almost no visible difference in the resolution between 25 °C (Figure 1B) and 40 °C (Figure 1C), but the analysis time is shorter for 25 °C. Moreover, 40 °C is the maximum recommended temperature by the manufacturer; hence, 25 °C is selected as optimum temperature for further experiments.

Maximum attention has been paid to the right chromatographic practice to reduce the fluctuation of retention times, which involves mainly the following precautions. Mobile phases are prepared every day fresh using solvents dried with molecular sieves and kept in tightly closed bottles to avoid evaporation. All measurements are performed in a single block of several weeks on the same system without changing between normal- and reversed-phase systems. Before any measurement, the columns are conditioned using the low flow rate of initial gradient composition (50 μL/min) overnight and the standard flow rate for 1 h before the analysis.

A remarkable improvement in the reproducibility of retention times has been achieved in comparison to traditional hexane–acetonitrile mobile phases previously used in our laboratory. The

Table 1. Basic APCI-MS Fragmentation Characteristics of Analyzed Regioisomeric TGs in Randomization Mixtures

TG	DB[a]	ratio of $[M + H - R_iCOOH]^+$ ions[b]
POP	1	$[OP]^+/[PP]^+ = 100:33$
OPP		$[OP]^+/[PP]^+ = 100:80$
PLP	2	$[LP]^+/[PP]^+ = 100:39$
LPP		$[LP]^+/[PP]^+ = 100:87$
OOP		$[OP]^+/[OO]^+ = 100:62$
OPO		$[OP]^+/[OO]^+ = 100:20$
PLnP	3	$[LnP]^+/[PP]^+ = 100:49$
LnPP		$[LnP]^+/[PP]^+ = 100:97$
OLP		$[OL]^+/[OP]^+/[LP]^+ = 100:72:84$
LOP		$[OL]^+/[OP]^+/[LP]^+ = 100:97:53$
OPL		$[OL]^+/[OP]^+/[LP]^+ = 58:100:85$
LLP	4	$[LP]^+/[LL]^+ = 100:81$
LPL		$[LP]^+/[LL]^+ = 100:33$
OLO		$[OL]^+/[OO]^+ = 100:45$
OOL		$[OL]^+/[OO]^+ = 100:88$
OLnP		$[OLn]^+/[OP]^+/[LnP]^+ = 100:60:93$
LnOP		$[OLn]^+/[OP]^+/[LnP]^+ = 95:100:33$
OPLn		$[OLn]^+/[OP]^+/[LnP]^+ = 49:100:92$
OLL	5	$[OL]^+/[LL]^+ = 100:81$
LOL		$[OL]^+/[LL]^+ = 100:34$
LLnP		$[LLn]^+/[LP]^+/[LnP]^+ = 100:78:88$
LPLn		$[LLn]^+/[LP]^+/[LnP]^+ = 44:100:82$
LnLP		$[LLn]^+/[LP]^+/[LnP]^+ = 100:93:47$
OLnO		$[OLn]^+/[OO]^+ = 100:23$
OOLn		$[OLn]^+/[OO]^+ = 100:76$
OLnL	6	$[OL]^+/[OLn]^+/[LLn]^+ = 62:95:100$
OLLn		$[OL]^+/[OLn]^+/[LLn]^+ = 94:54:100$
LOLn		$[OL]^+/[OLn]^+/[LLn]^+ = 100:78:56$
LnLnP		$[PLn]^+/[LnLn]^+ = 100:78$
LnPLn		$[PLn]^+/[LnLn]^+ = 100:28$
LLnL	7	$[LLn]^+/[LL]^+ = 100:36$
LLLn		$[LLn]^+/[LL]^+ = 100:68$
OLnLn		$[OLn]^+/[LnLn]^+ = 100:79$
LnOLn		$[OLn]^+/[LnLn]^+ = 100:34$
LLnLn	8	$[LLn]^+/[LnLn]^+ = 100:36$
LnLLn		$[LLn]^+/[LnLn]^+ = 100:61$

[a] DB, number of double bonds. [b] Listed values correspond to the arithmetic mean of at least three consecutive measurements.

Table 2. Peak Area Ratios of TG Regioisomeric Groups in Silver-Ion HPLC/MS after the Randomization of Equal Amounts of PPP, OOO, LLL, and LnLnLn

TG randomization mixture	TG regioisomeric group[a]	peak area ratio
OOO/PPP	OOP/OPO	65:35
	OPP/POP	63:37
OOO/LLL	OOL/OLO	68:32
	OLL/LOL	62:38
OOO/LnLnLn	OOLn/OLnO	66:34
	OLnLn/LnOLn	65:35
LLL/PPP	LLP/LPL	61:39
	LPP/PLP	60:40
LLL/LnLnLn	LLLn/LLnL	68:32
	LLnLn/LnLLn	62:38
LnLnLn/PPP	LnLnP/LnPLn	60:40
	LnPP/PLnP	61:39
OOO/LnLnLn/PPP	OLnP/LnOP/OPLn	33:34:33
OOO/LLL/PPP	OLP/LOP/OPL	29:35:36
OOO/LLL/LnLnLn	OLnL/OLLn/LOLn	30:33:37

[a] *sn*-1 and *sn*-3 positions are not differentiated in this study, e.g., OOP and POO are treated as equivalent.

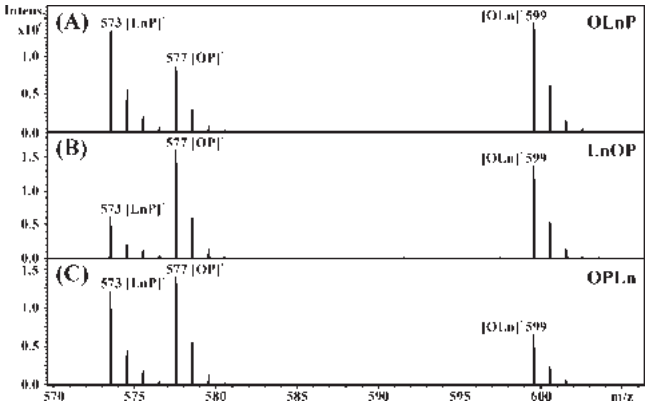

Figure 5. Positive-ion APCI mass spectra of (A) OLnP, (B) LnOP, and (C) OPLn in a zoomed region of *m*/*z* 570−605 with diacylglycerol fragment ions for peaks from the randomization mixture shown in Figure 4B.

reproducibilities (Figure 2) for three selected peaks with 2 (PLP), 4 (PLL), and 6 (LLL) DBs are acceptable now, as demonstrated on relative standard deviations of retention times of 0.4%, 1.0%, and 0.7% for 1 day measurements and 1.9%, 1.7%, and 1.4% for 2 days measurements. In hexane−acetonitrile mobile phases used in our laboratory previously, the 1 day reproducibility for these three peaks was 7.4%, 6.8%, and 5.2%. Some shifts in retention times can occur on longer time scale, but they can be efficiently eliminated by the use of the relative retention $r = (t_{R,TG} - t_M)/(t_{R,std} - t_M)$, as listed in Supporting Information Table S1. The retention in silver-ion mode is governed mainly by the DB number, but certain separation also occurs for TGs differing only in the length of the fatty acid chain (see Figure 3). The retention order of TGs within these groups with the constant DB number in sunflower oil analysis is the following: for XLL type (where X is the saturated fatty acid), LgLL < C23:0LL < BLL < ALL < SLL < LLMa < LLP < LLC15:0 < LLM; for XLO type, LgLO < C23:0LO < BLO < ALO < SLO < OLMa < OLP; for XLS and XLP types, LgLS < BLS + LgLP < ALS + BLP < SLS + ALP < SLP < PLP, etc. The reconstructed ion current traces for diacylglycerol fragment ions of XLL series are overlaid in Figure 3 to illustrate possible separation according to the chain length. Nonlabeled minor peaks in this figure correspond to mass interferences from other coeluting TGs (not XLL series) with identical diacylglycerol fragment ions. Retention characteristics of all TGs in particular DB groups identified in plant oils (sunflower, blackcurrant, olive, and palm) and animal fat (lard) are summarized in Supporting Information Table S1. Differences in retention times of logical XLL series are approximately 0.4 min per two methylene groups (see Figure 3). The retention order of regioisomers follows the rule that more DBs in *sn*-1/3 positions mean a stronger interaction with silver ions embedded in the stationary phase and hence higher retention in comparison with regioisomers having the same unsaturations

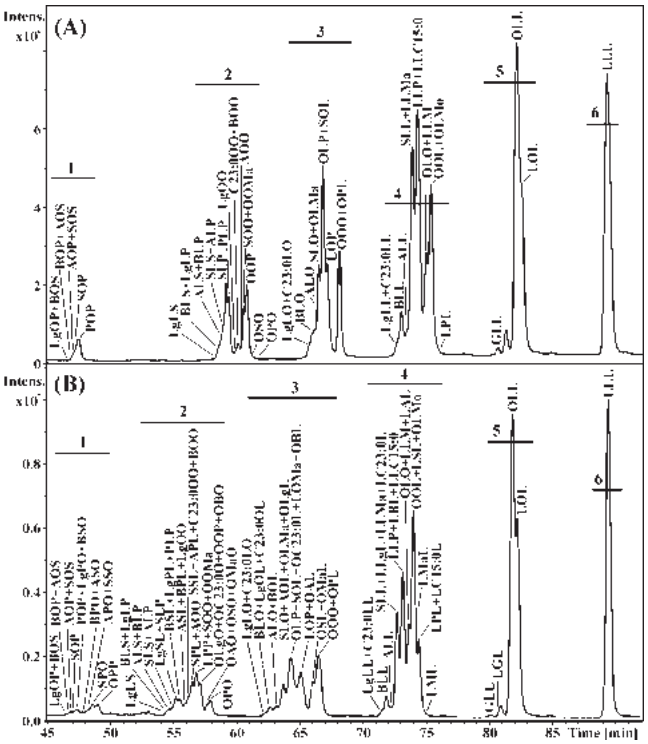

Figure 6. Silver-ion HPLC/APCI-MS analysis of (A) sunflower oil and (B) randomized sunflower oil.

in the middle *sn*-2 position. The probable explanation is a better steric availability of the DB in *sn*-1/3 positions. Regioisomers of XYO/YXO and XYL/YXL types (X and Y are saturated fatty acids) and saturated TGs are not differentiated.

Randomization of TG Mixtures and Their Separation. The chemical interesterification of fatty acids in TGs (randomization) is a known process used in industrial processing of oils and fats to modify physicochemical properties of food products.[28] In our work, the randomization is applied for the generation of standard mixtures of regioisomers (Figure 4), which are too expensive or often not commercially available at all. First, the randomization reaction has been optimized[31] resulting in a robust and reproducible procedure (see the Experimental Section for conditions). Theoretically, the randomization of binary mixtures of equal amounts of single-acid TGs $R_1R_1R_1$ and $R_2R_2R_2$ should provide eight combinations of TGs at identical concentrations: $R_1R_1R_1$, $R_1R_2R_1$, $R_1R_1R_2$, $R_2R_1R_1$, $R_1R_2R_2$, $R_2R_2R_1$, $R_2R_1R_2$, and $R_2R_2R_2$. In practice, enantiomers $R_1R_1R_2$ versus $R_2R_1R_1$ and $R_1R_2R_2$ versus $R_2R_2R_1$ cannot be resolved in a nonchiral environment; therefore, we obtain the following concentration ratios (in parentheses) for initial TGs and two regioisomeric pairs: $R_1R_1R_1$ (1), $R_1R_2R_1$ (1), $R_1R_1R_2 + R_2R_1R_1$ (2), $R_1R_2R_2 + R_2R_2R_1$ (2), $R_2R_1R_2$ (1), $R_2R_2R_2$ (1). The theoretical calculation fits well with experimental results for randomization reactions, as illustrated in Figure 4A and Table 2 for binary randomization mixtures, which confirms that the chemical interesterification is really a random process applicable for the generation of regioisomeric standards at defined concentration ratios. Figure 4B shows the chromatogram of the ternary randomization mixture of OOO, LnLnLn, and PPP providing six regioisomeric doublets at concentration ratios 2:1 and one triplet OLnP/LnOP/OPLn with identical concentrations. This way the standard mixtures of TG regioisomers are generated for the optimization of regioisomeric silver-ion separation. Chromatograms of randomization mixtures (Figure 5 and Supporting Information Figures S2 and S3) also demonstrate the stereoselectivity of our HPLC method providing the baseline separation for regioisomers containing up to three DBs and at least partial separation for TGs with four to eight DBs. As a rule, the bigger the difference in the DB number of fatty acids means better separation of corresponding TG regioisomers, e.g., the baseline separation of P/L and P/Ln regioisomers is relatively easily achieved (Figure 5 and Supporting Information Figure S2). The example of partial resolution of LnOLn/OLnLn regioisomers (Figure 4B) containing seven DBs shows that the number of DBs is probably not a limiting factor for the regioisomeric separation, but the critical requirement for the successful separation of highly polyunsaturated regioisomeric TGs is the difference in the DB number between fatty acids. Polyunsaturated TGs containing fatty acids differing only by one DB are critical pairs for regioisomeric separation, e.g., O/L (peak splitting) and L/Ln (only peak shoulder) pairs. Fatty acids differing by two and more DBs are well-separated for TGs containing up to four DBs and partially for five and more DBs. Some improvement may be expected with further extension of column length at the expense of very long retention times and also rather high costs of multiple columns.

APCI Mass Spectra of Regioisomeric TGs. The randomization is used for the generation of regioisomeric mixtures of TGs, which can be subsequently separated in silver-ion HPLC, and APCI mass spectra of separated regioisomers can be recorded regardless the physical absence of pure regioisomeric standards. Figure 5 shows the differences in mass spectra of regioisomeric triplet OLnP/LnOP/OPLn, which is chromatographically separated unlike all previous papers. APCI mass spectra shown in Figure 5 correspond to the spectra of pure standards. The advantage of silver-ion HPLC/MS determination of regioisomers is the fact that regioisomers do not differ in their relative responses (see ratios in Table 2); hence, peak area ratios correspond to concentration ratios. Table 1 lists exact ratios of DG fragment ions obtained only from randomization experiments to be sure that these results are not affected by possible coelutions common in complex natural samples. Two MS approaches are used for *sn*-2 fatty acid characterization. The simple approach just determines the prevailing fatty acid in the middle *sn*-2 position based on lower relative abundance of the corresponding DG fragment ion,[5,16,19,17,20,21,25] but it has been demonstrated recently[34−37] that the type of fatty acids (mainly DB number and positions) affects the relative abundances of corresponding DG fragment ions. More exact approach is based on the construction of calibration curves using identical standards of regioisomeric pairs mixed at different ratios,[21−23,26,33] but the precision of this determination may be affected by certain fluctuations of fragment ion ratios. Ratios of DG fragment ions shown in Table 1 can be applied for NARP-HPLC determination of regioisomeric ratios measured on the same instrument, because the calibration curves are linear and

(34) Li, X.; Evans, J. J. *Rapid Commun. Mass Spectrom.* **2005**, *19*, 2528–2538.
(35) Li, X.; Collins, E. J.; Evans, J. J. *Rapid Commun. Mass Spectrom.* **2006**, *20*, 171–177.
(36) Gakwaya, R.; Li, X.; Wong, Y. L.; Chivukula, S.; Collins, E. J.; Evans, J. J. *Rapid Commun. Mass Spectrom.* **2007**, *21*, 3262–3268.
(37) Lísa, M.; Holčapek, M.; Řezanka, T.; Kabátová, N. *J. Chromatogr., A* **2007**, *1146*, 67–77.

Table 3. Calculation of Theoretical TG Composition after the Randomization of TGs in Sunflower Oil (*n* Is the Number of Fatty Acids, R_i Is Variable Fatty Acid, and x_{Ri} Is the Weight Fraction of R_i)[a]

	no. of TGs		relative concentration of TGs[b]	
type[b]	theoretical	sunflower oil	theoretical	sunflower oil
$R_1R_1R_1$	n	6	$x_{R_1}{}^3$	LLL (23.3), OOO (1.2), PPP (0.05), SSS (0.01), BBB (<0.01), AAA (<0.01)
$R_1R_1R_2$	$n(n-1)$	30	$3x_{R_1}{}^2x_{R_2}$	OLL (26.0), OOL (9.7), LLP (8.7), SLL (5.8), BLL (1.3), OOP (1.2), LPP (1.1), SOO (0.80), ALL (0.56), SSL (0.49), OPP (0.41), BOO (0.18), SSO (0.18), SPP (0.09), AOO (0.08), SSP (0.06), BBL (0.02), BPP (0.02), APP (0.01), BSS (0.01), BBO (0.01), ASS (<0.01), BBP (<0.01), SBB (<0.01), BBA (<0.01), AAO (<0.01), AAL (<0.01), AAP (<0.01), AAS (<0.01), BAA (<0.01)
$R_1R_2R_3$	$[n(n-1)(n-2)]/6$	20	$6x_{R_1}x_{R_2}x_{R_3}$	OLP (6.5), SLO (4.4), SLP (1.5), BLO (0.97), SOP (0.55), ALO (0.41), BLP (0.32), SLB (0.22), ALP (0.14), BOP (0.12), ASL (0.09), BSO (0.08), AOP (0.05), BSP (0.03), ASO (0.03), BAL (0.02), BAO (0.01), ASP (0.01), BAP (<0.01), BAS (<0.01)
total	$[n(n+1)(n+2)]/6$	56		sum of TGs is 96.91%; the rest corresponds to TGs containing trace fatty acids

[a] Analyzed sunflower oil has the following weight fractions in % of main fatty acids (ref 5): linoleic (L) 61.52%, oleic (O) 22.94%, palmitic (P) 7.69%, stearic (S) 5.15%, behenic (B) 1.14%, arachidic (A) 0.49%, and the rest (1.07%) corresponds to trace fatty acids. [b] Stereospecific configuration is not distinguished in this table.

Table 4. Relative Peak Areas of Main TGs in Sunflower Oil before the Randomization Compared with the Experimental and Theoretical Relative Concentrations after the Randomization

	relative peak areas [%]		
TG	before randomization (exptl)	after randomization (exptl)	after randomization (theor)
SLP	1.8	0.7	0.5
PLP	1.6	0.6	0.4
LPP/SOO	0/1.1	0.9/0.8	0.7/0.5
OOP	1.9	1.0	0.8
OSO	0.1	0.4	0.3
OPO	0.1	0.4	0.4
SLO	2.4	1.5	1.5
OLP/SOL	2.0/4.3	1.8/2.7	1.5/2.2
OBL/LOP	0/3.1	0.4/2.5	0.3/2.2
OSL	0	1.4	1.5
OOO/OPL	3.7/0.1	1.5/2.7	1.2/2.2
BLL	1.6	0.9	0.9
SLL	7.5	4.1	3.9
LLP	9.7	5.8	5.8
OLO	3.0	3.6	3.2
OOL	6.5	7.7	6.5
LPL	0.4	3.0	2.9
OLL	16.4	16.0	17.3
LOL	4.9	9.4	8.7
LLL	17.2	20.0	23.3

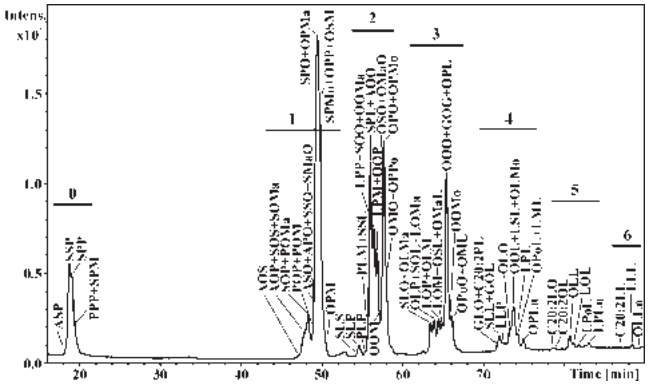

Figure 7. Silver-ion HPLC/APCI-MS analysis of lard.

Table 5. Comparison of Regioisomeric Occupation of the *sn*-2 Position for Saturated (Palmitic) and Unsaturated (Oleic and Linoleic) Fatty Acids in Plant Oil (Sunflower) and Animal Fat (Lard)

regioisomeric pair	sunflower oil	lard
POP/OPP	100/0	8/92
OOP/OPO	98/2	12/88
PLP/LPP	100/0	1/99
LLP/LPL	97/3	9/91
OLP/LOP/OPL	63/36/1	3/12/85

the effect of mobile phase on the ratio of DG fragment ions is negligible. This way the lack or high prices of pure regioisomers can be overcome.

Analysis of Complex Natural Mixtures. The randomization process has been applied for sunflower, blackcurrant, olive, and palm oils and lard as a representative of animal fats. Retention times of all identified TGs in these samples are summarized in Supporting Information Table S1. The comparison of chromatograms before and after randomization (Figure 6) is useful for the verification of *sn*-2 determination, because the *sn*-2 occupation is truly random after the interesterification, as shown in randomization reactions of TG standard mixtures (Figure 5 and Supporting Information Figures S2 and S3). Table 3 shows the calculation of theoretical TG composition in the randomized mixture[28] applied for the real sample of sunflower oil with known fatty acid composition.[5] To keep reasonable the complexity of this table, only six main fatty acids are included in the calculation, while remaining fatty acids form about 1%, and they are referred as trace fatty acids. This calculation provides 56 combinations of TGs (neglecting regioisomers in this table), but 27 of them have negligible concentrations (<0.1%). The comparison of initial TG composition of sunflower oil with experimental and theoretical TG composition after the randomization is illustrated in Table 4. Good correlation between theoretical and experimental values

confirms that this model is applicable for the calculation of TG concentrations after the randomization on the condition that the initial fatty acid composition is correctly determined.

The generally accepted opinion is that unsaturated fatty acids (mainly linoleic) preferentially occupy the *sn*-2 position in plant oils, whereas it is just opposite for animal fats, where unsaturated fatty acids are found mainly in *sn*-1/3 positions. The established method for regiospecific determination is the enzymatic hydrolysis of whole plant oils or animal fats, which provides overall information on *sn*-2 average preference for all TGs found in this sample. In our work, a representative plant oil (sunflower—Figure 6) and animal fat (lard—Figure 7) are compared concerning the quantitative data for *sn*-2 preferences of fatty acids in intact TGs. Table 5 lists regioisomeric ratios of TGs composed of three common fatty acids (palmitic, oleic, and linoleic) occurring both in plant and animal samples. This is a clear quantitative proof based on the silver-ion separation of intact TGs that *sn*-2 occupation for saturated versus unsaturated fatty acids is selective with opposite preferences for plants and animals. The interesting example is TG composed of P, O, and L, where the *sn*-2 occupation preference for sunflower oil is in the order of increasing DB number (OLP/LOP/OPL = 63/36/1), but it is just opposite for the lard sample (OLP/LOP/OPL = 3/12/85). Peak area ratios are obtained using the reconstruction of suitable ion currents considering masses of coeluting peaks. The data for other analyzed plant oils (palm, olive, and blackcurrant oils—data not shown) are in agreement with this conclusion. The knowledge of *sn*-2 preference in TGs is very important due to the bioavailability of particular fatty acids, because human lipases first cleave fatty acids in *sn*-1/3 positions and therefore fatty acids present in the *sn*-2 position can be worse accessible for the human organism.

CONCLUSIONS

Silver-ion chromatography is a powerful method for the analysis of TG regioisomers found in plant oils and animal fats. The optimization of HPLC conditions together with the coupling of three 25 cm silver-ion ChromSpher Lipids columns in series provides the best separation selectivity reported so far for the regioisomeric analysis of TGs enabling the determination of individual regioisomeric ratios for TGs found in natural samples. In this work, our HPLC/APCI-MS has enabled the identification of 196 TGs containing 0−11 DBs and fatty acid chain length from 14 to 24 carbon atoms. The comparison of representative plant oil (sunflower) and animal fat (lard) provides quantitative data (Table 5) for the preferential occupation of the *sn*-2 position by unsaturated fatty acids in plant oils and saturated fatty acids in animal fats. The randomization is used here as a new approach for the generation of regioisomeric standards of TGs. The randomization of selected plant oils shows that there is a clear preference of certain fatty acid combinations and regioisomeric order in TGs before the randomization process, whereas the TG composition after the randomization is truly random. The position of fatty acids on the glycerol skeleton is very important from the nutrition point of view, and the presented method can contribute to this area, because the absence of reliable quantitative methods applicable for complex natural and biological samples limits such research.

ACKNOWLEDGMENT

This work was supported by the Grant Project No. MSM-0021627502 sponsored by the Ministry of Education, Youth and Sports of the Czech Republic and Project Nos. 203/06/0219 and 203/09/P249 sponsored by the Czech Science Foundation.

SUPPORTING INFORMATION AVAILABLE

Additional information as noted in text. This material is available free of charge via the Internet at http://pubs.acs.org.

Received for review January 21, 2009. Accepted March 23, 2009.

AC900150J

analytical chemistry

Article

pubs.acs.org/ac

Characterization of Triacylglycerol Enantiomers Using Chiral HPLC/APCI-MS and Synthesis of Enantiomeric Triacylglycerols

Miroslav Lísa* and Michal Holčapek

Department of Analytical Chemistry, Faculty of Chemical Technology, University of Pardubice, Studentská 573, 53210 Pardubice, Czech Republic

Supporting Information

ABSTRACT: In this work, the first systematic characterization of triacylglycerol (TG) enantiomers in real samples using chiral high-performance liquid chromatography (HPLC) with atmospheric pressure chemical ionization mass spectrometry (APCI-MS) is performed. Our chiral HPLC/APCI-MS method is based on the use of two cellulose-tris-(3,5-dimethylphenylcarbamate) columns connected in series using a gradient of hexane-2-propanol mobile phase. All TG enantiomers containing 1−8 DBs and different fatty acyl chain lengths are separated using our chiral HPLC method except for TGs having a combination of saturated and di- or triunsaturated fatty acyls in *sn*-1 and *sn*-3 positions. In our work, the randomization reaction of monoacyl TG standards is used for the preparation of all TG enantiomers and regioisomers in a mixture, while the stereospecific esterification of 1,2- or 2,3-isopropylidene-*sn*-glycerols by selected fatty acids is used for the synthesis of TG enantiomers. The composition of TG enantiomers and regioisomers in hazelnut oil and human plasma samples is determined. Unsaturated fatty acids are preferentially esterified in *sn*-2 position in hazelnut oil, while no significant preference of saturated or unsaturated fatty acyls is observed in case of human plasma sample. Fatty acids with the higher number of DBs are preferred in *sn*-1 position of TG enantiomers in hazelnut oil unlike to moderate *sn*-3 preference in human plasma. The characterization of cholesteryl esters from TG fraction of human plasma sample using our chiral HPLC/APCI-MS method is presented as well.

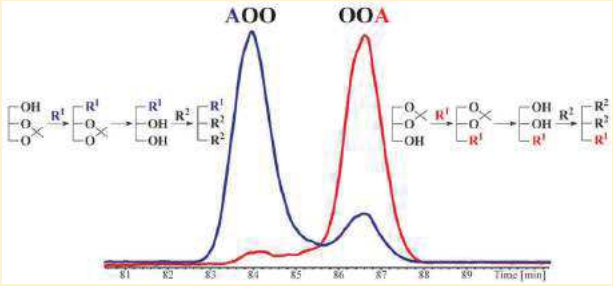

Triacylglycerols (TGs) are important components of human diet used as a source of energy, fatty acids (including essential ones), fat soluble vitamins, and other nonpolar compounds. The variety of TG species is enormous due to a high number of fatty acids present in natural samples. They differ in fatty acyl chain lengths, number, positions, and cis-/trans- configuration of double bonds (DBs) and their position on the glycerol skeleton (regioisomers, enantiomers), all having great differences in their biological and nutritional properties. Nonaqueous reversed-phase (NARP) and silver-ion HPLC/MS represent the most widespread analytical techniques used for the characterization of natural TG mixtures. NARP-HPLC enables the separation of tens to hundreds TGs in natural samples[1−12] according to their equivalent carbon number (ECN)[3−6,9] even with the separation of cis-/trans-isomers,[13−15] DB positional isomers,[16−19] and linear/branched isomers.[15,20] Silver-ion chromatography provides the separation of TGs mainly according to their degree of unsaturation,[21−28] DB positional isomers[25,26] and cis-/trans-isomers.[13,21,23] Moreover, regioisomers can also be resolved under carefully optimized chromatographic conditions.[13,21,26] Good orthogonality of NARP and silver-ion chromatographic modes is used in two-dimensional HPLC in online[29−31] or off-line[13,32] setup for the characterization of complex TG mixtures. Gas chromatography with liquid stationary phase[33] can be also applied for the characterization of complex mixtures of cis-/trans-isomers as their fatty acid methyl esters. The prevailing fatty acid in *sn*-2 position can be determined using atmospheric pressure chemical ionization (APCI)[6,14,28,34] due to the lower relative abundance of fragment ion $[M+H-R^2COOH]^+$ formed by the neutral loss of fatty acid from this position.

The stereospecific analysis of individual TGs represents a challenging task in the lipidomics due to different stereoavailability of fatty acyls in the stereospecific environment of human body. The stereospecific analysis using silver-ion HPLC or APCI mass spectra enables the determination of fatty acids in *sn*-2 position (TG regioisomers), but without the resolution of *sn*-1 and *sn*-3 positions for TG enantiomers. Nowadays, the analysis of TG enantiomers is usually performed using chemical derivatization methods or chiral HPLC after their partial hydrolysis to diacylglycerols (DGs) by *sn*-1/3 stereoselective pancreatic lipase[35,36] or more often by Grignard reagent[37−39] without the specificity to any fatty acid and less fatty acyl migration. The chemical derivatization method uses the conversion of formed DGs to different derivatives (e.g., phospholipids[35]) followed by another *sn*-2 specific hydrolysis (e.g., using phospholipase A). Drawbacks of stereospecific

Received: November 7, 2012
Accepted: January 8, 2013
Published: January 8, 2013

   dx.doi.org/10.1021/ac303237a | *Anal. Chem.* 2013, 85, 1852−1859

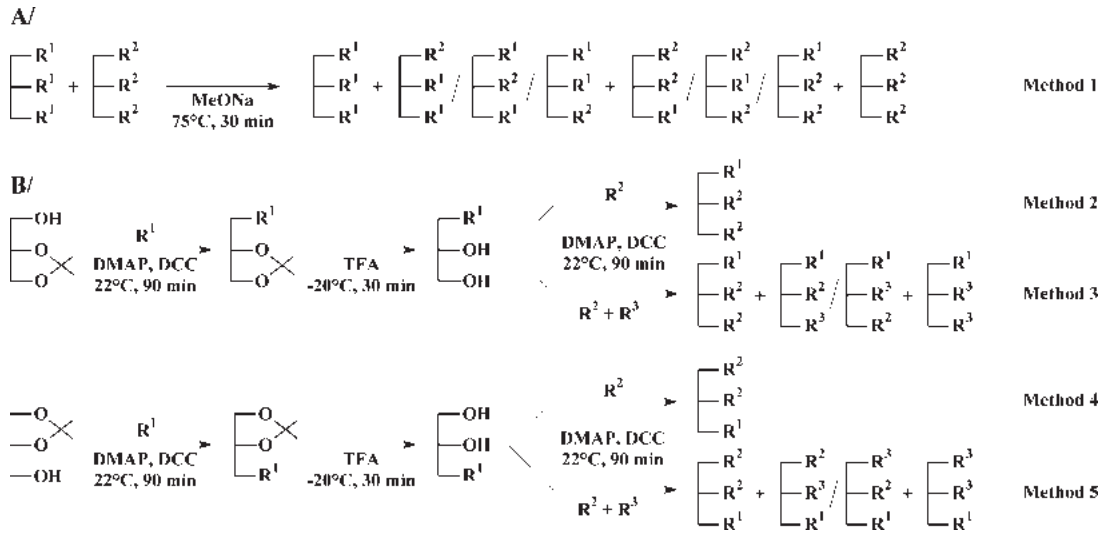

Figure 1. Scheme of synthetic procedures used for the preparation of triacylglycerol isomers: A/synthesis of the mixture of triacylglycerol regioisomers and enantiomers using the randomization reaction of monoacyl triacylglycerol standards, B/synthesis of enantiomers using the stereospecific esterification of 1,2- and 2,3-isopropylidene-*sn*-glycerols. MeONa, sodium methoxide; DMAP, 4-dimethylaminopyridine; DCC, dicyclohexylcarbodiimide; TFA, trifluoroacetic acid; R^1, R^2, R^3, different fatty acids esterified on the glycerol skeleton.

analysis using the chemical derivatization are laborious and time-consuming derivatization steps with a potential risk of fatty acyl migration strongly depending on reaction conditions.

The chiral HPLC uses the derivatization of DGs with chiral agents to form diastereoisomers (e.g., diastereoisomeric naphthylethylurethanes[37,39,40] or phenylethylcarbamates[36]), which can be easily separated using the conventional silicagel column in nonchiral normal-phase HPLC systems. Nonchiral agents can be used to form chiral derivatives (e.g., 3,5-dinitrophenylurethanes[38,41−43]), which are easily resolved using the chiral column. Intact DGs[44] or monoacylglycerols (MGs)[45−47] can also be directly separated by chiral HPLC without any derivatization. No systematic study of retention behavior of intact TG enantiomers or the analysis of real samples by chiral HPLC have been published so far. Polysaccharide-based chiral HPLC column with cellulose-tris-3,5-dimethylphenylcarbamate coated on the silicagel as a stationary phase and hexane-2-propanol mobile phase have been used for the separation of two pairs of intact TG enantiomers,[48] but only with fatty acyls with a great difference in the fatty acyl chain length and saturation degree (combination of two C8:0 with C20:5 or C22:6 fatty acyls). Such combinations do not occur in nature, where C16 and C18 fatty acyls with 0 to 3 DBs are strongly prevailing. The same column with methanol as the mobile phase has been used with so-called recycle chromatography for the partial separation of three TG enantiomeric pairs with retention times in the range of 150−190 min.[49] A great challenge in the stereospecific analysis of TGs is the lack of commercial standards of TG enantiomers. These standards are usually synthesized in the laboratory, which involves laborious synthesis in several steps using glycerol with blocked hydoxyl groups in specific positions, that is, 1,2- and 2,3-isopropylidene-*sn*-glycerols.[50,51]

The main goal of our work is the development of chiral HPLC/APCI-MS method for the analysis of TG enantiomers using polysaccharide based chiral HPLC columns. Two different approaches for the synthesis of TG standards are developed based on the randomization reaction and stereospecific esterification of glycerol applied for the synthesis of wide range of TG regioisomers and enantiomers used for the characterization of their retention behavior in the chiral HPLC. The developed method is applied for the stereospecific analysis of TGs in biological samples and preferences of individual fatty acyls in specific positions are discussed as well.

EXPERIMENTAL SECTION

Materials. Hexane, dichloromethane, chloroform (all HPLC grade), 2-propanol (HPLC/MS grade), methanol (HPLC gradient grade), sodium methoxide, sodium hydroxide, 1,2-isopropylidene-*sn*-glycerol, and 2,3-isopropylidene-*sn*-glycerol, 4-dimethylaminopyridine (DMAP), dicyclohexylcarbodiimide (DCC), and trifluoroacetic acid (TFA) (99%) were purchased from Sigma-Aldrich (St. Louis, MO, USA). The model mixture of TG standards GLC#435 (all saturated monoacyl TGs from C7:0 to C22:0), tripalmitin (PPP, C16:0), tristearin (SSS, C18:0), triarachidin (AAA, C20:0), trielaidin (EEE, Δ*9t*-C18:1), tripetroselinin (PePePe, Δ*6*-C18:1), tri-*cis*-vaccenin (cVacVacVa, Δ*11*-C18:1), triolein (OOO, Δ*9*-C18:1), trilinolein (LLL, Δ*9,12*-C18:2), trilinolenin (LnLnLn, Δ*9,12,15*-C18:3), trigamma-linolenin (γLnγLnγLn, Δ*6,9,12*-C18:3), and palmitic (P, C16:0), stearic (S, C18:0), arachidic (A, C20:0), oleic (O, Δ*9*-C18:1), linoleic (L, Δ*9,12*-C18:2), and linolenic (Ln, Δ*9,12,15*-C18:3) acids were purchased from Nu-ChekPrep (Elysian, MN, USA).

Sample Preparation. The fraction of TGs from plasma sample was collected after the HILIC separation of total lipid extract prepared using chloroform−methanol−water extraction procedure[52] (see Supporting Information). TGs from hazelnuts were extracted using hexane[7] (see Supporting Information). The samples were dissolved in hexane at the appropriate concentration before the HPLC analysis.

Synthesis of TG Isomers Using the Randomization Reaction. Mixtures of TG enantiomers and regioisomers with equal molar concentrations were prepared from monoacyl TG standards (i.e., AAA, OOO, LLL, etc.) using the randomization procedure[26] (Figure 1**A**, Method 1). Twenty mg of each TG standard and 100 mg of sodium methoxide were weighed into a

dx.doi.org/10.1021/ac303237a | *Anal. Chem.* 2013, 85, 1852−1859

Table 1. Composition of Triacylglycerols in Synthesized Randomization Mixtures According to Method 1 Described in Figure 1

randomization mixture	composition of triacylglycerols[a]
AAA/OOO/LnLnLn	AAA; AAO/AOA/OAA; AOO/OAO/OOA; OOO; ALnA/AALn/LnAA; ALnO/OLnA/LnAO/LnOA/AOLn/OALn; OLnO/LnOO/OOLn; LnLnA/ALnLn/LnALn; LnLnO/OLnLn/LnOLn; LnLnLn
OOO/LLL/LnLnLn	OOO; OLO/LOO/OOL; OLnO/LnOO/OOLn; LLO/OLL/LOL; LLnO/LnLO/OLnL; LnOL/OLLn/LOLn; LLL; LnLnO/OLnLn/LnOLn; LnLL/LLnL/LLLn; LnLnL/LLnLn/LnLLn; LnLnLn
PPP/LLL/OOO	PPP; PPO/POP/OPP; POO/OPO/OOP; OOO; PLP/LPP/PPL; PLO/OLP/POL/LOP/LPO/OPL; OLO/LOO/OOL; LLP/PLL/LPL; LLO/OLL/LOL; LLL
SSS/LLL	SSS; SSL/SLS/LSS; SLL/LLS/LSL; LLL
PPP/LLL	PPP; PLP/LPP/PPL; LLP/PLL/LPL; LLL

[a]Sorted according to retention times in our chiral HPLC/APCI-MS method.

dry boiling flask with the addition of 2 mL of hexane dried with molecular sieves. The mixture was heated at 75 °C for 30 min in water bath under the reflux.Then, the mixture was extracted with water and methanol to remove sodium methoxide. The hexane phase containing synthesized TGs was evaporated using the gentle stream of nitrogen and redissolved before the HPLC/MS analysis in hexane at the appropriate concentration.

Stereospecific Synthesis of TG Enantiomers. TG enantiomers of $R^1R^2R^2$ (Method 2)/$R^2R^2R^1$ (Method 4) type and enantiomers with mixed fatty acyls $R^1R^2R^3$ (Method 3)/$R^3R^2R^1$ (Method 5) (Figure 1B) were synthesized from 1,2- and 2,3-isopropylidene-*sn*-glycerols. Ten milligrams of 1,2- or 2,3-isopropylidene-*sn*-glycerol, 20 mg of fatty acid, 10 mg of DMAP and 15 mg of DCC in 1 mL of dichlormethane were stirred in a vial for 1.5 h at ambient temperature. Then, residual hydroxyl groups in glycerol were deprotected by the reaction with 0.25 mL of ice cold TFA for 30 min at −20 °C and then TFA was neutralized with 2 mL of 2 mol/L ice cold sodium hydroxide. Formed MGs were extracted from the reaction mixture using 3 mL of chloroform - methanol (4:1, v/v) mixture and the chloroform layer was evaporated using the gentle stream of nitrogen. Prepared 1-MG (Methods 2 and 3) or 3-MG (Methods 4 and 5) were stirred with the total amount of 40 mg of fatty acids (one fatty acid in the case of Methods 2 and 4 or more fatty acids for Methods 3 and 5), 20 mg of DMAP and 30 mg of DCC in 1 mL of dichlormethane for 1.5 h at ambient temperature. Synthesized TG enantiomers were extracted from the reaction mixture using hexane, evaporated using the gentle stream of nitrogen and redissolved before the HPLC/MS analysis in hexane at the appropriate concentration.

Chiral HPLC/APCI-MS. HPLC experiments were performed on a liquid chromatograph Agilent 1200 Series (Agilent Technology, Waldbronn, Germany). The final HPLC method for analyses of TGs used the following conditions: two chiral chromatographic columns Lux Cellulose-1 with cellulose-tris-(3,5-dimethylphenylcarbamate) coated silicagel as the stationary phase (250 mm × 4.6 mm, 3 μm, Phenomenex, Torrance, CA, U.S.A.) connected in series, the flow rate 1 mL/min, the injection volume for standard mixtures and analyzed samples 1 μL, column temperature 35 °C and the mobile phase gradient: 0 min −90% A + 10% B, 180 min 60% A + 40% B, where A is hexane and B is hexane-2-propanol (99:1, v/v) mixture. The column was conditioned 60 min before each analysis to achieve good reproducibility. The ion trap analyzer Esquire 3000 (Bruker Daltonics, Bremen, Germany) with positive-ion APCI was used in the mass range m/z 50−1200 with the following setting of tuning parameters: pressure of the nebulizing gas 50 psi, drying gas flow rate 3 L/min, temperatures of the drying gas and APCI heater 350 and 400 °C, respectively. Reconstructed ion current chromatograms of protonated molecules and fragment ions were used to support the identification and integration of coeluting peaks.

Definition of Abbreviations. Identified TG species were annotated using initials of fatty acid trivial names sorted according to their stereochemical positions (*sn*-1, *sn*-2, and *sn*-3), for example, 1-octadec-9-enoyl-2-octadeca-9,12-dienoyl-3-hexadecanoyl-*sn*-glycerol was annotated as OLP. Abbreviations of fatty acids: M, myristic (C14:0); P, palmitic (C16:0); Po, palmitoleic (Δ9-C16:1); Ma, margaric (C17:0); S, stearic (C18:0); Pe, petroselinic (Δ*6*-C18:1); O, oleic (Δ*9*-C18:1); E, elaidic (Δ*9t*-C18:1); cVa, *cis*-vaccenic (Δ*11*-C18:1); L, linoleic (Δ*9,12*-C18:2); Ln, linolenic (Δ*9,12,15*-C18:3); γLn, gamma-linolenic (Δ*6,9,12*-C18:3); A, arachidic (C20:0).

RESULTS AND DISCUSSION

Synthesis of TG Standards. Two different synthetic procedures are applied for the preparation of TG isomers in this work as shown in Figure 1. The randomization reaction (Method 1, Figure 1A) of monoacyl TG standards catalyzed by sodium methoxide is used for the synthesis of all enantiomeric and regioisomeric TGs in one mixture based on our previously developed randomization procedure.[26] During the randomization process, individual fatty acyls in TGs are randomly distributed by inter- and intraesterification on the glycerol skeleton providing TGs with a random combination of fatty acyls including their regioisomers and enantiomers (Table 1). Figure 2A shows a chiral HPLC separation of randomization mixture prepared from AAA, OOO, and LnLnLn standards. The randomization reaction provides an equimolar mixture of all TG isomers due to the random distribution of fatty acyls without any visible preference of individual fatty acids. Various randomization mixtures of TGs containing fatty acyl chain lengths with 16, 18, and 20 carbon atoms and the number of DBs from 0 to 3 have been prepared. These mixtures have been applied for the optimization of chiral HPLC method and the characterization of retention behavior of TG isomers (Figure 2A and Supporting Information Figures S-1 and S-2).

Although the randomization reaction is very simple and fast method for the synthesis of both types of isomers, it provides only their mixture and individual enantiomers have to be identified based on retention times of individual standards. Figure 1B shows a scheme of the synthesis of TG enantiomers based on the stereospecific esterification of free hydroxyl groups in 1,2- and 2,3-isopropylidene-*sn*-glycerols with protected hydroxyl groups in *sn*-1,2 or *sn*-2,3 positions, respectively. In the first step, the free hydroxyl group of isopropylidene is esterified with selected fatty acid (R^1) catalyzed by DMAP and DCC coupling agents. Then, protected hydroxyl groups are hydrolyzed using TFA acid at low temperature (−20 °C) yielding optically pure 1-MG

dx.doi.org/10.1021/ac303237a | *Anal. Chem.* 2013, 85, 1852−1859

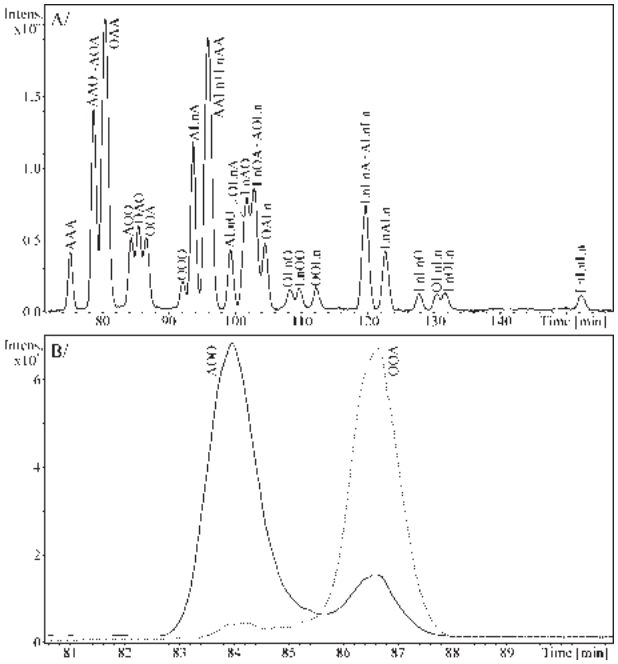

Figure 2. Comparison of chiral HPLC/APCI-MS chromatograms of synthesized triacylglycerol standards: A/mixture of all triacylglycerol isomers prepared by the randomization reaction of AAA, OOO, and LnLnLn standards according to Method 1, B/overlay of chromatograms of AOO and OOA enantiomers synthesized by the stereospecific esterification of 2,3- and 1,2-isopropylidene-*sn*-glycerols according to Methods 2 and 4, respectively. HPLC conditions: two Lux Cellulose-1 columns (250 mm × 4.6 mm, 3 μm, Phenomenex) connected in series, flow rate 1 mL/min, column temperature 35 °C, gradient 0 min −90% A + 10% B, 180 min 60% A + 40% B, where A is hexane and B is a mixture of hexane-2-propanol (99:1, v/v).

(Methods 2 and 3) or 3-MG (Methods 4 and 5). These MGs are esterified in the next step with another fatty acid (R^2, Methods 2 and 4) providing TG enantiomers. TG enantiomers composed from two different fatty acyls are prepared by this procedure (Figure 2B). Mixed-acyl TG enantiomers are obtained, if two or more fatty acids are added in the second esterification step (Methods 3 and 5). These TGs (Figure 3) are composed from selected fatty acyl (R^1) in *sn*-1 (Method 3) or *sn*-3 (Method 5) positions and randomly distributed fatty acyls (R^2 + R^3) on remaining *sn*-2,3 or *sn*-1,2 hydroxyl groups, respectively. The set of 8 mixtures of enantiomeric mixed-acyl TGs (Figure 3 and Supporting Information Figures S-3−S-5) has been prepared by this procedure from stearic, oleic, linoleic, and linolenic acids as C18 fatty acids with 0−3 DBs covering a wide range of most common combinations of fatty acids in natural TG samples. Individual fatty acids are first specifically esterified in *sn*-1 or *sn*-3 position and after the deprotection step an equimolar mixture of selected fatty acids is added for the random esterification of remaining hydroxyl groups. Table 2 shows a composition of synthesized mixtures of enantiomeric mixed-acyl TGs using this procedure (Methods 3 and 5).

A special attention have to be given to reaction conditions to prevent the fatty acyl migration during the synthesis. Low temperature of deprotection step is crucial for the prevention of fatty acyl migration on the glycerol skeleton. If deprotection temperature is higher or reagents are not properly cooled before the reaction, increased rate of fatty acyl migration is

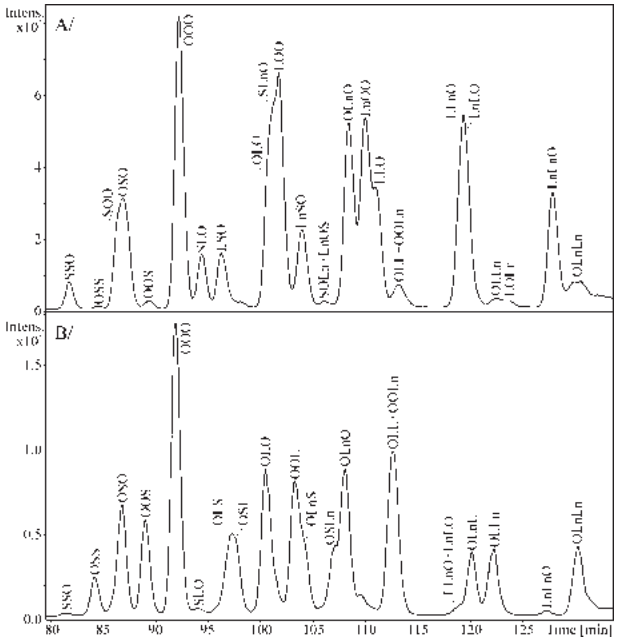

Figure 3. Chiral HPLC/APCI-MS chromatograms of synthesized mixtures of enantiomeric triacylglycerols of R^1R^2O type (A/Method 5) and OR^2R^3 type (B/Method 3), where R^i are randomly distributed stearic (S), oleic (O), linoleic (L) and linolenic (Ln) acyls in *sn*-1/2 or *sn*-2/3 positions. HPLC conditions are identical as for Figure 2.

Table 2. Composition of Enantiomeric Triacylglycerols in Mixtures Synthesized by Stereospecific Esterification of 1,2- and 2,3-Isopropylidene-*sn*-glycerols According to Method 3 and 5 Described in Figure 1

general triacylglycerol formula[a]	composition of triacylglycerols[b]
SR^2R^3	SSS; SSO/SOS; SOO; SSL/SLS; SLO/SOL; SLnS/SSLn; SLnO/SOLn; SLL; SLnL/SLLn; SLnLn
R^1R^2S	SSS; SOS/OSS; OOS; SLS/LSS; OLS/LOS; SLnS/LnSS; OLnS/LnOS; LLS; LLnS/LnLS; LnLnS
OR^2R^3	OSS; OSO/OOS; OOO; OLS/OSL; OLO/OOL; OLnS/OSLn; OLnO/OOLn; OLL; OLnL/OLLn; OLnLn
R^1R^2O	SSO; SOO/OSO; OOO; SLO/LSO; OLO/LOO; SLnO/LnSO; OLnO/LnOO; LLO; LLnO/LnLO; LnLnO
LR^2R^3	LSS; LSO/LOS; LOO; LLS/LSL; LLO/LOL; LLnS/LSLn; LLnO/LOLn; LLL; LLnL/LLLn; LLnLn
R^1R^2L	SSL; SOL/OSL; OOL; SLL/LSL; OLL/LOL; SLnL/LnSL; OLnL/LnOL; LLL; LnLL/LLnL; LnLnL
LnR^2R^3	LnSS; LnSO/LnOS; LnOO; LnLS/LnSL; LnLO/LnOL; LnLnS/LnSLn; LnLnO/LnOLn; LnLL; LnLnL/LnLLn; LnLnLn
R^1R^2Ln	SSLn; SOLn/OSLn; OOLn; SLLn/LSLn; OLLn/LOLn; SLnLn/LnSLn; OLnLn/LnOLn; LLLn; LLnLn/LnLLn; LnLnLn

[a] R^1, R^2, R^3 = different fatty acyls in *sn*-1, 2, 3 positions including S, stearic; O, oleic; L, linoleic; and Ln, linolenic acyls. [b] Sorted according to retention times in our chiral HPLC/APCI-MS method.

observed, which may result in the racemic mixture of both isomers. The optical purity of synthesized TG enantiomers under optimized reaction conditions is sufficient to obtain retention times of individual isomers and in most cases it is better than 93%.

Chiral HPLC/APCI-MS Analysis. The chiral polysaccharide column packed with cellulose-tris-(3,5-dimethylphenylcarba-

dx.doi.org/10.1021/ac303237a | *Anal. Chem.* 2013, 85, 1852−1859

mate) selector has been used for this study as the most promising chiral stationary phase for the separation of nonpolar TG enantiomers based on literature[48,49] and manufacturers information. The separation in normal-phase mode is selected due to nonpolar character of TGs and their low solubility in polar solvents typical for the reversed-phase mode. The careful optimization of chromatographic conditions has been done with the goal to achieve the best separation of chiral isomers (regardless the analysis time) including the optimization of column length, separation temperature, mobile phase and gradient composition. The change of separation temperature (Supporting Information Figure S-6) does not show any significant trend in the chromatographic resolution of TGs unlike to NARP-HPLC analysis of TGs, where the chromatographic resolution increases with decreasing separation temperature.[9] The best separation of individual isomers is achieved at 35 °C (Supporting Information Figure S-6C). Hexane-based mobile phases with acetonitrile, 2-propanol and their mixtures have been tested (Supporting Information Figures S-7 and S-8). The hexane-2-propanol mobile phase (Supporting Information Figure S-7A) shows the best separation of TG isomers. Hexane−acetonitrile−2-propanol (Supporting Information Figure S-7B) and hexane−acetonitrile (Supporting Information Figure S-8) phases provide similar chromatographic separation as hexane-2-propanol mobile phase for TG isomers with 5−7 DBs, but enantiomeric pairs with 1 to 3 DBs are not separated at all.

The concentration of 2-propanol in the mobile phase and gradient steepness strongly influence retention times of TGs and also their chromatographic resolution. The final change of 2-propanol concentration in our gradient is 0.1%/hour, therefore, the precision of mobile phase preparation is especially important to achieve a good reproducibility of retention times of TGs using chiral HPLC. The column conditioning for 60 min with a flow rate of 1 mL/min is used between two runs, because it also shows a significant effect on the chromatographic reproducibility. The final chiral HPLC method provides retention times of TGs (Supporting Information Table S-1) with a standard deviation typically lower than 1.5 min among different days, which is still acceptable for the analysis in normal-phase mode and retention times up to 150 min.

Molecular weights and esterified fatty acyls of TGs are identified based on both protonated molecules and fragment ions in their positive-ion APCI mass spectra. TG regioisomers and enantiomers provide the same APCI mass spectra, but differences in relative abundances of fragment ions can be used for the differentiation of regioisomers (Supporting Information Figure S-9) based on well-known fact that the neutral loss of fatty acid from *sn*-2 position is less preferred.[6,14,28,34] For example, the ratio of fragment ions $[OO]^+/[AO]^+$ = 15/100 for OAO regioisomer (Supporting Information Figure S-9A) is lower due to the loss of arachidic acid from the *sn*-2 position compared to 43/100 for AOO (Supporting Information Figure S-9B) and 40/100 for OOA (Supporting Information Figure S-9C) enantiomers. On the other hand, negligible differences in the range of several percent are observed for the relative abundance of fragment ions of enantiomers, which is not sufficient for their differentiation and is attributed to common experimental variation of relative abundances, for example, $[OO]^+/[AO]^+$ = 43 ± 5/100 for AOO (Supporting Information Figure S9-B) and 40 ± 6/100 for OOA (Supporting Information Figure S9-C) (data obtained from 4 consecutive runs). No measurable differences in ratios of relative abundances of protonated molecules vs fragment ions are observed for TG isomers. For this reason, individual TG enantiomers are synthesized for the determination of their retention order.

Retention Behavior of TGs in Chiral HPLC. Figure 4 shows the chiral HPLC/APCI-MS analysis of monoacyl TG

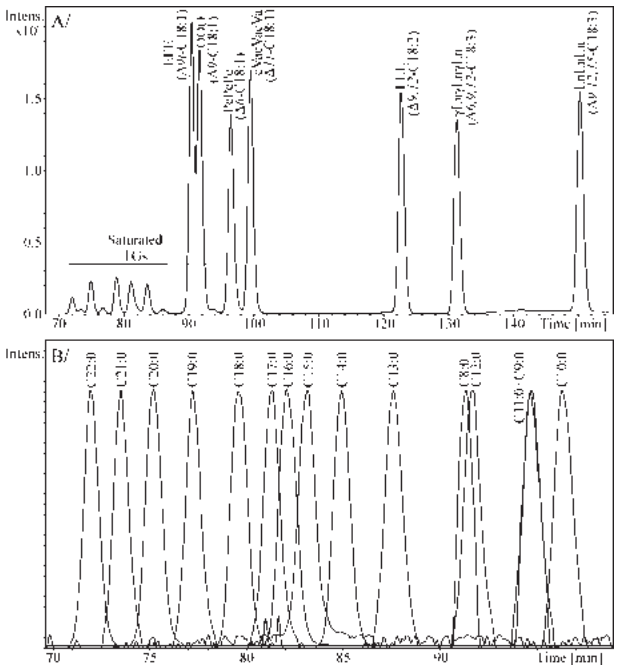

Figure 4. Effect of degree of unsaturation, double bonds configuration and position on the retention behavior of triacylglycerols in the chiral HPLC/APCI-MS analysis. A/Mixture of monoacyl triacylglycerol standards with saturated (from C8:0 to C22:0), monounsaturated (E, elaidic; O, oleic; Pe, petroselinic; cVa, *cis*-vaccenic), diunsaturated (L, linoleic), and triunsaturated (Ln, linolenic; γLn, gamma linolenic) fatty acyls, B/reconstructed ion current chromatograms of diacylglycerol fragment ions $[R^1R^1]^+$ of saturated triacylglycerols. HPLC conditions are identical as for Figure 2.

standards with saturated fatty acyls from C8:0 to C22:0 and C18 unsaturated fatty acyls containing 1 to 3 DBs with the different cis-/trans-configuration (Δ9-C18:1-OOO/EEE) and the position (C18:1-PePePe/OOO/cVacVacVa and C18:3-γLnγLnγLn/LnLnLn) of DBs. In general, the retention of TGs is governed by the number of DBs and their retention times increase with increasing number of DBs in fatty acyls. Retention times of TGs also strongly depend on cis-/trans-configuration of DBs, positions of DBs and lengths of fatty acyl chains. EEE (t_R = 90.2 min) with trans-configuration of DBs have slightly lower retention time compared to OOO (t_R = 91.7 min) with cis-configuration, which is the same pattern as observed for silver-ion HPLC,[13,21,23] but the difference between retention times of both isomers is significantly lower. All DB positional isomers with C18:1 and C18:3 fatty acyls are baseline separated, but their retention order cannot be predicted as the dependence on the increasing or decreasing distance of the first DB from the carbonyl group unlike to other chromatographic modes. In silver-ion HPLC, TG positional isomers elute in the order Δ*11*-C18:1 < Δ*9*-C18:1 < Δ6-C18:1 and Δ*9,12,15*-C18:3 < Δ*6,9,12*-C18:3 (ref 28 and our unpublished

dx.doi.org/10.1021/ac303237a | *Anal. Chem.* 2013, 85, 1852−1859

data) compare to Δ9-C18:1 < Δ6-C18:1 < Δ11-C18:1 using chiral HPLC. Moreover, the reversed order of Δ6,9,12-C18:3 < Δ9,12,15-C18:3 positional isomers compared to Δ9-C18:1 < Δ6-C18:1 isomers is observed in the chiral HPLC. TGs are also partially separated according to fatty acyl chain lengths, as clearly demonstrated on the separation of saturated TGs (Figure 4B). Their retention times increase with decreasing fatty acyl chain length from C22:0 to C10:0 fatty acyls, but the retention order of shorter TGs is reversed, that is, C8:0 < C9:0 < C10:0. Unusual chromatographic behavior of TG positional isomers and TGs with different fatty acyl chain lengths is probably caused by the combination of different retention mechanisms in the chiral HPLC given by the column containing nonpolar chiral selector coated on silicagel stationary phase, where mechanisms of nonaqueous reversed-phase and normal-phase modes together with chiral interactions are combined. The accurate characterization of contributions of individual retention mechanism would require more systematic study on different chiral columns.

The separation of TG enantiomers using chiral HPLC is governed by the number of DBs of esterified fatty acyls in *sn*-1 and *sn*-3 positions without significant influence of fatty acyl in *sn*-2 position. In the case of enantiomeric pairs containing only one DB in *sn*-1 and *sn*-3 positions (i.e., combination of oleic and saturated fatty acyls), enantiomers with DB in *sn*-1 position have higher retention times compared to *sn*-3 position. For example, enantiomer OOA (86.5 min) with oleic acid in *sn*-1 position has higher retention time than AOO (84.3 min) isomer (Figure 2**A**). The effect of the number of DBs in *sn*-2 position on the separation of enantiomers can be demonstrated on the enantiomeric pair OLnA (101.0 min) and ALnO (98.9 min), where linolenic acyl with 3 DBs in *sn*-2 position has no significant effect on the retention of isomers and their difference in retention times (Δ 2.1 min) is the same as for OOA/AOO pair (Δ 2.2 min). TGs with three and more DBs in outer positions have the reversed retention order of isomers. The enantiomer with fatty acyl containing more DBs in *sn*-3 position has higher retention time compared to *sn*-1 position, for example, OALn (t_R = 104.3 min) with linolenic acid in *sn*-3 position has higher retention time compared to LnAO (101.2 min), OOLn (112.5 min) compared to LnOO (109.3 min), etc. All enantiomers are at least partially separated except for some TGs having combinations of saturated and di- (linoleic) or triunsaturated (linolenic) fatty acyls in *sn*-1 and *sn*-3 positions, without visible separation, that is, LPP/PPL, LOP/POL, LLP/PLL, AALn/LnAA, LnOA/AOLn and LnLnA/ALnLn enantiomeric pairs. On the other hand, TGs with the combination of monounsaturated and saturated fatty acyls in *sn*-1/3 positions are well separated, for example, AAO (78.6 min)/OAA (80.3), AOO (84.3)/OOA (86.5), etc. The fatty acyl chain length has also a partial effect on the separation of enantiomers, as illustrated on TG enantiomers containing palmitic or stearic acyls in the combination with linoleic acyl (Supporting Information Figure S-2). PPL/LPP and LLP/PLL enantiomeric pairs (Supporting Information Figure S-2B) are not separated at all unlike to SSL/LSS and SLL/LLS pairs (Supporting Information Figure S-2A), which are partially separated. The complex retention behavior can be demonstrated on enantiomeric pairs composed from three fatty acyls having identical fatty acyl composition, but in different stereochemical positions. For example, enantiomers in the randomization mixture prepared from AAA, OOO, and LnLnLn elute in the order ALnO (98.9 min, higher number of DB in *sn*-3 position) < OLnA (101.0, *sn*-1), LnAO (101.2, *sn*-1) < OALn (104.3, *sn*-3), and LnOA (102.8, *sn*-1) = AOLn (*sn*-3) (Figure 2**A**). The retention behavior of TG enantiomers in the chiral HPLC is rather complex and cannot be generalized for all isomers, therefore the use of identical standards for the initial identification of all enantiomers is essential. For this reason, individual enantiomeric isomers presented in analyzed samples are synthesized in this work to confirm their retention order.

Analysis of Real Samples. The developed chiral HPLC/APCI-MS method is applied for the characterization of composition of TG isomers in natural samples represented by plant (hazelnut oil) and human (plasma) samples. Figure 5 shows chiral HPLC/APCI-MS chromatograms of hazelnut oil and human plasma samples with identified TG isomers. TGs marked by asterisk mean that the determination of enantiomer is not unambiguous due to the coelution of both isomers (e.g., LOP* and LLP* in hazelnut oil) or missing identical standard for low abundant TGs (e.g., SPP*, SPO*, and OSP* in the plasma sample). For these TGs, fatty acyls in *sn*-2 positions are identified based on APCI mass spectra and fatty acyls in *sn*-1 and *sn*-3 positions are arranged according to decreasing molecular masses, that is, LPP, LOP, LLP, etc. In total, 19 (hazelnut oil) and 26 (human plasma) TGs including enantiomers and regioisomers are identified. The number of identified TGs in analyzed samples is lower compared to our previous NARP-HPLC/MS and 2D-HPLC/MS methods, that is, 30 TG species have been identified in hazelnut oil NARP-HPLC/MS.[10] On the other hand, these methods do not provide any information about the enantiomeric composition. The lower number of identified TGs can be probably explained by the fact that small peaks of trace TGs are further resolved into individual stereoisomers resulting in the decrease of their

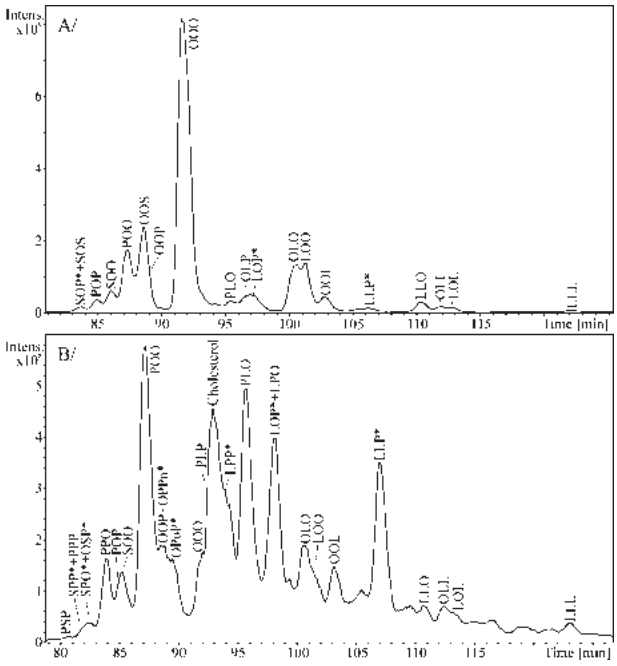

Figure 5. Chiral HPLC/APCI-MS chromatograms of: A/hazelnut oil, and B/human plasma samples. HPLC conditions are identical as for Figure 2. TGs marked by asterisk mean that the determination of enantiomer is not unambiguous because of the coelution of both isomers or missing identical standard for low abundant TGs.

dx.doi.org/10.1021/ac303237a | *Anal. Chem.* 2013, 85, 1852−1859

peak areas. In complex biological samples, these small peaks can be overlapped by peaks of more abundant TGs. The next step will be the use of two-dimensional HPLC (NARP × chiral), which should yield the same number of identified TGs together with their enantiomeric resolution. Ionization efficiencies of enantiomers are identical, therefore peak ratios of resolved enantiomers correspond to their concentration ratios.

Cholesterol and 12 cholesteryl esters (CEs) containing 9 fatty acyls are identified in TG fraction from the total lipid extract of human plasma sample (Supporting Information Figure S-10 and Table S-2) because of the coelution of cholesterol and CEs with TGs in the HILIC mode used for the fractionation. CE species are annotated by the carbon number (CN) and the number of DBs (CN:DB-CEs) without the identification of DB position in fatty acyl chains or the chirality of sterol part, which is not the goal of this work. Individual fatty acyls are identified based on the neutral loss of corresponding fatty acid providing the most abundant fragment ion in positive-ion APCI mass spectra of CEs (Supporting Information Figure S-11). The relative abundance of protonated molecules in APCI spectra of CEs strongly depends on the saturation degree of esterified fatty acyls and it is higher for unsaturated fatty acyls (4% for C18:2-CE and 10% for C20:4-CE), while $[M + H]^+$ ion is completely missing for monounsaturated and saturated fatty acyls. Molecular weights of these CEs are determined based on potassium adducts $[M + K]^+$. The adduct of molecule with the fragment ion m/z = 369 is also observed for CEs with unsaturated fatty acyls (e.g., Supporting Information Figure S-11). The most abundant CEs in human plasma are C18:2-CE, C18:1-CE, and C16:0-CE. This corresponds with the fatty acid composition of identified TGs, where TGs containing L, O, and P acyls are also the most abundant species. CEs with the identical fatty acyl composition in different retention times are detected (Supporting Information Table S-2), that is, two species of C16:1-CE (t_R = 16.0 and 17.3 min), C18:1-CE (16.6 and 17.8 min), and C18:2-CE (20.1 and 27.0 min), but without the identification of the isomerism (cholesterol enantiomers or positional isomer of DBs) due to the lack of identical standards.

The relative abundance of TG enantiomers and regioisomers in hazelnut oil and human plasma is listed in Table 3. The sum of peak areas from reconstructed ion chromatograms of fragment ions and protonated molecules is used for the determination of isomeric ratios, that is, the sum of $[M + H]^+$ at m/z 883 and fragment ions $[OO]^+$ at m/z 603 and $[OL]^+$ at m/z 601 is used for the determination of OLO, LOO, and OOL ratios. The ratio of coeluted enantiomers cannot be determined (e.g., LLP and PLL), because they provide the same fragment ions with comparable relative abundances. In the case of the coelution of enantiomers and regioisomers (e.g., POP and OPP in hazelnut oil and human plasma samples), the presence of regioisomer (OPP) in the peak can be confirmed or excluded based on the comparison of fragment ion ratio in the chromatographic peak with the ratio known for pure standards, that is, the ratio of fragment ions $[OP]^+/[PP]^+$ = 100:23 in hazelnut oil or 100:26 in plasma compared to 100:31 for POP and 100:75 for OPP standards exclude possible coelution of OPP isomer in the peak. If both isomers are present in the peak, the ratio of fragment ions is between these two values.

Table 3. Relative Ratios of Triacylglycerol Isomers in Hazelnut Oil and Human Plasma Samples Determined by Chiral HPLC/APCI-MS

triacylglycerol isomers	hazelnut oil	plasma
SSO/(SOS + OSS)	0/100 (SOS)[a]	0/0
PPO/(POP + OPP)	0/100 (POP)[a]	61/39 (POP)[a]
SOO/OSO/OOS	39/0/61	100/0/0
POO/(OPO + OOP)	54/46 (OOP)[a]	82/18 (OOP)[a]
PLP/(LPP + PPL)	0/0	23/77[b]
PLO/OLP/(POL + LOP + LPO)/OPL	27/29/44 (POL +LOP)[a,b]/0	55/0/45[b]/0
OLO/LOO/OOL	46/39/15	43/30/27
LPL/(LLP + PLL)	0/100[b]	0/100[b]
LLO/OLL/LOL	55/23/22	35/46/19

[a]Prevailing triacylglycerol isomer. [b]Relative ratios of these enantiomers cannot be determined due to the coelution.

TGs in both samples are composed mainly from P, O and L acyls with similar combinations in TGs, but their distribution in individual stereochemical positions is different (Table 3). The *sn*-2 position in hazelnut oil TGs is preferentially esterified by unsaturated fatty acyls, because no isomer with saturated fatty acyl in this position is identified. These results fit well with our previously published data on the sunflower oil using silver-ion HPLC.[15] Human plasma TGs contain both saturated and unsaturated fatty acyls in *sn*-2 position without a clear preference of one type. For example, groups of TG isomers PPO/POP/OPP = 61:39:0 and PLP/(LPP + PPL) = 23:77 show higher abundances of TGs containing saturated fatty acyls in *sn*-2 position (i.e., PPO and LPP+PPL) compared to groups POO/OPO/OOP = 82:0:18 and LPL/(LLP + PLL) = 0:100, where no isomers with saturated fatty acyls in *sn*-2 position are identified. Preferences in the esterification of fatty acyls in *sn*-1 and *sn*-3 positions are probably caused by the different selectivity of enzymes involved in the synthesis of TGs. Fatty acyls with the higher number of DBs are preferred in *sn*-1 position in hazelnut oil, while they are slightly preferred in *sn*-3 position in plasma, i.e., the ratio of enantiomers SOO/OOS = 39/61 in hazelnut oil and 100/0 in plasma, LOO/OOL = 39:15 and 30:27, and LLO/OLL = 55:33 and 35:46.

CONCLUSIONS

The first ever reported method for the routine chiral analysis of enantiomeric TGs in natural samples is presented here. This work opens new field of chiral lipidomic analysis, because differences between *sn*-1 and *sn*-3 positions have been neglected so far. Our chiral HPLC/APCI-MS method under optimized chromatographic conditions enables the separation of most TG enantiomers and regioisomers according to the DB composition of fatty acyls. Two different approaches are applied for the synthesis of TG isomers. The randomization reaction of monoacyl TG standards is applied for the preparation of mixtures of TG enantiomers and regioisomers, which are then used for the characterization of retention behavior. The synthesis of TG enantiomers even with mixed fatty acyls is developed for the determination of individual enantiomers using the stereospecific esterification of 1,2- or 2,3-isopropylidene-*sn*-glycerol. The optimized chiral HPLC/APCI-MS method is applied for the characterization of TG isomer composition in real samples represented by hazelnut oil and human plasma samples, where the preference of saturated or unsaturated fatty acyls in different positions is recognized. Unsaturated fatty acyls in *sn*-2 position and fatty acyls with a higher number of DBs in *sn*-1 position are preferred in hazelnut oil, while no significant preference of fatty acyl in *sn*-2 position and only moderate preference of fatty acyls with the higher number of DBs in *sn*-3 position is observed in plasma sample.

Our results show that natural distribution of fatty acids is not random, but different for various organisms.

■ ASSOCIATED CONTENT

Supporting Information

Additional information as noted in text. This material is available free of charge via the Internet at http://pubs.acs.org.

■ AUTHOR INFORMATION

Corresponding Author

*E-mail: Miroslav.Lisa@upce.cz. Tel: +420466037090.

Notes

The authors declare no competing financial interest.

■ ACKNOWLEDGMENTS

This work was supported by the grant project 203/09/0139 sponsored by the Czech Science Foundation. M. L. thanks to the project 203/09/P249 sponsored by the Czech Science Foundation for the partial financial support. Authors would like to acknowledge the help of Eva Cífková and Magdaléna Ovčačíková with the preparation of plasma sample.

■ REFERENCES

(1) Byrdwell, W. C.; Emken, E. A.; Neff, W. E.; Adlof, R. O. *Lipids* **1996**, *31*, 919.
(2) Cvačka, J.; Hovorka, O.; Jiroš, P.; Kindl, J.; Stránský, K.; Valterová, I. *J. Chromatogr. A* **2006**, *1101*, 226.
(3) Héron, S.; Tchapla, A. *Finger Prints of Triacylglycerols from Oils and Fats by HPLC Isocratic Elution and Evaporative Light Scattering Detection, ELSD Sedex 45*; Sedere: Alfortville, France, 1994.
(4) Holčapek, M.; Jandera, P.; Fischer, J. *Crit. Rev. Anal. Chem.* **2001**, *31*, 53.
(5) Holčapek, M.; Jandera, P.; Fischer, J.; Prokeš, B. *J. Chromatogr. A* **1999**, *858*, 13.
(6) Holčapek, M.; Jandera, P.; Zderadička, P.; Hrubá, L. *J. Chromatogr. A* **2003**, *1010*, 195.
(7) Holčapek, M.; Lísa, M.; Jandera, P.; Kabátová, N. *J. Sep. Sci.* **2005**, *28*, 1315.
(8) Kofroňová, E.; Cvačka, J.; Vrkoslav, V.; Hanuš, R.; Jiroš, P.; Kindl, J.; Hovorka, O.; Valterová, I. *J. Chromatogr. B* **2009**, *877*, 3878.
(9) Lísa, M.; Holčapek, M. *Chem. Listy* **2005**, *99*, 195.
(10) Lísa, M.; Holčapek, M. *J. Chromatogr. A* **2008**, *1198*, 115.
(11) Lísa, M.; Lynen, F.; Holčapek, M.; Sandra, P. *J. Chromatogr. A* **2007**, *1176*, 135.
(12) Mottram, H. R.; Woodbury, S. E.; Evershed, R. P. *Rapid Commun. Mass Spectrom.* **1997**, *11*, 1240.
(13) Holčapek, M.; Velínská, H.; Lísa, M.; Česla, P. *J. Sep. Sci.* **2009**, *32*, 3672.
(14) Mottram, H. R.; Crossman, Z. M.; Evershed, R. P. *Analyst* **2001**, *126*, 1018.
(15) Lísa, M.; Netušilová, K.; Franěk, L.; Dvořáková, H.; Vrkoslav, V.; Holčapek, M. *J. Chromatogr. A* **2011**, *1218*, 7499.
(16) Laakso, P. *J. Am. Oil Chem. Soc.* **1997**, *74*, 1291.
(17) Lísa, M.; Holčapek, M.; Řezanka, T.; Kabátová, N. *J. Chromatogr. A* **2007**, *1146*, 67.
(18) Lísa, M.; Holčapek, M.; Sovová, H. *J. Chromatogr. A* **2009**, *1216*, 8371.
(19) van den Berg, J. D. J.; Vermist, N. D.; Carlyle, L.; Holčapek, M.; Boon, J. J. *J. Sep. Sci.* **2004**, *27*, 181.
(20) Schreiberová, O.; Krulikovská, T.; Sigler, K.; Čejková, A.; Řezanka, T. *Lipids* **2010**, *45*, 743.
(21) Adlof, R.; List, G. *J. Chromatogr. A* **2004**, *1046*, 109.
(22) Adlof, R. O. *J. High Resolut. Chromatogr.* **1995**, *18*, 105.
(23) Adlof, R. O.; Menzel, A.; Dorovska-Taran, V. *J. Chromatogr. A* **2002**, *953*, 293.
(24) Christie, W. W. *J. Chromatogr.* **1988**, *454*, 273.
(25) Laakso, P.; Voutilainen, P. *Lipids* **1996**, *31*, 1311.
(26) Lísa, M.; Velínská, H.; Holčapek, M. *Anal. Chem.* **2009**, *81*, 3903.
(27) Schuyl, P. J. W.; de Joode, T.; Vasconcellos, M. A.; Duchateau, G. *J. Chromatogr. A* **1998**, *810*, 53.
(28) Holčapek, M.; Dvořáková, H.; Lísa, M.; Girón, A. J.; Sandra, P.; Cvačka, J. *J. Chromatogr. A* **2010**, *1217*, 8186.
(29) Dugo, P.; Kumm, T.; Crupi, M. L.; Cotroneo, A.; Mondello, L. *J. Chromatogr. A* **2006**, *1112*, 269.
(30) Mondello, L.; Tranchida, P. Q.; Staněk, V.; Jandera, P.; Dugo, G.; Dugo, P. *J. Chromatogr. A* **2005**, *1086*, 91.
(31) van der Klift, E. J. C.; Vivó-Truyols, G.; Claassen, F. W.; van Holthoon, F. L.; van Beek, T. A. *J. Chromatogr. A* **2008**, *1178*, 43.
(32) Dugo, P.; Favoino, O.; Tranchida, P. Q.; Dugo, G.; Mondello, L. *J. Chromatogr. A* **2004**, *1041*, 135.
(33) Ragonese, C.; Tranchida, P. Q.; Dugo, P.; Dugo, G.; Sidisky, L. M.; Robillard, M. V.; Mondello, L. *Anal. Chem.* **2009**, *81*, 5561.
(34) Fauconnot, L.; Hau, J.; Aeschlimann, J. M.; Fay, L. B.; Dionisi, F. *Rapid Commun. Mass Spectrom.* **2004**, *18*, 218.
(35) Brockerhoff, H. *J. Lipid Res.* **1965**, *6*, 10.
(36) Rogalska, E.; Ransac, S.; Verger, R. *J. Biol. Chem.* **1990**, *265*, 20271.
(37) Agren, J. J.; Kuksis, A. *Lipids* **2002**, *37*, 613.
(38) Ando, Y.; Ota, T.; Matsuhira, Y.; Yazawa, K. *J. Am. Oil Chem. Soc.* **1996**, *73*, 483.
(39) Christie, W. W.; Nikolova-Damyanova, B.; Laakso, P.; Herslof, B. *J. Am. Oil Chem. Soc.* **1991**, *68*, 695.
(40) Laakso, P.; Christie, W. W. *Lipids* **1990**, *25*, 349.
(41) Itabashi, Y.; Takagi, T. *Lipids* **1986**, *21*, 413.
(42) Itabashi, Y.; Takagi, T. *J. Chromatogr.* **1987**, *402*, 257.
(43) Takagi, T.; Ando, Y. *Lipids* **1991**, *26*, 542.
(44) Piyatheerawong, W.; Iwasaki, Y.; Yamane, T. *J. Chromatogr. A* **2005**, *1068*, 243.
(45) Deng, L.; Nakano, H.; Iwasaki, Y. *J. Chromatogr. A* **2007**, *1165*, 93.
(46) Deng, L.; Nakano, H.; Iwasaki, Y. *J. Chromatogr. A* **2008**, *1198*, 67.
(47) Garcia, P.; Franco, P.; Alvarez, R.; de Lera, A. R. *J. Sep. Sci.* **2011**, *34*, 999.
(48) Iwasaki, Y.; Yasui, M.; Ishikawa, T.; Irimescu, R.; Hata, K.; Yamane, T. *J. Chromatogr. A* **2001**, *905*, 111.
(49) Nagai, T.; Mizobe, H.; Otake, I.; Ichioka, K.; Kojima, K.; Matsumoto, Y.; Gotoh, N.; Kuroda, I.; Wada, S. *J. Chromatogr. A* **2011**, *1218*, 2880.
(50) Fraser, B. H.; Perlmutter, P.; Wijesundera, C. *J. Am. Oil Chem. Soc.* **2007**, *84*, 11.
(51) Wijesundera, C. *Eur. J. Lipid Sci. Technol.* **2005**, *107*, 824.
(52) Lísa, M.; Cífková, E.; Holčapek, M. *J. Chromatogr. A* **2011**, *1218*, 5146.

Miroslav Lísa[1]
Rumen Denev[2]
Michal Holčapek[1]

[1]Department of Analytical Chemistry, Faculty of Chemical Technology, University of Pardubice, Pardubice, Czech Republic
[2]Institute of Organic Chemistry with Centre of Phytochemistry, Bulgarian Academy of Sciences, Sofia, Bulgaria

Received May 24, 2013
Revised July 1, 2013
Accepted July 3, 2013

Research Article

Retention behavior of isomeric triacylglycerols in silver-ion HPLC: Effects of mobile phase composition and temperature

A systematic study of the retention behavior of isomeric triacylglycerols (TGs) in silver-ion HPLC on a ChromSpher Lipids column has been performed between 10 to 40°C using the most widespread hexane- and dichloromethane-based mobile phases. The randomization of mono-acyl TG standards and the random esterification of glycerol with fatty acids are employed to produce mixtures of TG isomers. The mobile phase composition has no influence on the general retention pattern, but significant differences in the retention order of double bond (DB) positional isomers in hexane and dichloromethane mobile phases are described and compared with the previous literature data. Saturated TGs with fatty acyl chain length from C7:0 to C22:0 are partially separated using the hexane mobile phase but not at all with the dichloromethane mobile phase. The hexane mobile phase enables at least partial resolution of TG regioisomers with up to seven DBs, while the resolution of only ALA/AAL and ALnA/AALn isomers is achieved with the dichloromethane mobile phase. The effect of temperature differs significantly depending on the mobile phase composition. Retention times of TGs increase with increasing temperature in the hexane mobile phase, while an opposite effect is observed for the dichloromethane mobile phase.

Keywords: Double bond positional isomers / Regioisomers / Silver-ion HPLC / *Trans* isomers / Triacylglycerol
DOI 10.1002/jssc.201300550

Additional supporting information may be found in the online version of this article at the publisher's web-site

1 Introduction

Triacylglycerols (TGs) are one of the most important and widespread derivatives of natural fatty acids [1]. They are primary metabolites with great importance for the normal physiological function of all living organisms. TGs serve as the main energy supplies and important food components essential for the human diet. Their structure is rather simple (triesters of fatty acids and glycerol), but they represent one of the most complex natural mixtures due to the large variety of esterified fatty acyls. Natural samples may contain 3^n different TG species, where n represents the number of fatty acyls in the sample. This number includes all possible isomers of TGs with various fatty acyl chain lengths, number, position and *cis*/*trans* configuration of double bonds (DBs), and different positions of fatty acyl chains on the glycerol backbone (regioisomers and enantiomers). All of the possible isomers of TGs are not present in real samples because only certain combinations are preferred in each organism. Nevertheless, natural mixtures are usually very complex and the detailed analysis of the isomers is rather challenging [2].

The most powerful technique in the characterization of TG composition is HPLC, providing a separation of most TG isomers. Coupling with atmospheric pressure chemical ionization (APCI) MS [3–9] enables an unambiguous identification of TG species differing in the fatty acyl chain composition without the necessity of identical standards. Moreover, relative abundances of fragment ions can be used for the differentiation of TG regioisomers ($R^1R^1R^2$ *vs.* $R^1R^2R^1$) [3–5, 10] because experimental results show a lower preference of neutral loss of fatty acids from the *sn*-2 position compared to *sn*-1 and *sn*-3 positions providing the $[M+H-R^2COOH]^+$ fragment ion with a lower relative abundance than statistically expected. Nonaqueous RP HPLC mode provides the separation of TGs based on different fatty acyl chain lengths and degree of saturation, which can be applied even for very complex samples containing tens to hundreds of TG

Correspondence: Dr. Miroslav Lísa, Department of Analytical Chemistry, Faculty of Chemical Technology, University of Pardubice, Studentská 573, 53210 Pardubice, Czech Republic
E-mail: Miroslav.Lisa@upce.cz
Fax: +420-46-603-7068

Abbreviations: A, arachidic acid (C20:0); **APCI**, atmospheric pressure chemical ionization; **DBs**, double bonds; **E**, elaidic acid (Δ*9t*-C18:1); **L**, linoleic acid (Δ*9, 12*-C18:2); **Ln**, linolenic acid (Δ*9, 12, 15*-C18:3); **γLn**, γ-linolenic acid (Δ*6, 9, 12*-C18:3); **O**, oleic acid (Δ*9*-C18:1); **Pe**, petroselinic acid (Δ*6*-C18:1); ***t*Pe**, *trans*-petroselinic acid (Δ*6t*-C18:1); **TG**, triacylglycerol; **Va**, vaccenic acid (Δ*11t*-C18:1); ***c*Va**, *cis*-vaccenic acid (Δ*11*-C18:1)

species [6, 8, 9, 11, 12]. Silver-ion HPLC is widely used for the separation of TGs based on the formation of weak reversible charge-transfer complexes between the π electrons of DBs and silver ions immobilized on the stationary phase [13, 14]. Retention patterns are similar for all lipids containing fatty acyls irrespective of the silver-ion chromatography technique, i.e. the retention is governed by the number, configuration, and positions of DBs in the fatty acyl chains [13–15]. In general, TGs are retained in order of increasing unsaturation number, compounds containing *trans* DBs are eluted significantly earlier than *cis* DB compounds [16–18], and compounds with conjugated DBs are eluted prior to compounds with methylene-interrupted DBs [13]. Furthermore, DB positional isomers [7, 19] and TG regioisomers [16, 18, 19] can also be separated using silver-ion HPLC. The good orthogonality of silver-ion and nonaqueous RP chromatographic modes is used in 2D HPLC for the characterization of very complex TG mixtures [18, 20]. The separation of TG enantiomers differing in positions of fatty acyls on the *sn*-1 and *sn*-3 positions ($R^1R^1R^2$ *vs.* $R^2R^1R^1$) has been achieved on a cellulose-tris-(3,5-dimethylphenylcarbamate) column with a hexane/2-propanol gradient [21].

The chromatographic resolution of TGs using silver-ion HPLC is affected by three factors: column properties, mobile phase composition, and column temperature. Nowadays, almost all silver-ion HPLC–MS experiments are based on the strong cation-exchanger type of silver-ion columns prepared in the laboratory or the single commercially available ChromSpher Lipids column with comparable performance. The mobile phase composition strongly affects the chromatographic resolution of TGs using silver-ion HPLC and careful optimization of solvent composition and gradient steepness can significantly improve the separation including the resolution of regioisomers. Two types of mobile phases are most frequently used in silver-ion HPLC. Chlorinated solvents, such as dichloromethane or dichloroethane with the addition of other polar modifiers at low concentrations, typically acetonitrile, acetone, or methanol [7, 22–25]. The second type is a hexane-based mobile phase with acetonitrile as the polar modifier [16, 17, 26, 27]. Hexane/acetonitrile mobile phases have the unique property to enable the resolution of TG regioisomers, which has not been reported so far for chlorinated mobile phases. The disadvantage of these systems is the low solubility of acetonitrile in hexane and low stability of mobile phases [28], which causes a lower reproducibility of retention times. This drawback can be significantly reduced by the addition of a small amount of 2-propanol into the mobile phase [4, 18, 19, 29, 30] or by the substitution of acetonitrile for butyronitrile [28] providing more stable mobile phases and reproducible retention times. In addition to these two main types, some other solvent combinations have also been reported, for example, toluene- [31, 32] and acetone-based mobile phases [33], but the results do not differ significantly.

In silver-ion HPLC, the effect of temperature is rather complex and is still not fully understood. The change of temperature influences the strength of silver–DB complex, but it is also assumed to strengthen the complex between the silver ion and acetonitrile in the mobile phase [16]. The increase of retention times of TGs with increasing temperature has been described in hexane/acetonitrile mobile phases [16, 19, 34], which is rather unusual in HPLC. Species with higher numbers of *cis* DBs are affected more strongly [16, 24]. On the other hand, the temperature decrease from 20 to 0°C causes the lower retention of TGs in hexane/acetonitrile, but it significantly increases with a further decrease of temperature [34]. However, a comprehensive study of temperature effects depending on the mobile phase composition has not been performed so far.

The goal of our work is the systematic study of the retention behavior of TGs in silver-ion HPLC affected by hexane- and dichloromethane-based mobile phases and by the column temperature. The set of TG standards comprising a large number of isomers is prepared using the random transesterification of TG standards and the random esterification of glycerol by a mixture of selected fatty acids. The retention behavior of all synthesized TG isomers using different mobile phases and temperatures is described and discussed.

2 Materials and methods

2.1 Reagents and solvents

Acetonitrile, 2-propanol (HPLC gradient grade), dichloromethane, methanol and hexane (HPLC grade), glycerol, sodium methoxide, 4-dimethylaminopyridine, and *N,N′*-dicyclohexylcarbodiimide were purchased from Sigma-Aldrich (St. Louis, MO, USA). The model mixture of TG standards GLC#435 (all saturated mono-acyl TGs from C7:0 to C22:0), tripalmitin (PPP, C16:0), tristearin (SSS, C18:0), tripetroselinin (PePePe, Δ*6*-C18:1), triolein (OOO, Δ*9*-C18:1), trielaidin (EEE, Δ*9t*-C18:1), tri-*cis*-vaccenin (*c*Va*c*Va*c*Va, Δ*11*-C18:1), trilinolein (LLL, Δ*9, 12*-C18:2), trilinolenin (LnLnLn, Δ*9, 12,15*-C18:3), tri-γ-linolenin (γLnγLnγLn, Δ*6,9,12*-C18:3), triarachidin (AAA, C20:0) and petroselinic (Δ*6*-C18:1), *trans*-petroselinic (Δ*6t*-C18:1), *cis*-vaccenic (Δ*11*-C18:1) and vaccenic (Δ*11t*-C18:1) acids were purchased from Nu–ChekPrep (Elysian, MN, USA). All solvents and reagents used for HPLC analyses and synthetic procedures were dried with molecular sieves.

2.2 Synthesis of TG standards

2.2.1 Random transesterification of TGs (Method 1)

TG regioisomers were prepared from mono-acyl TG standards (OOO, LLL, etc.) using the randomization procedure described earlier [19]. Briefly, 10 mg of each TG standard and 50 mg of sodium methoxide were weighed into a dry boiling flask with the addition of 2 mL of hexane dried with molecular sieves. The mixture was heated at 75°C for 30 min in a water bath under reflux. Then, the mixture was extracted

Table 1. TG composition of mixtures used for silver-ion HPLC–APCI-MS experiments, initial compounds and methods used for their preparation

Mixture	Initial compounds	Method	TG composition[a)]
Mixture 1	Saturated TGs from C7:0 to C22:0, PePePe, OOO, EEE, *c*Va*c*Va*c*Va, LLL, LnLnLn, γLnγLnγLn	Mixture of TG standards	Saturated TGs from C7:0 to C22:0, EEE, *c*Va*c*Va*c*Va, OOO, PePePe, LLL, LnLnLn, γLnγLnγLn
Mixture 2	AAA, OOO, LnLnLn	Method 1	AAA, AOA, AAO, AOO, OAO, ALnA, OOO, AALn, ALnO, AOLn, OALn, OLnO, OOLn, ALnLn, LnALn, OLnLn, LnOLn, LnLnLn
Mixture 3	OOO, LLL, LnLnLn	Method 1	OOO, OLO, OOL, OLL, LOL, OLnO, OOLn, LLL, OLnL, OLLn, LOLn, LLnL, LLLn, OLnLn, LnOLn, LLnLn, LnLLn, LnLnLn
Mixture 4	AAA, LLL, LnLnLn + OOO	Method 1 (OOO added after reaction)	AAA, ALA, AAL, ALnA, OOO, AALn, ALL, LAL, ALnL, ALLn, LALn, LLL, ALnLn, LnALn, LLnL, LLLn, LLnLn, LnLLn, LnLnLn
Mixture 5	AAA, OOO, LLL	Method 1	AAA, AOA, AAO, ALA, AAL, AOO, OAO, ALO, AOL, OAL, OOO, ALL, LAL, OLO, OOL, OLL, LOL, LLL
Mixture 6	EEE, OOO	Method 1	EEE, EOE, OEE, OOE, OEO, OOO
Mixture 7	Pe, *t*Pe, glycerol	Method 2	*t*Pe*t*Pe*t*Pe, *t*Pe*t*Pe*t*Pe, Pe*t*Pe*t*Pe, Pe*t*Pe*t*Pe, Pe*t*PePe, PePePe
Mixture 8	*c*Va, Va, glycerol	Method 2	VaVaVa, Va*c*VaVa, *c*VaVaVa, *c*Va*c*VaVa, *c*VaVa*c*Va, *c*Va*c*Va*c*Va

a) Listed according to retention times in the hexane mobile phase.

with water and methanol to remove sodium methoxide. The hexane phase containing the synthesized TGs was evaporated using a gentle stream of nitrogen and redissolved in hexane at the appropriate concentration before HPLC–MS analysis.

2.2.2 Random esterification of glycerol (Method 2)

A total of 15 mg of each fatty acid, 9.5 mg of glycerol, 13 mg of 4-dimethylaminopyridine, and 22 mg of *N,N′*-dicyclohexylcarbodiimide were weighed into a dry vial with the addition of 1 mL of dichloromethane dried with molecular sieves. The mixture was stirred at room temperature for 1.5 h. Then, TGs were extracted with hexane, the solvent was evaporated using a gentle stream of nitrogen, and the residue was redissolved in hexane to an appropriate concentration before HPLC–MS analysis.

2.3 Silver-ion HPLC–APCI-MS

Silver-ion HPLC–MS experiments were performed on a liquid chromatograph Agilent 1200 Series (Agilent Technologies, Waldbronn, Germany) coupled to an ion-trap mass analyzer Esquire 3000 (Bruker Daltonics, Bremen, Germany). Positive-ion APCI was used in the mass range m/z 50–1200 with the following parameters: pressure of the nebulizing gas 50 psi, drying gas flow rate 3 L/min, temperature of the drying gas and APCI heater 350 and 400°C, respectively. Reconstructed ion current chromatograms of protonated molecules and fragment ions were used to support the identification of coeluting peaks.

A ChromSpher Lipids column (250 × 4.6 mm, 5 μm, Agilent Technologies) with a flow rate of 1 mL/min and injection volume of 1 μL was used for all silver-ion HPLC experiments with the following gradients:

(i) Hexane-based mobile phase: 0 min 100% A, 60 min 52% A + 48% B, where A is hexane/2-propanol/acetonitrile (99.8:0.1:0.1, v/v/v) and B is hexane/2-propanol/acetonitrile (96:2:2, v/v/v).
(ii) Dichloromethane-based mobile phase: 0 min 100% A, 60 min 33% A + 67% B, where A is dichloromethane and B is dichloromethane/acetonitrile (90:10, v/v).

HPLC experiments were performed at 10, 20, 25, 30, and 40°C for hexane and 10, 25, and 40°C for dichloromethane mobile phases. The column was conditioned 45 min before each analysis to achieve a good reproducibility.

3 Results and discussion

3.1 Silver-ion HPLC–APCI-MS analysis of TGs

A wide range of TG species was tested in this work using silver-ion HPLC in an effort to cover the retention behavior of naturally occurring TGs in plant and animal tissues including all possible isomers, that is, TGs with various fatty acyl chain lengths, number, position and *cis*/*trans* configuration

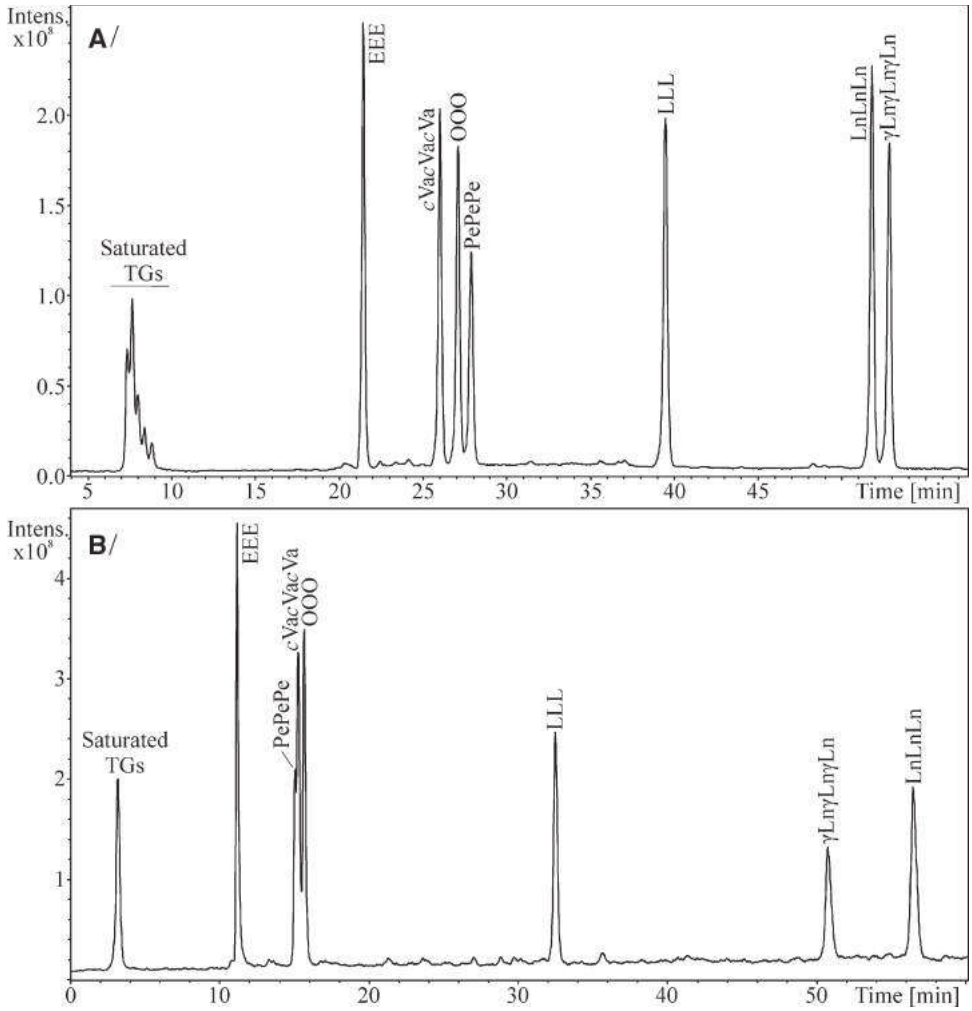

Figure 1. Effect of fatty acyl chain lengths, degree of unsaturation, DB configuration and position (Mixture 1) on the retention behavior of TGs in silver-ion HPLC–APCI-MS analysis: A/ hexane and B/ dichloromethane mobile phases. HPLC conditions: ChromSpher Lipids column (250 × 4.6 mm, 5 μm, Agilent Technologies), flow rate 1 mL/min, column temperature 25°C, gradient A/ 0 min 100% A, 60 min 52% A + 48% B, where A is hexane/2-propanol/acetonitrile (99.8:0.1:0.1, v/v/v) and B is hexane/2-propanol/acetonitrile (96:2:2, v/v/v), B/ 0 min 100% A, 60 min 33% A + 67% B, where A is dichloromethane and B is dichloromethane/acetonitrile (90:10, v/v).

of DBs, and different positions of fatty acyl chains on the glycerol skeleton (regioisomers). For this purpose, two synthetic procedures (the randomization of TGs and the random esterification of glycerol by fatty acids) have been applied to produce isomeric mixed-acyl TGs (Table 1). The randomization reaction (Method 1) of mono-acyl TG standards (AAA, OOO, etc.) catalyzed by sodium methoxide [19] provides an equimolar mixture of all possible TG isomers including regioisomers and enantiomers (Table 1) due to the random distribution of individual fatty acyls on the glycerol skeleton during the randomization process. The random esterification of glycerol by the mixture of selected fatty acids (Method 2) is used in cases when corresponding TG standards are not commercially available. This method provides an equimolar mixture of all possible TG isomers due to the random distribution of fatty acyls on the glycerol skeleton without any noticeable preference of individual fatty acids (Table 1).

Two different silver-ion HPLC methods using the most widespread hexane- and dichloromethane-based mobile phases and a ChromSpher Lipids column have been developed in this work. The hexane mobile phase is used according to our previously developed method [19], which enables the separation of TGs with different degrees of unsaturation, DB positional isomers and also TG regioisomers. This mobile phase contains acetonitrile as a polar modifier with the addition of 2-propanol. In this method, 2-propanol in the mobile phase does not influence the retention behavior of TGs as shown in Supporting Information Fig. S1, but it increases the miscibility of hexane and acetonitrile and improves the reproducibility of retention times [19]. Acetonitrile is also used as the polar modifier in the dichloromethane mobile phase. The presence of acetonitrile in both mobile phases partly eliminates the influence of modifier on the retention behavior of TGs so that mainly the effects of hexane and dichloromethane solvents should be observed. An identical silver-ion HPLC column is used for experiments with both mobile phases to guarantee the same properties of the column. First, the column was used in the hexane mobile phase, then properly flushed and used in the dichloromethane mobile phase. The column properties are significantly changed after use with dichloromethane in the mobile phase, which were tested with selected hexane experiments. The original performance of the column was reached after two days of conditioning with hexane mobile phase. Column temperatures

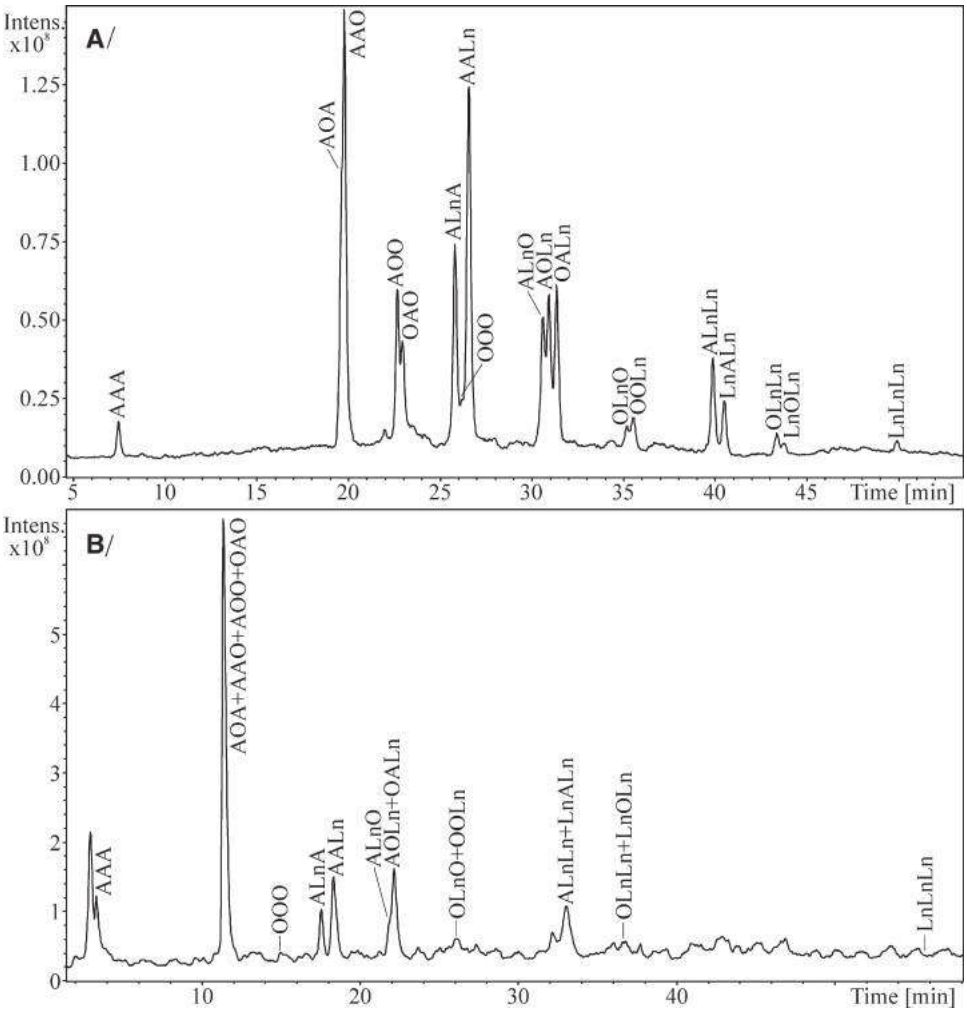

Figure 2. Comparison of silver-ion HPLC–APCI-MS chromatograms of synthesized TGs (Mixture 2) prepared by the randomization reaction of AAA, OOO, and LnLnLn standards according to Method 1: A/ hexane and B/ dichloromethane mobile phases. HPLC conditions are the same as stated for Fig. 1.

in the range from 10 to 40°C were used for testing the temperature effect on the retention behavior of TGs. This temperature range is commonly used for silver-ion HPLC experiments and it is dictated by the lower limit of the column thermostat used for these experiments and the upper limit of column stability recommended by the manufacturer.

Individual TGs are identified based on their APCI full mass spectra. Protonated molecules $[M+H]^+$ or ammonium adducts $[M+NH_4]^+$ are used for the determination of TG molecular weights, while fatty acyl composition is determined from $[M+H-R^iCOOH]^+$ fragment ions formed by neutral losses of fatty acids from the glycerol skeleton. TG regioisomers are identified based on the lower relative abundance of $[M+H-R^2COOH]^+$ fragment ion formed by the neutral loss of fatty acid from the *sn*-2 position, which is energetically less preferred compared to the *sn*-1 and *sn*-3 positions. TG enantiomers differing between the *sn*-1 and *sn*-3 fatty acyl chains cannot be resolved by silver-ion HPLC or identified by MS and require the use of chiral column [21]. Fatty acyls in *sn*-1 and *sn*-3 positions are ordered according to their decreasing molecular weight, for example, TG with arachidic and oleic acyls in the outer *sn*-1/3 positions and linoleic acyl in the *sn*-2 position is annotated with arachidic acyl in the *sn*-1 position as ALO (not OLA), because arachidic acyl has higher molecular weight (MW = 312) compared to oleic acyl (MW = 282). The APCI mass spectra of TGs in both hexane and dichloromethane mobile phases are almost identical, but significantly worse S/N is observed due to the increased baseline for dichloromethane given by a lower compatibility of chlorinated solvents with MS detection compared to hexane (based on our experience).

3.2 Effect of mobile phase composition

Figures 1–5 and Supporting Information Figs. S2–S4 show silver-ion HPLC–APCI-MS chromatograms of prepared TG mixtures using hexane (A/) and dichloromethane (B/) mobile phases at a column temperature of 25°C. In both silver-ion HPLC systems, general retention patterns are valid, that is, TGs are retained in order of increasing number of DBs, *trans* isomers elute prior to *cis* isomers and DB positional isomers are also separated. Nevertheless, large differences between both mobile phases are observed. Figure 1 shows

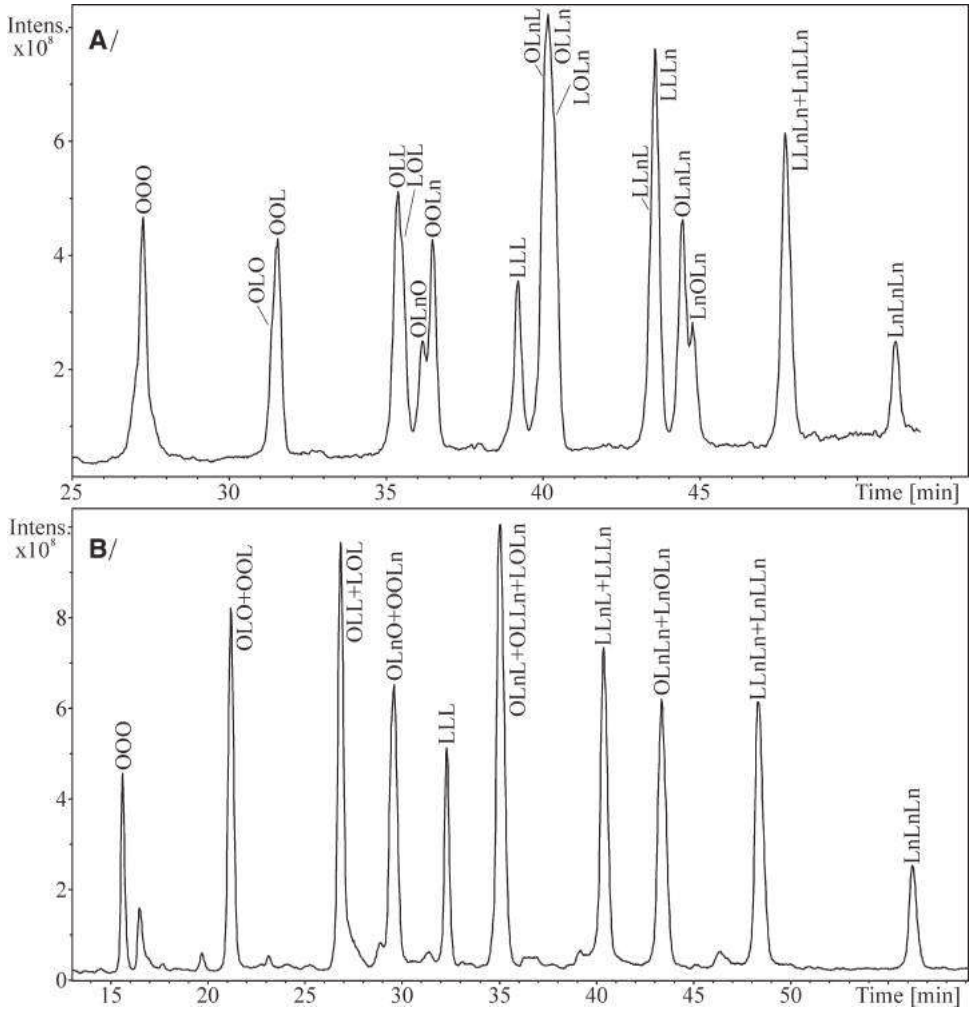

Figure 3. Comparison of silver-ion HPLC–APCI-MS chromatograms of synthesized TGs (Mixture 3) prepared by the randomization reaction of OOO, LLL, and LnLnLn standards according to Method 1: A/ hexane and B/ dichloromethane mobile phase. HPLC conditions are the same as stated for Fig. 1.

effects of different fatty acyl chain lengths, degree of unsaturation, DB configuration and position on the retention behavior of TGs in silver-ion HPLC using hexane (Fig. 1A) and dichloromethane (Fig. 1B) mobile phases. Significant differences are observed mainly for the separation of DB positional isomers. In the hexane mobile phase, retention times of DB positional isomers with C18:1 and C18:3 acyls increase with decreasing distance between the first DB and the carbonyl, that is, *c*Va*c*Va*c*Va < OOO < PePePe (Δ*11* < Δ*9* < Δ*6*) and LnLnLn < γLnγLnγLn (Δ*9, 12, 15* < Δ*6,9,12)*, respectively. The retention order of isomers is changed on using the dichloromethane mobile phase to PePePe < *c*Va*c*Va*c*Va < OOO (Δ*6* < Δ*11* < Δ*9*) and γLnγLnγLn < LnLnLn (Δ*6,9,12* < Δ*9, 12, 15*). The retention order of C18:3-TG isomers using our dichloromethane mobile phase corresponds to data achieved with chlorinated mobile phases, such as dichloromethane/1,2-dichloroethane/acetone/acetonitrile [7], but also with acetone/acetonitrile [35] (Table 2). All experiments in this work differ only in hexane and dichloromethane because the silver-ion HPLC column is identical, acetonitrile is the modifier in both mobile phases and 2-propanol does not influence the retention order of TGs (Supporting Information Fig. S1). Therefore, the change of retention order of DB positional isomers in this work is probably because of the different influence of hexane and dichloromethane on silver ion–DB complexation. In general, the change of retention order of DB positional isomers between hexane- and dichloromethane-based mobile phases cannot be unambiguously ascribed to the change of mobile phase solvent only, but this phenomenon is probably given by a more complex mechanism, as demonstrated for the separation of DB positional isomers of fatty acid phenacyl esters using different mobile phases (Table 2). For example, the change of retention order of some C20:1 and C18:3 fatty acid isomers has been demonstrated after the change of modifier from acetonitrile to 2-propanol [36], that is, the retention order of C20:1 fatty acid isomers is Δ13 < Δ11 < Δ5 < Δ8 using hexane/dichloromethane/acetonitrile *vs.* Δ13 < Δ11 < Δ8 < Δ5 using hexane/dichloromethane/2-propanol or the retention order of C18:3 isomers Δ9, 12, 15 < Δ6, 9, 12 using dichloromethane/acetonitrile *vs.* Δ6, 9, 12 < Δ9, 12, 15 using dichloromethane/2-propanol mobile phase. On the other hand, the retention order of C18:3 fatty acid isomers using dichloromethane/acetonitrile (Δ9, 12, 15 < Δ6, 9, 12) does

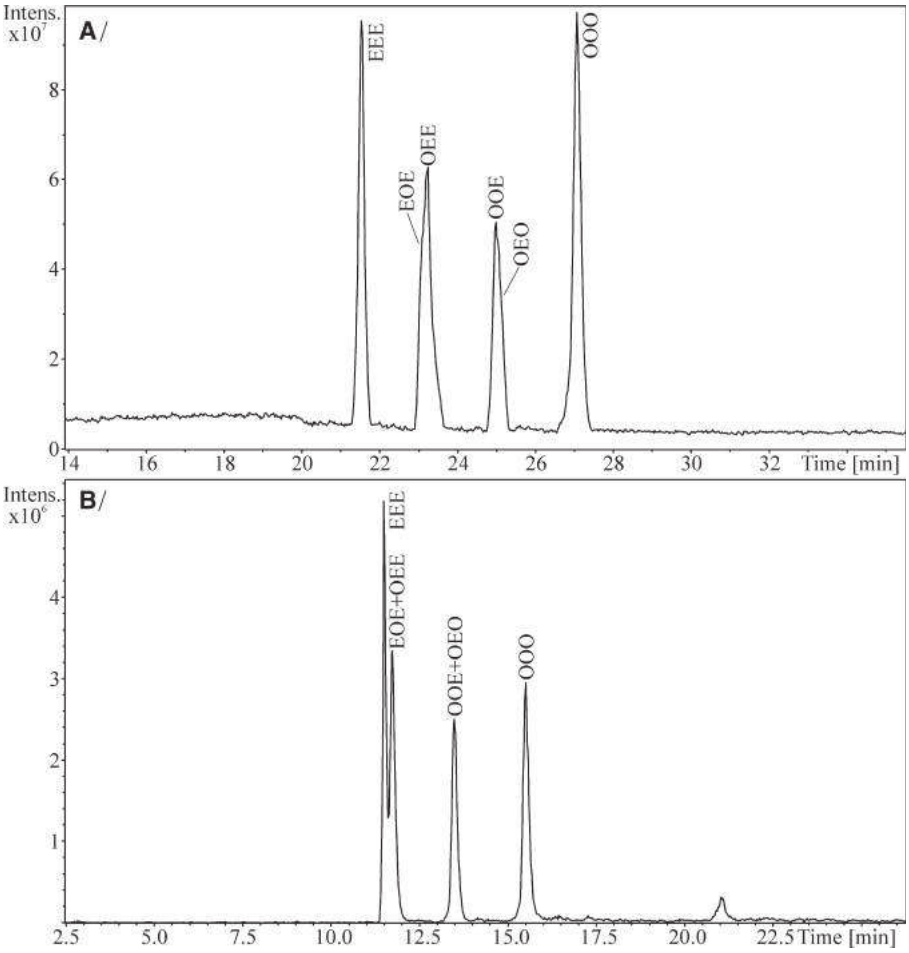

Figure 4. Comparison of silver-ion HPLC–APCI-MS chromatograms of synthesized TGs (Mixture 6) prepared by the randomization reaction of OOO and EEE standards according to the Method 1: A/ hexane and B/ dichloromethane mobile phases. HPLC conditions the same as stated for Fig. 1.

not correspond to the retention order of C18:3-TG isomers using our dichloromethane/acetonitrile mobile phase (Δ6, 9, 12 < Δ9, 12, 15), but to the hexane/acetonitrile/2-propanol mobile phase (Δ9, 12, 15 < Δ6, 9, 12). Moreover, other results show the identical retention order of C18:1 fatty acid isomers in 1,2-dichloroethane/dichloromethane/acetonitrile [24] and hexane/dichloromethane/2-propanol [37] mobile phases with acetonitrile and 2-propanol as modifiers, that is, Δ11 < Δ9 < Δ6, which also corresponds to the retention order of C18:1-TGs using our hexane/acetonitrile/2-propanol mobile phase.

The chromatographic behavior of TGs with different fatty acyl chain lengths varied in both silver-ion systems. While fully saturated mono-acyl TGs containing C7:0 to C22:0 acyls are partly separated in the hexane mobile phase (Fig. 1A), no separation is observed in the dichloromethane mobile phase (Fig. 1B). Retention times of saturated TGs increase with the decreasing number of carbon atoms in fatty acyl chains in the hexane mobile phase (Supporting Information Fig. S5), which is consistent with previously published data [4, 19, 38]. The separation of TG species without DBs using silver-ion HPLC has been ascribed to a normal-phase effect of silica-based silver-ion HPLC columns [38]. This phenomenon is probably suppressed by the higher polarity of dichloromethane and a different interaction with the stationary phase, because no separation of saturated species in dichloromethane mobile phase appeared using the same silver-ion HPLC column as for hexane experiments.

The dichloromethane mobile phase is less suitable for the separation of TG regioisomers, because only ALA/AAL and ALnA/AALn regioisomers (Fig. 2B, Supporting Information Figs. 2B and 3B) are separated in synthesized mixtures. In the hexane mobile phase, regioisomers with up to seven DBs (OLnLn/LnOLn) are at least partially resolved (Figs. 2A, 3A, Supporting Information Figs. 2A and 3A). Better separation of TG regioisomers is observed for TGs containing fatty acyl chains with substantial differences in DB number, for example, ALA/AAL isomers ($R = 0.97$ at 25°C) are partially but clearly resolved, while LLnLn/LnLLn isomers elute in a single peak ($R = 0$) (Table 3). In general, the separation of TG regioisomers with a combination of fatty acyl chains of higher unsaturation like O/L or L/Ln is very difficult [17, 19] and they are observed as broader peaks with shoulders in this work, for example, OLO/OOL and OLL/LOL or LLnL/LLLn and LLnLn/LnLLn (Fig. 3A). As a rule of thumb, regioisomers with fatty acyl chains with higher number of DBs in the *sn*-1 and *sn*-3 positions are retained more strongly, for example, ALnO (one DB in the *sn*-1 and *sn*-3 positions) < AOLn (three DBs) < OALn (four DBs) (Fig. 2A). The separation

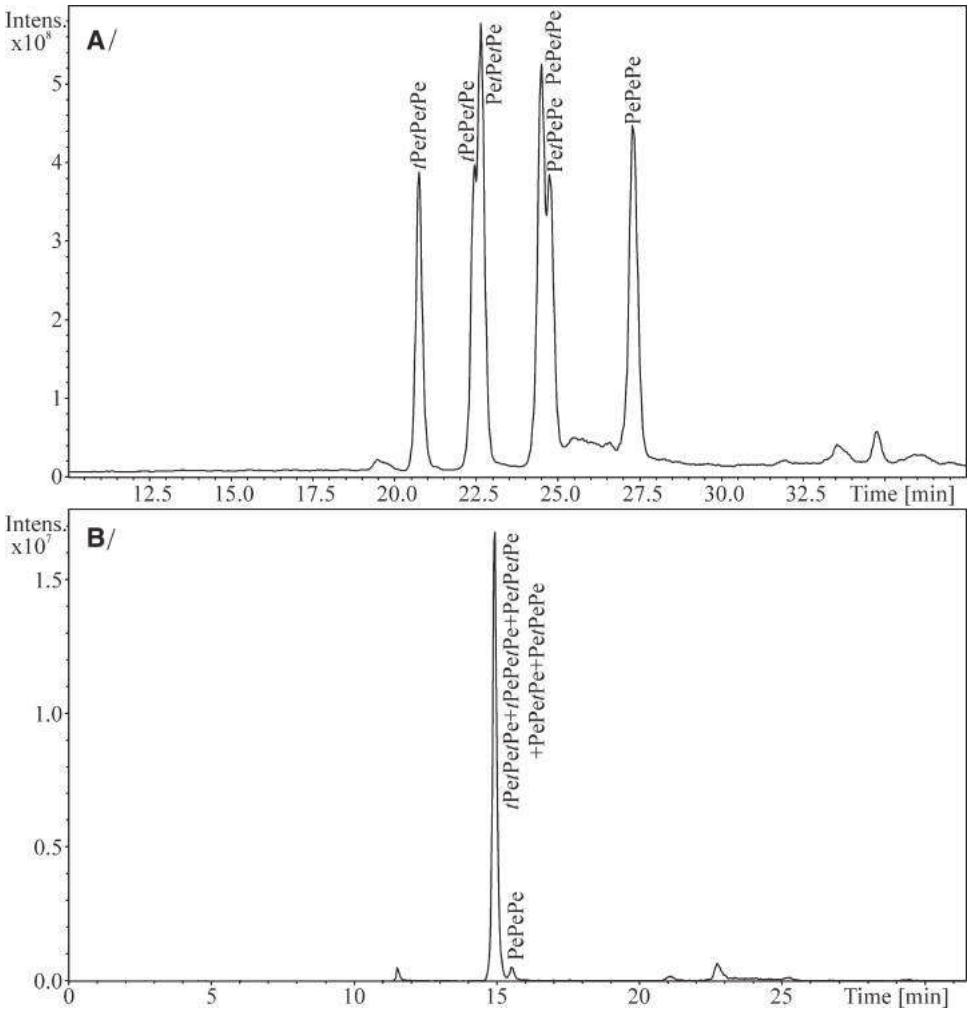

Figure 5. Comparison of silver-ion HPLC–APCI-MS chromatograms of synthesized TGs (Mixture 7) prepared by the random esterification of glycerol with Pe and *t*Pe fatty acid standards according to Method 2: A/ hexane and B/ dichloromethane mobile phases. HPLC conditions are the same as stated for Fig. 1.

of TG regioisomers with *cis* and *trans* configuration of DBs strongly depends on their positions in fatty acyl chains. Thus, while *t*PePe*t*Pe/Pe*t*Pe*t*Pe and PePe*t*Pe/Pe*t*PePe isomers (Δ6) are partially resolved at 25°C (Fig. 5A), no separation of E/O (Δ9) (Fig. 4A) and Va/*c*Va (Δ*11*) (Supporting Information Fig. S4A) isomers is observed. Individual TG regioisomers are identified based on relative ratios of $[M+H-R^iCOOH]^+$ fragment ions. These ratios are similar for both mobile phases, for example, the ratio of $[AA]^+/[ALn]^+ = 61{:}100$ for ALnA and 100:83 for AALn in the hexane mobile phase compared to 52:100 and 94:100 in the dichloromethane mobile phase, respectively.

Minor changes in the retention order of TGs in both systems can be observed inside TG groups with the same number of DBs. Groups of TGs containing one and two DBs are not resolved in the dichloromethane mobile phase compared to the hexane mobile phase (Fig. 2 and Supporting Information Fig. S3). OOO elutes between ALnA and AALn isomers in hexane (Fig. 2A and Supporting Information Fig. S2A), while it elutes ahead of these TGs in the dichloromethane mobile phase (Fig. 2B and Supporting Information Fig. S2B). Similarly, ALL/LAL isomers elute ahead of OLO/OOL isomers in hexane (Supporting Information Fig. S3A) compared to OLO/OOL isomers eluting ahead of ALL/LAL isomers in the dichloromethane mobile phase (Supporting Information Fig. S3B). Significant differences can be observed among the separation of *cis*/*trans* TG isomers with the different position of DBs using the dichloromethane mobile phase. While E/O isomers are resolved using the dichloromethane mobile phase (except from their regioisomers) (Fig. 4B), most of the *t*Pe/Pe isomers (Fig. 5B) and Va/*c*Va isomers (Supporting Information Fig. S4B) co-elute in one peak. The chromatographic resolution of TGs using the dichloromethane mobile phase is usually better than in the hexane mobile phase at these conditions (Table 3), but the dichloromethane mobile phase does not provide any resolution of most TG regioisomers, saturated TGs and some *cis*/*trans* TG isomers.

3.3 Effect of temperature

The effect of column temperature on the van't Hoff plots and relative retention times of synthesized mixtures using

Table 2. Influence of the mobile phase composition on the retention order of DB positional isomers of mono-acyl triacylglycerols (TGs) and fatty acid phenacyl esters (FAPEs)

Mobile phase composition	Species	Retention order of double bond positional isomers	Ref.
Hexane/acetonitrile/2-propanol	C18:1-TG	$\Delta11 < \Delta9 < \Delta6$	
Dichloromethane/acetonitrile	C18:1-TG	$\Delta6 < \Delta11 < \Delta9$	
1,2-Dichloroethane/dichloromethane/acetonitrile	C18:1-FAPE	$\Delta11 < \Delta9 < \Delta6$	[24]
Hexane/dichloromethane/2-propanol	C18:1-FAPE	$\Delta11 < \Delta9 < \Delta6$	[37]
Hexane/dichloromethane/acetonitrile	C20:1-FAPE	$\Delta13 < \Delta11 < \Delta5 < \Delta8$	[36]
Hexane/dichloromethane/2-propanol	C20:1-FAPE	$\Delta13 < \Delta11 < \Delta8 < \Delta5$	[36]
Hexane/acetonitrile/2-propanol	C18:3-TG	$\Delta9, 12, 15 < \Delta6, 9, 12$	
Dichloromethane/acetonitrile	C18:3-TG	$\Delta6, 9, 12 < \Delta9, 12, 15$	
Dichloromethane/1,2-dichloroethane/acetone/acetonitrile	C18:3-TG	$\Delta6, 9, 12 < \Delta9, 12, 15$	[7]
Acetone/acetonitrile	C18:3-TG	$\Delta6, 9, 12 < \Delta9, 12, 15$	[35]
Dichloromethane/acetonitrile	C18:3-FAPE	$\Delta9, 12, 15 < \Delta6, 9, 12$	[36]
Dichloromethane/2-propanol	C18:3-FAPE	$\Delta6, 9, 12 < \Delta9, 12, 15$	[36]

Table 3. Chromatographic resolution of selected TG pairs containing various combinations of fatty acyls (Sa—saturated, Mo—monounsaturated, D—diunsaturated, and T—triunsaturated fatty acyls) using silver-ion HPLC with hexane and dichloromethane mobile phases at different temperatures

TG pairs		Chromatographic resolution[a)]							
		Hexane					Dichloromethane		
		10°C	20°C	25°C	30°C	40°C	10°C	25°C	40°C
Sa/Sa	SSS/PPP	0.65	0.51	0.69	0.56	0.67	0	0	0
Mo/Mo	EEE/OOO	4.29	5.97	7.82	8.32	12.47	10.12	9.42	9.42
T/T	γLnγLnγLn/LnLnLn	1.38	1.07	1.27	1.23	1.43	4.06	4.36	4.36
Sa/Mo	AOA/AAO	1.15	1.62	0.64	0.25	0.49	0	0	0
	OOA/OAO	0.30	0.31	0.44	0.59	0.61	0	0	0
Sa/D	ALA/AAL	0.59	0.57	0.97	0.82	0.76	1.14	1.12	0
	ALL/LAL	0.41	0.50	0.35	0.41	0.51	0	0	0
Sa/T	ALnA/LnAA	0.60	0.71	0.73	0.67	0.68	0.89	0.82	0.80
	ALnLn/LnALn	0.54	0.69	0.32	0.49	0.43	0	0	0
Mo/Di	OLO/OOL	0	0	0	0	0	0	0	0
	OLL/LOL	0	0	0	0	0	0	0	0
Mo/T	OLnO/OOLn	0.38	0.37	0.77	0.40	0.37	0	0	0
	OLnLn/LnOLn	0.41	0.26	0.36	0.37	0.29	0	0	0
D/T	LLnL/LLLn	0	0	0	0	0	0	0	0
	LLnLn/LnLLn	0	0	0	0	0	0	0	0

a) Chromatographic resolution $R = 2\ (t_{RB} - t_{RA})/(w_A + w_B)$, where t_R are retention times of the TGs and w their peak widths.

hexane and dichloromethane mobile phases is shown in the Supporting Information (Supporting Information Charts S1–S9). Figures 6 and 7 show the effect of temperature on the retention times of mono-acyl TGs with fatty acyl chains differing in length, number, configuration and position of DBs using hexane and dichloromethane mobile phases (Supporting Information Table 1). The effect of temperature differs between the mobile phases. In the hexane mobile phase, retention times increase with higher temperature (in the range 10–40°C; Fig. 6), which is consistent with published data using a hexane/acetonitrile mobile phase [16, 34]. This phenomenon is rather unusual for most HPLC modes and has been explained by the fact that temperature induces changes in the stability of the acetonitrile–DB complex [16]. On the other hand, our dichloromethane mobile phase also contains acetonitrile as the modifier, but retention times of TGs decrease with increasing temperature (Fig. 7). This temperature effect has also been shown in the analysis of methyl and phenacyl esters of oleic acid using a 1,2-dichloroethane/dichloromethane/acetonitrile

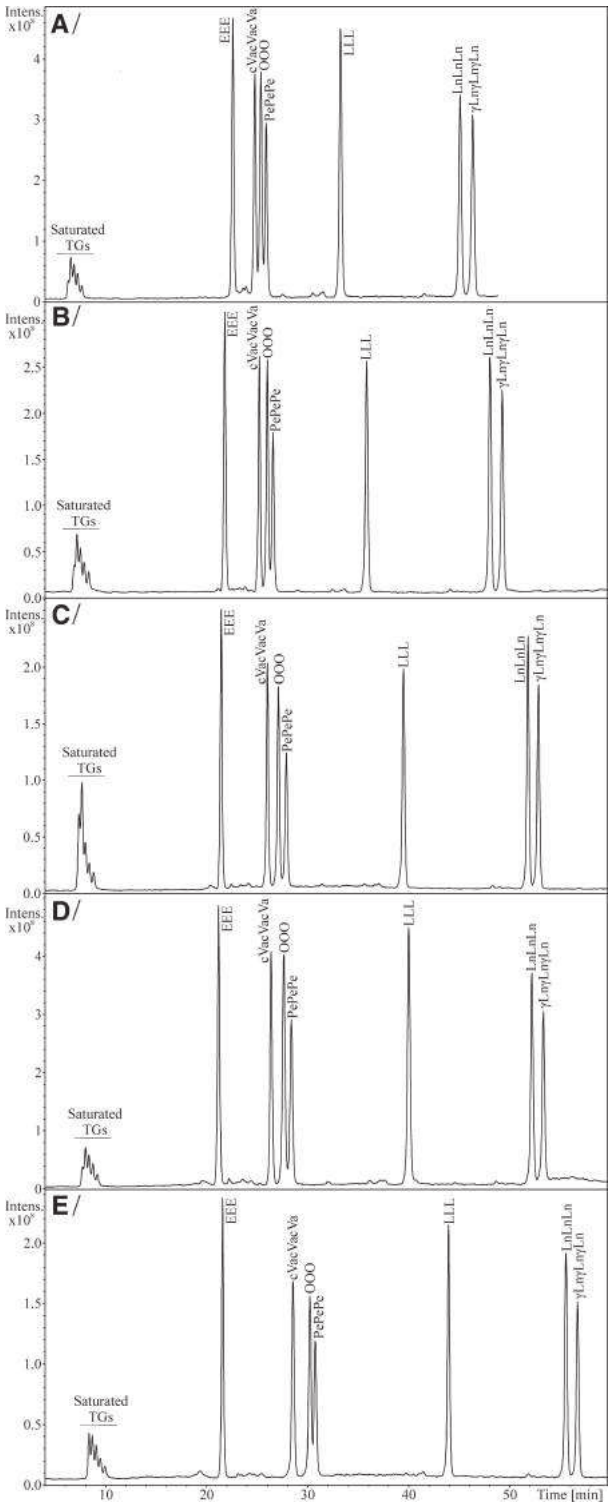

Figure 6. Effect of column temperature on the retention behavior of TGs with various fatty acyl chain lengths, degrees of unsaturation, DB configurations and positions (Mixture 1) in silver-ion HPLC–APCI-MS analysis using the hexane mobile phase: A/ 10, B/ 20, C/ 25, D/ 30, and E/ 40°C. HPLC conditions: ChromSpher Lipids column (250 × 4.6 mm, 5 μm, Agilent Technologies), flow rate 1 mL/min, gradient 0 min 100% A, 60 min 52% A + 48% B, where A is hexane/2-propanol/acetonitrile (99.8:0.1:0.1, v/v/v) and B is hexane/2-propanol/acetonitrile (96:2:2, v/v/v).

mobile phase [24]. Therefore, the different retention behavior is probably not caused by acetonitrile, which is identical for both mobile phases, but mainly by the effect of hexane and dichloromethane solvents on the stationary phase.

In the hexane mobile phase, the effect of temperature is stronger for TGs with the higher number of DBs. For example, the retention time of LnLnLn changes from 46.9 min at 10°C to 56.8 min at 40°C compared to retention times of saturated TGs or EEE (*trans* TGs), which are almost identical at all temperatures (Fig. 6, Supporting Information Table S1). The chromatographic resolution of C18:1-TG isomers slightly increases with increasing temperature mainly for EEE, *c*Va*c*Va*c*Va and OOO isomers (Table 3, Fig. 6). TGs with a higher number of DBs are also affected strongly in the dichloromethane mobile phase (Fig. 7), but the change of retention times is slightly lower compared to that in the hexane mobile phase, for example, the retention time of LnLnLn changes from 55.8 min at 10°C to 48.4 min at 40°C (Supporting Information Table S1). A stronger influence of temperature on the chromatographic resolution using the dichloromethane mobile phase is observed for C18:1-TG isomers, which are better resolved at higher temperature (Fig. 7).

The effect of temperature on the chromatographic resolution of TG regioisomers in the hexane mobile phase is significantly lower compared to the resolution of TGs with a different number of DBs (Supporting Information Fig. S6, Table 3). The chromatographic resolution of regioisomers with three and more DBs is almost identical at all temperatures (Table 3). The resolution of other isomers slightly increases at higher temperatures, except the AOA/AAO isomers, which have a higher resolution at 10 and 20°C (Table 3). A more significant effect of temperature on the chromatographic resolution of regioisomers is observed for *cis*/*trans* TG isomers (Fig. 8, Supporting Information Figs. S7 and S8). Their chromatographic resolution significantly improves when the temperature increases. While the *t*PePe*t*Pe/*t*Pe*t*PePe and PePe*t*Pe/Pe*t*PePe isomers are not resolved at 10°C (Fig. 8A), they are partially separated at 40°C (Fig. 8E). The EOE/EEO and OOE/OEO isomers (Supporting Information Fig. S7) are partially resolved at 40°C, but the Va*c*VaVa/*c*VaVaVa and Va*c*VaVa/*c*VaVaVa isomers (Supporting Information Fig. S8) are not separated at all. Temperature does not affect the chromatographic resolution of the ALA/AAL and ALnA/LnAA isomers using the dichloromethane mobile phase, except for the separation of ALA/AAL isomers at 40°C without any resolution (Table 3).

4 Concluding remarks

A comprehensive study of the retention pattern of a large number of TG isomers containing the most common fatty acyl chains is demonstrated here using silver-ion HPLC on a ChromSpher Lipids column and the most widely used hexane- and dichloromethane-based mobile phases. The hexane-based mobile phase with 2-propanol and acetonitrile as modifiers enables the resolution of TG regioisomers with up to seven DBs. The dichloromethane mobile phase provides

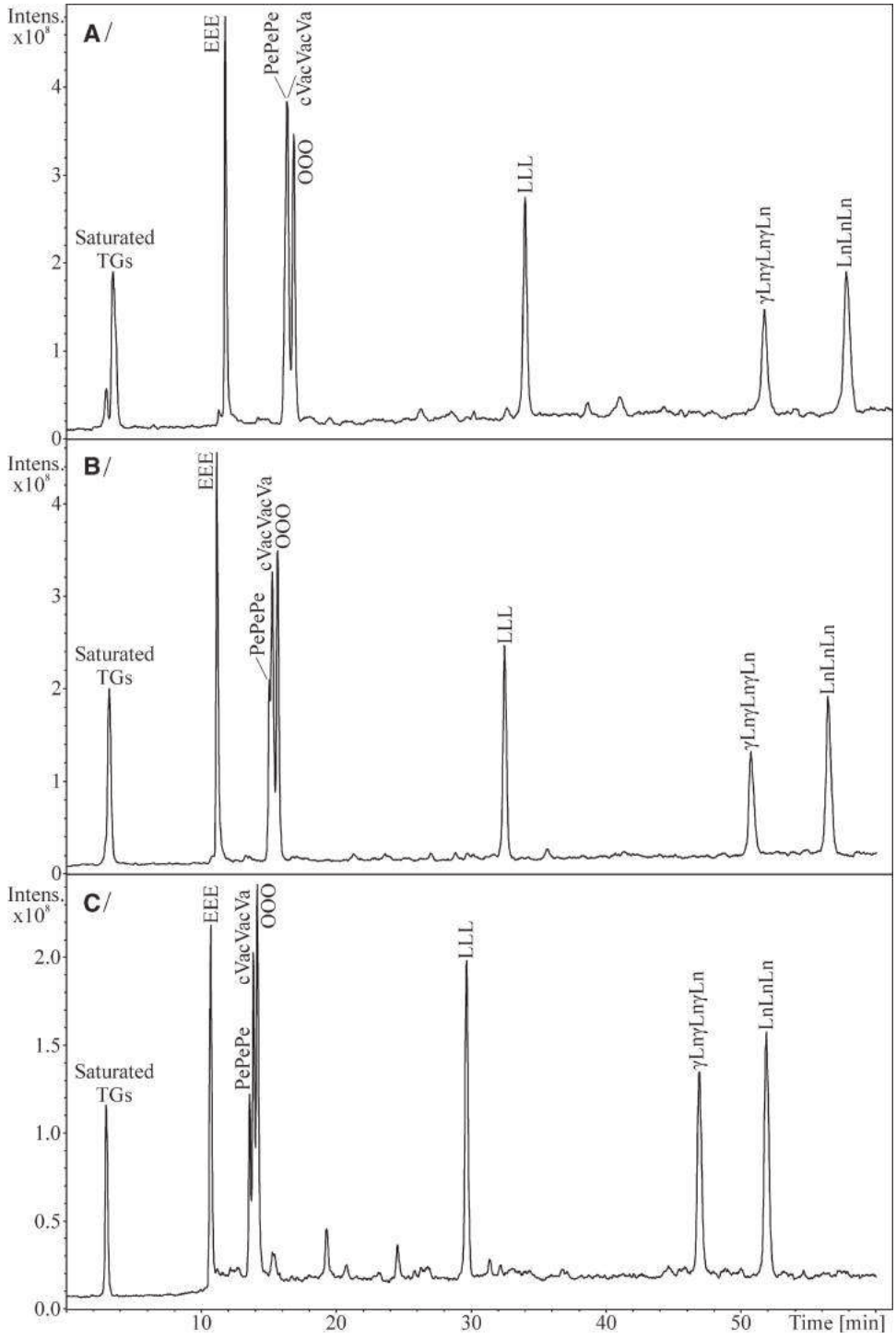

Figure 7. Effect of column temperature on the retention behavior of TGs with various fatty acyl chain lengths, degrees of unsaturation, DB configurations and positions (Mixture 1) in silver-ion HPLC–APCI-MS analysis using dichloromethane mobile phase: A/ 10, B/ 25, and C/ 40°C. HPLC conditions: ChromSpher Lipids column (250 × 4.6 mm, 5 μm, Agilent Technologies), flow rate 1 mL/min, gradient 0 min 100% A, 60 min 33% A + 67% B, where A is dichloromethane and B is dichloromethane/acetonitrile (90:10, v/v).

better chromatographic resolution of TG species compared to the hexane mobile phase, but does not enable the resolution of most TG regioisomers. Significant differences between the hexane and dichloromethane mobile phases are observed mainly in the retention order of TG species differing in positions of the DBs in the fatty acyl chains probably due to the different effect of hexane and dichloromethane on the stationary phase influencing the retention of TGs. Temperature affects the retention of TGs depending on the mobile phase composition. At elevated temperatures, TGs are retained more strongly in hexane and more weakly in the dichloromethane mobile phase. Temperature does not significantly influence

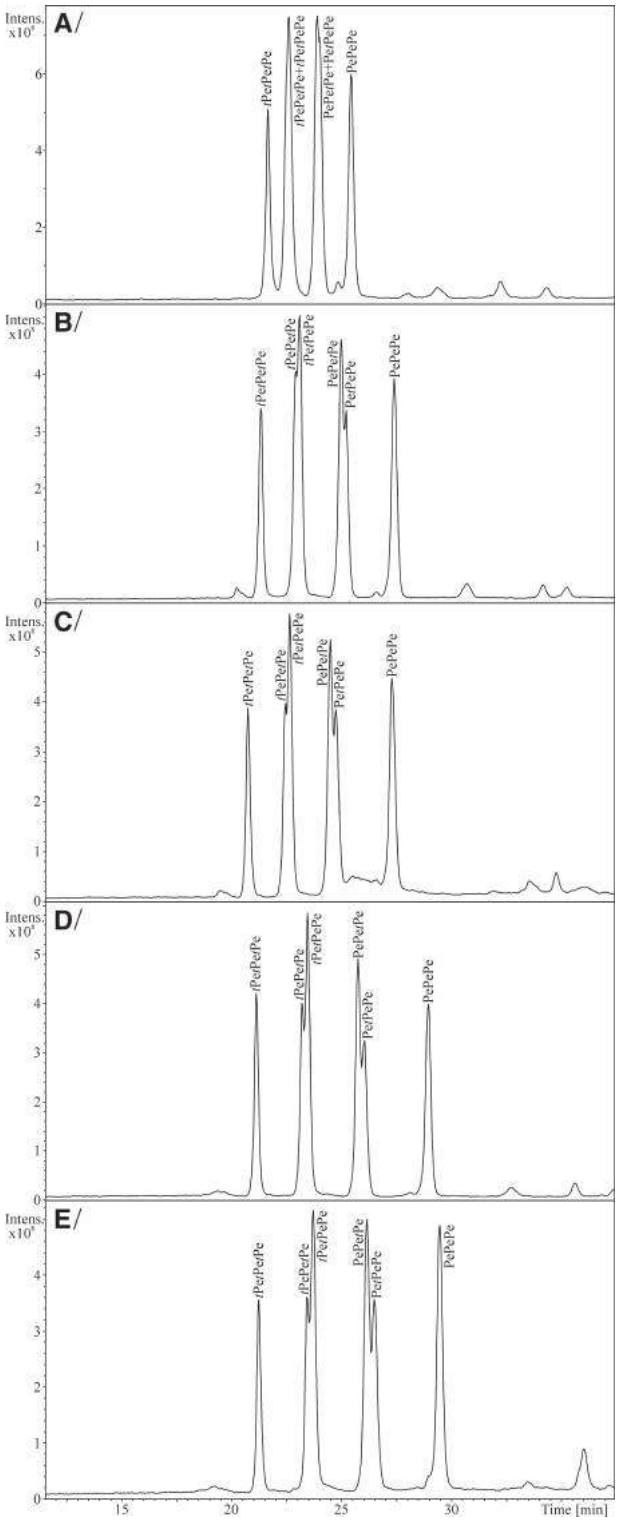

Figure 8. Effect of column temperature on the retention behavior of TGs (Mixture 7) prepared by the random esterification of glycerol with Pe and *t*Pe fatty acid standards according to Method 2 in silver-ion HPLC–APCI-MS analysis using the hexane mobile phase: A/ 10, B/ 20, C/ 25, D/ 30, and E/ 40°C. HPLC conditions are the same as those stated for Fig. 6.

the chromatographic resolution of TG regioisomers with the exception of *cis*/*trans* TG regioisomers using the hexane mobile phase. In general, the mobile phase composition affects the separation of TGs with silver-ion HPLC on a ChromSpher Lipid column more strongly than the temperature.

This work was supported by the grant project 203/09/0139 sponsored by the Czech Science Foundation. The authors would like to acknowledge Dr. B. Nikolova-Damyanova for fruitful discussions during the manuscript preparation.

The authors have declared no conflict of interest.

5 References

[1] Gunstone, F. D., *Modifying Lipids for Use in Food*, Woodhead Publishing, Cambridge 2006.

[2] Christie, W. W., Han, X., *Lipid Analysis – Isolation, Separation, Identification and Lipidomic Analysis (4th edition)*, Oily Press, Bridgwater 2010.

[3] Fauconnot, L., Hau, J., Aeschlimann, J. M., Fay, L. B., Dionisi, F., *Rapid Commun. Mass Spectrom.* 2004, *18*, 218–224.

[4] Holčapek, M., Dvořáková, H., Lísa, M., Girón, A. J., Sandra, P., Cvačka, J., *J. Chromatogr. A* 2010, *1217*, 8186–8194.

[5] Holčapek, M., Jandera, P., Zderadička, P., Hrubá, L., *J. Chromatogr. A* 2003, *1010*, 195–215.

[6] Holčapek, M., Lísa, M., Jandera, P., Kabátová, N., *J. Sep. Sci.* 2005, *28*, 1315–1333.

[7] Laakso, P., Voutilainen, P., *Lipids* 1996, *31*, 1311–1322.

[8] Lísa, M., Holčapek, M., *J. Chromatogr. A* 2008, *1198*, 115–130.

[9] Lísa, M., Holčapek, M., Boháč, M., *J. Agric. Food. Chem.* 2009, *57*, 6888–6898.

[10] Mottram, H. R., Crossman, Z. M., Evershed, R. P., *Analyst* 2001, *126*, 1018–1024.

[11] Lísa, M., Netušilová, K., Franěk, L., Dvořáková, H., Vrkoslav, V., Holčapek, M., *J. Chromatogr. A* 2011, *1218*, 7499–7510.

[12] Dugo, P., Beccaria, M., Fawzy, N., Donato, P., Cacciola, F., Mondello, L., *J. Chromatogr. A* 2012, *1259*, 227–236.

[13] Nikolova-Damyanova, B., *J. Chromatogr. A* 2009, *1216*, 1815–1824.

[14] Holčapek, M., Lísa, M., in: Byrdwell, W. C., Holčapek, M. (Eds.), *Extreme Chromatography – Faster, Hotter, Smaller*, American Oil Chemists' Society, AOCS Press, Urbana, 2011, pp. 197–230.

[15] Nikolova-Damyanova, B., in: Adlof, R. (Ed.), *Advances of Lipid Methodology – 5*, The Oily Press, Bridgwater 2003, pp. 43–123.

[16] Adlof, R., List, G., *J. Chromatogr. A* 2004, *1046*, 109–113.

[17] Adlof, R. O., *J. High. Resolut. Chromatogr.* 1995, *18*, 105–107.

[18] Holčapek, M., Velínská, H., Lísa, M., Česla, P., *J. Sep. Sci.* 2009, *32*, 3672–3680.

[19] Lísa, M., Velínská, H., Holčapek, M., *Anal. Chem.* 2009, *81*, 3903–3910.

[20] Dugo, P., Favoino, O., Tranchida, P. Q., Dugo, G., Mondello, L., *J. Chromatogr. A* 2004, *1041*, 135–142.

[21] Lísa, M., Holčapek, M., *Anal. Chem.* 2013, *85*, 1852–1859.

[22] Christie, W. W., *J. Chromatogr.* 1988, *454*, 273–284.

[23] Juaneda, P., Sebedio, J. L., Christie, W. W., *J. High. Resolut. Chromatogr.* 1994, *17*, 321–324.

[24] Nikolova-Damyanova, B., Herslof, B. G., Christie, W. W., *J. Chromatogr.* 1992, *609*, 133–140.

[25] Nikolova-Damyanova, B., Christie, W. W., Herslof, B., *J. Chromatogr. A* 1995, *693*, 235–239.

[26] Dugo, P., Kumm, T., Crupi, M. L., Cotroneo, A., Mondello, L., *J. Chromatogr. A* 2006, *1112*, 269–275.

[27] Mondello, L., Tranchida, P. Q., Staněk, V., Jandera, P., Dugo, G., Dugo, P., *J. Chromatogr. A* 2005, *1086*, 91–98.

[28] Harfmann, R. G., Julka, S., Cortes, H. J., *J. Sep. Sci.* 2008, *31*, 915–920.

[29] Cvačka, J., Hovorka, O., Jiroš, P., Kindl, J., Stránský, K., Valterová, I., *J. Chromatogr. A* 2006, *1101*, 226–237.

[30] Han, J. J., Iwasaki, Y., Yamane, T., *J. High. Resolut. Chromatogr.* 1999, *22*, 357–361.

[31] Jeffrey, B. S. J., *J. Am. Oil Chem. Soc.* 1991, *68*, 289–293.

[32] Schuyl, P. J. W., de Joode, T., Vasconcellos, M. A., Duchateau, G., *J. Chromatogr. A* 1998, *810*, 53–61.

[33] Nikolova-Damyanova, B., Christie, W. W., Herslof, B. G., *J. Chromatogr. A* 1995, *694*, 375–380.

[34] Adlof, R., *J. Chromatogr. A* 2007, *1148*, 256–259.

[35] Leskinen, H., Suomela, J. P., Pinta, J., Kallio, H., *Anal. Chem.* 2008, *80*, 5788–5793.

[36] Momchilova, S., Nikolova-Damyanova, B., *J. Liq. Chromatogr. Relat. Technol.* 2000, *23*, 2303–2316.

[37] Momchilova, S., Nikolova-Damyanova, B., *J. Liq. Chromatogr. Relat. Technol.* 2000, *23*, 2317–2325.

[38] Adlof, R. O., *J. Chromatogr. A* 1997, *764*, 337–340.

Journal of Chromatography A, 1217 (2010) 8186–8194

Contents lists available at ScienceDirect

Journal of Chromatography A

journal homepage: www.elsevier.com/locate/chroma

Regioisomeric analysis of triacylglycerols using silver-ion liquid chromatography–atmospheric pressure chemical ionization mass spectrometry: Comparison of five different mass analyzers

Michal Holčapek[a,*], Hana Dvořáková[a], Miroslav Lísa[a], Ana Jimenéz Girón[b], Pat Sandra[b], Josef Cvačka[c]

[a] University of Pardubice, Faculty of Chemical Technology, Department of Analytical Chemistry, Studentská 573, 53210 Pardubice, Czech Republic
[b] Ghent University, Krijgslaan 281 S4-bis, B-9000 Ghent, Belgium
[c] Institute of Organic Chemistry and Biochemistry, Academy of Sciences of the Czech Republic, v.v.i., Flemingovo nám. 2, 16610 Prague 6, Czech Republic

ARTICLE INFO

Article history:
Received 6 September 2010
Received in revised form 14 October 2010
Accepted 18 October 2010
Available online 23 October 2010

Keywords:
Triacylglycerols
Triglycerides
Silver-ion chromatography
Argentation chromatography
Regioisomer
Randomization

ABSTRACT

Silver-ion high-performance liquid chromatography (HPLC) coupled to atmospheric pressure chemical ionization mass spectrometry (APCI-MS) is used for the regioisomeric analysis of triacylglycerols (TGs). Standard mixtures of TG regioisomers are prepared by the randomization reaction from 8 mono-acid TG standards (tripalmitin, tristearin, triarachidin, triolein, trielaidin, trilinolein, trilinolenin and tri-*gamma*-linolenin). In total, 32 different regioisomeric doublets and 11 triplets are synthesized, separated by silver-ion HPLC using three serial coupled chromatographic columns giving a total length of 75 cm. The retention of TGs increases strongly with the double bond (DB) number and slightly for regioisomers having more DBs in *sn*-1/3 positions. DB positional isomers (linolenic *vs.* γ-linolenic acids) are also separated and their reverse retention order in two different mobile phases is demonstrated. APCI mass spectra of all separated regioisomers are measured on five different mass spectrometers: single quadrupole LC/MSD (Agilent Technologies), triple quadrupole API 3000 (AB SCIEX), ion trap Esquire 3000 (Bruker Daltonics), quadrupole time-of-flight micrOTOF-Q (Bruker Daltonics) and LTQ Orbitrap XL (Thermo Fisher Scientific). The effect of different types of mass analyzer on the ratio of $[M+H-R_iCOOH]^+$ fragment ions in APCI mass spectra is lower compared to the effect of the number of DBs, their position on the acyl chain and the regiospecific distribution of acyl chains on the glycerol skeleton. Presented data on $[M+H-R_iCOOH]^+$ ratios measured on five different mass analyzers can be used for the direct regioisomeric determination in natural and biological samples.

1. Introduction

Plant oils, animal fats and fish oils are natural sources of TGs in the human diet. They are important for our nutrition, as they supply energy, essential fatty acids (FAs), fat soluble vitamins, sterols, etc. [1]. The complexity of natural and biological TG mixtures is tremendous, since they may contain hundreds of different TGs. TGs are characterized by the total carbon number (CN), the number, position and configuration (*cis*/*trans*) of DBs in FA acyl chains and the stereospecific position of FAs on the glycerol skeleton (*sn*-1, 2 or 3). The knowledge of stereospecific positions of individual FAs is highly important, because human pancreatic lipases (secreted into the duodenum) or lipoprotein lipases (active in chylomicrons and very low density lipoproteins), preferentially catalyze the hydrolysis of FAs in *sn*-1/3 positions, which results in the different bioavailability of FAs depending on their *sn*-position. The severe problem in the regioisomeric analysis of TGs is the lack of standards. A limited range of standards is commercially available, but they are quite expensive. Randomization (*i.e.*, chemical interesterification) is a common industrial process used for the modification of physicochemical properties of TG mixtures in food and cosmetic products [1]. In our previous work [2], we have modified this procedure for the use in the micro scale range (milligram amounts), which overcomes the lack of standards by the synthesis of standard regioisomeric mixtures at well defined composition. The randomization reaction yields a truly random distribution of statistically expected regioisomers.

The most powerful separation technique used in the detailed characterization of complex TG mixtures is non-aqueous reversed-phase (NARP) HPLC [3–8], but unfortunately it is mostly not convenient for the separation of regioisomers with the exception of extremely long retention times up to 200 min causing peak broadening [9]. Silver-ion normal phase HPLC can be applied for the separation of TGs into groups differing in the DB number

* Corresponding author. Tel.: +420 466 037 087; fax: +420 466 037 068.
E-mail address: Michal.Holcapek@upce.cz (M. Holčapek).

0021-9673/$ – see front matter © 2010 Elsevier B.V. All rights reserved.
doi:10.1016/j.chroma.2010.10.064

[10–13], but it does not provide the same separation efficiency as NARP mode and it also suffers from a lower reproducibility. Unlike NARP, it provides a baseline resolution for regioisomers with up to three DBs and the partial resolution for highly unsaturated TGs [2]. The problem with the reproducibility in silver-ion systems can be partially solved by using a modified composition of commonly used hexane–acetonitrile mobile phases with the addition of 2-propanol to improve the mutual miscibility and therefore also the reproducibility. The principle of silver-ion chromatography is based on the formation of weak reversible complexes of π electrons from DBs with silver ions embedded in the stationary phase during the sample elution through the chromatographic column [11,12]. Two dimensional combination of NARP and silver-ion systems [10,14–17] provides quite good orthogonality in the analysis of TGs and therefore high peak capacity.

The main analytical techniques applicable for the regiospecific analysis of TGs are the following: (1) silver-ion HPLC [2,15–20], (2) MS [22–25], (3) enzymatic reactions [26], and (4) nuclear magnetic resonance (NMR) [27]. Each technique has certain limitations. NMR provides an absolute answer based on characteristic chemical shifts, but the practical applicability is severely limited by the need of pure compounds in milligram amounts. Enzymes with various levels of selectivity towards stereospecific positions or particular FA lengths are well known, but their application in a quantitative manner is often not as straightforward, because exact values of enzymatic stereoselectivity may not be known and also depends on experimental conditions. Furthermore, other analytical techniques (*e.g.*, HPLC) are required to detect products of enzymatic hydrolysis.

The ability of MS to distinguish regioisomers is known from the pioneering work published already in 1964 using electron ionization [28], which was 30 years later confirmed with APCI [29]. HPLC/APCI-MS is now often applied for characterization of prevailing FAs in the *sn*-2 position in complex natural mixtures [4–6,19–25]. Other ionization techniques, like electrospray ionization [30–35] or matrix-assisted laser desorption/ionization [36], can be used for the same purpose as well with the assistance of adduct formation with small cations (*e.g.*, ammonium, sodium or silver). Nevertheless, APCI is the most convenient ionization due to non-polar character of TGs, good compatibility with non-aqueous mobile phases and good sensitivity. All MS approaches rely on the fact that the neutral loss of FA from the middle *sn*-2 position is less energetically favored in comparison to cleavages from the side *sn*-1/3 positions [22–25,28,29]. This knowledge is often applied for the estimation of prevailing FA in the *sn*-2 position, but regioisomeric standards are essential for the quantitative determination [37–40].

The goal of this work is a systematic study of regioisomeric analysis of TGs based on our previously optimized silver-ion HPLC method and measurements of $[M+H-R_iCOOH]^+$ fragment ion ratios on five different types of mass analyzers. For this study, a broad range of regioisomeric standard mixtures is synthesized using the micro scale randomization procedure. This extensive data set measured in three different laboratories is used for the generalization of the fragmentation behavior in APCI mass spectra and the retention behavior in silver-ion chromatography, where the distribution of DBs in acyl chains has the highest importance.

2. Experimental

2.1. Chemicals

Acetonitrile, acetone, 2-propanol, methanol and hexane (HPLC grade solvents) and sodium methoxide were purchased from Sigma–Aldrich (St. Louis, MO, USA). Standards of tripalmitin (PPP, C16:0), tristearin (SSS, C18:0), triolein (OOO, Δ9-C18:1), trielaidin (EEE, Δ9trans-C18:1), trilinolein (LLL, Δ9,12-C18:2), trilinolenin (LnLnLn, Δ9,12,15-C18:3), tri-*gamma*-linolenin (γLnγLnγLn, Δ6,9,12-C18:3), triarachidin (AAA, C20:0), model mixtures of TG standards GLC#435 (all saturated single-acid TGs from C7:0 to C22:0) and GLC#437 (C16:0, C18:0, Δ9-C18:1, Δ9,12-C18:2, Δ9,12,15-C18:3 and C20:0) were purchased from Nu–ChekPrep (Elysian, MN, USA).

2.2. Randomization synthesis of regioisomeric TG mixtures

Standards of mixed-acid triacylglycerols ($R_1R_1R_2$, $R_1R_2R_2$, etc.) were prepared from mono-acid triacyglycerols ($R_1R_1R_1$) using the randomization procedure described recently [2]. The mixture of three mono-acid TGs were weighed (15 mg of each TG) into a dry boiling flask together with 90 mg of sodium methoxide and 2 mL of hexane dried with molecular sieves. The mixture was heated for 30 min in a water bath under reflux. The reaction temperature was kept constant at 75 °C. Then, the mixture was extracted with water and three times with 1 mL of methanol to remove sodium methoxide. The hexane phase containing randomized analytes was used for HPLC analyses. The same procedure was applied for the preparation of all randomization mixtures. The full list of synthesized TG regioisomers used in this study is shown in Table 1. Ratios of $[M+H-R_iCOOH]^+$ fragment ions shown in Tables 2 and 3 represent mean values of at least four points (mostly six points) with their standard deviations. Table 2 lists the data on all measured regioisomeric doubles including $R_1R_2R_3$ type TGs containing two different FAs with identical masses (O and E, Ln and γLn), while Table 3 shows the data on regioisomeric triplets.

2.3. Silver-ion HPLC

The final silver-ion HPLC method used for analyses of randomization mixtures is as follows. Three silver-ion chromatographic

Table 1
List of components of randomization mixtures and synthesized TG regioisomers (certain combinations in doublets occur multiple times).

Standards used for randomization	Regioisomers						
	Doublets						Triplets
PPP + OOO + LLL	POP/OPP	OOP/OPO	PLP/LPP	LLP/LPL	OOL/OLO	OLL/LOL	OLP/LOP/OPL
PPP + OOO + LnLnLn	POP/OPP	OOP/OPO	PLnP/LnPP	OLnO/OOLn	LnLnP/LnPLn	OLnLn/LnOLn	OLnP/LnOP/OPLn
PPP + LLL + LnLnLn	PLP/LPP	PLnP/LnPP	LLP/LPL	LnLnP/LnPLn	LLnL/LLLn	LLnLn/LnLLn	LLnP/LnLP/LPLn
SSS + OOO + LLL	SOS/SSO	SLS/SSL	SOO/OSO	SLL/LSL	OOL/OLO	OLL/LOL	SLO/SOL/OSL
SSS + OOO + LnLnLn	SOS/SSO	SOO/OSO	SLnS/SSLn	OLnO/OOLn	SLnLn/LnSLn	OLnLn/LnOLn	SLnO/SOLn/OSLn
AAA + OOO + LLL	AOA/AAO	ALA/AAL	AOO/OAO	ALL/LAL	OOL/OLO	OLL/LOL	ALO/AOL/OAL
AAA + OOO + LnLnLn	AOA/AAO	AOO/OAO	ALnA/AALn	OLnO/OOLn	ALnLn/LnALn	OLnLn/LnOLn	ALnO/AOLn/OALn
AAA + LLL + LnLnLn	ALA/AAL	ALnA/AALn	ALL/LAL	ALnLn/LnALn	LLnL/LLLn	LLnLn/LnLLn	ALnL/ALLn/LALn
OOO + LLL + LnLnLn	OOL/OLO	OLL/LOL	OLnO/OOLn	LLnL/LLLn	OLnLn/LnOLn	LLnLn/LnLLn	OLnL/OLLn/LOLn
PPP + OOO + EEE	PEP/EPP	POP/OPP	EEP/EPE	OOP/OPO	EEO/EOE	OEO/OOE	OEP/EOP/EPO
OOO + LnLnLn + γLnγLnγLn	OLnO/OOLn	OγLnO/OOγLn	OLnLn/LnOLn	OγLnγLn/γLnOγLn	LnLnγLn/LnγLnLn	γLnLnγLn/ γLnγLnLn	OLnγLn/OγLnLn/ LnOγLn

Table 2
Ratios of fragment ions for TG regioisomeric doublets recorded on five different mass spectrometers after silver-ion HPLC separation (see Section 2 for detailed conditions).

TG[a]	DB	Ratio of fragment ions $[R_1R_1]^+/[R_1R_2]^+$	Orbitrap (Thermo)	QqTOF (Bruker)	Ion trap (Bruker)	Single quadrupole (Agilent)	Triple quadrupole (AB SCIEX)
PEP	1	$[PP]^+/[EP]^+$	(30 ± 2):100	(32 ± 4):100	(25 ± 1):100	(28 ± 1):100	(26 ± 1):100
EPP		$[PP]^+/[EP]^+$	(94 ± 1):100	(85 ± 3):100	(93 ± 4):100	(86 ± 1):100	(88 ± 2):100
AOA		$[AA]^+/[AO]^+$	(31 ± 4):100	(27 ± 3):100	(31 ± 2):100	(27 ± 2):100	(30 ± 3):100
AAO		$[AA]^+/[AO]^+$	(94 ± 2):100	(87 ± 6):100	(79 ± 4):100	(78 ± 2):100	(80 ± 4):100
SOS		$[SS]^+/[SO]^+$	(27 ± 3):100	(40 ± 6):100	(33 ± 4):100	(35 ± 1):100	(38 ± 1):100
SSO		$[SS]^+/[SO]^+$	(90 ± 3):100	(94 ± 4):100	(91 ± 5):100	(86 ± 2):100	(80 ± 2):100
POP		$[PP]^+/[OP]^+$	(32 ± 1):100	(33 ± 5):100	(23 ± 2):100	(26 ± 1):100	(32 ± 2):100
OPP		$[PP]^+/[OP]^+$	(72 ± 3):100	(80 ± 5):100	(89 ± 6):100	(83 ± 3):100	(84 ± 1):100
EEP	2	$[EE]^+/[EP]^+$	(66 ± 1):100	(58 ± 3):100	(57 ± 1):100	(52 ± 1):100	(59 ± 2):100
EPE		$[EE]^+/[EP]^+$	(29 ± 2):100	(19 ± 1):100	(19 ± 1):100	(18 ± 1):100	(19 ± 1):100
EOP		$[OE]^+/[EP]^+$	(92 ± 2):100	(88 ± 4):100	(80 ± 5):100	(53 ± 1):100	(63 ± 1):100
OEP		$[OE]^+/[EP]^+$	(70 ± 1):100	(67 ± 2):100	(65 ± 3):100	(52 ± 1):100	(61 ± 1):100
OPE		$[OE]^+/[EP]^+$	(18 ± 1):100	(26 ± 1):100	(20 ± 1):100	(19 ± 1):100	(19 ± 1):100
ALA		$[AA]^+/[AL]^+$	(45 ± 3):100	(40 ± 6):100	(45 ± 2):100	(37 ± 2):100	(43 ± 1):100
AAL		$[AA]^+/[AL]^+$	(67 ± 3):100	(94 ± 3):100	(63 ± 3):100	(93 ± 2):100	(91 ± 5):100
SLS		$[SS]^+/[SL]^+$	(44 ± 1):100	(44 ± 2):100	(42 ± 3):100	(37 ± 1):100	(27 ± 1):100
SSL		$[SS]^+/[SL]^+$	(61 ± 1):100	(95 ± 3):100	(81 ± 3):100	(94 ± 3):100	(90 ± 4):100
PLP		$[PP]^+/[LP]^+$	(44 ± 3):100	(39 ± 1):100	(39 ± 2):100	(38 ± 2):100	(45 ± 1):100
LPP		$[PP]^+/[LP]^+$	(84 ± 3):100	(87 ± 2):100	(77 ± 5):100	(96 ± 1):100	(85 ± 2):100
AOO		$[OO]^+/[AO]^+$	(54 ± 1):100	(57 ± 4):100	(53 ± 1):100	(56 ± 2):100	(66 ± 1):100
OAO		$[OO]^+/[AO]^+$	(18 ± 2):100	(19 ± 3):100	(17 ± 1):100	(17 ± 1):100	(22 ± 1):100
SOO		$[OO]^+/[SO]^+$	(60 ± 4):100	(70 ± 5):100	(50 ± 5):100	(54 ± 1):100	(55 ± 1):100
OSO		$[OO]^+/[SO]^+$	(21 ± 3):100	(22 ± 2):100	(17 ± 1):100	(19 ± 1):100	(18 ± 1):100
OOP		$[OO]^+/[OP]^+$	(51 ± 1):100	(62 ± 2):100	(64 ± 1):100	(54 ± 2):100	(56 ± 1):100
OPO		$[OO]^+/[OP]^+$	(16 ± 1):100	(20 ± 1):100	(21 ± 1):100	(19 ± 1):100	(20 ± 1):100
ALnA	3	$[AA]^+/[ALn]^+$	(44 ± 1):100	(30 ± 2):100	(37 ± 1):100	(35 ± 2):100	(41 ± 2):100
AALn		$[AA]^+/[ALn]^+$	(81 ± 3):100	(86 ± 1):100	(92 ± 2):100	(89 ± 3):100	(89 ± 2):100
SLnS		$[SS]^+/[SLn]^+$	(42 ± 1):100	(30 ± 2):100	(36 ± 2):100	(34 ± 3):100	(25 ± 1):100
SSLn		$[SS]^+/[SLn]^+$	(82 ± 3):100	(87 ± 2):100	(83 ± 6):100	(82 ± 4):100	(83 ± 2):100
PLnP		$[PP]^+/[LnP]^+$	(47 ± 3):100	(49 ± 4):100	(32 ± 2):100	(32 ± 2):100	(41 ± 3):100
LnPP		$[PP]^+/[LnP]^+$	(92 ± 4):100	(97 ± 1):100	(77 ± 6):100	(86 ± 3):100	(88 ± 1):100
ALL	4	$[LL]^+/[AL]^+$	(83 ± 3):100	(73 ± 1):100	(89 ± 2):100	(83 ± 3):100	(86 ± 2):100
LAL		$[LL]^+/[AL]^+$	(31 ± 1):100	(30 ± 1):100	(36 ± 5):100	(32 ± 2):100	(37 ± 1):100
SLL		$[LL]^+/[SL]^+$	(77 ± 4):100	(75 ± 5):100	(90 ± 2):100	(80 ± 2):100	(89 ± 2):100
LSL		$[LL]^+/[SL]^+$	(23 ± 2):100	(16 ± 2):100	(25 ± 3):100	(11 ± 1):100	(34 ± 1):100
LLP		$[LL]^+/[LP]^+$	(91 ± 3):100	(81 ± 1):100	(78 ± 2):100	(77 ± 3):100	(78 ± 5):100
LPL		$[LL]^+/[LP]^+$	(39 ± 1):100	(33 ± 1):100	(48 ± 2):100	(29 ± 2):100	(33 ± 2):100
OLO		$[OO]^+/[OL]^+$	(46 ± 2):100	(45 ± 4):100	(32 ± 3):100	(43 ± 1):100	(36 ± 1):100
OOL		$[OO]^+/[OL]^+$	(60 ± 2):100	(88 ± 4):100	(71 ± 6):100	(68 ± 2):100	(77 ± 2):100
OLL	5	$[LL]^+/[OL]^+$	(89 ± 2):100	(81 ± 4):100	(88 ± 7):100	(71 ± 2):100	(79 ± 1):100
LOL		$[LL]^+/[OL]^+$	(46 ± 2):100	(34 ± 4):100	(42 ± 3):100	(36 ± 2):100	(40 ± 1):100
OLnO		$[OO]^+/[OLn]^+$	(29 ± 5):100	(23 ± 2):100	(24 ± 2):100	(26 ± 1):100	(26 ± 2):100
OOLn		$[OO]^+/[OLn]^+$	(72 ± 2):100	(76 ± 4):100	(67 ± 5):100	(64 ± 2):100	(79 ± 2):100
OOγLn		$[OO]^+/[O\gamma Ln]^+$	100:(41 ± 1)	100:(51 ± 2)	100:(50 ± 1)	100:(44 ± 1)	100:(49 ± 2)
ALnLn	6	$[LnLn]^+/[ALn]^+$	(81 ± 3):100	(89 ± 4):100	(90 ± 3):100	(86 ± 1):100	(91 ± 2):100
LnALn		$[LnLn]^+/[ALn]^+$	(36 ± 3):100	(31 ± 2):100	(37 ± 2):100	(31 ± 2):100	(44 ± 1):100
SLnLn		$[LnLn]^+/[SLn]^+$	(78 ± 1):100	(83 ± 1):100	(87 ± 3):100	(80 ± 2):100	(86 ± 2):100
LnSLn		$[LnLn]^+/[SLn]^+$	(30 ± 1):100	(32 ± 1):100	(48 ± 2):100	(29 ± 2):100	(29 ± 1):100
LnLnP		$[LnLn]^+/[LnP]^+$	(84 ± 3):100	(78 ± 3):100	(92 ± 7):100	(86 ± 1):100	(76 ± 1):100
LnPLn		$[LnLn]^+/[LnP]^+$	(33 ± 3):100	(28 ± 2):100	(45 ± 3):100	(29 ± 1):100	(37 ± 2):100
LLnL	7	$[LL]^+/[LLn]^+$	(38 ± 4):100	(36 ± 3):100	(41 ± 4):100	(44 ± 3):100	(44 ± 1):100
LLLn		$[LL]^+/[LLn]^+$	(68 ± 6):100	(68 ± 5):100	(67 ± 4):100	(71 ± 2):100	(74 ± 2):100
OLnLn		$[LnLn]^+/[OLn]^+$	(87 ± 2):100	(79 ± 2):100	(88 ± 4):100	(86 ± 2):100	(81 ± 3):100
LnOLn		$[LnLn]^+/[OLn]^+$	(38 ± 3):100	(34 ± 2):100	(43 ± 3):100	(32 ± 2):100	(45 ± 2):100
γLnOγLn		$[\gamma Ln\gamma Ln]^+/[O\gamma Ln]^+$	(10 ± 1):100	(11 ± 1):100	(18 ± 3):100	(12 ± 1):100	(15 ± 1):100
LLnLn	8	$[LnLn]^+/[LLn]^+$	(75 ± 4):100	(61 ± 2):100	(73 ± 5):100	(62 ± 3):100	(75 ± 2):100
LnLLn		$[LnLn]^+/[LLn]^+$	(46 ± 1):100	(36 ± 4):100	(44 ± 2):100	(44 ± 2):100	(47 ± 1):100

[a] TGs within double bond groups are sorted according to their retention times.

columns ChromSpher Lipids (250 mm × 4.6 mm, 5 μm, Varian, Palo Alto, CA, USA) were connected in series, the flow rate was set at 1 mL/min, the injection volume was 1 μL, the column temperature was 25 °C, and the mobile phase gradient was: 0 min – 100% A, 140 min – 61% A + 39% B, where A is the mixture of hexane–2-propanol–acetonitrile (99.8:0.1:0.1, v/v/v) and B is the mixture of hexane–2-propanol–acetonitrile (96:2:2, v/v/v). The mobile phase was prepared fresh every day. Silver-ion columns were conditioned at 50 μL/min of the initial mobile phase composition overnight and at 1 mL/min for 1 h before the first analysis. The injector needle was washed with the mobile phase before each injection. The chromatographic system was equilibrated between injections at least for 30 min.

2.4. Mass spectrometers used for comparative study

Positive-ion APCI and the mass range m/z of 50–1200 were used in all cases.

Table 3
Ratios of fragment ions for TG regioisomeric triplets recorded on five different mass spectrometers after silver-ion HPLC separation (see Section 2 for detailed conditions).

TG[a]	DB	Ratio of fragment ions $[R_1R_3]^+/[R_1R_2]^+/[R_2R_3]^+$	Orbitrap (Thermo)	QqTOF (Bruker)	Ion trap (Bruker)	Single quadrupole (Agilent)	Triple quadrupole (AB SCIEX)
ALO	3	$[AO]^+/[AL]^+/[OL]^+$	(42 ± 3):(75 ± 1):100	(56 ± 1):(83 ± 2):100	(50 ± 4):(84 ± 2):100	(71 ± 2):(81 ± 1):100	(49 ± 2):(74 ± 2):100
AOL		$[AL]^+/[AO]^+/[OL]^+$	(30 ± 2):(84 ± 3):100	(38 ± 1):(95 ± 3):100	(36 ± 2):(91 ± 4):100	(38 ± 2):(94 ± 1):100	(32 ± 2):(73 ± 2):100
OAL		$[OL]^+/[AO]^+/[AL]^+$	(46 ± 2):100:(80 ± 2)	(46 ± 1):100:(79 ± 3)	(54 ± 1):100:(89 ± 1)	(44 ± 2):100:(81 ± 3)	(53 ± 2):100:(91 ± 4)
SLO		$[SO]^+/[SL]^+/[OL]^+$	(48 ± 2):(67 ± 2):100	(62 ± 2):(86 ± 1):100	(42 ± 1):(77 ± 3):100	(56 ± 3):(91 ± 2):100	(46 ± 2):(86 ± 1):100
SOL		$[SL]^+/[SO]^+/[OL]^+$	(33 ±2):(87 ± 2):100	(49 ± 1):(95 ± 1):100	(38 ± 2):(88 ± 4):100	(44 ± 2):(89 ± 1):100	(43 ± 1):(90 ± 1):100
OSL		$[OL]^+/[SO]^+/[SL]^+$	(54 ± 2):100:(98 ± 1)	(46 ± 1):100:(81 ± 1)	(58 ± 4):100:(92 ± 4)	(25 ± 2):100:(63 ± 1)	(36 ± 1):100:(75 ± 1)
OLP		$[OP]^+/[OL]^+/[LP]^+$	(55 ± 1):100:(73 ± 1)	(72 ± 1):100:(84 ± 1)	(40 ± 5):100:(56 ± 4)	(56 ± 2):100:(78 ± 2)	(48 ± 2):100:(70 ± 2)
LOP		$[LP]^+/[OL]^+/[OP]^+$	(39 ± 2):100:(95 ± 3)	(53 ± 5):100:(97 ± 1)	(29 ± 2):100:(83 ± 3)	(39 ± 1):100:(91 ±1)	(35 ± 1):100:(85 ± 4)
OPL		$[OL]^+/[OP]^+/[LP]^+$	(47 ± 2):100:(77 ± 3)	(58 ± 1):100:(85 ± 2)	(75 ± 4):100:(89 ± 3)	(46 ± 1):100:(74 ± 3)	(64 ± 1):100:(89 ± 2)
ALnO	4	$[AO]^+/[ALn]^+/[OLn]^+$	(52 ± 1):(88 ± 1):100	(54 ± 2):(96 ± 4):100	(54 ± 4):(88 ± 1):100	(55 ± 1):(94 ± 1):100	(56 ± 3):(93 ± 2):100
AOLn		$[ALn]^+/[AO]^+/[OLn]^+$	(37 ± 1):100:(82 ± 2)	(42 ± 4):100:(76 ± 1)	(43 ± 2):100:(84 ± 1)	(38 ± 1):100:(88 ± 2)	(40 ± 1):100:(84 ± 1)
OALn		$[OLn]^+/[AO]^+/[ALn]^+$	(43 ± 3):(83 ± 1):100	(48 ± 3):(79 ± 4):100	(47 ± 3):(88 ± 3):100	(45 ± 1):(90 ± 2):100	(42 ± 2):(86 ± 2):100
SLnO		$[SO]^+/[SLn]^+/[OLn]^+$	(54 ± 2):100:(97 ± 2)	(44 ± 1):100:(90 ± 2)	(42 ± 2):100:(96 ± 2)	(50 ± 4):100:(95 ± 2)	(50 ± 1):100:(86 ± 2)
SOLn		$[SLn]^+/[SO]^+/[OLn]^+$	(41 ± 2):100:(88 ± 3)	(43 ± 2):100:(91 ± 4)	(58 ± 1):100:(97 ± 2)	(42 ± 3):100:(91 ± 1)	(52 ± 2):100:(90 ± 2)
OSLn		$[OLn]^+/[SO]^+/[SLn]^+$	(41 ± 3):100:(82 ± 2)	(36 ± 2):100:(91 ± 3)	(51 ± 2):100:(85 ± 2)	(50 ± 1):100:(96 ± 1)	(47 ± 2):100:(93 ± 3)
OLnP		$[OP]^+/[OLn]^+/[LnP]^+$	(55 ± 2):100:(91 ± 1)	(60 ± 5):100:(93 ± 1)	(49 ± 2):100:(70 ± 2)	(54 ± 3):100:(96 ± 1)	(46 ± 2):100:(90 ± 2)
LnOP		$[LnP]^+/[OLn]^+/[OP]^+$	(36 ± 1):(90 ± 3):100	(33 ± 1):(95 ± 4):100	(50 ± 1):(88 ± 3):100	(44 ± 1):(86 ± 1):100	(35 ± 2):(92 ± 2):100
OPLn		$[OLn]^+/[OP]^+/[LnP]^+$	(55 ± 2):100:(86 ± 1)	(49 ± 2):100:(92 ± 4)	(61 ± 2):100:(81 ± 4)	(44 ± 2):100:(95 ± 1)	(50 ± 1):100:(90 ± 2)
ALnL	5	$[AL]^+/[ALn]^+/[LLn]^+$	(70 ± 2):(88 ± 2):100	(79 ± 1):(90 ± 2):100	(48 ± 5):(77 ± 5):100	(63 ± 1):(69 ± 2):100	(50 ± 3):(64 ± 1):100
ALLn		$[ALn]^+/[AL]^+/[LLn]^+$	(51 ± 2):(91 ± 1):100	(66 ± 4):(93 ± 3):100	(46 ± 4):(82 ± 2):100	(54 ± 3):(81 ± 4):100	(35 ± 2):(57 ± 1):100
LALn		$[LLn]^+/[AL]^+/[ALn]^+$	(87 ± 2):100:(95 ± 1)	(49 ± 1):100:(83 ± 1)	(64 ± 1):100:(81 ± 4)	(49 ± 2):100:(82 ± 2)	(75 ± 2):100:(85 ± 2)
LLnP		$[LP]^+/[LLn]^+/[LnP]^+$	(45 ± 1):100:(92 ± 2)	(78 ± 3):100:(88 ± 6)	(36 ± 2):100:(57 ± 2)	(63 ± 1):100:(70 ± 1)	(50 ± 2):100:(62 ± 2)
LnLP		$[LnP]^+/[LLn]^+/[LP]^+$	(47 ± 1):100:(92 ± 1)	(44 ± 3):100:(82 ± 3)	(42 ± 2):100:(80 ± 2)	(57 ± 2):100:(82 ± 2)	(42 ± 2):100:(80 ± 2)
LPLn		$[LLn]^+/[LP]^+/[LnP]^+$	(38 ± 2):100:(87 ± 1)	(47 ± 1):100:(93 ± 2)	(67 ± 3):100:(89 ± 2)	(47 ± 1):100:(82 ± 2)	(73 ± 2):100:(89 ± 3)
OLnL	6	$[OL]^+/[OLn]^+/[LLn]^+$	(71 ± 1):(88 ± 3):100	(62 ± 3):(95 ± 4):100	(54 ± 4):(71 ± 4):100	(63 ± 3):(84 ± 3):100	(55 ± 2):(72 ± 2):100
OLLn		$[OLn]^+/[OL]^+/[LLn]^+$	(70 ± 4):(82 ± 2):100	(54 ± 3):(94 ± 2):100	(73 ± 5):(84 ± 5):100	(70 ± 1):(87 ± 3):100	(79 ± 2):(92 ± 2):100
LOLn		$[LLn]^+/[OL]^+/[OLn]^+$	(61 ± 1):100:(90 ± 5)	(56 ± 2):100:(78 ± 1)	(76 ± 2):100:(87 ± 2)	(69 ± 3):100:(93 ± 2)	(83 ± 3):100:(86 ± 4)

[a] TGs within double bond groups are sorted according to their retention times.

(1) Quadrupole time-of-flight (QqTOF) analyzer micrOTOF-Q (Bruker Daltonics, Bremen, Germany) – flow rate of the nebulizing and drying gas 5 and 3 L/min, respectively, temperatures of the drying gas and APCI heater 300 °C and 400 °C, respectively. QqTOF was coupled to an Agilent 1200 Series liquid chromatograph (Agilent Technologies, Waldbronn, Germany).
(2) Ion trap (IT) analyzer Esquire 3000 (Bruker Daltonics, Bremen, Germany) – pressure of the nebulizing gas 70 psi, drying gas flow rate 3 L/min, temperatures of the drying gas and APCI heater were 350 °C and 400 °C. The ion trap was coupled to the Agilent 1200 Series liquid chromatograph.
(3) Single quadrupole (Q) LC/MSD (Agilent Technologies, Waldbronn, Germany) – pressure of the nebulizing gas 50 psi, drying gas flow rate 7 L/min, temperatures of the drying gas and APCI heater were 300 °C and 400 °C. The Q was coupled to the Agilent 1100 Series liquid chromatograph.
(4) Triple quadrupole (QqQ) API 3000 (AB SCIEX, Foster City, CA, USA) – pressure of the nebulizing and curtain gas 15 psi and 6 psi, respectively, and temperature of APCI 400 °C. The QqQ was coupled to the Waters 2690 Alliance liquid chromatograph (Waters, Milford, MA, USA).
(5) LTQ Orbitrap XL (Thermo Fisher Scientific, Waltham, MA,USA) – flow rate of the sheath and auxiliary gases 55 and 25 arbitrary units, respectively, vaporizer temperature 300 °C and capillary temperature 200 °C. The Orbitrap was coupled to the Rheos Allegro quaternary gradient UHPLC pump (Thermo

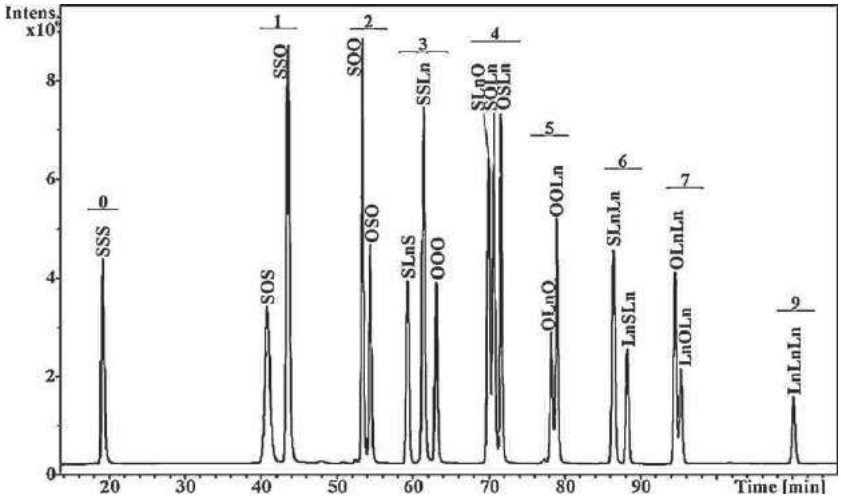

Fig. 1. Silver-ion HPLC/APCI-MS chromatogram of the randomization mixture prepared from tristearin (SSS, C18:0), triolein (OOO, Δ9-C18:1) and trilinolenin (LnLnLn, Δ9,12,15-C18:3), see Section 2 for conditions. Numbers correspond to the double bond number.

Fisher Scientific), HTSPAL autosampler (CTC Analytics AG, Zwingen, Switzerland), and DeltaChromTM CTC 100 column oven (Watrex, Prague, Czech Republic).

2.5. Notation of TGs and FAs

TGs are annotated using initials of trivial names of FAs arranged according to their *sn*-1, *sn*-2 and *sn*-3 positions. Positions *sn*-1 and *sn*-3 cannot be distinguished by silver-ion HPLC, therefore the order in these side positions follow decreasing masses in accordance with our previously established convention [2–5,7,9,10,23,38], *i.e.*, OLP but not PLO. If FA residues have identical masses, then sn-1 position is used for more common FA, *e.g.*, LnOγLn but not γLnOLn, OPE but not EPO. Abbreviations of FAs used in this work: P, palmitic (C16:0); S, stearic (C18:0); O, oleic (Δ9-C18:1); E, elaidic (Δ9t-C18:1); L, linoleic (Δ9,12-C18:2); Ln, linolenic (Δ9,12,15-C18:3); γLn, *gamma*-linolenic (Δ6,9,12-C18:3); A, arachidic (C20:0).

3. Results and discussion

The first problem in the regioisomeric analysis of TGs is the use of appropriate regioisomeric standards. Some TG regioisomers are commercially available from Larodan (Malmö, Sweden), but their prices are rather high. In our previous work [2], we have developed a method for the preparation of regioisomeric mixtures based on the well known randomization procedure used in food and cosmetic industries for the production of lipid mixtures with required properties, called functional lipids. Table 1 lists 11 performed randomization reactions providing 32 different doublets and 11 triplets of regioisomeric TGs. The synthesis has required a total reaction time of 11 h (30 min for preparation + 30 min for reaction = 1 h * 11 reactions) and the total analytical time is 55 h (2 h for the chromatographic run, 2 analyses per sample, 1 h for the system equilibration = 5 h * 11 reactions); in total it is about 66 h of working time. This laborious synthetic part of the work is essential

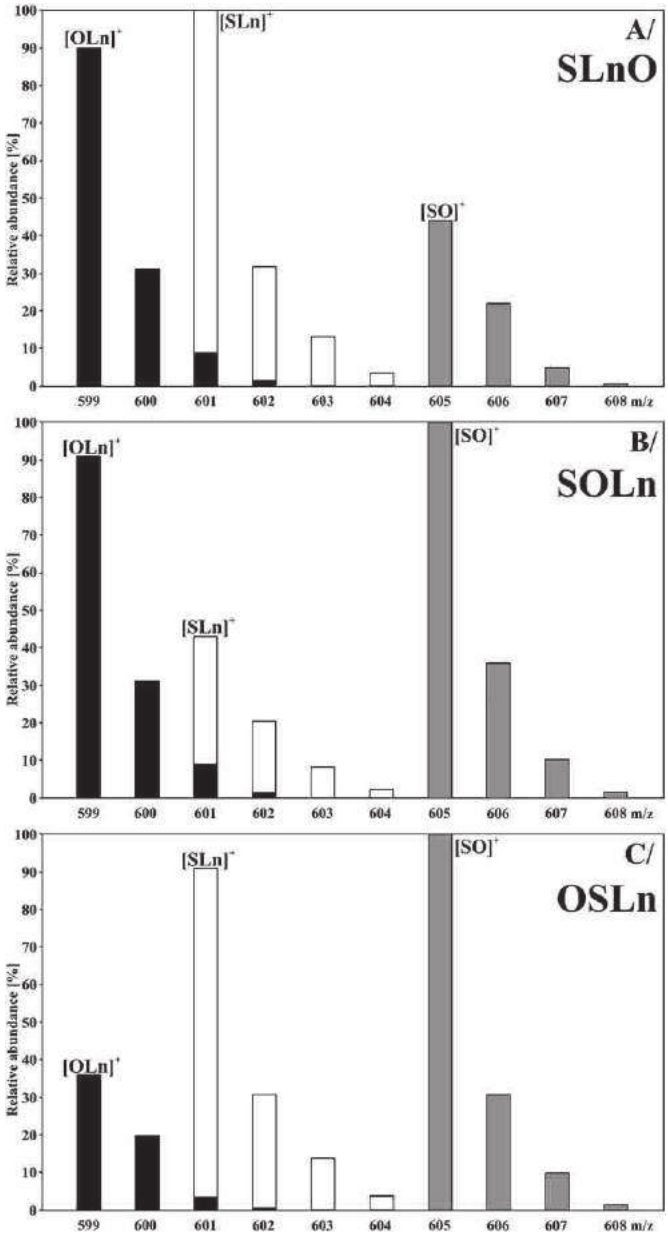

Fig. 2. Normalized relative abundances of $[M+H-R_iCOOH]^+$ fragment ions in APCI mass spectra of regioisomeric triplet SLnO (A), SOLn (B) and OSLn (C) obtained from the chromatogram shown in Fig. 1.

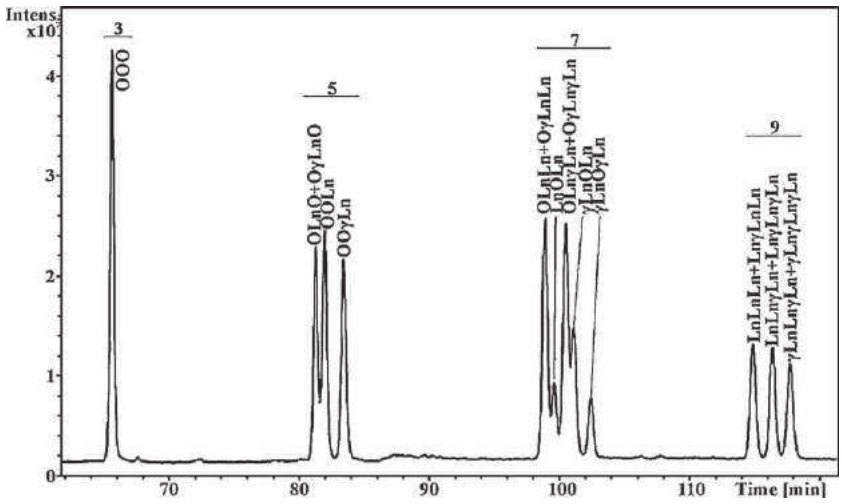

Fig. 3. Silver-ion HPLC/APCI-MS chromatogram of the randomization mixture prepared from triolein (OOO, Δ9-C18:1), trilinolenin (LnLnLn, Δ9,12,15-C18:3) and tri-γ-linolenin (γLnγLnγLn, Δ6,9,12-C18:3), see Section 2 for conditions. Numbers correspond to the double bond number.

for a systematic study of retention and fragmentation behavior of regioisomeric TGs.

Fig. 1 shows a typical chromatogram of the randomization mixture of three mono-acid TGs (SSS, OOO and LnLnLn) with the baseline resolution of most peaks, while some of them have only partial resolution (*e.g.*, OLnO/OOLn, OLnLn/LnOLn) but still sufficient for reliable peak integration. Fig. 2 shows regions of APCI mass spectra with diacylglycerol fragments of the regioisomeric triplet SLnO (A), SOLn (B) and OSLn (C). For the identification of *sn*-2 FA, contributions of A + 2 and A + 3 isotopes should be subtracted from $[M+H-R_iCOOH]^+$ fragment ions with *m*/*z* values higher by two units, *e.g.*, A + 2 isotopic peak from $[OLn]^+$ fragment ion contributes to the peak of $[SLn]^+$ at *m*/*z* 601. Tables 2 and 3 show raw data without A + 2 isotopic subtraction for all measured regioisomers. The neutral loss of FA from the middle *sn*-2 position is less preferred, therefore the smallest peak among $[M+H-R_iCOOH]^+$ ions corresponds to the neutral loss from *sn*-2 position, *e.g.*, the smallest peak of $[SO]^+$ in Fig. 2A confirms that Ln is in the *sn*-2 position (SLnO). DBs in outer *sn*-1/3 positions have a stronger effect on the retention probably caused by a better steric availability of DBs for interaction with the silver-ions embedded in the stationary phase. The same retention pattern is valid for all studied regioisomers which can be expressed as a simple rule of thumb: more DBs in outer *sn*-1/3 positions result in a slightly higher retention in silver-ion HPLC.

A highly complex retention pattern is observed in the case of TGs containing isomers differing only in the position of DBs (Fig. 3), such as linolenic (Δ9,12,15-C18:3) and γ-linolenic (Δ6,9,12-C18:3) acids. When the only difference between two TGs is in the DB positions for *sn*-2 FA (OLnO *vs.* OγLnO), then no visible chromatographic separation is observed (Fig. 3). On the other hand, the same difference occurring in *sn*-1/3 positions (OOLn *vs.* OOγLn) leads to a very good resolution with the difference of retention times about 1.6 min. The identification of the individual peaks in Fig. 3 is based on the combination of several known facts: (A) the knowledge of retention behavior of TGs containing Ln based on the measurement of other randomization mixtures, (B) differences in fragment ion ratios for *sn*-1,3 *vs.* *sn*-2, (C) differences in $[M+H]^+/[M+H-R_iCOOH]^+$ ratios between Ln and γLn, (D) differences in retention times between Ln and γLn, (E) agreement of statistical ratios of peak areas in individual DB groups and the theoretical calculation, *e.g.*, the identification of the DB = 7 group in Fig. 3 is as follows: OLnLn/LnLnO + OγLnLn/LnγLnO (theoretical relative abundance 4; experimental 4), LnOLn (1; 1.1), OLnγLn/γLnLnO + OγLnγLn/γLnγLnO (4; 4), γLnOLn/LnOγLn (2; 2),

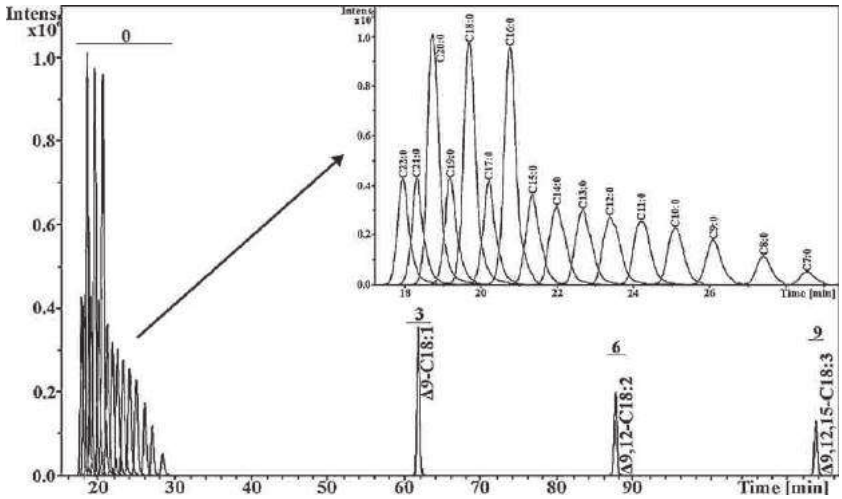

Fig. 4. Silver-ion HPLC/APCI-MS chromatogram of all mono-acid TG standards. Numbers correspond to the double bond number. Inset zoom shows the resolution of saturated TGs from C7:0 to C22:0. Concentrations of all standards are identical except for C16:0, C18:0 and C20:0 with doubled concentrations.

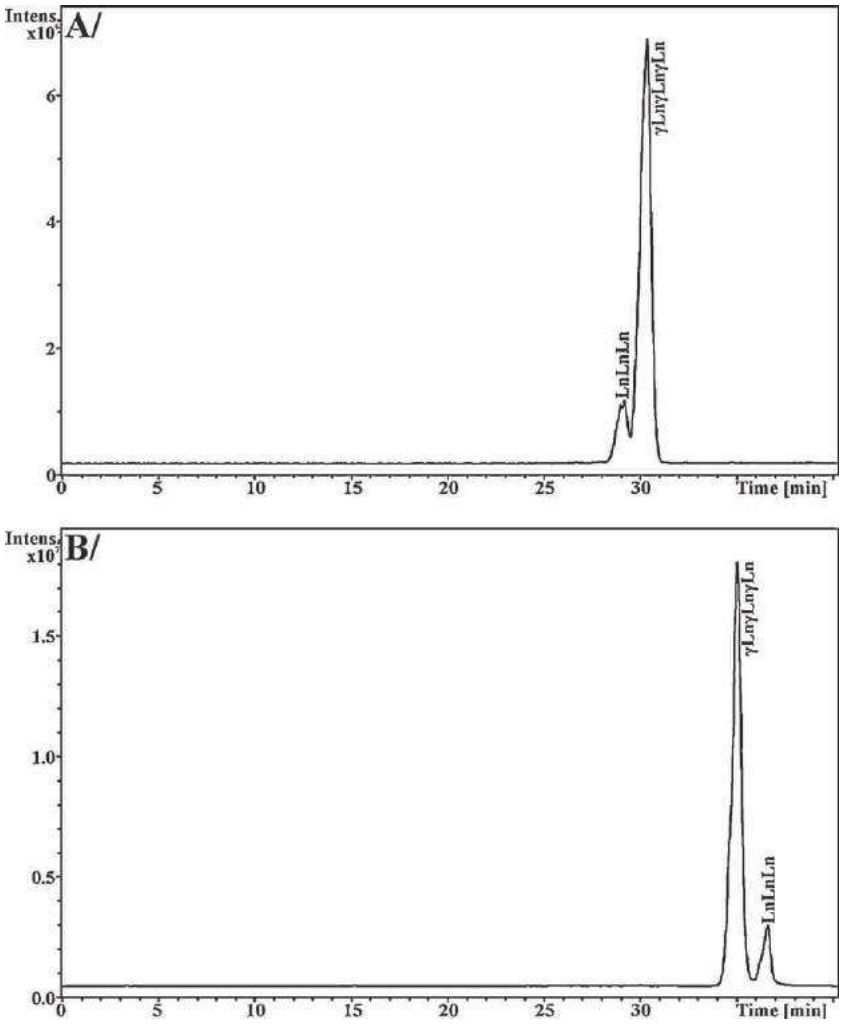

Fig. 5. Comparison of retention behavior of LnLnLn and γLnγLnγLn in two different mobile phase systems: (A) 0 min – 100% A, 60 min – 50% A + 50% B, where A is hexane–2-propanol–acetonitrile (99.8:0.1:0.1, v/v/v) and B is hexane–2-propanol–acetonitrile (96:2:2, v/v/v) [2] and (B) 0 min – 100% acetone, 5 min – 100% acetone, 30 min – 94% acetone + 7% acetonitrile, 40 min – 89% acetone + 11% acetonitrile [20]. All other experimental conditions are identical as in Section 2.

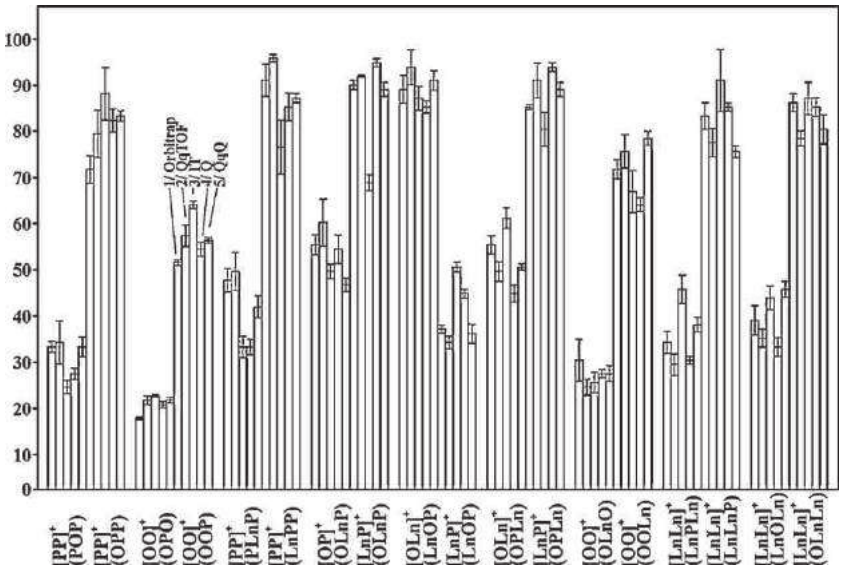

Fig. 6. Plots of relative abundances of $[R_1R_1]^+$ related to $[R_1R_2]^+$ fragment ions (100%) with their standard deviations for the randomization mixture PPP/OOO/LnLnLn measured on five different instruments: (1) LTQ Orbitrap XL (Thermo Fisher Scientific), (2) quadrupole time-of-flight micrOTOF-Q (Bruker Daltonics), (3) ion trap Esquire 3000 (Bruker Daltonics), (4) single quadrupole LC/MSD (Agilent Technologies) and (5) triple quadrupole API 3000 (AB SCIEX).

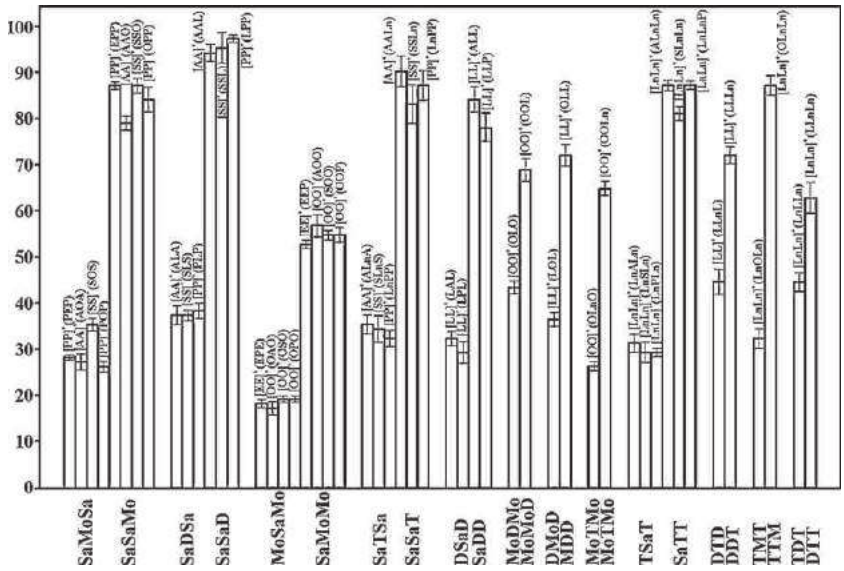

Fig. 7. Plots of relative abundances of $[R_1R_1]^+$ related to $[R_1R_2]^+$ fragment ions (100%) with their standard deviations for randomization mixtures measured on the single quadrupole mass spectrometer; annotation of *x* axis: Sa – saturated, Mo – monounsaturated, D – diunsaturated, T – triunsaturated; annotation of particular columns correspond to individual $[M+H-R_2COOH]^+$ ions fragmented from TGs written in parentheses.

γLnOγLn (1; 0.9). The fragmentation behavior of TGs containing γLn is significantly different, as illustrated on the example of OOγLn (see Table 2), where the ratio of $[R_1R_1]^+/[R_1R_2]^+$ is reversed in comparison to all other measured TGs.

The retention in silver-ion chromatography increases with an increasing number of DBs. Optimized conditions can provide at least the partial separation even for saturated TGs, as shown in the chromatogram (Fig. 4) of standard mixtures containing saturated TGs with C7:0 to C22:0 and unsaturated TGs with C18:1, C18:2 and C18:3. If the response factor (RF) of C18:1 (triolein) is set to 1.00, then RFs of saturated TGs from C14:0 to C22:0 are in the range of 0.59–0.64 (relative difference is lower than 8%), the RF of LLL is 1.37 and of LnLnLn 1.86. Regioisomers have identical RFs. The best chromatographic resolution of regioisomers has been published by our method [2] using hexane–2-propanol–acetonitrile as the mobile phase and in separations published by Adlof [18] using conventional hexane–acetonitrile mobile phase. The addition of 2-propanol does not bring any improvement in the chromatographic resolution, but it improves the limited miscibility of hexane and acetonitrile and therefore yields much better intra- and inter-day reproducibility, which is a serious problem with hexane–acetonitrile mobile phases. It is interesting that the retention order of TGs containing Ln and γLn in our work is reversed in comparison to all published articles so far [11,20,41,42]. For that reason, we repeated the experiment [20] using the previously reported mobile phase composition. Fig. 5 confirms that the retention order of DB positional isomers strongly depends on the mobile phase composition and that the order of LnLnLn and γLnγLnγLn is really reversed in the two systems. Other interesting example of strong effect of DB position is the ratio of $[R_1R_1]^+/[R_1R_2]^+$ fragment ions, which is completely reversed in case of OOγLn unlike to all other regioisomers listed in Table 2.

The main goal of our inter-instrument comparison of APCI mass spectra of TG regioisomers has been to study to what extent are published ratios of $[M+H-R_iCOOH]^+$ ions [30,33,34,39,40] applicable for different instruments and laboratories. Five different types of mass analyzers from various manufacturers have been selected and all regioisomeric mixtures have been measured by a single person using identical conditions. Fig. 6 shows a visual comparison for some regioisomers (the full data set is shown in Tables 2 and 3). Mostly, differences among instruments are within the common experimental errors expressed by the standard deviation but not in all cases. These values of $[M+H-R_iCOOH]^+$ ratios can be used for quantitation without the need of silver-ion HPLC separation of regioisomers. For example, NARP-HPLC provides the separation of TGs but without regioisomeric distinction but by comparing the ratio of $[M+H-R_iCOOH]^+$ ions with those in Tables 2 and 3, the regioisomeric ratio can be determined. This assumption is based on the known fact [6,24,37–39] that calibration curves for regioisomeric mixtures are linear and therefore accurately determined $[M+H-R_iCOOH]^+$ ratios of pure regioisomers can be used for the construction of this linear dependence. We have not detected any dependence of $[M+H-R_iCOOH]^+$ ratios on the mobile phase composition. Measurements of regioisomeric standards on the same instrument should generate, of course, more accurate results, but this level of precision is often not required in the regioisomeric analysis, since the common practice often relies only on the determination of the prevailing FA in the middle *sn*-2 position based on the deviation from statistically expected ratios of $[M+H-R_iCOOH]^+$ ions.

Ratios of $[M+H-R_iCOOH]^+$ fragment ions strongly depend on the DB number and position in individual FAs, while the DB geometry and FA length have only minor influence (Fig. 7). The data measured on the quadrupole analyzer are grouped according to the unsaturation level of individual FAs, *i.e.*, saturated (Sa), monounsaturated (Mo), diunsaturated (D) and triunsaturated (T). Good correlation is observed among values in individual groups, especially considering the fact that differences in *cis*/*trans* isomerism (*e.g.*, PEP *vs.* POP in SaMoSa group, EPP *vs.* OPP in SaSaMo group) or high differences in alkyl chain lengths (*e.g.*, AOA *vs.* POP in SaMoSa group differs by eight carbon atoms) are neglected. On the other hand, the positions of DBs have a much stronger effect on $[M+H-R_iCOOH]^+$ ratios, as illustrated by the difference between LnOLn and γLnOγLn (32 *vs.* 12%, see Tables 2 and 3) in agreement with previous works [43–45]. Fig. 7 suggests that the data for a TG with a given unsaturation pattern can be generalized for other TGs with the same unsaturation pattern, which can solve the lack of unusual standards but still provide accurate regioisomeric determination. It can be concluded that the number and distribution of DBs have major effects on both retention behavior in silver-ion mode and ratios of

$[M+H-R_iCOOH]^+$ ions, while the alkyl chain length of FAs and the geometry of DBs have only very minor effects.

4. Conclusions

Possibilities and limitations of two basic approaches (silver-ion HPLC and ratios of $[M+H-R_iCOOH]^+$ fragment ions) in the regioisomeric analysis of TGs have been systematically studied. The randomization synthesis of a broad range of standard regioisomeric mixtures, their silver-ion HPLC separation and subsequent measurements of APCI mass spectra on five different mass analyzers (single quadrupole, triple quadrupole, ion trap, hybrid QqTOF and Orbitrap) produce an extensive data set for the generalization of retention and fragmentation behavior of regioisomeric TGs. The randomization enables the preparation of any regioisomeric combination, because mono-acid TG standards are commercially available for both common and unusual TGs. Silver-ion chromatograms show a clear separation of TGs into groups differing in the number of DBs. Our optimized silver-ion system also provides a good resolution inside DB groups, where the DB position and stereospecific position on the glycerol skeleton (*sn*-1/3 or 2) play an important role. DBs in outer *sn*-1/3 positions cause slightly stronger retention compared to *sn*-2 regioisomers. If the only difference between two TGs is in the position of DB (*e.g.*, linolenic *vs.* γ-linolenic acids), then no separation is observed for different DB positions occurring in *sn*-2 FA, while the same situation for *sn*-1/3 positions results in a good chromatographic resolution. The instrument type, for those instruments tested, has only minor effect on $[M+H-R_iCOOH]^+$ ratios, therefore published values can be used for the *sn*-2 identification and rough quantitation on other instruments as well. We recommend three alternative approaches for the TG regioisomeric analysis depending on the laboratory equipment and skills: (A) ratios of chromatographic peak areas in silver-ion HPLC (no need for regioisomeric standards due to the known retention order and identical response factors for regioisomers), (B) fragment ion ratios and (C) combination of both approaches which should provide the most reliable results.

Acknowledgments

This work was supported by the grant project no. MSM0021627502 sponsored by the Ministry of Education, Youth and Sports of the Czech Republic and project no. 203/09/0139 sponsored by the Czech Science Foundation. M.H. would like to kindly appreciate the mental contribution of Dr. W.C. Byrdwell (USDA, Beltsville, MD, USA), because our mutual discussion has initiated this work, but he could not participate in this study later on.

References

[1] C.C. Akoh, D.B. Min, Food Lipids: Chemistry, Nutrition, and Biotechnology, second edition, Marcel Dekker, New York, 2002.
[2] M. Lísa, H. Velínská, M. Holčapek, Anal. Chem. 81 (2009) 3903.
[3] M. Holčapek, M. Lísa, P. Jandera, N. Kabátová, J. Sep. Sci. 28 (2005) 1315.
[4] M. Lísa, M. Holčapek, J. Chromatogr. A 1198 (2008) 115.
[5] M. Lísa, M. Holčapek, M. Boháč, J. Agric. Food Chem. 57 (2009) 6888.
[6] W.C. Byrdwell, W.E. Neff, Rapid Commun. Mass Spectrom. 16 (2002) 300.
[7] M. Lísa, F. Lynen, M. Holčapek, P. Sandra, J. Chromatogr. A 1176 (2007) 135.
[8] S. Momchilova, Y. Itabashi, B. Nikolova-Damyanova, A. Kuksis, J. Sep. Sci. 29 (2006) 2578.
[9] M. Lísa, M. Holčapek, H. Sovová, J. Chromatogr. A 1216 (2009) 8371.
[10] M. Holčapek, H. Velínská, M. Lísa, P. Česla, J. Sep. Sci. 32 (2009) 3672.
[11] W.W. Christie, J. Chromatogr. 454 (1988) 273.
[12] W.W. Christie, J. Chromatogr. B 671 (1995) 197.
[13] B. Nikolova-Damyanova, J. Chromatogr. A 1216 (2009) 1815.
[14] P. Dugo, O. Favoino, P.Q. Tranchida, G. Dugo, L. Mondello, J. Chromatogr. A 1041 (2004) 135.
[15] P. Dugo, T. Kumm, A. Fazio, G. Dugo, L. Mondello, J. Sep. Sci. 29 (2006) 567.
[16] I. Francois, A.D. Pereira, P. Sandra, J. Sep. Sci. 33 (2010) 1504.
[17] E.J.C. van der Klift, G. Vivó-Truyols, F.W. Claassen, F.L. van Holthoon, T.A. van Beek, J. Chromatogr. A 1178 (2008) 43.
[18] R.O. Adlof, J. High Resol. Chromatogr. 18 (1995) 105.
[19] J. Cvačka, O. Hovorka, P. Jiroš, J. Kindl, K. Stránský, I. Valterová, J. Chromatogr A 1101 (2006) 226.
[20] H. Leskinen, J.P. Suomela, J. Pinta, H. Kalli, Anal. Chem. 80 (2008) 5788.
[21] P.J.W. Schuyl, T. De Joode, M.A. Vasconcellos, G.S.M.J.E. Duchateau, J. Chromatogr. A 810 (1998) 53.
[22] W.C. Byrdwell, Lipids 36 (2001) 327.
[23] M. Holčapek, P. Jandera, J. Fischer, B. Prokeš, J. Chromatogr. A 858 (1999) 13.
[24] A. Jakab, I. Jablonkai, E. Forgacs, Rapid Commun. Mass Spectrom. 17 (2003) 2295.
[25] H.R. Mottram, S.E. Woodbury, R.P. Evershed, Rapid Commun. Mass Spectrom. 11 (1997) 1240.
[26] H.G. Janssen, K. Hrnčiřík, A. Szórádi, M. Leijten, J. Chromatogr. A 1112 (2006) 141.
[27] I.B. Standal, D.E. Axelson, M. Aursand, J. Am. Oil Chem. Soc. 86 (2009) 401.
[28] M. Barber, T.O. Merren, Tetrahedron Lett. 17 (1964) 1063.
[29] H.R. Mottram, R.P. Evershed, Tetrahedron Lett. 37 (1996) 8593.
[30] R. Gakwaya, X. Li, Y.L. Wong, S. Chivukula, E.J. Collins, J.J. Evans, Rapid Commun. Mass Spectrom. 20 (2007) 3262.
[31] L.C. Herrera, M.A. Potvin, E. Melanson, Rapid Commun. Mass Spectrom. 24 (2010) 2745.
[32] N.L. Leveque, S. Heron, A. Tchapla, J. Mass Spectrom. 45 (2010) 284.
[33] X. Li, E.J. Collins, J.J. Evans, Rapid Commun. Mass Spectrom. 20 (2006) 171.
[34] X. Li, J.J. Evans, Rapid Commun. Mass Spectrom. 19 (2005) 2528.
[35] M. Malone, J.J. Evans, Lipids 39 (2004) 273.
[36] E. Pittenauer, G. Allmaier, J. Am. Soc. Mass Spectrom. 20 (2009) 1037.
[37] L. Fauconnot, J. Hau, J.M. Aeschlimann, L.B. Fay, F. Dionisi, Rapid Commun. Mass Spectrom. 18 (2004) 218.
[38] M. Holčapek, P. Jandera, P. Zderadička, L. Hrubá, J. Chromatogr. A 1010 (2003) 195.
[39] H. Leskinen, J.P. Suomela, H. Kallio, Rapid Commun. Mass Spectrom. 21 (2007) 2361.
[40] W.C. Byrdwell, Lipids 40 (2005) 383.
[41] R.G. Harfmann, S. Julka, H.J. Cortes, J. Sep. Sci. 31 (2008) 915.
[42] P. Laakso, P. Voutilainen, Lipids 31 (1996) 1311.
[43] B. Nikolova-Damyanova, B.G. Herslof, W.W. Christie, J. Chromatogr. 609 (1992) 133.
[44] H. Leskinen, J.P. Suomela, J. Pinta, H. Kallio, Anal. Chem. 80 (2008) 5788.
[45] M. Lísa, M. Holčapek, T. Řezanka, N. Kabátová, J. Chromatogr. A 1146 (2007) 67.

Research Article

Rapid Communications in Mass Spectrometry

Received: 11 September 2015 Revised: 13 October 2015 Accepted: 18 October 2015 Published online in Wiley Online Library

Rapid Commun. Mass Spectrom. **2016**, *30*, 256–264
(wileyonlinelibrary.com) DOI: 10.1002/rcm.7430

Determination of triacylglycerol regioisomers using differential mobility spectrometry

Martin Šala[1,2], Miroslav Lísa[1], J. Larry Campbell[3] and Michal Holčapek[1]*

[1]University of Pardubice, Faculty of Chemical Technology, Department of Analytical Chemistry, Studentská 573, 532 10 Pardubice, Czech Republic
[2]National Institute of Chemistry, Laboratory for Analytical Chemistry, Hajdrihova 19, 1000 Ljubljana, Slovenia
[3]SCIEX, 71 Four Valley Drive, , Concord, Ontario L4K 4V8, Canada

RATIONALE: Triacylglycerols (TG) contain three fatty acyls attached to the glycerol backbone in stereochemically numbered positions *sn*-1, 2 and 3. Isobaric TG with exchanged fatty acyl chains in positions *sn*-1/3 *vs*. *sn*-2 are referred to as regioisomers and the determination of their regioisomeric ratios is important for nutrition purposes.
METHODS: Differential mobility spectrometry (DMS) coupled to electrospray ionization mass spectrometry (ESI-MS) is applied for the separation of simple unsaturated TG regioisomers extracted from porcine adipose tissue using their silver-ion molecular adducts.
RESULTS: Four pairs of TG regioisomers containing combinations of unsaturated and saturated fatty acyl chains are successfully separated using DMS with 1-butanol or 1-propanol as the chemical modifier. Various experimental parameters are carefully optimized, such as the separation and compensation voltages applied to DMS electrodes, the type and flow rate of chemical modifier and the dwell time of analyte ions in the DMS cell. The optimized DMS approach is used for the characterization of TG regioisomers in less than one minute, compared to tens of minutes typical for silver-ion or reversed-phase high-performance liquid chromatography/mass spectrometry approaches.
CONCLUSIONS: The application of this method for the characterization of TG regioisomers in porcine adipose tissue shows the method suitability for analyses of other animal fats.

Lipidomics deals with the comprehensive characterization of lipids in dynamic biological systems. Lipids can be divided into eight main categories: fatty acyls, glycerolipids, glycerophospholipids, sphingolipids, sterol lipids, prenol lipids, saccharolipids, and polyketides.[1] Triacylglycerols (TG) – nonpolar lipids belonging to the glycerolipids family – are abundant in many biological samples, forming the major part of plant oils and animal fats.[2–4] TG molecules consist of a glycerol backbone bonded to three fatty acyl chains that can be of different chain lengths and can contain carbon–carbon double bonds (DB) of varying number, position, and geometry (*cis* or *trans*). These acyl chains can also be positioned differently on the glycerol skeleton (*sn*-1, *sn*-2, and *sn*-3). TG with fatty acyl chains differing in *sn*-1/3 *vs*. *sn*-2 positions are regioisomers. Two different fatty acyl chains in the *sn*-1 and *sn*-3 positions represent two enantiomers, and this isomerism creates an enormous complexity in analyses of TG due to the number of possible isomers occurring in biological samples. The determination of the identity of the *sn*-2 fatty acyl is important for nutrition purposes due to the different bioavailability of essential fatty acyl chains depending on *sn*-position.[5]

* *Correspondence to:* M. Holčapek, Department of Analytical Chemistry, Faculty of Chemical Technology, University of Pardubice, Studentská 573, 532 10 Pardubice, Czech Republic. E-mail: Michal.Holcapek@upce.cz

In recent years, mass spectrometry (MS) has become an almost essential tool for many lipidomics applications.[6] The nonpolar character of TG makes atmospheric pressure chemical ionization (APCI) a logical first choice for ionization, as reported in the majority of lipidomic studies focused only on TG.[2–4,7–9] Atmospheric pressure photoionization (APPI) is an alternative ionization technique providing comparable results to APCI.[10] Unfortunately, both APCI and APPI are less convenient for polar lipid classes, so electrospray ionization (ESI) is generally chosen for lipidomic studies covering multiple nonpolar and polar lipid classes.[6,11] Positive-ion APCI or APPI mass spectra of TG show protonated molecules $[M+H]^+$ with lower relative abundances of $[M+Na]^+$ or $[M+NH_4]^+$ adducts, while these adduct ions dominate in ESI mass spectra with the total absence of protonated molecules. The additional information on individual fatty acyl chains in the TG molecule requires the fragmentation of the intact ionized TG to form $[M+H–R_iCOOH]^+$ fragment ions, where R_i is the *sn*-position of the lost fatty acyl chain. These fragments are typically observed in full scan mass spectra measured with all atmospheric pressure ionization techniques, but their relative abundances are lower in ESI than APCI/APPI. Hence, tandem mass spectrometry (MS/MS) is used for the identification of fatty acyl chains in ESI-MS.[11] The ratios of fragment ions arising from the cleavage of fatty acids from the *sn*-1/3 positions ($[M+H–R_1COOH]^+$ and $[M+H–R_3COOH]^+$ ions) and the *sn*-2 position ($[M+H–R_2COOH]^+$ ion) are commonly used for the identification of the prevailing fatty

Rapid Communications in Mass Spectrometry

acyl in the *sn*-2 position, because the neutral loss of the acyl chain from the *sn*-2 position is less preferred.[2–4,7,8,12] Another possibility for the differentiation of the *sn*-2 position is based on the formation of regiospecific 'G' and 'J' product ions using high-energy collision-induced dissociation MS/MS.[13,14]

Various analytical methods have been explored to improve the identification of TG regioisomers, including (1) silver-ion high-performance liquid chromatography (HPLC),[4,12,15–17] (2) the ratio of $[M+H–R_iCOOH]^+$ fragment ions in APCI mass spectra,[2,18] (3) the stereospecific enzymatic hydrolysis followed by another suitable analytical technique,[19] and (4) nonaqueous reversed-phase (NARP)-HPLC using two columns with very long retention times (100–500 min).[20,21] The silver-ion HPLC provides accurate results due to the separation of most TG regioisomers and it can be considered as a reference method, but analysis times range from 60 to 120 min. The fragment ion ratios of $[M+H–R_iCOOH]^+$ are typically used in coupling with NARP-HPLC, with analysis times in the range of tens of minutes; however, the accuracy and robustness is lower than with the silver-ion HPLC determination of TG regioisomers. NARP is a frequently employed method due to its potential to separate numerous TG according to the equivalent carbon number, which is defined as the number of carbon atoms in fatty acyl chains minus two times the number of double bonds (DB).[2–4] Silver-ion HPLC separates TG according to the number, positions and geometry of any DB present.[12,15–17] It also enables the regioisomeric separation of TG differing in the DB distributions between the *sn*-1/3 and *sn*-2 positions.[12,16,22] TG enantiomers and also many TG regioisomers can be also distinguished by chiral HPLC in normal-phase systems.[23,24] Silver ions have also been doped into LC effluent to produce adducts with TG,[25] with regioisomeric analyses derived from MS^5 level fragmentation of $[TG+Ag+AgNO_3]^+$ adduct ions.

More recently, various ion mobility spectrometry (IMS) techniques have been employed instead of or in addition to HPLC for the improvement of TG analyses by MS. At present, different types of IMS systems are commercially available and have been applied for the analysis of lipids, i.e., drift tube IMS,[26] traveling wave IMS (TWIMS),[27] high-field asymmetric waveform IMS (FAIMS)[28] and differential mobility spectrometry (DMS).[29] The drift tube IMS and TWIMS systems are typically mounted within the vacuum manifold (low-pressure region) of a mass spectrometer, while FAIMS and DMS techniques are positioned at an elevated pressure (atmospheric pressure) between the ionization source and the MS orifice.

The DMS method employed in this work has shown potential in lipidomics as demonstrated by its ability to separate glycerophospholipid and sphingolipid classes[29] and to separate phosphatidylcholine (PC) regioisomers.[30] Other examples of the separation capabilities of DMS include differentiation of structural isomers,[31–35] stereoisomers[36,37] or ions differing only in their protonation sites.[38] In the DMS cell, ions are transmitted between two planar electrodes by a flow of gas at atmospheric pressure. A high-voltage radiofrequency asymmetric waveform is applied across these electrodes, where the difference between the mobility of ions during the high- and low-field portions of the waveform determines their trajectories. The separation is achieved as a function of the direct current voltage (the compensation voltage, CV) required to steer the trajectory of ions toward the MS inlet. In addition, vapors of organic chemical modifiers can be introduced into the DMS transport gas, which affects the solvation state of analyte ions and alters the apparent mobility of such species.[39] This phenomenon is described by the dynamic cluster/decluster model, because analyte ions are clustered with modifier molecules in the lower field part and declustered in the higher field part of the radiofrequency waveform.[34,39] Further improvements in the selectivity can be achieved with the use of so-called throttle gas, which is a variable flow of nitrogen gas added into the chamber that effectively reduces the transport gas flow through the DMS towards the mass spectrometer, increasing the residence time of ions in the DMS cell and improving the resolution.[37]

The goal of this work is the development of a new DMS-MS method for the determination of TG regioisomers, specifically for the analysis of these regioisomers in porcine adipose tissue, where the most abundant TG regioisomers are combinations of monounsaturated and saturated fatty acyl chains. Different types and concentrations of chemical modifiers and also different types of molecular adducts are investigated with the goal of achieving the regioisomeric separation of these TG. This new DMS-MS method for the regioisomeric analysis is also compared with previously published results with silver-ion HPLC and ratios of fragment ions in mass spectra in terms of the regioisomeric resolution (RR), analysis times, limits of detection and quantitation, with favorable comparisons drawn.

EXPERIMENTAL

Materials

Methanol, ethanol, 2-propanol (all LC/MS grade), 1-propanol, 1-butanol, hexane (all HPLC grade), sodium methoxide and silver nitrate were purchased from Sigma-Aldrich (St. Louis, MO, USA). Standards of tristearin (SSS, C18:0), triolein (OOO, C18:1 (9Z)), trilinolein (LLL, C18:2 (9Z,12Z)) and tripalmitin (PPP, C16:0) used for the randomization reaction were purchased from Nu-ChekPrep (Elysian, MN, USA) with 99% purity. TG regioisomers (OSO, SOO, SOS, SSO, POP, OPP, OPO and OOP) were purchased from Larodan Fine Chemicals AB (Malmo, Sweden) with 99% purity. The stereospecific numbering (*sn*-) of fatty acyls is reflected by TG abbreviation, e.g., OSO means 1-oleoyl-2-stearoyl-3-oleoyl-*sn*-glycerol. The porcine adipose tissue was purchased from a local butcher in Pardubice, Czech Republic.

Standards and sample preparation

Silver nitrate ($AgNO_3$) solution was prepared in 2-propanol/water (1:1, v/v) at the concentration of 1 mg/mL. Stock solutions of TG regioisomers standards were prepared in hexane at concentration of 1 mg/mL and then diluted to 25 µg/mL in hexane/2-propanol (1:1, v/v). A 2% $AgNO_3$ solution was added to this solution and left under ambient

conditions for 30 min to induce the formation of silver-ion adducts. The porcine adipose tissue sample was prepared according to an established method.[9] One mg of tissue was weighed and homogenized with 1 mL of hexane. The suspension was filtered through a 0.22 µm cellulose filter (Teknokroma, Barcelona, Spain). Then 20 µL of the filtrate was diluted with 1 mL of hexane/2-propanol (1:1, v/v) with the addition of a 2% $AgNO_3$ solution and left under ambient conditions for 30 min. The porcine adipose tissue extract was analyzed directly by DMS without any fractionation.

DMS-MS conditions

Experiments were performed on a 6500 QTRAP mass spectrometer equipped with a SelexION™ DMS cell (SCIEX, Concord, ON, Canada) using the positive-ion ESI mode. The systematic optimization of all relevant parameters was performed with the goal of achieving the best regioisomeric separation, sensitivity and robustness. These parameters included the type of chemical modifier and its flow rate (120–290 µL/min), the separation voltage (SV) (1500–4100 V), the pressure of throttle gas (30–46 psi) and the DMS temperature (DT) (150–300 °C). After the initial screening of several chemical modifiers commonly used in DMS (acetonitrile, acetone and alcohols), only alcohols (methanol, ethanol, 1-propanol, 2-propanol and 1-butanol) were further investigated due to the best results for TG regioisomers. Two selected reaction monitoring (SRM) transitions were used for monitoring of TG: *m/z* 937–655 and 937–653 for OPP/POP, *m/z* 963–681 and 963–679 for OPO/OOP, *m/z* 995–713 and 995–711 for SSO/SOS and *m/z* 993–711 and 993–709 for OSO/SOO. The optimized conditions used for final measurements were as follows: flow rate of analyte of 10 µL/min, 1-butanol as the modifier at the flow rate of 120 µL/min in nitrogen (10 or 20 psi) as the curtain gas, SV of 4100 V, electrospray voltage 5500 V, DT of 225 °C, DMS offset of –5 V, and source temperature of 50 °C. The pressure of the throttle gas (differential resolution, DR) was adjusted for the DMS resolution of each regioisomeric pair (see Table 1). SRM data were acquired for CV ramped from 0 to +10 V in 0.10 V steps.

RESULTS AND DISCUSSION

Optimization of DMS separation using OSO/SOO as a model TG regioisomeric mixture

The resolution of TG regioisomers is a very demanding analytical task in lipidomics analyses, so the careful optimization of all relevant experimental parameters is essential to achieve successful separation. The initial optimization of the DMS-MS system began with the selection of the TG molecular adduct. For $[M+Na]^+$ or $[M+NH_4]^+$ adducts, no separation was observed for the equimolar mixture of the regioisomeric pair OSO and SOO. However, the separation of $[M+Ag]^+$ adducts of those same TG regioisomers was next attempted. This choice is based on the analogy with silver-ion HPLC of TG regioisomers[12,22] and in light of earlier DMS-based separation of silver-ion adducts of PC 16:0/18:1 and PC 18:1/16:0 regioisomers.[30] Recently, drift-time ion mobility spectrometry has shown promise in separating the same regioisomeric ions,[40] albeit with initial lower overall sensitivity.

Figures 1–4 illustrate the optimization of key parameters affecting the DMS separation of $[OSO+Ag]^+$ and $[SOO+Ag]^+$ ions, such as the type (Fig. 1) and the flow rate (Fig. 2) of the chemical modifier, the separation voltage (Fig. 3), and the DR (Fig. 4). Several parameters are mutually interconnected, so optimization was done iteratively with the best settings of other parameters; however, these figures should illustrate the effects of individual parameters on the regioisomeric resolution (RR) and the signal intensity. SRM transitions representing neutral losses of oleic (*m/z* 993–711) or stearic (*m/z* 993–709) acid from these $[M+Ag]^+$ ions were used for the method development. Different ratios in SRM traces also confirm the separation of regioisomers, because TG regioisomers have a lower preference for neutral losses of fatty acids from the *sn*-2 position and therefore $[M+H–R_2COOH]^+$ fragment ions have lower relative abundances than $[M+H–R_1COOH]^+$ and $[M+H–R_3COOH]^+$ ions.

Previous studies showed strong effects of chemical modifiers used in the DMS analysis on the resolution,[32–37,40–43] but these effects greatly depend on the type of analyte. Alcohols provide the most promising results based on our initial tests with acetonitrile, acetone, methanol, ethanol, 1-propanol, 2-propanol and 1-butanol. A general trend is observed that the RR is improved with the increasing length of alkyl chain

Table 1. Parameters used for measurements of calibration curves $y = a.x + b$ for individual TG regioisomers: compensation voltage (CV), slope (a), intercept (b), regression coefficient (r^2), differential resolution (DR), scanned *m/z* range, limit of detection (LOD) at signal-to-noise (S/N) = 3 and limit of quantitaton (LOQ) at S/N = 10

TG regioisomer	CV (V)	*a* (*10^4)	*b* (*10^5)	r^2	DR (psi)	*m/z* range	LOD (µg/mL)	LOQ (µg/mL)
POP	3.7	0.41	0.24	0.977	45	937–947	4.1	13.8
OPP	2.6	1.7	2.5	0.947			2.7	9.1
OPO	5.8	0.6	0.74	0.946	42	962–972	0.8	2.6
OOP	6.7	1.7	0.68	0.967			2.1	7.0
SOS	3.9	0.64	0.66	0.989	45	992–1002	2.5	8.3
SSO	3.3	0.86	1.6	0.992			1.5	4.9
OSO	5.2	3.8	3.2	0.973	42	992–1002	3.4	11.6
OOS	6.2	9.3	8.2	0.951			1.9	6.4

Rapid Communications in Mass Spectrometry

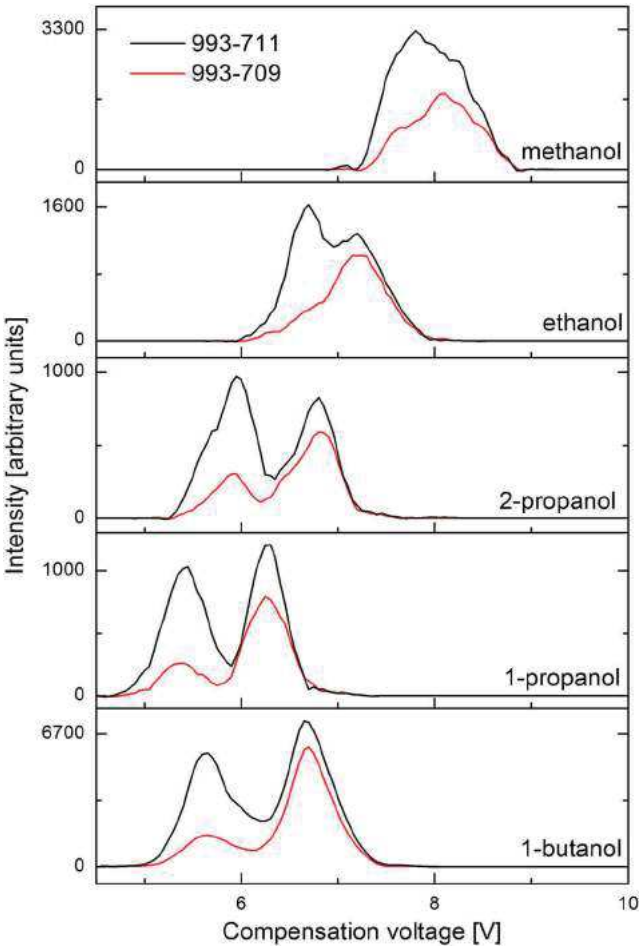

Figure 1. Effect of the type of chemical modifier on the DMS separation of the OSO/SOO regioisomeric pair. Two SRM transition traces for neutral losses of oleic (*m/z* 993–711) or stearic (*m/z* 993–709) acid are shown. The flow rate of the chemical modifier is 250 μL/min except for 1-butanol, where the flow rate is reduced to 120 μL/min due to the sensitivity. All other DMS-MS parameters are kept constant: sample flow rate 10 μL/min, DR 43 psi, SV 4100 V and DT 225 °C.

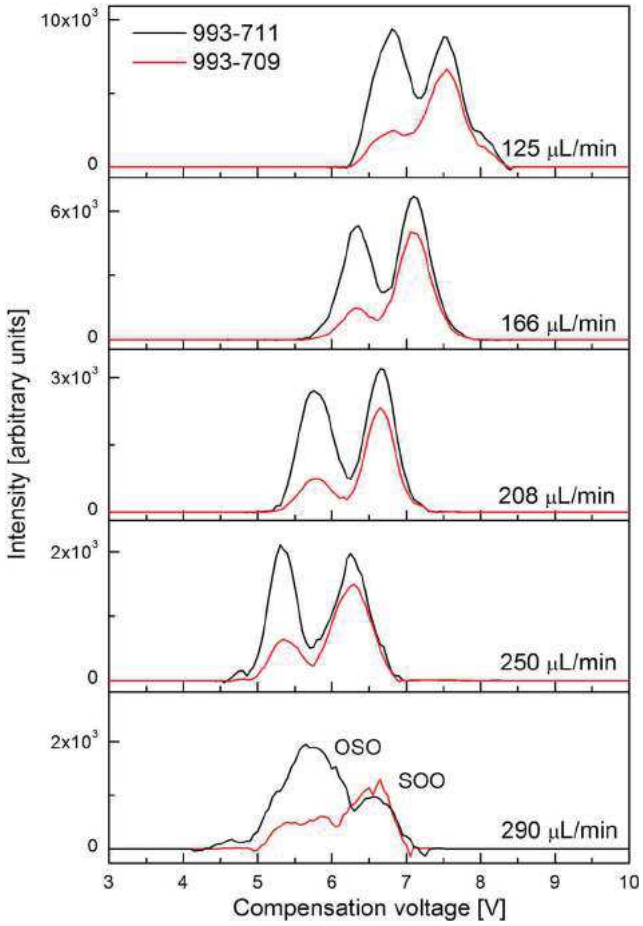

Figure 2. Effect of the flow rate of 1-propanol as the modifier in nitrogen as the curtain gas on the DMS separation of the OSO/SOO regioisomeric pair. Other experimental conditions are the same as for Fig. 1.

in the alcohol (butanol > propanol > ethanol > methanol), albeit with the loss of signal intensity accompanying improvements in the resolution (Fig. 1). The comparison between the primary (1-propanol) and secondary (2-propanol) alcohols shows slightly better resolution and sensitivity for the primary alcohol. The compromise between the resolution and the sensitivity is the selection of 1-butanol (better resolution and lower sensitivity) or 1-propanol (lower resolution and higher sensitivity). More importantly, in cases where the most abundant TG in animal fats and plant oils are being analyzed, or when sample availability is not a limiting factor, TG regioisomer separation and time savings – not sensitivity – are the critical parameters for optimization. Hence, 1-butanol was selected in the final method (see Experimental section).

Figures 2–4 show the optimization of the DMS separation for OSO and SOO using 1-propanol as the chemical modifier. When the modifier flow rate was increased, the resolution was improved, to the detriment of the signal intensity (see Fig. 2). SV is also a critical parameter for the optimization of DMS separation (Fig. 3), since no regioisomeric separation is observed at SV below 3100 V, with the best resolution being achieved at the maximum SV value of the system (4100 V). At this maximum SV, the signal intensity is somewhat reduced and an increased probability of discharges is observed, but almost baseline separation of these TG regioisomers is achieved. To mitigate these deleterious effects, the flow rate of the modifier can be reduced. In the previous study of Blagojevic *et al.*,[43] various multicomponent modifiers were tested to overcome these issues. Attempts of separations with higher potentials have already been reported in the literature and yielded promising results.[44–46]

Overall, the DMS regioisomeric separation has the following prerequisites: (1) the formation of silver-ion adducts, (2) the alcoholic modifier at the optimal flow rate, (3) the highest possible SV, and (4) the optimized DR value. Figure 4 illustrates the difference between nonresolved peaks at 36 psi and well-resolved peaks at 45 psi. However, this improved resolution results in an overall decrease in sensitivity (Fig. 4). Again, such compromises in sensitivity and regioisomeric resolution in the SRM-based experiments could be offset by using linear ion trap based scans (e.g., accumulating ion signals for several ms).

Separation of other TG regioisomers common in animal fats

After the complete optimization of the DMS-MS separations of the OSO/SOO regioisomeric pair, these conditions were applied to the analysis of other combinations of TG containing

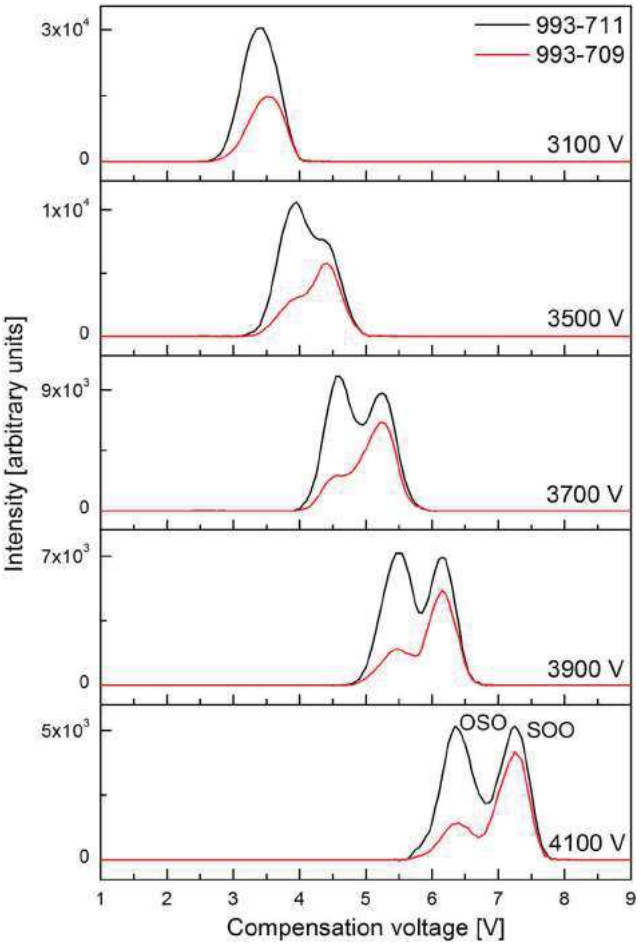

Figure 3. Effect of the separation voltage (SV) on the DMS separation of the OSO/SOO regioisomeric pair. The flow rate of 1-propanol as the chemical modifier is 166 μL/min. Other experimental conditions are the same as for Fig. 1.

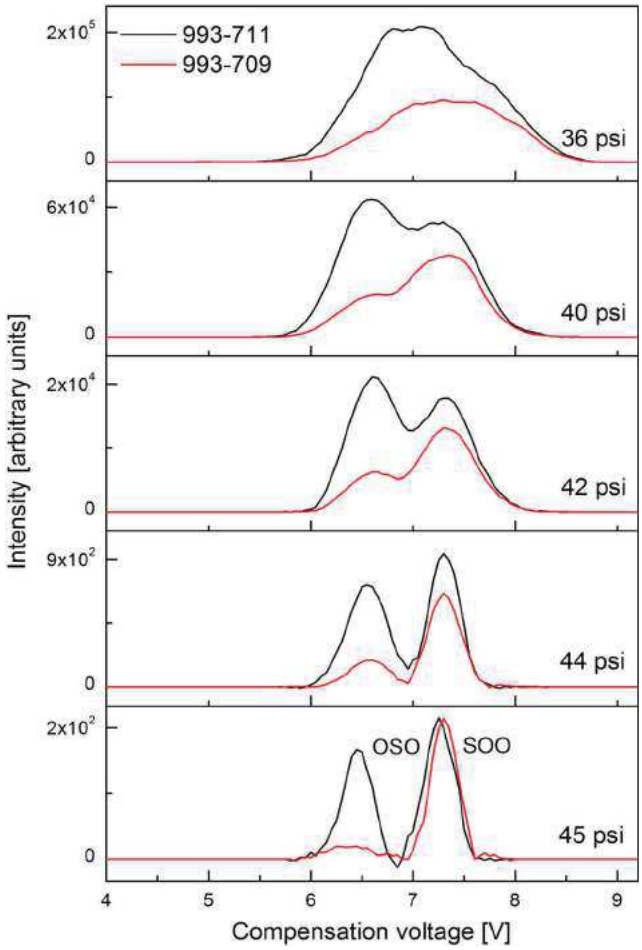

Figure 4. Effect of the pressure of throttle gas (DR) on the DMS separation of the OSO/SOO regioisomeric pair using 1-propanol as the chemical modifier and SV 4100 V. Other experimental conditions are the same as for Fig. 3.

unsaturated and saturated fatty acyl chains, which are common for animal adipose tissues. These analytes were measured at equimolar concentrations (25 μg/mL) using the Q1 scan in the appropriate *m/z* range for monitoring of $[M+Ag]^+$ ions (Table 1). The data presented in Fig. 5 and Tables 1 and 2 for OPP/POP, OPO/OOP, SSO/SOS and OSO/SOO regioisomeric pairs suggest that this DMS-MS workflow could be generally applied for the regioisomeric determination of TG containing monounsaturated and saturated fatty acyl chains.

The best results obtained for this DMS-MS technique employed standards of TG regioisomers for the construction of calibration curves. This was due to the interesting observation that the relative intensities of TG regioisomers injected at identical concentrations (Fig. 5) yielded nonequivalent peak areas for each regioisomer in a pair. For example, one of the regioisomers (OPP, OOP, SSO and SOO) provided a higher peak intensity than its matched regioisomer (POP, OPO, SOS and OSO). Lower intensities are observed in two cases (POP and SOS) for species with higher CV while the situation is just reversed for another two cases (OPO and OSO). When compounds are infused separately with the DMS cell turned off, the relative abundances are identical, which is well known from silver-ion HPLC[12,22] and confirms that the ionization efficiencies of these TG regioisomers are identical. This behavior is under investigation as it differs from the DMS-MS separation observed for smaller lipid regioisomer pairs (e.g., PC 16:0/18:1 and PC 18:1/16:0).[28] However, the use of calibration curves fully eliminates this discrimination and ultimately provides accurate results (Table 2).

Determination of TG regioisomers in the porcine adipose tissue extract

To demonstrate the applicability of the optimized DMS-MS method for real biological sample analysis, porcine adipose tissue was chosen as a representative sample of animal fat (Fig. 6), in which unsaturated fatty acyl chains preferentially occupy the *sn*-1/3 positions.[4] In addition, the regioisomeric ratios of this tissue type of several TG containing combinations of saturated and monounsaturated fatty acyls have already been measured using silver-ion HPLC/MS[22] and fragment ion ratios in NARP-HPLC/MS[18] (Table 2). For DMS-MS results, the RR was calculated in a similar way as the chromatographic resolution, with the difference in CV values (instead of retention times) between two regioisomers being divided by the mean peak width (w) at the half maximum:

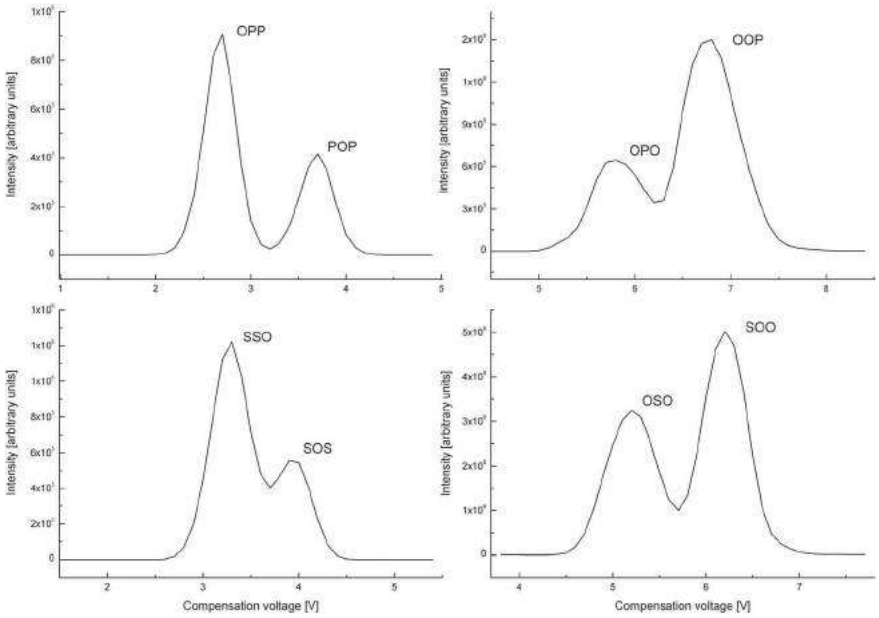

Figure 5. DMS separation of the regioisomeric pairs OSO/SOO, SOS/SSO, POP/OPP and OPO/OOP (the concentration is 12.5 μg/mL for all TG) monitored by Q1 scan. The flow rate of 1-butanol as the chemical modifier is 120 μL/min and DR values are listed in Table 1. Other experimental conditions are the same as for Fig. 3.

Table 2. Comparison of determined TG regioisomeric ratios in porcine adipose tissue using various analytical approaches together with their regioisomeric resolution (RR)

	DMS method		Silver-ion HPLC/MS[22]		
TG regioisomeric pair	Concentration ratio	RR	Concentration ratio	RR[a]	Fragment ion ratios in HPLC/MS[18]
POP/OPP	5/95	3.1	8/92	2.3	0/100[b]
OPO/OOP	90/10	1.8	88/12	2.1	100/0[b]
SOS/SSO	30/70	1.2	n.d.[c]	3.9	30/70
OSO/SOO	n.d.[c]	2.1	n.d.[c]	1.7	n.d.[c]

[a]RR calculated from previously published data.[12,22]
[b]Only the prevailing fatty acyl in the *sn*-2 position is determined.
[c]n.d.: not determined.

$$RR = 2*(CV_2–CV_1)/(w_1 + w_2) \quad (1)$$

Note that the RR cannot be calculated for the fragment ratio method because the principle of this method does not enable this calculation.

The comparison between DMS-MS and silver-ion HPLC (Table 2) shows slightly better RR for POP/OPP (3.1 *vs.* 2.3) and OSO/SOO (2.1 *vs.* 1.7) pairs and slightly worse RR for OPO/OOP (1.8 *vs.* 2.1) and SOS/SSO (1.2 *vs.* 3.9) pairs. The RR for TG containing unsaturated and saturated fatty acyl chains can be considered as comparable for both methods. For TG containing polyunsaturated fatty acyl chains (e.g., LSL/SLL and SLS/SSL pairs), the DMS-MS method could not provide satisfactory RR, while silver-ion HPLC can be applied for the partial RR of polyunsaturated TG with fatty acyl chains differing at least by two DB, such as OLnO/OOLn and OLnLn/LnOLn.[22] However, both analytical techniques are hindered for fully saturated TG regioisomers, because no DB are available for either gas-phase or liquid-phase binding of Ag^+. The regioisomeric ratio of OSO/SOO cannot be determined in the porcine adipose samples, because their concentration is below the detection limit of our method, similarly to previous works.[18,22]

The precision of different analytical methods used for the regioisomeric determination is also compared. Fragment ratios in mass spectra typically exhibit a certain level of fluctuation, so the accurate determination is rather difficult, with most papers reporting only the prevailing fatty acyl in the *sn*-2 position[2,3] or at maximum values rounded to the nearest multiple of 10% with correlation coefficients in the range 0.970–0.986.[2,18] Thus far, silver-ion HPLC/MS provides the most accurate results due to good chromatographic resolution of many TG regioisomers, but the serious drawback is the analysis time in the range of 60–120 min plus time needed for the system equilibration (typically overnight before the first injection) to achieve a good reproducibility of retention times. Thus, a new analytical method with higher throughput would be highly desirable, and the DMS-MS

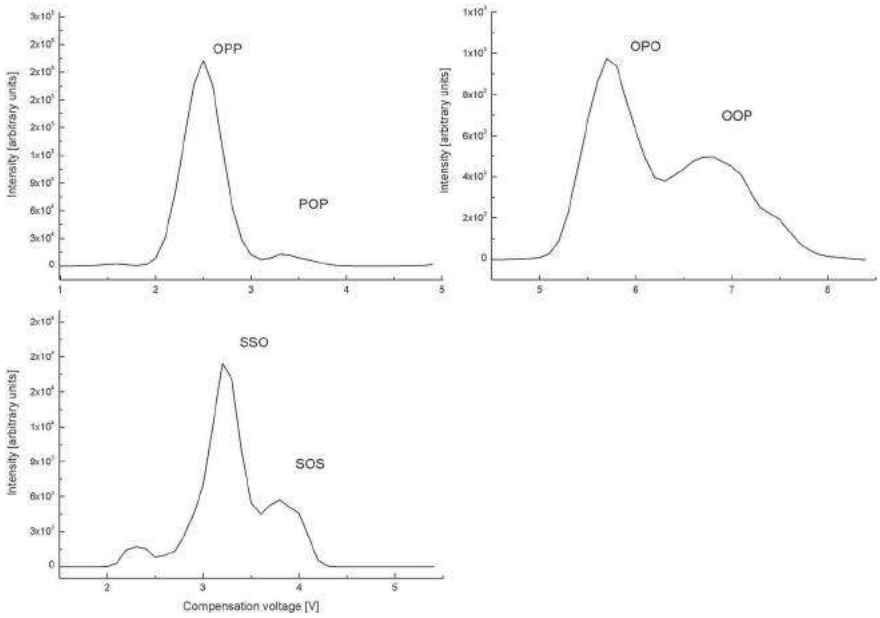

Figure 6. DMS analysis of TG regioisomers containing combinations of saturated and monounsaturated fatty acyls in the sample of porcine adipose tissue monitored by Q1 scan. Experimental conditions are the same as for Fig. 5.

method shows promise in this area with typical separations requiring less than 1 min of analysis time per sample. Several improvements are required for the DMS-MS method to be generally applicable to TG regioisomer separation, including achieving better correlation coefficients and the applicability for polyunsaturated TG, where the sufficient regioisomeric resolution for their quantitation has not been achieved yet.

CONCLUSIONS

The DMS-MS separation of TG regioisomers is reported for the first time using their silver adducts and 1-butanol or 1-propanol as the chemical modifier. This work serves as a proof-of-concept that DMS provides the selectivity for the regioisomeric resolution of several combinations of monounsaturated and saturated fatty acyl chains by separating regioisomeric TG. DMS-MS yields quantitative data for OSO/SOO, SOS/SSO, POP/OPP and OPO/OOP regioisomeric pairs determined in the porcine adipose tissue extract and compares well with previously published results obtained with established methods. This DMS-MS technique is suggested as a complementary approach to silver-ion HPLC with much higher throughput, because DMS-MS is accomplished in less than 1 min compared to 1 h and more for silver-ion HPLC. DMS-MS can be applied for fast determination of regioisomeric ratios of TG containing combinations of saturated and monounsaturated fatty acyls, which are typical for mammal adipose tissues and also occurring in plant oils.

Acknowledgements

This work was supported by the ERC CZ Project No. LL1302 sponsored by the Ministry of Education, Youth and Sports of the Czech Republic. M.Š. acknowledges the support of the Slovenian Research Agency (P1-0034).

REFERENCES

[1] Available: http://www.lipidmaps.org/ (accessed August 19, 2015).
[2] M. Holčapek, P. Jandera, P. Zderadička, L. Hrubá. Characterization of triacylglycerol and diacylglycerol composition of plant oils using high-performance liquid chromatography-atmospheric pressure chemical ionization mass spectrometry. *J. Chromatogr. A* **2003**, *1010*, 195.
[3] M. Lísa, M. Holčapek. Triacylglycerols profiling in plant oils important in food industry, dietetics and cosmetics using high-performance liquid chromatography-atmospheric pressure chemical ionization mass spectrometry. *J. Chromatogr. A* **2008**, *1198*, 115.
[4] M. Lísa, K. Netušilová, L. Franěk, H. Dvořáková, V. Vrkoslav, M. Holčapek. Characterization of fatty acid and triacylglycerol composition in animal fats using silver-ion and non-aqueous reversed-phase high-performance liquid chromatography/mass spectrometry and gas chromatography/flame ionization detection. *J. Chromatogr. A* **2011**, *1218*, 7499.
[5] M. Ramírez, L. Amate, A. Gil. Absorption and distribution of dietary fatty acids from different sources. *Early Hum. Develop.* **2001**, *65*, S95.
[6] K. Ekroos. *Lipidomics: Technologies and Applications*. Wiley-VCH, Weinheim, **2012**.
[7] W. C. Byrdwell. Atmospheric pressure chemical ionization mass spectrometry for analysis of lipids. *Lipids* **2001**, *36*, 327.
[8] W. C. Byrdwell. The bottom-up solution to the triacylglycerol lipidome using atmospheric pressure chemical ionization mass spectrometry. *Lipids* **2005**, *40*, 383.
[9] M. Holčapek, M. Lísa, P. Jandera, N. Kabátová. Quantitation of triacylglycerols in plant oils using HPLC with APCI-MS, evaporative light-scattering, and UV detection. *J. Sep. Sci.* **2005**, *28*, 1315.
[10] S. S. Cai, J. A. Syage. Atmospheric pressure photoionization mass spectrometry for analysis of fatty acid and acylglycerol lipids. *J. Chromatogr. A* **2006**, *1110*, 15.
[11] J. L. Kerwin, A. M. Wiens, L. H. Ericsson. Identification of fatty acids by electrospray mass spectrometry and tandem mass spectrometry. *J. Mass Spectrom.* **1996**, *31*, 184.

[12] M. Holčapek, H. Dvořáková, M. Lísa, A. J. Girón, P. Sandra, J. Cvačka. Regioisomeric analysis of triacylglycerols using silver-ion liquid chromatography atmospheric pressure chemical ionization mass spectrometry: Comparison of five different mass analyzers. *J. Chromatogr. A* **2010**, *1217*, 8186.
[13] C. Cheng, M. L. Gross, E. Pittenauer. Complete structural elucidation of triacylglycerols by tandem sector mass spectrometry. *Anal. Chem.* **1998**, *70*, 4417.
[14] E. Pittenauer, G. Allmaier. The renaissance of high-energy CID for structural elucidation of complex lipids: MALDI-TOF/RTOF-MS of alkali cationized triacylglycerols. *J. Am. Soc. Mass Spectrom.* **2009**, *20*, 1037.
[15] H. Kallio, P. Rua. Distribution of the major fatty acids of human milk between sn-2 and sn-1,3 positions of triacylglycerols. *J. Am. Oil Chem. Soc.* **1994**, *71*, 985.
[16] R. O. Adlof. Analysis of triacylglycerol positional isomers by silver ion high-performance liquid-chromatography. *J. High Res. Chromatogr.* **1995**, *18*, 105.
[17] M. Lísa, R. Denev, M. Holčapek. Retention behavior of isomeric triacylglycerols in silver-ion HPLC: Effects of mobile phase composition and temperature. *J. Sep. Sci.* **2013**, *36*, 2888.
[18] L. Fauconnot, J. Hau, J. M. Aeschlimann, L. B. Fay, F. Dionisi. Quantitative analysis of triacylglycerol regioisomers in fats and oils using reversed-phase high-performance liquid chromatography and atmospheric pressure chemical ionization mass spectrometry. *Rapid Commun. Mass Spectrom.* **2004**, *18*, 218.
[19] H. G. Janssen, K. Hrnčirík, A. Szórádi, M. Leijten. An improved method for sn-2 position analysis of triacylglycerols in edible oils and fats based on immobilised lipase D (Rhizopus delemar). *J. Chromatogr. A* **2006**, *1112*, 141.
[20] S. Momchilova, K. Tsuji, Y. Itabashi, B. Nikolova-Damyanova, A. Kuksis. Resolution of triacylglycerol positional isomers by reversed-phase high-performance liquid chromatography. *J. Sep. Sci.* **2004**, *27*, 1033.
[21] S. Momchilova, Y. Itabashi, B. Nikolova-Damyanova, A. Kuksis. Regioselective separation of isomeric triacylglycerols by reversed-phase high-performance liquid chromatography: Stationary phase and mobile phase effects. *J. Sep. Sci.* **2006**, *29*, 2578.
[22] M. Lísa, H. Velínská, M. Holčapek. Regioisomeric characterization of triacylglycerols using silver-ion HPLC/MS and randomization synthesis of standards. *Anal. Chem.* **2009**, *81*, 3903.
[23] M. Lísa, M. Holčapek. Characterization of triacylglycerol enantiomers using chiral HPLC/APCI-MS and synthesis of enantiomeric triacylglycerols. *Anal. Chem.* **2013**, *85*, 1852.
[24] T. Řezanka, I. Kolouchová, A. Čejkova, T. Cajthaml, K. Sigler. Identification of regioisomers and enantiomers of triacylglycerols in different yeasts using reversed- and chiral-phase LC-MS. *J. Sep. Sci.* **2013**, *36*, 3310.
[25] N. L. Lévêque, S. Héron, A. Tchapla. Regioisomer characterization of triacylglycerols by non-aqueous reversed-phase liquid chromatography/ electrospray ionization mass spectrometry using silver nitrate as a postcolumn reagent. *J. Mass Spectrom.* **2010**, *45*, 284.
[26] J. C. May, C. R. Goodwin, N. M. Lareau, K. L. Leaptrot, C. B. Morris, R. T. Kurulugama, A. Mordehai, C. Klein, W. Barry, E. Darland, G. Overney, K. Imatani, G. C. Stafford, J. C. Fjeldsted, J. A. McLean. Conformational ordering of biomolecules in the gas phase: nitrogen collision cross sections measured on a prototype high resolution drift tube ion mobility-mass spectrometer. *Anal. Chem.* **2014**, *86*, 2107.
[27] J. Castro-Perez, T. P. Roddy, N. M. M. Nibbering, V. Shah, D. G. McLaren, S. Previs, A. B. Attygalle, K. Herath, Z. Chen, S.-P. Wang, L. Mitnaul, B. K. Hubbard, R. J. Vreeken, D. G. Johns, T. Hankemeier. Localization of fatty acyl and double bond positions in phosphatidylcholines using a dual stage CID fragmentation coupled with ion mobility mass spectrometry. *J. Am. Soc. Mass Spectrom.* **2011**, *22*, 1552.
[28] A. A. Shvartsburg, G. Isaac, N. Leveque, R. D. Smith, T. O. Metz. Separation and classification of lipids using differential ion mobility spectrometry. *J. Am. Soc. Mass Spectrom.* **2011**, *22*, 1146.
[29] T. Lintonen, P. R. S. Baker, M. Suoniemi, B. Ubhi, K. Koistinen, E. Duchoslav, J. L. Campbell, K. Ekroos. Differential mobility spectrometry-driven shotgun lipidomics. *Anal. Chem.* **2014**, *86*, 9662.
[30] A. T. Maccarone, J. Duldig, T. W. Mitchell, S. J. Blanksby, E. Duchoslav, J. L. Campbell. Rapid and unambiguous characterization of acyl chains in phosphatidylcholines using differential mobility and mass spectrometry. *J. Lipid. Res.* **2014**, *55*, 1668.
[31] D. A. Barnett, B. Ells, R. Guevremont, R. W. Purves. Separation of leucine and isoleucine by electrospray ionization-high field asymmetric waveform ion mobility spectrometry-mass spectrometry. *J. Am. Soc. Mass Spectrom.* **1999**, *10*, 1279.
[32] V. Blagojevic, A. Chramow, B. B. Schneider, T. R. Covey, D. K. Bohme. Differential mobility spectrometry of isomeric protonated dipeptides: modifier and field effects on ion mobility and stability. *Anal. Chem.* **2011**, *83*, 3470.
[33] W. B. Parson, B. B. Schneider, V. Kertesz, J. J. Corr, T. R. Covey, G. J. Van Berkel. Rapid analysis of isomeric exogenous metabolites by differential mobility spectrometry - mass spectrometry. *Rapid Commun. Mass Spectrom.* **2011**, *25*, 3382.
[34] J. L. Campbell, M. Zhu, W. S. Hopkins. Ion-molecule clustering in differential mobility spectrometry: Lessons learned from tetraalkylammonium cations and their isomers. *J. Am. Soc. Mass Spectrom.* **2014**, *25*, 1583.
[35] C. Liu, J. C. Y. Le Blanc, J. Shields, J. S. Janiszewski, C. Ieritano, G. F. Ye, G. F. Hawes, W. S. Hopkins, J. L. Campbell. Using differential mobility spectrometry to measure ion solvation: An examination of the roles of solvents and ionic structures in separating quinoline-based drugs. *Analyst* **2015**, *140*, 6897.
[36] W. Jin, M. Jarvis, M. Star-Weinstock, M. Altemus. A sensitive and selective LC-differential mobility-mass spectrometric analysis of allopregnanolone and pregnanolone in human plasma. *Anal. Bioanal. Chem.* **2013**, *405*, 9497.
[37] B. B. Schneider, T. R. Covey, S. L. Coy, E. V. Krylov, E. G. Nazarov. Planar differential mobility spectrometer as a pre-filter for atmospheric pressure ionization mass spectrometry. *Int. J. Mass Spectrom.* **2010**, *298*, 45.
[38] J. L. Campbell, J. C. Y. Le Blanc, B. B. Schneider. Probing electrospray ionization dynamics using differential mobility spectrometry: The curious case of 4-aminobenzoic acid. *Anal. Chem.* **2012**, *84*, 7857.
[39] B. B. Schneider, T. R. Covey, S. L. Coy, E. V. Krylov, E. G. Nazarov. Chemical effects in the separation process of a differential mobility/mass spectrometer system. *Anal. Chem.* **2010**, *82*, 1867.
[40] M. Groessl, S. Graf, R. Knochenmuss. High resolution ion mobility-mass spectrometry for separation and identification of isomeric lipids. *Analyst* **2015**, *140*, 6904.
[41] J. L. Campbell, J. C. Y. LeBlanc, R. G. Kibbey. Differential mobility spectrometry: A valuable technology for analyzing challenging biological samples. *Bioanalysis* **2015**, *7*, 853.
[42] T. Porta, E. Varesio, G. Hopfgartner. Gas-phase separation of drugs and metabolites using modifier-assisted differential ion mobility spectrometry hyphenated to liquid extraction surface analysis and mass spectrometry. *Anal. Chem.* **2013**, *85*, 11771.

[43] V. Blagojevic, G. K. Koyanagi, D. K. Bohme. Multi-component ion modifiers and arcing suppressants to enhance differential mobility spectrometry for separation of peptides and drug molecules. *J. Am. Soc. Mass Spectrom.* **2014**, *25*, 490.
[44] A. A. Shvartsburg, R. D. Smith. High-resolution differential ion mobility spectrometry of a protein. *Anal. Chem.* **2013**, *85*, 10.
[45] A. A. Shvartsburg, D. C. Prior, K. Q. Tang, R. D. Smith. High-resolution differential ion mobility separations using planar analyzers at elevated dispersion fields. *Anal. Chem.* **2010**, *82*, 7649.
[46] A. A. Shvartsburg, K. Q. Tang, R. D. Smith, M. Holden, M. Rush, A. Thompson, D. Toutoungi. Ultrafast differential ion mobility spectrometry at extreme electric fields coupled to mass spectrometry. *Anal. Chem.* **2009**, *81*, 8048.

Journal of Chromatography A, 1218 (2011) 5146–5156

Contents lists available at ScienceDirect

Journal of Chromatography A

journal homepage: www.elsevier.com/locate/chroma

Lipidomic profiling of biological tissues using off-line two-dimensional high-performance liquid chromatography–mass spectrometry

Miroslav Lísa, Eva Cífková, Michal Holčapek*

University of Pardubice, Faculty of Chemical Technology, Department of Analytical Chemistry, Studentská 573, 532 10 Pardubice, Czech Republic

ARTICLE INFO

Article history:
Received 3 March 2011
Received in revised form 19 May 2011
Accepted 23 May 2011
Available online 30 May 2011

Keywords:
Lipidomics
Lipids
Phospholipids
Hydrophilic interaction liquid chromatography
Two-dimensional liquid chromatography
Regioisomers

ABSTRACT

Lipids are important components in all biological tissues having many essential roles associated with the proper function of the organism. Their analysis in the biological tissues and body fluids is a challenging task due to the extreme sample complexity of polar lipids and to their amphiphilic character. In this work, we describe a new method for the characterization of the lipid composition in various tissues, using off-line two-dimensional coupling of hydrophilic interaction liquid chromatography (HILIC) and reversed-phase (RP) high-performance liquid chromatography coupled to electrospray ionization (ESI) and atmospheric pressure chemical ionization (APCI) mass spectrometry. In the first dimension the total lipid extracts are fractioned using HILIC into individual lipid classes. In total, 19 lipid classes (+3 regioisomeric pairs) that cover a wide range of polarities are separated in one analytical run, which is the highest number of analyzed lipid classes reported so far. The lysophospholipid regioisomers are also separated in HILIC mode followed by the identification based on the characteristic ESI mass spectra. The collected fractions of the various lipid classes are further separated in the RP mode, which offers an excellent resolution of the individual lipid species. Their ESI or APCI mass spectra give correct information on the fatty acid composition and on the individual regioisomeric positions on the glycerol skeleton. Off-line coupling of both modes enables the comprehensive analysis of plant and animal samples as illustrated on the analysis of egg yolk, soya and porcine brain tissues.

1. Introduction

Lipidomics is a branch of metabolomics that involves the identification and quantification of cellular lipid molecular species and their interactions with other lipids, proteins and metabolites [1]. Lipidomics contributes towards the understanding how lipids function in a biological system and for the elucidation of the mechanism of lipid-based diseases including atherosclerosis, diabetes, cancer, cardiovascular diseases, obesity, Alzheimer's disease, etc. [1,2]. Lipids may be broadly defined as hydrophobic or amphiphilic small molecules that originate entirely or in part by carbanion-based condensations of thioesters and/or by carbocation-based condensations of isoprene units [3]. Lipids are mostly water-insoluble molecules that represent a wide range of various polar and nonpolar compounds containing fatty acids and their derivatives [4]. Lipids have a variety of functions within cells including the source of energy, fat-soluble vitamins, essential fatty acids, structural components of cell membranes, transmission of information in cells, biosynthetic precursor, etc. Lipids can be divided into eight basic categories according to Fahy et al. [3,5]: fatty acyls, glycerolipids, glycerophospholipids, sphingolipids, sterol lipids, prenol lipids, saccharolipids and polyketides. The first and very important step in the lipid analysis involves the extraction of lipids from the biological material. The standard method of the lipid extraction was introduced by Folch et al. [6] and later modified by Bligh and Dyer [7]. This method is based on the use of chloroform/methanol/water as a ternary solvent mixture, which separates into two layers: upper (aqueous) layer containing non-lipid compounds and bottom (chloroform) layer containing lipid compounds.

High-performance liquid chromatography (HPLC), thin-layer chromatography (TLC) and gas chromatography (GC) can be applied for specific tasks in the lipidomic analysis. GC is a routine method for the fatty acid profiling after the transesterification to fatty acid methyl esters. In the hydrophilic interaction liquid chromatography (HILIC), individual lipid classes are separated according to their polarity using various silica [8–12] or diol columns [13–17]. Common types of mobile phase systems are the following: chloroform/methanol/water [13,14] and hexane/2-propanol/water [12,15–17]. Formic acid, ammonium acetate, ammonium hydroxide, ammonia, triethylamine and methyl tert-butyl ether can be used as additives. Various types of C_{18} [18–25] and C_8 [26,27] columns in reversed-phase (RP) HPLC systems with mobile phases containing methanol/acetonitrile/water [20,22,28], methanol/water [21,23,25], acetonitrile/water [24,26]

* Corresponding author. Tel.: +420 466037087; fax: +420 466037068.
E-mail address: Michal.Holcapek@upce.cz (M. Holčapek).

0021-9673/$ – see front matter © 2011 Elsevier B.V. All rights reserved.
doi:10.1016/j.chroma.2011.05.081

and 2-propanol/acetonitrile/water [18,19] have been reported. Non-aqueous RP (NARP) HPLC with various types of C_{18} columns and the mixtures of organic solvents as the mobile phase (acetonitrile, 2-propanol, hexane, dichloromethane, etc.) is used for the separation of non-polar triacylglycerols (TGs) [29–33].

The lipidomic analysis deals with an enormous sample complexity, therefore one-dimensional chromatographic separation may not be sufficient for comprehensive lipidomic characterization. More abundant species can mask trace components, which leads to the loss of information with the potential biological relevance. Two-dimensional (2D) HPLC offers the opportunity to separate complex lipidomic mixtures according two molecular properties, *e.g.*, hydrophobic character of the molecule (RP-HPLC) and electrostatic forces related to the compound polarity (HILIC). 2D-HPLC of lipids can be performed either in on-line [30,34–36] or off-line [37–39] mode. The advantage of off-line 2D is the full optimization of separation conditions in both dimensions [37], but this technique is more laborious and time consuming. On-line 2D-HPLC can be automated, but the chromatographic resolution in the second dimension is sacrificed at cost of sampling time at the first dimension, typically 1 min [30,34,35]. Numerous papers can be found on the detailed 2D-HPLC characterization of one lipid class (typically TGs) [30,34,35,37], but only few works are devoted to the comprehensive lipidomic analysis [36,38,39]. The best separation found in the literature has presented the identification of 721 lipid species from 12 lipid classes [36].

Electrospray ionization (ESI) [10,12,13,18,19,21–24,26,27,40–44] and matrix-assisted laser desorption–ionization (MALDI) [39,45–49] are the most widely used ionization techniques for the identification of polar lipids, while atmospheric pressure chemical ionization (APCI) [31–33,50] is preferred for non-polar lipids. ESI mass spectra in the positive-ion mode provide accurate information on the molecular weight (MW) and on the presence of individual polar head groups. In the ESI negative-ion mode, the presence of $[RCOO]^-$ fragment ions correspond to the individual fatty acids esterified on the glycerol skeleton. MALDI is often used in connection with TLC separation of lipid classes [45].

The main goal of our work is the development of non-target HPLC/MS method applicable for the comprehensive characterization of wide range of lipid classes in biological tissues, because the HPLC/MS methods used so far in lipidomics are based on the selected reaction monitoring of predefined mass transitions, but they cannot be applied for the determination of all unknown lipids. We use HILIC in the first dimension for the fractionation of total lipid extracts into individual lipid classes, which are then analyzed using RP separation with ESI or APCI-MS identification of individual species. The developed method is applied for the analysis of lipid composition in selected animal and plant tissues.

2. Experimental

2.1. Materials

Acetonitrile, 2-propanol, methanol (all HPLC gradient grade), chloroform (HPLC grade, stabilized by 0.5–1% ethanol) and ammonium acetate were purchased from Sigma–Aldrich (St. Louis, MO, USA). De-ionized water was prepared with Demiwa 5-roi purification system (Watek, Ledeč nad Sázavou, Czech Republic) and by Ultra CLEAR UV apparatus (SG, Hamburg, Germany). Standards of lipids containing oleic acid (Δ9*cis*-C18:1) (*i.e.*, TG, CE, FA, PG, LPG, PI, CA, LPI, pPE, PE, LPE, pPC, PC, SM and LPC – see Table 1 for the definition of lipid abbreviations) and cholesterol (Chol) were purchased from Avanti Polar Lipids (Alabaster, AL, USA). Individual lipid species are annotated according to their fatty acid composition, *e.g.*, 1-octadecenoyl-2-docosahexaenoyl-*sn*-glycero-3-phosphatidylcholine is annotated as 18:1/22:6-PC. Spherisorb Si (250 × 4.6 mm and 150 × 4.6 mm, 5 μm, Waters, Milford, MA, USA), Atlantis Si (150 × 2.1 mm, 3 μm, Waters), Nova-Pak Si (150 × 3.9 mm, 4 μm, Waters), SunFire Si (250 × 4.6 mm, 5 μm, Waters), Purospher Star NH_2 (250 × 4 mm, 5 μm, Merck, Darmstadt, Germany), porous shell particles column Ascentis Si (150 × 2.1 mm, 2.7 μm, Sigma–Aldrich), porous shell particles column Kinetex HILIC (150 × 2.1 mm, 2.6 μm, Phenomenex, Torrance, CA, USA), Ascentis HILIC (150 × 2.1 mm, 3 μm, Sigma–Aldrich) and SeQuant ZIC-HILIC (150 × 2.1 mm, 3.5 μm, SeQuant, Umea, Sweden) columns were used for the optimization of HILIC separation. Hypersil Gold C_{18} (150 × 3 mm, 5 μm, Thermo Scientific, Waltham, MA, USA), Luna C_{18} (250 × 4.6 mm, 150 × 4.6 mm and 250 × 3.0 mm, 5 μm, Phenomenex), Ultracarb ODS 30 (150 × 3.2 mm, 5 μm, Phenomenex), Nova-Pak C_{18} (300 × 3.9 mm and 150 × 3.9 mm, 4 μm, Waters), Purospher Star C_{18} (250 × 4 mm, 5 μm, Merck), Zorbax SB-C_{18} (150 × 4.6 mm, 3.5 μm, Agilent Technologies, Waldbronn, Germany), Eclipse XDB-C_{18} (150 × 4.6 mm, 5 μm, Agilent Technologies), porous shell particles column Ascentis Express C_{18} (150 × 2.1 mm, 2.7 μm, Sigma–Aldrich) and porous shell particles column Kinetex C_{18} (150 × 2.1 mm, 2.6 μm, Phenomenex) columns were used for the optimization of RP-HPLC separation. Samples of egg, soya and porcine brain were purchased at local stores.

Table 1
Abbreviations used for individual lipids classes in accordance with the literature [3,5] and typical neutral losses ($\Delta m/z$) from protonated molecules $[M+H]^+$ and characteristic ions (m/z) used for the identification in positive-ion ESI mass spectra.

Lipid class	Abbreviation	Neutral loss ($\Delta m/z$)	Characteristic ion (m/z)
Triacylglycerol	TG	–	$[M+H-R_iCOOH]^+$
Cholesterol	Chol	–	369
Cholesteryl ester	CE	–	–
Fatty acid	FA	–	–
Cytidine diphosphate-diacylglycerol	CDP-DG	–	$[M+H-R_iCOOH]^+$
Phosphatidylglycerol	PG	172	–
Lysophosphatidylglycerol	LPG	172	–
Glycosylceramide	GlcCER	162	–
Phosphatidylinositol	PI	260	–
Cardiolipin	CA	–	–
Lysophosphatidylinositol	LPI	260	–
Phosphatidylethanolamine plasmalogen	pPE	141	–
Phosphatidylethanolamine	PE	141	–
Lysophosphatidylethanolamine	LPE	141	–
Phosphatidylcholine plasmalogen	pPC	183	184
Phosphatidylcholine	PC	183	184
Sphingomyeline	SM	183	184
Lysophosphatidylcholine	LPC	183	184

2.2. Sample preparation

The total lipid extracts from lipid tissues were prepared according to Folch et al. [6] using chloroform/methanol/water system. Briefly, approximately 1 g of lipid tissue was homogenized with 20 mL mixture of chloroform/methanol (2:1, v/v) and the homogenate was filtered using a course filter paper. Then, 4 mL of 1 M NaCl was added and the mixture was centrifuged at 3000 rpm for 5 min at room temperature. The chloroform (bottom) layer containing lipids was evaporated by a gentle stream of nitrogen and redissolved in 2-propanol/water (1:1, v/v) for HILIC analysis.

2.3. HPLC/MS conditions

All HPLC experiments were performed on a liquid chromatograph Agilent 1200 series (Agilent Technologies). The UV detection at 205 nm and the Esquire 3000 ion trap analyzer with (Bruker Daltonics, Bremen, Germany) were coupled in series, where ESI is used for the detection of all polar phospholipid species, while APCI is preferred for non-polar lipids, such as TGs.

2.3.1. HILIC fractionation of lipid classes

In the first dimension, HILIC was used for the fractionation of total lipid extracts into lipid classes using Spherisorb Si column (250 × 4.6 mm, 5 μm, Waters), a flow rate of 1 mL/min, an injection volume of 10 μL, separation temperature of 40 °C and a mobile phase gradient: 0 min – 94% A + 6% B, 60 min – 77% A + 23% B, where A is acetonitrile and B is 5 mM aqueous ammonium acetate. The injector needle was washed with the mobile phase after each injection. Lipid classes were identified using ESI-MS in the mass range *m/z* 50–1500 with the following setting of tuning parameters: pressure of the nebulizing gas of 60 psi, the drying gas flow rate of 10 L/min and temperature of the drying gas 365 °C. Fractions of lipid classes were collected manually, evaporated by a gentle stream of nitrogen and redissolved in the initial mobile phase composition for the 2D analysis. The volume for redissolvation was selected according to the concentration of individual fractions in the range of 100–1000 μl.

2.3.2. RP-HPLC separation of polar lipids

In the second dimension, collected fractions of lipid classes were analyzed using two RP-HPLC methods according to their polarity. Fractions of polar lipids were analyzed using RP-HPLC with porous shell particles column Kinetex C_{18} (150 × 2.1 mm, 2.6 μm, Phenomenex), the flow rate of 0.3 mL/min, the injection volume of 1 μL, separation temperature of 40 °C and the mobile phase gradient: 0 min – 75% A + 25% B, 100 min – 88% A + 12% B, where A is the mixture of acetonitrile/2-propanol (1:1, v/v) and B is 5 mM aqueous ammonium acetate. Polar lipids were identified using ESI-MS in the mass range *m/z* 50–1500 with the following setting of tuning parameters: pressure of the nebulizing gas of 40 psi, the drying gas flow rate of 9 L/min and temperature of the drying gas 365 °C. The low energy collision induced dissociation tandem mass spectrometry (MS/MS) experiments were performed during HPLC/MS runs with the automatic precursor selection, the isolation width of *m/z* 4, the collision amplitude of 1 V and helium as a collision gas.

2.3.3. NARP-HPLC separation of non-polar lipids

Fractions of non-polar lipids were analyzed by non-aqueous reversed phase (NARP) HPLC/APCI-MS with C_{18} columns according to our previous work [31], *i.e.*, two Nova-Pak C_{18} columns (150 × 3.9 and 300 × 3.9 mm, 4 μm, Waters) connected in series, the flow rate of 1 mL/min, the injection volume of 1 μL, separation temperature of 25 °C and the mobile phase gradient: 0 min – 100% acetonitrile, 106 min – 31% acetonitrile + 69% 2 – propanol. Non-polar lipids were identified using APCI-MS in the mass range *m*/z 50–1200, pressure of the nebulizing gas of 70 psi, the drying gas flow rate of 3 L/min, temperatures of the drying gas and APCI heater 350 °C and 400 °C, respectively.

3. Results and discussion

3.1. Optimization of HILIC separation

The total lipid extracts prepared by the modified Folch extraction procedure, have been fractionated by HILIC into the individual lipid classes. First, chromatographic conditions have been carefully optimized (Figs. S1–S3) to achieve best separation of the maximum number of lipid classes. For this purpose, column packing, mobile phase composition (*i.e.*, type of organic solvent, concentration of water, concentration of additive and pH value), separation temperature and gradient steepness have been tested using a mixture of 16 standards of lipid classes represented by species containing oleic acid (Δ9*cis*-C18:1) and the total lipid extract from egg yolk containing lipid classes with a wide range of polarities. Nine commercially available silica columns with porous and porous shell particles designed especially for HILIC separation or conventional silica columns for NP-HPLC from various manufacturers have been tested (columns are listed in Section 2, representative chromatograms are shown in Fig. S1). Both types of HILIC and NP-HPLC columns provide the separation of lipid classes with similar results. Greater differences are observed among columns from different manufacturers due to diverse packing procedures and between porous vs. porous shell particles columns. Porous shell particles HILIC columns (Fig. S1A) permit a good resolution of the lipid classes, however, we have observed the limited sample capacity of these columns which makes them inconvenient for the fractionation. The best chromatographic resolution of critical classes with lower retention times and the ability to work with higher sample load are achieved with NP-HPLC silica column with porous particles (Spherisorb Si, 250 × 4.6 mm, 5 μm) (Fig. 1).

The mobile phase composition plays a critical role in the separation selectivity of HILIC. A number of common HPLC organic solvents in the mixture with aqueous ammonium acetate have been tested as the mobile phase components for the HILIC analysis of lipids, *e.g.*, acetonitrile, methanol, ethanol, 2-propanol, hexane and their mixtures. The type of organic solvent has a significant effect on the chromatographic resolution of lipids. Good resolution of lipid classes is obtained with the mixture of hexane/2-propanol/aqueous ammonium acetate, but poor reproducibility caused by a limited miscibility and increased background noise in HPLC/MS disfavors this mobile phase composition. The best selectivity, chromatographic resolution and low background noise are observed in acetonitrile/water mobile phase with the addition of ammonium acetate.

Water present in the mobile phase is adsorbed on the surface of the silica stationary phase and participates in the HILIC separation process [51]. Therefore, the water concentration is crucial for the separation selectivity and chromatographic resolution in HILIC separation of lipids, especially important is the initial percentage of water. The minimum amount of 4% of water in the mobile phase has been found as the basic prerequisite for the reasonable separation. The concentration of salts and pH value of mobile phase are also important parameters, especially for ionic lipids. The use of strong ion-pairing agents (*e.g.*, alkyl ammonium salts) can significantly improve the chromatographic resolution of charged compounds, but it causes a strong signal suppression and contamination of MS system. Volatile mobile phase modifiers (*e.g.*, ammonium acetate) yield almost comparable chromatographic separation. These agents are MS compatible, but their concentration should be kept as low as possible to reduce the ion suppression

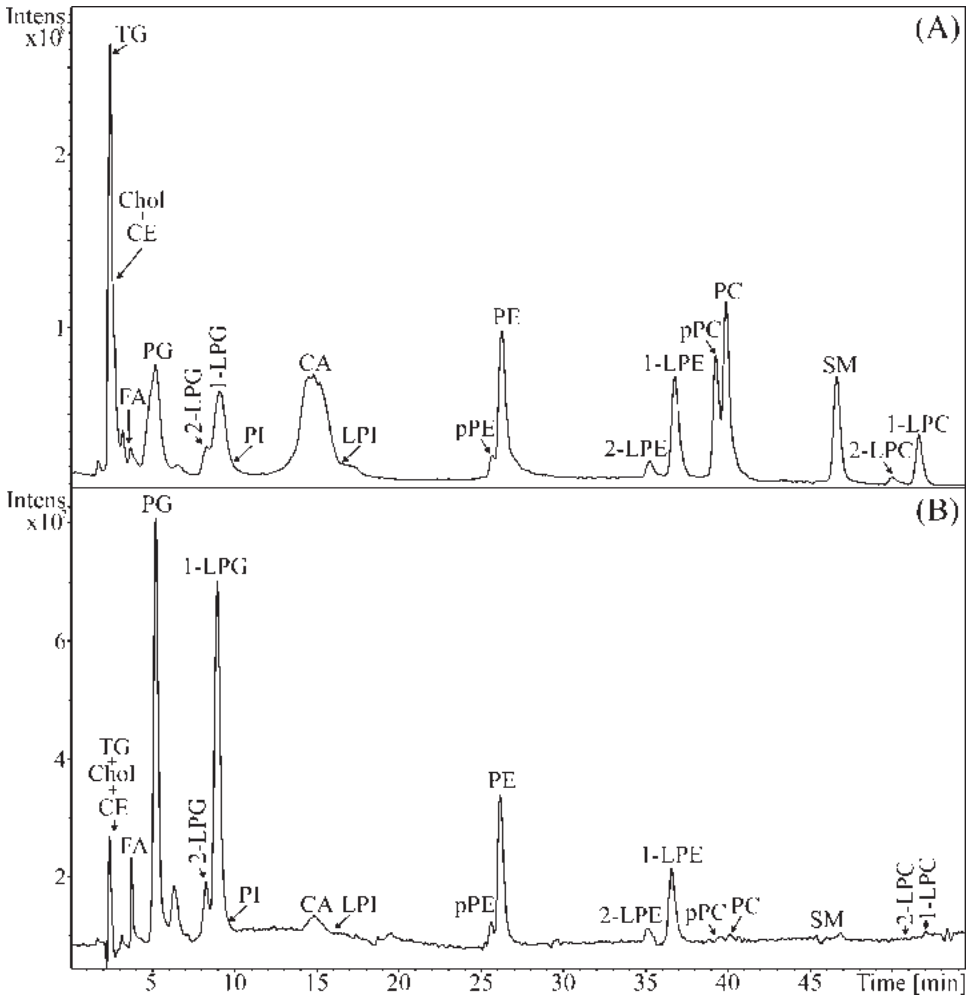

Fig. 1. HILIC/ESI-MS analysis of lipid classes represented by standards containing oleic acid (Δ9*cis*-C18:1) using Spherisorb Si column (250 × 4.6 mm, 5 μm) and ESI-MS detection in (A) positive-ion mode and (B) negative-ion mode. HPLC conditions: flow rate 1 mL/min, separation temperature 40 °C, gradient 0 min – 94% A + 6% B, 60 min – 77% A + 23% B, where A is acetonitrile and B is 5 mM aqueous ammonium acetate. Peak annotation: TG: triacylglycerol, Chol: cholesterol, CE: cholesteryl ester, FA: fatty acid, PG: phosphatidylglycerol, 2-LPG: 2-lysophosphatidylglycerol, 1-LPG: 1-lysophosphatidylglycerol, PI: phosphatidylinositol, CA: cardiolipin, LPI: lysophosphatidylinositol, pPE: phosphatidylethanolamine plasmalogen, PE: phosphatidylethanolamine, 2-LPE: 2-lysophosphatidylethanolamine, 1-LPE: 1-lysophosphatidylethanolamine, pPC: phosphatidylcholine plasmalogen, PC: phosphatidylcholine, SM: sphingomyeline, 2-LPC: 2-lysophosphatidylcholine, 1-LPC: 1-lysophosphatidylcholine.

[52]. In our method, ammonium acetate concentration and pH value have only a small effect on retention times of lipid classes with higher retention times (LPC, SM, PC, LPE and PE), but rather significant effect for classes with low retention times, *i.e.*, PG, LPG, CA (Figs. S2 and S3). The salt concentration and pH value strongly influence the ionization efficiency of lipids, which is significantly lower in mobile phases without ammonium acetate (Fig. S2) and at lower pH values (Fig. S3). The best separation and signal intensity have been achieved in mobile phases with 5 mM aqueous ammonium acetate at the neutral pH. Changes of gradient steepness and separation temperature have only negligible effects on the chromatographic resolution.

3.2. HILIC fractionation of lipids

In HILIC mode (Figs. 1 and 2), lipids are separated into classes that are identified based on the neutral losses of their polar head groups and characteristic product ions in full-scan positive-ion ESI mass spectra (Table 1). In general, the retention mechanisms in HILIC are based on the adsorption of the solute on the column packing and/or the partitioning of the solute into a water layer that is formed on the surface of the column packing. These interactions belong to the group of electrostatic forces. The typical rule for the retention of lipids in HILIC is that compounds with higher polarity or stronger dissociation are more retained, but other mechanisms are involved in case of Chol, FA, PG and LPG classes, where relatively low retention times in HILIC are observed that are comparable to neutral (non-polar) classes of TGs and CEs without any ionic or polar functional group (Fig. 1). Most lipid classes are baseline separated using our optimized HILIC method except for non-polar lipids (TG, Chol and CE) which are coeluting at retention times close to the void volume of the system. These classes are collected in one fraction, but TG and Chol can be easily separated using RP-HPLC mode in the second dimension. Lipids inside individual classes are partially separated according to the number of double bonds. Polyunsaturated species containing C22:6, C22:5 and C20:4 acids are less retained and they form partially separated peaks at the front of particular classes, for example, classes of PE, PC, SM (Fig. 2A and C) are partially separated into two or three peaks according to the unsaturation level of individual species.

The optimized HILIC method enables the partial separation of phospholipid plasmalogens from their phospholipid analogs, *i.e.*, pPE from PE (Figs. 1 and 2B and C) and pPC from PC (Figs. 1 and 2C). *Sn*-1 and *sn*-2 regioisomers of lysophospholipid are also separated in the HILIC mode (Fig. 1), *i.e.*, 2-LPG and 1-LPG, 2-LPE and 1-LPE, 2-LPC and 1-LPC. *Sn*-1 lysophospholipids have higher reten-

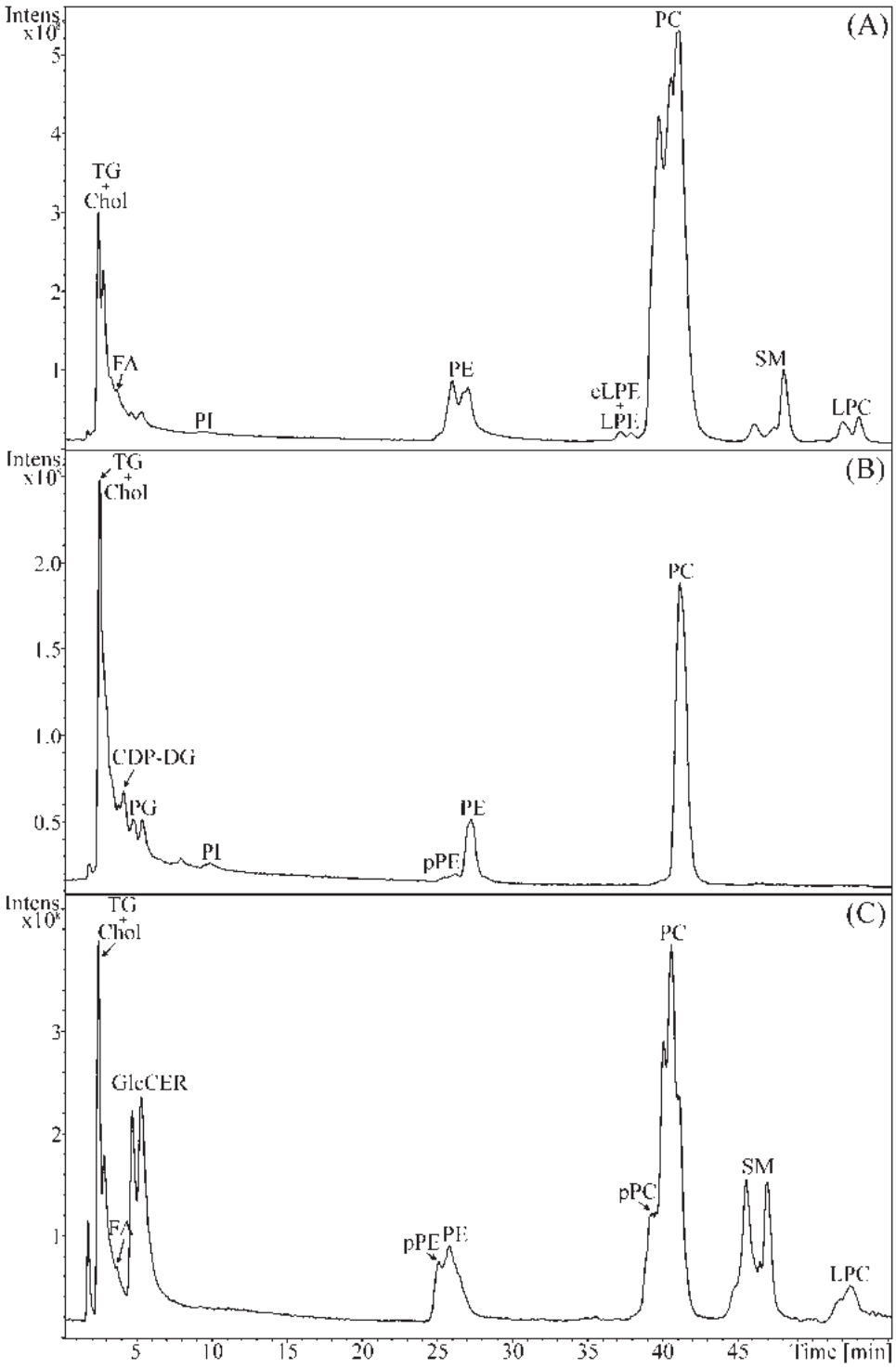

Fig. 2. HILIC with positive-ion ESI-MS detection of total lipid extracts from (A) egg yolk, (B) soya, and (C) porcine brain tissues. HPLC conditions and peak annotation are identical as for Fig. 1, CDP-DG: cytidine diphosphate-diacylglycerol, GlcCER: glycosylceramide.

tion in comparison to *sn*-2 isomers. Individual regioisomers are identified by negative-ion ESI full-scan mass spectra based on the relative abundance of carboxylate ions $[RCOO]^-$ (Fig. 3). The relative abundance of the $[RCOO]^-$ ion formed by cleavage of the fatty acid from the *sn*-2 position of phospholipids is higher in comparison to the ion formed by cleavage from the *sn*-1 position [12]. This rule has been applied for the identification of lysophospholipid regioisomers, *i.e.*, the higher intensity of $[RCOO]^-$ ion corresponds to *sn*-2 isomer. Ratios of relative abundances of $[RCOO]^-/[M-H]^-$ ions for lysophospholipid regioisomers are 100/27 for 2-LPE (Fig. 3A) and 100/70 for 1-LPE (Fig. 3B), 100/75 for 2-LPC and 45/100 for 1-LPC, 100/30 for 2-LPG and 62/100 for 1-LPG. The identification of *sn*-1 and *sn*-2 isomers is confirmed by identical standards. The synthesis of lysophospholipids produces mainly *sn*-1 isomers due to the thermodynamic preference. The small concentration of *sn*-2 isomers is formed via the fatty acyl migration on the glycerol during the purification process, which is in accordance with our results that significantly higher concentration is observed for *sn*-1 lysophospholipids in comparison to *sn*-2 isomers (Fig. 1).

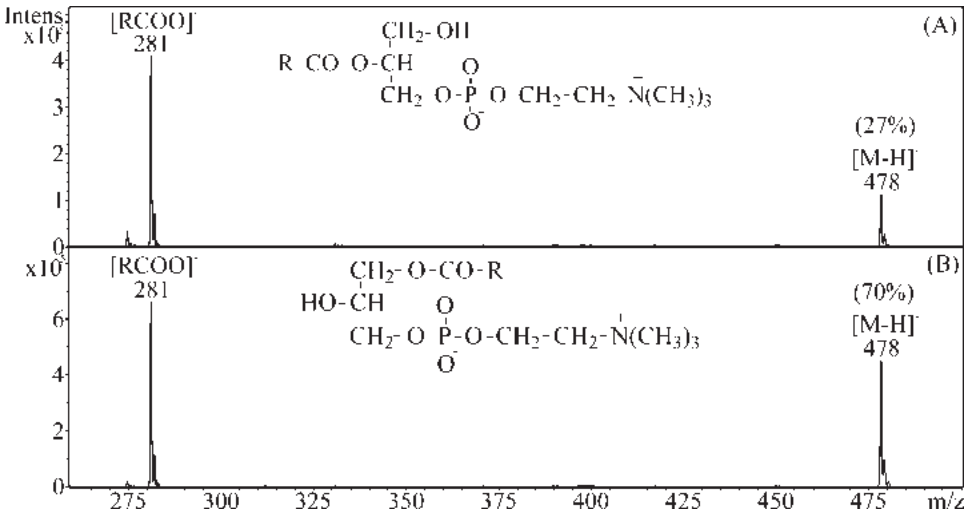

Fig. 3. Negative-ion ESI mass spectra of (A) 1-hydroxy-2-oleoyl-*sn*-glycero-3-phosphatidylethanolamine (2-LPE), and (B) 1-oleoyl-2-hydroxy-*sn*-glycero-3-phosphatidylethanolamine (1-LPE) standards.

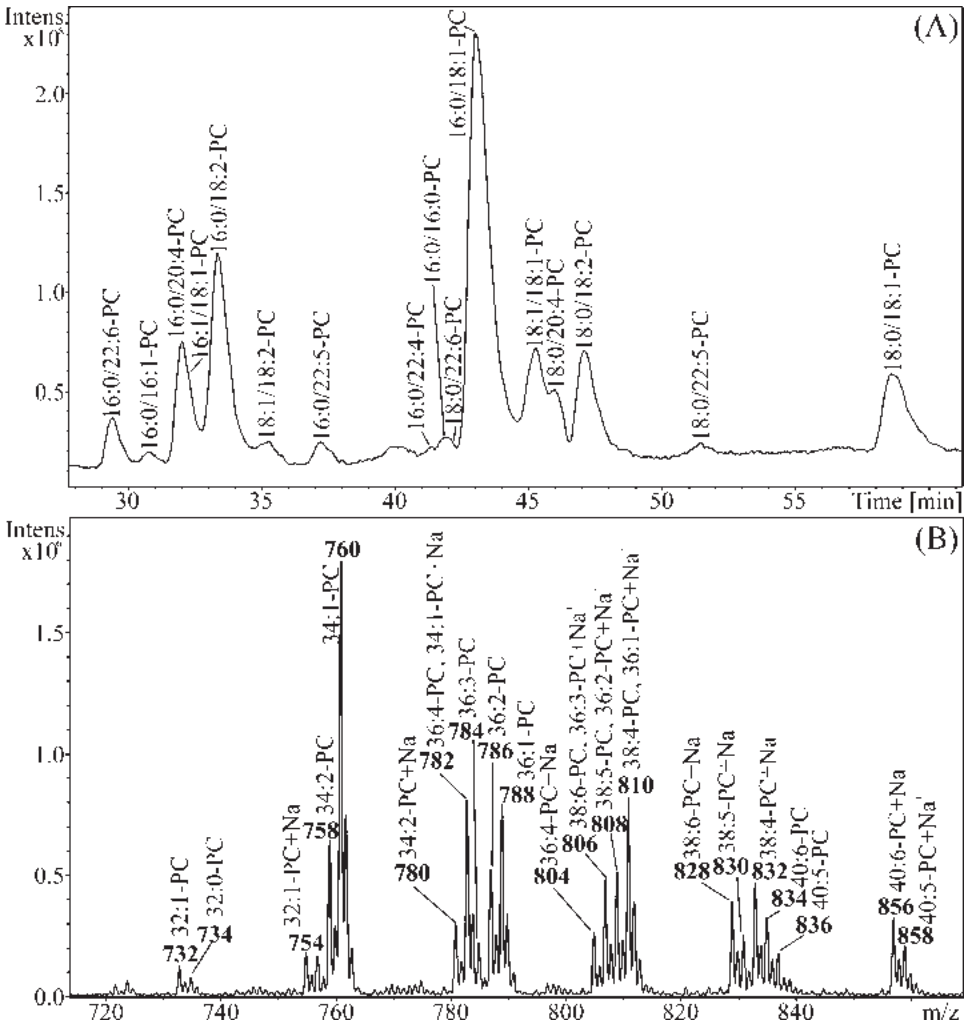

Fig. 4. Comparison of (A) RP-HPLC/ESI-MS analysis of PC fraction from egg yolk in the positive-ion mode and (B) positive-ion ESI mass spectrum of PC fraction from HILIC. HPLC conditions: porous shell particles column Kinetex C_{18} (150 × 2.1 mm, 2.6 μm), flow rate 0.3 mL/min, separation temperature 40 °C, gradient 0 min – 75% A + 25% B, 100 min – 88% A + 12% B, where A is the mixture of acetonitrile/2-propanol (1:1, v/v) and B is 5 mM aqueous ammonium acetate.

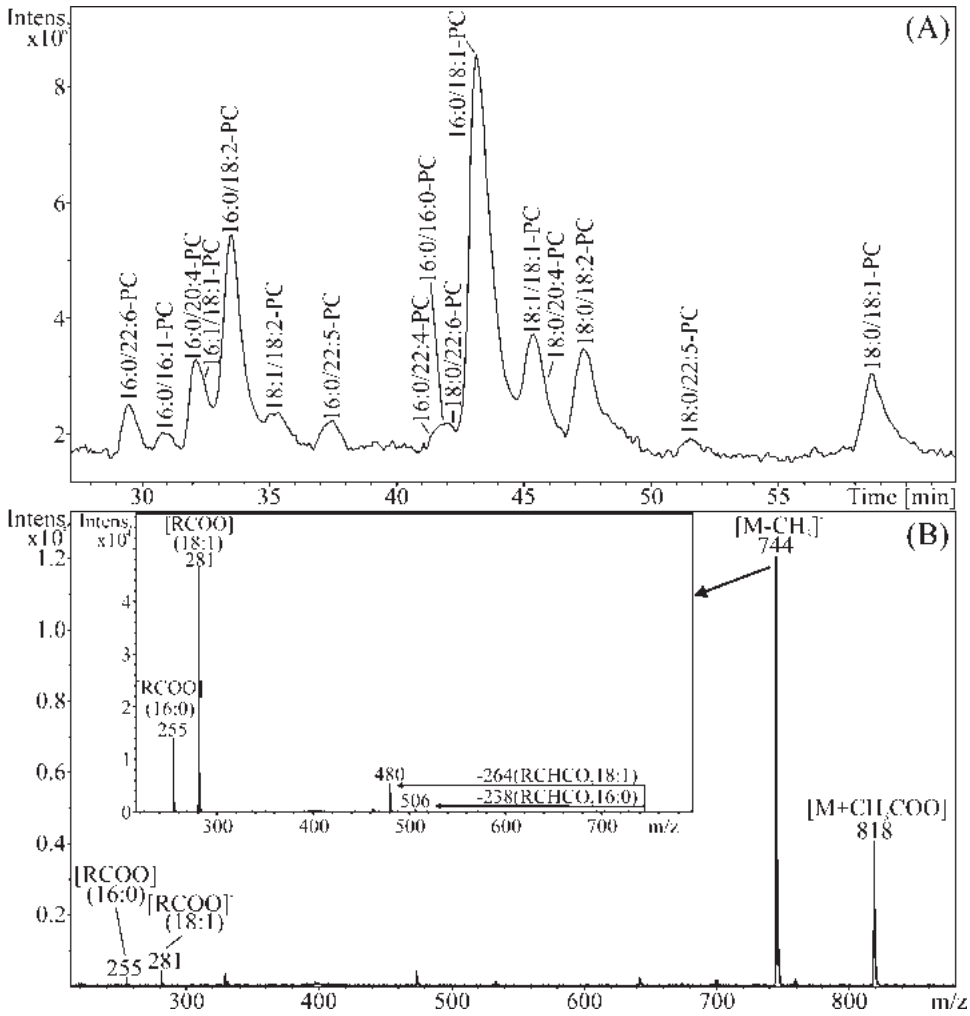

Fig. 5. RP-HPLC/ESI-MS analysis of (A) PC fraction from egg yolk in the negative-ion mode and (B) negative-ion ESI mass spectrum of 1-palmitoyl-2-oleoyl-*sn*-glycero-3-phosphatidylcholine (16:0/18:1-PC) with inset of MS/MS spectrum of *m/z* 744 used for determination of regioisomeric position of acyl chains. HPLC conditions are identical as for Fig. 4.

3.3. *Reversed-phase HPLC/MS analysis of lipids*

RP-HPLC method has been developed for the analysis of lipid fractions in the second dimension using C_{18} column and acetonitrile/2-propanol/aqueous ammonium acetate gradient. The special attention has been paid to the optimization of chromatographic conditions to achieve the highest number of separated species. Nine C_{18} columns with various column packing from different manufacturers have been tested (columns are listed in Section 2, representative chromatograms are shown in Fig. S4). Porous shell C_{18} column provides the best chromatographic resolution for most lipid species within a reasonable retention window (Figs. 4–7 and Fig. S4A). Similarly to HILIC, water concentration in the mobile phase is especially important at the beginning of gradient, which is one of the most critical parameter affecting the chromatographic resolution of lipids in RP-HPLC. Higher concentration of water significantly improves the chromatographic resolution and also the signal to noise ratio (Fig. S5). Water has also well pronounced impact on retention times of polyunsaturated species, which are retained more strongly at higher concentrations of water than other species, which can result in changed retention order (Fig. S5). The concentration of ammonium acetate does not show a visible effect on the chromatographic resolution or retention times of lipids, but it improves the ionization efficiency of lipids (Fig. S6). Other parameters, such as pH value of mobile phase (Fig. S7), gradient steepness (Fig. S8) and separation temperature, have negligible effects on the RP-HPLC separation.

In the RP-HPLC method (Figs. 4–7), lipid species are separated according to the acyl chain lengths and the number of double bonds. The chromatographic pattern partially fits to the well known model used for TGs [31–33] (Fig. 8), where the equivalent carbon number (ECN) is defined as the total carbon number (CN) of fatty acyls minus two times the double bond (DB) number (ECN = CN − 2DB). The retention of lipids in RP-HPLC increases proportionally to their ECN, except for polyunsaturated species containing fatty acyls with four and more double bonds, which are retained more strongly and they elute in higher ECN groups. For example, 16:0/22:6-PC with ECN = 26 and 16:0/20:4-PC with ECN = 28 elute in the group with ECN = 30 (Fig. 4A). The same chromatographic behavior is observed for all lipid classes in RP-HPLC (Figs. 4–7). Plasmalogen (pPE) and ether (eLPE) lipids (Fig. 6) have higher retention times in RP-HPLC in comparison to their phospholipid (PE and LPE) analogs.

ESI-MS and MS/MS spectra in both the positive-ion and negative-ion modes are used in the RP-HPLC/MS analysis of complex lipids. Full-scan positive-ion ESI mass spectra (Fig. 4B) allows the determination of molecular weights based on protonated molecules $[M+H]^+$, sodium $[M+Na]^+$ and potassium $[M+K]^+$ adducts. In the positive-ion ESI-MS mode, the neutral losses of polar head groups afforded characteristic fragment ions are observed

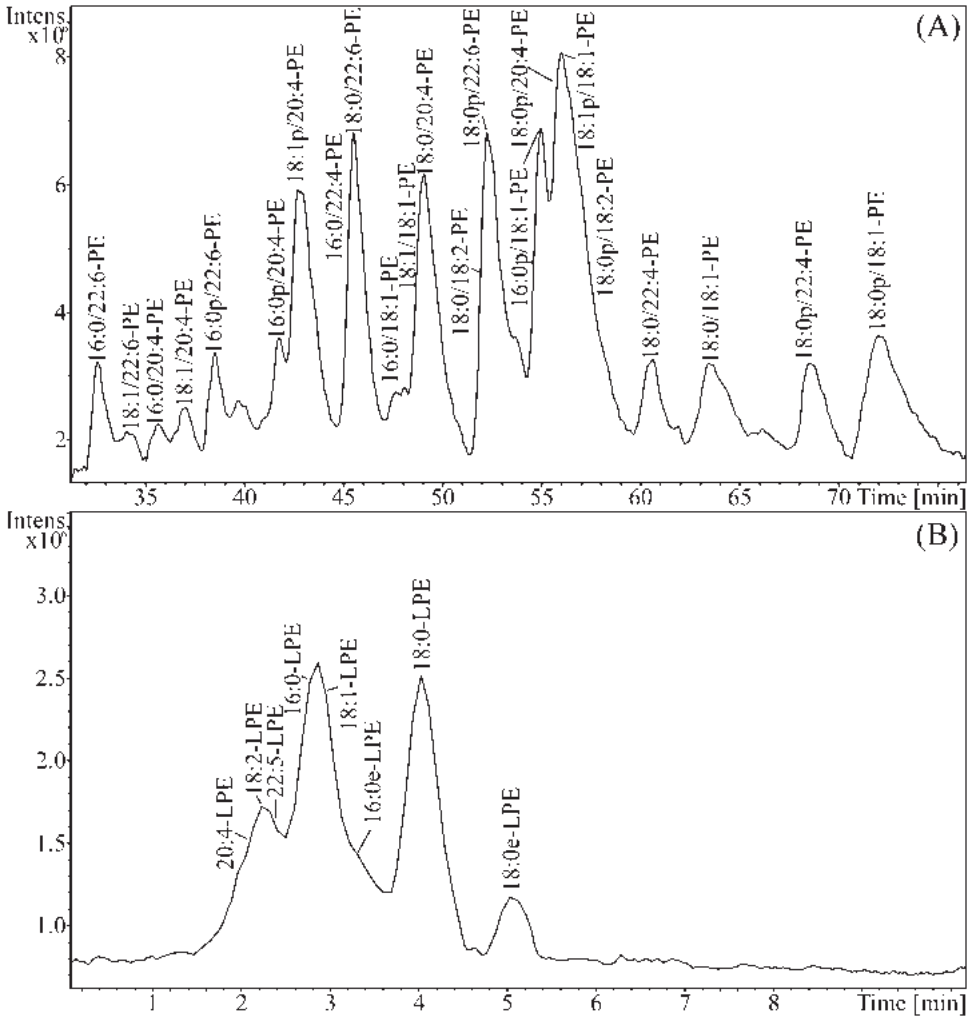

Fig. 6. RP-HPLC/ESI-MS analysis in the negative-ion mode of (A) PE fraction containing plasmalogens (pPE) from porcine brain and (B) LPE fraction containing alkyl ethers (eLPE) from egg yolk. p refers to plasmalogens and e refers to alkyl ethers. HPLC conditions are identical as for Fig. 4.

(Table 1). Whereas, in the negative-ion ESI-MS mode (Fig. 5B), we observed the deprotonated molecules $[M-H]^-$, the adducts with chloride $[M+Cl]^-$, acetate $[M+CH_3COO]^-$ and/or the loss of methyl $[M-CH_3]^-$ with low relative abundances of fatty acyl fragment ions $[RCOO]^-$. The latter are used for the determination of the fatty acid composition of the individual species. The relative abundances of aforementioned product ions in the low-energy MS/MS analyses (inset of Fig. 5B) provide clear information for the determination of their *sn*-1 or *sn*-2 positions based on the higher intensity of $[RCOO]^-$ product ions formed by losses from the *sn*-2 position. Fig. 4 shows the comparison of RP-HPLC/ESI-MS analysis of PC fraction and ESI mass spectrum of the peak of whole PC group from HILIC. First, the fraction of PC is collected during the HILIC analysis and then this fraction can be either analyzed by RP-HPLC/ESI-MS (Fig. 4A) or measured directly by ESI-MS without a chromatographic separation (Fig. 4B). RP-HPLC/ESI-MS enables the determination of fatty acid combinations in individual lipids including the determination of their *sn*-1 or *sn*-2 positions even for trace concentrations (Fig. 4A), while the direct ESI-MS is sufficient only for the determination of carbon number and double bond number (Fig. 4B). In addition, the presence of sodiated molecules $[M+Na]^+$ complicates the identification in the spectra measured by direct infusion ESI-MS, because they have identical nominal masses as protonated molecules of lipids differing by two methylene units and three double bonds, *e.g.*, protonated 36:4-PC has the same nominal mass $m/z = 782$ as sodiated 34:1-PC. Their resolution requires a high-resolution mass analyzer or chromatographic separation (Fig. 4A).

The fraction of non-polar TGs containing cholesterol has been analyzed using our previously developed NARP-HPLC method with APCI-MS detection using C_{18} column in the total length of 75 cm, separation temperature 25 °C and the gradient of acetonitrile/2-propanol [31] (Fig. 8). Cholesterol is clearly separated from TGs in NARP-HPLC. Individual TGs are separated according to their ECN as described in more details earlier [31–33]. Most TGs inside one ECN group are separated according to acyl chain lengths and the double bond number. TGs with higher number of double bonds have lower retention times than saturated TGs with the same ECN, *e.g.*, 18:1/18:1/18:1-TG has slightly lower retention in comparison to 18:1/18:1/16:0-TG or even 16:0/18:1/16:0-TG, all with ECN = 48. APCI-MS is suitable for the identification of TGs due to their non-polar character. Individual TG species and their fatty acid composition are identified based on their full-scan positive-ion APCI mass spectra containing both abundant fragment ions and $[M+H]^+$ and $[M+NH_4]^+$ ions. Ratios of fragment ions $[M+H-RCOOH]^+$ are used for the determination of fatty acids stereochemical positions, because the neutral loss of fatty acid from *sn*-2 position provides the fragment ion with lower relative abundance in comparison to *sn*-1 and *sn*-3 positions.

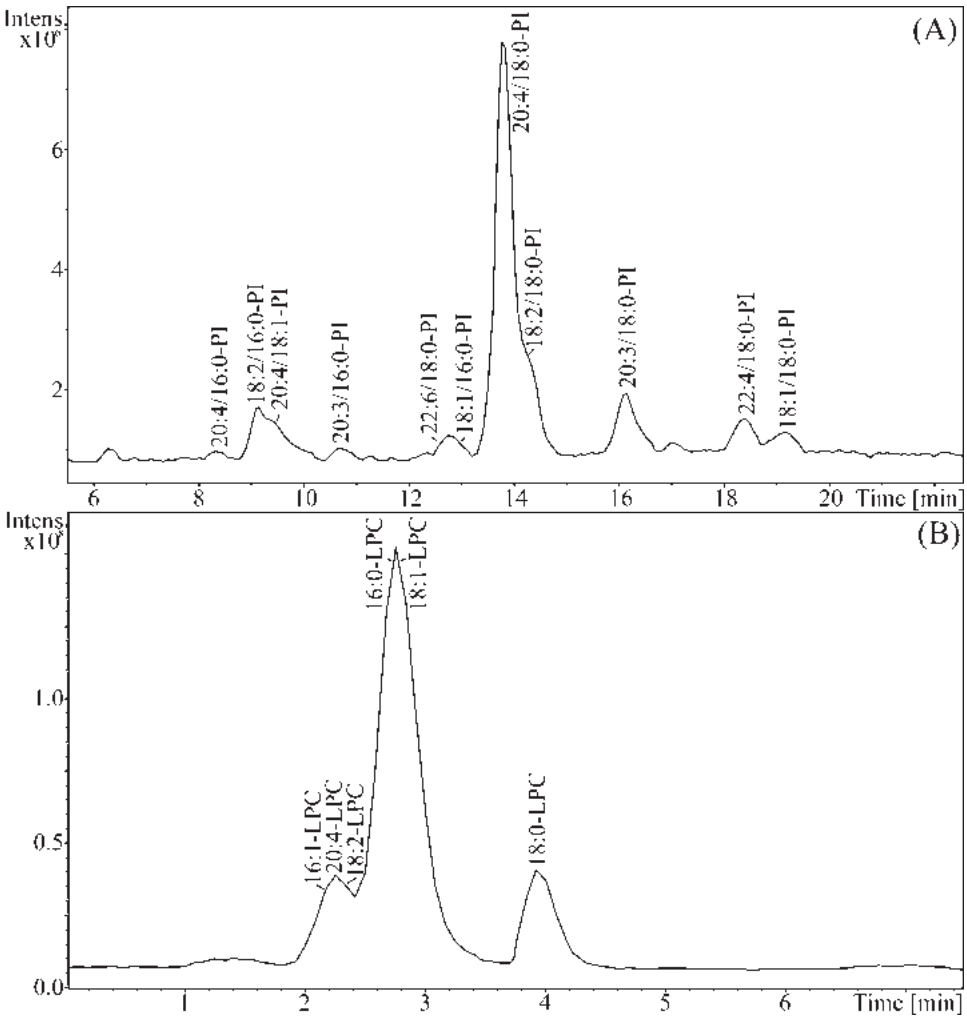

Fig. 7. RP-HPLC/ESI-MS analysis in the positive-ion mode of (A) PI, and (B) LPC fractions from egg yolk. HPLC conditions are identical as for Fig. 4.

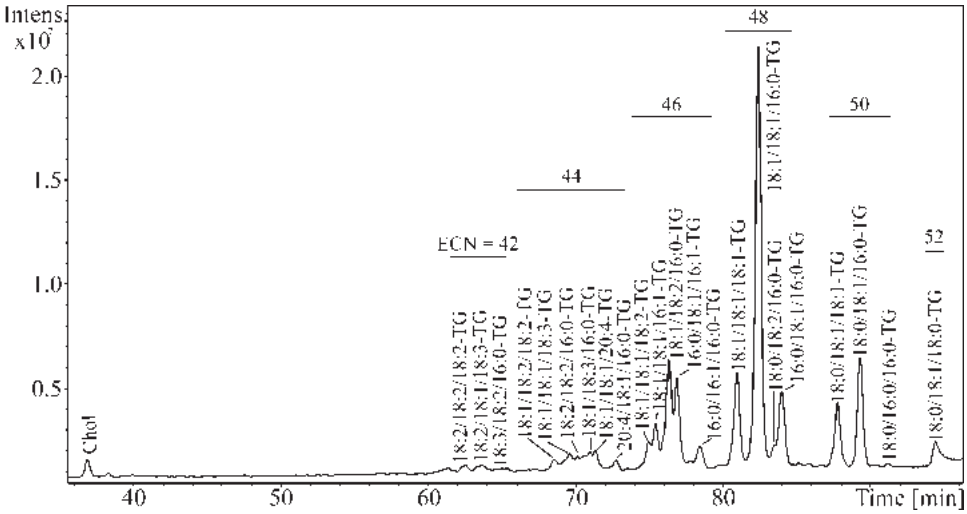

Fig. 8. NARP-HPLC/APCI-MS analysis in the positive-ion mode of TG fraction containing cholesterol from egg yolk. HPLC conditions: two Nova-Pak C_{18} columns (150 × 3.9 and 300 × 3.9 mm, 4 μm, Waters) connected in series, flow rate 1 mL/min, separation temperature 25 °C, gradient 0 min – 100% acetonitrile, 106 min – 31% acetonitrile + 69% 2-propanol.

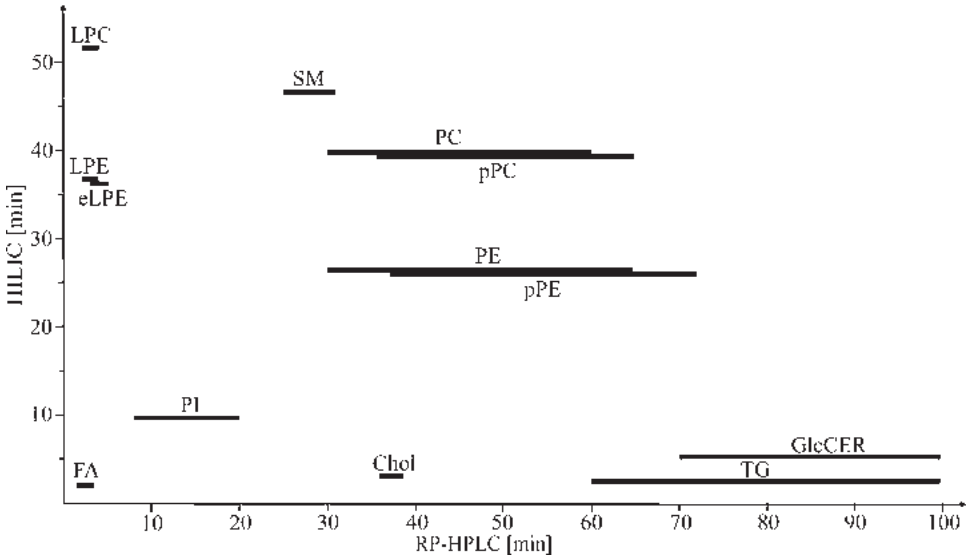

Fig. 9. 2D plot compiled from HILIC and RP-HPLC retention times of lipids detected in studied samples. Retention times of Chol and TG species are from NARP-HPLC analysis. HPLC conditions are listed in Section 2.

3.4. Off-line 2D-HPLC/MS analysis of samples

Optimized off-line 2D-HPLC/MS method is applied for the characterization of lipid composition in egg yolk, soya and porcine brain tissues (Figs. 2 and 4–8). Fig. 9 depicts 2D plot compiled from retention times of lipid classes using HILIC and individual lipid species using RP-HPLC. The plot shows an excellent orthogonality of both modes, which enables detailed lipidomic characterization and also the potential of this system for on-line 2D-HPLC/MS lipidomic analysis. In total, 15 lipid classes have been identified in analyzed samples using optimized HILIC method. The tested biological samples do contain 10 (egg yolk, porcine brain) or 8 (soya) different lipid classes. TG, Chol, PE and PC classes are present in all samples. The most abundant classes are TG and PC. eLPE in egg yolk (Figs. 2A and 6B) and pPC and pPE in soya (Fig. 2B) and porcine brain (Fig. 2C) samples are identified. In egg yolk and porcine brain samples, both *sn*-1 and *sn*-2 regioisomers of LPE and LPC are detected with a strong preference of *sn*-1 isomer over *sn*-2 isomer. More than 150 lipid species are identified using RP-HPLC/MS of fractions in analyzed samples. The number of lipid species varies among classes, which is given by fatty acid composition of the sample and their combinations on the glycerol skeleton. For example, the sample of egg yolk contains 22 species of TG and 1 Chol (Fig. 8), 6 FA (not shown), 11 PI (Fig. 7A), 14 PE (not shown), 6 LPE and 2 eLPE (Fig. 6B), 16 species of PC (Figs. 4A and 5A), 6 SM (not shown) and 6 LPC (Fig. 7B). TGs are composed from fatty acids containing 0–3 double bonds and 16 or 18 carbons except for 18:1/18:1/20:4-TG and 20:4/16:0:18:1-TG. Complex lipids are composed from the wide range of fatty acids containing 0–6 double bonds and 16–22 carbon atoms. They often have the combination of one saturated or monounsaturated acid and one polyunsaturated acid, *e.g.*, 16:0/22:6-PC. The strong preference of unsaturated fatty acids in the *sn*-2 position is observed for all identified glycerolipids except for PI, where saturated fatty acids are favored in *sn*-2 position (Fig. 7A). In total, 9 fatty acids in egg yolk, 6 in soya and 9 in porcine brain samples are observed.

4. Conclusions

This work presents off-line 2D combination of HILIC fractionation in the first dimension followed by the RP-HPLC analysis of collected fractions in the second dimension. Both systems show an excellent orthogonality enabling the comprehensive characterization of lipid composition in complex biological samples as demonstrated on egg yolk, soya and porcine brain tissues. Lipids are separated into classes according to their polarity and electrostatic interactions in HILIC mode, while the retention of lipids in RP-HPLC is governed by acyl chain lengths and the number of double bonds. The separation of *sn*-1 and *sn*-2 lysophospholipid regioisomers in HILIC mode is achieved by carefully optimized chromatographic conditions. Higher relative abundance of fatty acyl ions formed by the cleavage of fatty acid from *sn*-2 position in negative-ion ESI mass spectra enables the differentiation of lysophospholipid regioisomers. RP-HPLC mode also provides the resolution of plasmalogen and ether phospholipids in analyzed samples. Fatty acid composition of individual lipids and positions of fatty acyls on the glycerol skeleton are determined based on their mass spectra. Unsaturated fatty acids are preferentially esterified in *sn*-2 position in all lipid classes except for PIs, where saturated fatty acids are favored in this position for unknown reason. Off-line 2D-HPLC/MS analysis of lipids is time consuming method, but it provides valuable information for the identification of species at trace concentrations in comparison to one-dimensional HPLC or even the direct infusion analysis.

Acknowledgements

This work was supported by the Grant Project No. MSM0021627502 sponsored by the Ministry of Education, Youth and Sports of the Czech Republic and Projects No. 203/09/P249 sponsored by the Czech Science Foundation.

Appendix A. Supplementary data

Supplementary data associated with this article can be found, in the online version, at doi:10.1016/j.chroma.2011.05.081.

References

[1] A.D. Watson, J. Lipid Res. 47 (2006) 2101.
[2] M.R. Wenk, Nat. Rev. Drug Discov. 4 (2005) 594.
[3] E. Fahy, S. Subramaniam, R.C. Murphy, M. Nishijima, C.R.H. Raetz, T. Shimizu, F. Spener, G. van Meer, M.J.O. Wakelam, E.A. Dennis, J. Lipid Res. 50 (2009) S9.
[4] W.W. Christie, http://lipidlibrary.aocs.org/index.html, American Oil Chemists' Society, 2011.

[5] E. Fahy, S. Subramaniam, H.A. Brown, C.K. Glass, A.H. Merrill, R.C. Murphy, C.R.H. Raetz, D.W. Russell, Y. Seyama, W. Shaw, T. Shimizu, F. Spener, G. van Meer, M.S. VanNieuwenhze, S.H. White, J.L. Witztum, E.A. Dennis, J. Lipid Res. 46 (2005) 839.
[6] J. Folch, M. Lees, G.H.S. Stanley, J. Biol. Chem. 226 (1957) 497.
[7] E.G. Bligh, W.J. Dyer, Can. J. Biochem. Physiol. 37 (1959) 911.
[8] D.Y. Wang, W.M. Xu, X.L. Xu, G.H. Zhou, Y.Z. Zhu, C.B. Li, M.M. Yang, Food Chem. 112 (2009) 150.
[9] A. Cascone, S. Eerola, A. Ritieni, A. Rizzo, J. Chromatogr. A 1120 (2006) 211.
[10] P.M. Hutchins, R.M. Barkley, R.C. Murphy, J. Lipid Res. 49 (2008) 804.
[11] U. Sommer, H. Herscovitz, F.K. Welty, C.E. Costello, J. Lipid Res. 47 (2006) 804.
[12] M. Pulfer, R.C. Murphy, Mass Spectrom. Rev. 22 (2003) 332.
[13] E. Hvattum, C. Rosjo, T. Gjoen, G. Rosenlund, B. Ruyter, J. Chromatogr. B 748 (2000) 137.
[14] S. Uran, A. Larsen, P.B. Jacobsen, T. Skotland, J. Chromatogr. B 758 (2001) 265.
[15] L.Q. Pang, Q.L. Liang, Y.M. Wang, L. Ping, G.A. Luo, J. Chromatogr. B 869 (2008) 118.
[16] C. Wang, S.G. Xie, J. Yang, Q. Yang, G.W. Xu, Anal. Chim. Acta 525 (2004) 1.
[17] S. Harrabi, W. Herchi, H. Kallel, P.M. Mayer, S. Boukhchina, Food Chem. 114 (2009) 712.
[18] E.J. Ahn, H. Kim, B.C. Chung, G. Kong, M.H. Moon, J. Chromatogr. A 1194 (2008) 96.
[19] D.Y. Bang, E.J. Ahn, M.H. Moon, J. Chromatogr. B 852 (2007) 268.
[20] V. Ioffe, T. Kalendarev, I. Rubinstein, G. Zupkovitz, J. Pharm. Biomed. Anal. 30 (2002) 391.
[21] C.A. Lytle, Y.D. Gan, D.C. White, J. Microbiol. Methods 41 (2000) 227.
[22] K. Retra, O.B. Bleijerveld, R.A. van Gesteil, A.G.M. Tielens, J.J. van Hellemond, J.F. Brouwers, Rapid Commun. Mass Spectrom. 22 (2008) 1853.
[23] K. Sandra, A.D. Pereira, G. Vanhoenacker, F. David, P. Sandra, J. Chromatogr. A 1217 (2010) 4087.
[24] Y.Q. Xia, M. Jemal, Rapid Commun. Mass Spectrom. 23 (2009) 2125.
[25] F.G. Xu, L. Zou, Q.S. Lin, C.N. Ong, Rapid Commun. Mass Spectrom. 23 (2009) 3243.
[26] B. Barroso, R. Bischoff, J. Chromatogr. B 814 (2005) 21.
[27] N. Mazzella, J. Molinet, A.D. Syakti, A. Dodi, J.C. Bertrand, P. Doumenq, Rapid Commun. Mass Spectrom. 19 (2005) 3579.
[28] E.M. Hein, L.M. Blank, J. Heyland, J.I. Baumbach, A. Schmid, H. Hayen, Rapid Commun. Mass Spectrom. 23 (2009) 1636.
[29] J. Cvačka, O. Hovorka, P. Jiroš, J. Kindl, K. Stránský, I. Valterová, J. Chromatogr. A 1101 (2006) 226.
[30] P. Dugo, T. Kumm, M.L. Crupi, A. Cotroneo, L. Mondello, J. Chromatogr. A 1112 (2006) 269.
[31] M. Holčapek, M. Lísa, P. Jandera, N. Kabátová, J. Sep. Sci. 28 (2005) 1315.
[32] M. Lísa, M. Holčapek, J. Chromatogr. A 1198 (2008) 115.
[33] M. Lísa, M. Holčapek, H. Sovová, J. Chromatogr. A 1216 (2009) 8371.
[34] E.J.C. van der Klift, G. Vivó-Truyols, F.W. Claassen, F.L. van Holthoon, T.A. van Beek, J. Chromatogr. A 1178 (2008) 43.
[35] P. Dugo, T. Kumm, B. Chiofalo, A. Controneo, L. Mondello, J. Sep. Sci. 29 (2006) 1146.
[36] H.G. Nie, R.R. Liu, Y.Y. Yang, Y. Bai, Y.F. Guan, D.Q. Qian, T. Wang, H.W. Liu, J. Lipid Res. 51 (2010) 2833.
[37] M. Holčapek, H. Velínská, M. Lísa, P. Česla, J. Sep. Sci. 23 (2009) 3672.
[38] T. Houjou, K. Yamatani, M. Imagawa, T. Shimizu, R. Taguchi, Rapid Commun. Mass Spectrom. 19 (2005) 654.
[39] Y. Sato, T. Nakamura, K. Aoshima, Y. Oda, Anal. Chem. 82 (2010) 9858.
[40] P.H. Axelsen, R.C. Murphy, J. Lipid Res. 51 (2010) 1244.
[41] K. Ekroos, C.S. Ejsing, U. Bahr, M. Karas, K. Simons, A. Shevchenko, J. Lipid Res. 44 (2003) 2181.
[42] C.S. Ejsing, T. Moehring, U. Bahr, E. Duchoslav, M. Karas, K. Simons, A. Shevchenko, J. Mass Spectrom. 41 (2006) 372.
[43] A. Takatera, A. Takeuchi, K. Saiki, T. Morisawa, N. Yokoyama, M. Matsuo, J. Chromatogr. B 838 (2006) 31.
[44] A.A. Karlsson, P. Michelsen, A. Larsen, G. Odham, Rapid Commun. Mass Spectrom. 10 (1996) 775.
[45] B. Fuchs, R. Suss, J. Schiller, Prog. Lipid Res. 49 (2010) 450.
[46] N. Goto-Inoue, T. Hayasaka, T. Taki, T.V. Gonzalez, M. Setou, J. Chromatogr. A 1216 (2009) 7096.
[47] A. Rohlfing, J. Muthing, G. Pohlentz, U. Distler, J. Peter-Katalinic, S. Berkenkamp, K. Dreisewerd, Anal. Chem. 79 (2007) 5793.
[48] K.A. Al-Saad, W.F. Siems, H.H. Hill, V. Zabrouskov, N.R. Knowles, J. Am. Soc. Mass Spectrom. 14 (2003) 373.
[49] J. Cvačka, A. Svatoš, Rapid Commun. Mass Spectrom. 17 (2003) 2203.
[50] W.C. Byrdwell, Lipids 36 (2001) 327.
[51] P. Jandera, Extreme chromatography: faster, hotter, smaller, in: W.C. Byrdwell, M. Holčapek (Eds.), Hydrophilic Interaction Chromatography – An Excellent Method for Separation of Polar Samples, American Oil Chemists' Society, 2011, p. 47.
[52] M. Holčapek, K. Volná, P. Jandera, L. Kolářová, K. Lemr, M. Exner, A. Církva, J. Mass Spectrom. 39 (2004) 43.

Lipids (2013) 48:915–928
DOI 10.1007/s11745-013-3820-4

ORIGINAL ARTICLE

Nontargeted Lipidomic Characterization of Porcine Organs Using Hydrophilic Interaction Liquid Chromatography and Off-Line Two-Dimensional Liquid Chromatography–Electrospray Ionization Mass Spectrometry

Eva Cífková · Michal Holčapek · Miroslav Lísa

Received: 10 January 2013 / Accepted: 2 July 2013 / Published online: 3 August 2013

Abstract Lipids form a significant part of animal organs and they are responsible for important biological functions, such as semi-permeability and fluidity of membranes, signaling activity, anti-inflammatory processes, etc. We have performed a comprehensive nontargeted lipidomic characterization of porcine brain, heart, kidney, liver, lung, spinal cord, spleen, and stomach using hydrophilic interaction liquid chromatography (HILIC) coupled to electrospray ionization mass spectrometry (ESI/MS) to describe the representation of individual lipid classes in these organs. Detailed information on identified lipid species inside classes are obtained based on relative abundances of deprotonated molecules $[M-H]^-$ in the negative-ion ESI mass spectra, which provides important knowledge on phosphatidylethanolamines and their different forms of fatty acyl linkage (ethers and plasmalogens), phosphatidylinositols, and hexosylceramides containing nonhydroxy- and hydroxy-fatty acyls. The detailed analysis of identified lipid classes using reversed-phase liquid chromatography in the second dimension was performed for porcine brain to determine more than 160 individual lipid species containing attached fatty acyls of different acyl chain length, double-bond number, and positions on the glycerol skeleton. The fatty acid composition of porcine organs is determined by gas chromatography with flame ionization detection after the transesterification with sodium methoxide.

Keywords Lipidomics · Lipidome · Quantitation · Porcine organs · Hydrophilic interaction liquid chromatography · HPLC/MS · Phospholipids

Abbreviations

APCI	Atmospheric pressure chemical ionization
CE	Cholesteryl ester
Cer	Ceramide
Chol (C)	Cholesterol
CN	Carbon number
DB	Double bond
ESI	Electrospray ionization
ePC (PakCho)	Plasmanylphosphatidylcholine (ether)
ePE (PakEtn)	Plasmanylphosphatidylethanolamine (ether)
FAME	Fatty acid methyl ester
FID	Flame ionization detector
GC	Gas chromatography
HexCer	Hexosylceramide
HILIC	Hydrophilic interaction liquid chromatography
HPLC	High-performance liquid chromatography
IS	Internal standard
LPC (LysoPtdCho)	Lysophosphatidylcholine
LPE (LysoPtdEtn)	Lysophosphatidylethanolamine
MS	Mass spectrometry
NARP	Nonaqueous reversed-phase
PC (PtdCho)	Choline glycerophospholipids
PE (PtdEtn)	Ethanolamine glycerophospholipids

Electronic supplementary material The online version of this article (doi:10.1007/s11745-013-3820-4) contains supplementary material, which is available to authorized users.

E. Cífková · M. Holčapek (✉) · M. Lísa
Department of Analytical Chemistry, Faculty of Chemical Technology, University of Pardubice, Studentská 573, 532 10 Pardubice, Czech Republic
e-mail: michal.holcapek@upce.cz

PI (PtdIns)	Phosphatidylinositol
PG (PtdGro)	Phosphatidylglycerol
pPC (PlsCho)	Plasmenylphosphatidylcholine (plasmalogen)
pPE (PlsEtn)	Plasmenylphosphatidylethanolamine (plasmalogen)
PS (PtdSer)	Phosphatidylserine
QqQ	Triple quadrupole
RF	Response factor
RP	Reversed-phase
SM (CerPCho)	Sphingomyelin
SRM	Selected reaction monitoring
TG (TAG)	Triacylglycerol

Introduction

Lipids are important components of cellular organisms that serve as building blocks of membranes, sources of energy, essential fatty acids and fat-soluble vitamins, biosynthetic precursor of cellular components, transmission of information in cells, etc. [1–3]. They are divided according to their structural and biosynthetic complexity into the following categories: fatty acyls, glycerolipids, glycerophospholipids, sphingolipids, sterol lipids, prenol lipids, saccharolipids, and polyketides [1]. Fatty acids are building blocks for the synthesis of triacylglycerols (TG), which are mainly used for energy storage and signaling. The balance among saturated, monounsaturated, and polyunsaturated fatty acids is important for maintaining the optimum fluidity of membranes. In the human organism, polyunsaturated fatty acids (PUFA) are main components of brain and retina, and n-6 PUFA are essential for the biosynthesis of prostaglandins, which decreases the production of inflammatory agents [4]. Glycerophospholipids are key constituents of lipid bilayers, which form the separate environment of internal cells and participate in the cellular signaling and enzyme activation. In nature, glycerophospholipids containing ether-linked fatty acyls (plasmenyl and plasmanyl-lipids) instead of ester-linked fatty acyls are common, especially as membrane constituents. Plasmenyl-lipids (plasmalogens) form up to 50 % of glycerophospholipids of brain and heart tissues of human, while plasmanyl-lipids (ethers) occur at only a few percent, but elevated levels of plasmalogens have been reported in human cancer tissues [5–7]. Sphingolipids are contained in most cell membranes, mainly in nervous membranes (brain and spinal cord).

The comprehensive lipidomic analysis of biological samples is a daunting task due to the extreme complexity of the lipidome (amphipathic character of lipids with hydrophobic acyl tails and hydrophilic head groups). Two basic strategies are used in mass spectrometry (MS)-based analysis of lipids: (1) direct infusion approaches without any separation step (shotgun method), and (2) chromatographic separation followed by MS, typically high-performance liquid chromatography (HPLC)–MS. Gas chromatography with flame ionization detection (GC/FID) or MS detection can be used for fatty acid profiling after the transesterification to fatty acid methyl esters (FAME) [8, 9]. HPLC/MS is a powerful technique in the separation of complex mixtures of glycerolipids, glycerophospholipids, sphingolipids, etc. Nonaqueous reversed-phase (NARP) HPLC coupled to atmospheric pressure chemical ionization (APCI) MS is applicable for the separation and identification of nonpolar lipids, such as TGs [9–12]. Hydrophilic interaction liquid chromatography (HILIC) and reversed-phase (RP) HPLC coupled to electrospray ionization (ESI) MS has been used for the separation of glycerophospholipids and sphingolipids [13–18] in animal tissues. Furthermore, the coupling of thin-layer chromatography (TLC) and matrix-assisted laser desorption-ionization (MALDI) has also been applied for the analysis of biological samples [19–21]. Comprehensive lipidomic analysis is often performed using on-line or off-line two-dimensional HPLC, which offers the opportunity to separate complex lipidomic mixtures according to two molecular properties [18, 22, 23]. Another possibility for the characterization of lipid classes with different ionization behavior is dual parallel coupling of HPLC and MS, where a certain portion of effluent can be diverted into the second HPLC/MS with different chromatographic and ionization conditions than the first HPLC/MS configuration [24].

The lipidomic quantitation has been a challenge for long time, but several approaches for targeted and nontargeted quantitation of lipids are known using MS (direct infusion [25–27] or in HPLC/MS configuration [28]) or ^{31}P nuclear magnetic resonance (NMR) spectrometry [29, 30]. The most widespread shotgun approach applies the direct infusion ESI–MS using various scans typical for triple quadrupole (QqQ) [13, 14, 17, 31–35] or hydride quadrupole–linear ion trap mass analyzers [36], such as the precursor ion scan, the neutral loss scan, the product ion scan, and the selected reaction monitoring (SRM), together with the use of suitable internal standards (typically deuterated or odd carbon number analogs of determined lipids). The shotgun approach has been used in numerous lipidomic studies due to its simplicity, easy automation, and rapidity. The shotgun approach without HPLC separation is less convenient for the analysis of isobaric lipids [28]. Ion suppression/enhancement effects in the shotgun approach can be stronger compared to HPLC/MS [28]. The novel trend in the lipidomic quantitation is the use of high-resolution quadrupole–time-of-flight (Q-TOF) mass analyzer [36] or even an ultrahigh-resolution orbitrap analyzer with the Fourier transformation providing the resolving power

over 100,000 (FWHM) and sub-ppm mass accuracy [17]. HPLC/MS methods offer the separation of isobaric species and significantly reduce suppression effects, but on the other hand it takes longer and requires additional instrumentation and expertise. Typically, reversed-phase (RP) mode is used for the HPLC separation with possible identification of several hundred lipid species [17, 23]. Recently, we have introduced the nontargeted approach based on HILIC-HPLC separation of lipid classes and the determination based on the use of response factors (RFs) for individual lipid classes together with a single internal standard (sphingosyl PE, d17:1/12:0) [37]. Another nontargeted method for the lipid class quantitation is ^{31}P NMR [29, 30], which is an accurate and nondestructive method, but suffering from low sensitivity and therefore very long measurement times, and is not suitable for HPLC coupling.

The main goal of this work is the application of nontargeted a HILIC-HPLC/ESI–MS method for qualitative and quantitative characterization of the lipidome, mainly glycerophospholipids and sphingolipids, in biological tissues (porcine organs), with comparison of the results with previously published data [13, 14, 17, 30, 38–41]. In this work, we determine the distribution of individual lipid classes in porcine brain, heart, kidney, liver, lung, spinal cord, spleen, and stomach, together with the representation of fatty acyls within certain classes.

Materials and Methods

Chemicals and Standards

Acetonitrile, 2-propanol, and methanol (all HPLC gradient grade), hexane and chloroform stabilized by 0.5–1 % ethanol (both HPLC grade), sodium methoxide, and ammonium acetate were purchased from Sigma-Aldrich (St. Louis, MO, USA). 1,2-dimyristoyl-*sn*-glycero- 3-phosphoglycerol (14:0/14:0-PG), 1,2-dimyristoyl-*sn*-glycero-3-phosphoethanolamine (14:0/14:0-PE), 1-myristoyl-2-hydroxy-*sn*-glycero-3-phosphoethanolamine (14:0-LPE), 1,2-dimyristoyl-*sn*-glycero-3-phosphocholine (14:0/14:0-PC), and 1-myristoyl-2-hydroxy-*sn*-glycero-3-phosphocholine (14:0-LPC) for the determination of extraction yields, 1,2-dipalmitoyl-*sn*-glycero-3-phosphocholine (16:0/16:0-PC), 1,2-dioleoyl-*sn*-glycero-3-phosphocholine (18:1/18:1-PC), 1,2-distearoyl-*sn*-glycero-3-phosphocholine (18:0/18:0-PC), 1,2-diarachidonoyl-*sn*-glycero-3-phosphocholine (20:4/20:4-PC), 1,2-didocosahexaenoyl-*sn*-glycero-3-phosphocholine (22:6/22:6-PC), 1,2-diheptadecanoyl-*sn*-glycero-3-phosphoethanolamine (17:0/17:0-PE), and 1,2-dioleoyl-*sn*-glycero-3-phosphoethanolamine (18:1/18:1-PE) for determination of ionization efficiency, and *N*-dodecanoyl-heptadecasphing-4-enine-1-phosphoethanolamine (sphingosyl PE, d17:1/12:0) used as the IS for the nontargeted quantitation with RFs were purchased from Avanti Polar Lipids (Alabaster, AL, USA). Brain, heart, kidney, liver, lung, spinal cord, spleen, and stomach of pig (female at the age of 8 months) were obtained from the family farm of the first author.

Sample Preparation

Total lipid extracts for HILIC-HPLC/MS analyses were prepared according to the modified Folch procedure [42] using a chloroform–methanol–water system. Briefly, approximately 0.5 g of porcine organ and 50 µL of 3.3 mg/mL IS (sphingosyl PE, d17:1/12:0) were homogenized with 10 mL of chloroform–methanol (2:1, v/v) mixture for 5 min and the homogenate was filtered using a coarse filter paper. Then, 2 mL of 1 mol/L NaCl was added, and the mixture was centrifuged at 2,500 rpm for 4 min at ambient temperature. The chloroform (bottom) layer containing lipids was taken and evaporated by a gentle stream of nitrogen and redissolved in chloroform–2-propanol (1:1,v/v) mixture for subsequent HILIC analyses.

FAMEs for GC/FID analyses were prepared from total lipid extracts of porcine organs using a standard procedure with sodium methoxide [8]. Briefly, the amount of 200 µL of total lipid extract and 1.6 mL of 0.25 mol/L sodium methoxide in methanol was heated on a water bath for 10 min at 65 °C. After the reaction, 1 mL of water saturated with sodium chloride and 1 mL of hexane were added, and the mixture was centrifuged at 2,500 rpm for 3 min at ambient temperature. The hexane (upper) layer containing FAMEs was taken and used for GC/FID analyses.

HILIC-HPLC/ESI–MS of Individual Porcine Organs

Total lipid extracts of porcine organs were analyzed using a Spherisorb Si column (250 × 4.6 mm, 5 µm; Waters, Milford, MA, USA), a flow rate of 1 mL/min, an injection volume of 10 µL, column temperature of 40 °C and a mobile phase gradient: 0 min—94 % A + 6 % B, 60 min—77 % A + 23 % B, where A is acetonitrile and B is 5 mM aqueous ammonium acetate [18]. All HPLC/MS experiments were performed on the liquid chromatograph Agilent 1200 series (Agilent Technologies, Waldbronn, Germany) coupled to the Esquire 3000 ion trap analyzer with ESI (Bruker Daltonics, Bremen, Germany). Individual lipid classes were identified and quantified using the total ion current in positive-ion and negative-ion modes in the mass range *m/z* 50–1,000 with the following setting of tuning parameters: pressure of the nebulizing gas 60 psi, drying gas flow rate 10 L/min, and temperature of the drying gas 365 °C. Low-energy collision-induced

dissociation tandem mass spectrometry (MS/MS) experiments were performed during HPLC/MS runs with the automatic precursor selection, the isolation width of $\Delta m/z$ 4, the collision amplitude of 1 V, and helium as a collision gas. Data were acquired and evaluated using the Data Analysis software (Bruker Daltonics).

Off-Line 2D-HPLC/MS of Porcine Brain

Individual lipid classes from porcine brain were manually collected during the HILIC-HPLC analysis, fractions were evaporated by a gentle stream of nitrogen and redissolved in acetonitrile–2-propanol (1:1, v/v) mixture. The volume for the redissolvation was selected according to the concentration of individual fractions. In the second dimension, fractions of polar lipid classes were analyzed using RP-HPLC/MS with core–shell particles column Kinetex C_{18} (150 × 2.1 mm, 2.6 μm; Phenomenex, Torrance, CA, USA), flow rate of 0.3 mL/min, injection volume of 1 μL, separation temperature of 40 °C, and mobile phase gradient: 0 min—75 % A + 25 % B, 110 min—89 % A + 11 % B, where A is the mixture of acetonitrile–2-propanol (1:1, v/v) and B is 5 mM aqueous ammonium acetate. Polar lipids were identified using ESI–MS in the mass range *m/z* 50–1,500 with the following setting of tuning parameters: pressure of the nebulizing gas of 40 psi, drying gas flow rate of 9 L/min, and temperature of the drying gas 365 °C. The identification of individual lipids is done by their ESI mass spectra and the knowledge of their retention behavior in HILIC and RP modes [18, 37].

GC/FID Analyses of FAMEs

The gas chromatograph with flame ionization detection Agilent 7890 (Agilent Technologies) using TR-FAME column (70 % cyanopropyl polysilphenylene-siloxane), 60 m length, 0.25 mm ID, 0.25 μm film thickness (Thermo Scientific, Waltham, MA, USA), was used for the fatty acid profiling based on measurements of their corresponding FAMEs. GC conditions were as follows: injection volume 1 μL, split ratio 1:15, flow rate of helium as a carrier gas 1.025 mL/min, and temperature program: initial temperature 160 °C, ramp to 210 °C at 2 °C/min, and then ramp to 235 °C at 22 °C/min. Injector and detector temperatures were 250 and 280 °C, respectively.

Results and Discussion

Our nontargeted quantitation approach [37] is based on the measurement of response factors for individual lipid classes using representatives of all determined classes (i.e., lipid species containing oleic acids). This way, relative differences (i.e., response factors) for individual lipid classes are determined. The determination of basic analytical parameters of developed method has to been done before measurements of real samples, such as limit-of-quantitation (LOQ) determined at signal-to-noise ratio of 10 (10–100 nmol/g for all classes except for PI and LPE; Table S-1) and standard deviations determined from 10 replicates (below 5.5 % in all cases; Table S-1). Another issue for the reliable lipidomic quantitation is the knowledge of effects of fatty acyl chain length and the number of double bonds on the ionization efficiency, which is determined for both polarity modes (positive and negative) and both chromatographic systems (HILIC and RP) under identical conditions as used for the analysis of real samples (Table S-2). Measurements of 5 PC standards (16:0/16:0, 18:1/18:1, 18:0/18:0, 20:4/20:4, and 22:6/22:6) and 3 PE (14:0/14:0, 17:0/17:0, and 18:1/18:1) show that the relative differences in responses (related to 18:1 containing species set as 100 % response) are in the range 70–110 % for RP in both polarity modes and 77–130 % for HILIC in both polarity modes. It should be mentioned that the negative-ion mode is not convenient for the detection of choline-containing PLs due to the low sensitivity, but relative responses still fit into the above-mentioned intervals.

The rather important issue of our nontargeted quantitation of lipid classes is the verification that ratios of extraction yields among lipid classes for different samples are comparable. In addition to the determination of extraction yields reported in our previous work [37], we have performed the following spiking experiment for one lipid species per class not occurring in studied samples (Fig. S-1). The mixture of representative standards of selected lipid classes (PG, PE, LPE, PC, and LPC) containing C14:0 fatty acids (concentration 88 μg/mL of each standard) and sphingosyl PE (d17:1/12:0) as the IS (concentration 222 μg/mL) was prepared and measured by HILIC-HPLC/ESI–MS in the identical way to all other samples (annotation in Fig. S-1 as standards without extraction). Then, the same experiment was repeated, but including the extraction step as for real samples (standards after extraction in Fig. S-1). Relative extraction yields [i.e., ratios of extraction yields of representative standards of selected lipid classes containing C14:0 related to the extraction yield of sphingosyl PE (d17:1/12:0) as the IS] are in the range 90–92 %. The last step was the extraction of selected biological tissues (heart, lung, spleen, and stomach) and also body fluids (plasma and urine) spiked with C14:0 standards followed again by HILIC-HPLC/ESI–MS measurements. Relative extraction yields are between 70 and 96 % (related to standards without extraction) for all standards in Fig. S-1, which is considered as acceptable for such heterogeneous biological materials. The comparison of results obtained by this

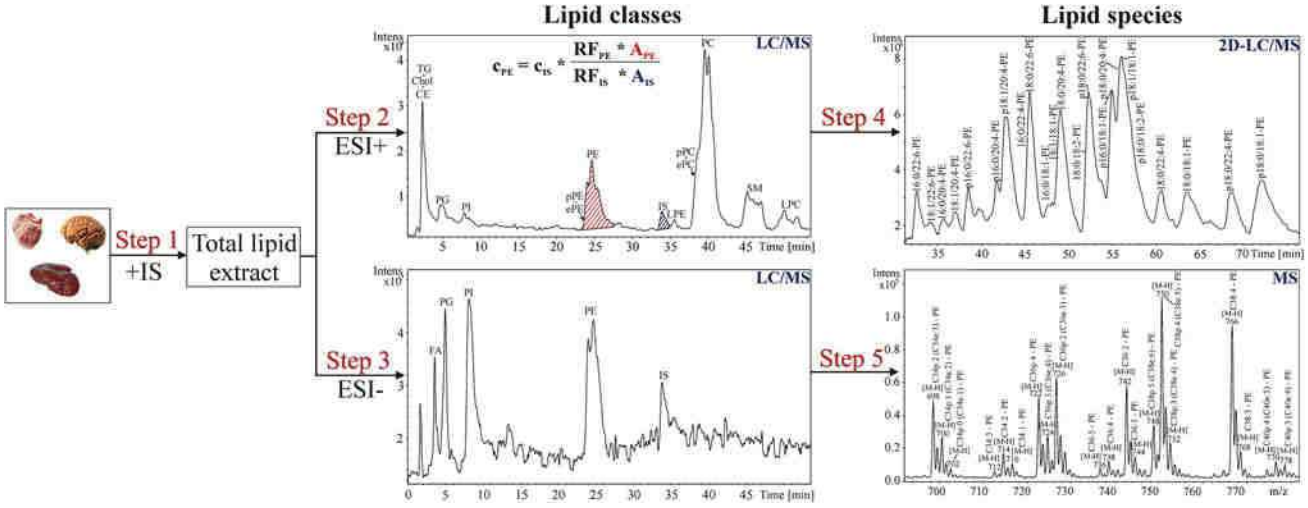

Fig. 1 Schematic overview of our nontargeted lipidomic approach: step 1: extraction with the addition of internal standard; step 2: HILIC-HPLC/MS in the positive-ion ESI; step 3/: HILIC-HPLC/MS in the negative-ion ESI; step 4: off-line 2D-HPLC/MS characterization of individual species inside lipid classes; step 5: negative-ion ESI mass spectrum of separated lipid class in HILIC-HPLC (details in "Materials and Methods")

approach and established quantitation method (SRM on triple quadrupole and ^{31}P NMR) were presented in our previous paper [37].

Lipid Classes Characterization of Porcine Organs Using HILIC-HPLC/ESI–MS

Figure 1 shows an overview of our approach used for the complex lipidomic characterization of eight porcine organs: brain, heart, kidney, liver, lung, spinal cord, spleen, and stomach (all HILIC chromatograms in Figs. S-2 and S-3). This approach is based on our HILIC-HPLC/ESI–MS method published recently [37] for the characterization of three nonpolar lipid classes (triacylglycerols, cholesterol, and cholesteryl esters) and 15 polar lipid classes, from which 10 lipid classes belong to the group of phospholipids such as phosphatidylglycerols (PG), phosphatidylinositols (PI), plasmenylphosphatidylethanolamines (pPE), plasmanylphosphatidylethanolamines (ePE), phosphatidylethanolamines (PE), lysophosphatidylethanolamines (LPE), phosphatidylserines (PS), plasmenylphosphatidylcholines (pPC), plasmanylphosphatidylcholines (ePC), and lysophosphatidylcholines (LPC), and 5 to the group of sphingolipids such as ceramides (Cer), sulfatides, hexosylceramides (HexCer), sphingosylphosphatidylethanolamine (IS), and sphingomyelins (SM). The nontargeted quantitation of lipid classes [37] is based on the peak integration of individual lipid classes separated in the HILIC mode multiplied by their response factors (RF) and correlated by a single IS (sphingosyl PE, d17:1/12:0). However, the HILIC-HPLC method does not enable the separation of non-polar lipids (TG, Chol, and CE), which coelute in one chromatographic peak close to the void volume of the system, and therefore their quantitation would not be reliable using this chromatographic system. Furthermore, the quantitation of Cer, HexCer, and sulfatides cannot be performed due to wide and only partially resolved peaks occurring in HILIC-HPLC. In the case of PS, the obtained data are semi-quantitative (labeled in Table 1) due to the peak tailing, which causes problems with the peak integration. Reliable quantitative data are obtained for PE, LPE, PC, SM, and LPC [33]. Table 1 shows the comparison of our quantitative data of porcine brain and previously reported data [30, 39, 40] for human or rat brain. Concentrations (in μmol/g) or relative abundances (in %) are similar despite different analytical methods and different types of brain samples (Table 2; Fig. 2). Relative abundances of individual lipid classes in all porcine organs are reported in Fig. 2, where the relative abundance of PC is in the range 32–40 %, PE 26–35 %, SM 5–19 %, PI up to 20 %, PS up to 12 %, LPE up to 8 %, LPC up to 7 %, and PG up to 5 %. Only spleen contains all quantified lipid classes (i.e., PC, PE, PI, SM, PS, LPE, LPC, and PG). In contrast to spleen, the lung and spinal cord are composed from the smallest number of lipid classes (i.e., PC, PE, PI, SM, and PG or PS). The comparison of lipid class concentrations in individual porcine organs (Table 2; Fig. S-4) confirms that PC and PE are the most abundant polar lipids in porcine organs. The highest concentrations of PC and PE are observed in the brain and the lowest in the lung and stomach. The HILIC-HPLC/ESI–MS method enables the determination of total concentrations of lipid classes, but the next step is the determination of concentrations of individual lipid species inside these classes. For this reason, the detailed characterization of

Table 1 Comparison of concentrations (μmol/g) or relative abundances (%) of individual lipid classes in the brain (porcine, human or rat) obtained by our HILIC-HPLC/ESI–MS method and previously published TLC [40], ^{31}P NMR [30], and HPLC/ELSD [39] data

Lipid class	HILIC-HPLC/ESI–MS		TLC [40]	^{31}P NMR [30]		HPLC/ELSD [39]
	Porcine		Human	Human	Rat	Rat
	Concentration (μmol/g)	Relative abundance (%)	Concentration (μmol/g)	Relative abundance (%)		Relative abundance (%)
PI	4.5	5.0	3.7	5.3	3.3	5.3
PE	30.7	34.3	29.0	37.6	37.6	37.6
LPE	2.0	2.3			1.4	
PS	10.6[a]	13.1[a]	9.0	12.5	12.7	15.6
PC	33.2	37.1	22.1	37.6	36.9	37.6
SM	6.5	7.3		1.9	4.8	1.9
LPC	0.8	0.9			1.5	
Others				0.7	0.95	2

[a] Only semi-quantitative data are determined for PS due to the peak tailing

Table 2 Concentrations (μmol/g) of individual lipid classes in porcine organs using the nontargeted quantitation with the single internal standard and response factor approach

Lipid classes	Concentration (μmol/g)							
	Brain	Heart	Kidney	Liver	Lung	Spinal cord	Spleen	Stomach
PG		1.71 ± 0.11	0.88 ± 0.05	0.67 ± 0.01	0.65 ± 0.04		0.27 ± 0.03	0.82 ± 0.01
PI	4.52 ± 0.10	4.99 ± 0.17	12.27 ± 0.63	7.79 ± 0.42	3.58 ± 0.11	5.29 ± 0.12	9.70 ± 0.17	5.02 ± 0.22
PE	30.67 ± 1.04	11.51 ± 0.48	16.22 ± 0.54	14.67 ± 1.26	8.32 ± 0.14	17.49 ± 0.20	16.27 ± 0.59	9.45 ± 0.35
LPE	2.04 ± 0.07[a]	1.60 ± 0.13		3.89 ± 0.17			0.97 ± 0.03[a]	1.48 ± 0.10[a]
PS	10.63 ± 0.83					1.35 ± 0.22	3.03 ± 0.29	
PC	33.21 ± 0.20	13.73 ± 0.87	23.99 ± 0.58	21.06 ± 0.68	11.24 ± 0.19	17.10 ± 0.65	22.51 ± 0.67	11.02 ± 0.22
SM	6.50 ± 0.23	1.87 ± 0.13	7.36 ± 0.29	2.64 ± 0.08	4.12 ± 0.14	9.66 ± 0.22	8.71 ± 0.20	4.38 ± 0.08
LPC	0.84 ± 0.01	1.62 ± 0.02	0.59 ± 0.02	1.78 ± 0.15			0.81 ± 0.04	2.50 ± 0.09

[a] Only semi-quantitation due to the bad peak shapes

selected lipid classes was carried out using two different approaches as described in the next two sections.

Analysis of Individual Lipid Species Using $[M-H]^-$ Ions in Negative-Ion ESI Mass Spectra

This approach enables the characterization of individual lipid species inside lipid classes based on relative abundances of deprotonated molecules $[M-H]^-$ in the negative-ion HILIC-HPLC/ESI–MS (i.e., PE, PI, PG, LPE, HexCer, and sulfatides). This approach cannot be applied for the positive-ion mode due to the presence of both protonated molecules $[M+H]^+$ and sodium adducts $[M+Na]^+$ ions, because $[M+Na]^+$ ions have identical nominal masses as $[M+H]^+$ ions of lipids having more than two methylene units and three double bonds (DB). The resolving power (RP) required for the differentiation of these species is over 300,000 [calculated from *m/z* 800: RP = 800/(21.98435 – 21.98195) = 333 × 10^3]. Such RP is achievable only on the ion cyclotron resonance mass spectrometer, therefore we have decided on the quantitation of PE, PI, and HexCer species in the negative-ion mode. For PE species, the type of fatty acyl linkage to the glycerol skeleton was also taken into account, i.e., the most commonly known ester-linked fatty acyls at both *sn*-1 and *sn*-2 positions (diacyl) are referred to as PE, ether-linked fatty acyls at the *sn*-1 position (1-alkyl-2-acyl) as ethers (ePE), and vinyl ether-linked fatty acyls at the *sn*-1 (1-alkenyl-2-acyl) as plasmalogens (pPE). Plasmalogens and ethers having identical retention times in the HILIC mode and identical $[M-H]^-$ ions (e.g., plasmalogen C38:4 has the same nominal mass *m/z* = 751 as ether C38:5) cannot be distinguished using this approach. Nevertheless, ether lipids are present in animal tissues as the minority, and therefore they are reported in parentheses (Fig. 3, and the text). The comparison of relative abundances of individual lipid species of PE and pPE (ePE) in all analyzed porcine organs is shown in Fig. 3a and b, respectively.

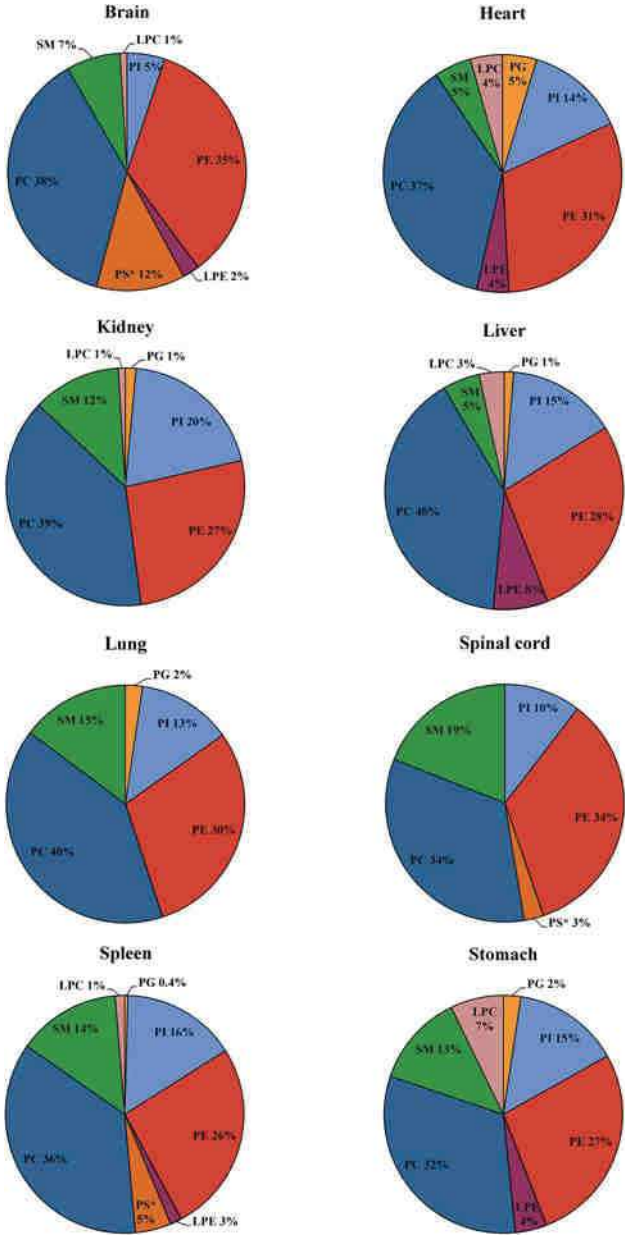

Fig. 2 Relative abundances (%) of monitored lipid classes in porcine organs using the nontargeted quantitation with the single internal standard and response factor approach (color figure online)

Concentrations of individual PE and pPE (ePE) species (Tables S-3, S-4) are calculated from the relative abundances of $[M-H]^-$ ions in ESI spectra multiplied by the total concentration of the whole lipid class obtained by nontargeted lipidomic quantitation (Table 2). Fatty acyls are annotated by their CN:DB (carbon number:double bond number). PE (Fig. 3a) containing saturated and monounsaturated fatty acyls with 16 and 18 carbon atoms prevail. The highest relative abundance of PE corresponds to species containing 38 carbon atoms and four DBs (typically C18:0 and C20:4 acyls). Polyunsaturated PE are present mainly in brain (typical composition C40:6, C40:5, and C40:4) and their lowest relative abundances are observed in heart. Lung, spinal cord, and spleen contain the long-chain (more than 20 carbon atoms) monounsaturated or saturated fatty acyls (C40:1 and C40:2 species), which are typical for sphingolipids, but they also occur in small amounts in phospholipids. There are two cases in which it is not possible to exclude the presence of pPE species in PE (mixtures of C36:0 with C38p:6 and C38:0 with C40p:6) due to identical *m/z* values observed in ESI spectra. Average parameters of aCN and aDB are calculated in the figure legend. Values of aCN are around 37 carbon atoms, but aDB varies from 2 for spinal cord to 3.3 for heart. Average parameters are useful for the simple overall characterization of particular sample types, as demonstrated earlier for TGs [43].

The representation of pPE (ePE) in various organs shows some interesting features (Fig. 3b). The highest relative abundance of pPE (ePE) is observed in kidney for C36:4 (typically C16:0 and C20:4). The most abundant pPE (ePE) species contains fatty acyls with four and more DBs, which shows that plasmalogens may serve as a source of polyunsaturated fatty acids [4]. Values of aCN in pPE (ePE) species are from 36.7 (heart and kidney) to 38.0 (liver). aDB of individual porcine organs varies from 3.3 (lung) to 4.2 (liver), except for spinal cord (2.8) with higher abundances of pPE (ePE) species containing fatty acyls with 0–3 DBs. In contrast to PE, long-chain saturated and monounsaturated fatty acyls in individual pPE (ePE) occur in spleen and stomach.

In general, plasmalogens can form up to 70 % of PE in animal tissues, where they have many important functions [5, 6]. Therefore, we compare the relative abundance of PE and pPE (ePE) in porcine organs (Fig. 4; Tables S-3, S-4). The lowest amount of pPE (ePE) is found in liver, which could be related to the biosynthesis of fatty acids in liver [5]. On the other hand, nervous tissues (brain and spinal cord) contain the highest amounts of pPE (ePE). The high relative proportion of pPE (ePE) is also observed in porcine heart and stomach. In these organs, plasmalogens have functions of antioxidants, signaling molecules, and modulators of membrane dynamics [5, 6]. Furthermore, individual lipid species of PI (Fig. S-5; Table S-5) were determined, where the highest relative abundance in all porcine organs corresponds to C18:0 and C20:4 fatty acyls (identical as for PE) with the highest abundance in spleen. High proportions of C34:0 and C34:1 PI species are determined in kidney unlike to other organs. Values of aCN are around 37, and aDB are from 2.4 (kidney) to 3.4 (spleen).

This approach was also used for the characterization of relative abundances of individual sphingolipids (i.e., HexCer) containing nonhydroxy-fatty acyls or hydroxy-fatty

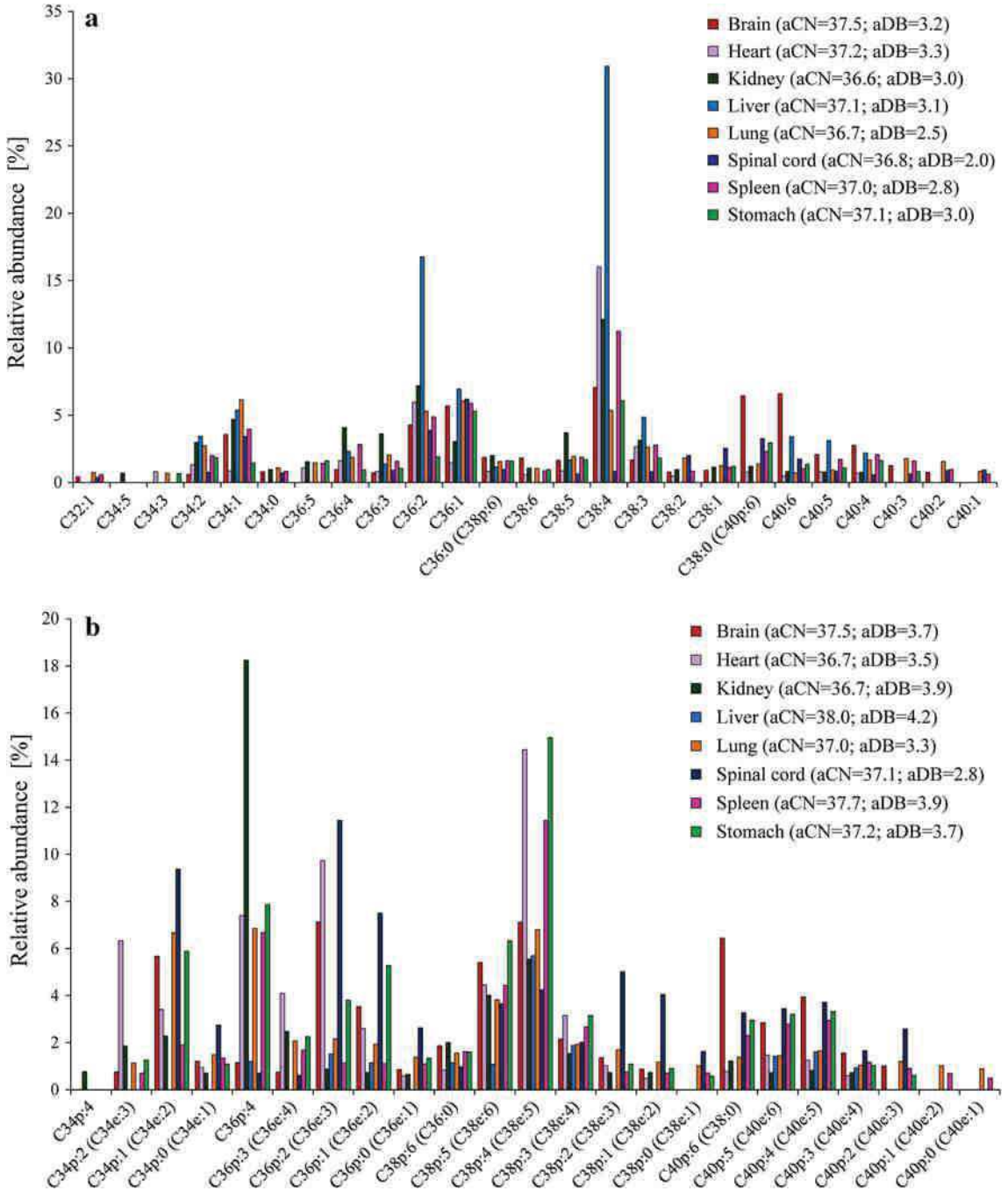

Fig. 3 Relative abundances (%) of individual species of (**a**) PE (1,2–diacyl) and (**b**) pPE (1-alkenyl-2-acyl) and ePE (1-alkyl-2-acyl) determined using relative abundances of $[M-H]^-$ ions in the negative-ion HILIC-HPLC/ESI–MS and calculated average carbon numbers (aCN) and average double bonds (aDB) numbers in porcine organs

acyls in porcine brain, kidney, spleen, spinal cord, and stomach (Fig. 5). HexCer are the most abundant in nervous tissues (brain and spinal cord), where they form important components of neurons [2]. Moreover, they are heavily represented in spleen due to various functions in the immune system [2]. Each organ has different HexCer with the highest relative abundance, i.e., C42:1-OH (C43:0) and C42:2-OH (C43:2) in brain and spinal cord, and C36:2-OH (C37:1) and C36:0-OH in stomach. Kidney and spleen contain the most abundant nonhydroxy-fatty acyls, such as C40:1 (C39:2-OH) and C40:0 (C39:1-OH) in kidney and C41:2 (C40:3-OH) and C39:2 (C38:3-OH) in spleen. As for plasmalogens and ethers, lipid species having identical values of $[M-H]^-$ ions for fatty acyls containing non-hydroxy- and hydroxy-forms (e.g., HexCer containing C42:2-OH has the same nominal value of $m/z = 825$ as

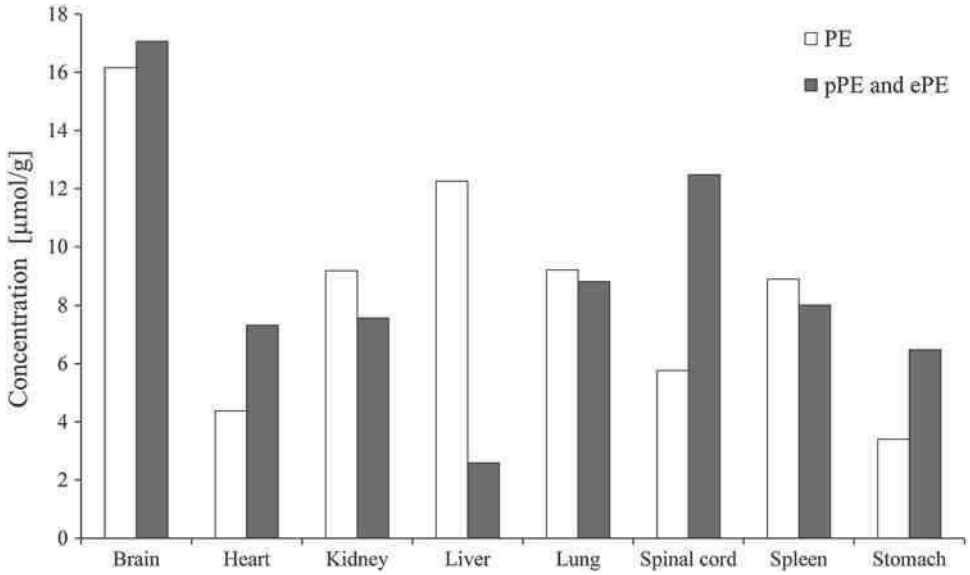

Fig. 4 Comparison of total concentrations of PE (individual species shown in Fig. 3a) and the sum of pPE and ePE species (individual species shown in Fig. 3b) in porcine organs

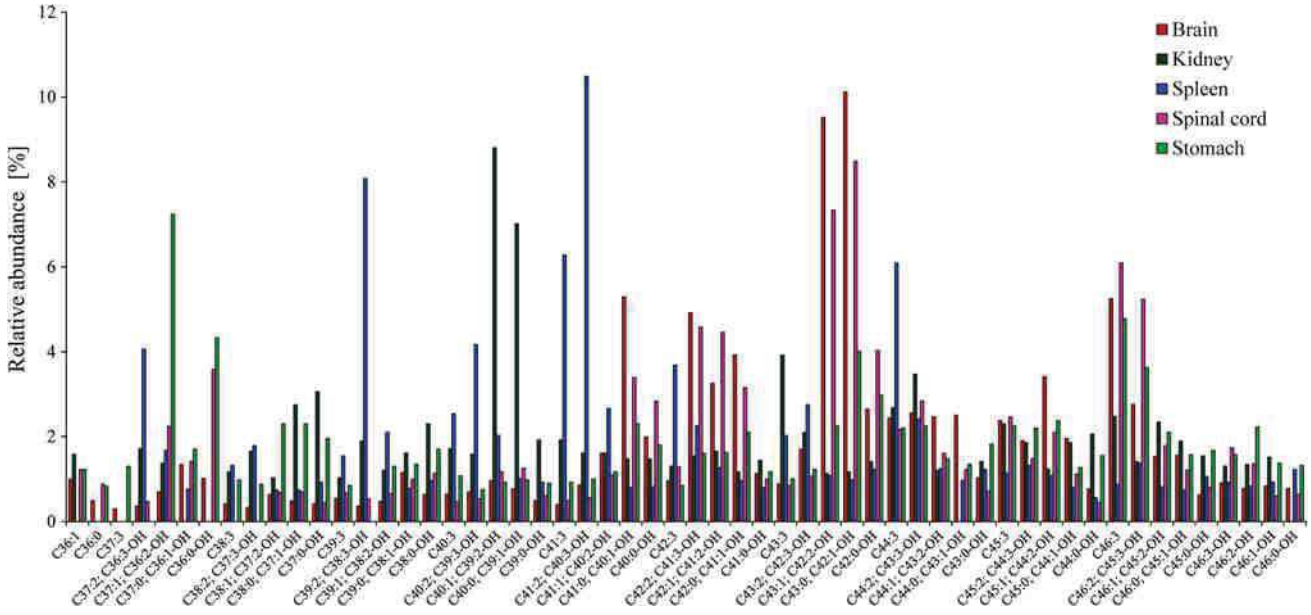

Fig. 5 Relative abundances (%) of individual HexCer containing nonhydroxy- or hydroxy-fatty acyls in brain, kidney, spleen, spinal cord, and stomach determined using relative abundances of $[M-H]^-$ ions in the negative-ion HILIC-HPLC/ESI–MS

HexCer containing C43:2) cannot be distinguished using this approach. Fatty acyls in parentheses are less probable due to the odd carbon number or higher number of DBs, because saturated and monounsaturated fatty acyls are typical for glycosphingolipids.

Off-Line 2D-HPLC/MS Detailed Analysis of Individual Lipid Species in Porcine Brain

The limitation of the first approach is that the only information on the total number of carbon atoms and DBs is obtained without the knowledge of the attached fatty acyls and their positions on the glycerol skeleton. For this reason, off-line two-dimensional HILIC × RP-HPLC/ESI–MS has been used for the detailed analysis of porcine brain. Individual fractions of lipid classes separated by HILIC-HPLC are isolated and used in the second dimension for the separation of individual lipid species inside lipid classes according to the fatty acyl chain lengths and the number of DBs using RP-HPLC. Almost 70 phospholipid (Table S-6) and 100 sphingolipid species are identified in the porcine brain. Namely, 11 PI (Fig. S-6A), 12 PE and 10 pPE published in [18], 7 LPE and 3 pLPE, 17 species of PC, 2 pPC and 2 ePC (Fig. 6a), and 5 LPC, and 42 are HexCer

and 2 Cer (Fig. 6b), 38 sulfatides (Fig. S-6B), and 12 SM. Phospholipids (PC, PE, and PI) are formed by the combination of 14 fatty acyls containing 16–22 carbon atoms and 0–6 DBs, where the most abundant fatty acyls are C16:0, C18:0, C18:1, and C20:4, whereas sphingolipids (HexCer, Cer, sulfatides, and SM) consist of 15 fatty acyls (nonhydroxy and hydroxy) containing 16–26 carbon atoms and 0–2 DBs. Fatty acyl positions on the glycerol skeleton are determined according to relative abundances of fatty acyls fragment ions $[RCOO]^-$ in the negative-ion ESI spectra. Higher relative abundances of $[RCOO]^-$ ions are typically related to the fragmentation from the *sn*-2 position compared to the *sn*-1 position for studied phospholipids (Fig. 7), but relative abundances of these fragment ions are also strongly affected by their unsaturation degree. Exceptions are observed in the case of some phospholipids containing combinations of C18:0 and C22:6, in which ratios of $[RCOO]^-$ ions are affected by the presence of $[RCOO]^-$ ion of polyunsaturated FA [44]. The second diagnostic ions for the determination of *sn*-2 are the neutral losses of ketene $[M\text{-}H\text{-}RCHCO]^-$ (Fig. 7) or fatty acid $[M\text{-}H\text{-}RCOOH]^-$. Neutral losses from the *sn*-2 position resulting in the formation of $[M\text{-}H\text{-}RCHCO]^-$ ions are always preferred without exception for PC, pPC, ePC, PE, pPE, ePE, PI, HexCer, and sulfatides studied in this work. It has been reported in the literature that the reversed ratio of above mentioned fragment ions has been observed for some lipid classes, such as PS and PA [44].

We observed a strong preference of polyunsaturated fatty acyls in the *sn*-2 position (Fig. 7a). The preference of *sn*-positions for two saturated fatty acyls (18:0/16:0-PC) is related to the acyl chain length, because fatty acyls containing more carbon atoms (C18:0) are favored in the *sn*-1 position unlike fatty acyls containing fewer carbon atoms (C16:0) in thes *sn*-2 position (Fig. 7b). HexCer (Fig. 6b) and sulfatides (Fig. S-6B) are separated in RP-HPLC according to nonhydroxy- or hydroxy-form of their fatty acyls, lengths, and the number of DBs. Nonhydroxy-forms

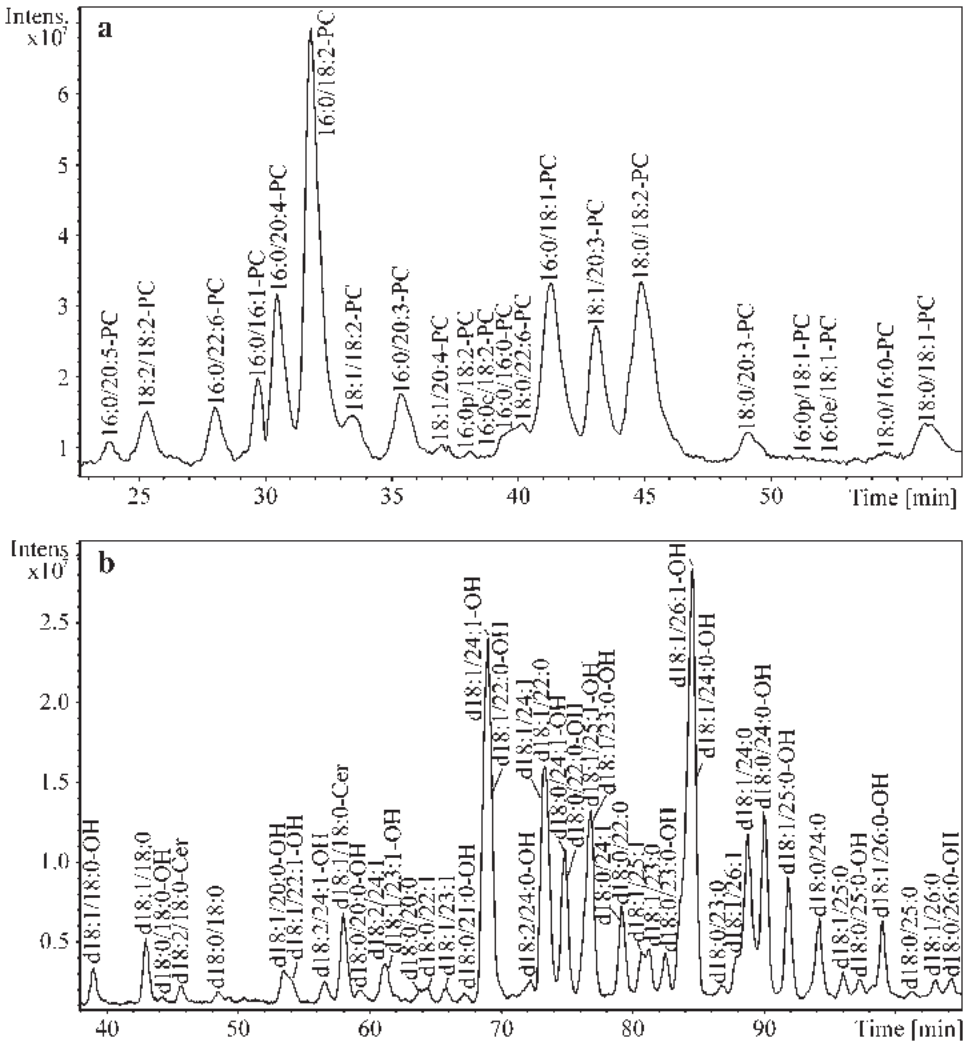

Fig. 6 Off-line 2D-HPLC/ESI–MS analysis of (**a**) PC and (**b**) HexCer and Cer fractions from the porcine brain. RP-HPLC conditions: flow rate 0.3 mL/min, separation temperature 40 °C, gradient 0 min—75 % A + 25 % B, 110 min—89 % A + 11 % B, where A is the mixture of acetonitrile–2-propanol (1:1, v/v) and B is 5 mM aqueous ammonium acetate

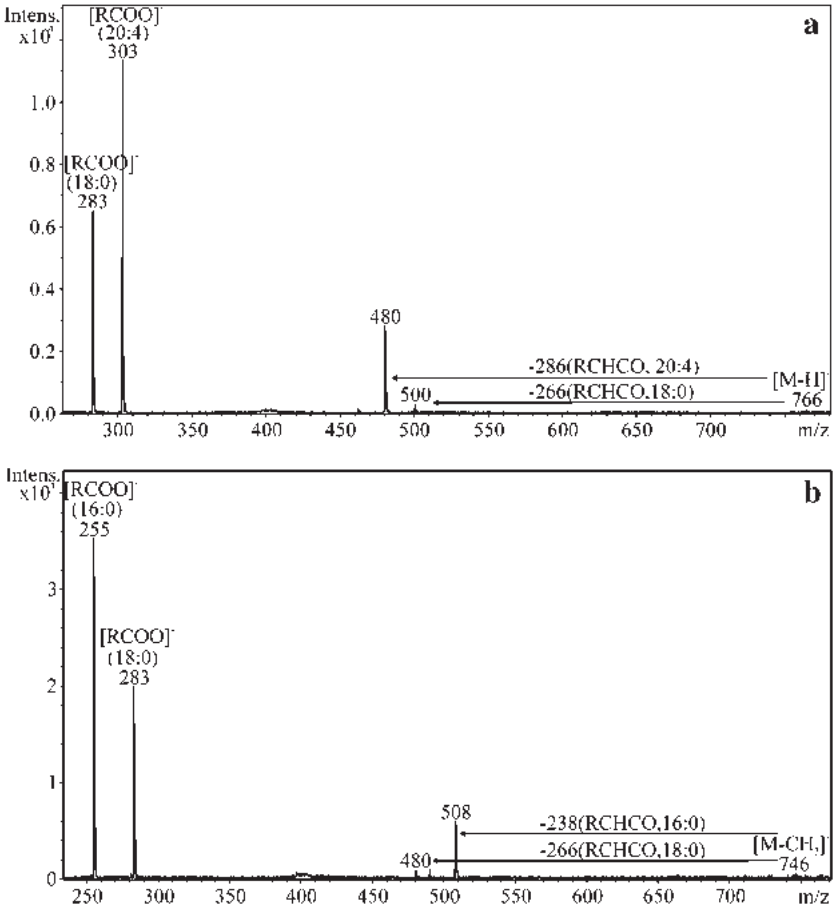

Fig. 7 Negative-ion ESI–MS/MS spectra of (**a**) *m/z* 766 for $[M-H]^-$ ion of 1-stearoyl-2-arachidonoyl-*sn*-glycero-3-phosphoethanolamine (16:0/20:4-PE), and (**b**) *m/z* 746 for $[M-CH_3]^-$ ion of 1-stearoyl-2-palmitoyl-*sn*-glycero-3-phosphocholine (18:0/16:0-PC)

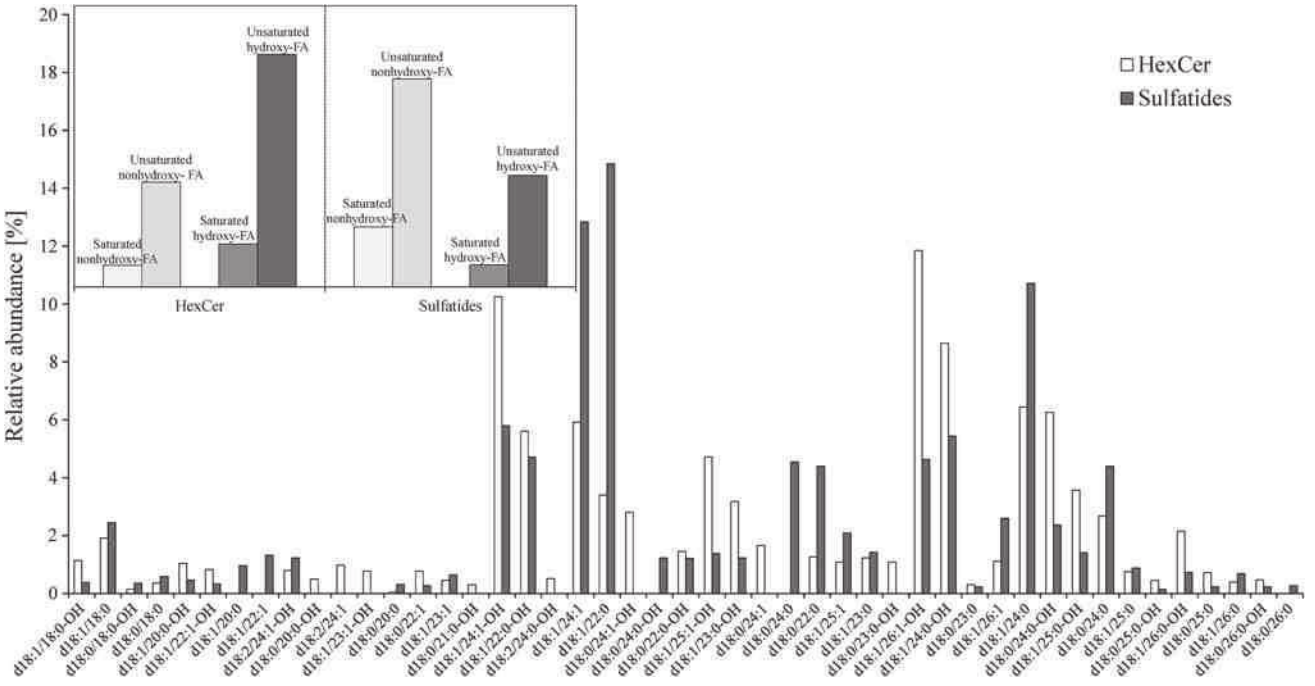

Fig. 8 Comparison of relative abundances of fatty acyl combinations in hexosylceramides (HexCer) and sulfatides in the porcine brain, and the distribution of saturated and unsaturated nonhydroxy- and hydroxy-fatty acyls in HexCer and sulfatides (inset)

Table 3 Relative molar concentrations (%) of fatty acids identified in porcine organs using GC/FID, retention times (t_R) of their FAMEs, response factors (RF), average carbon number (aCN) and average double bond (aDB) numbers

t_R [min]	Fatty acid	RF	Brain	Heart	Kidney	Liver	Lung	Spinal cord	Spleen	Stomach
8.7	C14:0	1.03	0.5	1.3	0.4		1.5	0.4	0.5	1.1
9.9	C15:0	1.04	0.1		0.2		0.3	0.1	0.5	0.3
11.4	C16:0	1.00	24.2	27.0	23.6	13.6	27.4	16.1	31.6	24.8
12.3	Δ*9*-C16:1	1.04	0.8	1.3	0.3	1.5	2.1	0.7	0.5	1.5
13.2	C17:0	0.99	0.3	0.5	1.0	0.3	0.6	0.4	1.2	1.5
15.2	C18:0	0.98	21.0	18.5	16.9	31.3	12.8	16.8	17.5	17.0
16.1	Δ*9*-C18:1	0.99	21.1	25.7	13.7	16.1	39.9	39.2	11.1	41.1
16.3	Δ*11*-C18:1	1.01	5.6	3.0	3.4	1.4	3.5	7.7	2.6	3.0
17.6	Δ*9,12*-C18:2	1.00	0.4	13.8	12.8	13.2	4.5	0.5	5.6	3.7
19.5	Δ*9,12,15*-C18:3	0.99		0.3	0.2		0.1		0.1	0.2
19.6	C20:0	0.98	0.1	0.2	0.2			0.6	0.1	0.2
20.6	Δ*11*-C20:1	0.99	0.7	0.5	0.4		0.9	6.2	0.4	1.0
21.8	C20:2	1.00[a]	0.3					0.5		
22.3	Δ*11,14*-C20:2	0.99	0.1	0.3	0.6		0.4	0.2	0.5	0.3
22.6	C20:3	1.00[a]	0.7		0.2	0.7		0.3	0.2	0.1
23.5	Δ*8,11,14*-C20:3	0.99	0.4	0.3	1.8	0.8	0.3	0.5	1.1	0.2
24.2	Δ*5,8,11,14*-C20:4	0.97	8.6	4.8	19.7	13.0	3.3	3.5	19.2	2.4
25.5	Δ*13*-C22:1	0.97	0.2		0.1			1.2	0.1	
26.2	Δ*5,8,11,14,17*-C20:5	1.00	0.2	0.3	1.5	1.7	0.2	0.1	0.5	0.1
26.3	C23:0	0.96	0.2					0.2		
26.9	C24:0[b]	1.00[a]	0.6					0.4	0.1	
28.0	Δ*7,10,13,16*-C22:4	0.97	3.5	0.6	0.6	1.0	0.9	2.1	2.8	0.6
28.5	Δ*4,7,10,13,16*-C22:5	0.96	1.0		0.1			0.1	0.2	
29.5	Δ*7,10,13,16,19*-C22:5	0.98	0.4	0.3	0.6	1.4	0.3	0.2	2.3	0.3
29.9	Δ*4,7,10,13,16,19*-C22:6	1.03	8.6		1.3	0.9	0.2	1.9	1.3	0.2
31.4	C26:0[b]	1.00[a]	0.2					0.1		
32.0	C27:0[b]	1.00[a]	0.3	1.3	0.4	3.0	1.0	0.2		0.3
*a*CN			18.5	17.8	18.2	18.6	17.7	18.3	18.2	17.6
*a*DB			1.5	0.9	1.6	1.3	0.8	1.0	1.5	0.7

[a] Not measured due to the lack of standard

[b] Branched fatty acids

of fatty acyls have higher retention times then their hydroxy-forms, as illustrated in examples for HexCer (Δt_R = 4–4.5 min) and sulfatides (2.5–3 min). The comparison of relative abundance of individual lipid species in HexCer and sulfatides is shown in Fig. 8. Major sphingolipids are composed of ceramide possessing 4-sphingenine (d18:1; prefix "d" designates a dihydroxy sphingoid base) with the hydroxy-form of C26:1, C24:1, and C24:0 acyls for HexCer and the nonhydroxy-form of C22:0, C24:1, and C24:0 acyls for sulfatides. The representation of nonhydroxy- and hydroxy-forms of fatty acyls in HexCer is in the ratio 30/70, which is exactly the opposite for sulfatides with the ratio 70/30 (Fig. 8 inset). HexCer are composed of 22 % saturated and 78 % unsaturated fatty acyls, while sulfatides have 43 % saturated and 57 % unsaturated fatty acyls.

Fatty Acid Profiling Using GC/FID

The fatty acid composition of porcine organs is characterized by the GC/FID analysis of FAMEs after the transesterification of total lipid extracts with sodium methoxide (Table 3). The previously optimized GC/FID method [9] enables the separation of FAMEs according to the acyl chain length and the number of DBs (Fig. S-7). Fatty acid profiles of analyzed porcine organs are obtained from peak areas of FAMEs in GC/FID chromatograms multiplied by the RFs of identical standards related to C16:0, and a total of 23 different fatty acids containing 14–26 carbon atoms and 0–6 DBs were determined. The most abundant fatty acid is C16:0 in brain, kidney, and spleen, Δ*9*-C18:1 in heart, lung, spinal cord, and stomach,

and C18:0 in liver. Large differences in the relative abundance of fatty acids are observed for arachidonic acid (C20:4), which is a key inflammatory intermediate [4]. Arachidonic acid forms approximately 20 % of identified fatty acids in porcine kidney and spleen, 14 % in liver, 9 % in brain, and 5 % or less in heart, lung, spinal cord, and stomach. The highest proportion of polyunsaturated fatty acids is determined in brain, while the lowest abundance is observed in heart. Average parameters are also calculated for fatty acid profiles of analyzed organs similar to the HPLC/MS determination of aCN and aDB in individual lipid classes. Values of aCN are around 18, but aDB varies from 0.7 for stomach to 1.6 for kidney.

Conclusions

The nontargeted HILIC-HPLC/ESI–MS method enables the characterization of individual lipid classes and their representation in vital porcine organs, such as brain, heart, kidney, liver, lung, spinal cord, spleen, and stomach. Concentrations of individual lipid classes in porcine organs were compared with previously published data. The determination of individual lipid species inside these classes was performed based on relative abundances of deprotonated molecules $[M-H]^-$ in the negative-ion ESI mode and off-line 2D-HPLC/MS. The first approach using $[M-H]^-$ ions provides important information on PE and their plasmalogens or ether analogs, PI, and HexCer in studied organs. Off-line 2D-HPLC/MS has been applied for the detailed analysis of porcine brain including the determination of attached fatty acyls and their positions on the glycerol ividual organs was performed using average parameters of CN and DB. The complementary information on fatty acid profiles was obtained by GC/FID. The comprehensive lipidomic analysis provides the detailed knowledge of the lipidome, which will be applied for future metabolic studies on human to investigate serious lipid-related human disorders.

Acknowledgments This work was supported by the Grant Project No. 203/09/0139 sponsored by the Czech Science Foundation. E.C. acknowledges the Grant CZ.1.07/2.3.00/30.0021 sponsored by the Ministry of Education, Youth and Sports of the Czech Republic.

References

1. Fahy E, Subramaniam S, Brown HA, Glass CK, Merrill AH, Murphy RC, Raetz CRH, Russell DW, Seyama Y, Shaw W, Shimizu T, Spener F, van Meer G, VanNieuwenhze MS, White SH, Witztum JL, Dennis EA (2005) A comprehensive classification system for lipids. J Lipid Res 46:839–861
2. Christie WW (2012) The lipid library. http://lipidlibrary.aocs.org/
3. Brown HA, Murphy RC (2009) Working towards an exegesis for lipids in biology. Nat Chem Biol 5:602–606
4. Calder PC (2006) n-3 polyunsaturated fatty acids, inflammation, and inflammatory diseases. Am J Clin Nutr 83:1505S–1519S
5. Braverman NE, Moser AB (2012) Functions of plasmalogen lipids in health and disease. Biochim Biophys Acta 1822:1442–1452
6. Nagan N, Zoeller RA (2001) Plasmalogens: biosynthesis and functions. Prog Lipid Res 40:199–229
7. Santos CR, Schulze A (2012) Lipid metabolism in cancer. FEBS J 279:2610–2623
8. Hamilton S, Hamilton RJ, Sewell PA (1992) Lipid analysis: practical approach. Oxford University Press, New York
9. Lísa M, Netušilová K, Franěk L, Dvořáková H, Vrkoslav V, Holčapek M (2011) Characterization of fatty acid and triacylglycerol composition in animal fats using silver-ion and non-aqueous reversed-phase high-performance liquid chromatography/mass spectrometry and gas chromatography/flame ionization detection. J Chromatogr A 1218:7499–7510
10. Cvačka J, Hovorka O, Jiroš P, Kindl J, Stránský K, Valterová I (2006) Analysis of triacylglycerols in fat body of bumblebees by chromatographic methods. J Chromatogr A 1101:226–237
11. Holčapek M, Lísa M, Jandera P, Kabátová N (2005) Quantitation of triacylglycerols in plant oils using HPLC with APCI-MS, evaporative light-scattering, and UV detection. J Sep Sci 28:1315–1333
12. Lísa M, Holčapek M (2008) Triacylglycerols profiling in plant oils important in food industry, dietetics and cosmetics using high-performance liquid chromatography-atmospheric pressure chemical ionization mass spectrometry. J Chromatogr A 1198:115–130
13. Ahn EJ, Kim H, Chung BC, Kong G, Moon MH (2008) Quantitative profiling of phosphatidylcholine and phosphatidylethanolamine in a steatosis/fibrosis model of rat liver by nanoflow liquid chromatography/tandem mass spectrometry. J Chromatogr A 1194:96–102
14. Axelsen PH, Murphy RC (2010) Quantitative analysis of phospholipids containing arachidonate and docosahexenoate chains in microdissected regions of mouse brain. J Lipid Res 51:660–671
15. Bang DY, Ahn EJ, Moon MH (2007) Shotgun analysis of phospholipids from mouse liver and brain by nanoflow liquid chromatography/tandem mass spectrometry. J Chromatogr B 852:268–277
16. Retra K, Bleijerveld OB, van Gesteil RA, Tielens AGM, van Hellemond JJ, Brouwers JF (2008) A simple and universal method for the separation and identification of phospholipid molecular species. Rapid Commun Mass Spectrom 22:1853–1862
17. Taguchi R, Ishikawa M (2010) Precise and global identification of phospholipid molecular species by an orbitrap mass spectrometer and automated search engine lipid search. J Chromatogr A 1217:4229–4239
18. Lísa M, Cífková E, Holčapek M (2011) Lipidomic profiling of biological tissues using off-line two-dimensional high-performance liquid chromatography mass spectrometry. J Chromatogr A 1218:5146–5156
19. Cvačka J, Svatoš A (2003) Matrix-assisted laser desorption/ionization analysis of lipids and high molecular weight hydrocarbons with lithium 2,5-dihydroxybenzoate matrix. Rapid Commun Mass Spectrom 17:2203–2207
20. Fuchs B, Schiller J (2009) Application of MALDI-TOF mass spectrometry in lipidomics. Eur J Lipid Sci Technol 111:83–98
21. Jackson SN, Wang HYJ, Woods AS (2005) In situ structural characterization of phosphatidylcholines in brain tissue using MALDI-MS/MS. J Am Soc Mass Spectrom 16:2052–2056
22. Dugo P, Kumm T, Crupi ML, Cotroneo A, Mondello L (2006) Comprehensive two-dimensional liquid chromatography

combined with mass spectrometric detection in the analyses of triacylglycerols in natural lipidic matrixes. J Chromatogr A 1112:269–275
23. Sandra K, Pereira AD, Vanhoenacker G, David F, Sandra P (2010) Comprehensive blood plasma lipidomics by liquid chromatography/quadrupole time-of-flight mass spectrometry. J Chromatogr A 1217:4087–4099
24. Byrdwell WC (2010) Dual parallel mass spectrometry for lipid and vitamin D analysis. J Chromatogr A 1217:3992–4003
25. Han XL, Yang K, Gross RW (2012) Multi-dimensional mass spectrometry-based shotgun lipidomics and novel strategies for lipidomic analyses. Mass Spectrom Rev 31:134–178
26. Yang K, Han X (2011) Accurate quantification of lipid species by electrospray ionization mass spectrometry—meets a key challenge in lipidomics. Metabolites 1:21–40
27. Yang K, Cheng H, Gross RW, Han XL (2009) Automated lipid identification and quantification by multidimensional mass spectrometry-based shotgun lipidomics. Anal Chem 81:4356–4368
28. Hu CX, van der Heijden R, Wang M, van der Greef J, Hankemeier T, Xua GW (2009) Analytical strategies in lipidomics and applications in disease biomarker discovery. J Chromatogr B 877:2836–2846
29. Culeddu N, Bosco M, Toffanin R, Pollesello P (1998) P-31 NMR analysis of phospholipids in crude extracts from different sources: improved efficiency of the solvent system. Magn Reson Chem 36:907–912
30. Pearce JM, Komoroski RA (2000) Analysis of phospholipid molecular species in brain by P-31 NMR spectroscopy. Magn Reson Med 44:215–223
31. Berdeaux O, Juaneda P, Martine L, Cabaret S, Bretillon L, Acar N (2010) Identification and quantification of phosphatidylcholines containing very-long-chain polyunsaturated fatty acid in bovine and human retina using liquid chromatography/tandem mass spectrometry. J Chromatogr A 1217:7738–7748
32. Hsu FF, Turk J (2001) Studies on phosphatidylglycerol with triple quadrupole tandem mass spectrometry with electrospray ionization: fragmentation processes and structural characterization. J Am Soc Mass Spectrom 12:1036–1043
33. Quehenberger O, Armando AM, Brown AH, Milne SB, Myers DS, Merrill AH, Bandyopadhyay S, Jones KN, Kelly S, Shaner RL, Sullards CM, Wang E, Murphy RC, Barkley RM, Leiker TJ, Raetz CRH, Guan ZQ, Laird GM, Six DA, Russell DW, McDonald JG, Subramaniam S, Fahy E, Dennis EA (2010) Lipidomics reveals a remarkable diversity of lipids in human plasma. J Lipid Res 51:3299–3305
34. Shaner RL, Allegood JC, Park H, Wang E, Kelly S, Haynes CA, Sullards MC, Merrill AH (2009) Quantitative analysis of sphingolipids for lipidomics using triple quadrupole and quadrupole linear ion trap mass spectrometers. J Lipid Res 50:1692–1707
35. Sommer U, Herscovitz H, Welty FK, Costello CE (2006) LC-MS-based method for the qualitative and quantitative analysis of complex lipid mixtures. J Lipid Res 47:804–814
36. Stahlman M, Ejsing CS, Tarasov K, Perman J, Boren J, Ekroos K (2009) High-throughput shotgun lipidomics by quadrupole time-of-flight mass spectrometry. J Chromatogr B 877:2664–2672
37. Cífková E, Holčapek M, Lísa M, Ovčačíková M, Lyčka A, Lynen F, Sandra P (2012) Nontargeted quantitation of lipid classes using hydrophilic interaction liquid chromatography–electrospray ionization mass spectrometry with single internal standard and response factor approach. Anal Chem 84:10064–10070
38. Dreissig I, Machill S, Salzer R, Krafft C (2009) Quantification of brain lipids by FTIR spectroscopy and partial least squares regression. Spectrochim Acta A 71:2069–2075
39. Homan R, Anderson MK (1998) Rapid separation and quantitation of combined neutral and polar lipid classes by high-performance liquid chromatography and evaporative light-scattering mass detection. J Chromatogr B 708:21–26
40. Igarashi M, Ma KZ, Gao F, Kim HW, Greenstein D, Rapoport SI, Rao JS (2010) Brain lipid concentrations in bipolar disorder. J Psychiatr Res 44:177–182
41. Kakela R, Somerharju P, Tyynela J (2003) Analysis of phospholipid molecular species in brains from patients with infantile and juvenile neuronal-ceroid lipofuscinosis using liquid chromatography-electrospray ionization mass spectrometry. J Neurochem 84:1051–1065
42. Folch J, Lees M, Stanley GHS (1957) A simple method for the isolation and purification of total lipides from animal tissues. J Biol Chem 226:497–509
43. Lísa M, Holčapek M, Boháč M (2009) Statistical evaluation of triacylglycerol composition in plant oils based on high-performance liquid chromatography-atmospheric pressure chemical ionization mass spectrometry data. J Agric Food Chem 57:6888–6898
44. Hsu FF, Turk J (2009) Electrospray ionization with low-energy collisionally activated dissociation tandem mass spectrometry of glycerophospholipids: mechanisms of fragmentation and structural characterization. J Chromatogr B 877:2673–2695

Anal Bioanal Chem (2015) 407:5033–5043
DOI 10.1007/s00216-015-8528-2

PAPER IN FOREFRONT

Continuous comprehensive two-dimensional liquid chromatography–electrospray ionization mass spectrometry of complex lipidomic samples

Michal Holčapek · Magdaléna Ovčačíková · Miroslav Lísa · Eva Cífková · Tomáš Hájek

Received: 2 December 2014 / Revised: 22 January 2015 / Accepted: 28 January 2015 / Published online: 19 February 2015

Abstract A new continuous comprehensive two-dimensional liquid chromatography–electrospray ionization mass spectrometry method has been developed for the lipidomic characterization of complex biological samples. The reversed-phase ultra-high-performance liquid chromatography with a C_{18} column (150 mm × 1 mm, 1.7 μm) used in the first dimension makes the separation of numerous lipid species differing in their hydrophobic part of the molecule, mainly fatty acyl chain lengths and the number and positions of double bonds, possible. Coeluted lipid species in the first dimension are resolved by the fast hydrophilic interaction liquid chromatography separation (50 mm × 3 mm, 2.7 μm, core–shell particles) of lipid classes according to their different polarities in the second dimension. Retention times in both dimensions, accurate *m/z* values, and tandem mass spectra provide high confidence in the identification of lipid species. The retention behavior of individual lipids in reversed-phase mode follows the equivalent carbon number pattern, which provides an additional tool for unambiguous identification. This analytical method is applied for the lipidomic characterization of total lipid extracts of human plasma and porcine brain samples, which resulted in the identification of 143 lipid species from four lipid categories and ten lipid classes.

Published in the topical collection *Lipidomics* with guest editor Michal Holčapek.

Electronic supplementary material The online version of this article (doi:10.1007/s00216-015-8528-2) contains supplementary material, which is available to authorized users.

M. Holčapek (✉) · M. Ovčačíková · M. Lísa · E. Cífková · T. Hájek
Department of Analytical Chemistry, Faculty of Chemical Technology, University of Pardubice, Studentská 573, 53210 Pardubice, Czech Republic
e-mail: Michal.Holcapek@upce.cz

Keywords Lipids · Lipidomics · Comprehensive 2D liquid chromatography · Mass spectrometry · Plasma · Brain

Introduction

Lipids have numerous important functions in cells, tissues, and body fluids, such as the formation of lipid bilayers, cell signaling, and energy storage [1]. Lipids are defined as small molecules formed by carbanion-based condensations of thioesters and/or by carbocation-based condensations of isoprene units. The most widely used LIPID MAPS classification system divides lipids into eight categories, namely, fatty acyls, glycerolipids, glycerophospholipids (GP), sphingolipids (SP), sterol lipids (ST), prenol lipids, saccharolipids, and polyketides, with many further classes and subclasses [1–3]. Lipidomics is a subset of metabolomics, which is aimed at the comprehensive analysis of lipids isolated from cells, tissues, or biological fluids and the study of their biological roles with respect to health and disease states [4–6]. Three major analytical platforms are known in lipidomic analysis [7]: shotgun electrospray ionization (ESI) mass spectrometry (MS) using direct infusion without any chromatographic separation [8–10], liquid chromatography (LC)/MS using various chromatographic modes [11–19], and MS imaging, providing information on the spatial lipid distribution in tissues [20, 21].

Shotgun lipidomics is a simple approach for lipidomic characterization, where the crude lipid extract typically in chloroform–methanol–2-propanol containing additives is infused directly into an ESI tandem MS (MS/MS) instrument. The aim is to identify and quantify as many lipid molecular species as possible from biological samples [8–10]. The

advantages of the shotgun approach are the short analysis time and easy automation, but on the other hand it may be difficult to obtain information on isomeric lipids, and attention must be paid to ion suppression effects. In practice, shotgun lipidomics is often used for the high-throughput automated quantitation of lipids, whereas LC/MS is preferred for more demanding tasks, including isomeric resolution.

Several chromatographic modes can be used in a liquid-phase separation of various types of lipid isomers, such as reversed-phase (RP) LC [11], normal-phase (NP) LC [12, 13], hydrophilic interaction LC (HILIC) [14, 15], silver-ion LC [16–18], and chiral LC [19]. RP-LC is used for lipid separation according to the length of the fatty acyl chains and the number and positions of double bonds (DB) [11]. NP-LC is typically used for the separation of only nonpolar lipid classes on the basis of their polarity using conventional NP mobile phase systems using hexane with polar additives [12]. However, the separation of polar lipid classes can be achieved on a poly(vinyl alcohol)–silica column with a more polar mobile phase (2-propanol–methyl *tert*-butyl ether–methanol with 4 mM ammonium formate), but the resolution of nonpolar lipid classes is sacrificed [13]. HILIC is frequently used for the analysis of polar compounds using various types of chromatographic columns, such as bare silica gel, polar stationary phases (amino, cyano, diol, etc.) chemically bonded to the silica gel support, and zwitterionic or ion-exchanger materials [22–26]. HILIC on silica columns provides very good lipid class separation [14, 15]. The previously discussed work [13] using more polar mobile phases results in a chromatogram very similar to that obtained using HILIC, so the retention mechanisms are probably similar as well. Silver-ion LC [16–18] is a special chromatographic mode typically used for the analysis of triacylglycerols (TG) and other nonpolar lipids and is based on the formation of weak reversible complexes of silver ions in the stationary phase with the π electrons of DB. Chiral LC has been successfully applied for the enantiomeric separation of TG [19].

However, one-dimensional separation may not be sufficient for complex lipidomic mixtures. Two dimensional (2D) LC is based on the combination of two different chromatographic modes, where the orthogonality of the separation mechanisms in both dimensions is a major requirement for such systems [22–26]. Various off-line and online 2D configurations are known, and each have their advantages and limitations. The commonest combination of separation mechanisms is based on lipid class separation in one dimension using either the NP mode or the HILIC mode coupled with lipid species separation in another dimension using RP separation [24–27]. The alternative for nonpolar lipid classes is the combination of silver-ion LC and nonaqueous RP separation in either an off-line setup [28] or an online setup [29, 30]. The advantage of the offline configuration [27, 28] is the possibility of full optimization in both dimensions regardless of the analysis time, which could yield the highest number of identified species, but a serious limitation is the very long analysis times, which are not suitable for high throughput or automation. The online combination [22–26] offers three alternative methods: (1) heart-cut 2D-LC is used for the analysis of a selected fraction [31, 32], (2) stopped-flow 2D-LC is a hybrid approach combining the advantages of the offline and online approaches, where the analysis in the first dimension is stopped for the time of the second-dimension analysis and then the flow is reestablished [33, 34], (3) the continuous comprehensive 2D-LC system allows all fractions eluted from the first dimension to be analyzed in the second dimension as well, and this is the fastest approach and the one with the greatest potential for automation. The major drawback of the continuous comprehensive 2D-LC setup is the limited analysis time in the second dimension caused by the modulation time, which compromises the resolution in the second dimension. To the best of our knowledge, no article has been published on continuous comprehensive 2D-LC/MS of multiple lipid classes. Another possibility on the edge between stopped-flow and continuous comprehensive 2D-LC is the use of a trapping column with a non-stopped-flow system [35, 36].

The main goal of our work was the development of a new continuous comprehensive 2D-LC/MS method for the characterization of the lipidomic composition of various biological samples. For this purpose, RP-LC mode with a C_{18} column is used in the first dimension, and HILIC with a silica column was used in the second dimension of a comprehensive 2D-LC/MS setup applied for lipid extracts of human plasma and porcine brain, where lipids were identified on the basis of retention times in two dimensions, and accurate *m*/*z* values of molecular adducts and characteristic fragment ions in their MS/MS spectra.

Experimental

Chemicals and standards

Acetonitrile, 2-propanol, methanol (all LC/MS gradient grade), chloroform (LC grade, stabilized by 0.5–1 % ethanol), ammonium acetate, sodium formate, sodium chloride, and cholest-5-en-3β-yl nonadecanoate [cholesteryl ester (CE) 19:0] were purchased from Sigma-Aldrich (St Louis, MO, USA). Deionized water was prepared with a Demiwa 5-roi purification system (Watek, Ledeč nad Sázavou, Czech Republic) and with an Ultra CLEAR UV apparatus (SG, Hamburg, Germany). Standards of polar lipid classes—1,2-di-[(9*Z*)-octadecenoyl)]-*sn*-glycero-3-phosphoethanolamine [phosphatidylethanolamine (PE) 18:1/18:1], 1,2-di-[(9*Z*)-octadecenoyl)]-*sn*-glycero-3-phosphocholine [phosphatidylcholine (PC) 18:1/18:1], 1-[(9*Z*)-octadecenoyl)]-*sn*-glycero-3-phosphocholine

[lysophosphatidylcholine (LPC) 18:1], *N*-(octadecanoyl)-sphing-4-enine-1-phosphocholine [sphingomyelin (SM) 18:1]—were purchased from Avanti Polar Lipids (Alabaster, AL, USA). The standard of 1,2,3-tri-[(9*Z*)-octadecenoyl)]-*sn*-glycerol (TG 18:1/18:1/18:1) was purchased from Nu-Chek Prep (Elysian, MN, USA). The lipid nomenclature follows the shorthand notation for lipid structures published by Liebisch et al. [37] and the LIPID MAPS [1] classification system.

Sample preparation

Total lipid extracts of human plasma and porcine brain were prepared according to the well-established Folch procedure [38] using a chloroform–methanol–water system with minor modifications [14, 15]. Human plasma (500 μL) or porcine brain (500 mg) was homogenized with 10 mL of a chloroform–methanol mixture (2:1, v/v). The homogenate was filtered using a coarse filter paper. Then, 2 mL of 1 M NaCl was added, and the mixture was centrifuged at 2,500 rpm for 3 min under ambient conditions. The chloroform (bottom) layer containing lipids was collected, evaporated by a gentle stream of nitrogen, and redissolved in a chloroform–2-propanol (1:2, v/v) mixture for analysis.

Continuous comprehensive 2D-LC conditions

Continuous comprehensive 2D-LC analysis of lipids was performed with an Agilent 1290 Infinity 2D-LC Solution system (Agilent Technologies, Santa Clara, CA, USA) containing two Agilent 1290 Infinity pumps, a thermostatted column compartment with a two-position eight-port switching valve (pressure limit 1,200 bar) for 2D-LC, and two identical 20-μL sampling loops. An Acquity UPLC BEH C_{18} column (150 mm×1 mm, 1.7 μm, Waters, Milford, MA, USA) was used in the first dimension under the following conditions: flow rate of 20 μL/min; injection volume of 1 μL; column temperature of 25 °C; mobile phase gradient of 78.5 % solvent B at 0 min and 100 % solvent B at 150 min, where solvent A was 5 mM aqueous ammonium acetate and solvent B was a mixture of 99.5 % acetonitrile and 2-propanol (1:2, v/v) and 0.5 % 5 mM aqueous ammonium acetate. A core–shell silica CORTECS HILIC column (50 mm×3 mm, 2.7 μm, Waters) was used in the second dimension under the following conditions: flow rate of 5 mL/min; column temperature of 40 °C; mobile phase gradient 92 % solvent B at 0 min, 80 % solvent B at 0.7 min, and 92 % solvent B at 1 min, where solvent A was 5 mM aqueous ammonium acetate and solvent B was acetonitrile. The modulation time between dimensions was 60 s. A T-piece mobile phase splitter was used before the effluent introduction into the MS system at a splitting ratio of 8 (MS system):100 (waste).

MS conditions

A hybrid quadrupole time-of-flight mass spectrometer (micrOTOF-Q, Bruker Daltonics, Bremen, Germany) with an ESI source was used as the detector with the following parameter settings: capillary voltage of 4.5 kV; nebulizing gas pressure of 1.6 bar; drying gas flow rate of 12 L/min; drying gas temperature of 220 °C. ESI mass spectra were measured in the range of *m*/*z* 50–1,500 in positive-ion mode. Negative-ion MS/MS mode was used only for the identification of fatty acyls in case of PE. A collision energy of 20–25 eV and argon as the collision gas were used for MS/MS experiments. The external calibration of the mass scale was performed with sodium formate clusters before individual measurements. The data were acquired and evaluated using DataAnalysis (Bruker Daltonics) and were visualized with GCImage (University of Nebraska, Lincoln, NE, USA).

Results and discussion

General considerations for the method development

The Agilent 1290 Infinity 2D-LC Solution system with a two-position eight-port switching valve was used for the development of the continuous comprehensive 2D-LC/MS method for lipidomic characterization, where a fully porous 1.7-μm-particle column was used in the first dimension and a core–shell sub-3-μm-particle column was used in the second dimension. The principal issue of the method development is the selection of the orthogonal separation mechanisms and also the appropriate order of these modes in the 2D arrangement. One separation mechanism should be applied for the lipid class separation, where NP and HILIC modes can be considered. NP-LC is typically used only for nonpolar lipid classes owing to the too strong retention of polar GP and SP classes [12], but the meaningful separation of both nonpolar and polar lipids under NP conditions has also been reported [13]. In our case of continuous comprehensive 2D-LC, HILIC separation is preferred owing to easy reequilibration and good compatibility with the aqueous mobile phases used in RP-LC. The RP mode is an obvious choice for the separation of lipids from all classes according to differences in the hydrophobic part of the molecule, mainly the length of the fatty acyl chains, and the number and positions of DB. The order of the RP and HILIC modes in the comprehensive 2D-LC concept is determined by a simple fact that RP-LC cannot provide a highly efficient separation of so many species within only 1 min as a typical modulation time used for comprehensive 2D-LC, but the HILIC class separation can be achieved in such a time frame with a certain level of compromise. Moreover, HILIC allows a partial separation of lipid species within individual

Table 1 Lipid species identified in total lipid extracts of human plasma and porcine brain

No.	Retention times (min)		Lipid species level[a]	Fatty acyl/alkyl level[a]	ECN
	D1	D2			
LPC					
1	7.4	0.68	LPC 22:6	PC 22:6_0:0	10
2	7.7	0.68	LPC 20:4	PC 20:4_0:0	12
3	8.7	0.71	LPC 18:2	PC 18:2_0:0	14
4	9.7	0.70	LPC 18:1	PC 18:1_0:0	16
5	9.7	0.72	LPC 16:0	PC 16:0_0:0	16
6	13.7	0.71	LPC 18:0	PC 18:0_0:0	18
SM					
7	38.7	0.66	SM 32:1		30
8	45.2	0.65	SM 34:2		30
9	51.7	0.65	SM 34:1		32
10	52.3	0.65	SM 36:2		32
11	64.6	0.64	SM 36:1		34
12	76.6	0.62	SM 42:3		36
13	77.6	0.63	SM 38:1		36
14	78.6	0.62	SM 40:2		36
15	83.6	0.62	SM 41:2		37
16	84.6	0.62	SM 39:1		37
17	89.6	0.61	SM 42:2		38
18	90.6	0.62	SM 40:1		38
19	92.1	0.62	SM 43:2		39
20	95.6	0.62	SM 40:0		40
21	97.6	0.62	SM 41:1		39
22	103.3	0.62	SM 42:1		40
Cer, HexCer, and Hex2Cer					
23	63.8	0.15	Cer 36:1 (OH)		34
24	65.3	0.18	Hex2Cer 36:1	Hex2Cer d18:1/18:0	34
25	67.2	0.14	Cer 36:1		34
26	67.2	0.16	HexCer 36:1	HexCer d18:1/18:0	34
27	74.7	0.14	Cer 36:1	Cer d18:1/18:0	34
28	77.9	0.12	Cer 38:1 (OH)		36
29	81.7	0.12	Cer 38:1	Cer d18:1/20:0	36
30	90.1	0.12	Cer 40:1 (OH)		38
31	90.7	0.16	HexCer 42:2	HexCer d18:1/24:1	38
32	90.8	0.16	Cer 42:2	Cer d18:1/24:1	38
33	92.7	0.18	HexCer 40:1	HexCer d18:1/22:0	38
34	98.4	0.16	HexCer 41:1	HexCer d18:1/23:0	39
35	101.5	0.17	HexCer 44:2	HexCer d18:1/26:1	40
36	104.0	0.17	HexCer 42:1	HexCer d18:1/24:0	40
37	104.8	0.18	HexCer 42:0	HexCer d18:0/24:0	42
38	106.5	0.18	HexCer 44:0	HexCer d18:0/26:0	44
PC					
39	40.6	0.54	PC 34:3	PC 16:1_18:2	28
40	41.5	0.53	PC 36:5	PC 16:0_20:5	26
41	46.2	0.52	PC 38:6	PC 16:0_22:6	26
42	49.5	0.52	PC 38:5	PC 18:1_20:4	28
43	49.5	0.53	PC 36:4	PC 16:0_20:4	28
44	51.6	0.52	PC 36:3	PC 18:1_18:2	30
45	51.6	0.54	PC 34:2	PC 16:0_18:2	30
46	52.6	0.56	PC 32:1	PC 16:0_16:1	30
47	53.5	0.52	PC 38:5	PC 18:0_20:5	28
48	54.6	0.52	PC 36:3	PC 16:0_20:3	30
49	58.5	0.53	PC 40:6	PC 18:0_22:6	28
50	62.5	0.52	PC 38:4	PC 18:0_20:4	30
51	63.5	0.54	PC 34:1	PC 16:0_18:1	32
52	63.3	0.56	PC 32:0	PC 16:0_16:0	32
53	65.5	0.53	PC 36:2	PC 18:0_18:2	32
54	68.5	0.52	PC 38:3	PC 18:0_20:3	32
55	75.6	0.53	PC 36:1	PC 18:0_18:1	34
56	76.6	0.56	PC 34:0	PC 16:0_18:0	34
PE					
57	49.3	0.33	PE 38:6	PE 16:0/22:6	26
58	53.3	0.33	PE 38:5	PE 18:1_20:4	28
59	53.3	0.34	PE 36:4	PE 16:0/20:4	28
60	55.1	0.31	PE P-38:6	PE P-16:0/22:6	
61	55.4	0.35	PE 34:2	PE 16:1_18:1	30
62	58.3	0.32	PE P-38:5/ PE O-38:6		
63	58.3	0.33	PE P-36:4	PE P-16:0/20:4	
64	61.3	0.33	PE 40:6	PE 18:0/22:6	28
65	63.8	0.34	PE 38:4	PE 18:0/20:4	30
66	64.8	0.36	PE 34:1	PE 16:0/18:1	32
67	67.3	0.35	PE 36:2	PE 18:1/18:1	32
68	69.3	0.33	PE 40:5	PE 18:0/22:5	30
69	69.3	0.33	PE P-38:3/ PE O-38:4		
70	70.3	0.33	PE 38:3	PE 18:0_20:3	32
71	71.3	0.32	PE P-38:4	PE P-18:0/20:4	
72	74.3	0.35	PE P-36:2	PE P-18:1/18:1	
73	75.5	0.34	PE 40:4	PE 18:0/22:4	32
74	79.3	0.35	PE 36:1	PE 18:0/18:1	34
75	79.3	0.33	PE P-40:4	PE P-18:0/22:4	
76	82.3	0.35	PE P-38:2	PE P-18:1/20:1	
77	84.4	0.36	PE P-36:1/ PE O-36:2		
78	84.5	0.31	PE 40:2		36
TG					
79	119.5	0.11	TG 48:3	TG 12:0_18:1_18:2	42
80	120.0	0.11	TG 50:4	TG 16:1_16:1_18:2	42
81	120.2	0.11	TG 52:5	TG 16:1_18:2_18:2	42
82	120.4	0.11	TG 46:2	TG 12:0_16:1_18:1	42
83	120.7	0.11	TG 54:6	TG 18:2_18:2_18:2	42

Table 1 (continued)

No.	Retention times (min)		Lipid species level[a]	Fatty acyl/alkyl level[a]	ECN
	D1	D2			
84	120.9	0.11	TG 44:1	TG 12:0_16:0_16:1	42
85	121.0	0.11	TG 50:4	TG 16:0_16:1_18:3	42
86	121.4	0.11	TG 46:2	TG 12:0_16:0_18:2	42
87	122.0	0.11	TG 48:3	TG 14:0_16:0_18:3	42
88	122.5	0.11	TG 52:5	TG 16:0_18:2_18:3	42
89	123.2	0.11	TG 54:6	TG 18:1_18:2_18:3	42
90	124.0	0.11	TG 52:5	TG 16:0_16:1_20:4	42
91	124.5	0.11	TG 54:6	TG 16:0_18:2_20:4	42
92	124.9	0.11	TG 50:4	TG 14:0_16:0_20:4	42
93	125.7	0.11	TG 54:6	TG 16:0_18:2_20:4	42
94	126.2	0.11	TG 52:4	TG 16:1_18:1_18:2	44
95	126.6	0.12	TG 54:5	TG 18:1_18:2_18:2	44
96	126.7	0.11	TG 48:2	TG 14:0_16:1_18:1	44
97	127.0	0.12	TG 50:3	TG 16:0_16:1_18:2	44
98	127.3	0.11	TG 52:4	TG 16:0_18:2_18:2	44
99	128.0	0.11	TG 48:2	TG 14:0_16:0_18:2	44
100	128.8	0.11	TG 46:1	TG 12:0_16:0_18:1	44
101	128.9	0.11	TG 52:4	TG 16:0_18:1_18:3	44
102	129.2	0.12	TG 50:3	TG 16:0_16:0_18:3	44
103	130.0	0.12	TG 56:6	TG 18:1_18:1_20:4	44
104	130.9	0.12	TG 54:5	TG 16:0_18:2_20:3	44
105	131.2	0.12	TG 56:6	TG 18:0_18:2_20:4	44
106	131.9	0.11	TG 52:4	TG 16:0_16:0_20:4	44
107	132.5	0.12	TG 56:6	TG 16:0_18:1_22:5	44
108	132.8	0.12	TG 54:4	TG 18:1_18:1_18:2	46
109	133.4	0.11	TG 50:2	TG 16:0_16:1_18:1	46
110	133.7	0.12	TG 52:3	TG 16:1_18:1_18:1	46
111	133.9	0.12	TG 54:4	TG 16:0_18:1_20:3	46
112	134.6	0.12	TG 48:1	TG 14:0_16:0_18:1	46
113	134.8	0.11	TG 50:2	TG 16:0_16:0_18:2	46
114	134.9	0.12	TG 52:3	TG 16:0_18:1_18:2	46
115	136.3	0.12	TG 56:5	TG 16:0_18:1_22:4	46
116	136.7	0.12	TG 46:0	TG 14:0_16:0_16:0	46
117	136.9	0.12	TG 52:3	TG 16:0_18:0_18:3	46
118	138.3	0.12	TG 56:5	TG 18:0_18:1_20:4	46
119	138.6	0.11	TG 54:3	TG 18:1_18:1_18:1	48
120	139.5	0.12	TG 52:2	TG 16:0_18:1_18:1	48
121	139.7	0.11	TG 54:3	TG 18:0_18:1_18:2	48
122	140.6	0.12	TG 50:1	TG 16:0_16:0_18:1	48
123	142.0	0.12	TG 52:2	TG 16:0_18:0_18:2	48
124	142.9	0.13	TG 48:0	TG 14:0_16:0_18:0	48
125	143.0	0.12	TG 56:4	TG 16:0_18:0_22:4	48
126	144.9	0.12	TG 56:3	TG 18:1_18:1_20:1	50
127	145.0	0.12	TG 54:2	TG 18:0_18:1_18:1	50
128	145.7	0.12	TG 56:3	TG 18:0_18:1_20:2	50
129	146.1	0.12	TG 52:1	TG 16:0_18:0_18:1	50
130	147.3	0.12	TG 50:0	TG 16:0_16:0_18:0	50
131	148.5	0.13	TG 56:2	TG 18:0_18:1_20:1	52
132	149.8	0.12	TG 54:1	TG 18:0_18:0_18:1	52
133	151.2	0.13	TG 52:0	TG 16:0_18:0_18:0	52
134	155.7	0.12	TG 54:0	TG 18:0_18:0_18:0	54
ST and SE					
135	45.2	0.12	ST 27:1_OH	Chol	
136	122.2	0.11	SE 27:1/20:5	CE 20:5	10
137	125.1	0.12	SE 27:1/22:6	CE 22:6	10
138	127.2	0.12	SE 27:1/18:3	CE 18:3	12
139	129.2	0.12	SE 27:1/20:4	CE 20:4	12
140	134.2	0.12	SE 27:1/18:2	CE 18:2	14
141	142.2	0.12	SE 27:1/18:1	CE 18:1	16
142	143.1	0.13	SE 27:1/16:0	CE 16:0	16
143	150.2	0.12	SE 27:1/18:0	CE 18:0	18

Cer ceramide (Cer), *Chol* cholesterol, *D1* first dimension, D2 second dimension, *ECN* equivalent carbon number, *HexCer* hexosyl ceramide, *Hex2Cer* dihexosyl ceramide, *LPC* lysophosphatidylcholine, *PC* phosphatidylcholine, *PE* phosphatidylethanolamine, *SE* steryl ester, *SM* sphingomyelin, *ST* sterol, *TG* triacylglycerol

[a] The lipid notation follows the shorthand nomenclature recommended by Liebisch et al. [37], where a slash separator denotes a proven *sn* position, and an underscore separator is used when the *sn* position of fatty acyls is not known.

$[M+H]^+$

$[M+NH_4]^+$

$[M+H-H_2O]^+$

classes (Table 1), which is maintained only in the case of the RP–HILIC configuration, but these minor retention differences would be lost in the opposite HILIC–RP configuration. This explains why our choice of RP–HILIC is superior to the HILIC–RP arrangement in continuous comprehensive 2D-LC/MS lipidomic applications. The opposite configuration is typically selected for off-line, stopped-flow, and heart-cut 2D-LC setups [29–32], where the analysis time in the second dimension is not limited as strictly as in the case of continuous comprehensive 2D-LC.

HILIC separation when dealing with phospholipid analysis has the important advantage of achieving a partial separation of molecular species within a single phospholipid class. The order of RP separation and HILIC separation in a consecutive manner is fully understandable. In fact, in “continuous” 2D-LC especially when analyzing lipids with a broad range of equivalent carbon numbers (ECN), the separation time frame becomes critical.

Optimization of RP separation in the first dimension

The basic prerequisites for the RP ultra-high performance LC (UHPLC) method optimization in the first dimension are as follows: a long column (i.e., 150 mm) packed with sub-2-μm particles to provide the best efficiency, a narrow column diameter (i.e., 1 mm) to maintain flow rates lower than 50 μL/min, which are essential for comprehensive 2D-LC/MS coupling, and sufficient peak widths to ensure that each chromatographic peak from the first dimension appears in at least two fractions in the second dimension [22–25]. These requirements result in a rather low flow rate in the first dimension (20 μL/min) and a long analysis time (165 min). The best separation is achieved on an Acquity UPLC BEH C_{18} column (150 mm×1 mm, 1.7 μm, Waters) using an aqueous ammonium acetate–acetonitrile–2-propanol gradient (details are given in "Experimental") optimized on the basis of our previous experience [15, 27]. The overlay of reconstructed ion current (RIC) chromatograms of RP-UHPLC/ESI-MS analysis is shown for the mixture of lipid standards in Fig. 1a and the total ion current chromatogram for the lipid extract of human plasma is shown in Fig. 1b. Figure S1a shows the total ion current chromatogram of RP-UHPLC/ESI-MS analysis of the porcine brain extract, which is selected owing to it having a high lipidomic complexity in comparison with plasma samples, mainly in the area of ceramides and hexosylated ceramides occurring in brain tissues (see Table S1 for a detailed comparison).

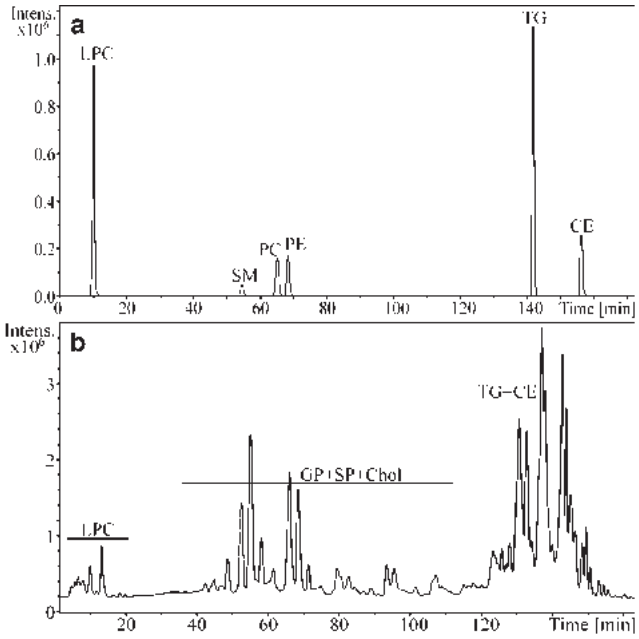

Fig. 1 Reversed-phase ultra-high-performance liquid chromatography (RP-UHPLC)/electrospray ionization mass spectrometry (ESI-MS) chromatograms: **a** overlay of reconstructed ion current (RIC) chromatograms of the mixture of lipid standards; **b** total ion current chromatogram of the lipid extract of human plasma. The RP-UHPLC conditions are reported in "Experimental." *CE* cholesteryl esters, *Chol* cholesterol, *GP* glycerophospholipids, *LPC* lysophosphatidylcholines, *PC* phosphatidylcholines, *PE* phosphatidylethanolamines, *SM* sphingomyelins, *SP* sphingolipids, *TG* triacylglycerols

The retention of individual lipid species is governed by the ECN, which is calculated as the total carbon number of fatty acyls minus two times the DB number. The ECN concept of the retention behavior was extensively discussed in our previous works on TG analysis [39–41], but it is also applicable for the other lipid classes analyzed in this work (Table 1). The LPC class exhibits the lowest retention (7–14 min) in RP mode, because members of this class have the smallest hydrophobic part of the molecule, i.e., one fatty acyl only in comparison with two fatty acyls for GP and SP and three fatty acyls for TG (Table 1). Moreover, the free hydroxyl group also reduces the retention in RP mode. Seven classes of polar lipids (LPC, SM, ceramides, hexosyl ceramides, dihexosyl ceramides, PC, and PE) and cholesterol are eluted over a broad range of retention times in accordance with the literature [11] . Nonpolar lipid classes (TG and CE) exhibit the highest retention in RP mode (120–160 min). Lipid species are partially resolved within ECN groups. Palmitoyl-containing TG typically exhibit higher retention than oleoyl-containing TG with the same ECN, e.g., for ECN=44 (TG 18:1_18:2_18:2< TG 16:0_18:2_18:2), ECN=48 (TG 18:1_18:1_18:1<TG 16:0_18:1_18:1<TG 16:0_16:0_18:1), etc., in accordance with our previous works [39–41]. Lipid species are well separated within lipid classes according to their ECN, but overlap of retention may occur among different classes, which is solved by HILIC separation in the second dimension.

Optimization of HILIC separation in the second dimension

Our initial intention was to use a short column (50 mm) with a wider diameter (3 mm) and sub-2 μm particles in the second dimension. An Acquity UPLC BEH HILIC column (50 mm× 3 mm, 1.7 μm, Waters) with an aqueous ammonium acetate–acetonitrile gradient was used for this purpose, but the column back pressure limited the maximum flow rate to only 4 mL/min. Anyway, relatively good separation with a total analysis time of 1 min was achieved (Fig. S2) in the comprehensive 2D-LC setup, but a serious problem arose from the limited column lifetime under such flow rates. The column back pressure gradually increased depending on the number of analyses until the system pressure limit (1,200 bar) was reached or complete deterioration of the column was observed, as experienced with three columns tested. For this reason, we changed the column to a core–shell sub-3-μm column with 50-mm length to develop a robust method capable to reaching the maximum flow rate of 5 mL/min in the second dimension, good separation of lipid classes, and improved column lifetime. This goal was achieved with a CORTECS HILIC column (50 mm×3 mm, 2.7 μm, Waters) and an aqueous ammonium acetate–acetonitrile gradient (details in "Experimental"),

as illustrated by the overlay of the RIC chromatograms in Fig. 2a for the mixture of lipid standards, Fig. 2b for the lipid extract of human plasma, and Fig. S1b for the lipid extract of porcine brain. Nonpolar lipid classes (TG and CE) together with cholesterol are eluted in the void volume of the system, similarly as in our previous works [12, 27], whereas polar lipid classes (PE, PC, SM, and LPC) exhibit acceptable separation according to their polarity within a 1-min separation window. A T-piece flow splitter was used between the second-dimension column and the mass spectrometer with a splitting ratio of 8 (MS system):100 (waste) so that the flow was within the limit of the quadrupole time-of-flight mass spectrometer.

Identification of individual lipids based on ESI mass spectra

The ionization and fragmentation behavior of individual lipid classes and species within classes are well known from previous works [7–11, 15], so this knowledge was applied for the identification of individual lipids in this work. Table S1 reports only unambiguous identifications for human plasma (Fig. 3a) and porcine brain (Fig. 3b) samples; no tentative suggestions without confident conclusions are reported here. The slash separator shows the known preference of the *sn* position according to the shorthand lipid notation suggested by Liebisch et al. [37], but it does not refer to a 100 %/0 % ratio of possible lipid regioisomers, because in most cases both regioisomers are present in a mixture with a certain stereospecific preference. The underscore separator is used when *sn* position is not known. The following essential requirements are taken into account for the identification of the lipids reported in Table 1: (1) retention times in both dimensions determined using RIC chromatograms, (2) accurate *m/z* values (mostly better than 5 ppm), and (3) characteristic fragmentation behavior in positive-ion and/or negative-ion MS/MS spectra depending on the signal. The characteristic fragment ion for all lipid classes containing a choline moiety (PC, SM, and LPC) is *m/z* 184, which can be used for better visualization of these classes using the RIC of *m/z* 184 in a 2D projection, as shown in Fig. 4, chromatogram A for human plasma and Fig. S3, chromatogram A for porcine brain. The fragment ion *m/z* 369 is characteristic of all lipid species containing cholesterol (Fig. 4, chromatogram B and Fig. S3, chromatogram B). ESI mass spectra of ceramides, hexosyl ceramides, and dihexosyl ceramides exhibit characteristic ions related to the type of base, *e.g.*, *m/z* 264 for 18:1 and *m/z* 266 for 18:0, which makes possible the accurate identification of fatty acyl positions (Table 1). The neutral loss of $\Delta m/z$ 141 is observed in positive-ion ESI mass spectra of PE, whereas negative-ion ESI-MS/MS provides information on the positions of attached fatty acyls based the ratio of $[R_1COO]^-$ and $[R_2COO]^-$ ions, where the $[R_2COO]^-$ ion is more abundant. This ratio changes for the combination of saturated and highly polyunsatured (C20:5 or C22:6) fatty acyls in PE owing to the formation of $[R_i]^-$ ions from $[R_iCOO]^-$ ions caused by the neutral loss of carbon dioxide [42]. The interpretation of positive-ion ESI mass spectra of TG is based on $[M+NH_4]^+$ and $[M+H-R_iCOOH]^+$ ions.

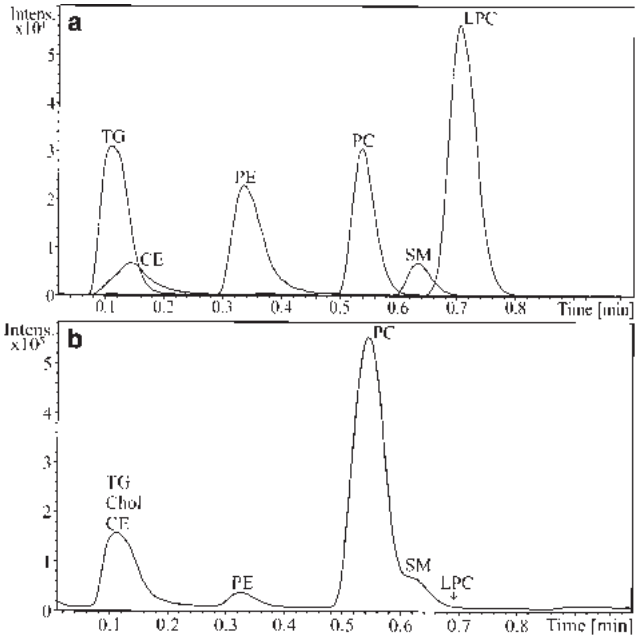

Fig. 2 Hydrophilic interaction liquid chromatography (HILIC)/ESI-MS chromatograms: **a** overlay of RIC chromatograms of the mixture of lipid standards; **b** total ion current chromatogram of the lipid extract of human plasma. The HILIC conditions are reported in "Experimental"

Continuous comprehensive 2D-LC/MS of lipids

The optimized continuous comprehensive 2D-LC method was applied for the analysis of human plasma (Fig. 3a) and porcine brain (Fig. 3b) lipidomic extracts. Human plasma is one of the most frequently analyzed biofluids, with the potential for biomarker screening of some diseases. The lipidome of brain tissue is a rather complex biological tissue containing numerous lipid classes, including ceramides and hexosylated ceramides. Use of porcine brain is preferred over use of human brain for ethical reasons. We visualized 2D chromatograms with GCImage using the conventional color scheme, where red corresponds to the most abundant species, and orange, yellow, and green correspond to species of decreasing abundance (Figs. 3 and 4, S3). The absence of a peak is represented by white. Figures 4 and S3 illustrate the potential of RIC chromatograms for better visualization of selected compound classes with common features in their mass spectra; for example, Fig. 4, chromatogram A and Fig. S3, chromatogram A highlight lipid classes containing a choline moiety (PC, SM, and LPC) using the RIC of *m*/z 184, whereas Fig. 4, chromatogram B and Fig. S3, chromatogram B show the RIC of *m/z* 369, which is characteristic of cholesterol and CE. Table 1 shows the individual lipid species identified in the samples studied. In total, we identified 97 lipid species from seven

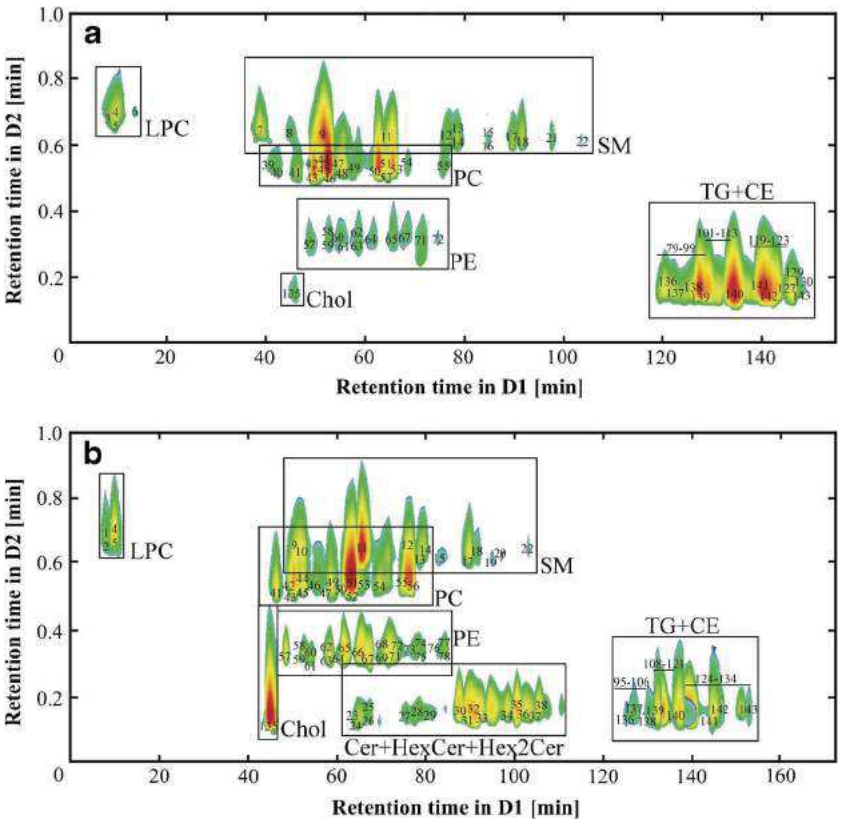

Fig. 3 Two-dimensional liquid chromatography (2D-LC)/ESI-MS chromatograms of total lipid extracts: **a** human plasma; **b** porcine brain. The conditions for the first dimension (*D1*) and the second dimension (*D2*) are identical to those for Figs. 1 and 2, respectively. The annotation of the peak numbers corresponds to the numbers in Table 1. *Cer* ceramides, *HexCer* hexosyl ceramides, H*ex2Cer* dihexosyl ceramides

different lipid classes (LPC, cholesterol, SM, PC, PE, TG, and CE) in the human plasma sample and 115 lipid species from ten different lipid classes (LPC, ST, ceramides, hexosyl ceramides, dihexosyl ceramides, SM, PC, PE, TG, and CE) in the porcine brain sample. The typical fatty acyls occurring in glycerolipids, GP, SP, and ST are 16:0, 16:1, 18:0, 18:1, 18:2, 20:0, 20:3, 20:4, 20:5, and 22:6. Highly polyunsaturated fatty acyls with five or six DB are not common for TG, but

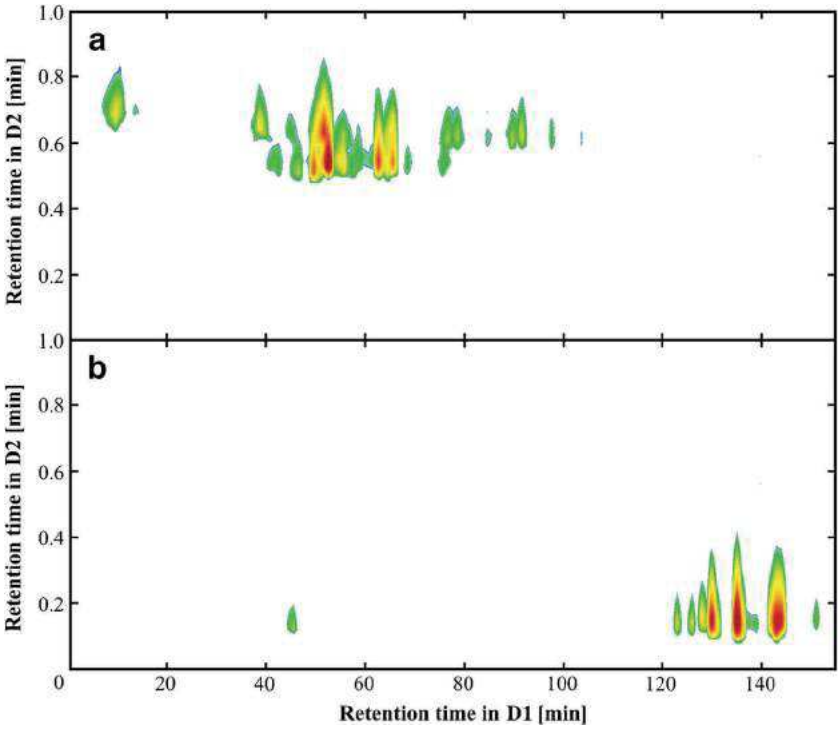

Fig. 4 RIC chromatograms of lipid class characteristic ions from 2D-LC/ESI-MS analysis of human plasma: *m/z* 184 characteristic of PC, SM, and LPC classes (*A*), and *m/z* 369 characteristic of cholesterol and CE (*B*)

18:3 is quite common and shorter fatty acyls 12:0 and 14:0 may occur as well. The occurrence of very long fatty acyls is observed for ceramides and hexosylated ceramides, such as 23:0, 24:0, 24:1, 26:0, and 26:1 (see Table 1 for details).

Conclusions

This work shows for the first time the application of continuous comprehensive 2D-LC/ESI-MS for the complex lipidomic characterization of polar and nonpolar lipid classes in human plasma and porcine brain samples. The logical combination for 2D-LC separation of lipids is species separation in one dimension (RP mode) and lipid class separation in another dimension (HILIC mode). An RP-UHPLC column with sub-2-μm particles was used in the first dimension to obtain the best separation of the maximum number of lipid species according to acyl chain lengths and the number of DB, and the fast HILIC analysis in the second dimension allows the separation of overlapped lipids in the first dimension on the basis of their different polarities. The advantages of our continuous comprehensive 2D-LC/MS method are the shorter analysis time and easier automation, but a drawback is the reduced number of identified lipids in comparison with off-line and stopped-flow 2D-LC/MS configurations. The present work is a proof of concept of possible application of continuous comprehensive 2D-LC/MS in lipidomics, but its implementation into quantitative lipidomic workflows requires further research and system improvements. Another aspect for future improvement is the sensitivity, because well-optimized one-dimensional LC/MS yields a higher number of identified lipid species compared with 2D-LC/MS systems using the identical sample [14, 15, 27].

Acknowledgments This work was supported by ERC CZ project no. LL1302 sponsored by the Ministry of Education, Youth, and Sports of the Czech Republic. E.C. acknowledges the support of project no. CZ.1.07/2.3.00/30.0021 sponsored by the Ministry of Education, Youth, and Sports of the Czech Republic.

References

1. LIPID MAPS (2014) LIPID MAPS Lipidomics Gateway. http://www.lipidmaps.org/. Accessed 2 Dec 2014
2. Fahy E, Subramaniam S, Brown HA, Glass CK, Merrill AH, Murphy RC, Raetz CRH, Russell DW, Seyama Y, Shaw W, Shimizu T, Spener F, van Meer G, VanNieuwenhze MS, White SH, Witztum JL, Dennis EA (2005) A comprehensive classification system for lipids. Eur J Lipid Sci Technol 107:337–364
3. Fahy E, Subramaniam S, Murphy RC, Nishijima M, Raetz CRH, Shimizu T, Spener F, van Meer G, Wakelam MJO, Dennis EA (2009) Update of the LIPID MAPS comprehensive classification system for lipids. J Lipid Res 50:S9–S14
4. Santos CR, Schulze A (2012) Lipid metabolism in cancer. FEBS J 279:2610–2623
5. van Meer G, Voelker DR, Feigenson GW (2008) Membrane lipids: where they are and how they behave. Nat Rev Mol Cell Biol 9:112–124
6. Oresič M, Hanninen VA, Vidal-Puig A (2008) Lipidomics: a new window to biomedical frontiers. Trends Biotechnol 26:647–652
7. Li M, Yang L, Bai Y, Liu HW (2014) Analytical methods in lipidomics and their applications. Anal Chem 86:161–175
8. Han XL, Gross RW (2005) Shotgun lipidomics: electrospray ionization mass spectrometric analysis and quantitation of cellular lipidomes directly from crude extracts of biological samples. Mass Spectrom Rev 24:367–412
9. Han X, Yang K, Gross RW (2012) Multi-dimensional mass spectrometry-based shotgun lipidomics and novel strategies for lipidomic analyses. Mass Spectrom Rev 31:134–178
10. Papan C, Penkov S, Herzog R, Thiele C, Kurzchalia T, Shevchenko A (2014) Systematic screening for novel lipids by shotgun lipidomics. Anal Chem 86:2703–2710
11. Sandra K, Pereira AD, Vanhoenacker G, David F, Sandra P (2010) Comprehensive blood plasma lipidomics by liquid chromatography/quadrupole time-of-flight mass spectrometry. J Chromatogr A 1217:4087–4099
12. Holčapek M, Cífková E, Červená B, Lísa M, Vostálová J, Galuszka J (2015) Determination of nonpolar and polar lipid classes in human plasma, erythrocytes and plasma lipoprotein fractions using ultrahigh-performance liquid chromatography-mass spectrometry. J Chromatogr A 1377:85–91
13. Sokol E, Almeida R, Hannibal-Bach HK, Kotowska D, Vogt J, Baumgart J, Kristiansen K, Nitsch R, Knudsen J, Ejsing CS (2013) Profiling of lipid species by normal-phase liquid chromatography, nanoelectrospray ionization, and ion trap–orbitrap mass spectrometry. Anal Biochem 443:88–96
14. Cífková E, Holčapek M, Lísa M, Ovčačíková M, Lyčka A, Lynen F, Sandra P (2012) Nontargeted quantitation of lipid classes using hydrophilic interaction liquid chromatography-electrospray ionization mass spectrometry with single internal standard and response factor approach. Anal Chem 84:10064–10070
15. Cífková E, Holčapek M, Lísa M (2013) Nontargeted lipidomic characterization of porcine organs using hydrophilic interaction liquid chromatography and off-line two-dimensional liquid chromatography-electrospray ionization mass spectrometry. Lipids 48:915–928
16. Lísa M, Netušilová K, Franěk L, Dvořáková H, Vrkoslav V, Holčapek M (2011) Characterization of fatty acid and triacylglycerol composition in animal fats using silver-ion and non-aqueous reversed-phase high-performance liquid chromatography/mass spectrometry and gas chromatography/flame ionization detection. J Chromatogr A 1218:7499–7510
17. Adlof RO (1997) Normal-phase separation effects with lipids on a silver ion high-performance liquid chromatography column. J Chromatogr A 764:337–340
18. Holčapek M, Dvořáková H, Lísa M, Girón AJ, Sandra P, Cvačka J (2010) Regioisomeric analysis of triacylglycerols using silver-ion liquid chromatography–atmospheric pressure chemical ionization mass spectrometry: comparison of five different mass analyzers. J Chromatogr A 1217:8186–8194
19. Lísa M, Holčapek M (2013) Characterization of triacylglycerol enantiomers using chiral HPLC/APCI-MS and synthesis of enantiomeric triacylglycerols. Anal Chem 85:1852–1859
20. Murphy SA, Nicolaou A (2013) Lipidomics applications in health, disease and nutrition research. Mol Nutr Food Res 57:1336–1346
21. Römpp A, Spengler B (2013) Mass spectrometry imaging with high resolution in mass and space. Histochem Cell Biol 139:759–783
22. Dugo P, Cacciola F, Kumm T, Dugo G, Mondello L (2008) Comprehensive multidimensional liquid chromatography: theory and applications. J Chromatogr A 1184:353–368

23. François I, Sandra K, Sandra P (2009) Comprehensive liquid chromatography: Fundamental aspects and practical considerations—a review. Anal Chim Acta 641:14–31
24. Česla P, Hájek T, Jandera P (2009) Optimization of two-dimensional gradient liquid chromatography separations. J Chromatogr A 1216: 3443–3457
25. D'Attoma A, Grivel C, Heinisch S (2012) On-line comprehensive two-dimensional separations of charged compounds using reversed-phase high performance liquid chromatography and hydrophilic interaction chromatography. Part I: orthogonality and practical peak capacity considerations. J Chromatogr A 1262:148–159
26. Jandera P, Hájek T, Staňková M, Vyňuchalová K, Česla P (2012) Optimization of comprehensive two-dimensional gradient chromatography coupling in-line hydrophilic interaction and reversed phase liquid chromatography. J Chromatogr A 1268:91–101
27. Lísa M, Cífková E, Holčapek M (2011) Lipidomic profiling of biological tissues using off-line two-dimensional high-performance liquid chromatography mass spectrometry. J Chromatogr A 1218:5146–5156
28. Holčapek M, Velínská H, Lísa M, Česla P (2009) Orthogonality of silver-ion and non-aqueous reversed-phase HPLC/MS in the analysis of complex natural mixtures of triacylglycerols. J Sep Sci 32:3672–3680
29. Dugo P, Kumm T, Crupi ML, Cotroneo A, Mondello L (2006) Comprehensive two-dimensional liquid chromatography combined with mass spectrometric detection in the analyses of triacylglycerols in natural lipidic matrixes. J Chromatogr A 1112:269–275
30. Yang Q, Shi X, Gu Q, Zhao S, Shan Y, Xu G (2012) On-line two dimensional liquid chromatography/mass spectrometry for the analysis of triacylglycerides in peanut oil and mouse tissue. J Chromatogr B 895–896:48–55
31. Ling YS, Liang HJ, Lin MH, Tang CH, Wu KY, Kuo ML, Lin CY (2014) Two-dimensional LC-MS/MS to enhance ceramide and phosphatidylcholine species profiling in mouse liver. Biomed Chromatogr 28:1284–1293
32. Sun C, Zhao Y-Y, Curtis JM (2014) Elucidation of phosphatidylcholine isomers using two dimensional liquid chromatography coupled in-line with ozonolysis mass spectrometry. J Chromatogr A 1351:37–45
33. Dugo P, Fawzy N, Cichello F, Cacciola F, Donato P, Mondello L (2013) Stop-flow comprehensive two-dimensional liquid chromatography combined with mass spectrometric detection for phospholipid analysis. J Chromatogr A 1278:46–53
34. Wang SY, Li J, Shi XZ, Qiao LZ, Lu X, Xu GW (2013) A novel stop-flow two-dimensional liquid chromatography-mass spectrometry method for lipid analysis. J Chromatogr A 1321:65–72
35. Li M, Feng BS, Liang Y, Zhang W, Bai Y, Tang W, Wang T, Liu HW (2013) Lipid profiling of human plasma from peritoneal dialysis patients using an improved 2D (NP/RP) LC-QToF MS method. Anal Bioanal Chem 405:6629–6638
36. Bang DY, Moon MH (2013) On-line two-dimensional capillary strong anion exchange/reversed phase liquid chromatography-tandem mass spectrometry for comprehensive lipid analysis. J Chromatogr A 1310:82–90
37. Liebisch G, Vizcaino JA, Kofeler H, Trotzmuller M, Griffiths WJ, Schmitz G, Spener F, Wakelam MJO (2013) Shorthand notation for lipid structures derived from mass spectrometry. J Lipid Res 54: 1523–1530
38. Folch J, Lees M, Stanley GHS (1957) A simple method for the isolation and purification of total lipides from animal tissues. J Biol Chem 226:497–509
39. Holčapek M, Jandera P, Fischer J, Prokeš B (1999) Analytical monitoring of the production of biodiesel by high-performance liquid chromatography with various detection methods. J Chromatogr A 858:13–31
40. Holčapek M, Jandera P, Zderadička P, Hrubá L (2003) Characterization of triacylglycerol and diacylglycerol composition of plant oils using high-performance liquid chromatography–atmospheric pressure chemical ionization mass spectrometry. J Chromatogr A 1010:195–215
41. Lísa M, Holčapek M (2008) Triacylglycerols profiling in plant oils important in food industry, dietetics and cosmetics using high-performance liquid chromatography–atmospheric pressure chemical ionization mass spectrometry. J Chromatogr A 1198–1199:115–130
42. Berdeaux O, Juaneda P, Martine L, Cabaret S, Bretillon L, Acar N (2010) Identification and quantification of phosphatidylcholines containing very-long-chain polyunsaturated fatty acid in bovine and human retina using liquid chromatography/tandem mass spectrometry. J Chromatogr A 1217:7738–7748

Michal Holčapek is currently a Full Professor and Head of the Mass Spectrometry Group in the Department of Analytical Chemistry, University of Pardubice. His research interests are mass spectrometry and its coupling with liquid-phase separation techniques, with specialization in lipidomic analysis and clinical applications. He is the author or co-author of over 100 articles in international peer-reviewed journals, and has an *h* index of 30.

Magdaléna Ovčačíková is a PhD student in the Mass Spectrometry Group in the Department of Analytical Chemistry, University of Pardubice. She is working on the characterization of lipids in biological samples using liquid chromatography–mass spectrometry coupling.

Miroslav Lísa is a Research Worker in the Department of Analytical Chemistry, University of Pardubice. He is working mainly on the development of new methods for the analysis of lipids using mass spectrometry and its coupling with high-performance liquid chromatography and supercritical fluid chromatography.

Tomáš Hájek is an Assistant Professor in the Department of Analytical Chemistry, University of Pardubice. His research interests are the development of online two-dimensional liquid chromatography, and the prediction and optimization of high-performance liquid chromatography separations.

Eva Cífková is a Research Worker in the Department of Analytical Chemistry, University of Pardubice. She focuses on the development of new mass-spectrometry-based methods for comprehensive lipidomic analysis and applications in biomarker discovery.

Journal of Chromatography A, 1450 (2016) 76–85

Contents lists available at ScienceDirect

Journal of Chromatography A

journal homepage: www.elsevier.com/locate/chroma

Retention behavior of lipids in reversed-phase ultrahigh-performance liquid chromatography–electrospray ionization mass spectrometry

Magdaléna Ovčačíková, Miroslav Lísa, Eva Cífková, Michal Holčapek*

University of Pardubice, Faculty of Chemical Technology, Department of Analytical Chemistry, Studentská 573, 53210 Pardubice, Czech Republic

ARTICLE INFO

Article history:
Received 4 March 2016
Received in revised form 10 April 2016
Accepted 29 April 2016
Available online 3 May 2016

Keywords:
Lipids
Lipidomics
Ultrahigh-performance liquid chromatography
Mass spectrometry
Human plasma
Retention behavior

ABSTRACT

Reversed-phase ultrahigh-performance liquid chromatography (RP-UHPLC) method using two 15 cm sub–2 μm particles octadecylsilica gel columns is developed with the goal to separate and unambiguously identify a large number of lipid species in biological samples. The identification is performed by the coupling with high-resolution tandem mass spectrometry (MS/MS) using quadrupole – time-of-flight (QTOF) instrument. Electrospray ionization (ESI) full scan and tandem mass spectra are measured in both polarity modes with the mass accuracy better than 5 ppm, which provides a high confidence of lipid identification. Over 400 lipid species covering 14 polar and nonpolar lipid classes from 5 lipid categories are identified in total lipid extracts of human plasma, human urine and porcine brain. The general dependences of relative retention times on relative carbon number or relative double bond number are constructed and fit with the second degree polynomial regression. The regular retention patterns in homologous lipid series provide additional identification point for UHPLC/MS lipidomic analysis, which increases the confidence of lipid identification. The reprocessing of previously published data by our and other groups measured in the RP mode and ultrahigh-performance supercritical fluid chromatography on the silica column shows more generic applicability of the polynomial regression for the description of retention behavior and the prediction of retention times. The novelty of this work is the characterization of general trends in the retention behavior of lipids within logical series with constant fatty acyl length or double bond number, which may be used as an additional criterion to increase the confidence of lipid identification.

1. Introduction

Lipids fulfill multiple essential roles within all eukaryotic cells in living organisms [1]. Living cells contain thousands of different lipid molecules that fall into eight lipid categories according to LIPID MAPS classification, namely fatty acyls, glycerolipids (GL), glycerophospholipids (GP), sphingolipids (SP), sterol lipids (ST), prenol lipids, saccharolipids and polyketides [1–5] containing many classes and subclasses. The dysregulation of the lipid metabolism contributes to numerous serious human diseases, such as obesity, diabetes, cardiovascular diseases and cancer. Therefore, they are investigated as possible biomarkers of these diseases [6–9].

Lipidomic analysis starts with the liquid – liquid lipid extraction from biological materials using organic solvents. The most frequently used extraction procedures are based on chloroform – methanol – water systems according to Folch et al. [10] or Bligh and Dyer [11], or the extraction using methyl *tert*-butyl ether solvent instead of chloroform [12]. Gas chromatography–mass spectrometry is an established approach for fatty acyl profiling [13]. Various analytical strategies are used in the lipidomic analysis using nontargeted and targeted lipidomic approaches [14–18]. Another possible division of lipidomic approaches is according to used analytical methodology. Shotgun lipidomics using triple quadrupole instruments and characteristic precursor ion and neutral loss scans [19–21] is well established approach for the fast quantitation of lipid molecular species from extracts of biological samples without a chromatographic separation. The second approach is the use of liquid chromatography–mass spectrometry (LC/MS) coupling, where various chromatographic modes can be selected depending on the required type of separation, such as reversed-phase (RP) LC [22–25], normal-phase (NP) LC [26,27], hydrophilic interaction liquid chromatography (HILIC) [14,15], silver-ion LC [13,28,29] and chiral LC [30,31]. The RP separation mode coupled with MS is widely used in a comprehensive lipidomic analysis to identify individual molecular species in different biological samples [22,32–34], where lipids are separated according to the length of fatty acyl chains and

* Corresponding author.
E-mail address: Michal.Holcapek@upce.cz (M. Holčapek).

http://dx.doi.org/10.1016/j.chroma.2016.04.082
0021-9673/

the number and position of double bonds (DB) [22]. In the RP mode, mobile phases are typically composed of mixture of water containing volatile buffers and polar organic solvents, such as methanol, acetonitrile and 2-propanol. RP mode provides intra- and interclass separation of lipid species, especially in ultrahigh-performance liquid chromatography (UHPLC) configuration [22], but on the other hand the quantitation is more demanding, because the lipid class internal standards do not coelute with analytes unlike the lipid class separation in HILIC or NP modes. NP-LC is particularly suitable for the separation of nonpolar lipid classes, where individual nonpolar lipid classes are separated based on their polarity [27]. HILIC separation allows the lipid class separation, where individual lipid classes are separated according to their polarity and electrostatic interactions [14,15]. HILIC and RP modes have relatively good complementarity of retention mechanisms, therefore various modes of their 2D-LC coupling have been already applied for the lipidomic analysis [35–37]. The HILIC-like separation can be also achieved in ultrahigh-performance supercritical fluid chromatography (UHPSFC) on silica columns, but with shorter analysis time and more efficient separation [38]. The silver-ion LC is a special chromatographic mode based on the formation of weak reversible complexes of silver ions with π electrons of DB, which enables the resolution of triacylglycerols (TG) and diacylglycerols (DG) isomers differing in the number, positions and geometry of DB [13,28,29]. The most demanding separation task is a chiral resolution, which has been applied to TG enantiomers [30,31].

The main goal of our work is the study of the retention behavior of individual lipids in RP-UHPLC to describe general dependences of retention times on the carbon number (CN) and the DB number. For this purpose, RP-UHPLC method with two C18 columns in series is optimized and coupled to high-resolution MS/MS to unambiguously identify the large number of lipids. The retention data are collected for lipid extracts of human plasma, human urine and porcine brain samples. Individual lipid species are identified based on accurate *m*/*z* values of their molecular adducts and characteristic fragment ions in their MS/MS spectra measured in positive- and negative-ion modes. Relative dependences of retention times on the CN or the DB number are fitted with the second degree polynomial regressions.

2. Material and methods

2.1. Chemicals and standards

Acetonitrile, 2-propanol, methanol, (all LC/MS gradient grade), hexane (HPLC grade), chloroform (HPLC grade, stabilized by 0.5–1% ethanol), ammonium acetate, sodium chloride, sodium methoxide, standards of cholest-5-en-3ß-yl octadecanoate [cholesteryl ester (CE) 18:1] and 3ß-hydroxy-5-cholestene [cholesterol (Chol)] were purchased from Sigma-Aldrich (St. Louis, MO, USA). Deionized water was prepared with a Milli-Q Reference Water Purification System (Molsheim, France). Standards of polar lipid classes containing C18:1(9Z) fatty acyl(s), lysophosphatidylcholine (LPC), lysophosphatidylethanolamine (LPE), phosphatidylserine (PS), phosphatidylglycerol (PG), phosphatidic acid (PA), phosphatidylcholine (PC), phosphatidylethanolamine (PE), sphingomyelin (SM), ceramide (Cer), and sphingomyelin (SM d18:1/12:0), ceramide (Cer d18:1/12:0), cholesteryl (d7) ester (Chol d7 16:0) and oleic acid-d9 (FA d9 18:1) were purchased from Avanti Polar Lipids (Alabaster, AL, USA). Nonpolar lipid standards of TG 18:1/18:1/18:1, TG 19:1/19:1/19:1 and DG 18:1/18:1 were purchased from Nu-Chek Prep (Elysian, MN, USA). The lipid nomenclature follows the shorthand notation for lipid structures published by Liebisch et al. [39] and the LIPID MAPS [2] classification system. Samples of human plasma and urine were obtained from healthy volunteers from the research team. Porcine brain was obtained from the local store.

2.2. Sample preparation

Blood was collected to heparin-lithium tubes and ultracentrifuged to obtain plasma. The total lipid extracts of human plasma, human urine and porcine brain tissue were prepared according to Folch procedure [10] using the chloroform – methanol – water solvent system with minor modifications [14,15]. Human plasma (50 μL) was homogenized with 3 mL of the chloroform – methanol (2:1, v/v) mixture, while porcine brain tissue (50 mg) and human urine (2 mL) were homogenized with 6 mL of the chloroform-methanol mixture (2:1, v/v) in the ultrasonic bath at 40 °C for 10 min. Then, deionized water (600 μL for human plasma and 1200 μL for porcine brain) was added (no additional water for human urine), and the mixture was centrifuged at 3000 rpm for 3 min under ambient conditions. The chloroform (bottom) layer containing lipids was collected, evaporated by a gentle stream of nitrogen and redissolved in 1 mL of the chloroform – 2-propanol (1:1, v/v) mixture for the RP-UHPLC/ESI-MS analysis.

2.3. RP-UHPLC conditions

Experiments were performed with an Agilent 1290 Infinity series (Agilent Technologies, Santa Clara, CA, USA). Two identical Acquity UPLC BEH C_{18} columns (150 mm × 2.1 mm, 1.7 μm, Waters, Milford, MA, USA) were coupled in series and used for the separation of total lipid extracts under the following conditions. Flow rate 180 μL/min, injection volume 2 μL, column temperature 40 °C, mobile phase gradient 0 min – 21.5% of solvent A and 78.5% of solvent B, 160 min – 100% of solvent B, where solvent A was 5 mmol/L aqueous ammonium acetate and solvent B was the mixture of 99.5% of acetonitrile – 2-propanol (1:2, v/v) and 0.5% water, the concentration of ammonium acetate in solvent B was also 5 mmol/L. The system backpressure reached 1000 bar during the gradient analysis.

2.4. ESI-MS conditions

The hybrid QTOF mass spectrometer (micrOTOF-Q, Bruker Daltonics, Bremen, Germany) with an ESI source was used as the detector under the following conditions: capillary voltage 4.5 kV, nebulizing gas pressure 1.0 bar, drying gas flow rate 8 L/min and drying gas temperature 200 °C. ESI mass spectra were measured in the range of *m*/*z* 50–1500 in positive- and negative-ion modes. Argon as the collision gas at the collision energy of 20–25 eV was used for MS/MS experiments. MS/MS spectra are recorded in both polarity modes using the data independent mode for all ions exceeding the instrumental intensity threshold of 10^4. The external calibration of the mass scale was performed with sodium formate clusters before individual measurements together with the internal recalibration using the most abundant known lipids. The data were acquired using the DataAnalysis software (Bruker Daltonics).

3. Results and discussion

3.1. RP-UHPLC separation of lipids

The goal of our RP-UHPLC analysis is the identification of the large number of lipid species, which is then used for the study of the retention behavior of individual lipids in logical series with the constant number of carbon atoms or DB. For this purpose, we have selected the coupling of two 15 cm C18 columns with sub–2 μm particles (150 mm × 2.1 mm, 1.7 μm) and aqueous ammonium acetate – acetonitrile – 2-propanol gradient, which

Table 1
Numbers of identified lipids in studied biological samples.

Lipid class	Human plasma	Human urine	Porcine brain	Total
FA	31	20	39	39
LPC	10	0	8	11
LPE	5	0	6	6
SM	33	1	21	33
PI	13	0	6	13
PG	1	0	5	6
PE	30	18	28	33
PC	50	2	40	57
Sulfatides	0	0	7	7
Cer	0	0	13	13
HexCer	0	0	12	12
DG	12	0	11	15
Chol + SE	22	0	9	22
TG	139	6	106	149
Total	346	47	311	416

provided the best performance in our previous work on 2D-LC/MS using single C18 column in the first dimension [35]. Optimized conditions with two C18 columns (details in Section 2) result in higher peak capacity ($P_C = 377$ calculated as $Pc = 1 + (t_g/1.7 \times w_{1/2})$ [40]) in comparison to one C18 column ($P_C = 140$) [40]. The number of real identifications in case of optimized RP separation (416) is 10% higher than the theoretical peak capacity due to the use of reconstructed ion currents. The analysis time of 160 min is acceptable for the study of retention behavior but not for the routine lipidomic analysis, where faster gradients on shorter columns are preferred.

Individual lipid species are separated in the RP mode according to the CN and the DB number, which is defined as the equivalent carbon number (ECN) and calculated as the total CN of all fatty acyls minus two times the DB number (ECN = CN-2DB). The ECN model has been initially developed for TG and other nonpolar lipids [41–43], but it is also applicable for polar lipid classes [35,44]. Few exceptions from this rule can be observed for phospholipids containing the combination of highly polyunsaturated and saturated fatty acyls, which are retained more strongly and elute in higher ECN groups, *e.g.*, PC 18:0/20:5 and PC 18:0/22:6 (both with ECN 28) elute in the group with ECN 30. The similar behavior is observed for all polar lipid classes in RP-UHPLC. Polar lipid classes (FA, LPC, LPE, SM, PI, PG, PE, PC, sulfatides, Cer, and HexCer) and DG are eluted over a broad range of retention times. Nonpolar lipids (CE and TG) have the highest retention in the RP mode, while the most polar lysophospholipids are retained the least (Fig. 1 and Table S1).

3.2. Identification of individual lipids using RP-UHPLC/ESI-MS

The identification of individual lipids is based on our previous experiences with retention, ionization and fragmentation behavior of various classes of lipids [6,14,15,35,38,44,45]. Table S1 lists only unambiguously identified lipids based on retention behavior characteristics, accurate *m/z* values (better than 5 ppm in most cases) and characteristic fragmentation behavior in both polarity modes. In total, 416 lipid species from 14 lipid classes including FA, LPC, LPE, SM, PI, PG, PE, PC, sulfatides, Cer, HexCer, DG, Chol, CE and TG have been positively identified in total lipid extracts of human plasma, human urine and porcine brain (Tables 1 and S1). The Venn's diagram shows differences among studied samples, how many lipids are shared among individual matrices and what identifications are unique for some samples (Fig. S2). The lipid species level (*e.g.*, PE 36:4) is the first annotation style based just on retention times and accurate *m/z* values in full-scan mass spectra. The fatty acyl/alkyl level (*e.g.*, PE 16:0_20:4) is used when the information of attached fatty acyls is known from MS or MS/MS spectra, but without *sn*-differentiation. The slash separator (*e.g.*, PE 16:0/20:4) indicates the known preference of *sn*-position according to the shorthand lipid notation recommended by Liebisch et al. [39]. Reported lipids are also correlated with our previous papers on the lipidomic characterization of biological tissues [6,44,45] and body fluids [38] to confirm the identification and avoid any error in the list of identified lipids.

The identification of FA, PI, PE, sulfatides and PG classes is based on deprotonated molecules $[M-H]^-$ in negative-ion ESI mass spectra. The characteristic fragment ion for lipid classes containing choline moiety (LPC, SM and PC) is *m/z* 184 in the positive-ion mode. Further observed ions for lipid classes containing choline moiety are protonated $[M+H]^+$ and sodiated $[M+Na]^+$ molecules in the positive-ion mode. The neutral loss of $\Delta m/z$ 141 is typical for positive-ion ESI mass spectra of PE, while negative-ion ESI-MS/MS provides information on the position of attached fatty acyls based on the ratio of $[R_1COO]^-/[R_2COO]^-$ ions, where $[R_2COO]^-$ ion is more abundant. This ratio is changed for the combination of saturated and highly polyunsaturated (C20:5 or C22:6) fatty acyls in PE due to the formation of $[R_i]^-$ ions from $[R_iCOO]^-$ ions caused by the neutral loss of carbon dioxide [46]. This approach is used for other phospholipid classes as well, as discussed in more details in our previous works [14,15]. The regioisomeric determination of lysophospholipids (LPL) is based on the knowledge of retention order of 1-LPL and 2-LPL standards. Observed ions for DG are protonated $[M+H]^+$ and sodiated $[M+Na]^+$ molecules and loss of water $[M+H-H_2O]^+$ in the positive-ion mode. The characteristic fragment ion for lipid species containing cholesterol (Chol and CE) is *m/z* 369. ESI mass spectra of Cer and HexCer exhibit characteristic ions related to the type of base, *e.g.*, *m/z* 264 for 18:1 and *m/z* 266 for 18:0, which enables the accurate identification of fatty acyl position. The interpretation of positive-ion ESI mass spectra of TG is based on $[M+NH_4]^+$ and $[M+H-R_iCOOH]^+$ ions. In some cases, more lipids with identical formula are reported with different retention times, such as FA 18:1 (9.8 and 10.4 min), FA 17:0 (10.6 and 11.3 min), FA 21:0 (21.2 and 22.8 min), PC 18:1/22:6, (40.0 and 40.6 min), PC 16:0/20:4 (41.0 and 44.0 min), *etc.* The most likely explanation for observed isomers is different positions of DB for unsaturated fatty acyls and branching for saturated fatty acyls, but we cannot report this information in tables due to missing verification with standards.

Fig. S1 shows TIC chromatograms of RP-UHPLC/ESI-MS analysis of the lipid standard mixture in positive-ion (Fig. S1A) and negative-ion (Fig. S1B) modes. The lipid standard mixture contains CE, Cer, Chol, DG, FA, GlcCer, LacCer, LPC, LPE, PA, PC, PE, PG, PS, SM and TG lipid class representatives with 18:1 fatty acyls and it is used throughout this work for the method development. Table S2 reports the major ions for individual lipid classes observed in both polarity modes. Fig. 1 depicts TIC chromatograms of measured lipid extracts: **A/**human plasma containing 11 lipid classes (FA, LPC, LPE, SM, PI, PG, PE, PC, DG, CE and TG), **B/**human urine containing 5 lipid classes (FA, SM, PE, PC and TG), and **C/**porcine brain containing 14 lipid classes (FA, LPC, LPE, SM, PI, PG, PE, PC, sulfatides, Cer, HexCer, DG, CE and TG). The porcine brain extract is selected due to known lipidomic complexity, which yields the detection of additional lipid classes not occurring in other studied samples, *i.e.,* sulfatides, Cer and HexCer. The type of glycosylation cannot be determined, therefore HexCer annotation is used instead of GluCer for the standard. These RP conditions with very long gradient time are purposely selected for the description of retention behavior of various lipid classes, but our conclusions are also applicable for shorter gradients used in the routine lipid analysis. This identification list will be used as the supporting information in our future quantitative lipidomic studies using either faster UHPLC/MS or shotgun MS approaches.

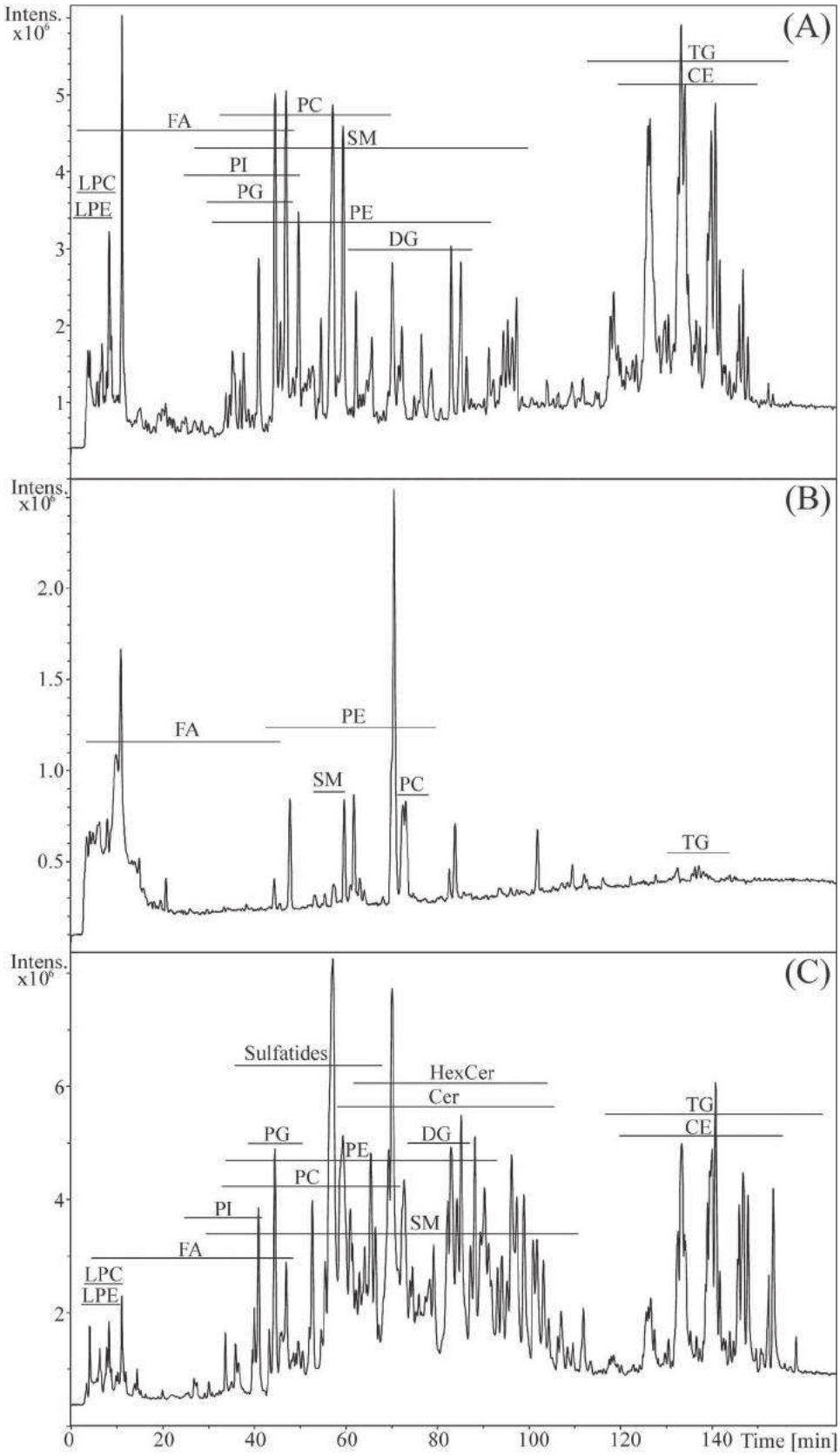

Fig. 1. Positive-ion RP-UHPLC/ESI-MS total ion current chromatograms of total lipid extracts of: (**A**) human plasma, (**B**) human urine, and (**C**) porcine brain. Conditions: two Acquity UPLC BEH C_{18} columns (150 mm × 2.1 mm, 1.7 μm) coupled in series, flow rate 180 μL/min, injection volume 2 μL, column temperature 40 °C, mobile phase gradient of acetonitrile, 2-propanol and 5 mmol/L aqueous ammonium acetate (other details in Material and methods). FA are detected only in the negative-ion mode. *Abbreviations:* CE – cholesteryl ester, Cer – ceramide, DG – diacylglycerol, FA – fatty acid, HexCer – hexosyl ceramide, LPC – lysophosphatidylcholine, LPE – lysophosphatidylethanolamine, PC – phosphatidylcholine, PE – phosphatidylethanolamine, PI – phosphatidylinositol, PG – phosphatidylglycerol, SM – sphingomyelin, and TG – triacylglycerol.

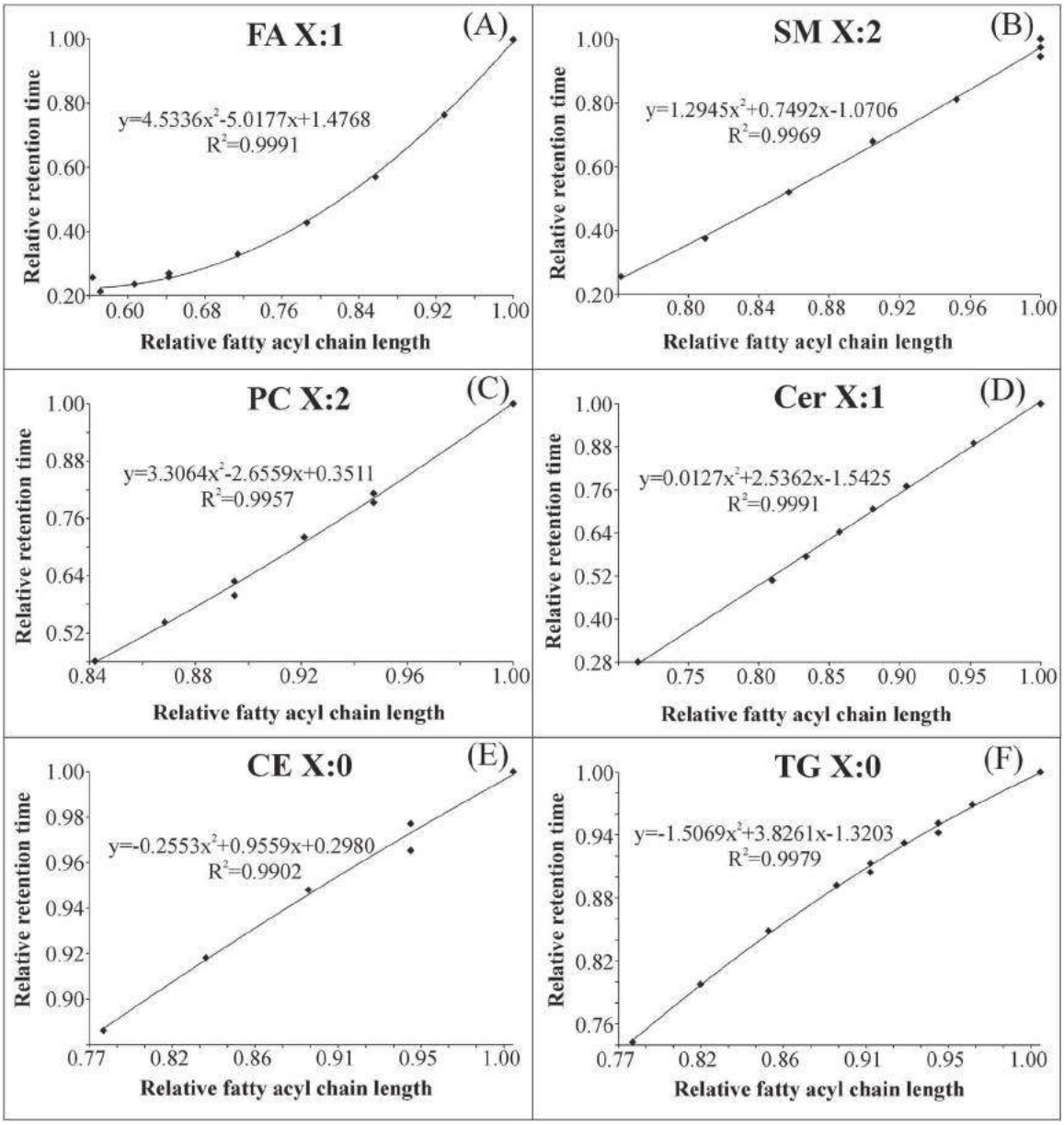

Fig. 2. Plots of polynomial dependences of relative retention times of lipids on the relative CN: (**A**) FA X:1 (X is from 16 to 28), (**B**) SM X:2 (X is from 32 to 42), (**C**) PC X:2 (X is from 32 to 38), (**D**) Cer X:1 (X is from 34 to 42), (**E**) CE X:0 (X is from 14 to 18), and (**F**) TG X:0 (X is from 42 to 54).

3.3. Study of retention behavior of various lipid classes

For all lipid classes studied, dependences of retention times on the CN (X) or the DB number (Y) can be fitted with the second degree polynomial regression $y = ax^2 + bx + c$. These curves can be plotted either as retention times *vs.* CN (or DB number) or as relative retention times *vs.* relative CN (or relative DB number). The use of relative units is more universal, because coefficients of polynomial regression do not depend on the column length or diameter. The highest value in a particular plot is equal to 1.00 and other values are recalculated. Typical dependences are shown in Fig. 2 for dependences on the CN for **A**/FA X:1, **B**/SM X:2, **C**/PC X:2, **D**/Cer X:1, **E**/CE X:0, and **F**/TG X:0. Table 2 shows that correlation coefficients R^2 are mostly better than 0.99, especially for curves containing more data points. Fig. 3 and Table 3 summarize results of dependences on DB number for: A/FA 18:Y, B/PI 36:Y, C/PE 40:Y, D/PC 34:Y, E/CE 18:Y, and F/TG 56:Y. Correlation coefficients are slightly worse for DB dependences, which is caused by a lower number of data points per curve compared to fatty acyl chain dependences and also multiple points caused by lipids with identical CN:DB composition but different fatty acyl composition. Polynomial equations still enable satisfactory prediction of retention times, because relative errors of retention time calculations using polynomial equations are better than 5%, which confirms the applicability of polynomial regressions as the supplementary identification criterion in addition to MS data.

Polynomial equations can be also applied for the prediction of retention times of missing lipids in their logical series. Fig. 4 shows an illustration how this approach can be used for the identification of unknown lipid inside the measured series. These lipid standards are not occurring in measured biological samples, therefore these standards are added and then experimental retention times are correlated with predicted retention times with relative errors lower than 5%, as illustrated on the example of TG 19:1/19:1/19:1 (Fig. 4**A**). Mass accuracies of molecular adducts (Fig. 4**B**) and product ions (Fig. 4**C**) are better than 5 ppm, which results in very high confidence of such identification. Other examples are shown in

Table 2
Parameters of polynomial regressions $y = ax^2 + bx + c$ of relative retention times of individual lipid series on the relative CN.

Lipid series	a	b	c	R^2	X
FA X:0	3.7991	−3.8555	1.0368	0.9949	12, 14, 15, 16, 17, 18, 20, 21,22, 23, 24, 25, 26
FA X:1	4.5336	−5.0177	1.4768	0.9991	16, 17, 18, 20, 22, 24, 26, 28
FA X:3	6.9790	−9.0233	3.0443	0.9910	18, 20, 22
SM X:0	−1.2578	5.3851	−3.1273	1.0000	34, 36, 40
SM X:1	0.3365	2.1286	−1.4651	0.9960	30, 32, 33, 34, 36, 38, 39, 40, 41, 42, 43
SM X:2	1.2945	0.7492	−1.0706	0.9969	32, 34, 36, 38, 40, 42
PI X:1	21.0477	−35.6225	15.5747	1.0000	32, 34, 36
PE X:1	−6.9475	15.1790	−7.2317	1.0000	34, 36, 40
PE X:2	−2.2415	7.0608	−3.8193	1.0000	34, 36, 40
PE X:4	−11.2849	24.7328	−12.4479	1.0000	36, 38, 40
PE X:5	3.0113	−1.6411	−0.3695	0.9999	36, 38, 40, 42
PE X:6	44.5140	−82.0360	38.5210	1.0000	38,40,42
PC X:1	6.2750	−8.6052	3.3241	0.9952	32, 34, 36
PC X:2	3.3064	−2.6559	0.3511	0.9957	32, 33, 34, 35, 36, 38
PC X:3	6.3464	−8.0278	2.6421	0.9626	34, 36, 38
PC X:4	−8.3879	19.8431	−10.4552	0.9458	36, 38, 40
Sulfatides X:1	1.6537	0.4987	−1.1487	1.0000	36, 38, 41, 42
Sulfatides X:2	−1.5463	6.9934	−4.4471	1.0000	42, 43, 44
Cer X:1	0.0127	2.5362	−1.5425	0.9991	34, 35, 36, 37, 38, 40, 42
Cer X:2	−2.7252	7.9161	−4.1909	1.0000	36, 38, 42
HexCer X:0	1.4186	−1.3316	0.9035	0.9620	36, 40, 42, 44
CE X:0	−0.2553	0.9559	0.2980	0.9902	14, 15, 16, 17, 18
CE X:1	−0.2321	0.9920	0.2383	0.9994	14, 16, 17, 18
TG X:0	−1.5069	3.8261	−1.3203	0.9979	42, 44, 46, 48, 49, 50, 51, 52, 54
TG X:1	−1.7123	4.2233	−1.5138	0.9921	44, 46, 48, 49, 50, 52, 53, 54, 56
TG X:2	−1.5937	4.0467	−1.4598	0.9930	46, 48, 49, 50, 51, 52, 53, 54, 56, 58
TG X:3	−0.9837	3.0144	−1.0457	0.9787	48, 49, 50, 51, 52, 53, 54, 56, 58
TG X:4	−0.1748	1.8097	−0.6370	0.9219	50, 52, 54, 56
TG X:5	1.6848	−1.6437	0.9517	0.9339	52, 54, 56

Table 3
Parameters of polynomial regressions $y = ax^2 + bx + c$ of relative retention times of individual lipid series on the relative DB number.

Lipid series	a	b	c	R^2	Y
FA 18:Y	0.5002	−1.2249	1.0007	0.9934	0, 1, 2, 3
FA 20:Y	0.8193	−1.6202	0.9707	0.9882	0, 1, 2, 3, 4, 5
FA 22:Y	0.7217	−1.5616	1.0041	0.9998	0, 1, 3, 4, 5, 6
FA 24:Y	1.3396	−2.2112	1.0000	1.0000	0, 1, 6
LPC 18:Y	0.4519	−1.0203	0.9452	0.9799	0, 1, 2
LPE 18:Y	−0.2105	−0.0351	1.0000	1.0000	0, 1, 2
SM 34:Y	−0.1743	−0.1677	1.0000	0.9830	0, 1, 2
SM 40:Y	−0.0247	−0.1926	1.0000	0.9870	0, 1, 2
SM 42:Y	0.1313	−0.5940	1.1834	0.9783	1, 2, 3
PI 36:Y	0.6095	−1.3926	1.3181	0.9863	1, 2, 3, 4
PI 38:Y	0.4390	−1.5755	1.6932	0.9622	3, 4, 5, 6
PE 34:Y	0.0870	−0.4319	1.0000	1.0000	0, 1, 2
PE 36:Y	0.0886	−0.7954	1.1483	0.9725	1, 2, 3, 4, 5
PE 38:Y	0.6683	−1.7895	1.7471	0.9208	3, 4, 5, 6
PE 40:Y	−0.3108	−0.4074	1.0724	0.9977	1, 2, 4, 5, 6, 7
PC 32:Y	0.0229	−0.4313	1.0000	0.9895	0, 1, 2
PC 34:Y	0.1973	−0.6858	0.9998	0.9878	0, 1, 2, 3
PC 36:Y	0.1975	−0.9098	1.1679	0.9830	1, 4, 5
PC 38:Y	0.0965	−0.8828	1.2945	0.9658	2, 3, 4, 5, 6
DG 34:Y	0.0535	−0.3395	1.0000	0.9980	0, 1, 2
DG 36:Y	0.1018	−0.5536	1.1673	0.9978	1, 2, 3
CE 18:Y	0.0210	−0.1889	1.0000	0.9995	0, 1, 2, 3
CE 20:Y	−0.2639	0.1622	0.9977	0.9945	3, 4, 5
TG 46:Y	−0.0151	−0.1126	1.0000	0.9828	0, 1, 2
TG 48:Y	0.0069	−0.1685	1.0002	0.9731	0, 1, 2, 3
TG 50:Y	−0.0221	−0.1716	0.9977	0.9744	0, 1, 2, 3, 4
TG 52:Y	0.0014	−0.2243	0.9999	0.9854	0, 1, 2, 3, 4, 5
TG 54:Y	−0.0160	−0.2182	0.9965	0.9720	0, 2, 3, 4, 5, 6
TG 56:Y	−0.0263	−0.2148	1.0268	0.9856	1, 2, 3, 4, 5, 6, 7

Table S3 for FA d9 18:1 (relative error 2.3%), SM d18:1/12:0 (4.9%), Cer d18:1/12:0 (1.9%) and CE d7 16:0 (1.8%).

The prediction of retention times with defined accuracy better than 5% yields additional identification point together with accurate *m*/*z* values of (de)protonated molecules, molecular adducts and diagnostic fragment ions, which increases the confidence of identification. The regularity in retention times of homologous series is known for long time, but we report here for the first time the well-defined identification criteria for lipids with possible applicability as additional identification point similarly as for LC/MS determination of compounds in forensic toxicology and doping analysis [47].

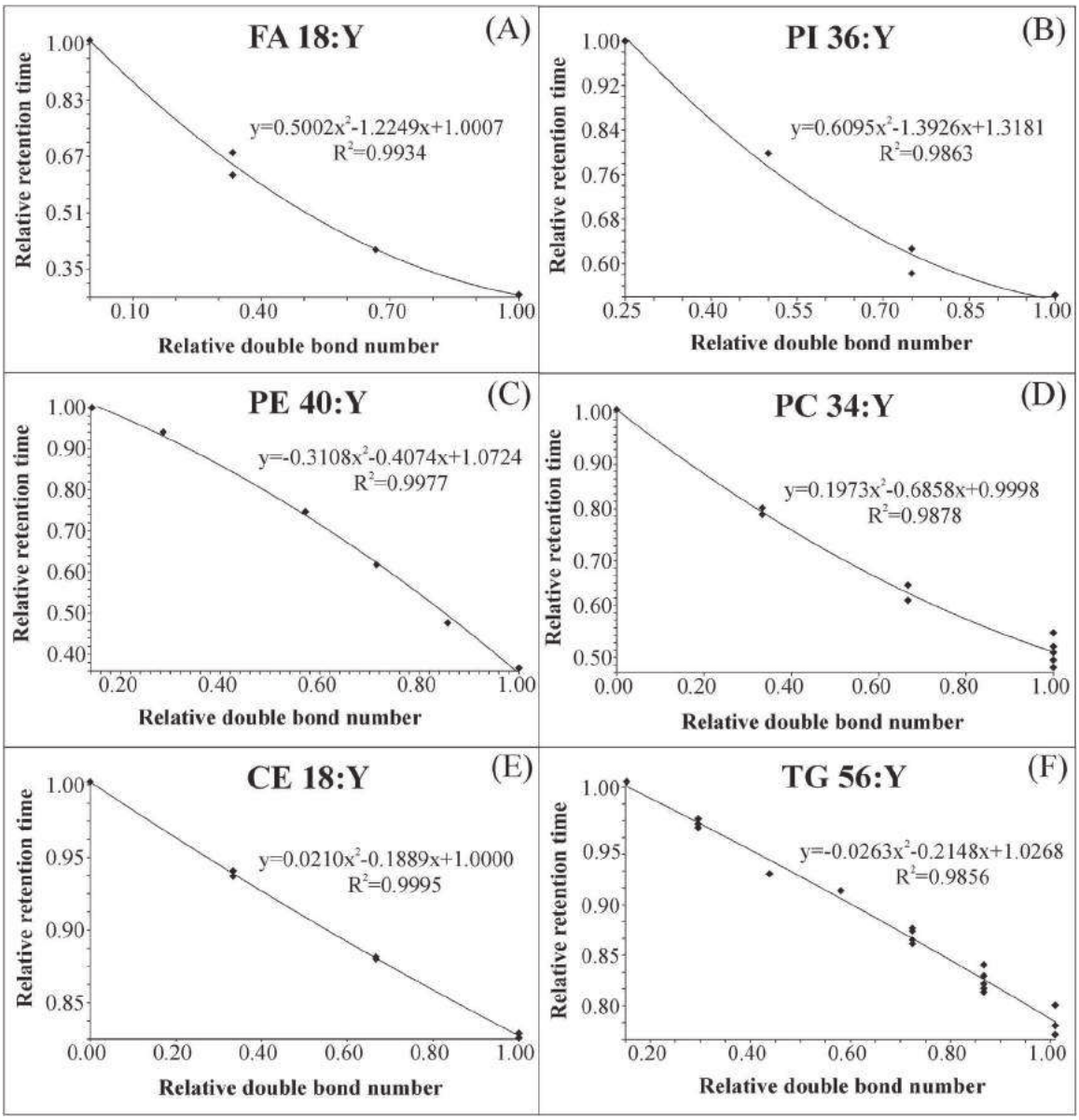

Fig. 3. Plots of polynomial dependences of relative retention times of lipids on the relative DB number: (**A**) FA 18:Y (Y is from 0 to 3), (**B**) PI 36:Y (Y is from 1 to 4), (**C**) PE 40:Y (Y is from 1 to 7), (**D**) PC 34:Y (Y is from 0 to 3), (**E**) CE 18:Y (Y is from 0 to 3), and (**F**) TG 56:Y (Y is from 1 to 7).

3.4. Comparison of retention behavior with other studies

The general applicability of our approach for the construction of retention times dependences has been tested on RP-LC/MS data previously published by a different group [48] and our UHPSFC/MS data [38] obtained by the chromatographic mode with the different retention mechanism. Results are illustrated on examples of **A**/PC X:2, **B**/TG X:1, **C**/PC 38:Y, and **D**/TG 58:Y in Fig. 5, Tables S4 and S5 for RP-LC and of **A**/PC X:1, **B**/TG X:1, **C**/PC 36:Y, and **D**/TG 54:Y in Fig. 6, Tables S6 and S7. Polynomial regressions have a general applicability for the correlation of relative retention times *vs.* the relative CN or relative DB number. In few cases, *a* quadratic coefficients are so small that these curves can be considered as the linear regression. Relative errors in case of UHPSFC data [38] are affected by very small retention times (*ca.* 1 min) and resulting negligible differences among individual TG (in the range of tens of milliseconds), but relative errors of retention time calculation are always better than 5% without any exception. We suggest this approach as other identification point to be generally used in UHPLC/MS and UHPSFC/MS to strengthen the advantage of chromatographic separation for the confident lipidomic identification based on the regularity in retention times of lipid homologous series.

4. Conclusions

The RP-UHPLC/ESI-MS method enables the separation and identification of large number of individual lipid species in human plasma, human urine and porcine brain samples. This method is applied for the study of retention behavior of various polar and nonpolar lipid classes, where polynomial dependences of relative retention times both on relative CN and relative DB number are observed. The regularity in the retention behavior of lipid homologous series is systematically studied, which results in the suggestion of the second degree polynomial regressions for the description of retention patterns of lipid logical series. Polynomial regressions of retention times can be applied as an additional criterion for the identification of unknown lipids in addition to MS and MS/MS data, which increases the confidence of LC/MS identi-

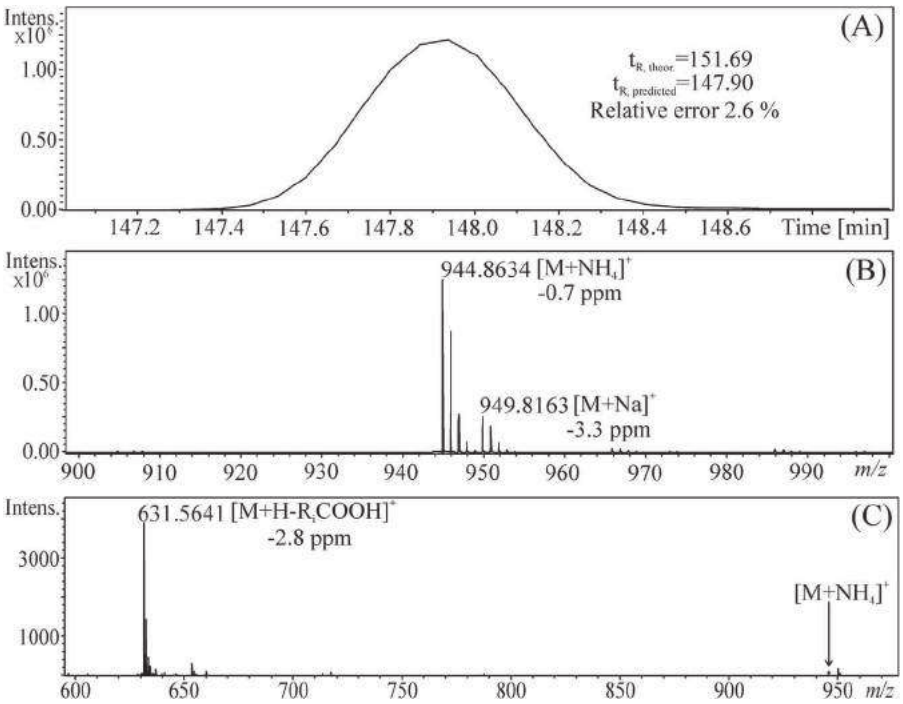

Fig. 4. RP-UHPLC/ESI-MS records of TG 19:1/19:1/19:1 standard: (**A**) reconstructed positive-ion chromatogram, (**B**) ESI-MS spectrum, and (**C**) MS/MS spectrum of $[M+NH_4]^+$ at *m/z* 944.8634.

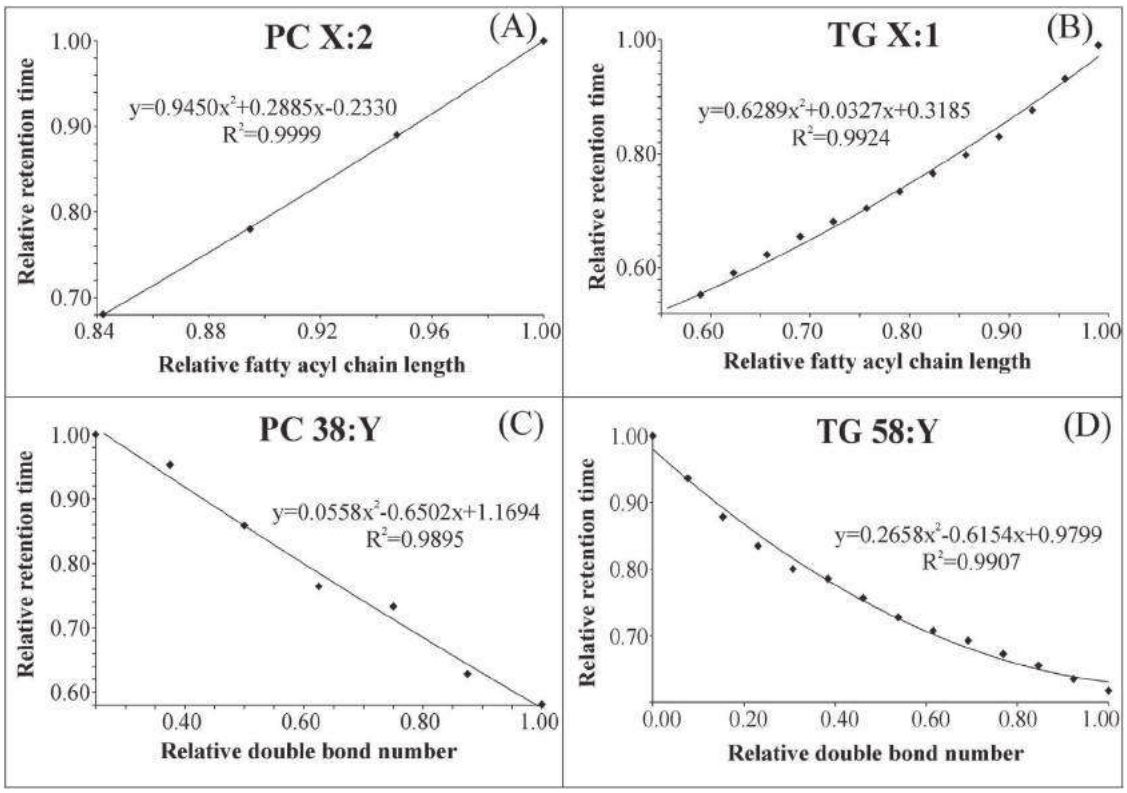

Fig. 5. Plots of polynomial dependences of relative retention times of PC and TG on the relative CN (X) and the relative DB number (Y) from RP-HPLC data [48]: (**A**) PC X:2 (X is from 32 to 38), (**B**) TG X:1 (X is from 34 to 60), (**C**) PC 38:Y (Y is from 2 to 8), and (**D**) TG 58:Y (Y is from 0 to 13).

fication. Another possible application is the prediction of retention times of missing lipids in their logical series, which may bring additional identifications of lipids at expected time windows, which is worthy mainly for trace species or lipids suffering from low ionization efficiencies, because a good quality MS and MS/MS data may not be available in such cases. The logical series with different fatty acyl lengths are based on the higher number of data points and they provide slightly better correlation coefficients, therefore they are recommended as the first choice for the identification.

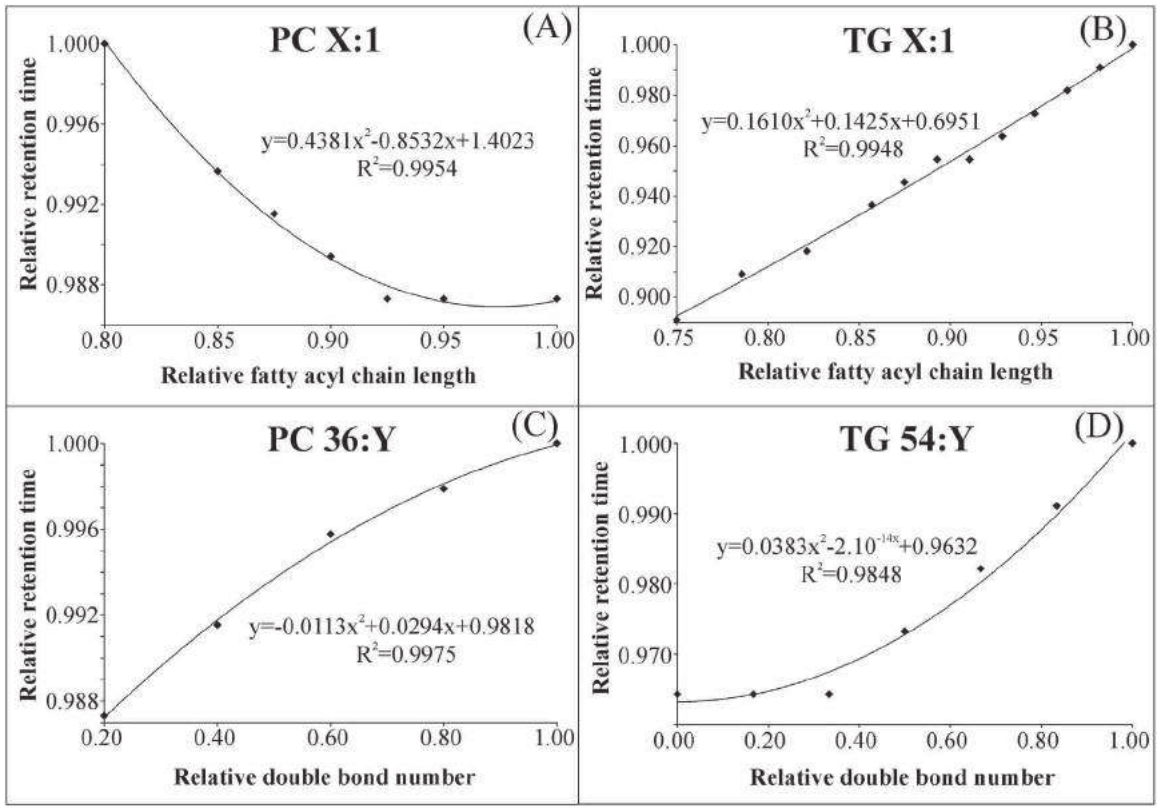

Fig. 6. Plots of polynomial dependences of relative retention times of PC and TG on the relative CN (X) and the relative DB number (Y) from UHPSFC data [38]: (**A**) PC X:1 (X is from 32 to 40), (**B**) TG X:1 (X is from 42 to 56), (**C**) PC 36:Y (Y is from 1 to 5), and (**D**) TG 54:Y (Y is from 0 to 6).

Acknowledgments

This work was supported by the ERC CZ grant project LL1302 sponsored by the Ministry of Education, Youth and Sports of the Czech Republic.

Appendix A. Supplementary data

Supplementary data associated with this article can be found, in the online version, at http://dx.doi.org/10.1016/j.chroma.2016.04.082.

References

[1] G. van Meer, D.R. Voelker, G.W. Feigenson, Membrane lipids: where they are and how they behave, Nat. Rev. Mol. Cell Biol. 9 (2008) 112–124.
[2] LIPID MAPS, LIPID MAPS Lipidomics Gateway, 2016 (accessed 2.01.16.) http://www.lipidmaps.org/.
[3] E. Fahy, S. Subramaniam, H.A. Brown, C.K. Glass, A.H. Merrill, R.C. Murphy, C.R.H. Raetz, D.W. Russell, Y. Seyama, W. Shaw, T. Shimizu, F. Spener, G. van Meer, M.S. VanNieuwenhze, S.H. White, J.L. Witztum, E.A. Dennis, A comprehensive classification system for lipids, Eur. J. Lipid Sci. Technol. 107 (2005) 337–364.
[4] E. Fahy, S. Subramaniam, R.C. Murphy, M. Nishijima, C.R.H. Raetz, T. Shimizu, F. Spener, G. van Meer, M.J.O. Wakelam, E.A. Dennis, Update of the LIPID MAPS comprehensive classification system for lipids, J. Lipid Res. 50 (2009) S9–S14.
[5] O. Quehenberger, A.M. Armando, A.H. Brown, S.B. Milne, D.S. Myers, A.H. Merrill, S. Bandyopadhyay, K.N. Jones, S. Kelly, R.L. Shaner, C.M. Sullards, E. Wang, R.C. Murphy, R.M. Barkley, T.J. Leiker, C.R.H. Raetz, Z.Q. Guan, G.M. Laird, D.A. Six, D.W. Russell, J.G. McDonald, S. Subramaniam, E. Fahy, E.A. Dennis, Lipidomics reveals a remarkable diversity of lipids in human plasma, J. Lipid Res. 51 (2010) 3299–3305.
[6] E. Cífková, M. Holčapek, M. Lísa, D. Vrána, J. Gatěk, B. Melichar, Determination of lipidomic differences between human breast cancer and surrounding normal tissues using HILIC-HPLC/ESI-MS and multivariate data analysis, Anal. Bioanal. Chem. 407 (2015) 991–1002.
[7] M. Holčapek, B. Červená, E. Cífková, M. Lísa, V. Chagovets, J. Vostálová, M. Bancířová, J. Galuszka, M. Hill, Lipidomic analysis of plasma, erythrocytes and lipoprotein fractions of cardiovascular disease patients using UHPLC/MS MALDI-MS and multivariate data analysis, J. Chromatogr. B 990 (2015) 52–63.
[8] C. Hu, R. van der Heijden, M. Wang, J. van der Greef, T. Hankemeier, G. Xu, Analytical strategies in lipidomics and applications in disease biomarker discovery, J. Chromatogr. B 877 (2009) 2836–2846.
[9] J. Suburu, Y.Q. Chen, Lipids and prostate cancer, Prostaglandins Other Lipid Mediators 98 (2012) 1–10.
[10] J. Folch, M. Lees, G.H.S. Stanley, A simple method for the isolation and purification of total lipids from animal tissues, J. Biol. Chem. 226 (1957) 497–509.
[11] E.G. Bligh, W.J. Dyer, A rapid method of total lipid extraction and purification, Can. J. Biochem. Physiol. 37 (1959) 911–917.
[12] V. Matyash, G. Liebisch, T.V. Kurzchalia, A. Shevchenko, D. Schwudke, Lipid extraction by methyl-*tert*-butyl ether for high-throughput lipidomics, J. Lipid Res. 49 (2008) 1137–1146.
[13] M. Lísa, K. Netušilová, L. Franěk, H. Dvořáková, V. Vrkoslav, M. Holčapek, Characterization of fatty acid and triacylglycerol composition in animal fats using silver-ion and non-aqueous reversed-phase high-performance liquid chromatography/mass spectrometry and gas chromatography/flame ionization detection, J. Chromatogr. A 1218 (2011) 7499–7510.
[14] E. Cífková, M. Holčapek, M. Lísa, M. Ovčačíková, A. Lyčka, F. Lynen, P. Sandra, Nontargeted quantitation of lipid classes using hydrophilic interaction liquid chromatography–electrospray ionization mass spectrometry with single internal standard and response factor approach, Anal. Chem. 84 (2012) 10064–10070.
[15] E. Cífková, M. Holčapek, M. Lísa, Nontargeted characterization of porcine organs using hydrophilic interaction liquid chromatography and off-line two-dimensional liquid chromatography–electrospray ionization mass spectrometry, Lipids 48 (2013) 915–928.
[16] G. Astarita, A.C. Kendall, E.A. Dennis, A. Nicolaou, Targeted lipidomic strategies for oxygenated metabolites of polyunsaturated fatty acids, Biochim. Biophys. Acta 1851 (2015) 456–468.
[17] M.A. Masood, C. Yuan, J.K. Acharya, T.D. Veenstra, J. Blonder, Quantitation of ceramide phosphorylethanolamines containing saturated and unsaturated sphingoid base cores, Anal. Biochem. 400 (2010) 259–269.
[18] C.S. Ejsing, E. Duchoslav, J. Sampaio, K. Simons, R. Bonner, C. Thiele, K. Ekroos, A. Shevchenko, Automated identification and quantification of glycerophospholipid molecular species by multiple precursor ion scanning, Anal. Chem. 78 (2006) 6202–6214.
[19] X.L. Han, R.W. Gross, Shotgun lipidomics: electrospray ionization mass spectrometric analysis and quantitation of cellular lipidomes directly from crude extracts of biological samples, Mass Spec. Rev. 24 (2005) 367–412.

[20] X. Han, K. Yang, R.W. Gross, Multi-dimensional mass spectrometry-based shotgun lipidomics and novel strategies for lipidomic analyses, Mass Spec. Rev. 31 (2012) 134–178.
[21] C. Papan, S. Penkov, R. Herzog, C. Thiele, T. Kurzchalia, A. Shevchenko, Systematic screening for novel lipids by shotgun lipidomics, Anal. Chem. 86 (2014) 2703–2710.
[22] K. Sandra, A.D. Pereira, G. Vanhoenacker, F. David, P. Sandra, Comprehensive blood plasma lipidomics by liquid chromatography/quadrupole time-of-flight mass spectrometry, J. Chromatogr. A 1217 (2010) 4087–4099.
[23] K. Retra, O.B. Bleijerveld, R.A. van Gesteil, A.G.M. Tielens, J.J. van Hellemond, J.F. Brouwers, A simple and universal method for the separation and identification of phospholipid molecular species, Rapid Commun. Mass Spectrom. 22 (2008) 1853–1862.
[24] M. Beccaria, G. Sullini, F. Cacciola, P. Donato, P. Dugo, L. Mondello, High performance characterization of triacylglycerols in milk and milk-related samples by liquid chromatography and mass spectrometry, J. Chromatogr. A 1360 (2014) 172–187.
[25] P. Dugo, M. Beccaria, N. Fawzy, P. Donato, F. Cacciola, L. Mondello, Mass spectrometric elucidation of triacylglycerol content of *Brevoortia tyrannus* (menhaden) oil using non-aqueous reversed-phase liquid chromatography under ultra high pressure conditions, J. Chromatogr. A 1259 (2012) 227–236.
[26] E. Sokol, R. Almeida, H.K. Hannibal-Bach, D. Kotowska, J. Vogt, J. Baumgart, K. Kristiansen, R. Nitsch, J. Knudsen, C.S. Ejsing, Profiling of lipid species by normal-phase liquid chromatography nanoelectrospray ionization, and ion trap–orbitrap mass spectrometry, Anal. Biochem. 443 (2013) 88–96.
[27] M. Holčapek, E. Cífková, B. Červená, M. Lísa, J. Vostalová, J. Galuszka, Determination of nonpolar and polar lipid classes in human plasma, erythrocytes and plasma lipoprotein fractions using ultrahigh-performance liquid chromatography–mass spectrometry, J. Chromatogr. A 1377 (2015) 85–91.
[28] M. Holčapek, H. Dvořáková, M. Lísa, A.J. Girón, P. Sandra, J. Cvačka, Regioisomeric analysis of triacylglycerols using silver-ion liquid chromatography–atmospheric pressure chemical ionization mass spectrometry: comparison of five different mass analyzers, J. Chromatogr. A 1217 (2010) 8186–8194.
[29] R.O. Adlof, Normal-phase separation effects with lipids on a silver ion high-performance liquid chromatography column, J. Chromatogr. A 764 (1997) 337–340.
[30] M. Lísa, M. Holčapek, Characterization of triacylglycerol enantiomers using chiral HPLC/APCI-MS and synthesis of enantiomeric triacylglycerols, Anal. Chem. 85 (2013) 1852–1859.
[31] T. Řezanka, K. Sigler, Separation of enantiomeric triacylglycerols by chiral-phase HPLC, Lipids 49 (2014) 1251–1260.
[32] R. t'Kindt, L. Jorge, E. Dumont, P. Couturon, F. David, P. Sandra, K. Sandra, Profiling and characterizing skin ceramides using reversed-phase liquid chromatography-quadrupole time-of-flight mass spectrometry, Anal. Chem. 84 (2012) 403–411.
[33] X.L. Gao, Q.B. Zhang, D. Meng, G. Isaac, R. Zhao, T.L. Fillmore, R.K. Chu, J.Y. Zhou, K.Q. Tang, Z.P. Hu, R.J. Moore, R.D. Smith, M.G. Katze, T.O. Metz, reversed-phase capillary ultra-performance liquid chromatography-mass spectrometry (UPLC-MS) method for comprehensive top-down/bottom-up lipid profiling, Anal. Bioanal. Chem. 402 (2012) 2923–2933.
[34] T. Yamada, T. Uchikata, S. Sakamoto, Y. Yokoi, E. Fukusaki, T. Bamba, Development of a lipid profiling system using reverse-phase liquid chromatography coupled to high-resolution mass spectrometry with rapid polarity switching and an automated lipid identification software, J. Chromatogr. A 1292 (2013) 211–218.
[35] M. Holčapek, M. Ovčačíková, M. Lísa, E. Cífková, T. Hájek, Continuous comprehensive two-dimensional liquid chromatography–electrospray ionization mass spectrometry of complex lipidomic samples, Anal. Bioanal. Chem. (2015) 5033–5043.
[36] S.Y. Wang, J. Li, X.Z. Shi, L.Z. Qiao, X. Lu, G.W. Xu, A novel stop-flow two-dimensional liquid chromatography–mass spectrometry method for lipid analysis, J. Chromatogr. A 1321 (2013) 65–72.
[37] P. Dugo, N. Fawzy, F. Cichello, F. Cacciola, P. Donato, L. Mondello, Stop-flow comprehensive two-dimensional liquid chromatography combined with mass spectrometric detection for phospholipid analysis, J. Chromatogr. A 1278 (2013) 46–53.
[38] M. Lísa, M. Holčapek, High-throughput and comprehensive lipidomic analysis using ultrahigh-performance supercritical fluid chromatography–mass spectrometry, Anal. Chem. 87 (2015) 7187–7195.
[39] G. Liebisch, J.A. Vizcaino, H. Köfeler, M. Trotzmüller, W.J. Griffiths, G. Schmitz, F. Spener, M.J.O. Wakelam, Shorthand notation for lipid structures derived from mass spectrometry, J. Lipid Res. 54 (2013) 1523–1530.
[40] U.D. Neue, Theory of peak capacity in gradient elution, J. Chromatogr. A 1079 (2005) 153–161.
[41] M. Holčapek, P. Jandera, J. Fischer, B. Prokeš, Analytical monitoring of the production of biodiesel by high-performance liquid chromatography with various detection methods, J. Chromatogr. A 858 (1999) 13–31.
[42] M. Holčapek, P. Jandera, P. Zderadička, L. Hrubá, Characterization of triacylglycerol and diacylglycerol composition of plant oils using high-performance liquid chromatography–atmospheric pressure chemical ionization mass spectrometry, J. Chromatogr. A 1010 (2003) 195–215.
[43] M. Lísa, M. Holčapek, Triacylglycerols profiling in plant oils important in food industry, dietetics and cosmetics using high-performance liquid chromatography–atmospheric pressure chemical ionization mass spectrometry, J. Chromatogr. A 1198–1199 (2008) 115–130.
[44] M. Lísa, E. Cífková, M. Holčapek, Lipidomic profiling of biological tissues using off-line two-dimensional high-performance liquid chromatography mass spectrometry, J. Chromatogr. A 1218 (2011) 5146–5156.
[45] E. Cífková, M. Holčapek, M. Lísa, D. Vrána, B. Melichar, V. Študent, Lipidomic differentiation between human kidney tumors and surrounding normal tissues using HILIC-HPLC/ESI-MS and multivariate data analysis, J. Chromatogr. B 1000 (2015) 14–21.
[46] O. Berdeaux, P. Juaneda, L. Martine, S. Cabaret, L. Bretillon, N. Acar, Identification and quantification of phosphatidylcholines containing very-long-chain polyunsaturated fatty acid in bovine and human retina using liquid chromatography/tandem mass spectrometry, J. Chromatogr. A 1217 (2010) 7738–7748.
[47] L. Rivier, Criteria for the identification of compounds by liquid chromatography–mass spectrometry and liquid chromatography-multiple mass spectrometry in forensic toxicology and doping analysis, Anal. Chim. Acta 492 (2003) 69–82.
[48] A. Fauland, H. Köfeler, M. Trotzmüller, A. Knopf, J. Hartler, A. Eberl, C. Chitraju, E. Lankmazr, F. Spener, A comprehensive method for lipid profiling by liquid chromatography-ion cyclotron resonance mass spectrometry, J. Lipid Res. 52 (2011) 2315–2322.

Journal of Chromatography A, 1377 (2015) 85–91

Contents lists available at ScienceDirect

Journal of Chromatography A

journal homepage: www.elsevier.com/locate/chroma

Determination of nonpolar and polar lipid classes in human plasma, erythrocytes and plasma lipoprotein fractions using ultrahigh-performance liquid chromatography-mass spectrometry

Michal Holčapek[a,*], Eva Cífková[a], Blanka Červená[a], Miroslav Lísa[a], Jitka Vostálová[b], Jan Galuszka[c]

[a] Department of Analytical Chemistry, Faculty of Chemical Technology, University of Pardubice, Studentská 573, 53210 Pardubice, Czech Republic
[b] Department of Medical Chemistry and Biochemistry, Faculty of Medicine and Dentistry, Palacký University, 77515 Olomouc, Czech Republic
[c] Department of Internal Medicine I–Cardiology, University Hospital Olomouc, IP Pavlova 6, 77520 Olomouc, Czech Republic

ARTICLE INFO

Article history:
Received 14 August 2014
Received in revised form
11 November 2014
Accepted 5 December 2014
Available online 12 December 2014

Keywords:
Lipids
Normal-phase
HILIC
Plasma, Erythrocytes
LC/MS

ABSTRACT

A novel normal-phase (NP) ultrahigh-performance liquid chromatography-mass spectrometry (UHPLC/MS) method is developed for a separation and quantitation of nonpolar lipid classes occurring in human plasma, erythrocytes and plasma lipoprotein fractions. The baseline class separation of cholesteryl esters (CE), cholesterol, triacylglycerols (TG), regioisomers of 1,2- and 1,3-diacylglycerols (DG) and 1-monoacylglycerols (1-MG) is achieved using an optimized hexane - 2-propanol–acetonitrile mobile phase within 18 min for all nonpolar lipid classes or only 9 min excluding monoacylglycerols not detected in studied samples. The determination of individual nonpolar lipid classes is performed by the response factor approach and the use of dioleoyl ethylene glycol as a single internal standard. Polar lipid classes, such as phosphatidylglycerols (PG), phosphatidylethanolamines (PE), phosphatidylcholines (PC), sphingomyelins (SM) and lysophosphatidylcholines (LPC), are separated by hydrophilic interaction liquid chromatography (HILIC) using 5 mmol/L aqueous ammonium acetate–methanol–acetonitrile gradient within 13 minutes. The quantitation of polar lipid classes is done by a similar approach as for nonpolar lipid classes, but a different internal standard (sphingosyl PE d17:1/12:0) is used. The complementary information on fatty acyl profiles after the transesterification of the total lipid extract is obtained by gas chromatography with flame ionization detection (GC/FID). The applicability of developed methodology for fast and comprehensive characterization of blood lipidome is illustrated on samples of human plasma, erythrocytes, high-density lipoprotein (HDL), low-density lipoprotein (LDL) and very low-density lipoprotein (VLDL) fractions.

1. Introduction

Lipids are hydrophobic or amphipathic small molecules that may originate entirely or in part by carbanion-based condensations of thioesters and/or by carbocation-based condensations of isoprene units [1,2]. Lipids can be divided into eight basic groups according to the Lipid MAPS consortium: fatty acyls, glycerolipids, glycerophospholipids, sphingolipids, sterol lipids, prenol lipids, saccharolipids and polyketides [1,3,4]. The division for polar (mainly glycerophospholipids, sphingolipids and saccharolipids) and nonpolar (glycerolipids, sterol lipids and fatty acyls) lipids is frequently used in the analytical chemistry [5], because polar and nonpolar lipids require different procedures for their sample preparation, chromatographic separation and mass spectrometric detection. Lipids are transported throughout the human body using lipoprotein particles, which can be divided according to their relative densities into chylomicrons, VLDL, LDL and HDL [5]. The disruption of lipid synthesis and processing can be correlated with serious human diseases, such as obesity, diabetes, cancer or cardiovascular diseases (CVD) [6,7]. Risk factors of CVD are elevated levels of total cholesterol, LDL cholesterol, triacylglycerols (TG), decreased HDL cholesterol [8,9], obesity, hypertension and hyperglycemia [10].

Chromatographic techniques coupled to mass spectrometry (MS) are typically used for a comprehensive lipidomic analysis of biological samples. Thin-layer chromatography (TLC) is a simple

* Corresponding author. Tel.: +420 466037087; fax: +420 466037068.
E-mail address: Michal.Holcapek@upce.cz (M. Holčapek).

http://dx.doi.org/10.1016/j.chroma.2014.12.023
0021-9673/

and cheap separation method, which can provide the basic information on phospholipid, glycerolipid and sphingolipid classes, but it can be also coupled with matrix-assisted laser desorption/ionization (MALDI) to obtain detailed information on lipid molecular species [11,12]. The routine analytical method for a fatty acyl profiling after the transesterification to fatty acid methyl esters (FAME) is GC/FID or GC/MS [13–16]. High-performance liquid chromatography (HPLC) enables the separation of individual polar lipid classes using HILIC [17–24] or nonpolar lipid classes using NP HPLC [22,24–26]. Reversed-phase (RP) HPLC [18,20,27–30] systems are frequently used for the separation of individual polar lipid species inside lipid classes, while nonaqueous reversed-phase (NARP) HPLC [14,31–33] is preferred for nonpolar lipid species, such as TG. At present, ultrahigh-performance liquid chromatography (UHPLC) offers significant advantages over conventional HPLC, such as the reduction of analysis time, the sensitivity increase and the reduced solvent consumption [34]. Electrospray ionization (ESI) is the most widespread ionization technique used in the MS analysis of polar lipids, while atmospheric pressure chemical ionization (APCI) is more convenient for nonpolar lipids. The quantitation of lipids using MS can be performed by several approaches, e.g., the shotgun approach [35–38] using precursor ion, neutral loss and selected reaction monitoring scans on triple quadrupole or hydride quadrupole–linear ion trap mass spectrometers, HPLC/MS class quantitation using the combination of single internal standard (IS) and response factors (RF) for individual lipid classes related to this IS [39] or HPLC/MS using IS per each lipid class [6].

The main goal of this work is the development of high-throughput methods for the comprehensive lipidomic analysis of blood fractions. We describe the novel NP-UHPLC/APCI-MS method for the quantitation of nonpolar lipid classes and improved HILIC-UHPLC/ESI-MS method for the quantitation of polar lipid classes with good repeatability of retention times and peak areas, which is an essential requirement for the reliable quantitation. The quantitation is performed using IS and RF approach. This methodology may provide the quantitative information on six nonpolar and five polar lipid classes together with the possibility of species quantitation based on mass spectra of peaks of individual lipid classes, which is applicable in the biomarker discovery research of serious human diseases related to lipids.

2. Experimental

2.1. Materials

Acetonitrile, 2-propanol, methanol (all HPLC/MS grade), chloroform stabilized with 0.5–1% ethanol, hexane (both HPLC grade) and ammonium acetate, sodium chloride and sodium methoxide were purchased from Sigma–Aldrich (St. Louis, MO, USA). Deionized water was prepared with Demiwa 5-roi purification system (Watek, Ledeč nad Sázavou, Czech Republic) and by ultra CLEAR UV apparatus (SG, Hamburg, Germany). Standards of CE, TG, 1,2-DG, 1,3-DG and 1-MG containing oleoyl acyls and nonadecanoyl acyls and cholesterol were purchased from Sigma-Aldrich. Standards of polar lipids containing oleoyl acyls (PG, PE, PC, SM and LPC), the IS for nonpolar lipids (dioleoyl ethylene glycol, IS_1), the IS for polar lipids (sphingosyl PE d17:1/12:0, IS_2) and deuterated cholesterol-d7 were purchased from Avanti Polar Lipids (Alabaster, AL, USA). Biological samples (plasma, erythrocytes, VLDL, LDL and HDL) were obtained from healthy volunteers and CVD patients in the cooperation with the University Hospital Olomouc. The experimental setup was approved by the Ethical committee at the University Hospital Olomouc.

2.2. Sample preparation

Blood of healthy volunteer (man, age group 40–55 years, body mass index 25.7) was collected to heparin-lithium tubes and centrifuged to obtain erythrocytes and plasma. Plasma was further separated into lipoprotein fractions by the ultracentrifugation. Nonpolar lipids were extracted according to the modification of previously published procedure [40]: 50 μL of the plasma sample and 5 μL of IS_1 (3.325 mg/mL) were mixed with 150 μL hexane–methanol (98:2, v/v). The mixture was incubated for 10 min, then 300 μL of methanol–water mixture (95:5, v/v) and 300 μL of hexane–methanol mixture (98:2, v/v) were added. The sample was centrifuged for one minute at 25 rpm, and the upper hexane layer was collected. The lower layer was washed twice with 300 μL of hexane–methanol (98:2, v/v), and the upper hexane layer was collected. The combined hexane extract containing nonpolar lipids was evaporated by a gentle stream of nitrogen, then redissolved in hexane and used for NP-UHPLC/APCI-MS analysis.

Total lipid extracts were prepared according to the modified Folch procedure [39,41]. 500 μL of the plasma sample (applicable for the plasma volume at least from 50 to 500 μL) and 50 μl of IS_2 (3.333 mg/mL) were homogenized with 10 mL of chloroform–methanol mixture (2:1, v/v). This mixture was filtered using a rough filter paper. Then 2 mL of 1 mol/L NaCl was added and centrifuged for 3 minutes at 25 rpm. The chloroform layer containing lipids was evaporated by the gentle stream of nitrogen and dissolved in chloroform–2-propanol (1:1, v/v) for the HILIC-UHPLC/ESI-MS analysis. FAME were prepared according to the procedure with sodium methoxide [14,42]. 100 μL of the sample (plasma, erythrocytes or lipoprotein fractions) and 1.6 mL of 0.25 mol/L sodium methoxide in methanol were heated on a water bath for 10 min at 65 °C. 1 mL of 1 mol/L NaCl and 1 mL of hexane were added after the reaction. The upper hexane layer containing FAME was used directly for the GC/FID analysis.

2.3. NP-UHPLC/APCI-MS conditions

Experiments were performed with a liquid chromatograph Agilent 1200 infinity series (Agilent Technologies, Santa Clara, CA, USA). Acquity UPLC HILIC column (50 × 2.1 mm, 1.7 μm, Waters, Milford, MA, USA) was used for the separation of nonpolar classes of lipids (CE, TG, DG, cholesterol and MG). The flow rate was 1 mL/min, the column temperature 30 °C, the mobile phase gradient 0 min – 99% A + 1% B, 20 min – 32% A + 68% B, where A is hexane and B is a mixture of hexane-2-propanol–acetonitrile (96:2:2, v/v/v). Esquire 3000 ion trap mass spectrometer (Bruker Daltonics, Bremen, Germany) operating in the positive-ion APCI mode was used for the detection of nonpolar lipids under the following conditions: mass range *m/z* 50–1000, corona voltage 4 μA, pressure of nebulizer gas 65 psi, flow rate of drying gas 3 L/min, drying temperature 350 °C and vaporizer temperature 375 °C. Nonpolar lipids were identified based on *m/z* values of $[M+H]^+$ ions and characteristic fragment ions and also retention times of individual compounds.

2.4. HILIC-UHPLC/ESI-MS conditions

Experiments were performed with a liquid chromatograph Agilent 1290 infinity series (Agilent Technologies). Acquity UPLC HILIC column (50 × 2.1 mm, 1.7 μm, Waters) was used for the separation of polar lipid classes (PG, PE, PC, SM and LPC). The flow rate was 0.5 mL/min, the column temperature was 40 °C, the mobile phase gradient 0 min – 0.5% A + 99.5% B, 20 min 20.5% A + 79.5% B, where A is the mixture of 5 mmol/L aqueous ammonium acetate - methanol (9:1, v/v) and B is acetonitrile. Hybrid quadrupole-time-of-flight (Q-TOF) micrOTOF-Q mass spectrometer (Bruker Daltonics) operating in the positive-ion ESI mode was used for the detection of polar

lipids under the following conditions: mass range *m/z* 50–1500, capillary voltage 4.5 kV, pressure of nebulizer gas 1.6 bar, flow rate of drying gas 9 mL/min and drying temperature 220 °C. Polar lipids were identified based on accurate *m/z* values of $[M+H]^+$ ions and characteristic fragment ions and also retention times of individual compounds.

2.5. GC/FID conditions

GC/FID experiments were performed on the gas chromatograph Agilent 7890 (Agilent Technologies) using TR-FAME column (60 m length, 0.25 mm ID, 0.25 μm film thickness, Thermo Scientific, Waltham, MA, USA) under the following conditions [18]: the injection volume 3 μL, the split ratio 1:15, the flow rate of helium as a carrier gas 1.025 mL/min. The temperature program was the following: the initial temperature 160 °C, ramp to 210 °C at 2 °C/min, ramp to 235 °C at 22 °C/min. Injector and detector temperatures were 250 °C and 280 °C, respectively.

3. Results and discussion

3.1. Sample preparation

The sample preparation is a rather important step in the lipidomic analysis, because inappropriate extraction procedures can cause lower recoveries for some lipid classes and systematic errors in the quantitative analysis. The essential requirement for any LC/MS quantitative assay is the use of appropriate IS for the quantitation. The use of isotopically labeled IS is the best quantitation approach, but it is not applicable for the lipidomic analysis due to the large range of analyzed molecules and the lack of such standards. In the present work, we follow the strategy developed in our previous work [39] based on the use of RF for individual lipid classes combined with the single IS well separated from other lipid classes and not occurring in biological samples.

The new method for the extraction of nonpolar lipids is optimized based on two phase liquid-liquid system with hexane–methanol–water (final conditions in Section 2.2 Sample preparation), where nonpolar lipids are concentrated in the upper hexane layer. After the collection of upper hexane layer, the bottom aqueous methanol layer is washed two times with hexane–methanol mixture (98:2, v/v) to increase the extraction efficiency. Combined hexane extracts are evaporated to dryness, then redissolved in pure hexane and used for further NP-UHPLC/APCI-MS analysis. Extraction recoveries for representatives of nonpolar lipid classes (CE 19:0, TG 19:0/19:0/19:0, cholesterol-d7 and DG 19:0/0:0/19:0) and IS_1 are shown in Table S1. Extraction recoveries for the stock solution without any matrix are in the range 97–110% and for the plasma matrix 93–100%, which clearly confirm the applicability of this method for the real analysis of body fluids without negative matrix effects. The extraction recovery of spiked samples cannot be determined for CE due to the common fragment ion *m/z* 369 corresponding to the loss of fatty acyl chain from CE, which is observed for both lipid class standard of CE and CE in plasma.

The extraction method for polar lipids is used according to previously developed procedure [18,39] based on the modified Folch method (details in Experimental, section 2.2 Sample preparation).

3.2. NP-UHPLC/APCI-MS of nonpolar lipid classes

The class separation of nonpolar lipids cannot be achieved under HILIC conditions, because nonpolar lipids elute unresolved in the void volume of the system [20] and the systematic optimization of separation does not help to increase their retention. For this reason, we have decided to develop new NP-UHPLC/APCI-MS method for

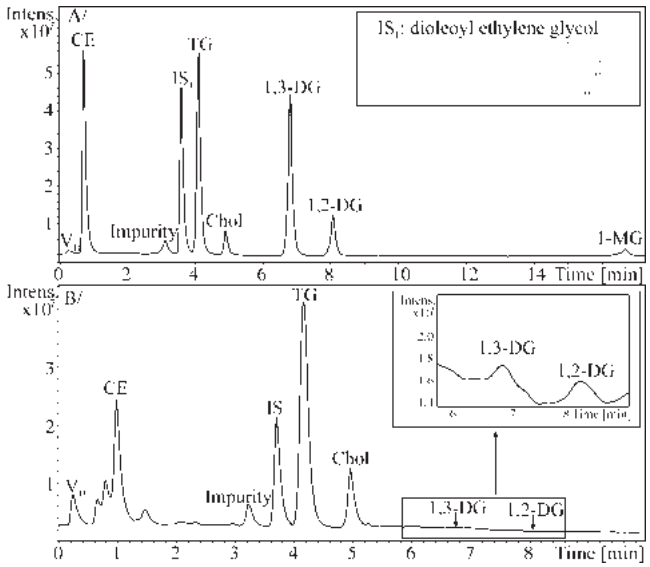

Fig. 1. NP-UHPLC/APCI-MS chromatogram of the separation of nonpolar lipid classes (CE, TG, cholesterol, 1,3-DG, 1,2-DG and 1-MG) and the internal standard IS_1 (dioleoyl ethylene glycol): (A) lipid class standards containing oleoyl acyls and cholesterol, (B) human plasma sample. Conditions: Acquity UPLC HILIC column (50 × 2.1 mm, 1.7 μm), flow rate 1 mL/min, column temperature 30 °C, gradient 0 min – 99% A + 1% B, 20 min – 32% A + 68% B, where A is hexane and B is a mixture of hexane-2-propanol–acetonitrile (96:2:2, v/v/v), positive-ion APCI-MS detection. Peak annotation: CE–cholesteryl esters; TG–triacylglycerols; Chol–cholesterol; 1,3-DG–1,3-diacylglycerols; 1,2-DG - 1,2-diacylglycerols; 1-MG - 1-monoacylglycerols.

the class separation and quantitation of main nonpolar lipid classes (TG, DG, MG, CE and cholesterol) in the shortest possible time suitable for high-throughput clinical analysis of blood samples. The appropriate IS has to be selected before the optimization of separation conditions, because the IS must be well separated from all lipid classes, it must be absent in analyzed samples and exhibit structural similarity with determined classes. Dioleoyl ethylene glycol is selected as the IS for the determination of nonpolar lipids (IS_1), because it fulfills all above mentioned criteria and moreover it is relatively cheap.

The first experiments have been performed on 150 × 2.1 mm silica column packed with 3 μm particles, but obtained results are unsatisfactory due to wider peaks, longer analysis times, low retention of CE and the coelution of IS_1, TG and the peak of impurity from hexane (antioxidant Irgafos 168 providing a signal at *m/z* 663). The column packed with sub-2 μm particles (Acquity UPLC HILIC column, 150 × 2.1 mm, 1.7 μm particles) provides narrower peaks (Fig. S1A), but the retention of CE is still too close to the system void volume and the critical pair of IS_1/TG is not resolved using a generic gradient of 2-propanol in hexane from 5% to 100% B within 30 minutes. A good separation of DG regioisomers, MG and cholesterol can be achieved relatively easily at a wide range of chromatographic conditions. The increased retention of CE further away from V_D can be achieved by decreased initial percentage of 2-propanol as the stronger solvent, but it does not help with the resolution of TG/IS_1 pair (Fig. S1B). Combined effects of the addition of acetonitrile into the polar modifier (2-propanol/acetonitrile, 1:1, v/v) and lowering the gradient steepness lead to the resolution of this critical pair. Increased temperature from 20 °C to 30 °C slightly increases the retention and improves the reproducibility. The low system back-pressure in NP system allows increasing the flow rate from the initial 0.4 mL/min (Figs. S1A and B) through 0.6 mL/min (Fig. S1C) to the final value of 1.0 mL/min (Fig. 1) without the negative effect on the system performance and the back-pressure is still below 200 bars. The final method (Fig. 1A) allows the baseline separation of all nonpolar lipid classes within 18 min or excluding MG

Table 1
Parameters of calibration curves, response factors and the repeatability of measurements for nonpolar and polar lipid class representatives containing oleoyl residues and for internal standards.

Lipid class	Retention time [min]	Slope	Intercept	Regression coefficient	Response factor	Repeatability [%] [a]	
						Retention times	Peak areas
Nonpolar lipids							
CE	0.74	4.519	75.676	0.999	1.06	1.1	3.8
IS_1 [b]	3.59	4.804	13.853	0.999	1.00	0.1	1.3
TG	4.12	6.005	45.665	0.996	0.80	0.4	0.5
Chol	4.88	0.903	−0.113	0.999	5.32	0.2	4.1
1,3-DG	6.81	6.102	10.195	1.000	0.79	0.1	2.3
1,2-DG	8.07	4.447	0.842	1.000	1.08	0.1	4.7
MG	16.65	0.463	−0.324	1.000	10.38	0.1	4.7
Polar lipids							
PG	4.34	0.249	2.569	0.982	2.80	0.2	1.1
PE	7.94	0.699	7.113	0.999	1.00	0.1	0.5
IS_2 [c]	9.63	0.697	7.685	1.000	1.00	0.1	1.6
PC	10.77	0.570	2.788	1.000	1.22	0.1	3.1
SM	11.86	0.293	2.092	0.999	2.38	0.1	4.1
LPC	12.49	0.313	0.676	0.999	2.23	0.1	1.0

[a] Standard deviations based on five consecutive measurements.
[b] Dioleoyl ethylene glycol is used as the internal standard for the determination of nonpolar lipids (IS_1).
[c] Sphingosyl PE d17:1/12:0 is used as the internal standard for the determination of polar lipids (IS_2).

in 9 min only. MG are not detected in studied blood samples, so the final method has been shortened excluding MG class. Fig. 1B illustrates the separation of nonpolar lipids in human plasma sample with abundant presence of CE, TG and cholesterol. 1,3- and 1,2-DG regioisomers are present only at the trace concentration. TG and DG elute in single peaks without a visible resolution of individual molecules within these lipid classes, while individual CE are partially separated (Fig. 1B).

The quantitation is based on the same strategy published recently for polar lipid classes [39] using the RF for individual lipid classes and the single IS. Calibration curves for lipid class representative standards containing oleoyl acyls and IS_1 have been measured. Ratios of slopes of calibration curves for IS_1 over lipid class representative is used for the determination of RF of particular lipid class (Table 1) based on the assumption that differences of relative responses of lipids within one class are small. The same assumption is used in the majority of quantitative approaches both for LC/MS and shotgun lipidomics due to the lack of quantitative lipidomic standards or their high prices. Individual lipoprotein fractions of human plasma and erythrocytes exhibit rather large differences in concentrations of nonpolar lipid classes, as illustrated in Fig. 2 and numerical values are listed in Table 2. Plasma shows similar concentrations of TG, CE and cholesterol, while only cholesterol is detected in erythrocytes. Large differences are found among particular plasma lipoprotein fractions. Some classes are more abundant in LDL compared to VLDL (e.g., CE almost 10 times and cholesterol 4 times), while it is vice versa for DG (e.g., 1,2-DG have almost 10 times higher concentration in VLDL compared to LDL). These concentration differences are in accordance with known metabolic functions of individual lipoprotein fractions [3,5].

Concentrations of individual lipid species within classes can be determined as well (Table S2) based on the assumption used in the majority of lipidomic quantitation that differences in RF within the class can be neglected. Then the concentration of lipid species is calculated by the multiplication of the total lipid class concentration by the relative abundances of individual lipids in the mass spectrum of whole lipid class. Table S2 also shows the comparison of our concentration with previously published work [38] on the NIST human plasma by nine different laboratories within the Lipid MAPS consortium. We obtain a satisfactory correlation despite the simplified way of our quantitation (single IS for all lipid classes instead of IS for each lipid class), different samples of human plasma, different extraction procedures (generic method *vs.* dedicated protocols for individual lipid classes). Over 50% of results in Table S2 differ less than 2 folds, almost 70% of concentrations differ less than 3 folds and only 8 values differ more than ten times, which is acceptable considering all discussed differences. There is also good agreement between identified lipid species in both data sets, while some lipids are not detected in one of these works, typically at low concentration levels. We have a lower number of identified nonpolar lipids due to necessity to use APCI in NP mode, which causes more extensive fragmentation (especially for CE) resulting in less detected intact lipid molecules.

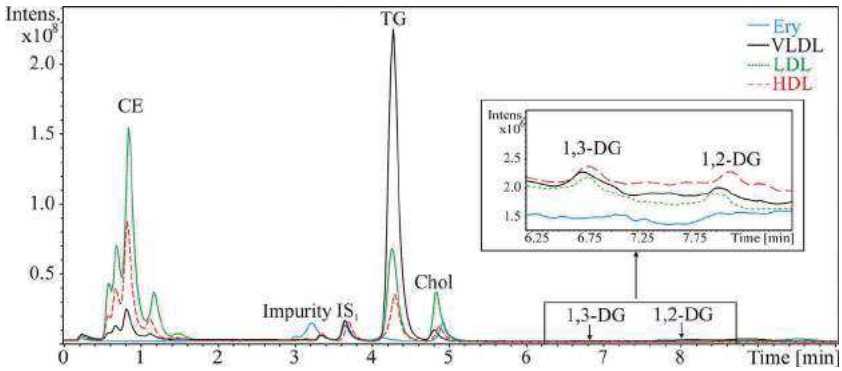

Fig. 2. NP-UHPLC/APCI-MS chromatograms of nonpolar lipid classes in human plasma lipoprotein fractions (HDL, LDL and VLDL) and erythrocytes. NP-UHPLC conditions are identical as for Fig. 1.

Table 2
Retention times and concentrations of nonpolar lipid classes by NP-UHPLC/APCI-MS and polar lipid classes by HILIC-UHPLC/ESI-MS determined in human plasma, erythrocytes and lipoprotein fraction samples.

Lipid class	Concentration [μg/mL]				
	Plasma	Erythrocytes	VLDL	LDL	HDL
Nonpolar lipids					
CE	770.5	n.d.[a]	470.2	4037.4	2180.8
TG	817.9	n.d.[a]	1845.8	1153.2	574.2
Chol	645.4	1946.1	578.7	2458.3	746.3
1,3-DG	2.1	n.d.[a]	8.9	4.0	13.6
1,2-DG	5.2	n.d.[a]	21.9	2.4	11.0
Polar lipids					
PE	60.7	159.3	34.6	48.9	68.4
PC	615.2	262.3	447.8	651.4	709.1
SM	264.4	159.5	123.4	307.9	197.3
LPC	189.5	23.3	22.0	72.1	55.3

[a] n.d. – not detected, below the limit of detection: 0.028 μg/mL for CE, 0.016 μg/mL for TG, 0.11 μg/mL for Chol, 0.015 μg/mL for 1,3-DG and 0.028 μg/mL for 1,2-DG.

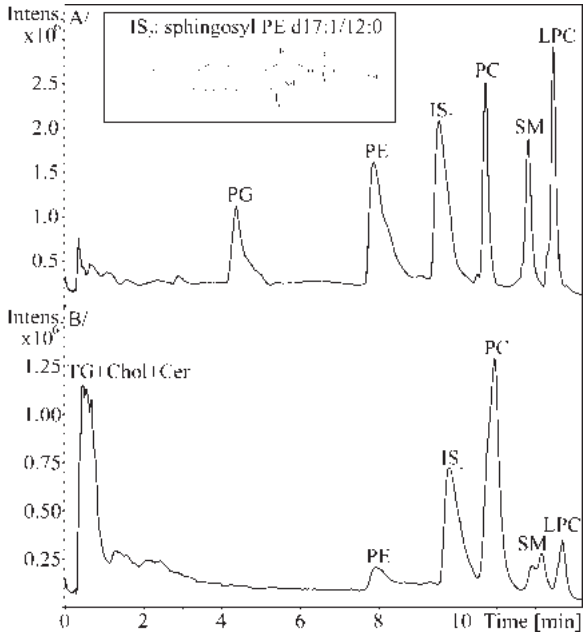

Fig. 3. HILIC-UHPLC/ESI-MS chromatograms of the separation of polar lipid classes (PG, PE, PC, SM and LPC) and the internal standard IS_2 (sphingosyl PE d17:1/12:0): (A) lipid class standards containing oleoyl acyls, and (B) human plasma sample. Conditions: Acquity UPLC HILIC column (50 × 2.1 mm, 1.7 μm), flow rate 0.5 mL/min, column temperature 40 °C, gradient 0 min – 0.5% A + 99.5% B, 20 min 20.5% A + 79.5% B, where A is a mixture of 5 mmol/L aqueous ammonium acetate–methanol (9:1, v/v), and B is acetonitrile, positive-ion ESI-MS detection. Peak annotation: PG–phosphatidylglycerols; PE–phosphatidylethanolamines; PC–phosphatidylcholines; SM–sphingomyelins; LPC–lysophosphatidylcholines.

3.3. HILIC-UHPLC/ESI-MS of polar lipid classes

The method development of polar lipid classes separation has started from our previously published HILIC-HPLC/ESI-MS method for the separation of multiple polar lipid classes [39]. The analysis time of this older method (60 min) is not acceptable for high-throughput clinical analysis and some lipid classes are not present in plasma and erythrocytes, so the optimization of their separation is useless. The first step for the reduction of analysis time is the selection of appropriate particle size and column geometry. The particle size of sub-2 μm and short 50 mm column is selected for the fast separation of all polar lipid classes determined in blood fractions (PE, PC, SM and LPC). The best results are achieved on the identical column as for NP separation (Acquity UPLC HILIC column, 50 × 2.1 mm, 1.7 μm), but one column is used only for nonaqueous NP and the second one for aqueous HILIC systems without changing columns between systems to avoid problems with the column equilibration while changing between nonaqueous and aqueous mobile phase systems. It was reported previously [26] and verified in our preliminary experiments that the use of mobile phase system combining nonaqueous part of gradient for nonpolar lipid classes followed by the aqueous gradient step used for the elution of polar lipid classes results in a lower repeatability of retention times (up to 6%) and peak areas (up to 10.5%) in comparison to separate methods used in this work (Table 1).

Total ion current chromatograms obtained with the final HILIC-UHPLC/ESI-MS method are shown for the mixture of standards of lipid class representatives (Fig. 3A) and the real sample of human plasma (Fig. 3B). The quantitative approach is based on the identical principle as for nonpolar lipids described in the previous chapter. The IS for the polar lipid class determination is sphingosyl PE d17:1/12:0 (IS_2) in accordance with our previous work [39]. Parameters of calibration dependencies with the lipid class RF are listed in Table 1. Differences in polar lipid composition among plasma lipoprotein fractions and erythrocytes (Fig. 4) are lower than in case of nonpolar lipids (Table 2). Only erythrocytes exhibit higher concentrations of PE and lower concentration of PC in comparison to other blood fractions. Concentrations of individual lipid species are determined (see Table S2) the same way for nonpolar lipid classes discussed above.

3.4. GC/FID

GC/FID is well established technique routinely used for the determination of fatty acyl profiles, which provide useful complementary information during the interpretation of mass spectra of

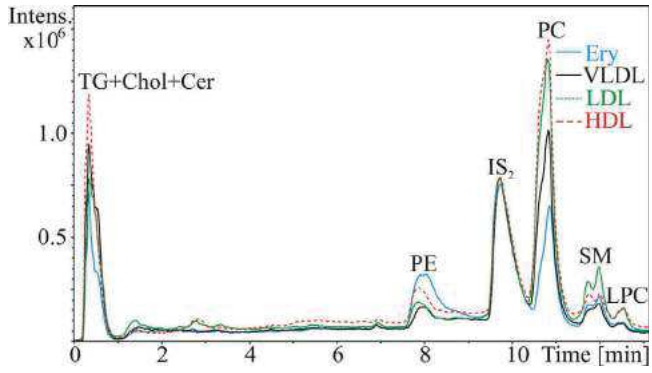

Fig. 4. HILIC-UHPLC/ESI-MS chromatograms of polar lipid classes in human plasma lipoprotein fractions (HDL, LDL and VLDL) and erythrocytes. Conditions are identical as for Fig. 3.

complex lipids. Fig. S3 illustrates the optimized GC separation of FAME in plasma, erythrocytes, VLDL, LDL and HDL of one person together with the quantitative data shown in Table S2.

4. Conclusions

Two complementary methods are developed for the determination of both nonpolar and polar lipid classes detected in human blood samples. NP-UHPLC/APCI-MS is used for five nonpolar lipid classes (CE, cholesterol, TG, 1,2-DG and 1,3-DG), while HILIC-UHPLC/ESI-MS is applied for five polar lipid classes (PG, PE, PC, SM and LPC). Both methods are optimized in terms of good separation of individual lipid classes, method robustness and applicability for high-throughput lipidomic characterization of large series of human plasma, erythrocytes and lipoprotein fraction samples typical for biomarker discovery studies. The quantitation approach is identical for both methods using RF of individual lipid classes, but different IS are used for the determination of nonpolar and polar lipid classes. GC/FID of FAME provides additional information on fatty acyl profiles, which shows differences among individual blood fractions. The applicability of these methods is already verified in the running project devoted to CVD, where hundreds of samples are measured and above mentioned lipid classes are quantified. Concentrations of lipid species inside particular classes are determined from their relative abundances within the class multiplied by the total class concentration and compared with the previously published work on the human plasma [38].

Acknowledgments

This work was supported by the project No. 206/11/0022 sponsored by the Czech Science Foundation. E.C. acknowledges the support of the grant project No. CZ.1.07/2.3.00/30.0021 sponsored by the Ministry of Education, Youth and Sports of the Czech Republic.

Appendix A. Supplementary data

Supplementary data associated with this article can be found, in the online version, at http://dx.doi.org/10.1016/j.chroma.2014.12.023.

References

[1] E. Fahy, S. Subramaniam, H.A. Brown, C.K. Glass, A.H. Merrill, R.C. Murphy, C.R.H. Raetz, D.W. Russell, Y. Seyama, W. Shaw, T. Shimizu, F. Spener, G. van Meer, M.S. VanNieuwenhze, S.H. White, J.L. Witztum, E.A. Dennis, A comprehensive classification system for lipids, J. Lipid Res. 46 (2005) 839–861.
[2] E. Fahy, S. Subramaniam, R.C. Murphy, M. Nishijima, C.R.H. Raetz, T. Shimizu, F. Spener, G. van Meer, M.J.O. Wakelam, E.A. Dennis, Update of the LIPID MAPS comprehensive classification system for lipids, J. Lipid Res. 50 (2009) S9–S14.
[3] E.A. Dennis et al., http://www.lipidmaps.org/, downloaded June 2014.
[4] E. Fahy, D. Cotter, M. Sud, S. Subramaniam, Lipid classification, structures and tools, Biochim. Biophys. Acta Mol. Cell Biol. Lipids 1811 (2011) 637–647.
[5] W.W. Christie, http://lipidlibrary.aocs.org/, downloaded June 2014.
[6] K. Ekroos (Ed.), Lipidomics, Technologies and Applications, Wiley-VCH, Weinheim, 2012.
[7] A.D. Watson, Lipidomics: a global approach to lipid analysis in biological systems, J. Lipid Res. 47 (2006) 2101–2111.
[8] P. Loria, G. Marchesini, F. Nascimbeni, S. Ballestri, M. Maurantonio, F. Carubbi, V. Ratziu, A. Lonardo, Cardiovascular risk, lipidemic phenotype and steatosis. A comparative analysis of cirrhotic and non-cirrhotic liver disease due to varying etiology, Atherosclerosis 232 (2014) 99–109.
[9] R. Martinez-Beamonte, J.M. Lou-Bonafonte, M.V. Martinez-Gracia, J. Osada, Sphingomyelin in high-density lipoproteins: Structural role and biological function, Int. J. Mol. Sci. 14 (2013) 7716–7741.
[10] P. Mathieu, P. Pibarot, E. Larose, P. Poirier, A. Marette, J.P. Despres, Visceral obesity and the heart, Int. J. Biochem. Cell Biol. 40 (2008) 821–836.
[11] B. Fuchs, Analysis of phospolipids and glycolipids by thin-layer chromatography–matrix-assisted laser desorption and ionization mass spectrometry, J. Chromatogr. A 1259 (2012) 62–73.
[12] B. Fuchs, R. Suss, K. Teuber, M. Eibisch, J. Schiller, Lipid analysis by thin-layer chromatography – A review of the current state, J. Chromatogr. A 1218 (2011) 2754–2774.
[13] J. Ecker, M. Scherer, G. Schmitz, G. Liebisch, A rapid GC–MS method for quantification of positional and geometric isomers of fatty acid methyl esters, J. Chromatogr. B 897 (2012) 98–104.
[14] M. Lísa, K. Netušilová, L. Franěk, H. Dvořáková, V. Vrkoslav, M. Holčapek, Characterization of fatty acid and triacylglycerol composition in animal fats and fish oils using silver-ion and non-aqueous reversed-phase high-performance liquid chromatography - mass spectrometry and gas chromatography - flame ionization detection, J. Chromatogr. A 1218 (2011) 7499–7510.
[15] T. Seppänen-Laakso, I. Laakso, R. Hiltunen, Analysis of fatty acids by gas chromatography, and its relevance to research on health and nutrition, Anal. Chim. Acta 465 (2002) 39–62.
[16] E. Tvrzická, M. Vecká, B. Staňková, A. Žák, Analysis of fatty acids in plasma lipoproteins by gas chromatography-flame ionization detection. Quantitative aspects, Anal. Chim. Acta 465 (2002) 337–350.
[17] B. Barroso, R. Bischoff, LC–MS analysis of phospholipids and lysophospholipids in human bronchoalveolar lavage fluid, J. Chromatogr. B 814 (2005) 21–28.
[18] E. Cífková, M. Holčapek, M. Lísa, Nontargeted lipidomic characterization of various porcine organs tissues using hydrophilic liquid chromatography - electrospray ionization mass spectrometry, Lipids 48 (2013) 915–928.
[19] A.A. Karlsson, P. Michelsen, A. Larsen, G. Odham, Normal-phase liquid chromatography class separation and species determination of phospholipids utilizing electrospray mass spectrometry/tandem mass spectrometry, Rapid Commun. Mass Spectrom. 10 (1996) 775–780.
[20] M. Lísa, E. Cífková, M. Holčapek, Lipidomic profiling of biological tissues using off-line two-dimensional high performance liquid chromatography - mass spectrometry, J. Chromatogr. A 1218 (2011) 5146–5156.
[21] C. Wang, S.G. Xie, J. Yang, Q. Yang, G.W. Xu, Structural identification of human blood phospholipids using liquid chromatography/quadrupole-linear ion trap mass spectrometry, Anal. Chim. Acta 525 (2004) 1–10.
[22] U. Sommer, H. Herscovitz, F.K. Welty, C.E. Costello, LC-MS-based method for the qualitative and quantitative analysis of complex lipid mixtures, J. Lipid Res. 47 (2006) 804–814.
[23] M. Pulfer, R.C. Murphy, Electrospray mass spectrometry of phospholipids, Mass Spectrom. Rev. 22 (2003) 332–364.
[24] P. Olsson, J. Holmback, B. Herslof, Separation of lipid classes by HPLC on a cyanopropyl column, Lipids 47 (2012) 93–99.
[25] P.M. Hutchins, R.M. Barkley, R.C. Murphy, Separation of cellular nonpolar neutral lipids by normal-phase chromatography and analysis by electrospray ionization mass spectrometry, J. Lipid Res. 49 (2008) 804–813.
[26] D.G. McLaren, P.L. Miller, M.E. Lassman, J.M. Castro-Perez, B.K. Hubbard, T.P. Roddy, An ultraperformance liquid chromatography method for the normal-phase separation of lipid, Anal. Biochem. 414 (2011) 266–272.
[27] E.J. Ahn, H. Kim, B.C. Chung, G. Kong, M.H. Moon, Quantitative profiling of phosphatidylcholine and phosphatidylethanolamine in a steatosis/fibrosis model of rat liver by nanoflow liquid chromatography/tandem mass spectrometry, J. Chromatogr. A 1194 (2008) 96–102.
[28] O. Berdeaux, P. Juaneda, L. Martine, S. Cabaret, L. Bretillon, N. Acar, Identification and quantification of phosphatidylcholines containing very-long-chain polyunsaturated fatty acid in bovine and human retina using liquid chromatography/tandem mass spectrometry, J. Chromatogr. A 1217 (2010) 7738–7748.
[29] K. Sandra, A.D. Pereira, G. Vanhoenacker, F. David, P. Sandra, Comprehensive blood plasma lipidomics by liquid chromatography/quadrupole time-of-flight mass spectrometry, J. Chromatogr. A 1217 (2010) 4087–4099.
[30] Y. Sato, I. Suzuki, T. Nakamura, F. Bernier, K. Aoshima, Y. Oda, Identification of a new plasma biomarker of Alzheimer's disease using metabolomics technology, J. Lipid Res. 53 (2012) 567–576.
[31] J. Cvačka, O. Hovorka, P. Jiroš, J. Kindl, K. Stránský, I. Valterová, Analysis of triacylglycerols in fat body of bumblebees by chromatographic methods, J. Chromatogr. A 1101 (2006) 226–237.
[32] M. Lísa, M. Holčapek, T. Řezanka, N. Kabátová, High-performance liquid chromatography–atmospheric pressure chemical ionization mass spectrometry and gas chromatography–flame ionization detection characterization of (5-polyenoic fatty acids in triacylglycerols from conifer seed oils, J. Chromatogr. A 1146 (2007) 67–77.
[33] M. Holčapek, P. Jandera, P. Zderadička, L. Hrubá, Characterization of triacylglycerol and diacylglycerol composition of plant oils using high-performance liquid chromatography - atmospheric pressure chemical ionization mass spectrometry, J. Chromatogr. A 1010 (2003) 195–215.
[34] L. Nováková, H. Vlčková, A review of current trends and advances in modern bio-analytical methods: chromatography and sample preparation, Anal. Chim. Acta 656 (2009) 8–35.
[35] X.L. Han, K. Yang, R.W. Gross, Multi-dimensional mass spectrometry-based shotgun lipidomics and novel strategies for lipidomic analyses, Mass Spectrom. Rev. 31 (2012) 134–178.
[36] D. Schwudke, G. Liebisch, R. Herzog, G. Schmitz, A. Shevchenko, Shotgun lipidomics by tandem mass spectrometry under data-dependent acquisition control, Methods Enzymol. 433 (2007) 175–191.
[37] K. Yang, H. Cheng, R.W. Gross, X.L. Han, Automated lipid identification and quantification by multi-dimensional mass spectrometry-based shotgun lipidomics, Anal. Chem. 81 (2009) 4356–4368.
[38] O. Quehenberger, A.M. Armando, A.H. Brown, S.B. Milne, D.S. Myers, A.H. Merrill, S. Bandyopadhyay, K.N. Jones, S. Kelly, R.L. Shaner, C.M. Sullards, E. Wang, R.C. Murphy, R.M. Barkley, T.J. Leiker, C.R.H. Raetz, Z.Q. Guan, G.M. Laird, D.A. Six,

D.W. Russell, J.G. McDonald, S. Subramaniam, E. Fahy, E.A. Dennis, Lipidomics reveals a remarkable diversity of lipids in human plasma, J. Lipid Res. 51 (2010) 3299–3305.
[39] E. Cífková, M. Holčapek, M. Lísa, M. Ovčačíková, A. Lyčka, F. Lynen, P. Sandra, Non-targeted quantitation of lipid classes using hydrophilic interaction liquid chromatography - electrospray ionization mass spectrometry using single internal standard and response factor approach, Anal. Chem. 84 (2012) 10064–10070.
[40] L. Lofgren, M. Stahlman, G.B. Forsberg, S. Saarinen, R. Nilsson, G.I. Hansson, The BUME method: a novel automated chloroform-free 96-well total lipid extraction method for blood plasma, J. Lipid Res. 53 (2012) 1690–1700.
[41] J. Folch, M. Lees, G.H.S. Stanley, A simple method for the isolation and purification of total lipids from animal tissues, J. Biol. Chem. 226 (1957) 497–509.
[42] R.J. Hamilton, S. Hamilton (Eds.), Lipid Analysis: A Practical approach, IRL Press at Oxford University Press, Oxford, 1992.

analytical chemistry

Article

pubs.acs.org/ac

High-Throughput and Comprehensive Lipidomic Analysis Using Ultrahigh-Performance Supercritical Fluid Chromatography–Mass Spectrometry

Miroslav Lísa* and Michal Holčapek

Department of Analytical Chemistry, Faculty of Chemical Technology, University of Pardubice, Studentská 573, 53210 Pardubice, Czech Republic

Supporting Information

ABSTRACT: New analytical approach for high-throughput and comprehensive lipidomic analysis of biological samples using ultrahigh-performance supercritical fluid chromatography (UHPSFC) with electrospray ionization-mass spectrometry (ESI-MS) is presented in this work as an alternative approach to established shotgun MS or high-performance liquid chromatography-MS. The lipid class separation is performed by UHPSFC method based on 1.7 μm particle-bridged ethylene hybrid silica column with a gradient of methanol–water–ammonium acetate mixture as a modifier. All parameters of UHPSFC conditions are carefully optimized and their influence on the chromatographic behavior of lipids is discussed. The final UHPSFC/ESI-MS method enables a fast separation of 30 nonpolar and polar lipid classes within 6 min analysis covering 6 main lipid categories including fatty acyls, glycerolipids, glycerophospholipids, sphingolipids, sterols, and prenols. Individual lipid species within lipid classes are identified based on positive and negative-ion full-scan and tandem mass spectra measured with high mass accuracy and high resolving power. Developed UHPSFC/ESI-MS method is applied for the analysis of porcine brain extract as a complex lipidomic sample, where 24 lipid classes containing 436 lipid species are identified. The method is validated for the quantitative analysis of lipid species in biological tissues using internal standards for each lipid class. This high-throughput, comprehensive and accurate UHPSFC/ESI-MS method is suitable for the lipidomic analysis of large sample sets in the clinical research.

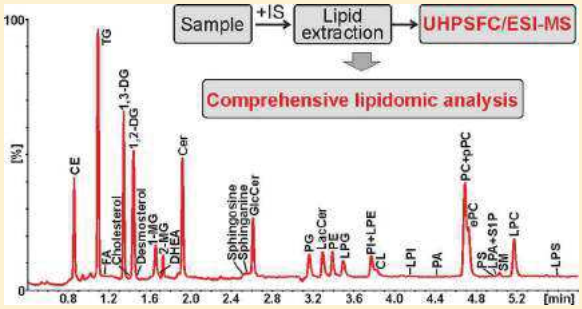

Lipidomics has had growing interest in recent decades because lipids are recognized as biologically active compounds having many functions in the human organism. They are a major form of energy storage in mammals, a source of fat soluble vitamins and essential fatty acids, main structural components of biological membranes, or act as cell signaling molecules.[1−3] According to the definition suggested by the LIPID MAPS consortium, lipids are hydrophobic or amphipathic small molecules that may originate entirely or in part by carbanion-based condensations of ketoacyl thioesters and/or by carbocation based condensations of isoprene units.[4] This definition covers a wide range of compounds, which can be divided into 8 categories and many subcategories according to their structures.[5] The extreme structural diversity of lipids in real biological samples is challenging for analytical techniques used in the lipidomic analysis due to large differences in physicochemical properties of individual species. At present time, two main analytical strategies are used in lipidomics,[6,7] such as the direct infusion mass spectrometry (MS) approach (known as shotgun MS) and the high-performance liquid chromatography (HPLC)/MS approach.

The shotgun MS methods use the characteristic fragmentation behavior of individual lipid classes detected by MS/MS scans (i.e., precursor ion, neutral loss and selected reaction monitoring scans) on triple quadrupole or quadrupole-linear ion trap mass spectrometers[2,8−10] or based on the measurement of MS and MS/MS spectra using mass analyzers with high resolving power and high mass accuracy.[11−14] In general, shotgun MS methods are considered to be high-throughput (analysis time is usually 10−30 min according to the number of scans) and easier to automate with robotic systems compared to HPLC techniques. On the other hand, these methods are less convenient for the direct resolution of some isobaric species or isomers and the identification of low abundant species because of possible ion suppression. Shotgun lipidomics with differential ion mobility have been used for the resolution of some isobaric and isomeric species.[15]

HPLC/MS methods usually provide more comprehensive information about the lipid composition, but they are typically more time-consuming with the analysis time in tens of minutes up to several hours in case of special methods for the separation of isomers. Hydrophilic-interaction liquid chromatography (HILIC)[16−21] enables the separation of lipids into lipid classes according to their polarity, but usually nonpolar lipids (e.g., TG,

Received: March 19, 2015
Accepted: June 19, 2015
Published: June 20, 2015

DOI: 10.1021/acs.analchem.5b01054
Anal. Chem. 2015, 87, 7187−7195

CE, Chol, etc.) elute nonresolved close to the system void volume. Therefore, normal-phase (NP) HPLC is used for the resolution of nonpolar lipid classes.[16,21−24] Reversed-phase (RP)-HPLC is widely used for the separation of individual lipid species according to the carbon number (CN) and the double bond (DB) number.[17,19,25−28] Nonaqueous reversed-phase (NARP)-HPLC[29−31] systems are preferred for the separation of nonpolar lipid species, such as TG. Nowadays, ultrahigh-performance liquid chromatography (UHPLC) with sub-two-micrometer particles is often used in the lipidomic analysis,[27,32,33] because it offers a significant reduction of the analysis time, the peak width (sensitivity increase) and the solvent consumption.

Supercritical fluid chromatography (SFC), especially using subtwo μm particles as ultrahigh-performance SFC (UHPSFC),[34] shows a great potential as the comprehensive and high-throughput screening method for the large number of samples in different omic fields including lipidomics. UHPSFC is not yet widely established in the lipidomic analysis and so far only SFC using conventional HPLC columns with 5 μm particles has been used. In general, C18 columns are most frequently used in SFC lipidomic analysis. SFC using C18 column has been used for the profiling of lipids in samples as intact molecules[35,36] or after their derivatization (methylation),[37] for the separation of TG,[38] oxidized PC,[39] carotenoids,[40] or TG regioisomers.[41] SFC using silver-ion HPLC columns has been used for the separation of TG from vegetable oils.[42]

The goal of our work is the development of new analytical strategy for the high-throughput and comprehensive lipidomic analysis of biological samples applicable for large clinical studies. We present new high-throughput UHPSFC/ESI-MS method using subtwo μm particle bridged ethylene hybrid silica column for the separation of wide range of nonpolar and polar lipid classes in one analysis including the identification and quantitation of individual lipid species using ESI-MS. The potential of this lipidomic method is demonstrated on the analysis of porcine brain extract as a complex lipidomic sample.

EXPERIMENTAL SECTION

Materials. Acetonitrile, 2-propanol, methanol (all HPLC/MS grade), *n*-hexane, chloroform stabilized with 0.5−1% ethanol (both HPLC grade), ammonium acetate, ammonium formate and acetic acid were purchased from Sigma-Aldrich (St. Louis, MO, USA). Deionized water was prepared with Demiwa 5-roi purification system (Watek, Ledeč nad Sázavou, Czech Republic) and by ultra CLEAR UV apparatus (SG, Hamburg, Germany). Carbon dioxide 4.5 grade (99.995%) was purchased from Messer Group Gmbh (Bad Soden, Germany). Standards of lipid class representatives were used for UHPSFC/ESI-MS method development, that is, CE, TG, FA, 1,3-DG, 1,2-DG, and 1-MG containing oleoyl acyls and cholesterol purchased from Sigma-Aldrich and Cer, PG, PE, LPG, PI, LPE, CL, LPI, PA, PC, pPC, ePC, PS, LPA, SM, LPC, and LPS containing oleoyl acyls, sphingosine, sphinganine, GlcCer d18:1/16:0, LacCer d18:1/16:0, S1P d17:1, desmosterol and DHEA purchased from Avanti Polar Lipids (Alabaster, AL, USA). Internal standards (IS) were used for the validation and quantitation, that is, CE 19:0, TG 19:0/19:0/19:0, FA 14:0, DG 19:0/0:0/19:0, and MG 19:0/0:0/0:0 purchased from Nu-ChekPrep (Elysian, MN, USA), D7-cholesterol, Cer d18:1/17:0, GlcCer d18:1/12:0, PG 14:0/14:0, LacCer d18:1/12:0, PE 14:0/14:0, LPG 14:0/0:0, LPE 14:0/0:0, PC 22:1/22:1, PC 14:0/14:0, SM d18:1/17:0, and LPC 17:0/0:0 purchased from Avanti Polar Lipids. Stock solutions of individual IS at the concentration of 2 mg/mL were prepared in a chloroform−2-propanol mixture (1:4). Stock solution of all IS was prepared by the mixing of 20 μL of each IS. Calibration solutions were prepared by the dilution in a hexane−chloroform mixture (7:3, v/v). Porcine brain was purchased at a local store. The total lipid extract of porcine brain for nontargeted identification of lipid species was prepared from 50 mg of the sample according to the modified Folch procedure,[18] then evaporated by a gentle stream of nitrogen and redissolved in 1 mL of a chloroform−2-propanol mixture (1:1, v/v). Ten microliters of the extract stock solution was diluted into 1 mL of the hexane−chloroform mixture (7:3, v/v) for nontargeted UHPSFC/ESI-MS analysis. The same procedure was used for the preparation of the total lipid extract for UHPSFC/ESI-MS quantitation with the addition of IS into the porcine brain sample before the extraction. Two microliters of LPE and DG, 4 μL of TG, Cer, PG, LPC, and MG, and 40 μL of FA, GlcCer, CE, D7-cholesterol, sulfatide, PE, PI, PC, and SM stock solutions of IS were added.

UHPSFC/ESI-MS Conditions. All UHPSFC experiments were performed on an Acquity UPC^2 instrument (Waters, Milford, MA, USA). The final method for lipidomic analyses used the following conditions: Acquity BEH UPC^2 column (100 mm × 3 mm, 1.7 μm, Waters), the flow rate 1.9 mL/min, the injection volume 1 μL, the column temperature 60 °C, the active back pressure regulator (ABPR) pressure 1800 psi and the gradient of methanol−water mixture (99:1, v/v) containing 30 mM of ammonium acetate as a modifier: 0 min, 1%; 5 min, 51%; 6 min, 51%. The injector needle was washed with the hexane−2-propanol−water mixture (2:2:1, v/v/v) after each injection.

UHPSFC instrument was connected with the mass spectrometer via the commercial interface kit (Waters) composed of two T-pieces enabling the backpressure control and mixing of column effluent with a makeup liquid. The mixture of methanol−water (99:1, v/v) at the flow rate 0.25 mL/min delivered by HPLC 515 pump (Waters) was used as a makeup liquid. The hybrid quadrupole−traveling wave ion mobility−time-of-flight mass spectrometer Synapt G2Si (Waters) in high-resolution mode with both positive-ion and negative-ion ESI modes was used in the mass range m/z 50−1600 with the following setting of tuning parameters: capillary voltages 3.0 kV and 2.5 kV for positive-ion and negative-ion modes, respectively, the sampling cone 20 V, the source offset 90 V, the source temperature 150 °C, the drying temperature 500 °C, the cone gas flow 0.8 L/min, the drying gas flow 17 L/min, and the nebulizer gas flow 4 bar. Leucine enkephaline was used as the lock mass for all experiments. MS/MS experiments were performed on a transfer cell with the collision energy ramp from 20 to 35 eV.

Method Validation. The linearity, the limit of detection (LOD), and the limit of quantitation (LOQ) of developed UHPSFC/ESI-MS method were determined based on the analysis of spiked lipid brain extract as a matrix by IS with the final concentration 0.4, 2, 4, 40, 400, 1000, and 3000 ng/mL. Ten microliters per milliliter of the extract stock solution was used for the experiments. The linearity was determined from calibration curves of individual IS plotted as peak abundances vs concentrations of standard solutions and calculated by the linear regression. Each calibration point was measured in triplicate from one calibration solution. LOD and LOQ were

DOI: 10.1021/acs.analchem.5b01054
Anal. Chem. 2015, 87, 7187−7195

determined from signal-to-noise ratios 3 and 10, respectively. Matrix effects were determined based on comparing the peak abundances of pure IS and IS spiked into the lipid brain extract as a matrix. The reproducibility of peak area was determined from 6 consecutive measurements of spiked porcine brain extract with IS for low (2 ng/mL) and high (1000 ng/mL) concentrations. The reproducibility of retention times was calculated as a standard deviation from 6 consecutive injections of the sample.

Quantitative Analysis. Final UHPSFC/ESI-MS conditions were used for quantitative analysis of lipid species in the porcine brain sample. Concentrations of lipid species were calculated from peak abundances of corresponding ions in lipid class ESI mass spectra after the isotopic correction related to the peak abundance of IS. Concentrations were calculated in pmol/mg of wet sample with average standard deviation of ±1.9%.

Lipid Nomenclature. LIPID MAPS nomenclature[4,5] and shorthand notation[43] were followed throughout this manuscript.

RESULTS AND DISCUSSION

UHPSFC/ESI-MS Method Development. Precise, comprehensive, and high-throughput methods are required for the analysis of large sample sets in current lipidomics. Our lipidomic approach is based on UHPSFC lipid class separation followed by ESI-MS identification and quantitation of individual species. UHPSFC with 1.7 μm particle size column is used in this work as the method providing high chromatographic efficiency together with high speed of analyses. First, the comprehensive nontargeted UHPSFC/ESI-MS analysis of representative or pooled sample is performed to describe the lipidomic composition of studied samples. The total lipid extract is separated into lipid classes using UHPSFC enabling their direct identification according to retention times. Individual lipid species within lipid classes are identified using positive-ion and negative-ion MS and MS/MS spectra with high mass accuracy and high resolving power. Then, the targeted quantitative analysis of identified lipid species in individual samples is performed using the UHPSFC/ESI-MS. Concentrations of individual lipid species are obtained from their relative abundances related to the IS.

In our work, we follow a generally accepted strategy of quantitative lipidomic analysis using IS per each lipid class added before the extraction, which covers different extraction efficiencies and MS responses among lipid classes, while differences among individual species within the class given by different acyl composition are not considered. IS are selected based on the detailed knowledge of lipidomic composition from the nontargeted UHPSFC/ESI-MS analysis of representative sample without IS. Lipid species which are not detected in the representative sample or having concentrations below LOQ are used as IS (see Experimental Section), that is, species containing deuterium atoms (D7-cholesterol), odd number fatty acyls (e.g., CE 19:0, DG 19:0/0:0/19:0, etc.), short or long fatty acyls (e.g., PE 14:0/14:0, PC 22:1/22:1, etc.) similarly to previous works.[10,13] Prerequisite for the precise quantitation is identical ionization conditions for IS and determined lipids, mainly a mobile phase composition and a matrix, which is especially important for the gradient elution. This requirement cannot be fulfilled with widely used C18 columns in the SFC analysis, where species within the lipid class are separated according to the composition of fatty acyls and elute in different retention times under the different mobile phase composition within the gradient. For this reason, we have decided to use HILIC-like separation of lipids into lipid classes, where lipid species and lipid class IS coelute in one peak under the identical mobile phase and matrix composition. Moreover, ion suppression effects among lipid classes are avoided as they are separated into individual peaks. For this purpose, UHPSFC dedicated column with bridged ethylene hybrid silica stationary phase is selected for the lipid class separation and individual parameters of the UHPSFC separation are carefully optimized with respect to the separation of the highest number of lipid classes within the shortest analysis time.

A polar modifier has to be used to increase the polarity of mobile phase for the analysis of lipids due to their wide range of polarities from rather nonpolar up to ionic species. The composition of the modifier is one of the most critical parameters influencing the UHPSFC separation of lipids. Different organic solvents have been tested, such as 2-propanol, ethanol, methanol, acetonitrile and their mixtures. Methanol is the best compromise between the chromatographic and ionization efficiency and also provides the best solubility of ammonium acetate necessary for the separation of lipids, which is poorly soluble in 2-propanol and almost insoluble in acetonitrile. Mixtures of acetonitrile or 2-propanol with methanol have also been tested, but they do not bring significant improvement compared to pure methanol. The partial improvement of the peak shape mainly for polar lipids (eluting after 2.7 min) is achieved with the addition of small amount of water into the modifier (Supporting Information Figure S-1). The selectivity is not influenced by the addition of water into the modifier except for LacCer and PE species, which are baseline resolved at 1% of water in the modifier (3.45 and 3.59 min), but coelute at 3% (3.46 min). The significant effect mainly on the peak shape of polar species is observed for the concentration of ammonium acetate in the modifier (Figure 1). Without ammonium acetate, only nonpolar lipid classes eluting before 2.0 min are separated, while polar lipids provide very broad peaks. The peak shape of polar lipids is significantly improved by increasing the concentration of ammonium acetate, while the separation of nonpolar lipids is not influenced. The ionization efficiency of lipids is also influenced by the addition of ammonium acetate into the modifier. The peak areas of TG, MG, GlcCer, and LacCer are reduced to half with addition of 5 mM of ammonium acetate, but the peak area of CE is doubled (Supporting Information Table S-1). The ionization efficiency of lipids is almost constant within the range from 5 to 30 mM of ammonium acetate and starts slightly deteriorate at 50 mM, therefore the concentration of 30 mM is selected. The addition of acetic acid or ammonium hydroxide has also been tested, but the effect on the chromatographic separation is negligible, so they are not used in the final method.

The analysis time is shorter with increased initial concentration of the modifier, but the low concentration (1%) is selected for the gradient, because it significantly improves the separation of nonpolar lipid classes (Supporting Information Figure S-2). Peak widths are slightly improved with the increase of the modifier gradient steepness, while the separation of lipids is not significantly influenced, which perfectly fits with the requirement for the high-throughput method (Supporting Information Figure S-3). As expected, the increased flow rate does not influence too much the chromatographic resolution using UHPSFC (Supporting

DOI: 10.1021/acs.analchem.5b01054
Anal. Chem. 2015, 87, 7187−7195

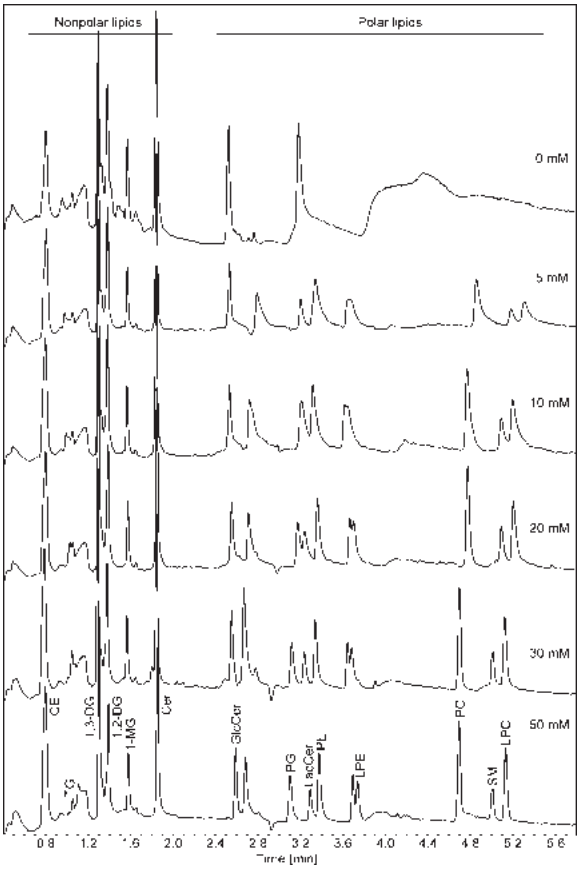

Figure 1. Effect of ammonium acetate concentration in the modifier on the UHPSFC/ESI-MS analysis of lipid class standards. UHPSFC conditions: Acquity BEH UPC^2 column (100 × 3 mm, 1.7 μm, Waters), the flow rate 1.9 mL/min, column temperature 60 °C, the ABPR pressure 1500 psi and the gradient of methanol with ammonium acetate as a modifier: 0 min, 2%; 5 min, 52%; 6 min, 52%. Peak annotation: CE, cholesteryl esters; TG, triacylglycerols; DG, diacylglycerols; MG, monoacylglycerols; Cer, ceramides; GlcCer, glucosylceramides; PG, phosphatidylglycerols; LacCer, lactosylceramides; PE, phosphatidylethanolamines; LPE, lysophosphatidylethanolamines; PC, phosphatidylcholines; SM, sphingomyelins; LPC, lysophosphatidylcholines.

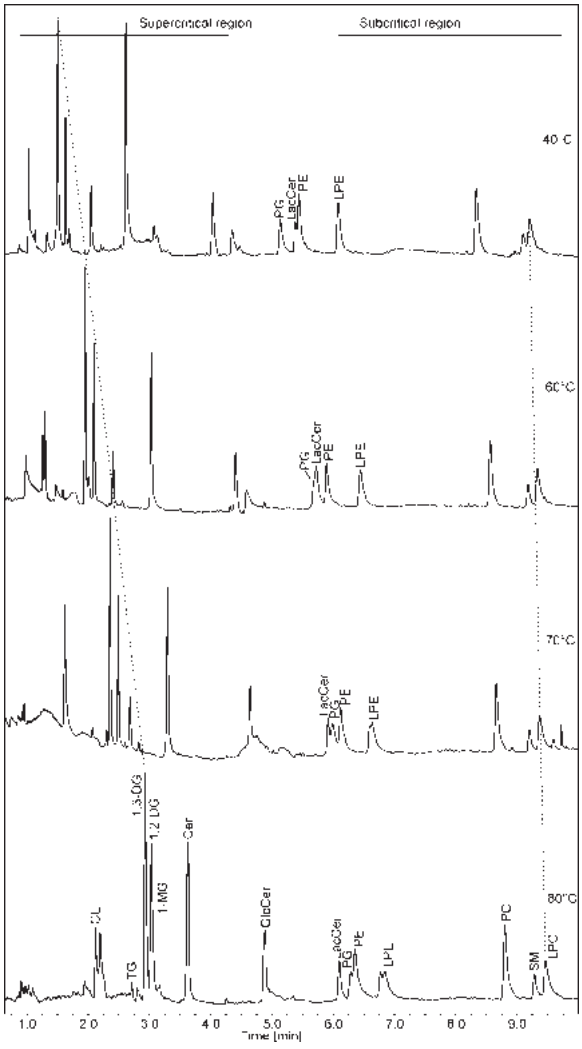

Figure 2. Effect of column temperature on the UHPSFC/ESI-MS analysis of lipid class standards. Dashed lines highlight changes of the retention behavior of TG (left) and LPC (right) species. UHPSFC conditions: Acquity BEH UPC^2 column (100 × 3 mm, 1.7 μm, Waters), the flow rate 1.9 mL/min, the ABPR pressure 1500 psi and the gradient of methanol with 10 mM of ammonium acetate as the modifier: 0 min, 0%; 10 min, 50%; 11 min, 50%. Peak annotation: CE, cholesteryl esters; TG, triacylglycerols; DG, diacylglycerols; MG, monoacylglycerols; Cer, ceramides; GlcCer, glucosylceramides; PG, phosphatidylglycerols; LacCer, lactosylceramides; PE, phosphatidylethanolamines; LPE, lysophosphatidylethanolamines; PC, phosphatidylcholines; SM, sphingomyelins; LPC, lysophosphatidylcholines.

Information Figure S-4), which is in accordance with well-known fact that the optimum theoretical plate height lies in a wide range of linear velocities.[34] It has to be noted that multiple parameters are changed by the change of flow rate, such as the column pressure drop and the gradient volume to column volume ratio. The flow rate of 1.9 mL/min is used, which enables the high-throughput analysis with short retention times and acceptable system backpressure.

In this work, no significant effect on the chromatographic efficiency is observed with the change of active back pressure regulator pressure (Supporting Information Figure S-5), therefore the pressure of 1800 psi is used as the lowest recommended value for a good reproducibility of retention times. The column temperature (Figure 2) does not significantly influence the chromatographic efficiency, but it causes some minor changes in the chromatographic selectivity. This can be demonstrated on the retention order of PG and LacCer standards, that is, PG elutes before LacCer at 40 and 60 °C, but after at 70 and 80 °C. The temperature 60 °C is used, which is a common value for UHPSFC analyses and provides a lower resistance and system backpressure.

UHPSFC effluent is mixed with the makeup fluid to ensure the ionization of lipids using ESI. The flow rate and the composition of makeup fluid have been optimized with respect to the ionization efficiency of lipids. The separated species are diluted by the makeup fluid lowering their concentration and sensitivity; therefore, the lowest possible flow rate of 0.25 mL/min is used, which is sufficient for stable electrospray and good ionization efficiency of lipids. The composition of the makeup fluid has also been optimized with the best results obtained for the mixture of methanol−water (99:1, v/v), which corresponds to the composition of the modifier in the final method.

DOI: 10.1021/acs.analchem.5b01054
Anal. Chem. 2015, 87, 7187−7195

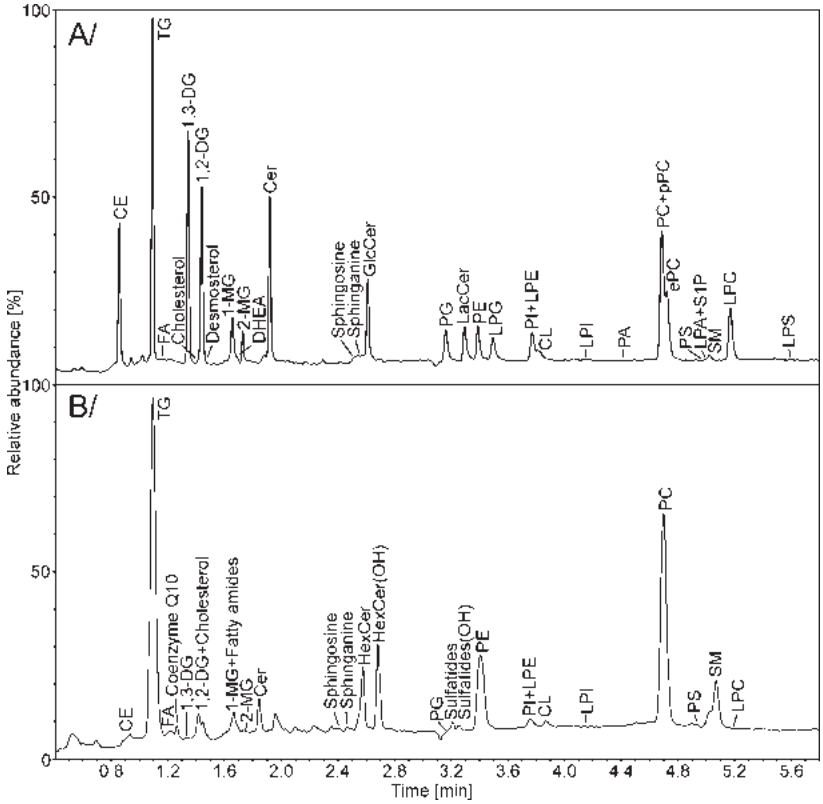

Figure 3. Positive-ion UHPSFC/ESI-MS chromatograms of the mixture of lipid class standards (A) and the total lipid extract of porcine brain (B). UHPSFC conditions: Acquity BEH UPC^2 column (100 × 3 mm, 1.7 μm, Waters), the flow rate 1.9 mL/min, the column temperature 60 °C, the ABPR pressure 1800 psi and the gradient of methanol−water mixture (99:1, v/v) containing 30 mM of ammonium acetate as the modifier: 0 min, 1%; 5 min, 51%; 6 min, 51%. Peak annotation: CE, cholesteryl esters; TG, triacylglycerols; FA, fatty acids; DG, diacylglycerols; MG, monoacylglycerols; DHEA, dehydroepiandrosterone; Cer, ceramides; GlcCer, glucosylceramides; HexCer, hexosylceramides; PG, phosphatidylglycerols; LacCer, lactosylceramides; pPE, 1-alkenyl-2-acyl phosphatidylethanolamines (plasmalogens); ePE, 1-alkyl-2-acyl phosphatidylethanolamines (ethers); PE, phosphatidylethanolamines; LPG, lysophosphatidylglycerols; PI, phosphatidylinositols; LPE, lysophosphatidylethanolamines; CL, cardiolipins; LPI, lysophosphatidylinositols; PA, phosphatidic acids; PC, phosphatidylcholines; pPC, 1-alkenyl-2-acyl phosphatidylcholines; ePC, 1-alkyl-2-acyl phosphatidylcholines; PS, phosphatidylserines; LPA, lysophosphatidic acids; S1P, sphingosine-1-phosphate; SM, sphingomyelins; LPC, lysophosphatidylcholines; LPS, lysophosphatidylserines.

UHPSFC Separation of Lipids. Figure 3 shows the separation of lipid class representatives (Figure 3A) and the total lipid extract of porcine brain (Figure 3B) using the final UHPSFC method (see Experimental Section). In our UHPSFC method, lipids are mainly separated according to their polarity into lipid classes. Retention times increase with the increased lipid polarity similarly to HILIC or NP-HPLC separations. In total, up to 30 lipid classes from 6 different lipid categories covering the wide range of nonpolar and polar lipids are separated within 6 min analysis. Under optimized UHPSFC conditions, most of lipid classes are baseline or at least partially separated. Similarly to HPLC separations, the strong peak tailing is observed for UHPSFC of acidic lipids, such as PA, PS, LPA, S1P and LPS, which complicates their precise quantitation. This behavior can be overcome by the use of stronger additives, such as alkylamines,[44] but these additives are not compatible with MS detection, because they cause severe memory effects.[45]

In addition to the class separation, lipid species within individual lipid classes are partially separated according to the fatty acyl composition (Figure 4). Retention times of all lipids increase with increased DB number, as demonstrated on reconstructed ion chromatograms of TG with 54 carbon atoms and the different number of DB (Figure 4A). The different situation is observed for the species differing in fatty acyl lengths, where the retention behavior of lipids differs for individual lipid classes. Retention times of TG increase with the fatty acyl length (Figure 4B), which is observed also for other nonpolar lipid classes, such as CE, FA, DG, MG, fatty amides and Cer (Supporting Information Table S-2). On the other hand, retention times of polar lipids decrease for longer fatty acyls, which can be demonstrated on the separation of PC species (Figure 4C). The retention behavior of nonpolar and polar lipids using UHPSFC can be correlated with HPLC using HILIC and NP modes.[17,22] Retention times of nonpolar lipids increase with the higher number of DB both in NP-HPLC and UHPSFC systems, but UHPSFC also provides the partial separation of lipid species differing in fatty acyl lengths. No separation is observed in the HILIC mode for polar lipids containing 0 to 3 DB, but species with 4 and more DB are less retained, which is reversed to UHPSFC. On the other hand, lower retention times for longer fatty acyl species are observed for HILIC mode, which is the same as for UHPSFC of polar lipids. It seems that there is a mixed-mode retention mechanism using our UHPSFC method changing from NP mechanism for nonpolar lipids to HILIC mechanism for polar lipids. This

DOI: 10.1021/acs.analchem.5b01054
Anal. Chem. 2015, 87, 7187−7195

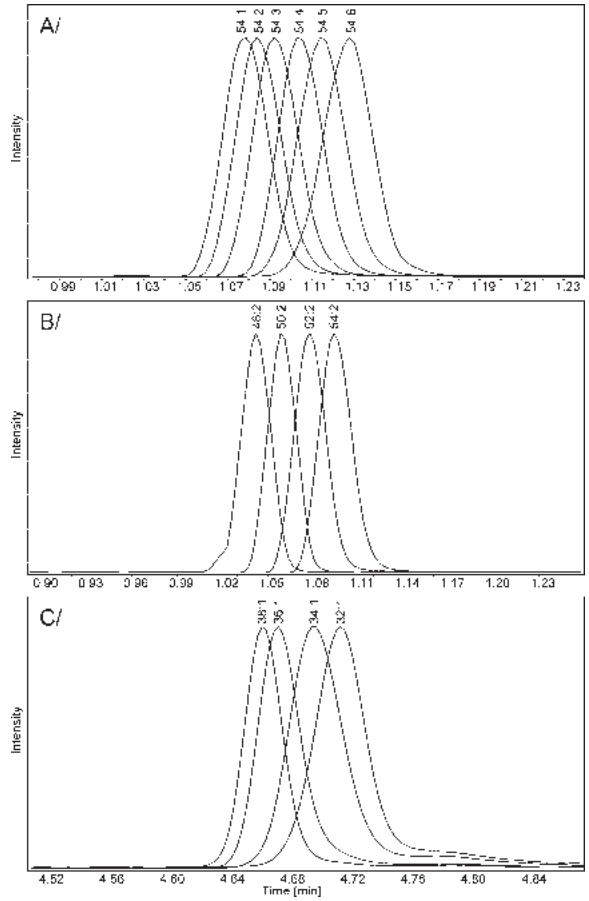

Figure 4. Effects of DB number and fatty acyl chain length on the retention behavior of lipids using UHPSFC/ESI-MS. Reconstructed ion chromatograms from the analysis of porcine brain extract: A/TG with 54 carbon atoms and the different number of DB, B/TG with 2 DB and the different number of carbon atoms and C/PC with 1 DB and the different number of carbon atoms. UHPSFC conditions are identical as for Figure 2.

phenomenon is probably caused by the mobile phase composition during the gradient. Almost pure CO_2 is used at the beginning of the analysis close to nonpolar mobile phases used in NP-HPLC. Then, the concentration of polar modifier is increased during the analysis changing from NP to HILIC conditions. This behavior enables the separation of both nonpolar and polar species in one analysis, which is not usually achieved by NP or HILIC modes or with poor reproducibility of retention times.

The addition of modifier changes the critical point of the mobile phase and usually 20−30% of modifier at maximum can be used to keep supercritical conditions. In this work, up to 51% of the modifier had to be used for the elution of polar lipid classes (e.g., PC, SM, LPC, etc.). It is evident that the mobile phase changes from the supercritical to subcritical fluid during the analysis due to high increase of modifier concentration. This can be clearly demonstrated by the influence of column temperature on retention times of lipids (Figure 2). In general, higher temperature induces a lower density of mobile phase leading to the increase of retention times.[34] Retention times of lipids increase with higher temperature using UHPSFC (as shown in Figure 2), but this effect is more pronounced in the supercritical region corresponding to approximately 1% to 26% of the modifier (up to 5 min). For example, the change of retention time of TG is 1.43 min between 40 and 80 °C, while the change for LPC is only 0.26 min. The similar behavior is observed for the ABPR pressure (Supporting Information Figure S-5). Retention times of lipids decrease with higher pressure under supercritical conditions due to the increase of mobile phase density, but changes in the subcritical region are slightly lower. Although properties of used mobile phase change significantly during the analysis, the reproducibility of retention times is very good.

UHPSFC/ESI-MS Identification of Lipids. Retention times from the UHPSFC analysis and the ESI mass spectra measured with high mass accuracy and high resolving power in both positive- and negative-ion modes are used for the unambiguous identification of individual lipid species (Supporting Information Table S-2). The total lipid extract is separated into lipid classes using the UHPSFC enabling the direct identification of lipid class based on the comparison of retention times with standards. The class separation of lipids also avoids the ion suppression effects among different lipid classes and improves the identification of isobaric (e.g., PC 36:1 vs PS 36:2) and trace species. Then, the averaged mass spectrum of lipid class chromatographic peak is used for the determination of lipid species level (Supporting Information Figure S-6), that is, the number of carbon atoms and DB of attached fatty acyl/alkyls. The partial separation of individual species within lipid classes according to fatty acyl lengths and the number of DB provides another supporting information for their identification. The fatty acyl composition of individual species can be determined using $[RCOO]^-$ ions in negative-ion MS/MS spectra.[17]

The ionization and fragmentation behavior of individual lipid classes using the UHPSFC/ESI-MS is similar to HPLC/ESI-MS. The most abundant ions in positive-ion UHPSFC/ESI-MS full scan mass spectra are protonated molecules $[M + H]^+$ (base peaks for fatty amides, sphinganine, LacCer, PE, LPE, CL, PC, SM, and LPC), adducts with ammonium ion $[M + NH_4]^+$ (TG and coenzyme Q10) and neutral losses of water $[M + H - H_2O]^+$ (DG, cholesterol, MG, Cer, sphingosine and LacCer), attached fatty acyls $[M + H - acyl]^+$ (CE) or phosphoglycerol $[M + H - H_2PO_4CH_2CHOHCH_2OH]^+$ (PG and LPG) and sulfo $[M + H - SO_3]^+$ (sulfatides) groups. UHPSFC/ESI-MS mass spectra provide relatively low abundance of sodium adduct ions, which reduces the risk of incorrect identification between $[M + H]^+$ and $[M + Na]^+$ ions, because the difference $\Delta m/z = 22$ also corresponds to additional 2 methylene units minus 3 DB. The relative abundance of $[M + Na]^+$ ions is below 1.5% for CE, TG, PC, SM, and LPC, from 3 to 10% for DG, Cer, PG, PE, LPG, and LPE and more than 20% only for MG, GlcCer and LacCer. The data are also correlated with negative-ion mass spectra and retention times of lipid species within lipid classes to unambiguously confirm the identification of all reported lipids. Positive-ion MS/MS spectra of identified classes provide well-known characteristic fragment ions and neutral losses observed in HPLC/MS, such as the phosphocholine fragment ion $m/z = 184$ ($[H_2PO_4CH_2CH_2N(CH_3)_3]^+$) for moieties containing choline (PC, LPC, and SM), $m/z = 369$ ($[M + H - H_2O]^+$ or $[M + H - acyl]^+$) for cholesterol containing lipids (cholesterol and CE) or fragment ions corresponding to ceramide bases (Cer, GlcCer, and LacCer). The neutral loss of phosphoethanolamine $\Delta m/z = 141$ ($H_2PO_4CH_2CH_2NH_2$) is observed for PE and neutral losses of fatty acyls for TG, DG, and MG. In the negative-ion mode,

DOI: 10.1021/acs.analchem.5b01054
Anal. Chem. 2015, 87, 7187−7195

Table 1. Calibration Parameters of Internal Standards (IS) in the Porcine Brain Matrix Using UHPSFC/ESI-MS Method

IS	calibration range [pmol/mL]	slope	correlation coefficient	LOD[a] [pmol/mL]	LOQ[b] [pmol/mL]	matrix effect
			positive-ion mode			
CE 19:0	0.5−4200	0.624	0.994	0.1	0.4	100
TG 19:0/19:0/19:0	0.4−1200	69.590	0.993	0.07	0.2	78
FA 14:0	n.d.[c]	n.d.[c]	n.d.[c]	n.d.[c]	n.d.[c]	n.d.[c]
DG 19:0/0:0/19:0	0.6−1600	35.354	0.996	0.2	0.7	103
D7-cholesterol	100−7100	0.043	0.992	74	247	76
MG 19:0/0:0/0:0	1−2800	7.561	0.993	1.4	4.6	91
Cer d18:1/17:0	0.8−1900	22.926	0.996	0.1	0.4	89
GlcCer d18:1/12:0	65−4300	0.678	0.991	66	220	86
PG 14:0/14:0	60−4100	0.403	1.000	99	329	78
LacCer d18:1/12:0	55−3600	0.403	0.997	33	111	108
PE 14:0/14:0	65−4400	0.444	0.998	90	298	147
LPG 14:0/0:0	95−6400	0.169	1.000	114	379	157
LPE 14:0/0:0	100−6500	0.150	0.998	375	1252	83
PC 22:1/22:1	0.5−3100	1.402	0.999	0.4	1.5	87
PC 14:0/14:0	6−4100	1.688	0.998	12	41	78
SM d18:1/17:0	0.6−3900	2.235	0.997	0.4	1.3	83
LPC 17:0/0:0	9−5700	1.833	0.999	18	61	85
			negative-ion mode			
CE 19:0	n.d.[c]	n.d.[c]	n.d.[c]	n.d.[c]	n.d.[c]	n.d.[c]
TG 19:0/19:0/19:0	n.d.[c]	n.d.[c]	n.d.[c]	n.d.[c]	n.d.[c]	n.d.[c]
FA 14:0	2−4600	1.338	0.996	0.3	1.0	92
DG 19:0/0:0/19:0	0.6−1600	4.611	1.000	1.1	3.5	83
D7-Cholesterol	n.d.[c]	n.d.[c]	n.d.[c]	n.d.[c]	n.d.[c]	n.d.[c]
MG 19:0/0:0/0:0	6−2800	0.870	0.999	7.3	24	86
Cer d18:1/17:0	0.8−1900	19.708	0.998	0.01	0.03	96
GlcCer d18:1/12:0	3−4300	1.261	0.993	4.2	14	82
PG 14:0/14:0	3−4100	1.235	1.000	4.8	16	94
LacCer d18:1/12:0	3−3600	0.971	0.991	5.1	17	85
PE 14:0/14:0	3−4400	0.855	0.994	5.8	19	98
LPG 14:0/0:0	5−6400	0.930	0.997	5.0	17	87
LPE 14:0/0:0	5−6500	0.561	1.000	5.5	18	88
PC 22:1/22:1	0.5−3100	0.326	0.999	0.8	2.5	89
PC 14:0/14:0	0.6−4100	0.337	0.999	0.5	1.7	84
SM d18:1/17:0	0.6−3900	0.523	0.992	0.02	0.06	97
LPC 17:0/0:0	0.9−5700	0.266	0.999	0.6	2.1	96

[a]LOD: limit of detection (S/N = 3). [b]LOQ: limit of quantitation (S/N = 10). [c]n.d.: not detected.

base peaks of spectra are mostly deprotonated molecules $[M - H]^-$, except for DG, PC, SM, and LPC providing mainly adduct ions with acetate $[M + CH_3COO]^-$. Relatively high abundances of $[M + CH_3COO]^-$ ions are also observed for Cer, GlcCer, and LacCer (70−95%). CL species exhibit $[M - 2H]^{2-}$ ions, which can be used for their identification even in the lower mass range, such as m/z = 50−1000 usually used in lipidomic analyses. Negative-ion MS/MS spectra show mainly $[RCOO]^-$ ions corresponding to the fatty acyl/alkyl composition.

Validation of UHPSFC/ESI-MS Method. Developed UHPSFC/ESI-MS method has been tested for the analysis of real samples represented by porcine brain extract as a complex lipidomic matrix. Table 1 shows calibration parameters of IS spiked into the porcine brain lipid extract using positive- and negative-ion ESI-MS. Obtained calibration curves (Supporting Information Figure S-7) of IS are linear within tested calibration ranges with correlation coefficients better than 0.991 in all cases. The positive-ion mode can be used for the quantitation of all tested lipid classes except for FA. In the negative-ion mode, CE, TG, and cholesterol are not detected. On the other hand, the negative-ion mode provides a better sensitivity for most classes indicated by lower LOD. Slopes of PC species slightly differ in the positive-ion mode (1.402 vs 1.688), while the difference is negligible in the negative-ion mode (0.326 vs 0.337). Slightly different ionization efficiencies can be expected for species differing by 16 carbon atoms and two double bonds in fatty acyls (i.e., 28:0 vs 44:2), but the same ionization behavior should be observed in both ionization modes. Another explanation of such behavior can be different influence of the matrix used for validation experiments to saturated and unsaturated species only in the positive-ion mode. The effect of the matrix on the response of IS (Table 1) has been evaluated from the analysis of pure IS and IS spiked into the porcine brain matrix. In negative-ion mode, the matrix effects for all IS are not significant ranging between 82% to 98%. The different behavior is observed in the positive-ion mode, where the influence of the matrix is much more pronounced. Especially ionization efficiencies of PE and LPG standards are significantly enhanced in the matrix (matrix effects 147% and 157%, respectively). The matrix has significant effect on the ionization efficiency of lipids, but these effects are identical for both lipid species and IS coeluting in one chromatographic peak. The reproducibility of peak areas has

DOI: 10.1021/acs.analchem.5b01054
Anal. Chem. 2015, 87, 7187−7195

been calculated for IS added into the porcine brain lipid extract for 6 consecutive analyses. Average standard deviations of peak areas of IS are 2.9% and 8.2% for concentrations 1000 and 2 ng/mL, respectively.

The final UHPSFC/ESI-MS method provides an excellent intraday stability of retention times in the range ±0.01 min. A small continuous reduction of retention times of mainly polar lipids is observed during multiple consecutive days. This phenomenon of small retention shift on SFC columns is probably given by the formation of silyl ethers on the particle surface with alcohols from the mobile phase leading to the decrease of hydrophilicity,[46] but it does not affect the identification and quantitation of lipids. The process is reversible and silanols can be hydroxylated again using water. For this reason, the column is regenerated daily by 5 consecutive injections of 10 μL of water and acetonitrile into 100% of CO_2 at 0.5 mL/min flow rate (Supporting Information Figure S-8) or occasionally is flushed with water−acetonitrile mixture (1:1, v/v), which minimizes this effect.

UHPSFC/ESI-MS Analysis of Porcine Brain. Figure 3B shows the separation of the total lipid extract from the porcine brain using the final UHPSFC/ESI-MS method. The porcine brain is selected as a testing sample due to its high lipidomic complexity, which covers a high number of nonpolar and polar lipid classes with a wide range of polarities. 436 lipid species are identified and quantified in the porcine brain using the UHPSFC/ESI-MS method (Supporting Information Table S-2) from 24 different lipid classes and 6 main lipid categories including fatty acyls, glycerolipids, glycerophospholipids, sphingolipids, sterols, and prenols. The number and profile of the identified species is comparable to recently published characterization of brain samples using conventional lipidomic methods. For example, 311 lipid species from 20 lipid classes have been identified in mouse cerebellum and hippocampus using the shotgun MS method, the instrument with 450 000 resolving power and different MS/MS methods.[47] 325 lipid species from 22 lipid classes have been quantified using HILIC and two RP-HPLC/MS methods in mouse and human brain tissues.[48]

The highest number of lipid species is identified for TG (72 species), PC (46), HexCer (40), sulfatides (35), PE (34), CL (32), FA (32), 1,2-DG (25), and SM (21). Glycosyl moieties in ceramide species, such as glucose and galactose, are not resolved using the UHPSFC/ESI-MS method and therefore they are annotated as hexosyl ceramides (HexCer). Lipid species with the various DB number are identified, from fully saturated up to highly polyunsaturated species containing 15 DB in case of CL 80:15. The lowest number of DB is observed for ceramides (Cer, HexCer, and sulfatides) and SM with 2 or at maximum 3 DB. Coenzyme Q10 as a representative of prenols is also identified in the porcine brain. The large number of PE and PC species with ether (ethers, ePE, ePC) and vinylether (plasmalogens, pPE, pPC) linkage are identified (Supporting Information Table S-2), but these species (ethers vs vinylethers) cannot be differentiated, so we report both possibilities.

CONCLUSIONS

The application of lipid class separation using the UHPSFC/ESI-MS for the high-throughput and comprehensive lipidomic analysis is presented for the first time in this work. The main advantage of this method is short analysis time for the separation of both nonpolar and polar lipid classes comparable to established shotgun MS methods, but the separation dimension provides other benefits over direct infusion methods, such as easier identification of isobaric lipids based on retention times and the identification of trace species using reconstructed ion chromatograms. The quantitative analysis of lipids is also significantly improved, because the class separation completely avoids the ion suppression effects among lipid classes and individual species within the class are ionized together with IS under the same matrix effects. Results from the optimization of individual chromatographic parameters show a different behavior of lipid species under supercritical and subcritical conditions. The comprehensive analysis using the UHPSFC/ESI-MS method for a wide range of nonpolar and polar lipid classes is demonstrated on analyses of lipid class standards and the complex lipidomic sample. Obtained validation parameters show the applicability of the developed UHPSFC/ESI-MS method for the lipidomic analysis of real samples. The present work is a proof-of-concept of the use of UHPSFC/ESI-MS method for lipidomic analysis of large sample sets in clinical studies.

ASSOCIATED CONTENT

Supporting Information

Effects of water concentration, the modifier initial concentration, modifier gradient steepness, flow rate, and ABPR pressure on the UHPSFC analysis of lipid class standards, examples of ESI mass spectra of lipid classes, examples of calibration curves, effect of column regeneration on the UHPSFC analysis, effect of ammonium acetate concentration in the modifier on the peak areas of lipid class standards using UHPSFC/ESI-MS, and lipid species identified in porcine brain extract. The Supporting Information is available free of charge on the ACS Publications website at DOI: 10.1021/acs.analchem.5b01054.

AUTHOR INFORMATION

Corresponding Author

*E-mail: Miroslav.Lisa@upce.cz. Tel: +420466037090.

Notes

The authors declare no competing financial interest.

ACKNOWLEDGMENTS

This work was supported by the grant project LL1302 sponsored by the Ministry of Education, Youth and Sports of the Czech Republic.

REFERENCES

(1) Dennis, E.A.; et al. Lipidomics Gateway. http://www.lipidmaps.org/ (accessed September 2014).

(2) Quehenberger, O.; Armando, A. M.; Brown, A. H.; Milne, S. B.; Myers, D. S.; Merrill, A. H.; Bandyopadhyay, S.; Jones, K. N.; Kelly, S.; Shaner, R. L.; Sullards, C. M.; Wang, E.; Murphy, R. C.; Barkley, R. M.; Leiker, T. J.; Raetz, C. R. H.; Guan, Z.; Laird, G. M.; Six, D. A.; Russell, D. W.; McDonald, J. G.; Subramaniam, S.; Fahy, E.; Dennis, E. A. *J. Lipid Res.* **2010**, *51*, 3299.

(3) van Meer, G.; Voelker, D. R.; Feigenson, G. W. *Nat. Rev. Mol. Cell Biol.* **2008**, *9*, 112.

(4) Fahy, E.; Subramaniam, S.; Brown, H. A.; Glass, C. K.; Merrill, A. H.; Murphy, R. C.; Raetz, C. R. H.; Russell, D. W.; Seyama, Y.; Shaw, W.; Shimizu, T.; Spener, F.; van Meer, G.; VanNieuwenhze, M. S.; White, S. H.; Witztum, J. L.; Dennis, E. A. *J. Lipid Res.* **2005**, *46*, 839.

(5) Fahy, E.; Subramaniam, S.; Murphy, R. C.; Nishijima, M.; Raetz, C. R. H.; Shimizu, T.; Spener, F.; van Meer, G.; Wakelam, M. J. O.; Dennis, E. A. *J. Lipid Res.* **2009**, *50*, S9.

DOI: 10.1021/acs.analchem.5b01054
Anal. Chem. 2015, 87, 7187−7195

(6) Li, M.; Yang, L.; Bai, Y.; Liu, H. *Anal. Chem.* **2014**, *86*, 161.
(7) Čajka, T.; Fiehn, O. *TrAC, Trends Anal. Chem.* **2014**, *61*, 192.
(8) Yang, K.; Cheng, H.; Gross, R. W.; Han, X. *Anal. Chem.* **2009**, *81*, 4356.
(9) Heiskanen, L. A.; Suoniemi, M.; Ta, H. X.; Tarasov, K.; Ekroos, K. *Anal. Chem.* **2013**, *85*, 8757.
(10) Wiesner, P.; Leidl, K.; Boettcher, A.; Schmitz, G.; Liebisch, G. *J. Lipid Res.* **2009**, *50*, 574.
(11) Jonasdottir, H. S.; Nicolardi, S.; Jonker, W.; Derks, R.; Palmblad, M.; Ioan-Facsinay, A.; Toes, R.; van der Burgt, Y. E. M.; Deelder, A. M.; Mayboroda, O. A.; Giera, M. *Anal. Chem.* **2013**, *85*, 6003.
(12) Li, F.; Qin, X.; Chen, H.; Qiu, L.; Guo, Y.; Liu, H.; Chen, G.; Song, G.; Wang, X.; Li, F.; Guo, S.; Wang, B.; Li, Z. *Rapid Commun. Mass Spectrom.* **2013**, *27*, 24.
(13) Schuhmann, K.; Almeida, R.; Baumert, M.; Herzog, R.; Bornstein, S. R.; Shevchenko, A. *J. Mass Spectrom.* **2012**, *47*, 96.
(14) Fhaner, C. J.; Liu, S. C.; Ji, H.; Simpson, R. J.; Reid, G. E. *Anal. Chem.* **2012**, *84*, 8917.
(15) Lintonen, T. P. I.; Baker, P. R. S.; Suoniemi, M.; Ubhi, B. K.; Koistinen, K. M.; Duchoslav, E.; Campbell, J. L.; Ekroos, K. *Anal. Chem.* **2014**, *86*, 9662.
(16) Sommer, U.; Herscovitz, H.; Welty, F. K.; Costello, C. E. *J. Lipid Res.* **2006**, *47*, 804.
(17) Lísa, M.; Cífková, E.; Holčapek, M. *J. Chromatogr. A* **2011**, *1218*, 5146.
(18) Cífková, E.; Holčapek, M.; Lísa, M.; Ovčačíková, M.; Lyčka, A.; Lynen, F.; Sandra, P. *Anal. Chem.* **2012**, *84*, 10064.
(19) Cífková, E.; Holčapek, M.; Lísa, M. *Lipids* **2013**, *48*, 915.
(20) Scherer, M.; Schmitz, G.; Liebisch, G. *Clin. Chem.* **2009**, *55*, 1218.
(21) Olsson, P.; Holmback, J.; Herslof, B. *Lipids* **2012**, *47*, 93.
(22) Holčapek, M.; Cífková, E.; Červená, B.; Lísa, M.; Vostálová, J.; Galuszka, J. *J. Chromatogr. A* **2015**, *1377*, 85.
(23) Hutchins, P. M.; Barkley, R. M.; Murphy, R. C. *J. Lipid Res.* **2008**, *49*, 804.
(24) McLaren, D. G.; Miller, P. L.; Lassman, M. E.; Castro-Perez, J. M.; Hubbard, B. K.; Roddy, T. P. *Anal. Biochem.* **2011**, *414*, 266.
(25) Ahn, E. J.; Kim, H.; Chung, B. C.; Kong, G.; Moon, M. H. *J. Chromatogr. A* **2008**, *1194*, 96.
(26) Berdeaux, O.; Juaneda, P.; Martine, L.; Cabaret, S.; Bretillon, L.; Acar, N. *J. Chromatogr. A* **2010**, *1217*, 7738.
(27) Sandra, K.; Pereira, A. d. S.; Vanhoenacker, G.; David, F.; Sandra, P. *J. Chromatogr. A* **2010**, *1217*, 4087.
(28) Sato, Y.; Suzuki, I.; Nakamura, T.; Bernier, F.; Aoshima, K.; Oda, Y. *J. Lipid Res.* **2012**, *53*, 567.
(29) Lísa, M.; Netušilová, K.; Franěk, L.; Dvořáková, H.; Vrkoslav, V.; Holčapek, M. *J. Chromatogr. A* **2011**, *1218*, 7499.
(30) Holčapek, M.; Lísa, M.; Jandera, P.; Kabátová, N. *J. Sep. Sci.* **2005**, *28*, 1315.
(31) Lísa, M.; Holčapek, M. *J. Chromatogr. A* **2008**, *1198*, 115.
(32) Ollero, M.; Astarita, G.; Guerrera, I. C.; Sermet-Gaudelus, I.; Trudel, S.; Piomelli, D.; Edelman, A. *J. Lipid Res.* **2011**, *52*, 1011.
(33) Gao, X.; Zhang, Q.; Meng, D.; Isaac, G.; Zhao, R.; Fillmore, T. L.; Chu, R. K.; Zhou, J.; Tang, K.; Hu, Z.; Moore, R. J.; Smith, R. D.; Katze, M. G.; Metz, T. O. *Anal. Bioanal. Chem.* **2012**, *402*, 2923.
(34) Nováková, L.; Perrenoud, A. G.-G.; Francois, I.; West, C.; Lesellier, E.; Guillarme, D. *Anal. Chim. Acta* **2014**, *824*, 18.
(35) Yamada, T.; Uchikata, T.; Sakamoto, S.; Yokoi, Y.; Nishiumi, S.; Yoshida, M.; Fukusaki, E.; Bamba, T. *J. Chromatogr. A* **2013**, *1301*, 237.
(36) Bamba, T.; Shimonishi, N.; Matsubara, A.; Hirata, K.; Nakazawa, Y.; Kobayashi, A.; Fukusaki, E. *J. Biosci. Bioeng.* **2008**, *105*, 460.
(37) Lee, J. W.; Nishiumi, S.; Yoshida, M.; Fukusaki, E.; Bamba, T. *J. Chromatogr. A* **2013**, *1279*, 98.
(38) Lesellier, E.; Latos, A.; de Oliveira, A. L. *J. Chromatogr. A* **2014**, *1327*, 141.
(39) Uchikata, T.; Matsubara, A.; Nishiumi, S.; Yoshida, M.; Fukusaki, E.; Bamba, T. *J. Chromatogr. A* **2012**, *1250*, 205.
(40) Matsubara, A.; Bamba, T.; Ishida, H.; Fukusaki, E.; Hirata, K. *J. Sep. Sci.* **2009**, *32*, 1459.
(41) Lee, J. W.; Nagai, T.; Gotoh, N.; Fukusaki, E.; Bamba, T. *J. Chromatogr. B* **2014**, *966*, 193.
(42) Sandra, P.; Medvedovici, A.; Zhao, Y.; David, F. *J. Chromatogr. A* **2002**, *974*, 231.
(43) Liebisch, G.; Vizcaino, J. A.; Kofeler, H.; Trotzmuller, M.; Griffiths, W. J.; Schmitz, G.; Spener, F.; Wakelam, M. J. O. *J. Lipid Res.* **2013**, *54*, 1523.
(44) Bure, C.; Ayciriex, S.; Testet, E.; Schmitter, J.-M. *Anal. Bioanal. Chem.* **2013**, *405*, 203.
(45) Holčapek, M.; Jirásko, R.; Lísa, M. *J. Chromatogr. A* **2010**, *1217*, 3908.
(46) Fairchild, J. N.; Brousmiche, D. W.; Hill, J. F.; Morris, M. F.; Boissel, C. A.; Wyndham, K. D. *Anal. Chem.* **2015**, DOI: 10.1021/ac5035709.
(47) Almeida, R.; Pauling, J. K.; Sokol, E.; Hannibal-Bach, H. K.; Ejsing, C. S. *J. Am. Soc. Mass Spectrom.* **2015**, *26*, 133.
(48) Chan, R. B.; Oliveira, T. G.; Cortes, E. P.; Honig, L. S.; Duff, K. E.; Small, S. A.; Wenk, M. R.; Shui, G.; Di Paolo, G. *J. Biol. Chem.* **2012**, *287*, 2678.

DOI: 10.1021/acs.analchem.5b01054
Anal. Chem. 2015, 87, 7187−7195

Journal of Chromatography A, 1439 (2016) 65–73

Contents lists available at ScienceDirect

Journal of Chromatography A

journal homepage: www.elsevier.com/locate/chroma

Hydrophilic interaction liquid chromatography–mass spectrometry of (lyso)phosphatidic acids, (lyso)phosphatidylserines and other lipid classes

Eva Cífková, Roman Hájek, Miroslav Lísa, Michal Holčapek*

Department of Analytical Chemistry, Faculty of Chemical Technology, University of Pardubice, Studentská 573, 53210 Pardubice, Czech Republic

ARTICLE INFO

Article history:
Received 9 November 2015
Received in revised form 15 January 2016
Accepted 25 January 2016
Available online 29 January 2016

Keywords:
Phosphatidic acid
Phosphatidylserine
Phospholipids
Lysophospholipids
HILIC
LC/MS

ABSTRACT

The goal of this work is a systematic optimization of hydrophilic interaction liquid chromatography (HILIC) separation of acidic lipid classes (namely phosphatidic acids—PA, lysophosphatidic acids—LPA, phosphatidylserines—PS and lysophosphatidylserines—LPS) and other lipid classes under mass spectrometry (MS) compatible conditions. The main parameters included in this optimization are the type of stationary phases used in HILIC, pH of the mobile phase, the type and concentration of mobile phase additives. Nine HILIC columns with different chemistries (unmodified silica, modified silica using diol, 2-picolylamine, diethylamine and 1-aminoanthracene and hydride silica) are compared with the emphasis on peak shapes of acidic lipid classes. The optimization of pH is correlated with the theoretical calculation of acidobasic equilibria of studied lipid classes. The final method using the hydride column, pH 4 adjusted by formic acid and the gradient of acetonitrile and 40 mmol/L of aqueous ammonium formate provides good peak shapes for all analyzed lipid classes including acidic lipids. This method is applied for the identification of lipids in real samples of porcine brain and kidney extracts.

1. Introduction

Phosphatidic acids (PA) are found in small amounts in biological membranes, but they are crucial biosynthetic precursors of all phospholipids (PL) and signaling molecules in biochemical and physiological processes in cells [1–3]. PA are a source of diacylglycerols (DG), which are precursors for triacylglycerols (TG), phosphatidylcholines (PC) and phosphatidylethanolamines (PE) via the Kennedy pathway [4], and precursors of phosphatidylglycerols (PG), phosphatidylserines (PS), phosphatidylinositols (PI) and cardiolipins via cytidine diphosphate DG (CDP-DG) pathway [1]. Lysophosphatidic acids (LPA) are biosynthetic precursors with regulatory functions in the mammalian reproduction system. PS are important components of cellular membranes, where they comprise 5–10% of total PL with important roles in the regulation of apoptosis, lipid synthesis and transport [1,3]. Lysophosphatidylserines (LPS) belong to signaling PL with the important role during inflammatory processes [5]. PA and PS are acidic lipids with the potential to carry two negative charges—both charges on the phosphate group for PA, while one negative charge is on the phosphate and the second one on the carboxylate group in case of PS (Fig. 1).

The comprehensive lipidomic analysis of various biological tissues is a challenging task due to the extreme complexity of individual lipid classes varying in the structure, attached functional groups, polarity, dissociation and ionization behavior, *etc.* The important part of lipidomic analysis is the quantitation, which can be performed using the MS with the direct infusion (shotgun lipidomics) [6–8] or the liquid chromatography–mass spectrometry (LC/MS) approaches [9,10]. Shotgun lipidomics enables fast and robust analysis using precursor ion and neutral loss scans characteristic for the fragmentation behavior of functional group of individual lipid classes [6–8]. LC/MS approaches can be divided into the lipid class separation according to the polarity using HILIC mode for polar lipid classes [9–11] or normal phase (NP) LC for nonpolar lipid classes [12,13]. Individual lipid species can be separated according to the fatty acyl chain length and the number of double bonds using reversed phase (RP) LC [11,14–16] or non-aqueous reversed-phase (NARP) LC [17–19]. Recently, the coupling of ultrahigh-performance supercritical fluid chromatography and mass spectrometry (UHPSFC/MS) approach [20] has

* Corresponding author. Fax: +420 466037068.
E-mail address: Michal.Holcapek@upce.cz (M. Holčapek).

http://dx.doi.org/10.1016/j.chroma.2016.01.064
0021-9673/

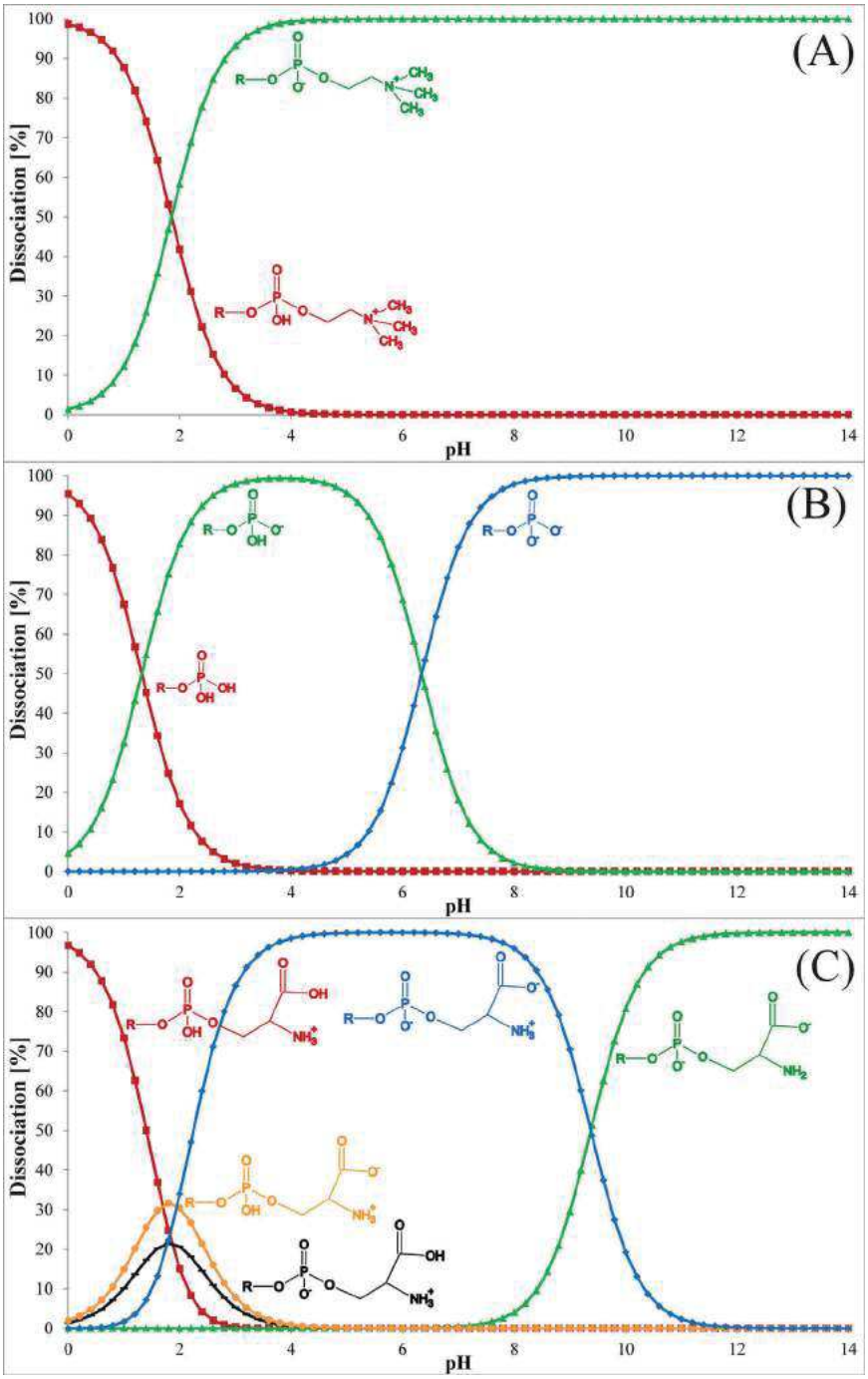

Fig. 1. Dissociation equilibria of (A) PC, (B) PA and (C) PS calculated by the Marvin demo software in the pH range 0–14, where R means $C_{17}H_{33}COOCH_2(C_{17}H_{33}COO)CHCH_2$-.

been introduced with the applicability for both polar and nonpolar lipid classes. The quantitative analysis in LC/MS approaches was described using internal standards (IS) per each lipid class [9] or the combination of single IS and response factors of individual lipid classes related to this IS [21]. The lipid class separation using HILIC or NP mode is more convenient for LC/MS quantitation, because lipid class IS are coeluting with lipid species inside particular lipid classes, therefore they are ionized at identical matrix conditions similarly as for shotgun lipidomics. This way of lipidomic quantitation should provide the most reliable data. Successful separations of PA and PS in HILIC mode have been previously reported [22–28], but they are based on the use of additives not well compatible with MS detection with possible strong ion suppression and memory effects, such as the use of alkyl ammonium salts as ion-pairing agents [29].

The main goal of this work is the optimization of HILIC/MS method for the analysis of the highest number of individual lipid classes with the emphasis on acidic lipid classes, such as PA, PS and their lysoderivatives using MS compatible conditions. We describe the separation in HILIC mode using a silica hydride column, which enables the characterization of 18 lipid classes including PA, PS and regioisomeric pairs of lysoderivatives in one analytical run. The developed method is applied for the analysis of lipid class composition of porcine brain and kidney.

2. Experimental

2.1. Chemicals and standards

Acetonitrile, 2-propanol, methanol (all HPLC/MS grade), chloroform stabilized by 0.5–1% ethanol (HPLC grade), ammonium formate, ammonium acetate, formic acid, acetic acid and sodium chloride were purchased from Sigma-Aldrich (St. Louis, MO, USA). Deionized water was prepared with a Milli-Q Reference Water Purification System (Molsheim, France). Standards of 1,2-dioleoyl-*sn*-glycero-3-phosphocholine (PC 18:1/18:1), 1-oleoyl-2-hydroxy-*sn*-glycero-3-phosphocholine (2-LPC 18:1), 1,2-dioleoyl-*sn*-glycero-3-phosphoethanolamine (PE 18:1/18:1), 1-oleoyl-2-hydroxy-*sn*-glycero-3-phosphoethanolamine (2-LPE 18:1), 1,2-dioleoyl-*sn*-glycero-3-phosphoglycerol (PG 18:1/18:1), 1-oleoyl-2-hydroxy-*sn*-glycero-3-phosphoglycerol (2-LPG 18:1), 1,2-dioleoyl-*sn*-glycero-3-phosphoserine (PS 18:1/18:1), 1-oleoyl-2-hydroxy-*sn*-glycero-3-phosphoserine (2-LPS 18:1), 1,2-dioleoyl-*sn*-glycero-3-phosphatidic acid (PA 18:1/18:1), 1-oleoyl-2-hydroxy-*sn*-glycero-3-phosphatidic acid (2-LPA 18:1), *N*-oleoyl-sphing-4-enine (Cer d18:1/18:1), *N*-palmitoyl-1-glucosyl-sphing-4-enine (HexCer d18:1/16:0), *N*-palmitoyl-1-lactosyl-sphing-4-enine (Hex2Cer d18:1/16:0) and *N*-oleoyl-sphing-4-enine-1-phosphocholine (SM d18:1/18:1) were purchased from Avanti Polar Lipids (Alabaster, AL, USA). Standards of 2-lysophospholipids contain small amounts of regioisomeric 1-lysophospholipids. The lipid nomenclature follows the LIPID MAPS system and the shorthand notation for lipid structures [30]. Biological samples (porcine brain and kidney) were obtained from the local farm.

2.2. Sample preparation

Briefly, 1 mg of lipid class standard was dissolved in a mixture of 200 μL of chloroform and 800 μL of 2-propanol. The lipid standard mixture was prepared by mixing of 10 μL of PC, 2-LPC, PE, 2-LPE, PG, 2-LPG, Cer, HexCer, Hex2Cer, SM and 50 μL of PA, 2-LPA, PS and 2-LPS. Biological samples (porcine brain and kidney) were prepared according to a modified Folch extraction [31] using a chloroform–methanol–water system. Briefly, 250 mg of tissue was homogenized for 3 min with 5 mL of chloroform–methanol (2:1, v/v) mixture and the homogenate was filtered using 0.2 μm Teknokroma syringe filter with regenerated cellulose (Teknokroma, Barcelona, Spain). Subsequently, 1 mL of 1 mol/L NaCl was added, and the mixture was centrifuged at 3000 rpm for 5 min at the ambient temperature. The chloroform bottom layer containing lipids was evaporated by a gentle stream of nitrogen and redissolved in chloroform-2-propanol (1:1, v/v) mixture for HILIC/MS analyses.

2.3. LC/MS conditions

Lipidomic analyses were performed on a liquid chromatograph Agilent 1290 Infinity series (Agilent Technologies, Waldbronn, Germany) coupled with the Esquire 3000 ion trap analyzer (Bruker Daltonics, Bremen, Germany). The optimization of HILIC method was performed using Acquity UPLC BEH HILIC column (150 × 2.1 mm, 1.7 μm, Waters, Milford, MA, USA), Ascentis Si (150 × 2.1 mm, 3 μm, Sigma–Aldrich), Kinetex HILIC (150 × 2.1 mm, 2.6 μm, Phenomenex, Torrance, CA, USA), Spherisorb Silica (150 × 4.6 mm, 10 μm, Waters), Acquity UPC^2 Torus DEA (100 × 3 mm, 1.7 μm, Waters), Acquity UPC^2 Torus 2-PIC (100 × 3 mm, 1.7 μm, Waters), Acquity UPC^2 Torus Diol (100 × 3 mm, 1.7 μm, Waters), Acquity UPC^2 Torus 1-AA (100 × 3 mm, 1.7 μm, Waters), and Cogent Diamond Hydride (250 × 4.6 mm, 4 μm, Microsolv, Eatontown, NJ, USA).

The final LC/MS method for the analysis of individual lipid classes in biological samples is the following: Cogent Diamond Hydride column (250 × 4.6 mm, 4 μm, Microsolv), a flow rate of 1 mL/min, an injection volume of 3 μL, column temperature of 40 °C and a mobile phase gradient: 0 min—99.7% A + 0.3% B, 60 min—75% A + 25% B, where A was acetonitrile with formic acid and B was 40 mmol/L aqueous ammonium formate with pH 4 adjusted by formic acid. The pH was measured by portable pH meter Checker (Hanna Instruments, Woonsocket, RI, USA). For all mobile phases used in this work, acetonitrile (phase A) contained the identical amount of formic acid as used for pH adjustment of aqueous solution (phase B) to keep the constant concentration of formic acid during the gradient elution. Individual lipid classes were detected in positive- and negative-ion ESI modes in the mass range *m*/*z* 50–1000 with the following setting of tuning parameters: scan speed 13,000 *m*/*z* /s, pressure of the nebulizing gas 60 psi, drying gas flow rate 10 L/min and temperature of the drying gas 365 °C, high-voltage capilary 4000 V and the target mass 800.

3. Results and discussion

3.1. Dissociation equilibria of lipids in aqueous solutions

Our previously published LC/MS method [11] using silica column Spherisorb Si (250 × 4.6 mm; 5 μm, Waters) and the mobile phase consisting of acetonitrile and 5 mmol/L of aqueous ammonium acetate enables the separation of most commonly occurring polar lipid classes except for acidic lipid classes (PA, LPA, PS and LPS) due to very broad tailing peaks under these conditions. For this purpose, we have reoptimized the selection of column packing material and the mobile phase composition (mainly pH, the type and concentration of additives). The dissociation equilibria for selected lipid classes in aqueous solutions are theoretically calculated using the Marvin demo software (ChemAxon, Budapest, Hungary) in the whole pH range from 0 to 14 (Fig. 1). The acidobasic dissociation equilibrium of PC (Fig. 1A) is a representative example of neutral PL. The pH 4 and higher should be selected to ensure that only one dissociation form is present in the solution (as zwitterions, see Fig. 1A). The similar behavior is observed for all neutral lipid classes. PA may occur in three forms depending on the pH (Fig. 1B): neutral molecules for pH < 2, deprotonated molecules in between pH 2 and 6 and doubly deprotonated molecules for pH > 6. Only one ionization form should be present in the solution to avoid the deterioration of chromatographic peaks, such as almost exclusive presence of deprotonated form at a narrow pH range of 3.6–4.0 (Fig. 1B). The most complicated situation is observed for PS class, where five different forms exist (Fig. 1C), which results in serious difficulties observed in HILIC separations of PS. The singly negatively charged molecule is present for the pH region from 4 to 7. The overlap of three above described pH regions is extremely narrow, because only at pH 4 all lipid classes are present in one dissociation form without the equilibrium with another form. This calculation is performed only for the aqueous solution, not considering the methanolic part of the mobile phase, but experimentally determined optimal separation conditions at pH 4 perfectly match with these considerations, as discussed in more detail later. The addition of formic acid is used for pH adjustment of aqueous part of the mobile phase. The identical amount of formic acid is also added to acetonitrile to keep the constant concentration of formic acid during the gradient run.

The dissociated ionic species formed from acidic lipids (see Fig. 1) in aqueous solutions compete for protons from silanol groups on the surface of silica stationary phase, so the quality and purity of the stationary phase is a basic prerequisite for the successful separation in addition to the pH selection. Properties of the sta-

Table 1
Tailing factors and normalized peak capacities per 1 cm of column length for individual lipid standards using nine different columns.

	Tailing factor [*1]									Normalized peak capacity/cm [*2]								
	Acquity	Ascentis	Kinetex	Spherisorb	Diol	2-PIC	DEA	1-AA	Hydride	Acquity	Ascentis	Kinetex	Spherisorb	Diol	2-PIC	DEA	1-AA	Hydride
Cer	1.4	1.1	0.9	1.3	1.0	1.3	1.5	1.3	1.1	4	3	6	4	10	15	17	12	6
HexCer	1.2	0.9	1.1	1.8	2.9	3.4	1.1	2.6	1.3	1	1	1	2	3	4	4	2	2
Hex2Cer	1.8	1.1	1.1	2.6	n.d.[*3]	n.d.[*3]	n.d.[*3]	n.d.[*3]	1.3	1	1	1	2	n.d.[*3]	n.d.[*3]	n.d.[*3]	n.d.[*3]	2
PG	1.6	4.1	1.5	2.2	1.5	1.3	1.6	1.3	1.0	2	2	2	2	5	15	17	12	3
PA	n.d.[*3]	n.d.[*3]	n.d.[*3]	n.d.[*3]	n.d.[*3]	n.d.[*3]	n.d.[*3]	n.d.[*3]	1.6	n.d.[*3]	n.d.[*3]	n.d.[*3]	n.d.[*3]	n.d.[*3]	n.d.[*3]	n.d.[*3]	n.d.[*3]	2
LPG	1.1	1.0	0.9	1.3	2.2	1.6	1.3	2.4	1.0	3	1	2	1	2	5	9	12	2
PE	2.1	1.0	1.4	2.0	2.2	1.7	1.7	1.4	1.1	4	4	4	4	2	15	9	3	4
PS	n.d.[*3]	2.6	1.4	0.9	n.d.[*3]	1.7	2.2	n.d.[*3]	1.3	n.d.[*3]	1	1	1	n.d.[*3]	8	2	n.d.[*3]	4
LPA	n.d.[*3]	n.d.[*3]	n.d.[*3]	n.d.[*3]	n.d.[*3]	n.d.[*3]	n.d.[*3]	n.d.[*3]	1.6	n.d.[*3]	n.d.[*3]	n.d.[*3]	n.d.[*3]	n.d.[*3]	n.d.[*3]	n.d.[*3]	n.d.[*3]	1
LPE	1.5	1.1	1.5	1.1	1.8	1.7	1.4	1.4	1.0	5	6	6	5	5	15	17	3	6
LPS	n.d.[*3]	1.0	n.d.[*3]	n.d.[*3]	n.d.[*3]	1.4	1.1	n.d.[*3]	1.4	n.d.[*3]	2	n.d.[*3]	n.d.[*3]	n.d.[*3]	8	6	n.d.[*3]	3
PC	1.6	1.4	1.1	1.5	1.8	1.8	1.7	1.6	1.4	5	4	6	4	10	15	6	6	2
LPC	1.3	1.3	1.2	1.3	1.6	1.6	1.3	1.6	1.0	5	4	6	4	5	15	9	3	4

[*1] The tailing factor is calculated as the ratio of the full width in 5% of peak height and two times of the front half width, $T_f = w_{0.05}/2 \times f$ [32].
[*2] The peak capacity is calculated as the ratio of the gradient time and full width in half of peak maximum, $P_C = 1 + (t_g/1.7 \times w_{1/2})$ [33], divided by the column length in cm.
[*3] n.d. – not determined due to wide tailing peaks.

tionary phase could seriously affect peak shapes of acidic lipids, which may result in the peak tailing. Silica columns contain free silanol groups, which exhibit the dissociation equilibrium of acidic protons depending on the mobile phase composition. Dissociated molecules of acidic analytes can also participate in the competition for protons, which could result in the stronger retention of deprotonated acids on the stationary phase and also peak tailing.

3.2. Unmodified silica columns

First, 4 commercially available silica columns (Fig. 2) with porous, porous shell and sub- 2 μm particles are tested using the lipid standard mixture, as described in the Experimental part. Representative chromatograms from different silica columns are measured under the same LC/MS conditions (except for the optimal flow rates used for particular columns) with the mobile phase consisting of acetonitrile, 20 mmol/L of aqueous ammonium formate and pH adjustment by formic acid. Silica columns varying in the particle size and manufacturers provide different results in terms of peak shapes and chromatographic resolution of separated lipid classes, but the retention order of lipid classes is almost identical (see Fig. 2). Table 1 shows the chromatographic efficiency of tested columns for individual lipid classes reported as their tailing factors and peak capacities per cm of the column length. The tailing factor is calculated as the ratio of the full width in 5% of peak height and two times of the front half width of peak, $T_f = w_{0.05}/2 \times f$ [32]. The peak capacity is calculated as the ratio of the gradient time and the full width in the half of peak height, $P_C = 1 + (t_g/1.7 \times w_{0.5})$, divided by the column length in cm [33]. The retention order of regioisomers of lysoderivates is assigned by negative-ion ESI mass spectra using relative abundances of carboxylate ions $[RCOO]^-$, which has been described in our previous work [11]. Acquity UPLC BEH HILIC column provides good peak shapes of all lipid classes except for wide and tailing peaks of PA, LPA, PS and LPS classes (Figs. 2 A and S1). The similar situation is observed for Kinetex HILIC (Fig. 2C) and Spherisorb Si (Fig. 2D) columns. The best peak shapes for acidic lipid classes are observed on Ascentis Si column (Fig. 2B).

The next step is the optimization of mobile phase composition, such as the concentration of ionic additives and pH. Ascentis Si column is used for this optimization due to the best results obtained in the previous step. Effects of pH of the mobile phase on the separation are illustrated in Figs. S2 and S3. The effect of pH on the retention behavior of PA and LPA is better visualized in the graph of normalized retention times *vs.* pH (Fig. 3) showing notable increases of PA and LPA retention at increased pH values. Differences in the retention behavior of most lipid classes except for PA and LPA are negligible, but significant changes of both retention times and peak shapes are observed for PA and LPA even for fine tuning of pH shown in Fig. S3. Peak shapes of acidic lipid classes are also seriously affected by the concentration of ammonium formate (20 and 60 mmol/L) in the mobile phase with the constant pH (Fig. S4). Increased concentration of ammonium formate improves peak shapes of PS and LPS, but on the other hand reduces the overall signal intensity of acidic lipids probably due to suppression effects. Unfortunately, peak shapes of PA and LPA are not improved at all (Fig. S4). The best separation on the silica column is achieved with fully porous particle column Ascentis, the mobile phase consisting of acetonitrile and 20 mmol/L of aqueous ammonium formate and pH adjusted to 3.4 by formic acid, but except for acidic lipid classes with strongly tailing peaks (Fig. 2B).

3.3. Modified silica columns

The comprehensive optimization of HILIC separation described in the previous chapter did not result in acceptable peak shapes of acidic lipid classes, therefore the investigation has continued with modified silica columns with different chemistries (Fig. 4). The knowledge of the role of pH and modifier concentration from the previous optimization is also taken into account. The diol column is the second most widespread column in the HILIC mode recommended mainly for acidic compounds. The retention behavior of lipids on Acquity UPC^2 Torus Diol (100 × 3 mm, 1.7 μm) is different in comparison with unmodified silica columns (Figs. 4 A and S5A). All lysoderivates are strongly retained on the diol column and they elute at higher retention times. PA, LPA, PS and LPS are not detected due to the strong peak tailing. Acquity UPC^2 Torus 2-PIC (100 × 3 mm, 1.7 μm) column containing bonded 2-picolylamine on the silica surface is recommended for a wide range of acidic, basic or neutral compounds. The application to the lipid standard mixture provides a significant improvement of chromatographic resolution and peak shapes of PS and LPS classes (Figs. 4 B and S5B), but unfortunately not for PA and LPA. The retention behavior of some ceramides (Cer and HexCer) is similar with unmodified silica surface, but the peak tailing of Hex2Cer containing large glycosylated part is worse. Acquity UPC^2 Torus DEA (100 × 3 mm, 1.7 μm) column containing bonded diethanolamine should be orthogonal to Torus 2-PIC phase, however in reality both types of stationary phases provide similar retention behavior and peak shapes of all lipid classes but with the lower signal intensity (Figs. 4 C and S5C). The last type of modified silica column is Acquity UPC^2 Torus 1-AA (100 × 3 mm, 1.7 μm) containing bonded 1-aminoanthracene, which is recommended for neutral compounds, such as polar and

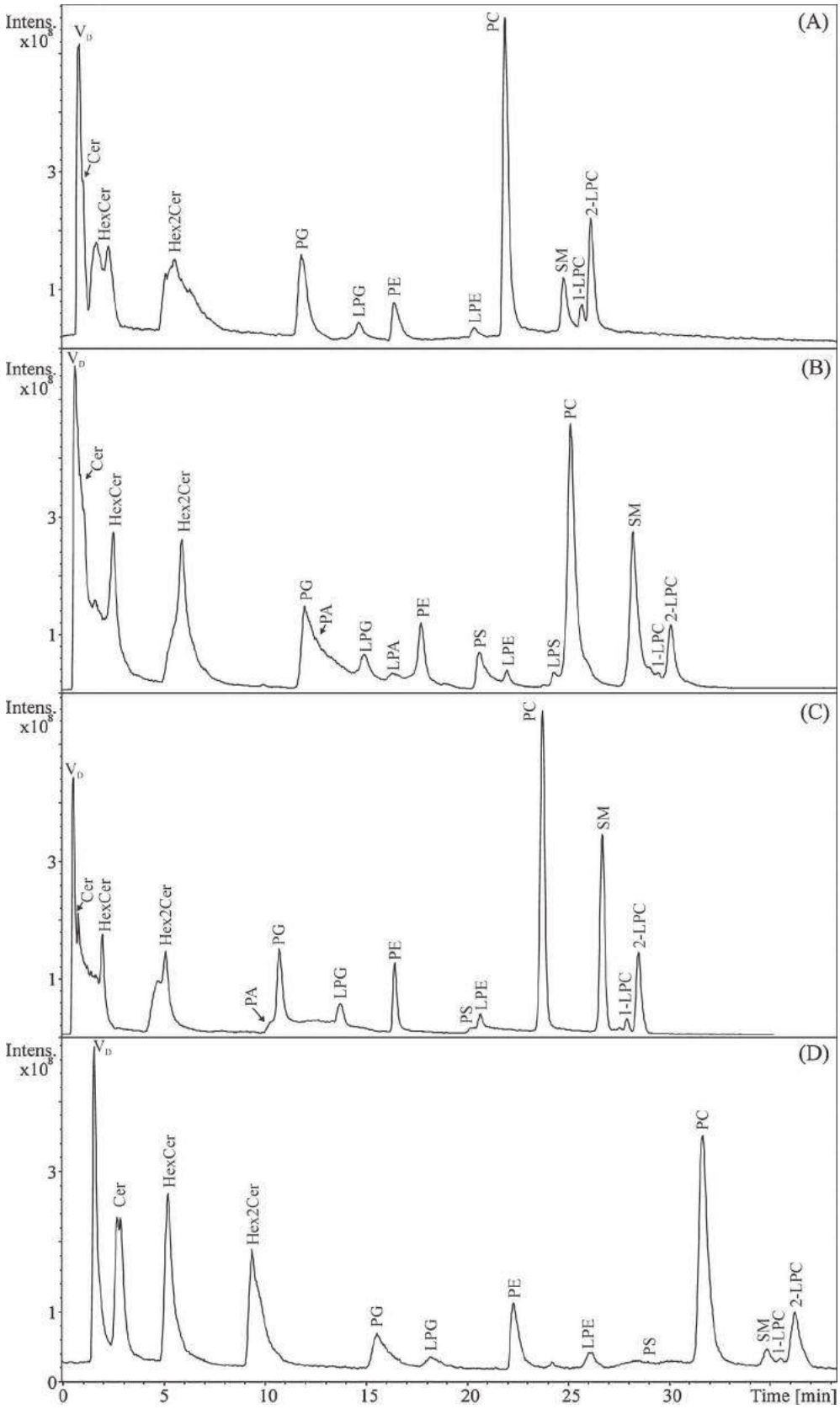

Fig. 2. Positive-ion HILIC/ESI–MS of lipid standard mixture measured using unmodified silica columns: (A) Acquity UPLC BEH HILIC (150 × 2.1 mm, 1.7 μm) column, flow rate 0.5 mL/min, (B) Ascentis Si (150 × 2.1 mm, 3 μm) column, flow rate 0.6 mL/min, (C) Kinetex HILIC (150 × 2.1 mm, 2.6 μm) column, flow rate 0.6 mL/min, and (D) Spherisorb Si (150 × 4.6 mm, 10 μm) column, flow rate 1 mL/min. Conditions: gradient 0 min—99.7% A + 0.3% B, 40 min—79.9% A + 20.1% B, where A is acetonitrile and B is 20 mmol/L of aqueous ammonium formate, pH 3.5 adjusted by formic acid. Peak annotation: Cer—ceramide, HexCer—hexosylceramide, Hex2Cer—dihexosylceramide, PG—phosphatidylglycerol, LPG—lysophosphatidylglycerol, PA—phosphatidic acid, LPA—lysophosphatidic acid, PE—phosphatidylethanolamine, LPE—lysophosphatidylethanolamine, PS—phosphatidylserine, LPS—lysophosphatidylserine, PC—phosphatidylcholine, SM—sphingomyelin, LPC—lysophosphatidylcholine.

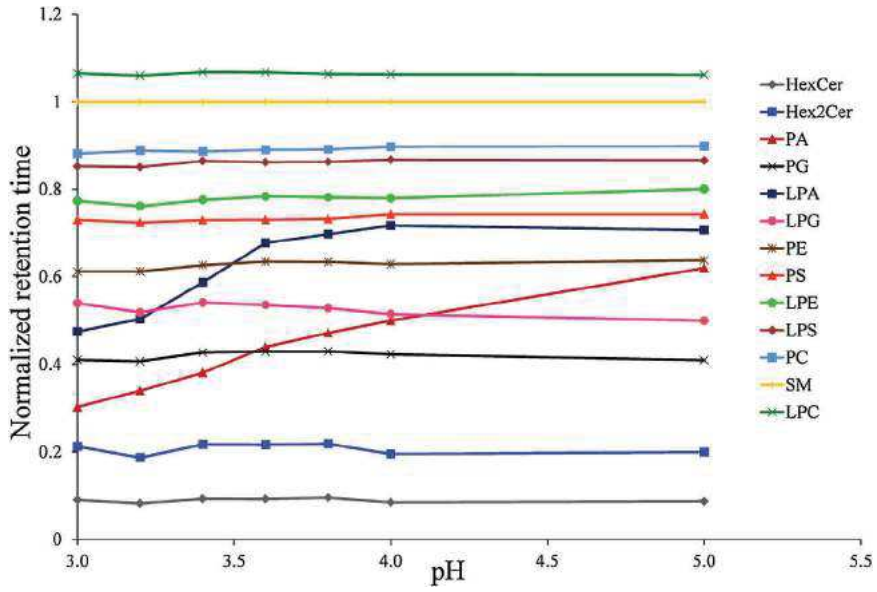

Fig. 3. Dependencies of normalized retention times (related to SM peak) of lipid standard mixture on pH using Ascentis Si column. Chromatograms are shown in Figs. S2 and S3.

nonpolar steroids, lipids and hydrophobic compounds. This column exhibits a higher retention of Cer, which results in their separation from the peak of system void volume. On the other hand, peak shapes of other lipid classes (Figs. 4 D and S5D) are the worst among all modified silica columns tested. The best separation is achieved on Acquity UPC^2 Torus 2-PIC column, but except for bad peak shapes of PA, LPA and Hex2Cer classes. Modified silica columns provide the best results in terms of the peak capacity (Table 1), but the major goal of this work to detect acidic lipid classes is not achieved similarly as for unmodified silica columns.

3.4. Hydride silica columns

Free silanol groups (Si—OH) on the surface of common silica columns are replaced by silicon-hydride (Si—H) bonds in case of so called hydride columns, which eliminates the acidic protons from silanols, but this reaction probably does not have 100% coverage. The silanol surface has a strong association with water, but silica hydride particles are slightly hydrophobic with only weak attraction of water. This type of columns can be operated in three chromatographic modes: RP, NP and aqueous NP [34]. The hydride column could enable the separation of both polar and nonpolar lipids using the dual retention mechanism RP and aqueous NP modes, which depends on the solvent composition. The separation of lipid standards using the hydride column provides excellent results for acidic classes PA, LPA, PS and LPS, and also the separation of Cer from the peak of system void volume (Fig. 5). The relative standard deviations for six consecutive injections are in the range of 0.5–2.2% (Table S2). The pH (Fig. S6), type and concentration of additives (Figs. S7 and S8) and the slope of mobile phase gradient are carefully optimized as well. Higher pH (Fig. S6) has a positive effect on peak shapes of most PL but the negative effect of sphingolipids (Cer, HexCer, Hex2Cer and SM). Significant changes in signal intensities are observed for Cer, which is approximately ten times lower at pH 6 compared to pH 3.5 (Fig. S6). Ammonium formate and ammonium acetate buffers as typical LC/MS volatile additives are compared (Fig. S7). The signal intensities are approximately two times higher for ammonium acetate buffer (Fig. S7A), but peak shapes and resolution of acidic lipid classes are significantly better for ammonium formate buffer (Fig. S7B). The optimization of ammonium formate concentration (Fig. S8) shows that most lipid classes have almost identical retention times except for PA and LPA, which have higher retention and better peak shapes with higher concentration of ammonium formate. However, increased concentrations also cause certain loss of sensitivity due to suppression effects, so the best compromise is 40 mmol/L of aqueous ammonium formate. The application of final method using the mobile phase consisting of acetonitrile and 40 mmol/L of aqueous ammonium formate and pH 4 adjusted by formic acid for lipid standard mixture is shown both for positive-ion (Fig. 5A) and negative-ion (Fig. 5B) ESI–MS. The optimal pH correlates well with dissociation equilibria shown in Fig. 1. The hydride column provides higher peak capacities for most lipid classes than unmodified silica columns, but lower than some modified silica columns (Table 1). The tailing factors for the most lipid classes are close to 1 except for PA and LPA (1.6 in both cases), but it is by far the best result among all tested conditions in this study, where tailing factors cannot be calculated at all due to completely deteriorated peak shapes of PA and LPA.

3.5. LC/MS analysis of biological samples

The final LC/MS method using hydride column is applied for the characterization of lipid composition of total lipid extracts of porcine brain (Fig. 5C) and kidney (Fig. S9). 13 lipid classes are detected, namely sulfatides, Cer, HexCer, Hex2Cer, PG, PI, PA, PE, LPE, PS, PC, LPC and SM. More than 140 individual lipid species are identified based on characteristic ions (Table S1) observed in positive- and negative-ion ESI modes. Individual lipid species differ in attached fatty acyls, which are annotated by their total carbon number and double bond number (CN:DB). The annotation of lipids is done on the assumption that abundant lipids typically contain even number of carbon atoms and also supported by our knowledge of the composition of these samples from our previous works [11,35,36]. We identify 25 sulfatides, 1Cer, 19HexCer, 3Hex2Cer, 5 PI, 2 PA, 33 PE, 3 LPE, 12 PS, 21 PC, 7 SM and 3 LPC in the porcine brain, which is a comparable number of lipids with our previous work using off-line two-dimensional HILIC x RP-HPLC/ESI–MS method, which is extremely time-consuming and does not enable the analysis of acidic lipids classes [35]. In the porcine kidney, 21 sulfatides, 1Cer, 17HexCer, 3Hex2Cer, 3 PG, 5 PI, 33 PE, 11 PS, 15 PC, 6 SM and 3 LPC are detected.

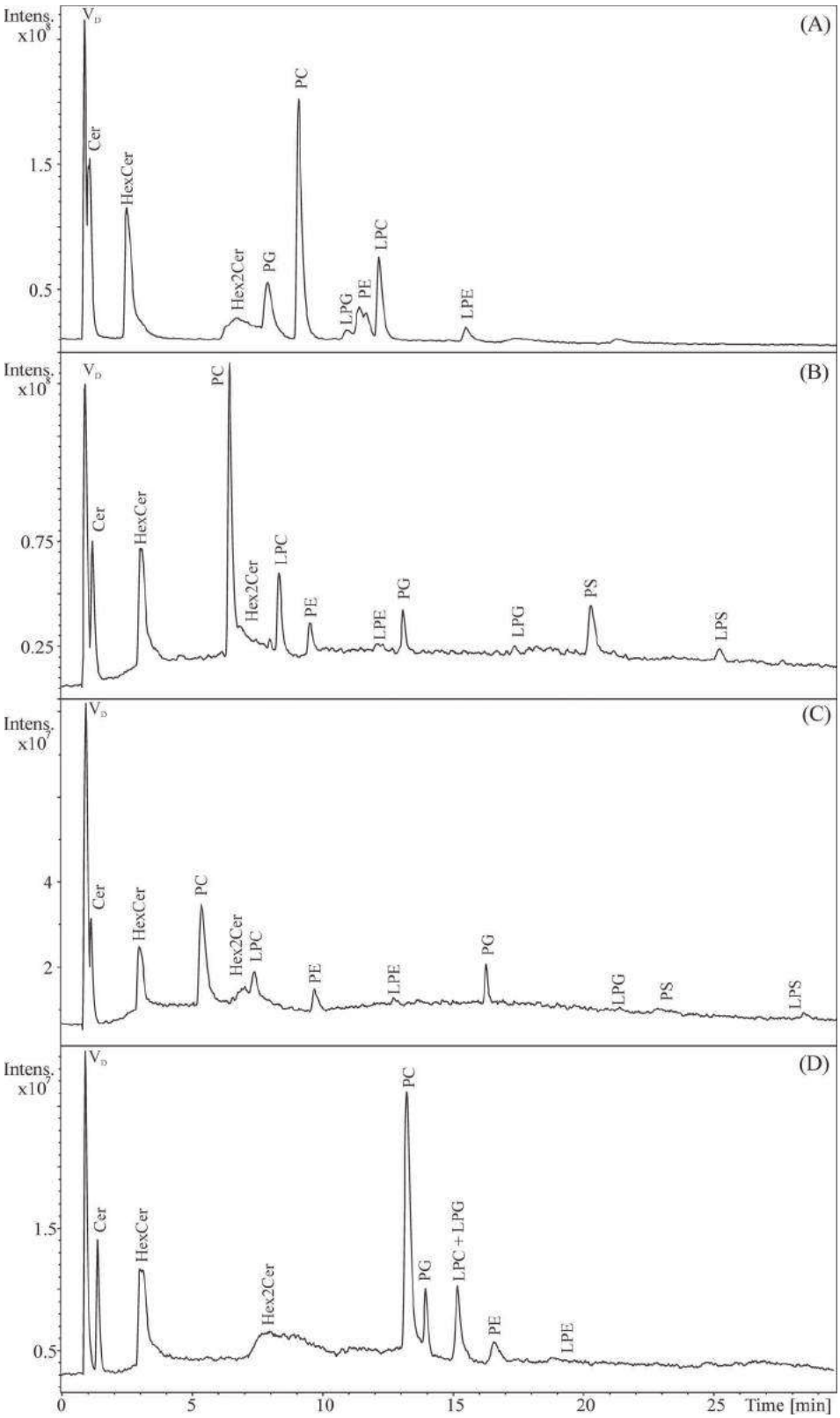

Fig. 4. Positive-ion HILIC/ESI-MS of lipid standard mixture measured using modified silica columns: (A) Acquity UPC^2 Torus Diol (100 × 3 mm, 1.7 μm), (B) Acquity UPC^2 Torus 2-PIC (100 × 3 mm, 1.7 μm), (C) Acquity UPC^2 Torus DEA (100 × 3 mm, 1.7 μm) and (D) Acquity UPC^2 Torus 1-AA (100 × 3 mm, 1.7 μm). Conditions: gradient 0 min—99.7% A + 0.3% B, 30 min—75% A + 25% B, where A is acetonitrile and B is 20 mmol/L of aqueous ammonium formate, pH 4 adjusted by formic acid.

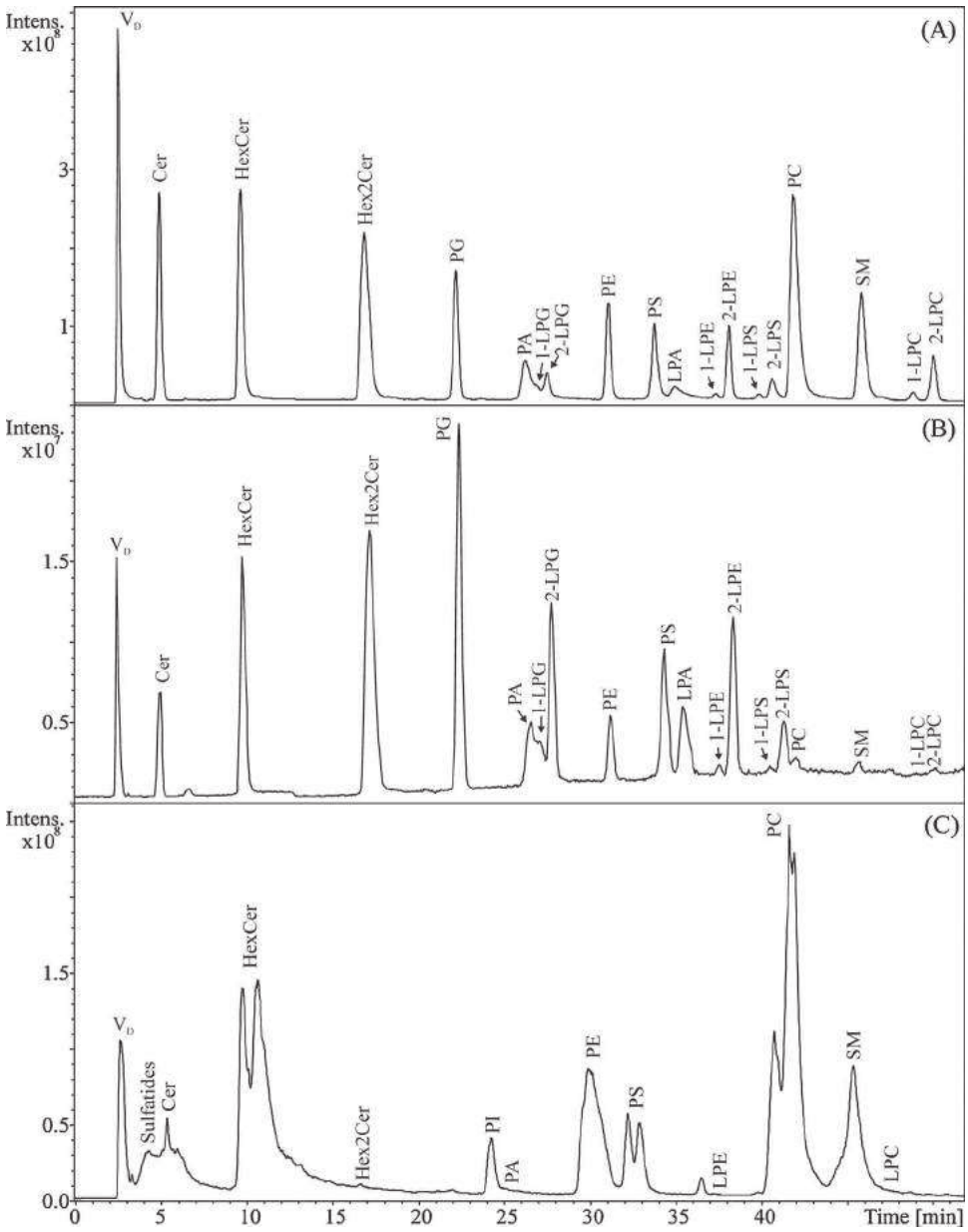

Fig. 5. Final HILIC/ESI-MS method using hydride column: (A) lipid standard mixture measured in the positive-ion mode, (B) lipid standard mixture measured in the negative-ion mode, (C) porcine brain extract measured in the positive-ion mode. Conditions: Cogent Diamond Hydride column (250 × 4.6 mm, 4 μm), flow rate 1 mL/min, gradient 0 min—99.7% A + 0.3% B, 60 min—75% A + 25% B, where A is acetonitrile and B is 40 mmol/L of aqueous ammonium formate, pH 4 adjusted by formic acid.

4. Conclusions

The optimized HILIC separation of acidic lipid classes PA, LPA, PS and LPS is convenient for the implementation in LC/MS lipidomic workflows, because the whole optimization is based only on conditions fully compatible with the MS detection, such as the use of volatile organic buffers and acids at lowest possible concentrations. The optimization of peak shapes of PA, LPA, PS and LPS has been a rather difficult task due to the necessity to optimize two critical parameters, such as the column type and pH value of mobile phase. Different dissociation forms for these acidic lipid classes can cause very broad and tailing chromatographic peaks and also seriously reducing the sensitivity, which explains why these lipid classes were not reported in previous works with HILIC/MS [9,10]. The best results are obtained on new hydride type column used under HILIC conditions and pH 4 selected in accordance with pH dependences of dissociation equilibria for PA and PS. The main advantage of hydride column is the replacement of acidic silanol groups Si—OH by hydride bonds Si—H, which reduces the risk of peak tailing of acidic lipids, as experimentally proved in our work.

Acknowledgments

This work was supported by the ERC CZ grant project LL1302 sponsored by the Ministry of Education, Youth and Sports of the Czech Republic.

Appendix A. Supplementary data

Supplementary data associated with this article can be found, in the online version, at http://dx.doi.org/10.1016/j.chroma.2016.01.064.

References

[1] V. Haucke, G. Di Paolo, Lipids and lipid modifications in the regulation of membrane traffic, Curr. Opin. Cell Biol. 19 (2007) 426–435.
[2] E.E. Kooijman, K.N.J. Burger, Biophysics and function of phosphatidic acid: a molecular perspective, Biochim. Biophys. Acta Mol. Cell Biol. Lipids 1791 (2009) 881–888.
[3] C.L. Stace, N.T. Ktistakis, Phosphatidic acid- and phosphatidylserine-binding proteins, Biochim. Biophys. Acta Mol. Cell Biol. Lipids 1761 (2006) 913–926.
[4] F. Gibellini, T.K. Smith, The Kennedy pathway-De novo synthesis of phosphatidylethanolamine and phosphatidylcholine, IUBMB Life 62 (2010) 414–428.
[5] S.C. Frasch, D.L. Bratton, Emerging roles for lysophosphatidylserine in resolution of inflammation, Prog. Lipid Res. 51 (2012) 199–207.
[6] X.L. Han, K. Yang, R.W. Gross, Multi-dimensional mass spectrometry-based shotgun lipidomics and novel strategies for lipidomic analyses, Mass Spectrom. Rev. 31 (2012) 134–178.
[7] D. Schwudke, G. Liebisch, R. Herzog, G. Schmitz, A. Shevchenko, Shotgun lipidomics by tandem mass spectrometry under data-dependent acquisition control, in: Lipidomics and Bioactive Lipids, Elsevier Academic Press Inc., San Diego, USA, 2007, pp. 175.
[8] K. Yang, X. Han, Accurate quantification of lipid species by electrospray ionization mass spectrometry—meets a key challenge in lipidomics, Metabolites 1 (2011) 21–40.
[9] M. Scherer, K. Leuthauser-Jaschinski, J. Ecker, G. Schmitz, G. Liebisch, A rapid and quantitative LC–MS/MS method to profile sphingolipids, J. Lipid Res. 51 (2010) 2001–2011.
[10] P.H. Axelsen, R.C. Murphy, Quantitative analysis of phospholipids containing arachidonate and docosahexenoate chains in microdissected regions of mouse brain, J. Lipid Res. 51 (2010) 660–671.
[11] M. Lísa, E. Cífková, M. Holčapek, Lipidomic profiling of biological tissues using off-line two-dimensional high-performance liquid chromatography mass spectrometry, J. Chromatogr. A 1218 (2011) 5146–5156.
[12] M. Holčapek, E. Cífková, B. Červená, M. Lísa, J. Vostálová, J. Galuszka, Determination of nonpolar and polar lipid classes in human plasma, erythrocytes and plasma lipoprotein fractions using ultrahigh-performance liquid chromatography–mass spectrometry, J. Chromatogr. A 1377 (2015) 85–91.
[13] D.G. McLaren, P.L. Miller, M.E. Lassman, J.M. Castro-Perez, B.K. Hubbard, T.P. Roddy, An ultraperformance liquid chromatography method for the normal-phase separation of lipids, Anal. Biochem. 414 (2011) 266–272.
[14] V. Ioffe, T. Kalendarev, I. Rubinstein, G. Zupkovitz, Reverse phase HPLC for polar lipids. Simple and selective HPLC procedures for analysis of phospholipid-based derivatives of valproic acid and various non-steroidal anti-inflammatory drugs, J. Pharm. Biomed. Anal. 30 (2002) 391–403.
[15] K. Sandra, A.D. Pereira, G. Vanhoenacker, F. David, P. Sandra, Comprehensive blood plasma lipidomics by liquid chromatography/quadrupole time-of-flight mass spectrometry, J. Chromatogr. A 1217 (2010) 4087–4099.
[16] Y. Sato, T. Nakamura, K. Aoshima, Y. Oda, Quantitative and wide-ranging profiling of phospholipids in human plasma by two-dimensional liquid chromatography/mass spectrometry, Anal. Chem. 82 (2010) 9858–9864.
[17] J. Cvačka, O. Hovorka, P. Jiroš, J. Kindl, K. Stránský, I. Valterová, Analysis of triacylglycerols in fat body of bumblebees by chromatographic methods, J. Chromatogr. A 1101 (2006) 226–237.
[18] P. Dugo, T. Kumm, M.L. Crupi, A. Cotroneo, L. Mondello, Comprehensive two-dimensional liquid chromatography combined with mass spectrometric detection in the analyses of triacylglycerols in natural lipidic matrixes, J. Chromatogr. A 1112 (2006) 269–275.
[19] M. Holčapek, M. Lísa, P. Jandera, N. Kabátová, Quantitation of triacylglycerols in plant oils using HPLC with APCI-MS evaporative light-scattering, and UV detection, J. Sep. Sci. 28 (2005) 1315–1333.
[20] M. Lísa, M. Holčapek, High-throughput and comprehensive lipidomic analysis using ultrahigh-performance supercritical fluid chromatography-mass spectrometry, Anal. Chem. 87 (2015) 7187–7195.
[21] E. Cífková, M. Holčapek, M. Lísa, M. Ovčačíková, A. Lyčka, F. Lynen, P. Sandra, Nontargeted quantitation of lipid classes using hydrophilic interaction liquid chromatography–electrospray ionization mass spectrometry with single internal standard and response factor approach, Anal. Chem. 84 (2012) 10064–10070.
[22] S.L. Abidi, T.L. Mounts, High-performance liquid-chromatography of phosphatidic-acid, J. Chromatogr. B-Biomed. Appl. 671 (1995) 281–297.
[23] C. Bure, S. Ayciriex, E. Testet, J.M. Schmitter, A single run LC–MS/MS method for phospholipidomics, Anal. Bioanal. Chem. 405 (2013) 203–213.
[24] A.A. Karlsson, P. Michelsen, A. Larsen, G. Odham, Normal-phase liquid chromatography class separation and species determination of phospholipids utilizing electrospray mass spectrometry tandem mass spectrometry, Rapid Commun. Mass Spectrom. 10 (1996) 775–780.
[25] M. Narvaez-Rivas, E. Gallardo, J.J. Rios, M. Leon-Camacho, A new high-performance liquid chromatographic method with evaporative light scattering detector for the analysis of phospholipids. Application to Iberian pig subcutaneous fat, J. Chromatogr. A 1218 (2011) 3453–3458.
[26] L.Q. Pang, Q.L. Liang, Y.M. Wang, L. Ping, G.A. Luo, Simultaneous determination and quantification of seven major phospholipid classes in human blood using normal-phase liquid chromatography coupled with electrospray mass spectrometry and the application in diabetes nephropathy, J. Chromatogr. B 869 (2008) 118–125.
[27] A. Triebl, M. Trotzmuller, A. Eberl, P. Hanel, J. Hartler, H.C. Kofeler, Quantitation of phosphatidic acid and lysophosphatidic acid molecular species using hydrophilic interaction liquid chromatography coupled to electrospray ionization high resolution mass spectrometry, J. Chromatogr. A 1347 (2014) 104–110.
[28] S. Uran, A. Larsen, P.B. Jacobsen, T. Skotland, Analysis of phospholipid species in human blood using normal-phase liquid chromatography coupled with electrospray ionization ion-trap tandem mass spectrometry, J. Chromatogr. B 758 (2001) 265–275.
[29] L. Kolařová, M. Holčapek, R. Jambor, L. Dostál, M. Nádvorník, A. Ružička, Structural analysis of 2,6-bis(alkyloxy) methyl phenyltin derivatives using electrospray ionization mass spectrometry, J. Mass Spectrom. 39 (2004) 621–629.
[30] G. Liebisch, J.A. Vizcaino, H. Kofeler, M. Trotzmuller, W.J. Griffiths, G. Schmitz, F. Spener, M.J.O. Wakelam, Shorthand notation for lipid structures derived from mass spectrometry, J. Lipid Res. 54 (2013) 1523–1530.
[31] J. Folch, M. Lees, G.H.S. Stanley, A simple method for the isolation and purification of total lipides from animal tissues, J. Biol. Chem. 226 (1957) 497–509.
[32] E. Grushka, M.N. Myers, P.D. Schettle, J.C. Giddings, Computer characterization of chromatographic peaks by plate height and higher central moments, Anal. Chem. 41 (1969) 889–892.
[33] U.D. Neue, Theory of peak capacity in gradient elution, J. Chromatogr. A 1079 (2005) 153–161.
[34] J. Pesek, M.T. Matyska, A comparison of two separation modes: HILIC and aqueous normal phase chromatography, LCGC N. Am. 25 (2007) 480–484.
[35] E. Cífková, M. Holčapek, M. Lísa, Nontargeted lipidomic characterization of porcine organs using hydrophilic interaction liquid chromatography and off-line two-dimensional liquid chromatography-electrospray ionization mass spectrometry, Lipids 48 (2013) 915–928.
[36] M. Holčapek, M. Ovčačíková, M. Lísa, E. Cífková, T. Hájek, Comprehensive two-dimensional liquid chromatography–electrospray ionization mass spectrometry of complex lipidomic samples, Anal. Bioanal. Chem. 407 (2015) 5033–5043.

Journal of Chromatography A, 1511 (2017) 107–121

Contents lists available at ScienceDirect

Journal of Chromatography A

journal homepage: www.elsevier.com/locate/chroma

Analysis of oxylipins in human plasma: Comparison of ultrahigh-performance liquid chromatography and ultrahigh-performance supercritical fluid chromatography coupled to mass spectrometry

Róbert Berkecz[a,b], Miroslav Lísa[a], Michal Holčapek[a,*]

[a] Department of Analytical Chemistry, Faculty of Chemical Technology, University of Pardubice, Studentská 573, 53210 Pardubice, Czech Republic
[b] Department of Medical Chemistry, Faculty of Medicine, University of Szeged, Dóm tér 8, H-6720 Szeged, Hungary

ARTICLE INFO

Article history:
Received 23 January 2017
Received in revised form 23 June 2017
Accepted 27 June 2017
Available online 29 June 2017

Keywords:
Oxylipin
Eicosanoid
Prostaglandin
Plasma
UHPSFC/MS
UHPLC/MS
SPE
ESI

ABSTRACT

The potential of ultrahigh-performance liquid chromatography–mass spectrometry (UHPLC/MS) and ultrahigh-performance supercritical fluid chromatography (UHPSFC) coupled to negative-ion electrospray ionization mass spectrometry (ESI–MS) for the analysis of 46 oxylipins and 2 fatty acid standards is compared in terms of their chromatographic resolution with the emphasis on distinguishing isobaric interferences and the method sensitivity. UHPLC provides the baseline separation of 24 isobaric oxylipins within 13 min, while UHPSFC enables the separation of only 20 isobaric oxylipins within 8 min. Moreover, the UHPLC/ESI–MS method provides an average improvement of sensitivity by 3.5-fold. A similar trend is observed in the analysis of human plasma samples, but lower ion suppression effects caused by lysophospholipids (LPL) are observed in case of UHPSFC/ESI–MS due to better separation of LPL. Both methods are fully applicable for the analysis of oxylipins, but UHPLC/ESI–MS method is preferred due to better separation and higher sensitivity, which results in the identification of 31 oxylipins in human plasma based on available standards and additional tentative 20 identifications based on accurate *m/z* values and the fragmentation behavior known from the literature.

1. Introduction

Oxylipins, including eicosanoids, docosanoids, and octadecanoids, are an important family of lipids, which are formed by the oxidation of polyunsaturated fatty acids (PUFA) [1]. They are derived mainly from arachidonic acid (AA), docosahexaenoic acid, eicosapentaenoic acid and dihomo-γ-linolenic acid. PUFAs are mostly generated from glycerophospholipids (PL) by the enzyme phospholipase A2, and then they are further metabolized to eicosanoids through enzymatic processes by free separate enzyme families, such as cyclooxygenase (COX), lipoxygenase (LOX), and cytochrome P450 (CYP). In addition, PUFA can be autooxidized forming bioactive lipids via nonenzymatic pathways as well [1,2]. In humans, eicosanoids have a wide range of physiological effects in inflammation, cardiovascular protection, blood clotting, and apoptosis. The important biological roles and excretion of these lipid mediators into body fluids, such as blood, urine, and cerebrospinal fluid, make them potential biomarker targets [2–6]. However, the concentration of eicosanoids (pmol/mL range) in human plasma is much lower compared to other endogenous lipids (nmol/mL range), such as glycerolipids, PL, sphingolipids, ceramides, and sterols.Therefore their analysis requires more sensitive analytical methods [7].

In past decades, the analysis of oxylipins was mainly performed by immunoassay techniques, such as radioimmunoassays (RIA) and enzyme immunoassays (EIA). The main disadvantage of these methods is the limited applicability for plasma and tissue samples due to immunological cross-reactivity and decreased sensitivity due to protein – eicosanoid interactions [2]. Gas chromatography–mass spectrometry (GC/MS) provides higher sensitivity and better selectivity than RIA and EIA, but the essential derivatization step during the sample preparation is time consuming and laborious [8,9]. Nowadays, liquid chromatography–mass spectrometry (LC/MS) is the most common technique used to simultaneously analyze eicosanoids and other oxylipins, especially in targeted tandem mass spectrometry (LC/MS/MS) mode using triple quadrupole (QqQ) instruments with the selected reaction monitoring (SRM) scanning mode [8], because it provides accu-

* Corresponding author.
E-mail address: Michal.Holcapek@upce.cz (M. Holčapek).

http://dx.doi.org/10.1016/j.chroma.2017.06.070
0021-9673/

rate quantitative information due to high sensitivity and selectivity without derivatization step and the opportunity of online sample extraction [9]. Mass spectrometry plays a major role in the identification and quantitation of eicosanoids. Negative-ion electrospray ionization (ESI) is the most sensitive ionization mode for eicosanoids due to the presence of carboxylic acid [10]. The comprehensive nontargeted analysis of eicosanoids using quadrupole time-of-flight (QTOF) mass spectrometer provides more qualitative information on analyzed samples, such as the identification of new compounds, information on matrix or other endogenous compounds, while SRM scans on QqQ are better for sensitive quantitation [8–10].

The LC separation is the most widespread technique for the analysis of wide range of oxylipins. Reversed-phase (RP) mode performed mainly on octadecylsilica (C18) or octylsilica (C8) column provides the highest selectivity for the resolution of isobaric oxylipins [2,6,8,9,11,12,14–18]. Oxylipins are determined in various body fluids, such as amniotic fluid, cerebrospinal fluid, urine, serum, and plasma [9,11–18]. LC/MS/MS method has been applied for the simultaneous determination of 32 oxylipins in human plasma samples in 29 min using C8 column and ammonium formate – acetonitrile gradient [12]. Vreeken and coworkers have detected 36 human plasma oxylipins in 26 min by UHPLC/MS/MS method using C18 column and aqueous acetic acid – 2-propanol – acetonitrile gradient [16]. Recently, UHPLC/MS/MS method has been used to identify and quantify 60 endogenous oxylipins in human plasma using C18 column in 5 min using aqueous acetic acid – acetonitrile – 2-propanol gradient [17]. Faccioli and coworkers have profiled 22 oxylipins in human plasma within 30 min with UHPLC/MS/MS method using C18 column and aqueous acetic acid – acetonitrile – 2-propanol gradient [18].

Supercritical fluid chromatography (SFC) successfully combines advantages of gas and liquid chromatography, and especially the novel approach based on the use of sub–2 μm particle columns yields ultrafast and efficient separations. This technique is referred as UHPSFC by the analogy to UHPLC, and may be easily coupled to mass spectrometry as well (UHPSFC/MS) [19]. Applications for various compounds classes illustrate the power of this new approach, *e.g.*, example for synthetic cannabinoids [20], pharmaceutical compounds [21], phospholipids, and sphingolipids [22]. However, UHPSFC/MS method for the analysis of oxylipins has not been reported so far.

The main goal of this study is a comparison of UHPLC/ESI–MS and UHPSFC/ESI–MS methods in terms of their suitability for the analysis of wide range of oxylipins in human plasma samples using the set of 46 standards typically occurring in biological systems. All parameters are carefully optimized to achieve the best selectivity and sensitivity of the final method, which is then applied for the analysis of endogenous oxylipins in the human plasma extract.

2. Experimental

2.1. Chemicals and standards

Methanol, acetonitrile, 2-propanol, ethanol (all LC/MS grade), chloroform stabilized by 0.5–1% ethanol (HPLC grade), ammonium formate, ammonium acetate, formic acid, and acetic acid were purchased from Sigma-Aldrich (St. Louis, MO, USA). Deionized water was prepared with a Milli-Q Reference Water Purification System (Molsheim, France). Carbon dioxide 4.5 grade (99.995%) was purchased from Messer Group Gmbh (Bad Soden, Germany).

8R-hydroxy-4Z,6E,10Z-hexadecatrienoic acid (**tetranor-12-HETE**), 12S-hydroxy-5Z,8E,10E-heptadecatrienoic acid (**12-HHTrE**), 13-oxo-9Z,11E-octadecadienoic acid (**13-OxoODE**), 9-oxo-10E,12Z-octadecadienoic acid (**9-OxoODE**), 13S-hydroxy-9Z,11E,15Z-octadecatrienoic acid (**13-HOTrE**), (±)13-hydroxy-9Z,11E-octadecadienoic acid (**13-HODE**), (±)9-hydroxy-10E,12Z-octadecadienoic acid (**9-HODE**), (±)12,13-dihydroxy-9Z-octadecenoic acid (**12,13-DiHOME**), (±)15-hydroxy-5Z,8Z,11Z,13E,17Z-eicosapentaenoic acid (**15-HEPE**), (±)5-hydroxy-6E,8Z,11Z,14Z,17Z-eicosapentaenoic acid (**5-HEPE**), (±)11,(12)-epoxy-5Z,8Z,14Z-eicosatrienoic acid (**11,12-EET**), (±)5,6-epoxy-8Z,11Z,14Z-eicosatrienoic acid (**5,6-EET**), (±)12-hydroxy-5Z,8Z,10E,14Z-eicosatetraenoic acid (**12-HETE**), (±)15-hydroxy-5Z,8Z,11Z,13E-eicosatetraenoic acid (**15-HETE**), (±)11-hydroxy-5Z,8Z,12E,14Z-eicosatetraenoic acid (**11-HETE**), (±)5-hydroxy-6E,8Z,11Z,14Z-eicosatetraenoic acid (**5-HETE**), 15S-hydroxy-8Z,11Z,13E-eicosatrienoic acid (**15-HETrE**), 9S-hydroxy-11,15-dioxo-2,3,4,5-tetranor-prostan-1,20-dioic acid (**tetranor-PGDM**), 9-oxo-15S-hydroxy-5Z,10Z,13E-prostatrienoic acid (**PGA2**), 11-oxo-15S-hydroxy-5Z,9,13E-prostatrienoic acid (**PGJ2**), 9S-hydroxy-11-oxo-5Z,12E,14E-prostatrienoic acid (**15-deoxy-δ-12,14-PGD2**), 15S-hydroxy-9-oxo-5Z,8(12),13E-prostatrienoic acid (**PGB2**), (±)5,6-dihydroxy-8Z,11Z,14Z,17Z-eicosatetraenoic acid (**5,6-DiHETE**), 5S,15S-dihydroxy-6E,8Z,10Z,13E-eicosatetraenoic acid (**5,15-DiHETE**), 8S,15S-dihydroxy-5Z,9E,11Z,13E-eicosatetraenoic acid (**8,15-DiHETE**), 5S,12R-dihydroxy-6Z,8E,10E,14Z-eicosatetraenoic acid (**LTB4**), 5S,12R-dihydroxy-6E,8E,10E,14Z-eicosatetraenoic acid (**6-trans LTB4**), (±)14,15-dihydroxy-5Z,8Z,11Z-eicosatrienoic acid (**14,15-DiHETrE**), (±)5,6-dihydroxy-8Z,11Z,14Z-eicosatrienoic acid (**5,6-DiHETrE**), 6-oxo-9S,11R,15S-trihydroxy-2,3-dinor-13E-prostaenoic acid, sodium salt (**2,3-dinor-6-keto-PGF1α**), 14S-hydroxy-4Z,7Z,10Z,12E,16Z,19Z-docosahexaenoic acid (**14-HDoHE**), (±)4-hydroxy-5E,7Z,10Z,13Z,16Z,19Z-docosahexaenoic acid (**4-HDoHE**), 9S,15S-dihydroxy-11-oxo-5Z,13E,17Z-prostatrienoic acid (**PGD3**), 9,15-dioxo-11R-hydroxy-5Z-prostenoic acid (**13,14-dihydro-15-keto-PGE2**), 9S,11R-epidioxy-15S-hydroxy-5Z,13E-prostadienoic acid (**PGH2**), 9-oxo-11R,15S-dihydroxy-5Z,13E-prostadienoic acid (**PGE2**), 9S,15S-dihydroxy-11-oxo-5Z,13E-prostadienoic acid (**PGD2**), 9S,11R-dihydroxy-15-oxo-5Z,13E-prostadienoic acid (**15-keto-PGF2α**), 9S,11S-dihydroxy-15-oxo-5Z-prostenoic acid (**13,14-dihydro-15-keto-PGF2α**), 9S,11R,15S-trihydroxy-5Z,13E-prostadienoic acid (**PGF2α**), 9S,11R,15S-trihydroxy-5Z,13E-prostadienoic acid-cyclo[8S,12R] (**8-iso-PGF2α**), (±)19,20-dihydroxy-4Z,7Z,10Z,13Z,16Z-docosapentaenoic acid (**19,20-DiHDPE**), 9α,11,15S-trihydroxythromba-5Z,13E-dien-1-oic acid (**TXB2**), 6-oxo-9S,11R,15S-trihydroxy-13E-prostenoic acid (**6-keto-PGF1α**), 7S,8R,17S-trihydroxy-4Z,9E,11E,13Z,15E,19Z-docosahexaenoic acid (**resolvin D1**), and 5S-hydroxy,6R-(S-cysteinyl),7E,9E,11Z,14Z-eicosatetraenoic acid (**LTE4**) standards (see Table S1 for structures) were purchased from Cayman Chemical (Ann Arbor, MI, USA). Fatty acid standards 6Z,9Z,12Z-octadecatrienoic acid (**γ-linolenic acid**), and 9Z,12Z,15Z-octadecatrienoic acid (**α-linolenic acid**) were purchased from Nu-Chek-Prep (Elysian, MN, USA).

The oxylipins nomenclature and abbreviations follow the LIPID MAPS structure database system [23]. Human plasma samples were obtained from healthy volunteers based on the ethical agreement.

2.2. Sample preparation

The stock solution containing 46 eicosanoid and 2 fatty acid standards at the concentration of 500 pg/μL except for tetranor-PGDM (2500 pg/μL), 2,3-dinor-6-keto-PGF1α (2500 pg/μL), PGD3 (2500 pg/μL), 5,6-EET (1000 pg/μL), PGH2 (2500 pg/μL), and LTE4 (5000 pg/μL) was prepared in ethanol. For UHPLC measurements, the stock solution was dried under nitrogen at ambient tem-

perature and redissolved in acetonitrile – water – acetic acid (45/55/0.02, v/v) mixture to prepare suitable concentration. In case of UHPSFC analysis, working solutions were prepared in chloroform – ethanol (50/50, v/v) mixture.

The solid phase extraction (SPE) was performed according to the method described by Schebb et al. [24] with minor modifications. Aliquots of 500 μL control plasma were diluted with 1.5 mL 90% aqueous methanol and vortexed for 10 s. Then the plasma solution was centrifuged (Hettich® EBA 20 centrifuge EBA 20) at 6000 rpm for 10 min at ambient temperature. The oxylipins were extracted using Strata™-X 33 μm (200 mg/3 mL) polymeric RP cartridges (8B-S100-FBJ-T, Phenomenex, Aschaffenburg, Germany). Cartridges were conditioned with 3 mL of methanol and then with 3 mL of water. Next, 2 mL of samples were loaded on cartridges, with a subsequent wash using 3 mL of water. Then oxylipins were eluted with 3 mL of methanol. The eluent was dried under nitrogen at ambient temperature and redissolved in 50 μL of the eluent A (acetonitrile – water – acetic acid (45/55/0.02, v/v/v) mixture) for UHPLC or 50 μL chloroform – ethanol (50/50, v/v) mixture in case of UHPSFC measurements. Finally, the solution was centrifuged at 6000 rpm for 1 min prior to transferring into 300 μL conical insert.

2.3. UHPLC/MS and UHPSFC/MS conditions

UHPLC/MS analyses were performed on a liquid chromatograph Agilent 1290 Infinity series (Agilent Technologies, Waldbronn, Germany) consisting of an Agilent 1290 Infinity LC binary pump, an Agilent 1290 Infinity well plate autosampler and an Agilent 1290 Infinity column thermostat. The UHPLC system was coupled to the Waters Synapt G2-Si quadrupole – ion mobility – time of flight mass spectrometer with ESI (Waters, Milford, MA, USA).

The final UHPLC/MS method for the analysis of oxylipins was as follows: Acquity UPLC BEH C18 column (150 × 2.1 mm, 1.7 μm, 130 Å, Waters), injection volume 1 μL, and column temperature 40 °C. The mobile phase A consisted of acetonitrile – water – acetic acid (45/55/0.02, v/v/v) mixture, and the eluent B was 2-propanol – acetonitrile (50/50, v/v) mixture. The gradient program was the following: 0 min – 2% B, 12 min – 62% B, 12.1 min – 99% B, 14.5 min – 99% B, 15 min – 2% B, and 20 min – 2% B. The flow rate was 0.4 mL/min during the analysis (from 0 to 13.5 min) and the equilibration before the next injection (from 18.5 to 20 min), and 0.65 mL/min during the column washing after the analysis (from 13.5 to 18.5 min). The injector needle was washed with strong (hexane – 2-propanol – water (2:2:1, v/v/v) mixture) and weak solvents (A eluent) after each injection.

All UHPSFC/MS experiments were done on an Acquity UPC^2 system (Waters, Milford, MA, USA) equipped with a binary solvent manager delivery pump, a sample manager maintained at 8 °C, 10 μL injection loop, a column oven, a backpressure regulator, and a Waters Model 515 pump for delivering make-up solvent. The chromatographic system was coupled to the mass spectrometer via dedicated interface kit (Waters) composed of two T-pieces enabling the backpressure control, and mixing of column effluent with a make-up solvent.

The following UHPSFC columns with the same column dimension (100 × 3 mm, 1.7 μm) were tested, i.e., Acquity UPC2 Torus 1-Aminoanthracene (1-AA), Acquity UPC2 Torus 2-Piycolylamine (2-PIC), Acquity UPC2 Torus Diol (1-DIOL), Acquity UPC2 Torus Diethylamine (DEA), and Acquity UPC2 HSS C18 SB (1.8 μm) (HSS C18).

The final UHPSFC method for the analysis of oxylipins was as follows: Acquity UPC^2 Torus 1-Aminoanthracene (1-AA) column (100 × 3 mm, 1.7 μm, Waters), active backpressure regulator (ABPR) pressure 1800 psi (124 bar), flow rate 1.7 mL/min, injection volume 1 μL, and column temperature 50 °C. The modifier 0.1% acetic acid in methanol was used as the eluent B. The gradient program was the following: 0 min – 4% B, 10 min – 30% B, 11 min – 30% B, 11.5 min – 4% B, and 15 min – 4% B. The injector needle was washed with hexane – 2-propanol – water (2:2:1, v/v/v) mixture after each injection. Pure methanol was delivered as a make-up eluent at the flow rate of 0.3 mL/min.

The mass spectrometer was operated in the negative-ion ESI sensitivity mode under the following conditions: mass range of m/z 50–950, capillary voltage 2.2 kV, source temperature 150 °C, sampling cone 20 V, source offset 90 V, drying temperature 500 °C, cone gas flow rate 50 L/h, desolvation gas flow rate 1000 L/h, and nebulizer gas pressure 4 bar. Leucine enkephaline was used as a lock mass for all experiments. The data dependent acquisition (DDA) experiments were performed on a transfer cell with the collision energy ramp from 17 to 40 eV with the selection of up to 3 ions. The setting of mass spectrometer was identical for both UHPLC/MS and UHPSFC/MS measurements except for decreased desolvation gas flow rate (800 L/h) used for UHPSFC/MS analysis in order to achieve the stable spray.

2.4. Data processing

The UHPLC system was controlled with Agilent OpenLAB software. The control of UHPSFC system, MS data acquisition and processing were conducted by MassLynx V4.1 SCN 901 and integrated TargetLynx softwares. Calculations were performed using Microsoft Excel software.

3. Results and discussion

A set of 46 oxylipin standards representing 36 eicosanoids, 4 docosanoids, 6 octadecanoids, and 2 fatty acids (see Table S1 for the complete list and structures) was used for the optimization of UHPLC/MS and UHPSFC/MS conditions. The previous occurrence of these standards in human plasma was an important aspect during their selection based on published works [7,12,16–18]. Chromatographic and mass spectrometric parameters were optimized to improve the separation and sensitivity. The final UHPLC/MS and UHPSFC/MS methods were compared, and the former one was applied for profiling of human plasma oxylipins. The MS sensitivity and chromatographic resolution were the main aspects during the optimization due to low natural abundances of oxylipins.

3.1. Optimization of UHPLC/MS method

3.1.1. Column selection and initial conditions

The Acquity UPLC BEH C18 column was selected for the RP analysis of oxylipins based on the literature [14,17,25]. The coelution of oxylipin isomers makes their identification and quantification complicated, therefore longer column (150 mm) was selected to improve the isomeric separation. The starting conditions were based on the mobile phase consisted of eluent A acetonitrile – water – acetic acid (60/40/0.02, v/v/v), eluent B 2-propanol – acetonitrile (50/50, v/v), and the gradient program from 0 min – 0.1% B to 6 min – 55.5% B, but too low retention was observed for **tetranor-PGDM**, **2,3-dinor-6-keto-PGF1α**, **PGD3**, **8-iso-PGF2α**, **PGF2α**, **6-keto-PGF1α**, **PGE2**, **PGH2**, and **TXB2** (retention factors lower than 1.2). Therefore, the amount of water in the eluent A was increased to 55% water to improve their retention. In parallel, the gradient program was also changed (0 min – 0.1% B, 6 min – 70.0% B, 6.75 min – 99.0% B, 7.50 min – 99% B, 7.65 min – 0.1% B, and 15 min – 0.1%B).

3.1.2. Effect of mobile phase composition

Effects of additives in the eluent A on the retention behavior and MS sensitivity of oxylipins were studied for the following additives: acetic acid (0.02 and 0.05%), formic acid (0.02 and 0.05%),

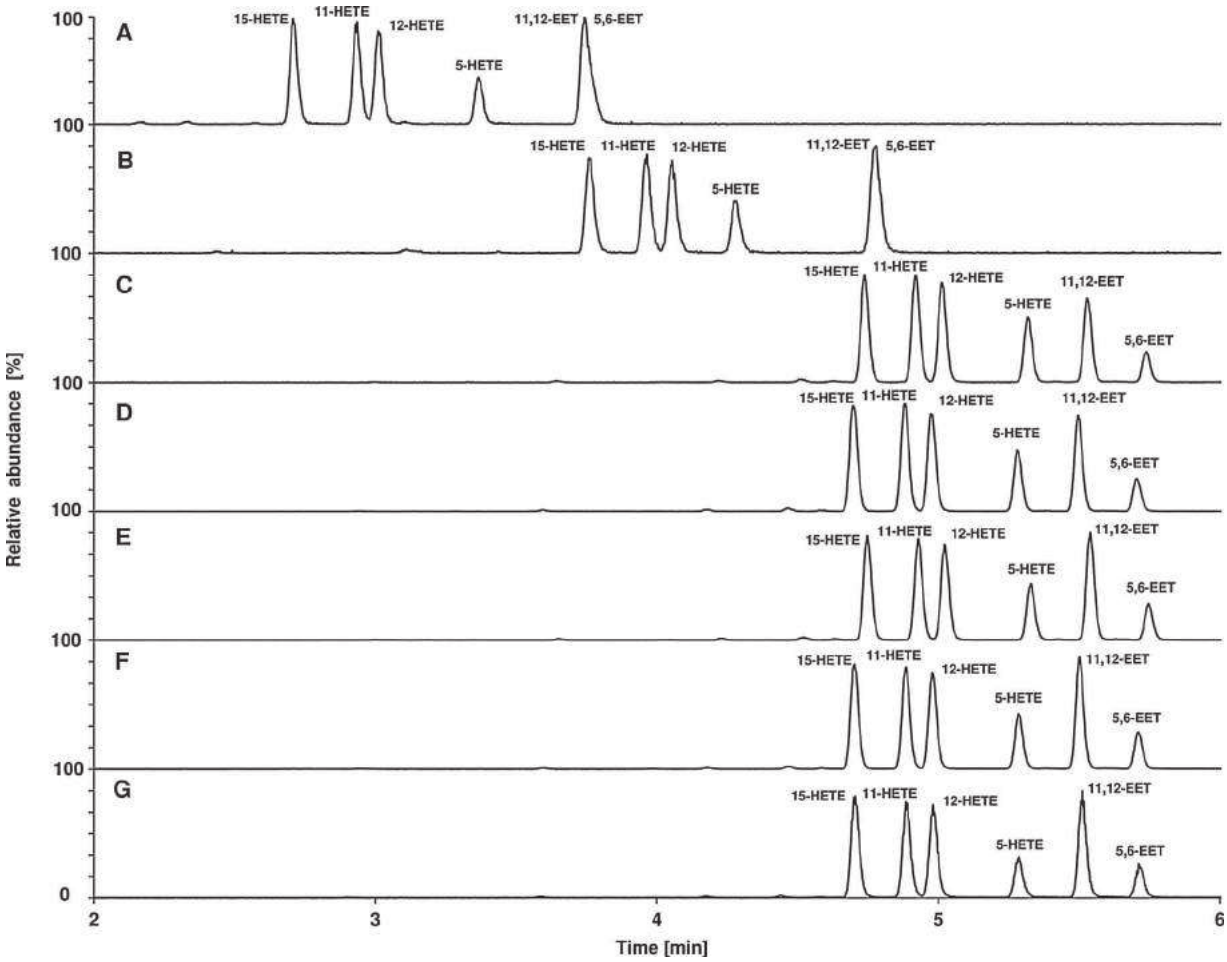

Fig. 1. Effect of additives in acetonitrile – water (45/55, v/v) mobile phases on negative-ion UHPLC/ESI–MS extracted ion chromatograms of the standard mixture of isomeric HETE/EET for the different composition of eluent A: (**A**) 5 mM ammonium acetate, (**B**) 5 mM ammonium formate, (**C**) 0.05% formic acid, (**D**) 0.02% formic acid, (**E**) 0.05% acetic acid, (**F**) 0.02% acetic acid, and (**G**) without any additive. Conditions: eluent B – 2-propanol – acetonitrile (50/50, v/v), Acquity UPLC BEH C18 column (2.1 × 150 mm, 1.7 μm, 130 Å, Waters), flow rate 0.5 mL/min, column temperature 40 °C, and gradient program 0 min – 0.1% B, 6 min – 70.0% B, and 6.75 min – 99.0% B.

5 mM ammonium acetate, and 5 mM ammonium formate (Fig. 1). The lowest retention was observed with ammonium acetate, while acetic and formic acids resulted in the highest retention times at 0.05%. The use of acetic and formic acids at the same concentration (0.02% or 0.05%) resulted in different pH values of the mobile phase, but the retention and resolution of isomers did not change significantly. For all compounds, higher retention times were observed for higher acid content (0.05%). The comparison of chromatographic resolution for isomers obtained with and without additives show that higher resolution was achieved with acetic acid, formic acid and without any additive, except for **γ-linolenic acid**, **α-linolenic acid**, **15-HETE**, **11-HETE**, **12-HETE**, **5-HETE**, **11,12-EET**, **5,15-DiHETE**, **6-trans LTB4**, **14-HDHA**, and **4-HDHA**, where the mobile phases with ammonium acetate provided better results. Peak shapes were not influenced considerably by additives. The serious peak tailing was observed for **LTE4** in the absence of any additive and in ammonium acetate or ammonium formate containing mobile phases. The peak shape was improved at higher acid concentrations, which can be explained by suppressed zwitterion formation of cysteinyl side chain (isoelectric point at pH 5.07) in more acidic environment [26]. The oxalic acid treatment of stationary phase using the injection of 20 μL of 10 mM oxalic acid two times [27] had also a substantial effect on the improvement of peak shape of **LTE4**.

Fig. 2 demonstrates the dependence of negative-ion ESI response on the type and concentration of additives. Acetic acid

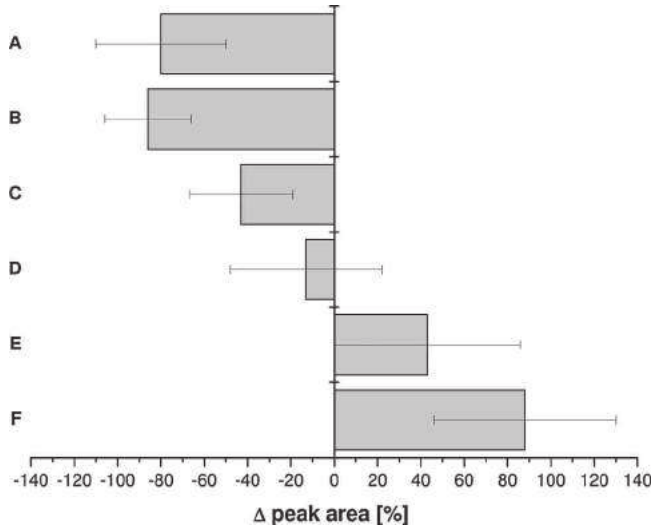

Fig. 2. Dependencies of peak areas of oxylipins standards in negative-ion UHPLC/ESI–MS on the composition of eluent A containing various additives in comparison to conditions without any additives: (**A**) 5 mM ammonium acetate, (**B**) 5 mM ammonium formate, (**C**) 0.05% formic acid, (**D**) 0.02% formic acid, (**E**) 0.05% acetic acid, and (**F**) 0.02% acetic acid. Other conditions are identical as for Fig. 1.

Table 1
Average relative changes in UHPLC for retention times (Δt_R), peak widths, peak areas, and resolution (R_s) for increased flow rates of 0.4 and 0.5 mL/min in comparison to the initial value of 0.3 mL/min.

Flow rate [mL/min]	Δt_R	Δpeak width	Δpeak area	ΔR_s
0.4	−33%	−21%	−31%	−6%
0.5	−54%	−33%	−51%	−14%

enhanced the ionization compared to the mobile phase without any additive (ca. 90% on the average for 0.02% and 40% for 0.05% of acetic acid). The use of formic acid caused the signal suppression (ca. 15% for 0.02% and 45% for 0.05% of formic acid). The addition of ammonium acetate or formate resulted in the drastic loss of sensitivity. 0.02% of acetic acid was selected as optimal for the further optimization of other parameters.

The retention and selectivity of the separation can be tuned by the composition of the organic solvent B. Four types of eluents B were investigated, such as 2-propanol – acetonitrile (50/50, v/v), 2-propanol – acetonitrile (10/90, v/v), acetonitrile, and methanol. The concentration of 2-propanol exhibited only a slight effect on retention, resolution, and sensitivity. The highest retention was observed for methanol, but it negatively influenced the separation, especially in case of **γ-linolenic acid**, **α-linolenic acid**, **13-HODE, 9-HODE,** and all **HETE**. Finally, 2-propanol – acetonitrile (50/50, v/v) was selected, because this was the most efficient in the removal of plasma phospholipid contaminants (in spite of SPE sample treatment) from the column during the washing step of gradient program.

3.1.3. *Effect of flow rate*

The increased flow rate reduces the analysis time, but on the other hand it also influences the resolution and sensitivity. Fig. 3 demonstrates the effect of flow rate in the range of 0.3–0.5 mL/min for isomers **15-HETE**, **11-HETE**, **12-HETE**, **5-HETE**, **11,12-EET**, and **5,6-EET**. Gradients for different flow rates are recalculated based on the ratio of squared column internal diameters. Average retention times and peak widths were decreased for all compounds, when the flow rate increased (Table 1), but it also reduced peak areas. The moderate reduction of resolution was observed with increased flow rates for isomers. 0.4 mL/min is chosen in the final method as a compromise among the short analysis time, high selectivity, and ESI response. The oxylipin and fatty acid standards eluted in the range of 1–12 min (Fig. 4 and Table 2). The flow rate gradient program was used during the washing and equilibration cycle to reduce the total run time.

3.2. *Development of UHPSFC/MS method*

3.2.1. *Column selection*

Five UHPSFC columns with the same column dimension (100 × 3 mm, 1.7 μm) and different chemistries were used in our column screening, *i.e.*, 1-AA, 2-PIC, 1-DIOL, DEA, and HSS C18, in order to find the optimal stationary phase for the anal-

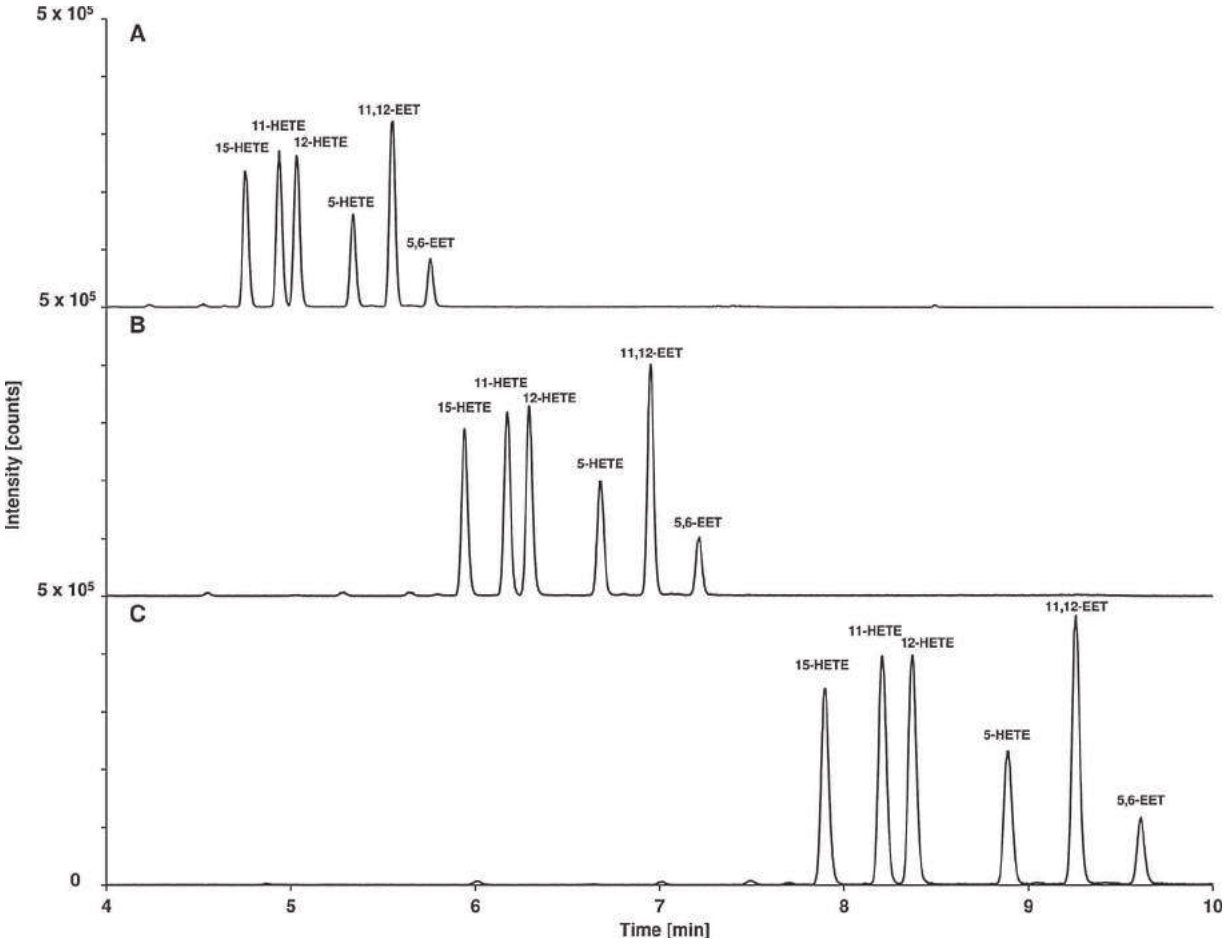

Fig. 3. Effect of the flow rate on negative-ion UHPLC/ESI–MS extracted ion chromatograms of the standard mixture of isomeric HETE/EET using 0.02% acetic acid as the additive in the eluent A: (**A**) 0.5 mL/min, (**B**) 0.4 mL/min, and (**C**) 0.3 mL/min. Gradient programs are adjusted for individual flow rates: (**A**) 0 min – 0.1% B, 6 min – 70.0% B, and 6.75 min – 99.0% B, (**B**) 0 min – 0.1% B, 7.52 min – 70.0% B, and 8.44 min – 99.0% B, and (**C**) 0 min – 0.1% B, 10.02 min – 70.0% B, and 11.25 min – 99.0% B. Other conditions are identical as for Fig. 1.

Table 2
Chromatographic and mass spectrometric data for oxylipin and fatty acid standards in the final UHPLC/MS method.

Abbreviation	Subclass	Isomeric group	Theoretical m/z of $[M-H]^-$	t_R in UHPLC/MS [min]	R_S	Indentified in plasma
tetranor-PGDM	Prostaglandins	–	327.1449	0.96		No
6-keto-PGF1α	Prostaglandins	1	369.2283	1.24	1.25	No
TXB2	Thromboxanes			1.53		Yes
8-iso-PGF2α	Prostaglandins	2	353.2334	1.52	1.53	Yes
PGF2α				1.73	4.96	Yes
13,14-dihydro-15-keto-PGF2α				2.43		No
2,3-dinor-6-keto-PGF1α	Prostaglandins	–	341.1970	1.71		No
PGD3	Prostaglandins	–	349.2021	1.71		No
PGH2	Prostaglandins	3	351.2177	1.88		No
PGE2				1.88	1.34	Yes
15-keto-PGF2α				2.03	0.68	No
PGD2				2.08	3.35	Yes
13,14-dihydro-15-keto-PGE2				2.48		No
Resolvin D1	Docosanoids	–	375.2177	2.37		No
PGA2	Prostaglandins	4	333.2071	3.15	0.96	No
PGJ2				3.33		No
PGB2				3.33	7.51	Yes
15-deoxy-δ-12,14-PGD2				4.51		No
8,15-DiHETE	Hydroxy/hydroperoxyeicosatetraenoic	5	335.2228	3.85	2.15	Yes
5,15-DiHETE	acids			4.14	0.71	Yes
6-trans LTB4	Leukotrienes			4.22	1.55	Yes
LTB4				4.48	6.33	No
5,6-DiHETE	Hydroxy/hydroperoxyeicosatetraenoic acids			5.54		Yes
12,13-DiHOME	Other octadecanoids	–	313.2384	4.75		Yes
19,20-DiHDPE	Docosanoids	–	361.2384	5.33		Yes
tetranor-12-HETE	Hydroxy fatty acids	–	265.1809	5.34		No
14,15-DiHETrE	Hydroxy/hydroperoxyeicosatrienoic	6	337.2384	5.40	8.46	Yes
5,6-DiHETrE	acids			7.18		Yes
12-HHTrE	Hydroxy/hydroperoxyeicosatrienoic acids	–	279.1966	5.50		Yes
LTE4	Leukotrienes	–	438.2320	5.60		No
13-HOTrE	Other octadecanoids	7	293.2122	6.34	7.77	Yes
13-OxoODE				7.83	1.72	Yes
9-OxoODE				8.22		Yes
15-HEPE	Hydroxy/hydroperoxyeicosapentaenoic acids	8	317.2122	6.70	4.94	Yes
5-HEPE	acids			7.55		Yes
13-HODE	Other octadecanoids	9	295.2279	7.56	1.10	Yes
9-HODE				7.73		Yes
15-HETE	Hydroxy/hydroperoxyeicosatetraenoic	10	319.2279	7.85	2.23	Yes
11-HETE	acids			8.26	1.20	Yes
12-HETE				8.48	3.39	Yes
5-HETE				9.13	3.05	Yes
11,12-EET	Epoxyeicosatrienoic			9.72	2.32	No
5,6-EET	acids			10.16		No
14-HDoHE	Docosanoids	11	343.2279	8.17	6.26	Yes
4-HDoHE				9.34		Yes
15-HETrE	Hydroxy/hydroperoxyeicosatrienoic acids	–	321.2435	8.68		Yes
α-Linolenic acids	Unsaturated fatty acids	12	277.2173	11.70	0.91	Yes
γ-Linolenic acids				11.90		Yes

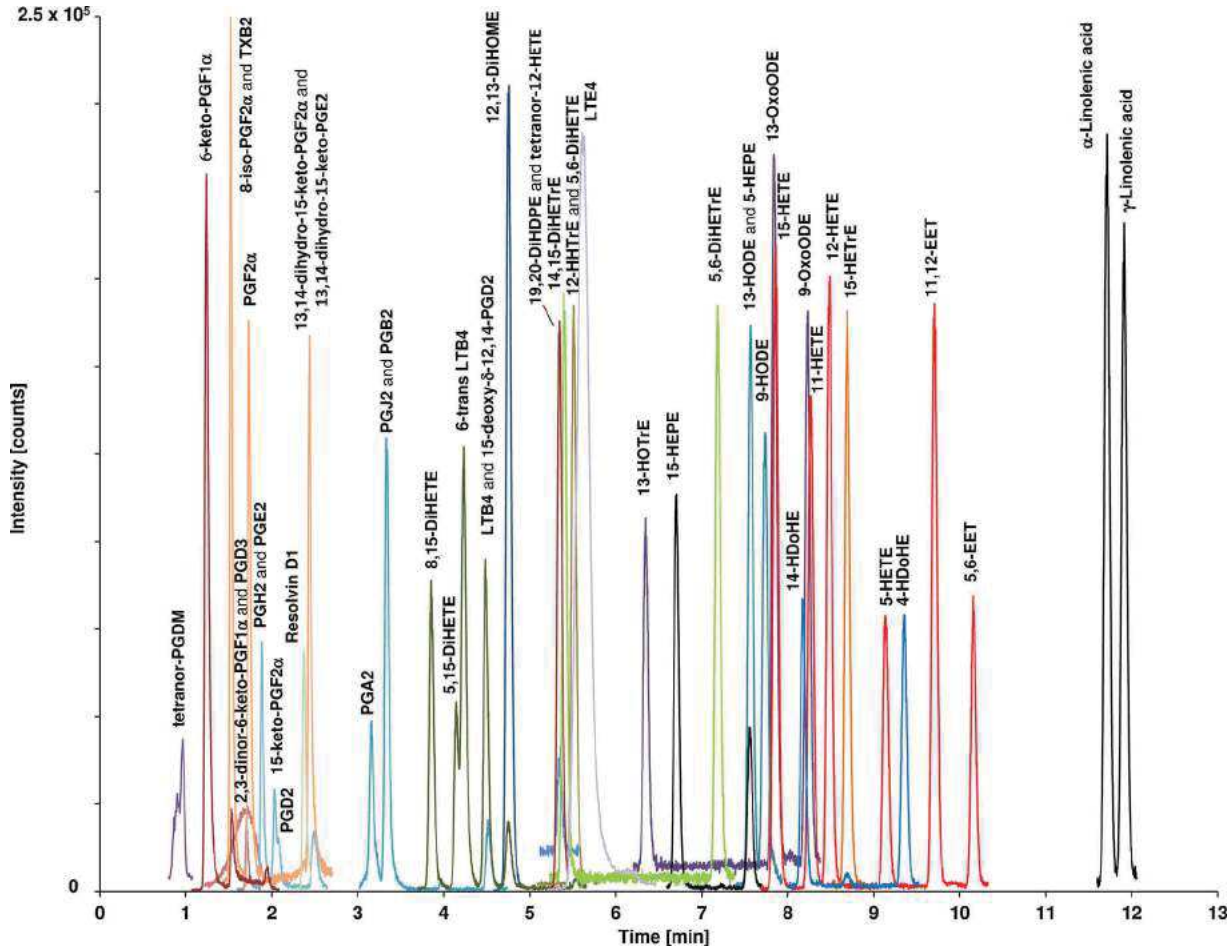

Fig. 4. Negative-ion UHPLC/ESI–MS extracted ion chromatograms of standard mixture obtained using final conditions: Acquity UPLC BEH C18 column (2.1 × 150 mm, 1.7 μm, 130 Å, Waters), flow rate 0.4 mL/min, column temperature 40 °C, eluent A acetonitrile – water – acetic acid (45/55/0.02, v/v/v), eluent B 2-propanol – acetonitrile (50/50, v/v), and gradient program 0 min – 2% B, 12 min – 62% B, and 12.1 min – 99% B. Details are in the Experimental.

ysis of oxylipins. The following parameters were chosen for the initial optimization: eluent B 10 mM ammonium acetate in methanol, methanol as the make-up eluent, ABPR pressure 1800 psi (124.1 bar), flow rate 1.0 mL/min, injection volume 1 μL, column temperature 50 °C, and the gradient program 0 min – 1% B, 5 min – 50% B, 12 min – 50% B, and 13 min – 1% B. First, the retention behavior of selected standards representing different types of isomerism was studied (**PGA2**, **15-deoxy-δ-12,14-PGD2**, **PGB2**, **PGD2**, **PGE2**, **PGF2α**, **8-iso-PGF2α**, **TXB2,** and **6-keto-PGF1α**). For all compounds, the lowest retention was observed on HSS C18 column compared with other stationary phases, moreover **PGF2α**, **8-iso-PGF2α**, **PGD2**, and **PGE2** are not separated. The obtained low retention and poor selectivity indicated the importance of electrostatic attraction between the carboxylate group from analytes and the basic functionality in the stationary phase, which is not occurring at all or only with mild effects on HSS C18 stationary phase due to the lack of additional ionizable functional groups beside residual silanols (pK_a = 7–8) [28,29]. DEA had the most basic functionality (calculated basic pK_a = 9.5), providing strong electrostatic interactions with deprotonated carboxyl groups of oxylipins, thus resulting in the highest retention times for all analytes, and generally accompanied by highest peak width, which resulted in the lower resolution. HSS C18 and DEA columns were excluded from further optimization based on above mentioned observations. Comparable retention and selectivity were observed on the remaining three stationary phases, therefore those were further tested. 1-DIOL provided lower retention of oxylipins compared to the basic stationary phases. Lower retention times were observed for all analytes on 1-AA relative to 2-PIC column [29]. Fig. 5 demonstrated that 1-AA stationary phase provided a superior chromatographic resolution for **11,12-EET**, **12-HETE**, **15-HETE**, **11-HETE**, and **5-HETE** isomers over 1-DIOL and 2-PIC columns. For **γ-linolenic acid** and **α-linolenic acid**, the partial separation was obtained only on 1-AA stationary phase. The bulky anthracene ring may improve the recognition process of isomers in at least two ways, such as the formation of additional hydrophobic interactions and steric hindrance. Finally, 1-AA column was selected for the development of UHPSFC/MS method considering the chromatographic data obtained for HETE, which exhibit numerous biologically important isomers in plasma.

3.2.2. *Effect of flow rate*

One of the main benefits of UHPSFC is the feasibility of using high flow rate [30,19], therefore 1.0, 1.5, 1.7, 2.0, and 2.3 mL/min flow rates were tested. The increased the flow rate from 1.0 mL/min resulted in the following average reductions of retention times: 36% at 1.5 mL/min, 44% at 1.7 mL/min, 53% at 2.0 mL/min, and 60% at 2.3 mL/min. The average resolution of isomers changed only moderately, and the maximum was found at 1.5 mL/min. The resolution was only slightly lower at 1.7 mL/min. The increase of the flow rate from 1.5 to 1.7 mL/min decreased peak widths, especially for **tetranor-PGDM** eluting at the beginning. The decrease of observed peak areas was very small (only 3%). Therefore, 1.7 mL/min was used in the final method.

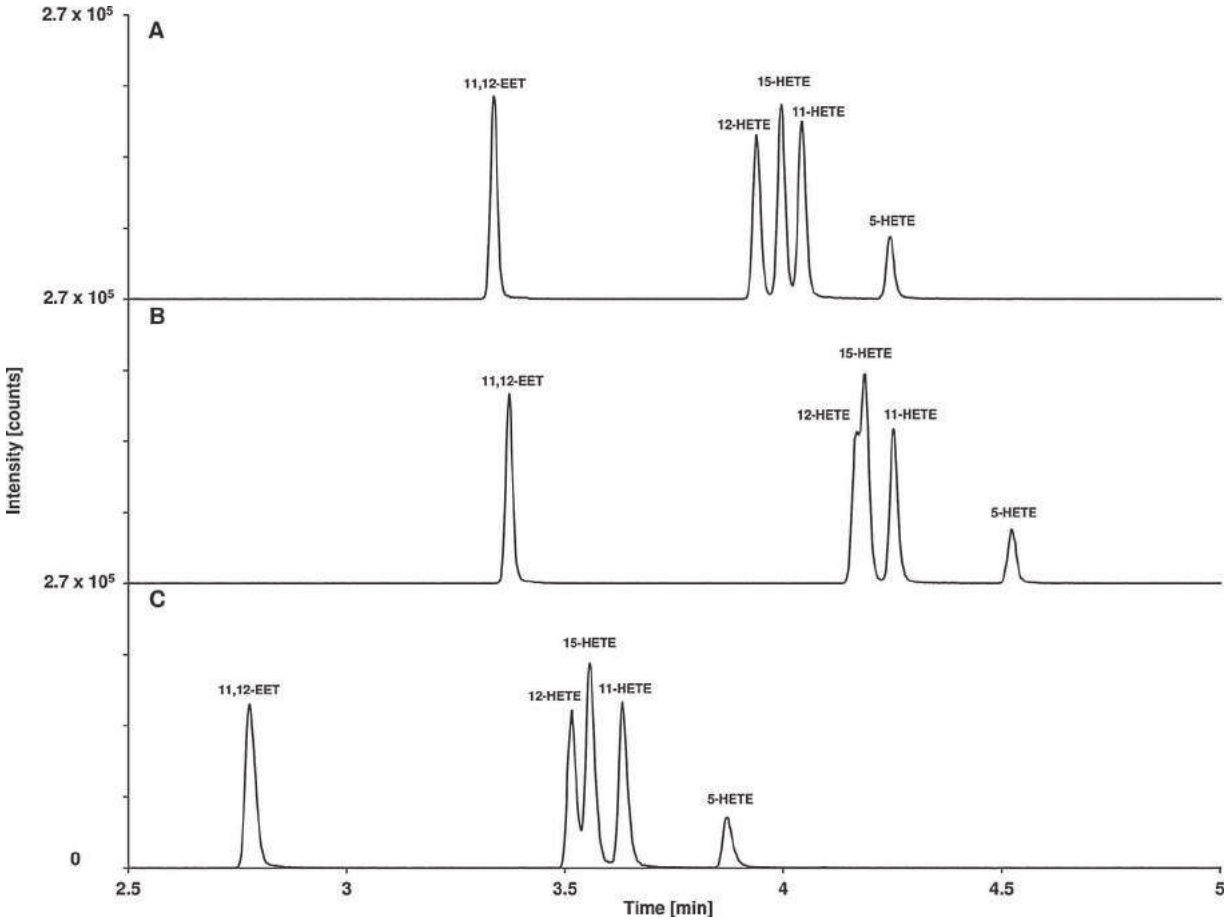

Fig. 5. Effect of the column type on negative-ion UHPSFC/ESI–MS extracted ion chromatograms of the standard mixture of isomeric HETE/EET: (**A**) Acquity UPC^2 Torus 1-Aminoanthracene (1-AA), (**B**) Acquity UPC^2 Torus 2-Pycolylamine (2-PIC), and (**C**) Acquity UPC^2 Torus Diol (1-DIOL) columns. Conditions: ABPR pressure 124 bar, flow rate 1 mL/min, column temperature 50 °C, modifier 10 mM ammonium acetate, gradient program 0 min – 1% B, 10 min – 50% B, and make-up pump flow rate 0.2 mL/min.

The effect of flow rate of make-up eluent on the sensitivity was also studied, and the trend of average signal reduction with increasing flow rate from 0.15 mL/min was the following: 10% at 0.2 mL/min, 13% at 0.25 mL/min and 20% at 0.30 mL/min. Despite the lower sensitivity at higher flow rate, 0.30 mL/min is essential to achieve stable spray in ESI–MS, especially at the beginning of analysis with low modifier content.

3.2.3. *Effect of temperature and backpressure*

The selectivity and mainly the retention in UHPSFC can be influenced by the density of mobile phase through the regulation of temperature and backpressure [31]. In order to study the effect of temperature on the chromatographic behavior of oxylipins, 40, 50, and 60 °C were selected at 124 bar backpressure. For all compounds, higher retention times are observed at higher temperature, while the separation of isomers was not influenced significantly. The effect of temperature on the change of retention was reduced by increasing the content of organic modifier in the mobile phase during the gradient program (Fig. S1). The distribution of data correlates with graphs obtained for diffusion coefficients of anthocyanins dependence on the methanol content in the mobile phase [32]. This retention behavior might be explained by decreased diffusion coefficients of oxylipins with increased organic solvent content and probably by the transition from supercritical to subcritical state in the range of 12–16% methanol [32,33]. The similar chromatographic behavior was found with decreased backpressure from 138 to 103 bar. The column temperature of 50 °C and the backpressure of 124 bar were selected in the final method.

3.2.4. *Effect of gradient steepness*

The retention and selectivity in UHPSFC can be influenced by the gradient steepness similarly as for other chromatographic techniques [31]. 30% of organic modifier provides sufficient elution strength even for the elution of more retained polar standards, for example **tetranor-PGDM** and **2,3-dinor-6-keto-PGF1α**. Thus, the range from 4% to 30% of the eluent B was used for the initial optimization step. In order to investigate the effect of gradient steepness on the chromatographic retention, a study was carried out with the gradient slope of 2.6, 5.2, and 10.4% of B/min. Retention times increased with decreased gradient steepness. This increase was 36% at 5.2% of B/min and 86% at 2.6% of B/min on the average. For the separation of isomers, a similar trend was found in the increase of resolution (57% and 152%) with the decrease of the gradient steepness.

3.2.5. *Selection of organic co-solvent and mobile phase additives*

The polarity of supercritical carbon dioxide is similar to hexane, thus the use of polar organic modifier in the mobile phase is essential for the elution of more polar compounds [19]. Methanol is the most common organic modifier in UHPSFC owing to its physical and chemical properties, such as its high elution strength, and the complete miscibility with supercritical fluid carbon dioxide at given temperature and pressure ranges. Moreover, the mobile phase additives (*e.g.*, ammonium acetate or formate) are well soluble in methanol at typically used concentrations [31]. Methanol with 10 mM of ammonium acetate was used as the organic modifier in the initial stage of optimization. The effect of other organic

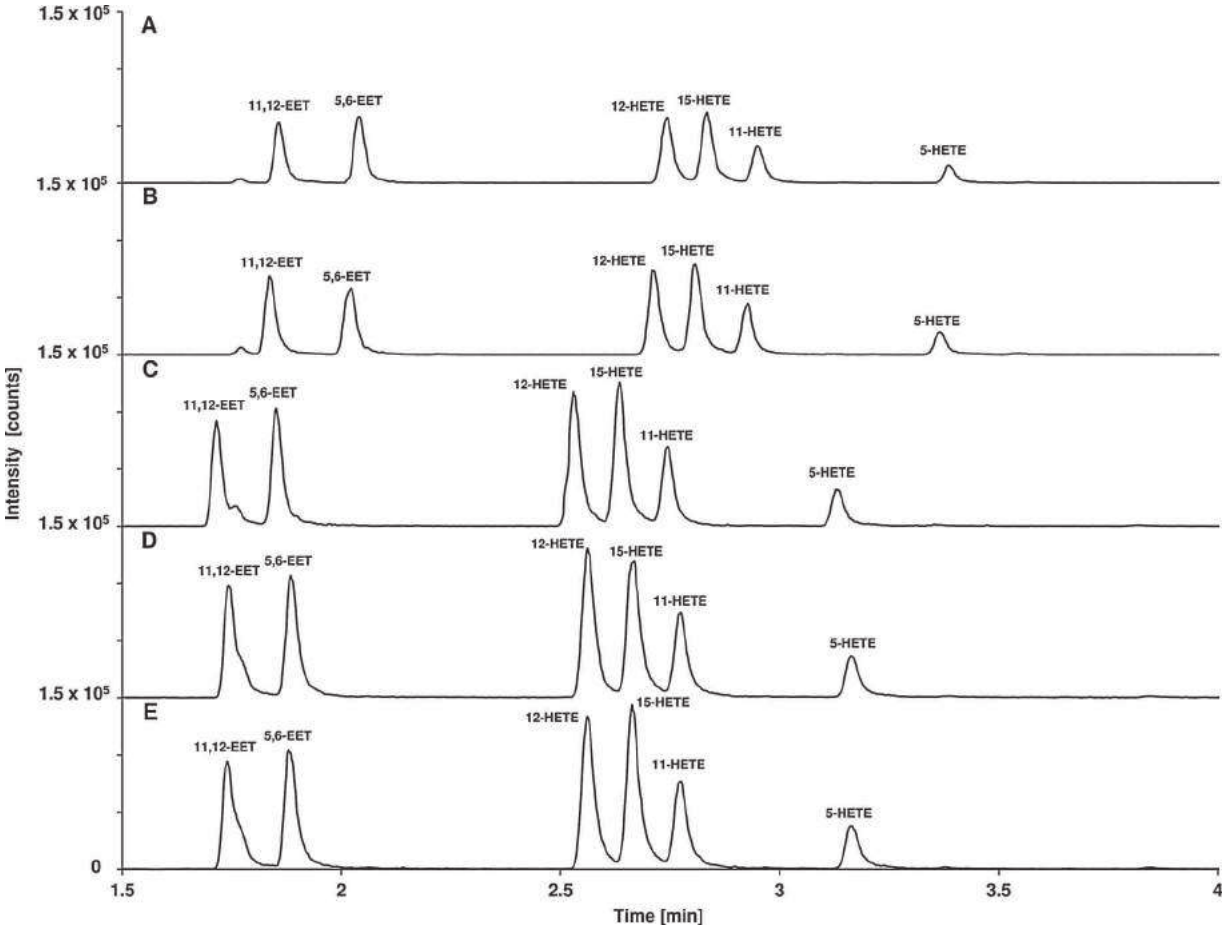

Fig. 6. Effect of different additives in methanol as a modifier on negative-ion UHPSFC/ESI–MS extracted ion chromatograms of the standard mixture of isomeric HETE/EET: (**A**) 10 mM ammonium acetate, (**B**) 10 mM ammonium formate, (**C**) 0.02% formic acid, (**D**) 0.02% acetic acid, and (**E**) without any additives. Conditions: 1-AA column, ABPR pressure 124 bar, flow rate 1.7 mL/min, column temperature 50 °C, gradient program 0 min – 4% B, 10 min – 30% B, and make-up pump flow rate 0.25 mL/min of methanol.

modifiers in methanol was tested for 10% or 20% of acetonitrile or 2-propanol in methanol. For all compounds, the addition of either acetonitrile or 2-propanol increased the retention moderately, while no influence on the separation of isomers was detected, therefore only methanol is used in further optimization steps.

The application of polar additives, such as acid, base, neutral salt or buffer in the mobile phase can influence the retention, selectivity and sensitivity through different ways depending on properties (mainly acid – base) of analyte, types of packed stationary phase and the detection mode [29,19,31]. Considering basic properties of 1-AA column and the detection of acidic oxylipins by negative-ion mode ESI–MS, the effects of acetic acid, formic acid, ammonium acetate, and ammonium formate on the chromatographic behavior and the sensitivity were investigated and compared with the mobile phase without any additive. The nature of additives showed only moderate effects on the retention, while the sensitivity was influenced considerably. Fig. 6 reveals that the use of different mobile phase additives for **1,12-EET**, **12-HETE**, **15-HETE**, **11-HETE**, and **5-HETE** isomers, slightly lower retention was observed for formic acid, while higher retention times were obtained when using salts, especially with ammonium acetate. Generally, increased retention and slightly improved resolution were obtained for increased concentration of ammonium acetate (1, 5, 10, 20, and 30 mM). However, the increase of acetic acid content (0.01, 0.02, 0.05, 0.1, and 0.2%) did not influence the retention and selectivity. The effect of additives on peak shape was negligible.

The concentration of acetic acid in the range of 0–0.2% does not show any visible effect on the retention. Fig. 6 shows the role of additives in the MS response. The use of ammonium acetate provided the lowest responses, as general trend for all compounds (47%), while the highest peak areas were obtained without any additives (*i.e.*, 100%) in methanol. Slightly higher response was found for ammonium formate (61%). The reduction of signal was more considerable for increased concentration of ammonium acetate, for example the mean intensity was reduced to approximately 50% with the change of concentration from 1 to 30 mM. Acetic acid (96%) provided a better sensitivity than formic acid (85%). The mean peak area showed a maximum at 0.1% of acetic acid within the tested range from 0 to 0.2%. The use of buffers in the mobile phase slightly improved the separation of isomers, but on the other hand it resulted in a serious loss of sensitivity, therefore 0.1% acetic acid was selected as the mobile phase additive.

The effect of water content (1, 2, and 5%) in the mobile phase containing 0.1% acetic acid on the retention and selectivity was studied. A slight improvement of peak shapes was achieved with 5% of water, but the ESI response was dramatically reduced by 65%. The similar signal reduction was observed for 1% water in methanol used as a make-up solvent, therefore water was not used either in the mobile phase or make-up solvent in further experiments.

3.2.6. *Effect of sample solvent and injected volume*

The type of solvent and injected volume can influence the peak shape and the retention time as well. Hexane and heptane are the best choice for dissolution solvent due to the similar polarity with supercritical carbon dioxide [19]. Hexane and chloroform were selected as commonly used nonpolar solvents in lipidomics.

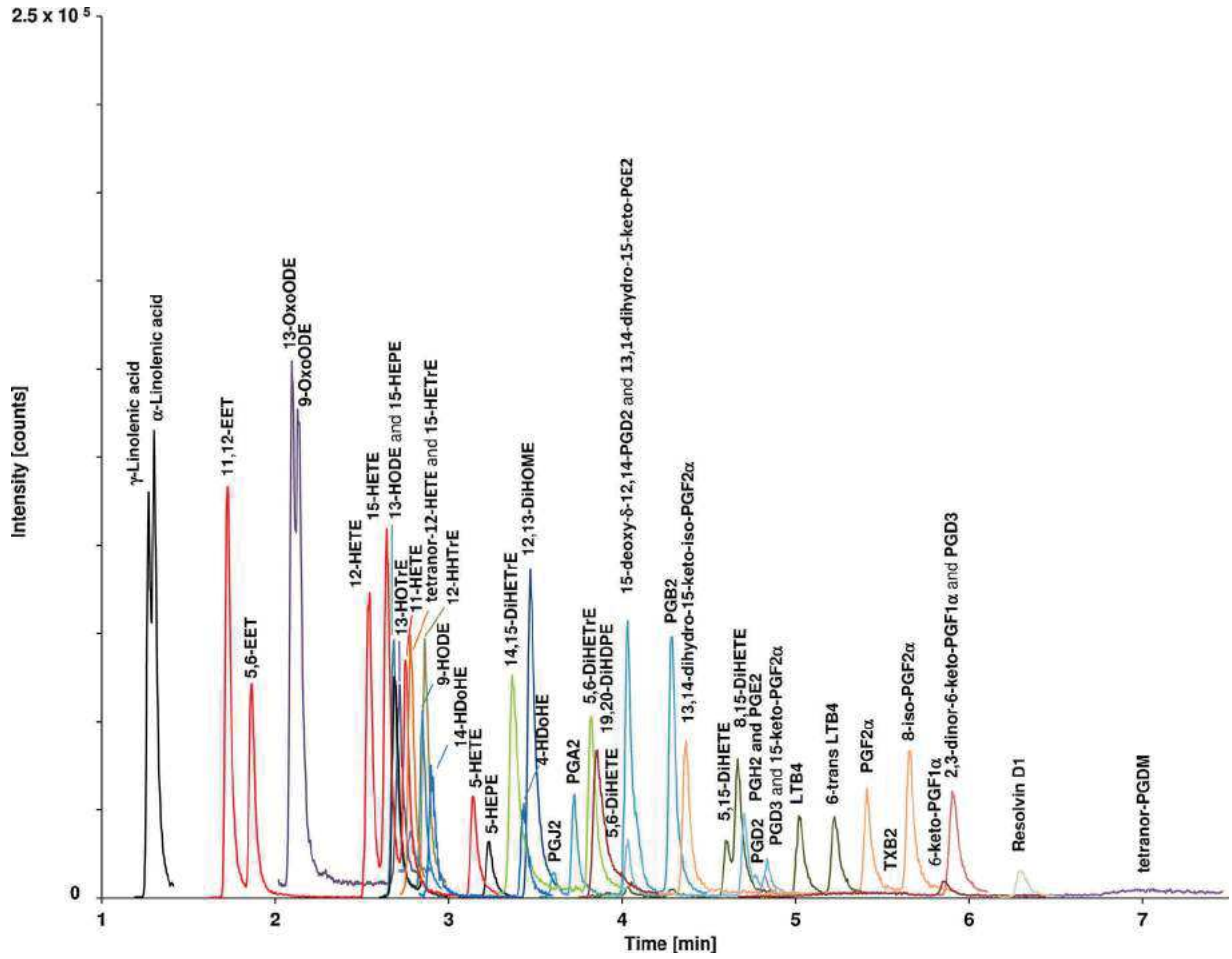

Fig. 7. Negative-ion UHPSFC/ESI–MS extracted ion chromatograms of the standard mixture obtained using final conditions: 1-AA column, modifier 0.1% acetic acid in methanol, ABPR pressure 124 bar, flow rate 1.7 mL/min, column temperature 50 °C, gradient program 0 min – 4% B, 10 min – 30% B, and make-up pump flow rate 0.30 mL/min of methanol. Details are in the Experimental.

However, the addition of polar organic solvent into chloroform was necessary for more polar standards. Thus, the effect of methanol and ethanol content and type of nonpolar solvents was investigated on chromatographic results. No significant changes were observed for retention times. The use of hexane and chloroform with 50% ethanol content showed that chloroform resulted in narrower peak widths. Concerning contribution of polar organic solvent (50%) in chloroform, the addition of ethanol resulted in better peak shape than methanol, additionally better separation occurred in case of low retained linolenic acid isomers. Interestingly, higher chloroform content did not provide any improvement in peak shapes. The selection of chloroform – ethanol (50/50, v/v) was the best compromise considering peak profiles, proper polarity, and low volatility. The injected volume may have the main effect on the peak distortion [19], therefore measurements were carried out for the injection volumes of 1, 2, 3, and 5 μL. The increase of injection volume resulted in no change in the retention, but it decreased the chromatographic resolution, as expected. This trend was more evident for less retained compounds. Thus, the injected volume was limited to 1 μL.

The final UHPSFC/MS method provided baseline separation for 20 oxylipin standards within 7 min (Fig. 7 and Table 3).

3.3. Comparison of UHPLC/MS and UHPSFC/MS

Fig. 8 demonstrated different retention mechanisms with a low degree of orthogonality ($r^2 = 0.8$) between UHPLC/MS and UHPSFC/MS methods. Generally, the increase of the compound hydrophobicity resulted in higher retention in RP-UHPLC, while the opposite trend was observed in UHPSFC. A different elution order between UHPLC and UHPSFC was observed for isomeric groups **1**, **2**, **3**, **4**, **5**, **7**, **10**, and **12**. For **γ-linolenic acid**, **α-linolenic acid, 11,12-EET**, and **5,6-EET**, the highest retention was observed in UHPLC, while lowest retention times were obtained in UHPSFC. **Resolvin D1**, **2,3-dinor-6-keto-PGF1α**, **TXB2**, and **6-keto-PGF1α** with 3 hydroxyl groups provided highest retention times in UHPSFC. For **TXB2,** broad (in UHPSFC) and tailing (in UHPLC) elution profiles may be associated with the interconversion between hemiacetal isomers [34]. The presence of additional carboxyl group in more polar analyte **tetranor-PGDM** caused the tailing peak with increased retention in UHPSFC. The contribution of polar cysteinyl side chain of **LTE4** may contribute to the peak shape distortion. This unfavorable effect was more pronounced in UHPSFC, where it disabled the detection of **LTE4** due to extremely tailing peaks. The degree of unsaturation also influenced the retention, mainly in UHPLC. Table 2 reveals that for **15-HETrE**, **15-HETE**, and **15-HEPE**, the reduction in retention times correlates with the increase in the number of double bonds.

Tables 2 and 3 show that UHPLC generally provides better separation of isomers than UHPSFC method except for positional isomeric groups of **2**, **4**, **5,** and **9**. Higher retention and resolution were observed for positional isomers **PGJ2**, **PGA2**, and **PGB2** in UHPSFC. It indicates that the position of the carbonyl group at C9 was more favorable for dipole–dipole interaction than at C11, thus

Table 3
Chromatographic and mass spectrometric data for oxylipin and fatty acid standards in the final UHPSFC/MS method.

Abbreviation	Subclass	Isomeric group	Theoretical m/z of $[M-H]^-$	t_R in UHPSFC/MS [min]	R_S	Indentified in plasma
tetranor-PGDM	Prostaglandins	–	327.1449	7.03		No
TXB2	Thromboxanes	1	369.2283	5.36	1.02	Yes
6-keto-PGF1α	Prostaglandins			5.86		No
13,14-dihydro-15-keto-PGF2α	Prostaglandins	2	353.2333	4.37	7.23	No
PGF2α				5.41	1.75	Yes
8-iso-PGF2α				5.66		Yes
2,3-dinor-6-keto-PGF1α	Prostaglandins	–	341.1970	5.90		No
PGD3	Prostaglandins	–	349.2021	4.82		No
13,14-dihydro-15-keto-PGE2	Prostaglandins	3	351.2177	4.03	4.81	No
PGH2				4.71		No
PGE2				4.71	0.68	Yes
PGD2				4.77	0.78	Yes
15-keto-PGF2a				4.83		No
Resolvin D1	Docosanoids	–	375.2177	6.30		No
PGJ2	Prostaglandins	4	333.2071	3.61	1.02	No
PGA2				3.73	3.07	No
15-deoxy-δ-12,14-PGD2				4.08	2.10	No
PGB2				4.28		Yes
5,6-DiHETE	Hydroxy/hydroperoxyeicosatetraenoic	5	335.2228	3.91	9.12	Yes
5,15-DiHETE	acids			4.60	0.73	Yes
8,15-DiHETE				4.67	2.40	Yes
LTB4	Leukotrienes			5.02	1.32	No
6-trans LTB4				5.22		Yes
12,13-DiHOME	Other octadecanoids	–	313.2384	3.47		Yes
19,20-DiHDPE	Docosanoids	–	361.2384	3.86		Yes
tetranor-12-HETE	Hydroxy fatty acids	–	265.1809	2.78		No
14,15-DiHETrE	Hydroxy/hydroperoxyeicosatrienoic	6	337.2384	3.37	2.60	Yes
5,6-DiHETrE	acids			3.82		Yes
12-HHTrE	Hydroxy/hydroperoxyeicosatrienoic acids	–	279.1966	2.87		Yes
LTE4	Leukotrienes	–	438.2320	n.d.		No
13-OxoODE	Other octadecanoids	7	293.2122	2.10	0.44	Yes
9-OxoODE				2.13	6.29	Yes
13-HOTrE				2.72		Yes
15-HEPE	Hydroxy/hydroperoxyeicosapentaenoic	8	317.2122	2.69	4.09	Yes
5-HEPE	acids			3.23		Yes
13-HODE	Other octadecanoids	9	295.2279	2.68	1.48	Yes
9-HODE				2.85		Yes
11,12-EET	Epoxyeicosatrienoic	10	319.2279	1.70	1.09	No
5,6-EET	acids			1.84	6.18	No
12-HETE	Hydroxy/hydroperoxyeicosatetraenoic			2.54	0.96	Yes
15-HETE	acids			2.64	0.90	Yes
11-HETE				2.75	2.76	Yes
5-HETE				3.14		Yes
14-HDoHE	Docosanoids	11	343.2279	2.90	3.78	Yes
4-HDoHE				3.43		Yes
15-HETrE	Hydroxy/hydroperoxyeicosatrienoic acids	–	321.2435	2.78		Yes
γ-Linolenic acids	Unsaturated fatty acids	12	277.2173	1.27	0.42	Yes
α-Linolenic acids				1.30		Yes

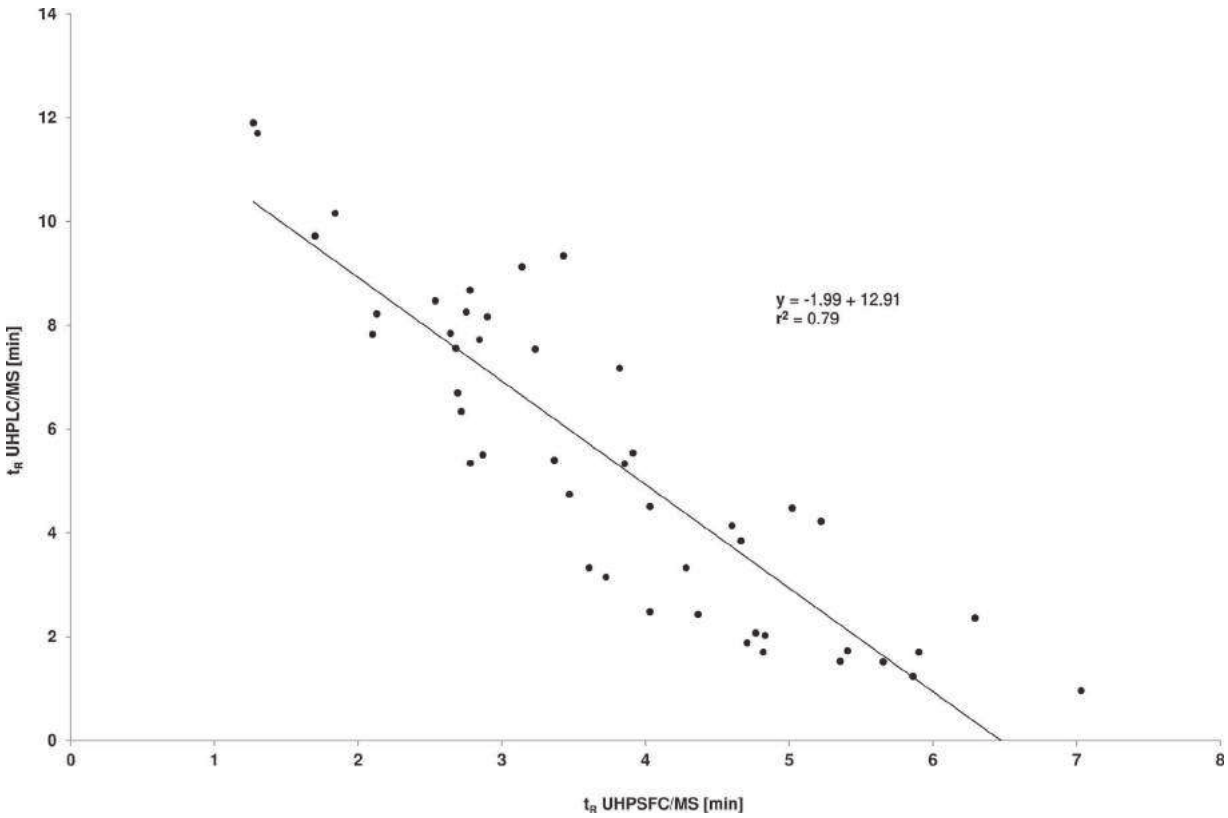

Fig. 8. Correlation of retention times in UHPLC/ESI–MS and UHPSFC/ESI–MS methods using final conditions.

position of double bond in the cyclopentane ring had higher contribution to the separation of isomers. For diastereoisomers **PGF2α** and **8-iso-PGF2α** and functional isomers of **15-keto-PGF2α** and **PGF2α**, higher retention was observed in UHPSFC, and this was accompanied by higher resolution.

The sensitivity of given analytical method was also an important aspect due to low concentrations of oxylipins in biological samples. Approximately 3.5-fold higher sensitivity on average was observed in UHPLC/MS in comparison to UHPSFC/MS. Figs. 4 and 7 with the same scale of intensity illustrate the different sensitivity in both methods. In UHPSFC, the signal reduction could be attributed to the following reasons: 1/applied higher flow rate, 2/lower ionization efficiency due to decreased sample solubility during carbon dioxide expansion, and 3/dilution and splitting of eluted sample prior to MS detection [35]. The lower concentration of compounds in the effluent might be caused by different diameters between UHPSFC (3 mm) and UHPLC (2.1 mm) columns [36].

3.4. Identification of oxylipins in human plasma

The enrichment of oxylipins through polar and nonpolar matrix removal is a critical step prior to their analysis due to their trace concentration in biological samples. Nowadays, SPE is one of the most efficient and widespread technique in the sample preparation procedure. The polymeric StrataX RP column showed a good recovery for oxylipins [7,17,24,37]. The application of relatively high volume of plasma sample was needed due to the limited injection volume in UHPSFC. Numerous glycerophospholipids (PL), mainly lyso species, enriched with oxylipins and fatty acids in the extracts, caused matrix effects due to the coelution with oxylipins, which eluted in the range of 2–7 min in UHPSFC and 1–10 min in UHPLC (Tables 2 and 3). This unfavorable effect was more pronounced in UHPLC owing to comparable retention of oxylipins and LPLs in the RP separation. For example, high abundant **LPI 20:4** and **LPI 18:2**, coeluted with **PGE2** and **PGD2** at 2.1 min. Retention times of other LPE and LPC were found in the range of 8–10 min, *e.g.*, **LPE 18:2**, **LPE 22:6**, **LPC 16:0**, and **LPC 22:6**, while in UHPSFC they eluted after 9 min, which reduces the risk of ion suppression effects. Fatty acids had higher retention times in UHPLC (after 9.5 min) and lower retention in UHPSFC (before 2.3 min), therefore the risk of ion suppression effects is relatively low in both cases.

Tables 2 and 3 show 31 oxylipins identified in human plasma based on 48 standards by both methods. Considering better separation of isomers and higher sensitivity, the optimized UHPLC/MS method was selected for the identification of additional plasma oxylipins. The further identification of additional oxylipins without available authentic standards was based on their retention times, accurate masses of precursor ions (7 ppm mass tolerance at maximum), and related fragment ions using homemade database created based on own measurements and literature sources [1–7,12,16–18,23,38,39]. Relevant chromatographic and MS data of additional 20 possible compounds in plasma including retention times, *m*/*z* of precursor ions, and observed fragment ions corresponding to structures are given in Table 4.

4. Conclusions

Optimized UHPLC/ESI–MS and UHPSFC/ESI–MS methods have been applied for the analysis of 46 oxylipins and 2 fatty acids standards. In UHPLC, mobile phase additives and their concentrations significantly influence the chromatographic retention and MS sensitivity, especially the use of acetic acid brings advantages over ammonium acetate or formate in terms of the resolution and sensitivity. The UHPSFC/ESI–MS method for oxylipins is reported for the first time here. 1-AA column yields a better separation of oxylipins than other dedicated sub–2 μm UHPSFC stationary phases (2-PIC, 1-DIOL, DEA, and HSS C18). The chromatographic resolution of

Table 4
UHPLC/MS/MS data for tentatively identified oxylipins without given standards in the human plasma sample.

Name	Abbreviation	Subclass	Experimental m/z of $[M-H]^-$	Mass accuracy [ppm]	t_R in UHPLC/MS [min]	m/z of observed fragment ions
5,9S,11R-trihydroxy-6E,14Z-prostadienoic acid-cyclo[8S,12R]	5-iso-PGF2α VI	Isoprostanes	353.2317	4.8	1.89	335, 317, 309, 115
9-oxo-11S,15S-dihydroxy-5Z,13E-prostadienoic acid	11β-PGE2	Prostaglandins	351.2164	3.7	1.95	333, 315, 271, 189
9,10-dihydroxy-12Z-octadecenoic acid	9,10-DiHOME	Other octadecanoids	313.2371	4.2	5.14	295, 277, 201, 177
9-hydroxy-10E,12Z,15Z-octadecatrienoic acid	9-HOTrE		293.2106	5.5	6.20	275, 231, 185, 171, 121
(+/−)-11-hydroxy-5Z,8Z,12E,14Z,17Z-eicosapentaenoic acid	11-HEPE	Hydroxy/hydroperoxyeicosapentaenoic acids	317.2115	2.2	6.28	299, 259, 255, 215, 195, 167, 149, 121
(+/−)-14(15)-epoxy-5Z,8Z,11Z,17Z-eicosatetraenoic acid	14(15)-EpETE	Other eicosanoids	317.2106	5.0	6.58	299, 255, 219, 207
(+/−)-20-hydroxy-4Z,7Z,10Z,13Z,16Z,18E-docosahexaenoic acid	20-HDoHE	Docosanoids	343.2280	−0.3	7.51	325, 299, 285, 281, 241, 187, 159, 133, 107
(+/−)-17-hydroxy-4Z,7Z,10Z,13Z,15E,19Z-docosahexaenoic acid	17-HDoHE		343.2276	0.9	8.02	325, 281, 273, 245, 229, 227, 201, 173, 147, 121, 111
15-oxo-5Z,8Z,11Z,13E-eicosatetraenoic acid	15-oxo-ETE	Hydroxy/hydroperoxyeicosatetraenoic acids	317.2107	4.7	8.05	299, 273, 139, 113
(+/−)-9,10-epoxy-12Z-octadecenoic acid	9(10)-EpOME	Other octadecanoids	295.2271	2.7	8.20	277, 183, 201, 171
(+/−)-10-hydroxy-4Z,7Z,11E,13Z,16Z,19Z-docosahexaenoic acid	10-HDoHE	Docosanoids	343.2278	0.3	8.22	325, 299, 281, 227, 181, 161, 153, 121
(+/−)-11-hydroxy-4Z,7Z,9E,13Z,16Z,19Z-docosahexaenoic acid	11-HDoHE		343.2277	0.6	8.41	325, 281, 227, 194, 165, 149, 133, 121, 95
8-hydroxy-5Z,9E,11Z,14Z-eicosatetraenoic acid	8-HETE	Hydroxy/hydroperoxyeicosatetraenoic acids	319.2276	0.9	8.60	301, 257, 163, 155
(+/−)-7-hydroxy-4Z,8E,10Z,13Z,16Z,19Z-docosahexaenoic acid	7-HDoHE	Docosanoids	343.2278	0.3	8.61	325, 281, 245, 227, 201, 147, 141, 121, 113, 97
(+/−)-8-hydroxy-4Z,6E,10Z,13Z,16Z,19Z-docosahexaenoic acid	8-HDoHE		343.2276	0.9	8.69	299, 281, 243, 189, 135, 109
9-hydroxy-5Z,7E,11Z,14Z-eicosatetraenoic acid	9-HETE	Hydroxy/hydroperoxyeicosatetraenoic acids	319.2272	2.2	8.77	301, 275, 257, 229, 203, 179, 167, 139, 123, 69
12-oxo-5Z,8Z,10E,14Z-eicosatetraenoic acid	12-oxo-ETE		317.2122	0.0	9.01	299, 273, 235, 153
(6E,8Z,11Z)-5-hydroxyicosa-6,8,11-trienoic acid	5-HETrE		321.2415	6.2	9.10	303, 259, 205, 115
(+/−)-12(13)-epoxy-9Z-octadecenoic acid	12(13)-EpOME	Other octadecanoids	295.2275	1.4	9.20	277, 195, 183
5-oxo-6E,8Z,11Z,14Z-eicosatetraenoic acid	5-oxo-ETE	Hydroxy/hydroperoxyeicosatetraenoic acids	317.2102	6.3	9.63	299, 273, 245, 203, 129

several critical isomeric pairs in UHPSFC is lower compared to RP-UHPLC, which shows that RP-like mode in UHPSFC is not really competitive to RP-UHPLC unlike to HILIC mode, where UHPSFC is superior to HILIC-UHPLC. This is probably caused by natural limitations of UHPSFC, where the typical mobile phase is nonpolar CO_2 with the addition of some polar modifier, which is far from the typical RP mobile phases used in UHPLC. In general, the sensitivity of UHPLC/MS is higher by a factor of ca. 3.5 times in comparison to UHPSFC/MS, but some opposite examples can be found as well, *e.g.*, prostaglandins. The sensitivity decrease is partially caused by different column diameters (the ratio of squared internal diameters is about 2). Finally, 31 oxylipins from 46 available standards are detected in the human plasma extract together with additional 20 tentatively identified endogenous oxylipins based on UHPLC/MS/MS measurements and home-made database of precursor and product ions and accurate m/z values of measured ions.

Acknowledgements

This work was supported by the ERC CZ grant project LL1302 sponsored by the Ministry of Education, Youth and Sports of the Czech Republic. Róbert Berkecz thanks for the financial support to the János Bolyai Research Scholarship of the Hungarian Academy of Sciences.

Appendix A. Supplementary data

Supplementary data associated with this article can be found, in the online version, at http://dx.doi.org/10.1016/j.chroma.2017.06.070.

References

[1] V.B. O'Donnel, B. Maskrey, G.W. Taylor, Eicosanoids: generation and detection in mammalian cells, in: B. Larijani, R. Woscholski, C.A. Rosser (Eds.), Lipid Signaling Protocols, Humana Press, New York, 2009, pp. 5–24.
[2] D. Wang, R.N. DuBois, Measurement of eicosanoids in cancer tissues, in: H.A. Brown (Ed.), Methods in Enzymology, vol. 433, Elsevier, 2007, pp. 27–50.
[3] D. Wang, R.N. DuBois, Eicosanoids and cancer, Nat. Rev. Cancer 10 (2010) 181–193.
[4] E.A. Dennis, P.C. Norris, Eicosanoid storm in infection and inflammation, Nat. Rev. Immunol. 15 (2015) 511–523.
[5] H. Tapiero, G. Nguyen Ba, P. Couvreur, K.D. Tew, Polyunsaturated fatty acids (PUFA) and eicosanoids in human health and pathologies, Biomed. Pharmacother. 56 (2002) 215–222.
[6] R. Loomba, O. Quehenberger, A. Armando, E.A. Dennis, Polyunsaturated fatty acid metabolites as novel lipidomic biomarkers for noninvasive diagnosis of nonalcoholic steatohepatitis, J. Lipid Res. 56 (2015) 185–192.
[7] O. Quehenberger, A.M. Armando, A.H. Brown, S.B. Milne, D.S. Myers, A.H. Merrill, S. Bandyopadhyay, K.N. Jones, S. Kelly, R.L. Shaner, C.M. Sullards, E. Wang, R.C. Murphy, R.M. Barkley, T.J. Leiker, C.R. Raetz, Z. Guan, G.M. Laird, D.A. Six, D.W. Russell, J.G. McDonald, S. Subramaniam, E. Fahy, E.A. Dennis, Lipidomics reveals a remarkable diversity of lipids in human plasma, J. Lipid Res. 51 (2010) 3299–3305.
[8] M. Puppolo, D. Varma, S.A. Jansen, A review of analytical methods for eicosanoids in brain tissue, J. Chromatogr. B 964 (2014) 50–64.
[9] C. Ferreiro-Vera, J.M. Mata-Granados, F. Priego-Capote, J.M. Quesada-Gómez, M.D. Luque de Castro, Automated targeting analysis of eicosanoid inflammation biomarkers in human serum and in the exometabolome of stem cells by SPE–LC–MS/MS, Anal. Bioanal. Chem. 399 (2011) 1093–1103.
[10] R.C. Murphy, R.M. Barkley, K.Z. Berry, K.Z. Berry, J. Hankin, K. Harrsion, C. Johnson, J. Krank, A. McAnoy, C. Uhlson, S. Zarini, Electrospray ionization and tandem mass spectrometry of eicosanoids, Anal. Biochem. 346 (2005) 1–42.
[11] K.R. Maddipati, R. Romero, T. Chaiworapongsa, Sen-Lin Zhou, Z. Xu, A.L. Tarca, J.P. Kusanovic, H. Munoz, K.V. Honn, Eicosanomic profiling reveals dominance of the epoxygenase pathway in human amniotic fluid at term in spontaneous labor, The FASEB J. Res. Commun. 28 (2016) 4835–4846.
[12] D.D. Shinde, K.B. Kim, K.S. Oh, N. Abdalla, K.H. Liu, S.K. Bae, J.H. Shon, H.S. Kim, D.-H. Kim, J.G. Shin, LC–MS/MS for the simultaneous analysis of arachidonic acid and 32 related metabolites in human plasma: basal plasma concentrations and aspirin-induced changes of eicosanoids, J. Chromatogr. B 911 (2012) 113–124.
[13] T. Nishisho, T. Tonai, Y. Tamura, T. Ikata, Experimental and clinical studies of eicosanoids in cerebrospinal fluid after spinal cord injury, Neurosurgery 39 (1996) 950–957.
[14] K. Sterz, G. Scherer, J. Ecker, A simple and robust UPLC-SRM/MS method to quantify urinary eicosanoids, J. Lipid Res. 53 (2012) 1026–1036.
[15] J. Song, X. Liu, J. Wuc, M.J. Meehan, J.M. Blevitt, P.C. Dorrestein, M.E. Milla, A highly efficient, high-throughput lipidomics platform for the quantitative detection of eicosanoids in human whole blood, Anal. Biochem. 433 (2015) 181–188.
[16] K. Strassburg, A.M.L. Huijbrechts, K.A. Kortekaas, J.H. Lindeman, T.L. Pedersen, A. Dane, R. Berger, A. Brenkman, T. Hankemeier, J. van Duynhoven, E. Kalkhoven, J.W. Newman, R.J. Vreeken, Quantitative profiling of oxylipins through comprehensive LC-MS/MS analysis: application in cardiac surgery, Anal. Bioanal. Chem. 404 (2012) 1413–1426.
[17] Y. Wang, A.M. Armando, O. Quehenberger, C. Yan, E.A. Dennis, Comprehensive ultra-performance liquid chromatographic separationand mass spectrometric analysis of eicosanoid metabolites in human samples, J. Chromatogr. A 1359 (2014) 60–69.
[18] A.F. Galvão, T. Petta, N. Flamand, V.R. Bollela, C.L. Silva, L.R. Jarduli, K.C.R. Malmegrim, B.P. Simões, L.A.B. de Moraes, L.H. Faccioli, Plasma eicosanoid profiles determined by high-performance liquid chromatography coupled with tandem mass spectrometry in stimulated peripheral blood from healthy individuals and sickle cell anemia patients in treatment, Anal. Bioanal. Chem. 408 (2016) 3613–3623.
[19] L. Nováková, A.G.G. Perrenoud, I. Francois, C. West, E. Lesellier, D. Guillarme, Modern analytical supercritical fluid chromatography using columns packed with sub-2 μm particles: a tutorial, Anal. Chim. Acta 824 (2014) 18–35.
[20] T. Berg, L. Kaur, A. Risnes, S.M. Havig, R. Karinen, Determination of a selection of synthetic cannabinoids and metabolites in urine by UHPSFC-MS/MS and by UHPLC-MS/MS, Drug Test. Anal. 8 (2016) 708–722.
[21] A.G.G. Perrenoud, J.L. Veuthey, D. Guillarme, Comparison of ultra-high performance supercritical fluid chromatography and ultra-high performance liquid chromatography for the analysis of pharmaceutical compounds, J. Chromatogr. A 1266 (2012) 158–167.
[22] M. Lísa, M. Holčapek, High-throughput and comprehensive lipidomic analysis using ultrahigh-performance supercritical fluid chromatography-mass spectrometry, Anal. Chem. 87 (2015) 7187–7195.
[23] M. Sud, E. Fahy, D. Cotter, A. Brown, E. Dennis, C. Glass, R. Murphy, C. Raetz, D. Russell, S. Subramaniam, LMSD: LIPID MAPS structure database, Nucleic Acids Res. 35 (2007) 527–532.
[24] A.I. Ostermann, Ina Willenberg, N.H. Schebb, Comparison of sample preparation methods for the quantitative analysis of eicosanoids and other oxylipins in plasma by means of LC-MS/MS, Anal. Bioanal. Chem. 407 (2015) 1403–1414.
[25] M. Mal, P.K. Koh, P.Y. Cheah, E.C.Y. Chan, Ultra-pressure liquid chromatography/tandem mass spectrometry targeted profiling of arachidonic acid and eicosanoids in human colorectal cancer, Rapid Commun. Mass Spectrom. 25 (2011) 755–764.
[26] J. McMurry, Biomolecules: amino acids, peptides, and proteins, in: J. McMurry (Ed.), Organic Chemistry, ninth edition, Cengage Learning, Boston, 2016, pp. 870–907.
[27] M. Müller, T.C. Sorrell, Quantitation of sulfidopeptide leukotrienes by reversed-phase high-performance liquid chromatography, J. Chromatogr. 343 (1985) 213–218.
[28] H.A. Claessens, A comparative study of test methods for stationary phases for reversed-phase column in HPLC, in: H.A. Claessens (Ed.), Characterization of Stationary Phases for Reversed-phase Liquid Chromatography: Column Testing, Classification and Chemical Stability, Technische Universiteit Eindhoven, Eindhoven, 1999, pp. 107–142.
[29] V. Desfontaine, J.L. Veuthey, D. Guillarme, Evaluation of innovative stationary phase ligand chemistries and analytical conditions for the analysis of basic drugs by supercritical fluid chromatography, J. Chromatogr. A 1438 (2016) 244–253.
[30] K. Hettiarachchi, A. Yun, M. Kong, J.R. Jacobsen, Q. Xue, The use of SFC in discovery sciences, in: G.K. Webster (Ed.), Supercritical Fluid Chromatography: Advances and Applications in Pharmaceutical Analysis, CRC Press Taylor & Francis Group, Boca Raton, 2014, pp. 15–41.
[31] J.W. Caldwell, W.B. Caldwell, G.K. Webster, Z. Wang, Method development of achiral SFC, in: G.K. Webster (Ed.), Supercritical Fluid Chromatography: Advances and Applications, in: Pharmaceutical Analysis, CRC Press Taylor & Francis Group, Boca Raton, 2014, pp. 65–96.
[32] C. Mantell, M. Rodríguez, E. Martínez de la Ossa, Measurement of the diffusion coefficient of a model food dye (malvidin 3,5-diglucoside) in a high pressure CO2+ methanol system by the chromatographic peak-broadening technique, J. Supercrit. Fluids 25 (2003) 57–68.
[33] T.A. Berger, Physical chemistry of mobile phases used in packed column SFC, in: R.M. Smith (Ed.), Packed Column SFC, The Royal Society of Chemistry, Cambridge, 1995, pp. 43–71.
[34] J.G. Bollinger, W. Thompson, Y. Lai, R.C. Oslund, T.S. Hallstrand, M. Sadilek, F. Turecek, M.H. Gelb, Improved sensitivity mass spectrometric detection of eicosanoids by charge reversal derivatization, Anal. Chem. 82 (2010) 6790–6796.
[35] Y. Zhao, SFC in process analytical chemistry, in: G.K. Webster (Ed.), Supercritical Fluid Chromatography: Advances and Applications in Pharmaceutical Analysis, CRC Press Taylor & Francis Group, Boca Raton, 2014, pp. 195–224.
[36] V. Desfontaine, L. Nováková, F. Ponzetto, R. Nicoli, M. Saugy, J.L. Veuthey, D. Guillarme, Liquid chromatography and supercritical fluid chromatography as

alternative techniques to gas chromatography for the rapid screening of anabolic agents in urine, J. Chromatogr. A 1451 (2016) 145–155.
[37] R. Deems, M.W. Buczynski, R. Bowers-Gentry, R. Harkewicz, E.A. Dennis, Detection and quantitation of eicosanoids via high performance liquid chromatography-electrospray ionization-mass spectrometry, in: H.A. Brown (Ed.), Methods in Enzymology, vol. 432, Elsevier, 2007, pp. 59–82.
[38] R.C. Murphy, Eicosanoid and bioactive lipid mediators, in: R.C. Murphy (Ed.), Tandem Mass Spectrometry of Lipids, Molecular Analysis of Complex Lipids, The Royal Society of Chemistry, Cambridge, 2015, pp. 40–74.
[39] R.C. Murphy, R.M. Barkley, K.Z. Berry, J. Hankin, K. Harrison, C. Johnson, J. Krank, A. McAnoy, C. Uhlson, S. Zarini, Electrospray ionization and tandem mass spectrometry of eicosanoids, Anal. Biochem. 346 (2005) 1–42.

analytical chemistry

Article

Cite This: Anal. Chem. 2017, 89, 12425-12432

pubs.acs.org/ac

Hydrophilic Interaction Liquid Chromatography–Mass Spectrometry Characterization of Gangliosides in Biological Samples

Roman Hájek, Robert Jirásko, Miroslav Lísa, Eva Cífková, and Michal Holčapek*

Department of Analytical Chemistry, Faculty of Chemical Technology, University of Pardubice, Studentská 573, 53210 Pardubice, Czech Republic

Supporting Information

ABSTRACT: The hydrophilic interaction liquid chromatography (HILIC) coupled to a negative-ion electrospray ionization tandem mass spectrometry (ESI-MS/MS) method has been developed for the identification of a wide range of gangliosides in biological samples. Gangliosides consist of a backbone of sphingoid base and a polar oligosaccharide chain containing at least one sialic acid. Gangliosides are extracted by chloroform–methanol–water mixture, where an upper aqueous layer containing gangliosides and other polar lipid subclasses is further purified by C18 solid-phase extraction. The optimization of chromatographic conditions includes the column selection, mobile-phase composition, pH value, buffer type, and concentration with the goal to achieve the best chromatographic resolution and MS sensitivity. The identification of gangliosides and other polar lipids is based on accurate m/z values of $[M-H]^-$ ions and fragment ions as well measured by high-resolution MS. The detailed interpretation of MS/MS spectra enables the generalization of fragmentation pathways, which is then used for the differentiation of *a*, *b*, and *c* series of gangliosides. The structural assignment is further confirmed by agreement with the predicted retention behavior in HILIC mode on the basis of the correlation among the ganglioside retention, the number of saccharide units, and their sequence. The final HILIC/ESI-MS/MS method is applied for the analysis of porcine brain, human kidney, lungs, plasma, and erythrocytes resulting in unambiguous identification of 145 ganglioside species from 19 subclasses, which represents the highest number of reported gangliosides. Moreover, 71 sulfatides and 59 polar phospholipids (phosphatidylserines, phosphatidylinositols, lysophosphatidylinositols, and phosphatidylglycerols) are detected within a 15 min run.

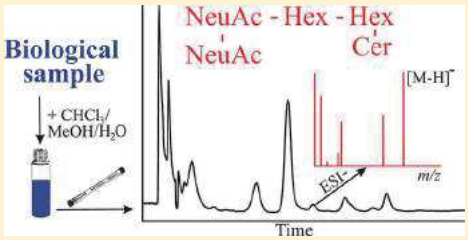

Sphingolipids are one of eight (fatty acyls, glycerolipids, glycerophospholipids, sterol lipids, prenol lipids, saccharolipids, polyketides, and sphingolipids) major lipid categories according to LIPID MAPS classification.[1] This category comprises highly diverse lipid species, where fatty acyls are linked via amide bond to a long chain base or sphingoid. The group of acidic sphingolipids contains gangliosides, which are sphingolipids containing the sphingoid base (ceramide) attached to mono- or polysialylated oligosaccharides. Gangliosides may have a different composition of sphingoid base, N-fatty acyls, and an oligosaccharide part, which results in a large complexity of natural gangliosides. Ceramide moiety can be attached to various sugars: (1) one or more uncharged sugars, such as glucose (Glc) or galactose (Gal), with possible further attachment of other neutral sugars, such as *N*-acetylgalactosamine (GalNAc), *N*-acetylglucosamine (GlcNAc), and fucose (Fuc); (2) ionized functional groups, such as sulfate attached to uncharged sugars or sialic acid residues. Sialic acid is a trivial name used for all derivatives of neuraminic acid,[2] where the most important is *N*-acetylneuraminic acid (NeuAc, SA) and less common is *N*-glycolylneuraminic acid (NeuGc). NeuAc and NeuGc are structurally similar, but they differ significantly in their natural occurrence. NeuAc is present in human unlike NeuGc, which is obtained only from the diet in a limited amount.[2−4] Gangliosides have important biological functions in mammalian cells.[2,5] They are present in almost all human tissues, and they are particularly abundant in neural tissues and extraneural organs, such as the lungs, spleen, and gut as well as in some biological fluids, such as milk.[6−10] Gangliosides are abundant in the central nervous system, and they play important roles in many physiological processes in cells, such as memory control, cell signaling, neuronal recovery, neuronal protection, apoptosis, adhesion, and differentiation.[2,11−15]

Gangliosides are complex lipids, and their analysis is critical for the understanding of their functions in the organism. The sample preparation is a crucial step due to low natural abundances of gangliosides. Typically, modifications of Folch extraction based on chloroform–methanol–water system are used[16] with further purification of upper aqueous phase by solid-phase extraction (SPE) using reversed-phase (RP)[9,17] or anion-exchange[18] modes to remove undesired salts and other contaminants. The extracts of gangliosides can be separated by liquid chromatography (LC)[5,18] using RP[9,18] or HILIC systems[5] and thin-layer chromatography (TLC).[6,19] The identification of gangliosides in biological tissues and fluids is a challenging task, which typically requires the use of tandem mass spectrometry (MS/MS) coupled to chromatographic

Received: August 29, 2017
Accepted: October 23, 2017
Published: October 23, 2017

DOI: 10.1021/acs.analchem.7b03523
Anal. Chem. 2017, 89, 12425−12432

techniques[20,21] or in shotgun configuration without chromatographic separation.[22,23] Negative-ion electrospray ionization (ESI) is the most convenient ionization mode for these acidic sphingolipids.[5,7,8,18,24] The derivatization can improve the sensitivity of gangliosides determination,[25] but it may be difficult to apply laborious derivatization procedure for high-throughput analysis of large series of clinical samples. The combination of mass spectrometry imaging and immunohistochemistry has been applied for multimodal detection of GM2 and GM3 in mice brain.[26] Another application of mass spectrometry imaging for spatial characterization of gangliosides in mice brain is based on the combination of imaging and ion mobility separation.[27]

In this study, the development and systematic optimization of HILIC/ESI-MS/MS method for the analysis of wide range of gangliosides is reported. The main parameters of the chromatographic optimization are the selection of the chromatographic column, the mobile-phase composition including pH value, type and concentration of buffers with the goal to achieve the best chromatographic resolution and also sensitivity with negative-ion ESI-MS detection. The fragmentation behavior of individual ganglioside subclasses in MS/MS mode is studied to elucidate the structure of both oligosaccharide and ceramide parts of ganglioside molecules. The developed method is applied for the analysis of biological samples, such as human kidney, lungs, plasma, erythrocytes, and porcine brain.

EXPERIMENTAL SECTION

Chemicals and Standards. Acetonitrile, methanol (both HPLC/MS grade), chloroform (HPLC grade, stabilized by 0.5−1% ethanol), ammonium formate, ammonium acetate, formic acid, and acetic acid were purchased from Sigma-Aldrich (St. Louis, MO, U.S.A.). Deionized water was prepared with a Milli-Q Reference Water Purification System (Molsheim, France). The standard of total ganglioside extract from porcine brain was purchased from Avanti Polar Lipids (Alabaster, AL, U.S.A.). The porcine brain was obtained from the local farm. Samples of plasma, erythrocytes, and kidney were obtained from the Department of Urology, Palacký University, Faculty of Medicine and Dentistry and University Hospital, Olomouc, Czech Republic. The sample of lungs was obtained from the Regional Hospital of Pardubice, Czech Republic. The study was approved by the hospital Ethical Committee, and patients signed documents giving their informed consent.

Sample Preparation. Two milligrams of total ganglioside extract from porcine brain was dissolved in 1100 μL of chloroform−methanol−water (600:425:75, v/v/v) mixture. Human blood was collected to heparin-lithium tubes and ultracentrifuged to obtain plasma. Samples of human kidney and human lungs were obtained during surgery, immediately frozen, and stored at −80 °C until the sample processing and the analysis. Human kidney, lungs, plasma, erythrocytes, and porcine brain tissue extracts were obtained by chloroform−methanol−water extraction according to Folch method[28] with minor modifications.[16,29,30] Initially, 25 mg of each tissue (human kidney, human lungs, or porcine brain) was cut by scalpel and homogenized in 6 mL of a chloroform−methanol mixture (2:1, v/v) using an ultrasonic bath at 40 °C for 10 min, while human plasma (200 μL) and erythrocytes (200 μL) were homogenized in 3 mL of chloroform−methanol mixture (2:1, v/v) using an ultrasonic bath at 40 °C for 10 min. Then, deionized water (1200 μL for tissues and 600 μL for plasma and erythrocytes) was added, and the mixture was centrifuged at 3000 rpm for 3 min under ambient conditions. The upper aqueous layer containing gangliosides was collected, evaporated by gentle stream of nitrogen to dryness, redissolved in 1 mL of water, and purified by SPE. First, 200 mg of tC18 cartridge (Sep-Pak Vac, 37−55 μm particle size) (Waters, Milford, MA, U.S.A.) was conditioned with 3 × 1 mL of methanol followed by 3 × 1 mL of water. Then, 1 mL of sample dissolved in water was loaded on the column, washed 3 times with 1 mL of water, and finally eluted by 3 × 1 mL of methanol. The eluate was collected, then evaporated by a gentle stream of nitrogen to dryness and redissolved in 500 μL of methanol−water−chloroform (300:150:50, v/v/v) mixture for the HILIC/ESI-MS analysis. The extraction recovery tested for GM3 subclass was 106% for high-level concentration and 103% for low-level concentration.

HILIC/ESI-MS Conditions. All LC experiments were performed on a liquid chromatograph Agilent 1290 Infinity series (Agilent Technologies, Waldbronn, Germany). The final method for the analysis of individual lipid subclasses used the following conditions: Ascentis Si column (150 × 2.1, 3 μm, Sigma-Aldrich), flow rate 0.3 mL/min, injection volume 1 μL, column temperature 40 °C, and mobile-phase gradient as follows—0 min: 87.7% A + 12.3% B; 15 min: 77.9% A + 22.1% B, where phase A was acetonitrile with acetic acid, and phase B was 10 mM aqueous ammonium acetate with pH 6.1 adjusted by acetic acid. The reequilibration time between runs is 15 min. The pH was measured by portable pH meter Checker (Hanna Instruments, Woonsocket, RI, U.S.A.). For all mobile phases used in this work, acetonitrile (phase A) contained the identical amount of formic or acetic acid as used for the pH adjustment of aqueous solution (phase B). The concentration of 10 mM of ammonium formate or ammonium acetate is used for the experimental optimization of the best pH value for the separation of gangliosides. The pH value is adjusted by the addition of formic or acetic acid to aqueous phase and subsequently pH measured by pH meter. The longer gradient was used during the method optimization—0 min: 99.5% A + 0.5% B; 55 min: 75.4% A + 24.6% B and flow rate 0.4 mL/min. Other conditions were identical as for the final method described above.

The following setting of hybrid quadrupole time-of-flight mass spectrometer (micrOTOF-Q, Bruker Daltonics, Bremen, Germany) in ESI mode was used: capillary voltage 2.5 kV, nebulizing gas pressure 1.2 bar, drying gas flow rate 9.3 L/min, and drying gas temperature 210 °C. ESI mass spectra were measured in the range of m/z 50−3000 in the negative-ion mode using the following setting of funnel 1 RF 400 Vpp, funnel 2 RF 400 Vpp, ISCID energy 0 eV, hexapole RF 400 Vpp, quadrupole ion energy 5 eV, low mass 300 m/z, collision cell energy 10 eV, collision RF 600 Vpp, transfer time 80 μs, and prepulse storage 12 μs. MS/MS spectra of up to 4 most abundant ions from the inclusion list were measured after each full MS scan in the data-dependent mode using the scan time of 0.5 s with 0.01 s of interscan time. The total cycle time is 0.51 s. The collision energy ramp was used for the fragmentation starting from m/z 700 as the low mass (collision energy 20 eV) up to m/z 2000 as the high mass (collision energy 70 eV).

The hybrid quadrupole−traveling wave ion mobility−time-of-flight mass spectrometer Synapt G2Si (Waters) in the resolution mode was used for the identification with the following conditions: negative-ion ESI, mass range m/z 50−2000, capillary voltage 2.2 kV, sampling cone 20 V, source offset 90 V, source temperature 150 °C, drying temperature

DOI: 10.1021/acs.analchem.7b03523
Anal. Chem. 2017, 89, 12425−12432

500 °C, cone gas flow 0.8 L/min, drying gas flow 17 L/min, and nebulizer gas flow 4 bar. Leucine enkephaline was used as the lock mass for all experiments. MS/MS experiments were performed on the transfer cell with the collision energy ramp from 20 to 70 eV.

RESULTS AND DISCUSSION

Nomenclature of Gangliosides. The first nomenclature of gangliosides was introduced by Svennerholm[31] and later approved by IUPAC.[32] In the shorthand notation system of gangliosides, the first letter G means ganglioside, the second letter indicates the number of sialic acids (M = mono, D = di, T = tri, and Q = tetra), then the number of neutral sugars is calculated as 5−*n* saccharide units, which may be followed by small letter *a*, *b*, or *c* defining the position of sialic acid(s). This notation may be explained on the example of GM1a (see Figure 1), which is ganglioside (G) containing one sialic acid (M), four neutral sugars (*n* = 4, i.e., 5−4 = 1), and the final small letter *a* describes the position of sialic acid. The abbreviation Ac means additional acetylation, for example, in the case of GD1−Ac. The colon-separated numbers (e.g., 36:1) behind ganglioside abbreviations provides the information on the total number of carbon atoms and double bonds (CN:DB) of N-linked fatty acyl and sphingoid base of ceramide part, and this annotation is based on the common assumption of sphingoid base with two hydroxyl groups and no hydroxylation of *N*-acyl. In the case of the presence of additional hydroxyl on the ceramide part without any specification of its position, the OH in parentheses is space separated and placed behind the ceramide DB number.

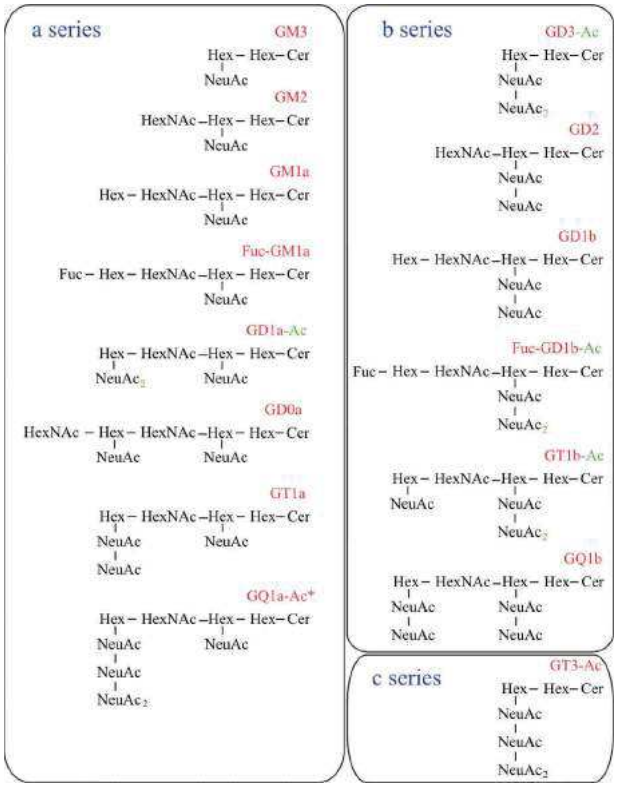

Figure 1. Structures of gangliosides identified in this work. Annotation:[32] the first letter G means ganglioside, the second letter indicates the number of sialic acids (M = mono, D = di, T = tri, and Q = tetra), then the number of neutral saccharide units is calculated as 5−*n*, the series *a* is −Hex(NeuAc)−Hex−Cer, the series *b* is −Hex(NeuAc−NeuAc)−Hex−Cer, and the series *c* is −Hex-(NeuAc−NeuAc−NeuAc)−Hex−Cer. The asterisk (GQ1a−Ac*) means that the structure is not confirmed by MS/MS spectra.

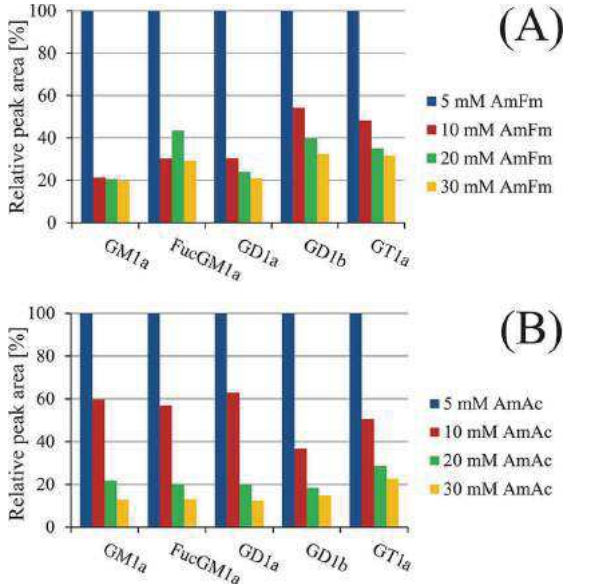

Figure 2. Comparison of relative peak areas vs molar concentrations of (A) ammonium formate (AmFm) and (B) ammonium acetate (AmAc) for major individual gangliosides GM1a 36:1 (RIC of $[M-H]^-$ at m/z 1544.9), Fuc−GM1a 36:1 (RIC of $[M-H]^-$ at m/z 1690.9), GD1a 36:1 (RIC of $[M-H]^{2-}$ at m/z 917.5), GD1b 36:1 (RIC of $[M-H]^{2-}$ at m/z 917.5), and GT1b 38:1 (RIC of $[M-H]^{2-}$ at m/z 1077.0).

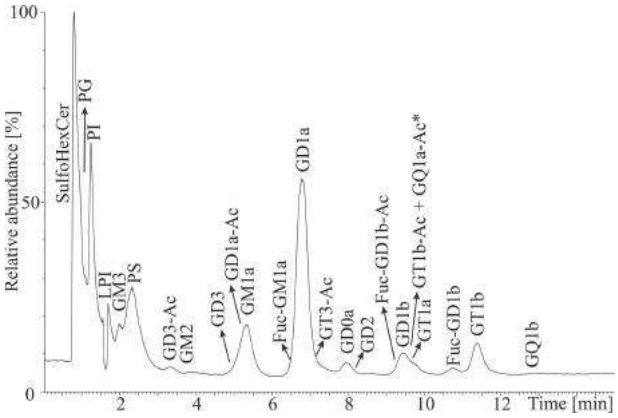

Figure 3. Negative-ion HILIC/ESI-MS total ion current chromatogram of porcine brain extract. Conditions: Ascentis Si column (150 × 2.1, 3 μm, Sigma-Aldrich), flow rate 0.3 mL/min, injection volume 1 μL, column temperature 40 °C, and mobile-phase gradient—0 min: 87.7% A + 12.3% B; 15 min: 77.9% A + 22.1% B, where phase A was acetonitrile with acetic acid, and phase B was 10 mM aqueous ammonium acetate with pH 6.1 adjusted by acetic acid (more details in Experimental Section).

Dissociation Equilibria of Gangliosides. In general, ganglioside molecules may be multiply charged depending on the pH value and the number of sialic acids containing a carboxylic functional group, which may be easily deprotonated to form carboxylate. The first step in the optimization of HILIC conditions is the selection of an optimal pH value, where all

DOI: 10.1021/acs.analchem.7b03523
Anal. Chem. 2017, 89, 12425−12432

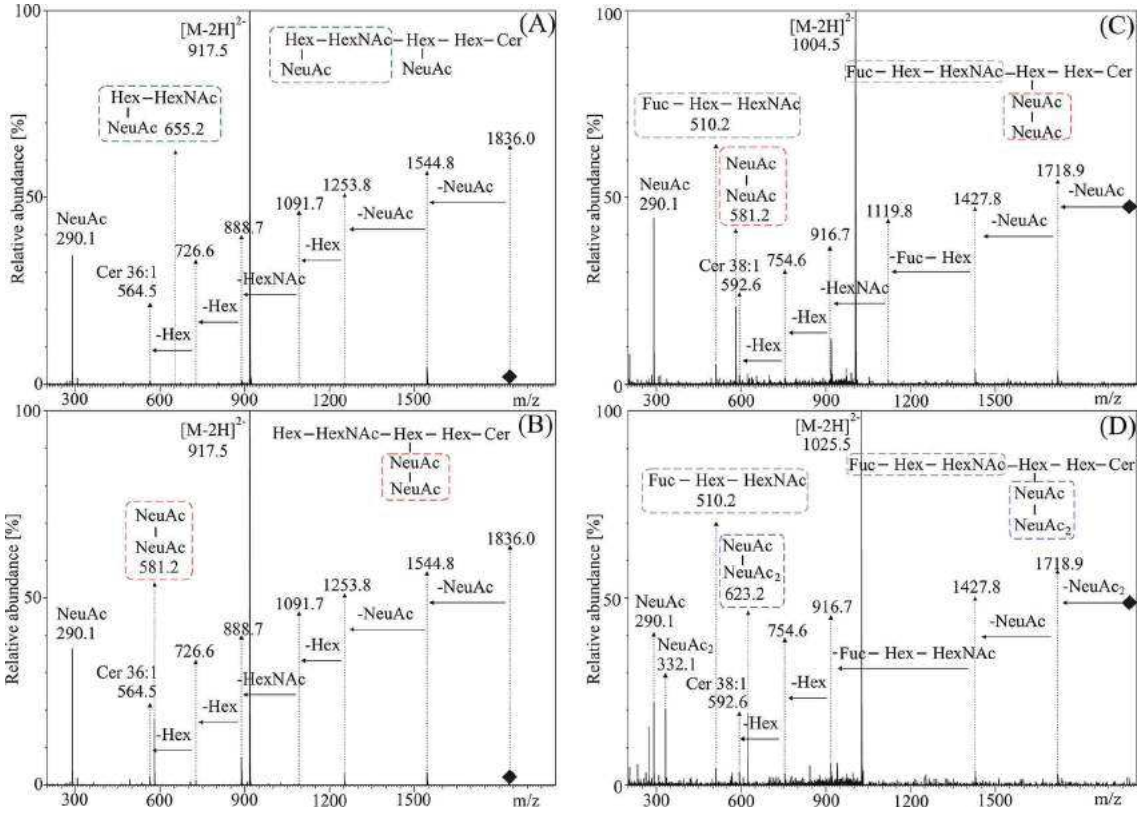

Figure 4. HILIC/ESI-MS/MS fragmentation behavior of (A) $[M-2H]^{2-}$ ion of GD1a 36:1 at m/z 917.5, (B) $[M-2H]^{2-}$ ion of GD1b 36:1 at m/z 917.5, (C) $[M-2H]^{2-}$ ion of Fuc−GD1b 38:1 at m/z 1004.5, and (D) $[M-2H]^{2-}$ ion of Fuc−GD1b−Ac 38:1 at m/z 1025.5.

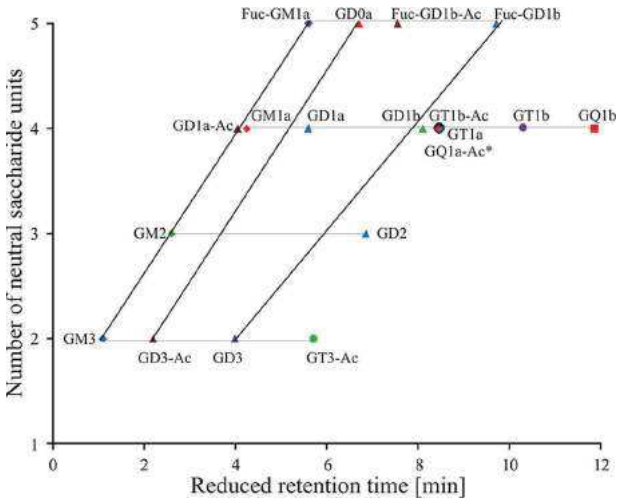

Figure 5. Dependence of reduced retention times in HILIC/ESI-MS on the number of neutral saccharide units. Annotation of gangliosides according to the number of sialic acids: GM, diamond; GD, triangle; GT, circle; and GQ, square. Abbreviations of gangliosides are depicted in Figure 1.

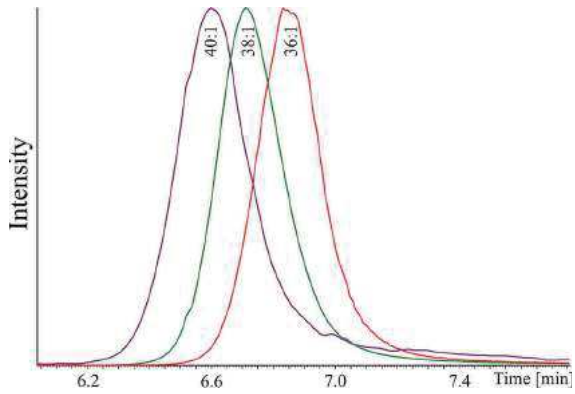

Figure 6. Overlay of RIC chromatograms of individual ganglioside species inside GD1a subclass with the number of carbon atoms and double bonds in fatty acyl chains.

studied gangliosides are present in one ionic form. The equilibrium of more charged forms should be avoided, because it may cause a peak tailing. Figure S-1 shows the calculated dissociation equilibria for GT1, GD1, and GM1. Only one triply charged form of GT1 is present in the pH range from 5 to 10 (Figure S-1A, red line). Negative charges are placed on carboxylates of three sialic groups in GT1. The neutral form is present at pH lower than 3 (Figure S-1A, blue line); however, it coexists with singly charged GT1 (yellow line, maximum at pH 2.4) and doubly charged GT1 (violet line, maximum at pH 3.2). Quadruply charged GT1 (green line) is predicted for pH higher than 10, where the addition charge is placed on the amino group of the *N*-acetylgalactosamine moiety. The similar interpretation can be described for GD1 (Figure S-1B) and GM1 (Figure S-1C), where the same region of pH from 5 to 10 corresponds to the single form for both GD1 (doubly charged, red line, Figure S-1B) and GM1 (singly charged, red line, Figure S-1C). Dissociation curves for *a*, *b*, and *c* series of

DOI: 10.1021/acs.analchem.7b03523
Anal. Chem. 2017, 89, 12425−12432

Table 1. Overview of Lipid Molecular Species Identified for Individual Lipid Subclasses in Porcine Brain, Human Kidney, Lungs, Plasma, and Erythrocyte Extracts Using HILIC/ESI−MS/MS Method

		sample type					
lipid subclass	retention time window [min]	porcine brain	human kidney	human lungs	human plasma	human erythrocytes	total
SulfoHexCer	0.6−1.7	38	25	3	2	4	43
SulfoHex$_2$Cer	0.6−1.7	-	25	-	-	4	25
PG	1.0−1.5	7	4	5	-	-	9
PI	1.0−1.5	10	20	13	8	9	20
LPI	1.7−2.4	8	8	4	5	-	10
PS	2.0−2.9	17	7	8	-	10	20
GM3	1.9−2.5	2	16	15	15	4	22
GD3-Ac	2.8−3.8	13	-	2	-	-	14
GM2	3.3−4.1	3	3	2	-	-	6
GD3	4.5−5.7	9	9	13	-	-	17
GD1a-Ac	4.8−5.5	3	-	-	-	-	3
GM1a	4.9−5.8	10	-	-	-	5	11
Fuc-GM1a	6.2−7.2	7	-	-	-	-	7
GD1a	6.3−7.1	7	4	2	-	-	10
GT3-Ac	6.3−7.3	6	-	-	-	-	6
GD0a	7.3−8.3	7	-	-	-	-	7
GD2	7.5−8.4	2	-	-	-	-	2
Fuc-GD1b-Ac	8.3−9.0	3	-	-	-	-	3
GD1b	8.8−9.6	8	-	-	-	-	8
GT1b-Ac	9.2−9.9	4	-	-	-	-	4
GQ1-Ac	9.2−9.9	2	-	-	-	-	2
GT1a	9.3−9.9	4	-	-	-	-	4
Fuc-GD1b	10.3−11.3	5	-	-	-	-	5
GT1b	10.8−12.0	12	-	-	-	-	12
GQ1b	12.4−13.5	2	-	-	-	-	2
total		189	122	67	30	36	272

ganglioside isomers are identical. The conclusion is that the optimal pH value should be in the range from 5 to 10.

Optimization of Buffer Composition. Based on the previous development of HILIC/ESI-MS method for acidic phospholipids,[33] Ascentis Si column has been tested for the separation of gangliosides. This column provides high efficiency for this type of acidic sphingolipids as well; therefore, it is further used in this work. The previous section describes the suggestion of optimal pH range based on theoretical calculations of dissociation equilibria, but it is essential to verify experimentally the best conditions for real separations. Moreover, the optimization of buffer type and concentration may have a critical importance, as known from our previous studies of acidic lipids.[33] The major ganglioside subclasses GM1a, Fuc−GM1a, GD1a, GD1b, and GT1b from the total ganglioside extract of porcine brain are used during the method development. Ammonium formate and acetate have been selected as volatile organic salts suitable for LC/MS operation in the concentration range from 0 to 30 mM (Figures 2, S-2, and Table S-1). The highest signal for ammonium formate or acetate is observed at 5 mM (Figure 2), but the best compromise between the sensitivity and peak shape is 10 mM. Mobile phases without any additives cannot be used for the separation due to the unacceptable peak tailing and no chromatographic resolution of isomeric GD1a and GD1b (Table S-1).

The pH range from 3.0 to 5.8 is tested for 10 mM of ammonium formate using the addition of formic acid (Figure S-3A and Table S-2) and from 3.0 to 6.5 for 10 mM of ammonium acetate using the addition of acetic acid (Figure S-3B and Table S-2). The direct comparison of optimum conditions for both tested buffers in Figure S-3C shows that the best results are obtained for ammonium acetate at pH 6.1. The peak width and tailing factors are illustrated in Figure S-4, Tables S-3 and S-4, where the worst results are obtained for most acidic mobile phases (pH 3) without any resolution of GD1a and GD1b. Measurements for all other pH values provide comparable results. Therefore, the best compromise among the sensitivity, tailing factors, and the chromatographic resolution is 10 mM of ammonium acetate, because it also provides a partial separation of Fuc−GM1a and GD1a unlike to 5 mM of ammonium acetate, but at cost of reduced sensitivity and longer analysis time, as shown in Figure S-5 with reconstructed ion current (RIC) chromatograms of GM1a, Fuc−GM1a, GD1a, GD1b, and GT1b.

Interpretation of MS/MS Spectra of Gangliosides. The application of the final method for the analysis of porcine brain extract is shown in Figure 3, where 19 ganglioside subclasses and 5 other polar lipid subclasses are detected. The full scan negative-ion ESI mass spectra are obtained for all peaks corresponding to individual subclasses of gangliosides, and the elemental composition is determined on the basis of accurate m/z measurements with the average mass accuracy of 3.1 ppm. Then, MS/MS spectra of $[M-H]^-$, $[M-2H]^{2-}$, or $[M-3H]^{3-}$ ions are recorded and interpreted. The charge state of precursor ion depends mainly on the number of sialic acids present in particular ganglioside. The fragmentation behavior of gangliosides (Figures 4 and S-6 to S-14) provides an excellent tool for sequencing of oligosaccharide part. The fragmentation is predictable and therefore provides unambiguous information on the sequence including the type of branching, i.e., the differentiation of *a*, *b*, and *c* series (see Figure 1).[5] All observed

DOI: 10.1021/acs.analchem.7b03523
Anal. Chem. 2017, 89, 12425−12432

fragment ions are singly charged with the only exception of m/z 931.5, which corresponds to $[M-2H-NeuAc_2]^{2-}$ ion in Figure S-12 or $[M-2H-NeuAc]^{2-}$ ion in Figures S-13 and S-14. The fragmentation of the most common gangliosides GM3, GM2, GM1a, and Fuc−GM1a has been well described in previous works.[18,34,35] The trace amount of GQ1a−Ac* does not allow the measurement of MS/MS spectra (labeled by asterisk), but the series *a* may be proposed on the basis of the characteristic retention behavior (Figure 5). The interpretation of MS/MS spectra of all other gangliosides subclasses (see structures in Figure 1) is described in the following figures: GD1a (Figure 4A), GD1b (Figure 4B), Fuc−GD1b (Figure 4C), Fuc−GD1b−Ac (Figure 4D), GD1a−Ac (Figure S-10), GD0a (Figure S-11), GT1b−Ac (Figure S-12), GQ1b (Figure S-13), GT1a (Figure S-14A), and GT1b (Figure S-14B). The symbol of black diamond highlights the precursor ions in MS/MS spectra.

Table S-5 lists characteristic neutral losses (NL) of individual saccharides units, and Table S-6 shows characteristic fragment ions related to the saccharide part of ganglioside molecules. There are several features in the fragmentation, which can be generally applied during the interpretation of unknown gangliosides. The fragmentation typically starts with the cleavage of sialic acids (NL of NeuAc, $\Delta m/z$ 291) until all sialic acids are lost. The Supporting Information is the presence of NeuAc fragment ion at m/z 290. The additional acetylation on the sialic acid ($NeuAc_2$) corresponds to the NL of $\Delta m/z$ 333 and the fragment ion $NeuAc_2$ at m/z 332. The position of $NeuAc_2$ can be determined according to the order of individual NL, as shown for example in Figure 4D. The presence of two or more neighboring sialic acids is identified on the basis of abundant characteristic fragment ions, such as NeuAc−NeuAc (m/z 581, Figure 4B,C), NeuAc−$NeuAc_2$ (m/z 623, Figure 4D), and NeuAc−NeuAc−$NeuAc_2$ (m/z 914, Figure S-9). The relative abundance of $[M-2H-2NeuAc]^-$ ion at m/z 1253.8 is higher in case of *b* series (Figure 4B), because it requires the cleavage of only one bond unlike to *a* series (Figure 4A), where two bonds have to be cleaved to obtain this fragment ion. The unambiguous proof of *b* series is the presence of abundant ion of NeuAc−NeuAc at m/z 581 in Figure 4B. This way the sequence of all sialic acids can be unambiguously assigned, which determines the series *a*, *b*, and *c* (see Figure 1). The further proof is the characteristic chromatographic behavior described in the next chapter. The presence of terminal fucose is recognized by the characteristic NL of $\Delta m/z$ 146 and also the fragment ion Fuc−Hex−HexNAc at m/z 510 (Figure 4C,D). The total fatty acyl composition in the ceramide part is indicated by characteristic fragment ions, such as m/z 564 for 36:1, m/z 592 for 38:1, and so on.

The identification of polar phospholipids and sulfatides follows well-known rules described in our previous works.[30,36−38] In case of sulfatides, frequent mass interferences occur for sulfatide species with the additional hydroxyl group (e.g., SulfoHexCer 38:2 (OH) at m/z 848.5563) vs sulfatides with the additional methylene group and one double bond less (e.g., SulfoHexCer 39:1 at m/z 848.5927). These species cannot be resolved by the resolving of our QTOF, which causes lower mass accuracy for these doublets, but the identification of all reported species is still clearly confirmed by the their fragmentation and retention behavior.

Retention Behavior of Gangliosides in HILIC Mode. The retention behavior of lipids follow the regular patterns related to the type of polar headgroup, the number of carbon atoms in fatty acyl chains and also the number of double bonds, as illustrated in numerous previous works.[21,29,30,33,39,40] Regularities in lipid retention behavior can be used for the prediction of retention times and then applied as an additional Supporting Information for the lipid identification. This approach is applicable both in reversed-phase[21,29,39] and HILIC[16,30,33,40] modes and recently in ultrahigh-performance supercritical fluid chromatography as well,[36] and therefore, the similar approach is tested for gangliosides with higher structural complexity caused by the presence of oligosaccharide part. Figure 5 shows the dependence of reduced retention times of gangliosides on the number of saccharide units with fitting of some observed logical series in this graph, for example, the series of GM3, GM2, GM1a, and Fuc−GM1a (see structures in Figure 1) shows an excellent fit. Higher number of saccharide units results in higher retention with the increment of approximately 1.5−3 min, but it depends on the type of saccharide units. This increase is about 1.5 min for the fucosylation, but the difference between GD3 and GD2 is up to 3 min. The same behavior is observed for sialic acids, where higher number of sialic acids strongly increases the retention by about 3.5−4 min. The retention of *a* series is 2−3 min lower in comparison to *b* series, which enables the assignment of *a* series in case of GQ1a−Ac*, which is the only ganglioside subclass without MS/MS due to very low concentration. The additional acetylation on the sialic acid ($NeuAc_2$) corresponds to the lower retention by slightly less than 2 min.

In HILIC mode, the partial separation inside peaks of individual ganglioside subclasses can be detected using the overlay of RIC chromatograms similarly as for other lipid subclasses investigated earlier.[16,30,36] The retention slightly decreases with increasing length of fatty acyls (Figures 6), which is the additional information for the structure confirmation.

LC/MS Analysis of Biological Samples. The final method is applied for measurements of human kidney, lungs, plasma, erythrocytes, and porcine brain extracts. The full list of all identified gangliosides and other polar lipid subclasses (phosphatidylserines (PS), phosphatidylinositols (PI), lyso-phosphatidylinositols (LPI), phosphatidylglycerols (PG), and sulfatides (SulfoHexCer)) is shown in Table S-7 with their relative intensities determined from RIC of individual species within particular subclasses together with mass accuracies. Only gangliosides that are identified with high confidence are reported here considering the following criteria: (1) accurate m/z values to determine the elemental composition (99% of measurements <10 ppm, 87% of measurements <5 ppm, and the average mass accuracy 3.1 ppm), (2) the interpretation of fragmentation behavior to sequence the oligosaccharide part of the molecule based on accurate m/z values, and (3) retention times in accordance with the predicted retention behavior shown in Figure 5. The previously reported information on the fragmentation behavior of gangliosides[5,18] is in agreement with our observations as well. The overview in Table 1 and the full list in Table S-7 clearly show that the brain tissue contains by far more gangliosides than other studied biological samples. Only GM3 is detected for all studied sample types with only few additional gangliosides in case of kidney (3 GD3−Ac, 3 GM2, 9 GD3, and 4 GD1a), lungs (2 GM2, 10 GD3, and 2 GD1a), and erythrocytes (4 GM1a).

DOI: 10.1021/acs.analchem.7b03523
Anal. Chem. 2017, 89, 12425−12432

CONCLUSIONS

Our new HILIC/ESI-MS/MS approach enables unambiguous identification of the highest number of gangliosides ever reported for studied biological samples. HILIC separation has been well-optimized, which results in the characterization of 145 ganglioside molecular species from 19 subclasses with additional identification of other 6 polar lipid subclasses (SulfoHexCer, SulfoHex$_2$Cer, PG, PI, LPI, and PS), which are known to be difficult for established MS-based lipidomic platforms. The identification of gangliosides and other lipids is based on high-resolution MS measurements providing high mass accuracy for both precursor and product ions, the agreement of fragmentation behavior in MS/MS with structure assignment, the correlation with the predicted retention behavior of ganglioside subclasses and also ganglioside species inside the individual subclass. The combination of this complementary information provides highly confident identification. The next step is the change of this qualitative method into the quantitative workflow using suitable internal standards and the method validation with application to real clinical samples. The present HILIC/ESI-MS is already optimized in terms of future planned quantitative high-throughput analysis, because the analysis time is fast, can be easily automated, and the lipid subclass separation is the best available approach for the lipidomic quantitation.

ASSOCIATED CONTENT

Supporting Information

The Supporting Information is available free of charge on the ACS Publications website at DOI: 10.1021/acs.analchem.7b03523.

Dissociation equilibria, comparison of peak widths, tailing factors, and relative peak areas at different mobile-phase composition, effect of ammonium acetate concentration on the separation, fragmentation behavior, characteristic neutral losses and fragment ions for individual ganglioside subclasses, list of lipids identified in porcine brain, human kidney, lungs, plasma, and erythrocytes (PDF)

AUTHOR INFORMATION

Corresponding Author

*Tel.: +420-466037087; Fax: +420-466037068; E-mail: Michal.Holcapek@upce.cz.

ORCID

Michal Holčapek: 0000-0003-3978-1249

Notes

The authors declare no competing financial interest.

ACKNOWLEDGMENTS

This work was supported by the ERC CZ grant project LL1302 sponsored by the Ministry of Education, Youth and Sports of the Czech Republic. Authors would like to thank Bohuslav Melichar and David Vrána (Palacky University, Medical School and Teaching Hospital, Department of Oncology, Olomouc, Czech Republic) for providing biological samples.

REFERENCES

(1) Fahy, E.; Subramaniam, S.; Brown, H. A.; Glass, C. K.; Merrill, A. H.; Murphy, R. C.; Raetz, C. R.; Russell, D. W.; Seyama, Y.; Shaw, W.; et al. *J. Lipid Res.* **2005**, *46*, 839−862.

(2) Aureli, M.; Mauri, L.; Ciampa, M. G.; Prinetti, A.; Toffano, G.; Secchieri, C.; Sonnino, S. *Mol. Neurobiol.* **2016**, *53*, 1824−1842.

(3) Schauer, R. *Zoology* **2004**, *107*, 49−64.

(4) Malykh, Y. N.; Schauer, R.; Shaw, L. *Biochimie* **2001**, *83*, 623−634.

(5) Ikeda, K.; Taguchi, R. *Rapid Commun. Mass Spectrom.* **2010**, *24*, 2957−2965.

(6) Lacomba, R.; Salcedo, J.; Alegría, A.; Lagarda, M. J.; Barberá, R.; Matencio, E. *J. Pharm. Biomed. Anal.* **2010**, *51*, 346−357.

(7) Giuffrida, F.; Elmelegy, I. M.; Thakkar, S. K.; Marmet, C.; Destaillats, F. *Lipids* **2014**, *49*, 997−1004.

(8) Ma, L.; MacGibbon, A. K.; Mohamed, H. J. B. J.; Loy, S.; Rowan, A.; McJarrow, P.; Fong, B. Y. *Int. Dairy J.* **2015**, *49*, 62−71.

(9) Fuller, M.; Duplock, S.; Hein, L. K.; Rigat, B. A.; Mahuran, D. J. *Anal. Biochem.* **2014**, *458*, 20−26.

(10) Valdes-Gonzalez, T.; Goto-Inoue, N.; Hirano, W.; Ishiyama, H.; Hayasaka, T.; Setou, M.; Taki, T. *J. Neurochem.* **2011**, *116*, 678−683.

(11) Sonnino, S.; Mauri, L.; Ciampa, M. G.; Prinetti, A. *J. Neurochem.* **2013**, *124*, 432−435.

(12) Sonnino, S.; Mauri, L.; Chigorno, V.; Prinetti, A. *Glycobiology* **2007**, *17*, 1R−13R.

(13) Lopez, P. H.; Schnaar, R. L. *Curr. Opin. Struct. Biol.* **2009**, *19*, 549−557.

(14) Hakomori, S.-I. *J. Biol. Chem.* **1990**, *265*, 18713−18716.

(15) Hakomori, S.-I.; Handa, K. *Glycoconjugate J.* **2015**, *32*, 1−8.

(16) Cífková, E.; Holčapek, M.; Lísa, M.; Ovčačíková, M.; Lyčka, A.; Lynen, F.; Sandra, P. *Anal. Chem.* **2012**, *84*, 10064−10070.

(17) Garcia, A. D.; Chavez, J. L.; Mechref, Y. *J. Chromatogr. B: Anal. Technol. Biomed. Life Sci.* **2014**, *947-948*, 1−7.

(18) Ikeda, K.; Shimizu, T.; Taguchi, R. *J. Lipid Res.* **2008**, *49*, 2678−2689.

(19) Prinetti, A.; Rocchetta, F.; Costantino, E.; Frattini, A.; Caldana, E.; Rucci, F.; Bettiga, A.; Poliani, P. L.; Chigorno, V.; Sonnino, S. *Glycoconjugate J.* **2009**, *26*, 623−633.

(20) Tsui, Z.-C.; Chen, Q.-R.; Thomas, M. J.; Samuel, M.; Cui, Z. *Anal. Biochem.* **2005**, *341*, 251−258.

(21) Hu, T.; Jia, Z.; Zhang, J. *Anal. Chem.* **2017**, *89*, 7808−7816.

(22) Sarbu, M.; Robu, A. C.; Ghiulai, R. M.; Vukelić, Z.; Clemmer, D. E.; Zamfir, A. D. *Anal. Chem.* **2016**, *88*, 5166−5178.

(23) Sarbu, M.; Robu, A. C.; Ghiulai, R. M.; Vukelić, Z.; Clemmer, D. E.; Zamfir, A. D. *Anal. Chem.* **2016**, *88*, 5166−5178.

(24) Fong, B.; Norris, C.; Lowe, E.; McJarrow, P. *Lipids* **2009**, *44*, 867−874.

(25) Huang, Q.; Liu, D.; Xin, B.; Cechner, K.; Zhou, X.; Wang, H.; Zhou, A. *Anal. Chim. Acta* **2016**, *929*, 31−38.

(26) Dufresne, M.; Guneysu, D.; Patterson, N. H.; Marcinkiewicz, M. M.; Regina, A.; Demeule, M.; Chaurand, P. *Anal. Bioanal. Chem.* **2017**, *409*, 1425−1433.

(27) Škrášková, K.; Claude, E.; Jones, E. A.; Towers, M.; Ellis, S. R.; Heeren, R. M. *Methods* **2016**, *104*, 69−78.

(28) Folch, J.; Lees, M.; Sloane-Stanley, G. *J. Biol. Chem.* **1957**, *226*, 497−509.

(29) Ovčačíková, M.; Lísa, M.; Cífková, E.; Holčapek, M. *J. Chromatogr. A* **2016**, *1450*, 76−85.

(30) Cífková, E.; Holčapek, M.; Lísa, M. *Lipids* **2013**, *48*, 915−928.

(31) Svennerholm, L. *J. Neurochem.* **1963**, *10*, 613−623.

(32) Chester, M. *Eur. J. Biochem.* **1998**, *257*, 293.

(33) Cífková, E.; Hájek, R.; Lísa, M.; Holčapek, M. *J. Chromatogr. A* **2016**, *1439*, 65−73.

(34) Fong, B. Y.; Ma, L.; Khor, G. L.; van der Does, Y.; Rowan, A.; McJarrow, P.; MacGibbon, A. K. *J. Agric. Food Chem.* **2016**, *64*, 6295−6305.

(35) Domon, B.; Costello, C. E. *Glycoconjugate J.* **1988**, *5*, 397−409.

(36) Lísa, M.; Holčapek, M. *Anal. Chem.* **2015**, *87*, 7187−7195.

(37) Lísa, M.; Cífková, E.; Holčapek, M. *J. Chromatogr. A* **2011**, *1218*, 5146−5156.

(38) Jirásko, R.; Holčapek, M.; Khalikova, M.; Vrána, D.; Študent, V.; Prouzová, Z.; Melichar, B. *J. Am. Soc. Mass Spectrom.* **2017**, *28*, 1562−1574.

DOI: 10.1021/acs.analchem.7b03523
Anal. Chem. 2017, 89, 12425−12432

(39) Fauland, A.; Köfeler, H.; Trötzmüller, M.; Knopf, A.; Hartler, J.; Eberl, A.; Chitraju, C.; Lankmayr, E.; Spener, F. *J. Lipid Res.* **2011**, *52*, 2314−2322.
(40) Cífková, E.; Holčapek, M.; Lísa, M.; Vrána, D.; Gatěk, J.; Melichar, B. *Anal. Bioanal. Chem.* **2015**, *407*, 991−1002.

DOI: 10.1021/acs.analchem.7b03523
Anal. Chem. 2017, 89, 12425−12432

analytical chemistry

Article

pubs.acs.org/ac

Nontargeted Quantitation of Lipid Classes Using Hydrophilic Interaction Liquid Chromatography–Electrospray Ionization Mass Spectrometry with Single Internal Standard and Response Factor Approach

Eva Cífková,[†] Michal Holčapek,*[,†] Miroslav Lísa,[†] Magdaléna Ovčačíková,[†] Antonín Lyčka,[‡,§] Frédéric Lynen,[⊥] and Pat Sandra[#]

[†]Department of Analytical Chemistry, Faculty of Chemical Technology, University of Pardubice, Studentská 573, 532 10 Pardubice, Czech Republic

[‡]Research Institute for Organic Syntheses, Rybitví 296, 533 54 Pardubice-Rybitví, Czech Republic

[§]Faculty of Science, University of Hradec Králové, Rokitanského 62, 500 03 Hradec Králové 3, Czech Republic

[⊥]Department of Organic Chemistry, Ghent University, Krijgslaan 281 S4-bis, B-9000 Ghent, Belgium

[#]Research Institute for Chromatography, President Kennedypark 26, B-8500 Kortrijk, Belgium

Supporting Information

ABSTRACT: The identification and quantitation of a wide range of lipids in complex biological samples is an essential requirement for the lipidomic studies. High-performance liquid chromatography–mass spectrometry (HPLC/MS) has the highest potential to obtain detailed information on the whole lipidome, but the reliable quantitation of multiple lipid classes is still a challenging task. In this work, we describe a new method for the nontargeted quantitation of polar lipid classes separated by hydrophilic interaction liquid chromatography (HILIC) followed by positive-ion electrospray ionization mass spectrometry (ESI-MS) using a single internal lipid standard to which all class specific response factors (RFs) are related to. The developed method enables the nontargeted quantitation of lipid classes and molecules inside these classes in contrast to the conventional targeted quantitation, which is based on predefined selected reaction monitoring (SRM) transitions for selected lipids only. In the nontargeted quantitation method described here, concentrations of lipid classes are obtained by the peak integration in HILIC chromatograms multiplied by their RFs related to the single internal standard (i.e., sphingosyl PE, d17:1/12:0) used as common reference for all polar lipid classes. The accuracy, reproducibility and robustness of the method have been checked by various means: (1) the comparison with conventional lipidomic quantitation using SRM scans on a triple quadrupole (QqQ) mass analyzer, (2) ^{31}P nuclear magnetic resonance (NMR) quantitation of the total lipid extract, (3) method robustness test using subsequent measurements by three different persons, (4) method transfer to different HPLC/MS systems using different chromatographic conditions, and (5) comparison with previously published results for identical samples, especially human reference plasma from the National Institute of Standards and Technology (NIST human plasma). Results on human plasma, egg yolk and porcine liver extracts are presented and discussed.

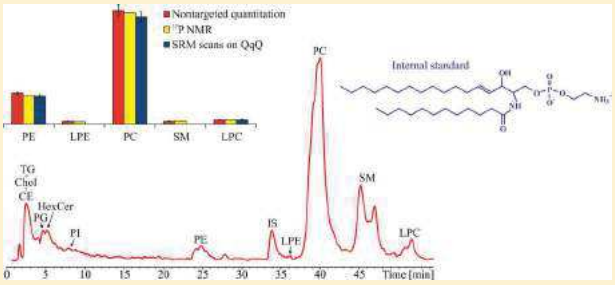

Lipids are hydrophobic or amphipathic small molecules that originate entirely or in part by carbanion-based condensations of thioesters (fatty acids, glycerolipids, glycerophospholipids, sphingolipids) or carbocation-based condensations of isoprene units (prenols and sterols).[1] Lipids are divided according to the structural and biosynthetic complexity into fatty acids, glycerolipids, glycerophospholipids, sphingolipids, sterol lipids, prenol lipids, saccharolipids, and polyketides categories.[1] Another division is based on the number of hydrolysis products into simple (nonpolar) and complex (polar) lipids.[2] The identification and quantitation of all lipids in complex biological samples can lead to the understanding how lipids function in a biological system and to the elucidation of mechanisms of lipid-related diseases including obesity, atherosclerosis, cancer, cardiovascular diseases, etc. The disruption of lipid metabolism may be associated with these diseases as well as the occurrence of modified lipids generated by free radicals oxidation.[2]

HPLC/MS is the most powerful analytical tool for nontargeted characterization of the lipidome in biological

Received: September 3, 2012
Accepted: October 17, 2012
Published: October 17, 2012

samples. HILIC and reversed-phase (RP) systems are typically used in the separation of lipids. Individual lipid classes can be separated according to their polarity using silica[3−6] or diol columns[7−10] in the HILIC mode or according to their hydrophobicity (the length of fatty acyl chains and the number of double bonds) using C_{18} columns[11−13] in the RP mode. Nonaqueous reversed-phase (NARP)[14−16] HPLC can be used in the separation of nonpolar lipids (triacylglycerols, diacylglycerols, monoacylglycerols, and fatty acids). Gas chromatography (GC) with flame ionization detection is typically applied for fatty acid profiling after transesterification into fatty acid methyl esters,[17] but it does not provide any information on intact polar lipids unlike HPLC/MS.

The most popular MS ionization techniques for the lipid analysis are electrospray ionization (ESI)[3,4,7,9,11−13,18,19] and matrix-assisted laser desorption/ionization (MALDI)[20−26] for the identification of polar lipids, while atmospheric pressure chemical ionization (APCI)[27,28] or atmospheric pressure photoionization (APPI)[27,29] are preferred for nonpolar lipids. MALDI has been coupled to the thin-layer chromatography (TLC)[23] for the analysis of phospholipids from egg yolk and for biological samples as well.[30]

The conventional method for quantitative analysis of lipids by MS is based on SRM scans on QqQ mass spectrometers.[3,13,19,31−35] This targeted quantitation can be used in the determination of lipids with known fragmentation behavior, because the previous knowledge of precursor ions and their specific product ions are required for SRM transitions. Advantages of the SRM approach are high sensitivity and selectivity, especially when combined with the analyte specific retention times in HPLC. On the other hand, the limitation of SRM quantitation is that this determination is, in principle, targeted and therefore limited to lipid molecules with predefined transitions, which may lead to the loss of information on unexpected lipids. The promising untargeted lipidomic quantitation has been introduced recently using the combination of ultrahigh resolving power (>100 000) and subppm mass accuracy of Fourier transform (orbitrap and ion-cyclotron resonance) instruments, which enables the identification and quantification of lipid species directly using nontargeted MS/MS data.[36−39] This strategy requires the most expensive Fourier transform mass spectrometers, which are not available to all lipid researchers. ^{31}P NMR is an alternative method for the absolute quantitation of the lipid classes containing phosphorus, because individual lipid species inside lipid classes have almost identical chemical shifts and NMR does not require any RFs for the quantitation.[23,40,41] Drawbacks of this approach are the lack of structural information unlike MS and very low sensitivity (high concentrations and several hours for the signal accumulation are required).

The goal of our work has been the development of a novel nontargeted broad spectrum lipidomic quantitation technique using HILIC-HPLC/ESI-MS applied to the determination of all separated lipid classes. Such a method should provide comprehensive information on the lipidome of biological samples without the loss of lipids and the need of defined SRM transitions and without the need of expensive internal standards (ISs) for each lipid class. Nontargeted quantitation is based on the peak integration of individual lipid classes in the HILIC mode multiplied by their RFs and correlated by only single IS (sphingosyl PE, d17:1/12:0) for all lipid classes. A similar quantitation approach based on the use of the RFs was successfully developed for the NARP-HPLC/APCI-MS analysis of triacylglycerols (TGs) and applied in several lipidomic studies focused on TGs.[15,17,42,43] In this work, this strategy is extended to the quantitation of several lipid classes with different polarities in one HPLC/MS run.

EXPERIMENTAL SECTION

Chemicals and Standards. Acetonitrile, 2-propanol, methanol (all HPLC gradient grade), chloroform (HPLC grade, stabilized by 0.5−1% ethanol), methyl-*tert*-butyl ether (MTBE), and ammonium acetate were purchased from Sigma-Aldrich (St. Louis, MO). 1,2-Dioleoyl-*sn*-glycero-3-phosphoglycerol (18:1/18:1-PG), 1-oleoyl-2-hydroxy-*sn*-glycero-3-phosphoglycerol (18:1-LPG), 1,2-dioleoyl-*sn*-glycero-3-phosphoethanolamine (18:1/18:1-PE), 1-oleoyl-2-hydroxy-*sn*-glycero-3-phosphoethanolamine (18:1-LPE), 1,2-dioleoyl-*sn*-glycero-3-phosphocholine (18:1/18:1-PC), 1-oleoyl-*sn*-sphing-4-enine-1-phosphocholine (18:1-SM), and 1-oleoyl-2-hydroxy-*sn*-glycero-3-phosphocholine (18:1-LPC) for the determination of RFs, 1,2-diheptadecanoyl-*sn*-glycero-3-phosphocholine (17:0/17:0-PC), 1,2-diheptadecanoyl-*sn*-glycero-3-phosphoethanolamine (17:0/17:0-PE), and 1-heptadecanoyl-2-hydroxy-*sn*-glycero-3-phosphocholine (17:0-LPC) as ISs for the conventional quantitation using SRM transitions, and N-dodecanoyl-heptadecasphing-4-enine-1-phosphoethanolamine (sphingosyl PE, d17:1/12:0) as the IS for nontargeted quantitation with RFs were purchased from Avanti Polar Lipids (Alabaster, AL). The human plasma standard reference material (NIST plasma) from the National Institute of Standards and Technology (Gaithersburg, MD) was prepared from plasma samples of 100 individuals between 40 and 50 years of age including an equal number of men and women and with a racial distribution that reflects the United States population. Egg and porcine liver samples were purchased at local stores.

Sample Preparation. Total lipid extracts from egg yolk, NIST human plasma, and porcine liver were prepared according to a modified Folch procedure[44] using a chloroform/methanol/water system. Briefly, approximately 0.5 g of lipid tissue and 50 μL of 3.3 mg/mL sphingosyl PE were homogenized with 10 mL of a mixture of chloroform/methanol (2:1, v/v), and the homogenate was filtered using a coarse filter paper. Then, 2 mL of 1 mol/L NaCl was added, and the mixture was centrifuged at 3000 rpm for 5 min at room temperature. The chloroform (bottom) layer containing the lipids was evaporated by a gentle stream of nitrogen and redissolved in a chloroform−2-propanol mixture (1:1, v/v) for the HILIC analysis. The modified Bligh and Dyer method[45] was performed in the same way as the Folch method, except that the mixture of chloroform−methanol was in the ratio 1:2 (v/v). For MTBE extraction,[46] approximately 0.5 g of lipid tissue and 50 μL of 3.3 mg/mL sphingosyl PE were homogenized with 15 mL mixture of MTBE/methanol (4:1, v/v). Then, 3 mL of water was added, and the organic (upper) layer containing the lipids was collected. The aqueous (bottom) layer was extracted again using the mixture MTBE/methanol/water (10:3:2.5, v/v/v). The organic (upper) layer was collected and combined with the organic extract from the previous step, evaporated by a gentle stream of nitrogen, and redissolved in chloroform−2-propanol mixture (1:1, v/v) for the HILIC analysis. Bligh and Dyer and MTBE extraction methods were used only for the comparison of extraction recoveries, but in all other measurements only the Folch extraction was used.

dx.doi.org/10.1021/ac3024476 | Anal. Chem. 2012, 84, 10064−10070

HILIC-HPLC/ESI-MS Conditions. Nontargeted quantitation with RFs was performed on a liquid chromatograph Agilent 1200 series (Agilent Technologies, Waldbronn, Germany) coupled to ESI-MS detection on the Esquire 3000 ion trap analyzer (Bruker Daltonics, Bremen, Germany). RFs of individual lipid classes and peak areas were determined using the total ion current chromatograms in the positive-ion ESI-MS mode in the mass range m/z 50−1000 with the following setting of tuning parameters: pressure of the nebulizing gas 60 psi, drying gas flow rate 10 L/min, and temperature of the drying gas 365 °C. Conditions used for measurements in the negative-ion mode were identical except for the polarity. The data were acquired and evaluated using the Data Analysis software (Bruker Daltonics). Total lipid extracts were fractionated into lipid classes using a Spherisorb Si column (250 × 4.6 mm, 5 μm, Waters, Milford, MA), a flow rate of 1 mL/min, an injection volume of 10 μL, column temperature of 40 °C, and a mobile phase gradient: 0 min, 94% A + 6% B; 60 min, 77% A + 23% B, where A was acetonitrile and B is 5 mM aqueous ammonium acetate. The injector needle was washed with the mobile phase before each injection.

Conventional quantitation using SRM transitions was performed on a liquid chromatograph Alliance 2690 (Waters) coupled to the Micromass Quattro Micro QqQ mass spectrometer (Waters). The following parameters of the ESI-MS source were set up for the positive-ion mode: mass range m/z 50−1000, capillary voltage 3.3 kV, extractor voltage 3 V, RF lens voltage 0.1 V, temperature of ESI source 100 °C, temperature of drying gas 300 °C, nebulization gas flow rate 500 L/h, collision energy 25 V for PE and 30 V for PC and LPC, the cone voltage 30 V for PE and 40 V for PC and LPC. SRM scans for lipid classes were performed with a dwell time of 0.2 s. The data were acquired and processed using MassLynx software (Waters).

^{31}P NMR Conditions. ^{31}P NMR spectra were measured on a Bruker Avance II 400 spectrometer at 202.46 MHz. The samples were dissolved in chloroform−2-propanol mixture (1:1, v/v). Deuterium oxide (placed in a 4 mm coaxial insert having a capillary in the measurement area) was used as a lock compound. ^{31}P chemical shifts were referred to the signal of PE ($\delta(^{31}P)$ = 0.01).

RESULTS AND DISCUSSION

Development of New Nontargeted Quantitation of Lipid Classes Using HILIC-HPLC/ESI-MS. The prerequisite for the development of our nontargeted lipidomic quantitation is a good chromatographic separation of individual lipid classes. For this purpose, we developed a HILIC-HPLC/ESI-MS method, which enables the separation of up to 19 lipid classes in a wide range of polarities in one analytical run.[5] The method has been applied to the analysis of NIST human plasma mixed with a known amount of IS and extracted using the modified Folch procedure[5] (Figure 1A). The HILIC chromatogram of human plasma shows 12 lipid classes eluting in order of polarity, i.e., nonpolar lipids (TG, Chol, CE), PG, HexCer, PI, PE, IS, LPE, PC, SM, and LPC. Unfortunately, the HILIC-HPLC method does not enable the separation of nonpolar lipids, because they coelute in one chromatographic peak close to the void volume of the system. The negative-ion ESI mode (Figure 1B) is more sensitive for anionic lipid classes, such as HexCer, PI, and PE.

The basic idea of the novel nontargeted lipidomic quantitation is based on the peak integration of lipid classes

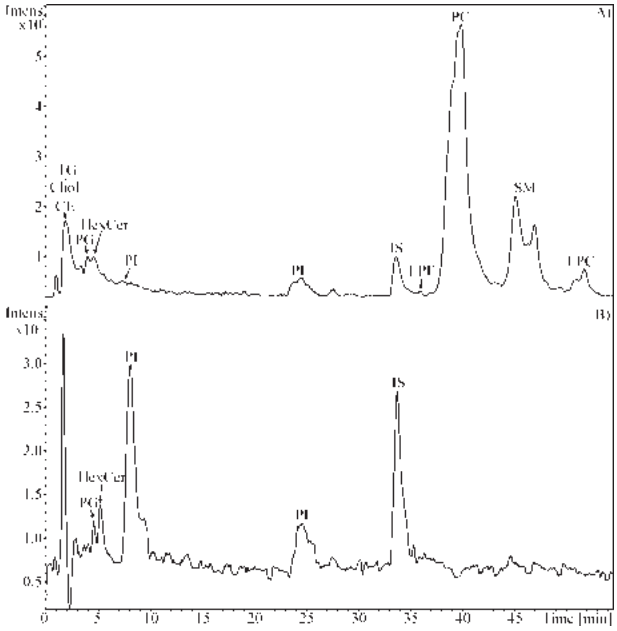

Figure 1. HILIC-HPLC/MS separation of total lipid extract from the NIST human plasma sample with the addition of internal standard (sphingosyl PE, d17:1/12:0) using Spherisorb Si column (250 × 4.6 mm, 5 μm) in: (A) positive-ion ESI-MS, and (B) negative-ion ESI-MS modes. HPLC conditions: flow rate 1 mL/min, separation temperature 40 °C, gradient 0 min−94% A + 6% B, 60 min−77% A + 23% B, where A is acetonitrile and B is 5 mM aqueous ammonium acetate. Peak annotation: TG, triacylglycerols; Chol, cholesterol; CE, cholesteryl esters; PG, phosphatidylglycerols; HexCer, hexosylceramides; PI, phosphatidylinositols; PE, phosphatidylethanolamines; IS, internal standard; LPE, lysophosphatidylethanolamines; PC, phosphatidylcholines; SM, sphingomyelins; LPC, lysophosphatidylcholines.

in the HILIC chromatogram followed by the multiplication of obtained peak areas by their RFs related to the single IS common for all lipid classes. The rather difficult task is the selection of a suitable IS with an appropriate retention behavior (i.e., no coelution with peaks of other lipid classes in HILIC chromatograms), which does not commonly occur in nature and has similar extraction behavior as for determined lipid classes. Polydeuterated phosphatidylcholine (18:0/18:0−PC, D79) was the first compound tested as IS with the assumption that polydeuterated and nondeuterated species could be separated. Unfortunately, the HILIC method did not provide any visible separation of polydeuterated and nondeuterated lipid species. The second compound tested as IS was N-dodecanoyl-heptadecasphing-4-enine-1-phosphoethanolamine (sphingosyl PE, d17:1/12:0) (Figure 2), which complies with all requirements for the IS in the nontargeted lipidomic quantitation. Sphingosyl PE elutes between the PE and LPE peaks, well separated from all lipid classes occurring in

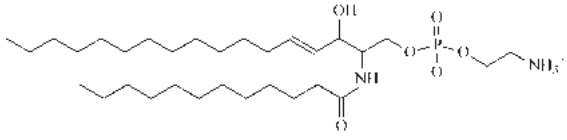

Figure 2. Structure of N-dodecanoyl-heptadecasphing-4-enine-1-phosphoethanolamine (sphingosyl PE, d17:1/12:0) used as an internal standard.

dx.doi.org/10.1021/ac3024476 | Anal. Chem. 2012, 84, 10064−10070

biological samples studied in our laboratory so far (lipid extracts from plants, animal and human body fluids and tissues such as plasma, serum, sebum, sperm, various organs with and without tumors, etc.). Moreover, sphingosyl PE provides an acceptable intensity in both positive-ion and negative-ion ESI-MS modes.

First, calibration curves were measured for the IS and these lipid classes (PG, LPG, PE, LPE, PC, SM, LPC) represented by standards containing oleoyl (Δ9*cis*-C18:1) acyls. The oleic acid has been selected as one of the most common fatty acids occurring in biological samples consistently with our previous method developed for TGs.[15] Calibration curves are linear at least in the concentration range from 5 to 1000 μg/mL for PC, SM, and LPC, and from 25 to 800 μg/mL for PG, LPG, PE, and LPE. Each lipid class is described by parameters of the linear dependency, $y = ax + b$, where y is the peak area, x is the concentration, and r^2 is the regression coefficients (Table 1).

Table 1. Parameters of Calibration Curves for Individual Lipid Classes Represented by Standards Containing Oleoyl (Δ9*cis*-C18:1) Acyl (retention times (t_R), Slopes (a), Intercepts (b), Regression Coefficients (r^2), and Response Factors (RF))

lipid class	t_R [min]	a	b	r^2	RF
PG	4.7	183.1	14.6	0.9996	0.318
LPG	8.4	271.8	23.1	0.9993	0.214
PE	24.8	196.6	2.2	0.9991	0.296
IS	**33.9**	**58.1**	**−0.6**	**0.9998**	**1.000**
LPE	36.1	112.7	−1.1	0.9984	0.516
PC	39.8	550.7	9.5	0.9997	0.106
SM	45.3	857.6	3.8	1.0000	0.068
LPC	51.2	488.6	2.8	0.9998	0.119

RFs are calculated as the ratio of the slope of the calibration dependency obtained for the IS to slopes of calibration dependencies of individual lipid classes. Obtained values of RFs are constant over months of measurements on the same instrument at identical conditions (deviation below 4%). This approach can be transferred to other instruments, but calibration dependencies must be measured first to obtain RFs valid for this particular instrument under given chromatographic conditions.

Peak areas of individual lipid classes and IS are integrated in the HILIC-HPLC/ESI-MS chromatogram of the total lipid extract with added IS. The concentration of IS is calculated from the calibration dependency, $c_{IS} = (A_{IS} + 0.6)/58.1$. Concentrations of individual lipid classes (Figure 3A) are calculated from the ratio of the peak area of lipid class to the peak area of IS multiplied by the RF_{class} and c_{IS}. For example, the concentration of PCs is calculated from the ratio of the peak area of PC to the peak area of IS multiplied by the RF_{PC} and c_{IS}. This new approach was compared with the conventional way of quantitation based on SRM transitions measured on a QqQ mass analyzer (Figure 3B), which is typically used in the shotgun setup without a chromatographic separation. However, identical HILIC conditions were applied here to ensure the direct comparison of quantitative data obtained by both approaches. Main disadvantages of quantitation using SRM scans are the necessity of ISs for each lipid class and the ability to quantify only lipids with previously determined SRM transitions. On the other hand, the requirement of our method

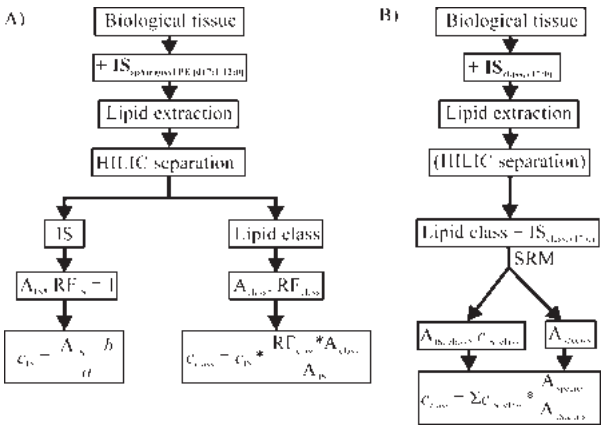

Figure 3. General schemes of both quantitation approaches: (A) novel nontargeted quantitation of lipid classes using single internal standard and response factor approach in HILIC-HPLC/ESI-MS, (B) conventional targeted quantitation using SRM scans on QqQ mass spectrometer. Abbreviations: IS, internal standard; A, peak area; RF, response factor; *c*, concentration; *a*, slope; *b*, intercept; SRM, selected reaction monitoring.

is the necessity of chromatographic resolution of lipid classes to be determined.

Extraction Recovery and Robustness of the Whole Method. Three basic extraction approaches are used in the lipidomic analysis and compared in this paper: (A) chloroform−methanol (2:1, v/v) extraction according to Folch,[44] (B) chloroform−methanol (1:2, v/v) extraction according to Bligh and Dyer,[45] and (C) MTBE extraction according to Shevchenko et al.[46] Extraction recoveries of these three extraction approaches (details in Experimental Section) are compared for Cer, PE, LPE, PC, SM, and LPC standards containing oleoyl acyl (Figure 4). White columns show chromatographic peak areas obtained from the standard solution without any extraction (100%), while other columns show extraction recoveries of individual approaches calculated as the mean peak area from six measurements together with standard deviations. All methods mostly provide results with good mutual agreement with few exceptions, e.g., lower recovery of LPE for Folch extraction, but all other values are in the interval 62−99%. The use of IS is essential for the reliable quantitation in accordance with established practice in HPLC/MS. When extraction recoveries are measured in human plasma and related to the IS (Figure S-1), then variability among individual extraction methods is rather low and in principle any of these methods can be used in the quantitation, as illustrated on the example of PE, PC, SM, and LPC. The additional test on the robustness was performed by the analysis of the porcine liver sample by three different persons, who extracted the same sample using the Folch extraction and each extract was injected two times into HPLC/MS, i.e., in total 6 chromatograms for one sample (Figure S-2). The mutual agreement is again satisfactory.

Verification of General Applicability of Our Method. Principal questions about the general applicability of our method based only on one IS and the use of RFs are the following: (1) stability of RFs over longer period of time, (2) applicability of the method on different HPLC/MS systems with different chromatographic conditions, (3) the verification that the approach based only on the single IS and RF approach can provide accurate results for various biological samples in

dx.doi.org/10.1021/ac3024476 | *Anal. Chem.* 2012, 84, 10064−10070

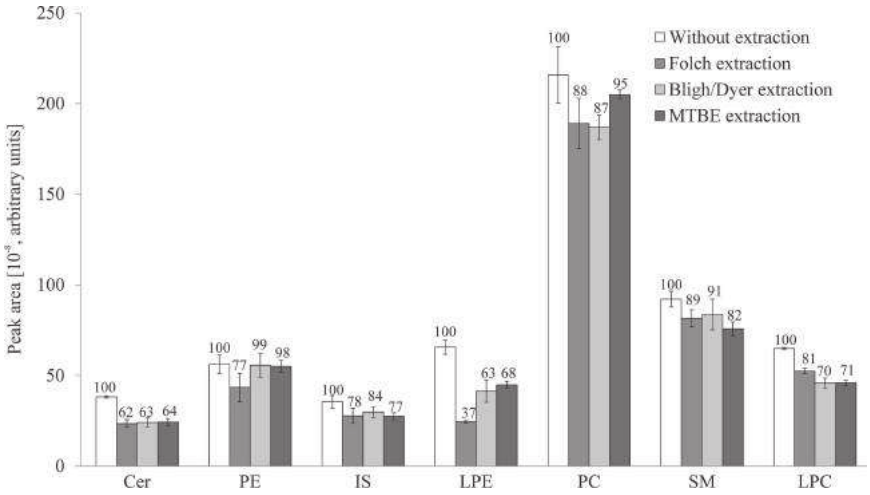

Figure 4. Comparison of extraction efficiency of Folch, Bligh and Dyer, and methyl-*tert*-butyl ether (MTBE) methods for ceramides (Cer), PE, IS, LPE, PC, SM, and LPC standards containing oleoyl (Δ9*cis*-C18:1) acyl. Reported relative recoveries (in percentages) are the standard mean of six measurements (three times extraction, each extract measured two times) together with standard deviations.

agreement with established techniques used in lipidomic quantitation. First, calibration curves were remeasured after a few months, and relative differences of RFs were lower than 4%. Then calibration curves were also measured on a different type of instrument (Q-TOF) using faster analysis under ultrahigh-performance liquid chromatography conditions optimized for main phospholipid and sphingolipid classes occurring in human plasma (clinical study in progress), and again good correlation was obtained in the measurement of identical human plasma samples.

The next step of the method validation was the comparison with reference methods used in lipidomic quantitation (SRM approach on QqQ and ^{31}P NMR) supported by the comparison with previously reported data on identical samples. Lipid species containing fatty acids with an odd carbon number are used as ISs in the SRM-based quantitation, PE (17:0/17:0), PC (17:0/17:0), and LPC (17:0). Individual SRM transitions (Table S-1) were assigned in previous off-line two-dimensional HILIC × RP-HPLC/MS measurements.[5] The first comparison is shown for the total lipid extract from egg yolk (Figure 5 and Table S-2), which was divided into three identical parts and

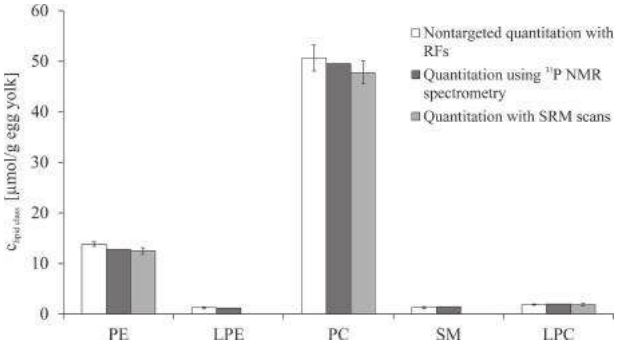

Figure 5. Comparison of concentrations (μmol/g) of PE, LPE, PC, SM, and LPC in the egg yolk using nontargeted quantitation of lipid classes using single internal standard and response factor approach in HILIC-HPLC/ESI-MS (white columns), the quantitation using ^{31}P NMR spectroscopy (dark columns), and the quantitation using SRM scans on QqQ mass spectrometer (gray columns).

used for measurements by three techniques. In general, the agreement between three completely different approaches is acceptable. In the case of PE and PC, values obtained by nontargeted quantitation with RFs are slightly higher compared to values obtained by targeted SRM approach, which could be explained by the fact that some minor lipid species are not defined in the SRM approach. Relative differences between nontargeted and targeted approaches are 0.5% for LPC, 5.6% for PC, and in the worst case 9.8% for PE (calculated from Table S-2). Values for LPE and SM with SRM are missing due to the lack of IS for these classes. Figure 6 shows an example of

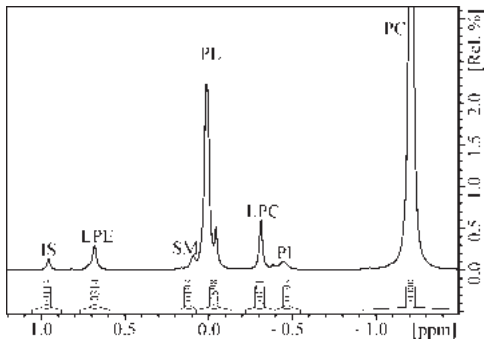

Figure 6. ^{31}P NMR spectrum of egg yolk extract measured in the chloroform−2-propanol mixture (1:1, v/v) at 202.46 MHz.

the ^{31}P NMR spectrum of egg yolk extract measured in chloroform−2-propanol mixture (1:1, v/v) at 202.46 MHz. The main advantage of NMR spectroscopy is no need of any RFs, because the signal is directly proportional to the number of measured nuclei, i.e., ^{31}P in our case.[23,40,41] The effect of fatty acyl chain length as well as the number and positions of double bonds on chemical shifts of individual lipids inside classes is rather small; therefore, the ^{31}P NMR spectrum of total lipid extract (Figure 6) shows peaks of lipid classes in a fashion very similar to that for HILIC-HPLC (Figure 1), which brings an ideal situation for the mutual comparison of obtained results. The last comparison is provided for the analysis of NIST human plasma (Figure 7 and Table S-3) by nontargeted

dx.doi.org/10.1021/ac3024476 | *Anal. Chem.* 2012, 84, 10064−10070

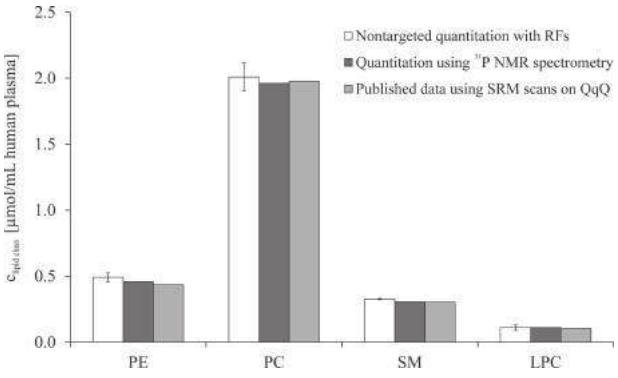

Figure 7. Comparison of concentrations (μmol/mL) of PE, PC, SM, and LPC in the NIST human plasma using nontargeted quantitation of lipid classes using single internal standard and response factor approach in HILIC-HPLC/ESI-MS (white columns), the quantitation using ^{31}P NMR spectroscopy (dark columns), and previously published data[34] (gray columns).

lipidomic quantitation with RFs in HILIC-HPLC/ESI-MS, ^{31}P NMR, and previously published data[34] obtained in eight different laboratories mainly by SRM on QqQ, except for classes of fatty acids and sterols quantified by GC/MS. The mutual correlation among three different analytical methods is rather good, especially considering the complexity of lipidomic plasma extracts and the number of individual lipid molecules inside particular lipid classes. Our method provides slightly higher concentrations for most lipid classes, which can be explained the same way as for the egg yolk.

Quantitation of Individual Lipid Species. The HILIC-HPLC/ESI-MS method can also be used in quantitation of lipid molecular species within individual lipid classes using relative intensities of characteristic ions in ESI mass spectra obtained by the peak integration in the HILIC chromatogram. Relative abundances of SM species have been determined based on $[M + H]^+$ ions (Table 2) and compared with the literature data.[47] The comparison of results shows a good match except for d24:1/18:1-SM. Moreover, absolute concentrations of lipid species can be calculated for the known total SM concentration in the egg yolk (in μmol/g) determined from the SM peak area in the HILIC chromatogram multiplied by the relative peak area of individual SM species. This approach is applicable for other lipid classes as well, but in certain cases the exact quantitation of individual species inside the class can be complicated by isobaric interferences of $[M + Na]^+$ ions with $[M + H]^+$ ions for lipids with the fatty acyl chain longer by two carbon atoms and additional three double bonds, e.g., protonated 36:4-PC has the same nominal mass m/z 782 as sodiated 34:1-PC, which requires either the ultrahigh-resolution typical for Fourier transform ion cyclotron resonance mass spectrometer or negative-ion mode, as illustrated on the example of PI determined in NIST human plasma and compared with previously published data on the same sample (Figure S-3). Another possible solution is the preferential formation of desired adduct ions achieved by the addition of a selected ion into the mobile phase.[48] Isobaric interferences do not occur for the SM class due to the absence of fatty acyl chains with three or more double bonds, so the accurate quantitation (Table 2) can be performed.

Table 2. Comparison of Relative Abundances (%) of Individual SM in the Egg Yolk Sample between Our Data Obtained by HILIC-HPLC/ESI-MS and Previously Published High-Performance Thin-Layer Chromatography Data[47] and the Absolute Concentrations (μmol/g) of Individual SM Species

sphingomyelin	HILIC-HPLC/ESI-MS (%)	HPTLC[47] (%)	HILIC-HPLC/ESI-MS (concentration, μmol/g)
d16:0/18:1	61	66	0.78
d18:0/18:1	9	10	0.12
d18:1/18:1	2	1	0.03
d20:0/18:1	2	4	0.03
d22:0/18:1	5	6	0.06
d22:1/18:1	1	1	0.01
d23:0/18:1	2	2	0.03
d24:0/18:1	4	5	0.05
d24:1/18:1	14	3	0.18
others	0	2	0.00
total	100	100	1.28

CONCLUSIONS

The novel nontargeted lipidomic quantitation method for the comprehensive lipidomic analysis enables the quantification of all lipid classes separated by HILIC-HPLC. Concentrations of individual lipid classes are obtained by the peak integration in the HILIC mode multiplied by their RFs related to a single IS. Concentrations of individual lipid species inside lipid classes can be also determined as relative abundances of particular peaks in mass spectra multiplied by the total concentration of the lipid class. The correlation with earlier published data on the lipidomic characterization of NIST human plasma,[34] egg yolk,[47] our comparison with established SRM approach on QqQ mass spectrometer, and also the ^{31}P NMR quantitation confirms the accuracy and precision of our results and applicability for various types of biological samples. In general, our nontargeted method is better suited for the quantitation of lipid classes, while the conventional SRM targeted approach has better sensitivity for selected lipid molecules and is faster compared to rather long HPLC/MS runs in the HILIC mode. Nontargeted HILIC-HPLC/ESI-MS quantitation can be used in the comprehensive lipidomic characterization of multiple lipid classes, such as clinical studies searching for lipidomic differences between healthy volunteers and disease patients. Two comprehensive lipidomic studies are in progress in our group using the described quantitative method, namely the lipidomic characterization of porcine organs and tissues and the clinical study of lipoprotein plasma fractions and erythrocytes of cardiovascular disease patients (over 1000 samples per year). The preliminary results confirm the robustness and reliability of this quantitative assay.

ASSOCIATED CONTENT

Supporting Information

Additional information as noted in text. This material is available free of charge via the Internet at http://pubs.acs.org.

AUTHOR INFORMATION

Corresponding Author

*Tel.: +420-466037087. Fax: +420-466037068. E-mail: Michal.Holcapek@upce.cz.

Notes

The authors declare no competing financial interest.

■ ACKNOWLEDGMENTS

This work was supported by the grant project No. 206/11/0022 sponsored by the Czech Science Foundation (E.C., M.H., M.L., and M.O.). We acknowledge the help of Pawel Pasikowski and Blanka Červená with the validation of the extraction procedure and Vitaliy Chagovets for the critical reading of the manuscript.

■ REFERENCES

(1) Fahy, E.; Subramaniam, S.; Brown, H. A.; Glass, C. K.; Merrill, A. H.; Murphy, R. C.; Raetz, C. R. H.; Russell, D. W.; Seyama, Y.; Shaw, W.; Shimizu, T.; Spener, F.; van Meer, G.; VanNieuwenhze, M. S.; White, S. H.; Witztum, J. L.; Dennis, E. A. *J. Lipid Res.* **2005**, *46*, 839.
(2) Christie, W. W. http://lipidlibrary.aocs.org/ downloaded April 2012.
(3) Axelsen, P. H.; Murphy, R. C. *J. Lipid Res.* **2010**, *51*, 660.
(4) Hutchins, P. M.; Barkley, R. M.; Murphy, R. C. *J. Lipid Res.* **2008**, *49*, 804.
(5) Lísa, M.; Cífková, E.; Holčapek, M. *J. Chromatogr. A* **2011**, *1218*, 5146.
(6) McLaren, D. G.; Miller, P. L.; Lassman, M. E.; Castro-Perez, J. M.; Hubbard, B. K.; Roddy, T. P. *Anal. Biochem.* **2011**, *414*, 266.
(7) Uran, S.; Larsen, A.; Jacobsen, P. B.; Skotland, T. *J. Chromatogr. B* **2001**, *758*, 265.
(8) Harrabi, S.; Herchi, W.; Kallel, H.; Mayer, P. M.; Boukhchina, S. *Food Chem.* **2009**, *114*, 712.
(9) Pang, L. Q.; Liang, Q. L.; Wang, Y. M.; Ping, L.; Luo, G. A. *J. Chromatogr. B* **2008**, *869*, 118.
(10) Wang, C.; Xie, S. G.; Yang, J.; Yang, Q.; Xu, G. W. *Anal. Chim. Acta* **2004**, *525*, 1.
(11) Retra, K.; Bleijerveld, O. B.; van Gesteil, R. A.; Tielens, A. G. M.; van Hellemond, J. J.; Brouwers, J. F. *Rapid Commun. Mass Spectrom.* **2008**, *22*, 1853.
(12) Sandra, K.; Pereira, A. D.; Vanhoenacker, G.; David, F.; Sandra, P. *J. Chromatogr. A* **2010**, *1217*, 4087.
(13) Shaner, R. L.; Allegood, J. C.; Park, H.; Wang, E.; Kelly, S.; Haynes, C. A.; Sullards, M. C.; Merrill, A. H. *J. Lipid Res.* **2009**, *50*, 1692.
(14) Cvačka, J.; Hovorka, O.; Jiroš, P.; Kindl, J.; Stránský, K.; Valterová, I. *J. Chromatogr. A* **2006**, *1101*, 226.
(15) Holčapek, M.; Lísa, M.; Jandera, P.; Kabátová, N. *J. Sep. Sci.* **2005**, *28*, 1315.
(16) Lísa, M.; Velínská, H.; Holčapek, M. *Anal. Chem.* **2009**, *81*, 3903.
(17) Lísa, M.; Netušilová, K.; Franěk, L.; Dvořáková, H.; Vrkoslav, V.; Holčapek, M. *J. Chromatogr. A* **2011**, *1218*, 7499.
(18) Lytle, C. A.; Gan, Y. D.; White, D. C. *J. Microbiol. Methods* **2000**, *41*, 227.
(19) Sommer, U.; Herscovitz, H.; Welty, F. K.; Costello, C. E. *J. Lipid Res.* **2006**, *47*, 804.
(20) Cvačka, J.; Svatoš, A. *Rapid Commun. Mass Spectrom.* **2003**, *17*, 2203.
(21) Al-Saad, K. A.; Siems, W. F.; Hill, H. H.; Zabrouskov, V.; Knowles, N. R. *J. Am. Soc. Mass Spectrom.* **2003**, *14*, 373.
(22) Fuchs, B.; Schiller, J. *European J. Lipid Sci. Technol.* **2009**, *111*, 83.
(23) Fuchs, B.; Schiller, J.; Suss, R.; Schurenberg, M.; Suckau, D. *Anal. Bioanal. Chem.* **2007**, *389*, 827.
(24) Rohlfing, A.; Muthing, J.; Pohlentz, G.; Distler, U.; Peter-Katalinic, J.; Berkenkamp, S.; Dreisewerd, K. *Anal. Chem.* **2007**, *79*, 5793.
(25) Stubiger, G.; Belgacem, O. *Anal. Chem.* **2007**, *79*, 3206.
(26) Stubiger, G.; Belgacem, O.; Rehulka, P.; Bicker, W.; Binder, B. R.; Bochkov, V. *Anal. Chem.* **2010**, *82*, 5502.
(27) Holčapek, M.; Jandera, P.; Zderadička, P.; Hrubá, L. *J. Chromatogr. A* **2003**, *1010*, 195.
(28) Lísa, M.; Holčapek, M. *Chem. Listy* **2005**, *99*, 195.
(29) Cai, S. S.; Short, L. C.; Syage, J. A.; Potvin, M.; Curtis, J. M. *J. Chromatogr. A* **2007**, *1173*, 88.
(30) Stubiger, G.; Pittenauer, E.; Belgacem, O.; Rehulka, P.; Widhalm, K.; Allmaier, G. *Rapid Commun. Mass Spectrom.* **2009**, *23*, 2711.
(31) Ahn, E. J.; Kim, H.; Chung, B. C.; Kong, G.; Moon, M. H. *J. Chromatogr. A* **2008**, *1194*, 96.
(32) Berdeaux, O.; Juaneda, P.; Martine, L.; Cabaret, S.; Bretillon, L.; Acar, N. *J. Chromatogr. A* **2010**, *1217*, 7738.
(33) Hsu, F. F.; Turk, J. *J. Am. Soc. Mass Spectrom.* **2001**, *12*, 1036.
(34) Quehenberger, O.; Armando, A. M.; Brown, A. H.; Milne, S. B.; Myers, D. S.; Merrill, A. H.; Bandyopadhyay, S.; Jones, K. N.; Kelly, S.; Shaner, R. L.; Sullards, C. M.; Wang, E.; Murphy, R. C.; Barkley, R. M.; Leiker, T. J.; Raetz, C. R. H.; Guan, Z. Q.; Laird, G. M.; Six, D. A.; Russell, D. W.; McDonald, J. G.; Subramaniam, S.; Fahy, E.; Dennis, E. A. *J. Lipid Res.* **2010**, *51*, 3299.
(35) Takatera, A.; Takeuchi, A.; Saiki, K.; Morisawa, T.; Yokoyama, N.; Matsuo, M. *J. Chromatogr. B* **2006**, *838*, 31.
(36) Fauland, A.; Kofeler, H.; Trotzmuller, M.; Knopf, A.; Hartler, J.; Eberl, A.; Chitraju, C.; Lankmayr, E.; Spener, F. *J. Lipid Res.* **2011**, *52*, 2314.
(37) Sato, Y.; Nakamura, T.; Aoshima, K.; Oda, Y. *Anal. Chem.* **2010**, *82*, 9858.
(38) Schuhmann, K.; Almeida, R.; Baumert, M.; Herzog, R.; Bornstein, S. R.; Shevchenko, A. *J. Mass Spectrom.* **2012**, *47*, 96.
(39) Taguchi, R.; Ishikawa, M. *J. Chromatogr. A* **2010**, *1217*, 4229.
(40) Schiller, J.; Arnold, K. *Med. Sci. Monit.* **2002**, *8*, MT205.
(41) Spyros, A.; Dais, P. *Prog. Nucl. Magn. Reson. Spectrosc.* **2009**, *54*, 195.
(42) Lísa, M.; Holčapek, M. *J. Chromatogr. A* **2008**, *1198*, 115.
(43) Lísa, M.; Holčapek, M.; Boháč, M. *J. Agric. Food Chem.* **2009**, *57*, 6888.
(44) Folch, J.; Lees, M.; Stanley, G. H. S. *J. Biol. Chem.* **1957**, *226*, 497.
(45) Bligh, E. G.; Dyer, W. J. *Can. J. Biochem. Physiol.* **1959**, *37*, 911.
(46) Matyash, V.; Liebisch, G.; Kurzchalia, T. V.; Shevchenko, A.; Schwudke, D. *J. Lipid Res.* **2008**, *49*, 1137.
(47) Ramstedt, B.; Leppimaki, P.; Axberg, M.; Slotte, J. P. *Eur. J. Biochem.* **1999**, *266*, 997.
(48) Hsu, F. F.; Bohrer, A.; Turk, J. *J. Am. Soc. Mass Spectrom.* **1998**, *9*, 516.

Research Article

Rapid Communications in Mass Spectrometry

Received: 24 March 2015 Revised: 19 September 2015 Accepted: 20 September 2015 Published online in Wiley Online Library

Rapid Commun. Mass Spectrom. **2015**, *29*, 2374–2384
(wileyonlinelibrary.com) DOI: 10.1002/rcm.7404

Effects of fatty acyl chain length, double-bond number and matrix on phosphatidylcholine responses in matrix-assisted laser desorption/ionization on an Orbitrap mass spectrometer

Vitaliy Chagovets, Miroslav Lísa and Michal Holčapek*

Department of Analytical Chemistry, Faculty of Chemical Technology, University of Pardubice, Studentská 573, 532 10 Pardubice, Czech Republic

RATIONALE: Matrix-assisted laser desorption/ionization mass spectrometry (MALDI-MS) is used for the fast qualitative and quantitative analysis of phosphatidylcholines (PC). Fatty acyl chain lengths and the number of double bonds (DB) affect relative responses of PC; hence the determination of correction factors of individual PC is important for the accurate quantitation. The signal intensity in MALDI-MS strongly depends on the matrix; therefore, the following matrices typically used in lipidomics are studied in the present work: 2,5-dihydroxybenzoic acid (DHB), 1,5-diaminonaphthalene (DAN) and 9-aminoacridine (9AA).
METHODS: Series of PC with various fatty acyl chain lengths are synthesized for this study. PC concentrations over two orders of magnitude are studied with MALDI-MS. These experiments provide sets of calibration curves for each of the synthesized PC and the further analysis of parameters of calibration curves is performed.
RESULTS: Correction factors for PC decrease with increasing fatty acyl chain length for all matrices. These dependences are steeper for unsaturated PC than for saturated ones. MALDI matrices also have a significant effect on this dependence. The weakest dependence on fatty acyl chain length is found for saturated PC in 9AA. In the case of the other matrices, the effect of fatty acyl chain length on the response is essential for both saturated and unsaturated PC. Calibration curves and parameters of calibration curves for both saturated and monounsaturated PC are fitted by a linear function with regression coefficients decreasing in the order 9AA > DAN > DHB.
CONCLUSIONS: Differences in relative responses for PC in MALDI-MS measurements must be taken into account for accurate quantitation. Parameters of calibration curves can be used for the determination of PC concentrations using a single internal standard (IS). This method gives good results for the 9AA matrix, but the reproducibility of measurements for the DHB and DAN matrices is lower and the method can be used for a rough estimation only. These matrices are less convenient for the quantitation of PC. Copyright © 2015 John Wiley & Sons, Ltd.

Phosphatidylcholines (PC) are important and highly abundant lipids in biological samples. They play essential roles as constituents of biomembranes,[1] regulators for various biological processes such as homeostasis, metabolism, cell signaling and organ physiology.[2] These functions of PC are associated with several diseases connected with deviations from the normal lipid expression.[3–6] Quantitative lipidomic analysis can be used for disease biomarker discoveries. Electrospray ionization mass spectrometry (ESI-MS) is commonly used in lipidomic studies.[7–11] Matrix-assisted laser desorption/ionization mass spectrometry (MALDI-MS) is also widely embedded in such investigations due to its high sensitivity, high speed of analysis, robustness and easy sample preparation.[12,13] MALDI-MS is mainly used in qualitative analysis, but MALDI-MS applications in quantitative analysis have been reported as well.[14–16]

A key problem for the accurate quantitation of lipids is different MS responses of various lipid classes and species. This means that the molar ratio of some lipid species is not equal to corresponding MS peak intensities ratio, i.e., different lipids may have different detection efficiency.[17–19] Several factors influence the overall detection efficiency, such as the ionization efficiency, the fragmentation efficiency, the efficiency of transfer to the gas phase, etc. Some of these factors are dependent on the molecular structure, while others are dependent on the composition and properties of a sample in general. PC consist of polar head groups containing choline and phosphoric acid residues, the glycerol backbone and fatty acyl, alkyl or alkenyl hydrophobic chains attached to *sn*-1 and *sn*-2 positions on the glycerol backbone. MS studies of lipids showed that PC are preferentially ionized and detected as protonated molecules or adducts with alkali metal ions.[13,20–23] Mainly the type of polar head group determines differences in the detection efficiency between classes of phospholipids. These differences could even result in the signal suppression of one lipid class by another

* *Correspondence to:* M. Holčapek, Department of Analytical Chemistry, Faculty of Chemical Technology, University of Pardubice, Studentská 573, 532 10 Pardubice, Czech Republic.
E-mail: Michal.Holcapek@upce.cz

Rapid Communications in Mass Spectrometry

one.[19] Fatty acyl chains determine differences in detection efficiency between lipid species within one class. The effect of fatty acyls is not as strong as for the polar head group, but it is not negligible. Previous ESI-MS studies have shown that both fatty acyl chain length and its degree of unsaturation have a significant influence.[17,18] To the best of our knowledge, no systematic study has been done so far for MALDI-MS quantitation of PC and therefore only an assumption is used that differences among MALDI responses are negligible inside the same lipid class.[24] The effect of fatty acyls could differ for MALDI and ESI techniques, because ionization mechanisms are not identical as well. One of the assumptions of the acyl chain influence in ESI-MS was that the difference in chains causes differences in the surface activity and, hence, different ionization efficiency in electrospray droplets and also can influence evaporation of molecules to the gas phase from the surface of a droplet.[18] In MALDI, the ionization depends on the matrix and its cocrystallization with sample molecules.[12] MALDI strongly depends on the sample structure, which is influenced by the analyte concentration, the ratio of analyte and matrix, solvent used for analyte and matrix preparation.[12,13,22,25,26] The detection efficiency can be dramatically different for the same species with various matrices or solvents used for the sample preparation.[13,25–27] Therefore, these factors must be taken into account during the development of MALDI-MS methods applicable for the quantitation.

Reliable quantitation in MS requires the use of an internal standard (IS) with a composition similar to quantified compounds, preferably isotopically labeled analogues. This approach is not feasible in the lipidomic quantitation, because tens to hundreds of lipid species may be present inside some lipid classes; therefore, certain simplifications must be introduced. Typically, the quantitation of lipid species inside the class is related to one or more IS from this class, but the IS cannot occur in studied samples, e.g., lipids with odd numbers of carbon atoms in fatty acyl chains.

The goal of the present work is the determination of effects of fatty acyl chain lengths and the DB number on the detection efficiency of PC in MALDI-MS experiments using 2,5-dihydroxybenzoic acid (DHB), 1,5-diaminonaphthalene (DAN) and 9-aminoacridine (9AA) as matrices, which are typically used for the lipidomic analysis.[27–29] The applicability of the final method with correction factors is used in the quantitation of PC in a human plasma sample.

EXPERIMENTAL

Materials

Dichloromethane, methanol, acetonitrile, 2-propanol, chloroform (all HPLC/MS grade), 4-dimethylaminopyridine (DMAP), dicyclohexylcarbodiimide (DCC), 2,5-dihydroxybenzoic acid (DHB), 1,5-diaminonaphthalene (DAN), 9-aminoacridine (9AA), and NaCl were purchased from Sigma-Aldrich (St. Louis, MO, USA). Myristic (FA 14:0), palmitic (FA 16:0), linolenic (FA 9Z,12Z,15Z-18:3), linoleic (FA 9Z,12Z-18:2), oleic (FA 9Z-18:1), stearic (FA 18:0), eicosapentaenoic (FA 5Z,8Z, 11Z,14Z,17Z-20:5), arachidic (FA 20:0), docosahexaenoic (FA 4Z,7Z,10Z,13Z,16Z,19Z-22:6), behenic (FA 22:0), and lignoceric (FA 24:0) fatty acids (FA) were purchased from NuChek Prep (Elysian, MN, USA); 1-heptadecanoyl-2-hydroxy-*sn*-glycero-3-phosphocholine (PC 17:0/0:0), 1-oleoyl-2-hydroxy-*sn*-glycero-3-phosphocholine (PC 18:1/0:0), 1,2-dipalmitoyl-*sn*-glycero-3-phosphocholine (PC 16:0/16:0), 1,2-diheptadecanoyl-*sn*-glycero-3-phosphocholine (PC 17:0/17:0), 1,2-dioleoyl-*sn*-glycero-3-phosphocholine (PC 18:1/18:1), 1,2-diarachidonoyl-*sn*-glycero-3-phosphocholine (PC 20:4/20:4), and 1,2-dibehenoyl-*sn*-glycero-3-phosphocholine (PC 22:0/22:0) were purchased from Avanti Polar Lipids (Alabaster, AL, USA).

Human plasma was obtained from healthy volunteers in cooperation with the Faculty Hospital Olomouc based on the approval of the ethical committee at the Faculty Hospital Olomouc.

Synthesis and sample preparation

The synthesis of PC from lysophosphatidylcholine (PC *x:y*/0:0) was performed with a procedure similar to this one used for triacylglycerol synthesis described earlier.[30] PC 17:0/0:0 (4.5 mg) or PC 18:1/0:0 (5.2 mg) was mixed with 5.6 mg of DMAP and 10.9 mg of DCC and dissolved in 1 mL of dichloromethane. Volumes of 25 µmol of each FA were mixed and dissolved in 7 mL of dichloromethane. Then 0.2 mL of one PC *x:y*/0:0 solution and 0.2 mL of FA mixture were stirred in a vial for 2 h at ambient temperature. The described synthetic procedure was repeated three times both for PC 17:0/0:0 and PC 18:1/0:0, which yielded six series of PC to check the reproducibility of synthesized lipids ratio. Synthesized PC series were used without further purification.

Solutions of synthesized lipids were prepared by the dilution with methanol and mixed with the matrix for MALDI-MS measurements. The IS (PC 17:0/17:0) was added for the construction of calibration curves at the concentration comparable to the measured PC.

Solutions of synthesized lipids were prepared by dilution with methanol. The series contained dilutions in 3, 6, 10, 30, 60, 100 times. The IS (PC 17:0/17:0) solution in methanol was added for the construction of calibration curves at the concentrations 3 µmol/L and 30 µmol/L for PC 17:0/*x:y* and PC 18:1/*x:y*, respectively. The matrix solution is added for MALDI-MS measurements. The final sample contained a dissolved solution of synthesized lipids, IS and matrix solution in the ratio 1:1:1 (v/v/v).

The blood was collected into heparin-lithium tubes and centrifuged to obtain plasma. The lipid extract from plasma was prepared according to the modified Folch method.[31] A volume of 500 µL of sample was homogenized with 10 mL of chloroform/methanol (2:1, v/v). This mixture was filtered using a rough filter paper. Then 2 mL of 1 mol/L NaCl was added and centrifuged for 3 min at 2500 rpm. The chloroform layer containing lipids was evaporated by a gentle stream of nitrogen and dissolved in chloroform/2-propanol (1:1, v/v).

MALDI-MS

The following matrix solutions were used for MALDI experiments: 10 mg/mL of 9AA in 2-propanol/acetonitrile 60:40 (v/v), 77 mg/mL of DHB in methanol and 10 mg/mL of DAN in 2-propanol/acetonitrile 60:40 (v/v). 5 µL of each sample was mixed with 5 µL of matrix solution and 5 µL of IS. 0.7 µL of this mixture was deposited on the stainless steel sample plate

and dried. Each sample was deposited in four wells and measured using an LTQ Orbitrap XL with a MALDI source (Thermo Scientific, Waltham, MA, USA). MALDI mass spectra were acquired in the positive-ion mode in the mass range *m/z* 400–1000 with the laser energy of 15 μJ per laser shot for the DHB and 9AA matrices and 7 μJ for the DAN matrix. The optimal laser energy was determined by means of the LTQ Orbitrap XL software. Each mass spectrum was obtained as a result of summation of 3 to 5 laser shots. The number of laser shots was determined by the analysis of total ion current profile after shooting several times in one position. The decisive criterion was the decrease in total ion current by 10–20%. Spectra for each well were measured from 50 randomly distributed points. The final spectrum for each sample was obtained by averaging of 200 spectra from four wells to obtain the representative averaged spectrum. Mass spectra were converted with msConvert tool[32] and preliminarily processed with a home-made program based on the MALDIquant package.[33] Lipids nomenclature through the paper is in accordance with LIPID MAPS[34] terminology and the shorthand notation summarized in Liebisch *et al.*[35]

RESULTS AND DISCUSSION

Synthesis of PC standards

Two series of PC with different fatty acyl chain lengths and number of DB were synthesized for the investigation of these effects on the MALDI-MS detection efficiency. The synthesis is performed on the basis of commercially available standards of saturated (PC 17:0/0:0) and monounsaturated (PC 18:1/0:0) lysophosphatidylcholines. Two kinds of PC sets are synthesized by the reaction of lysophosphatidylcholines and the mixture of FA standards to prepare PC 17:0/*x:y* and PC 18:1/*x:y* series, where *x* is the carbon number (CN) and *y* is the DB number in the following fatty acyls in the *sn*-2 position: 14:0, 16:0, 18:3, 18:2, 18:1, 18:0, 20:5, 20:0, 22:6, 22:0 and 24:0 (details in the Experimental section). Saturated FA are selected to produce series of data points to reveal the general trends. The number of DB is varied by choosing lysophosphatidylcholines with different numbers of unsaturations in its fatty acyl. Only saturated and monounsaturated lysophosphatidylcholines are commercially available; therefore, reaction products with saturated FA allowed the detailed study of PC with zero and one DB only. FA with higher unsaturation are added for rough estimation of their responses with respect to the main series. The lengths of saturated FA cover the typical range in biological samples. The synthesized PC together with *m/z* values of their $[M+H]^+$ and $[M+Na]^+$ ions are summarized in Table 1. In addition, the PC 16:0/*x:y* series were synthesized and analyzed (data not presented). This demonstrates properties similar to that of PC 17:0/*x:y*. Presentation of the data for the PC 17:0/*x:y* series is related to the fact that it can be added to biological samples for data correction as it has odd CN which is relatively rare in nature.

MALDI-MS analysis of synthesized PC

Products of synthesis were investigated by MALDI-MS to confirm the presence of the compounds of interest. Zoomed *m/z* regions of $[M+H]^+$ ions in the positive-ion mass spectra of

Table 1. Theoretical and experimental *m/z* values of protonated and sodiated molecules in the PC 17:0/*x:y* and PC 18:1/*x*:0 series with measured mass accuracy

	$[M+H]^+$			$[M+Na]^+$		
Lipid	Theoretical	Experimental	Mass accuracy [ppm]	Theoretical	Experimental	Mass accuracy [ppm]
PC 17:0/14:0	720.5538	720.5548	1.4	742.5357	742.5367	1.3
PC 17:0/16:0	748.5851	748.5860	1.2	770.5670	770.5700[a]	3.9
PC 17:0/18:3	770.5694	770.5700[a]	0.8	792.5514	792.5527	1.6
PC 17:0/18:2	772.5851	772.5866	1.9	794.5670	794.5700[b]	3.8
PC 17:0/18:1	774.6007	774.6021	1.8	796.5827	796.5827	0.0
PC 17:0/18:0	776.6164	776.6176	1.5	798.5983	798.5997	1.8
PC 17:0/20:5	794.5694	794.5700[b]	0.8	816.5514	816.5523	1.1
PC 17:0/20:0	804.6477	804.6487	1.2	826.6296	826.6307	1.3
PC 17:0/22:6	820.5851	820.5861	1.2	842.5670	842.5680	1.2
PC 17:0/22:0	832.6790	832.6799	1.1	854.6609	854.6622	1.5
PC 17:0/24:0	860.7103	860.7111	0.9	882.6922	882.6936	1.6
PC 18:1/14:0	732.5538	732.5546	1.1	754.5357	754.5367	1.3
PC 18:1/16:0	760.5851	760.5859	1.1	782.5670	782.5692[c]	2.8
PC 18:1/18:3	782.5694	782.5692[c]	0.3	804.5514	804.5523	1.1
PC 18:1/18:2	784.5851	784.5858	0.9	806.5670	806.5687[d]	2.1
PC 18:1/18:1	786.6007	786.6015	1.0	808.5827	808.5826	0.1
PC 18:1/18:0	788.6164	788.6170	0.8	810.5983	810.5989	0.7
PC 18:1/20:5	806.5694	806.5687[d]	0.9	828.5514	828.5520	0.7
PC 18:1/20:0	816.6477	816.6481	0.5	838.6296	838.6303	0.8
PC 18:1/22:6	832.5851	832.5855	0.5	854.5670	854.5678	0.9
PC 18:1/22:0	844.6790	844.6796	0.7	866.6609	866.6616	0.8
PC 18:1/24:0	872.7103	872.7107	0.5	894.6922	894.6929	0.8

[a, b, c, d] *m/z* values are not resolved in our measurements.

PC 17:0/*x:y* and PC 18:1/*x:y* series are presented for 9AA (Fig. 1), DHB (Supplementary Fig. S1) and DAN (Supplementary Fig. S2, see Supporting Information) matrices. Peaks present in mass spectra correspond to protonated or sodiated molecules of PC, which is confirmed by accurate *m/z* determination with the mass accuracy typically better than 3 ppm (Table 1). Peaks of sodiated PC are not observed at all or with a negligible intensity for samples measured with 9AA matrix, which is an advantage for the interpretation of spectra. Relative abundances of $[M+Na]^+$ ions for PC are about 10–60% related to $[M+H]^+$ ions for measurements with DHB and DAN matrices. Peaks at *m/z* 770, 794 (Supplementary Figs. S1(a), S2(a)) and *m/z* 782, 806 (Supplementary Figs. S1(b), S2(b)) correspond to overlapping signals of protonated and sodiated PC, which is known problem of MS analysis of phospholipids in the positive-ion mode,[36] because their resolution requires a resolving power of over 300,000. Tandem mass spectra are obtained to confirm the chemical structures of synthesized compounds. Supplementary Fig. S3 (see Supporting Information) shows a characteristic fragmentation of sodiated and protonated PC on the example of PC 18:1/18:1.[37,38] All calculations in the present investigation are performed for protonated species only to be able to compare results for the same ions for all three matrices. Besides, the ratio of intensities of sodiated and protonated PC can be different for different species because protonation is localized on the head group and the interaction with Na^+ can involve fatty acyl chains which wrap around the cation and such kinds of interaction with Na^+ may depend on chain lengths much stronger than the interaction of H^+.

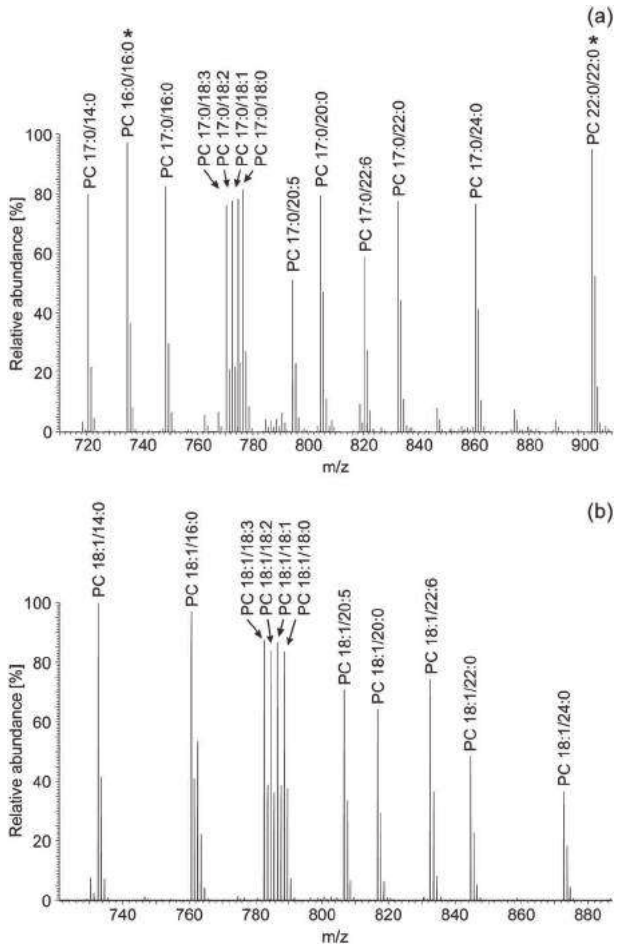

Figure 1. Positive-ion MALDI mass spectra of synthesized PC measured using 9AA as the matrix: (a) PC 17:0/*x:y* series with added PC 16:0/16:0 and PC 22:0/22:0 at identical concentrations (labeled by asterisks) and (b) PC 18:1/*x:y* series. The result after averaging of 200 mass spectra from four wells with the same sample is shown.

Concentrations of analyzed PC are estimated for each synthesized mixture using the standard addition analysis[16] to enable the selection of the appropriate IS concentration. Determined concentrations are around 0.06 mmol/L for the PC 17:0/*x:y* series and 0.8 mmol/L for the PC 18:1/*x:y* series with the relative standard deviation (RSD) approximately 5%. Based on this information, concentrations of IS added to each dilution of synthesized series are 3 μmol/L and 30 μmol/L for PC 17:0/*x:y* and PC 18:1/*x:y* correspondingly. Synthesized PC compounds were not purified and some amounts of initial substances (lysophosphatidylcholine and fatty acids) are present in the mixtures modeling the presence of other lipids. The crucial question of our work concept is the confirmation of the initial assumption that the reaction really provides equimolar mixtures of synthetized PC.[39–41] For this purpose, an equimolar mixture of two PC standards is added to synthesized samples (Fig. 1(a)). Peaks of added standards of PC 16:0/16:0 and PC 22:0/22:0 are labelled with asterisks. Slopes of trend lines built for intensities of equimolar standards and synthesized species have close values (–0.029 and –0.032, respectively). Peak intensities of synthesized PC in mass spectra obtained with 9AA matrix also demonstrate a similar dependence as for the equimolar mixture of standards known from the literature.[26] The reproducibility of normalized intensities of synthesized species produced in three different replicative reactions is demonstrated by standard deviations in Supplementary Fig. S4 (see Supporting Information).

MALDI mass spectra depend on the structure of measured compounds, matrix, solvent and the concentration ratio of matrix to analyte. Dependences of absolute intensities of PC in positive-ion MALDI mass spectra on the concentration are shown for the three studied matrices (Fig. 2). Dependences show the same trend for all studied matrices. Absolute intensities increase up to $5*10^{-4}$ mol/L, then the signal starts to decrease. This behavior could be explained by the spot structure after the cocrystallization with the matrix and the variation in matrix-to-analyte ratio. For example, in the case of DHB, the structure of the spot is uniform without visible matrix crystals for samples with high concentrations of lipids. The matrix-to-analyte ratio for these samples is about 50:1 to 500:1, while the optimal ratio is typically at 1000:1 and higher.[12] Such excess of lipids may result not in an increase in their MALDI-MS signal, but in hampering of the function of DHB as a matrix. With the increase in the matrix relative amount, polycrystals could be formed, which improves incorporation of lipids into the matrix structure and thus improving lipid-matrix interaction resulting in the increase in lipid signal intensities. The observed effect depends on the overall concentration of lipids, which may be attributed to the influence on the sample structure. Their measurement allows the

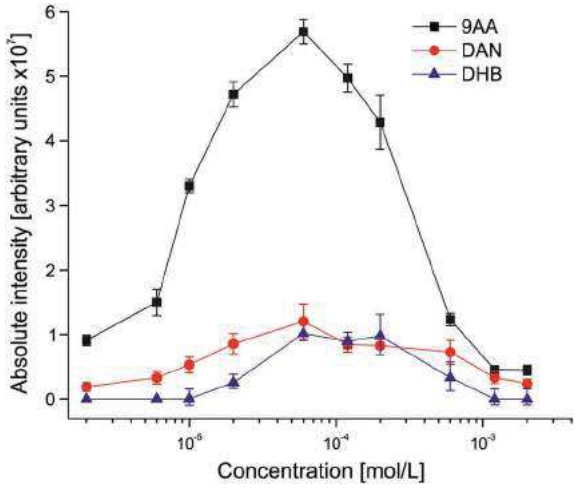

Figure 2. Dependences of absolute intensities of $[M+H]^+$ ions of PC 32:1 on the concentration measured using 9AA, DAN or DHB matrix.

concentration region with the monotonic dependence of peak intensities to be determined, which is used for further experiments.

Another parameter influencing MALDI mass spectra is the laser energy. The optimal laser energy is determined using standard procedures of the LTQ Orbitrap XL software and varied within ±30% around that value. No significant variations in responses to synthesized PC are observed.

One of the reasons that could cause discrimination in signal intensity is that during the sample drying, the moving edge of the evaporating droplet can support processes similar to those in the chromatography resulting in uneven analyte distribution. These processes may result in response differences over local regions of the sample spot. The measurement in multiple random points over a sample spot improves the representative data sampling. Relative intensities for synthesized PC from spectra corresponding to randomly distributed spots over one well with a sample are shown in Supplementary Figs. S5–S7 (see Supporting Information). Similar picture is observed for other spots. Figures represent data for matrices used in the study. Relative standard deviations of absolute intensities are relatively high. They are around 20, 16 and 38% for samples measured with 9AA, DHB and DAN, respectively. At the same time, relative intensities vary to a smaller extent. Relative standard deviations of intensities normalized to the internal standard are around 7.6, 8.9 and 13.6% for samples measured with 9AA, DHB and DAN. In addition, deviations of normalized intensities are correlated demonstrating relatively even distribution of compounds over the spot. Analysis of Supplementary Fig. S8 (see Supporting Information) shows that differences between observed values of normalized intensities for different PC are significant compared with ranges of signal deviation.

Response dependences on fatty acyl length and DB number

Calibration curves for the synthesized PC are constructed after the addition of PC 17:0/17:0 as the IS to prepared series with different concentrations. Logarithmic plots of the normalized signal of $[M+H]^+$ ions *vs.* the molar ratio of PC to IS are shown in Fig. 3 for 9AA matrix with the RSD approximately 3% (Supplementary Fig. S9, see Supporting Information, represents similar data for two other replicative syntheses). The average of the regression coefficients is 0.997 ± 0.003 (Supplementary Table S1, see Supporting Information). Calibration curves can be described by a linear equation:

$$y = s * x + i \quad (1)$$

where s and i are parameters corresponding to the slope and intercept of the calibration curves and

$$y = \log\left(\frac{I_x}{I_{IS}}\right), x = \log\left(\frac{c_x}{c_{IS}}\right) \quad (2)$$

where I_x, c_x are the intensity and concentration of synthesized PC, I_{IS} and c_{IS} are the intensity and concentration of the IS (PC 17:0/17:0). Parameters of these dependences are summarized in Supplementary Table S1 (see Supporting Information). Dependences of s and i on the CN of fatty acyls are constructed based on this data (Fig. 4). Dots corresponding to parameters of calibration curves of lipids that differ in chain length only can be well approximated with linear functions (Table 2):

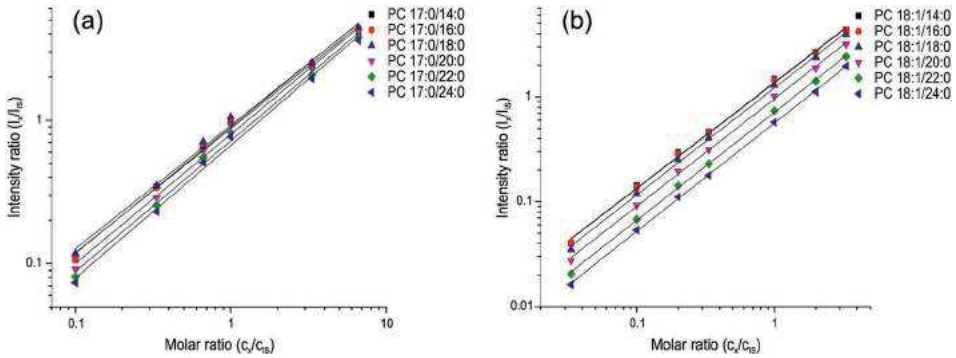

Figure 3. Logarithmic correlation of normalized intensities of $[M+H]^+$ ions and normalized molar ratios of synthesized PC to IS (PC 17:0/17:0) measured using 9AA as the matrix: (a) PC 17:0/*x*:*y* and (b) PC 18:1/*x*:*y* series. The result is for one synthetic procedure.

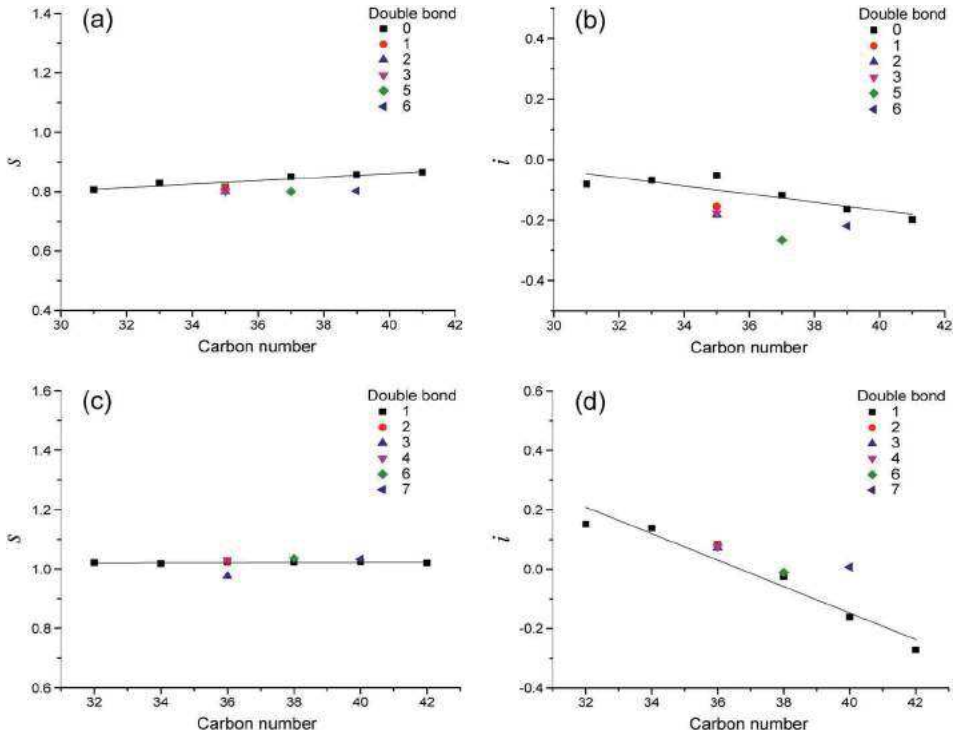

Figure 4. Linear dependences of: (a) slopes (*s*) for PC 17:0/*x vs.* the carbon number, (b) intercepts (*i*) for PC 17:0/*x:y vs.* the carbon number, (c) slopes (*s*) for PC 18:1/*x:y vs.* the carbon number, and (d) intercepts (*i*) for PC 18:1/*x:y vs.* the carbon number. Samples measured using 9AA as the matrix. The result is for one synthetic procedure.

Table 2. Coefficients of linear fitting of corresponding parameters (*s* and *i*) of calibration curves in their dependence on CN (Fig. 5 and Supplementary Figs. S6 and S7, see Supporting Information)

Matrix	Lipid series	Parameter of calibration curve	Slope[a]	Intercept[b]	Regression coefficient (r^2)	Power of analysis	p-value
9AA	PC 17:0/x:0	s^c	0.006	0.673	0.826	0.97	0.01
		i^d	–0.013	0.391	0.703	0.80	0.02
	PC 18:1/x:0	s^c	0.003	0.917	−0.153	-	0.59
		i^d	–0.041	1.470	0.924	1.00	0.00
DHB	PC 17:0/x:0	s^c	–0.038	2.108	0.956	1.00	0.00
		i^d	0.001	0.007	−0.248	-	0.94
	PC 18:1/x:0	s^c	–0.083	4.739	0.946	1.00	0.00
		i^d	–0.099	5.511	0.789	0.94	0.01
DAN	PC 17:0/x:0	s^c	0.031	–0.158	0.738	0.86	0.02
		i^d	0.021	–1.367	0.257	0.20	0.17
	PC 18:1/x:0	s^c	0.002	0.900	0.382	0.32	0.11
		i^d	–0.029	0.998	0.947	1.00	0.00

[a]Slope of the linear dependence of calibration curve parameter on the carbon number.
[b]Intercept of the linear dependence of calibration curve parameter on the carbon number.
[c]Slope of the calibration curve.
[d]Intercept of the calibration curve.

$$s = 0.006*\mathrm{CN} + 0.673 \quad (3)$$

$$i = -0.013*\mathrm{CN} + 0.391 \quad (4)$$

for the series of saturated PC and

$$s = 0.003*\mathrm{CN} + 0.917 \quad (5)$$

$$i = -0.041 * \mathrm{CN} + 1.470 \quad (6)$$

for monounsaturated PC. The dependence is not very steep, which is represented by the values of multipliers of CN close to zero. Values of the slope for PC 18:1/*x:y* are less dependent on CN than for PC 17:0/*x:y* and the trend is reversed for intercepts. Figure 4 illustrates the effects of CN and DB on the relative responses of PC. Intensities of saturated PC are very similar (Fig. 1(a), PC 17:0/*x*:0 series), but intensities of monounsaturated species decrease for

higher CN (Fig. 1(b), PC 18:1/*x*:0 series). The influence of DB number can be estimated from the series of PC 17:0/18:0, PC 17:0/18:1 and PC 17:0/18:2 showing a small incremental decrease in intensity for unsaturated PC. This effect is much stronger for polyunsaturated PC, e.g. the comparison of the pairs PC 17:0/20:0 and PC 17:0/20:5, PC 17:0/22:0 and PC 17:0/22:6 (Fig. 1(a)) with the relative signal decrease of *ca*. 25–30% for polyunsaturated fatty acyls related to saturated ones.

For the explanation of *s* and *i* values, the following expression can be deduced from Eqns. (1) and (2):

$$\frac{I_x}{I_{IS}} = 10^i \left(\frac{c_x}{c_{IS}}\right)^s \quad (7)$$

which demonstrates the relationship between MS peak intensity of a compound and its concentration and also influence of parameters of calibration curves on this relationship. It is obvious from Eqn. (7) that *s* determines the shape of the dependence and *i* plays a role in the determination of the scaling factor. Thus, taking into account Eqns. (3)–(6) and values in Supplementary Table S1 (see Supporting Information) and Fig. 4, one can conclude that the dependence of the intensity on the concentration is nearly linear as values of *s* are close to 1 and that the scaling factor in Eqn. (7) is more strongly influenced by the fatty acyl chain lengths in the case of monounsaturated PC than for saturated PC.

Several points corresponding to polyunsaturated PC are also depicted in Fig. 4. It is impossible to build dependences similar to PC 17:0/*x*:*y* and PC 18:1/*x*:*y* due to the lack of series of data points. Nevertheless, it is evident that these points are relatively close to the monounsaturated PC series (Figs. 4(c) and 4(d)) and, thus, Eqns. (5) and (6) can be used for a rough estimation of parameters of calibration curves for polyunsaturated PC as well.

Accounting the dependence of parameters of the calibration curve on CN for saturated PC may result in corrections to the determined concentration of about 10%, which is determined by the largest difference between the peak intensities of PC 17:0/14:0 and PC 17:0/24:0. This value is comparable to the experimental error in MALDI analysis of saturated PC with 9AA. The assumption about equal responses can be accepted. In the case of unsaturated PC, the picture is different and the value of correction can reach 60% for PC with CN difference equal to 10. Thus taking into account the influence of the acyl chain length can improve the estimation of concentration of unsaturated PC.

A similar study was performed for the same PC samples measured with DHB or DAN matrices. The results of this study are summarized in Supplementary Figs. S10–S13 and Supplementary Tables S2 and S3 (see Supporting Information). In general, lipids measured with DHB and DAN also show dependences of their responses on fatty acyls, but this dependence is much stronger than for the 9AA matrix. Parameters of linear dependences are fitted with regression coefficients on average equal to 0.91 ± 0.06 for DHB and 0.98 ± 0.00 for DAN, which is somewhat worse compared to 9AA. Relative standard deviations of peak intensities are also higher, on average18% for DHB and 40% for DAN. These facts make cautious the use of data and equations obtained with DHB and DAN for predictive measurements without using several IS.

Table 2 shows parameters of calibration curves for all three matrices. Similar data are calculated for all three replicate syntheses and obtained parameters are close to each other within errors of measurements and calculations.

Application of the developed method for PC standard mixtures and human plasma

The developed method was first applied for the analysis of mixtures of PC standards with known concentrations. Concentrations of these standards are calculated using information about mass spectrometric intensities with and without accounting for differences in relative responses of PC. In the first case, concentrations are obtained by multiplying the ratio of the PC intensity to IS with IS concentration. In the second case, they are calculated with Eqn. (7) using the data from Table 2. Comparisons of PC concentrations known from the mixture preparation with concentrations calculated from MS data are presented in Tables 3–5. Errors in Tables 3–5 are found as difference between concentrations known from preparation and from MS data divided by the concentration known from the preparation and multiplied by 100. Results show that

Table 3. Concentrations of lipid standards in mixtures 1 and 2 prepared by weighing and determined from MALDI measurements using 9AA matrix with and without the use of response correction

	Concentration [µmol/L]			Relative error [%]	
Lipid	Weighed	Without response correction	With response correction	Without response correction	With response correction
			Mixture 1		
PC 16:0/16:0	3.0	3.5 ± 0.3	2.8 ± 0.1	18	5
PC 18:1/18:1	3.0	2.7 ± 0.2	2.6 ± 0.1	10	13
PC 20:4/20:4	3.0	2.2 ± 0.2	3.2 ± 0.1	26	8
PC 22:0/22:0	3.0	3.2 ± 0.2	3.0 ± 0.1	6	1
			Mixture 2		
PC 16:0/16:0	1.2	1.8 ± 0.1	1.2 ± 0.0	47	2
PC 18:1/18:1	6.0	6.3 ± 0.4	5.9 ± 0.3	5	1
PC 20:4/20:4	0.4	0.3 ± 0.0	0.4 ± 0.0	30	10
PC 22:0/22:0	15.0	13.7 ± 1.0	15.2 ± 3.7	9	1

Rapid Communications in Mass Spectrometry

Table 4. Concentrations of lipid standards in mixtures 1 and 2 prepared by weighing and determined from MALDI measurements using DHB matrix with and without the use of response correction

	Concentration [μmol/L]			Relative error [%]	
Lipid	Weighed	Without response correction	With response correction	Without response correction	With response correction
			Mixture 1		
PC 16:0/16:0	3.0	4.0 ± 0.8	3.0 ± 1.7	32	2
PC 18:1/18:1	3.0	2.8 ± 0.8	2.7 ± 0.8	6	10
PC 20:4/20:4	3.0	2.5 ± 0.5	3.3 ± 0.7	17	10
PC 22:0/22:0	3.0	1.3 ± 0.8	3.3 ± 0.3	57	9
			Mixture 2		
PC 16:0/16:0	1.2	1.9 ± 0.4	1.4 ± 0.2	59	18
PC 18:1/18:1	6.0	6.5 ± 2.4	6.5 ± 2.2	8	9
PC 20:4/20:4	0.4	0.3 ± 0.1	0.4 ± 0.0	19	4
PC 22:0/22:0	15.0	3.3 ± 2.1	9.3 ± 5.8	78	38

Table 5. Concentrations of lipid standards in mixtures 1 and 2 prepared by weighing and determined from MALDI measurements using DAN matrix with and without the use of response correction

	Concentration [μmol/L]			Relative error [%]	
Lipid	Weighed	Without response correction	With response correction	Without response correction	With response correction
			Mixture 1		
PC 16:0/16:0	3.0	3.1 ± 1.0	2.8 ± 0.2	20	6
PC 18:1/18:1	3.0	3.1 ± 0.8	3.2 ± 0.2	3	8
PC 20:4/20:4	3.0	3.6 ± 0.7	3.5 ± 0.1	20	17
PC 22:0/22:0	3.0	1.9 ± 0.5	1.9 ± 0.1	36	36
			Mixture 2		
PC 16:0/16:0	1.2	1.3 ± 0.3	1.1 ± 0.1	12	5
PC 18:1/18:1	6.0	6.5 ± 1.6	6.3 ± 2.0	8	5
PC 20:4/20:4	0.4	0.5 ± 0.1	0.4 ± 0.0	19	12
PC 22:0/22:0	15.0	24.8 ± 7.0	7.4 ± 4.1	65	50

taking into account the effect of fatty acyl parameters on PC detection efficiency significantly improves the determination of concentration of PC by MALDI-MS. Parameters of monounsaturated PC are used in calculations for polyunsaturated PC due to the lack of polyunsaturated PC standards, so the precision of concentrations for highly unsaturated PC may be slightly reduced.

The method was also applied for a sample of human plasma from a healthy volunteer. The positive-ion MALDI mass spectrum of this sample is presented in Fig. 5. PC 34:1 and PC 36:2 species are quantified by the method of IS addition. The results of this quantitation are summarized in Table 6 together with concentrations calculated using the ratio of PC peak intensity to the IS without and with the response factor. The errors listed in Table 6 were calculated in a way similar to the errors in Tables 3–5, but the concentration found with the IS addition method is used as the reference. This data also demonstrates a satisfactory agreement between concentrations found with different methods and a decrease in error using response factors is observed in most cases. Table 7 demonstrates results on PC concentrations in the human plasma normalized to PC 34:0 with and without

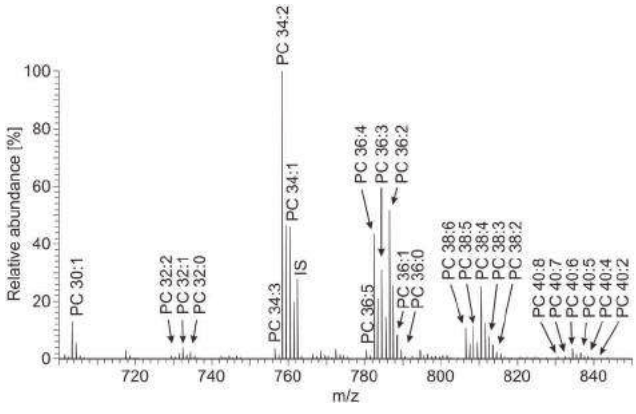

Figure 5. Positive-ion MALDI mass spectrum of human plasma lipid extract with added PC 17:0/17:0 as the internal standard (IS) and measured using 9AA as the matrix.

correction, compared with the normalized data from the literature.[42] The data for some PC correlate well, but in some cases higher differences are observed, which may be attributed to the fact that human plasma samples are not identical.

Table 6. Comparison of concentrations of selected PC in human plasma determined by the standard addition method and calculated from MALDI measurements with and without the use of response factors using different matrices

	Concentration [μmol/L]			Relative error [%]	
Lipids	Standard addition	Calculated without response factor	Calculated with response factor	Without response factor	With response factor
			9AA		
PC 34:1	82.2 ± 4.1	69.1 ± 6.7	74.0 ± 5.4	16	10
PC 36:2	96.8 ± 6.8	85.3 ± 7.7	102.9 ± 7.7	12	6
			DHB		
PC 34:1	82.2 ± 4.1	136.2 ± 29.5	111.8 ± 30.2	64	36
PC 36:2	96.8 ± 6.8	114.2 ± 24.4	115.1 ± 23.4	18	19
			DAN		
PC 34:1	82.2 ± 4.1	73.1 ± 10.6	71.78 ± 9.3	11	13
PC 36:2	96.8 ± 6.8	78.4 ± 12.2	88.8 ± 10.0	19	8

Table 7. Relative concentrations of PC in human plasma normalized on total PC content and multiplied by 1000 PC

	Relative concentration		
Lipid	Without response factor	With response factor	Literature data
PC 30:1	0.1 ± 0	0.1 ± 0	0.6 ± 0.1
PC 32:2	1.8 ± 0.1	1.2 ± 0.1	5.3 ± 0.2
PC 32:1	9.7 ± 0.2	6.3 ± 0.6	15.4 ± 1
PC 32:0	5.6 ± 0.4	3.6 ± 0.2	6.1 ± 0.3
PC 34:3	13.8 ± 0.7	10.8 ± 0.3	7.4 ± 0.5
PC 34:2	266 ± 25.1	196.9 ± 12	101.1 ± 7.5
PC 34:1	89 ± 1.2	92.5 ± 0.4	48 ± 4.4
PC 36:5	8.6 ± 0.5	8.3 ± 0.8	6.9 ± 0.6
PC 36:4	117.5 ± 11.2	108.3 ± 6.6	92.5 ± 5.9
PC 36:3	97.4 ± 2	90.1 ± 6.9	88.7 ± 7
PC 36:2	109.9 ± 0.5	128.7 ± 10.9	136.6 ± 9.7
PC 36:1	20 ± 1.6	19.1 ± 0.3	53.7 ± 7
PC 36:0	1.8 ± 0.1	1.8 ± 0	4.3 ± 0.8
PC 38:6	29 ± 0.4	33.7 ± 1.5	33.8 ± 2.6
PC 38:5	30.3 ± 0.9	35.2 ± 2.7	46.4 ± 4.8
PC 38:4	69.1 ± 1.9	78.9 ± 4	136.6 ± 11.3
PC 38:2	2.5 ± 0.1	3.1 ± 0.2	20.2 ± 3.1
PC 40:8	26.3 ± 2	37.6 ± 0.6	14.5 ± 1.3
PC 40:7	61.8 ± 4.7	86.7 ± 3	12.4 ± 2.4
PC 40:6	29.9 ± 2.9	42.6 ± 3.4	42.7 ± 5.5
PC 40:5	7.4 ± 0.3	10.9 ± 0.6	35.8 ± 5.4
PC 40:4	2.4 ± 0.1	3.6 ± 0.1	19.6 ± 3
PC 40:2	0 ± 0	0 ± 0	71.5 ± 8.6

Concentrations calculated from MALDI measurements using 9AA with and without the response factors and calculated from literature data.[42]

CONCLUSIONS

The present work demonstrates that the efficiency of PC detection in positive-ion MALDI-MS depends on fatty acyl chain length and DB number. Linear dependences are observed for all three matrices (9AA, DHB or DAN), while the steepness of these dependences differs for individual matrices and the saturation level of the PC. Relative responses of saturated PC with 9AA are the least dependent on the fatty acyl chain length and therefore the most convenient for quantitation applications. The effect of fatty acyl chain length on correction factors must be taken into account for DHB or DAN matrices with both saturated and unsaturated PC as well as with unsaturated PC with 9AA matrix. For a rough estimation, the results of PC quantitation obtained with 9AA matrix can be used without correction. Data obtained with DAN and especially with DHB are better to use mainly for the qualitative comparison or for the relative quantitation, taking into account the high signal deviation and strong dependence of PC responses on both CN and DB. Another way is to use one IS and the model for the calculation of PC concentrations, which accounts for differences in their responses. This model must be created in advance and based on preliminary investigation of PC with different compositions. This last approach provides good results for 9AA and slightly higher variations for DHB and DAN matrices.

Acknowledgements

This work was supported by ERC CZ Project No. LL1302 sponsored by the Ministry of Education, Youth and Sports of the Czech Republic. V.C. acknowledges the support of Grant Project No. CZ.1.07/2.3.00/30.0021 sponsored by the Ministry of Education, Youth and Sports of the Czech Republic. The help of Magdalena Ovčačíková (University of Pardubice) with the sample preparation is acknowledged. The authors also acknowledge the Faculty Hospital Olomouc for the supplied human blood samples.

REFERENCES

[1] W. Dowhan. Molecular basis for membrane phospholipid diversity: Why are there so many lipids? *Annu. Rev. Biochem.* **1997**, *66*, 199.
[2] A. Shevchenko, K. Simons. Lipidomics: coming to grips with lipid diversity. *Nat. Rev. Mol. Cell Biol.* **2010**, *11*, 593.
[3] A. Thomas, J. Deglon, S. Lenglet, F. Mach, P. Mangin, J. L. Wolfender, S. Steffens, C. Staub. High-throughput phospholipidic fingerprinting by online desorption of dried spots and quadrupole-linear ion trap mass

spectrometry: Evaluation of atherosclerosis biomarkers in mouse plasma. *Anal. Chem.* **2010**, *82*, 6687.
[4] L. A. Hammad, G. X. Wu, M. M. Saleh, I. Klouckova, L. E. Dobrolecki, R. J. Hickey, L. Schnaper, M. V. Novotny, Y. Mechref. Elevated levels of hydroxylated phosphocholine lipids in the blood serum of breast cancer patients. *Rapid Commun. Mass Spectrom.* **2009**, *23*, 863.
[5] K. Ekroos, in *Lipidomics*. Wiley-VCH, Weinheim, **2012**, p. 1.
[6] E. Cífková, M. Holčapek, M. Lísa, D. Vrána, J. Gatěk, B. Melichar. Determination of lipidomic differences between human breast cancer and surrounding normal tissues using HILIC-HPLC/ESI-MS and multivariate data analysis. *Anal. Bioanal. Chem.* **2015**, *407*, 991.
[7] M. R. Wenk. The emerging field of lipidomics. *Nat. Rev. Drug Discov.* **2005**, *4*, 594.
[8] H. Jiang, M. A. Kiebish, D. A. Kirschner, X. Han, in *Lipidomics*. Wiley-VCH, Weinheim, **2012**, p. 53.
[9] Y. Liu, Y. Chen, M. C. Sullards, in *Lipidomics*. Wiley-VCH, Weinheim, **2012**, p. 73.
[10] M. Ståhlman, J. Borén, K. Ekroos, in *Lipidomics*. Wiley-VCH, Weinheim, **2012**, p. 35.
[11] A. Thomas, S. Lenglet, P. Chaurand, J. Deglon, P. Mangin, F. Mach, S. Steffens, J. L. Wolfender, C. Staub. Mass spectrometry for the evaluation of cardiovascular diseases based on proteomics and lipidomics. *Thrombosis Haemostasis* **2011**, *106*, 20.
[12] F. Hillenkamp, M. Karas, in *MALDI MS*. Wiley-VCH, Weinheim, **2007**, p. 1.
[13] J. Schiller, J. Arnhold, S. Benard, M. Muller, S. Reichl, K. Arnold. Lipid analysis by matrix-assisted laser desorption and ionization mass spectrometry: A methodological approach. *Anal. Biochem.* **1999**, *267*, 46.
[14] H. Hidaka, N. Hanyu, M. Sugano, K. Kawasaki, K. Yamauchi, T. Katsuyama. Analysis of human serum lipoprotein lipid composition using MALDI-TOF mass spectrometry. *Ann. Clin. Lab. Sci.* **2007**, *37*, 213.
[15] T. Fujiwaki, M. Tasaka, S. Yamaguchi. Quantitative evaluation of sphingomyelin and glucosylceramide using matrix-assisted laser desorption ionization time-of-flight mass spectrometry with sphingosylphosphorylcholine as an internal standard Practical application to tissues from patients with Niemann-Pick disease types A and C, and Gaucher disease. *J. Chromatogr. B – Anal. Technol. Biomed. Life Sci.* **2008**, *870*, 170.
[16] M. W. Duncan, H. Roder, S. W. Hunsucker. Quantitative matrix-assisted laser desorption/ionization mass spectrometry. *Brief. Funct. Genomics Proteomics* **2008**, *7*, 355.
[17] B. Brugger, G. Erben, R. Sandhoff, F. T. Wieland, W. D. Lehmann. Quantitative analysis of biological membrane lipids at the low picomole level by nano-electrospray ionization tandem mass spectrometry. *Proc. Natl. Acad. Sci. USA* **1997**, *94*, 2339.
[18] M. Koivusalo, P. Haimi, L. Heikinheimo, R. Kostiainen, P. Somerharju. Quantitative determination of phospholipid compositions by ESI-MS: effects of acyl chain length, unsaturation, and lipid concentration on instrument response. *J. Lipid Res.* **2001**, *42*, 663.
[19] M. Petkovic, J. Schiller, M. Muller, S. Benard, S. Reichl, K. Arnold, J. Arnhold. Detection of individual phospholipids in lipid mixtures by matrix-assisted laser desorption/ionization time-of-flight mass spectrometry: Phosphatidylcholine prevents the detection of further species. *Anal. Biochem.* **2001**, *289*, 202.
[20] S. N. Jackson, H. Y. J. Wang, A. S. Woods. In situ structural characterization of phosphatidylcholines in brain tissue using MALDI-MS/MS. *J. Am. Soc. Mass Spectrom.* **2005**, *16*, 2052.
[21] H. Y. J. Wang, C. B. Liu, H. W. Wu. A simple desalting method for direct MALDI mass spectrometry profiling of tissue lipids. *J. Lipid Res.* **2011**, *52*, 840.
[22] J. Schiller, in *MALDI MS*. Wiley-VCH, Weinheim, **2007**, pp. 215.
[23] V. Zabrouskov, K. A. Al-Saad, W. F. Siems, H. H. Hill, N. R. Knowles. Analysis of plant phosphatidylcholines by matrix-assisted laser desorption/ionization time-of-flight mass spectrometry. *Rapid Commun. Mass Spectrom.* **2001**, *15*, 935.
[24] R. R. Landgraf, T. J. Garrett, M. C. Prieto Conaway, N. A. Calcutt, P. W. Stacpoole, R. A. Yost. Considerations for quantification of lipids in nerve tissue using matrix-assisted laser desorption/ionization mass spectrometric imaging. *Rapid Commun. Mass Spectrom.* **2011**, *25*, 3178.
[25] S. Benard, J. Arnhold, M. Lehnert, J. Schiller, K. Arnold. Experiments towards quantification of saturated and polyunsaturated diacylglycerols by matrix-assisted laser desorption and ionization time-of-flight mass spectrometry. *Chem. Phys. Lipids* **1999**, *100*, 115.
[26] G. Sun, K. Yang, Z. Zhao, S. Guan, X. Han, R. W. Gross. Matrix-assisted laser desorption/ionization time-of-flight mass spectrometric analysis of cellular glycerophospholipids enabled by multiplexed solvent dependent analyte-matrix interactions. *Anal. Chem.* **2008**, *80*, 7576.
[27] B. Fuchs, J. Schiller. Recent developments of useful MALDI matrices for the mass spectrometric characterization of apolar compounds. *Curr. Org. Chem.* **2009**, *13*, 1664.
[28] D. J. Harvey. Matrix-assisted laser-desorption ionization mass-spectrometry of phospholipids. *J. Mass Spectrom.* **1995**, *30*, 1333.
[29] A. Thomas, J. L. Charbonneau, E. Fournaise, P. Chaurand. Sublimation of new matrix candidates for high spatial resolution imaging mass spectrometry of lipids: Enhanced information in both positive and negative polarities after 1,5-diaminonapthalene deposition. *Anal. Chem.* **2012**, *84*, 2048.
[30] M. Lísa, M. Holčapek. Characterization of triacylglycerol enantiomers using chiral HPLC/APCI-MS and synthesis of enantiomeric triacylglycerols. *Anal. Chem.* **2013**, *85*, 1852.
[31] J. Folch, M. Lees, G. H. S. Stanley. *J. Biol. Chem.* **1957**, *226*, 497.
[32] M. C. Chambers, B. Maclean, R. Burke, D. Amodei, D. L. Ruderman, S. Neumann, L. Gatto, B. Fischer, B. Pratt, J. Egertson, K. Hoff, D. Kessner, N. Tasman, N. Shulman, B. Frewen, T. A. Baker, M. Y. Brusniak, C. Paulse, D. Creasy, L. Flashner, K. Kani, C. Moulding, S. L. Seymour, L. M. Nuwaysir, B. Lefebvre, F. Kuhlmann, J. Roark, P. Rainer, S. Detlev, T. Hemenway, A. Huhmer, J. Langridge, B. Connolly, T. Chadick, K. Holly, J. Eckels, E. W. Deutsch, R. L. Moritz, J. E. Katz, D. B. Agus, M. MacCoss, D. L. Tabb, P. Mallick. A cross-platform toolkit for mass spectrometry and proteomics. *Nat. Biotechnol.* **2012**, *30*, 918.
[33] S. Gibb, K. Strimmer. MALDIquant: a versatile R package for the analysis of mass spectrometry data. *Bioinformatics* **2012**, *28*, 2270.
[34] LipidMAPS. Available: http://www.lipidmaps.org.
[35] G. Liebisch, J. A. Vizcaino, H. Kofeler, M. Trotzmuller, W. J. Griffiths, G. Schmitz, F. Spener, M. J. O. Wakelam. Shorthand notation for lipid structures derived from mass spectrometry. *J. Lipid Res.* **2013**, *54*, 1523.
[36] R. Estrada, M. C. Yappert. Alternative approaches for the detection of various phospholipid classes by matrix-assisted laser desorption/ionization time-of-flight mass spectrometry. *J. Mass Spectrom.* **2004**, *39*, 412.
[37] P. Domingues, M. R. M. Domingues, F. M. L. Amado, A. J. Ferrer-Correia. Characterization of sodiated glycerol phosphatidylcholine phospholipids by mass spectrometry. *Rapid Commun. Mass Spectrom.* **2001**, *15*, 799.
[38] K. A. Al-Saad, W. F. Siems, H. H. Hill, V. Zabrouskov, N. R. Knowles. Structural analysis of phosphatidylcholines

by post-source decay matrix-assisted laser desorption/ionization time-of-flight mass spectrometry. *J. Am. Soc. Mass Spectrom.* **2003**, *14*, 373.
[39] Y. J. Liu, E. Lotero, J. G. Goodwin. Effect of carbon chain length on esterification of carboxylic acids with methanol using acid catalysis. *J. Catal.* **2006**, *243*, 221.
[40] B. Selmi, E. Gontier, F. Ergan, D. Thomas. Effects of fatty acid chain length and unsaturation number on triglyceride synthesis catalyzed by immobilized lipase in solvent-free medium. *Enzyme Microbial Technol.* **1998**, *23*, 182.
[41] A. E. M. Janssen, A. Vanderpadt, K. Vantriet. Solvent effects on lipase-catalyzed esterification of glycerol and fatty-acids. *Biotechnol. Bioeng.* **1993**, *42*, 953.
[42] O. Quehenberger, A. M. Armando, A. H. Brown, S. B. Milne, D. S. Myers, A. H. Merrill, S. Bandyopadhyay, K. N. Jones, S. Kelly, R. L. Shaner, C. M. Sullards, E. Wang, R. C. Murphy, R. M. Barkley, T. J. Leiker, C. R. Raetz, Z. Guan, G. M. Laird, D. A. Six, D. W. Russell, J. G. McDonald, S. Subramaniam, E. Fahy, E. A. Dennis. Lipidomics reveals a remarkable diversity of lipids in human plasma. *J. Lipid Res.* **2010**, *51*, 3299.

SUPPORTING INFORMATION

Additional supporting information may be found in the online version of this article at the publisher's website.

Journal of Chromatography A, 1525 (2017) 96–108

Contents lists available at ScienceDirect

Journal of Chromatography A

journal homepage: www.elsevier.com/locate/chroma

Lipidomic analysis of biological samples: Comparison of liquid chromatography, supercritical fluid chromatography and direct infusion mass spectrometry methods

Miroslav Lísa*, Eva Cífková, Maria Khalikova, Magdaléna Ovčačíková, Michal Holčapek

Department of Analytical Chemistry, Faculty of Chemical Technology, University of Pardubice, Studentská 573, 53210 Pardubice, Czech Republic

ARTICLE INFO

Article history:
Received 20 January 2017
Received in revised form
25 September 2017
Accepted 7 October 2017
Available online 8 October 2017

Keywords:
Lipidomics
Lipidomic analysis
UHPLC
UHPSFC
Direct infusion
Mass spectrometry

ABSTRACT

Lipidomic analysis of biological samples in a clinical research represents challenging task for analytical methods given by the large number of samples and their extreme complexity. In this work, we compare direct infusion (DI) and chromatography – mass spectrometry (MS) lipidomic approaches represented by three analytical methods in terms of comprehensiveness, sample throughput, and validation results for the lipidomic analysis of biological samples represented by tumor tissue, surrounding normal tissue, plasma, and erythrocytes of kidney cancer patients. Methods are compared in one laboratory using the identical analytical protocol to ensure comparable conditions. Ultrahigh-performance liquid chromatography/MS (UHPLC/MS) method in hydrophilic interaction liquid chromatography mode and DI-MS method are used for this comparison as the most widely used methods for the lipidomic analysis together with ultrahigh-performance supercritical fluid chromatography/MS (UHPSFC/MS) method showing promising results in metabolomics analyses. The nontargeted analysis of pooled samples is performed using all tested methods and 610 lipid species within 23 lipid classes are identified. DI method provides the most comprehensive results due to identification of some polar lipid classes, which are not identified by UHPLC and UHPSFC methods. On the other hand, UHPSFC method provides an excellent sensitivity for less polar lipid classes and the highest sample throughput within 10 min method time. The sample consumption of DI method is 125 times higher than for other methods, while only 40 μL of organic solvent is used for one sample analysis compared to 3.5 mL and 4.9 mL in case of UHPLC and UHPSFC methods, respectively. Methods are validated for the quantitative lipidomic analysis of plasma samples with one internal standard for each lipid class. Results show applicability of all tested methods for the lipidomic analysis of biological samples depending on the analysis requirements.

1. Introduction

Lipidomics [1] is a branch of metabolomics aimed at the analysis of lipid species and their biological functions in organism. Lipids play multiple roles in cellular functions, act as messengers in cell signaling, and they are potential biomarkers for some serious human diseases. According to their definition [2,3], lipids represent varied groups of compounds with large differences in their structures and physicochemical properties, which is demanding for analytical techniques used in the lipidomic analysis. Nowadays, mass spectrometry (MS) is a key technique in the lipidomic analysis of biological samples thanks to significant advances in last years. Mainly two approaches are used in the MS lipidomic analysis, such as direct infusion (DI)-MS lipidomics (often called shotgun lipidomics) and liquid chromatography/MS lipidomics, which are used almost equally in the literature [4,5].

DI-MS lipidomics represents analytical methods without any preseparation step. Lipid extracts are directly infused into the ion source of mass spectrometer, where all lipids are ionized together. Lipids are detected based on MS(/MS) spectra acquired by high resolving power/high mass accuracy analyzers [6–9] or more often using MS/MS scans (*i.e.*, precursor ion (PI), neutral loss (NL), and selected reaction monitoring (SRM) scans) based on the characteristic fragmentation behavior of individual lipid classes measured on

* Corresponding author.
E-mail address: miroslav.lisa@gmail.com (M. Lísa).

https://doi.org/10.1016/j.chroma.2017.10.022
0021-9673/

triple quadrupole or quadrupole-linear ion trap mass spectrometers [10–13]. These methods are widely used for the analysis of large sample sets in a clinical research, because they are high-throughput and easy to automate with robotic systems providing accurate and reproducible quantitative data. On the other hand, determination of isomers, isobaric species or trace species is often difficult as they are analyzed in the mixture.

These problems are overcome by separation step in the case of chromatography/MS lipidomics, where different chromatographic modes can be selected for the separation of all kinds of isomerism. Furthermore, the separation of lipids avoids of ion suppression effect during the ionization process, which can be serious mainly for species with ionic head groups. Liquid chromatography (LC) is the most widely used chromatographic technique for the comprehensive lipidomic analysis. Lipids can be separated into individual species using reversed-phase (RP) separation [14–21] according to their fatty acyl composition, *i.e.*, fatty acyl length and number of double bonds (DB). Hydrophilic interaction liquid chromatography (HILIC) enables a class separation of lipids according to their polarity and charge [14,15,22–26], while lipids differing in the fatty acyl composition coelute together in one chromatographic peak corresponding to the lipid class. HILIC methods usually do not provide the separation of nonpolar lipids, which are not retained and elute in the column void volume. These lipids are separated using normal phase (NP) mode according to their polarity [22,25,27–29], but this mode cannot be used for more polar lipids due to their strong retention under such conditions. Serial coupling of HILIC and RP columns in mixed-mode liquid chromatography combines lipid class separation of lipids with better selectivity of lipid species within the lipid class [30]. HILIC and DI methods have been combined into one mass spectrometry-based lipidomics platform for the analysis of phospholipids and sphingolipids [31]. In last years, supercritical fluid chromatography (SFC) has become more popular chromatographic technique in metabolomic analyses including lipidomics. We have demonstrated that SFC using sub-two μm hybrid silica column has a great potential as the comprehensive and high-throughput screening method enabling the class separation of nonpolar and polar lipids in one 6 min analysis [32]. C18 columns are often used for SFC separations of individual lipid species according to the fatty acyl composition, such as the lipidomic analysis of intact [33] or methylated [34] species, the separation of TG [35], oxidized PC [36], carotenoids [37] or TG regioisomers [38].

The quantitative lipidomic analysis brings many challenges for analysts due to enormous complexity of lipidomic samples, because the utilization of corresponding standards for all species is impossible. Selected exogenous lipids with unusual composition of fatty acyls are used as internal standards (IS) for each lipid class (*e.g.*, short/long fatty acyls, combination of odd and even carbon or deuterated fatty acyls) and the concentration of individual species is calculated as the ratio of their signals related to the signal of IS [6,9,11–13,24,32]. This simplification using IS for all species within given lipid class brings reliable quantitative data for case/control studies.

The aim of this work is a comparison of chromatography/MS and DI-MS approaches for the lipidomic analysis of biological samples. For this purpose, HILIC ultrahigh-performance liquid chromatography (UHPLC)/MS and ultrahigh-performance supercritical fluid chromatography (UHPSFC)/MS methods are compared with DI-MS method in one laboratory using identical analytical protocol. Lipids in tumor tissue, surrounding normal tissue, plasma and erythrocytes pooled samples of kidney cancer patients are identified using each method to demonstrate their capabilities for the analysis of various lipid classes in complex biological matrices. Each method is validated for the quantitative lipidomic analysis of plasma samples using IS per each lipid class and the lipidomic composition of 6 plasma samples is determined.

2. Experimental

2.1. Materials

Acetonitrile, 2-propanol, methanol (all HPLC/MS grade), hexane, chloroform stabilized with 0.5–1% ethanol (both HPLC grade), ammonium acetate, and acetic acid were purchased from Sigma-Aldrich (St. Louis, MO, USA). Deionized water was prepared with a Milli-Q ReferenceWater Purification System (Molsheim, France). Carbon dioxide 4.5 grade (99.995%) was purchased from Messer Group Gmbh (Bad Soden, Germany). Lipid class IS were used for the method validation and quantitative analysis, *i.e.*, DG 12:1/0:0/12:1, MG 19:1/0:0/0:0, and TG 19:1/19:1/19:1 purchased from Nu-ChekPrep (Elysian, MN, USA), D7-CE 16:0, Cer d18:1/12:0, HexCer d18:1/12:0 (Glucosyl(ß)Cer d18:1/12:0), D7-cholesterol, Hex2Cer d18:1/12:0 (Lactosyl(ß)Cer d18:1/12:0), LPC 17:0/0:0, LPE 14:0/0:0, LPG 14:0/0:0, LPS 17:1/0:0, PA 14:0/14:0, PC 14:0/14:0, PE 14:0/14:0, PG 14:0/14:0, PS 14:0/14:0, SM d18:1/12:0, and SulfoHexCer d18:1/12:0 (MonoSulfoGalactosyl(ß)Cer d18:1/12:0) purchased from Avanti Polar Lipids (Alabaster, AL, USA). Stock solutions of individual IS at the concentration of 2 mg/mL were prepared in a chloroform – 2-propanol (1:4, v/v) mixture. A stock solution of IS mixture for calibration samples was prepared by mixing of IS stock solutions at 1:1 ratio. Stock solutions of IS mixtures for the method validation and the quantitative analysis of plasma samples were prepared by mixing of IS stock solutions at ratios listed in Table S1.

2.2. Biological samples

Samples of tumor tissue, surrounding normal tissue, plasma, and erythrocytes were obtained from kidney cancer patients in cooperation with the Faculty Hospital Olomouc (Czech Republic) based on the approval of ethical committee at the Faculty Hospital Olomouc. The total lipid extracts were prepared from 25 μL of plasma/erythrocytes or 25 mg of tissue according to the modified Folch procedure [23], then evaporated by a gentle stream of nitrogen and redissolved in 0.5 mL of chloroform – 2-propanol (1:1, v/v) mixture. Plasma samples for the quantitative analysis were spiked before the extraction with appropriate IS mixture at middle concentration level (Table S1). Total lipid extract stock solutions were diluted 20 times by chloroform – 2-propanol (1:4, v/v) mixture for UHPLC/MS, 20 times by hexane – 2-propanol – chloroform (7:1.5:1.5, v/v/v) mixture for UHPSFC/MS and 12 times by chloroform – methanol – 2-propanol (1:2:4, v/v/v) mixture containing 7.5 mM of ammonium acetate and 1% of acetic acid for DI-MS analyses. The nontargeted identification and the method validation were carried out using pooled samples prepared from 20 random patient samples with males and females in equal proportions.

2.3. UHPLC/MS and UHPSFC/MS conditions

UHPLC experiments were performed on a liquid chromatograph Agilent 1290 Series (Agilent Technologies, Waldbronn, Germany) using the following conditions: Acquity UPLC BEH HILIC column (150 mm × 2.1 mm, 1.7 μm, Waters), the flow rate 0.4 mL/min, the injection volume 1 μL, the autosampler temperature 8 °C, the column temperature 40 °C, and the gradient: 0 min – 100% A, 10 min – 84% A + 16% B, where A was acetonitrile – water (96:4, v/v) mixture containing 7 mM of ammonium acetate, and B was water containing 7 mM of ammonium acetate.

UHPSFC experiments were performed on an Acquity UPC^2 instrument (Waters, Milford, MA, USA) using our previously devel-

Table 1
Observed ions and their average relative abundances in positive-ion ESI full-scan mass spectra of IS.

IS	Observed ion	Elemental formula	Theoretical *m*/*z*	Relative abundance [%]		
				UHPLC	UHPSFC	DI
D7-CE 16:0	$[M+K]^+$	$C_{43}H_{69}D_7KO_2$	670.5916		0.4	0.3
	$[M+Na]^+$	$C_{43}H_{69}D_7NaO_2$	654.6177		9.7	8.5
	$[M+NH_4]^+$	$C_{43}H_{73}D_7NO_2$	649.6623		0.4	100
	$[M+H]^+$	$C_{43}H_{70}D_7O_2$	632.6357		0.1	0
	$[M+H\text{-}FA]^+$	$C_{27}H_{38}D_7$	376.3955		100	3.3
Cer d18:1/12:0	$[M+K]^+$	$C_{30}H_{59}KNO_3$	520.4127		0.2	0.5
	$[M+Na]^+$	$C_{30}H_{59}NaNO_3$	504.4387		8.5	9.7
	$[M+H]^+$	$C_{30}H_{60}NO_3$	482.4568		2.7	100
	$[M+H\text{-}H_2O]^+$	$C_{30}H_{58}NO_2$	464.4462		100	17.1
	$[M+H\text{-}2H_2O]^+$	$C_{30}H_{56}NO$	446.4356		4.7	1.1
	$[M+H\text{-}FA\text{-}H_2O]^+$	$C_{18}H_{36}NO$	282.2791		0.7	0
	$[M+H\text{-}FA\text{-}2H_2O]^+$	$C_{18}H_{34}N$	264.2686		6.7	0.6
DG 12:1/0:0/12:1	$[M+K]^+$	$C_{27}H_{48}KO_5$	491.3133		0.1	1.0
	$[M+Na]^+$	$C_{27}H_{48}NaO_5$	475.3394		11.9	15.5
	$[M+NH_4]^+$	$C_{27}H_{52}NO_5$	470.3840		0	100
	$[M+H]^+$	$C_{27}H_{49}O_5$	453.3575		0.8	7.6
	$[M+H\text{-}H_2O]^+$	$C_{27}H_{47}O_4$	435.3469		100	21.9
	$[M+H\text{-}FA]^+$	$C_{15}H_{27}O_3$	255.1955		7.8	1.3
Hex2Cer d18:1/12:0	$[M+K]^+$	$C_{42}H_{79}KNO_{13}$	844.5183	2.6	0.1	0.7
	$[M+Na]^+$	$C_{42}H_{79}NNaO_{13}$	828.5444	27.1	43.4	22.3
	$[M+H]^+$	$C_{42}H_{80}NO_{13}$	806.5624	100	100	100
	$[M+H\text{-}H_2O]^+$	$C_{42}H_{78}NO_{12}$	788.5519	20.9	19.1	6.7
	$[M+H\text{-}Hex2]^+$	$C_{30}H_{58}NO_2$	464.4462	11.5	22.6	2.7
	$[M+H\text{-}Hex2\text{-}H_2O]^+$	$C_{30}H_{56}NO$	446.4356	0.9	1.9	0.8
	$[M+H\text{-}Hex2\text{-}FA\text{-}H_2O]^+$	$C_{18}H_{36}NO$	282.2791	0.3	0.4	0
	$[M+H\text{-}Hex2\text{-}FA\text{-}2H_2O]^+$	$C_{18}H_{34}N$	264.2686	2.7	5.2	0.4
HexCer d18:1/12:0	$[M+K]^+$	$C_{36}H_{69}KNO_8$	682.4655	3.6	0.3	0.8
	$[M+Na]^+$	$C_{36}H_{69}NNaO_8$	666.4915	34.7	27.8	5.8
	$[M+H]^+$	$C_{36}H_{70}NO_8$	644.5096	78.5	58.8	100
	$[M+H\text{-}H_2O]^+$	$C_{42}H_{78}NO_{12}$	626.4990	100	100	7.1
	$[M+H\text{-}Hex]^+$	$C_{30}H_{58}NO_2$	464.4462	26.8	28.1	2.4
	$[M+H\text{-}Hex2\text{-}FA\text{-}H_2O]^+$	$C_{18}H_{36}NO$	282.2791	0.6	0.4	0
	$[M+H\text{-}Hex2\text{-}FA\text{-}2H_2O]^+$	$C_{18}H_{34}N$	264.2686	4.8	4.4	0.3
D7-Cholesterol	$[M+H\text{-}H_2O]^+$	$C_{27}H_{38}D_7$	376.3955		100	100
LPC 17:0/0:0	$[M+K]^+$	$C_{25}H_{52}NO_7PK$	548.3113	1.1	0.1	3.4
	$[M+Na]^+$	$C_{25}H_{52}NO_7PNa$	532.3374	14.4	1.7	10.8
	$[M+H]^+$	$C_{25}H_{53}NO_7P$	510.3554	100	100	100
	$[M+H\text{-}H_2O]^+$	$C_{25}H_{51}NO_6P$	492.3449	0.8	0.5	0.3
	$[phosphocholine]^+$	$C_5H_{15}NO_4P$	184.0733	0.2	0.3	0.1
LPE 14:0/0:0	$[M+K]^+$	$C_{19}H_{40}KNO_7P$	464.2174	3.2	1.5	1.9
	$[M+Na]^+$	$C_{19}H_{40}NNaO_7P$	448.2435	50.0	14.4	5.7
	$[M+H]^+$	$C_{19}H_{41}NO_7P$	426.2615	100	100	100
	$[M+H\text{-}H_2O]^+$	$C_{19}H_{39}NO_6P$	408.2510	21.8	21.3	0.7
	$[M+H\text{-}phosphoethanolamine]^+$	$C_{17}H_{33}O_3$	285.2424	14.8	19.3	0.7
LPG 14:0/0:0	$[M+K]^+$	$C_{20}H_{41}KO_9P$	495.2120	24.4	5.6	2.3
	$[M+Na]^+$	$C_{20}H_{41}NaO_9P$	479.2380	48.8	23.8	31.5
	$[M+NH_4]^+$	$C_{20}H_{45}NO_9P$	474.2826	0	0	100
	$[M+H]^+$	$C_{20}H_{42}O_9P$	457.2561	3.5	6.3	92.8
	$[M+H\text{-}H_2O]^+$	$C_{20}H_{40}O_8P$	439.2455	22.1	18.5	11.0
	$[M+H\text{-}2H_2O]^+$	$C_{20}H_{38}O_7P$	421.2350	91.9	81.2	1.9
	$[M+H\text{-}phosphoglycerol]^+$	$C_{17}H_{33}O_3$	285.2424	100	100	6.4
LPS 17:1/0:0	$[M+K]^+$	$C_{23}H_{44}KO_9NP$	548.2385			2.8
	$[M+Na]^+$	$C_{23}H_{44}NaO_9NP$	532.2646			23.5
	$[M+H]^+$	$C_{23}H_{45}O_9NP$	510.2827			100
MG	$[M+Na]^+$	$C_{22}H_{42}NaO_4$	393.2975		52.9	17.7
19:1/0:0/0:0	$[M+NH_4]^+$	$C_{22}H_{46}NO_4$	388.3421		0	100
	$[M+H]^+$	$C_{22}H_{43}O_4$	371.3156		51.8	23.3
	$[M+H\text{-}H_2O]^+$	$C_{22}H_{41}O_3$	353.3050		100	4.0
PA 14:0/14:0	$[M+K]^+$	$C_{31}H_{61}KO_8P$	631.3736			0.8
	$[M+Na]^+$	$C_{31}H_{62}NO_8P$	615.3996			12.2
	$[M+NH_4]^+$	$C_{31}H_{65}NO_8P$	610.4442			100
	$[M+NH_4\text{-}H_3PO_4]^+$	$C_{31}H_{59}O_4$	495.4408			8.6
PC 14:0/14:0	$[M+K]^+$	$C_{36}H_{72}KNO_8P$	716.4627	2.5	0	6.2
	$[M+Na]^+$	$C_{36}H_{72}NNaO_8P$	700.4888	6.1	1.7	16.0
	$[M+H]^+$	$C_{36}H_{73}NO_8P$	678.5068	100	100	100
	$[phosphocholine]^+$	$C_5H_{15}NO_4P$	184.0733	0.3	0.2	0.5
PE 14:0/14:0	$[M+K]^+$	$C_{33}H_{66}KNO_8P$	674.4158	1.5	0.3	2.1
	$[M+Na]^+$	$C_{33}H_{66}NNaO_8P$	658.4418	8.8	7.9	10.9
	$[M+H]^+$	$C_{33}H_{67}NO_8P$	636.4599	100	100	100
	$[M+H\text{-}phosphoethanolamine]^+$	$C_{31}H_{59}O_4$	495.4408	22.1	20.1	5.0

Table 1 (*Continued*)

IS	Observed ion	Elemental formula	Theoretical *m/z*	Relative abundance [%]		
				UHPLC	UHPSFC	DI
PG 14:0/14:0	$[M+K]^+$	$C_{34}H_{67}KO_{10}P$	705.4103	7.1	0	1.6
	$[M+Na]^+$	$C_{34}H_{67}NaO_{10}P$	689.4364	14.5	7.7	11.0
	$[M+NH_4]^+$	$C_{34}H_{71}O_{10}P$	684.4810	5.6	3.7	100
	$[M+H]^+$	$C_{34}H_{68}O_{10}P$	667.4545	5.6	3.9	7.9
	$[M+H\text{-phosphoglycerol}]^+$	$C_{31}H_{58}O_4$	495.4408	100	100	18.4
PS14:0/14:0	$[M+K]^+$	$C_{34}H_{66}KO_{10}NP$	718.4056			1.4
	$[M+Na]^+$	$C_{34}H_{66}NaO_{10}NP$	702.4317			21.0
	$[M+H]^+$	$C_{34}H_{67}O_{10}NP$	680.4497			100
	$[M+H\text{-phosphoserine}]^+$	$C_{31}H_{59}O_4$	495.4408			6.7
SM d18:1/12:0	$[M+K]^+$	$C_{35}H_{71}KN_2O_6P$	685.4681	1.2	0.1	5.1
	$[M+Na]^+$	$C_{35}H_{71}N_2NaO_6P$	669.4942	22.4	2.1	7.6
	$[M+H]^+$	$C_{35}H_{72}N_2O_6P$	647.5123	100	100	100
	$[\text{phosphocholine}]^+$	$C_5H_{15}NO_4P$	184.0733	1.0	0.9	0.2
SulfoHexCer d18:1/12:0	$[M+Na]^+$	$C_{36}H_{69}NNaO_{11}S$	746.4484		0.5	14.9
	$[M+NH_4]^+$	$C_{36}H_{73}N_2O_{11}S$	741.4930		0	32.3
	$[M+H]^+$	$C_{36}H_{70}NO_{11}S$	724.4664		27.5	100
	$[M+H\text{-}SO_3]^+$	$C_{36}H_{70}NO_8$	644.5096		75.3	5.1
	$[M+H\text{-}H_2SO_4]^+$	$C_{36}H_{68}NO_7$	626.4990		100	19.0
	$[M+H\text{-Hex-FA-}H_2O]^+$	$C_{18}H_{36}NO$	282.2791		1.1	0
	$[M+H\text{-Hex-FA-}2H_2O]^+$	$C_{18}H_{34}N$	264.2686		9.3	0
TG 19:1/19:1/19:1	$[M+Na]^+$	$C_{60}H_{110}O_6Na$	949.8195		6.5	11.2
	$[M+NH_4]^+$	$C_{60}H_{114}NO_6$	944.8641		100	100
	$[M+H]^+$	$C_{60}H_{111}O_6$	927.8375		0.5	0
	$[M+H\text{-FA}]^+$	$C_{41}H_{75}O_4$	631.5660		39.8	1.7

oped UHPSFC/MS method for the lipidomic analysis [32] with the following conditions: Acquity BEH UPC^2 column (100 mm × 3 mm, 1.7 μm, Waters), the flow rate 1.9 mL/min, the injection volume 1 μL, the autosampler temperature 8 °C, the column temperature 60 °C, the active back pressure regulator (ABPR) pressure 1800 psi, and the gradient of methanol – water (99:1, v/v) mixture containing 30 mM of ammonium acetate as a modifier: 0 min – 1%, 5 min – 51%, 6 min – 51%.

Both UHPLC and UHPSFC experiments were performed using the identical hybrid quadrupole – travelling wave ion mobility – time of flight mass spectrometer Synapt G2Si (Waters) in the resolution mode with positive-ion ESI and the mass range *m/z* 50–1200 with the following setting of tuning parameters: the capillary voltage 3.0 kV, the sampling cone 20 V, the source offset 90 V, the source temperature 150 °C, the drying temperature 500 °C, the cone gas flow 0.8 L/min, the drying gas flow 17 L/min, and the nebuliser gas flow 4 bar. Leucine enkephaline was used as the lock mass for all experiments. UHPLC instrument was connected directly with the mass spectrometer by capillary from column to ESI probe. UHPSFC instrument was connected with the mass spectrometer *via* the commercial interface kit (Waters) composed of two T-pieces enabling the backpressure control and mixing of column effluent with a make-up liquid. The mixture of methanol – water (99:1, v/v) at the flow rate 0.25 mL/min delivered by HPLC 515 pump (Waters) was used as a make-up liquid.

2.4. DI-MS conditions

Experiments were performed on a quadrupole-linear ion trap mass spectrometer 6500 QTRAP (Sciex, Concord, ON, Canada) equipped by ESI probe with the following setting of tuning parameters: the ionspray voltage 5200 V, the curtain gas 20 psi, the source temperature 50 °C, the ion source gas(*1*) 15 psi, and the ion source gas(*2*) 10 psi. MS/MS scans were measured with the scan rate 1000 Da/s, the declustering potential 80 V, the entrance potential 10 V, and the collision energy 12 eV (cholesterol, CE), 20 eV (DG, MG), 25 eV (PA, SulfoHexCer), 30 eV (PE, LPE, PS, LPS, PG, LPG, TG), and 35 eV (PC, LPC, SM, Cer, HexCer, Hex2Cer). Samples were introduced by a flow injection using a liquid chromatograph Agilent 1290 Series (Agilent Technologies) consisted of Agilent 1290 binary pump and Agilent 1260 autosampler. 50 μL of sample was injected into the flow rate 3 μL/min of chloroform – methanol – 2-propanol (1:2:4, v/v/v) mixture containing 7.5 mM of ammonium acetate and 1% of acetic acid with the analysis time 12 min, and the autosampler temperature 20 °C. LC/MS system was washed after each analysis with methanol – 2-propanol – water (2:2:1, v/v/v) mixture containing 7.5 mM of ammonium acetate and 1% of acetic acid.

2.5. Method validation

The system suitability test was carried out before the validation procedure at two concentration levels. Calibration samples with dilution factors of 10 (high level) and 5000 (low level) were injected 6 times to evaluate the repeatability (relative standard deviation, RSD, %) of peak areas using UHPLC/MS and UHPSFC/MS methods and signal intensities using DI-MS method. Validation parameters such as selectivity, accuracy, precision, calibration curve, limits of detection and quantification, matrix effect, carry-over and stability were studied according to EMEA [39], extraction efficiency was studied according to FDA [40]. Individual parameters were determined for IS representing properties of the lipid class. The selectivity was determined using 6 extracts of randomly selected plasma samples spiked before the extraction with the IS mixture at middle concentration level (Table S1) and 6 extracts of appropriate non-spiked plasma samples. The accuracy and precision were studied using the pooled plasma sample spiked after the extraction at low and high concentration levels (Table S1). The intra-day accuracy and intra-day precision were studied in a single run using three samples per concentration level. The inter-day accuracy and inter-day precision were evaluated among three independent runs in two different days using three samples at the high concentration level. Two sets of 13 calibration samples of IS with and without matrix were prepared by dilution of the IS mixture stock solution (1:1) with dilution factors of 10, 25, 50, 75, 100, 500, 1000, 5000, 10,000, 25,000, 50,000, 75,000, and 100,000. Each calibration sample with matrix contained 5% of the pooled plasma extract. The lower limit of quantification (LLOQ) and the upper limit of quantification (ULOQ) corresponded to the first and the last points of linearity range, respectively. The limit of detection (LOD) was determined based on signal to noise ratio (S/N = 3) observed from reconstructed ion chro-

matogram (UHPLC/MS and UHPSFC/MS) or NL and PI mass spectra (DI-MS) of IS. Extracts of pooled plasma spiked with IS (Table S1) before the extraction and extracts of pooled plasma spiked after the extraction were prepared for each tested method separately and used to investigate the extraction efficiency. The matrix effect was evaluated according to Matuszewski [41] by comparison of the calibration slope of IS prepared in matrix (pooled plasma) with the slope of pure IS. The carry-over was evaluated for each IS by the injection of blank sample with the pure solvent after the calibration sample at high concentration level (dilution factor of 10). The reliability of results obtained within analysis of large sample sets was evaluated by on-instrument and freeze-and-thaw stability tests. The stability of spiked plasma extract at middle concentration level was measured in autosampler at certain time intervals: 0, 4, 8, 12, 16, and 24 h. Sample for freeze-and-thaw experiment was analyzed immediately after complete unassisted thawing in autosampler.

2.6. Data processing and quantitation

Ion intensities of positive-ion ESI full-scan mass spectra of lipid class peaks were used for the data evaluation of UHPLC/MS and UHPSFC/MS experiments, while intensities of MS/MS scans were used for DI-MS. Raw UHPLC/MS and UHPSFC/MS data were processed using MarkerLynx XS software, *i.e.*, individual ESI full-scans corresponding to lipid class peak were combined together (Fig. S1) with the peak separation 50 mDa and markers extracted with the intensity threshold 3000. Raw data from DI-MS experiments were extracted using LipidView software with the mass tolerance 0.3 Da, the minimum S/N = 5 and the minimum intensity 1%. All *.txt* data were further processed using our excel macro script for the detection and quantitation of lipids. Lipid species were detected according to accurate *m*/*z* values with the mass tolerance 10 mDa or MS/MS scans based on the database compiled from identified lipids in the pooled sample followed by the isotopic correction of ion intensities. Concentration of lipid specie was calculated from corrected ion intensity related to the intensity of lipid class IS. Ions and MS/MS scans of lipid classes used for the method validation and the quantitative analysis of lipids are listed in Table S2. Multivariate data analysis of quantitative results was performed using the SIMCA software, version 13.0 (Umetrics, Umeå, Sweden). Pareto scaling was used for data normalization defined as the mean-centered data divided by the square root of the standard deviation. Pareto scaling reduced the influence of intense peaks, while emphasizing weaker peaks. Logarithm function was used for data transformation to improve the normal distribution. The lipid nomenclature followed the LIPID MAPS system [2,3] and the shorthand notation for lipid structures [42].

3. Results and discussion

3.1. Lipidomic analysis

The goal of this work is the comparison of three different analytical methods for the lipidomic analysis of biological samples in a clinical research, such as chromatography/MS methods using UHPLC and UHPSFC together with DI-MS method. UHPLC/MS and DI-MS methods are used in this work as the most widespread methods for the lipidomic analysis, while UHPSFC/MS method is selected as a new method showing a great potential for the high-throughput and comprehensive lipidomic analyses [32]. These methods are compared in one laboratory using the standardized lipidomic analysis workflow as described in Fig. 1. First, the pooled sample is prepared from samples in the sample set to characterize averaged concentrations of individual lipids. Afterward, the total lipid extract of the pooled sample is prepared using chloroform – methanol – water extraction and used for the detailed nontargeted characterization of a lipid profile. The unambiguous identification of lipid species using UHPLC/MS and UHPSFC/MS methods is based on their retention times and positive/negative-ion full-scan and tandem mass spectra measured with high mass accuracy and high resolving power. MS/MS scans in positive and negative-ion modes based on the characteristic fragmentation behavior of lipid classes are used for identification of lipid species in case of DI-MS method. Total number of carbon atoms and double bonds (CN:DB) is identified for all lipid species, because species with identical CN:DB differing in fatty acyl composition are not resolved using tested methods. The detailed knowledge of the sample lipid profile is used for the selection of exogenous lipid species as IS, *i.e.*, lipids not identified in the sample or with concentrations bellow limit of quantitation. Then, each method is validated for the given type of sample and selected IS. Finally, validated methods are applied for the targeted quantitative analysis of individual samples with the addition of IS. Only species identified in the nontargeted characterization of pooled sample are quantified by the relation of their intensity in MS spectrum to the intensity of IS with known concentration. Obtained data are further processed and evaluated.

3.2. UHPLC and UHPSFC separation of lipids

The lipid class separation of total lipid extracts is used in this work, which brings several benefits over the lipid species separation. The main advantage is in the quantitative analysis, because IS coelute with species of the given lipid class in one peak under the identical composition of a gradient and matrix influencing the ionization efficiency of all species and IS at the same level. In case of the RP lipid species separation, IS differing in fatty acyl composition are separated from other species and elute under different conditions. The lipid class separation enables easier identification of lipid species, because all species from one lipid class differing in fatty acyl composition elute in one peak without the overlap with species from other lipid classes, which is typical for the RP separation of total lipid extracts [18,20]. Ion suppression effects among different lipid classes are also eliminated using the lipid class separation. Finally, lipid class separation methods can be generally faster due to the separation of only several lipid classes compared to the separation of hundreds species in the case of species separation mode.

HILIC-UHPLC method using 1.7 μm particle bridged ethylene hybrid silica column and a gradient of acetonitrile – water – ammonium acetate mobile phase is used based on our previous experiments. Our UHPSFC method for the lipidomic analysis [32] based on 1.7 μm particle bridged ethylene hybrid silica column with a gradient of methanol – water – ammonium acetate mixture as a modifier is used for UHPSFC experiments. Fig. 2A and B shows the UHPLC/MS and UHPSFC/MS chromatograms of the lipid class IS. The retention of lipids using both methods is governed mainly by their polarity, *i.e.*, retention times are higher for more polar lipid classes. Lipid species from one lipid class differing only in the fatty acyl composition have similar polarity, and they coelute in one peak corresponding to the given lipid class (Figs. 3 and 4). UHPLC method does not provide the resolution of some lipid classes eluting in the column void volume (Fig. 2A), which disables their proper identification and quantification. Mainly nonpolar lipids (CE and TG) show poor retention, but also species containing one hydroxyl group (Cer, DG, MG, and cholesterol), where the effect of their nonpolar part is more pronounced than the effect of the polar functional group. A similar behavior has been also observed for our previous HILIC methods with different silica columns [14,15] in agreement with general properties of HILIC mode showing lower selectivity for less polar species. On the other hand, UHPSFC method pro-

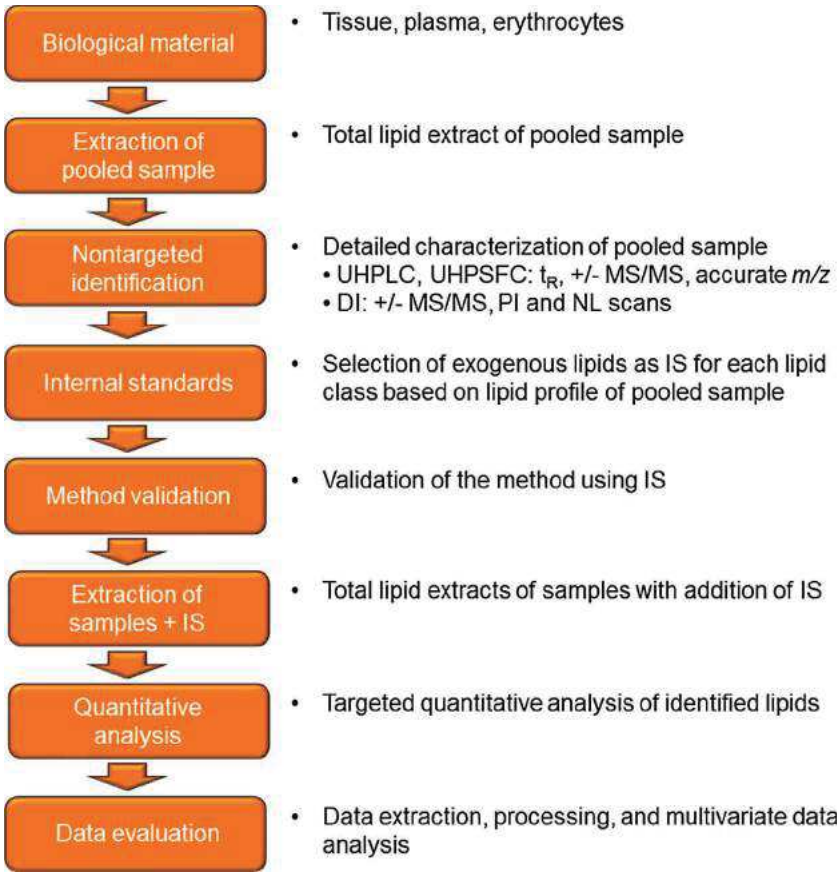

Fig. 1. Analysis workflow used in the lipidomic analysis of biological material.

vides the separation of all lipid classes in one analysis including nonpolar species (Fig. 2B). This selectivity is given by the nature of used mobile phase starting from normal-phase like conditions of nonpolar carbon dioxide with very low concentration of the polar modifier at the beginning of the gradient (1%) changing up to HILIC like conditions with high concentration of the modifier (51%) containing 1% of water. The retention behavior of lipids using UHPLC method is also influenced by a charge of lipid polar head group demonstrated by poor retention of SulfoHexCer containing very polar sulfate group, which is well retained using UHPSFC. The selectivity of both methods is similar except for LPG/PE and PC/LPE pairs showing an inverse retention order, *i.e.*, PE > LPG and LPE > PC using UHPLC compared to PE < LPG and LPE < PC using UHPSFC. 1,3-DG/1,2-DG and 1-MG/2-MG positional isomers are well resolved using UHPSFC, but positional isomers of more polar lyso- lipids are not resolved at all compared to the baseline resolution achieved by UHPLC (*i.e.*, 1-LPG/2-LPG, 1-LPE/2-LPE, and 1-LPC/2-LPC). UHPSFC method enables a partial resolution of lipid species within the lipid class peak according to the fatty acyl length and DB number, as described in our previous work [32]. This behavior is used as another tool for the unambiguous identification of lipids using UHPSFC. The partial separation of lipids according to the fatty acyl length is also achieved by UHPLC method, but no separation of species with 0–3 DB and only lower retention of species containing 4 and more DB are observed.

3.3. Nontargeted identification of lipids

ESI is used in this work for all tested methods and applied for the nontargeted identification of lipids in biological samples representing by tumor tissue, surrounding normal tissue, erythrocytes, and plasma pooled samples. The identical quadrupole – time of flight mass spectrometer with high resolving power/high mass accuracy is used for UHPLC and UHPSFC experiments to assure the same detection conditions for both methods differing only in used chromatographic technique. Individual lipids are identified from combined spectra of ESI full-scans corresponding to lipid class peaks (Fig. S1) based on accurate *m/z* with the mass error mostly bellow 5 ppm and based on fragment ions in tandem mass spectra. Different mass spectrometer is used for DI, because this approach requires mass analyzer for specific MS/MS scans (PI and NL scans). DI experiments are performed on a quadrupole-linear ion trap mass spectrometer with low resolving power and low mass accuracy. The identification of lipids using all methods is based on well-known fragmentation behavior of lipids, *i.e.*, characteristic fragment ions and neutral losses of individual lipid classes. The main observed ions and their relative abundances in positive-ion ESI full-scan mass spectra of IS are listed in Table 1. The comparison of UHPLC and UHPSFC shows clearly the effect of chromatographic method, because the same mass spectrometer is used for the detection. Relative abundances of fragment ions do not show significant differences between both methods for all lipids except for Hex2Cer d18:1/12:0, where fragment ions formed by the neutral losses of hexoses using UHPLC have half relative abundance compared to UHPSFC, *i.e.*, the relative abundance of $[M+H-Hex2]^+$ is 11.5% using UHPLC *vs.* 22.6% using UHPSFC, $[M+H-Hex2-H_2O]^+$ is 0.9% *vs.* 1.9% and $[M+H-Hex2-FA-2H_2O]^+$ is 2.7% *vs.* 5.2%. More significant differences are observed for $[M+Na]^+$ and $[M+K]^+$ adduct ions given by the combination of different nature of mobile phases and the concentration of water. The relative abundance of adduct ions for all species is significantly higher using UHPLC than UHPSFC except for $[M+Na]^+$ of Hex2Cer d18:1/12:0. The lower relative abundance of

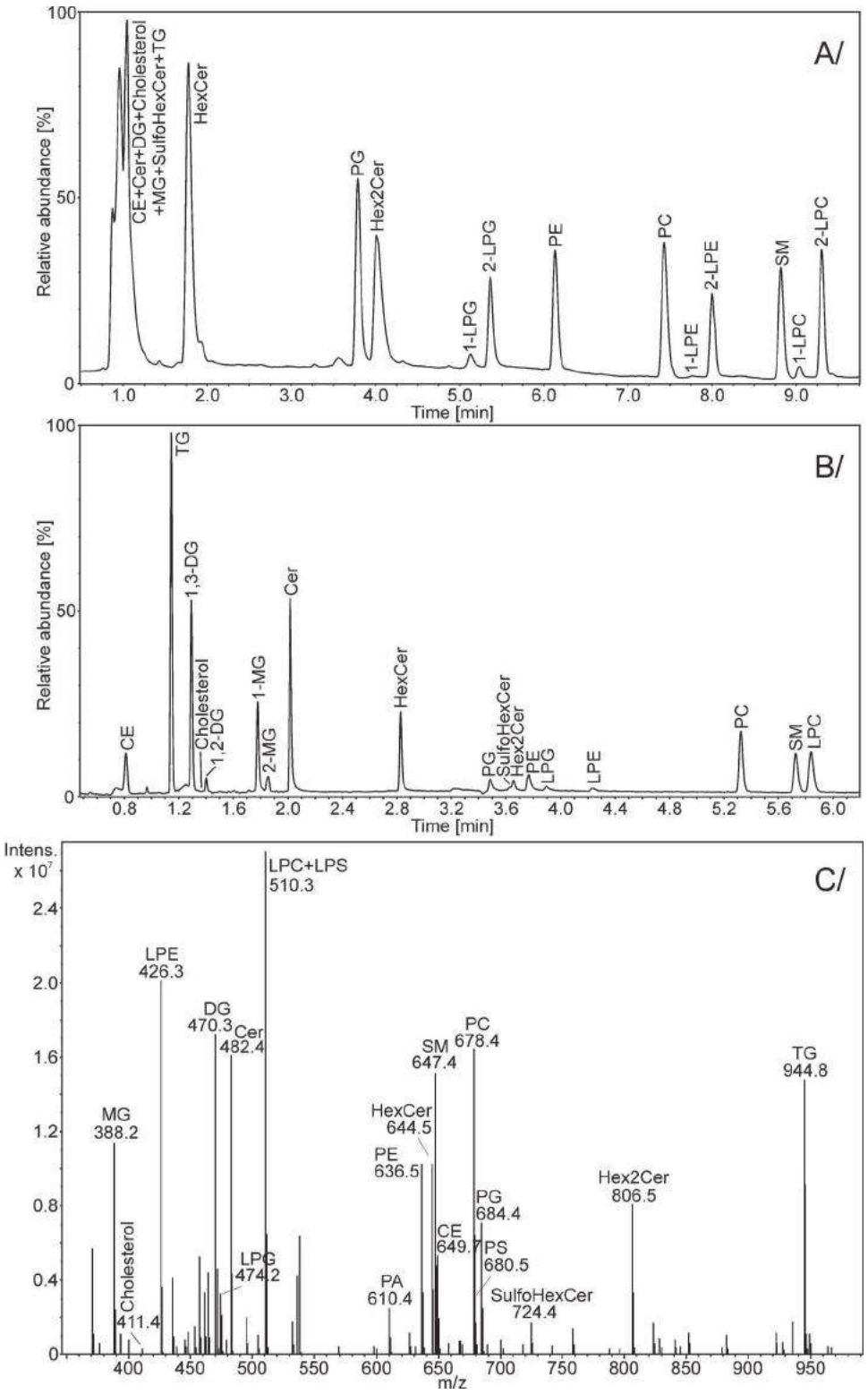

Fig. 2. Analyses of lipid internal standards using tested methods. ESI positive-ion total ion chromatograms using (A) UHPLC/MS and (B) UHPSFC/MS methods and (C) positive-ion full-scan ESI mass spectrum using DI-MS method. UHPLC conditions: Acquity UPLC BEH HILIC column (150 × 2.1 mm, 1.7 μm, Waters), the flow rate 0.4 mL/min, the column temperature 40 °C and the gradient: 0 min – 100% A and 10 min – 84% A + 16% B, where A is acetonitrile – water mixture (96:4, v/v) containing 7 mM of ammonium acetate, and B is water containing 7 mM of ammonium acetate. UHPSFC conditions: Acquity BEH UPC^2 column (100 × 3 mm, 1.7 μm, Waters), the flow rate 1.9 mL/min, the column temperature 60 °C, the ABPR pressure 1800 psi, and the gradient of methanol – water mixture (99:1, v/v) containing 30 mM of ammonium acetate as the modifier: 0 min – 1%, 5 min – 51%, and 6 min – 51%. Peak annotation: CE – cholesteryl ester, Cer – ceramide, DG – diacylglycerol, Hex2Cer – dihexosylceramide, HexCer – hexosylceramide, LPC – lysophosphatidylcholine, LPE – lysophosphatidylethanolamine, LPG – lysophosphatidylglycerol, LPI – lysophosphatidylinositol, LPS – lysophosphatidylserine, MG – monoacylglycerol, PA – phosphatidic acid, PC – phosphatidylcholine, PE – phosphatidylethanolamine, PI – phosphatidylinositol, PG – phosphatidylglycerol, PS – phosphatidylserine, SM – sphingomyelin, SulfoHexCer – sulfohexosylceramide, and TG – triacylglycerol.

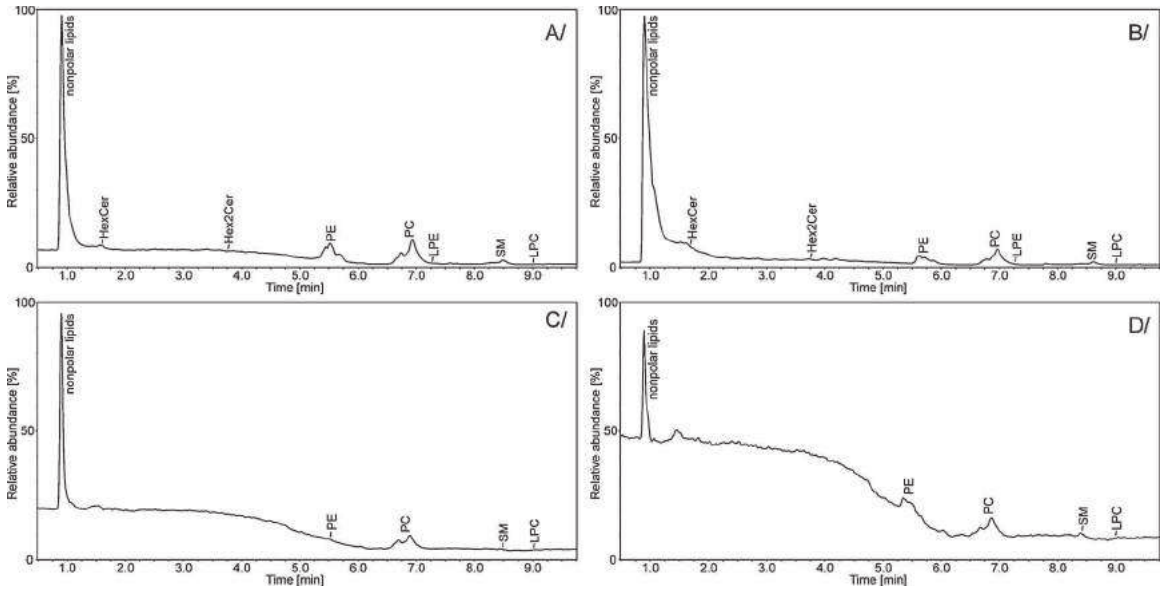

Fig. 3. Positive-ion UHPLC/ESI–MS chromatograms of (A) normal tissue, (B) tumor tissue, (C) plasma, and (D) erythrocytes pooled samples. UHPLC conditions and peak annotation are identical as for Fig. 2.

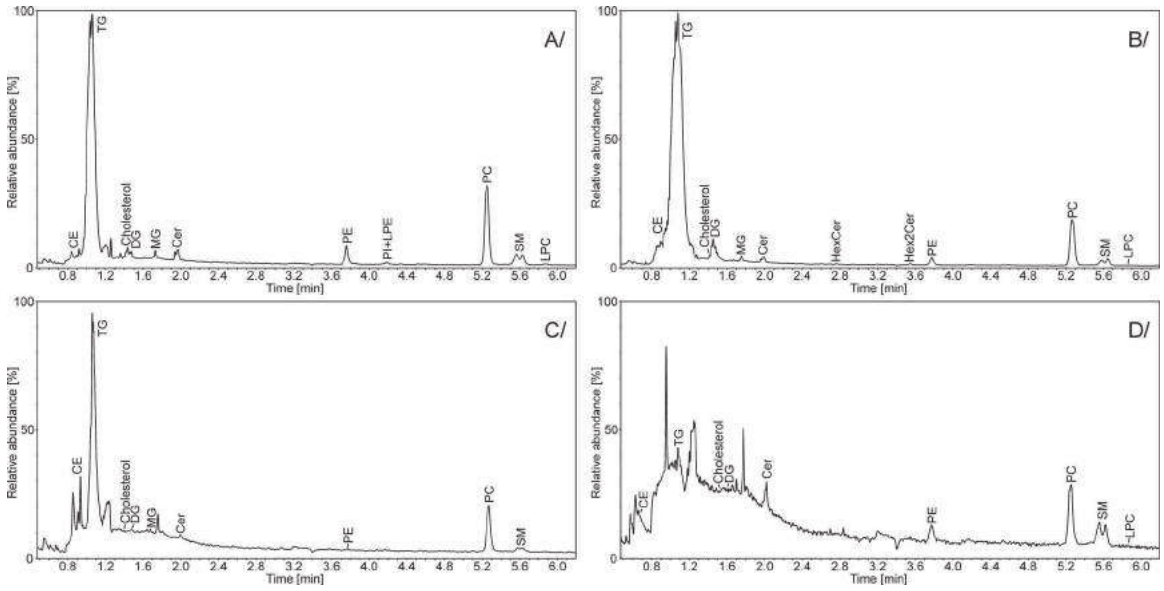

Fig. 4. Positive-ion UHPSFC/ESI–MS chromatograms of (A) normal tissue, (B) tumor tissue, (C) plasma, and (D) erythrocytes pooled samples. UHPSFC conditions and peak annotation are identical as for Fig. 2.

adduct ions using UHPSFC method is favorable for the analysis of complex samples, because adduct ions can overlap with protonated molecules of species with different composition of fatty acyls, and their resolution is more complicated requiring ultrahigh resolving power instrument or additional MS/MS experiments. Species with different CN:DB composition of fatty acyls are resolved by UHPSFC method due to their partial separation.

Relative abundances of $[M+Na]^+$ and $[M+K]^+$ using DI method are comparable to both chromatography/MS methods, but significantly higher abundances of $[M+NH_4]^+$ and $[M+H]^+$ is observed for many species, *i.e.*, higher relative abundance of $[M+NH_4]^+$ for D7-CE 16:0, MG 19:1/0:0/0:0, and PG 14:0/14:0, $[M+H]^+$ for Cer d18:1/12:0, and HexCer d18:1/12:0, and both ions for DG 12:1/0:0/12:1, LPG 14:0/0:0, and SulfoHexCer d18:1/12:0 species. On the other hand, significantly lower intensities of fragment ions in positive-ion ESI full-scan mass spectra of IS are observed in all cases, *e.g.*, the relative abundance of $[M+H-H_2O]^+$ of HexCer is 100% in both chromatography/MS methods compared to 7.1% in DI method, *etc.* This shows a softer ionization process using DI method given by the different composition of solvents with high concentration of the additives advancing the formation of molecular adducts, but also different construction of ion sources have to be considered.

Isobaric species with low differences in molecular weights (the same nominal mass) cannot be resolved using DI method due to a low resolving power and mass accuracy of quadrupole-linear ion trap mass spectrometry detection and the same characteristic fragment ions in positive-ion MS/MS spectra of both isobars. For example, protonated molecules of species differing by one additional methylene unit minus one DB and hydroxyl group (both $\Delta m/z = 16$) (*e.g.*, Cer d18:0/21:0 (611.6211) *vs.* Cer d18:0/20:1(OH) (611.5847)) or acyl and ether/plasmalogen species with one additional methylene unit (*e.g.*, PC 33:1 ($m/z = 746.5695$) *vs.* PC

Table 2
Number of identified lipid species in normal tissue, tumor tissue, plasma, and erythrocytes pooled samples.

Lipid class	Normal tissue			Tumor tissue			Plasma			Erythrocytes			Total
	UHPLC	UHPSFC	DI	UHPLC	UHPSFC	DI	UHPLC	UHPSFC	DI	UHPLC	UHPSFC	DI	
CE		13	10		26	13		13	11		6	6	28
Cer		22	14		22	15		13	13		21	13	35
Des			4			4			5			1	5
DG		42	18		43	18		19	13		10	9	47
Hex2Cer	3		5	4	4	5			4			1	6
HexCer	4		6	5	5	6			5			2	7
Cholesterol		1	1		1	1		1	1		1	1	1
LPA			1			1							1
LPC	5	8	11	5	8	11	4		9	2	2	4	13
LPE	7	7	7	4		10			8			4	13
LPG			2			2			6			5	7
LPI			4			4							4
LPS			3			3							3
MG		4	5		2	5		2	4			3	5
PA			9			8						10	10
PC	41	40	46	49	50	46	27	41	41	24	38	38	67
PE	35	29	42	35	30	48	9	5	39	27	23	41	50
PG			16			16			13			6	19
PI		6	25			27			12			12	30
PS			31			31			14			19	35
SM	24	30	26	23	24	26	12	22	20	11	30	24	33
SulfoHexCer			11			10			4				12
TG		135	34		153	34		111	28		42	8	179
Total	119	337	331	125	368	344	52	227	250	64	173	207	610

O-34:1/P-34:0 (746.6058)). Latter can be resolved in negative-ion mode MS^n spectra based on carboxylate fragment ions [43]. These isobars are resolved using UHPLC and UHPSFC methods thanks to higher resolving power/mass accuracy detection and different retention times.

In total, 610 lipid species have been identified in pooled samples of tumor tissue, surrounding normal tissue, plasma, and erythrocytes using three tested methods (Table S3). Table 2 shows numbers of identified lipid species within lipid classes using individual methods representing their different identification capability. The total number of identified species using UHPLC method is lower compared to other two methods, because less polar species are not identified/quantified due to their elution in the column void volume. These coeluted species can be resolved based on high resolving power ESI mass spectra, but their identification is very complicated mainly due to their overlap and response suppression by impurities eluted in the column void volume. The total numbers of identified species using UHPSFC and DI methods are comparable, but they differ significantly within individual lipid classes. In general, more species of nonpolar lipids are identified using UHPSFC compared to DI method, *i.e.*, CE, TG, Cer and DG. Mainly the number of TG species is significantly larger using UHPSFC showing higher sensitivity of this method for TG, *e.g.,* 135 *vs.* 34 TG in normal tissue, 153 *vs.* 34 in tumor tissue, *etc*. On the other hand, DI method shows better sensitivity for polar lipids, such as LPA, LPG, LPI, LPS, PA, PI, PG, PS, and SulfoHexCer. These species are usually not detected at all using both chromatography/MS methods due to low sensitivity given by the different composition of solvents and strong peak tailing using silica columns [44] in case of acidic lipids (*i.e.*, PA, LPA, PS, and LPS).

3.4. Method validation

Each method is validated for the quantitative analysis of lipids in plasma samples of kidney cancer patients. We apply a widely used strategy of lipidomic quantitation with one IS for each lipid class, while variations in ionization efficiency among individual species within given class differing in fatty acyl composition are neglected. The selection of appropriate IS for such kind of quantitative analysis is critical due to enormous complexity of lipidomic samples. Therefore, we select IS after the untargeted characterization of pooled samples based on the detailed knowledge of lipid profiles. It is difficult to find exogenous lipid species inside the lipidomic pattern with similar composition of fatty acyls, which are not present in samples or overlapped with isobaric species. Commercially available lipid quantitative standards provided by Avanti Polar Lipids use unusual combination of even and odd fatty acyls, but these species can be also overlapped with common endogenous species of identical nominal mass, especially when MS instruments with lower resolwing power are used. For example, PC 17:0/14:1 (PC 31:1, MW = 717.5309) can be overlapped with isobaric PC O-32:1/P-32:0 (MW = 717.5672), PC 17:0/20:4 (PC 37:4, MW = 795.5778) with PC O-38:4/P-38:3 (795.6142), PE 17:0/14:1 (PE 31:1, MW = 675.4839) with PE O-32:1/P-32:0 (675.5203), *etc*. We use mainly IS with shorter fatty acyls for the analysis of plasma samples, such as 14:0 or combinations of 18:1 and 12:0 fatty acyls in case of ceramide species (Table S1), because they are not detected in the plasma pooled sample. These IS are also widely used by other lipidomic groups [6,9,11,13].

IS are used for the method validation as representatives of all species within the lipid class. The system suitability test has been performed before the validation procedure showing acceptable values of RSD below 7.0% for all analyzed IS and tested methods. Pooled plasma spiked with the mixture of IS is used for the determination of linearity range, calibration slope, limits of detection, and quantitation (Table 3). Calibration curves are constructed for individual IS showing coefficient of determination (R^2) above 0.99. The linearity range of IS in the plasma matrix is in most cases two up to four orders of magnitude for all tested methods. LLOQ are usually lower in DI, while in UHPSFC vary among individual lipid classes due to wide differences in their responses. ULOQ is mostly lower using DI method and does not differ significantly among individual lipids, *i.e.*, ULOQ of most IS are between 2000 and 3000 pmol/mL in the calibration mixture. This is probably the critical concentration of lipids in the calibration mixture, where lipid-lipid interactions and/or aggregation of lipids start to have significant effect on the ionization efficiency of lipids limiting their linearity range [1].

Table 3
Results of the methods validation in plasma matrix.

IS	Linearity range [pmol/mL]			Calibration slope						Limit of detection [pmol/mL]		
	UHPLC	UHPSFC	DI	UHPLC		UHPSFC		DI		UHPLC	UHPSFC	DI
				with matrix	without matrix	with matrix	without matrix	with matrix	without matrix			
D7-CE 16:0		2–15832	2–2043			4.249	3.8135	0.0604	0.0726		0.4	1.3
Cer d18:1/12:0	5–4887	4–2077	1–2680	13.219	15.7370	9.7338	8.5860	0.1583	0.2334	2.1	0.2	0.3
DG 12:1/0:0/12:1		2–2211	3–2853			8.6865	8.2069	0.1024	0.1643		0.4	1.7
Hex2Cer d18:1/12:0	15–15335	130–2607	2–1602	6.1303	7.3858	0.0468	0.0458	0.0423	0.0457	6.2	75.3	0.8
HexCer d18:1/12:0	7–7313	6–6216	2–2005	7.6242	10.2260	1.339	1.1936	0.1583	0.1792	1.7	1.1	0.9
D7-Cholesterol		254–25400	8–1639			0.0156	0.0128	0.0009	0.0014		74.7	5.1
LPC 17:0/0:0	10–24252	8–4123	5–2658	3.823	4.6268	4.4757	4.2790	0.1707	0.2400	0.2	0.8	1.3
LPE 14:0/0:0	28–27665	47–9406	2–3034	0.9721	1.0059	0.1009	0.0806	0.0706	0.0893	0.3	1.8	1.2
LPG 14:0/0:0	10–10332	220–4391	3–2970	1.1144	1.5148	0.0435	0.0224	0.0289	0.0344	0.1	110.1	1.4
LPS 14:0/0:0			5–2660					0.0334	0.0519			2
MG 19:1/0:0/0:0		5–10802	2–1832			1.2084	1.3280	0.0399	0.0586		0.6	0.9
PA 14:0/14:0			1–2178					0.1235	0.1761			0.5
PC 14:0/14:0	7–17365	30–5904	4–1904	6.0489	7.7336	7.5383	4.6280	0.3334	0.5116	0.7	0.6	1.2
PE 14:0/14:0	7–7406	16–3147	1–2031	4.3202	5.6060	0.5294	0.4088	0.2201	0.2921	0.2	0.6	0.4
PG 14:0/14:0	7–6836	15–2905	1–1936	9.9834	12.5590	0.4008	0.3390	0.1646	0.2083	0.1	1.1	0.4
PS 14:0/14:0			1–1899					0.1414	0.1864			0.5
SM 18:1/12:0	7–18197	6–15468	10–1996	3.8316	4.7180	5.1779	4.8480	0.2653	0.3521	0.4	0.9	1.7
SulfoHexCer 18:1/12:0		68–900	2–892			0.1242	0.0852	0.0746	0.0828		42.1	0.9
TG 19:1/19:1/19:1		1–1439	4–3481			14.314	15.1920	0.0105	0.0151		0.3	1.4

Calibration curves of IS with and without pooled plasma as the matrix are measured to demonstrate the matrix effects. Responses of all IS are suppressed in the plasma matrix using UHPLC and DI methods, what can be demonstrated by the lower calibration slopes of IS with matrix than without matrix (Table 3). The average decrease of IS calibration slopes in the plasma matrix is 20% using UHPLC (from 16 to 26% for most lipids) and 27% using DI method (from 10% to 37%). The different effect is observed with UHPSFC method, where the response enhancement in the matrix is observed for the majority of IS with the average increase of calibration slopes of 21%. This behavior can be ascribed clearly to the properties of UHPSFC method, because the identical detection is used also for UHPLC while showing the response suppression of all IS. Quantitation limits obtained for studied methods show comparable results depending on the ionization efficiency of individual lipids. The lowest LOD are achieved for 6 IS using UHPLC, 6 using UHPSFC, and 4 using DI method, respectively. On-instrument and freeze-and-thaw stability tests show suitable results for all methods ranged from 80 to 120% and from 90 to 110%, respectively. All tested methods fulfill validation requirements for bioanalytical and clinical applications, showing variation in the extraction recovery within the range of 79–110% for most of IS, accuracy ranged from 85 to 114%, and precision up to 9.5% (Table S4).

3.5. Comparison of methods

The lipidomic analysis of biological samples in clinical research puts special requirements on analytical methods, such as throughput of samples, comprehensiveness, sample and solvent consumptions, *etc*. Selected parameters characterizing three tested lipidomic methods are compared in Table 4. The analysis time of UHPLC method is 10 min providing the separation of only polar lipid classes compared to 6 min analysis of both polar and nonpolar lipid classes using UHPSFC method. The method time including the time of analysis and the time of column equilibration is 20 min for UHPLC and 10 min for UHPSFC method. The equilibration time of UHPSFC is only 4 min without any compromise of retention time stability, while longer equilibration is required for UHPLC method (10 min) to achieve stable retention times due to generally slower equilibration of HILIC conditions and the use of lower flow rate compared to UHPSFC method. The analysis time of DI method is 12 min, which is double compared to UHPSFC, but provides comprehensive information about a wide range of lipid classes. The total method time is 23 min including time before analysis (2 min) to reach stable conditions after the sample injection and time for system washing after the analysis (9 min).

The highest number of lipid classes is identified using DI method including 23 nonpolar and polar lipids. Moreover, acidic lipids are determined using DI, which are not detected at all using UHPLC and UHPSFC methods. The number of identified lipid classes is lower using UHPLC method (7), because many nonpolar classes elute in the column void volume disabling their proper identification based on the MS and retention data. The highest total number of identified lipid species is achieved with UHPSFC method due to excellent ionization efficiency of nonpolar lipids, mainly TG.

The amount of injected sample is critical in some biological applications with limited quantity of sample. 1 μL of sample solution containing 0.05 μL of the total lipid extract is injected on column in UHPLC and UHPSFC analyses. Both methods provide comparable results of sensitivity depending on the ionization efficiency of individual lipid classes, which can differ between both methods, as demonstrated on slopes of calibration curves (Table 3). The similar sensitivity is also provided by DI method, but significantly higher amount of the sample is used. 50 μL of sample solution containing 6.25 μL of the total lipid extract is injected in DI method, which is 125 times more than using UHPLC and UHPSFC

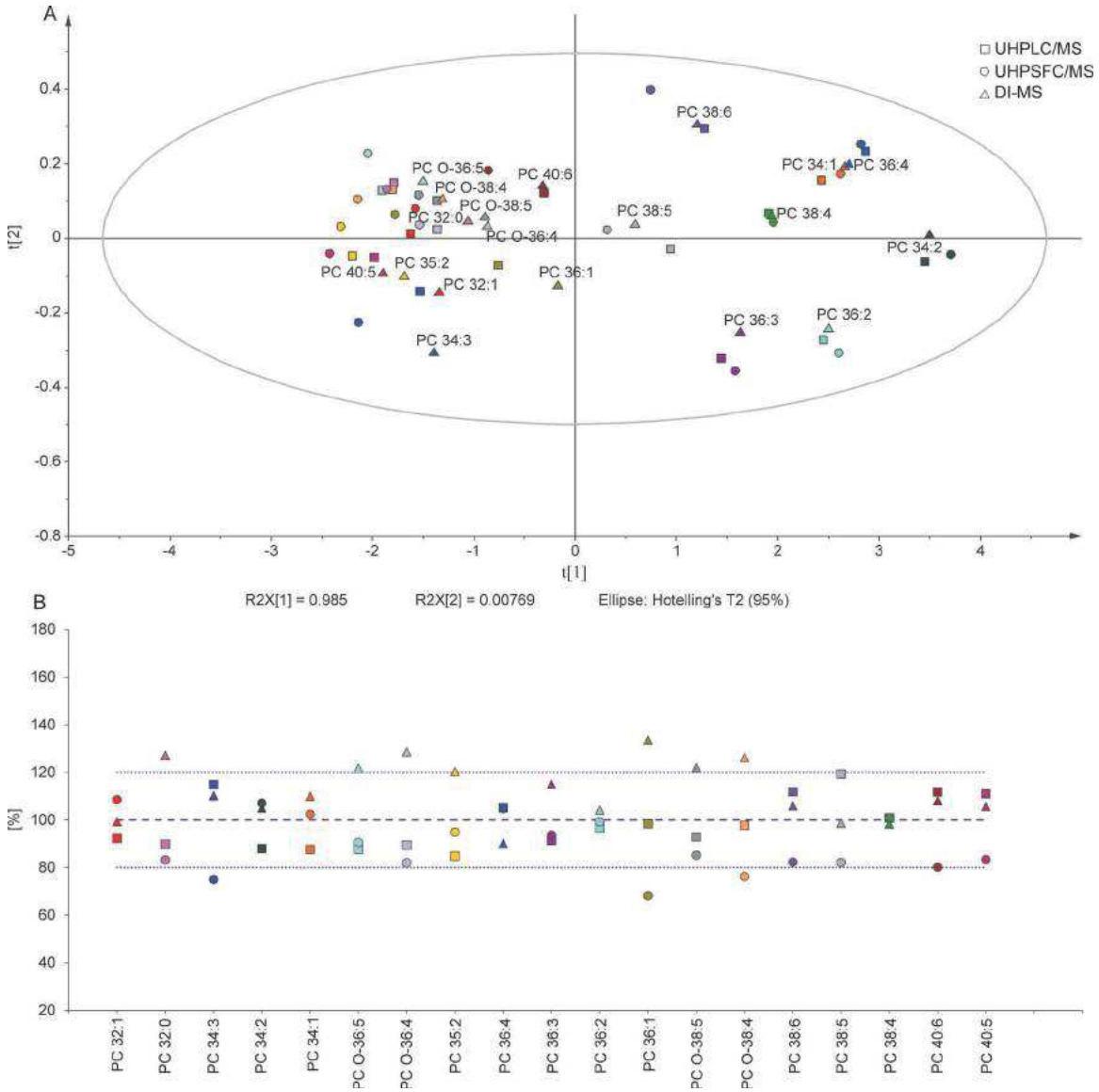

Fig. 5. Comparison of quantitation results of kidney cancer patient plasma samples using three tested methods. (A) The principal component analysis score plot of phosphatidylcholines of 6 plasma samples and (B) the difference plot of phosphatidylcholines of one sample using UHPLC/MS (square), UHPSFC/MS (circle), and DI-MS (triangle) methods.

Table 4
Comparison of selected parameters of tested lipidomic methods.

Method parameter	UHPLC	UHPSFC	DI
Analysis time [min]	10	6	12
Method time [min]	20	10	23
Identified lipid classes	7	14	23
Identified lipid species	132	450	390
Injection volume [μL]	1	1	50
Total lipid extract consumption [μL/analysis]	0.05	0.05	6.25
Flow rate [mL/min]	0.4	1.9	0.003
Organic solvent consumption [mL/analysis]	3.53	4.89[a]	0.04

[a] Consumption corresponds to both solvent of mobile phase (3.40 mL) and make-up liquid (1.49 mL) used for ESI.

methods. It is given by the fact that the sample is infused during the whole analysis, but individual lipids are measured only for short time corresponding to MS/MS scans. The sample consumption can be reduced by widely used nano-flow infusion system equipped by nanoESI with typical flow rates in hundreds of nL/min. On the other hand, the typical sample consumption for this experimental setup is 10 μL [9,12], which is only five times less compared to 50 μL injected in our DI method. The amount of organic solvent used for one analysis is very low for DI method, because only 3 μL/min flow rate of sample solution is used. The solvent consumptions for one analysis using UHPLC and UHPSFC methods are comparable (3.53 vs. 3.40 mL), but make-up liquid is used in case of UHPSFC to support ESI process with final consumption of organic solvent 4.89 mL.

Overall intensity of UHPLC and UHPSFC analyses obtained using the same mass spectrometer is comparable, but differences in response can be observed for individual lipid classes (Fig. 2, Table 3). UHPSFC method (Fig. 2B) shows excellent responses for nonpolar lipids (*e.g.*, Cer, DG, and TG), while responses of Hex2Cer, LPE, LPG, PE, and PG classes is lower compare to UHPLC (Fig. 2A). The lower response is given by different nature of mobile phases, because identical mass spectrometer is used for both UHPSFC and UHPLC methods. These classes elute in the time region, where UHPSFC mobile phase is changing from supercritical state to subcritical state due to higher amount of the modifier in the gradient [32]. ESI ionization efficiency is influenced causing lower response of lipid classes. UHPLC method shows more universal responses for separated polar lipids (Fig. 2A), but the response of nonpolar lipids cannot be compared due to their coelution. The DI method using the quadrupole – ion trap mass spectrometer provides lower distribution of lipid responses compared to UHPSFC method. Responses of lipids using DI can be also influenced by ion suppression effects according to the composition of sample, because all species are ionized together without any preseparation step. Especially charged species may compete for the charge during ESI process influencing their responses.

Validated methods are applied for the quantitative analysis of lipids in plasma samples of 6 kidney cancer patients. PC, SM and PE classes are identified using all tested methods, but PE species have concentration bellow the limit of quantification. Quantitative results of PC (Fig. 5A) and SM (Fig. S2A) species from 6 measured plasma samples using 3 tested methods are compared using the principal component analysis (PCA) score plot. Fig. 5A depicts the PCA score plot of 57 variables representing quantitative results of 19 PC species (labeled by different colors) measured using 3 methods (UHPLC/MS – square, UHPSFC/MS – circle, and DI-MS – triangle) in 6 samples. The first component in the PCA plot explains 98.5% and the second component explains 0.8% of the variation (Table S5). Each point in the PCA score plot represents concentrations of one PC in 6 measured plasma samples using given method. Individual PC species are represented by 3 points corresponding to 3 tested methods. Clustering of these 3 points shows a good correlation of measure concentrations in all samples among tested methods. The difference plot (Fig. 5B) is used to demonstrate relative differences of measured concentrations among tested methods for one plasma sample. Concentrations of individual PC species are related to the average species concentration from three tested methods. The variation of concentrations among tested methods is for most species within the range of ± 20%, which is good correlation of quantitative results among three different lipidomics methods based on the quantitation using only one IS for all lipid class species neglecting their various fatty acyls composition. Similar results are observed for SM species (Fig. S2) with slightly higher variation for species at low concentration in the plasma sample. These results confirm that this kind of quantitative analysis provides reliable quantitative results for clinical research especially for the case/control comparison.

4. Conclusions

The aim of this work is the comparison of three analytical methods (UHPLC/MS, UHPSFC/MS, and DI-MS) for the lipidomic analysis of biological samples in a clinical research. All experiments are performed in one laboratory using the same analytical protocol providing uniform conditions for the direct comparison of tested methods, which cannot be achieved using literature data measured under different conditions. Our goal is to demonstrate advantages and limitations of tested methods and not analytical techniques in general, because various conditions can be used by other authors providing different results. Obtained results show applicability of all tested methods for the lipidomic analysis of biological samples according to analysis requirements in respect to advantages and limitations of individual methods. UHPLC method can be applied mainly for the analysis of polar lipid classes, but is not convenient for the analysis of less polar lipids due to their elution in the column void volume disabling their proper identification and quantification. UHPSFC method can be used for comprehensive and high-throughput lipidomic analyses providing the separation and identification of lipids within the whole range of polarities in 6 min analysis. DI method provides the most comprehensive information about the composition of lipids covering 23 lipid classes in 12 min analysis. On the other hand, DI method does not enable the identification of isobaric species due to low resolving power/low mass accuracy MS detection. Calibration parameters of individual IS using all methods show generally similar sensitivity, but with response differences among individual lipid classes. UHPSFC method provides large differences among individual lipid classes with excellent response mainly for nonpolar lipids, but lower response for polar species. DI method provides more uniform response for most lipid classes bringing advantage for the identification of lipid classes with lower response in UHPLC and UHPSFC. The method time of UHPSFC method for the analysis of one sample is 10 min providing two times higher sample throughput than using UHPLC and DI methods. The main drawback of DI method is significantly higher sample consumption compared to other methods, but only 40 μL of organic solvent is used for one sample analysis compared to 3.5 and 4.9 mL using UHPLC and UHPSFC, respectively. Quantitative results using one IS for each lipid class show good correlation among tested methods.

Acknowledgments

This work was supported by the Ministry of Education, Youth and Sports of the Czech Republic [ERC CZ grant number LL1302]. Authors thank to Bohuslav Melichar, David Vrána, and Vladimír Študent for providing samples.

Appendix A. Supplementary data

Supplementary data associated with this article can be found, in the online version, at https://doi.org/10.1016/j.chroma.2017.10.022.

References

[1] X.L. Han, R.W. Gross, Global analyses of cellular lipidomes directly from crude extracts of biological samples by ESI mass spectrometry: a bridge to lipidomics, J. Lipid Res. 44 (2003) 1071–1079.
[2] E. Fahy, S. Subramaniam, H.A. Brown, C.K. Glass, A.H. Merrill, R.C. Murphy, C.R.H. Raetz, D.W. Russell, Y. Seyama, W. Shaw, T. Shimizu, F. Spener, G. van Meer, M.S. VanNieuwenhze, S.H. White, J.L. Witztum, E.A. Dennis, A comprehensive classification system for lipids, J. Lipid Res. 46 (2005) 839–861.
[3] E. Fahy, S. Subramaniam, R.C. Murphy, M. Nishijima, C.R.H. Raetz, T. Shimizu, F. Spener, G. van Meer, M.J.O. Wakelam, E.A. Dennis, Update of the LIPID MAPS comprehensive classification system for lipids, J. Lipid Res. 50 (2009) S9–S14.
[4] T. Čajka, O. Fiehn, Comprehensive analysis of lipids in biological systems by liquid chromatography-mass spectrometry, TrAC Trends Anal. Chem. 61 (2014) 192–206.
[5] M. Li, L. Yang, Y. Bai, H. Liu, Analytical methods in lipidomics and their applications, Anal. Chem. 86 (2014) 161–175.
[6] C.J. Fhaner, S.C. Liu, H. Ji, R.J. Simpson, G.E. Reid, Comprehensive lipidome profiling of isogenic primary and metastatic colon adenocarcinoma cell lines, Anal. Chem. 84 (2012) 8917–8926.
[7] H.S. Jonasdottir, S. Nicolardi, W. Jonker, R. Derks, M. Palmblad, A. Ioan-Facsinay, R. Toes, Y.E.M. van der Burgt, A.M. Deelder, O.A. Mayboroda, M. Giera, Detection and structural elucidation of esterified oxylipids in human synovial fluid by electrospray ionization-fourier transform ion-cyclotron mass spectrometry and liquid chromatography-ion trap-MS3: detection of esterified hydroxylated docosapentaenoic acid containing phospholipids, Anal. Chem. 85 (2013) 6003–6010.

[8] F. Li, X. Qin, H. Chen, L. Qiu, Y. Guo, H. Liu, G. Chen, G. Song, X. Wang, F. Li, S. Guo, B. Wang, Z. Li, Lipid profiling for early diagnosis and progression of colorectal cancer using direct-infusion electrospray ionization Fourier transform ion cyclotron resonance mass spectrometry, Rapid Commun. Mass Spectrom. 27 (2013) 24–34.
[9] K. Schuhmann, R. Almeida, M. Baumert, R. Herzog, S.R. Bornstein, A. Shevchenko, Shotgun lipidomics on a LTQ Orbitrap mass spectrometer by successive switching between acquisition polarity modes, J. Mass Spectrom. 47 (2012) 96–104.
[10] O. Quehenberger, A.M. Armando, A.H. Brown, S.B. Milne, D.S. Myers, A.H. Merrill, S. Bandyopadhyay, K.N. Jones, S. Kelly, R.L. Shaner, C.M. Sullards, E. Wang, R.C. Murphy, R.M. Barkley, T.J. Leiker, C.R.H. Raetz, Z. Guan, G.M. Laird, D.A. Six, D.W. Russell, J.G. McDonald, S. Subramaniam, E. Fahy, E.A. Dennis, Lipidomics reveals a remarkable diversity of lipids in human plasma, J. Lipid Res. 51 (2010) 3299–3305.
[11] K. Yang, H. Cheng, R.W. Gross, X. Han, Automated lipid identification and quantification by multidimensional mass spectrometry-based shotgun lipidomics, Anal. Chem. 81 (2009) 4356–4368.
[12] L.A. Heiskanen, M. Suoniemi, H.X. Ta, K. Tarasov, K. Ekroos, Long-term performance and stability of molecular shotgun lipidomic analysis of human plasma samples, Anal. Chem. 85 (2013) 8757–8763.
[13] P. Wiesner, K. Leidl, A. Boettcher, G. Schmitz, G. Liebisch, Lipid profiling of FPLC-separated lipoprotein fractions by electrospray ionization tandem mass spectrometry, J. Lipid Res. 50 (2009) 574–585.
[14] E. Cífková, M. Holčapek, M. Lísa, Nontargeted lipidomic characterization of porcine organs using hydrophilic interaction liquid chromatography and off-line two-dimensional liquid chromatography-electrospray ionization mass spectrometry, Lipids 48 (2013) 915–928.
[15] M. Lísa, E. Cífková, M. Holčapek, Lipidomic profiling of biological tissues using off-line two-dimensional high-performance liquid chromatography mass spectrometry, J. Chromatogr. A 1218 (2011) 5146–5156.
[16] E.J. Ahn, H. Kim, B.C. Chung, G. Kong, M.H. Moon, Quantitative profiling of phosphatidylcholine and phosphatidylethanolamine in a steatosis/fibrosis model of rat liver by nanoflow liquid chromatography/tandem mass spectrometry, J. Chromatogr. A 1194 (2008) 96–102.
[17] O. Berdeaux, P. Juaneda, L. Martine, S. Cabaret, L. Bretillon, N. Acar, Identification and quantification of phosphatidylcholines containing very-long-chain polyunsaturated fatty acid in bovine and human retina using liquid chromatography/tandem mass spectrometry, J. Chromatogr. A 1217 (2010) 7738–7748.
[18] K. Sandra, A.d.S. Pereira, G. Vanhoenacker, F. David, P. Sandra, Comprehensive blood plasma lipidomics by liquid chromatography/quadrupole time-of-flight mass spectrometry, J. Chromatogr. A 1217 (2010) 4087–4099.
[19] Y. Sato, I. Suzuki, T. Nakamura, F. Bernier, K. Aoshima, Y. Oda, Identification of a new plasma biomarker of Alzheimer's disease using metabolomics technology, J. Lipid Res. 53 (2012) 567–576.
[20] M. Holčapek, M. Ovčačíková, M. Lísa, E. Cífková, T. Hájek, Continuous comprehensive two-dimensional liquid chromatography-electrospray ionization mass spectrometry of complex lipidomic samples, Anal. Bioanal. Chem. 407 (2015) 5033–5043.
[21] M. Narvaez-Rivas, Q.B. Zhang, Comprehensive untargeted lipidomic analysis using core-shell C30 particle column and high field orbitrap mass spectrometer, J. Chromatogr. A 1440 (2016) 123–134.
[22] U. Sommer, H. Herscovitz, F.K. Welty, C.E. Costello, LC-MS-based method for the qualitative and quantitative analysis of complex lipid mixtures, J. Lipid Res. 47 (2006) 804–814.
[23] E. Cífková, M. Holčapek, M. Lísa, M. Ovčačíková, A. Lyčka, F. Lynen, P. Sandra, Nontargeted quantitation of lipid classes using hydrophilic interaction liquid chromatography-electrospray ionization mass spectrometry with single internal standard and response factor approach, Anal. Chem. 84 (2012) 10064–10070.
[24] M. Scherer, G. Schmitz, G. Liebisch, High-throughput analysis of sphingosine 1-phosphate, sphinganine 1-phosphate, and lysophosphatidic acid in plasma samples by liquid chromatography-tandem mass spectrometry, Clin. Chem. 55 (2009) 1218–1222.
[25] P. Olsson, J. Holmback, B. Herslof, Separation of lipid classes by HPLC on a cyanopropyl column, Lipids 47 (2012) 93–99.
[26] I. Losito, R. Patruno, E. Conte, T.R.I. Cataldi, F.M. Megli, F. Palmisano, Phospholipidomics of human blood microparticles, Anal. Chem. 85 (2013) 6405–6413.
[27] M. Holčapek, E. Cífková, B. Červená, M. Lísa, J. Vostálová, J. Galuszka, Determination of nonpolar and polar lipid classes in human plasma, erythrocytes and plasma lipoprotein fractions using ultrahigh-performance liquid chromatography – mass spectrometry, J. Chromatogr. A 1377 (2015) 85–91.
[28] P.M. Hutchins, R.M. Barkley, R.C. Murphy, Separation of cellular nonpolar neutral lipids by normal-phase chromatography and analysis by electrospray ionization mass spectrometry, J. Lipid Res. 49 (2008) 804–813.
[29] D.G. McLaren, P.L. Miller, M.E. Lassman, J.M. Castro-Perez, B.K. Hubbard, T.P. Roddy, An ultraperformance liquid chromatography method for the normal-phase separation of lipids, Anal. Biochem. 414 (2011) 266–272.
[30] S. Granafei, P. Azzone, V.A. Spinelli, I. Losito, F. Palmisano, T.R.I. Cataldi, Hydrophilic interaction and reversed phase mixed-mode liquid chromatography coupled to high resolution tandem mass spectrometry for polar lipids analysis, J. Chromatogr. A 1477 (2016) 47–55.
[31] T.T. Zhang, S. Chen, X.L. Liang, H. Zhang, Development of a mass-spectrometry-based lipidomics platform for the profiling of phospholipids and sphingolipids in brain tissues, Anal. Bioanal. Chem. 407 (2015) 6543–6555.
[32] M. Lísa, M. Holčapek, High-throughput and comprehensive lipidomic analysis using ultrahigh-performance supercritical fluid chromatography-mass spectrometry, Anal. Chem. 87 (2015) 7187–7195.
[33] T. Yamada, T. Uchikata, S. Sakamoto, Y. Yokoi, S. Nishiumi, M. Yoshida, E. Fukusaki, T. Bamba, Supercritical fluid chromatography/Orbitrap mass spectrometry based lipidomics platform coupled with automated lipid identification software for accurate lipid profiling, J. Chromatogr. A 1301 (2013) 237–242.
[34] J.W. Lee, S. Nishiumi, M. Yoshida, E. Fukusaki, T. Bamba, Simultaneous profiling of polar lipids by supercritical fluid chromatography/tandem mass spectrometry with methylation, J. Chromatogr. A 1279 (2013) 98–107.
[35] E. Lesellier, A. Latos, A.L. de Oliveira, Ultra high efficiency/low pressure supercritical fluid chromatography with superficially porous particles for triglyceride separation, J. Chromatogr. A 1327 (2014) 141–148.
[36] T. Uchikata, A. Matsubara, S. Nishiumi, M. Yoshida, E. Fukusaki, T. Bamba, Development of oxidized phosphatidylcholine isomer profiling method using supercritical fluid chromatography/tandem mass spectrometry, J. Chromatogr. A 1250 (2012) 205–211.
[37] A. Matsubara, T. Bamba, H. Ishida, E. Fukusaki, K. Hirata, Highly sensitive and accurate profiling of carotenoids by supercritical fluid chromatography coupled with mass spectrometry, J. Sep. Sci. 32 (2009) 1459–1464.
[38] J.W. Lee, T. Nagai, N. Gotoh, E. Fukusaki, T. Bamba, Profiling of regioisomeric triacylglycerols in edible oils by supercritical fluid chromatography/tandem mass spectrometry, J. Chromatogr. B 966 (2014) 193–199.
[39] European Medicines Agency, Guideline on bioanalytical method validation, Committee for Medicinal Products for Human Use, 192217/2009, Rev. 1 Corr. 2, 21 July 2011.
[40] Food and Drug Administration, Guidance for Industry on Bioloanalytical Method Validation, Federal Register, 23 May 2001.
[41] B.K. Matuszewski, Standard line slopes as a measure of a relative matrix effect in quantitative HPLC-MS bioanalysis, J. Chromatogr. B 830 (2006) 293–300.
[42] G. Liebisch, J.A. Vizcaino, H. Kofeler, M. Trotzmuller, W.J. Griffiths, G. Schmitz, F. Spener, M.J.O. Wakelam, Shorthand notation for lipid structures derived from mass spectrometry, J. Lipid Res. 54 (2013) 1523–1530.
[43] F.F. Hsu, I.J. Lodhi, J. Turk, C.F. Semenkovich, Structural distinction of diacyl-, alkylacyl, and alk-1-enylacyl glycerophosphocholines as M-15 (−) ions by multiple-stage linear ion-trap mass spectrometry with electrospray ionization, J. Am. Soc. Mass Spectrom. 25 (2014) 1412–1420.
[44] E. Cífková, R. Hájek, M. Lísa, M. Holčapek, Hydrophilic interaction liquid chromatography-mass spectrometry of (lyso)phosphatidic acids, (lyso)phosphatidylserines and other lipid classes, J. Chromatogr. A 1439 (2016) 65–73.

Journal of Chromatography B, 990 (2015) 52–63

Contents lists available at ScienceDirect

Journal of Chromatography B

journal homepage: www.elsevier.com/locate/chromb

Lipidomic analysis of plasma, erythrocytes and lipoprotein fractions of cardiovascular disease patients using UHPLC/MS, MALDI-MS and multivariate data analysis

Michal Holčapek[a,*], Blanka Červená[a], Eva Cífková[a], Miroslav Lísa[a], Vitaliy Chagovets[a], Jitka Vostálová[b], Martina Bancířová[b], Jan Galuszka[c], Martin Hill[d]

[a] Department of Analytical Chemistry, Faculty of Chemical Technology, University of Pardubice, Studentská 573, 53210 Pardubice, Czech Republic
[b] Palacký University, Department of Medical Chemistry and Biochemistry, Faculty of Medicine and Dentistry, 77515 Olomouc, Czech Republic
[c] University Hospital Olomouc, I. P. Pavlova 185/6, 77520 Olomouc, Czech Republic
[d] Institute of Endocrinology, Národní 8, 11694 Prague 1, Czech Republic

ARTICLE INFO

Article history:
Received 25 December 2014
Accepted 17 March 2015
Available online 23 March 2015

Keywords:
Lipids
Lipidomics
Cardiovascular diseases
Lipoprotein fractions
UHPLC/MS
Multivariate data analysis

ABSTRACT

Differences among lipidomic profiles of healthy volunteers, obese people and three groups of cardiovascular disease (CVD) patients are investigated with the goal to differentiate individual groups based on the multivariate data analysis (MDA) of lipidomic data from plasma, erythrocytes and lipoprotein fractions of more than 50 subjects. Hydrophilic interaction liquid chromatography on ultrahigh-performance liquid chromatography (HILIC-UHPLC) column coupled with electrospray ionization mass spectrometry (ESI-MS) is used for the quantitation of four classes of polar lipids (phosphatidylethanolamines, phosphatidylcholines, sphingomyelins and lysophosphatidylcholines), normal-phase UHPLC—atmospheric pressure chemical ionization MS (NP-UHPLC/APCI-MS) is applied for the quantitation of five classes of nonpolar lipids (cholesteryl esters, triacylglycerols, sterols, 1,3-diacylglycerols and 1,2-diacylglycerols) and the potential of matrix-assisted laser desorption/ionization mass spectrometry (MALDI-MS) is tested for the fast screening of all lipids without a chromatographic separation. Obtained results are processed by unsupervised (principal component analysis) and supervised (orthogonal partial least squares) MDA approaches to highlight the largest differences among individual groups and to identify lipid molecules with the highest impact on the group differentiation.

1. Introduction

Lipids are hydrophobic or amphipathic small molecules that may originate entirely or in part by the carbanion based condensation of ketoacylthioesters and/or the carbocation based condensation of isoprene units according to the Lipid MAPS classification system. Lipids are divided into eight categories: fatty acyls, glycerolipids, glycerophospholipids, sphingolipids, saccharolipids, polyketides, sterol lipids and prenol lipids [1–3]. For the chromatographic analysis of lipids, it is useful to divide them into groups of polar and nonpolar lipids. Lipids have several important functions in a human organism, such as a source of energy (triacylglycerols, TG), building blocks of cell membrane (glycerophospholipids), signaling molecules between organelles or cells (glycerophospholipids, diacylglycerols and fatty acyl derivatives), hormones (derivatives of cholesterol) and the role in the immune system (glycerolipids) [4–7]. Lipids are transported by lipoprotein particles in the human body due to their hydrophobicity. Dietary

Abbreviations: APCI, atmospheric pressure chemical ionization; BMI, body mass index; CE, cholesteryl esters; CVD, cardiovascular disease; DG, diacylglycerols; DHB, 2,5-dihydroxybenzoic acid; EDTA, ethylenediaminetetraacetic acid; ESI, electrospray ionization; g1, group 1; g2, group 2; g3, group 3; g4, group 4; g5, group 5; FWHM, full width at half maximum; HDL, high-density lipoproteins; HILIC, hydrophilic interaction liquid chromatography; HPLC, high-performance liquid chromatography; IS_1, internal standard 1 (sphingosyl PE d17:1/12:0); IS_2, internal standard 2 (dioleoyl ethylene glycol); LC, liquid chromatography; LDL, low-density lipoproteins; LPC, lysophosphatidylcholines; LVEF, left ventricular ejection fraction; MALDI, matrix-assisted laser desorption/ionization; MDA, multivariate data analysis; MS, mass spectrometry; NP, normal phase; OPLS, orthogonal partial least squares; PC, phosphatidylcholines; PCA, principal component analysis; PE, phosphatidylethanolamines; PLS, partial least squares; SM, sphingomyelins; TG, triacylglycerols; UHPLC, ultrahigh-performance liquid chromatography; VLDL, very low-density lipoproteins.

* Corresponding author. Tel.: +420 466 037 087; fax: +420 466 037 068.
E-mail address: Michal.Holcapek@upce.cz (M. Holčapek).

http://dx.doi.org/10.1016/j.jchromb.2015.03.010
1570-0232/

cholesterol, glycerophospholipids and TG are absorbed in the small intestine, transported by chylomicrons to the blood circulation, where the TG part of chylomicrons is degraded to fatty acids, which could be used as the source of energy. Liver generates very low-density lipoproteins (VLDL) containing TG, glycerophospholipids, cholesterol, cholesteryl esters (CE) and protein parts. The main function of VLDL is the transport of TG to extrahepatic tissues. Low-density lipoproteins (LDL) are responsible for the transfer of cholesterol and CE to cells. High-density lipoproteins (HDL) are the smallest lipoprotein particles and they transfer overflowing cholesterol from cells back to the liver and the interchange of CE, TG and glycerophospholipids with VLDL. HDLs have also numerous additional properties, such as the apoprotein source for other lipoproteins, anti-inflammatory, antioxidant and antithrombotic properties [8–10]. The dysregulation of lipid metabolism could lead to the development of CVD, cancer, Alzheimer disease, etc. [11].

The prevalence of major risk factors for CVD is increasing in the major population of countries of the developing world with subsequently increased rates of coronary and cerebrovascular events [12]. The major risk factors of CVD are obesity, high level of circulating lipids, age, gender, smoking, diabetes mellitus, hyperhomocysteinemia, etc. [5,11,13–16]. The obesity has a strong connection with the development of CVD [17]. Dietary fatty acids are accumulated in the adipose tissue until the storage capacity becomes saturated in case of the obesity, which induces a combined state of inflammation and insulin resistance [13,17,18]. The term CVD does not represent a single disease, but it includes, for example coronary heart disease, strokes, valvular heart disease and cardiomyopathy [19]. Lipids have a crucial role in the development of CVD and related diseases [20]. The downregulation of PC and plasmalogen-PE and the increase of PC/lysophosphatidylcholines (LPC) ratio have been reported for hyperlipidemic patients [21].

Two main analytical techniques are used for the lipidomic quantitation, shotgun without any chromatographic separation [22,23] and high-performance liquid chromatography–mass spectrometry (HPLC/MS) or UHPLC/MS approaches. Advantages of shotgun are an easier automation and higher throughput, while HPLC/MS is more prone to ion suppression effects and can provide more detailed information of various types of lipid isomerism. HILIC can be used for the separation of individual classes of polar lipids [24–28], while NP-HPLC is more convenient for nonpolar lipid classes [29–32]. The lipid species separation according to the acyl chain length and the number of the double bonds can be achieved by reversed phase (RP)-HPLC [25,33–36], while silver-ion HPLC is more convenient for nonpolar lipid regioisomers or double bond positional isomers [37,38]. MALDI provides the fast analysis without the requirement of chromatographic separation [39], which could be useful for high-throughput clinical screening.

MDA methods are typically used for the group differentiation in the lipidomic analysis using either unsupervised (principal component analysis, PCA) or supervised (partial least squares, PLS, and OPLS) methods [40]. PCA is used to reduce primary variables to the latent variables, which are called principal components due to the decreasing model dimensionality. Principal components are linear combinations of x_i, which are mutually uncorrelated. PLS relates two data matrices, *X* and *Y*, to each other by a linear multivariate model, which works with a maximum covariance between matrices *X* and *Y* [41,42]. OPLS divides a systematic variation in matrices *X* into two model parts, one part of the model expresses correlations between *X* and *Y* matrices and another part of the model expresses the variation that is not related (orthogonal) to *Y* [42,43]. Results of MDA are typically presented in in two forms, score plots and loading plots. The score plot displays two score vectors plotted against each other for the visualization of objects, *e.g.*, samples or patients. The loading plot is constructed using two loading vectors plotted against each other to visualize characteristic variables, such as lipid species [44]. The S-plot is a variant of the loading plot, where *X* axis is the variable of magnitude and *Y* axis is the reliability [44].

The main goal of this work is a lipidomic study of differences among CVD, healthy normal and healthy obese subjects using three MS-based methods: HILIC-UHPLC/ESI-MS for the analysis of polar lipid classes, NP-UHPLC/APCI-MS for the analysis of nonpolar lipid classes and MALDI-MS for the fast lipidomic screening. MDA methods (PCA and OPLS) are used for a better visualization of group differences.

2. Materials and methods

2.1. Materials

Acetonitrile, 2-propanol, methanol (all HPLC/MS grade), hexane (HPLC grade), chloroform (HPLC grade, stabilized with 0.5–1% ethanol), ammonium acetate, 2,5-dihydroxybenzoic acid (DHB), NaCl, KBr and EDTA $Na_2{\cdot}2H_2O$ were purchased from Sigma–Aldrich (St. Louis, MO, USA). Deionized water was prepared with Demiwa 5-roi purification system (Watek, Ledeč nad Sázavou, Czech Republic) and by ultra CLEAR UV apparatus (SG, Hamburg, Germany). Standards of polar lipids containing oleoyl acyls (PE, PC, SM and LPC), internal standards for polar lipids (sphingosyl PE d17:1/12:0, IS_1) and for nonpolar lipids (dioleoyl ethylene glycol, IS_2) were purchased from Avanti Polar Lipids (Alabaster, AL, USA). Standards of CE, cholesterol, TG, 1,3-DG and 1,2-DG containing oleoyl acyls were purchased from Sigma–Aldrich. Biological samples (plasma, erythrocytes, VLDL, LDL and HDL) were obtained from healthy volunteers and CVD patients in cooperation with the Faculty Hospital Olomouc based on the approval of the ethical committee at the Faculty Hospital Olomouc.

2.2. Characterization of studied subjects

Fifty eight men between 40 and 55 years were selected for the study with the following characterization of individual groups (details in Table S1): group 1 (g1): healthy subjects with body mass index (BMI) with the mean value of 25.1 kg/m^2 without medication; group 2 (g2): healthy subjects with BMI between 30 and 35 kg/m^2 without medication; group 3 (g3): subjects with the non-ischemic dilated cardiomyopathy and negative coronographic findings, chronic heart failure, left ventricular ejection fraction (LVEF) below 35% with stable therapy (diuretics, angiotensin-converting enzyme inhibitors, beta-blockers and acetylsalicylic acid); group 4 (g4): subjects with the chronic form of atrial fibrillation/flutter without valvular heart disease, myocardial infarction or chronic heart failure, LVEF more than 35% with antiarrhythmic agents, anticoagulants, statins and radiofrequency ablation therapy; group 5 (g5): subjects with ischemic heart diseases, post myocardial infarction, without the chronic heart failure, LVEF more than 35% with stable therapy of beta-blockers, statins and acetylsalicylic acid.

2.3. Sample preparation

Blood was collected to heparin-lithium tubes and centrifuged to obtain erythrocytes and plasma. Erythrocytes were washed three times by phosphate buffered saline. Plasma was further separated into lipoprotein fractions by the ultracentrifugation. The following ultracentrifugation steps were applied to obtain lipoprotein fractions (VLDL, LDL and HDL) according to literature [45]. The volume of plasma was divided into two polycarbonate tubes for the ultracentrifugation and refilled with the density solvent 1 (1.1 g NaCl + 37.6 mg EDTA $Na_2{\cdot}2H_2O$ dissolved in 100 mL of water). Samples were centrifuged for 11 h at 10 °C and 45,000 × *g* and then the VLDL fraction was collected. The remaining solution was mixed

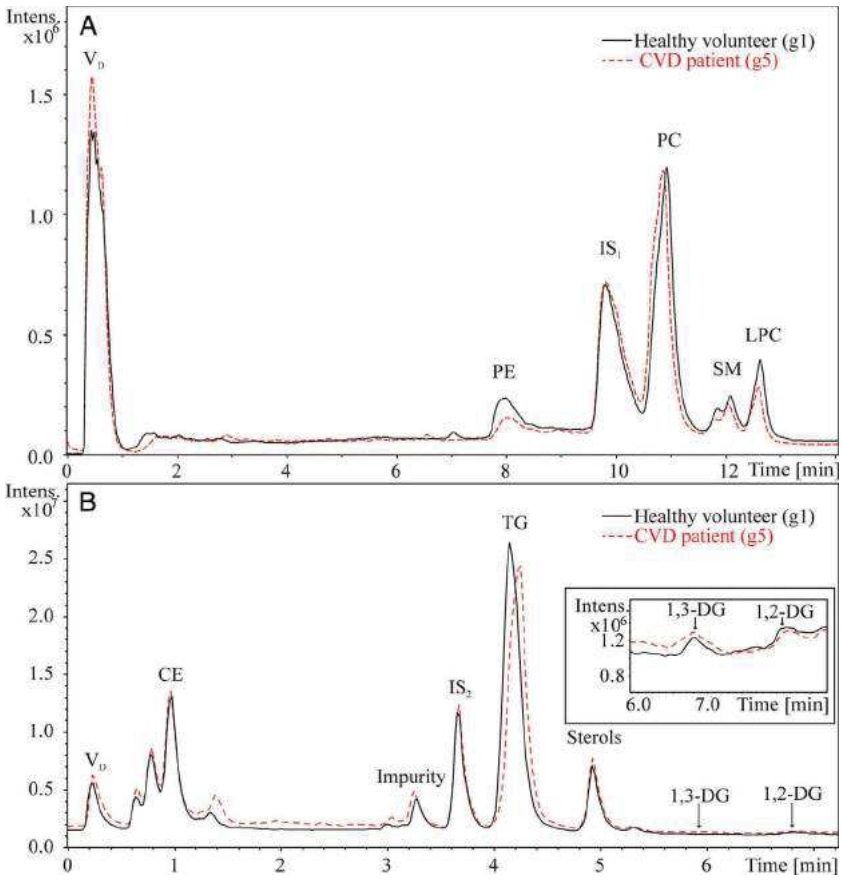

Fig. 1. Chromatograms of plasma samples of healthy volunteer (g1) and CVD patient (g5). (A) HILIC-UHPLC/ESI-MS separation of polar lipid classes (PE, PC, SM and LPC) and the internal standard IS_1 (sphingosyl PE d17:1/12:0). *Conditions*: Acquity UPLC HILIC column (50 mm × 2.1 mm, 1.7 μm), flow rate 0.5 mL/min, column temperature 40 °C, gradient 0 min; 0.5% A + 99.5% B, 20 min 20.5% A + 79.5% B, where A is a mixture of 5 mmol/L aqueous ammonium acetate and methanol (9:1, v/v) and B is acetonitrile. (B) NP-UHPLC/APCI-MS separation of nonpolar lipid classes (CE, TG, sterols, 1,3-DG and 1,2-DG) and the internal standard IS_2 (dioleoyl ethylene glycol). *Conditions*: Acquity UPLC HILIC column (50 mm × 2.1 mm, 1.7 μm), flow rate 1 mL/min, column temperature 30 °C, gradient 0 min; 99% A + 1% B, 20 min 32% A + 68% B, where A is hexane and B is the mixture of hexane–2-propanol–acetonitrile (96:2:2, v/v/v).

with 0.5 mL of the density solvent 2 (9.2 g KBr + 37.6 mg EDTA $Na_2{\cdot}2H_2O$ dissolved in 100 mL water). Samples were centrifuged again for 12 h at 10 °C and 45,000 × *g* and then the LDL fraction was collected. The remaining solution was mixed with 0.5 mL of the density solvent 3 (34.8 g KBr + 188.0 mg EDTA $Na_2{\cdot}2H_2O$ dissolved in 100 mL of water). Samples were centrifuged for 48 h at 10 °C and 20,000 × *g* and finally the HDL fraction was collected.

The total lipid extract was prepared according to the modified Folch method [46]. Five hundred microliter of sample with 50 μL (3.3 mg/mL) of IS_1 was homogenized with 10 mL of chloroform–methanol mixture (2:1, v/v). This mixture was filtered using a rough filter paper. Then 2 mL of 1 mol/L NaCl was added and centrifuged for 3 min at 2500 rpm. The chloroform layer containing lipids was evaporated by a gentle stream of nitrogen and dissolved in chloroform–2-propanol (1:1, v/v) for the HILIC analysis.

Nonpolar lipid extracts were prepared according to the previously developed method [32]. Fifty microliter of the sample with 5 μL (3.3 mg/mL) of IS_2 was mixed with 150 μL of hexane–methanol (98:2, v/v). The mixture was incubated for 10 min, then 300 μL of methanol–water mixture (95:5, v/v) and 300 μL of hexane–methanol mixture (98:2, v/v) were added. The sample was centrifuged for 1 min at 2500 rpm and then the upper hexane layer was collected. The lower layer was washed twice with 300 μL of hexane–methanol and the upper hexane layer was collected again and combined. Hexane solution containing nonpolar lipids was evaporated by the gentle stream of nitrogen, then dissolved in hexane and used for NP-UHPLC/APCI-MS analysis.

Ten microliter of the total lipid extract was mixed with 10 μL of 0.5 mol/L DHB in methanol and 0.7 μL of this mixture was deposited on the stainless steel sample plate and dried using the gentle stream of nitrogen. Each sample was deposited in six wells and used for the MALDI-MS analysis.

2.4. HILIC-UHPLC/ESI-MS conditions [32]

Experiments were performed with a liquid chromatograph Agilent 1290 Infinity Series (Agilent Technologies, Santa Clara, CA, USA). Acquity UPLC HILIC column (50 mm × 2.1 mm, 1.7 μm, Waters, Milford, MA, USA) was used for the separation of polar classes of lipids. The flow rate was 0.5 mL/min, the column temperature was 40 °C, the mobile phase gradient was 0 min: 0.5% A + 99.5% B; 20 min: 20.5% A + 79.5% B, where A was the mixture of 5 mmol/L aqueous ammonium acetate and methanol (9:1, v/v), B was acetonitrile. Hybrid quadrupole–time-of-flight mass spectrometer (MicroTOF-Q, Bruker Daltonics, Bremen, Germany) operating in the positive-ion ESI mode was used for the determination of polar lipid classes (PE, PC, SM and LPC) and IS_1 under the following conditions: capillary voltage 4.5 kV, pressure of nebulizer gas 1.6 bar, flow rate of drying gas 9 mL/min, drying temperature 220 °C and mass range *m/z* 50–1500.

2.5. NP-UHPLC/APCI-MS conditions [32]

Experiments were performed with a liquid chromatograph Agilent 1200 Infinity Series (Agilent Technologies). Acquity UPLC HILIC

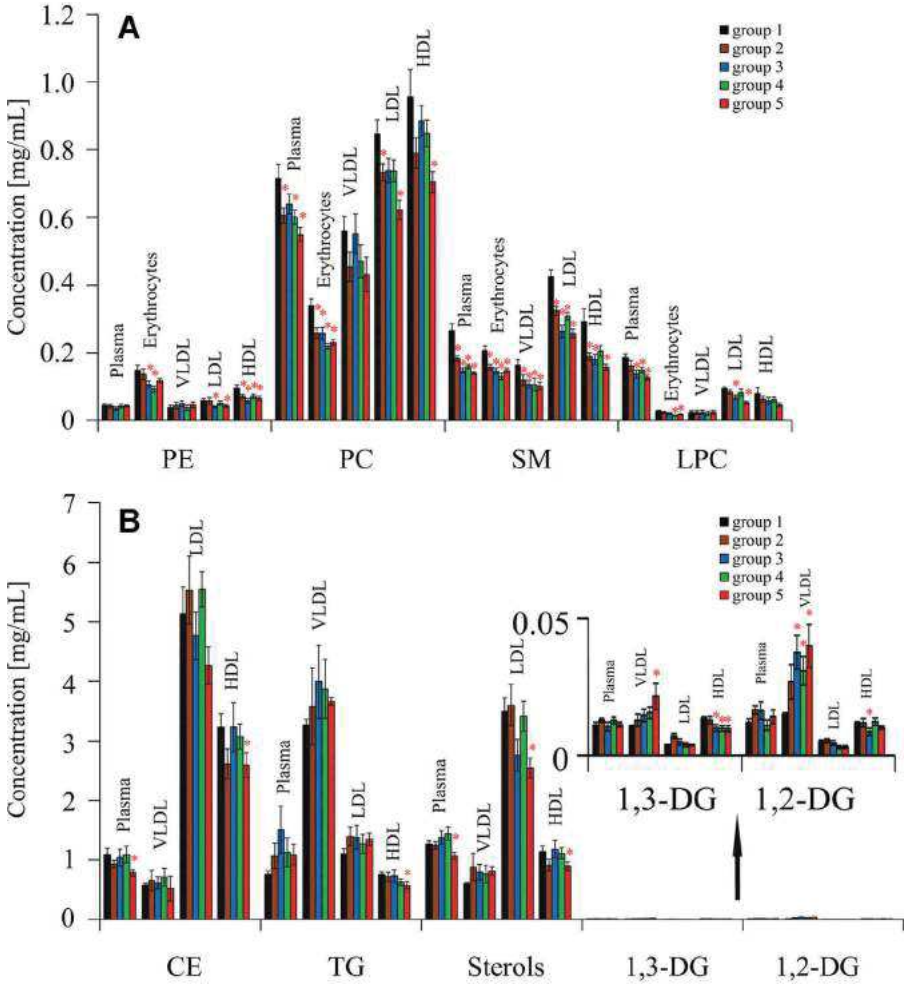

Fig. 2. Comparison of mean group concentrations with standard error bars for: (A) PE, PC, SM and LPC as polar lipid classes, and (B) CE, TG, sterols, 1,3-DG and 1,2-DG as nonpolar lipid classes determined in plasma, erythrocytes, VLDL, LDL and HDL. Lipid class concentrations significantly different from the group 1 ($p \leq 0.05$) according to the Student's *t*-test are labelled by an asterisk.

(50 mm × 2.1 mm, 1.7 μm, Waters) column was used for the separation of nonpolar classes of lipids. The flow rate was 1 mL/min, the column temperature was 30 °C, the mobile phase gradient was 0 min: 99% A + 1% B; 20 min: 32% A + 68% B, where A was hexane and B was the mixture of hexane–2-propanol–acetonitrile (96:2:2, v/v/v). Esquire 3000 ion trap mass spectrometer (Bruker Daltonics) operating in the positive-ion APCI mode was used for the determination of nonpolar lipid classes under the following conditions: corona current 4000 nA, pressure of nebulizer gas 65 psi, flow rate of drying gas 3 L/min, drying temperature 350 °C, vaporizer temperature 375 °C, target mass *m/z* 500 and mass range *m/z* 50–1000.

2.6. MALDI-MS conditions

Experiments were performed with hybrid linear ion trap–orbitrap mass analyzer LTQ Orbitrap XL (Thermo Scientific, Waltham, MA, USA) operating in the positive-ion MALDI in the mass range *m/z* 300–2000 with the resolving power of 100,000 and the laser energy of 15 μJ per laser shot. The mass spectrum from one point was obtained as a summation of 3 laser shots. Spectra for each well were measured from 50 randomly distributed positions. The final spectrum for each patient was obtained by averaging of 300 spectra from six wells to obtain the most representative spectrum. Mass spectra were converted with msConvert tool [47] and preliminarily processed with home-made program based on the MALDIquant package [48].

2.7. MDA of lipidomic data

MS data were evaluated by the Data Analysis software (Bruker Daltonics), the Progenesis QI software (Waters) and the Simca 13.0 software (Umetrics, Umeå, Sweden). MS data were processed by the Progenesis QI software using the high resolution positive-ion MS for polar lipids and the low resolution positive-ion MS for nonpolar lipids. The alignment, peak picking and identification of lipids were performed. Data sheets from Progenesis QI software were obtained and absolute intensities of all identified compounds were recalculated to relative abundances of lipid molecules. The data were transformed using the logarithmic transformation to obtain a Gaussian normal distribution and the Pareto scaling was used for final statistical models. The data were processed by unsupervised PCA and supervised OPLS methods to obtain group clusters. Lipid molecules with the highest impact on the group clustering were identified in S-plots.

3. Results and discussion

3.1. UHPLC/MS methods

The goal of this study is finding differences among the lipidomic composition of blood fractions (plasma, erythrocytes, VLDL, LDL and HDL) of three types of CVD patients (g3, g4 and g5) and healthy controls (g1). The obesity plays a rather important role in the

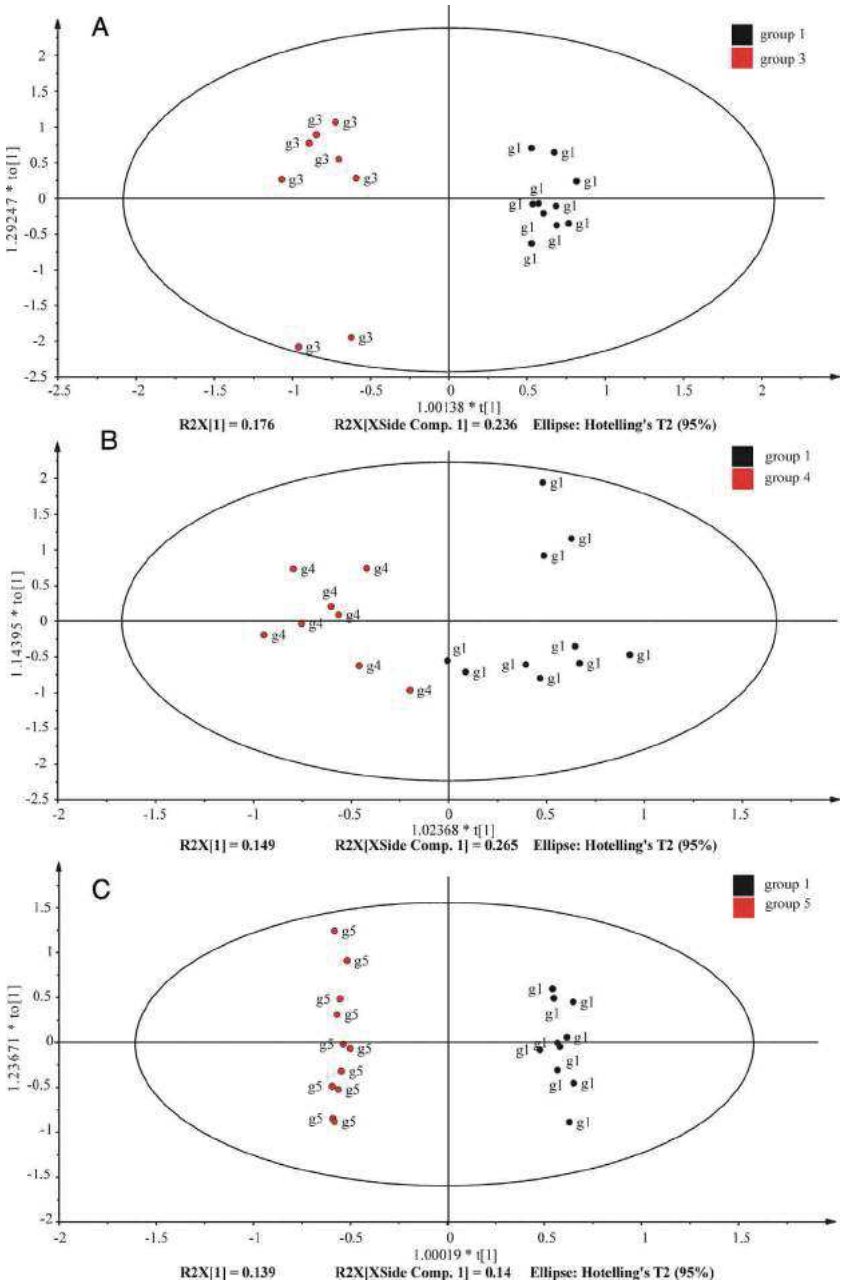

Fig. 3. OPLS score plots for polar and nonpolar lipid classes in human plasma samples: (A) g1 *vs.* g3, (B) g1 *vs.* g4, and (C) g1 *vs.* g5.

development of CVD [17] so the group of obese healthy control (g2) is included as well to differentiate effects of CVD and obesity on the lipidome. Details on the selection and size of individual groups, characteristic biochemical and anthropometric parameters are summarized the Experimental part and Table S1.

UHPLC/MS methods for the analysis of large series of clinical samples have been developed in our previous works [26,32,49]. Briefly, HILIC-UHPLC/ESI-MS method (Fig. 1A) is used for the determination of polar lipid classes (PE, PC, SM and LPC) using the IS_1 (sphingosyl PE d17:1/12:0) and response factors approach [26,32] to normalize different ionization efficiencies of individual lipid classes. IS_1 is not present in biological samples and well separated from chromatographic peaks of other lipid classes. Nonpolar lipid classes (CE, TG, ST, 1,3-DG and 1,2-DG) are determined in a similar fashion, but their separation is performed in NP-UHPLC/APCI-MS (Fig. 1B) mode, because they elute in the void volume using the previously mentioned HILIC method [25]. Dioleoyl ethylene glycol is used as IS_2. The quantitation of polar lipid classes in the HILIC mode and nonpolar lipid classes in NP mode is done by the multiplication of lipid class peak areas by response factors of this class and normalized to the IS_1 for polar lipids and IS_2 for nonpolar lipids to obtain absolute lipid class concentrations shown in Table S2. Then the lipid species composition is determined from the overall mass spectra of chromatographic peaks of lipid classes. Relative concentrations of lipid species are determined based on the assumption that differences in relative responses of individual lipid species can be neglected. Most lipidomic clinical studies are based on the comparison of healthy and disease states, so basically relative changes are measured and the extent of such changes is statistically evaluated by MDA methods. Mean group concentrations for individual lipid classes with their standard error bars are summarized in Fig. 2. Another way of data presentation is the use of relative concentrations in pie chart graphs (Fig. S1), which can better visualize some trends in concentration changes among

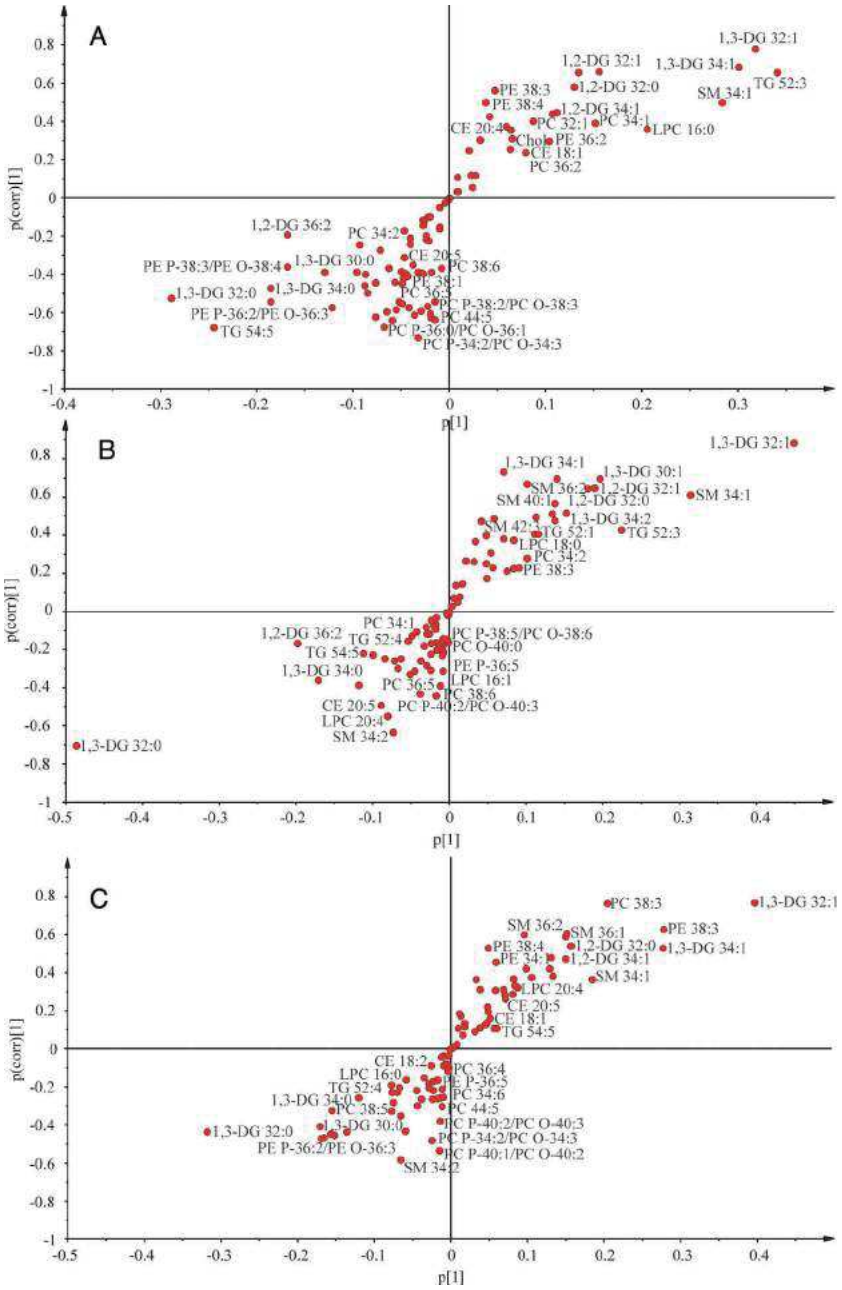

Fig. 4. S-plots from OPLS analysis (see Fig. 3) for lipid classes in human plasma samples with the most important upregulated lipid molecules in the upper right corner and downregulated lipid molecules in the lower left corner: (A) g1 *vs.* g3, (B) g1 *vs.* g4, and (C) g1 *vs.* g5.

individual lipid classes. Fig. S2 illustrates two selected examples of lipid molecules with large changes in concentrations among individual groups. The concentration of PC 32:0 (Fig. S2A) is downregulated in CVD patients, where the highest decrease but also high variation is observed for g3. The concentration of TG 52:3 (Fig. S2B) is upregulated in CVD patients, where the largest change is observed for g3, but again with the largest variability for this group.

3.2. MALDI-MS

MALDI-MS has the potential for the high-throughput clinical analysis of numerous samples without a chromatographic separation. The high-resolution (100,000 FWHM) full scan positive-ion mode is used for our measurements to reduce the risk of peak overlaps caused by missing chromatography. At the beginning, all important lipid molecules are identified based on the mass accuracy better than 1 ppm, verified by MS/MS spectra and also correlated with identified lipids in UHPLC/MS experiments. For routine measurements, only absolute intensities of monitored *m/z* values are recorded and their mass accuracies are checked. Then, absolute intensities are normalized to IS_1 in a similar way as described for UHPLC/MS experiments and processed by MDA methods. Conditions of MALDI measurements are carefully optimized in terms of selected matrix, laser energy and extensive signal averaging to obtain the highest possible robustness for quantitative MALDI measurements. MALDI-MS analysis is tested simultaneously with UHPLC/MS analysis to compare the potential of UHPLC/MS with MALDI-MS for the quantitative comparison of large data sets of samples. Some advantages but mainly limitations of MALDI-MS are observed in our study, such as lower robustness of the quantitation and more demanding data interpretation due to the lack

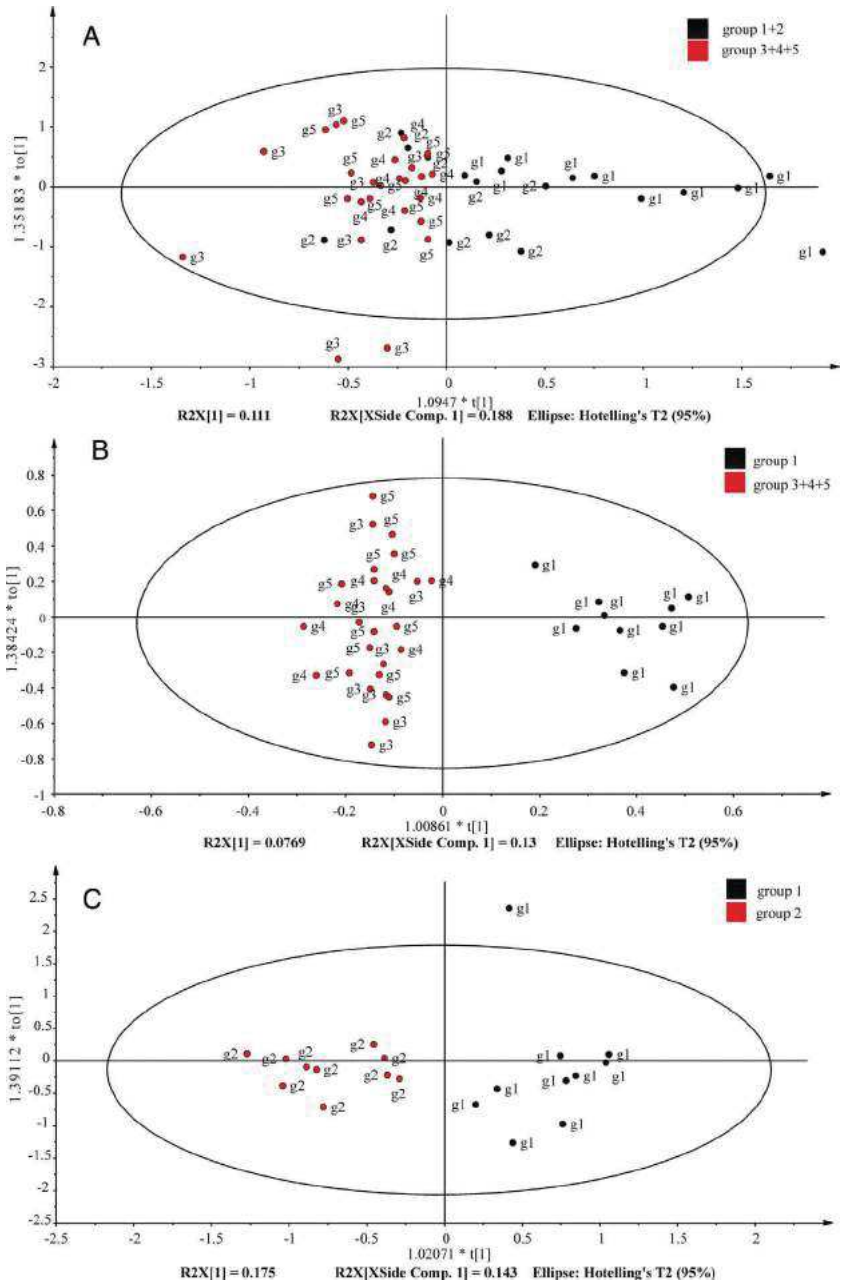

Fig. 5. OPLS score plots for polar and nonpolar lipid classes in human plasma samples: (A) g1 + g2 *vs.* g3 + g4 + g5, (B) g1 *vs.* g3 + g4 + g5, and (C) g1 *vs.* g2.

of retention time in UHPLC/MS, where the lipid class is easily determined by the characteristic retention of particular group. The main advantage of MALDI in our study is a reduced fragmentation in comparison to APCI, which has to be used in NP-UHPLC/MS setup, because mobile phases used in NP systems do not allow the use of ESI. This advantage of MALDI over APCI is dramatic in case of TG, where the significant fragmentation is observed with APCI (relative abundances of $[M+H]^+$ lower than 2% for saturated TG) compared to base peaks of molecular adducts in case of MALDI. Unfortunately, the MDA of MALDI-MS data is slightly worse compared to UHPLC/MS (Fig. S3), as concluded from the worse group clustering. Our conclusion on MALDI-MS *vs.* UHPLC/MS comparison is that UHPLC/MS is superior technique for the quantitative lipidomic studies due to the lower signal variation, easier species identification (possible combination of accurate *m/z* values and class characteristic retention times) and improved grouping in MDA.

3.3. Development of statistical models

Tables of absolute intensities of individual lipid species obtained by the Progenesis QI software are processed using the Simca 13.0 statistical software. First, the absolute intensity of each lipid molecule is normalized to the absolute intensity of the IS_1 for polar lipid classes and IS_2 for nonpolar lipid classes. The development of the best statistical model is explained on the example of plasma samples. First, an unsupervised PCA method (Fig. S4) is always applied to see the natural grouping of samples, as shown on examples of g1 + g2 *vs.* g3 + g4 + g5 using different ways of data scaling and normalization. Distinct group clusters can be expected only for samples with significantly different values of certain parameters, which is often not a case of lipidomic or metabolomic studies. Then, the supervised OPLS method is applied to improve the group clustering (Fig. S5). The important parameter is the way of data scaling. The conventional unit variance (UV) scaling does not provide the

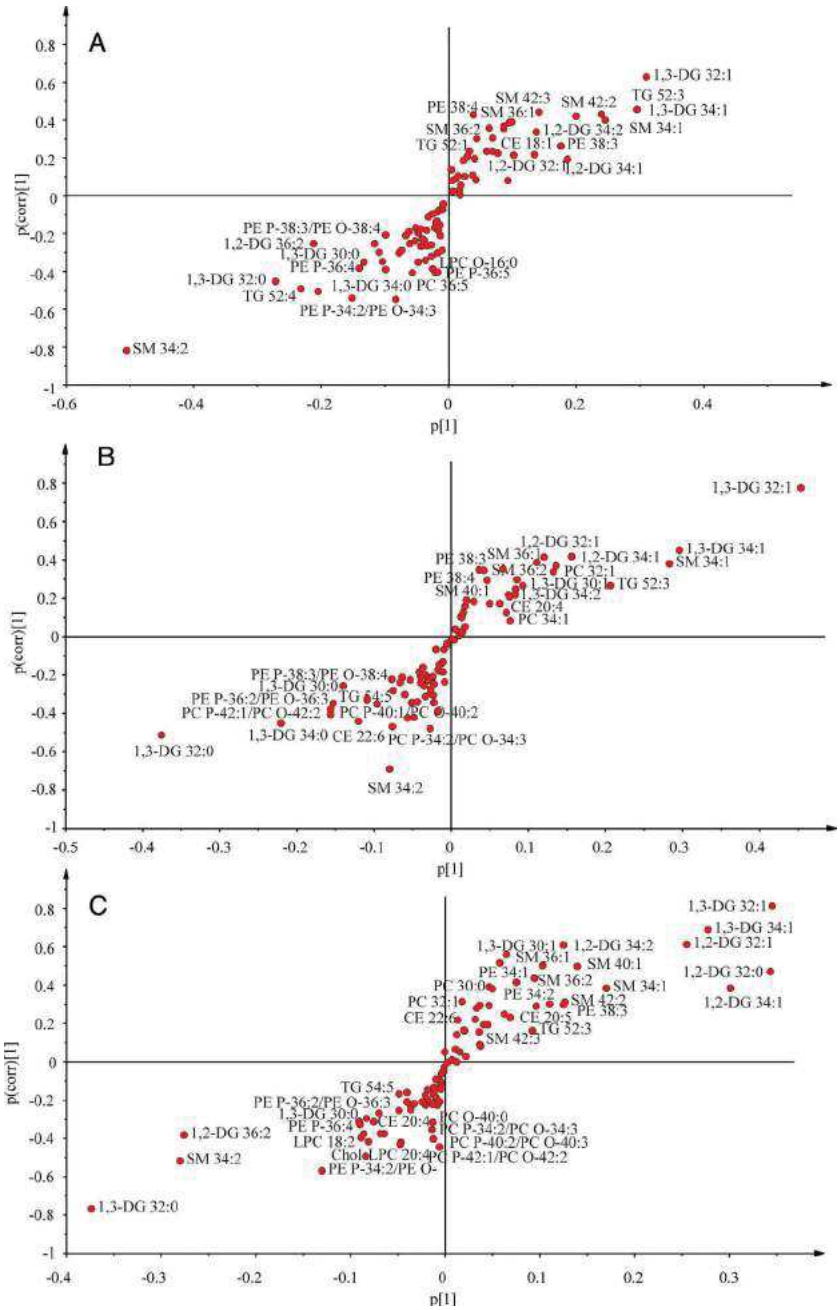

Fig. 6. S-plots from OPLS analysis (see Fig. 5) for lipid classes in human plasma samples with the most important upregulated lipid molecules in the upper right corner and downregulated lipid molecules in the lower left corner: g1 + g2 *vs.* g3 + g4 + g5, (B) g1 *vs.* g3 + g4 + g5, and (C) g1 *vs.* g2.

best results for the metabolomic data (Figs. S4A, S4B, S5A and S5B), where the Pareto scaling is recommended [42] and also in our case the group clustering is better with the Pareto scaling used in the rest of this work. Tables S3 and S4 show basic parameters of statistical models used in figures presented in this paper, where nonpolar and polar lipids can be processed either separately or jointly depending on quality of the statistical group differentiation.

3.4. *Effects of CVD and obesity on lipidomic profiles*

Various statistical correlations among individual groups are studied in our lipidomic data set and the most interesting results are presented here with the emphasis on the differentiation of healthy and CVD groups by MDA methods. The following main trends are observed (Fig. 2) for comparison of mean lipid class concentrations of individual groups in comparison to normal healthy group (g1). In general, quantitative data obtained by biochemical measurements (Table S1) and UHPLC/MS data (Fig. 2) are in a good agreement. PC and SM decrease in all fractions in comparison to g1. This decrease is statistically significant according to *t*-test for SM in most fractions and for PC in plasma and erythrocytes. PE decreases in many cases, the most pronounced and statistically relevant decrease is observed for HDL (g3, g4 and g5) and LDL (g3 and g5) in agreement with the previous work [50] and also for erythrocytes (g3 and g4). The decrease of LPC concentration is observed for all fractions except for VLDL. The statistically significant changes are reported for g3, g4 and g5 in plasma, g4 and g5 in erythrocytes, g3 and g5 in LDL. LPC with anti-inflammatory properties is decreased in obese and CVD patients [51]. LPC (18:2) decrease observed in obese patients is in agreement with the

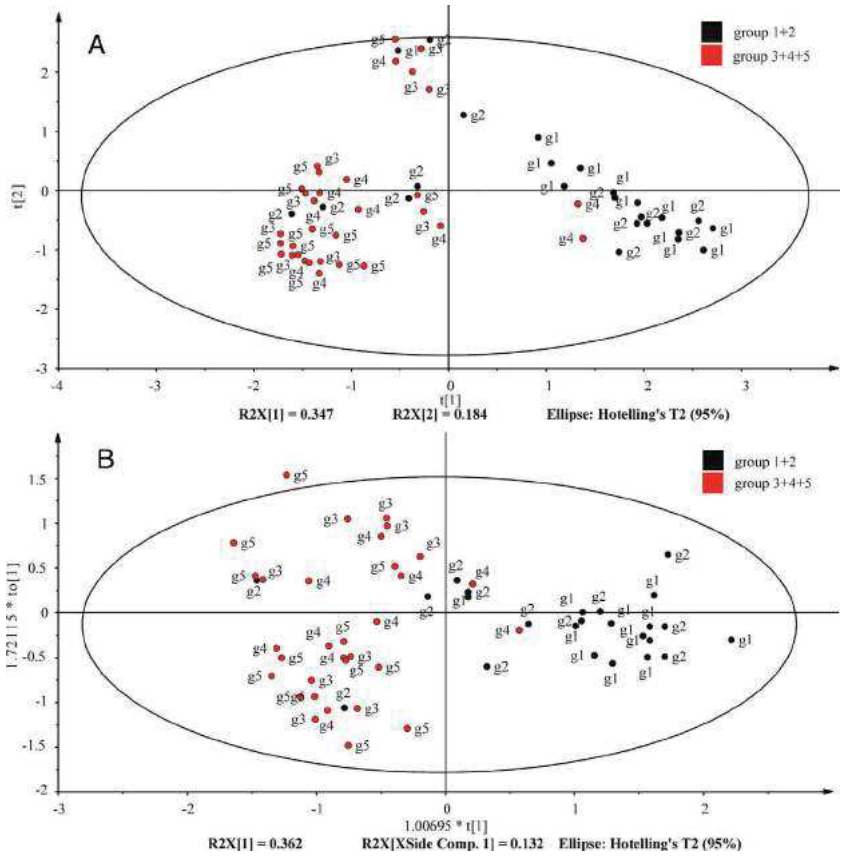

Fig. 7. Statistical plots for nonpolar lipid classes in HDL samples: (A) PCA score plot, and (B) OPLS score plot.

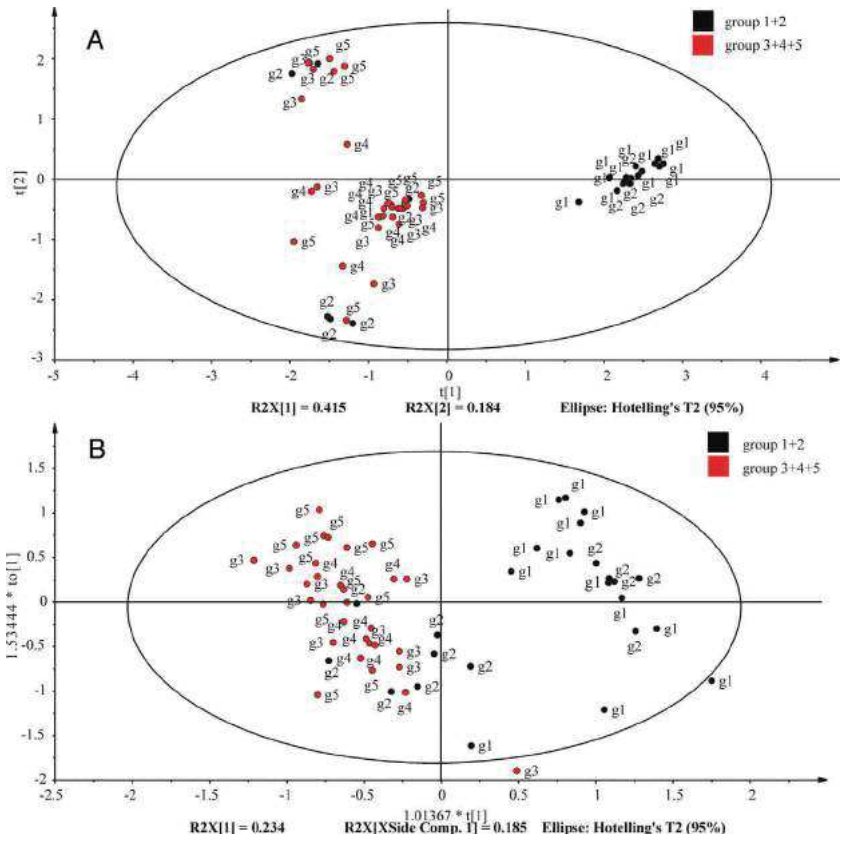

Fig. 8. Statistical plots for nonpolar lipid classes in LDL samples: (A) PCA score plot, and (B) OPLS score plot.

previous work [52]. Other works have reported the opposite effects, such as increased LPC concentration in the sperm of obese man [53] or in human plasma of rheumatoid arthritis patients [54], but this observation does not correspond to our data for plasma of CVD patients. Table S5 shows that ratios of PC/LPC and PC/SM are increased for CVD groups (g3, g4 and g5) compared to the healthy control in case of plasma, LDL and mainly HDL, which is in agreement with the previously published work [55], but another work [56] reports the increased cardiovascular risk for the elevated concentration of lipoprotein-associated phospholipase A2.

For nonpolar lipid classes, the concentration increase is observed for both 1,2- and 1,3-DG in VLDL, but not for other blood fractions. 1,3-DG concentrations even decrease in HDL (g3, g4 and g5). Concentrations of TG in most fractions (except for HDL) are increased, which is in agreement the previous study as well [57]. Large variations in TG concentrations are probably associated with the different diet and living style of individual objects. Changes are mostly not statistically significant due to large variations, but anyway the following trends are apparent: increase of TG concentration (the largest for g3) in plasma, VLDL and LDL, but TG concentration decreases in HDL (statistically significant for g5). Concentration trends for sterols and CE measured by UHPLC/MS (Fig. 2B) are in a full agreement with biochemical measurements (Table S1). The reduced concentration of most lipid classes is observed for g5 (Fig. 2), in many cases these decreases are statistically significant according to *t*-test, such as decreases of CE in plasma and HDL, TG in HDL, sterols in plasma, LDL and HDL, PC, SM and LPC in most fractions. This trend is probably related to the drug lowering therapy with statins, because g5 has a stable therapy of beta-blockers and statins. High blood TG level is associated with the increased risk of CVD [58]. The large increase of 1,2-DG and 1,3-DG in VLDL (Fig. 2B) could be associated with TG degradation by the lipoprotein lipase. Concentration profiles of DG and TG in VLDL show similar profiles.

The first step in MDA is the comparison of CVD groups separately for individual types of CVD (g3, g4 or g5) with healthy controls (g1) excluding healthy obese at this stage (Figs. S6 and 3). Unsupervised PCA score plots (Fig. S6) do not provide a clear group separation, but OPLS score plots (Fig. 3) show the distinct group separation of healthy and disease groups in all cases and there are also similarities in the most influential lipid molecules on the group separation visualized in S-plots (Fig. 4). The common features are the downregulation of some saturated DG (1,3-DG 32:0, 1,3-DG 34:0 and 1,3-DG 30:0) and several plasmalogen/ether PE and PC, the upregulation of some monounsaturated DG (*e.g.*, 1,3-DG 32:1, 1,3-DG 34:1, 1,2-DG 32:1). Another features are observed only for some CVD groups, such the upregulation of TG 52:3 for g3 (Fig. 4A), SM 34:1 for g3 (Fig. 4A) and g4 (Fig. 4B), PC 38:3 and PE 38:3 for g5 (Fig. 4C). When all three CVD groups are combined (g3 + g4 + g5) and correlated with combined healthy normal and healthy obese groups (g1 + g2), then the group clustering is not so clear (Fig. 5A) as in previous examples, but anyway all healthy normal and CVD subjects are clearly distinguished the score plot, but obese subjects (g2) are almost randomly distributed in this graph. The lipidomic composition of healthy obese is somewhere in between healthy state and CVD state in agreement with previous works and known facts that the obesity leads to proinflammatory conditions with the possible development of CVD [17]. If the obese group is excluded from the OPLS model, then the correlation g1 *vs.* g3 + g4 + g5 shows the excellent group separation again (Fig. 5B). Fig. 5C shows that healthy normal and healthy obese can also be easily differentiated by their lipidomic plasma composition. Lipid species with the highest impact on the group clustering are highlighted in S-plots (Fig. 6) showing similarities with the previous correlation of individual disease types (Fig. 4) as expected, but some features are better visualized here. The upregulation of SM 34:1 in g3 and g4, and of SM 36:1 and SM 36:2 in patients of all CVD is observed (Fig. 4). Obese participants (g2) have elevated SM 34:2, SM 36:1 and SM 36:2 (Fig. 6C).

In two cases, lipidomic differences between g1 + g2 *vs.* g3 + g4 + g5 are large enough that even unsupervised PCA yields the visible separation of group clusters, as shown for nonpolar lipid classes in Fig. 7A for HDL and in Fig. 8A for LDL. Only few obese subjects from g2 and two g4 subjects in case of HDL are incorrectly classified in these score plots. OPLS improves the group clustering only in part, but anyway the analysis of nonpolar lipids in HDL and LDL may be considered as the possible target in the future searches for CVD biomarkers. Another example of successful g1 + g2 *vs.* g3 + g4 + g5 MDA separation is shown for polar lipid classes in erythrocytes and VLDL, but the supervised OPLS has to be used for such group clustering (Fig. S7).

4. Conclusions

Three different MS-based methods are used for the lipidomic characterization of five groups containing healthy control, obese and three groups of different types of CVD patients. HILIC-UHPLC/ESI-MS provides the quantitative data on polar lipid classes and NP-HPLC/APCI-MS on nonpolar lipid classes. In both cases, relative lipid species concentrations are determined as well from mass spectra of chromatographic peaks of individual classes and further used for MDA. MALDI-MS is tested for the determination of all lipids without the chromatographic separation, but this approach is not superior to UHPLC/MS methods in terms of analytical information and also the quality of statistical differentiation of group clusters by MDA methods. The biological variability among individual people causes that unsupervised PCA method provides in most cases only a partial group clustering in PCA score plots, so the supervised OPLS has to be used for the better differentiation. CVD is a typical multifactorial type of diseases, where individual types of CVD exhibit also differences in their lipidomic composition. Another risk factor is the obesity, therefore the group of healthy obese is often in between healthy and CVD groups. If the obese group is excluded from our data, then the differentiation between healthy and disease samples is unambiguous in all cases, but such picture would be artificial. Finally, lipid molecules with the highest impact on the group clustering in OPLS score plots are identified using S-plots and increased/decreased concentrations of these lipids can be correlated with the development of CVD and the possible future research of their biomarker potential. Two most upregulated lipids in CVD groups are 1,3-DG 32:1 and 1,3-DG 34:1 and most downregulated species are SM 34:2 and 1,3-DG 32:0.

Acknowledgments

This work was supported by the project No. 206/11/0022 sponsored by the Czech Science Foundation. E. C. and V. C. acknowledge the support of the grant project No. CZ.1.07/2.3.00/30.0021 sponsored by the Ministry of Education, Youth and Sports of the Czech Republic.

Appendix A. Supplementary data

Supplementary data associated with this article can be found, in the online version, at http://dx.doi.org/10.1016/j.jchromb.2015.03.010.

References

[1] E.A. Dennis et al., http://www.lipidmaps.org/, downloaded December 2014.
[2] E. Fahy, S. Subramaniam, R.C. Murphy, M. Nishijima, C.R.H. Raetz, T. Shimizu, F. Spener, G. van Meer, M.J.O. Wakelam, E.A. Dennis, Update of the lipid maps comprehensive classification system for lipids, J. Lipid Res. 50 (2009) S9–S14.

[3] E. Fahy, D. Cotter, M. Sud, S. Subramaniam, Lipid classification, structures and tools, Biochim. Biophys. Acta Mol. Cell Biolog. Lipids 1811 (2011) 637–647.
[4] Y. Liu, V.A. Bankaitis, Phosphoinositide phosphatases in cell biology and disease, Prog. Lipid Res. 49 (2010) 201–217.
[5] F. Gunstone, J. Harwood, A.J. Dijkstra (Eds.), The Lipid Handbook with CD-ROM, third ed., CRC, Press, Boca Raton, FL, USA, 2007.
[6] O. Quehenberger, A.M. Armando, A.H. Brown, S.B. Milne, D.S. Myers, A.H. Merrill, S. Bandyopadhyay, K.N. Jones, S. Kelly, R.L. Shaner, C.M. Sullards, E. Wang, R.C. Murphy, R.M. Barkley, T.J. Leiker, C.R.H. Raetz, Z.Q. Guan, G.M. Laird, D.A. Six, D.W. Russell, J.G. McDonald, S. Subramaniam, E. Fahy, E.A. Dennis, Lipidomics reveals a remarkable diversity of lipids in human plasma, J. Lipid Res. 51 (2010) 3299–3305.
[7] G. van Meer, D.R. Voelker, G.W. Feigenson, Membrane lipids: where they are and how they behave, Nat. Rev. Mol. Cell Biol. 9 (2008) 112–124.
[8] M. Navab, S.T. Reddy, B.J. Van Lenten, A.M. Fogelman, HDL and cardiovascular disease: atherogenic and atheroprotective mechanisms, Nat. Rev. Cardiol. 8 (2011) 222–232.
[9] R. Martinez-Beamonte, J.M. Lou-Bonafonte, M.V. Martinez-Gracia, J. Osada, Sphingomyelin in high-density lipoproteins: structural role and biological function, Int. J. Mol. Sci. 14 (2013) 7716–7741.
[10] K.A. Rye, P.J. Barter, Cardioprotective functions of HDL, J. Lipid Res. 55 (2014) 168–179.
[11] E.Y. Cho, J.E. Manson, M.J. Stampfer, C.G. Solomon, G.A. Colditz, F.E. Speizer, W.C. Willett, F.B. Hu, A prospective study of obesity and risk of coronary heart disease among diabetic women, Diabetes Care 25 (2002) 1142–1148.
[12] D.S. Celermajer, C.K. Chow, E. Marijon, N.M. Anstey, K.S. Woo, Cardiovascular disease in the developing world, J. Am. Coll. Cardiol. 60 (2012) 1207–1216.
[13] M. Bastien, P. Poirier, I. Lemieux, J.-P. Després, Overview of epidemiology and contribution of obesity to cardiovascular disease, Prog. Cardiovasc. Dis. 56 (2014) 369–381.
[14] M. Boban, V. Persic, Z. Jovanovic, A. Brozina, B. Miletic, A. Rotim, N. Drinkovic, S. Manola, G. Laskarin, L. Boban, Obesity dilemma in the global burden of cardiovascular diseases, Int. J. Clin. Pract. 68 (2014) 173–179.
[15] A.M. Kanaya, D. Grady, E. Barrett-Connor, Explaining the sex difference in coronary heart disease mortality among patients with type 2 diabetes mellitus—a meta-analysis, Arch. Intern. Med. 162 (2002) 1737–1745.
[16] X.H. Qin, Y. Huo, D. Xie, F.F. Hou, X.P. Xu, X.B. Wang, Homocysteine-lowering therapy with folic acid is effective in cardiovascular disease prevention in patients with kidney disease: a meta-analysis of randomized controlled trials, Clin. Nutr. 32 (2013) 722–727.
[17] P. Mathieu, P. Pibarot, E. Larose, P. Poirier, A. Marette, J.P. Despres, Visceral obesity and the heart, Int. J. Biochem. Cell Biol. 40 (2008) 821–836.
[18] P. Codoner-Franch, S. Tavarez-Alonso, M. Porcar-Almela, M. Navarro-Solera, A. Arilla-Codoner, E. Alonso-Iglesias, Plasma resistin levels are associated with homocysteine, endothelial activation, and nitrosative stress in obese youths, Clin. Biochem. 47 (2014) 44–48.
[19] C. Mathers, J. Salomon, M. Ezzati, S. Begg, S. Vander-Hoorn, A. Lopez, Global Burden of Disease and Risk Factors, Oxford University Press, New York, NY, USA, 2006.
[20] A. Reis, A. Rudnitskaya, P. Chariyavilaskul, N. Dhaum, V. Melville, J. Goddard, D.J. Webb, A.R. Pitt, C.M. Spickett, Top-down lipidomics of low density lipoprotein reveal altered lipid profiles in advanced chronic kidney disease, J. Lipid Res. (2015), in press.
[21] G. Stubiger, E. Aldover-Macasaet, W. Bicker, G. Sobal, A. Willfort-Ehringer, K. Pock, V. Bochkov, K. Widhalm, O. Belgacem, Targeted profiling of atherogenic phospholipids in human plasma and lipoproteins of hyperlipidemic patients using MALDI-QIT-TOF-MS/MS, Atherosclerosis 224 (2012) 177–186.
[22] X.L. Han, R.W. Gross, Shotgun lipidomics: electrospray ionization mass spectrometric analysis and quantitation of cellular lipidomes directly from crude extracts of biological samples, Mass Spec. Rev. 24 (2005) 367–412.
[23] C. Papan, S. Penkov, R. Herzog, C. Thiele, T. Kurzchalia, A. Shevchenko, Systematic screening for novel lipids by shotgun lipidomics, Anal. Chem. 86 (2014) 2703–2710.
[24] B. Barroso, R. Bischoff, LC-MS analysis of phospholipids and lysophospholipids in human bronchoalveolar lavage fluid, J. Chromatogr. B 814 (2005) 21–28.
[25] M. Lísa, E. Cífková, M. Holčapek, Lipidomic profiling of biological tissues using off-line two-dimensional high-performance liquid chromatography–mass spectrometry, J. Chromatogr. A 1218 (2011) 5146–5156.
[26] E. Cífková, M. Holčapek, M. Lísa, M. Ovčačíková, A. Lyčka, F. Lynen, P. Sandra, Nontargeted quantitation of lipid classes using hydrophilic interaction liquid chromatography-electrospray ionization mass spectrometry with single internal standard and response factor approach, Anal. Chem. 84 (2012) 10064–10070.
[27] U. Sommer, H. Herscovitz, F.K. Welty, C.E. Costello, LC-MS-based method for the qualitative and quantitative analysis of complex lipid mixtures, J. Lipid Res. 47 (2006) 804–814.
[28] M. Pulfer, R.C. Murphy, Electrospray mass spectrometry of phospholipids, Mass Spec. Rev. 22 (2003) 332–364.
[29] P. Olsson, J. Holmback, B. Herslof, Separation of lipid classes by HPLC on a cyanopropyl column, Lipids 47 (2012) 93–99.
[30] P.M. Hutchins, R.M. Barkley, R.C. Murphy, Separation of cellular nonpolar neutral lipids by normal-phase chromatography and analysis by electrospray ionization mass spectrometry, J. Lipid Res. 49 (2008) 804–813.
[31] D.G. McLaren, P.L. Miller, M.E. Lassman, J.M. Castro-Perez, B.K. Hubbard, T.P. Roddy, An ultraperformance liquid chromatography method for the normal-phase separation of lipids, Anal. Biochem. 414 (2011) 266–272.
[32] M. Holčapek, E. Cífková, B. Červená, M. Lísa, J. Vostálová, J. Galuszka, Determination of nonpolar and polar lipid classes in human plasma, erythrocytes and plasma lipoprotein fractions using ultrahigh-performance liquid chromatography–mass spectrometry, J. Chromatogr. A 1377 (2015) 85–91.
[33] E.J. Ahn, H. Kim, B.C. Chung, G. Kong, M.H. Moon, Quantitative profiling of phosphatidylcholine and phosphatidylethanolamine in a steatosis/fibrosis model of rat liver by nanoflow liquid chromatography/tandem mass spectrometry, J. Chromatogr. A 1194 (2008) 96–102.
[34] O. Berdeaux, P. Juaneda, L. Martine, S. Cabaret, L. Bretillon, N. Acar, Identification and quantification of phosphatidylcholines containing very-long-chain polyunsaturated fatty acid in bovine and human retina using liquid chromatography/tandem mass spectrometry, J. Chromatogr. A 1217 (2010) 7738–7748.
[35] K. Sandra, A.D.S. Pereira, G. Vanhoenacker, F. David, P. Sandra, Comprehensive blood plasma lipidomics by liquid chromatography/quadrupole time-of-flight mass spectrometry, J. Chromatogr. A 1217 (2010) 4087–4099.
[36] Y. Sato, I. Suzuki, T. Nakamura, F. Bernier, K. Aoshima, Y. Oda, Identification of a new plasma biomarker of Alzheimer's disease using metabolomics technology, J. Lipid Res. 53 (2012) 567–576.
[37] M. Holčapek, H. Dvořáková, M. Lísa, A.J. Girón, P. Sandra, J. Cvačka, Regioisomeric analysis of triacylglycerols using silver-ion liquid chromatography atmospheric pressure chemical ionization mass spectrometry: comparison of five different mass analyzers, J. Chromatogr. A 1217 (2010) 8186–8194.
[38] M. Lísa, K. Netušilová, L. Franěk, H. Dvořáková, V. Vrkoslav, M. Holčapek, Characterization of fatty acid and triacylglycerol composition in animal fats using silver-ion and non-aqueous reversed-phase high-performance liquid chromatography/mass spectrometry and gas chromatography/flame ionization detection, J. Chromatogr. A 1218 (2011) 7499–7510.
[39] B. Fuchs, Analysis of phospolipids and glycolipids by thin-layer chromatography-matrix-assisted laser desorption and ionization mass spectrometry, J. Chromatogr. A 1259 (2012) 62–73.
[40] S. Wagner, K. Scholz, M. Sieber, M. Kellert, W. Voelkel, Tools in metabonomics: an integrated validation approach for LC-MS metabolic profiling of mercapturic acids in human urine, Anal. Chem. 79 (2007) 2918–2926.
[41] S. Wold, J. Trygg, A. Berglund, H. Antti, Some recent developments in PLS modeling, Chemom. Intell. Lab. Syst. 58 (2001) 131–150.
[42] L. Errikson, T. Byrne, E. Johansson, J. Trygg, C. Vikstrom, Multi- and Megavariate Data Analysis (Basic Principles and Application), Sweden, UMETRICS ACADEMY, Malmo, 2013.
[43] J. Trygg, S. Wold, Orthogonal projections to latent structures (O-PLS), J. Chemom. 16 (2002) 119–128.
[44] E.L. Donovan, S.M. Pettine, M.S. Hickey, K.L. Hamilton, B.F. Miller, Lipidomic analysis of human plasma reveals ether-linked lipids that are elevated in morbidly obese humans compared to lean, Diabetol. Metab. Syndr. 5 (2013) 24–38.
[45] R.J. Havel, H.A. Eder, J.H. Bragdon, Distribution and chemical composition of ultracentrifugally separated lipoproteins in human serum, J. Clin. Invest. 34 (1955) 1345–1353.
[46] J. Folch, M. Lees, G.H.S. Stanley, A simple method for the isolation and purification of total lipids from animal tissues, J. Biol. Chem. 226 (1957) 497–509.
[47] M.C. Chambers, B. Maclean, R. Burke, D. Amodei, D.L. Ruderman, S. Neumann, L. Gatto, B. Fischer, B. Pratt, J. Egertson, K. Hoff, D. Kessner, N. Tasman, N. Shulman, B. Frewen, T.A. Baker, M.-Y. Brusniak, C. Paulse, D. Creasy, L. Flashner, K. Kani, C. Moulding, S.L. Seymour, L.M. Nuwaysir, B. Lefebvre, F. Kuhlmann, J. Roark, P. Rainer, S. Detlev, T. Hemenway, A. Huhmer, J. Langridge, B. Connolly, T. Chadick, K. Holly, J. Eckels, E.W. Deutsch, R.L. Moritz, J.E. Katz, D.B. Agus, M. MacCoss, D.L. Tabb, P. Mallick, A cross-platform toolkit for mass spectrometry and proteomics, Nat. Biotechnol. 30 (2012) 918–920.
[48] S. Gibb, K. Strimmer, MALDIquant A versatile R package for the analysis of mass spectrometry data, Bioinformatics 28 (2012) 2270–2271.
[49] E. Cífková, M. Holčapek, M. Lísa, Nontargeted lipidomic characterization of porcine organs using hydrophilic interaction liquid chromatography and off-line two-dimensional liquid chromatography-electrospray ionization mass spectrometry, Lipids 48 (2013) 915–928.
[50] I. Yang, K.H. Kim, J.Y. Lee, M.H. Moon, On-line miniaturized asymmetrical flow field-flow fractionation-electrospray ionization-tandem mass spectrometry with selected reaction monitoring for quantitative analysis of phospholipids in plasma lipoproteins, J. Chromatogr. A 1324 (2014) 224–230.
[51] S. Heimerl, M. Fischer, A. Baessler, G. Liebisch, A. Sigruener, S. Wallner, G. Schmitz, Alterations of plasma lysophosphatidylcholine species in obesity and weight loss, PLoS ONE 9 (2014) e111348–e111354.
[52] M.N. Barber, S. Risis, C. Yang, P.J. Meikle, M. Staples, M.A. Febbraio, C.R. Bruce, Plasma lysophosphatidylcholine levels are reduced in obesity and type 2 diabetes, PLoS ONE 7 (2012) e41456–e41467.
[53] A. Nimptsch, S. Pyttel, U. Paasch, C. Mohr, J.-M. Heinrich, J. Schiller, A MALDI MS investigation of the lysophosphatidyl-choline/phosphatidylcholine ratio in human spermatozoa and erythrocytes as a useful fertility marker, Lipids 49 (2014) 287–293.
[54] B. Fuchs, J. Schiller, U. Wagner, H. Häntzschel, K. Arnold, The phosphatidylcholine/lysophosphatidylcholine ratio in human plasma is an indicator of the severity of rheumatoid arthritis: Investigations by 31P NMR and MALDI-TOF MS, Clin. Biochem. 38 (2005) 925–933.

[55] S.K. Byeon, J.Y. Lee, S. Lim, D. Choi, M.H. Moon, Discovery of candidate phospholipid biomarkers in human lipoproteins with coronary artery disease by flow field-flow fractionation and nanoflow liquid chromatography–tandem mass spectrometry, J. Chromatogr. A 1270 (2012) 246–253.
[56] I. Gonçalves, A. Edsfeldt, N.Y. Ko, H. Grufman, K. Berg, H. Björkbacka, M. Nitulescu, A. Persson, M. Nilsson, C. Prehn, J. Adamski, J. Nilsson, Evidence supporting a key role of Lp-PLA2-generated lysophosphatidylcholine in human atherosclerotic plaque inflammation, Arterioscler. Thromb. Vasc. Biol. 32 (2012) 1505–1512.
[57] M.J. Stampfer, R.M. Krauss, J. Ma, P.J. Blanche, L.G. Holl, F.M. Sacks, C.H. Hennekens, A prospective study of triglyceride level, low-density lipoprotein particle diameter, and risk of myocardial infarction, JAMA - J. Am. Med. Assoc. 276 (1996) 882–888.
[58] P.N. Hopkins, M. Nazeem Nanjee, L.L. Wu, M.G. McGinty, E.A. Brinton, S.C. Hunt, J.L. Anderson, Altered composition of triglyceride-rich lipoproteins and coronary artery disease in a large case-control study, Atherosclerosis 207 (2009) 559–566.

Anal Bioanal Chem (2015) 407:991–1002
DOI 10.1007/s00216-014-8272-z

RESEARCH PAPER

Determination of lipidomic differences between human breast cancer and surrounding normal tissues using HILIC-HPLC/ESI-MS and multivariate data analysis

Eva Cífková · Michal Holčapek · Miroslav Lísa · David Vrána · Jiří Gatěk · Bohuslav Melichar

Received: 15 June 2014 / Revised: 10 September 2014 / Accepted: 14 October 2014 / Published online: 29 October 2014

Abstract The comprehensive approach for the lipidomic characterization of human breast cancer and surrounding normal tissues is based on hydrophilic interaction liquid chromatography (HILIC)–electrospray ionization mass spectrometry (ESI-MS) quantitation of polar lipid classes of total lipid extracts followed by multivariate data analysis using unsupervised principal component analysis (PCA) and supervised orthogonal partial least square (OPLS). This analytical methodology is applied for the detailed lipidomic characterization of ten patients with the goal to find the statistically relevant differences between tumor and normal tissues. This strategy is selected for better visualization of differences, because the breast cancer tissue is compared with the surrounding healthy tissue of the same patient, therefore changes in the lipidome are caused predominantly by the tumor growth. A large increase of total concentrations for several lipid classes is observed, including phosphatidylinositols, phosphatidylethanolamines, phosphatidylcholines, and lysophosphatidylcholines. Concentrations of individual lipid species inside the abovementioned classes are also changed, and in some cases, these differences are statistically significant. PCA and OPLS analyses enable a clear differentiation of tumor and normal tissues based on changes of their lipidome. A notable decrease of relative abundances of ether and vinylether (plasmalogen) lipid species is detected for phosphatidylethanolamines, but no difference is apparent for phosphatidylcholines.

Keywords Breast cancer · Lipid biomarkers · HILIC-HPLC/ESI-MS · Quantitation · Statistical analysis

Published in the topical collection celebrating *ABCs 13th Anniversary.*

Electronic supplementary material The online version of this article (doi:10.1007/s00216-014-8272-z) contains supplementary material, which is available to authorized users.

E. Cífková · M. Holčapek (✉) · M. Lísa
Department of Analytical Chemistry, Faculty of Chemical Technology, University of Pardubice, Studentská 573, 532 10 Pardubice, Czech Republic
e-mail: Michal.Holcapek@upce.cz

D. Vrána · B. Melichar
Department of Oncology, Medical School and Teaching Hospital, Palacký University, I.P. Pavlova 6, 775 20 Olomouc, Czech Republic

J. Gatěk
Department of Surgery, Atlas Hospital, Tomáš Baťa University in Zlín, nám. T.G. Masaryka 5555, 760 01 Zlín, Czech Republic

Introduction

Breast cancer is the most common malignant tumor in women population and one of the most common causes of death from cancer [1, 2]. Breast cancer represents a group of different neoplastic disorders originating in the same organ rather than a single disease entity. At least four breast cancer subtypes with distinct biology and clinical presentation are currently recognized, including two subtypes characterized by the expression of hormone receptors (luminal A tumors and luminal B tumors), human epidermal growth factor (HER)-2 positive, and triple negative breast cancer. While tissue diagnosis is based on the histological evaluation of the tumor tissue, there is still an unmet medical need for biomarkers that would reliably reflect the disease burden.

Lipids are the building blocks of cell membranes, and the lipidomic composition can change during the malignant transformation. Lipid metabolism plays an important role in oxidative stress and is associated, among other parameters, with factors linked to the breast cancer risk including hormonal balance, body mass index, breast density, drug metabolism, and growth of insulin levels [3]. The potential effect of fat diet and changes of lipid metabolism on cancer progression and aggressiveness of cancer cells has been suggested by several lipidomic studies that compare fatty acid composition in tumor vs. normal tissues [4, 5] or blood of breast cancer patients

vs. healthy controls [6, 7] using gas chromatography (GC) coupled with flame ionization detection (FID) or mass spectrometry (MS). Several studies [4–6, 8, 9] report the ratio of *n*-6 polyunsaturated fatty acids (PUFA) to *n*-3 PUFA being a key factor for tumor angiogenesis that is essential for tumor growth and metastasis. The major *n*-6 PUFA is linoleic acid (FA 18:2), which can be metabolized into arachidonic acid (FA 20:4). *n*-3 PUFA are represented mainly by α-linolenic acid (FA 18:3), docosahexaenoic acid (FA 22:6), and eicosapentaenoic acid (FA 20:5). In past, the ratio of *n*-6/*n*-3 PUFA was close to 1:1, but the current Western diet has resulted in the change of this ratio up to 15:1 [8, 10], which is considered as a potential risk factor for many disorders including cancer.

Various lipidomic approaches have been used for the analysis of phospholipid composition in breast cancer cell lines [11–14], human tumor and normal tissues [15, 16], or human body fluids (blood or urine) [17, 18]. Reports on the differences of phospholipid composition between mammary epithelial cells and breast cancer cells with different biological behaviors show rather conflicting results mainly for phosphatidylethanolamines (PE), lysophosphatidylcholines (LPC), and cardiolipins in different cancer cells [11, 12]. In another study, total concentrations of phosphatidylcholines (PC) and PE are increased by more than 41 % in breast cancer patients compared with healthy controls [18].

The coupling of high-performance liquid chromatography and mass spectrometry (HPLC/MS) is the technique most frequently used for highly sensitive and selective lipidomic characterization with the possibility to identify and quantify complex mixtures of polar and nonpolar lipids, relatively rapid screening of various biological samples [19]. Reversed-phase HPLC makes possible to separate individual lipid species differing in fatty acyl chain lengths and the number of double bonds, while hydrophilic interaction liquid chromatography (HILIC) is more convenient for the separation of lipid classes. MS coupled with the direct infusion (shotgun approach) is the technique commonly used for rapid lipidomic analyses using product ion, neutral loss, and the selected reaction monitoring scans typical for triple quadrupoles (QqQ) and other hybrid tandem mass analyzers [20, 21].

Magnetic resonance imaging (MRI) [22–25] is used for the noninvasive in vivo characterization of breast tissues that can improve the specificity of tumor diagnostics, monitoring of tumor responses to systemic treatment, and analyses of tumor tissues in vivo and in vitro [1]. H MRI and [31] P MRI are used for the monitoring of significant differences in phospholipid metabolites in normal and tumor breast tissues. Increased relative abundances are reported for choline metabolites and most phospholipid classes except for PC, LPC, plasmalogen phosphatidylethanolamines (pPE), and phosphatidylserines (PS) [25]. MRI is used mainly as a diagnostic tool in medicine due to low sensitivity and selectivity.

The main challenge in the lipidomic studies of biological samples is the evaluation of data sets of large size and complexity [26]. At present, principal component analysis (PCA) and techniques based on partial least square projections to latent structures (PLS) are often used for multivariate data analysis (MDA) in multiple omics platforms [27]. The principle of PCA is finding a transformation that reduces the dimensionality of the data by conversion of a set of correlated variables to a new set of uncorrelated variables called principal components [27]. PLS finds the linear correlations (predictive variables) between dependent variables (Y matrix) and predictor variables (X matrix). There is a risk that variations in X matrix are not linearly correlated with Y matrix in PLS [27, 28]. For this reason, orthogonal partial least square (OPLS) [27, 29] is enhanced, and the latent variables are divided into linearly correlated (predictive) and nonlinearly (orthogonal) correlated variables between X and Y matrices (variables in X orthogonal to Y). In contrast to unidirectional correlations of PLS and OPLS (i.e., X→Y), orthogonal 2 projections to latent structures (O2PLS) [27, 30] is described using bidirectional correlations (i.e., X↔Y). Generally, latent variables in O2PLS are partitioned into predictive variables, variables in X orthogonal to Y and variables in Y orthogonal to X. Advantages of O2PLS in comparison to PLS are better data interpretability, clear selection of outliers, reduction of model complexity, determination the number of components, etc. [26, 27, 30].

This paper describes the application of our previously reported quantitative approach for the lipidomic characterization of changes in breast cancer tissues compared with surrounding normal tissues using HILIC-HPLC/electrospray ionization mass spectrometry (ESI-MS). The lipid class quantitation by HILIC is used for the first time for the clinical study, and this approach clearly shows differences in lipidomes of tumor and normal tissues. Observed differences in the lipidome caused by the tumor growth are visualized by both unsupervised and supervised MDA.

Experimental

Chemicals and standards

Acetonitrile, 2-propanol, methanol (all HPLC/MS grade), chloroform stabilized by 0.5–1 % ethanol and hexane (both HPLC grade), and ammonium acetate were purchased from Sigma-Aldrich (St. Louis, MO, USA). Deionized water was prepared with a Demiwa 5-roi purification system (Watek, Ledeč nad Sázavou, Czech Republic). *N*-Dodecanoyl-heptadecasphing-4-enine-1-phosphoethanolamine (d17:1/12:0) used as an internal standard (IS) for the nontargeted quantitation was purchased from Avanti Polar Lipids (Alabaster, AL, USA). Human breast tumor and surrounding normal

tissues of ten patients (see Electronic Supplementary Material (ESM) Table S1) were obtained from the Department of Surgery, Atlas Hospital Zlín in the Czech Republic. All patients have read and signed the informed consent approved by the Hospital Ethical Committee. No sample was excluded from the statistical evaluation.

Sample preparation

Human breast tumor tissues and surrounding normal tissues were extracted according to a modified Folch procedure [31] using a chloroform–methanol–water system. Briefly, 50–150 mg of human tissue and 25 μL of 3.3 mg/mL IS were homogenized with a 5-mL mixture of chloroform–methanol (2:1, *v*/*v*), and the homogenate was filtered using a coarse filter paper. Subsequently, 1 mL of 1 mol/L NaCl was added, and the mixture was centrifuged at 3000 rpm for 5 min at room temperature. The chloroform bottom layer (total lipid extract) containing the lipids was evaporated by a gentle stream of nitrogen and redissolved in chloroform–2-propanol mixture (1:1, *v*/*v*) for HILIC-HPLC/MS analyses. Total lipid extracts were purified using re-extraction with hexane–methanol–water system to remove the excess of nonpolar lipids, mainly triacylglycerols (TG). Briefly, 100 μL of total lipid extract was mixed with a 900-μL mixture of hexane–methanol–water (4:1:1, *v*/*v*/*v*). The extract was divided into hexane (upper) layer containing mainly nonpolar lipids and methanol–water (bottom) layer containing mainly polar lipids. Polar lipid extracts were evaporated by a gentle stream of nitrogen and redissolved in chloroform–2-propanol mixture (1:1, *v*/*v*) for HILIC analyses.

HILIC-HPLC/ESI-MS conditions

Lipidomic analyses were performed on a liquid chromatograph Agilent 1200 series (Agilent Technologies, Waldbronn, Germany) coupled with the Esquire 3000 ion trap analyzer (Bruker Daltonics, Bremen, Germany). Lipid extracts were separated into individual lipid classes using a Spherisorb Si column (250×4.6 mm, 5 μm, Waters, Milford, MA, USA), a flow rate of 1 mL/min, an injection volume of 10 μL, column temperature of 40 °C, and a mobile phase gradient: 0 min, 94 % A+6 % B and 60 min, 77 % A+23 % B, where A was acetonitrile and B was 5 mM aqueous ammonium acetate [32]. Individual lipid classes were detected in the positive- and negative-ion ESI modes in the mass range *m*/*z* 50–1000 with the following setting of tuning parameters: pressure of the nebulizing gas, 60 psi; drying gas flow rate, 10 L/min; and temperature of the drying gas, 365 °C. The acquired data were quantified using the nontargeted lipidomic analysis of individual lipid classes using the single IS and response factors described earlier [33]. Individual lipids within phosphatidylinositol (PI) and PE classes were identified and quantified using relative intensities of deprotonated molecules $[M\text{-}H]^-$ and PC using relative intensities of $[M\text{-}CH_3]^-$ ions in the negative-ion ESI mode [34], while individual sphingomyelins (SM) were quantified using protonated molecules $[M+H]^+$ in the positive-ion ESI mode [33].

Data analysis

Unsupervised multivariate data analyses were performed using PCA and supervised analyses using OPLS method in the SIMCA software version 13.0 (Umetrics AB, Umeå, Sweden) [27, 30]. The Pareto scaling was used before the statistical analysis. Multivariate models were described using R^2 and Q^2 parameters, where R^2 describes fractions of the sum of squares of all X (and Y for OPLS) that the model can explain using the latent variables, and Q^2 describes fractions of the sum of squares of all X (and Y for OPLS) predicted by the model according to the cross validation or how accurately the model can be expected to predict new data. These values for all models were shown in ESM Tables S2 and S3. All statistical evaluations using PCA and OPLS method described in this work were calculated from relative abundances.

Results and discussion

Quantitation of individual polar lipid classes using HILIC-HPLC/ESI-MS

Total lipid extracts of normal and tumor tissues are prepared using the modified Folch method and analyzed using HILIC-HPLC/ESI-MS [33]. The breast tissue contains a large amount of nonpolar lipids, mainly TG, which results in large tailing peak containing TG and other nonpolar lipids in the HILIC chromatogram interfering significantly with other lipid classes (see ESM Fig. S1). For this reason, we perform re-extraction of total lipid extracts using hexane–methanol–water mixture to remove excessive nonpolar lipids (see ESM Fig. S1). The removal of nonpolar lipids does not change the lipidomic profiles of polar lipids. HILIC-HPLC/ESI-MS analyses of purified fractions of polar lipids show significant differences in the composition of individual lipid classes for the normal (black line) and tumor (red line) tissues of the same patient (Fig. 1a). The quantitation of individual lipid classes is performed using the previously developed validated method based on the combination of a single IS and response factors for each class related to this IS [33, 34]. This approach neglects small differences in ionization efficiencies and fragmentation behavior of individual lipids within the class similarly as the large majority of both shotgun and LC/MS lipidomic quantitations due to the lack of standards for all lipids. All lipid classes presented in Fig. 1b show statistically

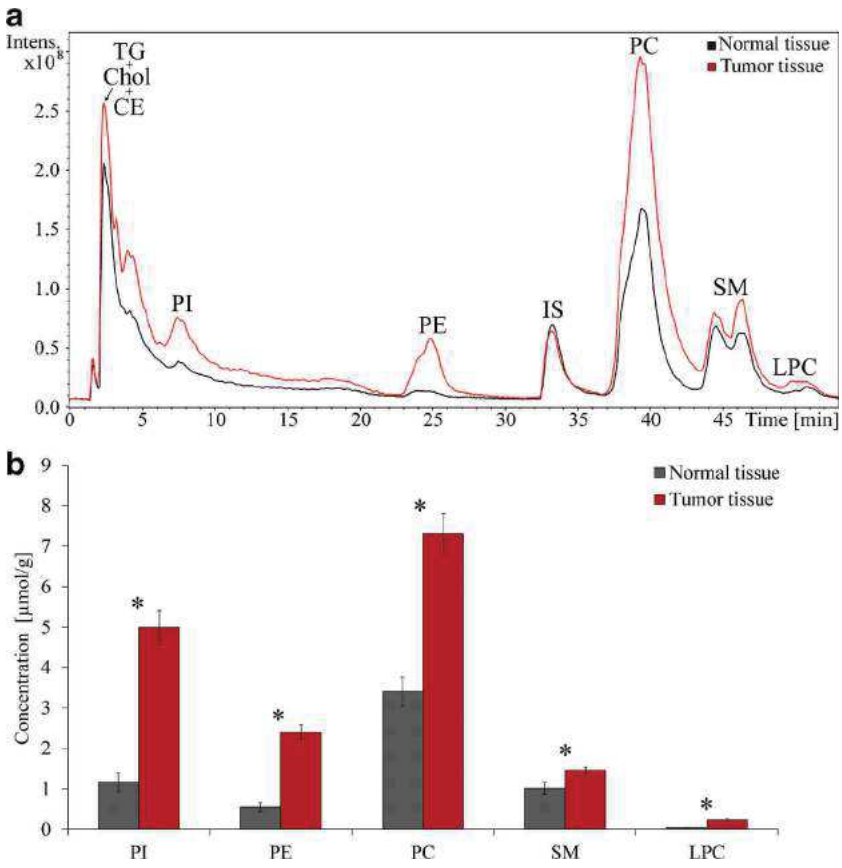

Fig. 1 **a** Positive-ion HILIC-HPLC/ESI-MS of polar lipid extracts of normal (*black line*) and tumor (*red line*) tissues of breast cancer patients. HPLC conditions: column Spherisorb Si (250×4.6 mm, 5 μm); flow rate, 1 mL/min; separation temperature, 40 °C; and gradient: 0 min, 94 % A+6 % B and 60 min, 77 % A+23 % B, where A is acetonitrile and B is 5 mM aqueous ammonium acetate. **b** Comparison of average concentrations [μmol/g] of individual lipid classes in normal and tumor tissues for ten patients with their standard errors. Peak annotation: *TG*, triacylglycerols; *Chol*, cholesterol; *CE*, cholesteryl esters; *PI*, phosphatidylinositols; *PE*, phosphatidylethanolamines; *IS*, internal standard; *PC*, phosphatidylcholines; *SM*, sphingomyelins; *LPC*, lysophosphatidylcholines. Statistically significant differences according to *T* test are indicated by an *asterisk*

significant differences in concentrations in normal tissues (gray columns) vs. tumor tissues (red columns) of ten breast cancer patients. The reliability of differences between groups under comparison is estimated with the Holm-Bonferroni method [35]. Numerical values are displayed in ESM Table S4. Average concentrations of PI, PE, and LPC increase more than four times and for PC more than twice in tumor tissues, which show large differences in the lipid composition of normal tissues and tumor tissues. Detailed analysis of individual lipids inside lipid classes can provide important information about the lipid metabolism in the breast cancer tissue.

Analysis of individual lipid species using $[M-H]^-$, $[M-CH_3]^-$, and $[M+H]^+$ ions

Individual lipid species concentrations are reported by two approaches. The first approach (Fig. 2) describes relative abundances of lipid species (in %) and their proportional changes between normal and tumor tissues, which is used for MDA with a good clustering of two groups. The second one (see ESM Fig. S2) describes absolute concentrations (in μmol/g) calculated using relative abundances of individual lipids multiplied by the total concentration of the whole lipid class. Individual lipid species differ in attached fatty acyls, which are annotated by their total carbon number and double bond number (CN:DB). Positions of individual fatty acyls on glycerol skeleton are not identified, and their shorthand notation corresponds with the established lipidomic terminology [36]. The lipid class of PI provides the greatest difference between concentrations of normal and tumor tissues (more than four times) for ten analyzed patients (Fig. 1b, ESM Table S4). Relative abundances of deprotonated molecules $[M-H]^-$ enable to describe the composition of 24 species (Fig. 2a). The highest relative abundance in both tissues corresponds to PI 38:4 species containing two attached fatty acyls with 38 carbon atoms and 4 double bonds. The most of individual PI species has higher relative abundances in the tumor tissue except for PI 38:4 (typically PI 18:0_20:4), PI 36:4 (PI 16:0_20:4), and PI 38:5 (PI 18:1_20:4). Figure 2Sb in the ESM shows concentrations in micromoles per gram for individual PI species and their differences for both tissues. Statistically significant differences according to *T* test are labeled by an asterisk (this annotation is used in all figures).

Fig. 2 Relative abundances [%] of individual **a** PI, **b** PE, **c** PC, and **d** SM ▶ in normal and tumor tissues of ten breast cancer patients determined using relative abundances of $[M-H]^-$ and $[M-CH_3]^-$ ions in negative-ion mass spectra or $[M+H]^+$ ions in positive-ion mass spectra obtained by HILIC-HPLC/ESI-MS. Statistically significant differences according to *T* test are indicated by an *asterisk*

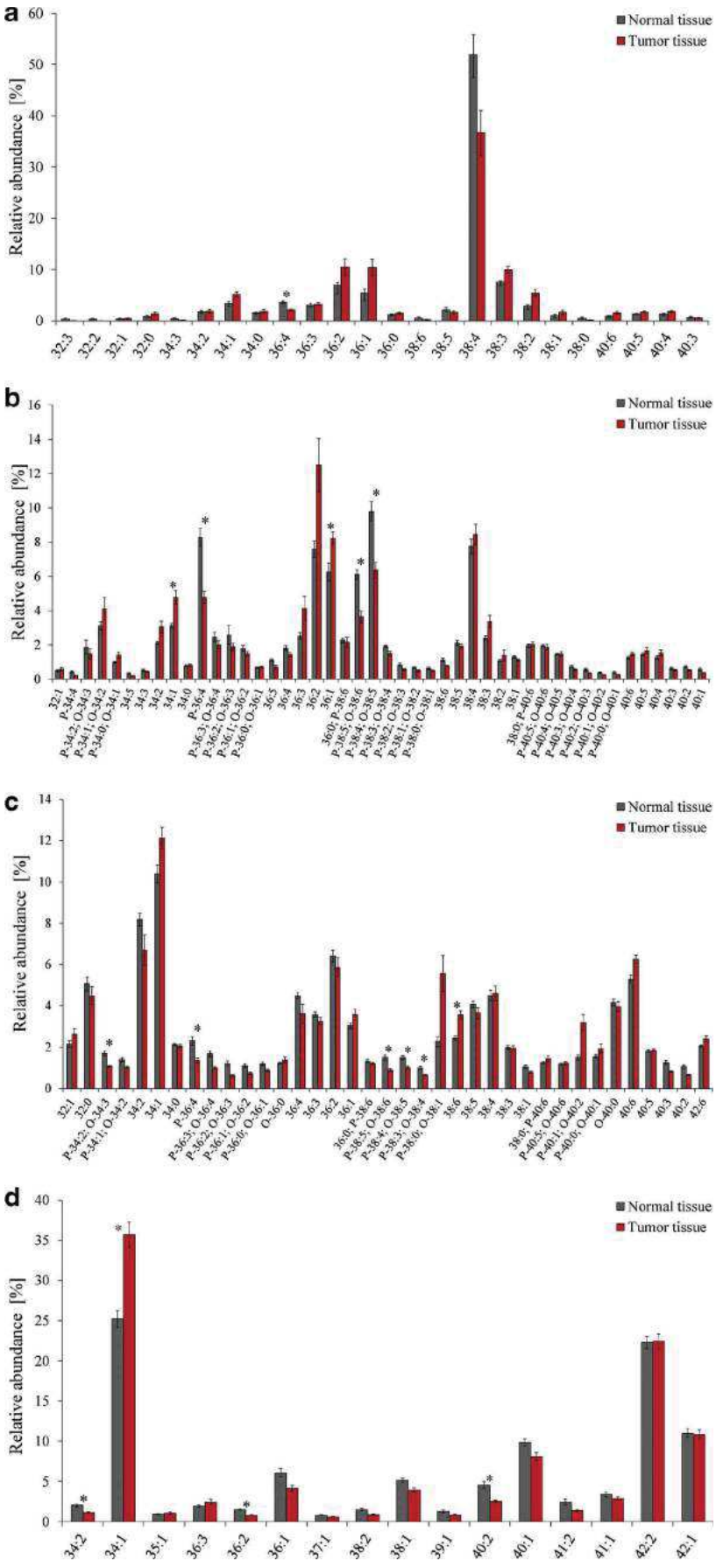
a
Normal tissue
Tumor tissue
Relative abundance [%]
32:3 32:2 32:1 32:0 34:3 34:2 34:1 34:0 36:4 36:3 36:2 36:1 36:0 38:6 38:5 38:4 38:3 38:2 38:1 38:0 40:6 40:5 40:4 40:3
b
Normal tissue
Tumor tissue
Relative abundance [%]
c
Normal tissue
Tumor tissue
Relative abundance [%]
d
Normal tissue
Tumor tissue
Relative abundance [%]
34:2 34:1 35:1 36:3 36:2 36:1 37:1 38:2 38:1 39:1 40:2 40:1 41:2 41:1 42:2 42:1

At first, unsupervised MDA using PCA was used for individual PI species in normal and tumor tissues (see ESM Table S2; Fig. 3a). The PCA model described using two principal components shows clearly indistinguished clusters of normal and tumor tissues. Supervised MDA using OPLS was used for more simple understanding of individual PI species influence on clustering of these groups (see ESM Table S3; Fig. 3b). The OPLS model for individual PI species (Fig. 4) is described using 1+2+0 components, where 1 predictive component summarizes the information contained

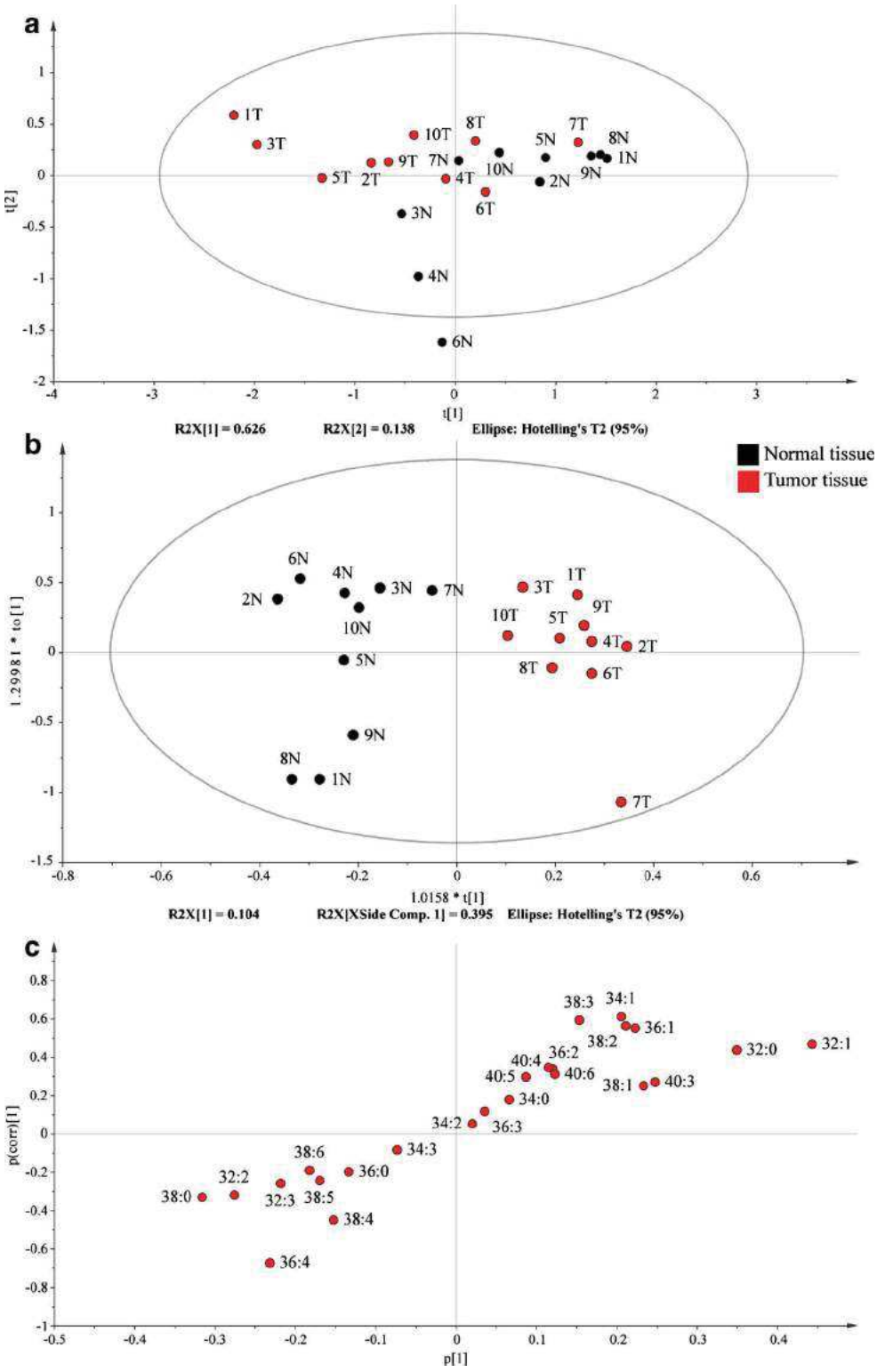

Fig. 3 Multivariate data analysis of relative abundances [%] of individual PI species in normal (*black*) and tumor (*red*) tissues: **a** PCA score plot, **b** OPLS score plot, and **c** OPLS S-plot

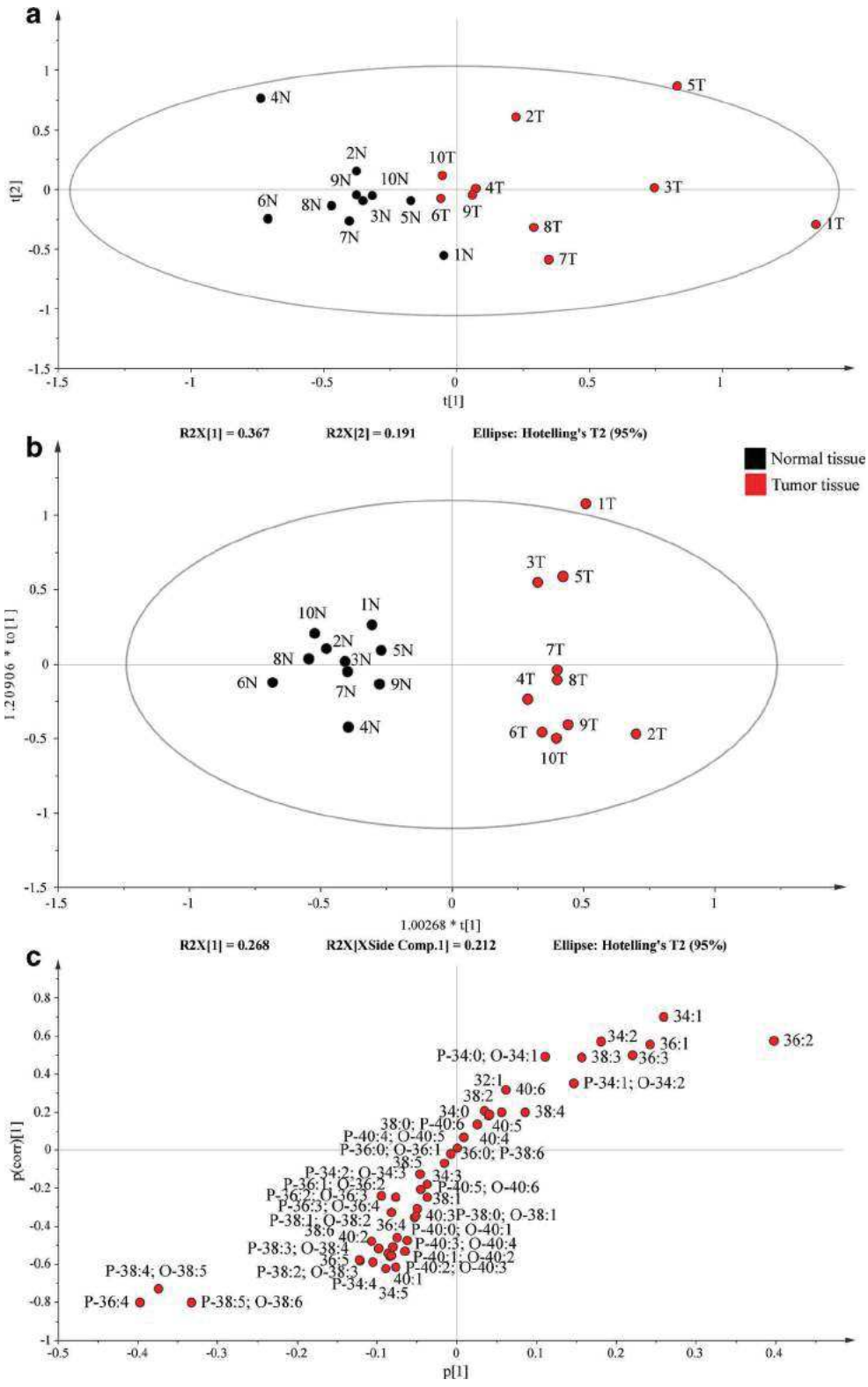

Fig. 4 Multivariate data analysis of relative abundances [%] of individual PE species in normal (*black*) and tumor (*red*) tissues: **a** PCA score plot, **b** OPLS score plot, and **c** OPLS S-plot

in X and Y matrices, 2 orthogonal in X components expresses the information that is unique to X matrix, and 0 orthogonal in Y component expresses the information that is unique to Y matrix. The score plot (Fig. 3b) shows the clear separation of two classes (normal vs. tumor tissue) of PI species, where the horizontal axis corresponds to the variability between classes and the vertical axis to the variability within classes. The S-plot (see ESM Fig. S3c) displays positively (PI 34:1, PI 32:1, PI 32:0) and negatively (PI 36:4, PI 38:0, PI 38:4) correlated lipids with tumor tissues. In general, the score plot is a

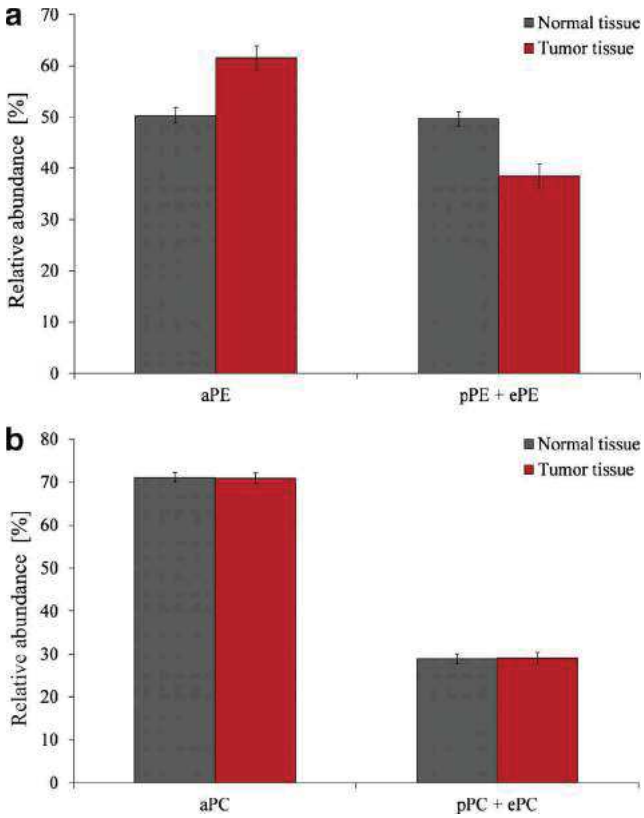

Fig. 5 Comparison of relative abundances of **a** the sum of aPE vs. the sum of pPE+ePE species and **b** the sum of aPC vs. the sum of pPC+ePC species in normal and tumor tissues with their standard errors of ten patients

summary of the relationship between normal and tumor tissues, while the S-plot interprets patterns observed in the score plot. The S-plot (Fig. 3c) shows the effect of attached fatty acyls in PI species on the partition into classes of normal and tumor tissues. PI 36:4 (PI 16:0_20:4), PI 38:4 (PI 18:0_20:4), and PI 34:1 (PI 16:0_18:1) are statistically the most reliable, where PI 36:4 and PI 38:4 are down-regulated in tumor tissues, while PI 34:1, 32:1 and 32:0 are up-regulated. On the other hand, PI species in the middle of the diagram close to the zero vertical axis (PI 34:2, PI 36:3, and PI 34:3) have a low statistical importance for the class differentiation. Obtained statistical results are comparable with Fig. 2a, but the loading plot provides a visualization of effects of individual PI on the group differentiation.

The lipid class of PE can be divided according to the type of fatty acyl linkage to the glycerol skeleton into the most commonly known group of ester-linked fatty acyls at both *sn*-1 and *sn*-2 positions (diacyls) referred as aPE, ether-linked fatty acyls in the *sn*-1 position (1-alkyl-2-acyl) referred as ethers (ePE), and vinyl ether-linked fatty acyls in the *sn*-1 position (1-alkenyl-2-acyl) referred as plasmalogens (pPE). Relative abundances and concentrations of 46 individual PE are shown in Fig. 5. Some combinations of PE (aPE, ePE, and pPE) having identical $[M\text{-}H]^-$ ions cannot be distinguished using this approach; therefore, all possible variants are reported regardless of probably lower concentrations of ePE according to the literature [37]. The comparison of relative abundances in both tissues (Fig. 2b) describes three statistically significant PE species (P-36:4, P-38:5/O-38:6, and P-38:4/O-38:5) with higher relative abundances in normal tissues. Figure S2b in the ESM illustrates differences of individual PE concentrations in normal and tumor tissues, which are statistically significant for all PE species having higher concentrations in tumors. Unsupervised MDA of individual PE using the PCA method (Fig. 4a; see ESM Table S2) shows again that smaller clusters for normal tissues and wider clusters for tumor tissues are similar. The MDA of individual PE using the OPLS model (Fig. 4b, c) is described using 1+1+0 components (see ESM Table S3). The score plot of PE species (Fig. 4b) depicts two well-separated groups. Differences within one group are larger for tumor tissues in comparison with normal tissues possibly due to various tumor subtypes. The S-plot (Fig. 4c) shows a significant down-regulated effect of three earlier mentioned PE species in tumor tissues and, moreover, PE 34:1 (PE 16:0_18:1) and PE 36:2 (PE 18:1_18:1) increased in tumor tissues, which can also be correlated with the data presented in Fig. 2b.

The PC class can be also divided according to fatty acyl linkage into diacyls (aPC), ethers (ePC), and plasmalogens (pPC) similarly as for PE. Relative abundances (Fig. 2c) and concentrations (see ESM Fig. S2c) of 36 PC species illustrate five statistically significant pPC or ePC and one aPC (namely PC 38:6) species by using the comparison of relative abundances and statistically significant differences in 26 PC species by using comparison of concentrations. The PCA model (see ESM Fig. S3a and Table S2) of relative abundances of PC described using two principal components shows similar clustering as for PE. The statistical evaluation of individual PC (see ESM Fig. S3b) using the OPLS method with 1+1+0 components (see ESM Table S3) enables to obtain the information about the differentiation of normal and tumor tissues. The S-plot (see ESM Fig. S3c) describes the important effect of most pPC and ePC (especially PC containing C20:4 and saturated fatty acyl) for normal tissues and PC 40:6 (PC 22:6_18:0), PC 38:6 (PC 22:6_16:0), and PC 34:1 (PC 16:0_18:1) for tumor tissues.

Plasmalogens play a critical role in cell membranes, for example in the structural function, signaling, or protection of membrane lipids against oxidation. Increased lipid oxidation associates with decreased plasmalogen levels and imbalances in lipid metabolism, which can lead to disease progression [38]. Therefore, we compare relative proportions of diacyls vs. plasmalogens and ethers in normal and tumor tissues (Fig. 5). The relative proportion of aPE in normal tissues is similar to that of pPE+ePE (50:50), but the relative proportion of aPE in tumor tissues is about one third higher than that of pPE+ePE (62:38) (Fig. 5a). Different results are obtained for the PC lipid class, where relative abundances of aPC vs. pPC+ePC are almost the same in both tissues (Fig. 5b).

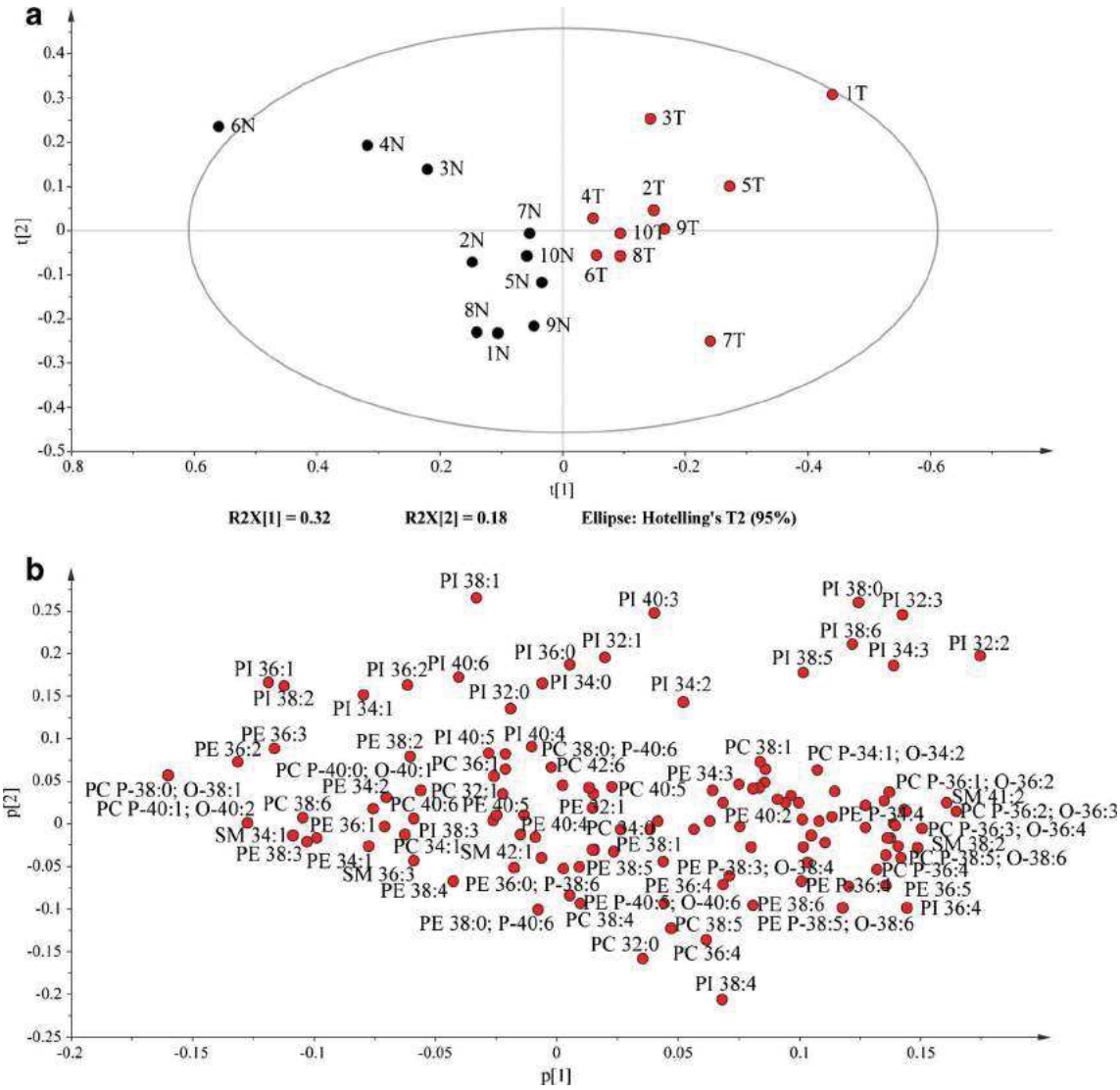

Fig. 6 Multivariate data analysis of relative abundances of all described lipid species in normal (*black circles*) and tumor (*red circles*) tissues using unsupervised PCA method: **a** the score plot and **b** the loading plot

The SM species are analyzed using protonated molecules $[M+H]^+$ in ESI mass spectra. This approach cannot be used for the analysis of SM 38:5 (SM 20:4_18:1) due to the presence of sodium adduct $[M+Na]^+$ ion of SM 36:2 with the identical nominal mass to $[M+H]^+$ ion of SM 38:5. Relative abundances (Fig. 2d) and concentrations (see ESM Fig. S2d) of 16 individual SM species (except for SM 38:5) are compared in normal and tumor tissues. SM 34:2 (SM 16:1_18:1), SM 34:1 (SM 16:0_18:1), SM 36:2 (SM 18:1_18:1), and SM 40:2 (SM 22:1_18:1) are described as statistically significant using the comparison of relative abundances, while SM 34:1 using the comparison of concentrations. Unsupervised MDA of individual SM using the PCA model described using two principal components (see ESM Fig. S4a and Table S2) shows worse clustering of normal and tumor groups in comparison with other lipid species. The statistical evaluation using the OPLS method with 1+1+0 components (see ESM Fig. S4b, c and Table S3) shows the most statistically reliable SM 34:1 (SM 16:0_18:1) increasing in tumor tissues and SM 36:2 and SM 40:2 decreasing in tumor tissues (see ESM Fig. S4c). The detailed analysis of LPC cannot be performed due to low concentrations and low intensities of protonated molecules $[M+H]^+$ in ESI mass spectra. Analysis of the total lipidome using unsupervised PCA method is shown in the score plot (Fig. 6). The loading plot (Fig. 6b) displays the relationship between X and Y matrices by using predictive components. The first component describes the separation of normal and tumor tissues—in this case, mainly PC P-38:0; O-38:1, PE 36:2, PC P-40:1; O-40:2, PI 32:2; and PC P-36:2; O-36:3. The second component shows a variability in tumor tissues, which is the most influenced by individual PI species (PI 38:1, PI 38:4). OPLS MDA of the total lipidome shows excellent results (Fig. 7a), where normal tissues form a compact group, while differences within the tumor group are larger. OPLS S-

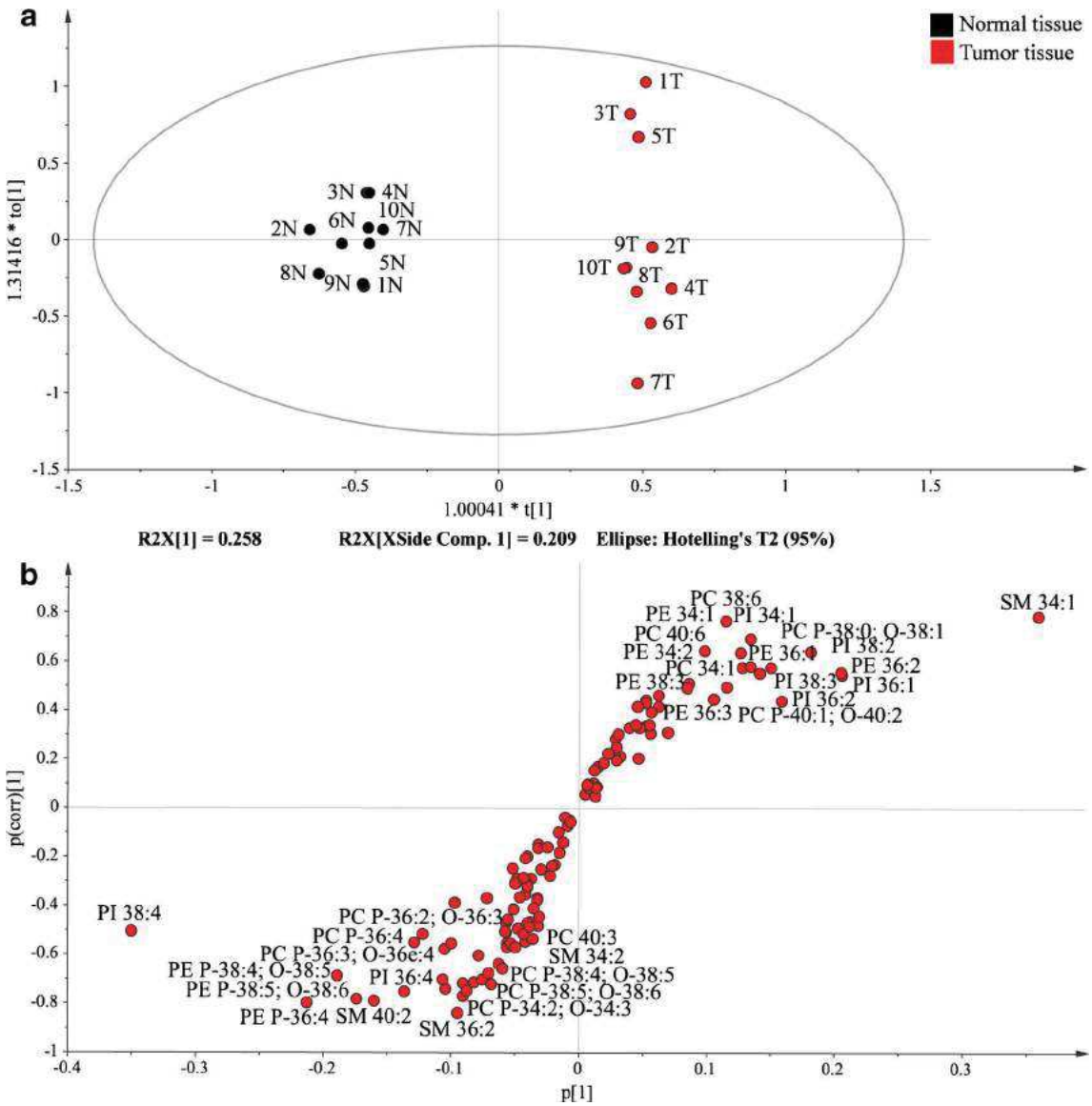

Fig. 7 Score plot of supervised multivariate data analysis of relative abundances of all lipids in normal and tumor tissues using OPLS method: **a** score plot and **b** S-plot

plot (Fig. 7b) shows that SM 34:1 (SM d18:1/16:0) has the highest positive correlation and PE P-36:4 (PE P-20:4_16:0) has the highest negative correlation with the tumor tissue. Both lipids exhibit high magnitude and high reliability in the OPLS model; therefore, they significantly contribute to the clustering of normal and tumor tissues.

Characterization of attached fatty acyls in phospholipids

The degree of lipid saturation plays an important role in de novo lipogenesis in cancer cells, because polyunsaturated fatty acyls are more susceptible to lipid peroxidation, which mediates cell death induced by oxidative stress or cytotoxic drugs [39, 40]. For this reason, we describe attached fatty acyls on the glycerol skeleton in normal and tumor tissues by using HILIC-HPLC/ESI-MS. Table 1 shows increased relative abundances of saturated (0 DB) and low unsaturated (1–3 DB) fatty acyls and decreased level of high unsaturated (4–6 DB) fatty acyls in tumor tissues in most phospholipid classes. The biggest differences between normal and tumor tissues for saturated and low unsaturated fatty acyls are observed for pPC+ePC and pPE+ePE, while lower relative abundances in tumor tissues are detected for aPE and aPC. PI is less unsaturated in tumors. Values of average carbon number (aCN) are from 36.0 (aPC) to 40.9 (pPE+ePE), and differences between normal and tumor groups are relatively small. Average double bond (aDB) number varies from 2.0 (pPC+ePE) to 3.8 (pPE+ePE) for phospholipid classes,

Table 1 Relative abundances [%] of saturated (0 DB), low unsaturated (1–3 DB), and high unsaturated (4–6 DB) fatty acyls on the glycerol skeleton in normal and tumor tissues, their average carbon number (aCN), and average double bond (aDB) number

Lipid class	Saturated (0 DB)		Low unsaturated (1–3 DB)		High unsaturated (4–6 DB)		aCN		aDB	
	Normal	Tumor	Normal	Tumor	Normal	Tumor	Normal	Tumor	Normal	Tumor
PI	4.1	4.8	34.2	49.5	61.7	45.7	37.3	37.1	3.2	2.8
PE	6.3	6.5	42.6	52.2	51.1	41.3	38.6	38.4	3.3	3.0
aPE	9.1	7.6	53.5	61.8	37.4	30.6	36.8	36.6	2.6	2.4
pPE+ePE	10.8	13.8	30.7	34.2	58.5	52.0	40.2	40.9	3.8	3.7
PC	17.0	19.3	50.6	50.9	32.4	29.9	37.4	37.6	2.6	2.5
aPC	11.0	10.3	56.4	55.6	32.6	34.1	36	36	2.5	2.6
pPC+ePC	28.3	35.0	39.8	42.6	31.9	22.5	37.6	38.1	2.5	2.0
SM	0	0	100	100	0	0	38.5	38	1.4	1.3
Average[a]	12.4	13.9	44.0	49.5	43.7	36.6	37.7	37.8	2.9	2.7

[a] Average parameters of phospholipids (excluding SM) obtained by averaging each column, i.e., average of values for PI, PE, aPE, pPE+ePE, PC, aPC, and pPC+ePC

and values of aDB are lower for tumor tissues in all lipid classes, except for aPC. The class of SM contains mainly monounsaturated attached fatty acyls, and all SM belong to low unsaturated fatty acyls. The described behavior of saturated, low unsaturated, and high unsaturated fatty acyls in tumor tissues is in agreement with that in the literature, but the present methodology provides tools for reliable quantitation and generalization of these trends for both class concentrations and individual lipid species as well.

Conclusions

The statistically significant increase of concentrations observed for several phospholipid classes and also lipid species within these classes is detected in breast tumor tissues of ten patients compared to surrounding normal tissues of the same patients. The decrease of relative abundances is observed for pPE and ePE (but not for pPC and ePC), which may be related to combined reasons not specific only to cancer, such as the oxidative stress and inflammation as side effects that accompany the tumor growth. The presence of phospholipids with the general formula C34:1 (mainly combination of C16:0 and C18:1) has shown marked association with tumor tissues for several lipid classes, while similar but less pronounced trend can be found for other phospholipids with low saturation level. The present study demonstrates a proof-of-concept of applicability of developed analytical methodology, but it also has certain limitations due to its pilot nature. All patients in this study are classified as luminal A or luminal B breast cancer, and less frequent subtypes, including hormone receptor-negative, HER-2 positive, and triple negative tumors, are not represented in this pilot cohort. The possible association between breast cancer subtype and phospholipid composition could be reliably addressed in future larger cohort of patients.

Acknowledgments This work was supported by ERC CZ project No. LL1302 sponsored by the Ministry of Education, Youth and Sports of the Czech Republic. E.C. acknowledges the support of the grant project no. CZ.1.07/2.3.00/30.0021 sponsored by the Ministry of Education, Youth and Sports of the Czech Republic. The help of Blanka Červená and Vitaliy Chagovets (University of Pardubice) in the extraction and data analysis and Martin Hill (Institute of Endocrinology) in the statistical evaluation is acknowledged.

References

1. Pelengaris S, Khan M (2013) Wiley: Oxford
2. Rosen L, Rosen G (2013) http://cancer.org/: Atlanta
3. Thomson CA, Thompson PA (2009) Future Oncol 5:1257–1269
4. Azordegan N, Fraser V, Le K, Hillyer LM, Ma DWL, Fischer G, Moghadasian MH (2013) Mol Cell Biochem 374:223–232

5. Pender-Cudlip MC, Krag KJ, Martini D, Yu J, Guidi A, Skinner SS, Zhang Y, Qu XY, He CW, Xu Y, Qian SY, Kang JX (2013) Cancer Sci 104:760–764
6. Lv WW, Yang TS (2012) Clin Biochem 45:127–133
7. Shannon J, King IB, Moshofsky R, Lampe JW, Gao DL, Ray RM, Thomas DB (2007) Am J Clin Nutr 85:1090–1097
8. Kang JX, Liu A (2013) Cancer Met Rev 32:201–210
9. Corsetto PA, Montorfano G, Zava S, Jovenitti IE, Cremona A, Berra B, Rizzo AM (2011) Lipids Health Dis. 10
10. Spencer L, Mann C, Metcalfe M, Webb M, Pollard C, Spencer D, Berry D, Steward W, Dennison A (2009) Eur J Cancer 45:2077–2086
11. Doria ML, Cotrim CZ, Simoes C, Macedo B, Domingues P, Domingues MR, Helguero LA (2013) J Cell Physiol 228:457–468
12. Doria ML, Cotrim Z, Macedo B, Simoes C, Domingues P, Helguero L, Domingues MR (2012) Breast Cancer Res Tr 133:635–648
13. Hua X, Zhou ZX, Yuan L, Liu SQ (2013) Anal Chim Acta 788:135–140
14. Chughtai K, Jiang L, Greenwood TR, Glunde K, Heeren RMA (2013) J Lipid Res 54:333–344
15. Hilvo M, Denkert C, Lehtinen L, Muller B, Brockmoller S, Seppanen-Laakso T, Budczies J, Bucher E, Yetukuri L, Castillo S, Berg E, Nygren H, Sysi-Aho M, Griffin JL, Fiehn O, Loibl S, Richter-Ehrenstein C, Radke C, Hyotylainen T, Kallioniemi O, Iljin K, Oresic M (2011) Cancer Res 71:3236–3245
16. Smith RE, Lespi P, Di Luca M, Bustos C, Marra FA, de Alaniz MJT, Marra CA (2008) Lipids 43:79–89
17. Hammad LA, Wu GX, Saleh MM, Klouckova I, Dobrolecki LE, Hickey RJ, Schnaper L, Novotny MV, Mechref Y (2009) Rapid Commun Mass Spectrom 23:863–876
18. Kim H, Min HK, Kong G, Moon MH (2009) Anal Bioanal Chem 393:1649–1656
19. Holčapek M, Jirásko R, Lísa MJ (2012) Chromatogr A 1259:3–15
20. Han XL, Yang K, Gross RW (2012) Mass Spectrom Rev 31:134–178
21. Yang K, Han X (2011) Metabolites 1:21–40
22. Begley JKP, Redpath TW, Bolan PJ, Gilbert FJ (2012) Breast Cancer Res. 14
23. Glunde K, Jie C, Bhujwalla ZM (2004) Cancer Res 64:4270–4276
24. Klomp DWJ, van de Bank BL, Raaijmakers A, Korteweg MA, Possanzini C, Boer VO, de Berg C, van de Bosch M, Luijten PR (2011) NMR Biomed 24:1337–1342
25. Merchant TE, Meneses P, Gierke LW, Denotter W, Glonek T (1991) Br J Cancer 63:693–698
26. Kirwan GM, Johansson E, Kleemann R, Verheij ER, Wheelock AM, Goto S, Trygg J, Wheelock CE (2012) Anal Chem 84:7064–7071
27. Eriksson L, Byrne T, Johansson E, Trygg J, Vikström C (2013) Multi- and megavariate data analysis. Basic principles and applications. Third revised edition. MKS Umetrics AB, Malmö
28. Wold S, Sjostrom M, Eriksson L (2001) Chemom Intell Lab Syst 58: 109–130
29. Trygg J, Wold S (2002) J Chemom 16:119–128
30. Trygg J (2002) J Chemom 16:283–293
31. Folch J, Lees M, Stanley GHS (1957) Biol Chem 226:497–509
32. Lísa M, Cífková E, Holčapek MJ (2011) Chromatogr A 1218:5146–5156
33. Cífková E, Holčapek M, Lísa M, Ovčačíková M, Lyčka A, Lynen F, Sandra P (2012) Anal Chem 84:10064–10070
34. Cífková E, Holčapek M, Lísa M (2013) Lipids 48:915–928
35. Holm S (1979) Scand J Stat 6:65–70
36. Liebisch G, Vizcaino JA, Kofeler H, Trotzmuller M, Griffiths WJ, Schmitz G, Spener F, Wakelam MJO (2013) Lipid Res 54:1523–1530
37. Nagan N, Zoeller RA (2001) Prog Lipid Res 40:199
38. Braverman NE, Moser AB (2012) Biochim Biophys Acta-Mol Basis Dis 1822:1442–1452
39. Rysman E, Brusselmans K, Scheys K, Timmermans L, Derua R, Munck S, Van Veldhoven PP, Waltregny D, Daniels VW, Machiels J, Vanderhoydonc F, Smans K, Waelkens E, Verhoeven G, Swinnen JV (2010) Cancer Res 70:8117–8126
40. Santos CR, Schulze A (2012) Febs J 279:2610–2623

Research Article

Rapid Communications in Mass Spectrometry

Received: 13 September 2016 Revised: 6 November 2016 Accepted: 9 November 2016 Published online in Wiley Online Library

Rapid Commun. Mass Spectrom. **2017**, *31*, 253–263
(wileyonlinelibrary.com) DOI: 10.1002/rcm.7791

Correlation of lipidomic composition of cell lines and tissues of breast cancer patients using hydrophilic interaction liquid chromatography/electrospray ionization mass spectrometry and multivariate data analysis

Eva Cífková[1], Miroslav Lísa[1], Roman Hrstka[2], David Vrána[3], Jiří Gatěk[4], Bohuslav Melichar[3] and Michal Holčapek[1]*

[1]University of Pardubice, Faculty of Chemical Technology, Department of Analytical Chemistry, Studentská 573, 53210 Pardubice, Czech Republic
[2]Masaryk Memorial Cancer Institute, Regional Centre for Applied Molecular Oncology, Žlutý kopec 7, 65653 Brno, Czech Republic
[3]Palacký University, Medical School and Teaching Hospital, Department of Oncology, I.P.Pavlova 6, 77520 Olomouc, Czech Republic
[4]Tomáš Baťa University in Zlín, Atlas Hospital, Department of Surgery, nám T. G. Masaryka 5555, 76001 Zlín, Czech Republic

RATIONALE: The goal of this work is the comparison of differences in the lipidomic compositions of human cell lines derived from normal and cancerous breast tissues, and tumor *vs.* normal tissues obtained after the surgery of breast cancer patients.
METHODS: Hydrophilic interaction liquid chromatography/electrospray ionization mass spectrometry (HILIC/ESI-MS) using the single internal standard approach and response factors is used for the determination of relative abundances of individual lipid species from five lipid classes in total lipid extracts of cell lines and tissues. The supplementary information on the fatty acyl composition is obtained by gas chromatography/mass spectrometry (GC/MS) of fatty acid methyl esters. Multivariate data analysis (MDA) methods, such as nonsupervised principal component analysis (PCA), hierarchical clustering analysis (HCA) and supervised orthogonal partial least-squares discriminant analysis (OPLS-DA), are used for the visualization of differences between normal and tumor samples and the correlation of similarity between cell lines and tissues either for tumor or normal samples.
RESULTS: MDA methods are used for differentiation of sample groups and also for identification of the most up- and downregulated lipids in tumor samples in comparison to normal samples. Observed changes are subsequently generalized and correlated with data from tumor and normal tissues of breast cancer patients. In total, 123 lipid species are identified based on their retention behavior in HILIC and observed ions in ESI mass spectra, and relative abundances are determined.
CONCLUSIONS: MDA methods are applied for a clear differentiation between tumor and normal samples both for cell lines and tissues. The most upregulated lipids are phospholipids (PL) with a low degree of unsaturation (e.g., 32:1 and 34:1) and also some highly polyunsaturated PL (e.g., 40:6), while the most downregulated lipids are PL containing polyunsaturated fatty acyls (e.g., 20:4), plasmalogens and ether lipids. Copyright © 2016 John Wiley & Sons, Ltd.

Breast cancer represents the most commonly diagnosed cancer and, after lung cancer, the second leading cause of cancer death in women.[1,2] The stimulation by the female hormones estrogen and progesterone plays an indispensable role in the pathogenesis of breast cancer, since the incidence in men is two orders of magnitude lower. Hormonal factors associated with age, lifestyle, or diet represent the principal cause of breast cancer, while exposure to radiation and other factors could also be responsible in individual cases. The germ-line mutations of *BRCA1* and *BRCA2* genes involved in maintenance of genome integrity represent additional factor responsible for almost 10% of breast cancer cases. Based on the tumor phenotype assessed by immunohistochemistry and molecular profiling, breast cancer is currently divided into several types with distinct biological features and therapeutic approaches, including luminal (luminal A and luminal B), HER-2-positive and basal (triple negative) breast carcinoma. The introduction of screening with early diagnosis resulting from the use of mammograms as well as the advances in multidisciplinary management of early breast cancer encompassing surgery, adjuvant (or neoadjuvant) systemic therapy including hormonal therapy, cytotoxic chemotherapy and targeted treatment, and adjuvant radiation have resulted

* *Correspondence to:* M. Holčapek, University of Pardubice, Faculty of Chemical Technology, Department of Analytical Chemistry, Studentská 573, 53210 Pardubice, Czech Republic.
E-mail: michal.holcapek@upce.cz

in a substantial reduction in mortality.[3] However, the success of multidisciplinary management is critically dependent on early detection. Although mammography represents the principal breast cancer screening method its sensitivity depends on the size of the tumor and density of the breast tissue. The necessary exposure to radiation limits the frequency of examinations and, not infrequently, breast cancer is detected within months of prior mammography (so-called interval breast cancer). Thus, biomarkers for early detection of breast cancer that could be determined in the biological fluids, and could be performed more frequently compared to mammography, are urgently needed.

The determination of biomarkers currently represents an indispensable component of the multidisciplinary management of cancer patients.[4] Circulating biomarkers currently used, e.g., carcinoembryonic antigen (CEA) or carbohydrate antigen (CA) 15-3, are not routinely used in cancer screening and the utilization in the follow-up of patients with breast cancer is also limited. Therefore, the search for new circulating biomarkers represents an unmet medical need in breast cancer.

The relation between lipid metabolism and breast cancer development has been investigated in various studies aimed at early diagnosis, identification of biomarkers and characterization of biochemical pathways.[5–9] Increased *de novo* production of fatty acids in tumor cells is associated with proliferation, aggressiveness and other aspects of malignant transformation,[7,8,10] because polyunsaturated fatty acids (PUFA), in contrast to saturated fatty acids, are more susceptible to oxidation and may subsequently induce cell death. For this reason, the increased concentrations of saturated fatty acids, such as palmitic (16:0) and stearic (18:0) acids, has been documented in breast carcinoma.[11,12] Furthermore, arachidonic (20:4; n-6 PUFA), docosahexaenoic (22:6; n-3 PUFA) and eicosapentaenoic (20:5; n-3 PUFA) acids are highlighted in many studies, because increased abundances of n-3 PUFA have been observed in tumor tissues.[8,13–18]

Comprehensive lipidomic analysis represents a challenging task due to the different structures of individual lipid classes and different physicochemical properties, such as polarity or solubility. The coupling of liquid chromatography and mass spectrometry (LC/MS) enables the separation of individual lipids and their sensitive identification and quantification, which has been frequently used in the breast cancer lipidomic research.[10,11,19–24] Many studies have reported an increased level of lipids containing saturated fatty acyls (14:0, 16:0 and 18:0) in breast tumor tissues, which is in agreement with increased *de novo* fatty acid synthesis.[11,20,22,23] The fatty acyl profiles can be measured by GC/MS after transesterification of intact lipids, which provides basic information on the fatty acyl distribution in all lipids.[12,13,15]

At the present time, MDA is an important part of most clinical studies due to the simplification and better visualization of large datasets.[25] PCA is an unsupervised statistical method providing an important overview on the sample clustering based on similarities and differences among all molecules determined. The unsupervised HCA method using the Ward linkage criterion clusters the objects according to similarities of the distance criterion using the smallest error of sum of squares. Results are visualized using a dendrogram, which merges individual samples into clusters starting from the smallest cluster of two up to the final cluster including all samples. The supervised OPLS-DA searches for similarities and differences between predefined two groups of samples, typically healthy compared to pathological ones.

The goal of the present work is the characterization of the lipid composition of various normal and tumor breast cell lines using HILIC/ESI-MS and GC/MS methods and identification of the most significant differences in the lipidomic compositions using MDA methods. The lipidomic composition of cell lines as the simplest model for cancer research is compared with tumor and surrounding normal tissues after breast tumor surgery to determine whether the same dysregulated lipids can be observed for both models.

EXPERIMENTAL

Chemicals and standards

Acetonitrile, 2-propanol, methanol (all LC/MS grade), chloroform stabilized by 0.5–1% ethanol (LC grade), ammonium acetate and sodium chloride were purchased from Sigma-Aldrich (St. Louis, MO, USA). Deionized water was prepared with a Milli-Q Reference water purification system (Millipore, Molsheim, France). *N*-Dodecanoyl-heptadecasphing-4-enine-1-phosphatidylethanolamine (d17:1/12:0) used as an internal standard (IS) was purchased from Avanti Polar Lipids (Alabaster, AL, USA). The lipid nomenclature follows the LIPID MAPS system[26] and the shorthand notation for lipid structures.[26] Breast cell lines were maintained at the Regional Center for Applied Molecular Oncology, Masaryk Memorial Cancer Institute in the Czech Republic (see Supplementary Table S1, Supporting Information), while human breast tumor and surrounding normal tissues of ten cancer patients were obtained from the Department of Surgery, Atlas Hospital Zlín, Czech Republic.

Sample preparation

Human cancer cell lines (Supplementary Table S1, Supporting Information) were obtained from the American Type Culture Collection (ATCC) and cultured in the recommended medium containing 10% fetal bovine serum, 0.3 mg/mL L-glutamine and 100 U/mL penicillin–streptomycin (all Invitrogen, Life Technologies, Paisley, UK) at 37°C and 5% CO_2. MCF10A cells were maintained in DMEM/F12 growth media supplemented with 5% horse serum, 100 U/mL penicillin–streptomycin (all Invitrogen, Life Technologies, Paisley, UK), 20 ng/mL EGF, 0.5 mg/mL hydrocortisone, 100 ng/mL cholera toxin and 10 µg/mL insulin (all Sigma-Aldrich) at 37°C and 5% CO_2.

All cell lines were grown in tissue culture plates (8–12 for each cell line, 2 biological replicates) with 100 mm diameter. During cultivation, the cells were periodically checked by microscopy and tested for Mycoplasma contamination. To form cell pellets, each plate was washed two times with ice-cold phosphate-buffered saline (PBS), then the cells were detached with cell scraper into 1 mL ice-cold PBS and subjected to centrifugation at 200 *g* for 10 min. Cell pellets were immediately stored at –80°C.

Rapid Communications in Mass Spectrometry

Cell lines were extracted using a chloroform/methanol/water system according to a modified Folch extraction.[27,28] Briefly, 70–300 mg of cell pellets and 25 µL of 3.3 mg/mL IS were homogenized for 3 min with 5 mL of chloroform/methanol (2:1, *v*/v) mixture and the homogenate was filtered using a coarse filter paper. Subsequently, 1 mL of 1 mol/L NaCl was added, and the mixture was centrifuged at 3000 rpm for 5 min at ambient temperature. The chloroform bottom layer (total lipid extract) containing lipids was evaporated by a gentle stream of nitrogen, redissolved in 500 µL of chloroform/2-propanol (1:1, *v*/v) mixture and filtered using a syringe filter with regenerated cellulose with a pore size 0.45 µm (Teknokroma, Barcelona, Spain).

Fatty acid methyl esters (FAME) were prepared from the lipid extract using sodium methoxide.[29] Briefly, 50 µL of lipid extract and 0.8 mL of 0.25 mol/L sodium methoxide in methanol were heated in a water bath for 10 min at 65°C. After the reaction, 0.5 mL of saturated solution of NaCl in water was added and, subsequently, FAME were extracted from the mixture using 1 mL hexane.

LC/MS conditions

Total lipid extracts were analyzed by a LC/MS method, as described previously.[28,30] A 1290 series liquid chromatograph (Agilent Technologies, Waldbronn, Germany) was coupled with an Esquire 3000 ion trap analyzer (Bruker Daltonics, Bremen, Germany). Separation of total lipid extracts was performed on a Spherisorb Si column (250 × 4.6 mm, 5 µm; Waters, Milford, MA, USA) using a flow rate of 1 mL/min, an injection volume of 1 µL, a column temperature of 40°C and a mobile phase gradient: 0 min – 94% A + 6% B, 60 min – 77% A + 23% B, where A was acetonitrile and B was

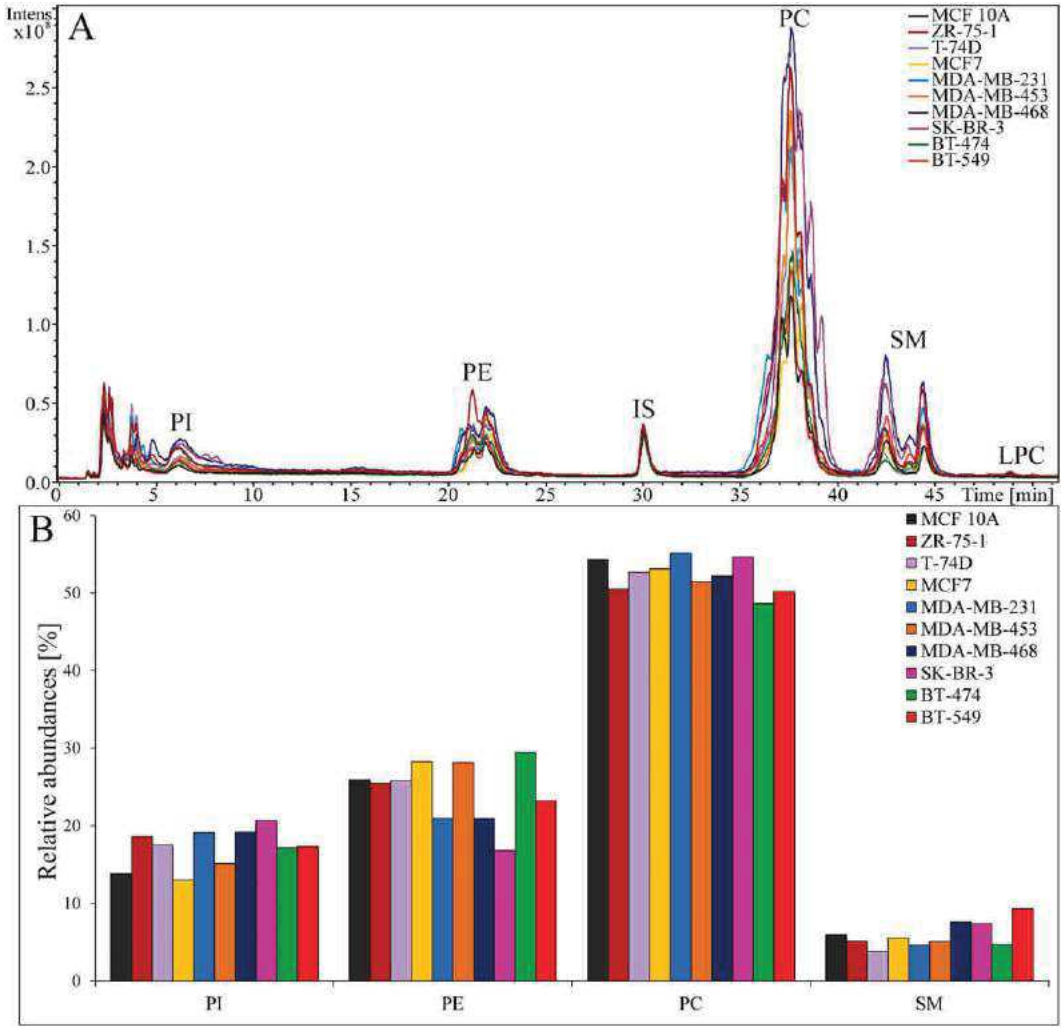

Figure 1. (A) Positive-ion HILIC/ESI-MS chromatograms of normal breast cell line MCF10A (black line) and nine tumor breast cell lines ZR-75-1, T-74D, MCF7, MDA-MB-231, MDA-MB-453, MDA-MB-468, SK-BR-3, BT-474, BT-549. LC conditions: column Spherisorb Si (250 × 4.6 mm, 5 µm), flow rate 1 mL/min, separation temperature 40°C, mobile phase gradient: 0 min – 94%A + 6%B, 60 min – 77%A + 23%B, where A is acetonitrile and B is 5 mM aqueous ammonium acetate. (B) Comparison of relative abundances of individual lipid classes in analyzed normal and tumor breast cell lines. Peak annotation: PI – phosphatidylinositols, PE – phosphatidylethanolamines, IS – internal standard, PC – phosphatidylcholines, SM – sphingomyelins, LPC – lysophosphatidylcholines.

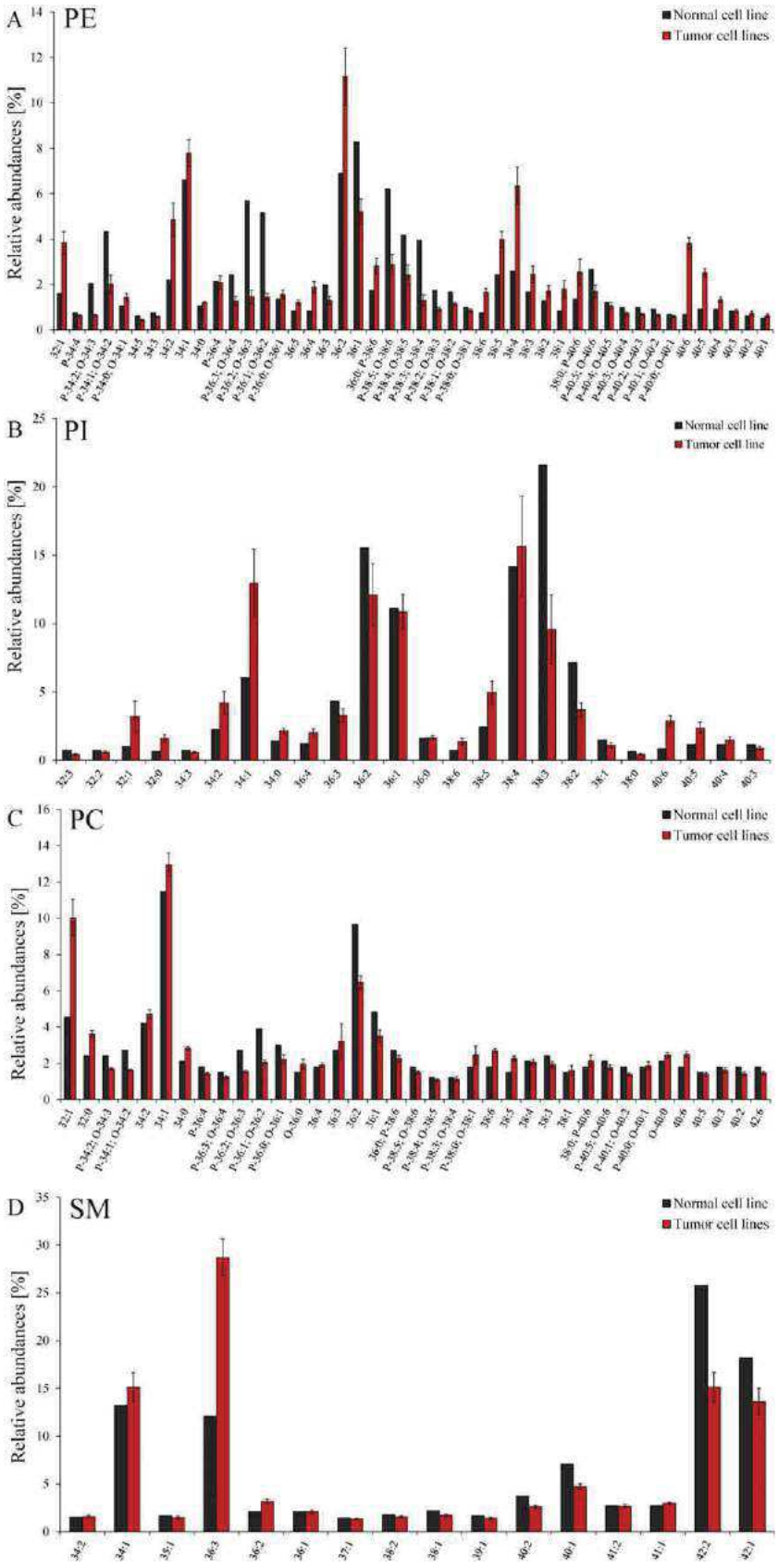

Figure 2. Relative abundances of individual lipids in normal breast cell line MCF10A (black columns) and average relative abundances from nine tumor breast cell lines (red columns, including standard errors of average value): (A) PE, (B) PI, (C) PC and (D) SM.

Rapid Communications in Mass Spectrometry

5 mmol/L aqueous ammonium acetate. Lipids were detected in positive- and negative-ion ESI-MS modes in the mass range *m/z* 50–1000 with the nebulizing gas 60 psi, drying gas flow rate 10 L/min and drying gas temperature of 365°C. Quantitation of individual lipid classes was achieved by the single IS and response factors[30] obtained from calibration curves. Individual lipid species were identified using relative abundances of deprotonated molecules $[M–H]^-$ for the PE and PI classes and $[M–CH_3]^-$ ions for the PC class in the negative-ion mode. SM species were identified as protonated molecules $[M + H]^+$ in the positive-ion mode. LPC could not be determined due to their low concentrations. Low-energy collision-induced dissociation tandem mass spectrometry (MS/MS) experiments were performed for the most abundant lipid species with an isolation width of *m/z* 4, collision energy of 1 V and helium as the collision gas.

GC/MS conditions

GC/MS experiments were performed on a model 7890 gas chromatograph (Agilent Technologies) using a TR-FAME column (60 m length, 0.25 mm ID, 0.25 µm film thickness; Thermo Scientific, Waltham, MA, USA) under the following conditions: injection volume 5 µL, split ratio 1:4 and flow rate of helium (99.996%) as a carrier gas 1.2 mL/min. The temperature gradient starting from the initial temperature 160°C, ramp to 235°C at 4°C/min and hold for 2 min, ramp to 250°C at 50°C/min. Detection was performed using a MSD 5977A quadrupole mass analyzer (Agilent Technologies) with an electron ionization (EI) source in the range *m/z* 50–500 under the following conditions: ionization energy 70 eV, gain factor 15, isolation width *m/z* 0.1, scanning frequency 10.9 scan/s, capillary temperature 235°C, EI source temperature 230°C and mass analyzer temperature 150°C. FAME were identified based on retention times, mass spectra compared with the Wiley Registry of Mass Spectral Data/NIST database as well as manual interpretation.

Statistical data analysis

MDA was performed using unsupervised HCA and PCA methods, and supervised OPLS-DA method using the SIMCA software (version 13.0; Umetrics, Umeå, Sweden). Data were preprocessed before statistical evaluation using Pareto scaling and logarithm transformation. OPLS-DA is cross-validated using leave group out method. The dendrogram was processed using the Ward linkage criterion, which minimizes the variation within the cluster. Box plots described the distribution of results using median, minimum, maximum and the variability of data sets in the first and third quartiles. Receiver operating characteristic (ROC) curves were constructed using MedCalc statistical software (version 15.8; MedCalc Software bvba, Ostend, Belgium).

RESULTS AND DISCUSSION

Lipidomic analysis of breast cell lines

A normal breast epithelium cell line (MCF10A) and nine breast cancer cell lines (ZR-75-1, T-74D, MCF7, MDA-MB-231, MDA-MB-453, MDA-MB-468, SK-BR-3, BT-474, BT-549, see Supplementary Table S1 (Supporting Information) for more details) were extracted according to a modified Folch procedure with chloroform/methanol/water mixture.[28] Total lipid extracts of cell lines obtained were analyzed using the HILIC/ESI-MS method. Quantitative analysis for each lipid class was performed using a combination of the single

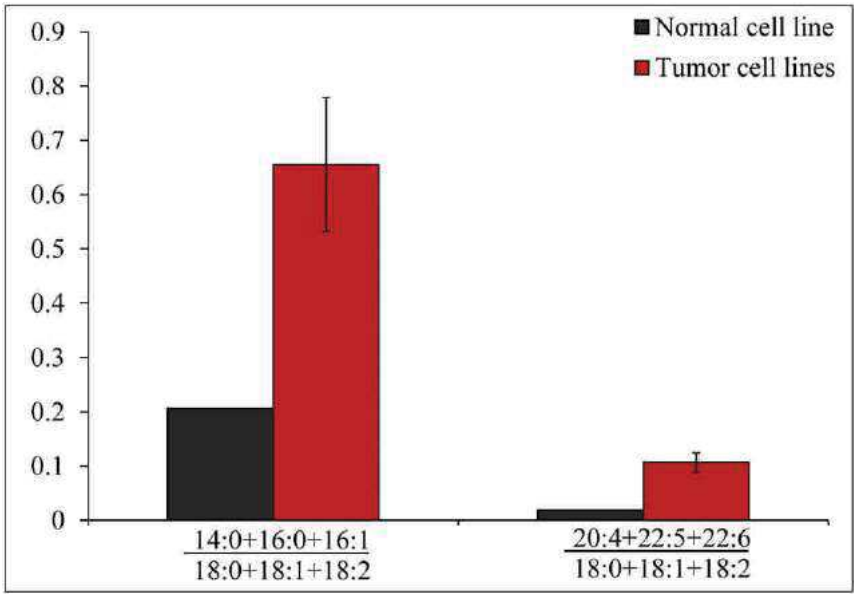

Figure 3. Ratios of sums of shorter acyls (14:0 + 16:0 + 16:1) to C18 acyls (18:0 + 18:1 + 18:2) and PUFA (20:4 + 22:5 + 22:6) to C18 acyls (18:0 + 18:1 + 18:2) in cell lines based on GC/MS data of FAME after the transesterification of intact lipids in normal breast cell line MCF10A (black columns) and average relative abundances from nine tumor breast cell lines (red columns, including standard errors of average value).

internal standard (IS) and response factors for each lipid class, which are normalized to the IS.[30] The HILIC/ESI-MS method enables the characterization of phosphatidylinositols (PI), phosphatidylethanolamines (PE), phosphatidylcholines (PC), sphingomyelins (SM) and lysophosphatidylcholines (LPC) in individual cell lines (Fig. 1), but concentrations of LPC are below the quantitation threshold of the present method. Figure 1(A) shows differences in peak shapes, which is caused by partially separated lipid species inside individual lipid classes according to the fatty acyl chain length and the number

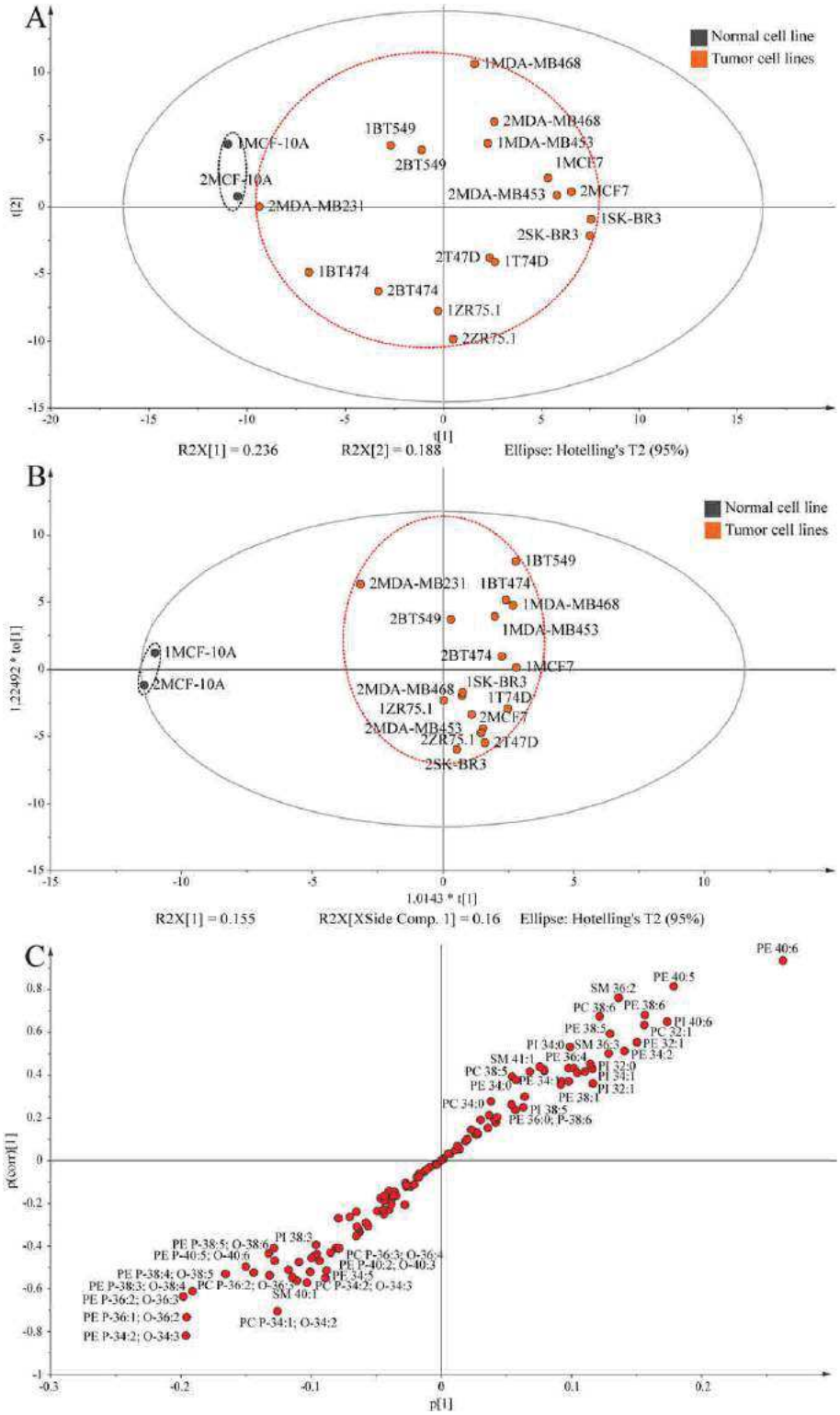

Figure 4. Multivariate data analysis of relative abundances of all lipids in normal and tumor breast cell lines: (A) the score plot of unsupervised PCA method, (B) the score plot, and (C) the S-plot of supervised OPLS-DA method.

of double bonds. Quantitative results of PI, PE, PC and SM are reported using relative abundances in % (Fig. 1(B)), but normal and tumor cell lines do not differ substantially in their phospholipid content, therefore the detailed analysis of individual lipid species inside classes is performed using characteristic ions in ESI mass spectra obtained by the peak integration of given lipid class in the HILIC chromatogram. The analysis of lipid species allows the characterization of relative abundances of 46 PE, 24 PI, 37 PC and 16 SM in normal and tumor cell lines (Supplementary Table S2 and Figs. S1–S4,

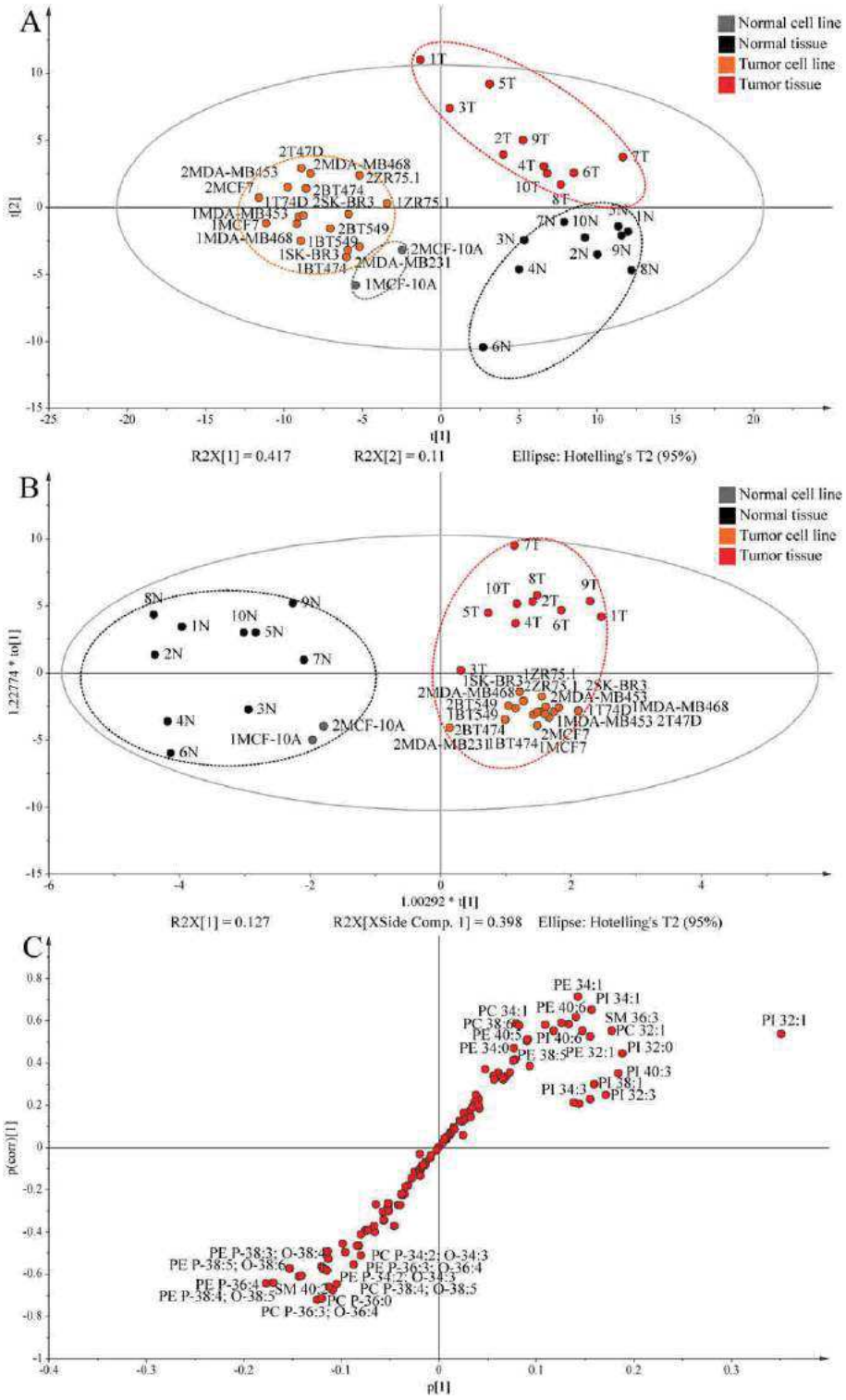

Figure 5. Multivariate data analysis of relative abundances of all lipids in normal and tumor breast cell lines and tissues of breast cancer patients: (A) the score plot of unsupervised PCA method, (B) the score plot, and (C) the S-plot of supervised OPLS-DA method.

Supporting Information). Figure 2 shows the comparison of relative abundances of individual lipid species inside lipid classes in the normal breast epithelial cell line and mean values for nine tumor breast cell lines. Individual lipid species are characterized by attached fatty acyls annotated by their total carbon number and double-bond number (CN:DB). Standard errors of average values are presented in figures for nine tumor samples, but they cannot be calculated for the normal sample, because only MCF10A is available. In the case of PE and PC, different types of fatty acyl linkages to the glycerol backbone in the *sn*-1 position are observed, where the ether linkage of fatty acyls in the *sn*-1 position (1-alkyl-2-acyl) is referred to as ethers (e.g., PE O-36:4) and the vinyl ether linkage in the *sn*-1 position (1-alkenyl-2-acyl) corresponds to plasmalogens (e.g., PE P-36:4). Isobaric ethers and vinyl ethers cannot be distinguished by common MS methods; therefore, we annotate them as a sum, e.g., PE P-34:2 and PE O-34:3. Figure 2 shows the significant differences between normal and tumor cell lines, which confirms the fact that tumor cells can be easily discriminated from normal cells for all studied cell lines based on their lipidomic composition. The most pronounced trend is a significant downregulation of most PE and PC ethers and plasmalogens (e.g., P-34:1/O-34:2, P-34:2/O-34:3, P-36:1/O-36:2 and P-36:2/O-36:3), while lipid species containing saturated and monounsaturated fatty acyls are significantly upregulated in tumor cell lines (e.g., species containing 34:0, 34:1, 32:1). Furthermore, lipid species containing some PUFA with more than three double bonds (e.g., 36:4, 38:4, 38:5, 38:6, 40:4, 40:5 and 40:6) are significantly upregulated in tumor cell lines. These trends are closely correlated with GC/MS results of the fatty acyl composition (Supplementary Fig. S5, Supporting Information). Saturated or monounsaturated fatty acyls with shorter acyl chains (14:0, 16:0 and 16:1) and PUFA containing four and more double bonds (20:4, 22:5, 22:6) are significantly upregulated in tumor cell lines. Plotted ratios of sums of shorter acyls to C18 (14:0 + 16:0 + 16:1/18:0 + 18:1 + 18:2) or PUFA to C18 (20:4 + 22:5 + 22:6/18:0 + 18:1 + 18:2) show upregulation of more than 3 times for shorter acyls and more than 5 times for PUFA (Fig. 3).

Statistical evaluation of breast cell lines data

MDA of relative abundances of detected polar lipid species was used as a tool for simplified visualization of the most significant differences between normal and tumor cell lines (Fig. 4). Cell lines were cultured, extracted and lipid composition measured using LC/MS in two batches within the time interval of 6 months (prefix 1 is the first batch, prefix 2 is the second batch, e.g., 1MCF10A and 2MCF10A) to verify the integrity of data. PCA clusters samples according to the similarities and differences between relative abundances of lipid species. Figure 4(A) shows clear clustering of the normal cell line and all tumor cell lines and significant similarities between samples in the first and second batch, providing a distinct proof of stability and reproducibility of all individual steps in sample preparation and analysis. The next step of MDA is application of the supervised OPLS-DA method (Figs. 4(B) and 4(C)), which improves the group clustering by the PCA method using predefined groups of samples (normal *vs.* tumor cell lines). The OPLS-DA score plot (Fig. 4(B)) shows excellent separation of clusters, while the S-plot (Fig. 4(C)) visualizes the lipids influencing this clustering. Upregulated lipids in tumor cell lines appear in the upper right corner and downregulated lipids in the lower left corner. The most upregulated species are PE 40:6 (PE 18:0/22:6), PE 40:5 (PE 18:0/22:5), PE 38:6 (PE 16:0/22:6), PI 40:6 (PI 18:0/22:6) and PC 32:1 (PC 16:0/16:1), and downregulated PE P-34:2 (PE P-16:0/18:2 and PE O-16:1/18:2), PE P-36:1 (PE P-18:0/18:1 and PE O-18:1/18:1), PE P-36:2 (PE P-18:0/18:2 and PE O-18:1/18:2), PC P-34:1 (PC P-18:0/16:1 and PC O-18:1/16:1) and PE P-38:3 (PE P-18:0/20:3 and PE

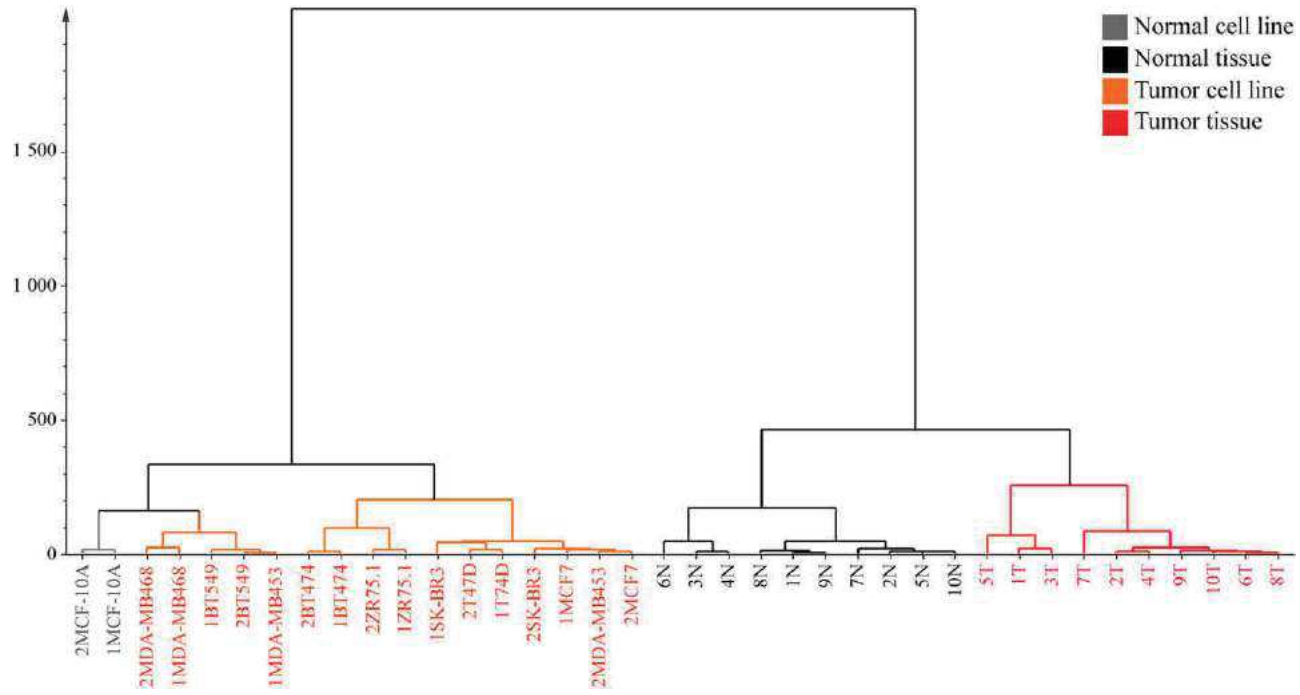

Figure 6. Dendrogram of normal and tumor breast cell lines and tissues calculated using the Ward linkage criterion.

Rapid Communications in Mass Spectrometry

O-18:1/20:3). The most abundant fatty acyl combinations on the glycerol skeleton were identified by MS/MS spectra in the negative-ion ESI mode.

Correlation of breast cell lines and breast tissues of cancer patients

LC/MS analysis enables the identification and characterization of differences in the lipidomic composition (see Supplementary Table S2, Supporting Information) of the breast normal cell line (MCF10A) and nine breast tumor cell lines (ZR-75-1, T-74D, MCF7, MDA-MB-231, MDA-MB-453, MDA-MB-468, SK-BR-3, BT-474 and BT-549). In our previous work we described changes in the lipidome of breast tumor tissue and surrounding normal tissue of breast cancer patients using the same LC/MS method.[24] However, these changes in breast tissues could also be caused by other factors in addition to cancer, such as inflammation and immune response. Moreover, the information is also diluted due to the presence of other cell types, adipose tissue, ducts, etc. On the other hand, the comparison of cell lines (tumor *vs.* normal) provides undiluted information on the lipidomic changes occurring in the tumor cell after the transformation from the normal cell. The goal of the present work is to determine the degree of similarity between tumor cell lines and tumor tissues and mainly to identify the most dysregulated lipids observed for both models.

Various MDA approaches are used for the statistical evaluation of relative abundances of 123 lipids from four lipid classes determined in this work: PCA, HCA, OPLS-DA, S-plots, dendrogram and ROC curves. The gap between cell lines (on the left) and tissues (on the right) in the PCA plot shown in Fig. 5(A) confirms the initial expectation that differences between cell lines and tissues are not negligible, but it is still possible to distinguish cancer samples from normal samples even in this unsupervised PCA plot. The same conclusion is obtained from the HCA plot as the second unsupervised MDA method that the primary separation criterion is the type of sample (cell line *vs.* tissue) and the second is cancer *vs.* normal (Fig. 6). When we switch from unsupervised methods to supervised OPLS-DA, then of course the group resolution is significantly improved and cancer *vs.* normal samples are clearly distinguished in all cases (Fig. 5(B)). The next step is the identification of most

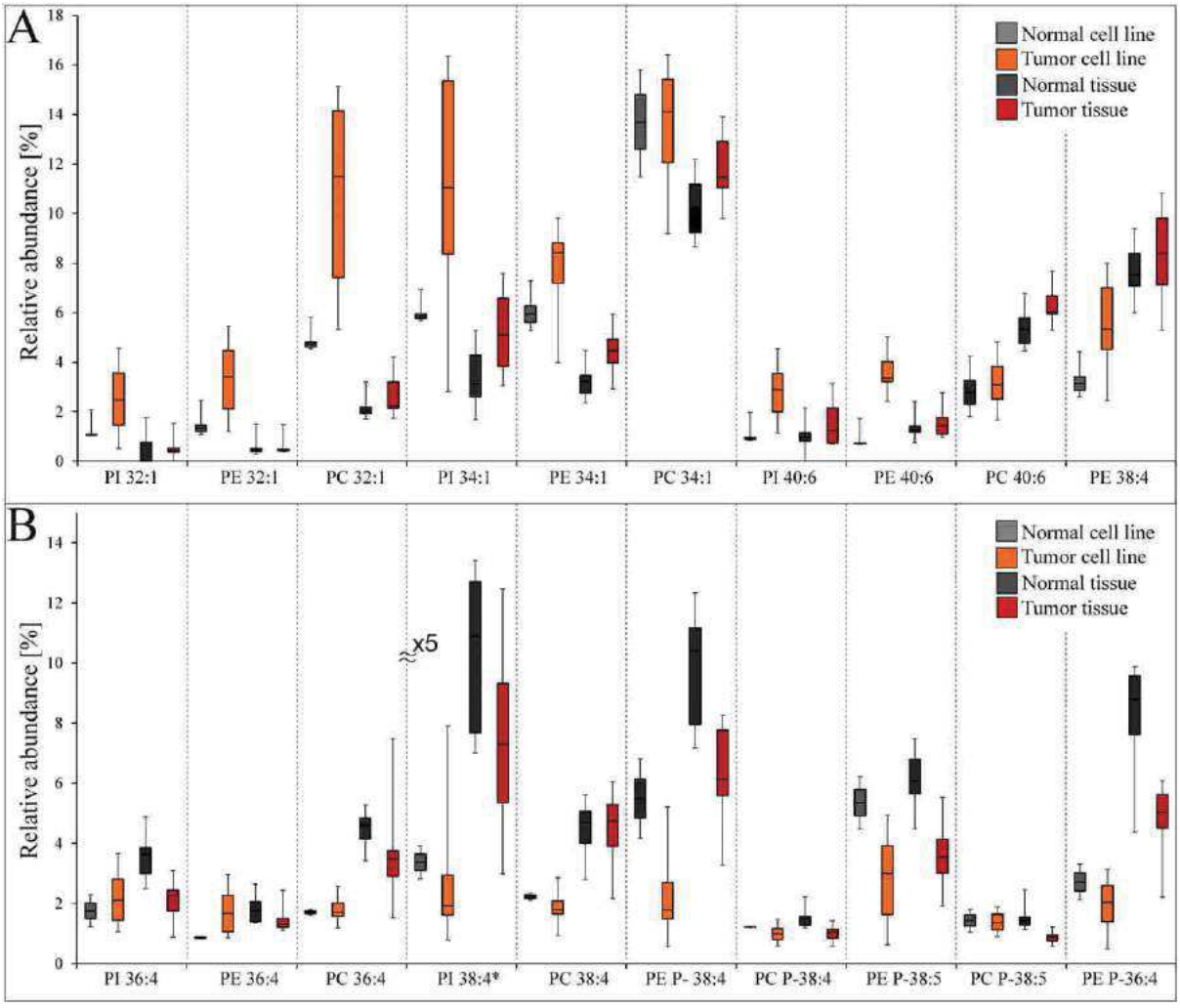

Figure 7. Box plots describing the most important (A) upregulated and (B) downregulated lipids in normal and tumor breast cell lines and tissues of breast cancer patients. *In the case of PI 38:4, *y* axes values are five times more than shown numbers, i.e., 0–70% range.

dysregulated lipids valid for both models using an S-plot (Fig. 5(C)). The logical series of the 10 most upregulated (Fig. 7 (A)) and 10 most downregulated (Fig. 7(B)) lipids are visualized by box plots with intervals of their relative abundances for all sample types. The central line in the box plot (Fig. 7) shows the value of the median, the lower part represents the first quartile and the upper part the third quartile. Extreme lines show minimum and maximum values. Some trends can be generalized and they are also in agreement with the state-of-the-art knowledge of lipidomic changes related to cancer. The significant upregulation is evident (Fig. 5 (C)) for lipids containing saturated and monounsaturated fatty acyls with shorter chains (32:0, 32:1, 34:0 and 34:1), which is illustrated in Fig. 7(A) for logical series of PL 32:1 and 34:1, but less pronounced upregulation could be observed for other low unsaturated PL as well. This is in perfect agreement with GC/MS data shown in Fig. 3 and Supplementary Fig. S5 (Supporting Information). Some PL with highly PUFA are upregulated (PI 40:6, PE 40:6, PC 40:6 and PE 38:4), while other polyunsaturated PL with general formulas 36:4 and 38:4 (combinations of 16:0/20:4 and 18:0/20:4) are downregulated (see Fig. 7(B)). The exception is the behavior of PE 38:4. It is clear that PL containing PUFA have important roles in cancer and changes could be also expected in the area of oxylipins formed by the oxidation of PUFA chains released from corresponding PL. Another general effect is the significant downregulation of ether and plasmalogen PE and PC, as shown in some examples in Fig. 7(B) and for the sum of all PE ethers and plasmalogens in Supplementary Fig. S6 (Supporting Information). Another way of visualization of the potential of most dysregulated lipids for distinguishing cancer *vs.* normal groups is the use of ROC curves (Supplementary Fig. S7, Supporting Information), which provides information on false positive/false negative rates. The area under the curve (AUC) in ROC graphs is a measure of reliability of used parameter for the differentiation of tumor *vs.* normal states. We plot sums of PE 32:1 + PI 32:1 + PC 32:1 in Supplementary Figs. S7(A) and S7(B) (Supporting Information) and of PE 36:4 + PI 36:4 + PC 36:4 in Supplementary Figs. S7(C) and S7(D) for cell lines (Figs. 7(A) and 7(C)) and tissues (Figs. 7(B) and 7(D)). The absolute resolution is obtained for PL 32:1 in cell lines (AUC = 1.00), but significantly decreased for tissues (AUC = 0.70), while results for PL 36:4 are comparable in both cases (AUC = 0.81 and 0.90, respectively).

CONCLUSIONS

This work confirms that changes observed in breast tumor tissues are caused mainly by different lipidomic profiles of tumor cells and these changes can be well correlated with the lipidomic composition of the nine breast cancer cell lines studied here. Although individual breast cancer cell lines show some differences in their lipidomic profiles, these differences do not cause problems in the differentiation between tumor and normal cells. The current research will continue with the analysis of human plasma of cancer patients and healthy volunteers with the emphasis on dysregulated lipids identified in tumor cell lines and tumor tissues and comparison between different types of breast cancer. Differences in lipid concentrations between normal and cancer groups are rather small for human plasma; therefore, the information on cancer-induced dysregulation of some PL with low unsaturation level (mainly 32:1 and 34:1), PL containing PUFA (36:4, 38:4, 38:5, 40:6, etc.) and plasmalogen and other ether lipids observed in cell lines and tissues could be helpful for the targeted lipidomic profiling of human plasma. These changes are also in agreement with GC/MS data showing the upregulation of shorter saturated (14:0 and 16:0) and monounsaturated (16:1) fatty acyls and some PUFA (20:4, 22:5 and 22:6).

Acknowledgements

This work was supported by the ERC CZ grant project LL1302 sponsored by the Ministry of Education, Youth and Sports of the Czech Republic. R.H. acknowledges the support of MEYS – NPS I – LO1413 and MH CZ - DRO (MMCI, 00209805) projects. The help of Blanka Červená and Magdaléna Ovčačíková (University of Pardubice) with the sample extraction is acknowledged.

REFERENCES

[1] D. Barh, A. Carpi, M. Verma, M. Gunduz. *Cancer Biomarkers: Minimal and Noninvasive Early Diagnosis and Prognosis*. CRC Press, Boca Raton, FL, USA, **2014**.
[2] *The Molecular Biology of Cancer*, (Eds: S. Pelengaris, M. Khan), (2nd edn.). Wiley-Blackwell, Oxford, UK, **2013**.
[3] B. Melichar, H. Studentova, H. Kalabova, D. Vitaskova, P. Cermakova, H. Hornychova, A. Ryska. Predictive and prognostic significance of tumor-infiltrating lymphocytes in patients with breast cancer treated with neoadjuvant systemic therapy. *Anticancer Res.* **2014**, *34*, 1115.
[4] B. Melichar. Laboratory medicine and medical oncology: the tale of two Cinderellas. *Clin. Chem. Lab. Med.* **2013**, *51*, 99.
[5] J. Baumann, C. Sevinsky, D. S. Conklin. Lipid biology of breast cancer. *Biochim. Biophys. Acta Mol. Cell Biol. Lipids* **2013**, *1831*, 1509.
[6] S. F. Nabavi, S. Bilotto, G. L. Russo, I. E. Orhan, S. Habtemariam, M. Daglia, K. P. Devi, M. R. Loizzo, R. Tundis, S. M. Nabavi. Omega-3 polyunsaturated fatty acids and cancer: lessons learned from clinical trials. *Cancer Metastasis Rev.* **2015**, *34*, 359.
[7] E. Rysman, K. Brusselmans, K. Scheys, L. Timmermans, R. Derua, S. Munck, P. P. Van Veldhoven, D. Waltregny, V. W. Daniels, J. Machiels, F. Vanderhoydonc, K. Smans, E. Waelkens, G. Verhoeven, J. V. Swinnen. De novo lipogenesis protects cancer cells from free radicals and chemotherapeutics by promoting membrane lipid saturation. *Cancer Res.* **2010**, *70*, 8117.
[8] C. R. Santos, A. Schulze. Lipid metabolism in cancer. *FEBS J.* **2012**, *279*, 2610.
[9] M. P. Wymann, R. Schneiter. Lipid signalling in disease. *Nat. Rev. Mol. Cell Biol.* **2008**, *9*, 162.
[10] S. M. Louie, L. S. Roberts, M. M. Mulvihill, K. X. Luo, D. K. Nomura. Cancer cells incorporate and remodel exogenous palmitate into structural and oncogenic signaling lipids. *Biochim. Biophys. Acta Mol. Cell Biol. Lipids* **2013**, *1831*, 1566.
[11] M. Hilvo, C. Denkert, L. Lehtinen, B. Muller, S. Brockmoller, T. Seppanen-Laakso, J. Budczies, E. Bucher, L. Yetukuri, S. Castillo, E. Berg, H. Nygren, M. Sysi-Aho, J. L. Griffin, O. Fiehn, S. Loibl, C. Richter-Ehrenstein, C. Radke, T. Hyotylainen, O. Kallioniemi, K. Iljin, M. Oresic. Novel

theranostic opportunities offered by characterization of altered membrane lipid metabolism in breast cancer progression. *Cancer Res.* **2011**, *71*, 3236.
[12] W. W. Lv, T. S. Yang. Identification of possible biomarkers for breast cancer from free fatty acid profiles determined by GC-MS and multivariate statistical analysis. *Clin. Biochem.* **2012**, *45*, 127.
[13] N. Azordegan, V. Fraser, K. Le, L. M. Hillyer, D. W. L. Ma, G. Fischer, M. H. Moghadasian. Carcinogenesis alters fatty acid profile in breast tissue. *Mol. Cell. Biochem.* **2013**, *374*, 223.
[14] P. A. Corsetto, G. Montorfano, S. Zava, I. E. Jovenitti, A. Cremona, B. Berra, A. M. Rizzo. Effects of n-3 PUFAs on breast cancer cells through their incorporation in plasma membrane. *Lipids Health Dis.* **2011**, *10*.
[15] M. C. Pender-Cudlip, K. J. Krag, D. Martini, J. Yu, A. Guidi, S. S. Skinner, Y. Zhang, X. Y. Qu, C. W. He, Y. Xu, S. Y. Qian, J. X. Kang. Delta-6-desaturase activity and arachidonic acid synthesis are increased in human breast cancer tissue. *Cancer Sci.* **2013**, *104*, 760.
[16] C. G. Skibinski, A. Das, K. M. Chen, J. Liao, A. Manni, M. Kester, K. El-Bayoumy. A novel biologically active acid stable liposomal formulation of docosahexaenoic acid in human breast cancer cell lines. *Chem.-Biol. Interact.* **2016**, *252*, 1.
[17] T. R. Witte, W. E. Hardman. The effects of omega-3 polyunsaturated fatty acid consumption on mammary carcinogenesis. *Lipids* **2015**, *50*, 437.
[18] J. X. Kang, A. Liu. The role of the tissue omega-6/omega-3 fatty acid ratio in regulating tumor angiogenesis. *Cancer Met. Rev.* **2013**, *32*, 201.
[19] J. Bergan, T. Skotland, T. Sylvanne, H. Simolin, K. Ekroos, K. Sandvig. The ether lipid precursor hexadecylglycerol causes major changes in the lipidome of HEp-2 cells. *PLoS One* **2013**, *8*.
[20] M. L. Doria, C. Z. Cotrim, C. Simoes, B. Macedo, P. Domingues, M. R. Domingues, L. A. Helguero. Lipidomic analysis of phospholipids from human mammary epithelial and breast cancer cell lines. *J. Cell. Physiol.* **2013**, *228*, 457.
[21] M. L. Doria, Z. Cotrim, B. Macedo, C. Simoes, P. Domingues, L. Helguero, M. R. Domingues. Lipidomic approach to identify patterns in phospholipid profiles and define class differences in mammary epithelial and breast cancer cells. *Breast Cancer Res. Tr.* **2012**, *133*, 635.
[22] H. Kim, H. K. Min, G. Kong, M. H. Moon. Quantitative analysis of phosphatidylcholines and phosphatidylethanolamines in urine of patients with breast cancer by nanoflow liquid chromatography/tandem mass spectrometry. *Anal. Bioanal. Chem.* **2009**, *393*, 1649.
[23] L. Yang, X. G. Cui, N. N. Zhang, M. Li, Y. Bai, X. H. Han, Y. K. Shi, H. W. Liu. Comprehensive lipid profiling of plasma in patients with benign breast tumor and breast cancer reveals novel biomarkers. *Anal. Bioanal. Chem.* **2015**, *407*, 5065.
[24] E. Cífková, M. Holčapek, M. Lísa, D. Vrána, J. Gatěk, B. Melichar. Determination of lipidomic differences between human breast cancer and surrounding normal tissues using HILIC-HPLC/ESI-MS and multivariate data analysis. *Anal. Bioanal. Chem.* **2015**, *407*, 991.
[25] L. Eriksson, T. Byrne, E. Johansson, J. Trygg, C. Vikström. *Multi- and Megavariate Data Analysis. Basic Principles and Applications*, (3rd revised edn.). MKS Umetrics AB, Malmö, Sweden, **2013**.
[26] G. Liebisch, J. A. Vizcaino, H. Kofeler, M. Trotzmuller, W. J. Griffiths, G. Schmitz, F. Spener, M. J. O. Wakelam. Shorthand notation for lipid structures derived from mass spectrometry. *J. Lipid Res.* **2013**, *54*, 1523.
[27] J. Folch, M. Lees, G. H. S. Stanley. A simple method for the isolation and purification of total lipids from animal tissues. *J. Biol. Chem.* **1957**, *226*, 497.
[28] M. Lísa, E. Cífková, M. Holčapek. Lipidomic profiling of biological tissues using off-line two-dimensional high-performance liquid chromatography mass spectrometry. *J. Chromatogr. A* **2011**, *1218*, 5146.
[29] S. Hamilton, R. J. Hamilton, P. A. Sewell. *Lipid Analysis: Practical Approach*, Oxford University Press, NY, **1992**.
[30] E. Cífková, M. Holčapek, M. Lísa, M. Ovčačíková, A. Lyčka, F. Lynen, P. Sandra. Nontargeted quantitation of lipid classes using hydrophilic interaction liquid chromatography–electrospray ionization mass spectrometry with single internal standard and response factor approach. *Anal. Chem.* **2012**, *84*, 10064.

SUPPORTING INFORMATION

Additional supporting information may be found in the online version of this article at the publisher's website.

Journal of Chromatography B, 1000 (2015) 14–21

Contents lists available at ScienceDirect

Journal of Chromatography B

journal homepage: www.elsevier.com/locate/chromb

Lipidomic differentiation between human kidney tumors and surrounding normal tissues using HILIC-HPLC/ESI–MS and multivariate data analysis

Eva Cífková [a], Michal Holčapek [a,*], Miroslav Lísa [a], David Vrána [b], Bohuslav Melichar [b], Vladimír Študent [c]

[a] University of Pardubice, Faculty of Chemical Technology, Department of Analytical Chemistry, Studentská 573, 532 10 Pardubice, Czech Republic
[b] Palacký University, Medical School and Teaching Hospital, Department of Oncology, I.P. Pavlova 6, 775 20 Olomouc, Czech Republic
[c] Palacký University, Faculty of Medicine and Dentistry, Department of Urology, I.P. Pavlova 6, 775 20 Olomouc, Czech Republic

ARTICLE INFO

Article history:
Received 27 January 2015
Received in revised form 24 March 2015
Accepted 5 July 2015
Available online 13 July 2015

Keywords:
Lipidomics
Kidney cancer
Glycerophospholipids
HILIC-HPLC/ESI–MS
Multivariate data analysis

ABSTRACT

The characterization of differences among polar lipid classes in tumors and surrounding normal tissues of 20 kidney cancer patients is performed by hydrophilic interaction liquid chromatography (HILIC) coupled to electrospray ionization mass spectrometry (ESI–MS). The detailed analysis of identified lipid classes using relative abundances of characteristic ions in negative- and positive-ion modes is used for the determination of more than 120 individual lipid species containing attached fatty acyls of different chain length and double bond number. Lipid species are described using relative abundances, providing a better visualization of lipidomic differences between tumor and normal tissues. The multivariate data analysis methods using unsupervised principal component analysis (PCA) and supervised orthogonal partial least square (OPLS) are used for the characterization of statistically significant differences in identified lipid species. Ten most significant up- and down-regulated lipids in OPLS score plots are also displayed by box plots. A notable increase of relative abundances of lipids containing four and more double bonds is detected in tumor compared to normal tissues.

1. Introduction

Kidney cancer ranks among 10 most common cancers for both men and women, representing approximately 3% of adult tumors [1,2]. Renal cell cancer (RCC) represents more than 90% of malignant kidney tumors. The principal histological RCC subtypes include clear cell RCC (70–80%), papillary RCC (10–15%) and chromophobe RCC (3–5%). RCC is characterized by the resistance to virtually all cytotoxic agents. Before the advent of targeted therapy, surgery was the only effective treatment of this tumor. However, only a small proportion of patients with metastatic disease could be cured with surgery. Cytokines, the only systemic agents with some reproducible activity, were effective only in a minority of patients. Targeted therapy has changed the natural course of metastatic RCC. In the last decade, a number of targeted agents have been introduced, including multiple tyrosine kinase inhibitors sunitinib, sorafenib, axitinib and pazopanib, the monoclonal antibody bevacizumab and mammalian target of rapamycin inhibitors everolimus and temsirolimus. Despite this progress, few, if any, patients are cured by currently available drugs. In the search of new effective therapies novel molecular targets associated with malignant transformation have to be identified.

Lipids play an essential role in many biological processes, including the formation of cellular or intracellular membranes and compartments, the energy storage, the synthesis of hormones and the signal transduction [2–4]. The disruption of lipid metabolism and associated signaling pathways alters cellular function resulting in a spectrum of disorders, including the cancer. For example, palmitic acid (16:0) is a substrate for the formation of lipids required for the cellular proliferation and tumorigenic

Abbreviations: aCN, average carbon number; aDB, average double bond; CE, cholesteryl esters; CN, carbon number; DB, double bond; ESI, electrospray ionization; HILIC, hydrophilic interaction liquid chromatography; HPLC, high-performance liquid chromatography; Chol, cholesterol; IS, internal standard; LPA, lysophosphatidic acids; LPC, lysophosphatidylcholines; MDA, multivariate data analysis; MS, mass spectrometry; NP, normal phase; OPLS, orthogonal partial least square; PC, phosphatidylcholines; PCA, principal component analysis; PE, phosphatidylethanolamines; PI, phosphatidylinositols; RCC, renal cell cancer; RF, response factor; RP, reversed phase; SM, sphingomyelins; TG, triacylglycerol.

* Corresponding author. Fax: +420 466037068.
E-mail address: Michal.Holcapek@upce.cz (M. Holčapek).

http://dx.doi.org/10.1016/j.jchromb.2015.07.011
1570-0232/

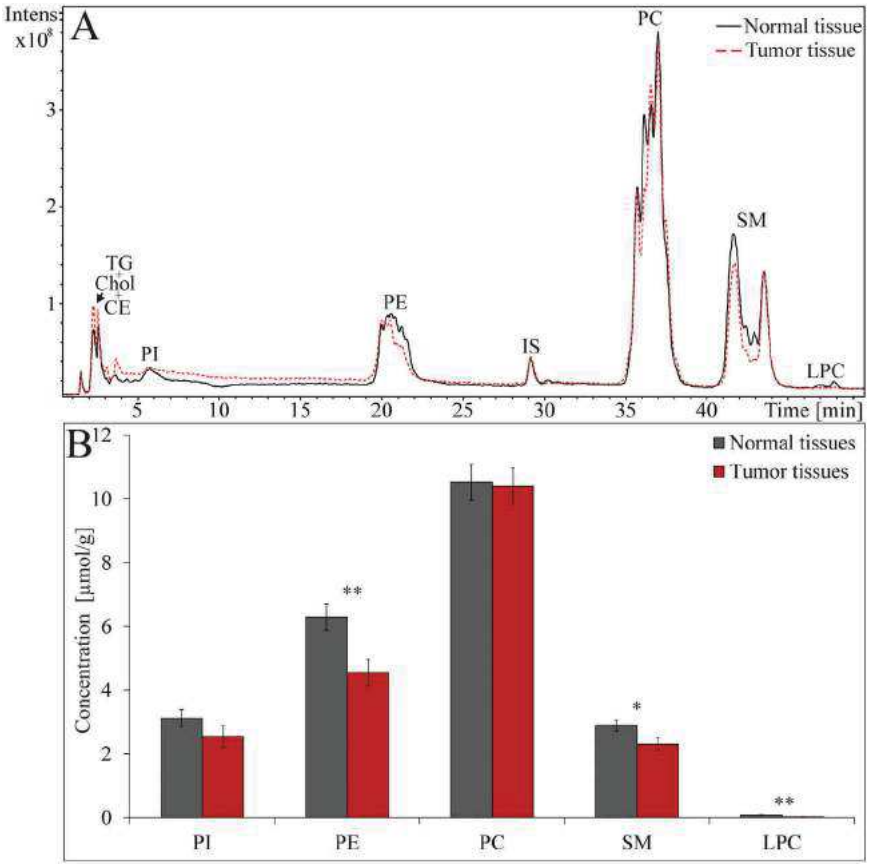

Fig. 1. (A) Positive-ion HILIC-HPLC/ESI–MS of total lipid extracts of normal (black line) and tumor (red line) tissues of a patient with clear cell type of kidney cancer. HPLC conditions: column Spherisorb Si (250 × 4.6 mm, 5 μm), flow rate 1 mL/min, separation temperature 40 °C, gradient 0 min – 94% A + 6% B, 60 min – 77% A + 23% B, where A is acetonitrile and B is 5 mM aqueous ammonium acetate. (B) Comparison of average concentrations [μmol/g] of individual lipid classes in normal and tumor tissues for 20 patients with their standard errors. Peak annotation: TG – triacylglycerols, Chol – cholesterol, CE – cholesteryl esters, PI – phosphatidylinositols, PE – phosphatidylethanolamines, IS – internal standard, PC – phosphatidylcholines, SM – sphingomyelins, LPC – lysophosphatidylcholines. Statistically significant differences according to *T*-test are indicated by an asterisk, where * refers to the significance $p \leq 0.05$ and ** $p \leq 0.01$. (For interpretation of the references to color in this figure legend, the reader is referred to the web version of this article.)

lipid signaling, while lysophosphatidic acids (LPA) and some specific eicosanoids serve as proliferative receptors. On the other hand, ceramides and sphingosines have antiproliferative and proapoptotic activity and are involved in the programed cell death [3–7]. Furthermore, arachidonic acid (20:4) belongs to major *n*-6 polyunsaturated fatty acids that affect increased production of inflammatory mediators [4].

Many studies addressing the lipidomic analysis of various biological samples benefit from high sensitivity and selectivity of the coupling of high-performance liquid chromatography and mass spectrometry (HPLC/MS). The separation in normal phase (NP) [8,9] or hydrophilic interaction liquid chromatography (HILIC) systems [10] enables the lipid class separation according to the polarity. Reversed phase (RP) HPLC on nonpolar stationary phases is frequently used for the separation of individual lipid species according to the fatty acyl chain length [11]. The quantitative analysis of lipids can be performed using the MS with the direct infusion (shotgun lipidomics) or HPLC/MS approaches. Shotgun is the most frequently used technique due to the rapid nontargeted analysis using precursor ion and neutral loss scans, which are well characterized for many lipid classes [12–14]. HPLC/MS approach was developed for the quantitation of separated lipid classes using the internal standard (IS) per each lipid class [15] or the combination of the single IS and response factors (RF) of individual lipid classes related with this IS [16,17].

Lipidomic analysis of RCC tissues and normal kidney tissues was performed using HPLC/MS [18], where significantly increased levels of cholesteryl esters (CE) and triacylglycerols (TG) and decreased levels of phosphatidylethanolamines (PE) and sphingomyelins (SM) in tumor tissues were reported. Mass spectrometry imaging using matrix-assisted laser desorption/ionization or desorption electrospray ionization was used for the relative comparison of tumor and surrounding normal tissues [19–22]. Increased absolute intensities for PI 18:0/20:4, PS 18:0/18:1 and PI 22:4/18:0 were reported [19,21] in kidney tumor tissues using the desorption electrospray ionization imaging. Analyses of lipids in plasma from RCC patients using ^{31}P nuclear magnetic resonance showed decreased concentrations of lysophosphatidylcholines (LPC) in comparison with healthy volunteers [23].

Multivariate data analysis (MDA) is a valuable approach for the evaluation of extensive data sets, providing significantly more information compared to the univariate data analysis [24–27]. The principal component analysis (PCA) is the most widespread nonsupervised method for the visualization of data sets using converted uncorrelated variables called principal components. Score plots serve for the projection of clustering of observed data, while loading plots describe clustering patterns. Orthogonal partial least square (OPLS) is a supervised method, where the group identification is set up in model parameters. OPLS method may use S-plots for a better visualization of clustering patterns including the influence of magnitude and reliability of variables.

The aim of the present study is to characterize lipidomic differences between kidney tumors and surrounding normal tissues in a cohort of 20 kidney cancer patients using our validated HILIC-

HPLC/ESI–MS method [17]. This method allows the quantitation of five lipid classes separated in HILIC mode and also the detailed analysis of individual lipid species inside these classes using relative abundances of characteristic ions in the negative- and positive-ion ESI mass spectra. The statistical evaluation of obtained data set for all patients using unsupervised PCA and supervised OPLS enables to identification of lipids with the highest impact on the group separation.

2. Experimental

2.1. Materials

Acetonitrile, methanol, 2-propanol (all HPLC/MS grade), chloroform (HPLC grade stabilized by 0.5-1% ethanol), ammonium acetate and sodium chloride were purchased from Sigma–Aldrich (St. Louis, MO, USA). Deionized water was prepared with a Demiwa 5-roi purification system (Watek, Ledeč nad Sázavou, Czech Republic). *N*-dodecanoyl-heptadecasphing-4-enine-1-phosphoethanolamine (d17:1/12:0) used as an internal standard (IS) for the quantitative analysis was purchased from Avanti Polar Lipids (Alabaster, AL, USA). Tumor tissues and surrounding normal tissues of 20 kidney cancer patients (Table S1) were obtained from the Department of Urology, Palacký University, Faculty of Medicine and Dentistry and University Hospital, Olomouc, Czech Republic. The study was approved by the Hospital Ethical Committee, and all patients signed informed consent.

2.2. Sample preparation

Samples of kidney tumor and normal kidney tissue were obtained during the surgery, immediately frozen and stored at −80 °C until the sample processing and the analysis. Human kidney tissues were prepared using chloroform–methanol–water extraction according to a Folch method [28]. Briefly, 250 mg of kidney tissue and 25 μL of 3.3 mg/mL IS were homogenized with 5 mL of chloroform–methanol (2:1, v/v) mixture. The filtered homogenate was mixed with 1 mL of 1 mol/L sodium chloride and centrifuged at 3000 rpm for 5 min at room temperature. Bottom chloroform layer containing lipids was evaporated by a stream of nitrogen and redissolved in 1 mL of chloroform–2-propanol mixture (1:1, v/v).

2.3. HPLC/MS conditions

Total lipid extracts were analyzed by HPLC/MS method described previously [10,17]. The liquid chromatograph Agilent 1290 series (Agilent Technologies, Waldbronn, Germany) was coupled with the Esquire 3000 ion trap analyzer (Bruker Daltonics, Bremen, Germany). The separation of individual lipid classes was performed on a Spherisorb Si column (250 × 4.6 mm, 5 μm, Waters, Milford, MA, USA), a flow rate of 1 mL/min, an injection volume of 1 μL, column temperature of 40 °C and a mobile phase gradient: 0 min – 94% A + 6% B, 60 min – 77% A + 23% B, where A was acetonitrile and B was 5 mmol/L aqueous ammonium acetate. Lipids were detected in positive- and negative-ion ESI–MS modes in the mass range m/z 50–1000 with the setting of pressure of the nebulizing gas 60 psi, drying gas flow rate 10 L/min and temperature of the drying gas 365 °C. The quantitation of individual lipid classes was achieved by the single IS and response factors obtained from calibration curves as described previously [17]. Individual lipid species were analyzed using relative abundances of deprotonated molecules $[M\text{-}H]^-$ for PE and PI classes and $[M\text{-}CH_3]^-$ ions for PC class in the negative-ion mode [17]. Individual SM species were analyzed using relative abundances of protonated molecules $[M+H]^+$ in the positive-ion mode due to the low signal intensity in the negative-ion mode. The low energy collision induced dissociation tandem mass spectrometry (MS/MS) experiments were performed for the most significant lipid species with the isolation width of *m/z* 4, the collision amplitude of 1 V and helium as a collision gas.

2.4. Statistical data analysis

MDA was performed using PCA and OPLS methods in the SIMCA software, version 13.0 (Umetrics, Umeå, Sweden). Data were preprocessed before the statistical analysis using the Pareto scaling. All models were characterized by score plots, loading plots and S-plots listed in Table S2. Statistically significant differences in graphs were calculated using the *T*-test, where * refers to the significance $p \leq 0.05$ (5%), ** $p \leq 0.01$ (1%) and *** $p \leq 0.01$ (0.1%). Box plots describe values of median, minimum, maximum and the variability of data sets using the first and third quartiles.

3. Results and discussion

3.1. Quantitative analysis of polar lipid classes

Among 20 samples analyzed, 19 cases are RCC (18 cases of clear cell RCC and one case of papillary RCC), while the rare Wilms tumor is diagnosed in one case. No statistically relevant differences are observed in our data for clear cell RCC, papillary RCC and Wilms tumor, so the data are treated as one group of kidney cancer. Total lipid extracts are analyzed using our previously developed HILIC-HPLC/ESI–MS method [17,29], which was validated for the quantitation of polar lipid classes using single IS (sphingosyl PE d17:1/12:0) and response factors calculated from their calibration curves [16,17]. Fig. 1A shows a baseline separation of PI, PE, PC, SM and LPC classes and the IS. Different peak shapes of some lipid classes are observed between normal (gray line) and tumor (red line) tissues for one patient, which is caused by different lipidomic composition inside these classes (Table S3). The present HILIC-HPLC/ESI–MS method is not applicable for the quantitation of nonpolar lipid classes, namely TG, CE and cholesterol (Chol), due to their elution in the system void volume. Mean lipid class concentrations of 20 kidney cancer patients significantly differ between normal (gray columns) and tumor (red columns) tissues for some lipid classes, with PE, LPC and SM showing the highest variance (Fig. 1B). Numerical values of mean concentrations and their standard deviations are listed in Table S4. Decreased levels of PE, SM and LPC in kidney tumor tissues in comparison with surrounding normal tissues are in agreement with previous reports [18,23].

3.2. Detailed analysis of individual lipid species

Individual lipid species inside classes are described using relative abundances of characteristic ions in ESI mass spectra obtained by the peak integration of given lipid class in the HILIC chromatogram. Deprotonated molecules $[M\text{-}H]^-$ are used for the analysis of individual PE and PI species and $[M\text{-}CH_3]^-$ ions for PC in the negative-ion mode, while protonated molecules $[M+H]^+$ are used for SM species in the positive-ion mode. In this study, the relative quantitation (in%) calculated based on relative abundances of their characteristic ions is preferred for individual lipid species (Figs. 2 and 3,), which is especially useful for better visualization of lipid changes between tumor and normal tissues. The absolute quantitative data (in μmol/g) are calculated as relative abundances of individual lipid species multiplied by the total concentration of this lipid class (Fig. S1 and S2). The deisotoping of mass spectra for all described lipid species is performed using the Excel script, where isotopic patterns are calculated using the Isotope pattern software (Bruker Daltonics). The identification of prevalent combination of

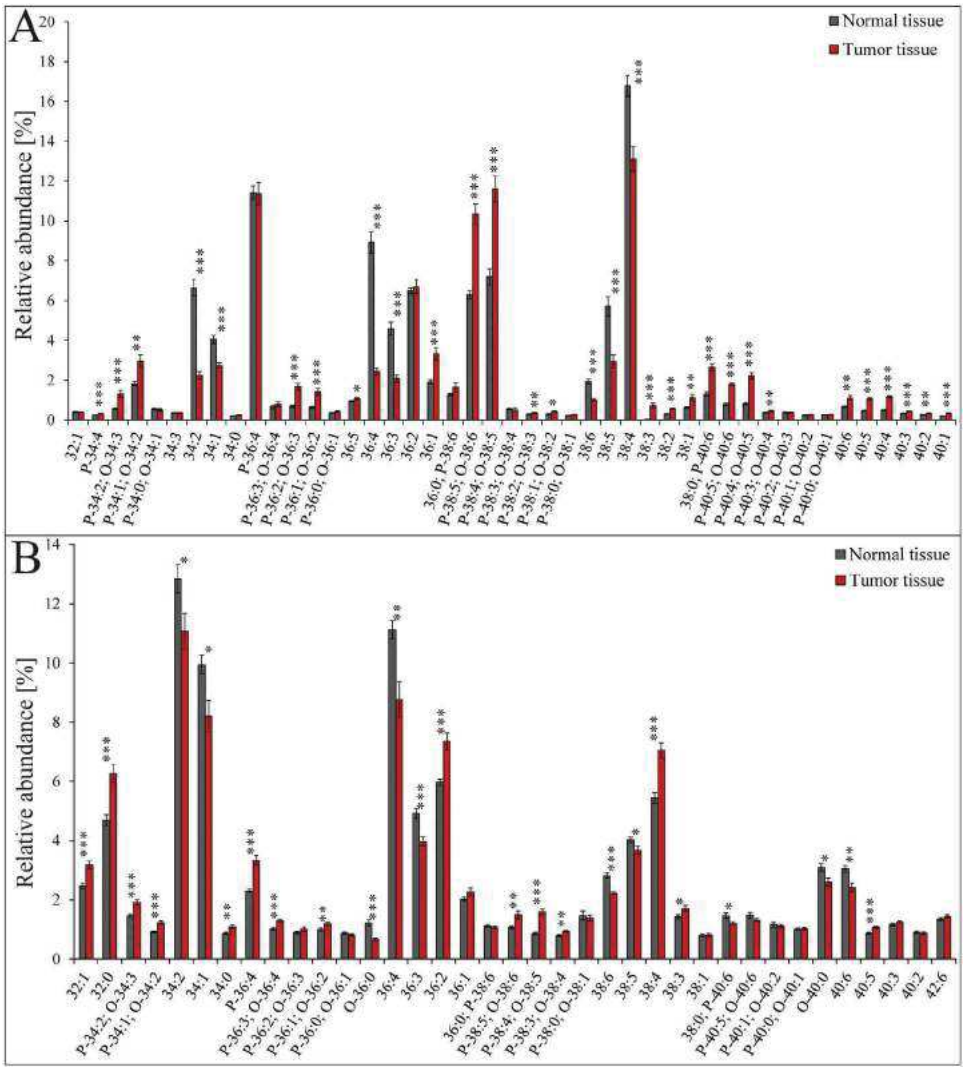

Fig. 2. Relative abundances [%] of individual species in normal and tumor tissues of 20 patients with kidney cancer: (A) PE and (B) PC determined by relative abundances of $[M\text{-}H]^-$ and $[M\text{-}CH_3]^-$ ions, respectively, in the negative-ion HILIC-HPLC/ESI–MS. Statistically significant differences according to *T*-test are indicated by an asterisk, where * refers to the significance $p \leq 0.05$, ** $p \leq 0.01$, and *** $p \leq 0.001$.

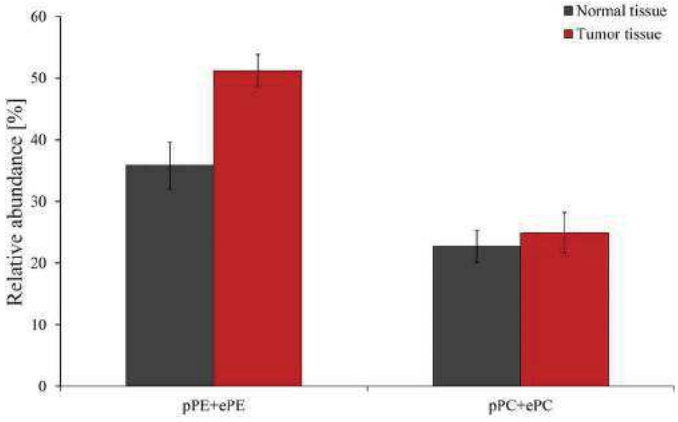

Fig. 3. Comparison of relative abundances of the sum of pPE+ePE species and the sum of pPC+ePC species in normal and tumor tissues for 20 patients. Bars indicate standard error.

attached fatty acyls and their positions on the glycerol skeleton of the most significant lipid species for differentiation of tumor and normal tissues was additionally performed using MS/MS spectra in the negative-ion mode. Individual lipid species are characterized by attached fatty acyls annotated by their total carbon number and double bond number (CN:DB). Some lipid species (e.g., PE and PC) can also differ in the type of fatty acyl linkage to the glycerol skeleton in the *sn*-1 position. The ester linkage of fatty acyls in both *sn*-1 and *sn*-2 positions (diacyls) is referred as aPE and aPC. The ether linkage of fatty acyls in *sn*-1 position (1-alkyl-2-acyl) is referred as ethers (ePE and ePC) and the vinyl ether linkage in *sn*-1 position (1-alkenyl-2-acyl) corresponds to plasmalogens (pPE and pPC).

3.3. Characterization of lipid species differences

Fig. 2A shows mean relative abundances of 45 PE species in tumor tissues (red columns) and surrounding normal tissues (gray columns) of 20 kidney cancer patients. The statistical significance is calculated using *T*-test. PE P-38:4 or O-38:5 (PE P-18:0/20:4 – prevalent combination of attached fatty acyls identified using MS/MS spectrum), PE P-38:5 or O-38:6 (PE P-18:0/20:5) and PE 36:1 (PE 18:0/18:1) are the most up-regulated PE species in tumor tissues, while PE 38:4 (PE 18:0/20:4), PE 36:4 (PE 16:0/20:4) and PE 34:2 (PE 16:0/18:2) are the most down-regulated species (Fig. 2A). All plasmalogen PE species containing more than 4 DB, which means one polyunsaturated fatty acyl on the glycerol skeleton, are up-regulated. Furthermore, the same trend is observed for PE

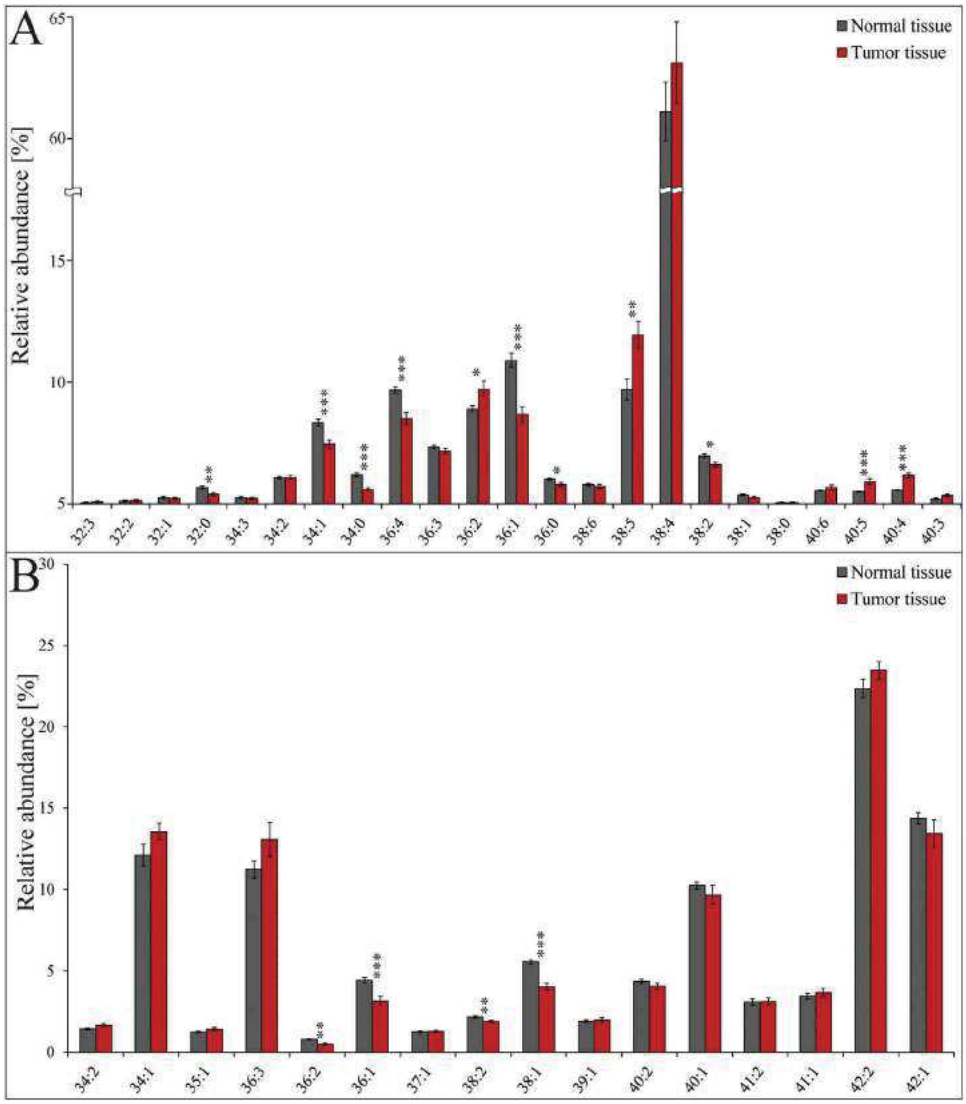

Fig. 4. Relative abundances [%] of individual species in normal and tumor tissues of 20 patients with kidney cancer: (A) PI and (B) SM determined using relative abundances of $[M-H]^-$ and $[M+H]^+$ ions, respectively, in the negative and positive-ion HILIC-HPLC/ESI–MS. Statistically significant differences according to *T*-test are indicated by an asterisk, where * refers to the significance $p \leq 0.05$, ** $p \leq 0.01$, and *** $p \leq 0.001$.

species with CN equal to 40. Relative abundances of saturated (0 DB), low unsaturated (1–3 DB) and high unsaturated (4–6 DB) fatty acyls, average CN (aCN) and average DB (aDB) are calculated in Table S3. The highest differences are observed for the group of aPE, where saturated fatty acyls decrease and high unsaturated acyls increase in tumor tissues. In other cases, differences are less pronounced.

The comparison of relative abundances of individual PC species (Fig. 2B) in tumor and normal tissues for 20 patients indicates 25 statistically significant differences in PC according to the *T*-test. The most up-regulated species are PC 38:4 (PC 18:0/20:4), PC 36:2 (PC 18:0/18:2) and PC 32:0 (PC 16:0/16:0), and down-regulated PC 34:2 (16:0/18:2), PC 36:4 (16:0/20:4) and PC 34:1 (16:0/18:1), which is in an excellent agreement with previous work [22]. Values of aCN and aDB for all PC species are similar, but significant differences between both tissues are observed for saturated and high unsaturated fatty acyls in pPC + ePC and aPC groups (Table S3). Relative abundance of saturated fatty acyls in pPC + ePC decrease about 22% in tumor tissues in comparison with surrounding normal tissues. The vinyl-ether bonds of plasmalogens are more sensitive to the oxidation by free radicals and protect membrane lipids against the oxidation associated with inflammatory response. Therefore, relative abundances of plasmalogens and ethers in PE and PC classes are reported for normal and tumor tissues in Fig. 3. The relative proportion of pPE + ePE group in PE lipid class forms 36% in normal tissues and 51% in tumor tissues, while pPC + ePC represents about 23% of all PC species in both tissues.

Relative abundances of 23 individual PI species are shown in Fig. 4A and indicate 5 statistically significant up-regulated PI species in tumor tissues, namely PI 38:5 (PI 16:0/22:5), PI 36:2 (PI 18:1/18:1), PI 40:5 (PI 18:0/22:5), PI 40:4 (PI 20:0/20:4) and PI 36:0 (18:0/18:0). These results are again in agreement with previous reports [19,21]. The species exhibiting highest down-regulated PI species are PI 36:1 (PI 18:0/18:1), PI 36:4 (PI 16:0/20:4) and PI 34:1 (PI 16:0/18:1). In comparison with other classes, the highest differences in the saturation of fatty acyls between normal and tumor tissues are observed for unsaturated fatty acyls, where low unsaturated decrease and high unsaturated increase in tumor tissues (Table S3).

Only 4 statistically significant SM species, namely SM 36:2, SM 36:1, SM 38:2 and SM 38:1, are identified using *T*-test by comparison of relative abundances of normal and tumor tissues (Fig. 4B). All

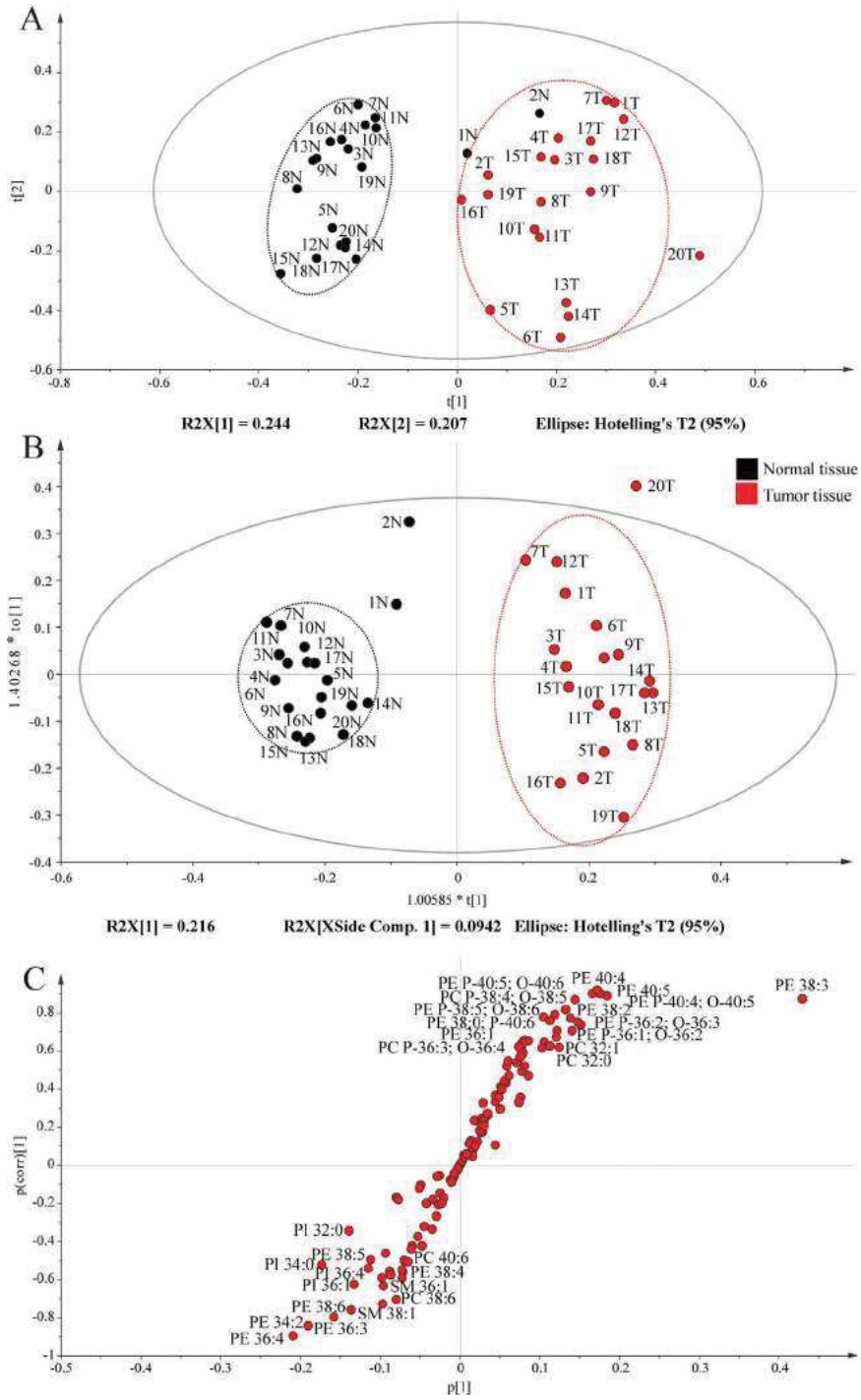

Fig. 5. Multivariate data analysis of relative abundances of all lipids in normal and tumor tissues: (A) the score plot of unsupervised PCA method, (B) the score plot and (C) the S-plot of supervised OPLS method describing up-regulated and down-regulated lipids in tumor tissues. (For interpretation of the references to color in the text, the reader is referred to the web version of this article.)

above mentioned SM species are down-regulated in tumor tissues and are formed by low unsaturated fatty acyls (Table S3). Individual fatty acyls on the glycerol skeleton cannot be identified using MS/MS spectra due to low signal intensities in the negative-ion mode. The analysis of individual LPC species cannot be performed due to low intensities of protonated molecules $[M+H]^+$ in the positive-ion ESI spectra.

HILIC-HPLC/ESI–MS method has already been used for the determination of lipidomic differences between tumor and surrounding normal tissues of 10 breast cancer patients [29]. A statistically significant increase of concentrations of all mentioned lipid classes and a decrease of relative abundances of pPE + ePE group were detected in breast tumor tissues. Lipids with the general formula 34:1 (combination of 16:0 and 18:1) are significantly increased in breast tumor tissues. Opposing trends are observed in kidney cancer. Nevertheless, glycerophospholipids with the general formula 36:4 (combination of 16:0 and 20:4) have shown marked decrease in tumor tissues for both cancer patient groups.

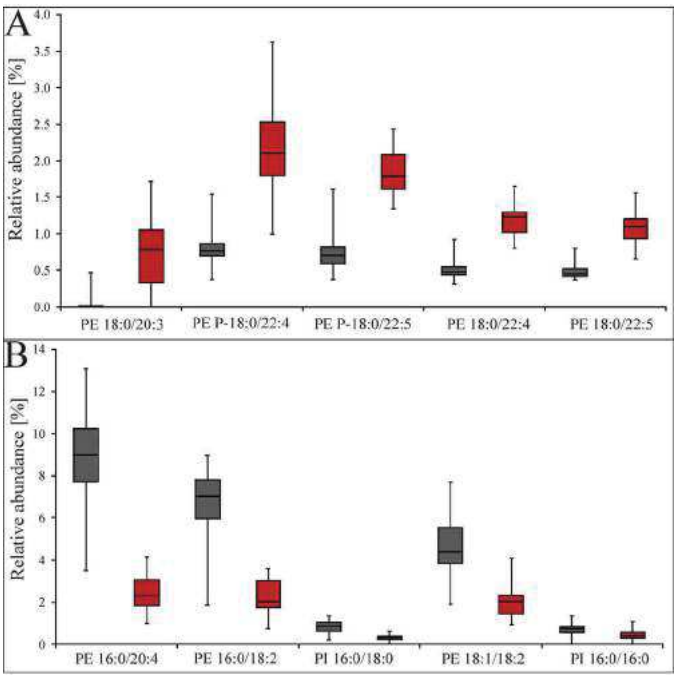

Fig. 6. Box plots describing the five most important (A) up-regulated and (B) down-regulated lipids in normal (gray) and tumor (red) tissues obtained using OPLS method. Each boxplot characterizes the variability of data sets using average values of median, first and third quartiles, minimum and maximum.

3.4. Statistical evaluation of identified lipid species

Relative abundances of all identified lipid species in normal and tumor tissues are statistically evaluated using the SIMCA software. At first, the data set is analyzed using unsupervised PCA method, which reduces the multidimensionality of the data to two-dimensional system characterized by principal components without any input specification of groups. The score plot of PCA method (Fig. 5A) shows a clear clustering of tumor tissues (red points) and normal tissues (gray points) except for 1N and 2N. The first component in PCA method explains 24.4% of the variation and the second component 20.7%. Subsequently, the supervised OPLS method is used to further improve the group clustering, because this statistical method has the input information on the group assignment. The score plot of OPLS method (Fig. 5B) shows the excellent group separation of normal and tumor tissues for all patients without any outliers. Larger variability is observed for the tumor group in contrast to the normal group, which can be probably explained by different tumor subtypes and tumor cell heterogeneity. Patterns of group clustering in OPLS score plot are visualized in the S-plot (Fig. 5C). The S-plot does not describe only the direction of regulation but also the reliability and magnitude of individual lipid species. The upper right corner of the S-plot shows up-regulated lipid species in tumor tissues, while the lower left corner down-regulated species. PE 38:3 is the up-regulated lipid with the highest reliability and high magnitude, while PE 36:4 is the most significant down-regulated lipid. Lipid species in the middle of the diagram close to zero on both axes have a low statistical significance for the group differentiation and therefore they are not annotated. The S-plot allows for the characterization of five most significant up-regulated species: PE 38:3 (PE 18:0/20:3), PE P-40:4 or O-40:5 (PE P-18:0/22:4), PE P-40:5 or O-40:6 (PE P-18:0/22:5), PE 40:4 (PE 18:0/22:4) and PE 40:5 (PE 18:0/22:5) and down-regulated: PE 36:4 (PE 16:0/20:4), PE 34:2 (16:0/18:2), PI 34:0 (16:0/18:0), PE 36:3 (PE 18:1/18:2) and PI 32:0 (PI 16:0/16:0) lipid species. These 10 lipids shown in box plots (Fig. 6) represent the largest differences between normal and tumor tissues with a low standard deviation of values. The central line in the box plot shows the value of median, the lower part represents the first quartile and the upper part is the third quartile. Extreme lines show minimum and maximum values.

Kidney cancer is a very heterogeneous group of malignant neoplasms. Most specimens examined in the present pilot study are clear cell RCC. With only a single case each of papillary RCC and Wilms tumor, no conclusions can be drawn about the lipid composition of these relatively rare kidney cancers. While currently the targeted treatment of advanced RCC relies on agents inhibiting the vascular endothelial growth factor and mammalian target of rapamycin pathways, novel drugs with other mechanisms of action start to emerge. With the advent of phosphatidylinositol 3 kinase inhibitors or other drugs targeting lipid-associated pathways, the understanding of changes of lipid metabolism in tumors may be of significance for the targeted therapy. Advances of targeted therapy are dependent on the development of predictive molecular biomarkers that may also include lipids. Present data open the way for the further research on the changes of lipid composition as biomarkers of response. The identification of lipid biomarkers could also aid in the early diagnosis, including the screening. The incidence of RCC in the Czech Republic is highest in the world, and depending on the availability of reliable diagnostic biomarkers screening programs can be envisaged.

4. Conclusions

HILIC-HPLC/ESI–MS method allows for the lipidomic characterization of tumors and surrounding normal tissues in a pilot study of 20 renal cell cancer patients. The decrease of total concentrations of PE, SM and LPC classes in tumor tissues compared to normal tissues is statistically significant according to the *T*-test. The most pronounced trend is observed for glycerophospholipids with a general formula 36:4 (PE 16:0/20:4, PC 16:0/20:4 and PI 16:0/20:4), which exhibit a significant decrease of relative concentrations in tumor tissues. PE 36:4 is the most markedly down-regulated lipid in the S-plot of OPLS method. Palmitic acyl (16:0) is associated with the proliferation and arachidonic acyl (20:4) with inflammatory processes in the organism and these effects are associated with the tumor progression. Most up-regulated lipid species are PE species containing one polyunsaturated fatty acyl (22:4 and 22:5) except for PE 38:3 (18:0 and 20:3), while all down-regulated lipid species contain mainly saturated or eventually low unsaturated fatty acyls except for PE 36:4 containing arachidonic acyl. The association of saturation level with the tissue type is noticed for 10 most significantly regulated lipids.

Acknowledgments

This work was supported by ERC CZ project No. LL1302 sponsored by the Ministry of Education, Youth and Sports of the Czech Republic. E.C. acknowledges the support of the grant project No. CZ.1.07/2.3.00/30.0021 sponsored by the Ministry of Education, Youth and Sports of the Czech Republic. The help of Blanka Červená and Magdaléna Ovčačíková (University of Pardubice) with the extraction procedure is acknowledged.

Appendix A. Supplementary data

Supplementary data associated with this article can be found, in the online version, at http://dx.doi.org/10.1016/j.jchromb.2015.07.011

References

[1] D. Barh, A. Carpi, M. Verma, M. Gunduz, Cancer Biomarkers, CRC Press, Boca Raton, FL, USA, 2014.
[2] S. Pelengaris, M. Khan, The Molecular Biology of Cancer. A Bridge from Bench to Bedside, Wiley-Blackwell, Oxford, UK, 2013.
[3] W. Al-Zhoughbi, J.F. Huang, G.S. Paramasivan, H. Till, M. Pichler, B. Guertl-Lackner, G. Hoefler, Tumor macroenvironment and metabolism, Semin. Oncol. 41 (2014) 281.
[4] M.P. Wymann, R. Schneiter, Lipid signalling in disease, Nat. Rev. Mol. Cell Biol. 9 (2008) 162.
[5] L. Arana, P. Gangoiti, A. Ouro, M. Trueba, A. Gomez-Munoz, Ceramide and ceramide 1-phosphate in health and disease, Lipids Health Dis. 9 (2010) 15.
[6] G.B. Mills, W.H. Moolenaar, The emerging role of lysophosphatidic acid in cancer, Nat. Rev. Cancer 3 (2003) 582.
[7] S.M. Louie, L.S. Roberts, M.M. Mulvihill, K.X. Luo, D.K. Nomura, Cancer cells incorporate and remodel exogenous palmitate into structural and oncogenic signaling lipids, Biochim. Biophys. Acta Mol. Cell Biol. Lipids 1831 (2013) 1566.
[8] D.G. McLaren, P.L. Miller, M.E. Lassman, J.M. Castro-Perez, B.K. Hubbard, T.P. Roddy, An ultraperformance liquid chromatography method for the normal-phase separation of lipids, Anal. Biochem. 414 (2011) 266.
[9] M. Holčapek, E. Cífková, B. Červená, M. Lísa, J. Vostálová, J. Galuszka, Determination of nonpolar and polar lipid classes in human plasma, erythrocytes and plasma lipoprotein fractions using ultrahigh-performance liquid chromatography-mass spectrometry, J. Chromatogr. A 1377 (2015) 85.
[10] M. Lísa, E. Cífková, M. Holčapek, Lipidomic profiling of biological tissues using off-line two-dimensional high-performance liquid chromatography mass spectrometry, J. Chromatogr. A 1218 (2011) 5146.
[11] K. Sandra, A.D. Pereira, G. Vanhoenacker, F. David, P. Sandra, Comprehensive blood plasma lipidomics by liquid chromatography/quadrupole time-of-flight mass spectrometry, J. Chromatogr. A 1217 (2010) 4087.
[12] X.L. Han, K. Yang, R.W. Gross, Multi-dimensional mass spectrometry-based shotgun lipidomics and novel strategies for lipidomic analyses, Mass Spectrom. Rev. 31 (2012) 134.
[13] D. Schwudke, G. Liebisch, R. Herzog, G. Schmitz, A. Shevchenko, Lipidomics and Bioactive Lipids, Elsevier Academic Press Inc, San Diego, USA, 2007, pp. 175.
[14] K. Yang, H. Cheng, R.W. Gross, X.L. Han, Automated lipid identification and quantification by multidimensional mass spectrometry-based shotgun lipidomics, Anal. Chem. 81 (2009) 4356.
[15] M. Scherer, K. Leuthauser-Jaschinski, J. Ecker, G. Schmitz, G. Liebisch, A rapid and quantitative LC–MS/MS method to profile sphingolipids, J. Lipid Res. 51 (2010) 2001.
[16] E. Cífková, M. Holčapek, M. Lísa, Nontargeted lipidomic characterization of porcine organs using hydrophilic interaction liquid chromatography and off-line two-dimensional liquid chromatography-electrospray ionization mass spectrometry, Lipids 48 (2013) 915.
[17] E. Cífková, M. Holčapek, M. Lísa, M. Ovčačíková, A. Lyčka, F. Lynen, P. Sandra, Nontargeted quantitation of lipid classes using hydrophilic interaction liquid chromatography–electrospray ionization mass spectrometry with single internal standard and response factor approach, Anal. Chem. 84 (2012) 10064.
[18] J.P. Sundelin, M. Stahlman, A. Lundqvist, M. Levin, P. Parini, M.E. Johansson, J. Boren, Increased expression of the very low-density lipoprotein receptor mediates lipid accumulation in clear cell renal cell carcinoma, PLoS One 7 (2012) e48694.
[19] A.L. Dill, L.S. Eberlin, C. Zheng, A.B. Costa, D.R. Ifa, L.A. Cheng, T.A. Masterson, M.O. Koch, O. Vitek, R.G. Cooks, Multivariate statistical differentiation of renal cell carcinomas based on lipidomic analysis by ambient ionization imaging mass spectrometry, Anal. Bioanal. Chem. 398 (2010) 2969.
[20] E.E. Jones, T.W. Powers, B.A. Neely, L.H. Cazares, D.A. Troyer, A.S. Parker, R.R. Drake, MALDI imaging mass spectrometry profiling of proteins and lipids in clear cell renal cell carcinoma, Proteomics 14 (2014) 924.
[21] V. Pirro, L.S. Eberlin, P. Oliveri, R.G. Cooks, Interactive hyperspectral approach for exploring and interpreting DESI–MS images of cancerous and normal tissue sections, Analyst 137 (2012) 2374.
[22] K. Yoshimura, L.C. Chen, M.K. Mandal, T. Nakazawa, Z. Yu, T. Uchiyama, H. Hori, K. Tanabe, T. Kubota, H. Fujii, R. Katoh, K. Hiraoka, S. Takeda, Analysis of renal cell carcinoma as a first step for developing mass spectrometry-based diagnostics, J. Am. Soc. Mass Spectrom. 23 (2012) 1741.
[23] F. Sullentrop, D. Moka, S. Neubauer, G. Haupt, U. Engelmann, J. Hahn, H. Schicha, P-31 NMR spectroscopy of blood plasma: determination and quantification of phospholipid classes in patients with renal cell carcinoma, NMR Biomed. 15 (2002) 60.
[24] L. Eriksson, T. Byrne, E. Johansson, J. Trygg, C. Vikström, Multi- and Megavariate Data Analysis. Basic Principles and Applications, MKS Umetrics AB, Malmö, Sweden, 2013.
[25] G.M. Kirwan, E. Johansson, R. Kleemann, E.R. Verheij, A.M. Wheelock, S. Goto, J. Trygg, C.E. Wheelock, Building Multivariate Systems Biology Models, Anal. Chem. 84 (2012) 7064.
[26] J. Trygg, S. Wold, Orthogonal projections to latent structures (O-PLS), J. Chemom. 16 (2002) 119.
[27] S. Wold, M. Sjostrom, L. Eriksson, PLS-regression: a basic tool of chemometrics, Chemom. Intell. Lab. Syst. 58 (2001) 109.
[28] J. Folch, M. Lees, G.H.S. Stanley, A simple method for the isolation and purification of total lipides from animal tissues, J. Biol. Chem. 226 (1957) 497.
[29] E. Cífková, M. Holčapek, M. Lísa, D. Vrána, J. Gatěk, B. Melichar, Determination of lipidomic differences between human breast cancer and surrounding normal tissues using HILIC-HPLC/ESI–MS and multivariate data analysis, Anal. Bioanal. Chem. 407 (2015) 991.